IJHSR International Journal of High School Research

April 2026 | Volume 8 | Issue 7
ijhsr.terrajournals.org
ISSN (Print) 2642-1046
ISSN (Online) 2642-1054

GENIUS OLYMPIAD

Let's build a better future together

International Project Fair focused on Sustainability and Environment for Grades 8-12



- Since 2011
- Hosted around 1400 participants in 2025 from 35+ states 70+ countries
- **Disciplines:** STEM, Coding, Robotics, AI, Speech, Entrepreneurship, Arts, Short Film, Music
- Applications start on December 1
- Application Deadline is March 1
- Finalists are announced by March 25
- Event is usually scheduled 2nd week of June
- Monday – Friday, includes a trip to Niagara Falls
- Hosted by large universities at Upstate New York
- Application Fee is $60/ project
- Participation Fee is $600/ person, w/ room and board
- Open buffet breakfast, lunch, and dinner
- Trip to Niagara Falls and boat tour is included
- **Instagram and Facebook @Geniusolympiad**
- For more information: **GENIUSOlympiad.org**
- Email: **info@geniusolympiad.org**

GENIUS Olympiad is organized by Terra Science and Education, a N.Y. based 501.c.3 non-profit organization dedicated for project-based learning



Marine Biology Research at Bahamas

Unique and exclusive partnership with the Gerace Research Center (GRC) in San Salvador, Bahamas to offer marine biology research opportunities for high school teachers and students.

- Terra has exclusive rights to offer the program to high school teachers and students around world.
- All trips entail extensive snorkeling in Bahamian reefs as well as other scientific and cultural activities.
- Terra will schedule the program with GRC and book the flights from US to the GRC site.
- Fees include travel within the US to Island, lodging, meals, and hotels for transfers, and courses.
- For more information, please visit terraed.org/bahamas.html

Terra is a N.Y. based 501.c.3 non-profit organization
dedicated for improving K-16 education

Table of Contents

April 2026| Volume 8| Issue 7

1 **Reconstructing Genomes Using Graph-Based Algorithms**
Aaron Kuang

8 **A Numerical Analysis of Stability in Zero-Sum Rock-Paper-Scissors Stochastic Replicator Dynamics**
Kyle Yang

14 **Photon Transport and Spectral Formation in Accreting Neutron Star Columns: A Monte Carlo Approach**
Andrew Gan

20 **The Effects of Chain-of-Thought Prompting on the Performance of Moderate-sized LLMs in Competitive Math**
Eric L. Min

27 **Digital Environment's Potential to Modulate Altered Decision-Making Pathways and Processes in Autism Spectrum Disorder**
Daniel D. Jackson

34 **The Economics of AI in the Music Industry: Impacts, Risks, and Opportunities**
Aashi Singh

43 **Genetic Factors in the Development and Diagnosis of Lymphedema and Lipedema**
Aditi S. Gandhi

50 **In Cancer Immunotherapy Using CAR T Therapy and Emerging Advances in Stem Cell Therapy**
Huseyn Ibrahimli

54 **Model Collapse: A Comprehensive Review of Causes, Detection, and Mitigation**
Murtaza S. Malik

65 **Predicting the Prognosis of Ulcerative Colitis with Machine Learning**
Aayushi Saxena

71 **Benchmarking Distinct Deep Learning Architectures for Forecasting ARIMA-Synthesized Non-Stationary Time Series**
Abdullah Shaikh

80 **Relationship and Comparison between Plasma, Neuroimaging, and Digital Biomarkers in Alzheimer's Disease**
Anaya Shabi

88 **A Systematic Review of Barriers and Solutions to Implementing Waste Reduction Strategies in Hospitals**
Shrey Aggarwal

96 **The Effects of Age and Sex on Symptom Severity and Brain Volumes of Irritable Bowel Syndrome Patients**
Anna Chia

105 **Capability of Dielectric Elastomer Actuators to Replace Natural Muscle**
Advait Swaminathan

115 **Comparative Structural Integrity of Miura-Ori and Flasher Origami Patterns for Deployable Solar Panels**
Aruzhan Muratbekova

122 **How Do Wing Length and Thickness Affect Flight Performance?**
Hannah Choo Ying En

128 **The War on Superbugs: Teixobactin, and a New Frontier in Antibiotic Resistance**
Michael Peng

133 **Temporal Lobe Epilepsy and Autoimmune Disorder Associations and Mechanisms: A Scoping Review**
Sanvi S. Singh

139 **The Role of Stem Cells in Cancer Treatments**
Amanda Chua

148 **A Review of Per- and Polyfluoroalkyl Substances (PFAS) and Age of Menarche among Adolescent Girls**
Ayaka Singh

154 **Biodegradable Textiles and Apparel as an Opportunity for Private Sector Environmental Impact**
Pranay Shrinivaas Balaji Shyam Sundar

162 **Investigation of Tensile and Soil Degradation Properties of Pure and Hybrid Homemade Bioplastics**
Kaiyue Chen

© 2026 Terra Science and Education

Table of Contents

April 2026| Volume 8| Issue 7

168 **A Role for Music in Slowing Memory Decline in Alzheimer's Disease**
Olivia Tu

177 **Reproductive Lifespan as a Proxy for Estrogen Exposure and Alzheimer's Disease Risk in Women: A Multisystem Perspective**
Sonya Komar

183 **An Automated Framework for Studying the Potential of AI Defaults in Assignments**
Audrey H. Koo

190 **The True Footprint of Clean Energy: A Life-Cycle Comparison of Solar, Wind, and Microalgae Biofuel**
Jun Kang

201 **CCR5 and Its Mutation in HIV Infection, and the Therapeutic Approach with CRISPR-Cas9**
Nana Shibuya

211 **Exploring Music Therapy as Adjunctive Care in Oncology: Insights from a Qualitative Case Study**
Sanskriti Varshney

219 **The Effects of Social Norms on Decision-Making in Game Theory**
Zhang Yiran

230 **Application of NASA's General Mission Analysis Tool (GMAT) in Replicating and Optimizing Historical Interplanetary Trajectories**
Adesh Krishnan

238 **Beyond Flavor: A Systematic Review of the Maillard Reaction's Impact on Health and Link to Carcinogenesis**
Fiona Zhong

244 **Exercise Therapy in Stress Management**
Haorui Zhang, Yi Wang

251 **Breaking Bad: Adversarial Prompting Targeting Feed Forward Neural Networks Within Transformers**
Luca Chang

259 **The Current State of Space Mining**
Naisha Thomre

264 **Cultural Frame Switching: A Russian-English Application to the Thematic Apperception Test**
Alexandra Denisova

273 **Assessing the Quality of Life of Palestinian Young Adult Refugees in Jordan: An Exploratory Study**
Antara Nayak

281 **A Comparative Analysis of Embedding Techniques and Their Importance in the Functionality of Large Language Models**
Elaine Jiang

290 **ADHD in Context: Gendered Presentation, Peer Relationships, and Family Challenges**
Kitty Men

296 **Finding Planets: Exoplanet Validation Using Overlapping Data from TESS And K2**
Mohammad Yawar Khan

301 **Evaluating the Accessibility of ChatGPT for Individuals with Dyslexia**
Shradha Sujeeth

308 **Sun-Aware Routing for Enhanced Driving Safety Using A* Search and Real-Time Atmospheric Conditions**
Rohin Vig

315 **The Relationship Between Stress and Fecundability: A Global Perspective**
Misaki Tsukada

321 **Ferrofluid and Its Application in Wound Healing**
Eldar Osmonov

326 **Climate Shockwaves: The Impact on Political Instability from Natural Disasters**
Haedam Lee

Editorial Board

International Journal of High School Research

EXECUTIVE PRODUCER

Dr. Fehmi Damkaci, President, Terra Science and Education

ASSISTANT PRODUCER

Nur Ulusoy

CHIEF EDITOR

Dr. Richard Beal, Terra Science and Education

COPY EDITORS

Ryan Smith, Terra Science and Education

LETTER FROM THE EDITOR

This issue of IJHSR features several papers that students produced for a scholarly event: Indigo Research's IRIS program, which immerses high school students in online college-level seminars. IRIS culminates in small symposia, where participating students present full-length research papers before their peers and professors. The dedicated scholars in this issue hail from both Indigo and NYAS (The New York Academy of Sciences), a prestigious global community comprising over 20,000 members, including leaders in science, industry, academia, government, and public policy.

All of the papers published in this issue underwent a rigorous single-blind peer review process, facilitated by IJHSR. Following this review, a selection of papers was accepted for further revisions, copy editing, and publication. All accepted submissions adhered to IJHSR's stringent quality standards, and the team responsible for organizing IRIS had no influence over the review process. IJHSR, Indigo Research, and the IRIS faculty are proud of the intellectual resilience that all student participants brought to the review process, whether or not their papers were accepted for this issue.

RESEARCH ADVISORY BOARD

Dr. Tammy L. Ingram

Dr. Steve Bullock

Dr. Audrey M. Wozniak

Dr. Samuel Lefcourt

Dr. Daria Sokolova

Dr. Feiyuan Long

Dr. Siddharth Krishnan

Dr. Kimberly Rose Clark

Dr. Kat Bochtler

Dr. Sinead M. Sinnott

Dr. Trinny Tat

Bre Calhoun

Dr. Barbara Biney

Malik A. Blackman

Aviezer Tucker

Dikshit Sarma Bhagabati

Monika Rybak

LJ Mun

Lauren M. Tetz

© 2026 Terra Science and Education

IJHSR
ijhighschoolresearch.org
RESEARCH ARTICLE

Reconstructing Genomes Using Graph-Based Algorithms

Aaron Kuang

Greenhill School, 4141 Spring Valley Road, Addison, TX, 75001, USA; aaron.kuang1228@gmail.com

ABSTRACT: Genome reconstruction is a crucial component of genome projects that aim to assemble an organism's complete genome sequence from short-fragmented DNA sequences. This task is fundamental and has wide-ranging applications in evolutionary research, medicine, conservation efforts, and synthetic biology. A common approach to genome reconstruction involves using graphs to identify overlapping sequences, known as k-mers, to recreate the entire genome. This study focuses on applying basic graph theory and Hierholzer's algorithm to efficiently identify Eulerian circuits and paths for genome assembly. The findings support the effectiveness of graph-based approaches as powerful tools in computational biology and genome research.

KEYWORDS: Graph Theory, Genome Analysis, Genetics, Genomics, Molecular Biology, Computational Biology.

Introduction

Genomic sequencing provides the foundation for understanding biological systems, from the genetic code of viruses to the human genome. A genome consists of the complete genetic information of an organism, encoded in DNA molecules. Each cell contains one DNA molecule, which is composed of long sequences of nucleotides forming a double helix structure. There are four types of nucleotides: adenine (A), cytosine (C), guanine (G), and thymine (T). The order of these nucleotides determines the sequence of the genome, which can be thought of as a long string of these four letters. Genomes are typically billions of nucleotides in length.[1]

Reading the genomes of organisms has many important applications. It has been used to study the evolution and relationships among species, identify genes and their functions, and advance medical research and treatments.[2,3] Genomic information has also improved agricultural practices, enabling the breeding of crops that are more resilient and yield.[4] New applications continue to emerge rapidly.

Each cell of an organism contains an identical copy of its genome. Thus, when a sample such as a drop of blood is taken, it contains billions of copies of the genome. Because genomes are so large, they cannot be read in one piece. Instead, sequencing technologies break the DNA into shorter fragments, typically a few hundred nucleotides long. These fragments are called k-mers, where k is the fragment length. Sequencing experiments read these k-mers, producing a large dataset of short DNA sequences. The challenge is to reconstruct the full genome from this collection of k-mers—a computational task known as the genome reconstruction problem. [5,6]

The rest of this article is organized as follows: In Section 2, we define the genome reconstruction problem precisely. Section 3 introduces directed graphs and the concept of Eulerian walks, which are essential for the reconstruction method. Section 4 explains how a directed graph can be constructed from lists of k-mers obtained in sequencing experiments. Section 5 shows why genome reconstruction reduces to finding an Eulerian walk in this graph and describes an algorithm to do so. Section 6 works through a simple example of genome reconstruction. Finally, Section 7 concludes with remarks and future directions. More information on the algorithms we explore in this article for the reconstruction of genomes, as well as different aspects of bioinformation, can be found in the references.[7-10]

The Genome Reconstruction Problem

As discussed in the introduction, every cell in a sample contains an identical copy of the genome. Thus, sequencing experiments are carried out, where the sections read are part of several identical copies of the genome/ This allows us to reconstruct the original sequence. We also recall that a k-mer is a section of the genome with k letters.

Consider the illustrative example in Table 1. We have four copies of the genome ACCTGTGTACC. Real genomes are much longer, but we use this short, simple example to illustrate the ideas. Each copy is broken into 4-mers. We start from the first letter on the first copy, from the second letter on the second copy, from the third letter on the third copy, and from the fourth letter on the fourth copy. This produces the 4-mers shown in black in the second column of Table 1. Shorter fragments, shown in red, are discarded.

Table 1: All the 4-mers of the genome ACCTGTGTACCT (in black).

Whole genome	4-mers in black
ACCTGTGTACCT	ACCT GTGT ACCT
ACCTGTGTACCT	A CCTG TGTA CCT
ACCTGTGTACCT	AC CTGT GTAC CT
ACCTGTGTACCT	ACC TGTG TACC T

From Table 1, we collect the 4-mers: ACCT, GTGT, ACCT, CCTG, TGTA, CTGT, GTAC, TGTG, TACC from the experiments. The goal is to develop an algorithm that takes as input this set of 4-mers and gives as output the genome

© 2026 Terra Science and Education

DOI: 10.36838/IJHSR87.1

ACCTGTGTACCT, which is not known. Note that some of the k-mers can be repeated, as ACCT appears twice in the list.

Of course, the situation described above is an idealized situation in which all the k-mers read have the same length. In real experiments, not all the k-mers read will have the same length. In this article, we will assume an ideal situation in which all k-mers read have the same length.

Thus, the goal is to use the list of k-mers read to infer the whole genome. We formalize this statement as follows:

The genome reconstruction problem: Let k be a positive integer. We are given an input list of k-mers. The goal is to find a genome whose k-mers are the list we were given, if such a genome exists. This genome is the output of the algorithm we will describe in this article.

It is instructive to look at the k-mers of a genome differently. Consider the example of the genome ACCTGTGTACCT. This genome has 12 letters. One of the 4-mers of this genome is the section of 4 letters that starts at the first letter, i.e., ACCT. A second 4-mer of this genome is the section of 4 letters that start at the second letter, i.e., CCTG. A third 4-mer of this genome is the section of 4 letters that starts at the third letter, CTGT. We can continue and obtain all the 4-mers. The list of the 4-mers obtained this way is: ACCT, CCTG, CTGT, TGTG, GTGT, TGTA, GTAC, TACC, ACCT. Note that this list is the same list that we obtained before, but in a different order.

When we are given the list of k-mers, it will not be sorted as described in the previous paragraph. In fact, our goal is to sort the k-mers as they appear in the genome, i.e., to have them as the list presented in the previous paragraph. Once sorted as in the last paragraph, reconstructing the genome is easy; simply start with the first k-mer, then add the last letter of the second k-mer, then the last letter of the third k-mer, and so on. This observation is at the heart of the algorithm we describe in this article.

The observation of the last paragraph is illustrated in Figure 1. Once sorted, the second k-mer is listed below the first k-mer and shifted one position to the right. Thus, the last k-1 letters of the first kmer are aligned on top of the first k-1 letters of the second k-mer. Note that these letters are the same. Similarly, the third k-mer is listed below the second k-mer and shifted one position to the right, etc. The result is shown in Figure 1. The letters in each column are the same. The genome can be reconstructed by dropping the letter of each column to the bottom line.



Figure 1:

In the rest of the article, we explain the mathematics and the algorithm needed to solve the genome reconstruction problem.

■ Directed Graphs

Graph Theory is a field of mathematics [11]. In this section, we introduce the concepts of Graph Theory that are needed by genome reconstruction algorithms.

Definition of directed graphs:

A directed graph is a pair of sets V and E. The elements of V are vertices, also known as nodes. In this paper, we will refer to them as nodes. The elements of E are edges. Each edge connects two nodes and has a specific direction, starting from one node, known as the tail, and ending at a node known as the head. We think of the edge as an arrow pointing from its tail to its head. The tail and the head of an edge are not necessarily different nodes. In visual representations, nodes are shown as circles, and edges as lines connecting the tail to the head of the edge with an arrow pointing toward the head. Figure 2 shows an example of a directed graph.

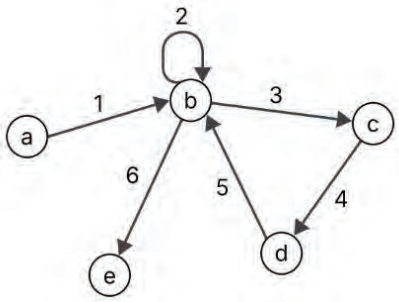

Figure 2: Example of a graph. The circles are the nodes. The arrows (not all straight) are the edges.

For reference, each node is labelled with a letter and each edge with a number. Table 2 lists the tail and head of each edge in Figure 2.

Table 2: List of the heads and tails of the edges of the graph of Figure 2.

Edge	Tail	Head
1	a	b
2	b	b
3	b	c
4	c	d
5	d	b
6	b	e

The graph of Figure 2 is a connected graph since it is in one piece. A disconnected graph, on the other hand, has two disjointed parts.

In-degree and out-degree of nodes:

The in-degree of a node is the number of edges that have that node as a head, and the out-degree of a node is the number of edges that have that node as a tail. In Table 3, we list the in-degree and out-degree of the Graph of Figure 2.

Table 3: List of the heads and tails of the edges of the graph of Figure 2. For each node of the graph of Figure 1, we list its in-degree, its out-degree, the edges that have the node as head, and the edges that have the node as tail.

Node	in-degree	out-degree	Edges with node as head	Edges with node as tail
a	0	1		1
b	3	3	1, 2, 5	2, 3, 6
c	1	1	3	4
d	1	1	4	5
e	1	0	6	

Walks and cycles:

A path is a sequence of edges where the head of one edge is the tail of the next. For example, the sequence of edges 1, 3, 4 is a path in the graph of Figure 2. Another path is e_1,e_2,e_2,e_3,e_4. These are the paths that particles can trace if they are only allowed to move along edges from the tails to the heads.

A walk is a path where each edge appears only once. For example, going back to the graph of Figure 2, the path 1, 3, 4 is also a walk, but the path 1, 2, 2, 3, 4 is not a walk because the edge 2 appears twice.

A cycle is a walk such that the tail of the first edge is the head of the last edge. This means that the particle moving along the cycle starts and ends at the same node. In Figure 2, the walk 3, 4, 5 is a cycle. The walk 2, 3, 4, 5 is also a cycle. The other cycle in that graph is the walk 3, 4, 5, 2.

Eulerian walks and cycles:

An Eulerian walk is a walk that contains all the edges in a graph. In the graph of Figure 2, the walk e_1,e_2,e_3,e_4,e_5,e_6 is an Eulerian walk. Note that not all graphs have Eulerian walks. We will later state a theorem providing the necessary and sufficient conditions for a graph to have an Eulerian path.

Naturally, an Eulerian cycle is a cycle that contains all the edges in a graph. Not all graphs have an Eulerian cycle. In fact, the graph of Figure 2 does not have an Eulerian cycle. Figure 3 shows an example of a graph with an Eulerian cycle. The cycle is e_1,e_2,e_3 is Eulerian.

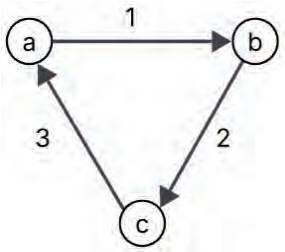

Figure 3: Example of a graph with an Eulerian cycle: 1, 2, 3.

The following theorem provides the necessary and sufficient conditions for a directed graph to have an Eulerian cycle.

Euler cycle theorem: For any directed, connected graph, there exists an Eulerian cycle if and only if, for each node in the graph, its in-degree and its out-degree are equal.

To illustrate this theorem, consider Table 4. The table shows that, for each node in the graph for Figure 3, its in-degree and its out-degree are equal. Thus, the graph has an Eulerian cycle.

Table 4: List of nodes of the graph of Figure 3 and their in-degree and out-degrees.

Nodes	In	Out	Difference
a	1	1	0
b	1	1	0
c	1	1	0

On the other hand, let's consider the graph of Figure 2. Note that the in-degree of node a is 0 and its out-degree is 1. They are different. Euler's theorem tells us that this graph has no Eulerian cycle. This is easily seen in a small graph, as the one in Figure 2, but when the graph has a large number of edges, Euler's theorem is useful in deciding if the graph has an Eulerian cycle.

For our purposes, we will need to find if a graph has an Eulerian walk that may or may not be a cycle. This leads to the next theorem, which is a natural extension of the Euler Cycle Theorem.

Euler walk theorem: A directed graph has an Eulerian walk that is not a cycle if all nodes have equal in-degrees and out-degrees except for two nodes. The out-degree of one of these nodes is equal to its in-degree plus one. This will be the starting node of the Eulerian walk. The out-degree of the other node of these nodes is equal to its in-degree minus one. This will be the ending node of the walk.

To illustrate the Euler walk theorem, consider the graph of Figure 2. The walk e_1,e_2,e_3,e_4,e_5,e_6 is an Eulerian walk. From Table 3, the in-degree of node a is 0, the out-degree of node a is 1; the in-degree of node e is 1, the out-degree of node e is 0; and for all other nodes, their in-degree equals their out-degree. The Euler walk theorem states that this graph has an Eulerian walk that starts at node a and ends at node e because the graph meets the conditions outlined above. In fact, e_1,e_2,e_3,e_4,e_5,e_6 is such an Eulerian walk.

Graph from a List k-mer

The input given is a list of k-mers, and the goal is to sort these k-mers into the sequence in which they appear in the genome we want to reconstruct, as in Figure 1. To that end, we will construct a graph and then find an Eulerian path on that graph. In this section, we explain how to construct the graph from the k-mers, and we also explain why finding an Eulerian path on this graph allows us to sort the k-mers and thus, reconstruct the genome.

We will explain and demonstrate the construction of a genome with an example. Suppose the list of k-mers that are given as input is ACCT, GTGT, GACC, CCTG, TGTG, ACCT, CTGT, GTGA, TGTG, TGAC. In this case, these are 4-mers. Our graph will have one edge for each of the 4-mers. Note that there may be different edges that have the same k-mer. This is the case in our example because the ACCT and TGTG appear twice in the list of k-mers.

Before describing the nodes, we remind the reader that the prefix of a k-mer is the (k-1)-mer that results from removing the last letter of the k-mer. For example, the prefix of ACCT is ACC. On the other hand, the suffix of a k-mer is the (k-1)-mer that results from removing the first letter of the k-mer. For example, the suffix of ACCT is CCT.

DOI: 10.36838/IJHSR87.1

The nodes will have (k-1)-mers associated with them. The (k-1)-mers of the tail node of an edge are the prefix of the k-mer of the edge, and the (k-1)-mer of the head node of an edge is the suffix of the k-mer of the edge. Unlike with the edges, there is no pair of nodes with the (k-1)-mer. For example, if an edge has the 4-mer ACCT, the 3-mer of its tail is ACC, and the 3-mer of its head is CCT. In Figure 4, we show just an edge, its head and its tail 4-mer, and the 3-mers of both the tail and head of the edge, but we do not show the rest of the graph.



Figure 4: An edge and its 4mer. The head and tail of this edge and their 3-mers.

The rules described in the previous paragraphs determine the graph from the list of k-mers. For short, we will refer to this graph as the graph from the k-mers. The graph of our example, i.e., the graph of the list of k-mers ACCT, GTGT, GACC, CCTG, TGTG, ACCT, CTGT, GTGA, TGTG, TGAC, is shown in Figure 5.

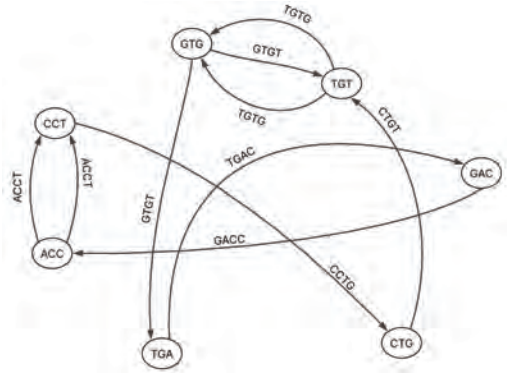

Figure 5: Graph of the list of 4-mers ACCT, GTGT, GACC, CCTG, TGTG, ACCT, CTGT, GTGA, TGTG, TGAC. The 4-mers of the edges and the 3-mers of the nodes are shown.

Assume we manage to find a Eulerian walk in this graph of Figure 5. Let $e_1,e_2,..,e_n$ be this Eulerian walk. This means that the head of e_{i-1} is equal to the tail of e_i. The label of this node is both the suffix of the label of e_{i-1}, and also the prefix of the label of e_i. Thus, the last k-1 letters of the label e_{i-1} are the same as the first k-1 letters of the label of e_i. Thus, we have the k-mers sorted as previously explained, as in Figure 1, and the reconstruction of the genome from this point is immediate. To illustrate this claim, we show, in Figure 6, the Eulerian walk $e_1,e_2,..,e_{10}$ in the graph of Figure 5. Figure 6 shows the same graph as in Figure 5. However, in Figure 6, we do not show the 4-mers of the edges and the 3-mers of the nodes. We show the labels of the edges. Assigning labels to the edges makes the description of the Eulerian path easier. Note that the labels can be chosen arbitrarily. To prevent the figure from becoming crowded, the 4-mers of each edge are shown in the table to the right of Figure 6. Note that we have not explained how to find Eulerian walks. This is done by applying the algorithm that we later explain in this article.

Edge	K-mer
e_1	TGTG
e_2	CTGT
e_3	TGAC
e_4	GACC
e_5	GTGA
e_6	ACCT
e_7	ACCT
e_8	CCTG
e_9	GTGT
e_{10}	TGTG

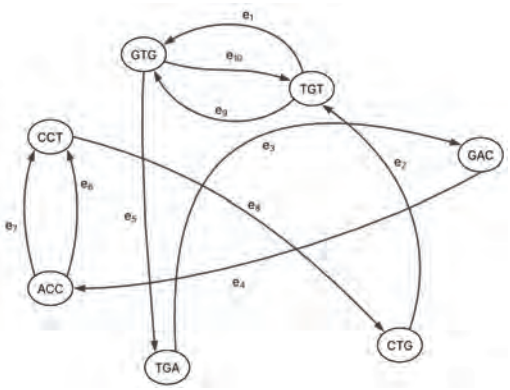

Figure 6: The left panel shows the same graph as in Figure 5.

We can list the 4-mers of the edges in the order of the path A, in this case ACCT, CCTG, CTGT, TGTG, GTGT, TGTG, GTGA, TGAC, GACC, ACCT. This is exactly the order in which the edges appear in Figure 1, from top to bottom. From where we can reconstruct the genome, as previously explained when we discussed Figure 1. This genome is ACCTGTGTGACCT.

Algorithm

As discussed in the previous section, our goal is to find an Eulerian path on the graph of k-mers. Before describing the algorithm to find such a path, we need to describe the algorithm to find an Eulerian cycle.

Algorithm to find an Eulerian Cycle:

In this section, we explain the algorithm we use to find an Eulerian cycle. We assume that, for all the nodes, their in-degree is equal to their out-degree. As previously described, this condition is necessary to guarantee that an Eulerian cycle exists.

There are two general algorithms to find an Eulerian cycle in a graph. The first is Fleury's algorithm, and the second is Hierholzer's algorithm, which is the method used in this paper. Hierholzer's algorithm is a stepwise construction by connecting cycles.

We explain the algorithm using the graph of Figure 7 as an example. We select an edge. We call this edge e_1. We create a walk with e_1 as its first edge. We extend the walk as much as possible. There may be more than one possible walk with e_1 as its first edge, but any walk will do. In our example, this walk we selected is the walk is $e_1e_2e_3e_4$, which is in green. Note that this walk can not be extended because there are no edges coming out of the last node, which is the head of the last edge, e_4 , that is not already part of the walk. Note that this walk is a cycle. This is a general fact, not just restricted to our example. This walk will always be a cycle.

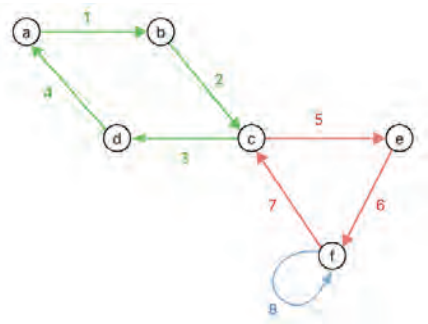

Figure 7: $e_1e_2e_3e_4$ is the first walk of Hierholzer's Algorithm shown in green.

If the cycle the algorithm obtained thus far by the algorithm had all the edges of the graph, this cycle would be Eulerian and would be the output of the algorithm. We would have accomplished our goal. In our example, the cycle $e_1e_2e_3e_4$, formed by the edges in green, does not contain all the edges of the graph and thus, it is not Eulerian.

If the cycle is not Eulerian, as in our example, the algorithm traces the cycle and stops at the first edge whose head is the tail of an edge not in the cycle. In our example, we start with the edge e_1 and travel to the node *b*. There are no edges coming out of *b* that are not in the cycle; this is the same as saying that there are no edges outside the cycle with *b* as a tail. We then travel through e_2 to the node *c*. The edge e_5 has *c* as a tail and is not in the walk. In other words, there is an edge not in the cycle that comes out of *c*. Thus, the edge e_2 is the edge in the cycle we were looking for.

The algorithm retraces the cycle, but starting at the edge following the one found in the previous paragraph. In our example, we start at the edge e_3. Thus, since we start at e_3, the cycle becomes is $e_3e_4e_1e_2$. Note that this walk can be extended because the endpoint of the cycle is now the node *c* and there are edges, e_5, not in the cycle yet, which have *c* as a tail. Thus, the algorithm can and does continue adding more edges to the walk.

The process continues as described in the last paragraph till all the edges in the graph are part of the cycle. Following our example, suppose the algorithm adds the red edges in Figure 7 to the cycle. Now the cycle is $e_3e_4e_1e_2\ e_5e_6e_7$. The algorithm is stuck again, but has 3 more edges than before. The whole process is repeated. The algorithm traces the cycle and stops at the edge e_6. It retraces the whole cycle starting from the next edge, the edge e_7, to get the cycle $e_7\ e_3e_4e_1e_2\ e_5e_6$. It can now continue and adds e_8. At this point, we have the Eulerian cycle $e_7\ e_3e_4e_1e_2\ e_5e_6e_8$.

Algorithm to find an Eulerian Walk:

Recall that our goal was to find an Eulerian walk, not necessarily an Eulerian cycle. In this section, we explain how the algorithm described in the previous section is extended to find Eulerian walks. There are two cases to consider.

First, if all nodes have equal in-degrees and out-degrees, the algorithm described in the previous section, Hierholzer's algorithm, finds an Eulerian cycle, which is also an Eulerian walk. No changes to the algorithm are necessary.

The second case is when all nodes have equal in-degrees and out-degrees except for two nodes. For one of the two nodes, its out-degree is equal to its in-degree plus one. We call this node the starting node. For the other node, its out-degree is equal to its in-degree minus one. We call this node the final node. The left panel of Figure 6 illustrates this case. *f* is the starting node and *a* is the final node.

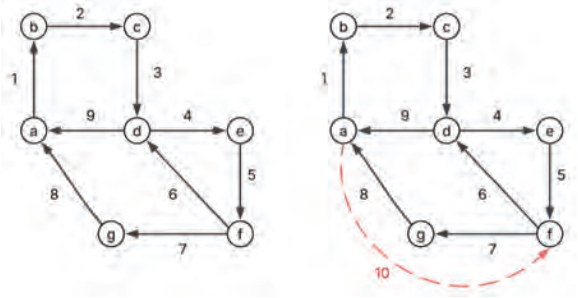

Figure 8:

We modify the graph by adding an edge that has the final node as the tail and the starting node as the head. We call this edge the added edge. In the example of Figure 8, this edge is *e*10, the edge in red in the right panel. Now, for all the nodes in this modified graph, their in-degrees equal their out-degrees.

We apply the algorithm explained in the last section to find an Eulerian cycle in the modified graph. Assume the cycle found in our example is $e_7e_8e_{10}e_4\ e_6e_9e_1e_2\ e_3e_4e_5$. We retrace the cycle till we find the added edge, e_{10} in our example. We now retrace the cycle starting at the edge that follows the added edge, i.e., starting at e_4 and ending at the edge before the added edge e_{10}, i.e., we stop at the edge e_8. This gives us the path $e_4\ e_6e_9e_1e_2\ e_3e_4e_5e_7e_8$. We have accomplished our goal. This is an Eulerian path of the original graph and is the output of the algorithm.

■ Example

In this section, we review the whole process of genome reconstruction by working out a small example.

We are given as input the list of *k*-mers ACCT, GTGT, GACC, CCTG, TGTG, ACCT, CTGT, GTGA, TGTG, TGAC. This is the same list of *k*-mers considered in Section 4. Note that *k*=4 in this example. Next, we construct the graph from this list of *k*-mers. This was also done in Section 4. The resulting graph is displayed in Figure 4.

The next step is to find an Eulerian walk in the graph. We find this path using the algorithm described in Section 5. Instead of just displaying the result, we practice the ideas of the algorithm on this example by working out its steps in detail.

The algorithm first checks the in-degree and out-degree of each node. In our example, all the nodes have the same in-degree and out-degree, except for 2 nodes. The out-degree of the node with label ACC is equal to its in-degree plus 1. The in-degree of the node with label CCT is equal to its out-degree plus 1. This means that this graph has an Eulerian path.

Next, the algorithm creates a new edge from the node with out-degree smaller than its indegree, this is the node with label CCT to the node with in-degree smaller than its out-degree.

DOI: 10.36838/IJHSR87.1

We show the graph again in Figure 9, where we are also including this new edge in red. We call this new edge e_{11}.

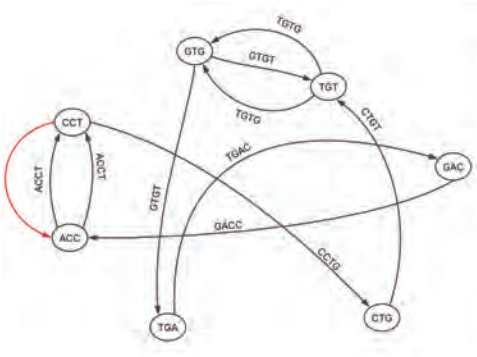

Edge	K-mer
e_1	TGTG
e_2	CTGT
e_3	TGAC
e_4	GACC
e_5	GTGA
e_6	ACCT
e_7	ACCT
e_8	CCTG
e_9	GTGT
e_{10}	TGTG

Figure 9:

Next, the algorithm finds an Eulerian cycle in the augmented graph, i.e., the graph with the red edge. To accomplish that task, we first select any edge. We select e_3. We construct a walk starting at e_3. We are free to select any such walk. This walk is extended as much as possible. The walk we select is $e_3e_4e_6e_8e_2e_3e_9e_5$. This walk can not be extended because all the edges coming out of the head of the last edge of the walk, i.e., e_5, are already in the walk. An edge coming out of a node means that the node is the tail of the edge. The walk found is always a cycle.

Next, the algorithm travels through the walk and stops at the first edge whose head is the tail of an edge not in the walk if there is such an edge. The head of e_3 is the node whose label is GAC. The only edge coming out of this node is e_4, since this edge is already in the walk, we continue through the walk. The edge in the walk coming after e_3 is e_4. The head of e_4 is the node whose label is ACC. The edges coming out of this node are e_6 and e_7. The edge e_7 is not in the walk. We have found the first edge whose head is the tail of an edge not in the walk. This is the edge e_4. The algorithm re-traces the cycle, but starting with the edge coming after e_4, the edge found in this step. The cycle has become $e_6e_8e_2e_3e_9e_5e_3e_4$. Note that now, there is an edge not in the cycle coming out of the last edge in the cycle, e_4. Thus, the cycle can be extended. This is what the algorithm does. In our example, we obtain the cycle $e_6e_8e_2e_3e_9e_5e_3e_4e_7e_{11}$.

The process of the last paragraph is repeated. We find that the first edge of the cycle whose head has an edge that is coming out of it and is not in the cycle is the edge e_2. Thus, retracing the cycle but starting at the edge after e_2, the cycle becomes $e_3e_9e_5e_3e_4e_7e_{11}e_6e_8e_2$. Next, we extend the cycle to obtain $e_3e_9e_5e_3e_4e_7e_{11}e_6e_8e_2e_1e_{10}$.

Now that the cycle contains all the edges, the algorithm retraces the cycle till it finds the edge that was added to the graph of k-mers, the red edge, which in our example is the edge e_{11}. Finally, the algorithm retraces the cycle starting from the edge after e_{11}, and stops at the edge before e_{11}. In our example, this is the edge e_7. We end up with the path $e_6e_8e_2e_1e_{10}e_3e_9e_5e_3e_4e_7$. This is the Eulerian walk in the graph of k-mers.

Once the Eulerian path is found, the genome is reconstructed as follows. Start with the label of the edge in the Eulerian walk. In our example, this is the e_6. Its label is ACCT. Then, add at the end the last letter of the second edge. In our example, this edge e_8. Its label is CCTG, so its last letter is G. Thus, we add G at the end of ACCT to get ACCTG. We do the same with the third edge. This is the edge e_2. Its label is CTGT. Its last letter is T. We add this last letter at the end of ACCTG to get ACCTGT. This process is continued through the whole walk to get the genome ACCTGTGGCTAC… This is the genome we were looking for. This is the output of the algorithm.

■ Results and Discussion

Algorithm Performance:

The algorithm reconstructs the original sequence by traversing each edge exactly once, thereby preserving the overlap information encoded in the k-mers. In the test case, the reconstructed genome matches the true sequence, and execution completes in under 1 millisecond on standard hardware.

Ambiguities and Repeats:

In larger and more complex genomes, multiple Eulerian paths may exist, creating ambiguities in reconstruction. Such cases arise from repeated k-mers, palindromic sequences, or variability in read lengths. To resolve these issues in practice, genome assemblers employ additional strategies such as error correction, assigning edge weights based on read coverage, or incorporating paired-end read information. Notable examples include assemblers such as Velvet and SPAdes, which integrate these heuristics into their pipelines.

Scalability:

The present implementation is designed for clarity rather than raw performance. Its runtime scales linearly with the number of k-mers, but efficiency can be improved through the use of optimized data structures. For large-scale datasets, techniques such as de Bruijn graph compression and parallelization are essential to ensure computational feasibility.

■ Conclusion

We presented a clean, accessible Python implementation of genome reconstruction using Eulerian paths in de Bruijn graphs. This approach illustrates how fundamental concepts from graph theory can be applied to support biological discovery.

Our implementation assumes an idealized setting where reads are error-free, of uniform length, and cover the genome completely. In practice, sequencing introduces additional challenges: k-mers often vary in length, some k-mers may be missing while others appear multiple times, and read errors introduce noise. Addressing these issues requires incorporating statistical models, error correction, and abundance information.

Furthermore, while the algorithm described here demonstrates the essential idea, practical genome assembly demands more sophisticated data structures, graph compression techniques, and parallelization for scalability. These challenges continue to drive research in the fast-growing field of bioinformatics, where advances in algorithms and computational tools directly impact our ability to interpret complex genomic data.

References

1. Dale, J.W., Von Schantz, M. and Plant, N., 2011. From genes to genomes: concepts and applications of DNA technology.
2. Muffato, M., Louis, A., Nguyen, N.T.T., Lucas, J., Berthelot, C. and Roest Crollius, H., 2023. Reconstruction of hundreds of reference ancestral genomes across the eukaryotic kingdom. *Nature Ecology & Evolution*, *7*(3), pp.355-366.
3. Ouzounis, C.A., 2005. Ancestral state reconstructions for genomes. *Current opinion in genetics & development*, *15*(6), pp.595-600.
4. https://institute.global/insights/public-services/what-genomic-sequencing-and-why-does-it-matter-future-health
5. Gregory, T.R. ed., 2011. *The evolution of the genome*. Elsevier.
6. Liberles, D.A. ed., 2007. *Ancestral sequence reconstruction*. OUP Oxford.
7. Pevzner, P.A.; Tang, H.; Waterman, M.S. An Eulerian path approach to DNA fragment assembly. *Proc. Natl. Acad. Sci. USA* **2001**, *98*(17), 9748–9753. https://www.pnas.org/doi/abs/10.1073/pnas.171285098
8. Compeau, P.E.; Pevzner, P.A.; Tesler, G. How to apply de Bruijn graphs to genome assembly. *Nat. Biotechnol.* **2011**, *29*(11), 987–991. https://www.nature.com/articles/nbt.2023
9. Kingsford, C.; Schatz, M.C.; Pop, M. Assembly complexity of prokaryotic genomes using de Bruijn graphs. *Genome Biol.* **2010**, *11*(12), R119. https://link.springer.com/article/10.1186/1471-2105-11-21
10. Pop, M., 2009. Genome assembly reborn: recent computational challenges. *Briefings in bioinformatics*, *10*(4), pp.354-366. https://academic.oup.com/bib/article/10/4/354/299108
11. Bollobás, B., 1998. *Modern graph theory* (Vol. 184). Springer Science & Business Media.

Authors

Aaron Kuang is a high school senior at Greenhill School. He is passionate about mathematics and computer science and enjoys developing algorithms for real-world problems.

DOI: 10.36838/IJHSR87.1

IJHSR

ijhighschoolresearch.org

RESEARCH ARTICLE

A Numerical Analysis of Stability in Zero-Sum Rock-Paper-Scissors Stochastic Replicator Dynamics

Kyle Yang

Deerfield Academy, 7 Boyden Lane, Deerfield, MA, 01342, USA; kyangsh2016@gmail.com

ABSTRACT: Stochastic differential equations have a wide range of applications across various disciplines, including finance, physics, and biology. There are usually two primary ways to evaluate them: Stratonovich, which samples midpoints, and Ito, which samples left endpoints. However, unlike deterministic calculus, these two schemes give different results upon evaluation. This article primarily analyzes the dynamics of the neutral equilibria of zero-sum replicator dynamics when subject to noise under both the Ito and Stratonovich schemes. We add noise because in real-world modeling scenarios, almost all natural systems are subject to some form of it. We find that intrinsically symmetric Brownian noise acts asymmetrically in zero-sum games, thereby decreasing a system's stability. Hence, neutral equilibria with noise behave like deterministic, asymptotically unstable equilibria. Additionally, the Stratonovich scheme exhibits greater variation than the Ito scheme in both mean and variance for all of the cases we study.

KEYWORDS: Chemistry, Organic Chemistry, Spectrophotometry, Carbinolamide, Kinetics.

Introduction

Stochastic Differential Equations:

This subsection largely follows Øksendal's textbook on SDEs, including notation and derivations.[1] In the modeling of various phenomena with random fluctuations, a special type of differential equation called a stochastic differential equation (SDE) is used. SDEs typically take the form:

$$dX(t) = \mu(t, X(t))\,dt + \sigma(t, X(t))\,d\xi(t) \quad (1)$$

Here, $X(t)$ is a variable probability distribution based on time, μ is a function from time and the distribution X (the state space) to codomain $\mathbb{R}$, σ is also a function from time and the state space to codomain $\mathbb{R}$, and $\xi(t)$ represents the random "noise" that is introduced to the system at time t. Essentially, the first term represents the driving movement of the system, while the second represents the random noise added.

The $\xi(t)$ can represent many types of noise. However, for this paper, we will assume $\xi(t)$ is a Wiener process (which models Brownian noise)—that is, we will assume $\xi(t) = W(t)$ to have the following properties, in accordance with Øksendal:[1]

i. $W(0) = 0$ almost surely (a.s.)

ii. $W(t)$ has independent increments

iii. $W(t+u) - W(t)$ is normally distributed with mean 0 and variance u: $W(t+u) - W(t) \sim \mathcal{N}(0,u)$

iv. $W(t)$ has a.s. continuous paths

Properties i) and iii) allow us to maintain symmetry, properties ii) and iii) give us nice probabilistic properties, and property iv) maintains well-definedness. Intuitively, the Wiener process helps us model a normal distribution whose variance increases linearly with time. At any time, we effectively 'sample' a random point from the distribution.

Having defined the terms in the SDE, we would now like to evaluate it. However, due to problems brought up by the Wiener process's lack of smoothness, the evaluated result changes based on the point sampled within each interval of a partition. We will demonstrate this difference between the Ito and Stratonovich schemes, which sample from the left endpoints and midpoints, respectively. These two schemes have different physical assumptions. While the Ito scheme accounts for the "unsmooth" nature of the noise, resulting in an extra term in its version of the chain rule, the Stratonovich scheme assumes a more symmetrical structure, maintaining the traditional deterministic chain rule. Following calculus intuition, we would like to "integrate both sides" of Equation 1 to determine the distribution of X. Since dW doesn't behave like a standard differential, we need to consider a (not necessarily even-spaced) partition of the interval $[0, T]$. Denote the finite collection of times dividing this interval as:

$$0 = t_1 < t_2 < \ldots < t_n = T$$

Now, we can assess the following discretized differentials and summations:

$$\Delta t_k = t_{k+1} - t_k, \qquad \Delta W_k = W(t_{k+1}) - W(t_k) \quad (2)$$

Left-endpoint (Ito) scheme:

$$X(t_n) = X(0) + \sum_{k=0}^{n-1} \mu(t_k, X(t_k))\,\Delta t_k + \sum_{k=0}^{n-1} \sigma(t_k, X(t_k)) \quad (3)$$

Midpoint (Stratonovich) scheme:

$$X(t_n) = X(0) + \sum_{k=0}^{n-1} \mu\left(\frac{t_k + t_{k+1}}{2}, \frac{X(t_k) + X(t_{k+1})}{2}\right)\Delta t_k + \sum_{k=0}^{n-1} \sigma\left(\frac{t_k + t_{k+1}}{2}, \frac{X(t_k) + X(t_{k+1})}{2}\right)\Delta W_k \quad (4)$$

Note that taking the limit as the size of each interval in the partition approaches 0 gives us the concept of "stochastic integrals." However, it is not too important for our purposes in this paper, as we will be adopting a discrete-time approach. We now demonstrate the difference between Ito (Equation 3) and Stratonovich (Equation 4) by taking their difference, which Øksendal terms the "correction term":[1]

$$\frac{1}{2}\sum_{k=0}^{n-1} \Delta X_k \Delta W_k \quad (5)$$

Generalizing these two schemes, we can sample from any point between intervals — say $\tau \in [t_k, t_{k+1})$. We denote α as

© 2026 Terra Science and Education

DOI: 10.36838/IJHSR87.8

the relative distance from t_k compared to t_{k+1}. In fact, regardless of which set of points we choose for the summation, our result remains mathematically consistent. However, despite mathematical consistency, the result of the summation yields nontrivial differences as we have demonstrated.

This paper will mainly analyze the differences between the $\alpha = 0$ (Ito) and $\alpha = ½$ (Stratonovich) schemes in the stochastic version of replicator dynamics. To contrast them, we will write Stratonovich SDEs with the notation $\circ\, dW_t$ and Ito SDEs with just dW_t, as Øksendal does.

Because the left–midpoint formulation of the Ito integral only uses information from time t_k to determine the state at time t_{k+1}, it doesn't "see into the future" (independent increments). In other words, this means the Ito scheme ensures that the mean is bounded and the conditional expectation up to a time is precisely the value at that time (martingale property). And, as mentioned previously, Ito integrals do not preserve the usual chain rule since an extra quadratic term from the Taylor expansion of $f(dX(t))$ appears due to the asymmetry of sampling the left midpoint and innate quadratic variation of W, giving the famous Ito's lemma:

$$df(X(t)) = \left[\mu(t)X(t)\frac{\partial f}{\partial X} + \tfrac{1}{2}\sigma(t)^2 X(t)^2 \frac{\partial^2 f}{\partial X^2}\right]dt + \sigma(t)X(t)\frac{\partial f}{\partial X}\,dW(t) \qquad (6)$$

A more detailed derivation using the Taylor expansion can be found in Øksendal's textbook.[1]

On the other hand, the Stratonovich integral preserves the classical chain rule. Because of its midpoint sampling, an extra quadratic term is generated, which cancels the quadratic term from the Taylor expansion. However, for the same reason, the Stratonovich integral does not have the martingale property; the midpoint sampling, in a certain sense, "peeks into the future."

Replicator Dynamics:

In this section, the definitions and derivations for deterministic replicator dynamics largely follow from Taylor and Jonker's 1978 paper and Hofbauer and Sigmund's 1998 book.[2,3] Replicator dynamics is a model that predicts frequencies of a set of competing phenotypes given a payoff matrix, which holds all the fitness information about the population ("rules" for when each pair of phenotypes "compete"). Mathematically, we describe this using a system of differential equations, with phenotype i adhering to:

$$dx_i = x_i\left[f_i(\mathbf{x}) - \phi(\mathbf{x})\right]dt, \qquad \phi(\mathbf{x}) = \sum_{j=1}^{n} x_j f_j(\mathbf{x}) \qquad (7)$$

Here, $\boldsymbol{x}$ is a column vector containing the frequencies of each phenotype; $\boldsymbol{\phi}$ is a function of $\boldsymbol{x}$, denoting the average fitness across all phenotypes; f_i denotes the fitness of phenotype i; and x_i is the frequency of phenotype i. The fitness of phenotype i is usually calculated by taking the i-th entry of the vector given by $\boldsymbol{Ax}$, where A is the payoff matrix. Essentially, the model compares each phenotype's fitness to the average fitness and determines the subsequent relative frequency of each phenotype based on the comparison. Furthermore, the model preserves the normalization of the x_i's, guaranteeing that they sum to 1. This can be easily shown by considering a function of the sum of all the x_i's and proving the derivative is 0.

We will follow Hofbauer and Sigmund's definitions of equilibrium points as those that have each $dx_i = 0$, *stable equilibria* as points that return to themselves under small perturbations, and *unstable equilibria* as points that become further *unstable*. Otherwise, we will call them *neutral*.[3]

The classic example of replicator dynamics is the *rock-paper-scissors* game, where A beats B, B beats C, and C beats A. It occurs frequently in nature, typically in the form of competing traits within a species. We will mainly study the zero-sum version in the rest of this paper, which means the winner and loser of each interaction gain/lose the same. As an example, we consider the following payoff matrix:

$$\begin{pmatrix} 0 & -1 & 1 \\ 1 & 0 & -1 \\ -1 & 1 & 0 \end{pmatrix}$$

Each ij-entry indicates the comparative fitnesses of phenotypes i and j, and more specifically, the outcome for type i. For example, when type 1 is compared to type 2, it will lose. Meanwhile, when type 1 is compared to type 3, it will win. Notice that to preserve the zero-sum nature, we must have an antisymmetric payoff matrix.

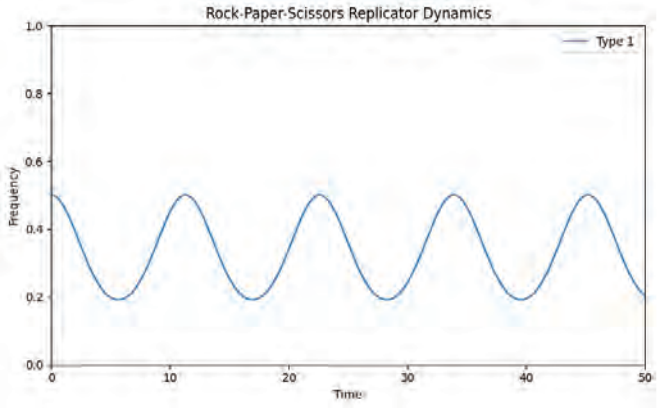

Figure 1: Frequency of phenotype x_1 as a function of time. The frequency never converges to the equilibrium point ⅓ because there is no attractive behavior in zero-sum replicator dynamics. Modeled using Heun's method, $\Delta t = 0.0001$.

Setting up the differential equations, initial values (0.5, 0.25, 0.25), and simulating the trajectories, we observe oscillatory behavior in Figure 1 due to the lack of attraction/repulsion exhibited by the neutral equilibrium point (⅓, ⅓, ⅓).

The majority of the following derivation of Ito replicator dynamics comes from Fudenberg and Harris's.[4] A more complete derivation with the individual calculations can be found in Delesse's work.[5] The derivation of the Stratonovich version is rather trivial, as it follows directly from the traditional chain rule.

When we consider adding a stochastic term to the differential equation, we can't directly add it, as the replicator differential equation is of frequency, not population. Thus, we must first consider the total populations and then convert them into their respective replicator equations. We have:

$$dr_i(t) = r_i(t)\left(\left[B(t, r(t)) - D(t, r(t))\right]dt + u_i[x(t)]dt + \sigma_i\, dW_i(t)\right) \qquad (8)$$

Where B is the background fitness ("base" number of successors), D is the death rate, u is the payoff function, σ_i is a scalar, and W_i is a Wiener process. Essentially, we are adding an extra stochastic term to each SDE in the system. Note that the quantity B-D differs from fitness, as we are considering the full population, not just frequencies. Now we would like to derive the differential equation for $x_i(t)$. Since we know $x_i(t) = r_i(t)/R(t)$, where $R(t)$ is the sum of all the ri's, we can apply the chain rule for Stratonovich and Ito's Lemma (Equation 6) for Ito on the function $f_i(r(t)) = r_i(t)/R(t)$, where $r(t)$ is a vector function containing the ri's. After expanding and simplifying:

Ito:

$$dx_i = x_i\left(f_i - \phi - \sigma_i^2 x_i + \sum_j \sigma_j^2 x_j^2\right)dt + x_i\left(\sigma_i\, dW_i - \sum_j \sigma_j x_j\, dW_j\right) \quad (9)$$

Stratonovich:

$$dx_i = x_i(f_i - \phi)\,dt + x_i\left(\sigma_i \circ dW_i - \sum_j x_j\sigma_j \circ dW_j\right) \quad (10)$$

Notice that the Ito version of replicator dynamics generates two extra terms in the drift term, which can be attributed to Ito's Lemma.

It has been shown that, given a stable equilibrium point, stochastic replicator dynamics frequently display behavior that also converges towards a neighborhood within that stable strategy. In other words, given that the noise is small enough, a stable equilibrium will still behave as a stable equilibrium. Additionally, a quantitative bound for the maximal magnitude of the noise that still maintains this stable behavior is known.6

It has also been demonstrated that, in certain instances, the stable states of the stochastic variant may differ substantially from those of the deterministic variant.[7] In other words, stochastic terms can cause the equilibria to shift. In addition, when there are multiple equilibrium points, it is also possible for trajectories to go back and forth between them, provided the noise and time are large enough.[8] The noise can push the trajectory into the attractive region of another equilibrium.

Together, these results demonstrate that equilibria cannot be treated in the same way when an extra stochastic term is added.

Despite the abundance of theory on the topic, very little numerical research has been done to observe the system's actualized behavior, especially in zero-sum stochastic models. To make new observations and test past claims regarding this topic, we will numerically simulate trajectories of zero-sum stochastic replicator dynamics, calculating the means and variances of phenotypes as a function of time. In the rest of this paper, we will analyze the speed of "divergence" for various magnitudes of noise in the stochastic version of the zero-sum rock-paper-scissors game when compared to the deterministic cycles illustrated in Figure 1.

Methods

To simulate individual trajectories for both Ito and Stratonovich processes, we used Heun's method with a time step of Δt = 0.001 in a Python script. We used Heun's method because it applies to both Ito and Stratonovich SDEs and maintains a relatively high level of accuracy.[9] Heun's method is as follows, in which each subsequent step takes the average of a "predictor" and "corrector":

$$\tilde{X}_{n+1} = X_n + f(t_n, X_n)\,\Delta t + G(t_n, X_n)\,\Delta W_n \quad (11)$$

$$X_{n+1} = X_n + \tfrac{1}{2}[f(t_n, X_n) + f(t_{n+1}, \tilde{X}_{n+1})]\Delta t + \tfrac{1}{2}[G(t_n, X_n) + G(t_{n+1}, \tilde{X}_{n+1})]\Delta W_n \quad (12)$$

We will assume that the variance (σ) of each phenotype is the same, ranging from the set: {0.05, 0.10, 0.15, 0.20, 0.25}. For each σ, we ran N = 10000 simulations for a duration of T = 50.0 with the initial condition $\boldsymbol{x}$ = (0.5, 0.25, 0.25). We ran this simulation several times for each σ and found similar results. Furthermore, the general trends observed in our N = 1000 test runs are almost identical to those in our N = 10000 runs. These suggest that our results are converging.

Each random variable W was generated using CuPy's built-in random number generator, which adheres to the rules specified above for a Wiener process. Since each path runs independently, using parallel computing can significantly speed up a simulation while retaining the simulation's integrity. Therefore, we utilized a GPU and CuPy's intrinsic GPU optimizations to accelerate the simulation.

To generate a frequency-time heatmap, we partitioned the time axis into 500 sections and the frequency axis into 50 sections, calculating probabilities by counting the number of trajectories passing through each partitioned section relative to the entire vertical strip. We collected data on the simulated mean and variance of the dataset in addition to the heatmaps.

Results and Discussion

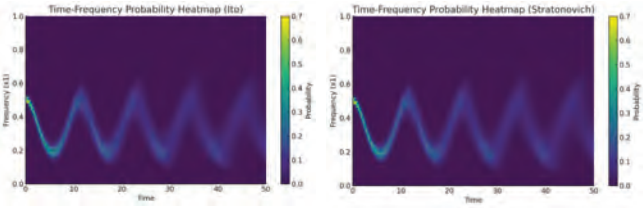

(A) (B)

Figure 2: Simulated results for σ = 0.05. The colors in the heatmap also begin to fade over time, indicating dispersion in individual trajectories. However, the general neighborhood of trajectories is still visible. A) Ito heatmap B) Stratonovich heatmap.

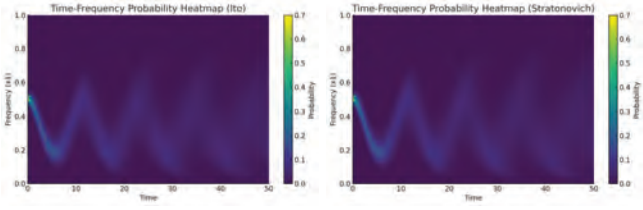

(A) (B)

Figure 3: Simulated results for σ = 0.10. The colors in the heatmap also begin to fade over time, indicating dispersion in individual trajectories. The general neighborhood of trajectories is still slightly visible. A) Ito heatmap B) Stratonovich heatmap.

DOI: 10.36838/IJHSR87.8

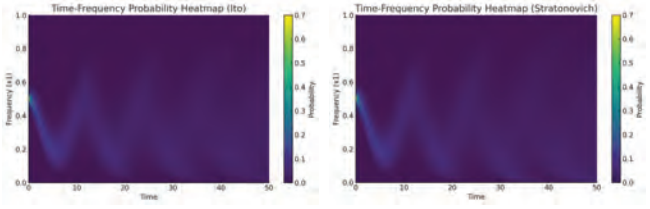

(A) (B)

Figure 4: Simulated results for σ = 0.15. The colors in the heatmap also begin to fade over time, indicating dispersion in individual trajectories. The general neighborhood of trajectories becomes unclear at about halfway, but generally concentrates more at lower frequencies. A) Ito heatmap B) Stratonovich heatmap.

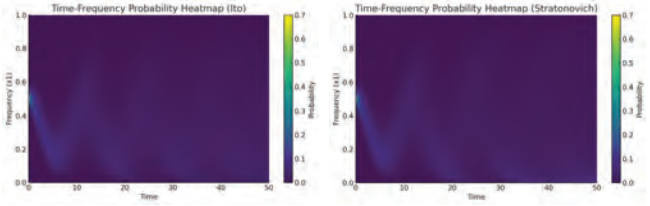

(A) (B)

Figure 5: Simulated results for σ = 0.20. The colors in the heatmap also begin to fade over time with a larger concentration in a low-frequency range, indicating dispersion in individual trajectories, which favors larger oscillations. The general neighborhood of trajectories becomes unclear quickly. A) Ito heatmap B) Stratonovich heatmap.

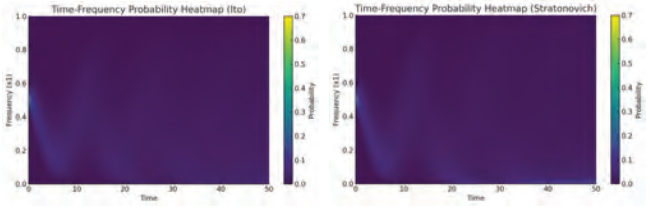

(A) (B)

Figure 6: Simulated results for σ = 0.25. The colors in the heatmap also begin to fade over time, with a larger concentration in a low-frequency range, indicating dispersion in individual trajectories, which favors larger oscillations. The general neighborhood of trajectories becomes unclear quickly. A) Ito heatmap B) Stratonovich heatmap.

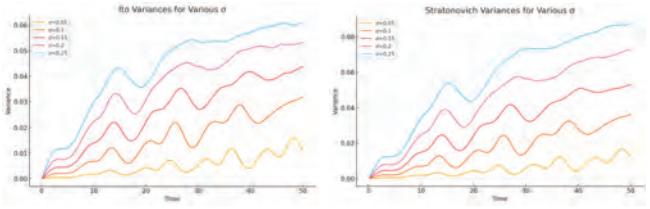

(A) (B)

Figure 7: Variances for various values of σ. They remain mostly evenly spaced in the time sampled. They all appear to dampen over time, although at different rates. A) Ito variances B) Stratonovich variances

Variance Behavior:

As seen in Figures 2-6 (a) and Figures 2-6 (b), over time, the paths disperse and stray from the orbits of the deterministic version. It is also clear that the size of the oscillations increases. However, the rate of this increase is variable. In Figures 7 (a)-(b), we observe that the rate at which variance increases over time is roughly proportional to the size of σ before beginning to dampen.

Notice that in Figure 7, the variances mostly remain evenly spaced and exhibit the behavior of "flattening out" as time goes on. We can attribute the second result to the fact that frequency is bounded between 0 and 1, and hence its variance is also bounded.

Furthermore, in Figure 7, oscillations are mirroring those in Figures 2-6 (a) and Figures 2-6 (b). This can be attributed to the fact that trajectories are "most misaligned" when the graph reaches its peak, as seen by the wider range of values in Figures 2-6 (a) and Figures 2-6 (b) at that point.

Ito vs. Stratonovich:

From observation, the Stratonovich variance is greater than the Ito variance. This result is due to the extra terms in the Ito version (especially the negative term), which act as an opposing force to any phenotype getting too big. We will provide a mathematical bound for when the Ito form's extra terms are guaranteed to limit the SDE's growth.

In the SDE, notice that the - $\sigma_i^2 x_i$ has a linear xi, while every other $\sigma_j^2 x_j^2$ has quadratic x_j. Also, note that each $0 < x_k < 1$, and they sum to 1. We would like the negative term to "overpower" the positive terms. Equivalently, we need that $\sigma_i^2 x_i > \Sigma\, \sigma_j^2 x_j^2$. Specifically, when we assume each $\sigma_i = \sigma$, as we did in our simulation, we can cancel the σ's as follows:

$$x_i > \sum_{j \neq i} x_j^2 \tag{13}$$

Since each $x_j > 0$, which is true by hypothesis, we can apply the ℓ1-ℓ2 norm inequality:

$$\left(\sum_{j \neq i} x_j\right)^2 \geq \sum_{j \neq i} x_j^2 \tag{14}$$

Since the sum of the x_i's is 1, we can make a substitution for the left-hand side of equation 14 and use the following inequality chain relating equations 13 and 14 to determine a bound for x_i :

$$x_i > (1 - x_i)^2 = \left(\sum_{j \neq i} x_j\right)^2 \geq \sum_{j \neq i} x_j^2 \tag{15}$$

Since any x_i satisfying the first inequality in equation 15 will automatically satisfy equation 13, we can solve this inequality to generate a bound for when the Ito terms are *guaranteed* to limit the SDE's growth. It is clear by algebra that this inequality is satisfied when $x_i > 0.382$. Interestingly, this is equal to one minus the inverse of the golden ratio. Thus, when some phenotype xi even slightly dominates the other phenotypes, the extra term in the Ito scheme dampens further growth. Additionally, we hypothesize that as time increases, the Ito scheme (Equation 9) will exhibit a lower maximum variance than the Stratonovich scheme (Equation 10).

Mean Behavior:

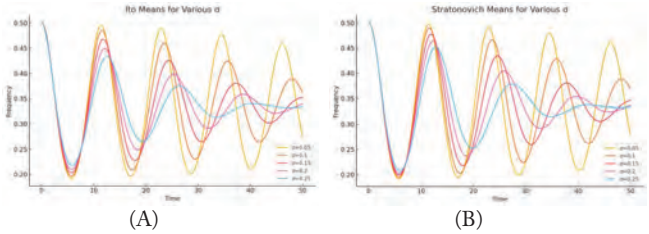

(A) (B)

Figure 7: Means trajectories for various values of σ. The rate of convergence increases as the magnitude of the noise increases. A) Ito means B) Stratonovich means.

While the variances and sizes of oscillations tend to increase for each σ, the means tend to stabilize towards the center equilibrium ⅓, as shown in Figure 8. Rather unintuitively, the speed of stabilization increases with σ, as shown in Figure 8; notice that as σ increases, the mean converges to ⅓ faster.

This effect can be attributed to the fact that noise can cause the periods of the cycles to change. This results in an average that involves the sum of many misaligned cycles, which cancel each other out and converge towards equilibrium. Hence, we have shown that a converging average does not necessarily indicate converging trajectories; in fact, a converging average often indicates increasingly chaotic trajectories. Essentially, the system exhibits some ergodicity.

Implications:

Together, these results indicate that asymptotically neutral equilibrium points are closer in nature to asymptotically unstable points. In other words, when a system has no "preferences," it tends to grow more chaotic rather than remain stable. The noise does not act symmetrically.

Furthermore, these results indicate that neutral equilibria and their associated cycles are susceptible to noise-induced changes, as the system lacks an intrinsic counterbalance. This can be observed in the dispersive behavior shown in Figures 2-6 and the steady increase in variance illustrated in Figure 7.

Since underlying neutral equilibrium points tend to be unstable, this result implies that cycles either have underlying stable behavior or have a near-negligible noise (small-noise limit). In the first case, the noise counteracts the underlying stability. In the second case, the system is inherently neutral in nature and typically adopts the deterministic variant.

Similar cyclic behavior can be commonly observed in nature's ecosystems, whether it be in the form of predator-prey cycles or competing phenotypes in a rock-paper-scissors-type relationship. As we have shown, these structures are incredibly brittle and easily disturbed by changes in the magnitude of noise to which the system is subject. In ecosystems, climate change, overfishing, and other human activities can all contribute to this environmental variance. Although noise does not immediately cause extinction events (i.e., one frequency approaches 0), increases in variance and cycle amplitude, seen in Figures 2-7, can significantly increase the risk. Notice that in each heatmap, a large percentage of the data concentrates at the more extreme frequencies. This behavior renders ecosystems far more susceptible to disasters, which can turn these extreme events into extinction-level occurrences.

Regarding the Ito vs. Stratonovich question, both the theory and results indicate that the Ito scheme is more resilient to noise than the Stratonovich scheme. These differences result from the assumed properties of the noise. While the Ito scheme assumes a martingale, the Stratonovich scheme assumes smoothness in the noise. Ultimately, the better model depends on the underlying conditions of the noise, which should be chosen carefully.

Further Questions:

Although we have provided a numerical approximation for the effect of noise on zero-sum games, several questions remain unanswered. What is the generalized behavior and stability of the system for any generic antisymmetric payoff matrix? What if the noise vector is asymmetric, where some $\sigma_i \neq \sigma_j$? Is there an explicit formula for the mean's speed of convergence and the variance's speed of increase? How do we express the sizes of the oscillations for the variance and mean graphs quantitatively? Which more accurately models noise in the context of rock-paper-scissors: Ito or Stratonovich?

■ Conclusion

We have illustrated that despite a converging mean, individual trajectories may diverge wildly within a system. In zero-sum games, adding a stochastic term often increases the system's instability, resulting in larger oscillations. In these cases, the magnitude of the system's variance also increases proportionally with the underlying variance before dampening. Specifically, our studied payoff matrix is

$$\begin{pmatrix} 0 & -1 & 1 \\ 1 & 0 & -1 \\ -1 & 1 & 0 \end{pmatrix}$$

Furthermore, as σ increases, the mean converges more quickly towards the neutral equilibrium point, with each peak decreasing steadily before evening out.

In both mean and variance, Ito dynamics (Equation 9) display less movement than Stratonovich dynamics (Equation 10), attributed to the "Ito correction" resulting from Ito's Lemma (Equation 6). This difference is non-negligible and should be carefully considered in modeling settings. We have also given an inequality, xi > 0.382, for the threshold at which the Ito scheme is guaranteed to limit growth more than the Stratonovich scheme.

Since symmetric Brownian noise acts asymmetrically on neutral equilibrium points and cycles, such equilibria behave very similarly to intrinsically asymptotically unstable equilibria. Hence, it is unlikely that observed neutral equilibria are intrinsically neutral unless the noise is sufficiently small. Additionally, without any attractive counterbalance, these equilibria are very susceptible to noise, which can significantly alter a trajectory's path. These alterations typically manifest as increased cycle amplitudes and concentrations at more extreme frequencies. In nature, environmental variance often comes from factors such as climate change, overfishing, and other human activities. These can significantly offset a system's balance and lead to extinction events.

■ Acknowledgments

The author thanks Professor J.S.W. Lamb for his guidance and mentorship.

■ References

1. Øksendal, B., Stochastic Differential Equations: An Introduction with Applications, 6th ed.; Springer: 2003.

DOI: 10.36838/IJHSR87.8

2. Taylor, P. D.; Jonker, L. B. Evolutionarily Stable Strategies and Game Dynamics. Mathematical Biosciences 1978, 40, 145–156.
3. Hofbauer, J.; Sigmund, K., Evolutionary Games and Population Dynamics; Cambridge University Press: Cambridge, 1998.
4. Fudenberg, D.; Harris, C. Evolutionary Dynamics with Aggregate Shocks. Journal of Economic Theory 1992, 57, 420–441.
5. Delesse, F. Stochastic Replicator Dynamics, Mémoire d'initiation à la recherche, PSL Research University – Université Paris-Dauphine, 2016.
6. Imhof, L. A. The Long-run Behavior of the Stochastic Replicator Dynamics. The Annals of Applied Probability 2005, 15, 1019–1045.
7. Foster, D. P.; Young, H. P. Stochastic Evolutionary Game Dynamics. Theoretical Population Biology 1990, 38, 219–232.
8. Avrachenkov, K.; Borkar, V. S. Metastability in Stochastic Replicator Dynamics. Dynamic Games and Applications 2019, 9, 366–390.
9. Hairer, E.; Nørsett, S. P.; Wanner, G., Solving Ordinary Differential Equations I: Nonstiff Problems, 2nd ed.; Springer: 1993.

Author

Kyle Yang attends Deerfield Academy (G11) in Massachusetts, USA. He is interested in both pure and applied mathematics, especially statistical theory, abstract algebra, and number theory. He plans on studying mathematics in college.

IJHSR
ijhighschoolresearch.org
RESEARCH ARTICLE

Photon Transport and Spectral Formation in Accreting Neutron Star Columns: A Monte Carlo Approach

Andrew Gan

Raffles Institution, 1 Raffles Institution Lane, Singapore 575954; ganandrew10@gmail.com

ABSTRACT: We present a Monte Carlo model for radiative transfer in the accretion columns of super-critical X-ray pulsars. The simulation follows individual X-ray photons as they propagate through the dense, magnetically confined plasma, focusing on Compton scattering as the dominant interaction process. The physical setup assumes a cylindrical accretion column characterized by the mass accretion rate, bulk inflow velocity, plasma temperature, and column geometry. Both thermal and bulk Comptonisation are treated self-consistently, and relativistic kinematics is included via Lorentz transformations between the electron and laboratory frames. We explore how variations in density, temperature, and flow velocity affect the emergent photon spectra and angular distributions. The results demonstrate the strong sensitivity of the escaping radiation to local plasma conditions in the sinking region, highlighting the importance of Compton scattering in shaping the observed X-ray emission of accreting neutron stars. This framework provides a basis for future models incorporating magnetic effects, cyclotron scattering, and pair production in highly luminous X-ray pulsars.

KEYWORDS: Physics and Astronomy, Astronomy and Cosmology, Neutron Stars, Accretion, Scattering, Radiative Transfer.

Introduction

Accreting strongly magnetized neutron stars (NSs) manifest themselves as X-ray pulsars (XRPs).[1] In these systems, material from a companion star is accelerated in the gravitational field of an NS and reaches the NS surface with velocity $v \simeq c(R_g/R) \sim 0.5c$, where $R_g \simeq 3\ (M/M_\odot)$ km is the gravitational radius of the NS, and M and R are the mass and radius of the NS, respectively.

At the NS surface, the kinetic energy of the accretion flow is transformed into heat and is emitted predominantly in the form of X-rays. The luminosity of XRPs is related to the mass accretion rate $\dot{M}$ as

$$L = \frac{GM\dot{M}}{R} \qquad (1)$$

and covers a wide range from $\sim 10^{33}$ erg s^{-1}, where it is limited by transition into the propeller state[2] or state of stable accretion from cold recombined disc,[3] and up to $\sim 10^{40}$ erg s^{-1}, where XRPs manifest themselves as ultra-luminous X-ray sources (ULXs).[4]

The strong magnetic field of an NS, which is expected to be $\gtrsim 10^{12}$G in XRPs,[5] shapes the geometry of the accretion flow in a region of size $\sim 10^8$ cm around an NS, which is called the NS magnetosphere. Hot plasma in the magnetosphere follows magnetic field lines and reaches the NS surface in a small region of area $\sim 10^9$ cm^2 located close to the magnetic poles of a NS.

Depending on the mass accretion rate, XRPs operate in two distinct regimes.[6] Sub-critical pulsars, with luminosities below a critical threshold of approximately $L_{crit} \sim 10^{37}$ erg s^{-1}, lack a fully developed radiative shock. In this regime, the infalling matter is decelerated primarily by Coulomb collisions or gas pressure near the surface,[7] and the X-ray emission emerges from a hot spot rather than an extended column. In contrast, super-critical XRPs exceed L_{crit}, at which point radiation pressure dominates the dynamics of the flow. A radiative shock forms several stellar radii above the surface, creating an optically thick accretion column in which photons diffuse sideways and escape through the walls.[6,8,9] The resulting geometry and radiation field are fundamentally different between these regimes.

The accretion column structure in the super-critical case is governed by magnetic confinement, radiation pressure, and gravity. The upper region contains the radiative shock, where the supersonic inflow is abruptly decelerated. Below the shock, the sinking region features dense, slowly settling plasma through which radiation diffuses and interacts extensively with electrons. The emergent X-ray spectrum is shaped in this region, with Compton scattering acting as the dominant radiative process.[10] At sufficiently high plasma temperatures, photon-photon interactions can produce electron-positron pairs, increasing the effective scattering opacity and further modifying the dynamics.[11,12]

The goal of this work is to develop a numerical Monte Carlo code to model radiative transfer of X-ray photons in the sinking region of the accretion column of a super-critical XRP. We focus on the kinematics of Compton scattering, which governs energy redistribution between photons and the hot, partially relativistic electron population. Our approach tracks individual photon histories, incorporating bulk inflow velocities, thermal electron motions, and potential pair creation effects. This allows us to examine how local plasma conditions determine the emergent radiation field and the observable spectra of accreting X-ray pulsars.

© 2026 Terra Science and Education

DOI: 10.36838/IJHSR87.14

Methods

Physical Framework:

We model a filled accretion column of cylindrical shape located at the magnetic pole of an NS. The geometry is characterized by a base radius d and a height H, the latter potentially extending up to a significant fraction of the NS radius R. The accretion column is assumed to be stationary and uniformly filled with plasma channeled along the magnetic field lines.

The mass inflow rate $\dot{M}$ is treated as a global parameter of the simulation, with values in the range $\dot{M} \gtrsim 10^{17}$ gs^{-1} appropriate for bright, super-critical XRPs. Together with the flow velocity v and the column cross-sectional area $A=\pi d^2$, the local mass density of the plasma is determined by

$$\rho = \frac{\dot{M}}{2\pi d^2 v} \tag{2}$$

where the factor of 2 accounts for the presence of two symmetric accretion columns.

We assume a fully ionized hydrogen plasma, so that the number density of free electrons is directly given by $n_e=\rho/m_p$, where m_p is the mass of the plasma. The number density is crucial because it affects the mean free path of the photon, or the average distance it travels between scattering events, and therefore the frequency of such events occurring:

$$l_{fp} = \frac{1}{2\sigma n_e} \tag{3}$$

where σ is the scattering cross-section, which will be discussed later.

The temperature T of the accretion flow is another key parameter of the model. We assume that electrons and protons are thermally coupled so that both species share the same kinetic temperature. In the plasma rest frame, the particle velocities follow a Maxwell–Boltzmann distribution, which gives the probability of any selected particle having a velocity v at temperature T:

$$f(v) = 4\pi v^2 \left(\frac{m}{2\pi k_B T}\right)^{3/2} \exp\left[-\frac{mv^2}{2k_B T}\right] \tag{4}$$

with the characteristic thermal speed $v_t=\sqrt{3k_BT/m}$. The corresponding cumulative distribution is

$$F(v) = \mathrm{erf}\left(\frac{v}{\sqrt{2}v_t}\right) - \frac{\sqrt{2}}{\sqrt{\pi}}\frac{v}{v_t}\exp\left[-\frac{v^2}{2v_t^2}\right] \tag{5}$$

The distributions given by the above equations are used to randomly select the thermal electron velocity for each scattering event, providing an adequate description of the electron gas for $T \lesssim 40$ keV, where the characteristic electron thermal velocities satisfy $v \ll c$. In this work, we focus on the radiative transfer of X-ray photons through the relatively dense sinking region of the column, where photons undergo multiple scatterings before escaping.

We assume that Compton scattering is the dominant process coupling radiation and matter. This is justified by the high electron temperatures and densities expected in super-critical accretion columns, which render free–free absorption and emission comparatively weak at X-ray energies.[13]

The scattering cross section, which represents the probability of a scattering event taking place, is taken to be the standard non-magnetic Klein-Nishina values, appropriate when the local magnetic field does not strongly quantize electron motion or when we are interested in the zeroth-order effect of Comptonisation. For a photon of energy E = hν scattering off an electron at rest, the total Klein-Nishina cross section is

$$\sigma_{KN} = \frac{3\sigma_T}{4}\left[\frac{1+x}{x^3}\left\{\frac{2x(1+x)}{1+2x} - \ln(1+2x)\right\} + \frac{\ln 1+2x}{2x} - \frac{1+3x}{(1+2x)^2}\right] \tag{6}$$

where $x=E/(m_ec^2)$ is the dimensionless photon energy and $\sigma_T \approx 6.65\times10^{-25}$ cm^2 is the Thomson cross section.[14] In the low-energy limit $x \ll 1$, this reduces to the Thomson value:

$$\sigma_{KN} \approx \sigma_T\left(1 - 2x + \frac{26}{5}x^2 + \cdots\right) \tag{7}$$

Since $x \approx 0$, this value is taken to be equal to σ_T, and used in the calculation of the mean free path.

Aside from the path the photon takes, the simulation also calculates and records how the photon energies are affected by scattering. The change in photon energy during a Compton scattering event depends on both the scattering angle and the electron's initial momentum. For the case of an electron initially at rest, the scattered photon energy E' is given by the standard Compton formula,[14]

$$E' = \frac{E}{1 + \frac{E}{m_ec^2}(1 - cos\theta)} \tag{8}$$

Where θ is the scattering angle in the laboratory frame. This expression shows that the photon loses more energy (larger wavelength shift) for larger scattering angles and for higher initial photon energies.

When the electron is moving in the lab frame with a relativistic velocity v, equation (8) is applied after transforming to the electron's rest frame.[14] The incident photon energy in the electron rest frame is obtained via a Lorentz transformation:

$$E_e = \gamma E(1 - \beta cos\psi) \tag{9}$$

Where $\beta = v/c$, $\gamma=(1-\beta^2)^{-1/2}$, and ψ is the angle between the photon propagation direction and the electron velocity in the lab frame. The scattering is then computed using the same Compton formula in (8), but with E_e as the incoming photon energy. If the scattering angle in the electron rest frame is θ_e, the scattered photon energy in that frame is thus:

$$E_e' = \frac{E_e}{1 + \frac{E_e}{m_ec^2}(1 - \cos\theta_e)} \tag{10}$$

Finally, the scattered photon energy in the lab frame is obtained by transforming E_e' back:

$$E' = \gamma E_e'(1 + \beta cos\psi') \tag{11}$$

where ψ' is the angle between the scattered photon direction and the electron velocity in the electron rest frame. This two-step Lorentz transformation procedure allows consistent treatment of Compton scattering on electrons with arbitrary momenta, which is essential for modelling hot plasmas and relativistic outflows.[14]

Bulk and thermal Comptonisation are included in the framework to investigate the significance of both effects. The bulk velocity of the accretion flow v can reach a substantial fraction of the speed of light, so special-relativistic transformations are applied at each scattering to properly account for Doppler shifts and aberration effects. The combined effect of bulk and thermal electron motions produces complex energy redistribution, which our Monte Carlo approach captures by simulating individual photon trajectories and interactions.

The free parameters of the physical framework are therefore: the base radius d and height H of the accretion column, the mass accretion rate $\dot{M}$, the flow velocity v, and the plasma temperature T. These quantities fully specify the density, electron number density, and velocity distribution of the scatterers, providing the input conditions for the radiative transfer simulation.

Monte Carlo Method:

To model the transport of X-ray photons through the accretion column, we employ a Monte Carlo approach in which individual photon trajectories are followed until they escape. The only interaction process considered is Compton scattering, which dominates under the high-temperature, high-density conditions expected in super-critical XRPs.[13] The relevant cross sections and energy–angle relations are given in the previous section and are used here without approximation.

In each simulation run, 10^3 photons are propagated through the cylindrical column. Their evolution is computed iteratively through the following sequence:

1. ***Photon injection:*** A photon is placed at a random position within the column. Its initial propagation direction is chosen isotropically in the plasma rest frame, and its initial energy E_i is set according to the assumed source spectrum.
2. ***Free path sampling:*** The mean free path l_{fp} is calculated from the local electron density n_e and the cross section σ_T. The actual travel distance l is drawn from an exponential distribution:

$$l = -l_{fp}\log(r) \tag{12}$$

Where r is a random value between 0 and 1.

3. ***Boundary check:*** If the updated photon position lies outside the column geometry, the photon is considered to have escaped, and its final energy and direction are recorded. Otherwise, a scattering event is simulated.
4. ***Scattering event:*** A thermal electron velocity is sampled from the Maxwell–Boltzmann distribution. The total electron momentum is then obtained by combining the sampled thermal velocity with the bulk inflow velocity v of the column. Next, a Lorentz transformation to the instantaneous electron rest frame is performed. The scattering is then computed using the relativistic Compton formula, with two random angles determining the outgoing photon direction. Finally, the scattered photon energy and direction are transformed back to the laboratory frame via the inverse Lorentz transformation, accounting for both bulk and thermal motions.
5. ***Iteration:*** The photon's updated position and energy are used as inputs for the next free path sampling step. The process continues until the photon exits the accretion column or a maximum number of scatterings is reached, to prevent the simulation from running for too long.

For each simulation, we also compute the average energy of the photons that successfully escape the accretion column.

If $E_f^{(i)}$ denotes the final energy of the i-th escaping photon and N is the total number of escaping photons, the mean energy is calculated as

$$\langle E_f \rangle = \frac{1}{N}\sum_{i=1}^{N} E_f^{(i)} \tag{13}$$

To quantify the spectral spread, we additionally evaluate the second moment

$$\langle E_f^2 \rangle = \frac{1}{N}\sum_{i=1}^{N} \left(E_f^{(i)}\right)^2 \tag{14}$$

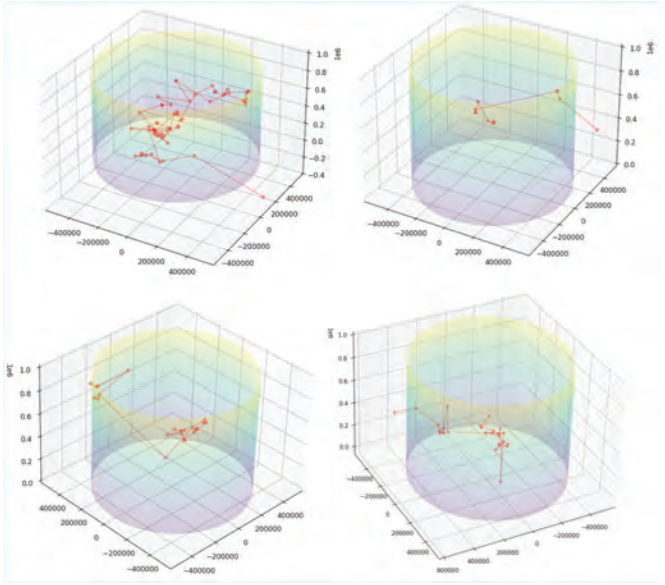

Figure 1: Examples of different photon trajectories inside the accretion column under identical physical conditions. Each dot represents a single Compton scattering event, after which the photon's direction of movement is randomized. The electron number density is artificially reduced for clarity; in reality, the number of scatterings is significantly higher.

which allows us to compute the standard deviation of the emergent photon energies via

$$\sigma_E = \sqrt{\langle E_f^2 \rangle - \langle E_f \rangle^2} \tag{15}$$

These quantities provide a compact measure of the energy redistribution produced by multiple Compton scatterings in the column. For the angular distribution, we also compute the mean final angle θ_f between the photon momentum vector

DOI: 10.36838/IJHSR87.14

and the normal to the neutron star surface, where $0<\theta_f<\pi$. If $\theta_f^{(i)}$ is the final angle of the i-th escaping photon, the average is obtained as

$$\langle\theta_f\rangle = \frac{1}{N}\sum_{i=1}^{N}\theta_f^{(i)} \quad (16)$$

This quantity provides a compact measure of the overall beaming of the escaping radiation relative to the accretion column geometry. This Monte Carlo algorithm naturally incorporates both bulk and thermal Comptonisation as well as special-relativistic Doppler and aberration effects. The resulting ensemble of photon histories yields the emergent angular distribution and energy spectrum for a given set of accretion column parameters. Examples of simulated photon trajectories are shown in Figure 1.

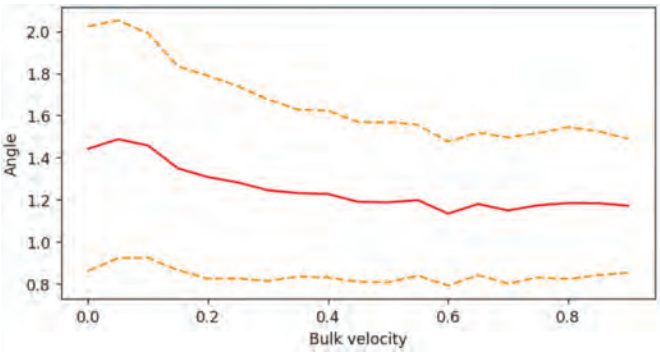

Figure 2: The solid line shows the average angle, in radians, between the normal to the NS surface and the final direction of photon motion for different bulk velocities in terms of c. An angle of $\pi/2$ represents photon escape parallel to the NS.

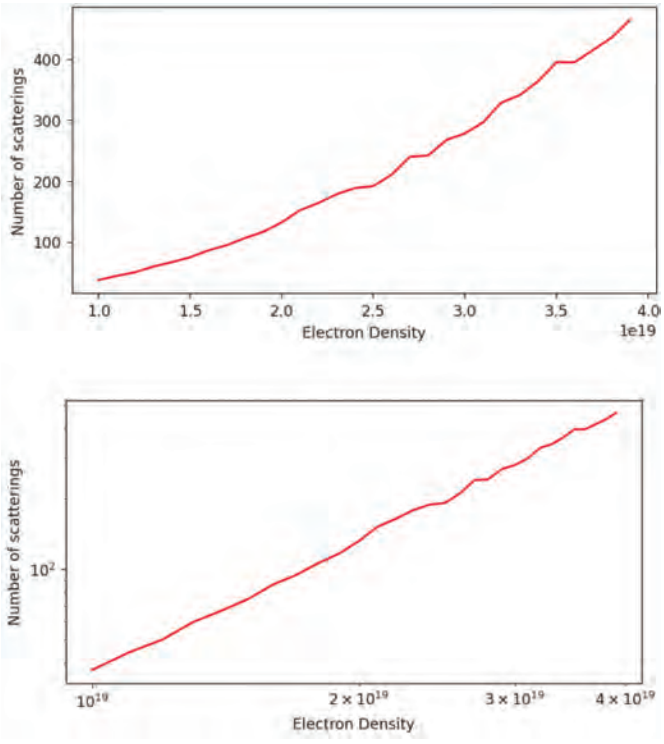

Figure 3: Average number of scatterings for different electron number densities (in cm^{-3}) on linear (top) and logarithmic (bottom) scales.

Results and Discussion

We compute the velocity distribution of electrons, the mean number of scatterings as a function of optical depth, and the spectrum and angular distribution of escaping photons. Additional analysis examines the effect of bulk inflow velocity and the potential contribution of electron– positron pairs to the scattering opacity. Figure 2 demonstrates that the bulk motion of the plasma inside the accretion column strongly affects the final angular distribution of escaping X-ray photons. At high inflow velocities directed towards the neutron star surface, the radiation field becomes increasingly beamed along the direction of the bulk velocity (i.e., downwards) with a lower dispersion, with a significant fraction of photons emerging at angles tilted towards the stellar surface. For all bulk velocities, the average angle $\langle\theta\rangle$ is below $\pi/2$, which reflects the fact that the initial photon source is located near the very bottom of the accretion channel and thus introduces a mild geometric asymmetry even in the static case. The numerical result that increasing β produces a pronounced downward beaming of X-rays is in good agreement with theoretical expectations proposed previously in the literature for super-critical accretion columns.[15-17]

Figure 3 shows the mean number of scatterings as a function of electron density. As expected, increasing n_e reduces the mean free path and significantly raises the number of interactions. This scaling is important in the context of pair creation: under typical accretion column conditions, high-energy photons can generate electron–positron pairs, boosting the scattering opacity. Using the standard low-temperature approximation,18 a temperature $T = 10^9$K yields $n\pm \approx 10^{26}\text{cm}^{-3}$, comparable to characteristic electron densities in XRPs, meaning the increase in n_e due to pair creation is non-negligible. The resulting increase in optical depth extends the photon diffusion time and can suppress the emergent luminosity.

The effect of bulk inflow velocity on the scattering statistics is shown in Figure 4. For any fixed density, the mean number of scatterings decreases with β at low velocities and then levels off for $\beta \gtrsim 0.6$. This saturation is a geometric effect: at high inflow speeds, photons are dragged deeper into the column and reflected multiple times from the base before escaping, leading to a quasi-steady mean interaction count. The expected upward trend with density is also evident; higher n_e pushes the system deeper into the optically thick regime, where the Monte Carlo code converges to a diffusion-like limit.

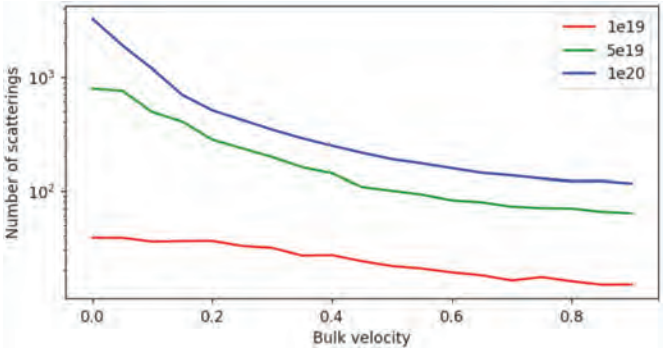

Figure 4: Average number of scatterings as a function of bulk velocity (in terms of c) for different electron densities. The vertical axis is logarithmic.

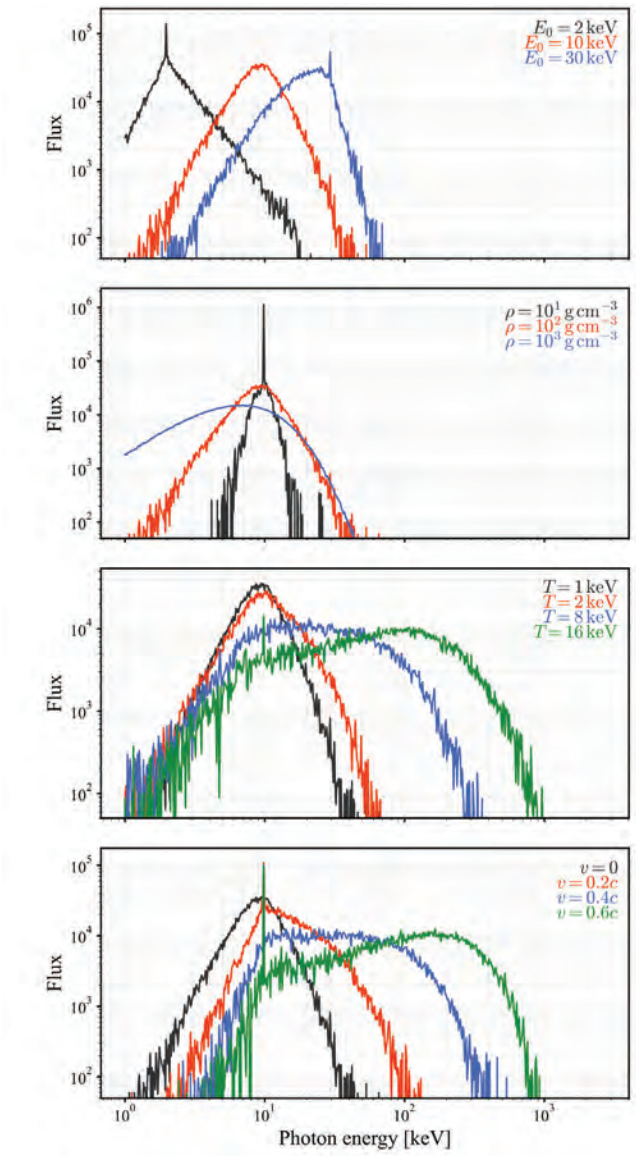

Figure 5: Emergent photon spectra from Monte Carlo simulations of Comptonisation in the accretion column under varying plasma conditions. Both axes are logarithmic. Spectral broadening and hardening are evident in both thermal and bulk Compton regimes.

Figure 5 summarizes the spectral impact of key plasma parameters. The top panel illustrates the dependence on the initial photon energy E_0 : higher E_0 photons retain a larger fraction of their energy and produce extended high-energy tails due to reduced energy loss per scattering and the onset of Klein–Nishina suppression. The second panel shows the effect of density: as ρ increases, the spectrum broadens and approaches a quasi-Wien distribution at $\rho = 10^3$ gcm^{-3} , indicating near-equilibration with the electron gas. The third panel demonstrates the role of electron temperature: higher T yields systematically harder spectra and shifts the peak to higher energies, in line with expectations from the Kompaneets equation.[14] The bottom panel highlights the impact of bulk inflow: increasing v from 0 to 0.6c causes a clear hardening and energy shift of the spectrum due to bulk Comptonisation, a process distinct from purely thermal scattering. These results confirm that both bulk and thermal Comptonization must be treated simultaneously when modelling super-critical XRPs. The angular redistribution, energy diffusion, and spectral formation are all tightly coupled to the local density, temperature, and inflow velocity in the sinking region of the accretion column.

Conclusion

We have developed a Monte Carlo model to study radiative transfer in the accretion columns of super-critical XRPs, focusing on the role of Compton scattering in shaping the emergent Xray spectra. The Python simulation code was written from scratch specifically for this project and designed to be modular for future extensions. The physical framework assumes a stationary, magnetically confined cylindrical column characterized by the accretion rate, flow velocity, plasma temperature, and geometry. Both bulk and thermal Comptonisation are treated selfconsistently, with full relativistic kinematics included via Lorentz transformations between the electron and laboratory frames.

A Monte Carlo approach was chosen because of its flexibility in handling complex geometries and boundary conditions in the emitting region. This method also allows for straightforward future upgrades to include cross sections that depend strongly on photon energy, propagation direction, and polarization state. A known drawback of the Monte Carlo technique is the increased computational cost in optically thick media due to the large number of scattering events. However, this is partially offset by the ease with which such simulations can be parallelized across multiple processors, making it well-suited for high-performance computing environments.

Our simulations track individual photon histories as they undergo multiple scatterings in the dense sinking region of the column. The results demonstrate that the spectral formation is highly sensitive to the local plasma conditions. In particular:

a) The mean number of scatterings and the angular distribution of escaping photons are strongly dependent on the electron density and the Klein–Nishina cross section, confirming the importance of Comptonisation in optically thick columns.

b) Thermal Comptonization produces systematic spectral hardening as the electron temperature increases, with the emergent spectrum approaching a quasi-Wien distribution at the highest densities.

c) Bulk Comptonization due to coherent inflow at v ~0.1c – 0.6c leads to significant energy amplification, distinct from pure thermal effects, and can shift the entire spectrum toward higher energies.

d) The combined effect of bulk and thermal motions creates complex energy redistribution that cannot be captured by either process in isolation.

e) Multiple scatterings of electrons participating in bulk inflow produce a pronounced downward beaming of escaping X-rays towards the neutron star surface. This behavior, observed in our simulations, is in good agreement with previous theoretical expectations for super-critical accretion columns[15-17] and provides a quantitative framework for modelling the illumination pattern of the stellar surface by the accretion flow.

DOI: 10.36838/IJHSR87.14

f) Pair production at $T \gtrsim 10^9$ K can raise the effective scattering opacity to values comparable to the electron density, prolonging photon diffusion times and reducing the column luminosity.

These findings emphasize that accurate modelling of X-ray pulsar spectra requires simultaneous treatment of both thermal and bulk Compton scattering in the dense sinking region. The beaming effect generated by bulk Comptonisation highlights the need to account for angular redistribution when predicting the geometry of the emitted radiation. Our Monte Carlo approach provides a flexible framework for such studies and can be used in the future to calculate the illumination pattern of the neutron star surface by accretion columns and to link it with observed pulse profiles and surface heating.

Future extensions of this work will incorporate the effects of strong magnetic fields,[19] including quantisation of electron motion and cyclotron resonant scattering, as well as the geometry of fan and pencil beam emission patterns.[20,21] The present results form a baseline for interpreting observations of bright XRPs and ULXs, and for constraining the plasma conditions in their accretion columns.

Acknowledgments

The author would like to thank his mentor, Alexander Mushtukov, for his invaluable guidance during the research project.

References

1. Mushtukov, A.; Tsygankov, S. Accreting Strongly Magnetised Neutron Stars: X-Ray Pulsars. *arXiv (Cornell University)* 2022. https://doi.org/10.48550/arxiv.2204.14185.
2. Illarionov, A. F.; Sunyaev, R. A. Why the Number of Galactic X-Ray Stars Is so Small? *Astronomy and Astrophysics* 1975, *39*, 185–196.
3. Tsygankov, S. S.; Mushtukov, A. A.; Suleimanov, V. F.; Doroshenko, V.; Abolmasov, P. K.; Lutovinov, A. A.; J. Poutanen. Stable Accretion from a Cold Disc in Highly Magnetized Neutron Stars. *Astronomy and Astrophysics* 2017, *608*, A17–A17. https://doi.org/10.1051/0004-6361/201630248.
4. Fabrika, S. N.; Atapin, K. E.; Vinokurov, A. S.; Sholukhova, O. N. Ultraluminous X-Ray Sources. *Astrophysical Bulletin* 2021, *76* (1), 6–38. https://doi.org/10.1134/s1990341321010077.
5. Rüdiger Staubert; Joachim Trümper; Eckhard Kendziorra; D. Klochkov; Konstantin Postnov; Kretschmar, P.; Pottschmidt, K.; Haberl, F.; Rothschild, R. E.; Santangelo, A.; Wilms, J.; I. Kreykenbohm; Fürst, F. Cyclotron Lines in Highly Magnetized Neutron Stars. *Astronomy and Astrophysics* 2019, *622*, A61–A61. https://doi.org/10.1051/0004-6361/201834479.
6. Basko, M. M.; Sunyaev, R. A. The Limiting Luminosity of Accreting Neutron Stars with Magnetic Fields. *Monthly Notices of the Royal Astronomical Society* 1976, *175* (2), 395–417. https://doi.org/10.1093/mnras/175.2.395.
7. Zel'dovich, Ya. B.; Shakura, N. I. X-Ray Emission Accompanying the Accretion of Gas by a Neutron Star. *Astronomicheskii Zhurnal* 1969, *46*, 225.
8. E, L. Y.; A, S. R. Accretion Column Structure. *Soviet Astronomy Letters* 1988, *14*, 390.
9. Wang, Y.-M.; Frank, J. Plasma Infall and X-Ray Production in the Magnetic Funnel of an Accreting Neutron Star. *Astronomy and Astrophysics* 1981, *93*, 255–268.
10. Becker, P. A.; Wolff, M. T. Thermal and Bulk Comptonization in Accretion-Powered X-Ray Pulsars. *The Astrophysical Journal* 2007, *654* (1), 435–457. https://doi.org/10.1086/509108.
11. Mushtukov, A. A.; Ognev, I. S.; Nagirner, D. I. Electron-Positron Pairs in Hot Plasma of Accretion Column in Bright X-Ray Pulsars. *Monthly Notices of the Royal Astronomical Society Letters* 2019, *485* (1), L131–L135. https://doi.org/10.1093/mnrasl/slz047.
12. Suleimanov, V. F.; Mushtukov, A. A.; Igor Ognev; Doroshenko, V. A.; Werner, K. Mean Opacities of a Strongly Magnetized High-Temperature Plasma. *Monthly Notices of the Royal Astronomical Society* 2022, *517* (3), 4022–4033. https://doi.org/10.1093/mnras/stac2935.
13. Frank, J.; King, A.; Raine, D. J. *Accretion Power in Astrophysics*; Cambridge University Press: Cambridge, 2002.
14. Rybicki, G. B.; Lightman, A. P. *Radiative Processes in Astrophysics*; 1986.
15. Kaminker, A. D.; Fedorenko, V. N.; Tsygan, A. I. A Radiating Accretion Column as a Model for an X-Ray Pulsar. *Astronomicheskii Zhurnal* 1976, *53*, 773.
16. Juri Poutanen; Mushtukov, A. A.; Suleimanov, V. F.; Tsygankov, S. S.; Nagirner, D. I.; Doroshenko, V.; Lutovinov, A. A. A REFLECTION MODEL for the CYCLOTRON LINES in the SPECTRA of X-RAY PULSARS. *The Astrophysical Journal* 2013, *777* (2), 115–115. https://doi.org/10.1088/0004-637x/777/2/115.
17. Postnov, K. A.; Gornostaev, M. I.; D. Klochkov; Laplace, E.; Lukin, V. V.; Shakura, N. I. On the Dependence of the X-Ray Continuum Variations with Luminosity in Accreting X-Ray Pulsars. *Monthly Notices of the Royal Astronomical Society* 2015, *452* (2), 1601–1611. https://doi.org/10.1093/mnras/stv1393.
18. Zeldovich, Ya. B.; Novikov, I. D. *Relativistic Astrophysics. Vol 1: Stars and Relativity*; 1971.
19. Harding, A. K.; Lai, D. Physics of Strongly Magnetized Neutron Stars. *Reports on Progress in Physics* 2006, *69* (9), 2631–2708. https://doi.org/10.1088/0034-4885/69/9/r03.
20. Gnedin, Y. N.; Sunyaev, R. A. The Beaming of Radiation from an Accreting Magnetic Neutron Star and the X-Ray Pulsars. *Astronomy and Astrophysics* 1973, *25*, 233.
21. Lutovinov, A. A.; Tsygankov, S. S.; Suleimanov, V. F.; Mushtukov, A. A.; Doroshenko, V.; Nagirner, D. I.; J. Poutanen. Transient X-Ray Pulsar v 0332+53: Pulse-Phase-Resolved Spectroscopy and the Reflection Model. *Monthly Notices of the Royal Astronomical Society* 2015, *448* (3), 2175–2186. https://doi.org/10.1093/mnras/stv125.

Author

Andrew Gan is a high school student at Raffles Institution, Singapore. He has a strong interest in physics and research, which he plans to pursue at university.

IJHSR
ijhighschoolresearch.org
RESEARCH ARTICLE

The Effects of Chain-of-Thought Prompting on the Performance of Moderate-sized LLMs in Competitive Math

Eric L. Min

Westwood High School, 12400 Mellow Meadow Dr, Austin, TX, 78750, USA, eric.lin.min7@gmail.com

ABSTRACT: Modern state-of-the-art large language models (LLMs), such as Deepseek V3 and GPT-4o, demonstrate significantly better performance on a variety of reasoning-related tasks when compared with small-scale (SLMs) and moderate-sized LLMs (MSLMs). *Chain-of-Thought* (CoT) prompting, where models are guided towards generating intermediate reasoning steps, has been shown to improve performance in LLMs. It produces notable gains across arithmetic, commonsense, and symbolic benchmarks, such as GSM8K. However, the effects of CoT prompting in MSLMs, particularly more recent models, remain unclear. This is often due to high degrees of prompt sensitivity, and thus, we explore the impact of CoT prompting in MSLMs, evaluating the degree to which encouraging these relatively smaller models to "think out loud" can enhance a model's rigorous task performance. In this paper, we evaluate the abilities of CoT-prompted MSLMs in the reasoning-reliant field of mathematics, particularly competitive mathematics, contrasting these results with zero-shot baselines and prompt variants to produce conclusions. The empirical gains reveal striking connections between prompt architecture and MSLM capacity. For example, the Llama-4-Maverick model exhibited signs of inherent internal prompting, supporting the result that the model performed the best when prompted with a specific example with a high degree of task alignment.

KEYWORDS: Robotics and Intelligent Machines, Cognitive Systems, Large Language Model, Chain of Thought (CoT), Competitive Mathematics.

Introduction

LLMs have achieved remarkable fluency in natural language tasks.[1,2] However, despite their apparent proficiency, these models are not actually capable of reasoning in the human sense.[3] LLMs fundamentally lack true reasoning because they operate as sophisticated pattern matchers, essentially stochastic parrots, that are trained via next token prediction on large-scale text collections, optimizing for the statistical likelihood of word sequences rather than the derivation of logically coherent and logic-driven conclusions.[4]

LLMs are evolving from static prompt response systems to dynamic cognitive agents, and progress hinges on structured prompting (*Chain-of-Thought, Tree-of-Thought, Forest-of-Thought*),[5,6] and tool usage (*ReAct, PAL*).[7] CoT functions by attempting to guide language models towards generating intermediate reasoning steps before answering; however, these linear reasoning chains are fragile with error propagation. Tree-of-Thought explores a branching space of thought hypotheses, generating and evaluating multiple reasoning chains before backtracking to the most common answer. ReAct (Reasoning + Acting) and PAL (Program-aided language) integrate external results from external code, API calls, or tools mid-reasoning to enhance their performance.

CoT stands out as a strong paradigm in language model reasoning since it strategically structures how the model "thinks,"[2] often significantly improving accuracy, transparency, and task performance.[8] CoT prompting enables LLMs to tackle multi-step reasoning tasks with noticeably improved accuracy.[9] It has been demonstrated that integrating intermediate reasoning steps often dramatically enhances performance on arithmetic, commonsense, and symbolic benchmarks. By eliciting an explicit sequence of reasoning steps, CoT offers users visibility into the model's cognitive process. This transparency is invaluable for debugging and evaluating trustworthiness.

Recent advances in MSLMs and SLMs underscore their growing significance beyond niche tasks, offering a combination of efficiency, control, and domain specialization that makes them particularly suited for enterprise and edge deployment scenarios. These lightweight models typically require far fewer computational resources than large-scale models, enabling deployment on devices like smartphones or edge servers while delivering low-latency and cost-effective inference.[10] By training or fine-tuning MSLMs and SLMs on domain-specific datasets, such as healthcare,[11] legal documents, and finance, organizations can achieve higher contextual accuracy and reduce hallucination risk compared to general-purpose LLMs, which is critical in regulated industries. Moreover, because MSLMs and SLMs can be deployed entirely on-device or within a secure network, they address privacy and compliance concerns inherent to cloud-based models, ensuring full data control as well as facilitating alignment with regulations such as GDPR or HIPAA. Some further argue that SLMs are not only sufficiently powerful but also inherently more suitable and economically advantageous as the core of agentic AI systems, proposing a modular architecture where heterogeneous dialogue is required.[12] Contemporary research further advocates for these smaller-scale language models in building agentic AI systems - models that perform specialized, repetitive tasks efficiently - highlighting their tailored fit for large-scale modular AI frameworks where smaller models complement larger,

© 2026 Terra Science and Education

DOI: 10.36838/IJHSR87.20

more general ones. However, they are not without certain drawbacks, as these models exhibit limitations in generality and robustness, particularly in complex reasoning or out-of-domain scenarios, and may be more susceptible to security vulnerabilities like jailbreak attacks.[13] Collectively, these findings imply that while MSLMs and SLMs may not necessarily replace LLMs for deep reasoning tasks, they offer a strategically powerful, accessible, and responsible alternative for many real-world applications where scale, cost, and control play a significant role.

Recent work has shown that CoT prompting can substantially improve reasoning in very large models, with reported gains across arithmetic, commonsense, and symbolic reasoning tasks.[2] These results support the idea that certain reasoning abilities are emergent, appearing once models exceed a sufficient scale. However, evidence also indicates that CoT may be ineffective, or even harmful, for smaller models, with accuracy drops of 15-30% observed on reasoning benchmarks.[14] Research on smaller and moderate-sized models has largely prioritized efficiency, domain specialization, and deployment constraints. While valuable, this focus has a significant shortcoming: it often treats reasoning capability as a secondary concern or an input for distillation, rather than systematically evaluating how in-context prompting strategies like CoT interact with these more constrained architectures.

This gap between well-established CoT gains in very large LLMs and the lack of systematic evidence for moderate-sized models frames our central question: can CoT prompting reliably enhance reasoning in MSLMs, and if so, to what extent and in which contexts?

In light of this, our work directly investigates the effectiveness of CoT prompting in moderate-sized and small language models. Specifically, we study CoT-augmented reasoning in Phi-4, Gemma-3-27b-it, and Llama 4 Maverick, evaluating their performance on competitive mathematical reasoning benchmarks relative to zero-shot baselines and internal prompting variations. This research aims to systematically establish the benefits of CoT for these resource-efficient architectures, moving beyond prior work that focuses predominantly on either very large LLMs or distilled small models. Through this analysis in multi-step, higher-level mathematics, we seek to illuminate how prompt architecture and model capacity in determining reasoning capability, thereby identifying when and how CoT prompting yields reliable improvements in models accessible to a wider range of users and applications.

Methods

In this paper, we evaluate the impact of various types of CoT prompts on the performance of MSLMs by drawing comparisons between the baseline performance (no prompting),[15] and the performance of the MSLMs when using 4 different CoT prompts to solve AMC12 competitive math questions.[16] Reasoning algorithms such as CoT are best evaluated with AMC12 math problems due to their multi-step structure, requiring chaining of operations (intermediate value calculations, applying formulas, reinterpretation), as well as their objective verifiability, since answers are binary and easy to check. AMC12 problems are a useful metric also due to their moderate difficulty and high discrimination, as the problems are neither trivial nor hyper-technical, and they challenge LLMs with stepwise logical and multi-concept problem-solving while maintaining strong discrimination across solver levels.[17] These questions offer distinct advantages over other benchmarks, serving as a good balance between the basic arithmetic of GSM8K math sets and the depth and challenge of greater difficulty benchmarks such as AIME or MATH that often make problems unsolvable by LLMs. AMC12 problems are also characterized by cognitive complexity beyond basic arithmetic, requiring parsing, deduction, and inference, skills central to deeper reasoning capabilities. Language models struggle with the precise symbol manipulation and algorithmic thinking needed for such problems, and CoT prompting helps bridge this symbolic-execution gap.

In our experiment, we use the MSLMs Gemma-3-27b-it, Llama-4-Maverick, and Phi-4, with the first two having been released 3 months prior to our experiment, and the latter being released 6 months prior, as shown in Appendix B. We classify these LLMs as MSLMs due to their model parameters, model families, and model pricing. According to IBM (2024), the families of these three models are all classified as small language models for their number of parameters used during computation. The three models also have significantly cheaper pricing than state-of-the-art LLMs, and LLMs such as Gemini 2.5 Pro have more than 8 times the price of Llama 4 Maverick, even with Llama 4 Maverick being the most expensive out of the three MSLMs. Despite being described as "lightweight,"[18] the three models have 27.4 billion, 17 billion, and 14.7 billion parameters, respectively, which all exceed the typically accepted model parameter upper bound of 14 billion when identifying SLMs.

Shown in Appendix A, we utilize 4 different CoT approaches, labeled CoT1, CoT2, CoT3, and CoT4. Both CoT1 and CoT2 are classified as one-shot CoT prompts, using a single handcrafted exemplar embedded with stepwise rationales. CoT1 possesses the longest input length in terms of both characters and words, followed by CoT2, CoT3, and CoT4. CoT1 provides a rigorous, expert-crafted solution that demonstrates the level of reasoning quality and structural clarity we aim to achieve. The remaining prompts were generated by the state-of-the-art LLM Deepseek-V3, allowing us to test whether AI-generated prompts can approximate this level of rigor while also enhancing replicability, reducing dependency on manual craftsmanship, and enabling scalable application cross-domains.

CoT1 utilized an ABA layout (introduction-example-task restated), starting with a general zero-shot prompt, then introducing an example question of great difficulty, solving it with stepwise rationales, before restating the zero-shot prompt and stating the problem to be solved. The question used for CoT1 was an AMC12 problem consisting of a combination of algebra, number theory, and combinatorics, three of the four major subjects in competitive mathematics. Geometry was not included, as multi-domain problems rarely span all four categories simultaneously, and geometric reasoning in particular

relies on diagrammatic and spatial intuition that text-based CoT prompting does not easily capture. The idea behind this prompt is for structured priming of expert reasoning, and this high-quality solution demonstrates domain-specific heuristics, logical sequencing, and mathematical formalisms. In particular, this example acts as a behavioral template, guiding the model toward producing output that mirrors the structure, clarity, and rigor expected in expert-level problem solving. The significance of this prompt is also highlighted by its alignment with the target problem distribution. The AMC12 contest is characterized by problems that require multi-step algebraic, number theoretic, combinatorial, and logical reasoning. Framing the prompt around this distribution helps ensure that the model applies reasoning strategies that are both appropriate in depth and transferable across a wide range of problems.

CoT2 provided a detailed framework for problem solving, consisting of problem decomposition, strategy selection, rigorous execution, and validation, and then applied this framework to an elementary computation math problem before stating certain critical rules and introducing the problem to be solved. This prompt emphasized expert emulation through role conditioning, as well as procedural decomposition of problem-solving. This structured prompt functions as a general-purpose reasoning blueprint for high-level mathematical problem solving. By combining role priming, procedural scaffolding, strategic heuristics, and validation mandates, it trains LLMs not only to solve problems accurately but also to explain and verify their work in a way that mirrors expert human mathematics.

Both CoT3 and CoT4 are classified as zero-shot CoT prompts, as neither introduces an example problem. CoT3 is greatly similar to CoT2 in idea, utilizing a similar 4-stage framework but being more concise and omitting the worked example. This streamlined, scaffold-based CoT prompt strikes a balance between structure and brevity, guiding LLMs through expert-level mathematical problem solving without the need for worked examples. By emphasizing decomposition, strategy selection, stepwise execution, and validation, it reinforces mathematically sound reasoning patterns while remaining general-purpose and token-efficient.

Finally, CoT4 utilized a short, general CoT prompt. This minimalistic prompt serves to guide LLMs to engage in basic Chain-of-Thought reasoning through lightweight instructions. It achieves broad applicability with minimal structure overhead. While it lacks the modular scaffolding of more elaborate prompts, its fluency, domain alignment, and efficiency make it suitable as a baseline prompt in symbolic math pipelines, especially when interpretability and prompt brevity are priorities.

These four prompts were chosen to vary along two key dimensions: exemplar inclusion and degree of structural scaffolding. CoT1, with an expert-crafted solution, represents an upper bound on the domain alignment. CoT2 and CoT3 explore the role of explicit procedural scaffolding with and without examples, respectively, while CoT4 provides a lightweight baseline for measuring the value of added structure. These dimensions are remarkable because they represent two of the most widely recognized and manipulable parameters of prompt design: whether to anchor the model with concrete demonstrations or leave it to infer strategies, and whether to provide explicit stepwise frameworks or rely on the model's internal reasoning habits. Together, this set lets us evaluate how exemplar priming and structural decomposition influence mathematical reasoning in MSLMs.

For our dataset, we use 3 years of AMC12 exam questions (2022,2023,2024), for a total of 150 questions, as two exams are released each year with 25 questions per exam. Since LLMs are probabilistic generators, each call can produce different reasoning or answers.[19,20] Thus, each question is attempted a total of 5 times to capture stochastic behavior, avoid outlier bias, and follow evaluation best practices. This helps to reflect true model variability, averaging out randomness, improving correctness via majority voting, and enhancing comparability and reliability. Therefore, we use three distinct MSLMs, a set of 5 prompts (including the baseline), an evaluation dataset of 150 questions, and 5 attempts per evaluation item, for a total of 11250 LLM calls. All data are available on GitHub upon request.

To analyze the results produced from these calls, we define four evaluation metrics: the Aggregate Attempt Accuracy Metric (AAA), Thresholded Problem-Solving Rate Metric (TSPR-2), Majority-Consensus Problem Accuracy Metric (MCPA), as well as a Challenging-Subset Aggregate Attempt Accuracy Metric (CSAAA). Together, these metrics form a hierarchy of evaluation, capturing raw potential, minimal understanding, robust reliability, and elite reasoning.

The AAA metric evaluates the total number of correct responses across all individual problem-solving attempts, calculated as $\sum_{i=1}^{n}(x_i)$ where x_i represents the number of correct responses for problem i, and n is the total number of problems. For example, a problem with 4 correct solves out of 5 would add 4 to the score. This measures overall performance across attempts, regardless of consistency, as even problems solved with low frequency earn credit.

The TSPR-2 metric applies a thresholding criterion: a problem is deemed "solved" if the model answers it correctly in at least 2 out of 5 attempts. TSPR-2 can be calculated as $\sum_{i=1}^{n} I(x_i \geq 2)$ where I represents the indicator function, evaluating to 1 when the condition is met, and 0 otherwise. For example, a question with 2 correct solves would add 1 to the score, while a question with 1 correct solve would not. This metric captures minimal reliability, identifying whether the model demonstrates some grasp of the problem-solving method, even if inconsistently, akin to recognizing early signs of understanding in student work.

MCPA is also a threshold metric, but with a stricter threshold: a problem is only deemed "solved" if the model answers it correctly in at least 3 out of 5 attempts. This can be expressed as $\sum_{i=1}^{n} I(x_i \geq 3)$. For example, a question with 3 correct solves would add 1 to the score, while a question with 2 correct solves would not. This metric captures robust mastery, requiring the model's reasoning to be dominant and repeatable across attempts, much like human grading standards that demand consistency before awarding full credit.

DOI: 10.36838/IJHSR87.20

CSAAA is a subset of the AAA metric, and it instead considers only the hardest questions in each exam. These are regarded as the "final fives", the last five questions of the AMC12, and these questions are widely recognized for their disproportionate difficulty relative to the earlier portions of the exam. These problems typically demand a significantly higher level of abstract reasoning, problem-solving creativity, and multi-step logic, distinguishing themselves from the more procedural or recall-based problems that appear earlier in the test. Since these problems often resist solution through brute-force computation or superficial pattern recognition, they serve as an effective benchmark for assessing whether a model is capable of reasoning in a structured and context-aware manner.

The following tables summarize results across these four metrics for different prompting strategies. The "Baseline" column reports raw values as fractions, where the numerator indicates the metric-observed score and the denominator indicates the maximum possible score under that metric. The subsequent columns (CoT1-CoT4) report percentage changes relative to the baseline, with positive values denoting improvement and negative values denoting deterioration. This presentation facilitates cross-metric comparison by normalizing results to relative deviations from a common reference point.

Results and Discussion

Below are the results of the Gemma-3-27b-it model when prompted with the four prompts, relative to a zero-shot baseline, as well as the baseline performance. A negative value would indicate a deterioration in performance.

Table 1: Gemma-3-27b-it evaluation dataset performance. CoT prompting leads to consistent improvements over the zero-shot baseline across all four evaluation metrics, with the strongest relative gains appearing in CoT1 and CoT4.

	Baseline	CoT1	CoT2	CoT3	CoT4
AAA	431/750	11.37%	6.26%	2.32%	9.28%
TSPR-2	95/150	14.74%	9.47%	6.32%	12.63%
MCPA	86/150	17.44%	12.79%	5.81%	6.98%
CSAAA	30/150	20.00%	20.00%	6.67%	33.33%

Below are the performances of the Llama-4-Maverick model when prompted with the four prompts, relative to a zero-shot baseline. The baseline performance is included as well.

Table 2: Llama-4-Maverick evaluation dataset performance. CoT prompting generally improves performance over the zero-shot baseline, with the strongest relative gains in CoT1 and moderate gains in CoT2.

	Baseline	CoT1	CoT2	CoT3	CoT4
AAA	426/750	7.75%	0.23%	-2.34%	-2.11%
TSPR-2	97/150	11.34%	3.09%	-4.12%	-3.09%
MCPA	87/150	1.15%	-5.75%	-2.30%	-2.30%
CSAAA	33/150	21.21%	21.21%	24.24%	12.12%

Below are the performances of the Phi-4 model when prompted with the four prompts, relative to a zero-shot baseline.

Table 3: Phi-4 evaluation dataset performance. Across the four evaluation metrics, CoT1-CoT3 generally reduce performance relative to the zero-shot baseline, indicating that these prompt styles do not transfer well to Phi-4. In contrast, CoT4 yields consistently positive gains, with especially large improvements on CSAAA.

	Baseline	CoT1	CoT2	CoT3	CoT4
AAA	340/750	0.29%	-7.94%	-7.65%	8.24%
TSPR-2	82/150	2.44%	-8.54%	-6.10%	8.54%
MCPA	69/150	-4.35%	-14.49%	-11.59%	8.70%
CSAAA	12/150	16.67%	8.33%	-25.00%	58.33%

Below is a chart of the AAA performances of the MSLMs when prompted with the prompt variants.

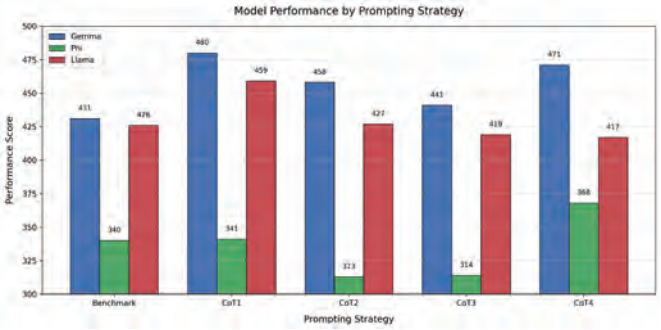

Figure 1: Model performance by prompting strategy. Note the truncated y-axis starting at a score of 300. CoT1 yields performance gains for all three models, while CoT4 produces especially large improvements for Phi-4 and strong gains for Gemma but a slight decrease for Llama relative to its baseline.

Under the zero-shot baseline, the Gemma-3-27b-it model could not produce labeled stepwise rationales. After introducing the four CoT prompts, it began doing so. This shift confirms that CoT prompting can induce reasoning behaviors not naturally present in the model's zero-shot outputs. From the results collected, shown in Table 1, it can be observed that both CoT1 and CoT4 generally led to better increases in performance than CoT2 and CoT3. These findings show that the quality and relevance of instructional structure directly influence the downstream. Despite its brevity, CoT4 resulted in a noticeable improvement, suggesting that even lightweight CoT prompts can elicit structured reasoning behavior within MSLMs. This result underscores the intrinsic latent capability of the Gemma-3-27b-it model to perform multi-step reasoning when nudged appropriately, and confirms findings from prior work on zero-shot prompting.[21]

The modest accuracy gains observed for CoT2 and especially CoT3 are a key finding. These two prompts often reduced accuracy compared with the benchmark (Tables 1-3). This degradation aligns with two well-documented failure modes in language models: hallucination and catastrophic forgetting. These phenomena highlight how mismatches in prompt structure or abstraction level can lead to degradation in reasoning quality. CoT2 presented a problem-solving framework along

with a generic arithmetic example, but this example lacked alignment with the structural and conceptual complexity of the AMC12 tasks. As a result, the model likely relied on superficial pattern matching, producing computationally valid but logically incorrect reasoning chains, a hallmark of hallucination in LLMs.[22]

An important characteristic of the benchmark performance of the Llama-4-Maverick model is the existence of labeled stepwise rationales without the aid of explicit prompting, suggesting the existence of a structured internal reasoning schema encoded during pretraining or fine-tuning, and this characteristic is shown in Appendix C. This behavior may indicate that the model has internalized procedural norms for explanation, possibly through exposure to datasets containing math problem solutions or CoT demonstrations.

This observed emergent behavior may reduce the model's responsiveness to certain types of external prompting, particularly when such prompts introduce incompatible or underspecified reasoning formats. In the case of CoT4, which used a minimal zero-shot prompt, it is likely the prompt failed to align with the model's pre-learned schema for rational generation. CoT4 was designed to elicit labeled stepwise rationales. However, this behavior was already present in the baseline results. This is supported by CoT4's noticeably worse performance when compared to CoT1, CoT2, and CoT3, shown in Table 2. While CoT3 used an AMC12-specific framework, this framework was generalized. As a result, rather than reinforcing the model's internal reasoning patterns, these prompts may have introduced prompt interference, where the model is forced to reconcile a vague or foreign framework with an already established reasoning process.[23] CoT2 likely also suffered from this interference, as the example and worked solution provided was a trivial arithmetic computation, and the framework included was also overgeneralizing. CoT2 was also much longer than CoT3 and CoT4. Although it seems intuitive that more context would improve performance, several recent studies reveal that excessively long prompts can degrade language model reasoning capabilities, even well before reaching their context window limits.[24,25] However, it can be seen that CoT1, CoT2, and CoT3 demonstrated similar degrees of improvement on the CSAAA metric, suggesting that the model potentially experienced reduced interference and improved alignment when attempting harder questions.

Despite the input length of CoT1 being significantly longer than that of the other prompts, the Llama-4-Maverick model demonstrated the best overall performance when prompted with CoT1. This is likely due to the high degree of alignment between the worked example and the evaluation dataset, as well as the domain-appropriate vocabulary.[26]

Figure 1 shows that the Phi-4 model performed notably worse overall. This suggests that minimal zero-shot prompting may align more closely with its internal capabilities than complex or structured alternatives. Consequently, specific or multi-step prompts such as CoT1, CoT2, and CoT3 may introduce format misalignment or overload for the MSLM, reducing coherence and increasing illogical or incomplete answers. This phenomenon mirrors findings in prompting sensitivity, as models with less robust conditioning capacities are more vulnerable to format-induced variability and may underperform when prompted with overly structured templates.[27] These ideas are all supported by the significant and notably better performance of the Phi-4 model when prompted with CoT4, as shown in Table 3.

Future Work

The reasoning capabilities within MSLMs can be advanced through frameworks similar to the following three, ensuring consistency, efficiency, and robustness. The first framework is blueprint guidance via LLM-generated templates, and this can ensure consistency,[28] as these blueprints provide structure for stepwise solutions, helping MSLMs systematically approach complex tasks without increasing model size.

Chain-of-Thought feeds into the blueprint process, and although CoT reveals the full reasoning chain, the blueprint framework distills it into a more abstract, MSLM-compatible scaffold, enabling consistent, structured guidance tailored to each model's capacity. Efficiency can be obtained through targeted scaffolding, providing necessary LLM hints during uncertain reasoning steps, leading to an accuracy boost with minimal overhead.[29] In this framework, the MSLM generates its own reasoning trajectory: $R = (r_1, r_2, r_3 \dots r_m)$ for a given prompt, each step r_i is evaluated. Flagged steps are replaced with alternative reasoning suggestions r_i' generated by an LLM: $r_i' \sim P_{LLM}(r_i' \mid Q, r_{<1})$, ensuring interventions are sparse and targeted, focusing on key decision points rather than full chain assistance. Finally, robust reasoning and self-verification can be promoted through a self-play framework,[30] where independent MSLMs generate and critique reasoning trajectories in tandem. Only reasoning trajectories that pass mutual agreement or validation are accepted, reducing noise and hallucination, and these methods don't rely on training data, making them scalable across tasks.

Causal inference within MSLMs and SLMs remains an emerging frontier, largely unexplored compared to its study in relatively larger LLMs, but it holds significant promise for advancing lightweight, domain-specialist AI systems. Recent surveys on causal inference and LLMs review how causal methodologies, such as causal discovery and treatment effect estimation,[31] can enrich causal inference. Potential future work includes adapting and evaluating MSLMs and SLMs on causal benchmarks such as Cladder and CRAB; developing domain-specific, smaller-scale agents that integrate structured knowledge graphs for causal discovery and treatment effect estimation; designing blueprint prompting strategies to scaffold causal reasoning in smaller models; and analyzing whether causal structure is internally represented within SLM and MSLM activations. Collectively, these directions promise to make causal reasoning accessible in lightweight, efficient models, expanding the utility of SLMs and MSLMs in high-stakes, resource-constrained, or privacy-preserving settings.

Conclusion

We observe that CoT prompting - guiding models to articulate intermediate reasoning steps - can yield notable per-

DOI: 10.36838/IJHSR87.20

formance gains in small and moderate-sized language models. Understanding a model's inherent capabilities, particularly its strengths, weaknesses, and latent biases, is crucial for crafting prompts that align well with its internal reasoning processes. Tailoring prompts effectively requires more than just clarity or examples; it relies on how compatible the prompt is with the model's built-in affordances. Capacity-aware prompt design involves diagnosing the model's strengths (e.g., numeral reasoning, understanding of text) and weaknesses (e.g., multi-step inference, nuanced instruction following) and then adjusting prompt structure accordingly. For instance, models at a smaller-scale or with lower computational affinity for complex inference may perform best with minimal zero-shot prompts (as demonstrated by the Phi-4 model, as well as, to a significantly less drastic degree, the Gemma-3-27b-it model) with short, clear instructions that avoid unnecessary examples or reasoning chains, while more capable models benefit from richer scaffolding (as demonstrated by both the Llama-4-Maverick model and the Gemma-3-27b-it model). Established benchmarks can be utilized to systematically identify domains where the model excels or struggles, and taken together, these findings advocate for prompting strategies that prioritize clarity, repeatability, and alignment with model capabilities, thereby fostering outputs that are both accurate and consistent.

Appendix

Appendix A: List of four prompts.



Appendix B: Model specification comparison, including state-of-the-art models Gemini 2.5 pro and Deepseek v3 0324.

	Gemma 27B	Phi-4	Llama 4 Maverick	Gemini 2.5 Pro	Deepseek V3 0324
Active Parameters (Billions)	27.4	14.7	17	Undisclosed	37
Openrouter Input pricing ($/M tokens)	0.09	0.06	0.15	1.25	0.25
Openrouter Output pricing ($/M tokens)	0.17	0.14	0.60	10.00	0.85
Release Date (MM/DD/YYYY)	03/12/2025	12/12/2024	04/05/2025	06/17/2025	03/24/2025

Appendix C: Llama-4-Maverick's (baseline) response to 2022 AMC12A problem 1.

```
"""## Step 1: Understand the given problem and the expression to be evaluated\nWe need to
evaluate the expression \\[3+\\frac{1}{3+\\frac{1}{3+\\frac13}}.\\]\n\n
## Step 2: Start simplifying from the innermost fraction\nFirst, simplify the innermost fraction:
$3 + \\frac{1}{3} = \\frac{9}{3} + \\frac{1}{3} = \\frac{10}{3}$.\n\n
## Step 3: Substitute the simplified innermost fraction back into the expression\nNow the
expression becomes \\[3+\\frac{1}{3+\\frac{1}{\\frac{10}{3}}} =
3+\\frac{1}{3+\\frac{3}{10}}.\\]\n\n
## Step 4: Simplify the next level of fraction\nSimplify the next innermost fraction: $3 +
\\frac{3}{10} = \\frac{30}{10} + \\frac{3}{10} = \\frac{33}{10}$.\n\n
## Step 5: Substitute this simplified fraction back into the expression\nNow the expression
becomes \\[3 + \\frac{1}{\\frac{33}{10}} = 3 + \\frac{10}{33}.\\]\n\n
## Step 6: Simplify the expression further\n$3 + \\frac{10}{33} = \\frac{99}{33} + \\frac{10}{33}
= \\frac{109}{33}$.\n\n
## Step 7: Convert the improper fraction to a mixed fraction as required\nTo convert
$\\frac{109}{33}$ to a mixed fraction, divide the numerator by the denominator: $109 \\div 33 =
3$ with a remainder of $10$. So, $\\frac{109}{33} = 3\\frac{10}{33}$.\n\nThe final answer is:
$\\boxed{3\\frac{10}{33}}$","""
```

Acknowledgments

I am deeply grateful to my advisor, Professor Siddharth Krishnan, for his invaluable mentorship, insightful feedback, and unwavering support throughout this research. His guidance has been instrumental in shaping the conceptual framework, methodology, and presentation of this work. I attest that the ideas, graphics, and writing in this paper are entirely my own.

References

1. OpenAI; Achiam, J.; Adler, S.; Agarwal, S.; Ahmad, L.; et al. GPT-4 Technical Report. *arXiv preprint 2023*, arXiv:2303.08774.
2. Wei, J.; Wang, X.; Schuurmans, D.; Bosma, M.; Ichter, B.; Xia, F.; Chi, E. H.; Le, Q. V.; Zhou, D. Chain-of-Thought Prompting Elicits Reasoning in Large Language Models. *NeurIPS 2022, 36*, 2201.11903. DOI: 10.48550/arXiv.2201.11903.
3. Ahn, J.; Verma, R.; Lou, R.; Liu, D.; Zhang, R.; Yin, W. Large Language Models for Mathematical Reasoning: Progresses and Challenges. *arXiv 2024*. DOI: 10.48550/arXiv.2402.00157.
4. Yan, J.; Wang, C.; Huang, J.; Zhang, W. Do Large Language Models Understand Logic or Just Mimic Context? *arXiv 2024*. DOI: 10.48550/arXiv.2402.12091.
5. Patil, A.; Jadon, A. Advancing Reasoning in Large Language Models: Promising Methods and Approaches. *arXiv [cs.CL] 2025*, *2502.03671v2*, *License: CC BY-SA 4.0*. DOI: 10.48550/arXiv.2502.03671.
6. Bi, Z.; Han, K.; Liu, C.; Tang, Y.; Wang, Y. Forest-of-Thought: Scaling Test-Time Compute for Enhancing LLM Reasoning. *arXiv [cs.CL] 2024*, 2412.09078. DOI: doi.org/10.48550/arXiv.2412.09078. License: CC BY-SA 4.0.
7. Yao, S.; Zhao, J.; Yu, D.; Du, N.; Shafran, I.; Narasimhan, K.; Cao, Y. ReAct: Synergizing reasoning and acting in language models. *arXiv:2210.*03629 2022. DOI: doi.org/10.48550/arXiv.2210.03629.
8. Wang, B.; Min, S.; Deng, X.; Shen, J.; Wu, Y.; Zettlemoyer, L.; Sun, H. Towards Understanding Chain-of-Thought Prompting: An Empirical Study of What Matters. *ACL 2023*.
9. Renze, M.; Guven, E. The Benefits of a Concise Chain of Thought on Problem-Solving in Large Language Models. *arXiv 2024*, 2401.05618. DOI: 10.48550/arXiv.2401.05618
10. John Johnson. Small Language Models (SLM): A Comprehensive Overview. *HuggingFace*, February 22, 2025 https://huggingface.co/blog/jjokah/small-language-model.
11. Aralimatti, R.; Shakhadri, S. A. G.; KR, K.; Angadi, K. B. Fine-Tuning Small Language Models for Domain-Specific AI: An Edge AI Perspective. *arXiv 2025*, 2503.01933. DOI: 10.48550/arXiv.2503.01933
12. Belcak, P.; Heinrich, G.; Diao, S.; Fu, Y.; Dong, X.; Muralidharan, S.; Lin, Y. C.; Molchanov, P. Small Language Models are the Future of Agentic AI. *arXiv 2025*, 2506.02153. DOI: 10.48550/arXiv.2506.02153.

13. Zhang, W.; Xu, H.; Wang, Z.; He, Z.; Zhu, Z.; Ren, K. Can Small Language Models Reliably Resist Jailbreak Attacks? A Comprehensive Evaluation. *arXiv 2025*, 2503.06519. DOI: 10.48550/arXiv.2503.06519.
14. Shim, J.; Dong Ho, S.; Kim, J. CoT Harms Performance of Rather Smaller Language Models. *Proceedings of the International Conference on Industrial Engineering and Operations Management (1st World Congress)* 2024, 504-508. DOI: 10.46254/WC01.20240169.
15. Radford, A.; Wu, J.; Child, R.; Luan, D.; Amodei, D.; Sutskever, I. Language Models Are Unsupervised Multitask Learners. *OpenAI blog 2019*
16. Mathematical Association of America. American Mathematics Competitions. MAA Website. https://maa.org/student-programs/amc/ (accessed 2025-07-24).
17. Zhang, J.; Zhao, Y.; Zhang, L.; Hu, J.; Luan, X.; Xu, Z.; Yang, F. Psychometric-Based Evaluation for Theorem Proving with Large Language Models. *arXiv 2025*, abs/2502.00855. DOI: 10.48550/arXiv.2502.00855.
18. Google DeepMind. Gemma 3 model card. https://huggingface.co/google/gemma-3-27b-it (accessed 2025-06-30).
19. Atil, B.; Aykent, S.; Chittams, A.; Fu, L.; Passonneau, R. J.; Radcliffe, E.; Rajagopal, G. R.; Sloan, A.; Tudrej, T.; Ture, F.; Wu, Z.; Xu, L.; Baldwin, B. Non-Determinism of "Deterministic" LLM Settings. *arXiv 2024*, 2408.04667. DOI: 10.48550/arXiv.2408.04667.
20. Ahn, J.; Yin, W. Prompt-Reverse Inconsistency: LLM Self-Inconsistency Beyond Generative Randomness and Prompt Paraphrasing. *arXiv 2025*, 2504.01282. DOI: 10.48550/arXiv.2504.01282.
21. Kojima, T.; Gu, S. S.; Reid, M.; Matsuo, Y.; Iwasawa, Y. Large Language Models Are Zero-Shot Reasoners. *arXiv 2022*, 2205.11916. DOI: 10.48550/arXiv.2205.11916.
22. Ji, Z.; Yu, T.; Xu, Y.; Lee, N.; Ishii, E.; Fung, P. Towards Mitigating Hallucination in Large Language Models via Self-Reflection. Findings of the Association for Computational Linguistics: *EMNLP 2023* 2023, Findings, 1827–1843. DOI: 10.18653/v1/2023.findings-emnlp.123.
23. Shi, F.; Chen, X.; Misra, K.; Scales, N.; Dohan, D.; Chi, E. H.; Schärli, N.; Zhou, D. Large Language Models Can Be Easily Distracted by Irrelevant Context. *Proceedings of the 40th International Conference on Machine Learning* 2023, 202, 31210-31227
24. Levy, M.; Jacoby, A.; Goldberg, Y. Same Task, More Tokens: the Impact of Input Length on the Reasoning Performance of Large Language Models. Proceedings of the Annual Meeting of the Association for Computational Linguistics (ACL 2024), Long Papers 2024, *1 (Long Papers)*, 15339–15353. DOI: 10.18653/v1/2024.acl-long.818.
25. Zhang, Z.; Li, J.; Lan, Y.; Wang, X.; Wang, H. An Empirical Study on Prompt Compression for Large Language Models. *Building Trust Workshop at ICLR 2025*, 2025. DOI: 10.48550/arXiv.2505.00019.
26. Schreiter, D. Prompt Engineering: How Prompt Vocabulary Affects Domain Knowledge. *arXiv 2025*, 2505.17037. DOI: 10.48550/arXiv.2505.17037.
27. Cao, B.; Cai, D.; Zhang, Z.; Zou, Y.; Lam, W. On the Worst Prompt Performance of Large Language Models. *arXiv 2024*, 2406.10248. DOI: 10.48550/arXiv.2406.10248.
28. Han, D.; Xia, M.; Madrigal Diaz, D.; Kessler, S.; Mallick, A.; Zhang, X.; Garcia, M. D. C. H.; Xu, J.; Rühle, V.; Rajmohan, S. Enhancing Reasoning Capabilities of Small Language Models with Blueprints and Prompt Template Search. *arXiv 2025*, 2506.08669. DOI: 10.48550/arXiv.2506.08669.
29. Kim, Y.; Yi, E.; Kim, M.; Yun, S. Y.; Kim, T. Guiding Reasoning in Small Language Models with LLM Assistance. *arXiv 2025*, 2504.09923. DOI: 10.48550/arXiv.2504.09923.
30. Qi, Z.; Ma, M.; Xu, J.; Zhang, L. L.; Yang, F.; Yang, M. Mutual Reasoning Makes Smaller LLMs Stronger Problem-Solvers. *arXiv 2024*, 2408.06195. DOI: 10.48550/arXiv.2408.06195.
31. Liu, X.; Xu, P.; Wu, J.; Yuan, J.; Yang, Y.; Zhou, Y.; Liu, F.; Guan, T.; Wang, H.; Yu, T.; McAuley, J.; Ai, W.; Huang, F. Large Language Models and Causal Inference in Collaboration: A Comprehensive Survey. *arXiv 2024*, 2403.09606. DOI: 10.48550/arXiv.2403.09606.

Author

Eric is currently a high school student in the United States. He is very passionate about both artificial intelligence and competitive mathematics, and has a strong background in competitive math, having qualified for the USAMO in 2025, and USAJMO in both 2023 and 2024.

DOI: 10.36838/IJHSR87.20

IJHSR
ijhighschoolresearch.org
REVIEW ARTICLE

Digital Environment's Potential to Modulate Altered Decision-Making Pathways and Processes in Autism Spectrum Disorder

Daniel D. Jackson

Procter R. Hug High School, 3530 Sullivan Lane, Sparks, Nevada, 89431, USA; danieldjackson08@gmail.com
Mentor: Jorge Avila, Bre Calhoun

ABSTRACT: Autism spectrum disorder (ASD) is characterized by atypical cognition and behavioral patterns, including atypical decision-making, risk processing, and moral reasoning. The digital age is expanding, and so are its impacts, especially on individuals with ASD. Research suggests that digital environments can alter the expression of genes and the connectivity of brain regions associated with decision-making tasks in individuals with ASD. This limited review highlights some of the potential of digital environments to act as external modulators that could either intensify or mitigate the atypical decision-making patterns in ASD by influencing the genetic and neural pathways involved in decision-making. This paper reviews decision-making, ASD, and digital environments from a neurogenetic and epigenetic perspective. Understanding connections between digital environments and biological mechanisms behind decision-making in individuals with ASD can uncover new directions for therapy, education, and technological intervention for neurodivergent individuals.

KEYWORDS: Cellular and Molecular Biology, Genetics, Neuroscience, Autism Spectrum Disorder, Decision-Making, Prefrontal Cortex, Digital Environment.

Introduction

The digital world is rapidly expanding, and so is its integration into our everyday lives. This increasingly virtual, fast-paced, and cognitively demanding environment has raised the importance of understanding how digital environments impact human cognition, specifically decision-making. This is especially important for neurodivergent populations like individuals with autism spectrum disorder (ASD), a neurological disorder characterized by its effects on communication, learning, and behavior.[1] There is an ample literature base regarding the neurogenetic pathways underlying the typical decision-making process and how digital environments alter behavior,[2,3] and similarly, ample information exists regarding the decision-making susceptibilities of people with ASD.[4–6] Still, there is a lack of knowledge on how digital environments specifically influence these neurogenetic pathways to modulate decision-making in individuals with ASD. Understanding how digital environments interact with underlying biological mechanisms of decision-making in individuals with ASD is ripe for exploration.

Decision-making involves the interaction of cognitive, emotional, and reward-based mechanisms.[7] Research has shown that individuals with ASD differ in their decision-making process from neurotypical individuals.[8] In a small study of 78 adults, individuals with autism spectrum conditions frequently experienced several problems in decision-making and were more likely to avoid decisions.[9] These difficulties may be exacerbated by the unpredictability of social situations and the fact that individuals with ASD struggle with social cue processing.[8] This is further illustrated by ASD individuals' association with emotional signals having less impact upon their decision-making capabilities.[5] In another example, the decisions of neurotypical and neurodivergent individuals differed depending on the type of decision and the context of the situation. For instance, individuals with ASD, compared to neurotypical peers, were less averse to ambiguity in gain situations and more risk-averse in loss contexts, and they showed reduced sensitivity changes in different situations.[4] In this context, gain situations involve positive outcomes, while loss scenarios are negative contexts involving adverse consequences.

While many genes are involved with decision-making pathways, this review's focus examines catechol-o-methyltransferase (*COMT*), dopamine receptors D2 and D4 (*DRD2* and *DRD4*), and serotonin transporter solute carrier family 6 member 4(*SLC6A4*). Variations in these genes have been linked to ASD and other neurodevelopmental disorders. The expression of these genes plays a role in the functioning of the prefrontal cortex (PFC), a brain region involved with higher-order executive functions (including planning, judgment, and flexible thinking).[10] This highlights the PFC's role in decision-making.[11] Exploring these genes and these PFC pathways provides new insight into the decision-making process and how it can be modified.

Digital environments and their increasing pervasiveness create novel cognitive conditions that normalize rapid information processing, immediate rewards, consistent and constant stimulus, and desensitization to content.[12] These environments have the potential to influence reward sensitivity, attention allocation, and emotional regulation.[3] These functions are already heavily altered in individuals with ASD, lending plausibility to the notion that digital landscapes modulate certain decision-making tendencies in individuals with ASD.[2] Moreover, ASD individuals are especially susceptible to increased media use due to the highly appealing nature of digital devices.[13]

© 2026 Terra Science and Education

DOI: 10.36838/IJHSR87.27

People spend a significant amount of time immersed in digital technology, such as VR headsets and video games. Individuals with ASD, compared with neurotypical peers, demonstrate neurogenetic and neuroanatomical differences in decision-making pathways.[8,9] Examining the interaction of the digital environment with neurogenetic and neuroanatomical pathways increases the understanding of technology's impact on cognitive development and its impact on neurotypical and neurodivergent populations. In particular, it raises the question: how do digital environments influence the *COMT, DRD2, DRD4*, and *SLC6A4* genes and the prefrontal cortex in individuals with autism spectrum disorder?

This paper explores the possibility of digital environments modulating changes, neurogenetically or epigenetically, leading to further atypical alterations in the PFC of individuals with ASD. These alterations could further differentiate the decision-making capabilities of people with ASD. Future research could examine how these differences can be altered through exposure to digital environments. Understanding the interaction of digital environments and the underlying pathways in decision-making can provide new insight into the decision-making process of individuals with ASD and others with neurodevelopmental disorders. These perspectives offer profound implications for future therapy of ASD.

Neurogenetic pathways underlying decision-making:

Decision-making can be defined as the process of evaluating available information to consider potential outcomes and selecting the outcome that most closely aligns with a person's goal. Decisions, big or small, are made every day. This review looks into aspects of decision-making, namely cognitive control, risk evaluation, and reward processing of individuals with ASD, and now considers some genetic influences. Understanding typical decision-making helps with differentiating atypical decision-making, providing additional insight into ASD and how digital environments may influence associated mechanisms.

The prefrontal cortex (PFC) is the most forward (anterior) brain region, and it plays a significant role in several processes. The brain matures from the back to the front; thus, the PFC does not fully develop until early adulthood, around age twenty-five.[14] The PFC plays a central role in decision-making by controlling short-term behavior in pursuit of a long-term goal. Additionally, the PFC is involved in other executive functions, including working memory, planning, judgment, and flexible thinking.[15] These are complex cognitive functions, so the PFC is unlikely to be the sole brain region responsible for them; nevertheless, the PFC has a critical role. Furthermore, damage to the PFC can cause people to jump to conclusions and inhibit their ability to consider alternative possibilities.11 Studying digital media's connection with this brain region has strong potential for understanding how decision-making is modulated in ASD.

The *COMT* gene creates the COMT enzyme, which is crucial to the breakdown of dopamine and influences cognitive, executive, memory, and attentional functions.[16] DRD2 and DRD4 influence reward processing and risk evaluation. Variations in the density of DRD2 and DRD4 influence dopamine levels, influencing impulsivity.[17] Another study found a correlation between a polymorphism and poor executive functioning.[18] A different study found a lack of conclusive evidence that DRD variations hinder executive functions in a financial risk-taking setting.[19] Further study is required to examine these differences and add to the scarce literature base. The *SLC6A4* gene regulates serotonin reuptake, influencing emotional regulation and impulse control, two functions critical to decision-making. It is important to note that these are not the only genes and processes involved in decision-making. Genes such as the *BDNF*,[20] *DARPP-32*, and *5-HT2A* include associations with general decision-making.[21]

Let's look at particular details. The *COMT* gene influences the decision-making pathways in the brain by regulating dopamine levels in the prefrontal cortex.[22] Dopamine influences decision-making through dopaminergic signaling between the PFC and other brain regions, allowing for goal-oriented behavior.[22] A polymorphism is two or more common genes or DNA sequences within individuals. The *COMT* gene has a Val158Met polymorphism, meaning there is a substitution of a guanine with an adenine base at codon 158, which causes the amino acid to become a methionine (Met) instead of a valine (Val).[16] Studies have shown that individuals possessing the Met/Met version of this polymorphism made worse decisions than individuals with the Val/Val variant.[16] This polymorphism also correlated with worse emotional decision-making.[20]

Two other genes involved in dopamine regulation are the dopamine D2 and dopamine D4 receptors (*DRD2* and *DRD4*). The *DRD2* gene controls the density of D2 receptors in the PFC, and people with lower D2-receptor density tend to make impulsive decisions, to have reduced reward anticipation, and to be susceptible to addictions.[23] This suggests that the *DRD2* gene influences decision-making by increasing a preference for instant gratification. The *DRD4* gene's influence on dopamine contributes to risk-taking, novelty-seeking, addictive behavior, and impulsivity.[17] A common polymorphism in this gene is the 7-repeat allele of the exon 3 variable number tandem repeats (VNTR) alleles. This polymorphism is believed to influence dopamine transmission, decreasing the performance of executive functions by increasing impulsive actions.

Serotonin is another neurotransmitter that impacts decision-making. The *SLC6A4* gene (5-HTT) facilitates serotonin reuptake, the transportation of serotonin from synaptic spaces into presynaptic neurons. Serotonin is associated with decision-making, particularly learning from negative outcomes and positive reward signals, facilitating dopamine reward processing, and influencing attentional capacity.[21] A common genetic variation is the 5-HTTLPR polymorphism with a short (S) allele in the region. This polymorphism is associated with increased emotional reactivity and a heightened response to negative stimuli.[24] This association appears to amplify risk aversion and create more negative reactions to a decision due to increased fear.

Together, *COMT, DRD2, DRD4,* and *SLC6A4* genes influence decision-making through their modulation of the neurotransmitters dopamine and serotonin in the PFC. These

genes significantly impact risk evaluation, reward sensitivity, impulsivity, and emotional regulation. I believe that a combination of these genes, and possibly others, has a significant influence on decision-making capabilities. Examination of these genetic mechanisms helps us grasp how the PFC regulates decision-making and how individuals with ASD experience deviations in these pathways. Understanding the neurogenetic pathways behind decision-making helps us explore the paper's purpose by allowing us to understand differences in function caused by ASD and points to the importance of researching how digital environments' interaction may change these pathways.

Neural and Genetic Pathways in Decision-Making Altered by ASD:

Autism spectrum disorder (ASD) is known to affect brain development and cognitive processes of impacted individuals from an early age, leading to differences and difficulties in learning, communication, and behavior.[25,26] These neurogenetic deviations in decision-making are shaped by irregular gene expression and atypical patterns of neural connectivity. Understanding these deviations helps us to comprehend the cognitive characteristics of individuals with ASD. This helps attribute results to digital environments and removes some potential confounding variables.

Individuals with ASD have abnormal dopamine transmission and activity in the PFC. The structure and the function of decision-making pathways are often disrupted. Parts of the brain communicate with each other inefficiently, impeding the integration of information and reducing intra-cortical connectivity.[26] This was further examined and supported by functional magnetic resonance imaging.[27] Reward-circuitry differences are also noticed in individuals with ASD.[25] Such atypical activation and connectivity in the PFC during decision-making tasks contribute to challenges in thinking flexibly and evaluating consequences. Acknowledging this atypical interaction helps when evaluating the digital landscape's impact on decision-making outcomes.

Given the decreased interconnectivity in the PFC of individuals with ASD, some changes in dopamine regulation, such as those affected by the *COMT, DRD2*, and *DRD4* genes, can enhance decision-making. Let's look at these studies of the *COMT* gene. Two studies reveal no significant difference between individuals with ASD and control groups for the Val/Val, Met/Val, and Met/Met genotypes.[28,29] The first study examined the relationship of the genotypes with other neurodevelopmental disorders, including anxiety and tics,[28] while the other study investigated hyperactivity.[29] They found no significant associations between individuals with ASD and the Val158Met polymorphism. However, the second study discovered that the association with hyperactivity and impulsivity was higher in the Val/Val genotype.[29] This finding suggests the possibility of certain genotypes in the *COMT* gene correlating with alterations in decision-making for individuals with ASD. Therefore, this is an important genetic mechanism to consider while examining how digital environments affect ASD.

One study of *DRD2* genes found that the gene correlated with susceptibility to ASD behaviors in affected male families and with the possibility of predicting ASD in families.[30] Another study found that individuals at high risk of developing ASD and who possessed *DRD4* and *DRD2* genotypes associated with less efficient dopaminergic functioning experienced more ASD behavior.[31] Since results varied, there is no conclusive evidence that the *DRD2* and *DRD4* genes are risk factors for ASD. However, this calls for further study. A meta-analysis of the 5-HTTLPR polymorphism of the SLC6A4 gene showed that the polymorphism does not have a statistically significant effect on ASD risk.[32] Multiple studies in the meta-analysis did find a correlation, but the studies lacked enough consistency to support causation. Thus, the *DRD* and *SLC6A4* genes are important genes to consider when studying how digital landscapes could influence decision-making in individuals with ASD.

COMT, DRD2, DRD4, and *SLC6A4* all appear plausibly related to decision-making mechanisms because of their effect on the PFC through dopamine and serotonin signaling. Mixed results fail to provide genotypic evidence tying these genes directly and consistently to ASD. The influence of these genes on decision-making lies mainly in their impact on behavior within individuals with ASD. Further research might explore the connection between these genes and ASD and their possible impacts on genetic circuits. This section provides a baseline for the decision-making effects in ASD populations, enabling the results of how decision-making is altered to be attributed to digital environments.

Epigenetic Regulation of ASD:

Epigenetics is the study of how molecular factors, such as behavior and environment, influence genetic activity without altering the DNA sequence.[33] While genetic polymorphisms in *COMT, DRD2, DRD4,* and *SLC6A4* genes have the potential to shape neurotransmitter signaling and decision-making and require further research to discover a consistent link with ASD, epigenetics has demonstrated a more coherent connection with ASD. Therefore, epigenetic changes provide a possible explanation for how environmental exposures can influence the neurogenetic mechanisms behind ASD risk, symptoms, and decision-making.

DNA methylation is a commonly used epigenetic marker. DNA methylation occurs when a methyl group attaches to the cytosine of a CpG dinucleotide.[34] This alters gene expression without changing the DNA sequence.[33] Numerous studies have found that dysregulation of DNA methylation has a strong relationship with ASD and other neurological disorders.[33–36] "Therefore, epigenetic alterations may significantly affect the function of autism-related genes," and such alterations show that the PFC is one of the brain regions most susceptible to environmental influences.[35] Furthermore, emerging evidence indicates that mild internet use is correlated with alterations in DNA methylation of *OXTR, DAT*, and other genes.[37] This highlights the importance of utilizing epigenetics to understand how digital environments regulate genes like *COMT, DRD*, and *SLC6A4*.

DOI: 10.36838/IJHSR87.27

Another common epigenetic biomarker is histone modifications. There are two types of modifications: acetylation and methylation. Acetylation occurs when the nucleosome dissolves, releasing genes that alter DNA composition. Histone tail methylation occurs when the nucleosomes tighten, inactivating the gene, preventing DNA from being altered.[36] Either way, histone modifications change the availability of DNA. Individuals with ASD showed an increased rate in cis-regulatory elements, an irregular connection between genes and ion channels, and reduced acetylation.[36] Thus, histone modifications serve as a biomarker for ASD. Research on how digital environments influence histone modifications remains limited, but such work could offer valuable insight into how digital landscapes shape decision-making genes.

These two processes show that dysregulation of histone acetylation and DNA methylation in genes associated with synaptic plasticity and neuronal differentiation is linked with ASD. This suggests that epigenetic regulation is important in understanding the environment's influence on genetic predisposition in individuals with ASD. Many of these studies focused on perinatal time periods, so future studies could explore the impact of the environment in later developing years after birth. Additionally, future research might examine changes in these biomarkers in decision-making genes for individuals with ASD. Epigenetic changes in ASD highlight how environmental factors can influence neurogenetic pathways, providing insight into atypical decision-making differences caused by digital environments.

Digital Environments' Influence on Decision-Making & ASD:

Digital environments (including video games, virtual reality, and social media) create unique experiences of sensory, cognitive, and social stimuli that influence neural mechanisms involved in decision-making. Addictive digital environments such as social media and video games have been associated with reduced activity in the prefrontal cortex.[3] This leads to addictive behaviors through the release of dopamine, activating the brain's reward system. Additionally, people "who frequently engage in media multitasking exhibited reduced reward self-control, leading to impulsive decision-making."[3] While digital environments can provide people with access to information, allowing for informed decisions, they can create cognitive overload, impairing decision-making skills.[3] Additionally, digital marketing has been shown to alter decision-making by creating cognitive biases through the integration of tailored options.[38] These cognitive biases can also be created through recommender systems, which prompt consumers to purchase items based on nudging mechanisms.[12] Lastly, digital environments have normalized automation, diminished attentional capabilities, promoted new biases, altered perception, and reduced cognitive abilities.[2] This information signifies just how important understanding digital environments is for not only ASD individuals but also the general population. Digital environments' ability to influence decisions signifies how important understanding this variable is for decision-making capabilities in ASD.

In addition to digital environments influencing decision-making, they have been associated with causing atypical neurodevelopment and impacting behaviors in individuals with ASD. Excessive screen time at a young age is correlated with developmental and behavioral problems, including the onset of ASD and other neurodevelopmental disorders.[39] Additionally, early digital media exposure was shown to create atypical sensory processing similar to that of autistic individuals.[40] Due to individuals with ASD's unique sensory characteristics, it is plausible that they are at increased risk of problematic media use and the implicated negative impacts.[13] This highlights how crucial understanding digital environments is for youth and ASD individuals.

On the other hand, digital environments are increasingly being tested for interventive methods, specifically in ASD samples. Serious games, games focused primarily on an educational function, show significant potential in positively impacting social skills in ASD.[41] While other mental processes aren't tested, serious games have promising implications for enhancing other cognitive outcomes, especially when considering how other executive functions influence social interactions. A small sample test of VR systems found a correlation between planning and social skills and associated the VR with improved social skills.[42] Furthermore, a meta-analysis suggested VR improves cognitive functions.[43] However, the analysis noted that the number of available studies was limited, and VR creates new problems with affordability, accessibility, and other important considerations. Another analysis found digital health interventions have optimistic results for all individuals with ASD.[44]

An alternative method being tested is applied behavioral analysis (ABA). Other treatments include "diets and vitamins, floor time, holding, medication, sensory integration, speech and music therapy, special education, and visual schedules."[45] These treatments lack conclusive evidence supporting their effectiveness in treating ASD. The meta-analysis of ABA did find associative outcomes between the therapy method and ASD symptoms. However, the effects were correlated with socialization and communication abilities, and there were no significant differences in adaptive behavior, cognition, or other ASD behaviors.[45] This illustrates the need for future study to show a significant connection between current ASD treatments and executive functions like decision-making. Additionally, literature could examine combining digital interventions with current therapy.

Overall, digital environments impair decision-making pathways by overloading cognitive processes and exacerbating conditions such as impulsivity. These environments are also associated with neurodevelopmental conditions and symptoms. However, these environments, implemented in interventive measures, show promising results in reducing ASD symptoms, especially in social contexts. Alternative methods for treating ASD symptoms lack associations with alleviating decision-making hindrances like impulsivity. Overall, future research is needed to understand how digital environments impact the *COMT, DRD2, DRD4*, and *SLC6A4* genes in neurotypical and neurodivergent populations. This research would

also provide new insights into how decision-making is affected and help create effective interventions.

Conclusion

This paper underscores the possibility that the interaction of ASD-linked genetic and neural variations with digital environments reshapes mechanisms of decision-making. Research is currently limited. This review exposes a) the need for understanding how digital environments impact the cognitive abilities of individuals with neurodevelopmental disorders, b) the possibility of utilizing digital tools to enhance and ease the experiences of these individuals, and c) the possibility of therapeutic methods. These are especially important concerns due to the heightened risk factors and susceptibility of individuals with ASD, in the context of digital landscapes, to addiction.

Future research could explore how these new ubiquitous environments modulate dopaminergic and serotonergic genes. Focusing on how digital environments impact pathways/processes of decision-making in development is crucial for understanding their effects on individuals.[46] Studies could also review the neurogenetic mechanisms underlying the interaction between ASD development and vulnerabilities to certain media. Future research would provide a more comprehensive understanding of the variations in the decision-making of individuals with ASD. Current literature associating digital interventions with decision-making is scarce. Furthermore, the potential for the combination of digital environments with current ASD treatment provides a novel avenue of study. Ultimately, leveraging digital environments to modulate decision-making in ASD could transform both research and therapy by bridging molecular, neural, and behavioral insight.[13]

Acknowledgments

Thank you to my mentors, Dr. Jorge Avila and Bre Calhoun. I would also like to thank my dad for supporting me.

References

1. Autism Spectrum Disorder - National Institute of Mental Health (NIMH). https://www.nimh.nih.gov/health/publications/autism-spectrum-disorder (accessed 2025-07-30).
2. Kirjakovski, A. Rethinking Perception and Cognition in the Digital Environment. Front. Cogn. **2023**, 2. https://doi.org/10.3389/fcogn.2023.1266404.
3. Shanmugasundaram, M.; Tamilarasu, A. The Impact of Digital Technology, Social Media, and Artificial Intelligence on Cognitive Functions: A Review. Front. Cogn. **2023**, 2. https://doi.org/10.3389/fcogn.2023.1203077.
4. Fujino, J.; Tei, S.; Hashimoto, R.; Itahashi, T.; Ohta, H.; Kanai, C.; Okada, R.; Kubota, M.; Nakamura, M.; Kato, N. Attitudes toward Risk and Ambiguity in Patients with Autism Spectrum Disorder. Mol. Autism **2017**, 8 (1), 45.
5. Shah, P.; Catmur, C.; Bird, G. Emotional Decision-Making in Autism Spectrum Disorder: The Roles of Interoception and Alexithymia. Mol. Autism **2016**, 7 (1), 43.
6. van der Plas, E.; Mason, D.; Happé, F. Decision-Making in Autism: A Narrative Review. Autism **2023**, 27 (6), 1532–1546. https://doi.org/10.1177/13623613221148010.
7. Crivelli, D.; Acconito, C.; Balconi, M. Emotional and Cognitive "Route" in Decision-Making Process: The Relationship between Executive Functions, Psychophysiological Correlates, Decisional Styles, and Personality. Brain Sci. **2024**, 14 (7), 734. https://doi.org/10.3390/brainsci14070734.
8. Robic, S.; Sonié, S.; Fonlupt, P.; Henaff, M.-A.; Touil, N.; Coricelli, G.; Mattout, J.; Schmitz, C. Decision-Making in a Changing World: A Study in Autism Spectrum Disorders. J. Autism Dev. Disord. **2015**, 45 (6), 1603–1613.
9. Luke, L.; Clare, I. C.; Ring, H.; Redley, M.; Watson, P. Decision-Making Difficulties Experienced by Adults with Autism Spectrum Conditions. Autism **2012**, 16 (6), 612–621.
10. Kennerley, S. W.; Walton, M. E. Decision Making and Reward in Frontal Cortex. Behav. Neurosci. **2011**, 125 (3), 297–317. https://doi.org/10.1037/a0023575.
11. Funahashi, S. Prefrontal Contribution to Decision-Making under Free-Choice Conditions. Front. Neurosci. **2017**, 11. https://doi.org/10.3389/fnins.2017.00431.
12. Jesse, M.; Jannach, D. Digital Nudging with Recommender Systems: Survey and Future Directions. Comput. Hum. Behav. Rep. **2021**, 3, 100052. https://doi.org/10.1016/j.chbr.2020.100052.
13. Lane, R.; Radesky, J. Digital Media and Autism Spectrum Disorders: Review of Evidence, Theoretical Concerns, and Opportunities for Intervention. J. Dev. Behav. Pediatr. JDBP **2019**, 40 (5), 364–368. https://doi.org/10.1097/DBP.0000000000000664.
14. Seemiller, L. R.; Ünsal, H. S.; Xie, Y.; Hossain, M. S.; Tuttle, K.; Johnson-Dendy, B.; McDonald, E. P.; Drew, P. J.; Zhang, N.; Crowley, N. A. Adolescent Alcohol Consumption Alters Sex-Specific Behaviors Associated with Prefrontal Functional Connectivity in Mice. bioRxiv **2025**, 2025.06.05.658112. https://doi.org/10.1101/2025.06.05.658112.
15. Miller, E. K.; Cohen, J. D. An Integrative Theory of Prefrontal Cortex Function. Annu. Rev. Neurosci. **2001**, 24 (Volume 24, 2001), 167–202. https://doi.org/10.1146/annurev.neuro.24.1.167.
16. Liu, D.; Schwieter, J. W.; Liu, W.; Mu, L.; Liu, H. The COMT Gene Modulates the Relationship between Bilingual Adaptation in Executive Function and Decision-Making: An EEG Study. Cogn. Neurodyn. **2023**, 17 (4), 893–907. https://doi.org/10.1007/s11571-022-09867-2.
17. Eisenberg, D. T.; MacKillop, J.; Modi, M.; Beauchemin, J.; Dang, D.; Lisman, S. A.; Lum, J. K.; Wilson, D. S. Examining Impulsivity as an Endophenotype Using a Behavioral Approach: A DRD2 TaqI A and DRD4 48-Bp VNTR Association Study. Behav. Brain Funct. **2007**, 3 (1), 2. https://doi.org/10.1186/1744-9081-3-2.
18. Ariza, M.; Garolera, M.; Jurado, M. A.; Garcia-Garcia, I.; Hernan, I.; Sánchez-Garre, C.; Vernet-Vernet, M.; Sender-Palacios, M. J.; Marques-Iturria, I.; Pueyo, R.; Segura, B.; Narberhaus, A. Dopamine Genes (DRD2/ANKK1-TaqA1 and DRD4-7R) and Executive Function: Their Interaction with Obesity. PLOS ONE **2012**, 7 (7), e41482. https://doi.org/10.1371/journal.pone.0041482.
19. Muda, R.; Kicia, M.; Michalak-Wojnowska, M.; Ginszt, M.; Filip, A.; Gawda, P.; Majcher, P. The Dopamine Receptor D4 Gene (DRD4) and Financial Risk-Taking: Stimulating and Instrumental Risk-Taking Propensity and Motivation to Engage in Investment Activity. Front. Behav. Neurosci. **2018**, 12. https://doi.org/10.3389/fnbeh.2018.00034.
20. Kang, J. I.; Namkoong, K.; Ha, R. Y.; Jhung, K.; Kim, Y. T.; Kim, S. J. Influence of BDNF and COMT Polymorphisms on Emotional Decision Making. Neuropharmacology **2010**, 58 (7), 1109–1113. https://doi.org/10.1016/j.neuropharm.2010.02.001.
21. Rogers, R. D. The Roles of Dopamine and Serotonin in Decision Making: Evidence from Pharmacological Experiments in Humans. Neuropsychopharmacology , 36 (1), 114–132. https://doi.org/10.1038/npp.2010.165.

DOI: 10.36838/IJHSR87.27

22. Wallace, D. L.; Aarts, E.; d'Oleire Uquillas, F.; Dang, L. C.; Greer, S. M.; Jagust, W. J.; D'Esposito, M. Genotype Status of the Dopamine-Related Catechol-O-Methyltransferase (COMT) Gene Corresponds with Desirability of "Unhealthy" Foods. Appetite **2015**, 92, 74–80. https://doi.org/10.1016/j.appet.2015.05.004.
23. Lee, B.; London, E. D.; Poldrack, R. A.; Farahi, J.; Nacca, A.; Monterosso, J. R.; Mumford, J. A.; Bokarius, A. V.; Dahlbom, M.; Mukherjee, J.; Bilder, R. M.; Brody, A. L.; Mandelkern, M. A. Striatal Dopamine D2/D3 Receptor Availability Is Reduced in Methamphetamine Dependence and Is Linked to Impulsivity. J. Neurosci. **2009**, 29 (47), 14734–14740. https://doi.org/10.1523/JNEUROSCI.3765-09.2009.
24. Munafò, M. R.; Brown, S. M.; Hariri, A. R. Serotonin Transporter (5-HTTLPR) Genotype and Amygdala Activation: A Meta-Analysis. Biol. Psychiatry **2008**, 63 (9), 852–857. https://doi.org/10.1016/j.biopsych.2007.08.016.
25. Dichter, G. S.; Felder, J. N.; Green, S. R.; Rittenberg, A. M.; Sasson, N. J.; Bodfish, J. W. Reward Circuitry Function in Autism Spectrum Disorders. Soc. Cogn. Affect. Neurosci. **2012**, 7 (2), 160–172. https://doi.org/10.1093/scan/nsq095.
26. Leisman, G.; Melillo, R.; Melillo, T. Prefrontal Functional Connectivities in Autism Spectrum Disorders: A Connectopathic Disorder Affecting Movement, Interoception, and Cognition. Brain Res. Bull. **2023**, 198, 65–76. https://doi.org/10.1016/j.brainresbull.2023.04.004.
27. Just, M. A.; Cherkassky, V. L.; Keller, T. A.; Kana, R. K.; Minshew, N. J. Functional and Anatomical Cortical Underconnectivity in Autism: Evidence from an fMRI Study of an Executive Function Task and Corpus Callosum Morphometry. Cereb. Cortex N. Y. N 1991 **2007**, 17 (4), 951–961. https://doi.org/10.1093/cercor/bhl006.
28. Gadow, K. D.; Roohi, J.; DeVincent, C. J.; Kirsch, S.; Hatchwell, E. Association of COMT (Val158Met) and BDNF (Val66Met) Gene Polymorphisms with Anxiety, ADHD, and Tics in Children with Autism Spectrum Disorder. J. Autism Dev. Disord. **2009**, 39 (11), 1542–1551. https://doi.org/10.1007/s10803-009-0794-4.
29. Karam, R. A.; Rezk, N. A.; Abdelrahman, H. M.; Hassan, T. H.; Mohammad, D.; Hashim, H. M.; Fattah, N. R. A. A. Catechol-O-Methyltransferase Val158Met Polymorphism and Hyperactivity Symptoms in Egyptian Children with Autism Spectrum Disorder. Res. Dev. Disabil. **2013**, 34 (7), 2092–2097. https://doi.org/10.1016/j.ridd.2013.04.002.
30. Hettinger, J. A.; Liu, X.; Hudson, M. L.; Lee, A.; Cohen, I. L.; Michaelis, R. C.; Schwartz, C. E.; Lewis, S. M.; Holden, J. J. DRD2 and PPP1R1B (DARPP-32) Polymorphisms Independently Confer Increased Risk for Autism Spectrum Disorders and Additively Predict Affected Status in Male-Only Affected Sib-Pair Families. Behav. Brain Funct. BBF **2012**, 8, 19. https://doi.org/10.1186/1744-9081-8-19.
31. Gangi, D. N.; Messinger, D. S.; Martin, E. R.; Cuccaro, M. L. Dopaminergic Variants in Siblings at High Risk for Autism: Associations With Initiating Joint Attention. Autism Res. Off. J. Int. Soc. Autism Res. **2016**, 9 (11), 1142–1150. https://doi.org/10.1002/aur.1623.
32. Wang, H.; Yin, F.; Gao, J.; Fan, X. Association Between 5-HTTLPR Polymorphism and the Risk of Autism: A Meta-Analysis Based on Case-Control Studies. Front. Psychiatry **2019**, 10, 51. https://doi.org/10.3389/fpsyt.2019.00051.
33. Loke, Y. J.; Hannan, A. J.; Craig, J. M. The Role of Epigenetic Change in Autism Spectrum Disorders. Front. Neurol. **2015**, 6, 107. https://doi.org/10.3389/fneur.2015.00107.
34. Tremblay, M. W.; Jiang, Y. DNA Methylation and Susceptibility to Autism Spectrum Disorder. Annu. Rev. Med. **2019**, 70, 151–166. https://doi.org/10.1146/annurev-med-120417-091431.
35. Nardone, S.; Elliott, E. The Interaction between the Immune System and Epigenetics in the Etiology of Autism Spectrum Disorders. Front. Neurosci. **2016**, 10, 329. https://doi.org/10.3389/fnins.2016.00329.
36. Oztenekecioglu, B.; Mavis, M.; Osum, M.; Kalkan, R. Genetic and Epigenetic Alterations in Autism Spectrum Disorder. Glob. Med. Genet. **2021**, 8 (4), 144–148. https://doi.org/10.1055/s-0041-1735540.
37. Annunzi, E.; Cannito, L.; Bellia, F.; Mercante, F.; Vismara, M.; Benatti, B.; Di Domenico, A.; Palumbo, R.; Adriani, W.; Dell'Osso, B.; D'Addario, C. Mild Internet Use Is Associated with Epigenetic Alterations of Key Neurotransmission Genes in Salivary DNA of Young University Students. Sci. Rep. **2023**, 13, 22192. https://doi.org/10.1038/s41598-023-49492-5.
38. Sharma, P.; Ueno, A.; Dennis, C.; Turan, C. P. Emerging Digital Technologies and Consumer Decision-Making in Retail Sector: Towards an Integrative Conceptual Framework. Comput. Hum. Behav. **2023**, 148, 107913. https://doi.org/10.1016/j.chb.2023.107913.
39. Qu, G.; Hu, W.; Meng, J.; Wang, X.; Su, W.; Liu, H.; Ma, S.; Sun, C.; Huang, C.; Lowe, S.; Sun, Y. Association between Screen Time and Developmental and Behavioral Problems among Children in the United States: Evidence from 2018 to 2020 NSCH. J. Psychiatr. Res. **2023**, 161, 140–149. https://doi.org/10.1016/j.jpsychires.2023.03.014.
40. Heffler, K. F.; Acharya, B.; Subedi, K.; Bennett, D. S. Early-Life Digital Media Experiences and Development of Atypical Sensory Processing. JAMA Pediatr. **2024**, 178 (3), 266–273. https://doi.org/10.1001/jamapediatrics.2023.5923.
41. Carneiro, T.; Carvalho, A.; Frota, S.; Filipe, M. G. Serious Games for Developing Social Skills in Children and Adolescents with Autism Spectrum Disorder: A Systematic Review. Healthcare **2024**, 12 (5), 508. https://doi.org/10.3390/healthcare12050508.
42. Kourtesis, P.; Kouklari, E.-C.; Roussos, P.; Mantas, V.; Papanikolaou, K.; Skaloumbakas, C.; Pehlivanidis, A. Virtual Reality Training of Social Skills in Adults with Autism Spectrum Disorder: An Examination of Acceptability, Usability, User Experience, Social Skills, and Executive Functions. Behav. Sci. **2023**, 13 (4), 336. https://doi.org/10.3390/bs13040336.
43. Mittal, P.; Bhadania, M.; Tondak, N.; Ajmera, P.; Yadav, S.; Kukreti, A.; Kalra, S.; Ajmera, P. Effect of Immersive Virtual Reality-Based Training on Cognitive, Social, and Emotional Skills in Children and Adolescents with Autism Spectrum Disorder: A Meta-Analysis of Randomized Controlled Trials. Res. Dev. Disabil. **2024**, 151, 104771. https://doi.org/10.1016/j.ridd.2024.104771.
44. Wang, T.; Ma, Y.; Du, X.; Li, C.; Peng, Z.; Wang, Y.; Zhou, H. Digital Interventions for Autism Spectrum Disorders: A Systematic Review and Meta-analysis. Pediatr. Investig. **2024**, 8 (3), 224–236. https://doi.org/10.1002/ped4.12417.
45. Yu, Q.; Li, E.; Li, L.; Liang, W. Efficacy of Interventions Based on Applied Behavior Analysis for Autism Spectrum Disorder: A Meta-Analysis. Psychiatry Investig. **2020**, 17 (5), 432–443. https://doi.org/10.30773/pi.2019.0229.
46. Kucker, S. C. Processes and Pathways in Development via Digital Media: Examples from Word Learning. Infant Behav. Dev. **2021**, 63, 101559. https://doi.org/10.1016/j.infbeh.2021.101559.

Author

Daniel Jackson is currently a senior in high school. He is interested in majoring in biology or public health. His interests in this research topic stem from his personal experiences. He hopes to go to medical school in the future.

DOI: 10.36838/IJHSR87.27

IJHSR
ijhighschoolresearch.org
RESEARCH ARTICLE

The Economics of AI in the Music Industry: Impacts, Risks, and Opportunities

Aashi Singh

Gems Modern Academy, Nad Al Sheba-3, Dubai, UAE; aashimsingh01@gmail.com

ABSTRACT: The global music industry, valued at over $28 billion in 2023, is undergoing a significant transformation driven by advancements in artificial intelligence (AI). From composition and production to distribution and consumption, AI is altering the economic and creative structure of the industry. Although AI offers novel creative possibilities and operational efficiencies, it also disrupts traditional revenue streams, threatens the livelihoods of music industry professionals, and raises ethical concerns around authenticity, ownership, and inequality. This paper examines the impact of advancements in AI across the music industry value chain through the lens of foundational economic concepts (e.g., creative destruction, substitution vs. complementarity, market efficiency). It also uses the Technology Acceptance Model (TAM), which explains why people choose to adopt a new technology, focusing on perceived usefulness, ease of use, risks, and external influences. Using industry data and published interviews with music professionals, the study shows a paradox: AI makes music easier to create and access, but it also disrupts jobs and redistributes value across the industry. The paper highlights the complex interplay between innovation and disruption in the music ecosystem, underscoring the need for balanced and responsible adaptation by stakeholders.

KEYWORDS: Behavioral and Social Sciences, Sociology and Social Psychology, Artificial Intelligence, Music Industry, Technology Acceptance Model.

Introduction

Music has long been both a form of artistic expression and a profession. Traditionally, music production required human creativity, technical skill, and expensive studio resources. Over the last two decades, digital technologies have revolutionized music distribution and monetization, first through streaming platforms and now through Artificial Intelligence (AI) driven tools, on both the production and consumption sides. The rise of Generative AI (Gen AI) has accelerated this shift, introducing tools capable of composing, producing, and even recommending music.

However, alongside these advancements come growing concerns: Revenues in music are projected to decline by 24% by 2028.[1] Studies indicate that a majority of musicians fear declining job security, and the erosion of fair compensation: 82% of over 4000 songwriters and composers surveyed in Australia and New Zealand fear AI threatens their livelihoods while in the UK, 68% of artists report job insecurity and declining value for their work.[2,3] Beyond financial risks, musicians worry about reduced creative freedom as algorithm-driven platforms are increasingly shaping both production and consumption of music.[4]

Despite these challenges, AI is also creating new pathways for creativity, lowering production costs, expanding access, and opening global markets to independent creators.[5,6] Audiences are also divided – some express skepticism toward AI-generated music,[7] while others are increasingly accepting of its presence in their listening habits.[8] In this evolving landscape, musicians and industry stakeholders are compelled to re-evaluate their roles, negotiating a delicate balance between embracing innovation and safeguarding human artistry.[9]

Against this background, the objective of this study is to explore how advancements in AI affect the music industry's value chain stages, such as creation, production, distribution, consumption, and monetization, and the resulting economic risks and opportunities for its stakeholders. This includes studying the impact on variables like efficiency, production costs, labor market change, market structure, consumer preferences, ownership issues, etc. The study uses an exploratory method examining the perceptions of music industry stakeholders related to the above parameters. It uses primarily two frameworks –AI Ripple Effect Waves (AIREW) and the Technology Acceptance Model (TAM). The analysis suggests that AI's impact on music is shaped by both economic structures and human responses.

Literature Review:

The global music industry has grown rapidly over the past decade and continues to evolve at a fast pace. According to the International Federation of the Phonographic Industry (IFPI), the recorded music market reached a valuation of over $28 billion in 2023, driven largely by the expansion of digital streaming services. Streaming now accounts for more than 80% of global recorded music revenues, reshaping both how audiences consume music and how the industry earns revenue.[10] This shift has enabled broader global reach, allowing artists from diverse regions to access international audiences.[11] It has also introduced challenges related to revenue distribution, with concerns about low payouts per stream impacting artist earnings.[12]

The economics of creative industries is considered unique because it involves the production and distribution of an intan-

© 2026 Terra Science and Education

DOI: 10.36838/IJHSR87.34

gible cultural good where creativity and innovation are central inputs.[13] Music, like other creative products, is an "experience good" whose value depends heavily on subjective consumer preferences and cultural context,[14] influencing pricing and investment decisions.[15] The music industry has high fixed costs and low marginal costs,[16] relies on project-based employment, and often experiences income volatility and 'superstar effects,' where a few artists capture most of the earnings.[17] Its value chain includes artists, record labels, publishers, distributors, and increasingly, tech platforms and intermediaries that control digital rights and data.[18] The rise of direct-to-fan models and independent music production has further diversified the market structure, reducing the dominance of major labels.[19] Studies have emphasized how these dynamics shape wage structures, bargaining power, and career trajectories.[20]

Generative AI (Gen AI), a form of machine learning that creates new content from training data,[21] represents the latest disruption in the industry. In music, AI tools are now integrated across the value chain: the creative process, production, and post-production, including distribution and marketing.[22] For composition, tools such as AIVA, Suno AI, and Amper Music assist musicians by generating melodies, harmonies, or soundscapes. For example, Orchidea provides orchestration suggestions, while Soundraw enables royalty-free compositions tailored to user preferences. Beyond creation, AI supports technical functions such as voice cloning, vocal synthesis, audio mixing and mastering, audio restoration, and transcription.[23] AI also enhances productivity by reducing the time required for editing and refining content.[24] Pre-production applications leverage machine learning algorithms to analyze musical databases, recommend new melodic structures, and inspire artists.[25] In the post-production and promotional stages, AI-driven algorithms can design marketing campaigns, test engagement strategies in real time, and optimize content for virality, enabling artists to interact more with audiences.[23]

Adoption of AI in the music industry is accelerating. A GEMA/SACEM survey revealed that 35% of respondents have used AI in music creation. The study also found that 63% of creators expect Gen AI to be most influential in composition, text writing, and creative processes, with additional applications in recording, editing, mixing, mastering, and promotional content. Genre-specific patterns are also emerging: AI adoption is highest in electronic music (54%), hip-hop (53%), advertising music (52%), and audio-visual work (46%). [26,27] However, 64% of respondents believed that the risks of AI outweigh its opportunities, compared to just 11% who saw it more positively. According to *Goldman Sachs' Music in the Air* (2024), [28] AI-generated music could account for as much as 25% of recorded songs by 2030, with tens of thousands already being uploaded to streaming platforms every week. Major record labels, including Universal Music Group and Warner Music Group, are lobbying for stronger regulations, while reports from the International Federation of the Phonographic Industry (IFPI) highlight declines in live session work where AI orchestration tools are widely used.

Independent composers, especially those working in advertising and gaming, have also reported fee reductions of 30–50% as AI substitutes for human-created content.

Empirical findings on AI's economic impact remain mixed. Li observed that moderate AI involvement in music creation correlated with higher profitability, suggesting that hybrid human-AI collaboration could be optimal.[29] However, he found no clear causal link. Makridis reported no negative effects of exposure to large language models on artists, such as a decrease in income or user engagement, contradicting much of the existing literature. [30] AI tools lower costs and make it possible for independent musicians to create professional-quality music without needing big budgets. This makes the music world more diverse, but it also means tougher competition and lower average income for many musicians.[31] In terms of jobs, AI often takes over technical tasks like mixing and mastering, but still relies on humans for creative decisions.[32] CISAC (2025) predicts that AI could cut musicians' income by nearly 25% by 2028.[1] As AI tools allow more people to make their own music, the need for professional singers, songwriters, and producers could go down. Even for those who stay in the business, the availability of AI tools lowers market rates, which threatens job security.[33] Schumpeter's idea of "creative destruction" explains how AI creates new opportunities but also replaces older ways of working.[34] This also matches Autor's polarization thesis that technology divides the job market into roles that are replaced and roles that are enhanced [31]. These changes reflect what Brynjolfsson and McAfee call the "Second Machine Age," when new technology changes how we work and produce.[35] These divergent findings highlight the need for further research into how AI affects artistic livelihoods and creative outcomes.

On the consumer side, AI-driven recommendation systems on platforms like Spotify and Apple Music reduce search costs and improve market efficiency.[36] However, these same algorithms may create "algorithmic lock-in," amplifying visibility for a limited group of artists while marginalizing others.[37] Audience behavior adds complexity to this study. Research shows that people often prefer music made by humans because they value the effort, uniqueness, and emotion behind it.[38] If fans find out that a song was partly or fully made with AI, they might feel less connected, spend less money, and become less loyal.[39]

Taken together, existing research illustrates both the opportunities and challenges of AI adoption in music. While AI lowers barriers to entry in the music industry and enriches creative potential, it disrupts established labor markets, challenges cultural authenticity, and introduces new questions of fairness in distribution. Table 1 maps and summarizes these dynamics using foundational economic concepts.

Table 1: This table shows that the impact of AI on the music industry value chain can be mapped to fundamental economic concepts.

Concept	AI Impact
Supply & Demand	AI reduces production costs, expands music supply, and lowers prices. Greater competition, however, compresses producer revenues.[37]
Opportunity Cost	Automation of routine tasks shifts opportunity costs, enabling artists to focus on creative, higher-value activities.[32]
Creative Destruction	AI disrupts traditional production and distribution, challenging incumbents and reshaping industry structures. [34,36];
Market Efficiency	Recommendation algorithms cut search costs and match music with listeners better, but the risk of "algorithmic lock-in," concentrating visibility among a few.[37]
Substitution & Complementarity	AI substitutes some technical jobs (e.g., sound engineering) while complementing creative roles, enhancing productivity and artistic output. [31,32].
Ethics & Responsibility	Raises issues of IP rights, cultural homogenization, and fair income distribution, highlighting the need for policy frameworks that balance innovation with equity.[11]

Despite the richness of existing research, a significant gap remains: There are only a few studies that have examined AI's impact across the entire music value chain or have captured the lived experiences of diverse industry actors. Addressing this gap, this study positions AI as an external technological shock that is reconfiguring the music industry. Specifically, it investigates how AI affects the different stages of the value chain and how industry professionals perceive the economic risks, opportunities, and challenges it presents.

Accordingly, this study seeks to answer the following research questions:

1. How is artificial intelligence affecting the music industry value chain stages?

2. How are industry professionals perceiving the economic risks, opportunities, and challenges posed by the advancement of AI and the usage of AI tools in music?

Conceptual Framework:

This study uses a conceptual lens that integrates economic theory with models of technology adoption. Two complementary frameworks guide the analysis: the AI Ripple Effect Waves (AIREW) Framework and the Technology Acceptance Model (TAM).

The AIREW Framework is an author-developed analytical framework to examine the impact of AI adoption across the music industry value chain. It is constructed through a synthesis of existing literature and conceptualizes AI as an '*external technological shock*' that triggers successive waves of transformation throughout the music industry. These waves ripple through different nodes of the value chain, reshaping costs, labor markets, consumer behavior, and market structures. By explicitly mapping AI's effects to foundational economic theories discussed in the literature review, the framework provides both an analytical structure for research and allows to bridge theory and observed practice.

As illustrated in Figure 1, the AIREW framework is composed of four analytical layers:

1. External Shock: AI-enabled tools are introducing new capabilities in the industry.

2. Value Chain Stages: The industry is organized into five stages: Creation, Production, Distribution, Consumption, and Monetization. These stages guided the organization of qualitative data.

3. Codes: Derived from existing literature, these codes are clustered observations around five economic categories: *Production Costs & Efficiency, Labor Market, Business models, Consumer Preferences, Intellectual Property & Ethics, and Ownership.*

4. Ripple Mapping: This captures how disruptions at one stage cascade into subsequent stages, creating cumulative effects across the value chain.

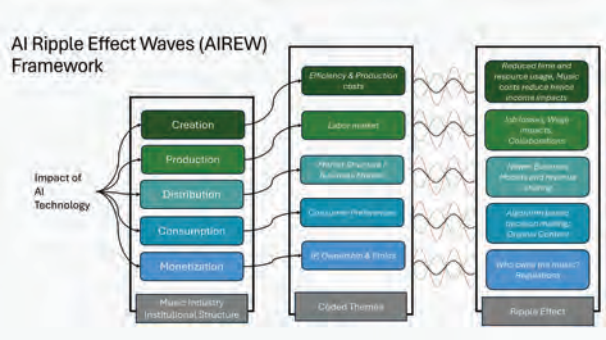

Figure 1: The AI Ripple Effect Waves (AIREW) framework represents AI as an external technological shock that impacts the music industry. It is shown as a ripple cascading to the value chain stages and creating cumulative effects. The framework also maps these changes to economic theories.

Complementing AIREW, the TAM Framework was applied to interpret the subjective perceptions of industry professionals. This is a framework explaining how users accept and use new technology, primarily based on a few factors like: Perceived Usefulness (does it help me?) and Perceived Ease of Use (is it easy to use?), External influences, and Risk perception.[40-42] This was conceptualized by Fred Davis, and since then, widely used in the technology space with improvisation. The model was particularly relevant for understanding divergent responses to AI adoption. Within this study, TAM was used to explore three key strands: (1) how artists and professionals perceive the utility of AI in their work, (2) how accessible they find these tools, and (3) how external factors such as industry norms, regulations, or ethical concerns shape their perceptions and adoption behaviors.

Taken together, AIREW and TAM form a dual-lens framework to look at AI's impact on music. AIREW sees AI as a powerful economic shock that spreads through the entire industry, while TAM focuses on how individuals such as musicians, producers, and listeners react to and adopt these changes. This integration ensures that both macro-level economic effects and micro-level adoption dynamics are accounted for, offering a holistic understanding of AI's impact on the music industry.

■ Research Method

This study adopts a qualitative empirical design using secondary data sources, with the goal of capturing how artificial intelligence (AI) is perceived and experienced by different stakeholders in the music industry. The focus is on understanding both structural economic effects across the value chain using the AIREW Framework and subjective adoption dynamics using the TAM model.

Data Collection:

The study used a purposive sampling method with an objective of capturing voices from diverse professionals of the music

DOI: 10.36838/IJHSR87.34

industry, and not limiting it to only musicians and directors. Further, it specifically identified interviews addressing the topic of the use of AI and its role in music creation, production, distribution, or consumption, allowing the study to capture informed perspectives on implication of AI adoption. These interviews are from recent years, ensuring the relevance to the current context and use of the use of Gen AI as an emerging technology.

Data used in this study were sourced from publicly available interviews of musicians, producers, sound engineers, composers, executives, and other professionals involved in the music ecosystem. Sources included trade journals, podcasts, YouTube interviews, industry reports, and social media commentary (Twitter/X, LinkedIn).

As the study extracted interviews published in English, data available in other languages could not be included. This limits the representation of samples from non-English-speaking regions of the world. Further, the industry has several stakeholders. While efforts were made to identify interviews from a diverse set of stakeholders, the lack of sufficient published information posed a limitation in representing the voices of a diverse set of stakeholders. Table 2 provides an overview of the selected interviewees and sources.

Table 2: The table provides an overview of the data sample used in this research, depicting the variety of data across roles and geographies.

Artist	Role	Geography	Source of Information
Curtiss King	Music Producer, Rapper, and Author	USA	Forbes Blog/Article - How musicians are fashioning creativity with AI[43]
Kyle Lehning	Music industry executive and producer	USA	Streaming platform [YouTube] (CBS Sunday morning news, 2024)[44,45]
Taryn Southern	YouTube Star, Singer, and Content Creator	USA	Forbes Article - How this YouTube star used AI for her new album [46]
Ross Malcom Boyd	Musician, Audio Engineer, Educator	Canada	[Video Interview]. YouTube. (2024, December 6th). *I asked 4 professional musicians about AI.* Channel: Sour_Vector [47]
Ryan Drew	Musician, AI Practitioner	Canada	
Ian Tomes	Jazz Guitarist	Canada	
Dr. Andrew Zinck	Doctor of Musicology, Composer, Teacher	Canada	
Holly Herndon	Musician, AI Practitioner	USA, Germany	Barry, R. (2024, February 8). *Holly Herndon's revolutionary AI music. Jacobin.*[48]
Armando Young	Electronic music producer	USA	Article in The Verge – Man Made Machine Music (2019).
Pharrell Williams	Singer and songwriter	USA	In Paris AI Action Summit .[49]
Golnar Khosrowshahi	CEO, Music Publishing Company	Iran, USA	The Journal [Hans Zimmer Isn't Scared of AI]. Wall Street Journal (Interview, 2024).[50]
Hans Zimmer	Music Composer and Producer	Germany	
Grimes	Singer, Songwriter, Record Producer	Canada	Grimes: Music, AI, and the Future of Humanity | Lex Fridman Podcast #281.[51] Twitter & Fortune Article – Feel Free 2023.[52]
A.R. Rahman	Musical Composer and Record Producer	India	Economic Times News Article, April 2025.[53]

Data Preparation and Analysis:

Where necessary, interviews were transcribed and cleaned to ensure consistency. The transcripts were then prepared for analysis using a deductive coding process. Codes were informed by literature-derived categories such as production efficiency, labor market effects, business model shifts, intellectual property, and consumer behavior. This was followed by thematic analysis, identifying recurring patterns and relationships across the data.

■ Results Findings

Table 3 presents the analysis of qualitative data. The analysis has been grouped into recurring themes, which highlight both the opportunities and challenges created by AI (Table 3), which are then further linked to relevant economic concepts and theories (Table 4). This approach offers a clear understanding of how AI adoption affects production processes, labor markets, intellectual property, and ethical issues in the music industry.

Table 3: The table presents the qualitative data analysis in the form of codes and themes. The analysis was done through an inductive coding process guided by the AIREW framework (Fig 1).

Excerpt	Codes	Themes
AI provides multiple possibilities but requires humans to arrange and finalize the song structure to fit the lyrics (Southern) *I think AI and Music will become another great tool and a great helper to help me figure out how to express emotion or give people an experience. (Hans Zimmer)*	Complementarity: AI supports, not replaces, human creativity	Human-AI collaboration
When you're at the start of your career, you usually lack in several key areas: 1)Resources, 2)Expertise, and 3)An industry network. AI, in the case of music creation, actually solves for all three. (Southern)	Lower marginal costs → greater market access, increased competition	Reduced barriers to entry
I think AI and Music will become another great tool and a great helper to help me figure out how to express emotion or give people an experience. (Hans Zimmer) *"AI helps when you're stuck, speeds up production, and avoids burnout." – Curtiss King.*	AI as a supportive creative tool Innovation reduces costs and opportunity costs.	Efficiency Gains
I don't think the music industry is going to die. I think it is going to follow a similar path that we've gone through many times in the music industry (Ross Malcolm Boyd)	Confidence in industry resilience despite technological change.	Human-AI collaboration
AI can mimic voices but lacks the emotional depth that human collaborators provide. *It's not about how it sounds, it's about how it feels, and that's not something a computer can figure out. (Kyle Lehning)* *AI, in particular, is trained on material from the past. Hans is looking to create something new (Hans Zimmer, Golnar)* *Can AI create music as good as Hans? AI conceded that it has challenges, especially about emotional depth, which is difficult to replicate without human experience.*	Emotional limitation of AI; Experience goods: human input is essential for emotional value	Limits of AI creativity
The models out there are being trained, but without any licenses or permissions. (Golnar Khosrowshahi) *We haven't yet figured out how to deal with intellectual property, and AI is like if a sample could sprout legs and run. It is recording technology 2.0, and we don't have an ethical framework. (Herndon)*	Intellectual property protection; Ethical concerns; Lack of established ethical and legal frameworks for AI in Music Institutional economics: importance of legal frameworks	Legal and ethical framework gaps
The question of whether I fear some sort of loss of employment? Personally, no. But I'm also recognizing that it is a trend that is happening, which is a disruption to the labor market. (Ryan Drew) *A lot of tracks have synthesized parts, if not the whole thing. Yeah, there'll be less, probably, studio musician work. (Ryan Drew)* *No, you're not going to have a hundred-piece orchestra. There's no budget for that. But you have a small orchestra, and then what you need to be able to do is flesh that out in your mix with your plug-ins, with your sample libraries. (Dr Andrew Zincks)*	Labor market disruption risk AI as a supportive tool; Labor market risks, Roles affected, Budget constraint driving technology adoption.	Labor market effects and creative adaptation

I see it as a tool when you are in a rut or stuck, or for budding songwriters to be able to use that as inspiration (Ross Malcolm Boyd)	AI as creative and supportive aid; Improve the artists' productivity.	Efficiency improvements
The question of whether I fear some sort of loss of employment? Personally, no. But I'm also recognizing that it is a trend that is happening, which is a disruption to the labor market. (Ryan Drew)	Fear of displacement; Labor market polarization: mid-tier jobs most vulnerable	Labor market anxiety and disruption
But that's the magic of the algorithm. Sometimes it knows your taste better than you do. That's amazing for listeners and efficient for the market, but the flip side is that it takes some of the humanity out of discovery and can influence what we listen to in hazy ways… Recommendation algorithms also have the habit of creating musical echo chambers, because they're reinforcing tastes rather than broadening them. (Armando Young) , New York-based musician	Algorithmic market shaping Hyper-personalization Algorithmic lock-in; Superstar effect	Market efficiency vs. fairness trade-offs
I think AI-generated work should instantly be in the public domain. It belongs to everybody because it was created by everybody essentially. (Ross Malcolm Boyd) *I think it's fundamentally incapable of doing any of this in a way that ensures that things like copyright, intellectual property, and bias issues are avoided. (Ian Tomes)* *We are in the music business, and our job is to advocate for IP and the protection of it, and we'll get there. (Golnar)*	Concept of communal creation; Ownership Concerns; Property rights economics: unresolved ownership tensions	IP challenges
We wouldn't use AI to write songs. AI is much more like a utility. It wouldn't replace creativity. It is no different from search engines being created. (Pharrell Williams) *When you're empowered with tools, you have to use them responsibly…You have a tool which can empower you to do things which you could never do before, or you could destroy people's lives….There should be rules, like certain things you can't do. This is also behavior in the software and digital world. (A.R Rahman)*	Ethical Use; Responsible Use Ethics and governance in technology adoption	Responsible AI adoption
I'll split 50% royalties on any successful AI-generated song that uses my voice. Same as I would with any artist I collab with. (Grimes)	Royalties sharing; evolving contracts for new realities	New economic arrangements and contracts
AI wasn't here to replace us as songwriters or producers, but to essentially assist us in being more efficient in our music-making process. I could use all the help I can to maximize my skills and time and avoid burnout. (Curtiss King)	AI reduces productivity and efficiency Opportunity cost: reallocation of time and effort	Productivity and well-being

Thematic Analysis:

The following eleven recurring themes emerged on the effect of artificial intelligence on the value chain of the music industry.

1. Human–AI collaboration: AI can assist in composition but requires human input for arrangement and emotional depth (*Southern, Zimmer*). This reflects the economic concept of complementarity, where technology supports human creative work instead of replacing it.

2. Reduced barriers to entry: AI tools give access to resources, expertise, and networks that were previously out of reach for emerging artists (*Southern*). Since these tools are easy to use, more musicians are adopting them. Economically, this represents the notion of lower marginal costs, which makes it easier for newcomers to enter the market, while also creating more competition.

3. Limits of AI creativity: Despite its technical abilities, AI struggles with emotional expression, originality, and cultural context (Lehning, Khosrowshahi). This limits the adoption of AI in areas where authenticity is highly valued. These findings support the theory of experience goods (Caves, 2000), [14] which emphasizes the importance of human input in creative industries.

4. Efficiency gains: The use of AI reduces time spent on routine tasks, offering inspiration and boosting productivity, speeds up production, and helps overcome creative blocks (*Curtiss King, Boyd*). This efficiency allows artists to focus more on creative work. This reflects technological innovation, lowering costs and increasing supply (Brynjolfsson & McAfee, 2014).35

5. Labor market effects: Session musicians and mid-tier roles face substitution, while hybrid roles emerge (Drew, Zincks). Some see AI as a threat, while others view it as a helpful tool. This illustrates polarization in labor markets (Autor, 2015),[31] where middle-tier jobs decline, but high-skill and entry-level roles remain resilient.

6. Productivity and well-being: AI can help reduce burnout by handling routine tasks and free time for creative focus (Curtiss King). This connects to opportunity cost, as AI frees up time for higher-value activities.

7. New Economic Arrangements and Contracts: AI is reshaping business models. For example, artists like Grimes have introduced royalty-sharing agreements for AI-assisted songs. These shifts reflect broader changes in the industry, where contracts evolve to meet new technological realities.

8. Market Efficiency vs. Fairness Trade-offs: Recommendation algorithms make music discovery easier but also reinforce concentration by promoting a limited number of artists (Young). This illustrates algorithmic lock-in and the superstar effect (Rosen, 1981), [17] where a few artists capture most of the attention and revenue.

9. Gaps in Legal and Ethical Frameworks: Concerns over licensing, ownership, and lack of frameworks persist in the absence of strong regulations (*Khosrowshahi, Herndon*). Weak or absent frameworks increase risk for artists and limit adoption. This highlights the importance of institutions in ensuring fair participation.

10. Intellectual Property Challenges: Debates continue over ownership of AI-generated music. Some argue for stricter protections, while others suggest placing AI works in the public domain (Boyd, Tomes). This reveals ongoing tensions related to property rights.

11. Responsible AI Adoption: Industry leaders call for balanced and ethical use of AI (Pharrell, Rahman). This highlights the role of ethics and governance in shaping technological trajectories.

Interpretation of the Findings using TAM:

To interpret the findings at a micro level, this study applies the TAM model, which focuses on three factors that influence the adoption of new technologies: perceived usefulness, perceived ease of use, and external influences.

1. Reduction in Costs and Barriers to Entry: The use of AI production tools reduces the cost of producing music in a studio, therefore making professional-level music quality more accessible to independent, small-scale musicians. These tools demonstrate the dimensions of TAM's specifically perceived usefulness (helping artists save time and money) and perceived ease of use (requiring little technical expertise). However, lower costs and easier access also result in higher competition and market saturation. This raises concerns about long-term sustainability for music artists' careers. In accordance with the TAM model, such risk perception is also a determinant of technology use.

DOI: 10.36838/IJHSR87.34

2. Labor Market Effects: The study reveals mixed perceptions, as some artists describe AI as a "*co-creator*" and others have issues like "*displacement risk*." From a TAM perspective, such inconclusive perceptions reflect different evaluations of usefulness. On one hand, AI is perceived to be capable of enhancing productivity; it is readily adopted, and on the other hand, it is perceived as a threat to employment security; adoption is resisted. Economically, these perceptions connect to the substitution-complementarity framework. Substitution occurs when AI displaces session musicians and mid-tier software engineers, but large-scale production for complex projects would still require human expertise, and thus, complementarity is observed when artists integrate AI into hybrid workflows. This creates "*skill polarization*", because while high-end and low-cost segments remain, the numbers and demand for mid-tier jobs might decline. High-profile artists can maintain their bargaining power through brand identity and revenues from live performances. Perceived ease of use also matters, as musicians who find AI tools accessible are more inclined to integrate them, while those facing technical or creative barriers may remain skeptical.

3. Consumer Behavior and Market Structure: Streaming platforms such as Spotify and Apple Music use AI-driven recommendation systems to influence the listening habits of their users, a classic example of TAM's dimension of external influences. While these systems reduce search time and help listeners discover new music, they can also lead to "algorithmic lock-in," where only a small number of artists receive most of the market visibility. Musicians think that visibility and audience engagement are shaped less by their own creative output and more heavily by algorithmic systems, and therefore market control lies with streaming companies who determine who gets discovered. This concentration of visibility can lead to unequal distribution of revenue, despite more artists participating in the market, because only certain artists benefit disproportionately from recommendation visibility (Rosen, 1981).[17] For consumers, this can result in "hyper-personalized pricing" and targeted advertising, thus changing the way revenue is distributed across the industry. However, as more content floods the market, per-stream payments may continue to decrease, which challenges artists' long-term sustainability.

4. Industrial Organization and Market Power: With AI-generated music having near-zero marginal costs, economic theory predicts downward pressure on prices. At the same time, large technology companies and streaming platforms hold significant power as they control algorithms, train data, and influence distribution channels. This reinforces existing power imbalances in the industry. TAM highlights the role of social and organizational influences that affect technology adoption. The observation that platforms hold disproportionate power introduces skepticism and perceived risk, potentially limiting broader AI acceptance.

5. Ethical and Distributional Considerations: Artists have raised ethical concerns such as "AI plagiarism" (allowing use of original work to train AI models without permission), loss of cultural authenticity, and unequal royalties. Such concerns affect not only how musicians use AI but also how an artist's audience responds to its use. Research suggests that listeners often value authenticity and human effort over AI-assisted work, which means that heavy reliance on AI could negatively impact an artist's reputation, even if the music itself is technically sound.

The findings show that AI adoption in music is not only about cost savings or efficiency. Using the TAM model, the findings explain why some artists adopt AI while others resist: those who perceive clear benefits in lowering costs or sparking creativity are more open to using it, while those who identify risks such as job loss, reduced diversity, or unfair royalties are more hesitant. Economically, this reflects the paradox of innovation: AI expands access to music creation but also disrupts traditional careers, increases inequality, and shifts power toward major platforms.

Synthesis:

Overall, the findings highlight what can be called a paradox of innovation. On one hand, the AIREW framework shows how AI, acting as an external shock, spreads through the music value chain by lowering production costs, changing labor market dynamics, and reshaping how music is distributed and consumed. On the other hand, the TAM model explains why the willingness to adopt is not uniform: artists' choices depend not only on technical benefits such as efficiency, but also on their perceptions of usefulness, potential risks, and the influence of social and cultural norms.

■ Discussions

The analysis shows that each theme can be understood through two perspectives: structural changes across the music industry value chain (AIREW) and individual adoption behaviors (TAM). Together, these lenses explain both the broad economic impact of AI and the personal decisions of artists and professionals.

- At the creation stage, AI is widely seen as useful and easy to use, helping artists collaborate and lowering barriers to entry. However, the lack of emotional authenticity limits its full acceptance, since many believe human input is still essential for creativity.
- In production and labor markets, AI introduces substitution pressures, where some jobs are replaced, the polarization of skills happens, and where mid-level roles are at risk the most. These structural effects are accompanied by individual perceptions of risk: some musicians adopt AI to improve efficiency, while others resist it due to fears of displacement.
- In distribution and consumption, Algorithms on streaming platforms make music discovery more efficient but also raise concerns related to fairness by concentrating visibility among a small group of artists. Platform policies and external influences strongly shape how artists adapt their strategies in this environment.
- On monetization and ownership, the new models of royalties and contracts, and debates about ethical use of AI, highlight the lack of clear legal and institutional

frameworks. These gaps create uncertainty, but they also drive discussions about responsibility and fairness in the industry.

To summarize, Table 4 provides a dual-lens mapping of each theme, connecting the structural effects identified through AIREW with the adoption dynamics explained by TAM, alongside relevant economic concepts.

Table 4: The table maps the themes that have emerged from the research with value chain impact as well as adoption dynamics. This shows how the effect of AI on the music industry can be understood both at the industry level and also on an individual level. The table further maps the themes with the relevant fundamental economic concepts.

S. No.	Theme	AIREW Lens (Value Chain Ripple)	TAM Lens (Adoption Dynamics)	Linked Economic Concept
1	Human–AI Collaboration in Music Creation	AI enables creative possibilities while humans finalize artistic direction	High perceived usefulness; AI seen as co-creator	Complementarity
2	Reduced Barriers to Entry & Market Access	Lower production costs; democratization of access	Ease of use & usefulness drive adoption for beginners	Lower marginal costs & market entry
3	Limits of AI Creativity & Human Input	Emotional depth & originality remain human strengths	Low usefulness & high risk perception constrain adoption	Experience goods & cultural value
4	Efficiency Gains & Creative Support	Streamlines workflows; reduces time on routine tasks	Strong perceived usefulness; higher opportunity cost of *not* adopting	Productivity & innovation
5	Labor Market Effects & Creative Adaptation	Substitutes mid-tier roles; creates hybrid workflows	Mixed perceptions: usefulness vs. risk (displacement fear)	Labor market polarization
6	Productivity & Well-being	Reduces burnout; sustains creative careers	Ease of use + usefulness → adoption for well-being	Opportunity cost & efficiency
7	New Economic Arrangements & Contracts	Emerging royalty-sharing & collaboration models	Shaped by external/ organizational influences	Industrial organization & contracts
8	Market Efficiency vs. Fairness	Music Platform Algorithms improve preference matching but reinforce concentration to few artists	External influence: Platform offering can influence consumer exposure, music taste, and artist choice	Algorithmic lock-in & superstar effect
9	Legal & Ethical Gaps	Lack of regulation on training data & ownership	High risk perception discourages adoption	Institutional economics
10	IP Challenges & Communal Creation	Proposals for public domain AI outputs	Conflicting perceptions: communal vs. private ownership	Property rights economics
11	Responsible AI Adoption	Governance structure needed in music industry ecosystem, e.g., related to norms around AI usage	The perception of society around the usage of AI in the creation of music influences their choice and hence guides adoption by the artist.	Ethics in economics & governance

Taken together, the dual-lens analysis suggests that AI's impact on music is shaped by both economic structures and human responses. This means that technological change in the music industry is never purely about innovation – it is also about how individuals, institutions, and society choose to interpret and adapt to it.

The results are consistent with studies done in other sectors also, e.g. in manufacturing sector, one of the study reported that use of AI has shown significant improvements across the value chain stages by improving processes, optimization, quality control etc., thus leading to internal competitiveness.[54] Another study reports that low skilled labor are more likely to be displaced with the deployment of AI. The same study also reports that the level of development of AI and the total amount of employment is a positive U-shaped relationship, where in the short term, the effect is dominated by the substitution effect, and in the long term, it is dominated by the creation effect.[55] In human resource-intensive industries like journalism, studies reported that AI is creating opportunities and tensions in the newsroom where it could enhance the capabilities of journalists by saving time, improving the efficiency of the news-making processes, and, therefore, improving the overall mass media industry's productivity. But there are also fears and related to ethical issues that call for control and supervision of the processes involved. [56]

By combining TAM with economic theory, this study contributes a nuanced understanding of how technological adoption in creative industries depends not only on financial benefits but also on various factors like perceived usefulness, ease of use, access, and various external factors such as social and organizational influences, alongside the risks and opportunities that come with it.

Limitations of research:

- As the research relied on published data, the researcher could not influence the framing of interview questions or context.
- Public interviews may carry biases, as participants shape responses for audiences.
- Only interviews in English were analyzed, which excludes potentially important perspectives from non-English-speaking markets.
- The music experts' purposefully sampled above are from the following regions: the US, Germany, Canada, Iran, India, and the UK. The industry experts sampled do not include many South and East Asian countries, as well as the Middle Eastern countries. Such geographical limitations limit the generalizability of the findings.
- The music industry has several stakeholders and roles. Efforts were made to identify interviews from a diverse set of stakeholders; however, the lack of sufficient published information available in English posed as a limitation towards representing the voices of all stakeholders.
- Future studies involving data from other regions and roles in the industry could potentially inform the research questions better.

■ Conclusion

Artificial intelligence is reshaping the music industry in multiple ways. It lowers production costs, alters patterns of labour demand, and transforms consumer behavior. From an economic perspective, AI makes music easier and cheaper to create, therefore opening doors for more people. But it also raises problems, such as unfair income distribution, reduced cultural variety, and the risk of large companies dominating the market.

This study provides a comprehensive examination of these changes by studying interviews and perspectives from people in the industry, using the AIREW framework, which traces how AI acts as an external shock that ripples through creation, production, distribution, consumption, and monetization stages of the music industry value chain. The TAM Framework enriched the analysis by showing that adoption patterns are not uniform and helped explain why artists and technicians

DOI: 10.36838/IJHSR87.34

decide to use (or avoid) AI, focusing on factors like usefulness, ease of use, risks, and external pressures such as market norms and policy environments. Importantly, TAM highlights how personal beliefs and social pressures affect whether AI is welcomed or resisted, connecting economic theories with the real experiences of artists.

The dual-lens analysis underscores that AI's impact on music is mediated by economic factors, perceptions, and institutions, and therefore not uniform. The findings also underscore a paradox: AI simultaneously fosters innovation and democratization while threatening cultural diversity, equitable income distribution, and professional sustainability.

Looking ahead, the long-term impact of AI on music will be shaped by regulatory responses, public attitudes toward machine-generated creativity, and the adaptive strategies of musicians and industry stakeholders. Future research should consider cross-regional studies (Comparative studies across global music markets could shed light on adoption patterns shaped by regional contexts) and include more quantitative analyses of royalty patterns, musician incomes, and whether audiences prefer human-made over AI-made music, which would give useful insights for both policy and industry. This is important to make sure AI brings innovation while also protecting fairness and cultural richness.

In the end, the real challenge for the music industry is not simply about harnessing AI's efficiency gains but also ensuring that technological adoption enhances rather than erodes the human essence of music.

Acknowledgments

The author expresses her gratitude to Prof. Dr. Iva Bimpli and Ms. Daryn Howland for their guidance and review throughout the development of this paper, as well as patiently explaining and teaching several economic concepts used in this research, and timely advising on the frameworks to explore. The support extended by the Indigo research team through the journey of research and review is deeply appreciated.

The author also expresses gratitude to her parents, who motivated her to pursue this research with dedication.

I attest that the ideas, graphics, and writing in this paper are entirely my own.

References

1. CISAC. *Annual Report 2023*; International Confederation of Societies of Authors and Composers: Paris, 2023; p 83.
2. APRA AMCOS. *Songwriter and Composer Survey 2024*; Australasian Performing Right Association and Australasian Mechanical Copyright Owners Society: Sydney, 2024.
3. Queen Mary University of London; Creative Industries Policy & Evidence Centre; Arts Council England. *AI and the Future of Creative Work: UK Artists' Report 2025*; Queen Mary University: London, 2025.
4. Bulayenko, O.; Heller, L.; Fratini, F. Algorithmic influence on music production and distribution. *Econ. Policy Rev.* 2022, 19 (3), 201–225.
5. Eiriz, V.; Leite, F. Innovation and music distribution: Digital technologies in creative work. *Creative Ind. J.* 2017, *10*(2), 146–162. https://doi.org/10.1080/17510694.2017.1282376.
6. Olayeni, T. AI tools in music production: Opportunities for emerging artists. *Int. J. Music Technol.* 2023, *12* (4), 201–215.
7. Tigre, P.; Maw, H. Audience perceptions of AI-generated songs. *J. Cult. Econ*. 2021, *45* (3), 567–589.
8. Zhou, Y.; Lee, J. Audience valuation of AI-generated creative works. *Digit. Creat. Econ. Rev.* 2024, *18* (1), 33–52.
9. Inie, N.; Falk, A.; Tanimoto, Y. Human–AI co-creation and transparency in design processes. *J. Human–AI Interact*. 2023, *5* (2), 77–95.
10. International Federation of the Phonographic Industry. *Global Music Report 2023: State of the Industry*; IFPI: London, 2023. https://www.ifpi.org/wp-content/uploads/2020/03/Global_Music_Report_2023_State_of_the_Industry.pdf (accessed Aug 20, 2025).
11. Aguiar, L.; Waldfogel, J. Platforms, promotion, and product discovery: Evidence from Spotify playlists. *NBER Working Paper*; National Bureau of Economic Research: Cambridge, MA, 2021.
12. Marshall, L. "Let's keep music special. F—Spotify": On-demand streaming and the controversy over artist royalties. *Creative Ind. J.* 2015, *8* (2), 104–118. https://doi.org/10.1080/17510694.2015.1051515.
13. Throsby, D. Modelling the cultural industries. *Int. J. Cult. Policy* 2008, *14*, 217–232.
14. Caves, R. E. *Creative Industries: Contracts Between Art and Commerce*; Harvard University Press: Cambridge, MA, 2000.
15. Hesmondhalgh, D. *The Cultural Industries*, 3rd ed.; SAGE Publications: London, 2013.
16. Towse, R. Economics of copyright in the age of AI. *J. Cult. Econ*. 2023, *47* (3), 395–415.
17. Rosen, S. The economics of superstars. *Am. Econ. Rev*. 1981, *71* (5), 845–858.
18. Wikström, P. *The Music Industry: Music in the Cloud*, 2nd ed.; Polity: Cambridge, UK, 2013.
19. Tschmuck, P. *Creativity and Innovation in the Music Industry*, 2nd ed.; Springer: New York, 2012.
20. Florida, R. *The Rise of the Creative Class: And How It's Transforming Work, Leisure, Community and Everyday Life*; Basic Books: New York, 2002.
21. Alabi, M. Generative AI and its applications in creative industries. *ResearchGate* 2024. https://www.researchgate.net/publication/382024251_Generative_AI_and_its_Applications_in_Creative_Industries(accessed Aug 20, 2025).
22. Larsen, B. C.; Narayan, J. Generative AI: A game-changer society needs to be ready for. *World Economic Forum*, January 9, 2023. https://www.weforum.org/agenda/2023/01/davos23-generative-ai-a-game-changer-industries-and-society-code-developers/ (accessed Aug 20, 2025).
23. Centre National de la Musique; BearingPoint. *AI in the Music Industry: State of Play and Prospects for the Deployment of Artificial Intelligence in the Industry and Analysis of the Anticipated Impacts on its Professions*; CNM: Paris, 2025. https://cnm.fr/wp-content/uploads/2025/06/20250617_CNM_IA_Study_EN_1.pdf (accessed Aug 20, 2025).
24. Sajjad, M.; Khan, A. Generative AI: Transforming creative industries with machine learning. *Res. Corridor J. Eng. Sci*. 2024, 2, 226–215.
25. Anantrasirichai, N.; Bull, D. Artificial intelligence and the creative industries: The future of human–machine interaction. *Int. Conf. Artif. Intell. Creat.*; Springer, 2021; pp 1–10.
26. Goldmedia. *AI and Music: Generative Artificial Intelligence in the Music Sector*; GEMA & SACEM, 2024.
27. Tencer, D. Global audio streams jumped 14% in 2024 to 4.8 trillion—With pop music the fastest-growing genre in the US. *Music Business*

Worldwide, January 21, 2025. https://www.musicbusinessworldwide.com/global-audio-streams-jumped-14-in-2024-to-4-8-trillion-as-pop-music-was-the-fastest-growing-genre-in-the-us/ (accessed Aug 20, 2025).
28. Goldman Sachs. *Music in the Air: AI and the Future of Music*; Goldman Sachs: New York, 2024.
29. Li, S. The impact of AI-driven music production software on the economics of the music industry. *Inf. Dev*. 2025, *41*(3), 957–967. https://doi.org/10.1177/02666669241312170.
30. Makridis, C. *The Impact of Generative Artificial Intelligence on Artists*; Stanford University; Institute for the Future (IFF); Univ. of Nicosia; The Gallup Organization; Arizona State University, 2025.
31. Autor, D. H. Why are there still so many jobs? The history and future of workplace automation. *J. Econ. Perspect*. 2015, *29* (3), 3–30. https://doi.org/10.1257/jep.29.3.3.
32. García, M. B. The paradox of artificial creativity: Challenges and opportunities of generative AI artistry. *Creativity Res. J*. 2024, 1–14. https://doi.org/10.1080/10400419.2024.2354622.
33. Drott, E. Fake streams, listening bots, and click farms: Counterfeiting attention in the streaming music economy. *Am. Music* 2020, *38* (2), 153–175. https://doi.org/10.5406/americanmusic.38.2.0153.
34. Schumpeter, J. A. *Capitalism, Socialism, and Democracy*; Harper & Brothers: New York, 1942.
35. Brynjolfsson, E.; McAfee, A. *The Second Machine Age: Work, Progress, and Prosperity in a Time of Brilliant Technologies*; W.W. Norton & Company: New York, 2014.
36. Jacques, S.; Flynn, M. Protecting human creativity in AI-generated music with the introduction of an AI-royalty fund. *GRUR Int*. 2024, *73* (12), 1137–1149. https://doi.org/10.1093/grurint/ikae134.
37. O'Connor, J.; Chen, J. Artificial intelligence in recommender systems. *Int. Conf. Artif. Intell. Eng. Technol*.; Springer, 2020; pp 1–10.
38. Tang, X. Intellectual property law as labor policy. *NYU L. Rev*. 2024, *100*, 62.
39. Lecamwasam, K.; Chaudhuri, T. R. Exploring listeners' perceptions of AI-generated and human-composed music for functional emotional applications. *arXiv*, June 3, 2025. https://arxiv.org/abs/2506.02856 (accessed Aug 20, 2025).
40. Davis, F. D. *A Technology Acceptance Model for Empirically Testing New End-User Information Systems: Theory and Results*; Ph.D. Dissertation, Massachusetts Institute of Technology, 1986; ProQuest Dissertations and Theses Global, Publication No. 8613430.
41. Venkatesh, V.; Davis, F. D. A theoretical extension of the technology acceptance model: Four longitudinal field studies. *Manag. Sci*. 2000, *46* (2), 186–204. https://doi.org/10.1287/mnsc.46.2.186.11926.
42. Venkatesh, V.; Thong, J. Y. L.; Xu, X. Consumer acceptance and use of information technology: Extending the unified theory of acceptance and use of technology. *MIS Q*. 2012, *36* (1), 157–178. https://doi.org/10.2307/41410412.
43. Zarczyński, A. How musicians are fashioning creativity with AI. *Forbes*. https://www.forbes.com/sites/andreazarczynski/2023/01/31/how-musicians-are-fashioning-creativity-with-ai/(accessed Aug 20, 2025).
44. YouTube. AI in music. https://youtu.be/zM2UzZ4TVGw?si=PZ-kqDQgdiyHqCB3X (accessed Aug 20, 2025).
45. Kyle's Korner. Song review: Randy Travis – Where That Came From. https://kyleskornerblog.wordpress.com/2024/05/06/song-review-randy-travis-where-that-came-from/ (accessed Aug 20, 2025).
46. Schawbel, D. Taryn Southern: How this YouTube star used AI for her new album. *Forbes*. https://www.forbes.com/sites/danschawbel/2017/09/26/taryn-southern-how-this-youtube-star-used-ai-for-her-new-album/ (accessed Aug 20, 2025).
47. YouTube. Musicians and AI. https://m.youtube.com/watch?v=U-0vqF8P-CQ4&pp=ygUNTXVzaWNpYW5zIEFJIA%3D%3D (accessed Aug 20, 2025).
48. *Jacobin*. Holly Herndon: AI and music composition. https://jacobin.com/2024/02/holly-herndon-ai-music-composition (accessed Aug 20, 2025).
49. United Nations. AI and the future of the music industry incomes. https://news.un.org/en/story/2025/02/1159996(accessed Aug 20, 2025).
50. *Wall Street Journal*. Hans Zimmer isn't scared of AI. https://www.wsj.com/video/hans-zimmer-isnt-scared-of-ai/D0434C33-6686-4831-8E79-832C2E0F9BD6 (accessed Aug 20, 2025).
51. *NME*. Grimes gives fans permission to use her voice in AI-generated songs. https://www.nme.com/news/music/grimes-gives-fans-permission-to-use-her-voice-on-songs-created-by-ai-3434810(accessed Aug 20, 2025).
52. YouTube. AI music demonstration. https://www.youtube.com/watch?v=KOwm7GUjcg8 (accessed Aug 20, 2025)
53. *Economic Times*. A.R. Rahman's views on AI in music. https://economictimes.indiatimes.com/magazines/panache/a-r-rahmans-chilling-take-on-ai-in-music-like-mixing-poison-with-oxygen/articleshow/120352403.cms?from=mdr(accessed Aug 20, 2025).
54. Gao, R. X.; Krüger, J.; Merklein, M.; Möhring, H.-C.; Váncza, J. Artificial Intelligence in Manufacturing: State of the Art, Perspectives, and Future Directions. *CIRP Ann*. 2024, *73* (2). https://doi.org/10.1016/j.cirp.2024.04.101.
55. Huo, Q.; Ruan, J.; Cui, Y. "Machine Replacement" or "Job Creation": How Does Artificial Intelligence Impact Employment Patterns in China's Manufacturing Industry? *Front. Artif. Intell*. 2024, *7*, 1337264. https://doi.org/10.3389/frai.2024.1337264.
56. Noain-Sánchez, A. Addressing the Impact of Artificial Intelligence on Journalism: The Perception of Experts, Journalists and Academics. *Communication. Society*. 2022, *35* (3), 105–121. https://doi.org/10.15581/003.35.3.105-121.

Author

Aashi Singh is a high school student at GEMS Modern Academy, Dubai, with strong academic interests in behavioral economics. Beyond academics, she is a published poet, a ballerina, and a student of music. She runs the platform Poets and Peace, providing a space for young poetic voices across the globe.

DOI: 10.36838/IJHSR87.34

IJHSR
ijhighschoolresearch.org
REVIEW ARTICLE

Genetic Factors in the Development and Diagnosis of Lymphedema and Lipedema

Aditi S. Gandhi

The Blake School, 511 Kenwood Parkway, Minneapolis, MN, 55403, USA; aditigandhi08@icloud.com

ABSTRACT: Lymphedema and Lipedema are chronic disorders that are often misdiagnosed, leading to complications ranging from infection to impaired mobility. While the genetic basis of lymphedema is well characterized, the genetic contributions to lipedema remain unclear despite clear familial hereditary patterns. This review examines current knowledge on the genetic foundations of both conditions, examining established causative genes in lymphedema and emerging evidence of heritability in lipedema. It also evaluates the role of genetic testing in diagnosis and classification. By emphasizing established findings and highlighting ongoing gaps, this review supports efforts to refine diagnosis and guide therapeutic development.

KEYWORDS: Lymphedema, Lipedema, Genetics, Inheritance, Misdiagnosis, Classification.

Introduction

Lymphedema is a chronic condition characterized by abnormal swelling that affects the arms and legs due to the failure of the lymphatic system, which is one of the important parts of the body that covers the immune system and fluid circulation (Figures 1 and 4). Lymphatic obstruction triggers chronic inflammation, leading to fibrosis and other lymphatic anomalies.[1] Symptoms commonly present swelling in the limbs, feeling heaviness or tightness in the skin, restricted range of motion, and fibrosis (pathologic thickening of the skin due to excess connective tissue) (Figure 1). Lymphedema is diagnosed clinically and based on a comprehensive evaluation and a physical examination. The diagnosis can be supported by >2 cm circumference or >200 mL volume difference between limbs.[2] Volume is measured using a tape (requires consistent technique), water displacement (accurate but unsuitable in patients with open wounds), or perometry (precise but expensive).[3] Non-invasive methods, such as tonometry and bioimpedance spectroscopy, assess tissue resistance and fibrosis.[4] Imaging methods, such as lymphoscintigraphy, ultrasound, CT, and MRI, help detect fluid accumulation and assist in diagnosis, especially when physical findings are unclear.[5]

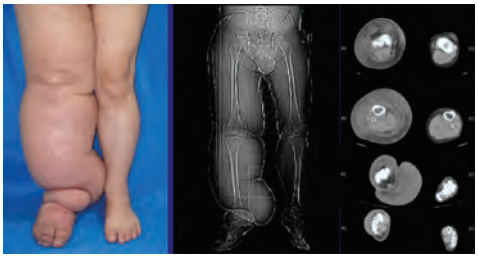

Figure 1: Clinical and radiologic features of unilateral lower-extremity lymphedema. (Left) Marked enlargement of the right leg with dorsal foot hump, papillomatosis, and deep skin folds consistent with advanced-stage lymphedema. (Middle) Coronal CT reconstruction demonstrates diffuse thickening of the subcutaneous compartment without bony abnormalities. (Right) Axial CT images at multiple levels show pronounced subcutaneous fat hypertrophy and fluid accumulation in the affected limb (R) compared with the normal contralateral side (L), with preservation of muscle architecture and absence of discrete mass lesions.

Lipedema, on the other hand, is a fat disorder causing symmetrical, painful fat buildup in mostly legs and sparing feet, but also can be seen in hips, thighs, buttocks, and sometimes upper arms. Lipedema has four distinct stages (Figure 2), each characterized by different cellular and immune characteristics. Pain, tenderness, and swelling may be prevalent in the affected areas. Lipedema diagnosis is also made clinically, but it has fewer validated tools available for confirmation. A basic evaluation consists of an assessment of familial history, manual evaluation, and a visual inspection with a focus on the known clinical features of lipedema. While both conditions rely heavily on clinical evaluation, the availability and use of diagnostic tools differ, with lymphedema having more established objective measures and imaging support than lipedema.[6] The pathophysiology of lipedema remains not fully understood but is thought to involve an interplay of genetic, hormonal, and vascular factors. Estrogen may contribute to lipedema by directly influencing fat storage through its receptors in white adipose tissue, leading to region-specific accumulation in lipedema typical areas such as the hips, legs, and buttocks (gynoid regions).[7] Because estrogen reduces fat breakdown (lipolysis) in these regions, fat gradually accumulates.[8] Additionally, vasculopathy, specifically microangiopathy damage to small blood vessels), has been observed in early stages of lipedema.[8] This may derive from a defect in the endothelial barrier function or from hypoxia (low oxygen), which impairs vascular structure.[10] Increased vascular permeability and abnormal angiogenesis (formation of new blood vessels), triggered by VEGF and other factors, can lead to fragile, leaky vessels that contribute to tissue changes and swelling seen in lipedema.[10]

© 2026 Terra Science and Education

DOI: 10.36838/IJHSR87.43

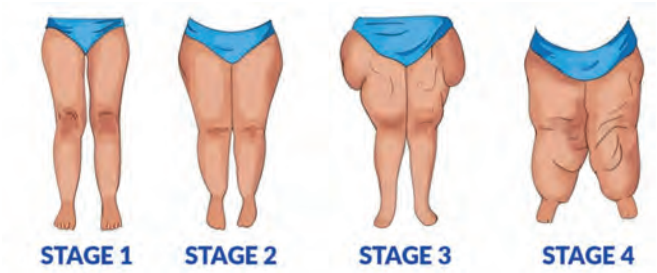

Figure 2: Stages of lipedema: In stage 1, the skin appears smooth, and the subcutaneous adipose tissue is soft and thickened, with small palpable nodules present. Stage 2 is distinguished by irregular skin texture and the occurrence of even larger skin nodules, alongside the development of interstitial fibrosis and gradual adipocyte enlargement. By stage 3, marked fat deposition results in large lobules and apparent limb abnormalities. This stage is also marked by pronounced adipocyte hypertrophy and a thick buildup of fibrous tissue. Stage 4, also known as lipo-lymphedema, includes the development of secondary lymphedema, severe edema, and dermal fibrosis.[12]

Lymphedema and lipedema are frequently misdiagnosed due to limited awareness and overlapping clinical features. Primary lymphedema (Figure 3) is rare, affecting 1 in 100,000 people, whereas secondary lymphedema affects 1 in 1,000 Americans.[13] The epidemiology of lipedema is uncertain, and the lack of data regarding the disease is a key contributor to its frequent misdiagnosis.[14] Prevalence rates vary widely, ranging from 11% to 39% among specific populations. Lipedema is frequently misdiagnosed as obesity due to overlapping clinical features. It predominantly affects women and most often occurs after pregnancy or menopause. Lipedema's specific etiology has not yet been identified, but it likely results from a combination of hormone disruptions, genetic factors, and anatomical irregularities in the lymphatic and vascular systems.[15]

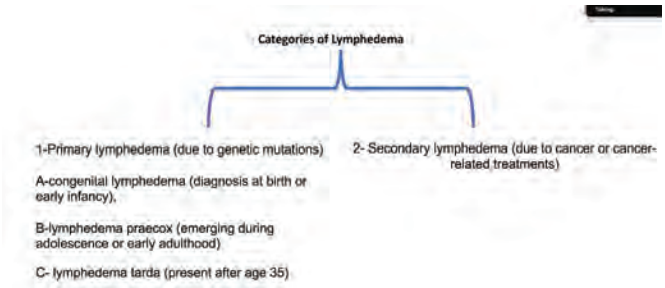

Figure 3: Categories of lymphedema: Lymphedema can be categorized into two types: primary lymphedema and secondary lymphedema.[16] Primary lymphedema is a hereditary disorder that results in deformity of the lymphatic system, caused most often by a genetic mutation.[16] While secondary lymphedema can be derived from injury or obstruction to the lymphatic system, most secondary lymphedema cases often result from cancer or cancer-related treatments. This includes surgical removal of lymph nodes, targeted radiation therapy, and medication-based treatment.[18] Primary lymphedema can be divided into three subcategories: congenital lymphedema (diagnosis at birth or early infancy), lymphedema praecox (emerging during adolescence or early adulthood), and lymphedema tarda (present after age 35).[19]

Lymphedema also has stages, and it is staged according to the increase of interstitial lymphatic fluid in the affected area, which stimulates subcutaneous fibroadipose formation. Its advancement is characterized in four stages. Stage 0 presents with clinically normal limbs, despite impaired lymphatic transport, which can be detected through imaging methods such as lymphoscintigraphy. Stage 1 is seen as early edema, which can be improved with elevation of the affected area. Stage 2 entails pitting edema, which does not improve with elevation, and stage 3 involves increased fibroadipose deposition and accompanied skin changes.[19]

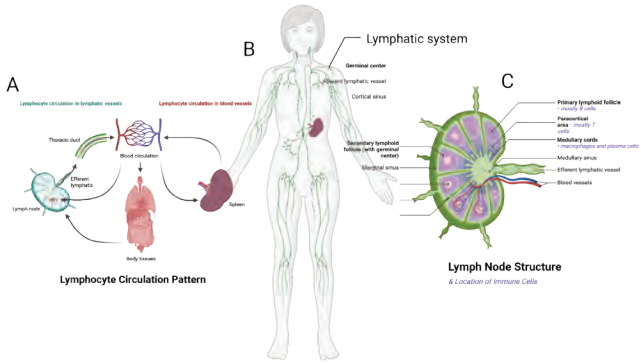

Figure 4: Overview of lymphocyte trafficking, lymphatic anatomy, and lymph node microarchitecture. (A) Schematic of lymphocyte circulation demonstrating coordinated movement between blood and lymphatic vessels. Lymphocytes enter lymph nodes through high endothelial venules (HEVs), transit through cortical and medullary regions, and exit via efferent lymphatics before returning to the bloodstream through the thoracic duct. (B) Anatomical map of the human lymphatic system, highlighting major lymphatic vessels and secondary lymphoid organs. (C) Cross-sectional structure of a lymph node showing the spatial organization of immune cell niches: B-cell–rich primary and secondary follicles, T-cell–dominant paracortex, and macrophage/plasma-cell–rich medullary cords, along with afferent/efferent lymphatic and blood vessel entry points (Figure done in Biorender).

This paper presents clinical features of lymphedema and lipedema, and describes their genetic pathways to highlight differences and different ways of diagnosis despite their similarities. It then explores the genetic and familial components of lipedema, including inheritance patterns and findings from different familial studies. Additionally, this paper integrates genetic findings across lymphedema and lipedema, uncovering shared genetic pathways and hormone-driven mechanisms that offer a new framework for understanding their overlapping features and persistent diagnosis challenges. Finally, it discusses the role of genetic testing in both conditions, including the use of next-generation sequencing in clinical practice. Understanding the genetic basis of lymphedema and advancing research into the genetics of lipedema are critical for preventing the misdiagnosis of these conditions. A confirmed genetic marker for lipedema and a broader clinical adoption of genetic panels for lymphedema are needed to prevent misdiagnosis and further complications.

Discussion

1.1. Genetics of Lymphedema:

Lymphedema can result from genetic mutations in the FLT4 gene, which codes for a protein called vascular endothelial growth factor receptor 3 (*VEGFR-3*).[21] This mutation interferes with lymphatic development and can cause swelling in both legs since birth. Most cases are inherited in an autosomal dominant pattern, but some recessive cases have been reported as well.[22] Mutations in the *VEGFR-3* reduce signaling and can lead to poorly formed lymphatic vessels.[1]

Similar symptoms can also occur from mutations in vascular endothelial growth factor receptor C (*VEGF-C*), the ligand for VEGFR-3, which can also damage lymphatic vessels.[7] Collagen and Calcium- binding EGF domain-containing protein 1 (CCBE1) and Protein Tyrosine Phosphatase Non-Receptor Type 14 (PTPN14) also influence this pathway. Their mutations can lead to more extensive lymphatic irregularities.[8] While lipedema does not have a confirmed genetic cause, it is seen to have an inheritance pattern that is not linked to a single gene. Family studies suggest a strong genetic component, with 60-80% of patients reporting a familial history. Whole-exome sequencing in families identified rare variants across many genes, but no single mutation was found consistent with all cases.[26] Instead, the results show genetic heterogeneity, where different genes contribute to the disease. Some detected genes include pro-opiomelanocortin (*POMC*), Stabilin-1 (*STAB1*), and Tenascin-X (*TNXB*). These genes are involved with connective tissue structure and fat metabolism.[21] Overall, larger population-based studies are needed to clarify the genetic basis of lipedema.

Apart from the the *VEGF-C/VEGFR-3* pathway, there are other essential pathways for lymphedema development. The PI3K/ATK pathway is important for cell proliferation and is activated by both *VEGFR-3* and *HGF/MET* signaling. Mutations in the AKT1 and PIK3CA can cause syndromic lymphatic malformations such as Proteus, CLAPO, and CLOVES syndrome, but other regulators such as *KIF11*, *PIEZO1, ARAP3, SYK, RELN*, and *SVEP1* may also contribute to the disruption of the *PI3K/AKT* pathway, leading to abnormal lymphangiogenesis and the development of primary lymphedema. Similarly, the *RAS/MAPK* pathway is also activated by *VEGFR-3* and HGF/MET signaling.[18] Mutations in *SOS1, RIT1, KRAS, NRAS, HRAS,* and *BRAF* are linked to Noonan spectrum disorders and Costello syndrome, all of which can include lymphedema as a clinical feature. The *HGF/MET* pathways regulate the growth and survival of lymphatic endothelial cells. Mutations in *HGF, MET, CBL,* and *PTPN11* are associated with primary lymphedema or lymphedema as a subset of broader syndromes. The *Rho/ROCK* pathway influences endothelial mobility and lymphatic pumping. Although mutations in this pathway are not directly linked to lymphedema, evidence suggests it may play an important role in lymphatic function through the regulation of endothelial mobility and lymphatic pumping. Additionally, several transcription factors are involved in lymphatic development and valve morphogenesis.[18] Mutations in *SOX18, GATA2*, and *FOXC2* are associated with various forms of syndromic lymphedema as well.[18]

Primary lymphedema can be inherited through both autosomal dominant and autosomal recessive modes of inheritance. Three genes: *FLT4 (VEGFR3)*, Forkhead Box *C2* (*FOXC2*), and SRY-box transcription factor 18 (*SOX18*) are known to cause primary lymphedema. More recent findings suggest hepatocyte growth factor (HGF) and its high-affinity receptor (MET) as additional candidate genes involved in lymphedema. The identification of genes that cause primary lymphedema has advanced both the understanding and diagnosis of the condition. For example, Milroy lymphedema is caused by mutations in the *VEGFR3* gene, whereas similar forms of congenital lymphedema may result from mutations in *VEGF-3* (which codes for the VEGFR3 ligand) or in Kinesin Family Member 11 (*KIF11*), which is associated with microcephaly-lymphedema syndrome.[29] Turner syndrome, caused by the absence or structural alteration of one X chromosome, may also present with congenital lymphedema.[29] Although these conditions appear clinically similar, genetic screening enables a clear diagnosis.

Lymphatic endothelial cell precursors develop from venous endothelial cells, explaining the close genetic and physiological relationship between veins and lymphatic vessels. Mutations in the *FOXC2* gene cause lymphedema-distichiasis syndrome. The underlying cause is lymphatic valve reflux, along with venous valve reflux affecting all superficial veins and about one-third of the deep veins. *FOXC2* was the first gene identified to cause venous disease. Although distichiasis is present at birth, lymphedema typically does not manifest until puberty or later in adulthood. This suggests that the *FOXC2* gene can cause early-onset (praecox) and late-onset (tarda) lymphedema. Other genetic forms, such as Milroy lymphedema, may also present with venous abnormalities, although these do not appear to directly cause swelling. Although treating venous reflux in genetic conditions might appear beneficial because it reduces lymphatic load, the benefits remain uncertain. In patients with *FOXC2* mutations, treatment shows little improvement, indicating that the primary role of the lymphatic system is to regulate chronic edema. Current research also suggests that lymphatic drainage, not venous reabsorption, is the main way for tissue fluid clearance.[29]

1.2. Genetics of Lipedema:

The etiology of lipedema remains clinically unknown, but evidence suggests a likely familial inheritance pattern. One study reported a positive family history in 60-80% of cases. To investigate inheritance patterns, recent research has examined groups of unrelated patients to explore the possibility of shared genetic influences. In a genome-wide association study (GWAS) involving 130 lipedema patients and matched controls, no single-nucleotide polymorphisms (SNPs) met the threshold for statistical significance. Michelini *et al.* developed a panel of 305 candidate genes potentially linked to lipedema, drawing on prior research.[30] Sequencing these genes in a cohort of 167 patients revealed 21 predicted damaging variants in 17 individuals.[31] Although the genetic factors contributing to the development of lipedema are unclear, multigene panels are important for further genetic investigations. Evidence also points to genetic heterogeneity, suggesting that the condition may arise from variants in different genes among affected individuals. While no single gene has been consistently observed in Lipedema cases, several genes have been reported in isolated patients or families, including POU Domain Class 1 Transcription Factor 1 (*POU1F1A*), Nuclear Receptor Binding SET Domain Protein 1 (*NSD1*), and Aldo-Keto Reductase Family 1 Member C1 (*AKR1C1*). Whole-exome sequencing was performed on 31 individuals, and 9 families was done in a study conducted by Morgan *et al.* Using the Genome Analysis

DOI: 10.36838/IJHSR87.43

Toolkit (GATK) best practices pipeline, researchers detected 2,786,094 single-nucleotide variants (SNVs) and indels. These variants were then filtered according to quality metrics, presumed inheritance patterns, gene tolerance to loss of function, predicted pathogenicity, and population allele frequencies. After filtering, the dataset included rare variants in 469 genes. Variants were found among individuals in all nine families studied, with 75 variants appearing in more than one family. However, no single variant was present in more than four families.[31]

Recent genetic studies have begun to clarify the molecular basis of lipedema. But as of right now, genetic testing for lipedema is for research use only.[30] Genetic testing methods of lipedema include: GWAS panels, whole exome sequencing, and candidate gene panels. The goal of these tests is to identify common SNP variants and rare mutations contributing to the disease. The first large-scale genetic analysis of lipedema was a genome-wide association study (GWAS) conducted using UK data. In this study, women clinically diagnosed with lipedema were compared to controls. This identified multiple single-nucleotide polymorphisms (SNPs) with significant associations. Particularly, variants in genes such as *LHFPL6, GATA2, ANGPT2,* and *VEGFA* had the strongest association signals.[33] These genes regulate fat distribution, angiogenesis, and lymphatic vessel development, suggesting that lipedema may stem from an interplay between adipose and lymphatic systems.[21]

Beyond common SNPs, rare variants not captured in GWAS may also drive lipedema, which are more effectively captured through exome sequencing. Candidate pathways linked to extracellular matrix remodeling and vascular signaling can potentially explain both the adipose tissue accumulation and the vascular fragility observed in patients.[33]

Targeted sequencing of genes already linked to lymphatic or adipose disorders has revealed areas of overlap between lipedema and other related conditions.[33] For example, *VEGFA* and *ANGPT2*, previously implicated in primary lymphedema, also appear in lipedema studies, further reinforcing the concept of shared molecular pathways across adipose-lymphatic diseases. Genetic testing for lipedema remains limited to research use only, with no clinically approved methods available. Several approaches are being explored, including genome-wide association studies, whole-exome sequencing, and candidate gene panels. The overarching aim of testing is to identify both common single-nucleotide polymorphisms (SNPs) and rare mutations that contribute to the development and progression of lipedema.[34]

Non-genetics of lipedema: hormonal regulations:

Studies of lipedema fat tissue show that adipocytes are often larger than normal. To investigate this, researchers have examined genes involved in adipocyte growth, metabolism, and hormone regulation. One gene, such as Uncoupling Protein 1 (UCP1), is typically expressed in brown adipose tissue and functions to burn energy and generate heat. Lower levels of UCP1 were expected in lipedema tissue due to slower metabolism in larger adipocytes, but no decrease was observed. Other common fat-related genes, such as leptin (LEP) and adiponectin (ADIPOQ), showed no significant differences between lipedema and healthy samples. However, some genes that regulate adipocyte development, including CCAT/enhancer-binding protein delta (CEBPD), Nuclear Receptor corepressor 2 (NCOR2), and Krüpel-like factor 4 (KLF4), were found at lower levels in lipedema tissue. These genes regulate Peroxisome Proliferator-Activated Receptor Gamma (PPARG), a key controller of fat cell formation.[29] However, not all results have been consistent. In one study, fat stem cells from lipedema patients showed higher levels of PPARG and LEP when grown and stimulated in the lab compared to controls.[29] These differences may be due to variations in study design or sample type.

These gene expression differences in fat tissue may help explain lipedema's inheritance pattern. Although no single genetic variant has been identified, the repeated involvement of genes linked to fat cell growth, hormone signaling, and tissue structure suggests that multiple genetic pathways may be involved in the condition. The strong female predominance in lipedema cases also points to hormonal factors, particularly estrogen, and how they may influence gene activity. One example is the gene Zinc Finger Protein 423 (ZNF423), which is involved in fat cell formation, can be activated by estrogen, and has been found at higher levels in lipedema tissue.[29] This hormonal association may help explain why symptoms often begin or worsen during periods of hormonal change, such as puberty, pregnancy, or menopause, when fluctuations in estrogen and progesterone influence fat distribution, fluid retention, and lymphatic function.[54]

1.3. Diagnosis and Testing of Lymphedema and Lipedema:

Although lymphedema symptoms are commonly prevalent even in early stages, it is often overlooked and insufficiently treated. Diagnosis is primarily done clinically, relying on a detailed and specific familial history of the patient along with a thorough physical examination that includes inspection, palpation, range of motion assessment, and physical evaluation.[35] Functional limitations and impacts on quality of life should be assessed using measurable methods, while psychological factors such as anxiety, depression, and sleep disturbances are also addressed. Lymphedema can be present individually or alongside other conditions such as lipedema, obesity, or chronic venous insufficiency.[35] It can also occur in malignant forms due to tumor infiltration or lymph node metastases.[36] A comprehensive diagnosis should also consider inflammatory disorders, venous disease, deep vein thrombosis, hypoalbuminemia, rheumatic disease, heart or kidney failure, and medication-induced edema.[37] Diagnostic laboratory tests (kidney, liver, thyroid function, D-dimer), chest X-ray, electrocardiography, echocardiogram, venous doppler ultrasonography (US), magnetic resonance imaging (MRI), or computed tomography (CT) may be used to confirm the diagnosis.[37]

Table 1: Imaging-based diagnostic techniques for lymphedema (ref: https://www.ahajournals.org/doi/10.1161/CIRCRESAHA.121.318307?url_ver=Z39.88-2003&rfr_id=ori:rid:crossref.org&rfr_dat=cr_pub%20%200pubmed)

Technique	Lymphatic application	Resolution	Depth limitation
Contrast lymphography	Central/visceral lymphatic visualization	≈1 mm	No limit
Radionuclide lymphoscintigraphy	Imaging of collecting lymphatic vessels and dermal backflow; quantitative assessment of lymphatic function	≈1.5 mm	No limit
Near infrared lymphography	Imaging of collecting lymphatic vessels and dermal backflow; quantitative assessment of lymphatic function	µm range	1.5 cm
MR lymphography	Central/visceral lymphatic visualization; functional and morphological evaluation of lymphatic vessel status	0.5–2 mm	No limit
CT	Assessment of lymphatic vessel status	50–200 µm	No limit
SPECT	Assessment of lymphatic vessel status	1–2 cm	No limit

Diagnosis of lipedema begins with a thorough clinical history focusing on the onset, duration, and progression of symptoms, factors that worsen them, and any previous treatments such as lymphatic massage, drainage, or compression garments, noting the effect of these treatments, which can indicate lymphatic involvement. Family history is very important, as lipedema often affects other female relatives with similar symptoms.[38] Physical examination should assess swelling in other areas to rule out systemic causes such as cardiac or renal disease and include a detailed evaluation of the lower limbs for asymmetry, prior surgical scars, and the location, extent, and texture of enlargement. The presence of fluid can be tested through pitting with prolonged pressure, though this may be absent in mild cases or those with advanced fibrosis.[39] In lipedema, the fatty tissue may feel soft or doughy, though it may be firmer in long-standing cases, and patients often have a history of easy bruising on the lower extremities, confirmed through history or direct observation.[40]

Clinical methods are available to help distinguish between different genetic forms of primary lymphedema when the causative gene is identified (Figure 6).[56] For cases where the gene is not yet identified, careful phenotyping is used.[57] Some vascular and combined lymphovascular malformations are caused by mosaic mutations, such as those in PIK3CA, which is linked to the mammalian target of rapamycin (mTOR) signaling pathway.[41] Targeting this pathway with drugs like sirolimus has shown promise in reducing symptoms, offering potential new treatment options for specific genetic forms of lymphedema.[18]

Table 2: Genes associated with primary lymphedema and their clinical features. This figure highlights three genes that play a role in primary lymphedema: FOXC2, FLT4/VEGFR3, and SOX18. Each gene is shown with its associated condition, inheritance pattern, function, and common clinical findings.

Gene Name	Associated Condition	Inheritance Pattern	Function/ Pathway	Clinical Features
FOXC2	Lymphedema-Distichiasis Syndrom (LDS)	Autosomal Dominant	regulates gene pathways + necessary for development of lymphatic vessels	• Bilateral lower limb swelling • Distichiasis (extra row of eyelashes) • sometimes varicose veins, ptosis, cleft palate, or heart valve abnormalities
FLT4 (VEGFR3)	Milroy Disease	Autosomal Dominant	necessary for lymphatic vessel formation and cardiovascular development	• Congenital lymphedema present in adolescence • bilateral swelling in legs + non-pitting edema • may have upslanting toenails or deep creases in toes
SOX18	Hypotrichosis-Lymphedema-Telangiectasia Syndrome (HLTS)	Autosomal Dominant or Autosomal Recessive	regulates blood and lymphatic vessel development during embryonic development and adult blood vessel formation	• scattered or absent scalp and body hair (hypotrichosis) • lymphedema developing in infancy or early childhood • Telangiectasia (small dilated blood vessels, often on upper face or body) • possible congenital heart defects in some cases

Progression flow of Lymphedema and Lipedema symptoms:

Symptoms of lymphedema often appear in early stages and include swelling, heaviness, skin tightness or firmness, pain, aching, soreness, numbness, tingling, stiffness, fatigue or weakness in the affected limb, and reduced mobility of nearby joints. These symptoms can serve as early indicators of rising interstitial pressure linked to the progression of lymphedema. As fluid retention increases, the limb swelling can increase with a noticeable difference in limb size (Figure 1 and Figure 5).[10] Clinicians and researchers have noted that lymphedema symptoms can appear in the earliest stages, even when objective diagnostic tools fail to detect measurable changes. This early phase may persist for months or even years before visible swelling develops. Recent studies show a strong link between individual symptoms and the presence of lymphedema and further indicate that a higher number of reported symptoms is associated with greater limb volume, as measured by infrared perimeter.[10]

In contrast, lipedema begins as abnormal fat deposition in the hips and buttocks and gradually progresses to the thighs and calves but stops at the ankles (Figure 5).[10] Many patients with lipedema are considered overweight or obese, and those who are not may deal with a disproportionate lower body compared to upper body, giving a pear-shaped appearance.[6] Swelling typically does not indent with pressure (pitting edema) unless edema has developed from another condition. Easy bruising, along with varicose veins and small spider veins near the skin surface, is also observed.[42] Swelling does not improve with elevation or weight loss. There is considerable variation in the severity and advancement of lipedema. Some patients obtain mild symptoms with barely any progression, while others can experience measured or accelerated progression.[42]



Figure 5: Clinical comparison of lymphedema and lipedema. Left: Lymphedema characterized by unilateral limb enlargement, distal involvement including the foot, and firm, non–pitting tissue consistent with lymphatic obstruction. Right: Lipedema showing bilateral, symmetrical fatty tissue deposition of the lower extremities with sparing of the feet, a nodular "peau d'orange" texture, and disproportionate adipose accumulation despite unaffected distal anatomy.

Genetic Testing and Diagnosis Yield in Lymphedema:

Genetic testing is important for the diagnosis of lymphedema because of its ability to recognize gene mutations linked to primary lymphedema. But currently, the effectiveness of genetic testing is very low. In a study including 147 patients diagnosed with primary lymphedema, genetic testing confirmed a contributing mutation in only 11 patients, meaning the current diagnostic yield of genetic testing is only 7%. Sev-

DOI: 10.36838/IJHSR87.43

enty-three patients had inconclusive results, while sixty-three had complete negative results, suggesting that current genetic panels are limited and more research is needed to identify additional causative genes. Mutations were most commonly identified in genes that play important roles in signaling pathways that regulate lymphangiogenesis and lymphatic valve development, such as CBL, CELSR1, FAT4, FLT4 (VEGFR-3), HGF, RIT1, and VEGFC.[18]

Discussion:

This review has examined the pathophysiology, diagnostic testing, and clinical treatment of both lymphedema and lipedema. It has also explored the current understandings of genetics in the onset and development of disease, and the impact of testing. Although advances in sequencing technologies have uncovered key mutations and pathways, the overall diagnostic yield of genetic testing remains low. For lymphedema, only a small number of patients receive a confirmed genetic diagnosis, and for lipedema, testing is still confined to research settings. These gaps show that many causative genes and mechanisms remain undiscovered.

At the same time, studies performed so far demonstrate the promise of genetics to reshape how we diagnose and treat these conditions. Shared pathways among lymphatic and adipose biology suggest that future work will need to bridge both paths instead of individual discoveries. Larger cohorts, advanced sequencing technologies (such as GWAS panels, exome sequencing, and targeted gene panels), and functional studies that test the biological impacts of genetic variants are essential for progression in treating vascular diseases.

■ Conclusion

In conclusion, genetic advancements have the potential to not only explain disease origin. They may also allow earlier diagnosis, more precise classification, and the development of targeted therapies. Continued collaboration between researchers and clinicians will be essential to translate these discoveries into benefits for patients.

■ Acknowledgments

The author would like to thank Professor Hamidreza Shaye for academic guidance during the preparation of this manuscript, Dr. Lauren Tetz for support during the writing process, and vascular medicine specialist Dr. Laxmana Godishala for providing valuable clinical information and feedback.

■ References

1. Li CY, Kataru RP, Mehrara BJ. Histopathologic Features of Lymphedema: A Molecular Review. Int J Mol Sci. 2020 Apr 6;21(7):2546.
2. Brouillard P, Boon L, Vikkula M. Genetics of lymphatic anomalies. J Clin Invest. 2014 Mar;124(3):898–904.
3. Buck DW, Herbst KL. Lipedema: A Relatively Common Disease with Extremely Common Misconceptions. Plast Reconstr Surg Glob Open. 2016 Sept;4(9):e1043.
4. Buso G, Depairon M, Tomson D, Raffoul W, Vettor R, Mazzolai L. Lipedema: A Call to Action! Obesity (Silver Spring). 2019 Oct;27(10):1567–76.
5. Campisi C, Campisi C, Accogli S, Campisi C, Boccardo F. Lymphedema staging and surgical indications in geriatric age. BMC Geriatr. 2010 May 19;10(1):A50.
6. Bonetti G, Paolacci S, Samaja M, Maltese PE, Michelini S, Michelini S, et al. Low Efficacy of Genetic Tests for the Diagnosis of Primary Lymphedema Prompts Novel Insights into the Underlying Molecular Pathways. Int J Mol Sci. 2022 July 3;23(13):7414.
7. Luta X, Buso G, Porceddu E, Psychogyiou R, Keller S, Mazzolai L. Clinical characteristics, comorbidities, and correlation with advanced lipedema stages: A retrospective study from a Swiss referral centre. PLOS ONE. 2025 Mar 20;20(3):e0319099.
8. Markarian B, Toro C, Moreira K, Polam S, Mathew N, Mayrovitz HN. Assessment Modalities for Lower Extremity Edema, Lymphedema, and Lipedema: A Scoping Review. Cureus. 2024 Mar;16(3):e55906.
9. Martin-Almedina S, Mortimer PS, Ostergaard P. Development and physiological functions of the lymphatic system: insights from human genetic studies of primary lymphedema. Physiological Reviews. 2021 Oct;101(4):1809–71.
10. Duhon BH, Phan TT, Taylor SL, Crescenzi RL, Rutkowski JM. Current Mechanistic Understandings of Lymphedema and Lipedema: Tales of Fluid, Fat, and Fibrosis. Int J Mol Sci. 2022 June 14;23(12):6621.
11. Fang J, Dagenais SL, Erickson RP, Arlt MF, Glynn MW, Gorski JL, et al. Mutations in FOXC2 (MFH-1), a forkhead family transcription factor, are responsible for the hereditary lymphedema-distichiasis syndrome. Am J Hum Genet. 2000 Dec;67(6):1382–8.
12. Ferrell RE, Kimak MA, Lawrence EC, Finegold DN. Candidate Gene Analysis in Primary Lymphedema. Lymphatic Research and Biology. 2008 June 1;6(2):69–76.
13. Greene A, Goss J. Diagnosis and Staging of Lymphedema. Seminars in Plastic Surgery. 2018 Feb;32(01):012–6.
14. Okhovat J-P, Alavi A. Lipedema: A Review of the Literature. Int J Low Extrem Wounds. 2014;14(3):262–267. doi:10.1177/1534734614554284
15. Hidding JT, Viehoff PB, Beurskens CHG, van Laarhoven HWM, Nijhuis-van der Sanden MWG, van der Wees PJ. Measurement Properties of Instruments for Measuring Lymphedema: Systematic Review. Phys Ther. 2016 Dec;96(12):1965–81.
16. Kayıran O, De La Cruz C, Tane K, Soran A. Lymphedema: From diagnosis to treatment. Turk J Surg. 2017;33(2):51–7.
17. Kim J, Jeon JY, Ko YM, Kang MS, Park SK, Roh K. Characteristics of Lymphedema in Patients Treated with Mammalian Target of Rapamycin Inhibitors. Lymphatic Research and Biology. 2021 Aug;19(4):365–71.
18. Klimentidis YC, Chen Z, Gonzalez-Garay ML, Grigoriadis D, Sackey E, Pittman A, et al. Genome-wide association study of a lipedema phenotype among women in the UK Biobank identifies multiple genetic risk factors. Eur J Hum Genet. 2023 Mar;31(3):338–44.
19. Michelini S, Herbst KL, Precone V, Manara E, Marceddu G, Dautaj A, et al. A Multi-Gene Panel to Identify Lipedema-Predisposing Genetic Variants by a Next-Generation Sequencing Strategy. Journal of Personalized Medicine. 2022 Feb;12(2):268.
20. Ferrell RE, Levinson KL, Esman JH, Kimak MA, Lawrence EC, Barmada MM, et al. Hereditary lymphedema: evidence for linkage and genetic heterogeneity. Hum Mol Genet. 1998 Dec;7(13):2073–8.
21. Characteristics of Lymphedema in Patients Treated with Mammalian Target of Rapamycin Inhibitors. Lymphat Res Biol. 2021. doi:10.1089/lrb.2020.0069

22. Child AH, Gordon KD, Sharpe P, Brice G, Ostergaard P, Jeffery S, et al. Lipedema: an inherited condition. Am J Med Genet A. 2010 Apr;152A(4):970–6.Aug;19(4):365–71.
23. Kruppa P, Georgiou I, Biermann N, Prantl L, Klein-Weigel P, Ghods M. Lipedema-Pathogenesis, Diagnosis, and Treatment Options. Dtsch Arztebl Int. 2020 June 1;117(22–23):396–403.
24. Mehrara BJ, Zampell JC, Suami H, Chang DW. Surgical management of lymphedema: past, present, and future. Lymphat Res Biol. 2011;9(3):159–67.
25. Poojari A, Dev K, Rabiee A. Lipedema: Insights into Morphology, Pathophysiology, and Challenges. Biomedicines. 2022 Nov 30;10(12):3081.
26. Schaverien MV, Coroneos CJ. Surgical Treatment of Lymphedema. Plast Reconstr Surg. 2019 Sept;144(3):738–58.
27. Senger JLB, Kadle RL, Skoracki RJ. Current Concepts in the Management of Primary Lymphedema. Medicina. 2023 May 6;59(5):894.
28. Szuba A, Rockson SG. Lymphedema: anatomy, physiology and pathogenesis. Vasc Med. 1997 Nov;2(4):321–6.
29. von Atzigen J, Burger A, Grünherz L, Barbon C, Felmerer G, Giovanoli P, et al. A Comparative Analysis to Dissect the Histological and Molecular Differences among
30. Morgan S, Reid I, Bendon C, Ishaq M, Shayan R, Pope B, Park D, Karnezis T. A Family-Based Study of Inherited Genetic Risk in Lipedema. Lymphat Res Biol. 2024. doi:10.1089/lrb.2023.0065
31. Grada AA, Phillips TJ. Lymphedema: Pathophysiology and clinical manifestations. J Am Acad Dermatol. 2017 Dec;77(6):1009–20.
32. Morgan S, Reid I, Bendon C, Ishaq M, Shayan R, Pope B, et al. A Family-Based Study of Inherited Genetic Risk in Lipedema. Lymphatic Research and Biology. 2024 Apr 1;22(2):106–11.

Authors

Aditi Gandhi is a high school junior at The Blake School in Minneapolis, Minnesota. Her academic interests include genetics, human biology, and biochemistry. She plans to pursue a career in medicine focused on improving care for individuals with lymphatic disorders.

DOI: 10.36838/IJHSR87.43

IJHSR
ijhighschoolresearch.org
REVIEW ARTICLE

In Cancer Immunotherapy Using CAR T Therapy and Emerging Advances in Stem Cell Therapy

Huseyn Ibrahimli

Baku, Azerbaijan; huseyn.ibrahimli2710@gmail.com

ABSTRACT: Chimeric antigen receptor (CAR) T-cell therapy has transformed cancer treatment by making precise antigen-specific tumor killing. However, its broader use remains limited by certain challenges such as T-cell exhaustion, short persistence, manufacturing complexity, high costs, and inconsistent patient-derived products. T-cell exhaustion is the progressive loss of function after chronic antigen exposure, while persistence describes the long-term survival of infused cells required for maintained tumor control. Recent innovations in stem cell reprogramming, or more specifically, induced pluripotent stem cells (iPSCs), allow for large-scale and easily gene-editable production of restored CAR T-cells with better longevity and stronger therapeutic function. This review goes over the advancements made in CAR receptor design from the first-generation models to the gene-edited armored CARs. It also includes workflows for generating iPSC-derived CAR T-cells and mentions strategies like cytokine engineering, receptor optimization, and gene editing to improve its effectiveness and safety. Clinical and preclinical findings are included too, adding extended persistence through co-stimulatory signaling, and promising early results in solid tumors such as gastric cancer and glioblastomas. Real-world impacts are also important, for example, the use of CAR T therapy in lower-income countries like India, and studies in China showed the survival benefits in patients with advanced cancers. These results show that the impact of CAR T therapy is already seen in clinics across different countries. Stem cell-based CAR T manufacturing is one of the biggest steps toward universal immunotherapies that can improve both access and patient outcomes in cancer treatment worldwide.

KEYWORDS: CAR T-cell Therapy, iPSC-derived CAR T-cells, Gene Editing, Cancer Immunotherapy, T-cell Exhaustion.

Introduction

Cancer immunotherapy uses the body's own immune system to find and kill harmful cells with the chimeric antigen receptor, with (CAR) T-cell therapy being one of the most important innovations in this field. In CAR T therapy, patient-derived T-cells or donor T-cells are genetically engineered to express synthetic receptors that identify specific tumor antigens, allowing MHC-free tumor cell killing.[1] This method has led to long-term recovery in some blood cancers, especially B-cell leukemia and lymphomas, frequently in patients who had no other remaining treatment alternatives.[2] A key factor in CAR T therapy is the balance of CD4+ helper cells, which support the immune response by producing cytokines and helping other cells, and CD8+ cytotoxic cells, which directly kill tumor cells. A balanced mix of these subsets has shown to improve persistence and overall outcomes.[3] However, this treatment still has many challenges. For example, autologous CAR T products are costly and time-consuming to produce; the engineered T-cells usually become exhausted, have limited persistence inside the body, and have reduced efficacy against solid tumors due to their immunosuppressive microenvironments. Manufacturing problems, donor cell limitations, and safety risks like cytokine release syndrome (CRS), neurotoxicity (ICANS), and graft versus host disease (GvHD) add even more problems when trying to make these therapies more widely available.[4] To find solutions to these problems, researchers are increasingly using induced pluripotent stem cells (iPSCs) as a renewable and easily engineerable source for CAR T manufacturing. iPSC-derived CAR T-cells can be produced at a large scale, gene edited to remove immunogenic features, add functional improvements, and be differentiated into balanced CD4+ helper and CD8+ cytotoxic subsets.[5] This review covers the biochemical advancements in CAR receptor design, the technical and clinical developments of iPSC-derived CAR T products, and the strategies being developed to move toward universal clinical cell-based immunotherapies.

Section 1: Evolution of CAR T Receptors Through Biochemical Innovation:

Over the last 2 decades, the chimeric antigen receptor (CAR) design has evolved from its basic prototype models into advanced therapeutic tools. The first-generation CARs were made of an antigen-binding single-chain variable fragment (scFv) linked to the CD247 signaling domain. This was enough to direct T-cell activation without the need for MHC, but they were very limited in their ability to expand, persist, and cause long-term tumor control.[6] Second-generation CARs added co-stimulatory domains such as CD28 or 4-1BB (CD137) improving T-cell activation and survival. The 4-1BB domain was shown to improve long-term persistence and boost mitochondrial fitness. CD28 provided faster expansion, but sometimes shorter activity and persistence.[7] These differences explain why some CAR T products persist for months or even years in patients, while others disappear faster. Third-generation CARs tried combining two co-stimulatory domains, CD28 and 4-1BB, together, but so far clinical outcomes have

© 2026 Terra Science and Education

DOI: 10.36838/IJHSR87.50

not shown clear advantages compared to second-generation CARs and, therefore, have led to mixed results.[8] The newest fourth-generation "armoured" CARs, also called TRUCKs, included additional features like cytokine secretion (IL-12 and IL-15) to resist tumor suppression and increase cell longevity. IL-15 helps CAR T-cells live longer in the body, while IL-12 can help beat the solid tumor microenvironment that normally blocks T-cells.[9] Safety switches, like inducible caspase-9, were also included and allowed the doctors to destroy the treatment quickly in case there was a toxic reaction from the patient. Finally, modern CAR design now uses gene editing tools like CRISPR to remove inhibitory pathways like PD-1 or TGFB-RII that normally cause T-cell exhaustion to help increase the persistence.[10] The structural and functional progression from first-generation CARs to fourth-generation armored CAR designs is shown in Figure 1.

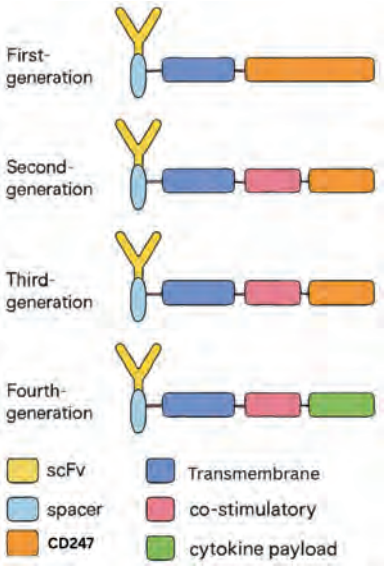

Figure 1: Structural evolution of CAR receptors from first to fourth generation designs. Figure created by Huseyn Ibrahimli. This progression shows how added co-stimulatory domains and cytokine engineering improved CAR T-cell persistence and effectiveness.

Section 2: Getting CAR T-Cells from Stem Cells:

The limits of autologous CAR T manufacturing, including the time, cost, donor variability, and complex procedures, have pushed a shift toward pluripotent stem cell products. iPSCs offer a limitless and easily engineered source for making CAR T-cells.[11] This scalability is especially important because iPSCs can be expanded much more easily while keeping the genetic stability, making them a better choice than donor-derived T-cells for regular production.[12] Research shows that mature T-cells can be reprogrammed into iPSCs and differentiated back into T-cells that keep their ability to target tumors.[13] The process of iPSC reprogramming, genome editing, and differentiation into functional CAR T-cells is shown in Figure 2. Clinical transition has focused on making the process safe and scalable, with GMP-compliant, Xeno-free, and feeder-free differentiation protocols.[14] Epigenetic tools like EZH1 inhibition have been used to improve cytokine secretion, cytotoxicity, and persistence *in vivo*.[15] In T-cell cancers, CD5-negative starting cells are used to avoid self-targeting.[16] At the same time, gene editing is used to delete TCR and HLA to reduce risks of GvHD and immune rejection, making "hypoimmunogenic" products that can be given to many patients without matching.[17] Several biotechnology companies like Fate Therapeutics are already testing these ideas, with iPSC-derived CAR T and NK therapies such as FT819 and FT576. Early results have shown good safety with no high-grade CRS or neurotoxicity.[18] Century Therapeutics is also developing iPSC-derived CAR NK products like Cnty 101, which has shown promising safety and activity in lymphoma.[19]

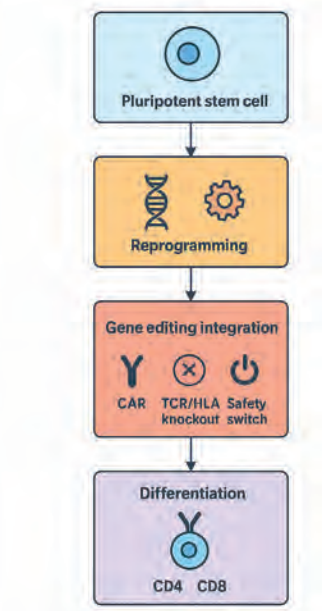

Figure 2: Workflow of iPSC reprogramming, genome editing, and differentiation into functional CAR T-cells. Figure created by Huseyn Ibrahimli. The workflow shows how stem cell engineering allows for scalable production of optimized CAR T-cells for broader clinical use.

Section 3: Enhancing CAR T Receptor Efficiency and Differentiation Strategies:

Enhancing receptor efficiency and cellular function is the main goal. Persistence is very important as long-lived CAR T-cells are strongly linked with durable remission. T-cell exhaustion happens when chronic antigen exposure decreases effector function, limiting its benefit. Strategies to improve persistence include co-stimulatory domains like 4-1BB.[20] Inserting cytokines like IL-15 under activation promoters can also help T-cells stay active longer without external support.[21] Deleting inhibitory receptors like PD-1 with CRISPR protects cells from exhaustion.[22] The balance of CD4 and CD8 subsets is another important factor since studies show that an even amount of CD4 to CD8 (about a 1:1 ratio) results in better persistence and antitumor activity.[23] Achieving a balanced CD4+ and CD8+ phenotype remains challenging for iPSC-derived products. Three-dimensional thymic organoid systems, including ligand 4 (DLL4), have been developed to restore physiological thymopoiesis.[24] Gene editing has also improved safety and performance. Deleting cytokine toxicity mediators like GM-CSF helps reduce CRS and neuroinflammation while keeping good antitumor activity.[25] Epigenetic modifications are being explored to make T-cells last longer

and resist exhaustion.[26] The receptor engineering approaches and iPSC differentiation strategies used to enhance CAR T-cell persistence and function are shown in Figure 3.



Figure 3: Summary of receptor engineering and iPSC differentiation strategies used to enhance CAR T-cell performance. Figure created by Huseyn Ibrahimli. These strategies improve CAR T-cell persistence, safety, and functionality in cancer treatment.

Clinical Developments and Real-World Impacts:

Clinical studies show the progress of CAR T in both blood cancers and solid tumors. In B-cell leukemias and lymphomas, remission rates of 70–90% have been reported.[27] Solid tumor progression is slower. A gastric cancer trial in China showed improved survival from 5.5 to 7.9 months.[28] Glioblastoma dual-target EGFR/IL13Ra2 CARs given into the cerebrospinal fluid caused tumor shrinkage in 62% of patients. Toxicities like CRS and ICANS remain challenges but are manageable.[27] Global access is also improving, with lower-cost CAR T therapy in India and the development of iPSC-derived products by industry.[29]

■ Conclusion

This review covered the evolution from early CAR receptor design to stem cell-based CAR T manufacturing and clinical use. CAR designs have evolved from first-generation models into advanced, gene-edited, multifunctional versions. iPSC-derived platforms allow large-scale universal products. Challenges like immune rejection, CD4/CD8 balance, neurological side effects, and solid tumor barriers remain. Advances in receptor design, differentiation methods, gene editing, and real-world clinical applications suggest a future with safer, more effective, globally accessible CAR T therapies.[1–29]

Declaration by Authors

Ethical Approval: Approved

Acknowledgement: None

Source of Funding: None

Conflict of Interest: The authors declare no conflict of interest.

■ Acknowledgments

Huseyn would like to thank Dr. Lauren Tetz for her guidance and support, and Dr. Hamidreza Shaye for his lessons and his knowledge throughout the course of this research.

■ References

1. Brudno JN, Kochenderfer JN. Toxicities of chimeric antigen receptor T cells: recognition and management. *Blood*. 2016;127(26):3321–3330. doi:10.1182/blood-2016-04-703751
2. Century Therapeutics. Clinical trial data on Cnty-101 CAR-NK therapy. 2023. Available from: https://centurytx.com Cho JH, Collins JJ, Wong WW. Universal chimeric antigen receptors for multiplexed and logical control of T cell responses. *Cell*. 2018;173(6):1426–1438.e11. doi:10.1016/j.cell.2018.04.013
3. Eyquem J, Mansilla-Soto J, Giavridis T, van der Stegen SJC, *et al.* Targeting a CAR to the TRAC locus with CRISPR/Cas9 enhances tumor rejection. *Nature*. 2017;543(7643):113–117. doi:10.1038/nature21405
4. Fate Therapeutics. FT-819 and FT-576 clinical trial updates. 2024. Available from: https://fatetherapeutics.com
5. Fesnak AD, June CH, Levine BL. Engineered T cells: the promise and challenges of cancer immunotherapy. *Nat Rev Cancer*. 2016;16(9):566–581. doi:10.1038/nrc.2016.97
6. Guedan S, Calderon H, Posey AD Jr, Maus MV. Engineering and design of chimeric antigen receptors. *Mol Ther Methods Clin Dev*. 2019;12:145–156. doi:10.1016/j.omtm.2018.11.003
7. Deuse T, Hu X, Gravina A, Wang D, *et al.* Hypoimmunogenic derivatives of induced pluripotent stem cells evade immune rejection in fully immunocompetent allogeneic recipients. *Nat Biotechnol*. 2019;37(3):252–258. doi:10.1038/s41587-019-0016-3.
8. June CH, O'Connor RS, Kawalekar OU, Ghassemi S, Milone MC. CAR T cell immunotherapy for human cancer. *Science*. 2018;359(6382):1361–1365. doi:10.1126/science.aar6711
9. Kawalekar OU, O'Connor RS, Fraietta JA, *et al.* Distinct signaling of coreceptors regulates metabolism and memory development in CAR T cells. *Immunity*. 2016;44(2):380–390. doi:10.1016/j.immuni.2016.01.011
10. Netsrithong R, Garcia-Perez L, Themeli M, *et al.* Engineered T cells from induced pluripotent stem cells: from research towards clinical implementation. *Front Immunol*. 2023;14:1325209. doi:10.3389/fimmu.2023.1325209.
11. Liu E, Marin D, Banerjee P, *et al.* Use of CAR-transduced natural killer cells in CD19-positive lymphoid tumors. *N Engl J Med*. 2020;382(6):545–553. doi:10.1056/NEJMoa1910607
12. Maude SL, Laetsch TW, Buechner J, *et al.* Tisagenlecleucel in children and young adults with B-cell lymphoblastic leukemia. *N Engl J Med*. 2018;378(5):439–448. doi:10.1056/NEJMoa1709866
13. Mardiana S, Gill S. Improving the efficacy and safety of CAR T cells for cancer therapy. *Nat Rev Clin Oncol*. 2019;16(8):461–474. doi:10.1038/s41571-019-0174-4
14. Miyahara Y, Nakagawa M, Lauren H, Johanna A, *et al.* Generation of iPSC-derived CD5 CAR-T cells avoiding fratricide in T-cell malignancies. *Blood*. 2023;142(Suppl 1):2029. doi:10.1182/blood-2023-2029
15. Neelapu SS, Locke FL, Bartlett NL, *et al.* Axicabtagene ciloleucel CAR T-cell therapy in refractory large B-cell lymphoma. *N Engl J Med.* 2018;377(26):2531–2544. doi:10.1056/NEJMoa1807447
16. Nishimura T, Kaneko S, Kawana-Tachikawa A, *et al.* Generation of rejuvenated antigen-specific T cells by reprogramming to pluripotency. *Cell Stem Cell*. 2013;12(1):114–126. doi:10.1016/j.stem.2012.09.003
17. Ren J, Liu X, Fang C, *et al.* Multiplex genome editing to generate universal CAR T cells resistant to PD-1 inhibition. *Clin Cancer Res*. 2017;23(9):2255–2266. doi:10.1158/1078-0432.CCR-16-1300
18. Sadelain M, Brentjens R, Rivière I. The basic principles of chimeric antigen receptor design. *Cancer Discov*. 2013;3(4):388–398. doi:10.1158/2159-8290.CD-12-0548

DOI: 10.36838/IJHSR87.50

19. Sterner RC, Sakemura R, Cox M, *et al.* GM-CSF inhibition reduces cytokine release syndrome and neuroinflammation but enhances CAR-T cell function. *Blood*. 2019;133(7):697–709. doi:10.1182/blood-2018-08-868639
20. Themeli M, Rivière I, Sadelain M. New cell sources for T cell engineering and adoptive immunotherapy. *Cell Stem Cell*. 2015;16(4):357–366. doi:10.1016/j.stem.2015.03.009
21. Vizcardo R, Masuda K, Yamada D, *et al.* Regeneration of human tumor antigen-specific T cells from iPSCs derived from mature CD8+ T cells. *Cell Stem Cell*. 2013;12(1):31–36. doi:10.1016/j.stem.2012.09.003
22. Netsrithong R, Garcia-Perez L, Themeli M, *et al.* Engineered T cells from induced pluripotent stem cells: from research towards clinical implementation. *Front Immunol*. 2023;14:1325209. doi:10.3389/fimmu.2023.1325209.
23. Zhao Z, Condomines M, van der Stegen SJC, *et al.* Structural design of engineered costimulation determines tumor rejection kinetics and persistence of CAR T cells. *Cancer Cell*. 2015;28(4):415–428. doi:10.1016/j.ccell.2015.09.004
24. Guedan S, Calderon H, Posey AD Jr, Maus MV, *et al.* Engineering and design of chimeric antigen receptors. *Mol Ther Methods Clin Dev*. 2019;12:145-156. doi:10.1016/j.omtm.2018.11.003.
25. Netsrithong R, Garcia-Perez L, Themeli M, *et al.* Engineered T cells from induced pluripotent stem cells: from research towards clinical implementation. *Front Immunol*. 2023;14:1325209. doi:10.3389/fimmu.2023.1325209.
26. Deuse T, Hu X, Gravina A, Wang D, *et al.* Hypoimmunogenic derivatives of induced pluripotent stem cells evade immune rejection in fully immunocompetent allogeneic recipients. *Nat Biotechnol*. 2019;37(3):252–258. doi:10.1038/s41587-019-0016-3.
27. Guedan S, Calderon H, Posey AD Jr, Maus MV, *et al.* Engineering and design of chimeric antigen receptors. *Mol Ther Methods Clin Dev*. 2019;12:145-156. doi:10.1016/j.omtm.2018.11.003.
28. Frontiers in Oncology. Advances in gene editing for safer CAR-T therapies. *Front Oncol*. 2024;14:1388475. doi:10.3389/fonc.2024.1388475
29. Turtle CJ, Hanafi LA, Berger C, *et al.* CD19 CAR–T cells of defined CD4+:CD8+ composition in adult B-cell ALL patients. *J Clin Invest*. 2016;126(6):2123–2138. doi:10.1172/JCI85309

Authors

Huseyn Ibrahimli has an academic interest in cancer immunotherapy, specifically CAR T-cell therapy and gene editing strategies for cancer treatment. His work focuses on reviewing advances that improve the effectiveness, persistence, and accessibility of the next generation of immunotherapies.

IJHSR
ijhighschoolresearch.org
RESEARCH ARTICLE

Model Collapse: A Comprehensive Review of Causes, Detection, and Mitigation

Murtaza S. Malik

Raha International School Gardens Campus, Khalifa City 'A, Al Raha Gardens Cnr. Al Mireef St, Abu Dhabi, 00000, UAE; murtaza.pog@gmail.com

ABSTRACT: As generative AI systems become increasingly trained on synthetic data, often produced by earlier iterations of the same models, concerns about model collapse have come to the forefront of AI research. Model collapse is the degradation of a model's output quality when it recursively learns from its outputs, leading to a loss of diversity, factuality, and generalization over time. Therefore, output starts to become increasingly repetitive and less creative, making it biased toward high-frequency or stereotypical patterns, because rare or nuanced examples gradually get filtered out. This makes the information users receive narrower, less trustworthy, and potentially discriminatory against marginalized groups whose experiences are underrepresented in high-probability data. These consequences of model collapse raise ethical dilemmas, especially for its applications in education, healthcare, hiring, and public services. This review investigates the detection and prevention of model collapse in generative AI, examining various studies on regression modeling, recursive training, and prompt evaluations. These studies compare synthetic and real data, track rare token loss, and analyze the compounding effects of low-diversity exposure. This project contributes to the field by consolidating current research showing collapse is measurable, mitigable via curated data, token-level editing, hybrid training, and unlearning, while proposing a hybrid benchmark for detection.

KEYWORDS: Model Collapse, Recursive Training, Synthetic Data, Output Bias, AI Ethics, Model Unlearning.

Introduction

At the core of generative AI, which is a subset of AI systems capable of creating original content,[1] lies a silent danger: these models may eventually lose sight of the richness of the human data they were trained on. A phenomenon known as "model collapse" occurs when AI systems are repeatedly trained on their own outputs, resulting in outputs that get increasingly bland, biased, and detached from reality.[2]

In recent years, large language models (LLMs), like LLaMA[3] and ChatGPT,[4] have made remarkable progress in generating text that is both fluent and relevant.[1] However, as developers use more and more synthetic data generated by previous iterations of these models for further training, concerns regarding long-term degradation have increased. Models that undergo recursive training eventually lose their rare token diversity, factual accuracy, and generalization ability.[2] The performance of models can drop even when synthetic data initially seems to be of high quality.[5] These effects can also result from overexposing models to repeated examples, even if they are clean and human-generated. When rare token loss sets in, the model's output becomes significantly dominated by a few high-frequency categories, and the long tail, less common ones, just disappear. As seen in Figure 1,[6] in this context, the model is finetuned with synthetic data, with the model collapsing onto a small set of nationalities, with most vanishing. Collectively, this literature indicates that collapse is increasingly recognized as a theoretical and practical threat.

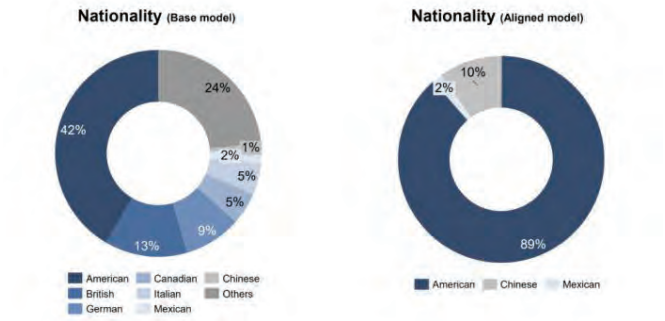

Figure 1: The preference-aligned model trained on simulated user outputs collapses to a narrow set of nationalities, demonstrating rare-token degradation compared to the more varied base model. Figure adapted from Devansh.[6]

Understanding model collapse is crucial because its implications extend beyond academic boundaries. As collapse progresses, model outputs become more homogeneous, overconfident, and reliant on high-probability patterns[5] which can lead to inaccurate information, the exclusion of minority voices, and a drop in user confidence.

Model collapse is a real and quantifiable phenomenon, but it can be lessened with intentional interventions. Our goal is to bridge the gap in the literature by integrating recent findings and collectively show that methods such as model confidence filtering, which filters synthetic outputs based on the model's certainty to retain higher-quality examples,[2] token-level editing, which replaces low-value or overly predictable tokens to preserve diversity,[7] and hybrid training with real data, which combines synthetic and human-generated data to maintain grounding in real-world distributions,[5] can all help lower the

© 2026 Terra Science and Education

DOI: 10.36838/IJHSR87.54

risk of collapse. Furthermore, to potentially reverse collapse, we suggest a novel approach that combines a model-testing framework to identify and reverse collapse in future AI pipelines with machine unlearning, a method for eliminating malicious data from machine learning (ML) systems.[8]

Our research methodology is mostly grounded in literature, referencing recent works that combine experimental benchmarks with theoretical modeling. Furthermore, we examine secondary data and suggest ways to incorporate it into upcoming AI development processes. Relevant papers were identified through systematic searches on Google Scholar using targeted keywords such as "model collapse," "rare token degradation", etc. Furthermore, we prioritized recent publications as well as applying citation snowballing by reviewing references within key papers to identify other relevant studies.

This is how the rest of the paper is organized:

Background information on synthetic data, generative AI, and the mechanisms underlying model collapse is given in Section 3. In Section we discuss and analyze a variety of model collapse monitoring methods 4. Prevention and mitigation techniques are discussed in Section 5. Additionally, we propose 2 methods for preventing and tracking model collapse through the use of model unlearning and hallucination tracking in Section 6, along with a discussion of their possible advantages and disadvantages. Finally, in Section 7, the paper's main conclusions are summarized, and the necessity of proactive collapse prevention in long-term AI deployment is emphasized.

Background

3.1. Generative AI and Synthetic Data:

Artificial intelligence is increasingly being integrated into our world today, from being used for customer service calls to medical imaging analysis, but all of this is thanks to generative AI systems. Generative AI systems, one of the most commonly used systems today, are a type of machine learning (ML) module that produces original content like text or images.1 These systems have rapidly transformed industries by automating tasks such as editing, writing, and summarization. As their capabilities grow, so too does their use. Millions of people now rely on generative AI tools in daily life, whether to draft emails, create social media posts, write essays, or generate blog content.[1] Due to this, a substantial portion of online content is now AI-generated. This rise in usage has led to the emergence of synthetic data, AI-created content that, once released publicly, blends into the broader web.[2] Since most modern AI models are trained on data scraped from the internet, this synthetic content often re-enters the training pipelines without filtering out. Even content with a small degree of AI involvement can be labeled as synthetic, and as AI usage becomes more common, this kind of data is leaking rapidly (see Figure 2). After a large pool of synthetic data eventually leaks into training data, it quietly evolves into a feedback loop (see Figure 2), where models are unintentionally trained on their own outputs. This phenomenon, if left unchecked, creates the conditions for a serious challenge in AI development: model collapse. Roman[9] describes how recursive training reduces sensitivity to rare events and shows how even a small overlap between training and evaluation data can obscure early signs of degradation. These risks are particularly important in professions where objectivity and accuracy are essential, such as healthcare, law, and education.[1]

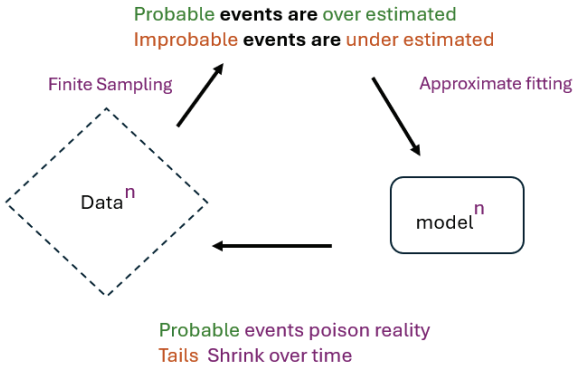

Figure 2: Model collapse is the downward spiral that occurs when a model keeps training on its own outputs, erasing low-probability events and reinforcing a biased view of reality. Adapted from Shumailov *et al.*[2]

3.2. Defining Model Collapse:

Model collapse is where a model's performance iteratively degrades as it recursively trains from its own low diversity outputs. Over time, this leads to "rare token" and "rare scenario" loss, such as when, in Gerstgrasser *et al.*,[10] models in later generations begin introducing irrelevant and implausible content or examples, shifting from factual architectural descriptions to surreal details like "black-tailed, white-tailed, blue-tailed, red-tailed, yellow-tailed jackrabbits" when describing churches (see Table 1). Furthermore, models can also hallucinate. In hallucination, models are displaying and outputting clearly false information or sources. The most well-known example is when Google's Gemini hallucinated in 2023 that the James Webb telescope claimed a discovery that never happened in the first place.[11]

The accuracy of the model is significantly impacted when rare token loss and hallucinations are allowed to continue, which causes the model to marginalize underrepresented data and favor high-probability, stereotypical responses. This is evident with the rise of gender bias and the decline of gender-neutral alternatives in generative AI models[10] where prompts such as "The doctor walked into the room and..." are nearly always completed with "he looked at the patient." [10]

This is a noteworthy example of a stereotypical response from a generative AI system. Additionally, the performance of these models starts to become more unreliable because of the growing gap between training data and real-world use cases.

3.3. Early and Late Collapse:

Researchers distinguish between early collapse, where rare or low-frequency tokens are lost, and late collapse, where output variance drops and the model drifts away from the original data distribution.[7] While catastrophic forgetting erases prior task knowledge when learning new ones, model collapse stems from the cumulative reuse of model-generated data (see Table 1).

Table 1: Model collapse- catastrophic forgetting. Adapted from Shumailov *et al.*[2] The table showcases progressive degradation in an OPT-125M language model when repeatedly trained on its own generated data, showing loss of semantic coherence, topic drift, and eventual nonsensical output across generations.

Example of text outputs of an OPT-125m model affected by Model Collapse. The model iteratively degrades where each new generation is trained on data produced by the previous generation.			
Inputs:			
some started before 1360 — was typically accomplished by a master mason and a small team of itinerant masons, supplemented by local parish labourers, according to Poyntz Wright. But other authors reject this model, suggesting instead that leading architects designed the parish church towers based on early examples of Perpendicular			
Outputs:			
Gen 0: Revival architecture such as St. John's Cathedral in London. The earliest surviving example of Perpendicular Revival architecture is found in the 18th @-@ century Church of Our Lady of Guernsey, which dates from the late 19th century. There are two types of perpendicular churches : those	**Gen 1:** architecture such as St. Peter's Basilica in Rome or St. Peter's Basilica in Buenos Aires. There is no evidence that any of these buildings were built during the reign of Pope Innocent III, but it is possible that they may have been built during the reign of his successor, Pope Innocent	**Gen 7:** architecture in England. In an interview with The New York Times, Wright said : " I don 't think there is anything wrong with me being able to do what I want to do. It just doesn't work for me. " He added : " I don 't know if you can call it funny.	**Gen 9:** architecture. In addition to being home to some of the world's largest populations of black @-@ tailed jackrabbits, white @-@ tailed jackrabbits, blue @-@ tailed jackrabbits, red @-@ tailed jackrabbits, yellow @-

3.4. Evidence That Model Collapse is Real:

Multiple empirical and theoretical studies demonstrate that model collapse is not a hypothetical failure mode, but a real and measurable phenomenon. In Shumailov *et al.*,[2] recursive training experiments on language models showed a sharp decline in lexical diversity and a measurable loss of rare tokens over successive generations. Additionally, it was also seen that there was a reduced recall for rare tokens and a drift toward high-frequency, less informative tokens, even when fluency remained stable.[12] Also, the test accumulates predictably with each iteration of self-training through regression-based modelling.[7] This is further confirmed by Feng *et al.*[13] that collapse is accompanied by semantic drift, disappearance of tail-distribution content, and factual inaccuracy. These findings together provide strong, cross-paper evidence that model collapse occurs in practice and can be reliably detected using quantitative metrics.

3.5. Effects of Model Collapse:

The harmful effects and consequences of model collapse are real and devastating. The loss of rare tokens and scenarios in their memory can erase minority group representation, which in turn narrows the diversity of model outputs and reinforces existing biases. The likelihood of factually incorrect outputs, undermining trust in high-stakes domains such as healthcare, law, and education, is greatly increased due to a rise in semantic drift and hallucination.[13] Along with that, late-stage collapse leads to embedding convergence,[7] reducing the model's ability to differentiate between contexts and degrading performance across a wide range of tasks. Overconfidence in incorrect answers further exacerbates harm by making failures less obvious to users. These effects collectively reduce the model's reliability, fairness, and alignment with real-world knowledge.

■ Monitoring Model Collapse

Monitoring model collapse is a key measure to ensure and protect the long-term reliability, fairness, and factuality of generative AI models.[2,13] It is seen that early-stage collapse is often invisible to conventional accuracy metrics because it first appears in rare or low probability outputs before affecting high frequency tokens. [2,12,13] It is noted that when collapse actually begins, its nature of self-reinforcing makes it difficult and costly to reverse, even in the smallest models.[2,7,10]

The stakes are greatly increased by environmental costs, as well as the retraining costs incurred.[14] The literature we studied identifies several monitoring approaches to catch collapse at this subtle stage. To compare these, this paper uses a four-factor evaluation scale, adapted from recurring evaluation priorities in the reviewed works:

1. **Sensitivity –** The ability to detect collapse onset before significant performance degradation on general benchmarks.
2. **Domain Adaptability –** A technique's efficacy across multiple domains, such as bio-med, financial, and legal.
3. **Computational Cost –** The resources that a method demands for continuous deployment and use.
4. **Diagnostic Depth –** The depth to which the method reveals not only the presence but also the likely cause of collapse.

Each method is rated High (H), Medium (M), or Low (L) for each factor, based on evidence from the reviewed literature.

4.1. Rare Token degradation:

Rare token degradation monitoring tracks and monitors a model's capability to be able to generate low-frequency tokens from its original training distribution.[2] These pertain to uncommon words, specialized domain terms, or even niche phrases that are more likely to disappear when models are trained recursively on synthetic outputs. For example, controlled recursion studies show token diversity decreasing sharply over generations, with rare vocabulary declining while common tokens persist.[12]

Rare tokens are much more sensitive to distributional drift than more naturally occurring frequent tokens, making them an early warning signal that often moves before overall benchmark accuracy.[13,15] In domain-specific continual pretraining (e.g., biomed), maintaining coverage of rare terms is critical; moreover, contamination between train and test sets can mask these early declines if not controlled.[7]

This method is applicable for use in both full pretraining and continual pretraining scenarios, particularly where domain-specific vocabulary is critical, such as in medicine or law.[2,12] Refer to Table 2 for a summary of the analysis.

Table 2: Rare Token degradation: Factor Ratings and Justifications. The table shows that rare-token–based metrics are a low-cost and sensitive early-warning signal for model collapse but offer limited diagnostic depth.

Factor	Rating	Justification
Sensitivity	High	It easily captures early signs of lexical narrowing, rare token loss, and tail erosion well before global accuracy drops.[2,12,10]
Domain Adaptability	Medium	This method works well across many fields but requires an extensively large list of rare tokens per domain (e.g., biomedical/legal), increasing setup time as it is quite time consumin.[16]
Computational Cost	Low	It could be run at evaluation time using fixed datasets (tail perplexity/recall and embedding drift checks), adding minimal overhead contrasted to retraining.[16]
Diagnostic Depth	Medium	It only picks up vocabulary loss and not the root cause unless paired with distributional or attribution analyses; training-data attribution helps trace whether drift stems from synthetic, duplicated, or contaminated sources.[7,10]

4.2. Embedding Drift Monitoring:

Embedding drift monitoring measures how the internal vector representation of rare or semantically important tokens changes across model checkpoints during training or continual pretraining. This method tracks cosine similarity between each token's current embedding and a reference embedding (usually from an early, pre-collapse checkpoint) to detect whether semantic meaning is eroding in the model's representation space.[10,16]

DOI: 10.36838/IJHSR87.54

For example, Dohmatob *et al.*[5] show that in over-parameterized regression models trained recursively on synthetic data, the parameter vector representing the ground-truth function progressively contracts toward zero when each generation is fit on independent data subsets. In their high-dimensional setup, this projection loses compounds over generations, leading the embeddings and thus the model's learned representation, to drift entirely away from the true target. By the later generations, the learned function norms drop close to that of a null predictor, confirming severe semantic drift.

Embedding drift is a structural health metric because embeddings encode semantic and syntactic relationships; distortions in their geometry often occur before surface-level performance declines. This allows it to be an early indicator of collapse that is sensitive to subtle degradation patterns invisible in perplexity or accuracy scores.[10,16]

Embedding drift is able to be used across domain-specific and domain-agnostic fields. It is valuable to implement this strategy for high-stakes fields (e.g., medical or legal NLP) where semantic precision is critical, as even small representational shifts can distort meaning in sensitive terms.[7] Refer to Table 3 for a summary of the analysis.

Table 3: Embedding Drift Monitoring: Factor Ratings and Justifications. The table shows that embedding drift is a highly sensitive and domain-agnostic indicator of early model collapse, offering strong diagnostic depth at moderate computational cost.

Factor	Rating	Justification
Sensitivity	High	Detects representational instability before it appears in text outputs; large embedding drift was observed generations before collapse in Dohmatob et al.'s regression experiments.[5]
Domain Adaptability	High	Works with any token set; only the reference embedding set needs to be domain-specific.[16]
Computational Cost	Medium	Requires periodic checkpoint saving and embedding-space comparisons; scales with vocabulary size but is less resource-intensive than full retraining.[10]
Diagnostic Depth	High	Can localize drift to specific token groups and, when paired with attribution tools, identify problematic synthetic data sources.[7]

4.3. Perplexity Gap Tracking:

Perplexity gap tracking compares a model's perplexity (PPL) over different token subsets, especially the long-tail, low-frequency portion, against its perplexity over the full evaluation set. The gap between these two scores acts as an early warning: a widening gap indicates that the model is losing the ability to predict rare or diverse sequences even if overall perplexity stays stable.[2,12]

For example, Shumailov *et al.*[2] conducted recursive training experiments and used the Wikitext-103 benchmark in them for assessment. While overall perplexity on the benchmark remained largely unchanged in early generations, tail perplexity climbed rapidly, reflecting the loss of low-probability events. This divergence between tail PPL and overall PPL appeared before standard benchmark accuracy degraded, confirming that the perplexity gap is an early indicator of collapse.

Perplexity gap tracking is effective because perplexity directly measures predictive uncertainty. Tail-specific perplexity magnifies the signal from low-frequency events, which are the first casualties of recursive synthetic training, making the gap a leading indicator of collapse risk.

Applicable in both general-domain and domain-specific benchmarks. Particularly useful in specialized areas like biomedical NLP, where monitoring perplexity on rare terminology is critical for early detection of semantic loss.[7] Refer to Table 4 for a summary of the analysis.

Table 4: Perplexity Gap Tracking: Factor Ratings and Justifications. The table shows that perplexity gap tracking provides a simple and scalable signal of distributional shift during model collapse, but is less sensitive to early-stage degradation compared to embedding or rare-token–based methods.

Factor	Rating	Justification
Sensitivity	High	It is able to identify tail-event degradation before full-set perplexity or accuracy drops.[2]
Domain Adaptability	Medium	It requires defining a tail-token list or tail-probability threshold for each domain.[12]
Computational Cost	Low	Uses standard evaluation runs; only requires calculating perplexity over token subsets, no retraining.[2]
Diagnostic Depth	Medium	Identifies tail loss, but not the exact cause without pairing with attribution or data-source analysis.[10]

4.4. Output Diversity Index (ODI) Monitoring:

ODI monitoring measures the diversity of generated outputs by computing metrics such as the number of type-token ratio and unique engrams or semantic cluster spread across a fixed set of prompts. The method detects when a model's responses begin favoring higher-probability sequences and forgetting rare cases or tokens, which is a sign of collapse.[10,12]

For example, Dohmatob *et al.*[5] note that in their experiments, the learned function's effective dimensionality shrinks each generation. This caused outputs to progressively increase the projection into a narrow subspace of possible responses, reducing variability in the predictions despite unchanged input diversity. By the final generations in their setup, the downstream model produced outputs statistically indistinguishable from a null predictor, reflecting minimal diversity.

ODI provides a direct behavioral signal of degeneration in generative space. Unlike perplexity-based metrics, which measure prediction uncertainty, ODI captures whether the range of content a model can produce is collapsing, even if the model remains confident in those fewer outputs.

This method applies to both text and non-text generative models (e.g., image diffusion models). In text, it is useful for domains requiring richness of expression, such as creative writing, policy drafting, or customer service, where repetition and narrowing of output styles are undesirable.

Additionally, ODI would apply to both text and non-text generative models. It would prove most useful where expressive range in writing matters, such as in creative writing, because ODI highlights early narrowing of output diversity.

Refer to Table 5 for a summary of the analysis.

Table 5: Perplexity Gap Tracking: Factor Ratings and Justifications. The table shows that perplexity gap tracking provides a simple and scalable signal of distributional shift during model collapse, but is less sensitive to early-stage degradation compared to embedding or rare-token–based methods.

Factor	Rating	Justification
Sensitivity	High	It is able to narrow the generative space before accuracy or perplexity shifts are visible.[5]
Domain Adaptability	High	It works for data like text, image, or code generation; domain-specificity only affects prompt design.[12]
Computational Cost	Medium	Requires generating and analyzing a large set of outputs periodically; cost grows with prompt set size.[10]
Diagnostic Depth	Medium	It as able to flag diversity loss but does not identify the cause without additional attribution or data-tracking tools.[7]

4.5. Benchmark Contamination Auditing:

Benchmark contamination auditing reviews whether training data contains material that overlaps with evaluation benchmarks. The technique works by matching similarities between benchmark items and training sets such as n-grams, hashes, or

embedding.[7] The problem is that contamination skews evaluation results, making it harder to detect early collapse because models can appear to perform well on benchmarks they have already "seen."

For example, Li *et al.*[7] reviewed that widely used benchmarks like PIQA and LAMBADA exhibited inflated accuracy scores when training data contained identical or near-identical items from those benchmarks. After removing these contaminated items, model performance dropped sharply in some cases by more than 20%, which revealed that earlier "good" results had masked underlying generalization problems. In the context of collapse monitoring, this means contamination can hide the early warning signs of degradation by artificially sustaining benchmark scores.

By ensuring benchmark cleanliness, contamination auditing removes a key source of false reassurance. It enables more accurate tracking of real model capabilities and makes collapse detection metrics, such as rare token loss or embedding drift, more reliable and accurate.

Works across general-purpose and domain-specific evaluation sets. Especially important in high-stakes testing environments (e.g., medical QA datasets), where contamination could make dangerous degradations invisible until they cause real-world harm. Refer to Table 6 for a summary of the analysis.

Table 6: Benchmark Contamination Auditing: Factor Ratings and Justifications. The table shows that benchmark contamination auditing is an extremely sensitive and broadly applicable method for uncovering hidden model degradation, even though it provides limited insight into root causes without follow-up analyses.

Factor	Rating	Justification
Sensitivity	High	It is able to reveal hidden degradation by removing artificial performance boosts from contaminated benchmarks.[7]
Domain Adaptability	High	It can be applied to any benchmark dataset with an accessible reference set.[7]
Computational Cost	Medium	It requires running similarity checks between large datasets, moderate overhead depending on detection method.[7]
Diagnostic Depth	Medium	It is able to identify the presence and extent of contamination but does not explain the underlying cause of performance drop without further analysis.[7]

4.6. Synthetic-to-Real Attribution Ratio (SRAR):

SRAR monitoring measures the proportion of synthetic versus original human-generated training sources based on a model's outputs. SRAR is able to achieve this through using influence functions, nearest-neighbor search in embedding space, data tracing tools, and other attribution methods.[10] If your ratio is increasing, it indicates that the model is relying more heavily on synthetic content, which often correlates with semantic drift and eventual collapse.

For example, Gerstgrasser *et al.*[10] applied an efficient attribution pipeline to track whether generations in LLaMA-derived models were anchored more in synthetic or real training segments. In their recursive training setup, later generations showed a marked increase in outputs whose nearest training neighbors were synthetic, even when those outputs appeared high-quality, signaling that the model's knowledge base was shifting away from human-grounded data.

SRAR directly quantifies the source composition behind outputs, making it a causal rather than purely correlational metric for collapse monitoring. This allows teams to detect shifts in data reliance before quality metrics degrade.

It can be applied to any model trained on mixed datasets, especially when synthetic loops are part of the training process. Particularly relevant for long-term model maintenance pipelines, where unintentional accumulation of synthetic traces can destabilize outputs. Refer to Table 7 for a summary of the analysis.

Table 7: SRAR: Factor Ratings and Justifications. The table shows that SRAR provides both early detection and strong diagnostic insight into model collapse by directly tracing degradation to rising reliance on synthetic data, at moderate computational cost.

Factor	Rating	Justification
Sensitivity	High	It is able to detect rising synthetic reliance before surface-level degradation appears.[10]
Domain Adaptability	High	It is able to function across domains if attribution-compatible datasets are available.[10]
Computational Cost	Medium	It requires storing embeddings for large portions of training data and running nearest-neighbor search.[10]
Diagnostic Depth	High	It is able to identify that degradation is occurring and why, by tracing it to synthetic data reliance.[10]

■ Model collapse mitigation

Mitigating model collapse is essential to ensuring the safe and effective use of AI systems, especially in high-stakes domains like law and medicine, where accuracy is critical and ethical risks leave no room for error.[2,8] Model collapse typically reduces output quality by promoting over-generalization, which undermines the reliability of AI in these sensitive fields. The compounding nature of collapse makes recovery more challenging and expensive, both monetarily and environmentally, as models must be retrained after they have been infected by collapse to a certain degree.[10]

It has been demonstrated that proactive measures like improved data curation, cautious use of synthetic data, and corrective mechanisms can slow or even reverse the effects of degradation[5]. Specifically, by eliminating collapse-inducing data from models without the need for retraining, our suggested machine unlearning technique provides a fresh and effective solution. This reduces resource usage and environmental impact in addition to restoring model performance.[8] To compare these strategies systematically, this paper evaluates them against four applied criteria drawn from recurring priorities in the reviewed literature:

Scalability – How well the approach performs when applied to large-scale, continuously updated models without prohibitive engineering or infrastructure changes.

Generalizability – An evaluation of the method's capacity to maintain or restore model quality across different data types, languages, and application domains, ensuring robustness beyond the environment in which it was originally designed or tested.

Detection-to-Action Speed – How quickly the strategy can be deployed after early collapse indicators appear, and how effectively it halts progression.

Sustainability and Cost Efficiency – The balance between computational, financial, and environmental costs versus the performance gains achieved.

Each strategy is rated High (H), Medium (M), or Low (L) for each criterion, based on evidence from the reviewed literature.

DOI: 10.36838/IJHSR87.54

5.1. Token-Level Editing:

Token-level editing is a form of post-processing that is narrower and is performed on model-generated text prior to the text being reintegrated into training. Its aims to circulate infrequent or domain-specific lexemes, to lessen the slip of factual accuracy, and to address long-tail thinning that is commonplace on recursive or synthetic-heavy training.[9,15,16]

Rather than accepting synthetic outputs exactly as they are, token-level editing selectively adjusts or replaces certain tokens, typically those that are overly generic or predicted with overly high confidence, to ensure that rare terms and factual anchors remain in the data. We found that this intervention actually preserves long-tail vocabulary, reduces the over-representation of common terms, and improves performance on de-contaminated validation sets,[15] reducing model collapse's effects. Moreover, we found that in recursive training without such controls, rare tokens disappear within a few generations.[2] Additionally, we find evidence that rare token embedding degradation can lead to broader representational collapse.[16] This makes token-level editing an effective way to interrupt collapse processes before they spread through the model's distribution.

This technique can be used in biomedical, legal, and financial domains to maintain coverage of rare or domain-critical terms, such as uncommon disease names, niche legal terminology, or rare financial instruments, when training large language models (LLMs). It can also be applied in multimodal models used in scientific and industrial contexts, where editing captions or answers preserves fine-grained object labels, specialist descriptors, or experimental terms across iterations. In VAEs and diffusion models used in creative and cultural preservation, editing local elements, such as patches that can help maintain stylistic diversity, heritage patterns, and less frequent visual motifs that could otherwise be lost through repeated synthetic reuse. Refer to Table 8 for a summary of the analysis.

Table 8: Token-Level Editing: Factor Ratings and Justifications. The table shows that token-level editing enables rapid, targeted intervention to mitigate early collapse signals, offering high generalizability and fast detection-to-action speed, but with moderate scalability and ongoing computational cost.

Factor	Rating	Justification
Scalability	Medium	It can be integrated into large-scale pipelines but requires probability estimation and token-level modifications across vast datasets, which increases processing overhead for continuously updated models.[15]
Generalizability	High	It can be applied to a wide range of domains and modalities, including text, multimodal captions, and even latent edits in generative models, with adaptation of editing criteria to domain-specific rare terms or features.[2]
Detection-to-Action Speed	High	Token editing can be triggered immediately upon detecting high-confidence overuse of generic tokens or loss of rare tokens, allowing for rapid corrective action before degradation spread.[15]
Sustainability and Cost Efficiency	Medium	More cost-efficient than full retraining and reduces long-term collapse risks, but continuous token-level scoring and selective resampling carry non-trivial computational costs at scale.[9,16]

5.2. Hybrid Training with Real and Synthetic Data:

Hybrid training encompasses combining high-quality human data with carefully controlled synthetic data during pretraining or continual updates. The method's goal is to expand coverage and reduce costs while avoiding the long-tail erosion and distribution shift seen in purely synthetic or recursive training.[9,15]

Hybrid training works by integrating vetted synthetic data into human data pipelines while enforcing safeguards to maintain distributional integrity. Gerstgrasser *et al.*[10] show that accumulating human data alongside new samples each round keeps test error bounded, whereas replacing earlier data causes error to grow over time.[5] and Zhu *et al.*[15] recommend gating synthetic content through selection or editing to preserve rare events and factual anchors, since naive mixing can distort scaling laws and truncate the long tail. These safeguarding techniques aid in preventing the consequences of model collapse, such as the loss of rare tokens and divergence from human distributions.[2,9]

This method can be used in biomedicine, law, and economic forecasting to ensure that LLMs retain rare clinical terms, jurisdiction-specific legal precedents, and low-frequency economic scenarios by blending curated human corpora with vetted synthetic continuations. It can also be applied to VAEs and diffusion models in scientific imaging and creative industries to preserve morphological diversity in medical scans, variability in architectural models, and stylistic range in art generation. In multimodal systems for specialized manufacturing and environmental monitoring, hybrid training helps maintain rare component labels, species identifiers, or environmental event descriptors by combining human-authored text and images with high-quality synthetic examples. Refer to Table 9 for a summary of the analysis.

Table 9: Hybrid Training with Real and Synthetic Data: Factor Ratings and Justifications. The table shows that hybrid training offers a highly scalable and sustainable long-term mitigation strategy against model collapse, balancing cost efficiency and generalizability, though it relies on prior detection signals to guide intervention.

Factor	Rating	Justification
Scalability	High	It is designed and built to work in large-scale, continuously updated pipelines by mixing curated human and synthetic data. Accumulation-based integration avoids prohibitive retraining cycles while maintaining data diversity.[10]
Generalizability	High	This is applicable across domains (biomedicine, law, economics, creative industries) and modalities (text, image, multimodal) by adjusting synthetic-data gating and selection criteria to domain-specific need.[2,15]
Detection-to-Action Speed	Medium	It needs prior detection of drift or model collapse indicators to adjust synthetic-to-human ratios, making it slightly slower to respond than purely post-processing intervention.[5]
Sustainability and Cost Efficiency	High	It is able to decrease the environmental and financial costs compared to full retraining by supplementing human datasets with vetted synthetic samples, while retaining rare-event coverage to prevent costly collapse recovery.[9,10]

5.3. Confidence-Based Filtering:

Confidence-based filtering is a technique applied to synthetic or model-generated data before it is used for further training. It can be classified as a quality control process as it removes low-quality, error-prone, or hallucinated outputs by evaluating the model's own confidence scores for each token or sequence. This method limits the spread of errors that could otherwise accelerate model collapse by excluding samples that the model is either uncertain about or confidently wrong on.[2,7,15]

Confidence-based filtering works by assigning a probability or confidence score to generated outputs and uses that score to decide whether the sample is edited, discarded, or kept. We see that removing low-confidence synthetic samples before training reduces noise and prevents the model from reinforcing incorrect patterns.[7] Furthermore, Zhu *et al.*[15] notes that in recursive setups, even small quantities of low-quality synthetic data can distort token distributions over time. Additional Shumailov *et al.*[2] emphasizes that collapse often starts with rare, low-probability events, making confidence-based screening a way to protect correctly generated rare events and discard unreliable ones. By enforcing quality thresholds, this method helps keep the training distribution stable.

This mitigation strategy is applicable in biomedical, legal, and financial domains as it can filter synthetic outputs for tasks such as clinical summarization, case law referencing, or market forecasting in LLMs, ensuring only high-confidence and accurate samples are used in training. Moreover, it can be used in multimodal models for scientific and industrial applications, where screening low-confidence captions or answers preserves the accuracy of fine-grained object descriptions, technical annotations, and experimental data. In VAEs and diffusion models for creative or research purposes, proxy confidence measures such as reconstruction likelihood or discriminator scores can be used to remove off-distribution or low-quality samples, maintaining diversity and coherence in generated outputs. Refer to Table 10 for a summary of the analysis.

Table 10: Confidence-Based Filtering: Factor Ratings and Justifications. The table shows that confidence-based filtering enables fast, pre-training intervention to block low-quality synthetic data, offering high generalizability and rapid response, but with moderate scalability and ongoing computational cost.

Factor	Rating	Justification
Scalability	Medium	Can be applied to large-scale pipelines, but continuous confidence scoring for every token or sequence increases computational overhead as dataset size grows.[7,15]
Generalizability	High	Works across text, multimodal, and generative models by adapting confidence metrics (e.g., token log-probabilities, reconstruction likelihoods, discriminator scores) to domain-specific outputs. [7]
Detection-to-Action Speed	High	Provides immediate quality gating at the point of data generation, allowing faulty outputs to be removed or corrected before entering the training pipeline.[15]
Sustainability and Cost Efficiency	Medium	Reduces long-term collapse recovery costs by preventing noisy data integration, but constant scoring and thresholding introduce ongoing computational expenses.[7]

5.4. Curated Data Selection Pipelines:

Curated data selection pipelines are structured processes for building training datasets that deliberately balance content diversity, quality, and representation. The pipelines are able to organize, filter, and then prioritize both human-generated and synthetic data using pre-defined, adjustable criteria that the training distribution maintains important rare events, factual consistency, and domain coverage.[17] Moreover, this aims to prevent the distributional drift and long-tail loss reported when models rely heavily on uncontrolled synthetic data sources.[2,15,18]

Curated pipelines usually work by selecting and screening data before it's entered into the training corpus. Mattioli *et al.*[18] shows that automated embedding signals usually give a misleading impression of data quality, showcasing that pipelines benefit from robust and strong layers of validation to make sure that filtering decisions preserve a meaningful and diverse set of training data. Zhu *et al.*[15] emphasize that the targeted inclusion of rare or domain-specific samples, especially in recursive or hybrid setups, can slow the erosion of the long tail. Furthermore, this also removes repetitive or low-quality synthetic sequences and stabilizes scaling trends. Shumailov *et al.*[2] show that recursive training without such curation leads to progressive narrowing of token frequency distributions and disappearance of low-probability items. By ensuring every refresh or augmentation of the dataset passes through a robust curation framework, the model is able to retain an increased amount of coverage and resist collapse dynamics.

This method can be applied in biomedical, legal, and economic domains to ensure datasets contain balanced coverage of rare disease cases, jurisdiction-specific rulings, and low-frequency market scenarios when training LLMs. It can be used in scientific and technical multimodal systems to maintain representation of infrequent object classes, rare environmental events, or specialist equipment by curating both text and image data. For VAEs and diffusion models used in creative industries and cultural preservation, curated pipelines can be designed to preserve underrepresented artistic styles, heritage motifs, or rare visual elements in generative datasets, ensuring diversity and authenticity in outputs. Refer to Table 11 for a summary of the analysis.

Table 11: Curated Data Selection Pipelines: Factor Ratings and Justifications. The table shows that curated data selection pipelines provide a generalizable and robust safeguard against model collapse by maintaining balanced, high-quality datasets, though they trade real-time responsiveness for moderate scalability and operational cost.

Factor	Rating	Justification
Scalability	Medium	Its automated filtering is able to scale well to large datasets, however incorporating human-in-the-loop validation for high-stakes domains increases operational complexity at scale.[15,18]
Generalizability	High	This method could be adapted to text, multimodal, and domain-specific datasets adjustable selection criteria, ensuring balanced coverage through of rare events and domain-critical data.[2,18]
Detection-to-Action Speed	Medium	It is able to detect and correct imbalances during dataset refreshes or augmentation cycles rather than in real time, making it slower than inline filtering approaches.[15]
Sustainability and Cost Efficiency	Medium	It is able to prevent costly retraining due to drift by maintaining balanced datasets, but ongoing validation and quality assurance incur moderate resource costs.[18]

5.5. Accumulation over Replacement in Iterative Training:

Accumulation over replacement is a data management strategy implemented in iterative training cycles where new training data is added to the existing dataset rather than replacing older data. The strategy aims to preserve valuable historical information, especially rare or low-frequency events, while still allowing the model to learn from new, diverse samples. This approach directly counters the error growth and long-tail loss observed when prior data is discarded in favor of new inputs during repeated fine-tuning or pretraining rounds.[10]

The principle is simple: maintain the cumulative dataset across training iterations, ensuring that each cycle retains all previously collected high-quality data alongside the newly added samples. This approach keeps test error bounded over many training generations, while replacement strategies cause error to grow linearly with each iteration.[10] Through retaining older data, accumulation ensures that domain-specific or rare content remains part of the distribution, in turn, reducing the likelihood of semantic drift or collapse. Shumailov *et al.*[2] investigate and find that replacing data in recursive setups accelerates the disappearance of low-probability tokens, allowing accumulation to be a direct countermeasure. Furthermore, accumulation can also be combined with other safeguards, such as curated selection or confidence-based filtering, to ensure that the growing dataset remains balanced and high quality.

This strategy can be used in biomedical, legal, and financial domains to keep rare disease case notes, jurisdiction-specific precedents, or low-frequency market events in the training set for LLMs across multiple updates. It can be applied in scientific multimodal systems to maintain infrequent object classes, rare environmental conditions, or specialized equipment annotations in both text and image modalities over successive training cycles. For VAEs and diffusion models in creative

DOI: 10.36838/IJHSR87.54

industries or cultural preservation, accumulation ensures that underrepresented motifs, styles, and niche subject matter remain in the dataset across model refreshes, aiding in preventing stylistic homogenization and mode collapse. Refer to Table 12 for a summary of the analysis.

Table 12: Accumulation over Replacement in Iterative Training: Factor Ratings and Justifications. The table shows that accumulation-based training is a highly scalable and generalizable strategy for mitigating model collapse by preserving rare and historical data across iterations, though it trades immediate responsiveness for moderate long-term resource costs.

Factor	Rating	Justification
Scalability	High	The approach integrates seamlessly into large-scale, continuously updated training pipelines, as adding new data to existing datasets avoids complex replacement logic and maintains stability over many iterations.[16]
Generalizability	High	It is quite effective across textual, multimodal, and generative domains by preserving both general and domain-specific rare content, ensuring robustness beyond the original application scope. [2]
Detection-to-Action Speed	Medium	It operates and works on an iteration-by-iteration basis, preserving rare data without requiring prior drift detection, but cannot react mid-cycle to emergent collapse signs.[16]
Sustainability and Cost Efficiency	Medium	Reduces retraining costs by avoiding loss of historical data, but ongoing storage and processing requirements grow with each cycle, adding to long-term resource usage.[2]

5.6. Synthetic Data Verification / Tail Preservation:

Synthetic data verification and tail preservation are a combination of two methods that ensure that synthetic samples added to the training dataset are of high quality and capable of maintaining coverage of rare, low-frequency events. The verification step focuses on screening synthetic outputs for factual accuracy, relevance, and cohesion. Moreover, tail preservation ensures that uncommon tokens, domain-specific terms, or rare features remain represented in the training distribution.[15,16]

Synthetic data verification begins with the generation of candidate synthetic samples, which are then assessed using a combination of automated quality metrics, human evaluation, or model-based tools to ensure factual accuracy and alignment with domain-specific requirements. However, if this is left unverified, synthetic data can distort token distributions, especially during recursive training by overrepresenting frequent patterns and diminishing the long tail.[15]

To counter this, verification filters are employed to remove or modify low-quality outputs, while tail-preservation mechanisms deliberately incorporate rare tokens sourced from domain glossaries or apply controlled resampling techniques to boost the representation of low-frequency content. Shumailov *et al.*[2] and Yu *et al.*[16] emphasize that maintaining rare token usage is vital for preventing embedding drift and preserving semantic diversity, both of which serve as early safeguards against model collapse.

Synthetic data verification can be implemented in biomedical, legal, and financial datasets to ensure that synthetic training data includes verified, high-accuracy outputs while preserving rare terminology such as uncommon disease names, niche case law terms, or infrequent financial instruments in large language models (LLMs). In scientific and technical multimodal systems, it can maintain coverage of rare experimental conditions, specialist equipment labels, or infrequent object classes by verifying and supplementing both text and image synthetic data. For VAEs and diffusion models in creative and cultural preservation, verification ensures synthetic samples meet authenticity and stylistic quality standards, while tail-preservation techniques maintain representation of rare artistic motifs, heritage designs, or niche cultural symbols that might otherwise vanish through repeated synthetic reuse.

Refer to Table 13 for a summary of the analysis.

Table 13: Synthetic Data Verification / Tail Preservation: Factor Ratings and Justifications. The table shows that synthetic data verification with tail-preservation mechanisms provides a generalizable and preventative safeguard against rare-token loss, though it introduces moderate scalability and cost trade-offs due to ongoing verification requirements.

Factor	Rating	Justification
Scalability	Medium	It could be integrated into large-scale pipelines, but verification and tail-preservation steps require additional processing such as automated scoring, human review, or targeted resampling, which can become resource-intensive at scale.[15]
Generalizability	High	It is adaptable across domains and modalities by adjusting verification criteria and rare-token lists to domain-specific requirements (e.g., biomedical glossaries, legal terminology, cultural heritage motifs).[2,16]
Detection-to-Action Speed	Medium	The quality verification can occur at the point of data generation, but tail-preservation measures often rely on periodic corpus audits rather than instant correction, which slows reaction to new collapse indicators.[15]
Sustainability and Cost Efficiency	Medium	Prevents costly retraining by ensuring synthetic data quality and rare-token retention, but ongoing verification and controlled resampling introduce moderate computational and financial costs.[2,16]

5.7. Data Deduplication and Multiplicity Control:

Data deduplication and multiplicity control are dataset management techniques aimed at reducing redundancy and excessive repetition in training data. Deduplication focuses on identifying and removing exact or near-duplicate samples, while multiplicity control addresses over-representation of similar patterns or repeated content in different forms. Both methods work to preserve diversity in the training distribution and avoid the representation collapse that can occur when models are repeatedly exposed to the same information.[2,5,15]

Excessive repetition in training datasets can bias model representations toward over-frequent features, leading to semantic narrowing and reduced capacity to generate rare or diverse outputs. Zhu *et al.*[15] show that data multiplicity, repeated exposure to the same or nearly identical data, can degrade model performance even if the duplicated data is high-quality, as it shifts probability mass away from the long tail. Deduplication uses exact matching, fuzzy matching, or embedding-based similarity to remove identical or overly similar samples. Multiplicity control goes further by monitoring dataset composition and capping the frequency of highly similar sequences, ensuring a balanced distribution of common and rare elements. Shumailov *et al.*[2] highlights that unchecked repetition exacerbates collapse in recursive setups, as duplicated content becomes disproportionately dominant. By enforcing these controls, the dataset maintains semantic variety and supports stable generalization.

This approach can be used in biomedical, legal, and financial domains to prevent models from overfitting to a small subset of frequently repeated documents, such as common clinical case summaries, boilerplate legal clauses, or widely circulated financial reports, thereby preserving the capacity to handle rare and novel cases in LLMs. In scientific and technical multimodal systems, deduplication and multiplicity control can ensure balanced representation of rare object classes, unique environmental events, or specialist equipment annotations in both text and image data. For VAEs and diffusion models in creative industries and cultural preservation, these techniques help maintain stylistic diversity by preventing certain motifs, genres, or cultural symbols from dominating the training corpus, re-

ducing the risk of mode collapse and homogenized outputs. Refer to Table 14 for a summary of the analysis.

Table 14: Data Deduplication and Multiplicity Control: Factor Ratings and Justifications. The table shows that deduplication and multiplicity control are broadly applicable safeguards against redundancy-driven collapse, offering stable long-term benefits while incurring moderate computational overhead.

Factor	Rating	Justification
Scalability	Medium	This technique can be scaled to large datasets using automated matching and similarity search, but embedding-based approaches are computationally heavy for massive corpora.[5,5]
Generalizability	High	It is applicable across text, multimodal, and generative datasets, with customization of similarity thresholds and frequency caps to fit domain-specific needs. [15]
Detection-to-Action Speed	Medium	Repetition and over-representation can be detected quickly with automated scanning, but full remediation often requires periodic batch processing rather than immediate correction.[5]
Sustainability and Cost Efficiency	Medium	It helps avoid the high costs of retraining from distributional collapse caused by redundancy, but frequent large-scale similarity computations can be resource-intensive.[2]

Discussion

(Note that all ideas discussed in this section are theoretical and not tested or proven to work)

6.1. Hybrid Monitoring Framework for Early Detection and Diagnosis of Model Collapse:

Now that we have delved into all monitoring methods and delved into their strengths and weaknesses (check section 4), we infer that they might work best if paired all together. For example, embedding drift or output diversity is able see how model behavior and internal representations are changing. Benchmark hygiene and attribution checks ensure that these signals reflect real degradation rather than noise or data leakage.[10,15] Additionally, there are other notable signals like tail-focused rare-token metrics that respond quickly when collapse begins.[2,16] Drawing on these complementary strengths, we outline a hybrid monitoring approach that combines fast, lightweight detection with deeper, periodic diagnostics and evaluation safeguards.

We suggest a hybrid monitor that blends deeper, recurring probes with light, always-on checks. As a first line of defense, we could monitor the perplexity gap between rare tokens and the entire set, as well as coverage and recall of rare tokens that are focused on the tail. While headline accuracy stays constant, early collapse frequently manifests as a fading long tail. Twelve. We could apply embedding-drift tests to a limited, carefully chosen set of crucial terms to determine what might be drifting. These would draw attention to modifications in internal representations before the emergence of surface-level errors.[16] We could run a monthly output-diversity panel to monitor for narrowing in generated outputs as a behavioral guardrail.[12] We would combine these with benchmark de-contamination to guarantee that assessments continue to be trustworthy. We could also estimate reliance on synthetic training neighborhoods by including a small synthetic-to-real attribution ratio (SRAR) sample when synthetic data is available.[10,15] We could try to gather actual data during iteration instead of replacing it, since theory and experiments indicate that this helps avoid the feedback loop that causes collapse.[10] Ultimately, when comparing these approaches, we found that each is ineffective in a particular area where another approach excels. As a result, we came to the conclusion that each approach was complementary to the others and considered combining these elements into a collapse-aware benchmark: a small prompt panel for diversity, a periodic drift or attribution slice, a fixed rare-token set for tail perplexity and recall (see Figure 3 for workflow). [2,15,16] However, a key limitation of this hybrid system is scalability. Running multiple overlapping monitors, such as attribution and drift checkers, becomes increasingly computationally heavy and expensive as model size and deployment scale grow with every check, limiting its feasibility for constant use.



Figure 3: Hybrid Monitoring Framework workflow. The figure illustrates an end-to-end hybrid framework that combines continuous monitoring, attribution, validation, and targeted intervention to detect, diagnose, and mitigate model collapse and hallucination risks across the full training–deployment lifecycle.

6.2. Model Unlearning for Collapse Mitigation:

Model unlearning is a technique that removes the influence of specific training data from a model's parameters without retraining from scratch. Model unlearning operates after training by modifying the model, so it behaves as though specific data had never been seen, rather than blocking problematic data beforehand.[8]

Model unlearning can be used to remove collapse-inducing data, such as over-represented synthetic samples, duplicated low-quality segments, or domain-specific content that has been degraded through recursive training. By selectively erasing the influence of this data, it may be possible to restore balance in the training distribution, recover lost diversity in rare tokens or features, and slow the progression of collapse. For example, in a biomedical question-answering model, unlearning can target repeatedly recycled synthetic case summaries that distort the overall variety of disease terminology. Periodic unlearning cycles could act as a "repair" stage in long-lived LLMs or multimodal systems when collapse indicators such as rare-token erosion or embedding drift reach a critical threshold.

Current unlearning work has mostly targeted privacy and compliance scenarios, such as meeting GDPR "right to be forgotten" requests. Applying it to model collapse raises open research questions:

- Whether unlearning can restore degraded embedding geometry and long-tail coverage.
- How to reliably identify collapse-inducing data segments.
- The maximum degree of recovery possible in late-stage collapse.

DOI: 10.36838/IJHSR87.54

- Developing scalable unlearning methods for multi-billion-parameter models.

Furthermore, model unlearning for collapse mitigation also has its drawbacks. Firstly, it needs extremely precise identification of harmful data, and errors could eliminate useful information, potentially leading to secondary distributional shift. Unlearning algorithms in use today are computationally costly and might not scale well. In particular, current techniques struggle to scale to multi-billion parameter models where unlearning steps become much slower and memory-intensive, and the intensive computational load may lead to the model becoming economically and environmentally unsustainable due to increased energy and cooling use as well as hardware demands.

6.3. Hallucination Tracking as an Early Collapse Signal:

Hallucination tracking methodically logs and examines situations in which a model produces content that is unsupported or factually inaccurate. It offers a behavioral indicator of model reliability over time by concentrating on the frequency, seriousness, and confidence of these errors.

Hallucinations could be a precursor to collapse. Particularly in rare or long-tail knowledge domains, models frequently generate more high-confidence but inaccurate outputs as token distributions get smaller and factual grounding deteriorates. Monitoring hallucination patterns may indicate the beginning of a collapse before more conventional indicators like token coverage or perplexity show appreciable shifts. This can be done by monitoring changes in hallucination rates along with other collapse metrics and conducting regular, domain-specific fact-checking evaluations against fixed reference sets (e.g., biomedical QA, legal facts).

The predictive value of hallucination detection for model collapse remains uncertain, despite its exploration for general AI reliability. Examining the relationship between recorded collapse events and hallucination patterns is one of the main areas of research.

- Creating scalable, automated pipelines for hallucination detection for ongoing observation.
- Assessing whether collapse risk across domains can be predicted by hallucination patterns in one domain.

Moreover, hallucination tracking as an early collapse signal also has its drawbacks. Firstly, false positives can occur in hallucination tracking caused by unrelated problems (prompting, retrieval errors), as well as false negatives on certain specific sub-domains. This, in turn, increases the computational cost of an already expensive tool, potentially making it economically unsustainable. Additionally, the method may face scalability challenges since constant fact-checking and high-frequency monitoring would become increasingly resource-intensive as model domains expand, making it environmentally unsustainable as well, given the energy demands associated with large-scale interference and verification.

■ Conclusion

A serious long-term risk to the dependability, equity, and factual foundation of generative AI systems is model collapse. Particularly in fields that require accuracy and domain coverage, the risk of distributional drift, rare-token loss, and embedding degradation increases as models are trained on their own outputs more frequently. This study examined the theoretical foundations of collapse, reviewed early detection techniques such as output diversity metrics, rare-token monitoring, perplexity gap tracking, and embedding drift analysis (refer to Table 15 for the summary of the analysis), and assessed a variety of mitigation techniques, including hybrid training, token-level editing, confidence-based filtering, curated data pipelines, accumulation, verification, and multiplicity control.

Building on this framework (refer to Table 16 for the summary of the analysis), we suggested two more lines of inquiry: hallucination tracking as a behavioral early-warning signal and machine unlearning to eliminate data that causes collapse after training. Both offer promising avenues, but further empirical investigation is required to determine their viability, scalability, and reliability for integration into large-scale AI development pipelines. Importantly, we also highlighted the shortcomings of the existing methods, including the computational cost of unlearning and the potential ambiguity in hallucination detection.

Our study showcases that no single approach is sufficient to prevent or reverse collapse. Instead, a robust strategy must include supplementary monitoring and mitigation tools, supported by continuous evaluation and domain-aware dataset management. For high-stakes applications in industries like medicine, law, finance, science, and cultural preservation, ensuring that generative models retain their accuracy, diversity, and dependability over the course of their operational lifetimes is not only a technical challenge but also an ethical requirement. However, the paper does not come without limitations.

This paper has several limitations. Experimental validation of the proposed Hybrid Monitoring Framework and Model Unlearning strategy was beyond the scope of this work, so both remain conceptual and grounded in analysis of existing empirical studies rather than controlled experimentation. In addition, the absence of a unified benchmark and the scarcity of detailed performance comparisons in the literature limited quantitative evaluation. Finally, research on model collapse remains fragmented and inconsistently reported, underscoring the need for more empirical studies, standardized benchmarks, and clearer reporting practices to establish reliable detection and mitigation strategies.

In the end, model collapse will require a shift from reactive fixes to proactive design, where data governance, quality assurance, and long-term distributional stability are incorporated into the development process. By combining advances in detection, mitigation, and post-hoc repair, the AI research community can develop systems that can withstand current challenges and long-term deployment pressures in an increasingly synthetic data ecosystem.

Table 15: All monitoring efforts analysis summary. Overall, hybrid training performs best due to its strong scalability, generalizability, and sustainability, while token-level editing performs worst overall as its moderate scalability and cost efficiency limit its effectiveness despite fast detection-to-action speed.

Method	Sensitivity	Domain Adaptability	Computational Cost	Diagnostic Depth
Rare token degradation	High	Medium	Low	Medium
Embedding drift monitoring	High	High	Medium	High
Perplexity gap tracking	High	Medium	Low	Medium
ODI monitoring	High	High	Medium	Medium
Benchmark contamination	High	High	Medium	Medium
Auditing	High	High	Medium	Medium
SRAR	High	High	Medium	High

Table 16: All mitigation efforts analysis summary. Overall, SRAR performs best due to its high sensitivity, strong domain adaptability, and high diagnostic depth, while rare token degradation performs worst overall as its limited domain adaptability and moderate diagnostic depth reduce its effectiveness despite low computational cost.

Method	Scalability	Generalizability	Detection-to-Action Speed	Sustainability & Cost Efficiency
Token-Level Editing	Medium	High	High	Medium
Hybrid Training	High	High	Medium	High
Confidence-Based Filtering	Medium	High	High	Medium
Curated Data Selection Pipelines	Medium	High	Medium	Medium
Accumulation over Replacement	High	High	Medium	Medium
Synthetic Data Verification / Tail Preservation	Medium	High	Medium	Medium
Data Deduplication & Multiplicity Control	Medium	High	Medium	Medium

■ Acknowledgments

I sincerely and wholeheartedly thank Professor Siddharth Krishnan and Dr. Plinio Zanini for their rigorous mentoring, productive feedback, and academic advice during the process of writing this paper. Their understanding, perspectives, and expertise were integral for this paper to even be written. Furthermore, I deeply appreciate the platform that the IRIS program has meticulously developed to create a venue that promotes inquisitiveness and critical thinking.

Last but not least, I extend my deepest thanks to the academic researchers whose papers and studies were the bones and the foundation of my own paper. Their work was and will always continue to be a fascinating topic of discussion. Furthermore, I attest to the idea that the graphics and writings in this paper are entirely my own.

■ References

1. NVIDIA. What is Generative AI? | NVIDIA. NVIDIA. https://www.nvidia.com/en-us/glossary/generative-ai. (accessed 2025-12-17).
2. Shumailov, I.; Shumaylov, Z.; Zhao, Y.; Gal, Y.; Papernot, N.; Anderson, R. The Curse of Recursion: Training on Generated Data Makes Models Forget. arXiv. https://doi.org/10.48550/arXiv.2305.17493.
3. META. Meta Platforms, Inc. Meta | Social technology company. https://www.meta.com/en-gb/about/?srsltid=AfmBOopMAuQZ-5tehzkVath6eWVD-_vAiwbojveyj4Se5KolZ3HZomMIE.
4. OpenAI. OpenAI. OpenAI. https://openai.com.
5. Dohmatob, E.; Feng, Y.; Yang, P.; Charton, F.; Kempe, J. A Tale of Tails: Model Collapse as a Change of Scaling Laws. arXiv.org. https://arxiv.org/abs/2402.07043.
6. Devansh. Addressing one of the Biggest Misunderstandings in AI. Medium. https://machine-learning-made-simple.medium.com/addressing-one-of-the-biggest-misunderstandings-in-ai-4d627821346.
7. Li, Y.; Lin, Z.; Yin, F.; Zhang, M. M. Preventing Model Collapse in Gaussian Process Latent Variable Models. arXiv.org. https://arxiv.org/abs/2404.01697.
8. Bourtoule, L.; Chandrasekaran, V.; Choo, C.; Jia, H.; Travers, A.; Zhang, B.; Lie, D.; Papernot, N. Machine Unlearning. ieeexplore.ieee.org. https://ieeexplore.ieee.org/abstract/document/9519428.
9. Roman, D. The Collapse of GPT. Acm.org 2025. https://doi.org/10.1145//3722476.
10. Gerstgrasser, M.; Schaeffer, R.; Dey, A.; Rafailov, R.; Sleight, H.; Hughes, J.; Korbak, T.; Agrawal, R.; Pai, D.; Gromov, A.; Roberts, D. A.; Yang, D.; Donoho, D. L.; Koyejo, S. Is Model Collapse Inevitable? Breaking the Curse of Recursion by Accumulating Real and Synthetic Data. arXiv.org. https://doi.org/10.48550/arXiv.2404.01413.
11. Twenty. AI Hallucinations vs Human Error. Twenty-four.it. https://www.twenty-four.it/insights/ai-hallucinations.
12. Villalobos, P.; Sevilla, J.; Heim, L.; Tamay Besiroglu; Marius Hobbhahn; Anson. Will We Run Out of Data? An Analysis of the Limits of Scaling Datasets in Machine Learning. arXiv (Cornell University) 2022. https://doi.org/10.48550/arxiv.2211.04325.
13. Feng, Y.; Dohmatob, E.; Yang, P.; Charton, F.; Kempe, J. Beyond Model Collapse: Scaling Up with Synthesized Data Requires Verification. arXiv.org. https://arxiv.org/abs/2406.07515.
14. Hao, K. Training a single AI model can emit as much carbon as five cars in their lifetimes. MIT Technology Review. https://www.technologyreview.com/2019/06/06/239031/training-a-single-ai-model-can-emit-as-much-carbon-as-five-cars-in-their-lifetimes.
15. Zhu, X.; Cheng, D.; Li, H.; Zhang, K.; Hua, E.; Lv, X.; Ding, N.; Lin, Z.; Zheng, Z.; Zhou, B. How to Synthesize Text Data without Model Collapse? arXiv.org. https://arxiv.org/abs/2412.14689.
16. Yu, S.; Song, J.; Kim, H.; Lee, S.; Ryu, W.-J.; Yoon, S. Rare Tokens Degenerate All Tokens: Improving Neural Text Generation via Adaptive Gradient Gating for Rare Token Embeddings. Proceedings of the 60th Annual Meeting of the Association for Computational Linguistics (Volume 1: Long Papers) 2022. https://doi.org/10.18653/v1/2022.acl-long.3.
17. PaperPile. Data Curation Pipeline. @emergentmind. https://www.emergentmind.com/topics/data-curation-pipeline.
18. Mattioli, L.; Ait-Hadichou, Y.; Chaouche, S.; Gonzalez, M. Data Curation Matters: Model Collapse and Spurious Shift Performance Prediction from Training on Uncurated Text Embeddings. Arxiv.org. https://arxiv.org/html/2506.17989v1.

■ Author

Murtaza S. Malik is an enthusiastic and extremely passionate research student fascinated with the field of AI. He aims to contribute to future AI policy and test his proposed solutions to model collapse as well as examining the economic and social effects of an AI-driven workforce.

DOI: 10.36838/IJHSR87.54

IJHSR
ijhighschoolresearch.org
RESEARCH ARTICLE

Predicting the Prognosis of Ulcerative Colitis with Machine Learning

Aayushi Saxena

The Lawrenceville School, 2500 Main St., Lawrenceville, New Jersey, 08648, USA; aayushi.saxena.me@gmail.com
Mentor: Rosalyn Abbott

ABSTRACT: Ulcerative Colitis is a chronic inflammatory bowel disease with unpredictable progression, often requiring invasive and costly procedures (e.g., colonoscopy) for monitoring. This study developed a Support Vector Machine classification model that integrates histological information (i.e., clinically established biomarkers), treatment history, lifestyle factors, and demographic variables to classify UC severity. First, a prototype was developed using a synthetic dataset of 50 simulated patient profiles containing age, calprotectin levels, and disease severity scores. The pipeline successfully classified unseen inputs, confirming basic functionality. This prototype was migrated to a clinician-facing web platform, which allows users to upload datasets, determine a train-test split, select the target variable, and visualize performance metrics. Validation with a publicly available biomedical drug-classification dataset yielded 90.0% accuracy and 91.3% precision, demonstrating system reliability. These results show that the platform can manage end-to-end workflows in a scalable and interpretable way. Once UC-specific patient datasets are incorporated, the system will be expanded to enable clinicians to input live patient data and receive severity predictions and relapse risk estimates. By considering a variety of factors, this tool has the potential to reduce reliance on invasive procedures, improve monitoring efficiency, and advance precision medicine approaches for UC management.

KEYWORDS: Computational Biology and Bioinformatics, Computational Biomodelling, Machine Learning, Ulcerative Colitis, Prognosis.

Introduction

Ulcerative Colitis (UC) is a chronic, idiopathic inflammatory bowel disease (IBD) that causes continuous mucosal inflammation in the colon and rectum.[1] While some risk factors, such as diet, stress, genetics, and microbiota, are correlated with inflammation, UC remains largely unpredictable in its progression. Associated symptoms (including bloody diarrhea, tenesmus, and abdominal pain) typically overlap with other gastrointestinal (GI) disorders, necessitating diagnostic tools such as colonoscopy, biopsy, and imaging, which are often invasive, expensive, and not practical for frequent monitoring.[2]

Despite advancements in treatment, patients remain at high risk for relapse, complications, and long-term consequences such as toxic megacolon and colorectal cancer.[3] Non-invasive biomarkers are increasingly used to monitor inflammation, but as stand-alone tools, they lack the specificity and sensitivity required to reliably predict prognosis.

Recent literature has explored novel biomarkers and applied machine learning techniques to IBD, yet relatively few studies focus specifically on prognosis prediction in UC using clinically relevant biomarkers in combination with demographic and lifestyle data. Moreover, many existing studies emphasize model development without addressing how such tools can be translated into practical platforms with clinical relevance and usability.[4]

This research addresses these gaps by developing a Support Vector Machine (SVM) model to classify UC severity using a combination of biomarker, histological, demographic, and medication history data. A web-based platform designed for practical use by clinicians and researchers was developed. The platform enables users to upload patient datasets, select the target column/outcome (i.e., severity score), and define how the dataset is divided between model training and validation (e.g., an 80/20 split means 80% of the data is used to train the model, while the remaining 20% is used to test its accuracy). Results are then displayed immediately through interactive charts and performance metrics (such as accuracy, precision, F-1 score, recall, etc.), making the outputs both interpretable and clinically relevant. While UC-specific patient data is still being acquired, the system has already been tested with publicly available biomedical datasets to demonstrate end-to-end functionality and scalability.

Ultimately, this research developed a clinician-facing web platform that includes a validated machine learning model for UC prognosis and a framework for integrating multidimensional patient data into precision medicine tools. This project offers a pathway from computational modeling to clinical applications in UC care, such as improved prognosis.

Methods

This project followed a multi-step research and development process to design and implement a machine learning model for predicting the prognosis of UC.[5]

Step #1: Literature Search and Variable Identification:

In order to select an appropriate machine learning model, it was first necessary to identify and define the types of variables that best represent the clinical and biological complexity

© 2026 Terra Science and Education

DOI: 10.36838/IJHSR87.65

of UC, which arises from a complex interplay between the gut microbiota, the mucosal immune system, and host genetics.[6,7] To capture this biological complexity, variables were selected to reflect both molecular indicators of inflammation and individual-level differences that influence immune function and disease severity.

The variable selection process was refined in consultation with IBD specialists (Dr. Soula Koniaris and Dr. Sarag Boukhar), who emphasized the central role of biomarkers in diagnosing and monitoring UC. Based on their guidance, four clinically significant serum and fecal biomarkers (C-reactive protein (CRP), erythrocyte sedimentation rate (ESR), calprotectin, and lactoferrin) were prioritized during the extensive literature search process. These biomarkers are routinely used to assess inflammatory burden and disease activity, providing quantifiable inputs well-suited for machine learning models. Additional demographic and lifestyle variables (including age, sex, diet, smoking status, and hospitalization history) were included to account for patient-specific variation in immune response and treatment outcomes.

Integrating patient-level characteristics with biomarker data produced a multidimensional feature set capturing the biological, behavioral, and demographic factors that shape UC progression. The final dataset combines biomarker values, clinical severity indices (e.g., Mayo Score, UCEIS), electronic medical records (diagnoses, history, problems, medication usage, lab test results), clinical data (relevant lab scores for biomarkers, medication journey, extraintestinal manifestations, disease phenotypes and locations, disease severity scores, etc.), and other demographic variables.[9] This comprehensive structure captures both systemic inflammation and individual variability, providing a strong foundation for developing and validating the machine learning model.

Step #2: Model Selection and Algorithm Capacity:

Because UC severity is influenced by a combination of immune, microbial, genetic, and lifestyle factors, a non-linear modeling approach was required to capture the complexity of these interactions. Based on the variable types identified earlier, both regression and multiclass classification frameworks were initially considered. Regression models predict continuous numeric outcomes (e.g., severity scores along a spectrum), whereas classification models assign cases to discrete categories (e.g., mild, moderate, severe).[10] Given that UC severity is typically evaluated through clinical categories, a classification approach was determined to be more appropriate.

Three supervised learning algorithms were evaluated: logistic regression, decision tree, and Support Vector Machine (SVM).[11] Logistic regression provides interpretability but is limited in modeling nonlinear biological relationships. Decision trees can model non-linearity but often overfit smaller or unbalanced datasets, reducing generalizability. The SVM algorithm was ultimately selected for its robustness in handling high-dimensional, non-linear, and limited-sample data, making it well-suited for biomedical contexts.[12]

To test the feasibility of this SVM model, an initial prototype was built in Python (Jupyter notebook), using the SVM model from the scikit-learn (sklearn) library, and trained on a synthetic dataset generated in Excel. The dataset consisted of 50 simulated UC patient profiles, generated based on clinically recognized biomarker ranges and severity indices reported in UC literature.[8] Each profile included two predictor variables—age and calprotectin level (μg/g)—and one target variable, disease severity, labeled on a 0–3 scale (0 = normal to 3 = severe). The SVM algorithm from the sklearn library was trained to map the predictor variables (defining the x vector as [age, calprotectin level]) to the output or target column (y = severity score). Although this dataset was artificial and limited in scope, it was instrumental in understanding how the dataset should be formatted later and allowed us to verify that the pipeline could successfully classify new inputs. Thereby, this step established a functional and replicable framework for future training on validated UC datasets.

Step #3: Prototype Development and User Testing:

To demonstrate user interaction and early data exploration workflows, an interactive prototype was developed using an R Shiny App (source code: https://github.com/aayushi-saxena-me/shinyapp). The app (hosted at https://aayushisaxena.shinyapps.io/shinyapp) allows for dataset/CSV upload, exploratory data analysis (summary statistics tables (with minimum, Q1, median, mean, Q3, and maximum values) and a one-sample hypothesis test), and a k-means clustering plot (a type of unsupervised machine learning algorithm). While this prototype provided proof-of-concept for user engagement, it lacked SVM integration and was not optimized for high-volume or clinical-grade deployment due to scalability limitations with the Shiny App framework.

Step #4: Platform Migration & Full Stack Development:

To overcome these limitations, the system was migrated to a full-stack architecture using Python/Django (source code: https://github.com/aayushi-saxena-me/statistical-analysis-app), with code development supported by Cursor (AI-powered IDE) and deployment via AWS CodeDeploy. The resulting web platform (https://statisticalanalysis.org) allows the user to upload patient datasets, define train-test splits, select the target/output variable, enable SVM learning analysis, and view performance metrics of the SVM classification, among other things. This architecture ensures scalability, reproducibility, and accessibility, making it possible for both researchers and clinicians to use advanced machine learning tools without requiring extensive programming expertise.

Step #5: Validation with External Datasets:

Since UC-specific datasets are still pending, platform validation was performed using a publicly available biomedical dataset (https://www.kaggle.com/datasets/prathamtripathi/drug-classification). This dataset was uploaded in CSV format, drug type was selected as the target column, RBF was selected as the SVM kernel, and a 20% Test / 80% Train split was selected. When the machine learning analysis was run, the SVM model achieved 90.0% classification accuracy, demonstrating the platform's ability to handle the full workflow (from data

upload to training and testing, to performance reporting) in a reliable and interpretable way. This confirms that the system works as intended and is ready to be applied to disease-specific data.

Once UC datasets are acquired, the same process can be repeated to produce clinically reliable predictions. Once trained on this UC dataset, in further iterations of the model, clinicians will be able to input new patient data and receive real-time outputs. For now, the focus is on demonstrating core functionality and evaluation workflows, not providing live patient predictions. Evaluating the model on new, unseen data provides a realistic measure of how well it will perform in real-world settings, an essential step toward developing a clinically dependable tool.

Results and Discussion

Literature Search: Biomarkers:

One of the initial focuses of this project was identifying biomarkers that could help predict the prognosis of Ulcerative Colitis (UC). While biopsy and endoscopy are effective diagnostic methods, their invasive nature and high cost limit their use in routine monitoring. Although some non-invasive imaging techniques have shown high diagnostic accuracy, they also require experienced personnel and sophisticated equipment, which can be costly and difficult to access regularly.[13]

Biomarkers, on the other hand, are medical signs different from symptoms that essentially act as measurable bodily substances which can provide information about both physiological and pathological conditions. These biomarkers can be found in various biological samples (e.g., blood, urine, tissues, etc.).[14] Some basic examples include vital signs from pulse and blood pressure to other serum, genetic, or inflammatory biomarkers, which require more complex laboratory tests. While biomarkers vary in specificity and sensitivity, they represent a practical alternative for monitoring disease progression. Through an extensive literature review and consultation with gastroenterologist Dr. Soula Koniaris, four clinically established biomarkers were prioritized: C-reactive protein (CRP), fecal calprotectin, lactoferrin, and erythrocyte sedimentation rate (ESR).

CRP is a well-known serum biomarker produced in the liver and elevated during acute-phase inflammatory responses. It has a relatively short half-life, making it a more dynamic indicator of inflammation. Although more sensitive for Crohn's disease than UC, CRP remains a useful indicator in UC.[15] Calprotectin, a calcium- and zinc-binding protein, is highly prevalent in phagocytic leukocytes (especially neutrophils) and constitutes about 60% of their cytosolic protein content. Neutrophil infiltration of the GI tract is a hallmark of UC, making calprotectin a strong indicator of active disease.[16] Fecal biomarkers such as calprotectin are particularly important in IBD diagnosis and prognosis because they reflect mucosal inflammation more directly. Fecal lactoferrin is another neutrophil-derived protein present in stool, and is significantly elevated in pediatric patients with active intestinal inflammation and IBD (for both UC and Crohn's disease).[17] ESR is a blood test that can indicate if there is inflammation (the immune system's response to injury, infection, and conditions such as immune system disorders (i.e., IBDs)) in your body. Erythrocytes are red blood cells, and the sedimentation rate is the time it takes for red blood cells to settle at the bottom of a test tube.[18] Though an elevated ESR is a less specific indicator of inflammation, compared to fecal lactoferrin, the biomarker still offers additional context as markers of systemic inflammation and neutrophil activity. According to Dr. Koniaris, elevated levels of these biomarkers described previously are commonly used in practice to assess whether inflammation is due to an intercurrent illness or not, and how to adjust their medication accordingly to prevent escalation of disease severity.

In addition to clinically validated biomarkers, emerging research highlights the potential of novel, more specific indicators. Several recent studies have used bioinformatic and machine learning approaches to identify differentially expressed mRNAs (DEMs) associated with immune activity in UC. One such study identified 216 DEMs related to neutrophil infiltration and leukocyte migration, with MST1L, OLFM4, and DPP10 standing out as potential prognostic markers.[19] Although these are not yet validated for clinical use, including them in future iterations of the model may help test their diagnostic utility.

Incorporating a wide range of biomarkers (established and experimental) along with basic patient information (e.g., age, gender, hospitalization history, diet, smoking, etc.) allows the model to account for the individualized nature of UC. Factoring these nuances increases the likelihood of building a tool that reflects real-world complexity and variation in disease behavior.

At this stage, we have a curated set of biomarkers and patient variables (including demographics) that will serve as the core features for the machine learning model. These inputs are both clinically meaningful and widely available, ensuring that the eventual tool will be feasible for real-world use while leaving space for incorporation of experimental biomarkers as the field evolves.

Computational & Model Selection:

Due to the complexity and non-linearity of UC progression, a Support Vector Machine (SVM) was selected as the primary model for classification. SVMs are a set of supervised learning algorithms effective for classification, regression, and outlier detection. They work by identifying a hyperplane that best separates data into classes, using kernel functions to project input into higher-dimensional space when necessary for non-linear separation.[20,21]

In this project, the model's input features include various clinical and biomarker data points, while the output is a severity score derived from UC scoring systems such as the Ulcerative Colitis Endoscopic Index of Severity (UCEIS) and the Mayo Score. For example, UCEIS scores range from 0-8, with higher scores indicating greater disease severity. These scores serve as the "y" values (labels) for training, while the "x" values are multidimensional input vectors consisting of variables like CRP, calprotectin, ESR, and patient demographics.

DOI: 10.36838/IJHSR87.65

SVMs require labeled training data, making them ideal for our objective: to classify the course and severity of UC into defined categories (e.g., mild, moderate, severe). Once trained, the model could help streamline clinical decision-making by suggesting potential treatment pathways or adjustments based on predicted risk of relapse.

Test Run and Prototype Tool:

To evaluate the viability of a machine learning model for UC prognosis, a Support Vector Machine (SVM) algorithm from the scikit-learn library was tested in Python.[22] The goal was to establish a working proof of concept while awaiting real clinical data. A synthetic dataset was created in Excel containing 50 hypothetical patient profiles. Each profile included two features—age (in years) and levels of fecal calprotectin (μg/g)—and was labeled with a correlating severity score from 0 to 3, representing disease intensity (mild to severe). This dataset was used to train the SVM in a Jupyter Notebook environment, and then the model was asked to classify new, unseen inputs using this training data.

For example, a 16-year-old patient with a calprotectin level of 400 μg/g was labeled as a 2 (moderate severity) in the dataset. When we asked the model to predict this same scenario ("clf.predict([[16, 400]])"), a score of 2 was returned as modeled in Figure 1. This prediction demonstrated that the model was functioning as intended, at least within the bounds of the simulated dataset.

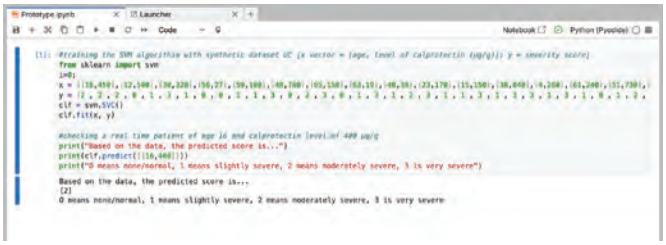

Figure 1: Implementation of a Support Vector Machine (SVM) in a Jupyter Notebook environment using a synthetic dataset of ulcerative colitis patient profiles. The model, trained on age and calprotectin level as predictive features, classified the test input [16, 400] with a severity score of 2, corresponding to moderate disease activity.

Although the dataset was small and artificially constructed, it validated the SVM's basic mechanics and confirmed the model pipeline, providing a foundation for interface and backend development. Future performance is expected to improve significantly with access to larger, clinically validated datasets.

Platform Development and External Dataset Validation:

In parallel to the Python-based modeling, an initial prototype was built using R Shiny and deployed at https://aayushisaxena.shinyapps.io/shinyapp to support clinical and user-facing interaction. This app enables users to upload CSV files, run summary statistics, perform hypothesis testing, and conduct unsupervised machine learning via k-means clustering. Though initially populated with a default brain tumor dataset, it can be used with any biomedical dataset. While the Shiny App was instrumental in shaping the user interface and front-end interaction, it could not run SVM models and would not scale effectively in a clinical setting.

To address the limitations of the prototype, a web-based platform (available at statisticalanalysis.org) was developed using Python/Django, migrated by Cursor, and deployed through AWS CodeDeploy to provide a unified environment for exploratory data analysis, statistical computation, and machine learning. Users can upload CSV or Excel datasets or generate sample data directly within the interface. Upon uploading, users can preview the data input and examine the key dataset information (number of rows, columns, and variable types) automatically produced by the system. Built-in visualization tools allow users to generate distribution plots, box plots, Q–Q plots, and correlation matrices, supporting a clear understanding of variable relationships and data distributions. The user can adjust which variables are the target columns in the analysis configuration on the left bar. The platform also computes descriptive statistics such as mean, standard deviation, variance, and percentile values, along with results from hypothesis testing modules, including t-tests and normality checks.

The platform also features a dedicated Machine Learning module that integrates an SVM classifier. Users can define the target column, choose a kernel function (e.g., Radial Basis, sigmoid, etc.), and specify the train-test split ratio (e.g., 80/20). The same number and type of input variables were used in both the training and validation datasets to maintain structural consistency and ensure the reliability of the model's evaluation. Once trained, the system automatically reports performance metrics (accuracy, precision, recall, and F1-score) along with a confusion matrix and performance summary chart for interpretability. While the prototype does not automatically normalize or standardize input data, users can manually format or preprocess their datasets prior to upload. This ensures flexibility for users who wish to control their own data preparation. Future iterations can be expanded to include built-in feature scaling to further optimize SVM performance and simplify the user workflow. The interactive interface allows users to refresh or rerun analyses without coding, making the platform suitable for both researchers and clinicians seeking to evaluate dataset trends or model outcomes efficiently.

To test this system, a publicly available biomedical dataset on drug classification was used. The dataset contained 200 samples (rows) and five drug classes as the target variable, with 5 input features: age, sex, blood pressure, cholesterol, and Na-to-K ratio.[23] The top of Figure 2 shows the performance metrics of the SVM classifier once it was trained (on 80%) and validated (with the remaining 20%) on the drug classification dataset. It produced an accuracy of 90.0% and precision of 91.3%, indicating that the SVM achieved balanced and reliable classification performance across all drug classes. The bottom half of Figure 2 shows another visualization of the performance metrics as well as the accompanying Confusion Matrix.

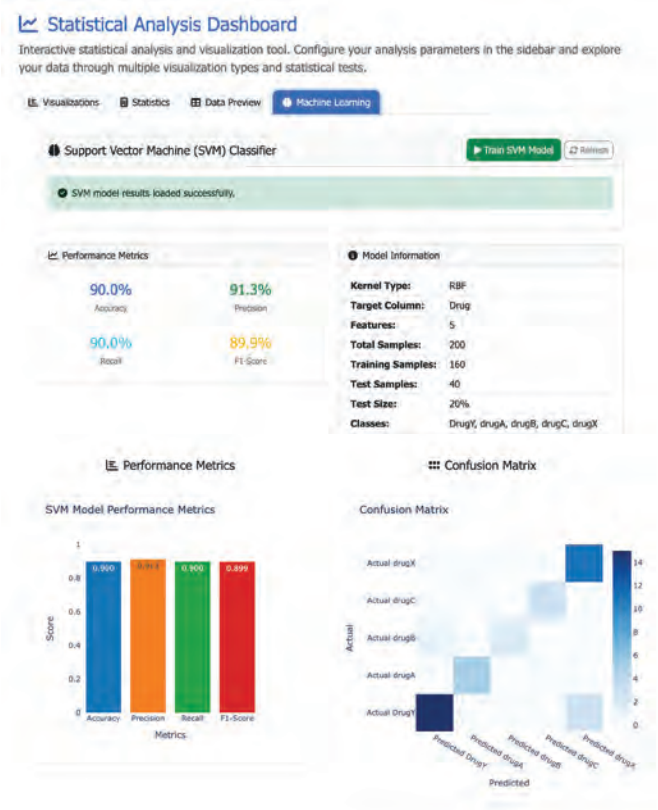

Figure 2: Web-based Statistical Analysis Dashboard demonstrating Support Vector Machine (SVM) model results on a drug classification dataset. At the top of the image, the dashboard interface displays model configuration and performance summary. On the bottom, the model outputs associated performance metrics and a confusion matrix showing classification accuracy (90.0%), precision (91.3%), recall (90.0%), and F1-score (89.9%).

While these datasets are not UC-specific, they effectively demonstrate the model's structure and performance. The architecture is ready to accept UC patient datasets, and once trained and validated on UC-specific data, the platform will not only evaluate predictive accuracy but also highlight which biomarkers and clinical variables most strongly influence disease prognosis.

This will enable refinement of the model by distinguishing between critical predictors and potential sources of noise. After validation, the system can expand beyond classification into a real-time decision-support tool, where clinicians may input patient-level data and immediately receive severity scores alongside probabilities of relapse, hospitalization, or treatment escalation. Producing performance metrics and actionable risk predictions for clinicians ensures that the platform is both scientifically robust and translationally relevant.

Limitations:

This study represents both a proof of concept and an applied framework for bridging innovation in machine-learning-based UC research with real-world clinical use; however, several limitations qualify its findings. First, the current system was developed on a synthetic dataset and validated on a drug-classification dataset that differs from UC in features and outcomes, so reported performance may not reflect UC prediction in practice. Second, the web app supports offline evaluation only: users upload a dataset, the platform performs a fixed 80/20 train–test split, and it reports metrics (accuracy, precision, recall, and F1 score) with a confusion matrix; per-patient, real-time prediction is not yet implemented. Preprocessing steps (e.g., feature scaling/normalization) are not fully specified, which matters for SVM stability and reproducibility. Before clinical use, the platform also requires testing and documentation for data security, scalability, and usability on UC-specific, multi-institutional datasets.

Conclusion

This study demonstrates the feasibility of applying machine learning to predict the prognosis of UC by integrating clinically established biomarkers, demographic variables, and treatment history into an SVM model. Through an extensive literature review and consultation with IBD experts, a relevant set of features was identified and used to build a classification system that distinguished UC severity in simulated data. This system was then migrated to a web-based platform and validated using an external biomedical dataset, showing reliable performance across key metrics including accuracy, precision, recall, and F1 score.

Overall, these results establish a functional proof of concept that bridges computational modeling with practical application. Moving forward, future implementations will involve incorporating UC-specific clinical datasets directly into the platform to train and evaluate the model on real patient data. This process will include structured data acquisition through clinical collaborations, evaluation of noisy or missing variables, and the development of automated preprocessing pipelines for normalization, feature scaling, and variable weighting to refine model accuracy. Once validated, the model will be expanded to enable clinicians to upload new de-identified patient data and automatically generate severity classifications based on the trained UC model. The platform will also allow users to visualize model outputs and identify which biomarkers and clinical variables most influence predictions, offering interpretability alongside performance. These updates will allow the system to be evaluated under real-world clinical conditions, improving its reliability and practical utility. Together, these advancements will transition the platform from a research prototype to a validated clinical decision-support tool, demonstrating how machine learning can be responsibly deployed to enhance predictive precision medicine and improve UC management.

Acknowledgments

This work was supported in part by the William Welles Bouton Award, which provided a $350 grant. I am deeply grateful to Dr. Soula Koniaris (Pediatric Gastroenterology, RWJBH Medical Group) for her guidance on the clinical relevance of IBD biomarkers, Dr. Sree Mallikarjun (UVA Data Science; Chief Data Scientist & Head of AI Innovation at Octus) for his mentorship and insights on model development and methodological planning in the ML framework, and to Dr. Sarag Boukhar (Pathology, RWJBH Medical Group) for his insights into the pathology of UC. I would also like to thank Dr. Rosa-

DOI: 10.36838/IJHSR87.65

lind Abbott (Carnegie Mellon University) for her mentorship and project advisement. Their expertise, support, and encouragement were invaluable in shaping this project.

References

1. Lynch, W. D.; Hsu, R. Ulcerative Colitis. In *StatPearls*; StatPearls Publishing: Treasure Island (FL), 2025.
2. *Diagnosis of Ulcerative Colitis - NIDDK*. National Institute of Diabetes and Digestive and Kidney Diseases. https://www.niddk.nih.gov/health-information/digestive-diseases/ulcerative-colitis/diagnosis (accessed 2025-07-27).
3. *Definition & Facts of Ulcerative Colitis - NIDDK*. National Institute of Diabetes and Digestive and Kidney Diseases. https://www.niddk.nih.gov/health-information/digestive-diseases/ulcerative-colitis/definition-facts (accessed 2025-08-27).
4. Kulkarni, C.; Liu, D.; Fardeen, T.; Dickson, E. R.; Jang, H.; Sinha, S. R.; Gubatan, J. Artificial Intelligence and Machine Learning Technologies in Ulcerative Colitis. *Ther. Adv. Gastroenterol.* **2024**, *17*, 17562848241272001. https://doi.org/10.1177/17562848241272001.
5. Mallikarjun, S.; Abbasi, A.; University of Virginia, McIntire School of Commerce. Big Data Projects. In *Quantitive Methods*; CFA Institute, 2020; pp 518–590.
6. Khor, B.; Gardet, A.; Xavier, R. J. Genetics and Pathogenesis of Inflammatory Bowel Disease. *Nature* **2011**, *474* (7351), 307–317. https://doi.org/10.1038/nature10209.
7. Porter, R. J.; Kalla, R.; Ho, G.-T. Ulcerative Colitis: Recent Advances in the Understanding of Disease Pathogenesis. *F1000Research* **2020**, *9*, F1000 Faculty Rev-294. https://doi.org/10.12688/f1000research.20805.1.
8. Singh, S.; Ananthakrishnan, A. N.; Nguyen, N. H.; Cohen, B. L.; Velayos, F. S.; Weiss, J. M.; Sultan, S.; Siddique, S. M.; Adler, J.; Chachu, K. A. AGA Clinical Practice Guideline on the Role of Biomarkers for the Management of Ulcerative Colitis. *Gastroenterology* **2023**, *164* (3), 344–372. https://doi.org/10.1053/j.gastro.2022.12.007.
9. *What is IBD Plexus? | Crohn's & Colitis Foundation*. https://www.crohnscolitisfoundation.org/research/plexus/what-is-ibd-plexus (accessed 2025-11-06).
10. Amazon Machine Learning - Developer Guide.
11. Gulati, J. *Logistic vs SVM vs Random Forest: Which One Wins for Small Datasets?*. MachineLearningMastery.com. https://machinelearningmastery.com/logistic-vs-svm-vs-random-forest-which-one-wins-for-small-datasets/ (accessed 2025-11-06).
12. Rodríguez-Pérez, R.; Bajorath, J. Evolution of Support Vector Machine and Regression Modeling in Chemoinformatics and Drug Discovery. *J. Comput. Aided Mol. Des.* **2022**, *36* (5), 355–362. https://doi.org/10.1007/s10822-022-00442-9.
13. Maconi, G.; Bolzoni, E.; Giussani, A.; Friedman, A. B.; Duca, P. Accuracy and Cost of Diagnostic Strategies for Patients with Suspected Crohn's Disease. *J. Crohns Colitis* **2014**, *8* (12), 1684–1692. https://doi.org/10.1016/j.crohns.2014.08.005.
14. Strimbu, K.; Tavel, J. A. What Are Biomarkers? *Curr. Opin. HIV AIDS* **2010**, *5* (6), 463–466. https://doi.org/10.1097/COH.0b013e32833ed177.
15. Alghoul, Z.; Yang, C.; Merlin, D. The Current Status of Molecular Biomarkers for Inflammatory Bowel Disease. *Biomedicines* **2022**, *10* (7), 1492. https://doi.org/10.3390/biomedicines10071492.
16. Zamani, H.; Barzin, G.; Yousefinia, M.; Mohammadkhani, A.; Ostovaneh, M. R.; Sharifi, A. H.; Tayebi, S.; Malekzadeh, R.; Ansari, R. Diagnostic Value of Fecal Calprotectin in Patient with Ulcerative Colitis. *Middle East J. Dig. Dis.* **2013**, *5* (2), 76–80.
17. Walker, T. R.; Land, M. L.; Kartashov, A.; Saslowsky, T. M.; Lyerly, D. M.; Boone, J. H.; Rufo, P. A. Fecal Lactoferrin Is a Sensitive and Specific Marker of Disease Activity in Children and Young Adults with Inflammatory Bowel Disease. *J. Pediatr. Gastroenterol. Nutr.* **2007**, *44* (4), 414–422. https://doi.org/10.1097/MPG.0b013e3180308d8e.
18. *Erythrocyte Sedimentation Rate (ESR): MedlinePlus Medical Test*. https://medlineplus.gov/lab-tests/erythrocyte-sedimentation-rate-esr/ (accessed 2025-08-28).
19. He, T.; Wang, K.; Zhao, P.; Zhu, G.; Yin, X.; Zhang, Y.; Zhang, Z.; Zhao, K.; Wang, Z.; Wang, K. Integrative Computational Approach Identifies Immune-relevant Biomarkers in Ulcerative Colitis. *FEBS Open Bio* **2022**, *12* (2), 500–515. https://doi.org/10.1002/2211-5463.13357.
20. *Support Vector Machine (SVM) Algorithm*. GeeksforGeeks. https://www.geeksforgeeks.org/machine-learning/support-vector-machine-algorithm/ (accessed 2025-07-27).
21. Saxena, V. Support Vector Machine and Its Applications in Information Processing. Thesis, Massachusetts Institute of Technology, 2004. https://dspace.mit.edu/handle/1721.1/29404 (accessed 2025-07-27).
22. *1.4. Support Vector Machines*. scikit-learn. https://scikit-learn/stable/modules/svm.html (accessed 2025-07-27).
23. *Drug Classification*. https://www.kaggle.com/datasets/prathamtripathi/drug-classification (accessed 2025-07-27).

Author

Aayushi Saxena is a senior at The Lawrenceville School. She is passionate about data science, humanities, and policy. Specifically, she wants to explore how technology innovation can be democratized and implemented to streamline convoluted systems (e.g., healthcare and law), improving access and creating meaningful impacts in people's everyday lives.

IJHSR
ijhighschoolresearch.org
RESEARCH ARTICLE

Benchmarking Distinct Deep Learning Architectures for Forecasting ARIMA-Synthesized Non-Stationary Time Series

Abdullah Shaikh

Jumeirah College, Dubai, UAE; abdshk21@gmail.com

ABSTRACT: Artificial Narrow Intelligence (ANI) systems now provide forecasting capabilities for non-stationary time series that match or exceed those of traditional statistical methods. Non-stationary processes are central to applications in finance, healthcare, and sports analytics, where accurate prediction is essential. To generate controlled datasets for benchmarking, we employed Autoregressive Integrated Moving Average (ARIMA) models as a classical framework for simulating non-stationary series. Using these sequences, we conducted a comparative evaluation of Long Short-Term Memory (LSTM) networks and Transformer architectures. Performance was quantified by mean squared error across a range of baseline block sizes, with data produced through custom Python pipelines. Results show that LSTMs consistently achieve lower prediction error than Transformers, with differences in mean squared error reaching statistical significance ($p < 0.05$). Transformer performance also degraded in the absence of moving average components, indicating sensitivity to residual noise. These findings suggest that LSTMs provide more stable and reliable forecasts for ARIMA-generated non-stationary data, while Transformers require additional constraints or modifications to achieve comparable robustness.

KEYWORDS: Robotics and Intelligent Machines, Machine Learning, Time Series Forecasting, Autoregressive Integrated Moving Average Models, Long Short-Term Memory, Transformer.

Introduction

Historically, classical Autoregressive Moving Average (ARMA) models assumed a stationary world, where statistical properties such as mean, variance, and autocorrelation remain constant over time. However, real-world data is rarely stationary since it exhibits stochastic volatility, regime shifts, long-term seasonality, evolving autocorrelation, and non-linear dependencies. These dynamics stretch beyond the capabilities of ARMA and its extensions, such as ARIMA (differencing) and SARIMA (seasonal). Nevertheless, recent advances in deep learning have offered promising alternatives for time series predictions. Chief amongst these are Long Short-Term Memory (LSTM) networks and Transformer-based models. In this study, we track how prediction errors evolve over block sizes, allowing us to characterize each model's stability and responsiveness in the face of non-stationary dynamics.

Traditional Statistical Models:

Diving deeper, models like ARIMA require data to be made stationary via transformations like differencing, which imposes rigidity and inhibits their capacity to adjust to volatile fluctuations. Furthermore, these models require extensive manual parameter tuning and frequently fail when confronted with noisy or sparse signals. In a comparative analysis of biomedical data, a Seasonal-ARIMA benchmark had a MAPE (Mean Absolute Percentage Error) of about 7.1%, whereas deep learning models had a MAPE of less than 3%.[1] Even more flexible statistical models, such as Meta's Prophet, outperformed ARIMA but struggled with the considerable unpredictability in patient vital signs, resulting in much greater RMSE (Root Mean Squared Error) and MAE (Mean Absolute Error) than neural networks.[1]

LSTM-Based Approaches:

In recent decades, LSTM networks have marked a paradigm shift in time series forecasting by introducing memory cells and gating mechanisms that selectively retain or discard past information. In a comparative study on the SSE 50 Index, it was found that an LSTM achieved an MAPE of 1.13%, thus significantly outperforming ARIMA in short-term forecasting accuracy, especially in the early prediction window.[2] Researchers who built upon these improvements had proposed a hybrid ensemble that integrates deep learning with gradient-boosted trees (XGBoost-DL). This model, when tested, achieved an even better accuracy, with an RMSE of 25.70 and an MAE of 19.82 on sunspot number forecasting. This model notably outperformed both SARIMA (RMSE: 54.11, MAE: 45.51) and a Transformer-based Informer model (RMSE: 29.90, MAE: 22.35).[3] The consistent reduction in error across these studies, from ARIMA to LSTM to XGBoost-DL, demonstrates the growing effectiveness of models that can flexibly learn complex, non-stationary dynamics.[3]

Transformer-Based Approaches:

Today, the latest evolution in time series forecasting is the introduction and development of Transformer-based models, consisting of a self-attention mechanism that is used to capture temporal relationships. Rather than processing inputs sequentially like an LSTM, a Transformer attends to all time steps simultaneously, learning which past observations are most relevant to forecasting the future. Transformers can learn

© 2026 Terra Science and Education

DOI: 10.36838/IJHSR87.71

seasonality, trends, and irregular patterns through positional encodings and attention weights, instead of assuming a fixed statistical structure. For example, recent studies introduced an Informer-based transformer for multi-domain forecasting, which considerably outperformed LSTM, GRU (Gated Recurrent Unit), and TCN (Temporal Convolutional Network) benchmarks by halving the MSE on traffic flow data (≈10.1 vs >20) and improving stock price forecast accuracy.[4] On the contrary, several other researchers note that for very long historical series or small datasets, a naive Transformer without architectural optimization may not automatically excel.[5] For example, they saw that a vanilla Transformer slightly underperformed an optimized LSTM on a decades-long stock dataset, with the LSTM yielding a lower RMSE (0.104 vs 0.232) for Hewlett–Packard stock forecasting.[5] However, the trend in recent research is that Transformer-based hybrid architectures tend to achieve the highest accuracy on non-stationary benchmarks. These include Temporal Fusion Transformers (which combine an LSTM encoder with multi-head attention for long-term features) and the Informer (which uses probabilistic sparse self-attention and a distillation mechanism to reduce redundant information).

Limitations of Current Literature:

The central tension in the current body of literature is that the pursuit of predictive accuracy is in a world governed by uncertainty, non-linearity, and evolving dynamics. While a range of models has been proposed, they come with constraints that limit generalizability and robustness across diverse real-world settings. Some of these constraints are explored ahead.

Firstly, many forecasting studies use real-world historical data where the true data-generating process is unknown, making it hard to discern which model is fundamentally better, as it might be highly likely that the deep learning network is simply overfitting the data and not necessarily learning the underlying structures within the dataset itself.[6] As a result, reliable forecasting benchmarks must no longer rely on a single test set or raw error difference alone. Instead, the need is to use statistical significance tests such as the Diebold-Mariano (DM) test[7] or the Wilcoxon signed-rank test to determine whether performance differences between models are truly meaningful or just due to chance. The widespread use of these in literature is currently not evident.

Another limitation is the inconsistent way some studies compare LSTMs and Transformers. Authors frequently evaluate proposed models against baseline architectures without performing equivalent hyperparameter tuning or ensuring consistent experimental settings, resulting in uncontrolled comparisons.[8] For example, in a recent finance study comparing LSTM and Transformer models across multiple financial instruments, the Transformer's MAPE varied from 1.34% to 2.7%, while the LSTM's MAPE remained between 1.33% and 1.51%, highlighting the Transformer's sensitivity to training conditions and data volatility.[8]

These findings indicate that unless experimental conditions are carefully controlled, one might draw wrong conclusions about which model is better.

Furthermore, several studies rely only on aggregate error metrics like MSE, RMSE, or MAE to compare models, without analyzing how errors evolve over the forecast horizon. Whilst these metrics summarize overall accuracy, they mask a model's failure to extrapolate trends or seasonality beyond the training data. For example, contemporary research demonstrated that an LSTM trained on a non-stationary series (with an upward trend) can fit short-term points well but then completely underestimate the continued growth, resulting in much larger errors farther out in time.[7] They also saw that two models with identical MSE may have very different behaviors: one might be consistently slightly off, while another is spot-on for short horizons but significantly off for long horizons. This type of long-term evaluation is currently limited in the present-day literature.

Additionally, it is also common to see papers proclaiming one model as "better" overall without accounting for contextual variability, such as the application domain and noise levels. For example, a study compared ARIMA and LSTM models for disease incidence forecasting at different time scales and found that no one model is universally best.[10] The classical ARIMA outperformed LSTM on coarser time scales (monthly and weekly predictions), while LSTM excelled on the daily forecasts.[10] The M4 and M5 forecasting competitions that involve thousands of series from finance, economics, and demographics also showed that no single method dominated across all categories.[11] Indeed, ensemble approaches and hybrids tended to do best overall by precisely adapting to different patterns. Therefore, a critical limitation in the literature currently is the lack of results stratified by context (domain type, data characteristics, forecast horizon). Without overcoming this issue, one might incorrectly assume that a model that works in one setting will work everywhere.

Key Intervention:

To address some of these gaps, this study introduces a controlled experimental framework for evaluating the performance of LSTM and Transformer models on non-stationary time series data generated using ARIMA pipelines. Unlike prior work that often relies on static benchmarks or uncontrolled real-world datasets, this setup enables fine-grained control over the degree and type of non-stationarity by systematically varying ARIMA parameters and block sizes. Model performance is evaluated over a forecast horizon using time-resolved Mean Squared Error (MSE), allowing us to examine how predictive accuracy stabilizes for each model and configuration.

In line with our commitment to overcome, or at the very least, mitigate the aforementioned limitations of existing literature, we ensured that both models are trained under consistent experimental settings with equivalent hyperparameter tuning. In addition, the Wilcoxon signed-rank test is used to statistically verify whether observed performance differences are robust or attributable to random variation. While this study focuses on baseline architectures, it also lays the groundwork for future experimentation with ensemble or hybrid forecasting models that may better accommodate contextual variability, such as application domain and noise level.

Methods

Research Design:

The research design is structured as a comparative simulation study. We generated a synthetic time series using explicitly defined ARIMA parameters. This approach offers a rare epistemic advantage: the data-generating process is fully known, allowing us to isolate model performance from the uncertainties of unknown external dynamics.

Such simulation-based forecasting benchmarks have been gaining traction for their rigor and reproducibility, as highlighted in various studies,[7] which emphasize the dangers of over-relying on real-world data without ground truth or reproducible baselines as outlined in depth previously.[9] Our methodological choice is aligned with these works but diverges by adding an incremental layer of variability: across both block sizes (from 5 to 95) and ARIMA parameter configurations ((0,1,1), (1,1,1), (2,1,2), (2,2,0))

For the purpose of acquiring an in-depth understanding of the data generation process, one must first understand the core logic behind the ARIMA model itself, which consists of three hyperparameters (p,d,q):

1. p (Autoregressive (AR)): The number of lagged observations included in the model (i.e., how many past values influence the current value). Increasing p allows the model to capture longer memory effects, but increases the risk of overfitting.

$y_t = \phi 1 y_{t-1} + \phi 2 y_{t-2} + \varepsilon_t$ for AR Order 2

2. d (Integrated (I)): The number of times the series is differenced to achieve stationarity. Differencing helps remove trends and seasonality.

- o $y_t' = y_t - y_{t-1}$ is the first difference
- o $y_t'' = y_t' - y_{t-1}$ is the second difference

3. q (Moving Average (MA)): The number of lagged forecast errors used in the model. Increasing q lets the model account for short-term shocks or noise patterns.

$y_t = \varepsilon_t + \theta_1 \varepsilon_{t-1}$ for MA(1)

The general form then becomes: $\Phi(L)(1-L)^d y_t = \Theta(L)\varepsilon_t$

Where:

- y_t is the original time series
- $\nabla^d y_t$ is the d-th order differenced time series
- ε_t is white noise error
- L is the lag operator ($L y_t = y_{t-1}$)
- $\Phi(L) = 1 - \phi_1 L - \phi_2 L^2 - \cdots - \phi_p L_p$
  - o The ϕ coefficients control how strongly past values at different lags influence the prediction.
- $\Theta(L) = 1 + \theta_1 L + \theta_2 L^2 + \cdots + \theta_q L_q$
  - o Each θ term controls how much past forecast errors influence the current value.

Another key component of the ARIMA model is the Block Size. It is the length of the forecast horizon, which represents how many time steps ahead the predictions are generated before retraining or updating the model. With smaller block sizes, it is widely believed that the accuracy will be greater as the predictions are likely to remain closer to the training range. However, with larger block sizes, the opposite is generally expected.

In the fitted ARIMA models, the estimated parameters are expressed through autoregressive (AR) and moving average (MA) coefficients, which are conventionally represented as denominator and numerator polynomials, respectively. The AR coefficients capture how past observations of the series influence its present value, while the MA coefficients reflect how past forecast errors propagate forward through the model. Together, these define the recursive structure of the time series in the time domain and can also be interpreted in the frequency domain as a transfer function given by the ratio of the two polynomials. This formulation allows insight into stability, persistence, and the filtering behavior of the model across different frequencies. Coefficients were computed in Python using the statsmodels library and are reported in the Results section to ensure transparency of model fitting and to provide a basis for comparison with the neural architectures benchmarked in this study.

For each p,d,q configuration used in this research, 1000 time steps were generated using the statsmodels library in Python, with Gaussian white noise input. The generated series were non-stationary by construction but structurally transparent, facilitating reproducibility and interpretability. To mimic batch-based processing common in neural forecasting pipelines, the full series was split into sliding window blocks of varying sizes (5 to 95, in increments of 10). Each block pair (input, target) was used to train and test the models.

Model Architectures:

In order to understand the specific model architecture used, it is imperative to first acknowledge how vanilla LSTMs and Transformers work, including the mathematical equations behind them.

LSTMs: LSTMs contain a memory cell and gating mechanisms that regulate the flow of information (Figure 1). These gates control what the network remembers, updates, and outputs at each time step, allowing LSTMs to learn both short- and long-range patterns in sequential data. The three gates are forget, input, and output gates that interact with a central cell state (memory) and a hidden state (output).[12] Below are the equations numbered sequentially from 1 to 6.

1. Forget Gate: This gate decides how much of the previous memory C_{t-1} to keep. The sigmoid function σ outputs values between 0 and 1 (0 means forget completely, 1 means keep entirely)

$f_t = \sigma(W_f \cdot [h_{t-1}, x_t] + b_f)$

2. Input Gate: This gate controls how much of the new input x_t should be written to the memory cell. Again, values close to 1 allow more new information in.

$i_t = \sigma(W_i \cdot [h_{t-1}, x_t] + b_i)$

DOI: 10.36838/IJHSR87.71

3. Candidate Memory (New Info to Add): This creates a candidate for new memory content, based on the current input and previous hidden state, passed through a tanh function to squash values between −1 and 1.

$\tilde{c_t} = tanh\,(W_C \cdot [h_{t-1},x_t] + b_C)$

4. Update Cell State: The memory cell is updated by combining the retained old memory C_{t-1} and the new candidate information, each weighted by its respective gate.

$C_t = f_t * C_{t-1} + i_t * \tilde{c_t}$

5. Output Gate: This gate decides how much of the memory to show as output, again using a sigmoid filter.

$o_t = \sigma_t(W_o \cdot [h_{t-1},x_t] + b_o)$

6. Compute Hidden State (Output): Finally, the hidden state output is calculated by applying tanh to the updated memory and scaling it by the output gate.

$h_t = o_t \cdot tanh\,(C_t)$

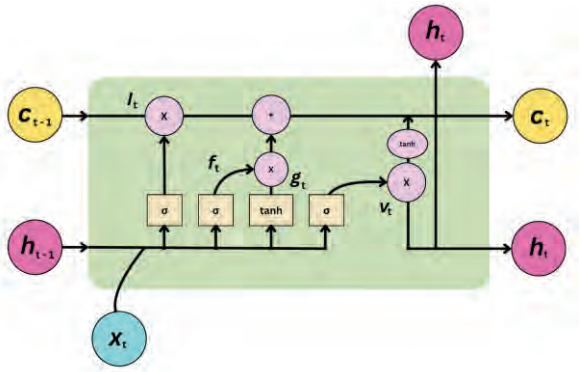

Figure 1: Diagrammatic representation of a vanilla LSTM cell. The figure illustrates how information flows through the forget gate (Equation 1), the input gate (Equation 2), and the output gate (Equation 5) to regulate updates to the cell state memory (Equation 4) and hidden state output (Equation 6). Each gate applies a sigmoid or tanh transformation to control what past information is retained and what new input is incorporated. This gating mechanism enables LSTMs to preserve long-term dependencies while flexibly adapting to short-term fluctuations, making them particularly effective for forecasting sequential and non-stationary data.

Transformers: In a transformer, there are two main parts: encoders and decoders (Figure 2). They process all steps in parallel using self-attention, allowing each input to weigh the importance of other inputs. Transformers learn patterns by passing this attention output through multilayer perceptrons, where residual connections and normalization ensure stable learning. The following steps elucidate the inner workings of a vanilla Transformer, like the one outlined by Vaswani *et al.*[13]

1. Input Embeddings and Positional Encoding: The raw input x_t is projected into a higher-dimensional space using weights W_e, and then a positional encoding is added to retain the order of the time steps.

$x_t' = x_t W_e + \mathrm{PosEnc}(t)$

2. Scaled Dot-Product Attention: Each input is then attended to all others using a weighted sum of values V, where the weights are based on the similarity (dot product) between queries Q and keys K. The division by $\sqrt{dk}$ stabilizes gradients.

$$\mathrm{Attention}(Q,K,V) = \mathrm{softmax}\left(\frac{QK^{\top}}{\sqrt{d_k}}\right)V$$

3. Multi-Head Attention: Instead of computing attention once, it is done in parallel across multiple heads, each learning different relationships. The results are then concatenated and linearly transformed.

$\mathrm{MultiHead}(Q,K,V) = \mathrm{Concat}(\mathrm{head}_1,\ldots,\mathrm{head}_h)W^O$

4. Individual Attention Head: Each head uses its own set of learned weights to compute queries, keys, and values. This lets the model learn diverse attention patterns.

$\mathrm{head}_i = \mathrm{Attention}(QW_i^Q, KW_i^K, VW_i^V)$

5. Feedforward Neural Network (FFNN): After attention, each position passes through the same fully connected network. The non-linearity (ReLU) helps capture complex patterns.

$\mathrm{FFNN}(x) = \mathrm{ReLU}(xW_1 + b_1)W_2 + b_2$

6. Residual Connection and Layer Normalization: A shortcut connection adds the input back to the sublayer output (either attention or FFNN), and the result is normalized. This helps stabilize and speed up training.

$\mathrm{Output} = \mathrm{LayerNorm}(x + \mathrm{Sublayer}(x))$

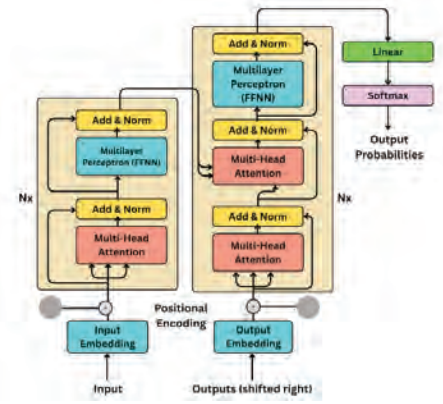

Figure 2: Diagrammatic representation of an encoder-decoder vanilla transformer, similar to the initial design presented by Vaswani *et al.* Figure highlights the parallel processing of all time steps via self-attention (Equations 2,3,4), where queries, keys, and values determine contextual relationships across the sequence. Multi-head attention allows the model to capture diverse dependencies, whilst residual connections and normalization stabilize learning. Positional encodings (Equation 1) supplement the absence of recurrence by embedding order information directly into the input.

Both models were trained on identical input–output configurations to ensure a fair comparison. Inputs consisted of single-feature time series segments of fixed block sizes (ranging from 5 to 95), with a forecasting horizon of 1. All models received the same preprocessed windowed data with no exogenous variables or pretrained components. The LSTM architecture followed a standard sequential design implemented in TensorFlow/Keras. It consisted of a single LSTM layer with 200 hidden units and ReLU activation, followed by a Dense layer with 50 ReLU units and a final Dense output layer with linear activation. No dropout was applied within the LSTM,

and the model was compiled using the Adam optimizer with a learning rate of 0.001 and an MSE as the loss function.

In our experiments, we used an encoder-only transformer, unlike the encoder-decoder Transformer in Figure 2. It is widely held true that encoders are more useful for natural language understanding, which makes them suitable for single-step regression forecasting, compared to decoders, which tend to be more apt for natural language generation instead. Our encoder-only transformer had two transformer blocks, each containing:

- Multi-head self-attention with 2 heads and head size = 64
- Layer normalization pre- and post-attention
- Dropout (0.2) applied to both attention outputs and feed-forward layers
- A feedforward sublayer using Conv1D with 64 filters and ReLU activation, followed by a linear Conv1D output layer.

Sequence outputs were aggregated using GlobalAveragePooling1D, followed by an MLP head with layers Dense(64, ReLU) → Dropout(0.2) → Dense(32, ReLU), and a final Dense output layer. Positional encodings were not used to retain simplicity. Architectural hyperparameters were selected to maintain a balance between model capacity and convergence stability, aligning with prior best practices. Both LSTM and Transformer models were trained using an 80/20 split on the ARIMA-generated datasets across all block sizes, with no separate validation set to maintain experimental consistency. Training was conducted for up to 50 epochs using the Adam optimizer (learning rate = 0.001, batch size = 64) and an MSE as the loss function. Early stopping with a patience of 10 was used to preserve generalization and retain the best model weights.

Analysis and Interrogation of Results:

For the evaluation process, we first compiled tables containing the Mean Squared Errors for each block size (from 5 to 95) for the 4 p,d,q parameters outlined earlier. In a nutshell, the MSE[14] measures how far the model's predictions are from the actual values. For each prediction, it finds the difference from the true value, squares it (to make all errors positive), and then takes the average of these squared differences. A lower MSE means the model is predicting more accurately.

$$\text{MSE} = \frac{1}{n}\sum_{i=1}^{n}(y_i - \hat{y}_i)^2$$

Where:

- y_i: the actual (true) value at position i
- $\hat{y}_i$: the predicted value at position i
- n: the total number of predictions

Following this calculation, the MSE was then passed through the Wilcoxon Signed Rank Test, which is a non-parametric test, in order to confirm whether any difference in the MSEs was legitimate or simply random variation. As noted earlier in the introduction, we could have also chosen the Diebold-Mariano (DM) test due to its prevalence in existing literature. However, it is key to understand that the DM test assumes covariance stationarity (constant mean, constant variance, and an autocovariance dependent solely on the lag). This is not the case for our ARIMA-generated time series, and thus, the core assumption of the DM test would break down if we were to use it on our MSEs. Given that the Wilcoxon signed-rank test does not hold any such assumptions, it was deemed to be the more adept test to use. Not just that, but the use of the Wilcoxon signed rank test has been widely supported in various older[15] and contemporary studies.[16] This calculation was implemented using scipy.stats.wilcoxon. The following steps outline how the Wilcoxon signed rank test values are calculated mathematically.

1. Firstly, the Wilcoxon Signed-Rank Test calculates the difference (D_i) in the performance scores (MSE) for each paired forecast (LSTM and Transformer).
$D_i = x_i - y_i$

2. Then it removes any zero differences, ranks the absolute values of the remaining differences ($|D_i|$), and assigns the original signs (+ or –) back to each rank. It then sums the positive and negative ranks separately, and the smaller of these sums becomes the test statistic (W).

$$W = \min\left(\sum_{R_i>0} R_i,\ \sum_{R_i<0} |R_i|\right)$$

3. The formula below (Z) standardizes the test statistic W so it can be compared to a normal distribution.

$$Z = \frac{W - \frac{n(n+1)}{4}}{\sqrt{\frac{n(n+1)(2n+1)}{24}}}$$

4. Then, the two-tailed p-value for a standard normal distribution can be calculated using the formula below. It represents the probability that a Z-score is at least as extreme as the observed value |z|, multiplied by 2 to account for both tails of the distribution.
$p = 2 \cdot P(Z \geq |z|)$

5. Finally, a statistically significant result is one where the p-value is below the actual significance level, indicating that one model consistently outperforms the other across the paired forecasts and that the results are not random.

Beyond the use of the MSE, we are also noting 2 other key metrics: MAE and MAPE.[17] These 2 metrics allow us to compare model performance in relative percentage terms and interpret the typical deviation better if needed.

On one hand, the MAE measures the average of the absolute differences between predicted values and actual values. The formula it utilizes is:

$$\text{MAE} = \frac{1}{n}\sum_{i=1}^{n}|y_i - \hat{y}_i|$$

On the other hand, the MAPE expresses prediction error as a percentage of the actual values. It tells us how large our errors are relative to the true values. The key equation here is:

DOI: 10.36838/IJHSR87.71

$$\text{MAPE} = \frac{100}{n}\sum_{i=1}^{n}\left|\frac{y_i - \hat{y}_i}{y_i}\right|$$

Additional Implementation Details:

For ARIMA, we employed a train–test split rather than introducing an additional validation set. In classical time-series modeling, the primary safeguard against overfitting lies in ensuring that model residuals remain well-behaved and that the fitted coefficients generalize across the observed series. Because ARIMA relies on sequential dependence, introducing a validation split would require withholding contiguous future values, which are more appropriately reserved for final out-of-sample evaluation. Moreover, the models exhibited stable convergence and consistent performance during training, reducing the need for iterative hyperparameter tuning through a separate validation set. Randomization of the data was not applied, as preserving temporal ordering is essential for autoregressive structures. Thus, the simpler train–test scheme was sufficient to evaluate forecasting performance while maintaining methodological rigor.

Also, all experiments were implemented in Python 3.10 and additional NumPy, SciPy and statsmodels libraries were used for time series data generation. Training and evaluation were conducted on Google Colab Pro, leveraging an NVIDIA T4 GPU for accelerated computation. Random seeds were fixed (np.random.seed(42)) at all stages to ensure reproducibility across runs and models. Visualizations were rendered using Matplotlib.

Results

To recap, for each configuration of the ARIMA Model, we evaluate model performance over varying block sizes (lag lengths) using Testing MSE as the primary metric. All experiments maintain d≥1 to ensure non-stationarity, in alignment with the study's focus. Additionally, the code was configured to follow a 'greedy' approach[18] where the number of epochs was not fixed, but rather depended on the point at which the validation loss plateaued or began to increase.

For reference, the ARIMA coefficients (AR and MA parts) for each configuration were:

- (0,1,1)
  - o Generated MA (Numerator) Coefficients: [1. -1.5]
  - o Generated AR (Denominator) Coefficients: [1.]
- (1,1,1)
  - o Generated MA (Numerator) Coefficients: [1. -1.5]
  - o Generated AR (Denominator) Coefficients: [1. -0.8]
- (2,1,2)
  - o Generated MA (Numerator) Coefficients: [1. 0. -2.25]
  - o Generated AR (Denominator) Coefficients: [1. 0. -0.64]
- (2,2,0)
  - o Generated MA (Numerator) Coefficients: [1.]
  - o Generated AR (Denominator) Coefficients: [1. 0. -0.64]

As mentioned earlier, the experiment incorporates the Wilcoxon Signed Rank Test to assess the significance of the results. This is explored further below:

Table 1: Wilcoxon signed-rank test results comparing LSTM and Transformer prediction errors across ARIMA configurations. Negative Z-scores indicate cases where LSTMs achieved lower mean squared errors than Transformers, while extremely small p-values ($p < 0.05$) confirm that these differences are statistically significant rather than random variation.

Dataset	W (Wilcoxon)	Z-Score	P-value
0,1,1	0	-8.862	3.90E-18
1,1,1	255	-7.805	5.95E-15
2,1,2	1920	-2.08	3.75E-02
2,2,0	970	-5.347	8.96E-08

The results in Table 1 indicate statistically significant differences in prediction errors between LSTM and Transformer models across all ARIMA configurations.

When interpreting the results seen in Figure 3, we can note the following for varying block size ranges:

• Small Block Sizes (5-25): LSTM consistently outperforms the Transformer in 3 out of 4 ARIMA configurations. It achieves particularly low MSE values in complex setups like ARIMA(2,1,2) and ARIMA(2,2,0), with averages around 0.028. In contrast, Transformer performance is highly unstable in these settings, with MSEs ranging between 0.015 and 0.315.

• Medium Block Sizes (35-65): LSTM models demonstrate consistent and stable performance across all ARIMA configurations, though without achieving the lowest errors, with MSE values typically ranging from 0.045 to 0.079 on average. Transformers show erratic behavior, performing well under ARIMA(2,1,2) with a low MSE of 0.019, but yielding significantly higher errors in ARIMA(0,1,1) and ARIMA(2,2,0), where MSE exceeds 0.09 and even 0.17.

• Large Block Sizes (75-95): LSTM models consistently achieve their lowest errors, most notably under ARIMA(2,1,2) with an average MSE of 0.014. Additionally, the Transformer model's performance can also be seen to improve.

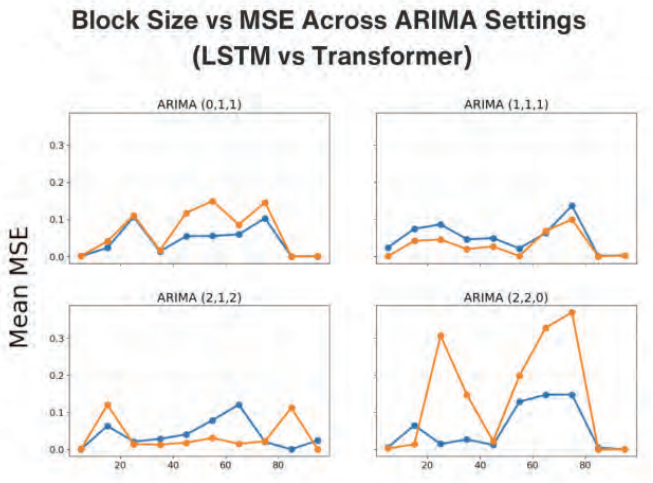

Figure 3: Mean testing MSE vs. block size for LSTM and Transformer models across different ARIMA configurations. Each subplot uses a consistent x and y-axis scale to enable direct visual comparison. The curves show that LSTMs generally maintain stable performance as block size increases, with error values clustering within a narrow band. In contrast, Transformer performance fluctuates sharply depending on block size and ARIMA parameters, with notable instability in (0,1,1) and (2,2,0).

Moreover, as seen below, Figure 4 displays the ΔMSE (LSTM MSE – Transformer MSE) across block sizes for all four ARIMA configurations, highlighting comparative model performance. Across most block sizes and configurations, negative ΔMSE values dominate, indicating that LSTM outperforms Transformer more frequently. The performance gap is especially pronounced under ARIMA(2,2,0), where LSTM achieves up to 0.29 lower MSE than Transformer, particularly in the small- to mid-range block sizes. ARIMA(2,1,2) shows more balanced results, with LSTM and Transformer alternating in dominance depending on block size. For ARIMA(1,1,1), Transformer generally maintains a slight edge throughout, while ARIMA(0,1,1) demonstrates the narrowest margins and highest variability in relative performance.

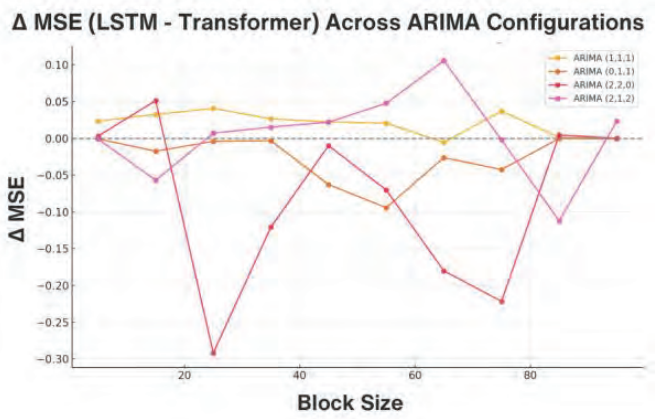

Figure 4: Difference in mean testing MSE (ΔMSE = LSTM – Transformer) across block sizes for each ARIMA configuration. Negative ΔMSE values indicate LSTM superiority, while positive values reflect cases where the Transformer performs better. These patterns underscore how LSTM resilience stems from its recurrent inductive bias, while Transformer performance is highly configuration-sensitive.

Beyond evaluating block size dependencies, it was imperative to investigate how variations in the ARIMA (p,d,q) parameters influence the performance. Across configurations, as seen in Figure 5, the LSTM consistently demonstrated a smooth and resilient performance curve. In contrast, the Transformer's performance was notably more configuration-sensitive. It only matched or slightly outperformed the LSTM under the baseline ARIMA(1,1,1) setting, which offers a balanced temporal dynamic. However, under more complex conditions, particularly with increased differencing (d) or autoregressive terms (p), its performance deteriorated significantly. In the ARIMA(0,1,1) configuration, where the autoregressive term is eliminated, LSTM performance remains relatively stable. However, Transformer models exhibit a moderate increase in MSE and greater variability across block sizes. Then, in the ARIMA(2,2,0) configuration, which removes the MA component while increasing differencing and autoregression, the most significant decline in Transformer performance takes place. Starkly high MSE values indicate a lack of adaptability to noise-driven or shock-driven memory structures. Lastly, in higher complexity configurations (a greater number of coefficients go into the ARMA), like ARIMA(2,1,2), both models exhibit improved performance, with LSTM maintaining a slight edge (although the difference in performance is negligible).

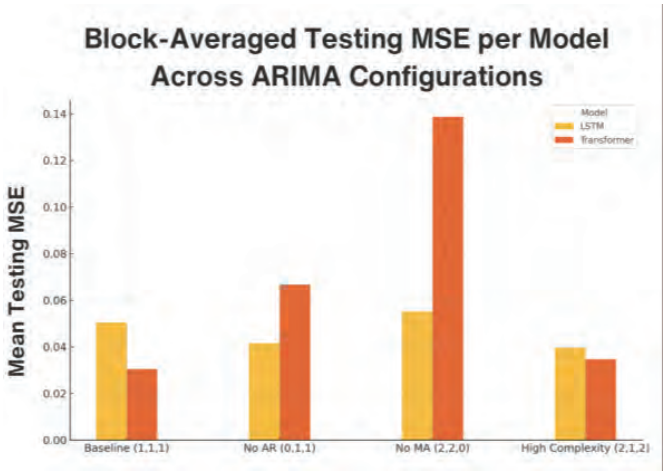

Figure 5: Average testing MSE of LSTM and Transformer models across four ARIMA configurations. When autoregressive or moving average components are removed, as in (0,1,1) and (2,2,0), Transformer performance deteriorates substantially while LSTMs remain stable. In the higher-complexity (2,1,2) setting, both models improve, though LSTM maintains a slight edge. This figure illustrates that while Transformers can excel in balanced conditions, they are far more sensitive to shifts in ARIMA dynamics, whereas LSTMs display consistent adaptability.

It is also essential to note that although MAE and MAPE were computed during experimentation, as outlined in the Methods section, they were not included in the main results for several reasons. Firstly, the models were trained to minimize MSE loss, so using MSE as the primary evaluation metric ensured direct alignment with the training objective. Additionally, relying on a single metric allowed for consistent and fair comparisons across different models and ARIMA configurations. Moreover, MAPE can become unstable or undefined when actual values are close to zero, a limitation encountered in almost all ARIMA configurations that use a block size of 85 and 95, making it less reliable for comprehensive reporting.

Discussion

Across all experimental configurations, the core insight was that vanilla LSTM models demonstrate greater resilience and adaptability than vanilla Transformers. Figure 4 reveals that the reason why LSTMs are better suited for sequential data is due to their recurrent design, which allows them to preserve contextual information over time and adapt robustly to changes in AR and MA components. Conversely, the Transformer, which relies on self-attention mechanisms rather than recurrence, exhibits greater sensitivity to the nature of the time series. Its performance peaks in the ARIMA(1,1,1) configuration, where both AR and MA components are present in moderate quantities. However, as the structure becomes skewed, either by removing AR in (0,1,1) or MA in (2,2,0), the Transformer struggles to adapt. Notably, the absence of the MA component results in a substantial performance drop, indicating potential difficulty in capturing residual-based or noise-driven correlations. These findings suggest that Transformers may lack the

DOI: 10.36838/IJHSR87.71

inductive bias necessary to generalize across varying degrees of non-stationarity.

The observed performance patterns offer several implications for practitioners working with non-stationary time series in domains such as finance, climate science, energy forecasting, and economics. First, the consistent superiority of LSTM models suggests that they are likely to perform better in real-world scenarios where there is a combination of noise-heavy settings, regime shifts, seasonal drifts, or shock-driven fluctuations. In contrast, Transformers may be appropriate in environments where the data exhibits balanced or well-structured dependencies, such as periodic sensor signals or clean transactional logs. However, their heightened sensitivity to block size and time series structure implies a greater need for configuration tuning and prior knowledge of the data-generating process.

Moreover, across all ARIMA configurations, the choice of block size (i.e., input sequence length) emerged as a key determinant of forecasting performance. LSTM models displayed a characteristic low U-shaped error curve, with degraded performance at both extremes while achieving optimal accuracy in the mid-to-high block size range. This suggests that LSTMs benefit from a balanced input window: one that is long but not so long that noise or redundant information accumulates. For Transformers, the relationship with block size was less stable and more configuration-dependent. In some settings, such as ARIMA(1,1,1), longer block sizes improved performance, whereas in others, like ARIMA(2,2,0), performance worsened with increasing sequence length. This inconsistency highlights the need for careful block size tuning. From a practical standpoint, these results position block size as a first-order hyperparameter, on par with learning rate or architecture depth. Selecting an inappropriate sequence length can lead to substantial drops in predictive accuracy, particularly for Transformer models. Therefore, automated tuning strategies or block-size-adaptive architectures may be worth exploring in future work.

While the experimental framework provides valuable insights into model behavior under controlled non-stationary settings, several limitations must be acknowledged. First, the analysis compares only baseline implementations of LSTM and Transformer architectures, without exploring architectural variants (e.g., BiLSTM, Informer, or Transformer-XL) that may offer enhanced performance on time series data. Additionally, only a fixed forecasting horizon and evaluation metric were used for comparison. Incorporating other perspectives, such as long-horizon degradation analysis, time-weighted metrics, or probabilistic error measures, could yield richer model diagnostics. Secondly, the statistical testing approach, while robust in comparing paired samples, relies on a finite set of repeated runs and does not fully capture within-run stochasticity. This may underrepresent variance in model training outcomes, particularly for Transformer models, which are known to be sensitive to initialization and convergence dynamics. Addressing these limitations in future work will help to strengthen the reliability and applicability of the study's conclusions.

Additionally, further investigation is warranted into the modeling of forecast error over time. The future direction of research would be to characterize how prediction errors evolve across the forecast horizon and attempt to fit polynomial models to time-resolved MSE curves. This may offer deeper insight into extrapolation dynamics and would directly address the open question of whether errors can be predictably modeled as a function of time in non-stationary settings. Given the sensitivity of both architectures to input sequence length, integrating dynamic lag windows or attention masks may lead to more stable and efficient forecasting pipelines. These extensions would further bridge theoretical understanding with practical forecasting performance.

Conclusion

In conclusion, these findings carry important implications for the broader research community working on deep learning for time series forecasting. While Transformers have recently garnered widespread attention for their success in natural language and vision tasks, this study reaffirms that their advantages do not straightforwardly translate to non-stationary time series prediction, especially under noisy or structurally imbalanced conditions. Our approach complements emerging studies that seek to reintroduce domain structure into neural forecasting (e.g., AR-Net,[19] N-BEATS[20]), positioning our work as both a caution and a contribution: cautioning against overgeneralizing Transformer utility in non-stationary domains, and contributing new methodology to diagnose temporal robustness in deep sequence models.

Acknowledgments

I would like to extend my heartfelt gratitude to Dr. Eric Sakk, Associate Professor of Computer Science at Morgan State University, for his mentorship and scholarly insight throughout this research. His deep expertise in artificial intelligence and time series analysis provided a valuable intellectual framework, particularly during the initial stages of experimental design. Moreover, Dr. Sakk's thoughtful feedback and academic encouragement greatly enhanced the rigor and clarity of my approach. I am truly grateful for his support and commitment to guiding young researchers in the pursuit of meaningful scientific inquiry. Additionally, I attest that the ideas, graphics, and writing in this paper are entirely my own.

References

1. Ni, H.; Meng, S.; Geng, X.; Li, P.; Li, Z.; Chen, X.; Wang, X.; Zhang, S. Time Series Modeling for Heart Rate Prediction: From ARIMA to Transformers; 2024; pp 584–589.
2. Hao, J.; Li, X.; Lv, Y.; Xiao, N. A Comparative Study on SSE 50 Index Prediction Based on ARIMA Model and LSTM Neural Network. In *2021 3rd International Conference on Machine Learning, Big Data and Business Intelligence (MLBDBI)*; IEEE: Taiyuan, China, 2021; pp 216–219. https://doi.org/10.1109/mlbdbi54094.2021.00049.
3. Dang, Y.; Chen, Z.; Li, H.; Shu, H. A Comparative Study of Non-Deep Learning, Deep Learning, and Ensemble Learning Methods for Sunspot Number Prediction. *Applied Artificial Intelligence* **2022**, *36* (1). https://doi.org/10.1080/08839514.2022.2074129.

4. Bhogade, V.; Nithya, B. Time Series Forecasting Using Transformer Neural Network. *International Journal of Computers and Applications* **2024**, *46* (10), 880–888. https://doi.org/10.1080/1206212x.2024.2396321.
5. Sonata, I.; Heryadi, Y. Comparison of LSTM and Transformer for Time Series Data Forecasting. In *2024 7th International Conference on Informatics and Computational Sciences (ICICoS), IEEE: Semarang, Indonesia*, 2024; pp 491–495. https://doi.org/10.1109/icicos62600.2024.10636892.
6. Hewamalage, H.; Ackermann, K.; Bergmeir, C. Forecast Evaluation for Data Scientists: Common Pitfalls and Best Practices. *Data Min Knowl Disc* **2023**, *37* (2), 788–832. https://doi.org/10.1007/s10618-022-00894-5.
7. Klyushin, D. Nonparametric Method for Estimation of Forecasting Models Using Small Samples. https://ceur-ws.org/Vol-3312/paper11.pdf (accessed 2025-07-23).
8. Bączek, J.; Zhylko, D.; Titericz, G.; Darabi, S.; Puget, J.-F.; Putterman, I.; Majchrowski, D.; Gupta, A.; Kranen, K.; Morkisz, P. TSPP: A Unified Benchmarking Tool for Time-Series Forecasting. arXiv January 8, 2024. https://doi.org/10.48550/arXiv.2312.17100.
9. Ruiru, D. K.; Jouandeau, N.; Odhiambo, D. LSTM versus Transformers: A Practical Comparison of Deep Learning Models for Trading Financial Instruments. In *Proceedings of the 16th International Joint Conference on Computational Intelligence*; SCITEPRESS - Science and Technology Publications: Porto, Portugal, 2024; pp 543–549. https://doi.org/10.5220/0012981100003837.
10. Zhang, R.; Song, H.; Chen, Q.; Wang, Y.; Wang, S.; Li, Y. Comparison of ARIMA and LSTM for Prediction of Hemorrhagic Fever at Different Time Scales in China. *PLoS ONE* **2022**, *17* (1), e0262009. https://doi.org/10.1371/journal.pone.0262009.
11. Makridakis, S.; Spiliotis, E.; Assimakopoulos, V. M5 Accuracy Competition: Results, Findings, and Conclusions. *International Journal of Forecasting* **2022**, *38* (4), 1346–1364. https://doi.org/10.1016/j.ijforecast.2021.11.013.
12. Hochreiter, S.; Schmidhuber, J. Long Short-Term Memory. Neural Computation 1997, 9 (8), 1735–1780. https://doi.org/10.1162/neco.1997.9.8.1735.
13. Vaswani, A.; Shazeer, N.; Parmar, N.; Uszkoreit, J.; Jones, L.; Gomez, A. N.; Kaiser, L.; Polosukhin, I. Attention Is All You Need. arXiv August 2, 2023. https://doi.org/10.48550/arXiv.1706.03762.
14. James, G.; Witten, D.; Hastie, T.; Tibshirani, R.; Taylor, J. *An Introduction to Statistical Learning with Applications in Python*; 2023.
15. Dems˘ar, J.; Demsar, J. Statistical Comparisons of Classifiers over Multiple Data Sets (2006).
16. Nguyen, T. S.; Nguyen, D. M. D.; Nguyen, V. T. Empirical Comparison of Lightweight Forecasting Models for Seasonal and Non-Seasonal Time Series. arXiv 2025. https://doi.org/10.48550/ARXIV.2505.01163.
17. Adhikari, R.; Agrawal, R. K. An Introductory Study on Time Series Modeling and Forecasting. **2013**. https://doi.org/10.48550/ARXIV.1302.6613.
18. Greedy Layer-Wise Training of Deep Networks. *Advances in Neural Information Processing Systems 19* **2007**, 153–160. https://doi.org/10.7551/mitpress/7503.003.0024.
19. Triebe, O.; Laptev, N.; Rajagopal, R. AR-Net: A Simple Auto-Regressive Neural Network for Time-Series. arXiv November 27, 2019. https://doi.org/10.48550/arXiv.1911.12436.
20. Oreshkin, B. N.; Carpov, D.; Chapados, N.; Bengio, Y. N-BEATS: Neural Basis Expansion Analysis for Interpretable Time Series Forecasting. arXiv February 20, 2020. https://doi.org/10.48550/arXiv.1905.10437.

Authors

Abdullah Shaikh, a rising senior from Jumeirah College, Dubai, is a dynamic innovator leading a Gen Z financial literacy movement by pioneering AI-driven financial tools and hosting insightful entrepreneurship podcasts. His research explores how deep learning techniques can aid in time series forecasting, especially for financial applications. Beyond academic pursuits, Abdullah has won global debate and STEM competitions, where he blends technical acumen with a passion for impact.

DOI: 10.36838/IJHSR87.71

IJHSR
ijhighschoolresearch.org
REVIEW ARTICLE

Relationship and Comparison between Plasma, Neuroimaging, and Digital Biomarkers in Alzheimer's Disease

Anaya Shabi

Global Indian International School SMART Campus, 27 Punggol Field Walk, Singapore, 828649; anaya.shabi10@gmail.com
Mentor: Dr. Bahaaeddin Attaallah

ABSTRACT: Alzheimer's disease (AD), the world's leading cause of dementia, presents significant diagnostic and therapeutic challenges due to its prolonged preclinical phase. This review critically examines three emerging biomarker modalities: plasma, neuroimaging, and digital biomarkers, evaluating their individual and combined utility in the detection and monitoring of AD. Plasma biomarkers provide minimally invasive, scalable measures of molecular pathology. Neuroimaging provides highly localized, anatomical detail necessary for diagnosis and monitoring of disease progression. Digital biomarkers from cognitive/behavioral measures via technological devices allow ecologically valid monitoring in real time. This comparative analysis weighs the respective strengths of each modality: accessibility (plasma), anatomic specificity (neuroimaging), and functionality (digital) against respective limitations. Within the ATN (Amyloid, Tau, Neurodegeneration) framework, this review synthesizes evidence to evaluate the rationale for an integrated biomarker approach for optimized early identification, personalized planning for therapeutics, and scalable mass-population screening.

KEYWORDS: Biomedical and Health Sciences, Pathophysiology, Alzheimer's Disease, Biomarkers, Plasma, Neuroimaging, Digital.

Introduction

Alzheimer's disease (AD) is a progressive neurodegenerative disorder that impairs memory, cognition, and the capacity to perform everyday activities.[1] AD is the most common type of dementia, affecting over 55 million people worldwide as of 2024 and projected to exceed 139 million by 2050.[1] AD typically begins with an extended preclinical phase during which pathological changes occur without any obvious symptoms, marked by amyloid-β aggregation and tau pathology.[2,3] Once clinical symptoms become apparent, irreversible neurodegeneration has usually occurred by which point most therapeutic interventions are ineffective.[4]

These pathological mechanisms underlie the ATN framework (Amyloid, Tau, Neurodegeneration), which is now used extensively to stage AD biomarkers.[2] Amyloid deposition ('A') can be assessed using amyloid PET or plasma *Aβ42/40*; tau pathology ('T') can be quantified using tau PET or plasma phosphorylated tau (*p-tau181, p-tau217, p-tau231*); neurodegeneration ('N') is reflected in MRI-based brain atrophy or functional decline measured through digital cognitive tools.[5–7] This framework depicts how different biomarker modalities assess complementary facets of AD pathology.

However, although each biomarker class has been extensively studied in isolation, few investigations have systematically compared plasma, neuroimaging, and digital modalities within a unified ATN framework.[2,5,7,8] This gap constrains our ability to elucidate how molecular, structural, and functional measures interact across the AD continuum, thereby limiting the translational value of biomarker research. Consequently, a more integrated comparative approach is necessary to align biomarker discovery with clinical application, improve diagnostic precision, and guide multimodal trial design.[9]

In recent decades, biomarkers have become essential tools for early diagnosis, disease monitoring, and therapeutic planning in AD.[9–11] Plasma biomarkers provide noninvasive measures of molecular pathologies;[5] neuroimaging biomarkers provide information about changes in brain structure and function;[3,6] digital biomarkers capture cognitive and behavioral changes through continuous or task-based assessments enabled by modern technological devices.[7] Each type of biomarker reveals different aspects of disease development, yet together they enrich understanding of pathophysiological processes underlying AD.

The literature reviewed was identified through searches on PubMed, Google Scholar, and Scopus conducted between 2015 and 2024, focusing on peer-reviewed studies of plasma, neuroimaging, and digital biomarkers in AD. This review prioritized large cohort studies, systematic reviews, and clinical trial data to ensure robustness of evidence. Previous reviews have frequently considered plasma, neuroimaging, or digital modalities in isolation. However, few studies have systematically compared these modalities within a unified framework, even as the ATN model increasingly emphasises their complementarity to represent amyloid ('A'), tau ('T'), and neurodegeneration ('N').[5,7–9] This lack of integrated analysis creates uncertainty regarding how distinct biomarker classes should be positioned relative to one another in both research and clinical contexts. Accordingly, this review synthesizes recent evidence across plasma, neuroimaging, and digital biomarkers, evaluating their diagnostic performance, scalability, and translational readiness when interpreted through the ATN framework.

© 2026 Terra Science and Education

DOI: 10.36838/IJHSR87.80

■ Comparative Relationships Between Biomarker Modalities

While plasma, neuroimaging, and digital biomarkers provide valuable insights individually, their full diagnostic and translational potential emerges when evaluated together.[2]

Pairwise comparisons clarify whether less invasive and scalable modalities can effectively complement or, in certain cases, replace more established but costly techniques. These comparisons correspond to the ATN framework: amyloid and tau pathology ('A' and 'T') are measured by plasma and imaging biomarkers, and neurodegeneration ('N') by imaging and digital measures.[2,7] Evaluating these relationships reveals where modalities converge or differ, which informs diagnostic approach, trial planning, and multimodal biomarker integration in clinical care. The following sections discuss these pairwise relationships in detail, starting with that between plasma and neuroimaging biomarkers.

Plasma and Neuroimaging:

Positron Emission Tomography (PET) and Magnetic Resonance Imaging (MRI) are cornerstone neuroimaging techniques for AD, providing *in vivo* quantification of amyloid plaques, tau tangles, and neurodegenerative alterations.[3,6,8] These techniques, for example, amyloid-PET, have been shown to reveal Aβ accumulation up to two decades before the onset of clinical disease symptoms, while tau-PET provides regional specificity useful for disease staging, which in turn correlates with the severity of clinical presentations.[3,5,6,8] These modalities are, however, expensive, invasive, and less accessible in nonspecialized centers.[8] Within the ATN framework, imaging captures amyloid ('A'), tau ('T'), and neurodegeneration ('N') with high spatial precision, whereas plasma biomarkers provide scalable molecular proxies for amyloid and tau pathology.[2]

As a result, plasma biomarkers, such as phosphorylated tau isoforms *p-tau181, p-tau217,* and *p-tau231*, are emerging as more viable, scalable alternatives.[12–14] These phosphorylated tau proteins reflect AD pathology and can be measured in blood with increasing sensitivity and specificity.

Various research studies demonstrated a strong association between neuroimaging biomarkers and plasma tau concentrations in AD. Plasma *p-tau217* closely mirrors tau-PET signals in early tau-deposition regions such as the entorhinal cortex and inferior temporal lobe, suggesting strong potential as a surrogate marker even in preclinical disease stages.[13,15]

Consistent with this concordance, longitudinal studies showed that plasma *p-tau217* predicts future tau-PET positivity as well as medial temporal lobe atrophy.[13,15] The robust association suggests that plasma *p-tau217* can serve as a surrogate marker during the preclinical stage of disease. Overall, these results support the conclusion that plasma *p-tau217* tracks with PET signals and is a scalable surrogate for early diagnosis.

Plasma *p-tau217* demonstrates high specificity (≈96%) for distinguishing AD from other neurodegenerative disorders in research cohorts. Plasma *p-tau217* results stem from relatively small clinical cohorts and thus cannot be assumed to be generalizable until they are replicated in larger, more diverse groups. These results indicate the potential of plasma markers as early identifiers, especially in those with no evident clinical symptoms.[15] In addition to diagnostic discrimination, spatial correlation of plasma and imaging markers indicates their complementary value. Plasma *p-tau231* levels correlate with Braak stage I–II areas and earliest tau pathology in the transentorhinal cortex.[14] Such anatomical correlations indicate that plasma biomarkers can reflect neuroanatomical changes identified by imaging, though they lack spatial resolution. This overlap implies that plasma assays can partially replicate spatial patterns normally obtained using imaging. Plasma biomarkers have also been shown to predict subsequent changes detectable by neuroimaging in longitudinal studies.

Individuals with elevated plasma *p-tau181* levels, despite normal baseline tau-PET scans, became tau-PET positive within two years.[13] A 2023 long-term follow-up revealed that higher plasma *p-tau217* predicted increasing tau-PET binding and medial temporal atrophy.[16] These findings demonstrate that plasma biomarkers not only indicate current pathology but may also predict future disease progression, a valuable feature for longitudinal monitoring. These longitudinal results further bolster the argument in favor of plasma assays as not only reflective, but predictive measures in the ATN cascade, well before imaging-detectable alterations.

Yet measurements are not always concordant between modalities, and in a minority of cases, plasma-imaging discordance may be of clinical importance in and of itself. Some patients have elevated tau-PET signal with low plasma tau, which can reflect late disease stages, where tau production has slowed, but deposition continues.[13] This discordance actually serves to emphasize that plasma and imaging are not equivalent but rather sample different points along the trajectory of tau pathology with possible diagnostic utility in distinguishing the stage of disease.

Notwithstanding such heterogeneity, the complementary strengths of these modalities have been demonstrated in clinical research to reduce costs and optimize participant selection. For instance, plasma *p-tau217* was employed in the AHEAD 3–45 trial as a prescreening test for cognitively normal individuals prior to more expensive amyloid- and tau-PET imaging.[10] Likewise, the TRAILBLAZER-ALZ 2 study used plasma *Aβ42/40* and *p-tau217* assays for prescreening participants receiving anti-amyloid treatment.[11]

These examples illustrate how plasma biomarkers can function as a cost-effective adjunct to neuroimaging by enabling large-scale prescreening prior to confirmatory testing. Such trial designs demonstrate that combining plasma-based screening with confirmatory imaging maximizes cost-efficiency and recruitment efficiency in AD research.[17,18]

Although these encouraging correlations do exist, there are some important limitations. Plasma–imaging concordance studies have most often been performed in small, fairly homogeneous populations,[12,13] rendering generalizability difficult. Plasma assays are not yet globally standardized and show significant variability across laboratories and assay platforms, which detracts from clinical utility.[19] Finally, apparent discor-

dance among modalities emphasizes the value of multimodal assessment over dependence on any one class of biomarkers.

In total, these results emphasize the complementarity of imaging and plasma biomarkers. Imaging offers anatomical resolution and staging across the 'A,' 'T,' and 'N' domains, whereas plasma assays offer noninvasive, scalable measures of amyloid and tau. These results demonstrate the complementarity of plasma and imaging, where plasma allows for low-cost scalability and imaging offers anatomical resolution.

Neuroimaging and Digital:

Neuroimaging biomarkers, such as PET and MRI, have provided important information regarding the structural and functional changes related to AD. Structural MRI data show that hippocampal atrophy, an important marker of episodic memory decline, develops at a very early stage, while fMRI studies show disturbances within the default mode network (DMN), a set of brain regions including the posterior cingulate cortex and medial prefrontal cortex that support introspective cognition and memory-related processes.[6,20,21] As imaging technologies have advanced, digital biomarkers have demonstrated convergent validity with imaging-based measures, offering accessible tools for assessing real-world functional impairments.[22] Within the ATN framework, MRI and fMRI act as spatial markers of neurodegeneration ('N'), whereas digital biomarkers capture functional manifestations of this domain in ecologically valid contexts. This complementarity underscores their potential for integrated monitoring of disease progression.[2,7]

Memory deficits are among the earliest clinical manifestations of AD and are closely associated with hippocampal atrophy on MRI.[6,20] Performance on digital memory assessments, such as narrative recall and object-location tasks administered via tablets, is associated with subsequent left hippocampal volume loss in a region essential for encoding verbal material.[22] However, most such studies were conducted in highly educated, predominantly Western cohorts,[23] limiting the generalizability of digital testing across diverse cultural and socioeconomic groups. Furthermore, performance on digital episodic memory tasks also correlates with medial temporal lobe atrophy.[23,24] These results indicate that, despite lacking spatial resolution, digital cognitive assessments can effectively reflect the neurodegeneration detected by imaging modalities.

Attention deficits, measured by reaction time variability (RTV), demonstrate strong concordance with fMRI-based disruptions. Elevated RTV, an index of attentional instability, has been associated with reduced DMN interconnectivity, even among cognitively normal individuals at risk for AD.[21] A 2024 follow-up analysis demonstrated that computerized attention measures predicted early network decline, reaffirming the potential of digital attention testing in preclinical AD.[24]

Beyond formal cognitive testing, spontaneous speech has also been investigated as an indirect measure of background neuroanatomical change. Executive function, one of the initial domains affected by AD, has also been associated with structural changes in the dorsolateral prefrontal cortex (DLPFC) and anterior cingulate cortex as observed on MRI.[20,23] Digital executive tests, such as the n-back and Stroop tasks, demonstrated sensitivity to dysfunction in affected brain regions. Digital administration of the Stroop test distinguished patients with MCI from controls and correlated with frontal lobe atrophy.[23] Speech-based digital biomarkers also demonstrate convergent validity with neuroimaging findings. A 2022 study found that increased silence duration in speech, a digital voice biomarker, correlated with early cognitive decline, and these speech patterns were associated with functional and structural brain changes in regions linked to AD.[25,26]

Longitudinal studies further strengthen evidence that digital biomarkers can predict neuroimaging outcomes. Earlier cognitive impairments detected by digital measures predicted subsequent hippocampal atrophy and tau deposition even when the baseline imaging was normal.[20,22] A 2024 validation study confirmed that digital memory impairments were associated with subsequent medial temporal lobe atrophy.[22] Together, these longitudinal findings suggest that digital tools may precede imaging-detectable decline by several years, reinforcing their utility as early screening instruments and continuous monitoring tools in at-risk populations.

Although findings are encouraging, several challenges persist. Digital biomarkers generally rely on heterogeneous platforms (e.g., tablets, smartphones, and wearable devices) and lack standardized protocols, complicating cross-study comparability. Wearable device integration into multimodal frameworks remains promising but underdeveloped, as wearable devices can provide continuous physiological measures that complement imaging and plasma-based markers. Test setting variability (home vs. clinic) and limited regulatory validation constrain translation to clinical trials or practice. Addressing these methodological and regulatory challenges will be essential for widespread clinical adoption.[7,27]

In summary, a substantial convergence of neuroimaging methods and digital cognitive biomarkers exists across many cognitive domains, particularly regarding memory, attention, and executive function. Neuroimaging tools provide accurate spatial representations of the brain, while digital tools track functional decline in ecologically valid settings at regular and economical intervals. This convergence supports combining both modalities for early detection and longitudinal monitoring of AD, with digital tools providing unique repeatability and ecological validity for both clinical trials and real-world applications.[7,27]

Digital and Plasma:

Plasma biomarkers such as phosphorylated tau isoforms (*p-tau181, p-tau217,* and *p-tau231*) and the amyloid-beta 42/40 ratio (*Aβ42/40*) are particularly effective in the identification of central pathological signs of AD.[12–14] Such biomarkers provide noninvasive tools that quantify molecular alterations indicative of amyloid deposition and tau pathology using scalable blood-based methods. Their clinical utility is greatly enhanced when linked with functional indicators from digital devices that record cognitive and behavioral performance.[7,22] Within the ATN framework, plasma biomarkers primarily reflect amyloid ('A') and tau ('T') pathology, whereas digital

DOI: 10.36838/IJHSR87.80

tools capture neurodegeneration ('N') through functional impairment. Integrating these modalities allows comprehensive assessment across all three domains.

Recent studies point to a rising correlation between plasma biomarker levels and performance deficits on digital cognitive tests. Plasma levels of *p-tau231* correlate with deficits in story recall and delayed recognition tests taken on tablet devices, even in cognitively healthy individuals.[22] These digital tests are found to be markers of medial temporal lobe function, an area that is the first to present tau pathology in AD. The presence of such a correlation suggests that functional deficits that are detected through digital means reflect underlying neurobiological processes, including elevated plasma tau levels.

Individuals with greater baseline plasma *p-tau217* levels declined more steeply in semantic fluency and learning ability over 18 months, according to web-based cognitive testing platforms.[15] These relationships were still significant after adjustment for possible confounding influences such as the APOE ε4 genotype and age, confirming the predictive validity of the plasma biomarker for functional decline. The findings also expand the role of internet-based testing in revealing subtle behavioral changes that result from molecular pathologies.

Beyond cognitive testing, speech-derived digital biomarkers offer a noninvasive alternative means of capturing the early molecular alterations. In a recent cohort study, poorer digital executive function performance predicted subsequent increases in plasma *p-tau181* and decreases in the *Aβ42/40* ratio.[22] This suggests that, in some preclinical cohorts, functional alterations may precede or coincide with peripheral biomarker changes, particularly in preclinical AD cohorts.

For instance, amyloid-positive status exhibited significantly more silent pauses and altered auditory parameters in remote speech recordings, demonstrating an association between speech-based digital biomarkers and underlying AD pathology.[26] However, most speech-derived digital biomarkers are still developed on prototype platforms, and standardized methods for integrating these tools into clinical practice have yet to be developed or validated.

In addition, remote digital cognitive testing, including working memory and semantic classification tasks, has shown promise as an early predictor of AD risk. Impaired performance on these tests predicted pathological plasma biomarker profiles one to two years later, particularly in cohorts with preclinical amyloid positivity.[28] These findings illustrate how digital performance can precede molecular change, rendering it amenable to risk stratification. Collectively, these studies suggest that digitally measured functional decline may foreshadow, and in some cases outpace, molecular alterations detected in plasma, highlighting the potential of digital tools for risk stratification in preclinical AD.

Despite encouraging results, key challenges remain. Most studies are limited by small, demographically homogeneous cohorts, raising concerns about generalizability. Digital tools also differ across platforms, complicating standardization, and few have yet been validated as regulatory endpoints. These limitations must be addressed before plasma and digital integration can be routinely implemented in clinical trials or practice.[7,22,27]

Collectively, current evidence confirms a bidirectional relationship between molecular and behavioral indicators, reinforcing the value of multimodal integration. When used together, these modalities enhance diagnostic precision, disease monitoring, and participant stratification in AD research. Importantly, integrating digital and plasma biomarkers offers a practical approach for prescreening and participant enrichment in large-scale clinical trials and remote longitudinal monitoring in real-world settings.

■ Comparison between Plasma, Neuroimaging, and Digital Biomarkers

The preceding paragraphs outlined the interaction of plasma, neuroimaging, and digital biomarkers and their molecular, structural, and functional qualities. Equally important is a systematic evaluation of each modality's comparative strengths. Each biomarker class offers distinct advantages and limitations depending on its use in presymptomatic detection, staging, therapeutic monitoring, or trial design. This section compares the three modalities on seven dimensions: diagnostic precision, temporal sensitivity, invasiveness, cost and scalability, clinical readiness, ecological validity, and primary limitations. This dimensional comparison highlights the usefulness of each modality in its domain and demonstrates how their differences allow for an integrated and complementary diagnostic framework. In the ATN framework, plasma biomarkers mainly index amyloid ('A') and tau ('T'), neuroimaging spans the three domains ('A', 'T', and 'N'), and digital biomarkers capture functional expressions of neurodegeneration ('N'). This comparative perspective illustrates how the three modalities align with distinct layers of the disease process. The following table summarizes these relationships, followed by a detailed analysis of each dimension.

Table 1: Comparison between plasma, neuroimaging, and digital biomarkers across different domains.

Dimension	Plasma Biomarkers (A/T)	Neuroimaging Biomarkers (A/T/N)	Digital Biomarkers (N)
Diagnostic Accuracy	High for *p-tau217* and *Aβ42/40* (AUC > 0.90) in research cohorts; real-world accuracy under validation	Gold standard for anatomical specificity and disease staging (amyloid/tau PET, MRI)	Moderate at present; improving with task diversity, AI, and multimodal tests
Temporal Sensitivity	Become abnormal ~7–10 years before symptom onset	Amyloid PET abnormal 15–20 years before onset; tau PET and MRI closer to symptoms	May detect very early functional changes (e.g., subtle speech, executive dysfunction), but less validated and temporally uncertain
Invasiveness & Burden	Minimally invasive (venipuncture)	Moderately to highly invasive; radiation exposure (PET), long scans	Noninvasive, home-based, frequent data capture
Cost & Scalability	Lower cost; scalable; increasingly feasible in primary care, though assays are not standardized	High cost; limited scalability; mainly tertiary centers or trials	Very low cost; highly scalable with consumer devices, but equity/digital divide issues limit reach
Clinical Readiness	Increasing adoption in trials; clinical uptake growing, but assay harmonization is lacking	Already established and regulatory-approved for diagnosis/staging	Experimental; platforms in pilot/validation stage; regulatory pathways emerging
Ecological Validity	Low; snapshot of molecular pathology in clinic setting	Moderate; in-clinic brain state measures	High; reflects real-world cognitive and behavioral function in daily life
Limitations	Affected by systemic factors; assay variability across labs, and standardization needed	Costly, centralized, logistically burdensome	Susceptible to device bias, environmental noise, and digital literacy/access variability

Diagnostic Accuracy:

Plasma *p-tau217* and *Aβ42/40* display excellent diagnostic accuracy (AUC > 0.90) in distinguishing AD from other dementias in large multicenter cohorts such as Janelidze *et al*. (n ≈ 1,200) and Palmqvist *et al*. (n ≈ 600).[5,15] Real-world accuracy may be reduced because such estimates are often derived from highly selected research cohorts.[29,30] Their accuracy, nonetheless, makes plasma assays promising candidates for large-scale early detection. Neuroimaging, especially tau-PET, remains the gold standard for anatomical staging, supplemented by longitudinal imaging studies of several hundred individuals across multisite consortia such as ADNI.[6,20] Digital biomarkers currently demonstrate modest accuracy (AUC ≈ 0.70–0.80) in small pilot groups of 100–300 subjects but are being refined at a high rate by multimodal assessments enhanced by machine learning.[7,24] AI approaches increasingly enable detection of subtle behavioral patterns such as reduced speech fluency or slowed response latency that may signal preclinical decline.[25,26] While imaging offers regional specificity and plasma biomarkers capture molecular signatures, digital technologies capture behavioral correlates that mirror more pervasive, early-stage cognitive disruptions that may precede discrete molecular or anatomical abnormalities. These accuracy differences reflect each modality's unique biological target rather than implying a diagnostic hierarchy.[2,9] In clinical practice, this means plasma assays are most promising for scalable early detection, imaging remains essential for staging and differential diagnosis, and digital tools may act as continuous functional readouts to track intervention response.[30] Together, these modalities demonstrate complementary accuracy profiles. Neuroimaging defines anatomical localization, plasma assays detect biochemical pathology, and digital tools capture functional impact.

Temporal Sensitivity:

Neuroimaging modalities such as amyloid PET document pathological deviations 15–20 years prior to symptom onset and hence serve as the earliest measurable indicators of pathological change.[3] Plasma tau biomarkers appear several years before clinical onset (estimated 7–10 years in longitudinal modeling).[13,29] Digital biomarkers, though still in early development, may detect subtle cognitive and functional changes even before measurable molecular abnormalities emerge.[7,21] Subtle impairments such as minor speech delays or executive dysfunction detected via digital tools may reflect compensatory neural responses that precede measurable pathological changes.[24,25] These signals remain less validated than molecular or imaging markers, and their temporal positioning within the ATN cascade is still under investigation. This temporal progression suggests a continuum of biomarker evolution: imaging often captures the earliest detectable deposition, while plasma assays reflect downstream molecular changes.

Invasiveness and Patient Burden:

The level of invasiveness itself is an important determinant of follow-up and longitudinal screening adherence. Plasma biomarkers are accessed by venipuncture alone and thus are convenient to sample repeatedly.[19] Neuroimaging, particularly PET, entails radiation exposure, prolonged scanning time, and clinical equipment with logistical inconveniences.[8,18] Digital biomarkers are remotely administered and completely noninvasive, permitting frequent data capture outside clinical settings.[27] These differences illustrate how plasma and digital approaches improve compliance in longitudinal research, while neuroimaging is still needed for definitive, multifactorial diagnosis.

Cost and Scalability:

Cost remains a decisive constraint in AD diagnostics. Neuroimaging is resource-intensive, with a single PET scan typically costing several thousand dollars when performed using state-of-the-art technology.[18,31] Plasma biomarkers, although still undergoing validation, represent a substantially more affordable option and are increasingly suited for deployment in primary care settings.[30,32] Digital biomarkers offer the highest scalability, as they require minimal infrastructure and enable passive, high-frequency measurement through consumer devices.[7,21] Formal cost-effectiveness modeling demonstrates that the use of blood-based or digital prescreening prior to PET imaging substantially reduces trial recruitment costs and participant burden.[18,31] These findings have broader health-economic implications, suggesting that plasma and digital biomarkers can reduce both trial-related and healthcare expenditures by decreasing reliance on high-cost imaging. Collectively, these cost differentials position plasma and digital biomarkers as promising first-line tools for scalable screening across diverse healthcare systems, supporting the adoption of tiered diagnostic models in AD.

Clinical Readiness:

Neuroimaging modalities are already being utilized via regulatory approval and integration into diagnostic criteria.[2] Plasma biomarkers are nearing clinical utility as they become integrated into trial designs and diagnostic algorithms, though the lack of assay standardization remains a major barrier to implementation.[30,32] Digital biomarkers are largely at the validation and preclinical research stages, with ongoing pilot studies in progress and unresolved regulatory questions.[27] The relative paucity of clinical readiness in digital biomarkers is a reflection of their recent discovery and continuing regulatory assessment.[27,33] Policy framework development and regulatory concordance will be needed to propel these devices from pilot trials to regular use in healthcare practice.[27,33] In summary, neuroimaging is clinically established, plasma biomarkers are undergoing translational adoption, and digital metrics remain pre-regulatory, reflecting the developmental gradient across modalities.

Ecological Validity:

Ecological validity has been conceptualized as the degree to which a biomarker captures daily functioning.[33] Digital biomarkers uniquely quantify behavior in real-world conditions, such as everyday speech or response latency.[25,27] Plasma and neuroimaging biomarkers, however, quantify biological processes under controlled conditions, providing precise but static

DOI: 10.36838/IJHSR87.80

snapshots of disease.[2,6] Digital tests should therefore be considered adjunctive tests that complement, rather than substitute for, traditional diagnostic tests.[7,27] Their use also raises equity concerns because access to smartphones, tablets, or stable internet may differ across age groups, socioeconomic groups, and cultural backgrounds. These synergistic strengths emphasize the need for integration of biological and behavioral data in minimizing access disparities to promote equitable clinical translation.

Modality Limitations:

Despite their promise, each biomarker modality faces distinct limitations. Plasma tests, while accurate and minimally invasive, lack global standardization and therefore limit the reproducibility of findings across populations.[5,19] Neuroimaging provides gold-standard anatomical precision but is constrained by cost, radiation exposure (in PET), and limited accessibility, which limits its utility to specialty centers and trials rather than broad clinical practice.[8,18] Digital biomarkers, though scalable and ecologically valid, suffer from heterogeneity in platforms and protocols, as well as disparities in digital literacy and device access that raise equity concerns.[21] Collectively, these limitations reinforce the complementary value of the three biomarker classes: plasma detects molecular pathology, imaging defines anatomical context, and digital tools capture functional consequences.

Synthesis and Implications:

This comparative analysis underscores the strategic complementarity of the three biomarker classes. Plasma assays allow for large-scale molecular screening;[19] neuroimaging provides spatial resolution for staging and diagnosis[6]; and digital technologies enable continuous, ecologically valid monitoring of cognitive and behavioral function.[27] While each modality has inherent limitations when used alone, together they align molecular, structural, and functional domains to a coherent diagnostic framework that encompasses the full trajectory of AD. In practice, recent prevention and treatment trials increasingly adopt this tiered model: plasma assays for prescreening, neuroimaging for confirmation and staging, and digital tests for longitudinal follow-up and monitoring of treatment.[7,10,11] This combined approach maximizes diagnostic specificity and enables patient-tailored therapeutic strategies, particularly as studies increasingly target presymptomatic intervention and long-term disease monitoring in heterogeneous populations.[2,32] Future research should prioritize the development of multimodal integration platforms that balance plasma, imaging, and digital biomarkers in integrated diagnostic algorithms for optimal analytical sensitivity, specificity, and scalability. Furthermore, standardized assay procedures, interoperable digital platforms, and shared data governance structures will be key to the translation of multimodal biomarkers from proof-of-concept studies into routine clinical practice.[19,32]

■ Conclusion

The clinical picture of AD is being transformed rapidly by advances in plasma, neuroimaging, and digital biomarkers. Each modality provides a unique, complementary perspective. Plasma biomarkers allow for minimally invasive, affordable identification of amyloid and tau pathology. Neuroimaging, and particularly PET and structural MRI, remains critical for anatomical accuracy and disease staging. Digital biomarkers provide ecologically valid assessments of cognition and behavior, documenting fine functional impairment in real-world settings. Within the ATN framework, the modalities provide a comprehensive picture of progression of the AD: plasma assays index ATN A (amyloid) and ATN T (tau), neuroimaging spans all sub-domains of ATN, and digital measures capture functional correlates of neurodegeneration.

Integration enables recruitment of participants for clinical studies and for individualized, adaptive monitoring and therapeutic approaches. Yet, translation of standardized diagnostic models to everyday clinical practice is still challenged by several difficulties, such as inter-assay variation between heterogeneous plasma platforms, the absence of complete international standardization of digital devices, and unanswered regulatory and validation dilemmas. For primary and community care, scalable plasma and digital biomarkers might be used as prescreening devices, thereby reducing the high costs of neuroimaging and enabling prospective clinical intervention at a shorter disease stage. At the clinical-trial level, multimodal prescreening approaches can reduce recruitment costs, expedite enrollment timelines, and enhance demographic diversity of study cohorts. At the health-system level, low-cost prescreening approaches can diminish economic burden while enhancing equitable access to evaluative diagnostic exploration for both high- and low-resource settings. Continued advances in wearable sensors and artificial intelligence will further expand the reach of biomarker-based monitoring, yet successful implementation will require investment in digital infrastructure, method standardization, and harmonized regulatory policies.

Despite rapid development, a number of challenges must be addressed before multimodal biomarker approaches are widely adopted for routine use in the clinical setting. Neuroimaging will continue to provide essential staging information despite its prohibitive cost and limited availability, which are current constraints for its universal adoption. Plasma biomarkers currently demonstrate the highest level of clinical readiness, but overarching large-scale harmonization of assays and convergent regulatory approaches must occur for routine adoption. Digital biomarkers, while highly scalable, remain the most investigational class. Device heterogeneity, scarce standardization, data protection concerns, and cultural variations continue to constrain their generalizability and regulatory approval.

Future research should emphasize large, multiethnic validation study cohorts across a variety of groups, globalization of assay harmonization, and regulatory framework development for digital endpoints. Real-world integration will also require the development of simplified clinical guidelines and reimbursement models to ease biomarkers' transition from

the research setting into everyday clinical practice. Of the three biomarker modalities, plasma biomarkers have by far the strongest evidence base for short-term clinical translation. Digital biomarkers, also derived from artificial intelligence and wearable sensor technologies, are investigational but extremely promising, assuming issues of privacy, interoperability, and data stewardship are appropriately managed. Together, these patterns indicate that plasma biomarkers are the most immediately translatable to clinical practice, neuroimaging will continue to serve as a foundation of disease confirmation and staging, and digital biomarkers have tremendous potential for changing continuous monitoring and patient engagement as soon as standardization, privacy, and equity concerns are appropriately overcome.

Acknowledgments

I would like to thank Dr. Bahaa Attaallah for all the support, mentorship, and guidance provided throughout my research journey.

References

1. 2024 Alzheimer's Disease Facts and Figures. *Alzheimers Dement*. **2024**, *20* (5), 3708–3821. https://doi.org/10.1002/alz.13809.
2. Jack, C. R.; Bennett, D. A.; Blennow, K.; Carrillo, M. C.; Dunn, B.; Haeberlein, S. B.; Holtzman, D. M.; Jagust, W.; Jessen, F.; Karlawish, J.; Liu, E.; Molinuevo, J. L.; Montine, T.; Phelps, C.; Rankin, K. P.; Rowe, C. C.; Scheltens, P.; Siemers, E.; Snyder, H. M.; Sperling, R.; Contributors; Elliott, C.; Masliah, E.; Ryan, L.; Silverberg, N. NIA-AA Research Framework: Toward a Biological Definition of Alzheimer's Disease. *Alzheimers Dement*. **2018**, *14* (4), 535–562. https://doi.org/10.1016/j.jalz.2018.02.018.
3. Villemagne, V. L.; Burnham, S.; Bourgeat, P.; Brown, B.; Ellis, K. A.; Salvado, O.; Szoeke, C.; Macaulay, S. L.; Martins, R.; Maruff, P.; Ames, D.; Rowe, C. C.; Masters, C. L.; Australian Imaging Biomarkers and Lifestyle (AIBL) Research Group. Amyloid β Deposition, Neurodegeneration, and Cognitive Decline in Sporadic Alzheimer's Disease: A Prospective Cohort Study. *Lancet Neurol*. **2013**, *12* (4), 357–367. https://doi.org/10.1016/S1474-4422(13)70044-9.
4. Cummings, J. New Approaches to Symptomatic Treatments for Alzheimer's Disease. *Mol. Neurodegener*. **2021**, *16* (1), 2. https://doi.org/10.1186/s13024-021-00424-9.
5. Janelidze, S.; Teunissen, C. E.; Zetterberg, H.; Allué, J. A.; Sarasa, L.; Eichenlaub, U.; Bittner, T.; Ovod, V.; Verberk, I. M. W.; Toba, K.; Nakamura, A.; Bateman, R. J.; Blennow, K.; Hansson, O. Head-to-Head Comparison of 8 Plasma Amyloid-β 42/40 Assays in Alzheimer Disease. *JAMA Neurol*. **2021**, *78* (11), 1375. https://doi.org/10.1001/jamaneurol.2021.3180.
6. Ossenkoppele, R.; Schonhaut, D. R.; Schöll, M.; Lockhart, S. N.; Ayakta, N.; Baker, S. L.; O'Neil, J. P.; Janabi, M.; Lazaris, A.; Cantwell, A.; Vogel, J.; Santos, M.; Miller, Z. A.; Bettcher, B. M.; Vossel, K. A.; Kramer, J. H.; Gorno-Tempini, M. L.; Miller, B. L.; Jagust, W. J.; Rabinovici, G. D. Tau PET Patterns Mirror Clinical and Neuroanatomical Variability in Alzheimer's Disease. *Brain J. Neurol*. **2016**, *139* (Pt 5), 1551–1567. https://doi.org/10.1093/brain/aww027.
7. Kourtis, L. C.; Regele, O. B.; Wright, J. M.; Jones, G. B. Digital Biomarkers for Alzheimer's Disease: The Mobile/ Wearable Devices Opportunity. *NPJ Digit. Med*. **2019**, *2*, 9. https://doi.org/10.1038/s41746-019-0084-2.
8. Leuzy, A.; Bollack, A.; Pellegrino, D.; Teunissen, C. E.; La Joie, R.; Rabinovici, G. D.; Franzmeier, N.; Johnson, K.; Barkhof, F.; Shaw, L. M.; Arkhipenko, A.; Schindler, S. E.; Honig, L. S.; Moscoso Rial, A.; Schöll, M.; Zetterberg, H.; Blennow, K.; Hansson, O.; Farrar, G. Considerations in the Clinical Use of Amyloid PET and CSF Biomarkers for Alzheimer's Disease. *Alzheimers Dement. J. Alzheimers Assoc*. **2025**, *21* (3), e14528. https://doi.org/10.1002/alz.14528.
9. Hampel, H.; Hardy, J.; Blennow, K.; Chen, C.; Perry, G.; Kim, S. H.; Villemagne, V. L.; Aisen, P.; Vendruscolo, M.; Iwatsubo, T.; Masters, C. L.; Cho, M.; Lannfelt, L.; Cummings, J. L.; Vergallo, A. The Amyloid-β Pathway in Alzheimer's Disease. *Mol. Psychiatry* **2021**, *26* (10), 5481–5503. https://doi.org/10.1038/s41380-021-01249-0.
10. Rafii, M. S.; Sperling, R. A.; Donohue, M. C.; Zhou, J.; Roberts, C.; Irizarry, M. C.; Dhadda, S.; Sethuraman, G.; Kramer, L. D.; Swanson, C. J.; Li, D.; Krause, S.; Rissman, R. A.; Walter, S.; Raman, R.; Johnson, K. A.; Aisen, P. S. The AHEAD 3-45 Study: Design of a Prevention Trial for Alzheimer's Disease. *Alzheimers Dement. J. Alzheimers Assoc*. **2023**, *19* (4), 1227–1233. https://doi.org/10.1002/alz.12748.
11. Mintun, M. A.; Lo, A. C.; Duggan Evans, C.; Wessels, A. M.; Ardayfio, P. A.; Andersen, S. W.; Shcherbinin, S.; Sparks, J.; Sims, J. R.; Brys, M.; Apostolova, L. G.; Salloway, S. P.; Skovronsky, D. M. Donanemab in Early Alzheimer's Disease. *N. Engl. J. Med.* **2021**, *384* (18), 1691–1704. https://doi.org/10.1056/NEJMoa2100708.
12. Palmqvist, S.; Stomrud, E.; Cullen, N.; Janelidze, S.; Manuilova, E.; Jethwa, A.; Bittner, T.; Eichenlaub, U.; Suridjan, I.; Kollmorgen, G.; Riepe, M.; Von Arnim, C. A. F.; Tumani, H.; Hager, K.; Heidenreich, F.; Mattsson-Carlgren, N.; Zetterberg, H.; Blennow, K.; Hansson, O. An Accurate Fully Automated Panel of Plasma Biomarkers for Alzheimer's Disease. *Alzheimers Dement*. **2023**, *19* (4), 1204–1215. https://doi.org/10.1002/alz.12751.
13. Karikari, T. K.; Pascoal, T. A.; Ashton, N. J.; Janelidze, S.; Benedet, A. L.; Rodriguez, J. L.; Chamoun, M.; Savard, M.; Kang, M. S.; Therriault, J.; Schöll, M.; Massarweh, G.; Soucy, J.-P.; Höglund, K.; Brinkmalm, G.; Mattsson, N.; Palmqvist, S.; Gauthier, S.; Stomrud, E.; Zetterberg, H.; Hansson, O.; Rosa-Neto, P.; Blennow, K. Blood Phosphorylated Tau 181 as a Biomarker for Alzheimer's Disease: A Diagnostic Performance and Prediction Modelling Study Using Data from Four Prospective Cohorts. *Lancet Neurol*. **2020**, *19* (5), 422–433. https://doi.org/10.1016/S1474-4422(20)30071-5.
14. Ashton, N. J.; Pascoal, T. A.; Karikari, T. K.; Benedet, A. L.; Lantero-Rodriguez, J.; Brinkmalm, G.; Snellman, A.; Schöll, M.; Troakes, C.; Hye, A.; Gauthier, S.; Vanmechelen, E.; Zetterberg, H.; Rosa-Neto, P.; Blennow, K. Plasma P-Tau231: A New Biomarker for Incipient Alzheimer's Disease Pathology. *Acta Neuropathol. (Berl.)* **2021**, *141* (5), 709–724. https://doi.org/10.1007/s00401-021-02275-6.
15. Palmqvist, S.; Janelidze, S.; Quiroz, Y. T.; Zetterberg, H.; Lopera, F.; Stomrud, E.; Su, Y.; Chen, Y.; Serrano, G. E.; Leuzy, A.; Mattsson-Carlgren, N.; Strandberg, O.; Smith, R.; Villegas, A.; Sepulveda-Falla, D.; Chai, X.; Proctor, N. K.; Beach, T. G.; Blennow, K.; Dage, J. L.; Reiman, E. M.; Hansson, O. Discriminative Accuracy of Plasma Phospho-Tau217 for Alzheimer Disease vs Other Neurodegenerative Disorders. *JAMA* **2020**, *324* (8), 772–781. https://doi.org/10.1001/jama.2020.12134.
16. Moscoso, A.; Heeman, F.; Dunås, T.; Schöll, M. Estimating the Time between Amyloid and Tau-pet Positivity: Implications for Alzheimer's Disease Prevention Trials. *Alzheimers Dement*. **2023**, *19* (S10). https://doi.org/10.1002/alz.082013.
17. Wittenberg, R.; Knapp, M.; Karagiannidou, M.; Dickson, J.; Schott, J. Economic Impacts of Introducing Diagnostics for Mild Cognitive Impairment Alzheimer's Disease Patients. *Alzheimers*

DOI: 10.36838/IJHSR87.80

Dement. N. Y. N **2019**, *5*, 382–387. https://doi.org/10.1016/j.trci.2019.06.001.
18. McMahon, P. M.; Araki, S. S.; Sandberg, E. A.; Neumann, P. J.; Gazelle, G. S. Cost-Effectiveness of PET in the Diagnosis of Alzheimer Disease. *Radiology* **2003**, *228* (2), 515–522. https://doi.org/10.1148/radiol.2282020915.
19. Verberk, I. M. W.; Misdorp, E. O.; Koelewijn, J.; Ball, A. J.; Blennow, K.; Dage, J. L.; Fandos, N.; Hansson, O.; Hirtz, C.; Janelidze, S.; Kang, S.; Kirmess, K.; Kindermans, J.; Lee, R.; Meyer, M. R.; Shan, D.; Shaw, L. M.; Waligorska, T.; West, T.; Zetterberg, H.; Edelmayer, R. M.; Teunissen, C. E. Characterization of Pre-Analytical Sample Handling Effects on a Panel of Alzheimer's Disease-Related Blood-Based Biomarkers: Results from the Standardization of Alzheimer's Blood Biomarkers (SABB) Working Group. *Alzheimers Dement. J. Alzheimers Assoc*. **2022**, *18* (8), 1484–1497. https://doi.org/10.1002/alz.12510.
20. Goyal, D.; Tjandra, D.; Migrino, R. Q.; Giordani, B.; Syed, Z.; Wiens, J.; Alzheimer's Disease Neuroimaging Initiative. Characterizing Heterogeneity in the Progression of Alzheimer's Disease Using Longitudinal Clinical and Neuroimaging Biomarkers. *Alzheimers Dement. Diagn. Assess. Dis. Monit*. **2018**, *10* (1), 629–637. https://doi.org/10.1016/j.dadm.2018.06.007.
21. Welhaf, M. S.; Balota, D. A.; Schindler, S. E.; Morris, J. C.; Hassenstab, J. J.; Aschenbrenner, A. J. Variability in Reaction Time Predicts Transition to Mild Alzheimer Disease and Is Sensitive to CSF Biomarkers in Cognitively Normal Older Adults. *Alzheimers Dement*. **2024**, *20* (S3), e087068. https://doi.org/10.1002/alz.087068.
22. Toniolo, S.; Zhao, S.; Scholcz, A.; Amein, B.; Ganse-Dumrath, A.; Heslegrave, A. J.; Thompson, S.; Manohar, S.; Zetterberg, H.; Husain, M. Relationship of Plasma Biomarkers to Digital Cognitive Tests in Alzheimer's Disease. *Alzheimers Dement. Amst. Neth.* **2024**, *16* (2), e12590. https://doi.org/10.1002/dad2.12590.
23. Marshall, G. A.; Dekhtyar, M.; Bruno, J. M.; Jethwani, K.; Amariglio, R. E.; Johnson, K. A.; Sperling, R. A.; Rentz, D. M. The Harvard Automated Phone Task: New Performance-Based Activities of Daily Living Tests for Early Alzheimer's Disease. *J. Prev. Alzheimers Dis*. **2015**, *2* (4), 242–253. https://doi.org/10.14283/jpad.2015.72.
24. Teng, J.; McKenna, M. R.; Gbadeyan, O.; Prakash, R. S.; Alzheimer's Disease Neuroimaging Initiative. Linking the Neural Signature of Response Time Variability to Alzheimer's Disease Pathology and Cognitive Functioning. *Netw. Neurosci. Camb. Mass* **2024**, *8* (3), 697–713. https://doi.org/10.1162/netn_a_00373.
25. Wang, H.-L.; Tang, R.; Ren, R.-J.; Dammer, E. B.; Guo, Q.-H.; Peng, G.-P.; Cui, H.-L.; Zhang, Y.-M.; Wang, J.-T.; Xie, X.-Y.; Huang, Q.; Li, J.-P.; Yan, F.-H.; Chen, S.-D.; He, N.-Y.; Wang, G. Speech Silence Character as a Diagnostic Biomarker of Early Cognitive Decline and Its Functional Mechanism: A Multicenter Cross-Sectional Cohort Study. *BMC Med*. **2022**, *20* (1), 380. https://doi.org/10.1186/s12916-022-02584-x.
26. García-Gutiérrez, F.; Marquié, M.; Muñoz, N.; Alegret, M.; Cano, A.; de Rojas, I.; García-González, P.; Olivé, C.; Puerta, R.; Orellana, A.; Montrreal, L.; Pytel, V.; Ricciardi, M.; Zaldua, C.; Gabirondo, P.; Hinzen, W.; Lleonart, N.; García-Sánchez, A.; Tárraga, L.; Ruiz, A.; Boada, M.; Valero, S. Harnessing Acoustic Speech Parameters to Decipher Amyloid Status in Individuals with Mild Cognitive Impairment. *Front. Neurosci.* 2023, 17, 1221401. https://doi.org/10.3389/fnins.2023.1221401.
27. Huang, J.; Zhou, S.; Xie, Q.; Yu, J.; Zhao, Y.; Feng, H. Digital Biomarkers for Real-Life, Home-Based Monitoring of Frailty: A Systematic Review and Meta-Analysis. *Age Ageing* 2025, 54 (4), afaf108. https://doi.org/10.1093/ageing/afaf108.
28. Chhatwal, J. P.; Schultz, S. A.; McDade, E.; Schultz, A. P.; Liu, L.; Hanseeuw, B. J.; Joseph-Mathurin, N.; Feldman, R.; Fitzpatrick, C. D.; Sparks, K. P.; Levin, J.; Berman, S. B.; Renton, A. E.; Esposito, B. T.; Fernandez, M. V.; Sung, Y. J.; Lee, J. H.; Klunk, W. E.; Hofmann, A.; Noble, J. M.; Graff-Radford, N.; Mori, H.; Salloway, S. M.; Masters, C. L.; Martins, R.; Karch, C. M.; Xiong, C.; Cruchaga, C.; Perrin, R. J.; Gordon, B. A.; Benzinger, T. L. S.; Fox, N. C.; Schofield, P. R.; Fagan, A. M.; Goate, A. M.; Morris, J. C.; Bateman, R. J.; Johnson, K. A.; Sperling, R. A.; Dominantly Inherited Alzheimer's Network Investigators. Variant-Dependent Heterogeneity in Amyloid β Burden in Autosomal Dominant Alzheimer's Disease: Cross-Sectional and Longitudinal Analyses of an Observational Study. *Lancet Neurol*. **2022**, *21* (2), 140–152. https://doi.org/10.1016/S1474-4422(21)00375-6.
29. Thijssen, E. H.; La Joie, R.; Wolf, A.; Strom, A.; Wang, P.; Iaccarino, L.; Bourakova, V.; Cobigo, Y.; Heuer, H.; Spina, S.; VandeVrede, L.; Chai, X.; Proctor, N. K.; Airey, D. C.; Shcherbinin, S.; Duggan Evans, C.; Sims, J. R.; Zetterberg, H.; Blennow, K.; Karydas, A. M.; Teunissen, C. E.; Kramer, J. H.; Grinberg, L. T.; Seeley, W. W.; Rosen, H.; Boeve, B. F.; Miller, B. L.; Rabinovici, G. D.; Dage, J. L.; Rojas, J. C.; Boxer, A. L.; Advancing Research and Treatment for Frontotemporal Lobar Degeneration (ARTFL) investigators. Diagnostic Value of Plasma Phosphorylated Tau181 in Alzheimer's Disease and Frontotemporal Lobar Degeneration. *Nat. Med*. **2020**, *26* (3), 387–397. https://doi.org/10.1038/s41591-020-0762-2.
30. Galasko, D. R.; Chhatwal, J. P.; Wijsman, E. M.; Rumbaugh, M. C.; Mozersky, J.; Blacker, D.; Shiley-Marcos Alzheimer's Disease Research Center. Incorporation of Plasma Biomarkers for Screening and Diagnosis in Primary Care. *Alzheimers Dement*. **2022**, *18* (S6), e059463. https://doi.org/10.1002/alz.059463.
31. Wittenberg, R.; Knapp, M.; Karagiannidou, M.; Dickson, J.; Schott, J. Economic Impacts of Introducing Diagnostics for Mild Cognitive Impairment Alzheimer's Disease Patients. *Alzheimers Dement. N. Y. N* **2019**, *5*, 382–387. https://doi.org/10.1016/j.trci.2019.06.001.
32. Palmqvist, S.; Tideman, P.; Mattsson-Carlgren, N.; Schindler, S. E.; Smith, R.; Ossenkoppele, R.; Calling, S.; West, T.; Monane, M.; Verghese, P. B.; Braunstein, J. B.; Blennow, K.; Janelidze, S.; Stomrud, E.; Salvadó, G.; Hansson, O. Blood Biomarkers to Detect Alzheimer Disease in Primary Care and Secondary Care. *JAMA* **2024**, *332* (15), 1245–1257. https://doi.org/10.1001/jama.2024.13855.
33. Kourtis, L. C.; Regele, O. B.; Wright, J. M.; Jones, G. B. Digital Biomarkers for Alzheimer's Disease: The Mobile/Wearable Devices Opportunity. *Npj Digit. Med.* **2019**, *2* (1), 9. https://doi.org/10.1038/s41746-019-0084-2.

Author

Anaya Shabi is a senior at Global Indian International School, Singapore. She plans to pursue a degree in medicine and is particularly interested in neuroscience and neurodegenerative diseases.

IJHSR
ijhighschoolresearch.org
REVIEW ARTICLE

A Systematic Review of Barriers and Solutions to Implementing Waste Reduction Strategies in Hospitals

Shrey Aggarwal

Abbey Park High School, 1455 Glen Abbey Gate, Oakville, Ontario, L6M 2G5, Canada; shreyaggarwal08@gmail.com
Mentor: Dr. Frank Glover

ABSTRACT: Hospitals, while cornerstones of modern medicine, consume substantial energy and generate significant amounts of waste, contributing to environmental pollution and associated health risks. This review examines studies on hospital waste management, identifying important barriers and investigating potential solutions to improve sustainability. While adhering to PRISMA guidelines, Google Scholar and PubMed were used to select papers using search terms like "waste management strategies" and "solutions to reducing hospital waste," resulting in 37 final papers. The findings of this paper show that rather than being the result of isolated deficiencies, waste management results are influenced by a variety of interconnected socio-technical factors, such as institutional policies, economic limitations, employee attitudes, and inadequate infrastructure. Various initiatives, including knowledge-based training programs and better segregation techniques, showed quantifiable short-term waste reductions; however, because of systemic challenges and a lack of resources, these solutions frequently failed to maintain their effects over time. Economic strategies, including expanding infrastructure and incorporating waste-related costs into financial planning, show strong potential to enhance long-term program effectiveness. Nevertheless, when people, budgets, systems, and laws are not handled collectively, even well-designed initiatives operate inadequately. Overall, this review highlights that effective hospital waste management requires coordinated action across policy, economic, and behavioral domains.

KEYWORDS: Science, Medical and Health Sciences, Environmental Health, Healthcare Systems, Waste Management.

Introduction

Environmental Impacts of Hospital Waste:

Hospitals and the invaluable services they provide have become a cornerstone of modern society.[1] Despite the well-known benefits of hospitals as places of healing and recovery, these industrial systems require large amounts of energy and produce significant amounts of waste that can pollute the environment and paradoxically lead to human illnesses.[2] Indeed, environmental pollution from healthcare waste byproducts poses a significant morbidity and mortality globally and is estimated to contribute to millions of deaths annually.[3] Despite various "green" initiatives to reduce the pollution burden from hospitals, 2-6 million tons of waste materials are produced annually, many of which are not properly sorted and ultimately disposed of via incineration, autoclaving, or microwave treatment.[4,5] The World Health Organization (WHO) categorizes healthcare waste into "non-hazardous" and "hazardous."[6] The hazardous stream encompasses distinct sub-types, including sharps (needles, scalpels), pathological and infectious waste (contaminated dressings, blood, tissue), and pharmaceutical/chemical waste. The different impacts of these categories drive the need for rigorous management. Sharps waste is responsible for hundreds of thousands of needle-stick injuries annually, directly transmitting severe infections like Hepatitis B/C and HIV. Chemical, pharmaceutical, and pathological waste introduces toxic, mutagenic, or antibiotic-resistant compounds into soil and water systems, linking them to chronic conditions, cancers, and respiratory illnesses.[7] The persistence of these severe public health and environmental risks necessitates an analysis of the barriers and solutions critical to the consistent implementation of proper waste management practices.

Different Pollutants and Chemicals in Materials:

Hospital waste consists of several hazardous chemicals. Some of the most commonly found chemicals include polychlorobiphenyls (PCBs), plastics, per- and polyfluoroalkyl substances (PFAS), and heavy metals.[8–10] PFAS are known to be exceptionally resistant to biodegradation, with half-lives of ~10+ years across various environmental and biological media.[10]

Additionally, contaminated biological specimens constitute another type of hospital waste that can harbor active pathogens, leading to illnesses among healthcare workers and the general population.[5] Proper disposal of these chemicals is crucial because many of these have been shown to bioaccumulate in the environment and can persist for many months or years before being chemically degraded.

Current Methods to Reduce Waste:

Currently, there are many different types of waste reduction and management programs in hospitals around the world. For example, a study conducted by Simmons *et al*. evaluated the effectiveness of a waste reduction quality improvement program, where ultimately formal teaching of how to dispose of sharps in the operating room (OR) after the operating room, properly led to a significant improvement in waste management knowledge and compliance with proper hazardous material disposal, and also resulted in an overall cost saving.[11] Another example of a hospital waste management program conducted by Palmi-

© 2026 Terra Science and Education

DOI: 10.36838/IJHSR87.88

sano *et al*. focused on reducing waste and slowing emissions by implementing a four-phase recycling program.[12]

The need to address the environmental and public health issues outlined in this study requires the implementation of organized waste management systems. These programs are fundamentally guided by the Waste Hierarchy, a systematic approach that prioritizes interventions aimed at minimizing contamination, ranking Reduction, Reuse, and Recycling above less sustainable methods like Recovery and final Disposal.[13] Effective waste management in a healthcare setting is therefore a holistic process that manages the entire lifecycle of medical consumables, not just final disposal.[14]

Well-developed methods often focus on shifting hospital practices towards this hierarchy. Reduction strategies include using electronic medical records to reduce paper waste or replacing disposable surgical basin sets with reusable ones. Recycling programs divert large volumes of clean, segregated plastic waste from operating rooms, which is rich in recoverable polymers.[13] Additionally, advances in treatment technology, such as advanced pyrolysis and plasma gasification, promise significant volume reduction (up to 97%) and provide sustainable substitutes for traditional disposal techniques.[14] These strategies show clear pathways to effective, sustainable healthcare waste management.

Despite the presence of these various initiatives, the majority of hospitals do not implement them.

Barriers to Waste Reduction:

Despite several well-developed methods and programs to reduce hospital waste pollution and to safely dispose of chemicals, many of these sustainability models are ineffective for several reasons, including a lack of awareness of existing programs among employers and staff at respective hospitals, implementation fatigue, cultural resistance to change, and the economic burden of sustaining programs.[15] Based on a survey of anesthesiologists, the principal barriers can be systematically categorized into three areas: knowledge and attitudes, economic considerations, and infrastructure.[16] This review will explore each of these categories. For example, an operating room analysis by McGain *et al*. found that around 41% of waste was potentially recyclable, but only just over half (55%) of these recyclable materials were placed in recycling bins.[17] Each of these issues can act independently or concurrently and ultimately hinder effective waste management efforts. In this systematic review paper, we examine the multifaceted barriers to effective healthcare waste management in hospitals, focusing on psychosocial, economic, infrastructural, and policy challenges, as well as summarizing potential solutions.

Methods

We performed a systematic literature review using PubMed and Google Scholar databases. This review paper adheres to the Preferred Reporting Items for Systematic Reviews and Meta-Analyses (PRISMA) guidelines to ensure rigor and reproducibility.[18] We limited our studies to only include peer-reviewed papers published from the year 2000 to the present. We included only papers published in the English language and deleted duplicate articles found between PubMed and Google Scholar. Search terms included "hospital waste," "waste management strategies," "operating room waste," and "solutions to reducing hospital waste," resulting in 37 final papers. We excluded editorials, internet blogs, and online forums (Figure 1). Additionally, each paper was categorized, and we ensured that a significant number of papers covered each domain of barriers and solutions (e.g., attitude and knowledge, economic, infrastructure, and policy).

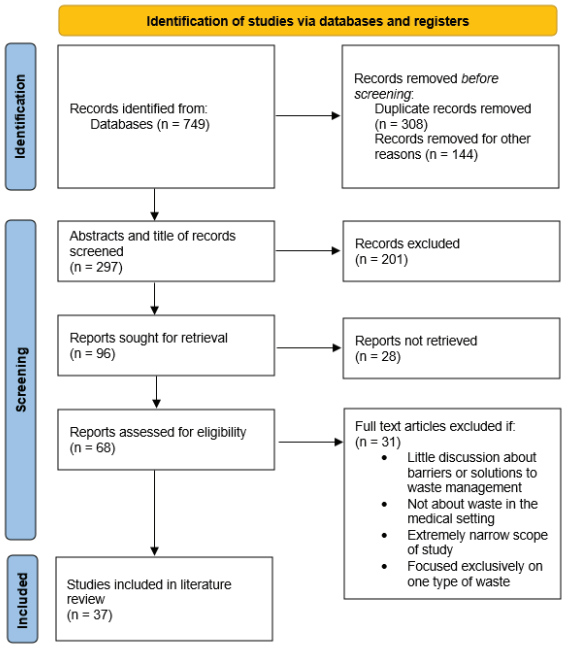

Figure 1: PRISMA flow diagram outlining methodology for selecting papers. The screening process narrowed 749 initial records down to 37 final papers, ensuring the review was based on high-quality, peer-reviewed evidence specifically focused on hospital waste barriers and solutions. Flowchart adapted from the PRISMA 2020 statement.[18]

Results

Attitude and Knowledge Barriers:

One of the most common barriers to efficient waste reduction, despite implemented hospital policies, is related to social attitudes among hospital staff who are responsible for waste disposal.[19] Numerous studies have implicated personal knowledge, awareness, and understanding of waste reduction as modifiable factors impeding proper waste disposal among healthcare workers. In a study by Azouz *et al*., researchers surveyed 524 participants at the Mayo Clinic to identify barriers to OR recycling and evaluate the effects of implementing a recycling improvement educational program.[20] Of the 524 participants, nearly half of the respondents stated they recycle less than 25% of waste, 56.7% did not know which operating room items were recyclable, 39% reported they 'only sometimes' or 'never' recycle in the OR, and 47.7% thought the greatest barrier to recycling was lack of knowledge. With this initial information, the authors performed a knowledge assessment after the implementation of the recycling educational program. The benefits of this program resulted in significant improvement in proper waste disposal, as well as cost savings of 10.3% ($p = 0.004$), which were related to improvements in

the sharps waste disposal when compared to the previous year at the surgery center. This study highlights the importance of proper waste disposal for not only improvements in environmental health but also cost savings, which can allow hospitals to run more efficiently. Equally important to these results was testing the proof of concept that interventions to target the lack of knowledge and awareness of recycling can increase proper waste disposal.

International studies have borne similar results. In a study conducted by Hakim *et al*. at Ain Shams University Hospitals, Cairo, Egypt, they assessed the knowledge, attitudes, and practices (KAP) of healthcare personnel regarding waste disposal through a cross-sectional study of 110 physicians, 151 nurses, and 89 housekeepers.[21] The authors administered a questionnaire concerning the knowledge of workers concerning waste disposal and the attitudes of workers towards waste disposal, such as whether safe waste disposal should be a priority. Satisfactory scores were defined by the study's authors as achieving a predetermined cutoff percentage, typically 50% or more, of the total correct answers on the knowledge questionnaire. It was found that physicians had the highest satisfactory knowledge scores of proper waste disposal (68.3%) compared to those of nurses (60.9%) and housekeepers (40.4%). Interestingly, while housekeepers scored the lowest in terms of knowledge, they had the highest satisfactory attitude scores (61.9%) compared with 49.0% among nurses and 56.4% among physicians. This suggests that while housekeepers may lack detailed procedural knowledge, they exhibit stronger values and commitment toward proper waste disposal. This could be due to the varying proximity of these individuals to the final act of waste management, and those who are more directly involved in waste disposal are more likely to be cognizant of proper disposal. For example, the surgeon's role in the OR focuses primarily on the operation, intending to have supplies handed and taken from him or her in an expedited and safe fashion. The OR nurses and cleaning staff are typically responsible for sorting the supplies and waste disposal at the end of the operation. The authors emphasized the importance of distinguishing between satisfactory knowledge, which is answering fact-based questions, and satisfactory attitude, which is the healthcare professionals' beliefs and willingness to participate in proper practices. As compared to the previous study from the Mayo Clinic, this study is a broad, cross-sectional survey that provides a systematic comparison of knowledge and attitudinal deficiencies across all hospital roles (physicians, nurses, housekeepers). Conversely, the previous Mayo Clinic study has many strengths over the other study because its narrow, focused methodology isolates the knowledge barrier (lack of clarity on recyclable items) to a single, high-waste area (the Operating Room), providing a highly precise and actionable insight into specialized personnel behavior.

Furthermore, in a study of Canadian anesthesiologists conducted by Matava *et al.*, researchers documented the anesthesiologists' current attitudes and perceived barriers towards sustainability and recycling in the OR.[22] The majority of those who responded (88.6%) reported that they agreed that the environmental burden of anesthesia-related products should be considered when in practice. Despite this, only 30.3% reported that their hospitals actively recycled OR waste. The biggest barriers that respondents cited were lack of support from the hospital and/or leadership (63.5%), inadequate information or education (62.8%), staff attitudes (52.2%), and lack of recycling facilities (51.5%). This shows the clear willingness among healthcare professionals regarding more sustainable practices in the OR, but also shows the need for more institutional backing. Despite the majority believing that environmental sustainability is important, the disconnect between individual motivation and institutional support is showing signs of implementation fatigue. Unresolved challenges can gradually erode enthusiasm, as seen by the frustration shown by several respondents over the stagnation of sustainability initiatives. These findings suggest that while education improves compliance, without institutional incentives or structural supports, the gains may be temporary.

Economic Barriers:

About 20–33% of all healthcare waste comes from the operating room (OR), and proper disposal can be expensive.[20] In a review of Indian health care units (HCU), researchers found that most hospitals lacked dedicated budgets for waste management, with an estimated ₹3000–4000 (USD 70–93) required to treat just one tonne of waste.[23] As a result, smaller HCUs frequently disregard proper waste practices altogether due to a lack of resources for even the most basic components, such as trained personnel, disinfectants, or on-site treatment facilities. The fact that these institutions are frequently left out of larger government waste initiatives because of their size or private ownership exacerbates these problems and causes a widening gap in waste compliance between urban and rural or lower-tier centers. Similarly, an expansive Australian study found that funding was often biased toward low-cost but unsustainable disposal options since the immediate cost of implementing waste management was frequently given priority over long-term environmental or economic benefits.[24] A study by Azouz *et al*. demonstrated a very minimal financial setback to initiate a recycling program; for example, many hospital ORs already have sharps containers and recycling bins in place, as well as established disposal protocols for each category of waste. This is one of several solutions that will be discussed later in this review.[20]

Although some studies have found otherwise, the initial economic investment needed for waste infrastructure, employee training, and technology might make it impossible for programs to be implemented, even when hospital administration supports sustainability in theory. This is especially true for smaller or underfunded healthcare facilities with limited resources. In a study of biomedical waste practices in Punjab, India, Kumar *et al*. found that many rural primary healthcare centers were unable to purchase even basic materials like color-coded bins or construct wash basins for proper disposal due to a lack of funds.[25] These institutions' lack of operational finances and trained personnel for educational programs further demonstrated how inadequate funding impedes both implementation and infrastructure. In the private sector, over 50%

DOI: 10.36838/IJHSR87.88

of respondents reported not seeing biomedical waste as a problem, yet still expected government or public-sector support to fund disposal. This shows the disconnect between financial responsibility and operational behavior. These results show that many institutions are discouraged from implementing sustainable systems due to the ongoing operational expenses of health care waste management, not only the initial investment, particularly when funding streams are fragmented or absent altogether.

Even when hospitals understand the importance of proper healthcare waste management, economic constraints impede implementation, especially in resource-limited contexts.[26] According to Taghipour & Mosaferi, incineration, while being the most effective disposal method, is also the most expensive, followed by autoclaving, with landfilling being the cheapest but environmentally worst option.[27] General operational budgets in Tabriz hospitals and developing countries usually leave little money for waste infrastructure or staff training since they prioritize urgent patient care over waste systems. Given their low waste volumes, smaller hospitals find it unfeasible to invest in treatment units. Even in cases where technology is available, the expenses of trained people, replacement parts, and continuous maintenance frequently outweigh the available funds. Some institutions resort to risky workarounds during these financial crunches, selling untreated biomedical waste to recyclers or scavengers despite the health risks. Compared to the previous study from Kumer *et al.*, this study analyzes the systemic failure across ten hospitals (Tabriz), comparing the explicit financial trade-offs between disposal methods (incineration being the most expensive but effective). In contrast, the previous study offers a broader quantitative evaluation across 120 diverse facilities (public vs. private, primary vs. secondary care), which objectively measures the impact of inadequate funding on essential operational infrastructure (e.g., color-coded bins).

Infrastructure and Policy Barriers:

One of the biggest barriers to efficient and sustainable OR waste management is infrastructure and associated challenges. The lack of on-site waste treatment facilities in many hospitals in developing Asian countries necessitates reliance on external services, which are often unreliable or inaccessible, particularly for rural healthcare facilities. In a review from Khan *et al.*, the authors find that transporting waste to centralized facilities presents extra logistical and financial issues for smaller rural hospitals, which can lead to delays or unsafe temporary storage.[28] Even in cases where treatment plants are present, they often suffer from poor maintenance, malfunctioning machinery, or outdated technologies that fail to comply with environmental safety regulations. Many facilities lack basic infrastructure for segregation, such as color-coded bins, designated storage locations, and secure transportation. This results in the mixing of hazardous and non-hazardous waste, raising the risk of pathogen exposure and chemical contamination. Due to a lack of basic infrastructure, hospitals frequently resort to open dumping or burning, which are low-cost practices but expose the environment to harmful pollutants and pathogens, contributing to environmental contamination. In HCWM, technical barriers relate to the accessibility, suitability, and intricacy of technology and techniques. Access to suitable and efficient technology for waste segregation, treatment, and disposal is a problem for many healthcare facilities. In environments with limited resources and restricted access to advanced technologies, this is particularly true.[26]

Beyond the geographical and logistical barriers, Raji *et al.* and Lino *et al.* draw attention to infrastructural deficits that affect waste management quality even within facilities that have access to treatment services. Raji *et al.* discuss a critical but often neglected gap with the lack of mechanisms to effectively handle liquid healthcare waste, such as the untreated discharge of greywater and blackwater, which introduces significant chemical and microbial hazards into surrounding environments.[29] They also note that many facilities rely on outdated incineration infrastructure without modern air pollution controls, directly worsening environmental safety. From a systems perspective, Lino *et al.* show that a major obstacle is the absence of infrastructure to support recycling, composting, and other circular economy initiatives.[30] Without these systems, a significant amount of potentially recoverable materials is thrown away. Both studies show that these shortcomings continue not only at the most technologically advanced levels but also at the most basic level of waste handling, where facilities may not have secure storage areas or clearly labeled segregation points, ultimately making it impossible to separate hazardous and non-hazardous waste at the source.

A lack of institutional leadership, along with policy and regulatory frameworks, is a major barrier to efficient hospital waste management. According to Khan *et al.*, legislation and regulations are often new in many developing Asian nations, and their implementation varies.[28] The author notes that many resource-constrained nations have only basic laws and limited regulatory bodies, whereas wealthy nations have established adequate policies and resources to enforce them. This creates a political barrier because local laws are not adequately monitored, and their value remains questionable, as many workers are not aware of them. The study makes the argument that international rules could be modified to satisfy standards if domestic regulations prove inadequate. Similarly, a review by Aboueid *et al.* notes that a key barrier is the absence of a top-down, unified strategy, noting that the adoption of sustainable practices might be hindered by a lack of leadership and clearly defined roles and duties within institutions.[31] They also identify specific political and regulatory barriers, such as a lack of incentives for hospitals to invest in sustainable solutions and conflicting protocols that create confusion. The authors emphasize that it is difficult to achieve broad and long-lasting improvement when the burden of implementing change unfairly rests on individual health professionals in the absence of strong, transformational leadership and a supportive institutional strategy. This stresses that the establishment of regulations at the national or provincial levels and policies at all governmental levels will be important to creating a space that will support a successful healthcare transformation.

Critically, these three categories of barriers are not independent factors but function as an interconnected socio-technical system where deficiencies in one area exacerbate problems in another. For example, economic limitations frequently make it impossible to invest in essential infrastructure, and staff cultural non-compliance becomes an issue with unclear institutional policies. The conceptual framework (Figure 2) illustrates this cyclical relationship between the barriers, suggesting that comprehensive, multifaceted solutions are necessary for effective waste management.

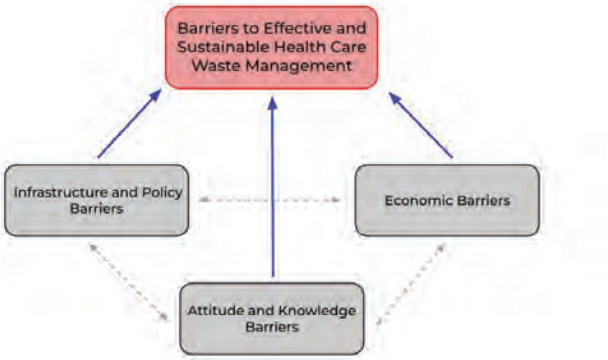

Figure 2: Interconnected barriers result in ineffective hospital waste management. This framework illustrates that waste management failures stem from a cyclical relationship where economic limits, infrastructure and policy gaps, and staff attitudes and knowledge reinforce one another.

Solutions:

- ***Attitude and Knowledge Barriers:***

Addressing attitudinal and behavioral barriers to healthcare waste management requires targeted interventions based on behavioral science and training. The Jungbluth *et al.* review provides a strong framework for this by emphasizing the need to use the COM-B model (Capability, Opportunity, and Motivation) and the Behavior Change Wheel to understand and influence recycling behavior in hospitals.[32] This method assists practitioners and researchers in moving past merely recognizing a lack of knowledge as a barrier. Rather, this framework can direct the creation of more effective, tailored interventions that directly address the root causes of behavioral shortfalls by systematically mapping influences to these components, such as an individual's physical and psychological Capability (knowledge and skills), social and physical Opportunity (access to bins and institutional support), and automatic and reflective Motivation (beliefs and intentions). A real-world example of such an intervention is the "educative skill-raising training" program implemented in a study by Hosny *et al.*[33] This study was conducted in Alexandria, Egypt, and was a direct and effective response to the attitudinal and knowledge-based barriers among medical waste handlers. The intervention was a structured, two-day training course delivered through lectures, group discussions, and demonstrations of practical skills. It specifically focused on topics such as the categorization of medical waste, safe handling and collection methods, proper use of personal protective equipment (PPE), and emergency procedures for accidental exposure or spills. A pre-made questionnaire was used as part of the study's methodology to gauge participants' knowledge, abilities, and practices before and after the training. The findings revealed a sharp rise in knowledge levels from a baseline of 9.6% to an impressive 97.3% after the intervention. Additionally, the percentage of employees demonstrating "good practice" increased from just 1.1% to 92.1%, proving that a well-designed and practical training program can effectively improve staff capability and result in major improvements in waste management and handling. Another paper by Saha *et al.* reinforces this point, that a shift to a circular economy in healthcare calls for sustainability education that aims to alter attitudes and embed these principles into training programs.[34] To overcome attitudinal barriers, this is an essential component that ensures sustainability and proper waste management become fundamental components of professional culture rather than temporary initiatives.

- ***Economic Barriers:***

Addressing the economic barriers of healthcare waste management requires targeted solutions focused on practical implementation. One study by Wormer *et al.* at the Carolinas Medical Center in North Carolina demonstrates how successful a committee-driven, bottom-up strategy may be.[35] This involves a focus on practical initiatives that lead to significant financial savings. For example, a "red bag initiative" that taught staff proper waste segregation led to a 75% reduction in biohazardous waste and an estimated $60,000 in annual savings, while also replacing disposable OR foam padding with reusable gel pads resulted in annual savings exceeding $50,000. By embracing a circular economy model, this institution also salvaged hundreds of pounds of discarded batteries for donation or redistribution, generating an additional $9,000 in annual savings. These actions show how a systematic committee-driven approach can help combat economic barriers. Furthermore, Cliff *et al.* emphasize the importance of a top-down, systemic approach to address these barriers.[36] Investing in modern, environmentally friendly waste treatment technologies, such as sterilization and incineration with energy recovery, which are proven to reduce both waste volume and operational costs, is a key solution. There is also a major institutional barrier: the lack of adequate environmental accounting systems. Hospitals' capacity to optimize resources is limited by their inability to appropriately integrate waste-related costs into their financial analysis in the absence of these systems. Implementing a framework that includes environmental accounting is crucial for improving financial efficiency and ensuring the long-term economic sustainability of waste management programs.

- ***Infrastructure and Policy:***

In many countries, the rapid expansion of the healthcare system has exacerbated existing challenges in hospital waste management, necessitating continuous efforts and the development of adequate infrastructure to ensure sustainable healthcare service delivery.[37] In a qualitative study using a descriptive phenomenological design, participants in Addis Ababa, Ethiopia, highlighted the crucial role of improving infrastructure and resource allocation and offered tangible solutions.[38] Data were collected through informant interviews and focus group discussions with the health care providers,

DOI: 10.36838/IJHSR87.88

waste management staff, and other stakeholders involved in infectious healthcare waste management. They stressed that the lack of essential resources, such as functional incinerators, proper waste containers, and adequate waste management equipment, hindered the implementation of waste management policies and recommended that funding resources from private and public donors be dedicated specifically to maintaining waste management policies. Additionally, participants in this study emphasized the need for regular evaluations and increased stakeholder engagement to enhance the monitoring and evaluation (M&E) systems in healthcare waste management. Many believed that routine assessments would help ensure that waste management policies remained both relevant and effective, adjusting to emerging needs and challenges.

Participants in the study also highlighted the big differences in waste recycling training between public and private healthcare facilities. Some of the key challenges include language barriers, low motivation of trainees, limited training material, and inconsistent access to specialized instruction in infectious waste management.[38] The authors propose focused resources to improve understanding of recycling policy by having instructions translated into several languages for workers to understand, focus groups to keep staff engaged, and standardized and tailored content teaching on proper waste sorting.

Furthermore, addressing policy barriers requires more than just guidelines. Findings from interviews and focus group discussions indicate that although policies are frequently in place, their implementation varies due to a lack of specific information and inadequate funding.[38] A solution proposed is to create more thorough regulations that specifically address specific challenges associated with hazardous waste, such as sharps, and ensure they are regularly evaluated to maintain their efficacy. The lack of participation of janitorial and frontline healthcare workers in the policy-making process is another major barrier, leading to policies that are not aligned with daily operational realities. To combat this, a recommendation is to foster broader stakeholder engagement and collaboration in policy development, as this not only guarantees that the strategies are more practical and implementable but also fosters a sense of accountability and ownership among waste management professionals. Finally, the authors emphasize the need for long-term planning to move away from ad hoc resource allocation. To guarantee sustainable and successful practices, this involves developing detailed plans that incorporate waste management into broader environmental and public health initiatives.

Discussion

The goal of this review was to investigate the barriers to hospital and operating room waste management and reduction, despite the proliferation of "green" initiatives and well-described technical options. We evaluated evidence across key domains: psychosocial attitudes and behaviors, economic constraints, infrastructure and policy gaps, and examined solutions to argue that waste outcomes are controlled by interrelated socio-technical forces rather than isolated deficiencies. In summary, even well-designed initiatives underperform if people, budgets, systems, and regulations are not all given adequate attention.

The literature shows evidence that failures in hospital waste management systems are rarely caused by a single isolated factor. The implementation of modern waste treatment technologies is significantly restricted by a lack of money, but this issue is exacerbated by inadequate institutional policies and poor staff awareness.[20,22] Educational initiatives, such as Mayo Clinic's recycling improvement program, for example, have shown that staff attitudes and knowledge have a significant impact on program performance.[20] However, as Lino *et al.* and Raji *et al.* show, infrastructural limitations, like outdated disposal technologies, inadequate segregation systems, and a lack of appropriate systems for handling liquid medical waste, undermine sustainable practices even when staff are motivated.[29,30] These challenges are made worse by economic pressures. Smaller healthcare facilities frequently deprioritize waste management because the costs of upgrading infrastructure, training personnel, and maintaining recycling programs are more expensive than urgent patient care costs.[27] Together, these results show that HCWM issues are compounded rather than independent, necessitating comprehensive interventions at the operational and regulatory levels.

After conducting research, the biggest barrier to improving HCWM isn't just one factor in isolation but the interaction of infrastructure limitations and institutional priorities. Initiatives for staff education and awareness are important, but they cannot be successful without adequate infrastructure, steady institutional support, and clear policy enforcement. Among the barriers identified, financial limitations and leadership inaction seem to be the most critical since they have a direct impact on the hospitals' ability to implement successful programs. A move toward integrated solutions that combine infrastructure investment with more robust regulatory frameworks and standardized waste segregation systems will be necessary for sustainable change. Equally important is recognizing that effective interventions require coordination at multiple levels, from frontline healthcare workers to hospital leadership and government funding. Without a coordinated strategy, even well-designed programs risk failing in practice. Fostering institutional accountability while giving long-term planning precedent over short-term cost reduction will be essential in closing the gap between proven, research-backed solutions and widespread adoption.

Strengths:

A key strength of this review is its comprehensive integration of findings from many contexts and methodologies, which enables a nuanced knowledge of healthcare waste management concerns. The paper offers insights that are applicable across a variety of healthcare systems by capturing both global patterns and region-specific dynamics by drawing on research from North America, Asia, and other regions. Another strength is the paper's focus on the interconnection between barriers, psychosocial factors, economic limitations, and inadequate infrastructure, rather than isolating them. This reflects the real-world complexity of putting efficient waste management

solutions into practice. Lastly, the focus on evidence-based solutions, which anchors the discussion in practical strategies that have been studied and, in some situations, successfully implemented, is another strength.

Limitations

While this review has a thorough synthesis of the barriers and solutions related to HCWM, several limitations should be acknowledged. First, research on ways to overcome policy and infrastructure-related barriers is notably lacking. This disparity makes it more difficult to assess the long-term efficacy of interventions in these areas and emphasizes the urgent need for more research on scalable, system-level changes. Second, the majority of the literature that is currently available concentrates on hospitals in underdeveloped nations, which may restrict the findings' applicability to higher-resource environments like North America, where waste generation patterns and regulatory frameworks differ. Third, inconsistencies in how studies define and measure healthcare waste management outcomes pose challenges for direct comparison and synthesis. Lastly, although there is evidence of effective short-term interventions, there are still insufficient longitudinal studies to assess the programs' long-term efficacy, which leaves gaps in the understanding of their long-term effects on financial and environmental outcomes.

■ Conclusion

To improve hospital waste management, this review points out several critical areas where future research is needed. While barriers such as inadequate infrastructure and weak policy enforcement are well-documented, few studies assess scalable interventions to address them. Future research should evaluate system-level waste management initiatives in various healthcare environments, especially those with limited resources and in rural areas, and investigate whether spending on modern infrastructure, such as advanced segregation systems, liquid waste treatment plants, and recycling programs, has long-term positive effects on the environment and finances. Furthermore, more research is required to determine whether policy changes, like mandatory sustainable guidelines or financial incentive models, are successful in overcoming institutional resistance. Moreover, as present educational initiatives frequently lack long-term follow-up, more research is needed about maintaining staff engagement over time. Lastly, using mixed-methods approaches could provide a better understanding of the interactions between psychosocial, infrastructure, and economic barriers, ultimately helping researchers develop better solutions.

This review paper highlights important barriers and solutions to hospital waste management in efforts to reduce environmental pollution and create healthier populations. Future studies are warranted to assess the efficacy and sustainability of interventions targeting these barriers.

■ Acknowledgments

I would like to acknowledge Dr. Frank Glover for his guidance in this project and Indigo Research for supporting this work. I attest that the ideas, graphics, and writing in this paper are entirely my own.

■ References

1. Garrick, R.; Sullivan, J.; Doran, M.; Keenan, J. The Role of the Hospital in the Healthcare System. In *The Modern Hospital*; Latifi, R., Ed.; Springer International Publishing: Cham, 2019; pp 47–60. https://doi.org/10.1007/978-3-030-01394-3_6.
2. Lenzen, M.; Malik, A.; Li, M.; Fry, J.; Weisz, H.; Pichler, P.-P.; Chaves, L. S. M.; Capon, A.; Pencheon, D. The Environmental Footprint of Health Care: A Global Assessment. *Lancet Planet. Health* **2020**, *4* (7), e271–e279. https://doi.org/10.1016/S2542-5196(20)30121-2.
3. Pépin, J. *Health-care waste*. https://www.who.int/news-room/fact-sheets/detail/health-care-waste.
4. Hossain, Md. S.; Santhanam, A.; Nik Norulaini, N. A.; Omar, A. K. M. Clinical Solid Waste Management Practices and Its Impact on Human Health and Environment – A Review. *Waste Manag.* **2011**, *31* (4), 754–766. https://doi.org/10.1016/j.wasman.2010.11.008.
5. Janik-Karpinska, E.; Brancaleoni, R.; Niemcewicz, M.; Wojtas, W.; Foco, M.; Podogrocki, M.; Bijak, M. Healthcare Waste-A Serious Problem for Global Health. *Healthc. Basel Switz.* **2023**, *11* (2), 242. https://doi.org/10.3390/healthcare11020242.
6. Y., C.; J., E.; U., P. *Safe Management of Wastes from Health-Care Activities: A Practical Guide*, 2nd ed.; Nonserial Publications; World Health Organization: Geneva, 2014.
7. Ghali, H.; Cheikh, A. B.; Bhiri, S.; Bouzgarrou, L.; Rejeb, M. B.; Gargouri, I.; Latiri, H. S. Health and Environmental Impact of Hospital Wastes: Systematic Review. *Dubai Med. J.* **2023**, *6* (2), 67–80. https://doi.org/10.1159/000529432.
8. Sabiha-Javied; Tufail, M.; Khalid, S. Heavy Metal Pollution from Medical Waste Incineration at Islamabad and Rawalpindi, Pakistan. *Microchem. J.* **2008**, *90* (1), 77–81. https://doi.org/10.1016/j.microc.2008.03.010.
9. Rizan, C.; Mortimer, F.; Stancliffe, R.; Bhutta, M. F. Plastics in Healthcare: Time for a Re-Evaluation. *J. R. Soc. Med.* **2020**, *113* (2), 49–53. https://doi.org/10.1177/0141076819890554.
10. Briassoulis, G.; Ilia, S.; Briassouli, E. Exposure to Per- and Polyfluoroalkyl Substances (PFASs) in Healthcare: Environmental and Clinical Insights. *Life Basel Switz.* **2025**, *15* (7), 1057. https://doi.org/10.3390/life15071057.
11. Plezia, D.; Sabol, V. K.; Nelson, C.; Simmons, V. C. Improving Waste Segregation in the Operating Room to Decrease Overhead Cost. *Qual. Manag. Health Care* **2024**, *33* (1), 44–51. https://doi.org/10.1097/QMH.0000000000000416.
12. Mastronardi, M.; Bortul, M.; Dragani, F.; Biloslavo, A.; de Manzini, N.; Palmisano, S. Implementing Recycling in the Operating Room: A Single-Center Experience. *Surg. Endosc.* **2025**, *39* (2), 1323–1332. https://doi.org/10.1007/s00464-024-11502-6.
13. Fletcher, C. A.; St. Clair, R.; Sharmina, M. A Framework for Assessing the Circularity and Technological Maturity of Plastic Waste Management Strategies in Hospitals. *J. Clean. Prod.* **2021**, *306*, 127169. https://doi.org/10.1016/j.jclepro.2021.127169.
14. Nematollahi, H.; Tuysserkani, M.; Nematollahi, A. Medical Waste Management in the Modern Healthcare Era: A Comprehensive Review of Technologies, Environmental Impact, and Sustainable Practices. *Results Eng.* **2025**, *28*, 107210. https://doi.org/10.1016/j.rineng.2025.107210.
15. Guetter, C. R.; Williams, B. J.; Slama, E.; Arrington, A.; Henry, M. C.; Möller, M. G.; Tuttle-Newhall, J. E.; Stein, S.; Crandall, M. Greening the Operating Room. *Am. J. Surg.* **2018**, *216* (4), 683–688. https://doi.org/10.1016/j.amjsurg.2018.07.021.

DOI: 10.36838/IJHSR87.88

16. McGain, F.; White, S.; Mossenson, S.; Kayak, E.; Story, D. A Survey of Anesthesiologists' Views of Operating Room Recycling. *Anesth. Analg*. **2012**, *114* (5), 1049–1054. https://doi.org/10.1213/ANE.0b013e31824d273d.
17. McGain, F.; Jarosz, K. M.; Nguyen, M. N. H. H.; Bates, S.; O'Shea, C. J. Auditing Operating Room Recycling: A Management Case Report. *Case Rep*. **2015**, *5* (3), 47–50. https://doi.org/10.1213/XAA.0000000000000097.
18. Page, M. J.; McKenzie, J. E.; Bossuyt, P. M.; Boutron, I.; Hoffmann, T. C.; Mulrow, C. D.; Shamseer, L.; Tetzlaff, J. M.; Akl, E. A.; Brennan, S. E.; Chou, R.; Glanville, J.; Grimshaw, J. M.; Hróbjartsson, A.; Lalu, M. M.; Li, T.; Loder, E. W.; Mayo-Wilson, E.; McDonald, S.; McGuinness, L. A.; Stewart, L. A.; Thomas, J.; Tricco, A. C.; Welch, V. A.; Whiting, P.; Moher, D. The PRISMA 2020 Statement: An Updated Guideline for Reporting Systematic Reviews. *BMJ* **2021**, n71. https://doi.org/10.1136/bmj.n71.
19. Tudor, T. L.; Barr, S. W.; Gilg, A. W. Linking Intended Behaviour and Actions: A Case Study of Healthcare Waste Management in the Cornwall NHS. *Resour. Conserv. Recycl*. **2007**, *51* (1), 1–23. https://doi.org/10.1016/j.resconrec.2006.06.009.
20. Azouz, S.; Boyll, P.; Swanson, M.; Castel, N.; Maffi, T.; Rebecca, A. M. Managing Barriers to Recycling in the Operating Room. *Am. J. Surg*. **2019**, *217* (4), 634–638. https://doi.org/10.1016/j.amjsurg.2018.06.020.
21. Hakim, S. A.; Mohsen, A.; Bakr, I. Knowledge, Attitudes and Practices of Health-Care Personnel towards Waste Disposal Management at Ain Shams University Hospitals, Cairo. *East. Mediterr. Health J. Rev. Sante Mediterr. Orient. Al-Majallah Al-Sihhiyah Li-Sharq Al-Mutawassit* **2014**, *20* (5), 347–354.
22. Petre, M.-A.; Bahrey, L.; Levine, M.; van Rensburg, A.; Crawford, M.; Matava, C. A National Survey on Attitudes and Barriers on Recycling and Environmental Sustainability Efforts among Canadian Anesthesiologists: An Opportunity for Knowledge Translation. *Can. J. Anaesth. J. Can. Anesth*. **2019**, *66* (3), 272–286. https://doi.org/10.1007/s12630-018-01273-9.
23. Muduli, K.; Barve, A. Barriers to Green Practices in Health Care Waste Sector: An Indian Perspective. *Int. J. Environ. Sci. Dev*. **2012**, 393–399. https://doi.org/10.7763/IJESD.2012.V3.254.
24. Pillay, L.; Winkel, K. D.; Kariotis, T. Developing the Green Operating Room: Exploring Barriers and Opportunities to Reducing Operating Room Waste. *Med. J. Aust*. **2024**, *221* (5), 279–284. https://doi.org/10.5694/mja2.52394.
25. Devi, A.; Ravindra, K.; Kaur, M.; Kumar, R. Evaluation of Biomedical Waste Management Practices in Public and Private Sector of Health Care Facilities in India. *Environ. Sci. Pollut. Res*. **2019**, *26* (25), 26082–26089. https://doi.org/10.1007/s11356-019-05785-9.
26. Quttainah, M. A.; Singh, P. Barriers to Sustainable Healthcare Waste Management: A Grey Method Approach for Barrier Ranking. *Sustainability* **2024**, *16* (24), 11285. https://doi.org/10.3390/su162411285.
27. Taghipour, H.; Mosaferi, M. The Challenge of Medical Waste Management: A Case Study in Northwest Iran-Tabriz. *Waste Manag. Res. J. Sustain. Circ. Econ.* **2009**, *27* (4), 328–335. https://doi.org/10.1177/0734242X08104132.
28. Khan, B. A.; Cheng, L.; Khan, A. A.; Ahmed, H. Healthcare Waste Management in Asian Developing Countries: A Mini Review. *Waste Manag. Res. J. Sustain. Circ. Econ*. **2019**, *37* (9), 863–875. https://doi.org/10.1177/0734242X19857470.
29. Raji, M. O.; Adeogun, A. G. Healthcare Waste Management: An Overview. *ABUAD J. Eng. Res. Dev. AJERD* **2024**, *7* (1), 14–27. https://doi.org/10.53982/ajerd.2024.0701.02-j.
30. Lino, F. A. M.; Ismail, K. A. R.; Castañeda-Ayarza, J. A. Municipal Solid Waste Treatment in Brazil: A Comprehensive Review. *Energy Nexus* **2023**, *11*, 100232. https://doi.org/10.1016/j.nexus.2023.100232.
31. Aboueid, S.; Beyene, M.; Nur, T. Barriers and Enablers to Implementing Environmentally Sustainable Practices in Healthcare: A Scoping Review and Proposed Roadmap. *Healthc. Manage. Forum* **2023**, *36* (6), 405–413. https://doi.org/10.1177/08404704231183601.
32. Jungbluth, L.; Goodwin, D.; Tull, F.; Bragge, P. Barriers and Facilitators to Recycling Waste in Hospitals: A Mixed Methods Systematic Review. *Resour. Conserv. Recycl. Adv*. **2024**, *21*, 200209. https://doi.org/10.1016/j.rcradv.2024.200209.
33. Hosny, G.; Samir, S.; El-Sharkawy, R. An Intervention Significantly Improve Medical Waste Handling and Management: A Consequence of Raising Knowledge and Practical Skills of Health Care Workers. *Int. J. Health Sci*. **2018**, *12* (4), 56–66.
34. Saha, K.; Farhanj, Z.; Kumar, V. A Systematic Review of Circular Economy Literature in Healthcare: Transitioning from a 'Post-Waste' Approach to Sustainability. *J. Clean. Prod*. **2025**, *512*, 145427. https://doi.org/10.1016/j.jclepro.2025.145427.
35. Wormer, B. A.; Augenstein, V. A.; Carpenter, C. L.; Burton, P. V.; Yokeley, W. T.; Prabhu, A. S.; Harris, B.; Norton, S.; Klima, D. A.; Lincourt, A. E.; Heniford, B. T. The Green Operating Room: Simple Changes to Reduce Cost and Our Carbon Footprint. *Am. Surg*. **2013**, *79* (7), 666–671.
36. Delgado, N.; Castillo, A. R. A. D.; Pilco-Chambilla, F. W.; Valencia, C. M. Z. Accounting and Healthcare Waste Management: Strategies to Improve Financial Efficiency and Reduce Environmental Impact. *South East. Eur. J. Public Health* **2024**, 355–363. https://doi.org/10.70135/seejph.vi.1680.
37. Yilma, M.; Taye, G.; Tefera, M.; Tassew, B.; Fentie, A. M.; Abebe, W. Exploring Barriers to and Facilitators of Infection Prevention and Control Practices in the Pediatrics and Child Health Department of Tikur Anbessa Specialized Hospital, Ethiopia. *Antimicrob. Resist. Infect. Control* **2024**, *13* (1), 121. https://doi.org/10.1186/s13756-024-01475-5.
38. Berhe, T. T.; Feleke, A. K.; Bekele, G. E.; Gebrihiwot, E. M.; Ali, Y. H.; Tedila, G. W. Facilitators and Barriers of Infectious Waste Management Practice in Public and Private Health Facilities of Addis Ababa, Ethiopia: A Qualitative Phenomenological Study. *Front. Public Health* **2025**, *13*, 1538124. https://doi.org/10.3389/fpubh.2025.1538124.

Author

Shrey is a senior at Abbey Park High School in Ontario with a strong interest in sustainability and healthcare. He is fascinated by the intersection between environmental systems and human health. He plans to study environmental science and medicine in college and continue research focused on solving pressing global health and sustainability challenges.

IJHSR
ijhighschoolresearch.org
RESEARCH ARTICLE

The Effects of Age and Sex on Symptom Severity and Brain Volumes of Irritable Bowel Syndrome Patients

By Anna Chia

Anglo-Chinese School (Independent), 121 Dover Rd, Singapore 139650, Singapore; annachia1906@gmail.com
Mentor: Barbara Biney

ABSTRACT: Irritable Bowel Syndrome is a common functional bowel disease that affects a large proportion of the general population. Often associated with changes in bowel habits and the manifestation of abdominal pain, IBS greatly impacts a patient's quality of life. This research paper analyzes a dataset to understand the relationship between sex, age, IBS symptom severity, and patient brain volumes. It was found that there were statistically significant differences in volumes of the left lateral orbitofrontal gyrus between the sexes. Female IBS patients in the dataset had comparable symptom severity to male IBS patients, and generally smaller brain volumes in individual brain regions. Older IBS patients were observed to have smaller brain volumes, but greater symptom severities. These results are contrary to the current consensus of IBS symptom severity in various populations.
KEYWORDS: Biomedical and Health Sciences, Pathophysiology, Neuroscience, Physiology, Neurobiology.

Introduction

Irritable Bowel Syndrome (IBS), a functional bowel disease (FBD), is a very common disorder, affecting 9-23% of the global population.[1] IBS is often defined as pain associated with a change in bowel habits. FBD refers to a gut disorder that does not show any structural or biochemical abnormalities, and according to the Rome criteria, is defined as symptoms stemming from the middle and lower gastrointestinal tract and symptoms appearing at least three days a month in the last three months.[2,3] Symptoms of IBS often include abdominal pain, either diarrhea or constipation, and bloating.[4] IBS has been associated with impaired quality of life and increased prevalence of mental disorders like depression.[5]

All forms of IBS, such as IBS with symptoms of constipation (IBS-C), diarrhea (IBS-D), or a mix of both (IBS-M), have been reported to manifest moderate to severe pain that interferes with daily life.[6] A meta-analysis by Tillisch, Mayer, and Labus noted that IBS participants showed greater brain activity in regions associated with visceral afferent processing and regions associated with emotional arousal.[7] IBS patients were also detailed to have reduced activation and decreased gray matter density in various areas of the brain, leading to impairment of the body's pain inhibitory system and possibly contributing to the pain levels of IBS.[8]

Recent studies also found associations between pain in IBS and brain morphology – research by Labus *et al.* observed that greater severity in IBS symptoms, such as heightened abdominal pain, was associated with lower brain region volumes.[9]

This study aimed to explore the correlation between sex and age and the pain severity of IBS. In addition, this paper aimed to investigate any correlation between sex or age and regional brain volume. It was hypothesized that females and younger age group individuals (18-29) would experience more severe IBS pain symptoms. It was also hypothesized that individuals experiencing greater pain symptoms would have lower brain volumes in regions associated with visceral sensation, emotional arousal, and attention.

Methodology

Source of Data:

The dataset (April 2011 NI IBS Pain) was obtained from the Statistics Online Computational Resource website by the University of Michigan.[10] This dataset originated from a brain imaging study of IBS patients and normal control participants.[11] The overall severity of gastrointestinal symptoms (BSQ_Overall, on a scale of 0 to 20), severity of the abdominal pain experienced (BSQ_abdominal pain, on a scale of 0 to 20) and general symptom severity (BSQ_severity, on a scale of 1 to 5) were determined using the Bowel Symptom Questionnaire, where increasing scores indicate increasing severity.[12] The proneness of the participants to anxiety was determined using the State-Trait Anxiety Inventory, where a higher score also indicated greater anxiety.[13] Neuroimaging data were also used to obtain volumes of regions of interest in the brain, reported in mm^3.[10]

Statistical Analysis:

Statistical analysis was conducted using RStudio (Version 2024.12.0+467). Participants with incomplete data were not included in the statistical analysis. Histograms for each variable's data were generated to identify outliers, which were then excluded from the analysis. Normality of the data was determined using a Shapiro-Wilk test, where a p-value of greater than 0.05 indicated a normal distribution.

An Independent Samples T-test was used to compare the data values between male and female participants if both data sets were normally distributed. The Independent Samples T-test is designed to compare the means of two normally

© 2026 Terra Science and Education

DOI: 10.36838/IJHSR87.96

distributed populations, which is also equivalent to the medians of these populations.[14,15] If one or both sets of data were not normally distributed, a Mann-Whitney U test was used instead. The Mann-Whitney U test is an alternative to the T-test that can compare groups that are not normally distributed by testing if one group tends to have higher values than the other group.[16]

For comparison across different age groups (18-29, 30-39, 40-49, and >50), a Kruskal-Wallis H test was performed. The Kruskal-Wallis H test is the non-parametric equivalent of the one-way ANOVA and can compare the medians of three or more groups of non-normally distributed data.[17] If the p-values, as calculated in the statistical tests, were less than 0.05, differences between groups were considered statistically significant.

Results

This section presents the results of the data analysis. Table 1 shows the characteristics of the dataset used.

Table 1: Characteristics of the dataset used.

Characteristics	IBS (n=87)
Sex	
Male	18
Female	69
Median Age, (Std)	30 (10.2)
Age groups	
18-29	41
30-39	20
40-49	21
>50	5

Comparison of Median Brain Volumes between Sex:

As shown in Figure 1, it was found that males have a significantly larger brain volume in the left lateral orbitofrontal gyrus than females (p-value of 0.0337 (<0.05)). While it was observed that males generally showed slightly larger volumes in individual brain regions, no other brain regions showed statistically significant differences in brain volumes. Other results can be found in Figures 2, 3, 4, and Tables 2, 3, and 4.

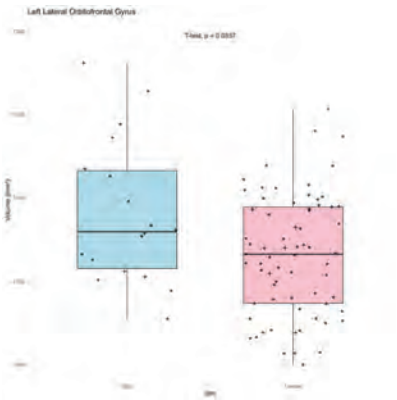

Figure 1: A box-and-whisker plot showing the difference in brain volume of the left lateral orbitofrontal gyrus between male and female IBS participants. Males were observed to have a larger brain volume than females in this brain region. The difference between these volumes was statistically significant.

Table 2: Table summarizing median brain volumes of regions in the frontal lobe for male and female IBS participants. The male IBS patients were generally observed to have greater brain volumes of regions in the frontal lobe. However, statistical tests for these comparisons suggest that the differences are not statistically significant, except for the left lateral orbitofrontal gyrus (p-value = 0.0337 (<0.05)).

Frontal lobe			
Brain Region	Median Male Brain volume (mm^3)	Median Female Brain volume (mm^3)	P-value
Left superior frontal gyrus	53827	51219	0.276
Right superior frontal gyrus	55871.5	53459	0.986
Left middle frontal gyrus	54586	53154	0.305
Right middle frontal gyrus	53519.5	51336	0.0773
Left inferior frontal gyrus	18714.5	17643	0.955
Right inferior frontal gyrus	24717.5	22941	0.0595
Left middle orbitofrontal gyrus	8556	8307	0.691
Right middle orbitofrontal gyrus	8959	9186	0.855
Left lateral orbitofrontal gyrus	4599.5	4329	0.0337 *
Right lateral orbitofrontal gyrus	4227.5	3840	0.0923
Left gyrus rectus	1970	1992	0.580
Right gyrus rectus	2426.5	2552	0.792

* indicates that the p-value is less than 0.05

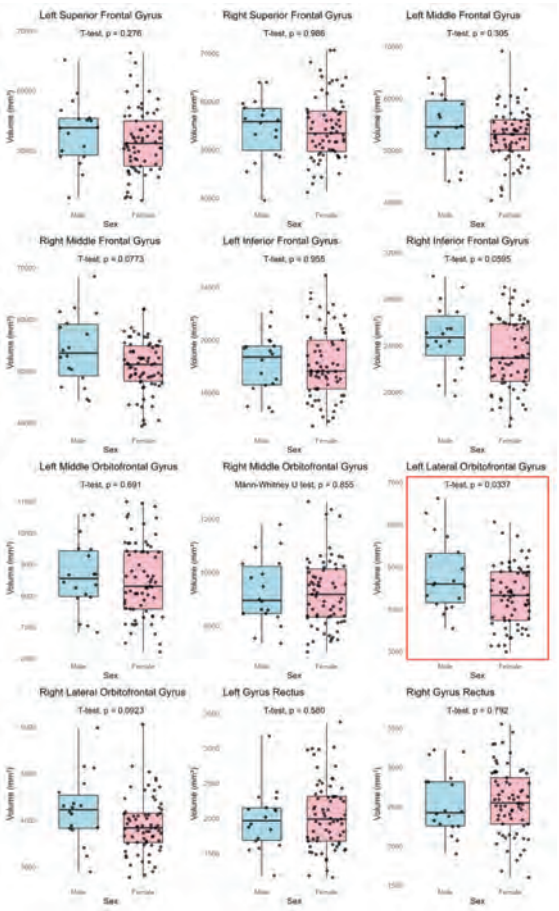

Figure 2: Box-and-whisker plots showing median brain volumes of regions in the frontal lobe of male and female IBS participants. The male IBS patients were generally observed to have greater brain volumes of regions in the frontal lobe. However, statistical tests for these comparisons suggest that differences are not statistically significant, except for the left lateral orbitofrontal gyrus (p-value = 0.0337 (<0.05)). The significant finding is highlighted with a red box above.

Table 3: Table of median brain volumes of regions in the limbic lobe of male and female IBS participants. Data analysis showed that female IBS participants had higher median brain volumes as compared to males in this region, except for in the right cingulate gyrus and the right hippocampus, but statistical analysis of these comparisons yielded p-values greater than 0.05.

Limbic Lobe			
Brain Region	Median Male Brain volume (mm^3)	Median Female Brain volume (mm^3)	P-value
Left cingulate gyrus	10618	10866	0.741
Right cingulate gyrus	11479	10798	0.399
Left hippocampus	3450.5	3616	0.876
Right hippocampus	4105	3917	0.431

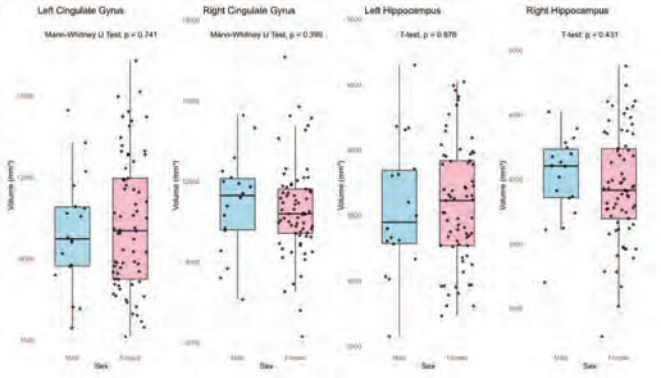

Figure 3: Box-and-whisker plots showing median brain volumes of regions in the limbic lobe of male and female IBS participants. Analysis shows that females had higher median brain volumes as compared to males in this region, except for in the right cingulate gyrus and the right hippocampus. These differences were not statistically significant.

Table 4: Table of median brain volumes of regions in the insular cortex, dorsal striatum (caudate and putamen), and brainstem of male and female IBS participants. Males displayed greater median brain volumes in most of these regions, though statistical analysis produced p-values greater than 0.05, suggesting that these differences had little statistical significance.

Insular cortex, dorsal striatum (caudate and putamen) and brainstem			
Brain Region	Median Male Brain volume (mm^3)	Median Female Brain volume (mm^3)	P-value
Left insular cortex	7920.5	7813	0.667
Right insular cortex	5136.5	5013	0.656
Left caudate	1565.5	1753	0.428
Right caudate	2037	2110	0.324
Left putamen	2802	2662	0.460
Right putamen	4037.5	3814	0.702
Brainstem	25931	26500	0.795

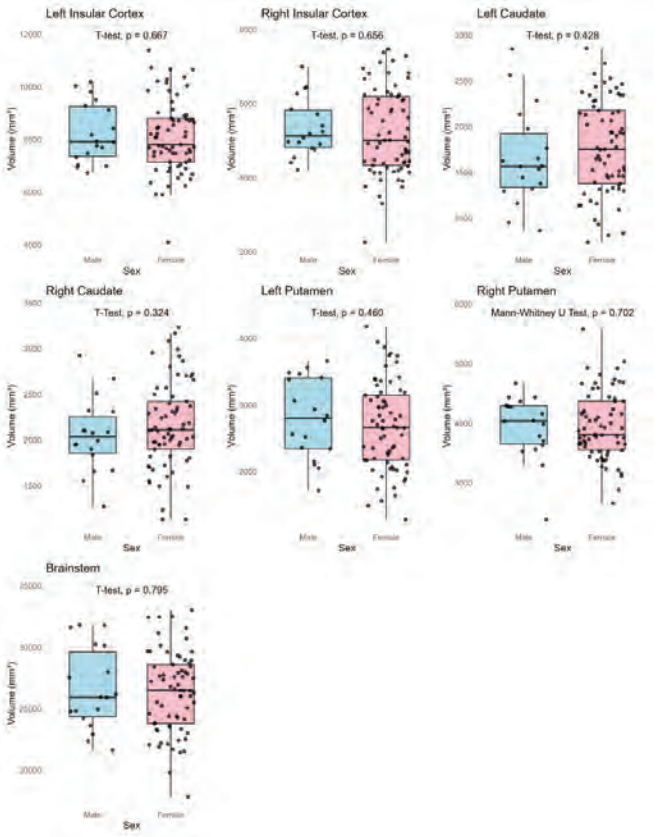

Figure 4: Box-and-whisker plots showing median brain volumes in the insular cortex, dorsal striatum (caudate and putamen), and brainstem of male and female IBS participants. Males displayed greater median brain volumes than females in most of these regions, apart from the caudate and the brainstem. Statistical analysis showed p-values greater than 0.05, suggesting that the differences had little statistical significance.

Female IBS patients also had a greater median brain volume than males, as seen in Figure 5 and Table 5, observing a larger median total brain volume, gray matter volume, and white matter volume. However, further statistical analysis showed no statistically significant difference when comparing these volumes between sexes.

Table 5: Table summarizing median overall brain volumes for male and female IBS participants. Female IBS participants are observed to have larger median total brain volumes, gray matter volumes, and white matter volumes. However, the Mann-Whitney U Test yielded p-values greater than 0.05, indicating that the differences from these comparisons had little statistical significance.

Brain Region	Median Male Brain volume (mm^3)	Median Female Brain volume (mm^3)	P-value
Total Brain	1143998.5	1226341	0.214
Gray Matter	528439.5	564193	0.0829
White Matter	489131	529262	0.278

DOI: 10.36838/IJHSR87.96

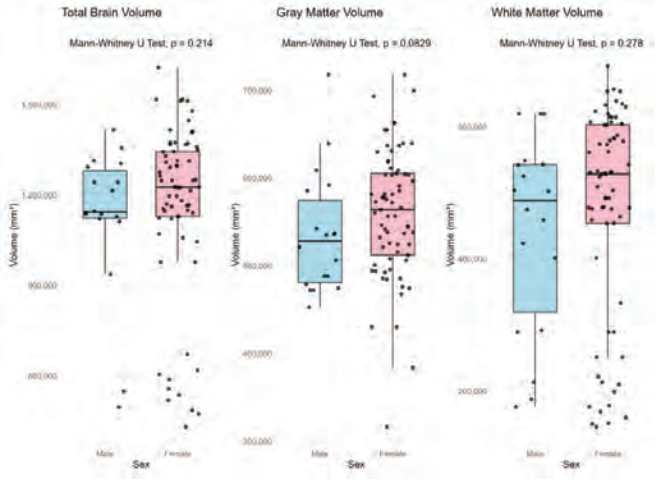

Figure 5: Box-and-whisker plots of median overall brain volumes of male and female IBS participants. Female IBS participants are observed to have larger median total brain volumes, gray matter volumes, and white matter volumes. However, the Mann-Whitney U Test yielded p-values greater than 0.05, indicating that the differences from these comparisons were statistically insignificant.

Comparison of IBS Symptom Severity between Sex:

Comparing symptom severity between sexes in Figure 6 and Table 6, women scored slightly higher on the BSQ questionnaire, and both male and female participants with IBS had similar median scores on the State-Trait Anxiety Inventory. Further statistical analysis reveals that these scores were not statistically significant, suggesting that male and female IBS patients experience comparable IBS symptom severities.

Table 6: Table summarizing IBS symptom severity data for male and female IBS participants. Analysis of the dataset showed that female participants with IBS had higher BSQ_Overall and BSQ_abdominal pain scores, while both male and female participants shared similar median scores for BSQ_severity and for the State-Trait Anxiety Inventory. However, statistical tests indicate that the differences in these comparisons of these scores were not statistically significant.

Symptom Measurement	Male Score	Female Score	P-value
BSQ Overall	10	12	0.693
BSQ abdominal pain	10	11	0.372
BSQ severity	3	3	0.752
Trait Anxiety (Raw)	34	34	0.892
Trait Anxiety	48.5	48	0.904

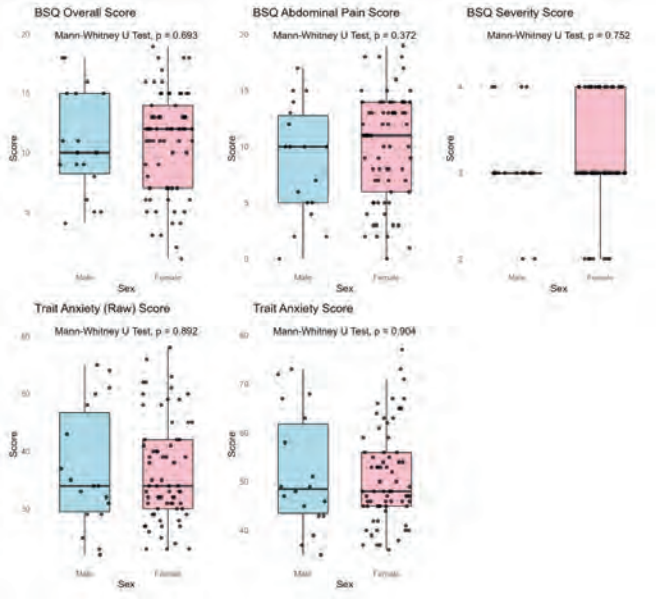

Figure 6: Box-and-whisker plots showing IBS symptom severity data of male and female IBS participants. Analysis of the dataset showed that female participants with IBS had higher BSQ_Overall and BSQ_abdominal pain scores, while both male and female participants shared similar median scores for BSQ_severity and for the State-Trait Anxiety Inventory. However, statistical tests indicate that the differences in these comparisons of these scores were not statistically significant.

Comparison of Median Brain Volumes between Age Groups:

Analysis of the brain volume data in Figure 7 and Table 7 showed that participants in the 30-39 age group were seen to have the greatest median total brain volume, while participants in the >50 age group had the greatest median gray matter volume. Participants in the 18-29 age group also had the greatest median white matter volume. In contrast, participants in the 40-49 age group had the lowest median total brain volume and white matter volume, and participants over 50 had the lowest median gray matter volume. These differences, however, were not statistically significant.

Table 7: Table summarizing median overall brain volumes for IBS participants of different age groups. Participants from the 40-49 age group and the >50 age group were found to have the lowest median total brain volumes, white matter volumes, and gray matter volumes. On the other hand, participants aged 30-39, >50, and 18-29 were determined to have the greatest median total brain volume, gray matter volume, and white matter volume, respectively. The results of the Kruskal-Wallis H tests indicate that these differences were not statistically significant.

Brain Region	Median Brain Volume for each age group (mm^3)				P-value
	18-29	30-39	40-49	>50	
Total Brain	1226341	1237565.5	1196812	1214995	0.707
Gray Matter	545699	569724	524661	603971	0.0614
White Matter	530256	501885.5	526213	459476	0.879



Figure 7: Box-and-whisker plots of median overall brain volumes for IBS participants of different age groups. Participants from the 40-49 age group and the >50 age group were found to have the lowest median total brain volumes, white matter volumes, and gray matter volumes. On the other hand, participants aged 30-39, >50, and 18-29 were determined to have the greatest median total brain volume, gray matter volume, and white matter volume, respectively. The results of the Kruskal-Wallis H tests indicate that these differences were not statistically significant.

In reference to the individual regions of interest in Figures 8, 9, 10, and Tables 8, 9, 10, individuals aged 18-29 and 30-39 typically had the greatest median brain volumes. Similarly, participants in the 40-49 and >50 age groups often showed the smallest median brain volumes. Further statistical analysis showed that the differences between these values were not statistically significant.

Table 8: Table summarizing median brain volumes of regions in the frontal lobe for IBS participants of different age groups. IBS patients aged between 40 and 49 and aged over 50 often showed the lowest median volumes in the frontal lobe, while participants in the 30-39 age group exhibited the highest median volumes in most regions. Further analysis of the dataset suggested that the differences between median volumes in each comparison had little statistical significance.

Frontal Lobe					
Brain Region	Median Brain Volume for each age group (mm^3)				P-value
	18-29	30-39	40-49	>50	
Left superior frontal gyrus	51514	54215.5	50542	52215	0.535
Right superior frontal gyrus	53210	56464.5	54094	53803	0.482
Left middle frontal gyrus	53900	53455	51160	53778	0.149
Right middle frontal gyrus	51499	52244.5	49685	52398	0.649
Left inferior frontal gyrus	17632	18540.5	17151	19132	0.275
Right inferior frontal gyrus	23292	24764	22084	22816	0.450
Left middle orbitofrontal gyrus	8634	8403.5	8307	8161	0.858
Right middle orbitofrontal gyrus	8995	9268.5	9257	8422	0.554
Left lateral orbitofrontal gyrus	4329	4476.5	4294	5123	0.387
Right lateral orbitofrontal gyrus	3840	3941.5	3886	3506	0.784
Left gyrus rectus	1921	2245	2114	1717	0.358
Right gyrus rectus	2541	2582	2552	2451	0.824

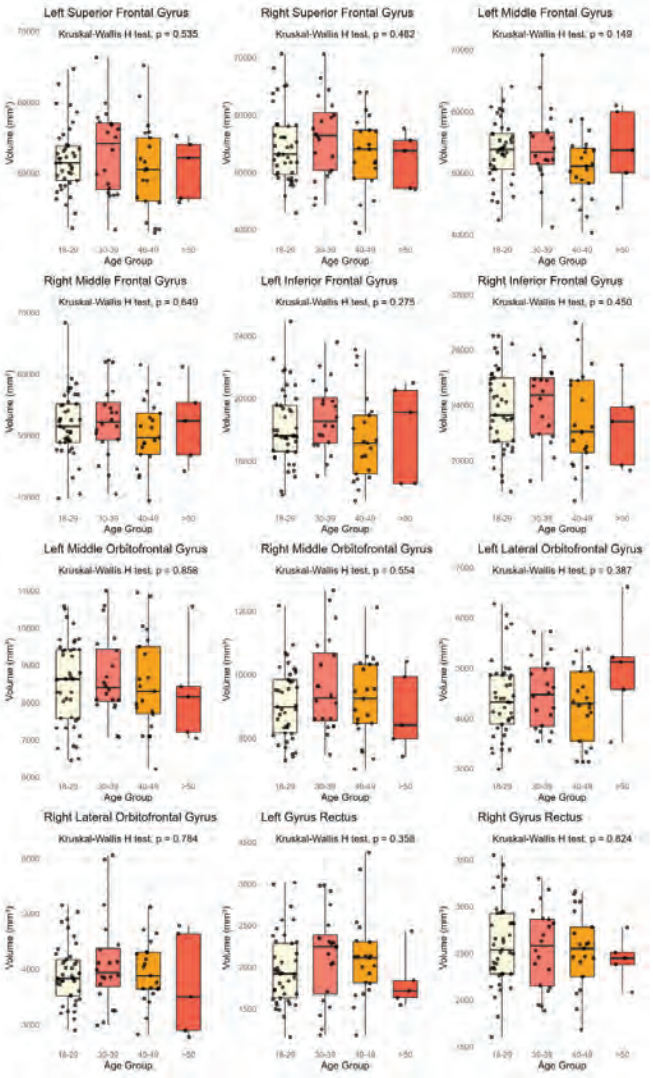

Figure 8: Box-and-whisker plots of median brain volumes of regions in the frontal lobe for IBS participants of different age groups. IBS patients aged between 40 and 49 and aged over 50 often showed the lowest median volumes in the frontal lobe, while participants in the 30-39 age group exhibited the highest median volumes in most regions. Further analysis of the dataset suggested that the differences between median volumes in each comparison had little statistical significance.

Table 9: Table summarizing median brain volumes of regions in the limbic lobe for IBS participants of different age groups. Participants from the 30-39 age group generally demonstrated the highest median brain volumes in this region, while the >50 and 18-29 age groups expressed the lowest median brain volumes. The Kruskal-Wallis H test showed little statistically significant difference within these comparisons.

Limbic Lobe					
Brain Region	Median Brain Volume for each age group (mm^3)				P-value
	18-29	30-39	40-49	>50	
Left cingulate gyrus	10222	11583	10954	9219	0.325
Right cingulate gyrus	10737	11645.5	10773	11679	0.321
Left hippocampus	3339	3680	3728	3410	0.251
Right hippocampus	3914	4130	3913	3667	0.632

DOI: 10.36838/IJHSR87.96

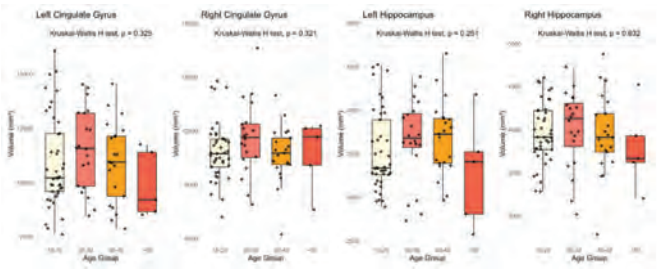

Figure 9: Box-and-whisker plots of median brain volumes of regions in the limbic lobe for IBS participants of different age groups. Participants from the 30-39 age group generally demonstrated the highest median brain volumes in this region, while the >50 and 18-29 age groups expressed the lowest median brain volumes. The Kruskal-Wallis H test showed little statistically significant difference within these comparisons.

Table 10: Table summarizing median brain volumes of regions in the insular cortex, dorsal striatum (caudate and putamen), and brainstem for IBS participants of different age groups. For most of these brain regions, participants in the 30-39 age group showed the greatest median brain volume, and participants over 50 years old generally showed the lowest median brain volumes. The p-values of these differences exceed 0.05, suggesting that the differences are not statistically significant.

Insular cortex, dorsal striatum (caudate and putamen) and brainstem					
Brain Region	Median Brain Volume for each age group (mm^3)				P-value
	18-29	30-39	40-49	>50	
Left insular cortex	7696	8221.5	8205	7135	0.513
Right insular cortex	4962	5546	5018	4679	0.546
Left caudate	1679	1730.5	1753	1625	0.991
Right caudate	2091	2198.5	2124	1805	0.297
Left putamen	2683	2708.5	2835	2149	0.468
Right putamen	3956	4125	3802	3530	0.259
Brainstem	26305	26548.5	25915	24827	0.999

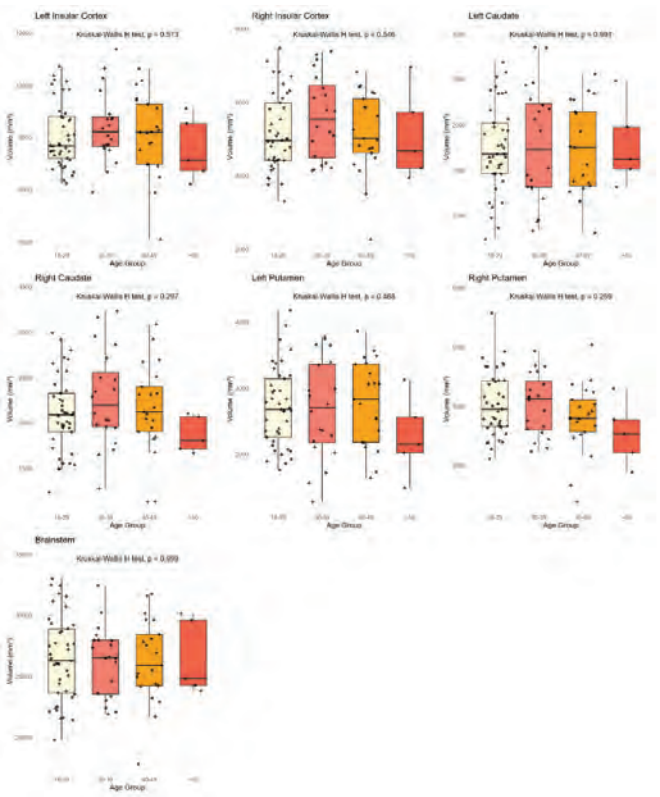

Figure 10: Box-and-whisker plots of median brain volumes of regions in the insular cortex, dorsal striatum (caudate and putamen), and brainstem for IBS participants of different age groups. For most of these brain regions, participants in the 30-39 age group showed the greatest median brain volume, and participants over 50 years old generally showed the lowest median brain volumes. The p-values of these differences exceed 0.05, suggesting that the differences are not statistically significant.

Comparison of IBS Symptom Severity between Age Groups:

In regard to age and symptom severity in Figure 11 and Table 11, participants in the age group of 40-49 showed higher median scores on the BSQ_questionnaire, while participants in the age groups 18-29 and >50 showed lower median scores for BSQ_overall and BSQ_abdominal pain, respectively. Participants aged >50 years old showed the highest median scores on the State-Trait Anxiety Inventory. Comparisons of the symptom measurements yielded p-values that suggested little statistical difference.

Table 11: Table summarizing IBS symptom severity data for IBS participants from different age groups. Participants aged 40-49 displayed higher median scores on most parts of the BSQ_questionnaire, while participants from the >50 age group showed the highest scores on the State-Trait Anxiety Inventory. These comparisons of the symptom measurements yielded few statistically significant differences.

Symptom Measurement	Median scores for each age group				P-value
	18-29	30-39	40-49	>50	
BSQ Overall	11	12	13	12	0.112
BSQ abdominal pain	8	12	13	5	0.0672
BSQ severity	3	3	3	3	0.950
Trait Anxiety (Raw)	34	39	32	53	0.124
Trait Anxiety	48	53	47	72	0.0794

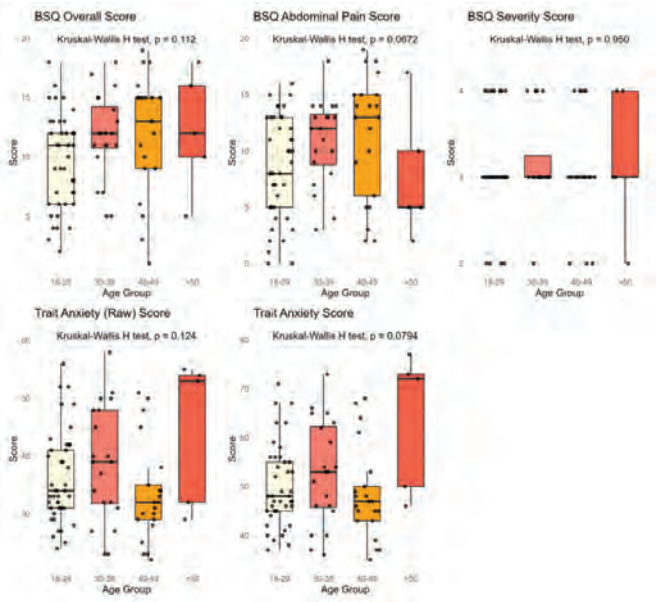

Figure 11: Box-and-whisker plots showing the different median IBS symptom severity scores for IBS participants of different age groups. Participants aged 40-49 displayed higher median scores on most parts of the BSQ questionnaire, while participants from the >50 age group showed the highest scores on the State-Trait Anxiety Inventory. The differences in symptom measurements were not statistically significant.

Discussion

This study compared the volumes of various brain regions of interest and symptom measurement scores between sexes and different age groups of IBS participants. While analysis of the dataset showed a statistically significant difference in comparisons of the left lateral orbitofrontal gyrus between sex and a general trend of females and patients above 40 years old having smaller median brain volumes, statistically significant differences were generally not found for most comparisons.

Statistically significantly greater volumes of the left lateral orbitofrontal gyrus were observed in males compared to females. The left lateral orbitofrontal gyrus is typically involved in changing emotional behavior, and lower volumes in this region have been associated with higher abdominal pain, due to reduced brain volumes altering the processing of visceral sensations.[18,19]

However, the lack of difference in symptom severity, despite the significant structural difference in the left lateral orbitofrontal gyrus and statistically insignificant structural differences in other brain regions, does not align with the anticipated inverse correlation between brain volume and pain. This may reflect a true lack of association between brain volumes and IBS pain severity or may be attributed to the limitations of this study. As such, this result should be interpreted cautiously.

The lack of significant differences in IBS symptom severity between sexes does not support this study's hypothesis and the general literature reporting that female IBS patients experience more severe abdominal pain during colorectal distention and significantly higher symptom scores.[20-22] The lack of significant differences in brain volumes also does not align with the literature, which shows significantly lower brain volumes in regions associated with pain processing.[12] However, this study had a sample size of 87 participants, which is smaller than the larger sample size often used for scientific studies. This dataset also observed a sample imbalance, with 69 females and only 18 males. This imbalance may have affected the observed trends and reduced the statistical significance between the two groups.

Similarly, comparisons of symptom severity and brain volumes between different age groups yielded non-significant differences in median values. The lack of significant differences in symptom severity across ages is inconsistent with the general understanding of younger IBS patients experiencing significantly greater abdominal pain and visceral hypersensitivity.[23,24] Once again, this lack of significant differences should be understood in consideration of the dataset's limited sample size and uneven sample distribution, with only 5 participants being above 50 years old.

The general statistically insignificant trend of younger patients having greater brain volumes, while patients older than 40 have the smallest brain volumes, aligns with prior studies that also reported statistically insignificant decreases in cortical thickness and gray matter in IBS patients as they aged.[25] However, as the differences between the groups did not reach statistical significance, which may be indicative of the limitations of the small and uneven sample size, the results cannot be directly correlated with existing literature.

Although most of the findings were non-significant, this data analysis can still contribute to broader literature. The lack of significant results reflects the limitations of the dataset's sample size and research design and highlights the importance of replication and larger-scale datasets in order to determine population trends. The results may also reflect a true lack of association between the volumes of most brain regions and IBS pain severity, and the trends observed may warrant further investigation with larger sample sizes. If future studies with larger sample sizes yield similar results, this may influence future counseling and patients' expectations of IBS symptoms and their severity. Women are currently expected to observe greater symptom severity, and many types of IBS medications, like Alosetron, cater towards female patients.[26,27] Similarly, younger patients are also expected to experience stronger psychological and abdominal pain symptoms and are thus anticipated to require more support.[28,29] As such, these exploratory results may help inform IBS diagnosis and treatment to promote more balanced care for both sexes and different age groups.

Conclusion

In conclusion, apart from volumes of the left lateral orbitofrontal gyrus between sexes, analysis of the data yielded mostly no statistically significant differences in IBS symptom severity and brain volumes between different sexes and age groups. Although the findings do not strongly support existing literature and hypotheses, these findings help to explore the relationship between brain volumes and IBS symptom severities, and the trends found can help guide the building of hypotheses in future, larger studies.

DOI: 10.36838/IJHSR87.96

The study experienced a few limitations. The study had a limited sample size, and the uneven distribution between variable groups may have also affected the trends observed. Although the findings explore correlations between IBS symptoms and brain volumes, their causal relationship cannot be confirmed. Moreover, inherent limitations of the Bowel Symptom questionnaire and the State-Trait Anxiety Inventory were that they rely on a participant's self-reported symptom severity, which may also be influenced by a patient's own perception of their pain and how they communicate it.

Future studies investigating relationships between sex/age and IBS should focus more on identifying the causal link between the different variables and pain severity for IBS, and determine the mechanism causing such a relationship, which can help provide a greater understanding of how IBS works.

Acknowledgments

I would like to thank Dr. Barbara Biney for her support and guidance throughout the research period. Data was obtained from the Statistics Online Computational Resource website by the University of Michigan, and figures were created by the author using RStudio (Version 2024.12.0+467).

References

1. Saha, L. Irritable Bowel Syndrome: Pathogenesis, Diagnosis, Treatment, and Evidence-Based Medicine. *World J. Gastroenterol.* **2014**, 20 (22), 6759–6773. https://doi.org/10.3748/wjg.v20.i22.6759.
2. Grundy, D.; De Giorgio, R.; Schemann, M. Enteric Nervous System: Disorders. In *Encyclopedia of Neuroscience*; Squire, L. R., Ed.; Academic Press, **2009**; pp. 1077–1082. https://doi.org/10.1016/B978-008045046-9.00661-6.
3. Häuser, W.; Layer, P.; Henningsen, P.; Kruis, W. Functional Bowel Disorders in Adults. *Dtsch. Ärztebl. Int.* **2012**, *109* (5), 83–89. https://doi.org/10.3238/arztebl.2012.0083.
4. Vahedi, H.; Ansari, R.; Mir-Nasseri, M. M.; Jafari, E. Irritable Bowel Syndrome: A Review Article. *Middle East J. Dig. Dis*. **2010**, *2* (2), 66–77.
5. Kopczyńska, M.; Mokros, Ł.; Pietras, T.; Małecka-Panas, E. Quality of Life and Depression in Patients with Irritable Bowel Syndrome. *Gastroenterol. Rev*. **2018**, *13* (2), 102–108. https://doi.org/10.5114/pg.2018.75819.
6. Bhinder, G.; Meza-Cardona, J. M.; Low, A.; Aumais, G.; Attara, G. P.; Gray, J. R. Irritable Bowel Syndrome Patient Experience: A Survey of Patient-Reported Symptoms by Irritable Bowel Syndrome Subtype and Impact on Quality of Life. *J. Can. Assoc. Gastroenterol.* **2023**, *6* (6), 219–228. https://doi.org/10.1093/jcag/gwad028.
7. Tillisch, K.; Mayer, E. A.; Labus, J. S. Quantitative Meta-Analysis Identifies Brain Regions Activated during Rectal Distension in Irritable Bowel Syndrome. *Gastroenterology* **2010**, *140* (1), 91–100. https://doi.org/10.1053/j.gastro.2010.07.053.
8. Elsenbruch, S. Abdominal Pain in Irritable Bowel Syndrome: A Review of Putative Psychological, Neural and Neuro-Immune Mechanisms. *Brain, Behavior, and Immunity* **2011**, *25* (3), 386–394. https://doi.org/10.1016/j.bbi.2010.11.010.
9. Labus, J.; Dinov, I. D.; Jiang, Z.; Ashe-McNalley, C.; Zamanyan, A.; Shi, Y.; Hong, J.-Y.; Gupta, A.; Tillisch, K.; Ebrat, B.; Hobel, S.; Gutman, B. A.; Joshi, S.; Thompson, P. M.; Toga, A. W.; Mayer, E. A. Irritable Bowel Syndrome in Female Patients Is Associated with Alterations in Structural Brain Networks. *Pain* **2013**, *155* (1), 137–149. https://doi.org/10.1016/j.pain.2013.09.020.
10. *SOCR Data April 2011 NI IBS Pain*. Statistics Online Computational Resource. University of Michigan. https://wiki.socr.umich.edu/index.php/SOCR_Data_April2011_NI_IBS_Pain (accessed 2025-11-22).
11. Mayer, E. A.; Berman, S.; Suyenobu, B.; Labus, J.; Mandelkern, M. A.; Naliboff, B. D.; Chang, L. Differences in Brain Responses to Visceral Pain between Patients with Irritable Bowel Syndrome and Ulcerative Colitis. *Pain* **2005**, *115* (3), 398–409. https://doi.org/10.1016/j.pain.2005.03.023.
12. Jiang, Z.; Dinov, I. D.; Labus, J.; Shi, Y.; Zamanyan, A.; Gupta, A.; Ashe-McNalley, C.; Hong, J.-Y.; Tillisch, K.; Toga, A. W.; Mayer, E. A. Sex-Related Differences of Cortical Thickness in Patients with Chronic Abdominal Pain. PLOS ONE **2013**, *8* (9), e73932. https://doi.org/10.1371/journal.pone.0073932.
13. Julian, L. J. Measures of Anxiety: State-Trait Anxiety Inventory (STAI), Beck Anxiety Inventory (BAI), and Hospital Anxiety and Depression Scale-Anxiety (HADS-A). *Arthritis Care Res*. **2011**, *63* (S11), S467–S472. https://doi.org/10.1002/acr.20561.
14. Rochon, J.; Gondan, M.; Kieser, M. To Test or Not to Test: Preliminary Assessment of Normality When Comparing Two Independent Samples. *BMC Med. Res. Methodol.* **2012**, *12*, 81. https://doi.org/10.1186/1471-2288-12-81.
15. Manikandan, S. Measures of Central Tendency: Median and Mode. *J. Pharmacol. Pharmacother.* **2011**, *2* (3), 214–215. https://doi.org/10.4103/0976-500X.83300.
16. Hart, A. Mann-Whitney Test Is Not Just a Test of Medians: Differences in Spread Can Be Important. *BMJ* **2001**, *323* (7309), 391–393. https://doi.org/10.1136/bmj.323.7309.391.
17. Yang, H. J.; Lee, H. S. Common Statistical Methods Used in Medical Research. *Kosin Med J.* **2025**, *40* (1), 21–30. https://doi.org/10.7180/kmj.24.160.
18. Rolls, E. T. Chapter 1 - The Neuroscience of Emotional Disorders. In *Handbook of Clinical Neurology*; Heilman, K. M., Nadeau, S. E., Eds.; Elsevier, 2021; Vol. 183, pp. 1–26. https://doi.org/10.1016/B978-0-12-822290-4.00002-5.
19. Su, Q.; Liu, L.; Hua, T.; Gong, J.; Tian, H.; Yun, J.; Cai, W. Selective Disruption of Gray Matter Volume Covariance in Orbitofrontal Cortex Subregions among Patients with Functional Constipation. Sci. Rep. **2025**, *15*, 15440. https://doi.org/10.1038/s41598-025-00148-6.
20. Kim, Y. S.; Kim, N. Sex-Gender Differences in Irritable Bowel Syndrome. *J. Neurogastroenterol. Motil.* **2018**, *24* (4), 544–558. https://doi.org/10.5056/jnm18082.
21. Marano, G.; Traversi, G.; Pola, R.; Gasbarrini, A.; Gaetani, E.; Mazza, M. Irritable Bowel Syndrome: A Hallmark of Psychological Distress in Women? *Life* **2025**, *15* (2), 277. https://doi.org/10.3390/life15020277.
22. Fan, W.; Chen, Y.; Fang, X.; Zhu, L.; Fei, G.; Lu, J.; Li, X. Gender Differences in Gastrointestinal, Biopsychosocial and Healthcare-Seeking Behaviors in Chinese Patients with Irritable Bowel Syndrome Predominant with Diarrhea. *BMC Gastroenterol.* **2024**, *24*. https://doi.org/10.1186/s12876-024-03153-7.
23. Beckers, A. B.; Wilms, E.; Mujagic, Z.; Kajtár, B.; Csekő, K.; Weerts, Z. Z. R. M.; Vork, L.; Troost, F. J.; Kruimel, J. W.; Conchillo, J. M.; Helyes, Z.; Masclee, A. A. M.; Keszthelyi, D.; Jonkers, D. M. A. E. Age-Related Decrease in Abdominal Pain and Associated Structural- and Functional Mechanisms: An Exploratory Study in Healthy Individuals and Irritable Bowel Syndrome Patients. *Front. Pharmacol.* **2021**, *12*, 806002. https://doi.org/10.3389/fphar.2021.806002.
24. Algera, J. P.; Blomsten, A.; Khadija, M.; Verbeke, K.; Vanuytsel, T.; Tack, J.; Simrén, M.; Törnblom, H. Distinct Age-Related Characteristics in Patients with Irritable Bowel Syndrome: Patient

Reported Outcomes and Measures of Gut Physiology. *npj Gut and Liver* **2024**, *1*, 10. https://doi.org/10.1038/s44355-024-00010-y.
25. Seminowicz, D. A.; Labus, J. S.; Bueller, J. A.; Tillisch, K.; Naliboff, B. D.; Bushnell, M. C.; Mayer, E. A. Regional Gray Matter Density Changes in Brains of Patients with Irritable Bowel Syndrome. *Gastroenterology* **2010**, *139* (1), 48–57. https://doi.org/10.1053/j.gastro.2010.03.049.
26. Voß, U.; Lewerenz, A.; Nieber, K. Treatment of Irritable Bowel Syndrome: Sex and Gender Specific Aspects. In *Sex and Gender Differences in Pharmacology*; Regitz-Zagrosek, V., Ed.; Springer Berlin Heidelberg: Berlin, Heidelberg, **2012**; pp. 473–498. https://doi.org/10.1007/978-3-642-30726-3.
27. Camilleri, M. Diagnosis and Treatment of Irritable Bowel Syndrome: A Review. *JAMA* **2021**, *325* (9), 865–877. https://doi.org/10.1001/jama.2020.22532.
28. Tang, Y.-R.; Yang, W.-W.; Liang, M.-L.; Xu, X.-Y.; Wang, M.-F.; Lin, L. Age-Related Symptom and Life Quality Changes in Women with Irritable Bowel Syndrome. *World J. Gastroenterol.* **2012**, *18* (48), 7175–7183. https://doi.org/10.3748/wjg.v18.i48.7175.
29. Yang, P.-L.; Kamp, K. J.; Burr, R. L.; Tang, H.-Y. (Jean); Dobra, A.; Shulman, R. J.; Heitkemper, M. M. Age Differences in Core Symptoms and Symptom Relationships in Patients with Irritable Bowel Syndrome: A Network Analysis. *The American Journal of Gastroenterology* **2023**, *118* (9), 1648–1655. https://doi.org/10.14309/ajg.0000000000002280.

Author

Anna Chia is currently attending Anglo-Chinese School (Independent) in Singapore. She is interested in pathophysiology and neuroscience. She aspires to pursue a career in the medical profession.

DOI: 10.36838/IJHSR87.96

IJHSR
ijhighschoolresearch.org
REVIEW ARTICLE

Capability of Dielectric Elastomer Actuators to Replace Natural Muscle

Advait Swaminathan

Singapore American School, 40 Woodlands Street 41, Singapore, 738547, Singapore; advait.swaminathan@gmail.com

ABSTRACT: From an engineering perspective, natural muscle is a remarkable actuator. Its properties, such as high actuation frequency, rapid response time, and lasting durability, have prompted research into artificial muscles that mimic the function of natural muscle. A promising candidate for an artificial muscle involves sandwiching a dielectric elastomer between two compliant electrodes. This assembly achieves large strains under an applied voltage and is known as a Dielectric Elastomer Actuator (DEA). DEAs have demonstrated exceptional performance in tests for actuation strain, efficiency, work density, modulus, and response time, making them a popular material for applications in artificial muscles. However, it remains unclear whether these performance metrics are sufficient to warrant their use as artificial muscles. Here, we evaluate the feasibility of DEA-based artificial muscles by comparing their metrics to those of natural muscle. We found that DEAs surpassed natural muscles at individual parameters, but they are still not capable of fully replacing natural muscles from a kinetic and dynamic standpoint, as there are numerous other functions of muscles that DEAs are not capable of accomplishing yet.

KEYWORDS: Biomedical Engineering, Biomechanics, Artificial Muscles, Dielectric Elastomer Actuators, Electroactive Polymer.

Introduction

Natural muscles possess exceptional mechanical capabilities such as a high force-to-weight ratio, resistance to deterioration, long stroke length, rapid response time, and high work densities.[1-3] Those properties not only allow muscles to perform complex functions but also enable them to do so reliably for years. Replicating this balance of power, efficiency, and longevity has become increasingly important in today's context of wearable robotics, biomedical prosthetics, and human–machine interfaces, where soft, lifelike actuation is essential. Such remarkable capabilities of natural muscles have long inspired scientists to develop artificial muscles that can mimic, or even replace, natural muscles.

Those efforts first came to fruition in the 18th century, when the Italian scientist Alessandro Volta reported an observation made by the scientist Felice Fontana: Leyden jars, the first version of a capacitor, exhibited a change in volume under electrification.[4-6] Later, demonstrated that a rubber band responds with a change in elongation when subject to an electric field.[7] This was the first ever introduction of an Electroactive Polymer (EAP) – a material which responds to electrical stimulation by changing size or shape.[8] In 1899, Sacerdote *et al.* determined a relationship between the electric field activation and strain response.[9] The invention of a piezoelectric polymer came in 1925, when Eguchi *et al.* experimented with carnauba wax, beeswax, and rosin, determining that they expanded when a DC bias field was applied across them.[10] These polymers exhibit two distinct behaviors. When a stress is applied, the material could become polarized in the direct piezoelectric effect, while when an electric field is applied, a strain could occur in the indirect piezoelectric effect. These effects are inherently reversible, making them useful mechanisms for designing artificial muscles that require multiple rapid actuations.[11] Since then, significant research has been made into the use of EAPs as artificial muscles.[12-16]

In general, EAPs can be divided into two main groups: ionic-based and field-based.[17] In an ionic EAP, a conductive polymeric matrix that facilitates ion transport is subjected to an electric field. This causes ion transport across the polymer, which corresponds to a shape change. Because the transport of ions can be done under a small potential difference, EAPs can operate under low voltages of around 1-2 V, and upon actuation, they tend to bend instead of actuating linearly. Examples include carbon nanotubes, Ionic Polymer-Metal Composites (IPMCs), ionic gels, and conductive polymers. In a field-based EAP, the deformation of a polymer relies on charge interactions in the presence of an electric field. These include polymer electrets, ferroelectric polymers, and dielectric elastomers (DEs). In all these materials, Coulombic forces drive the actuation, typically requiring high voltages on the order of 100 V/pm.[5] However, because of their polymeric nature, such conductors can undergo large deformation under an applied load.

Their energy density, defined as the area underneath the stress-strain curve, can be enormous. For example, the theoretical energy density of pre-stretched VHB 4910, 3M's acrylic elastomer, has an energy density of 3.4 MJ/m^3, significantly higher than that of skeletal muscle at 0.07 MJ/m^3.[18] They can be operated in a wider variety of environments due to fewer constraints.[8] Their ability to mimic biological muscle with large actuation strains and vibration dampening has earned them the name 'artificial muscles'.[13]

© 2026 Terra Science and Education

DOI: 10.36838/IJHSR87.105

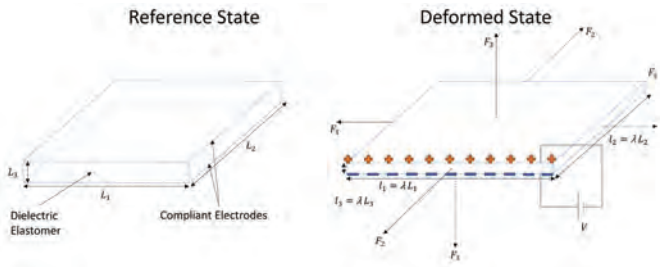

Figure 1: Reference and deformed state of a Dielectric Elastomer Actuator. Applying Voltage V compresses the elastomer in thickness and expands it in-plane, creating a stretch ratio of λ.

Of all field-based actuators, Dielectric Elastomer Actuators (DEAs) have emerged as the standout candidate for use as artificial muscles. In its simplest configuration, a DEA is a dielectric elastomer sandwiched between two compliant electrodes. A voltage is applied across the electrodes. This causes a compression in the thickness direction because of the attraction between the oppositely charged plates. Moreover, the actuator undergoes planar expansion due to the incompressibility of the elastomer. DEAs outperform natural muscle on multiple principal parameters. For example, DEAs can achieve a maximum actuation strain of 503% compared to 40% in natural muscle. DEAs also have a work density of 3.4 kJ/m^3 compared to 0.04 kJ/m^3 in natural muscle.[19] Moreover, the efficiency of a DEA can reach up to 90%, while the average efficiency of natural muscle is around 40%.[20]

So far, researchers have explored the use of DEAs as a variety of artificial muscles. Eckerle *et al.* have created a biologically inspired hexapedal robot that walks using DEA actuations.[21] Wu *et al.* have generated prototypes of a functioning artificial heart that pumps blood using DEA actuation.[22] Cao *et al.* have devised a prototype for a three-segment leg that extends and contracts using DEA actuation.[23] Liu *et al.* designed a prototype for a bicep muscle using a pre-stretched, spindle-shaped DEA to actuate the contraction.[24] A fish robot that is capable of swimming in all four directions was created by Shintake *et al.* They sandwiched multiple silicone DEAs together to create a large deformation for minimal voltages.[25] Carpi *et al.* created a design for contractions of an eye for a humanoid robot using buckling DEA structures.[26]

These diverse demonstrations, ranging from bioinspired locomotion to cardiac and ocular actuation, show that DEA research now bridges disciplines like materials science, robotics, and biomedical engineering and is central to developing next-generation soft machines and prosthetics. However, the performance of these prototypes remains constrained by differences in fabrication methods, material composition, and scaling behavior, making systematic comparison essential. Thus, are DEAs viable as actuators in artificial muscles, or is there significant ground to make up? This paper compares the important parameters for existing DEA designs and evaluates their feasibility in comparison to natural muscle. Section 2 will introduce the mechanism behind a DEA and the Physics involved as well. Section 3 describes some of the most used materials in DEAs and their various advantages and disadvantages. Section 4 analyzes 5 prominent parameters for natural muscle and DEAs in detail and evaluates whether, for that certain parameter, DEAs can replace natural muscle. Section 5 discusses the findings and collates the data collected into figures. It also talks about future research opportunities and some existing limitations of DEAs. Section 6 concludes the findings of the paper and summarizes the prominent ideas mentioned in this paper. The central research question guiding this study is: to what extent can dielectric elastomer actuators match or surpass the mechanical efficiency, strain capacity, and energy density of natural muscles while remaining safe and practical for real-world artificial muscle applications?

Discussion

We begin by reviewing the mechanics underlying DEAs.[27-29] Referring to Figure 1, consider a DEA of dimensions L_1, L_2, L_3 in the reference state. Because the DEA is highly deformable, two states are used to define its geometry. In the deformed state, the DEA has dimensions l_1, l_2, l_3. Corresponding to each deformation, we define the three principal stretches as $\lambda_1=l_1/L_1$, $\lambda_2=l_2/L_2$, and $\lambda_3=l_3/L_3$. To capture the electromechanical coupling, we look at the change in energy associated with actuating the DEA. In the deformed state, we represent forces on the DEA responsible for changing its dimensions l_1, l_2, l_3 as F_1, F_2, F_3 respectively. We denote the electric charge by Q, and the voltage by V, such that the electric field is given by: $E=V/L_3$. Recall that the work done (W) by a force, F in displacing an object a distance, x is given by:

$$W = \int F dx. \tag{1}$$

Consequently, when a DEA is actuated, the increment of mechanical work done (dW_m) by forces over infinitesimally small displacements dl_1, dl_2, dl_3 is given by:

$$dW_m = F_1 dl_1 + F_2 dl_2 + F_3 dl_3. \tag{2}$$

Similarly, the electrical work done dW_E done by the voltage V as an incremental charge dQ flows through it is given by:

$$dW_E = V dQ. \tag{3}$$

Under thermodynamic equilibrium, the total change in energy of the system dU, is equal to the work done by the mechanical and electrical forces:

$$dU = dW_m + dW_E. \tag{4}$$

Consequently, the total change in energy of the system can be represented using its mechanical and electrical contributions as:

$$dU = F_1 dl_1 + F_2 dl_2 + F dl_3 + V dQ. \tag{5}$$

We next convert all quantities in equation (6) quantities in the reference state. The stretches in each state relate to the lengths in the deformed state and reference state (Figure 2). Substituting $dl_i=L_i\lambda_i$ gives the total energy as:

$$dU = F_1 L_1 d\lambda_1 + F_2 L_2 d\lambda_2 + F_3 L_3 d\lambda_3 + V dQ. \tag{6}$$

Define the energy density (energy per unit reference volume) as $\psi = U/(L_1 L_2 L_3)$. Taking its differential, the variation of energy density can be written as:

$$d\psi = s_1 d\lambda_1 + s_2 d\lambda_2 + s_3 d\lambda_3 + E dD. \quad (7)$$

where s_1, s_2, s_3 are the three Cauchy normal stresses and are given by $s_1=F_1/A_1$, $s_2=F_2/A_2$, $s_3=F_3/A_3$, and D is the electric field displacement and is given by $D=Q/L_1L_2$.

When the energy per unit volume is prescribed, its variation is given by:

$$d\psi = \frac{\partial\psi}{\partial\lambda_1} d\lambda_1 + \frac{\partial\psi}{\partial\lambda_2} d\lambda_2 + \frac{\partial\psi}{\partial\lambda_3} d\lambda_3 + \frac{\partial\psi}{\partial D} dQ. \quad (8)$$

Equations (7) and (8) give the equations of state of the dielectric elastomer under equilibrium:

$$s_1 = \frac{\partial\psi}{\partial\lambda_1}, \quad (9a)$$

$$s_2 = \frac{\partial\psi}{\partial\lambda_1}, \quad (9b)$$

$$s_3 = \frac{\partial\psi}{\partial\lambda_3}, \quad (9c)$$

$$E = \frac{\partial\psi}{\partial D}. \quad (9d)$$

■ Materials Used in a DEA

As the primary component in DEAs, the material chosen for the Dielectric Elastomer significantly changes the performance of the DEA. Materials optimal for use as a DE tend to have low elastic modulus, high dielectric constants, low viscosity, and high electrical breakdown strength. These materials are divided into three predominant categories: polyurethanes (PU), acrylic, and silicone elastomers.

Out of the three, the most commonly used material tends to be acrylic elastomers, specifically 3M's acrylic elastomers VHB 4905 and 4910. This is because they tend to be inexpensive and commercially available. Recently, a DEA that integrated a 3M VHB acrylic elastomer generated a maximum strain of over 380%.[30] However, they tend to have slower response times because of the viscoelastic nonlinearities in the elastomer.

In contrast to the acrylic elastomers, silicone elastomers tend to have lower actuation strains. Since they have lower dielectric constants, they require large voltages to achieve sizable actuation strains. Chen *et al.* explored this phenomenon in a comparison between two rubber-based actuators, which use THERABAND YELLOW 11726 and OPPO BAND GREEN 8003, made of styrenic and natural rubber, respectively, and the acrylic elastomer VHB 4905 by 3M.[31] They found that the acrylic elastomers had mechanical dissipation due to viscoelastic response, while the rubber actuators had dissipation due to viscoplasticity. They also found that the acrylic elastomer is much more deformable than the rubber actuators, with maximum strains of λ = 7.4

DEAs made of a polyurethane material tend to have a higher dielectric constant, resulting in a higher force output at lower electric fields. However, their higher elastic modulus tends to have lower actuation strains, which holds them back from being used widely.[32]

The other important component of the DEA, for which material choice is pivotal, is the compliant electrode. A compliant electrode is a thin material that conducts electricity and is able to synchronously follow the large strains of the elastomer membrane, without generating an opposing strain or losing conductivity.[32] These compliant electrodes must be conductive and soft at the same time, while sustaining large strains and maintaining adhesion to the DE. The most common materials used for compliant electrodes tend to be metallic thin film, graphite and carbon powder, and carbon grease.[33,34] Although metals have lower resistance than carbon, they are rarely used because the particles of metal are bigger than those of Carbon and hence offer inferior contact with the DE.[35] Additionally, their powders tend to form an insulating oxidative layer on their surface when exposed to air.[36] However, Toth *et al.* and Jung *et al.* have reported DEAs created with compliant electrodes made of silver grease.[37,38]

Carbon and Graphite Powders are made of loose carbon particles directly applied onto the DE and hence don't contribute to the stiffness of the DE, allowing larger actuations. However, they tend to be difficult to handle because of their sensitivity to static charges. Additionally, these particles are not bonded together and tend to detach from the membrane over large strains. For the same reason, they could have a limited lifespan.[34] This is why they are generally found in combination with an adhesive acrylic elastomer such as 3M's VHB 4910. Because these layers are inherently sticky, they bind the individual powder particles to the elastomer, significantly reducing detachment, even over large strains.[34] Schlaak's group did use Carbon Powder paired with a Silicone Elastomer in their multilayered configuration.[39]

As a substitute for an adhesive acrylic elastomer, another way of solving the adhesion problem is binding the particles into one viscous matrix in the form of a grease. Carbon Grease electrodes are the most commonly used in the industry since they are cheap, easy to apply onto membranes, and have great adhesion capabilities.[32] They also provide great conductivity under large strains. However, their lifespan is relatively short due to drying of the grease or diffusion into the DE. This could cause short-circuits or swelling of the DE material. Additionally, this viscous material is not rigid and could flow due to gravity, especially affecting DEAs stored vertically.[34]

■ Parameters

Strain:

The first metric we will consider for comparing DEAs to natural muscle is elongation strain. This is defined as the deformation of a material from stress, or simply a ratio of the change in length to the original length.[40] For natural muscles, the typical strain is about 20%, while the maximum achieved strain with a pre-stretch for a DEA is 380%.[4] This was achieved under an applied electric field of approximately 65 MV/m using a biaxially pre-stretched (≈5×) VHB 4910 acrylic elastomer from 3M, as reported by Goh *et al.* Pre-stretching is the process of stretching out the Dielectric Elastomer uniaxially or biaxially using either a mechanical load or an interpenetrating network.[18,41] Pre-stretching the DE significantly improves actuation strain. Kofod *et al.* found that pre-stretching in the width direction by a factor of 5 increased the strain by approximately 100% for all loads.[42] It is important to note, however, that this is only true when endplane stress is not present.[42] As they increased pre-stretch from 1 to 5, actuation strain also

DOI: 10.36838/IJHSR87.105

increased, but only up to a point, after which it fell. This point is known as the 'optimum load region'. The typical strain for a DEA tends to be around 25%, which is higher than that of natural muscles at 20%.[2] Considering that pre-stretching can improve actuation strain, it is possible that in the future, even larger strains can be generated as pre-stretching technology improves. Because large pre-stretches thin the film and reduce its cross-sectional area, they also lower force output, indicating a trade-off between achieving high strain and maintaining mechanical strength. Optimizing this balance suggests that future DEA designs should combine moderate pre-stretch ratios with multilayer stacking or frame-supported geometries to achieve large deformations without compromising load-bearing capability. Thus, DEAs already demonstrate sufficient actuation strain to serve as artificial muscles in systems where flexibility and range of motion are prioritized.

Efficiency:

The second metric we will consider is efficiency, also known as the maximal energy coupling efficiency factor (k^2). We define efficiency as the ratio of output mechanical work to the input electrical energy.[43] Traditionally, DEAs have been modelled based on continuum mechanics. These models specifically account for large material deformations, viscoelasticity, and non-linear elasticity.[43] However, to model DEA efficiency, these models also need to account for another parameter – electrical losses. Using this theory, a study by Lochmatter *et al*. found that, in optimal conditions, DEA strip actuators could reach efficiencies of up to 90%, but electrical losses can rapidly lower this maximum.[44] They also pointed out that there was a significant difference between the theoretical and experimental efficiency of DEAs. Another study was conducted on diamond actuators using VHB's acrylic elastomer, operating under a constant voltage. It was observed that the actuator had an efficiency of only 18%, significantly lower than what was theorized. This was attributed to viscoelasticity and current leakage.[45] A study by Bigue *et al*. investigated the efficiency of Conical DEAs and multicell DEA rotary motors. They found that at lower electric fields, efficiency diminished by ~35% for acrylic cone actuators. However, at higher voltages, the average electromechanical efficiency was ~85%.[43] Madden *et al*. found that an average efficiency of 60% can be achieved with integrated energy recovery circuitry in the actuator.[46] In these studies, efficiencies above 80% were generally obtained for acrylic DEAs actuated around 60 MV/m and low frequencies (< 1 Hz), conditions that minimize viscoelastic losses and dielectric heating. Across all the actuators tested with various materials, it was found that the best efficiency was found at maximal electric fields of around 60 KV/mm.[43] Additionally, it is important to note that actuation frequency also has an effect on DEA efficiency. Generally, an increased actuation frequency results in a lower DEA efficiency.[47] Thus, it is clear that DEA efficiency is heavily dependent on the electric field applied, viscoelasticity, and current leakage. In comparison to the efficiency of a DEA, the average efficiency is ~30% for mammalian muscle, significantly lower than that of the aforementioned DEAs.[4] As technology is able to reduce current leakages and viscoelasticity in the future, DEA efficiency could improve significantly. At present, these efficiency levels already make DEAs promising for soft robotic systems and artificial limbs, where energy conservation and rapid actuation are critical feasibility factors. However, sustaining these high efficiencies under continuous operation would require improved insulation and heat management to prevent dielectric breakdown and ensure safe operation in wearable or biomedical devices. In addition, integrating energy-recovery circuitry and flexible encapsulation without increasing weight remains a key engineering challenge for deploying DEAs in portable, battery-powered systems.

Young's Modulus:

Next, we will consider Young's modulus. The modulus, Y is defined as the stress per unit strain and is a measure of the stiffness of a material. We will later use the shear modulus to characterize the mechanical behavior of the DEA, which relates to the Young's modulus as: $Y = 3\mu$, because the material is incompressible. For small strains, the Young's modulus is given by the formula $Y = 3\rho RT / M_C$ where Y is the modulus, ρ is the density of the elastomer, R is the gas constant, T is the absolute temperature, and MC is the average molecular weight of chain segments between crosslinking sites.[48] Using this formula, Hu *et al*. devised a DEA using an elastomer with a variable Young's Modulus. Through thermal treatment, they induced Dies-Alder (DA) reactions within the elastomer, either increasing or decreasing polymer chain segment length.[48] They chose this method specifically because it was reversible. Their design was able to create variable moduli between 0.17 and 0.52 MPa.[48] For natural muscles, the typical Young's Modulus is around 10-60 MPa.[46] Thus, with a significantly lower modulus, existing DE materials are capable of being used in DEAs to simulate natural muscle. However, it is important to note that Hu *et al.*'s study only generated a maximum strain of 30%.[48] This is much lower than many other designs, including those cited in the strain section. Non-variable-modulus DEAs can reach strains up to 380 % but with slightly higher moduli around 0.6–0.7 MPa, highlighting a trade-off between compliance and strength. Designs that spatially vary stiffness, using multilayer or gradient-modulus architectures, could maintain soft contact at the surface while reinforcing internal layers to generate greater specific forces. Such hybrid stiffness tailoring is a promising route toward actuators that combine comfort and high performance.

Response Time:

Next, we discuss response time–one of the greatest features of a DEA is its rapid response time. It is interesting to see that pre-stretching the DEA has no influence on its response time, and thus, response time will never be a limiting factor for maximizing strain.[49] In a study conducted by Winter *et al*., it was found that the average response time across various muscles in the body for men and women ranged from ~160 - 250 ms among young adults.[50] By solving the coupled boundary value problem of an axisymmetric DEA, found that the delay time (t_d) is given by:

$$t_d = 1.143R_0\sqrt{\frac{\rho}{\mu}} \quad (10a)$$

while response time (t_r) is given by:

$$t_r = 1.886R_0\sqrt{\frac{\rho}{\mu}} \quad (10b)$$

where ρ is the mass density of the elastomer in kg/m^3, μ is the shear modulus in Pascals (Pa), which represents the material's stiffness. We plot the response time equation (10b) taken from Jia *et al.* in Figure 2.[49] As the modulus of the DEA increases, the response time decreases. The response time is larger when the radius of the DEA is larger. As cited in the Young's Modulus section, the modulus of a DEA is on the order of 1 MPa. Since this modulus is still well below that of most natural muscles, there remains significant potential to lower the response time by increasing the modulus of the DEA.

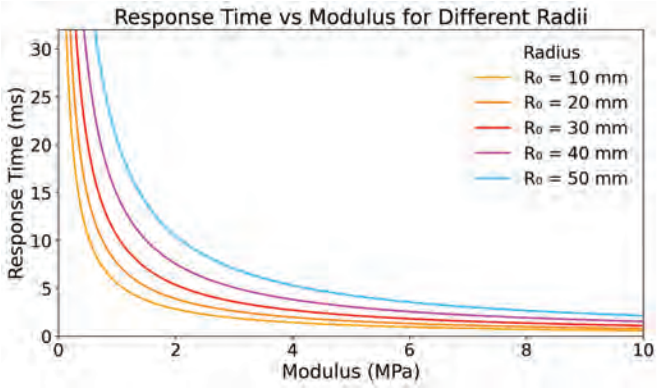

Figure 2: Response time as a function of elastomer stiffness (Young's modulus) for different actuator radii. Data adapted from Jia *et al.*[49] The model assumes a silicone-based DEA with a modulus of approximately 1 megapascal, an initial actuator radius of 50 millimeters, and an applied electric field of 30 megavolts per meter. Curves represent theoretical predictions for low-load, low-frequency operation.

Plugging in representative numbers, the modulus of the elastomer is $\mu = 10^6\ N/m^2$. For a DEA with a 50mm radius, the maximum response time is ~21.2 ms, which is significantly faster than natural muscle.[49] Such rapid actuation demonstrates the feasibility of DEAs for real-time control in soft robots and prosthetic devices. To translate this dynamic advantage into practical systems, minimizing electrode resistance and optimizing film thickness can sustain fast actuation speeds across varying loads, enabling smoother, more responsive motion control. However, under heavy loads or high-frequency operation, viscoelastic damping and heat buildup can slow performance, indicating that response optimization must be integrated with thermal management.

Energy Density:

Energy density in a muscle can be defined as the output work generated by the muscle upon excitation, normalized to the mass or volume of the muscle.[51] Looking back into the past, with the development of gunpowder in the 1400s, higher energy densities became available. In the 1670s, a Dutch Mathematician and Scientist designed a linear actuator where the combustion of gunpowder caused a piston to move inside the cylinder. According to Huygens' calculations, 1 pound of gunpowder could raise an object weighing 3000 pounds by approximately 30 feet, corresponding to a gunpowder specific energy density of 0.27 kJ/kg.[51] These initial formulations of actuator designs with respect to energy density have birthed DEAs with large energy densities of up to 3.4 MJ/m^3.

The maximum energy density for a natural muscle is ~ 0.15 Mj/m^3, significantly less than that of the DEA.[52] This is also true for the typical energy density of DEAs and natural muscle, at 0.15 Mj/m^3 and 0.008 Mj/m^3.[54] The highest reported DEA values correspond to acrylic films (VHB 4910) operated at 60–70 MV/m and 3–5× pre-stretch, conditions that also push close to dielectric breakdown limits. We now apply our theoretical framework to predict the theoretical energy density of a dielectric elastomer. Pelrine *et al.* provided an estimate by considering the Maxwell stress incurred on a DEA.[18] We now rederive their result using the non-linear continuum framework, which uses stresses defined in the current (deformed) configuration. The total differential of energy density can be expressed as:

$$d\psi = (\sigma_1 l_2 l_3 + l_3 l_2 ED)dl_1 + (\sigma_2 l_3 l_1 + l_3 l_1 ED)dl_2 + \sigma_3 l_1 l_2 dl_3 + El_1 l_2 l_3 dD \quad (11)$$

where $\sigma_1 = F_1/l_2 l_3$, $\sigma_2 = F_2/l_1 l_3$, $\sigma_3 = F_3/l_2 l_1$ are the true stresses acting in the deformed direction in the deformed state, and D is the electric field displacement as before. Under equilibrium, equation (11) yields the following constitutive relations in the deformed state:

$$\sigma_1 = \frac{\partial\psi}{\partial\lambda_1}\frac{1}{\lambda_2\lambda_3} - ED, \quad (12a)$$

$$\sigma_2 = \frac{\partial\psi}{\partial\lambda_2}\frac{1}{\lambda_1\lambda_3} - ED, \quad (12b)$$

$$\sigma_2 = \frac{\partial\psi}{\partial\lambda_3}\frac{1}{\lambda_1\lambda_2} - ED, \quad (12c)$$

$$E = \frac{\partial\psi}{\lambda_1\lambda_2\lambda_3\partial D}. \quad (12d)$$

Consider the ideal dielectric elastomer model given by Suo *et al.*, which combines a mechanical strain energy term and an electrostatic energy term: [27]

$$W = \mu/2\,(\lambda_1^{\ 2} + \lambda_2^{\ 2} + \lambda_1^{-2}\lambda_2^{-2} - 3) + 1/2D^2/E \quad (13)$$

In this equation, μ is the shear modulus of the elastomer and ϵ is its permittivity. The first term represents the entropic elastic energy stored in the polymer network, while the second corresponds to the electrostatic energy arising from charge accumulation.

Following the analysis from Suo *et al.*, under an applied electric field, the in-plane stretches are equal, $\lambda_1 = \lambda_2 = \lambda$ and incompressibility gives that $\lambda_3 = \lambda^{-2}$.[27] Applying equations (11a-d) and setting the external forces to zero gives:

$$\epsilon\Phi^2/(H\mu) = \lambda^{-2} - \lambda^{-8} \quad (14)$$

Equation (14) shows the non-linear relationship between the applied electric field E, the material's shear modulus μ , and its permittivity ϵ. Solving this for the maximum physically stable configuration gives a maximum stretch of λ_{max} =1.3. We now use this to calculate the maximum energy density. The general form of energy density can be written as:

DOI: 10.36838/IJHSR87.105

$$W = \mu/2\,(2\lambda_{max}^{\ 2} + \lambda_{max}^{\ -4} - 3) + 1/2\lambda_{max}^{\ 2}\epsilon^2(\phi/H) \quad (15)$$

Isolating Φ in equation (14), we get:

$$\Phi = \sqrt{\frac{(\lambda_{max}^{\ -2} - \lambda_{max}^{\ -6})(H\mu)}{\epsilon}} \quad (16)$$

Plugging equation (15) into equation (14), we get:

$$W_{max} = \mu/2\,(2\lambda_{max}^{\ 2} + \lambda_{max}^{\ -4} - 3) + (\mu\epsilon/2H)(1 - \lambda_{max}^{\ -6}). \quad (17)$$

Equation (17) gives the maximum amount of energy stored in a DEA per unit volume. Under small stretches, the the second term dominates and the maximum energy density scales as: $W_{max} \sim 3\mu\epsilon/H(\lambda_{max}-1)$. At larger stretches, the entropic term dominates and maximum energy density scales as $W_{max} \sim \mu\lambda^2_{max}$.

These relationships explain why thinner, highly pre-stretched films achieve greater energy densities but also face greater failure risk. To leverage this capability safely, future DEA designs should pair high-permittivity fillers with multilayer configurations that distribute field strength, reducing voltage requirements without sacrificing energy density. This strategy would make DEAs more practical for compact, power-dense actuation in wearable robotics, artificial limbs, and small autonomous systems, where natural muscle is limited by mass and efficiency.

Compiled Data and Discussion

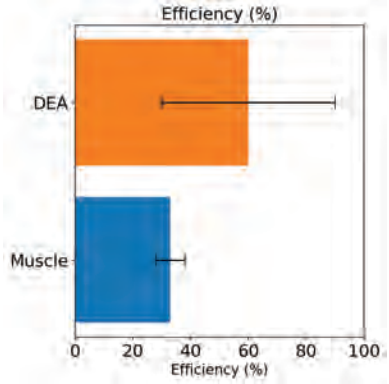

Figure 3: Comparison of efficiency between DEAs and Natural Muscle. Data extracted from [4,46]

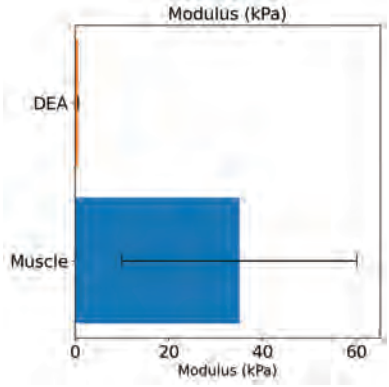

Figure 4: Comparison of energy density between DEAs and Natural Muscle. Data extracted from [52,54]

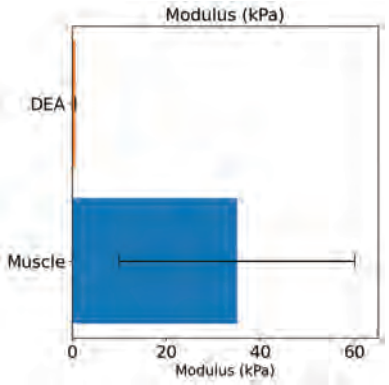

Figure 5: Comparison of elastic modulus between DEAs and Natural Muscle. Data extracted from [46,48]

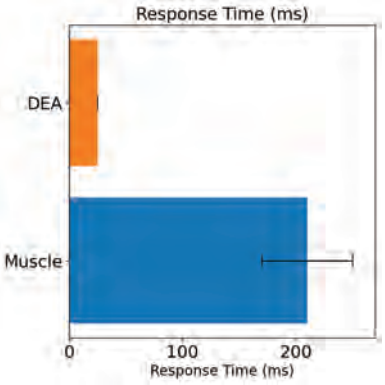

Figure 6: Comparison of response time between DEAs and natural muscle. Data extracted from [49,50]

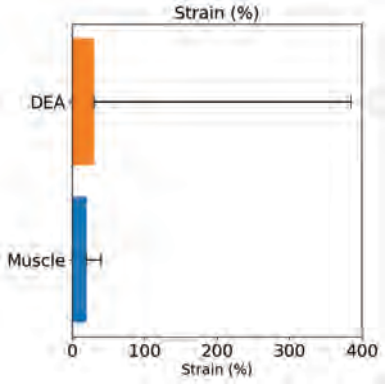

Figure 7: Comparison of strain between DEAs and natural muscle. Data extracted from [2,4]

We have summarized all the data we have collected in Figures 3-7. The horizontal bars displayed in Figures 3-7 are not statistical error bars but visual representations of the wide range of reported values for each parameter across multiple studies. They illustrate the variability observed in parameters such as efficiency, strain, and energy density rather than measurement uncertainty. The use of a logarithmic scale in some plots highlights that these ranges can span several orders of magnitude, underscoring the substantial variance in performance metrics due to differences in experimental setup, material formulation, and actuation conditions. In cases where only one-sided bars are shown, the asymmetry reflects that published data often

specify only an upper or lower bound for a given parameter, rather than a symmetric range around a mean value.

DEAs outperform natural muscles on all the parameters compared in this paper. They have significantly larger maximum and average strains, resulting in larger overall deformations. DEAs also exhibit faster response times, often on the order of milliseconds, allowing for faster actuation in dynamic environments in artificial muscles.

In terms of energy density, DEAs were able to reach 3.4 MJ/m^3, significantly higher than that of natural muscle, making them suitable for compact and power-dense systems. DEAs are also more efficient, converting more electrical energy into mechanical work, and have lower energy loss. This is critical to battery-powered, long-duration applications.

Finally, DEAs also had a markedly lower modulus than natural muscle, making them softer and more compliant. It is important to note, however, that even though the lower modulus is advantageous, the mechanical design must compensate for this. A lower modulus results in a lower force output for the DEA and could limit load-bearing capabilities. Thus, design choices such as pre-stretching or stacking need to be implemented along with the low-modulus elastomer.[55]

In addition, DEAs are difficult to isolate as independent components. They often require complex driving electronics, sensors, and high-voltage power supplies to function correctly. Holding the pre-stretch also necessitates a mechanical frame or fixture, which increases bulk and reduces space efficiency in compact robotic systems.

We plot the average quantity of each metric with the error bars showing the maximum and minimum values for each source we have found. When considering a single parameter at once, it is clear that DEAs are capable of replacing natural muscle as actuators.

It is important to note, however, that these results also highlight several limitations within current DEA research itself. Reported values across studies often vary widely due to non-standardized testing conditions, differing electrode materials, and inconsistent definitions of strain, energy density, or efficiency. Many studies measure performance under idealized laboratory conditions rather than in realistic, load-bearing scenarios, which makes direct comparison difficult. In some cases, authors selectively report peak values rather than averages or steady-state behavior, leading to optimistic bias in published data. Additionally, differences in measurement methodologies – such as whether strain is defined in area or length terms, or whether efficiency accounts for dielectric heating – introduce further uncertainty. These inconsistencies underscore the need for standardized benchmarking protocols in DEA research to ensure accurate cross-study comparison and reproducibility.

At the same time, these variations reveal important tradeoffs between actuation strain, energy density, response speed, and durability – no single DEA formulation currently optimizes all parameters simultaneously. Broader implications of these tradeoffs extend to the design of next-generation soft robotic systems, where DEAs may be tailored for specific functions such as wearable assistive devices, haptic interfaces, and bioinspired locomotion. Continued advances in materials processing and low-voltage actuation are likely to make DEAs increasingly viable for practical applications in prosthetics and soft exoskeletons.[18]

These parameters also cannot be considered in isolation and must be evaluated in the context of how the actuator will be used. Natural muscles have numerous other functions in the body other than mechanical movements. These include stabilizing joints, maintaining body posture, and generating heat through contraction.[51]

Existing DEA designs will rapidly develop towards optimizing specific parameters in their design. For example, an artificial muscle DEA could have the required properties, such as energy density or strain, to replace a human bicep from a mechanical standpoint. However, to replace it completely, the DEA's design needs to match the bicep's design from a kinematic and dynamic standpoint for the actuator to be optimal.

Additionally, DEAs use large electric fields to create large strains with a rapid response time. Hu *et al.*'s actuator used an electric field of 65 MV/m, and Bigue *et al.* found that the maximum efficiency for an actuator was at 60 MV/m.[43,48] However, it is important to note that such high electric fields are non-native to the human body. Dawson *et al.* suggested that the average electric field present in subcutaneous fat is only ~25 kV/m over a 100 ns duration.[56] Although it is under the assumption that the actuator will be designed to isolate the electric fields safely, these high electric fields are still dangerous and could lead to cardiac fibrillation.[56]

Such large electric fields are used because current manufacturing methods establish a limit on the minimum thickness of elastomers that can be consistently fabricated. Progress has been made towards creating elastomers suited to lower electric fields by creating processing methods that are more suitable for producing uniform dielectric elastomers. The Langmuir-Blodgett method ensures that Carbon Nanotubes are placed more uniformly throughout each layer. Silicone elastomers have relatively low dielectric permittivity, and hence, Carbon Nanotubes are used to improve it in order to reduce the electric field required for actuation.[57] This could also be done by adding materials such as TiO_2, $BaTiO_3$, and Al_2O_3.[58-63]

However, this will likely be the major limiting factor to lowering voltages in the future because of fabrication defects such as bubbles and dust. Thus, more research needs to go towards developing methods to manufacture thin dielectric elastomers on the order of 5 μm consistently, without defects, to reduce the electric fields across the DEA. There have been alternative methods explored to reduce the electric field across a DEA. They can be multilayered, which increases the breakdown field strength. For example, Lotz. *et al.* stacked 50 actuating layers, each of 20 μm, on top of each other and created a DEA that can be actuated at only 600 V, significantly lower than those that have been mentioned in this paper.[64]

■ Conclusion

DEAs surpass natural muscle in several key performance parameters, including strain, energy density, efficiency, response time, and compliance. They have achieved maximum strains

DOI: 10.36838/IJHSR87.105

up to 380%, energy densities as high as 3.4 MJ/m^3, and efficiencies approaching 90%, all while maintaining lower moduli than natural muscle. These features enable them to produce large deformations rapidly and efficiently, making them promising candidates for artificial muscles. Pre-stretching, advanced material choices like acrylic and silicone elastomers, and design strategies such as multilayer stacking have further enhanced DEA capabilities. In summary, this paper finds that DEAs can equal or exceed the mechanical performance of natural muscle in isolated metrics, establishing them as one of the most capable soft-actuation systems currently available.

However, despite their strong performance, DEAs are not yet capable of fully replacing natural muscles from a kinetic and dynamic standpoint. Natural muscles serve additional roles such as stabilizing joints, maintaining posture, and generating heat – functions that DEAs do not currently replicate. Furthermore, the high electric fields required for DEA operation, often exceeding 60 MV/m, are not native to the human body and pose potential risks like cardiac fibrillation. In addition to electrical hazards, the risk of dielectric breakdown or arcing under high-field conditions can cause device failure or local tissue damage if not properly isolated. Thermal buildup from dielectric losses and current leakage also presents a safety concern in sustained or repetitive actuation cycles. While methods such as carbon nanotube doping and novel fabrication techniques aim to reduce actuation voltages, significant research is still needed to address these challenges and develop DEAs that can safely and comprehensively replicate muscle function. Achieving safe and low-voltage operation (e.g., below 10 MV/m) without compromising strain performance will be a defining threshold for biomedical feasibility.

Looking forward, research should focus on the development of high-permittivity, defect-free elastomers capable of achieving comparable strain at reduced electric fields, alongside improved electrode designs that enhance durability and biocompatibility for long-term operation exceeding one million actuation cycles. Parallel efforts should target the integration of closed-loop control systems with embedded sensing and feedback to emulate the adaptive, proprioceptive behavior of natural muscle. Meeting these milestones would mark a pivotal step toward translating DEAs from high-performance experimental prototypes to safe, reliable, and responsive artificial muscles for biomedical and robotic applications.

Acknowledgments

A big thank you to Sammy Hassan for mentoring me through the paper-writing process and introducing me to the field of Soft Robotics. I would also like to extend my gratitude to Plinio Zanini for guiding me through the paper revision.

References

1. Pelrine, R.; Chiba, S. *Review of Artificial Muscle Approaches*; SRI International Information, Telecommunications, and Automation Division 333 Ravenswood Avenue, Menlo Park, California, 1992.
2. Ariano, P.; Accardo, D.; Lombardi, M.; Bocchini, S.; Draghi, L.; De Nardo, L.; Fino, P. Polymeric Materials as Artificial Muscles: An Overview. *Journal of Applied Biomaterials & Functional Materials* **2015**, *13* (1), 1–9. https://doi.org/10.5301/jabfm.5000184.
3. Mirfakhrai, T.; Madden, J. D. W.; Baughman, R. H. Polymer Artificial Muscles. *Materials Today* **2007**, *10* (4), 30–38. https://doi.org/10.1016/s1369-7021(07)70048-2.
4. Volta, A. Lettere Inedite Di Alessandro Volta, 1835.
5. Romasanta, L. J.; Lopez-Manchado, M. A.; Verdejo, R. Increasing the Performance of Dielectric Elastomer Actuators: A Review from the Materials Perspective. *Progress in Polymer Science* **2015**, *51*, 188–211. https://doi.org/10.1016/j.progpolymsci.2015.08.002.
6. Carpi, F.; Bauer, S.; De Rossi, D. Stretching Dielectric Elastomer Performance. *Science* **2010**, *330* (6012), 1759–1761. https://doi.org/10.1126/science.1194773.
7. Roentgen, W. C. About the Changes in Shape and Volume of Dielectrics Caused by Electricity; Annalen Der Physik und Chemie, 1880; pp 771–786.
8. Bar-Cohen, Y. Electroactive Polymers: Current Capabilities and Challenges. In *SPIE Proceedings*; Bar-Cohen, Y., Ed.; SPIE: San Diego, CA, 2002; Vol. 4695, pp 1–7. https://doi.org/10.1117/12.475159.
9. Sacerdote, M. P. *Journal of Physics, 3rd Series* **1899**, *8*.
10. Eguchi, M. *Philosophical Magazine* **1925**, *49*.
11. Smith, M.; Kar-Narayan, S. Piezoelectric Polymers: Theory, Challenges and Opportunities. *International Materials Reviews* **2022**, *67* (1), 65–88. https://doi.org/10.1080/09506608.2021.1915935.
12. Zhenyi, M.; Scheinbeim, J. I.; Lee, J. W.; Newman, B. A. High Field Electrostrictive Response of Polymers. *J Polym Sci B Polym Phys* **1994**, *32* (16), 2721–2731. https://doi.org/10.1002/polb.1994.090321618.
13. Bar-Cohen, Y. Electroactive Polymers as Artificial Muscles: Capabilities, Potentials and Challenges. In *Robotics 2000*; American Society of Civil Engineers: Albuquerque, New Mexico, United States, 2000; pp 188–196. https://doi.org/10.1061/40476(299)24.
14. Kornbluh, R. D.; Pelrine, R.; Pei, Q.; Heydt, R.; Stanford, S.; Oh, S.; Eckerle, J. Electroelastomers: Applications of Dielectric Elastomer Transducers for Actuation, Generation, and Smart Structures. In *SPIE Proceedings*; McGowan, A.-M. R., Ed.; SPIE: San Diego, CA, 2002. https://doi.org/10.1117/12.475072.
15. Electroactive Polymers as Artificial Muscles: A Review. Journal of *Spacecraft and Rockets* **2024**. https://doi.org/10.2514/jsr.
16. Kornbluh, R.; Bashkin, J.; Pelrine, R.; Prahlad, H.; Chiba, S. Medical Applications of New Electroactive Polymer Artificial Muscles. *Seikei-Kakou* **2004**, *16* (10), 631–637. https://doi.org/10.4325/seikeikakou.16.631.
17. Qiu, Y.; Zhang, E.; Plamthottam, R.; Pei, Q. Dielectric Elastomer Artificial Muscle: Materials Innovations and Device Explorations. *Acc. Chem. Res.* **2019**, *52* (2), 316–325. https://doi.org/10.1021/acs.accounts.8b00516.
18. Pelrine, R.; Kornbluh, R.; Pei, Q.; Joseph, J. High-Speed Electrically Actuated Elastomers with Strain Greater Than 100%. *Science* **2000**, *287* (5454), 836–839. https://doi.org/10.1126/science.287.5454.836.
19. Goh, Y. F.; Akbari, S.; Khanh Vo, T. V.; Koh, S. J. A. Electrically-Induced Actuation of Acrylic-Based Dielectric Elastomers in Excess of 500% Strain. *Soft Robotics* **2018**, *5* (6), 675–684. https://doi.org/10.1089/soro.2017.0078.
20. Guo, Y.; Liu, L.; Liu, Y.; Leng, J. Review of Dielectric Elastomer Actuators and Their Applications in Soft Robots. *Advanced Intelligent Systems* **2021**, *3* (10). https://doi.org/10.1002/aisy.202000282.
21. Eckerle, J.; Stanford, S.; Marlow, J.; Schmidt, R.; Oh, S.; Low, T.; Shastri, S. V. Biologically Inspired Hexapedal Robot Using Field-Effect Electroactive Elastomer Artificial. In *SPIE Proceed-*

ings; McGowan, A.-M. R., Ed.; SPIE: Newport Beach, CA, 2001; Vol. 4332, pp 269–280. https://doi.org/10.1117/12.429666.
22. Wu, W.; Zhang, S.; Wu, Z.; Qin, S.; Li, F.; Song, T.; Cao, X.; Wang, Z. L.; Zhang, L. On the Understanding of Dielectric Elastomer and Its Application for All-Soft Artificial Heart. *Science Bulletin* **2021**, *66* (10), 981–990. https://doi.org/10.1016/j.scib.2020.12.033.
23. Cao, C.; Gao, X.; Conn, A. T. Towards Efficient Elastic Actuation in Bio-Inspired Robotics Using Dielectric Elastomer Artificial Muscles. *Smart Mater. Struct*. **2019**, *28* (9), 095015. https://doi.org/10.1088/1361-665x/ab326b.
24. Liu, L.; Zhang, C.; Luo, M.; Chen, X.; Li, D.; Chen, H. A Biologically Inspired Artificial Muscle Based on Fiber-Reinforced and Electropneumatic Dielectric Elastomers. *Smart Mater. Struct*. **2017**, *26* (8), 085018. https://doi.org/10.1088/1361-665x/aa723f.
25. Shintake, J.; Cacucciolo, V.; Shea, H.; Floreano, D. Soft Biomimetic Fish Robot Made of Dielectric Elastomer Actuators. *Soft Robotics* **2018**, *5* (4), 466–474. https://doi.org/10.1089/soro.2017.0062.
26. Carpi, F.; Fantoni, G.; Guerrini, P.; De Rossi, D. Buckling Dielectric Elastomer Actuators and Their Use as Motors for the Eyeballs of an Android Face. In *SPIE Proceedings*; Bar-Cohen, Y., Ed.; SPIE: San Diego, CA, 2006; Vol. 6168, p 61681A. https://doi.org/10.1117/12.655254.
27. Suo, Z. Theory of Dielectric Elastomers. *Acta Mechanica Solida Sinica* **2010**, *23* (6), 549–578. https://doi.org/10.1016/s0894-9166(11)60004-9.
28. Qian, J. Mechanics of Dielectric Elastomers: Materials, Structures, and Devices. *JZUS-A* **2016**, *17*, 1–21. https://doi.org/10.1631/jzus.a1500125.
29. Lu, T.; Ma, C.; Wang, T. Mechanics of Dielectric Elastomer Structures: A Review. *Extreme Mechanics Letters* **2020**, *38*, 100752. https://doi.org/10.1016/j.eml.2020.100752.
30. *Electroactive Polymer (EAP) Actuators as Artificial Muscles: Reality, Potential, and Challenges, Second Edition*; Bar-Cohen, Y., Ed.; SPIE: 1000 20th Street, Bellingham, WA 98227-0010 USA, 2004. https://doi.org/10.1117/3.547465.
31. Chen, Y.; Agostini, L.; Moretti, G.; Fontana, M.; Vertechy, R. Dielectric Elastomer Materials for Large-Strain Actuation and Energy Harvesting: A Comparison between Styrenic Rubber, Natural Rubber and Acrylic Elastomer. *Smart Mater. Struct.* **2019**, *28* (11), 114001. https://doi.org/10.1088/1361-665x/ab3b32.
32. Gu, G.-Y.; Zhu, J.; Zhu, L.-M.; Zhu, X. A Survey on Dielectric Elastomer Actuators for Soft Robots. *Bioinspir. Biomim*. **2017**, *12* (1), 011003. https://doi.org/10.1088/1748-3190/12/1/011003.
33. Carpi, F.; Chiarelli, P.; Mazzoldi, A.; De Rossi, D. Electromechanical Characterisation of Dielectric Elastomer Planar Actuators: Comparative Evaluation of Different Electrode Materials and Different Counterloads. *Sensors and Actuators A: Physical* **2003**, *107* (1), 85–95. https://doi.org/10.1016/s0924-4247(03)00257-7.
34. Rosset, S.; Shea, H. R. Flexible and Stretchable Electrodes for Dielectric Elastomer Actuators. *Appl. Phys. A* **2013**, *110* (2), 281–307. https://doi.org/10.1007/s00339-012-7402-8.
35. S.-P., R.; F.-H., K.; K.-C., C. Dispersion of Carbon Black in a Continuous Phase: Electrical, Rheological, and Morphological Studies. *Colloid & Polymer Science* **2002**, *280* (12), 1110–1115. https://doi.org/10.1007/s00396-002-0718-8.
36. Huang, J. Carbon Black Filled Conducting Polymers and Polymer Blends. *Adv Polym Technol* **2002**, *21* (4), 299–313. https://doi.org/10.1002/adv.10025.
37. Toth, L. A.; Goldenberg, A. A. Control System Design for a Dielectric Elastomer Actuator: The Sensory Subsystem. In *SPIE Proceedings*; Bar-Cohen, Y., Ed.; SPIE: San Diego, CA, 2002; Vol. 4695, pp 323–334. https://doi.org/10.1117/12.475179.
38. Jung, K.; Kim, K. J.; Choi, H. R. A Self-Sensing Dielectric Elastomer Actuator. *Sensors and Actuators A: Physical* **2008**, *143* (2), 343–351. https://doi.org/10.1016/j.sna.2007.10.076.
39. Hau, S.; Rizzello, G.; Seelecke, S. A Novel Dielectric Elastomer Membrane Actuator Concept for High-Force Applications. *Extreme Mechanics Letters* **2018**, *23*, 24–28. https://doi.org/10.1016/j.eml.2018.07.002.
40. Mechanics of Materials: Strain. https://www.bu.edu/moss/mechanics-of-materials-strain/.
41. Ha, S. M.; Yuan, W.; Pei, Q.; Pelrine, R.; Stanford, S. Interpenetrating Polymer Networks for High-Performance Electroelastomer Artificial Muscles. *Advanced Materials* **2006**, *18* (7), 887–891. https://doi.org/10.1002/adma.200502437.
42. Kofod, G. The Static Actuation of Dielectric Elastomer Actuators: How Does Pre-Stretch Improve Actuation? *J. Phys. D: Appl. Phys.* **2008**, *41* (21), 215405. https://doi.org/10.1088/0022-3727/41/21/215405.
43. Bigue, J.-P. L.; Plante, J.-S. Experimental Study of Dielectric Elastomer Actuator Energy Conversion Efficiency. *IEEE/ASME Trans. Mechatron*. **2013**, *18* (1), 169–177. https://doi.org/10.1109/tmech.2011.2164930.
44. Lochmatter, P.; Kovacs, G.; Wissler, M. Characterization of Dielectric Elastomer Actuators Based on a Visco-Hyperelastic Film Model. *Smart Mater. Struct.* **2007**, *16* (2), 477–486. https://doi.org/10.1088/0964-1726/16/2/028.
45. Plante, J.-S.; Dubowsky, S. On the Performance Mechanisms of Dielectric Elastomer Actuators. *Sensors and Actuators A: Physical* **2007**, *137* (1), 96–109. https://doi.org/10.1016/j.sna.2007.01.017.
46. Madden, J. D. W.; Vandesteeg, N. A.; Anquetil, P. A.; Madden, P. G. A.; Takshi, A.; Pytel, R. Z.; Lafontaine, S. R.; Wieringa, P. A.; Hunter, I. W. Artificial Muscle Technology: Physical Principles and Naval Prospects. *IEEE J. Oceanic Eng.* **2004**, *29* (3), 706–728. https://doi.org/10.1109/joe.2004.833135.
47. Tang, C.; Du, B.; Jiang, S.; Wang, Z.; Liu, X.-J.; Zhao, H. A Review on High-Frequency Dielectric Elastomer Actuators: Materials, Dynamics, and Applications. *Advanced Intelligent Systems* **2024**, *6* (2). https://doi.org/10.1002/aisy.202300047.
48. Hu, W.; Ren, Z.; Li, J.; Askounis, E.; Xie, Z.; Pei, Q. New Dielectric Elastomers with Variable Moduli. *Adv Funct Materials* **2015**, *25* (30), 4827–4836. https://doi.org/10.1002/adfm.201501530.
49. Jia, K.; Lu, T.; Wang, T. J. Response Time and Dynamic Range for a Dielectric Elastomer Actuator. *Sensors and Actuators A: Physical* **2016**, *239*, 8–17. https://doi.org/10.1016/j.sna.2016.01.013.
50. Winter, E. M.; Brookes, F. B. C. Electromechanical Response Times and Muscle Elasticity in Men and Women. Eur. J. Appl. Physiol. 1991, 63 (2), 124–128. https://doi.org/10.1007/BF00235181.
51. Mirvakili, S. M.; Hunter, I. W. Artificial Muscles: Mechanisms, Applications, and Challenges. *Advanced Materials* **2018**, *30* (6). https://doi.org/10.1002/adma.201704407.
52. Wakeling, J. M.; Ross, S. A.; Ryan, D. S.; Bolsterlee, B.; Konno, R.; Domínguez, S.; Nigam, N. The Energy of Muscle Contraction. I. Tissue Force and Deformation During Fixed-End Contractions. *Front. Physiol.* **2020**, *11*. https://doi.org/10.3389/fphys.2020.00813.
53. Cai, Y.; Chen, Z.; Gao, Y.; Tang, J.; Mao, J.; Wang, D.; Chen, J.-F.; Luo, Y. Significantly Enhancing Electro-Actuation Performance of Dielectric Elastomer with ZrO2 Nanoparticles. *Composites Science and Technology* **2022**, *227*, 109543. https://doi.org/10.1016/j.compscitech.2022.109543.
54. Mirfakhrai, T.; Madden, J. D. W.; Baughman, R. H. Polymer Artificial Muscles. *Materials Today* **2007**, *10* (4), 30–38. https://doi.org/10.1016/s1369-7021(07)70048-2.

DOI: 10.36838/IJHSR87.105

55. Ghevondyan, M.; Davtyan, M.; Aghayan, M. Dielectric Elastomer Actuators: Medical Applications Review. *Discov Mater* **2025**, *5* (1). https://doi.org/10.1007/s43939-025-00225-7.
56. Stuchly, M. A.; Dawson, T. W. Interaction of Low-Frequency Electric and Magnetic Fields with the Human Body. *Proc. IEEE* **2000**, *88* (5), 643–664. https://doi.org/10.1109/5.849161.
57. Madsen, F. B.; Yu, L.; Daugaard, A. E.; Hvilsted, S.; Skov, A. L. Silicone Elastomers with High Dielectric Permittivity and High Dielectric Breakdown Strength Based on Dipolar Copolymers. *Polymer* **2014**, *55* (24), 6212–6219. https://doi.org/10.1016/j.polymer.2014.09.056.
58. Vudayagiri, S.; Zakaria, S.; Yu, L.; Hassouneh, S. S.; Benslimane, M.; Skov, A. L. High Breakdown-Strength Composites from Liquid Silicone Rubbers. *Smart Mater. Struct*. **2014**, *23* (10), 105017. https://doi.org/10.1088/0964-1726/23/10/105017.
59. Ouyang, G.; Wang, K.; Chen, X. Y. TiO2Nanoparticles Modified Polydimethylsiloxane with Fast Response Time and Increased Dielectric Constant. *J. Micromech. Microeng.* **2012**, *22* (7), 074002. https://doi.org/10.1088/0960-1317/22/7/074002.
60. Liu, H.; Zhang, L.; Yang, D.; Yu, Y.; Yao, L.; Tian, M. Mechanical, Dielectric, and Actuated Strain of Silicone Elastomer Filled with Various Types of TiO_2. *Soft Materials* **2013**, *11* (3), 363–370. https://doi.org/10.1080/1539445x.2012.661821.
61. Lotz, P.; Matysek, M.; Lechner, P.; Hamann, M.; Schlaak, H. F. Dielectric Elastomer Actuators Using Improved Thin Film Processing and Nanosized Particles. In *SPIE Proceedings*; Bar-Cohen, Y., Ed.; SPIE: San Diego, California, 2008; Vol. 6927, p 692723. https://doi.org/10.1117/12.776197.
62. Liu, Y.; Liu, L.; Zhang, Z.; Leng, J. Dielectric Elastomer Film Actuators: Characterization, Experiment and Analysis. *Smart Mater. Struct*. **2009**, *18* (9), 095024. https://doi.org/10.1088/0964-1726/18/9/095024.
63. Gallone, G.; Galantini, F.; Carpi, F. Perspectives for New Dielectric Elastomers with Improved Electromechanical Actuation Performance: Composites *versus* Blends. *Polymer International* **2010**, *59* (3), 400–406. https://doi.org/10.1002/pi.2765.
64. Lotz, P.; Matysek, M.; Schlaak, H. F. Fabrication and Application of Miniaturized Dielectric Elastomer Stack Actuators. *IEEE/ASME Trans. Mechatron*. **2011**, *16* (1), 58–66. https://doi.org/10.1109/tmech.2010.2090164.

Author

Advait is currently a high school student in Singapore. He has a strong interest in robotics through many years of training and participation in competitions, coursework, and internship experience in a drone manufacturing company. Advait is keen to pursue a degree in engineering to develop robotics technologies.

IJHSR
ijhighschoolresearch.org
RESEARCH ARTICLE

Comparative Structural Integrity of Miura-Ori and Flasher Origami Patterns for Deployable Solar Panels

Aruzhan Muratbekova

Haileybury Almaty, Al-Farabi Avenue 112, Almaty, 050040, Kazakhstan; muraaruzhan@gmail.com
Mentor: S. Bullock

ABSTRACT: With the introduction of origami folding patterns into deployable structures in space in the mid-2000s, the field of aerospace engineering experienced an innovative breakthrough with new benefits. The advantages of using origami principles in deployable structures are undeniable; from reduced weight and costs to enhanced functionality, origami in spacecraft has significantly increased efficiency. The deployment of solar panels, specifically, is heavily dependent on utilizing origami-inspired structures to maximize the surface area for energy absorption while minimizing the storage volume. For the better performance of solar panel deployment, the origami structure must have high structural integrity to withstand the space environment and external impacts. This paper presents two folding patterns, comparing their structural integrity: Miura-Ori and Flasher origami folds. The study focused on the comparison and evaluation, specifically assessing their strength and structural integrity through physical experimentation using smaller-scale Mylar and Flasher models. As a result of physical testing, the Flasher outperformed Miura-Ori by 16% in terms of strength, indicating it to be a more impact-resistant origami structure. It is hypothesized that the rotational symmetry of Flasher distributes compressive stress more evenly, yielding a higher peak load than the parallelogram tessellation of Miura-Ori.

KEYWORDS: Engineering Mechanics, Aerospace and Aeronautical Engineering, Solar Panels, Miura-Ori, Flasher.

Introduction

Solar cells (SCs) are single units that convert solar energy into electricity using the photovoltaic effect. Solar panels (SPs) are structures made up of multiple SCs to convert this energy on a larger scale. SPs are widely used and reliable for energy generation in aerospace applications, where photovoltaic devices can provide an uninterrupted and stable power supply.[1] Over the past 50 years since 1970, the power conversion efficiency of photovoltaic technologies has increased, reaching a mean value of 28.95% for different SC materials.[1] Considering the value of solar energy and the effective use of photovoltaic abilities, SPs have become one of the most valuable and widely used energy-generating technologies in spacecraft (including artificial satellites as well as exploration technologies), serving as the primary energy source for various space missions.[2] And one of the methods used for SPs to absorb sun energy and convert it to electricity is photovoltaics.[3]

Among the power generation systems, the photovoltaic cells remain a stronger option, specifically for long-term space missions, in contrast to nonrechargeable batteries and fuel cells.[1] The advantages and reasons why the use of SPs has become more widespread in spacecraft energy-generating systems include the following: Sustainability and independence from finite resources, Energy storage in advance, No refuelling necessity, Lightweight, Low cost, High availability, and stock.[4] All of these advantages maximize the convenience of using SPs in spacecraft. However, they do not completely exclude possible problems caused by the size of SPs in larger spacecraft, where more SCs are used to provide a bigger surface area for solar energy intake.[4] As a result, many designs struggle with limited power generation capabilities, leaving fewer opportunities for larger spacecraft maintenance.[4] This issue creates a need to develop simplified deployable mechanisms to create more compact designs, easing the launch of spacecraft.

These problems have been addressed by a Japanese paper-folding technique, origami, which has been implemented in space engineering as a promising approach to reduce the challenges associated with SP design.[4] The concept of using origami in space missions allows for the development of solar panels that can unfold or expand upon deployment, providing a larger surface area for energy collection.[1] Origami-inspired techniques in space engineering help alleviate multiple negative aspects of using large SPs. Consequently, there are several reasons why origami brings additional advantages to SPs, including higher cost efficiency, improved space and weight efficiency, reduced friction and wear, and increased precision due to more options for scalability.[4,5]

Despite the advantages that origami-based aerospace designs provide, solar panels are prone to structural failures due to the harsh conditions of space, including external impacts such as micrometeoroid impacts or space debris.[1] This is even more applicable in the case of larger surface area SPs, making them much more vulnerable and requiring them to withstand physical damage.[1] Structural integrity concerns can be addressed by designing specific origami patterns to distribute stress more evenly and better absorb external impacts.[6]

There are numerous origami patterns used for SP deployment. The Miura and Flasher designs stand out as the most common configurations utilized in SPs.[4] Researchers at Brigham Young University have indicated that engineers and

© 2026 Terra Science and Education

DOI: 10.36838/IJHSR87.115

scientists focus on the following properties of origami: 1) Stowability, 2) Portability, 3) Deployability, 4) Fewer components, 5) Manufacturability, 6) Lower volume and mass, and 7) Ease of miniaturization and assembly.[4,5] While meeting all of these requirements, the Miura and Flasher folding designs are also examples of rigid origami consisting of rigid folds. Rigid folds have surfaces surrounded by crease lines, and the ones that do not bend. Both Flasher and Miura satisfy the implementation of rigid origami without deformation due to flexible crease lines.[4] Each rigid section of origami can pivot around the creases, allowing these creases to be viewed as revolute joints in mechanical design. Likewise, the entire crease pattern with a single vertex can be considered a spherical linkage. This is because, when the paper is folded into a 3-D shape, the intersections of the creases and edges maintain equal distances from the vertex.[4] As this paper focuses on the structural integrity of origami folds, it is essential to examine each origami pattern's mechanical properties in detail.

Miura-Ori

One of the rigidly folded types, Miura-Ori, is an origami pattern consisting of several single units that consist of four identical parallelograms surrounding vertices, and consisting of a single mountain and valley creases. This single unit of four quadrangle plates repeats throughout the pattern, forming a tessellation, as shown in Figure 1.[7] It consists of interchanging, repeating mountain and valley creases in a sequence.[7] One unit of Miura-Ori has a single vertex angle (α) and a single span length (a), as well as the second span length (b).

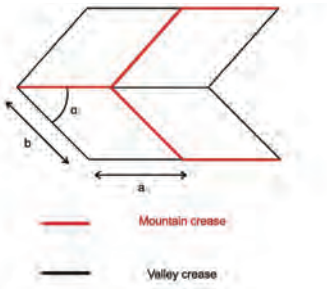

Figure 1: Single Miura-Ori unit showing a mountain and valley creases, as well as span lengths a and b along with vertex angle α.

Due to its characteristics, this pattern could be arranged for various performance purposes, for example, by adding another interchanging angle (β) or varying the span length.[7] There are also multiple variations in the design of Miura-Ori where both the angles and span length are changed to different quantities, making its structure fold in different ways while still retaining its original form, for example, by forming more of an arch figure.[7] To keep this research as fair as possible, the most common version of the Miura-Ori design has been kept for the physical testing.

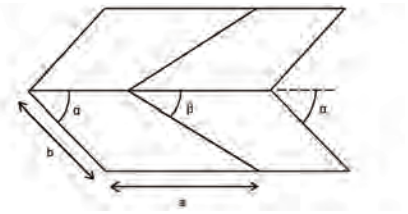

Figure 2: Single Miura-Ori unit with the introduction of angle β. All of the other dimensions shown are kept the same.

Figure 2 shows an example of another Miura-Ori single cell variation by introducing a new angle beta to the system. One of the most important mechanical features of Miura-Ori is the degree of freedom determined by the angle θ.[8] This is the angle between two faces and is responsible for the energy absorption capabilities and in-plane behaviors.[8] This tessellation pattern is widely used for engineering purposes due to its high stiffness-to-weight ratio and successful energy absorption performance, making Miura-Ori an extremely high stress-absorbing origami pattern.[8] Dihedral angle is the angle between the 2 creases within an origami that determines its strength. When span lengths a, b, and angle α are constant, the unit performance depends on the dihedral angle θ, as shown in Figure 3. It is also essential to mention that the span lengths a and b would be equal for this to work.[8] Because an optimal angle theta relies on the value of alpha, the optimal value for both will be used.[9]

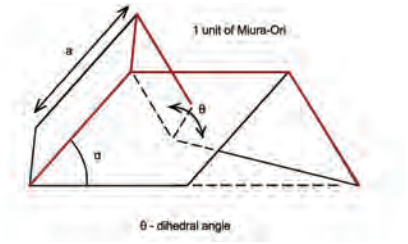

Figure 3: Showing a single Miura-Ori unit with the introduction of angle θ in a three-dimensional diagram.

Looking more specifically at the architectural role of Miura-Ori, its self-locking feature enables the opportunity for this tessellation to be used in terms of mechanics and structure, where it can form structures that resemble arches and shells when modified.[10] It is also shown that Miura-Ori's pattern parts could be removed without causing any changes in its origami behaviour, showing its advantages for architectural modifications.[10] For the physical testing part, the following dimensions were considered as optimal for the dihedral angle: θ=50°.[10]

Flasher:

Flasher is another type of rigid origami, similar to Miura-Ori; however, their fundamental structures differ. Origami Flashers have a cyclic symmetry within their structure, with the number of edges of the central regular polygon determining the number of identical sectors.[11] This rotationally symmetric set of creases is folded around the polygonal cylinder in the center.[12] The edges of the hub(central polygon) and the folds where they meet are considered valley folds. Lines that divide these valley folds are also added, creating the mountain folds

in between. The creases in the Flasher and the overall folding direction can only face clockwise or counterclockwise.[11]

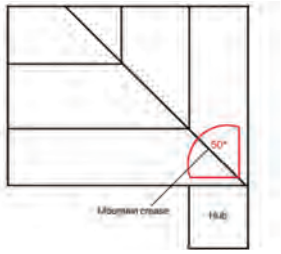

Figure 4: A fragment of the square Flasher showing the fold line at 50° for the mountain crease.

In Figure 4, the most basic Flasher pattern used is shown; the model is directed clockwise and has a pattern with the square central hub. Like any rigid origami, Flasher has alternating sequences of mountain and valley creases. To demonstrate this, Figure 3 below is shown.



Figure 5: Basic expanded Flasher model with different colours representing their corresponding mountain and valley creases.

Figure 5 illustrates the origami patterns of planar origami flashers considering four different central hubs. The red lines and black lines represent the mountain creases and valley creases, respectively.[11] Mechanical behavior is strongly dependent on folding dihedral angles at mountain and valley creases. These angles determine whether the pattern collapses into a flattened disk or cones, its deployment stiffness, and final unloaded shape.[13] Dihedral fold angle is directly linked to deployment path, strain energy, and mechanical fatigue performance, making it the most important factor in deciding the overall structural integrity of the origami Flasher model.[14] For the optimal performance of the flasher unit, it is essential to keep the dihedral angle θ at a value of 50°.[14]

There are numerous studies assessing each origami folding pattern in terms of their structural integrity and dynamic mechanical properties with different acute angles in quasi-static and fully static conditions, where the optimal acute angles at peaks and compression distances for the highest energy absorption have been investigated.[15] Taking this into account, this paper aims to produce a comparison between the two structures and set up its own testing method to evaluate which origami pattern between the two origami patterns would be stronger. This gap is significant because in space missions with the use of SPs, where the potential hazards are more prominent, the factor of structural integrity would play a crucial role in suppressing the negative effects of collisions. Hence, the choice of the origami pattern used for deployment would play a role in that, deciding the goal of this paper to compare the 2 most common patterns in terms of their ability to withstand external impacts. By analysing each folding pattern's performance in load and stretch testing, this study allows engineers to choose the strongest origami folding pattern for SPs. The significance of this study lies in its potential to use the design of SPs in spacecraft for missions with a high risk of external impact, ultimately contributing to more efficient and sustainable space exploration. The hypothesis guiding this research is that the Miura and Flasher origami patterns will demonstrate varying degrees of structural integrity in terms of strength and flexibility, impacting their effectiveness in SP applications in space.

Methods

This research aims to evaluate the structural integrity of deployable solar panels designed using Miura and Flasher origami patterns. These patterns were chosen due to their established effectiveness in optimizing space utilization and enhancing deployable structures in aerospace applications.[4] The methodology encompasses model design and fabrication, experimental setup, and a comprehensive assessment of performance metrics, including load-bearing capacity.

Design and Fabrication:

Models of deployable SPs will be constructed for the physical tests, where each model will be measuring 15 cm x 15 cm in their deployed state, representing a smaller scale of typical solar panels used in space missions. Each origami pattern will consist of five identical models for each origami folding type, resulting in a total of ten models. It has been decided that at least 5 models will be tested for each origami pattern to collect the mean and ensure the results are as reliable as possible with the inclusion of random error. In the experiment setup, a sample size of 5 has been considered a reasonable number to investigate the connection. The Miura origami fold will consist of 2 x 2 cells, like in Figure 6. Flasher origami fold will be made from a 7 x 7 square base with a square quadrilateral base, resulting in 4 clockwise vertices, like in Figure 6 as well. The paper prototypes could be seen and compared to the Mylar Miura and Flasher in the images below in Figure 7. And Figure 8.

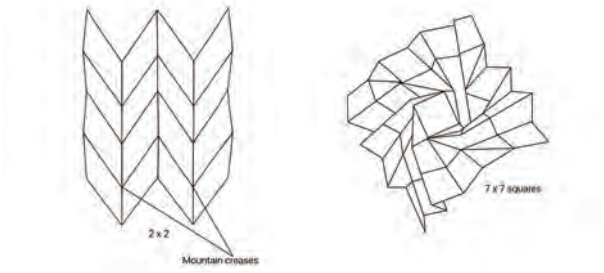

Figure 6: Upper view of the Miura (on the left) and Flasher (on the right) origami folds in a 2-D diagram.

DOI: 10.36838/IJHSR87.115

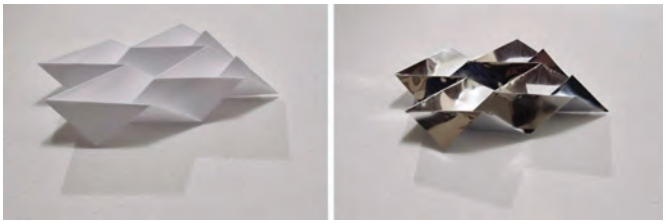

Figure 7: Paper Miura Fold on the left and Mylar Miura Fold on the right.

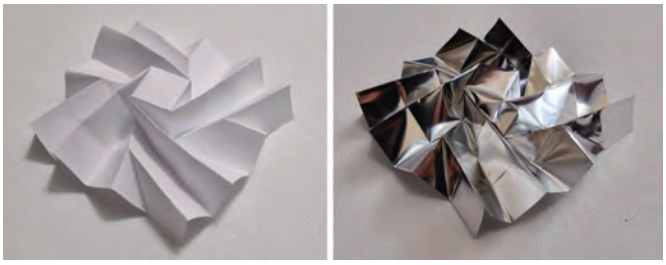

Figure 8: Paper Flasher Fold on the left and Mylar Flasher Fold on the right.

There are proven to be 4 possible materials suitable for the creation of origami-inspired SP designs. These include Mylar (type A), Tyvek, Kapton, and UHMWPE(Ultra-High Molecular Weight Polyethylene).[5] All of the materials were able to undergo 10000+ cycles of fatigue in a custom-designed fatigue tester consisting of a crank-slider mechanism without any tears or holes, making them a suitable choice for this study.[5] However, the chosen material used to recreate the models in the study will be Mylar, a polyester known for its exceptional strength-to-weight ratio. Mylar is a material that is able to withstand harsh environments while having paper-like properties and thickness. It has also been studied that in the Mylar Crease Fatigue Results, the thinner Mylar (177.8 μm) was able to withstand over 1000+ cycles before failure.[16] The physical property of flexibility is being compared to the materials from which the SCs are made. SCs are made of different materials and alloys, including the most popularly used Silicon(Si), Cu(In,Ga)Se2, and CH3NH3PbI3, which are nowadays used for SPs creation.[1] Even though Mylar is not sensitive to environmental changes, it is still significant to keep the environmental factors, such as temperature and humidity, the same during the experimentation process. The Mylar Type-A material is used in many reliable studies for structural integrity testing. For example, Mylar has been utilized as the main material for Kresling origami fold physical testing.[16]

Properties of Mylar relevant for this study include tensile strength, tear strength, elastic constants, and shrinkage. The following qualities for Type-A Mylar can be seen in Table 1.

Table 1: Mylar Type-A material characterization was used in the physical testing.[17] Properties of Mylar which are relevant for the physical testing are shown, including tear strength, tensile strength, elastic constraints, and shrinkage.

Tear strength	Tensile strength	Elastic constants	Shrinkage
23.6*10^6 g/m at 23°	172MPa at 23°	1.6*10^-10 Pa^-1 oriented	2.5%, 30 min at 150°

Potential uncertainties in the physical testing may arise from variations in material properties, inaccuracies in folds, and human factors during model construction. Assumptions include uniformity in the material properties of Mylar across all models, while limitations may involve the inability to replicate the full range of environmental conditions experienced in space (including other space environment features apart from the external impact, including plasma or solar wind, directly ionizing radiations, thermal cycles, solar activity, and neutral atmosphere with vacuum).[16]

Experimental setup:

The following paragraph contains information on the experimental setup for mechanical and physical testing on the origami models to determine their structural integrity. The setup involved 15 cm x 10 cm cardboard borderlines, inside of which one model at a time was placed.

The goal is to compare the strength of 2 origami patterns in the fairest way possible.

Below is a step-by-step description of the method to physically test the structural integrity and strength of the origami patterns:

1. Place a folded model vertically on a flat surface inside the fence-like cardboard area
2. Place a weight-distributing platform on top of the model(-for equal spread of the pressure and weight onto the mountain creases). Cardboard weight-distributing platform: 11 cm x 6.5 cm.
3. Add weights in increments of 10g onto the cardboard platform
4. Record the maximum weight each fold can withstand before collapsing
5. Repeat for 5 models of each origami pattern type

The weight loads at which each origami model collapses will be recorded, and the mean collapsing weight for each design will be calculated to compare structural performance and determine the strongest pattern. To ensure a fair comparison, weight distribution will be standardized by maintaining consistent contact between the cardboard and the same number of mountain creases on each model.

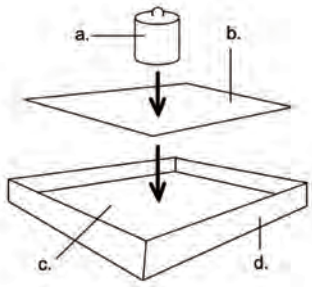

Figure 9: The setup for the experiment, where a is the weight load, b is a weight-distributing platform, c is a place where the origami piece will be trapped to undergo a physical test, and d is a cardboard fence to keep the origami model in the same shape.

In Figure 9 above, the setup for the experiment is shown. The only value getting changed is going to be the weights, where they will be added by 10g until the origami collapses.



Figure 10: The experimental setup images for Miura-Ori showing it in the cardboard fence.

Since 5 models were created for the 2 different origami patterns, the weights were tested on each one until collapse, to then collect the mean for the sample. The mean is a statistical measure of central tendency, defined as the sum of all observed values in a data set divided by the total number of observations. It represents the average value around which the data are distributed. The results for the weight until collapse could be seen in the results and discussions part. The cardboard platform, on which the weights were loaded, was able to cover all four mountain creases in the Miura fold and eight mountain creases in the Flasher fold, as shown in Figure 10. The cardboard outline was used to maintain a specific angle between the cells in the Miura and Flasher folds because the pressure applied may differ depending on the acuteness of this angle. A cardboard platform piece was needed to address the issue of uneven pressure created by the weights, thus spreading the weight force evenly across the creases. It was decided that the experiment would use an acute angle of 50° between the mountain crease vertices for both origami patterns since it is proven to be optimal for both origami folds.[14]

The metallic weights used vary from 10 g to 500 g. Overall, they make up 1 kilogram. The metal-made weights are placed exactly in the middle in each of the tests, making sure the weight is distributed evenly across the cardboard piece at the top.



Figure 11: Weights kit including weights of 10g, 20g, 20g, 50g, 100g, 100g, 200g, 500g, totalling 1 kg overall.

The weights used in the experiment are shown above in Figure 11. Added in intervals of 10g, they were placed in the middle piece of cardboard to test the origami structures in terms of their structural strength.

Comparison and assessment:

To assess the structural integrity, the maximum load that the origami folding technique can withstand will be measured and compared, and the record of its resistance, deformation, and failure points will be collected. Important factors to assess would also include stress distribution and deformation patterns, which will be recorded and identified by taking photos. To make the experiment as reliable as possible, five other copies of the origami patterns will be used. By calculating the mean and then comparing the values, the goal of the paper is to determine the most common weight needed to make the origami structure fail.

For the most accurate result, the origami models will be placed with the vertices at the same angles, with both origami patterns having 50-degree mountain creases, so that the pressure affecting the model is the same. To ensure the angles are measured correctly, the protractor has been used. However, there are twice as many mountain creases in the Flasher model, which could create a higher surface area. The difference in surface area would be mostly insignificant due to the mountain creases being extremely small in terms of surface area, so the weight will act almost equally.

Results

Table 2 represents the data obtained from physical and mechanical tests on the Miura and Flasher origami folds and the weight needed to cause a collapse of the origami structure under the same conditions. The mass in grams was recorded as soon as the origami model collapsed (by collapse, it means the model got compressed under the weight, unable to withstand the pressure). Figure 12 shows the consequences of collapse for both Miura-Ori and Flasher, respectively. As expected, due to Mylar Type-A's properties, the material did not show any signs of tears or stretches; however, the dents were visible as a result of pressure.

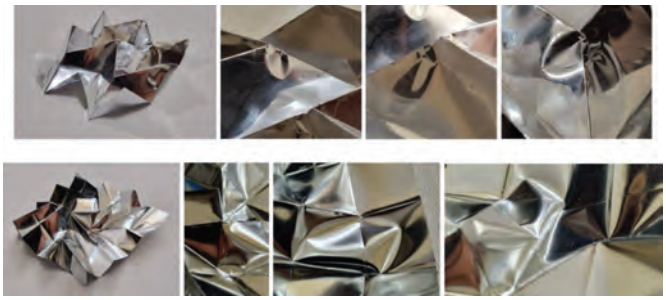

Figure 12: Examples of Miura-Ori (row above) and Flasher post collapse (row below).

As a result of physical testing, all of the data have been summarized in Table 2, where the maximum weight until collapse has been recorded for each origami model and its 5 copies. The mean has been calculated for all 5 attempts. The angle in degrees has also been indicated as a reference to show that the optimal angle for both Miura-Ori and Flasher has been kept the same throughout the experimentation.

DOI: 10.36838/IJHSR87.115

Table 2: Results of the physical experiments on the Miura and Flasher models with the mean. The mean weights at which the models collapsed have been recorded for the same optimal angle for both origami types.

Model	Miura 1	Miura 2	Miura 3	Miura 4	Miura 5	mean
Angle between the cells(°)	50	50	50	50	50	50
Max weight until collapse(g)	800	830	800	820	810	812
Model	**Flasher 1**	**Flasher 2**	**Flasher 3**	**Flasher 4**	**Flasher 5**	**mean**
Angle between the cells(°)	50	50	50	50	50	50
Max weight until collapse(g)	940	950	930	940	960	944

The data collected could be represented in a visual and more understandable way by using the bar chart as shown in Figure 13, where the light colour has been used to indicate results for Miura-Ori, and the darker colour has been used to indicate the results for Flasher.

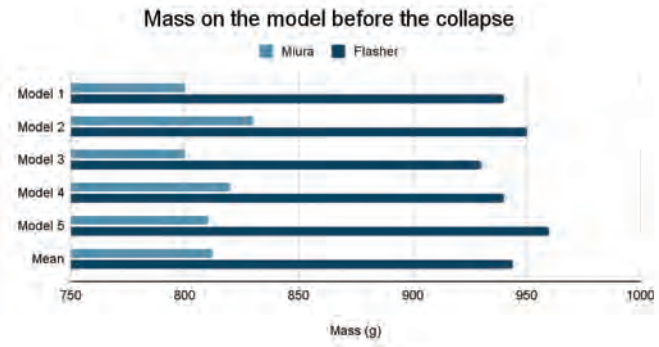

Figure 13: Bar chart results showing the mass needed to reach the collapse in Miura-Ori and Flasher models, including their mean mass withstood before the collapse on the x-axis, and the model number with mean on the y-axis.

Discussion

The Miura origami fold all snapped towards one of the two cell sides, where the highest vertices experienced the most pressure. It is common to observe bending within the cell angles and a dent (visible on the cells from one side), as well as deflection of the obtuse angles on the mountain convex creases. No issues were noticed in the valley concave creases. Interestingly, however, in Miura model 5 and Miura model 4, there was a dent seen in the middle of the parallelogram, which was not observed in the other models. This could be caused by excessive pressure on a specific mountain crease, resulting in one cell bending fully under the weight and disrupting its usual fold pattern.

The Flasher origami fold, however, experienced far less damage compared to the Miura. The damage was usually seen in one of the four clockwise sections, leaving a dent between the folds or resulting in incorrect bend lines for the folds. Like the Miura, the most significant damage was observed at the top of the mountain creases, where the bent creases with the largest dents were located. Interestingly, in Flasher model 2, there is a dent at the very edge of the origami. Similar to the anomaly in the Miura models, it is suggested that this dent could be caused by excessive pressure on this specific side of the Flasher, leaving its lower part deformed.

With a difference of 132 grams between the mean results for Flasher and Miura, it is evident that the Flasher folding pattern has higher structural integrity and resistance to external impacts. Even looking at Figure 14 is enough to understand that the ability to withstand the weight is drastically different between the two origami pattern folds. The strength and compressibility tests showed that both types of origami patterns have high structural strength; however, Flasher notably demonstrated better results for the SPs compared to the Miura origami technique. Flasher withstood a range of 930-960 grams, outperforming Miura's range of 800-830 grams. By calculating the Miura average as 815g and Flasher as 945g, their difference in averages is equivalent to 130. As a result, it is relevant to note that Flasher was able to outperform Miura-Ori by 16%, all due to its origami fold being more suitable to stand against higher pressure.

The experiment was fair, as both model types used the same acute angle for their dihedral angle (50 degrees), the same deployed area, and the same material, along with its thickness. While some limitations were discussed previously, overall, the experiment was successful in identifying a more robust origami folding technique for the deployment of SPs in space applications for spacecraft.

Conclusion

In conclusion, the paper's goal of comparing Miura-Ori and Flasher origami patterns concerning the structural integrity of deployable solar panels was to determine which origami type has higher structural integrity. With the physical testing and controlled conditions, both origami model types were tested on their ability to withstand the weight compressing them until the collapse point. Under quasi-static compression, Flasher-patterned 15 cm Mylar panels sustained 16% higher peak load than Miura-Ori equivalents (944 ±10 g vs. 812 ±12 g). The rotational symmetry of Flasher redistributes stress, delaying hinge buckling, making it a more suitable technique for deployable SPs that need better structural integrity for space missions. When translated into real size, even though geometrical similarities will be the same, the material will still differ. Given Mylar's unique similarity to PV cells, it ultimately is still different, and the % of weight with standard could differ from expectations as well. Another limitation of this study is the fact that only 5 models were tested for each; this encourages further research to use even more samples to ensure an even higher credibility. Still, his paper could be valuable for selecting the Flasher as a preferable choice for further spacecraft development for SP usage. Based on the research, it is suggested that similar studies in the future could expand on the topic by comparing Flasher to other origami fold patterns or by exposing it to space environmental stress simulations to further validate Flasher's potential in deployment scenarios.

Acknowledgments

I would like to express my gratitude to Dr. Bullock and Ms. Long for their invaluable assistance in the process of writing this research paper. The advice and guidance I have received made it key to conduct and finish this research successfully.

References

1. Verduci, R.; Romano, V.; Brunetti, G.; Yaghoobi Nia, N.; Di Carlo, A.; D'Angelo, G.; Ciminelli, C. Solar Energy in Space Applications: Review and Technology Perspectives. *Advanced Energy Materials* 2022, *12* (29), 2200125. https://doi.org/10.1002/aenm.202200125.
2. Rodgers, E.; Gertsen, E.; Sotudeh, J.; Mullins, C.; Hernandez, A.; Le, H.; Smith, P.; Reviewer, N.; Charania, A.; Colvin, T.; Meyers, R. *Office of Technology, Policy, and Strategy Space-Based Solar Power*; 2024. https://www.nasa.gov/wp-content/uploads/2024/01/otps-sbsp-report-final-tagged-approved-1-8-24-tagged-v2.pdf?emrc=744da1%0A (accessed 2025-08-06).
3. Yogesh, S.; Yogalakshmi, M.; Abishek, M.; Ari Prasath, R.; Madhusudanan, G. Origami-Based Folding Techniques for Solar Panel Applications. *Int. J. Electr. Eng. Technol.* 2021, *12* (3), 195–203. https://d1wqtxts1xzle7.cloudfront.net/67663917/IJEET_12_03_022-libre.pdf
4. Yue, S. A Review of Origami-Based Deployable Structures in Aerospace Engineering. *Journal of Physics* 2023, *2459* (1), 012137–012137. https://doi.org/10.1088/1742-6596/2459/1/012137.
5. Morgan, J.; Magleby, S. P.; Howell, L. L. An Approach to Designing Origami-Adapted Aerospace Mechanisms. *Journal of Mechanical Design* 2016, *138* (5). https://doi.org/10.1115/1.4032973.
6. Garcia, D. J.; Bettinger, R. A.; Hartsfield, C. Simulated Debris Impact Testing of Additively Manufactured Origami Mirror Structure for Space-Based SSA. Poster presented at the Advanced Maui Optical and Space Surveillance Technologies Conference (AMOS), Maui, HI, Sept 2023.
7. Huseynli, A. Geometric and Mobility Analysis of the Miura-Ori Pattern and Its Derivations; Master's Thesis, Izmir Institute of Technology, 2016. https://openaccess.iyte.edu.tr/bitstream/11147/5708/1/T001537.pdf
8. Liu, S.; Lu, G.; Chen, Y.; Leong, Y. W. Deformation of the Miura-ori Patterned Sheet. *Int. J. Mech. Sci.* 2015, *99*, 130–142. https://doi.org/10.1016/j.ijmecsci.2015.05.009
9. Karagiozova, D.; Zhang, J.; Lu, G.; You, Z. Dynamic In-Plane Compression of Miura-Ori Patterned Metamaterials. *Int. J. Impact Eng.* 2019, *129*, 80–100. https://doi.org/10.1016/j.ijimpeng.2019.02.012
10. Demir, D. *A Comprehensive Perspective into the Use of Origami in Architecture*; Abdullah Gül University, 2023.
11. Wang, S.; Gao, Y.; Huang, H.; Li, B.; Guo, H.; Liu, R. Design of Deployable Curved-Surface Rigid Origami Flashers. Mech. Mach. Theory 2022, 167, 104512. https://doi.org/10.1016/j.mechmachtheory.2021.104512
12. Srinivas, V.; Harne, R. L. Directing Acoustic Energy by Flasher-Based Origami Inspired Arrays. *The Journal of the Acoustical Society of America* 2020, *148* (5), 2935–2944. https://doi.org/10.1121/10.0002483.
13. Lu, L.; Leanza, S.; Zhao, R. Origami with Rotational Symmetry: A Review on Their Mechanics and Design. *Applied Mechanics Reviews* 2023, *75* (5). https://doi.org/10.1115/1.4056637.
14. Chen, Y.; Shi, P.; Bai, Y.; Li, J.; Feng, J.; Pooya Sareh. Engineered Origami Crease Perforations for Optimal Mechanical Performance and Fatigue Life. *Thin-Walled Structures* 2023, *185*, 110572–110572. https://doi.org/10.1016/j.tws.2023.110572.
15. Xiang, X.; Qiang, W.; Hou, B.; Tran, P.; Lu, G. Quasi-Static and Dynamic Mechanical Properties of Miura-Ori Metamaterials. *Thin-Walled Structures* 2020, *157*, 106993. https://doi.org/10.1016/j.tws.2020.106993.
16. Dunne, F.; Westra, K.; Mattox, C.; Leachman, J. Fatigue Life Characterization of Hand Folded and Vacuum Formed Kresling Origami Bellows at 77K. *IOP Conference Series: Materials Science and Engineering* 2022, *1241* (1), 012014. https://doi.org/10.1088/1757-899x/1241/1/012014.
17. Mark, J. E.; Allcock, H. R.; West, R. Properties of Films Are Given for Mylar Type A (DuPont) Biaxially Oriented and Crystalline Films. In Polymer Handbook; Brandrup, J., Immergut, E. H., Grulke, E. A., Eds.; Wiley: New York, 1999; pp 33–46.

Author

Aruzhan Muratbekova is an open-minded student who is highly interested in music, sciences, and art. Engineering, origami, and architecture are areas of her interest that she would want to explore on a deeper level in university. Being a part of the Haileybury Almaty school, she actively participates in the school life as a house leadership team member and violinist.

DOI: 10.36838/IJHSR87.115

IJHSR
ijhighschoolresearch.org
RESEARCH ARTICLE

How Do Wing Length and Thickness Affect Flight Performance?

Hannah Choo Ying En

Hwa Chong Institution (College Section), 661 Bukit Timah Rd, Singapore, Singapore 269734, Singapore; hannahchoo7375@gmail.com
Mentor: Naveen Pillai

ABSTRACT: With the rise of globalization, airplanes as a form of transportation are more important than ever. Besides merely transporting people and goods from one location to another, they are one of the main reasons countries are now more interdependent and interconnected as goods and people integrate across the globe. As the world continues to innovate and improve airplanes, there are many factors, such as the shape of the airfoil, that affect the flight performance of airplanes, and understanding how this affects airplanes is crucial in the development of airplanes. This paper will discuss the history of airplanes starting from the Wright Flyer, the possible dangers associated with airplanes, and the effect of changes in wing shape on the flight performance of airplanes.

KEYWORDS: Engineering Mechanics, Aerospace and Aeronautical Engineering, Wing Shape, Flight Performance.

Introduction

Created by Sir George Cayley of England,[1] aeronautics is the scientific study of flying. Over the past few years, advancements in technology and aeronautics have led to many significant innovations, like the creation of airplanes, which have resulted in globalization. Airplanes allow people to fly from one country or continent to another in a short amount of time. As such, countries are now more interconnected and interdependent. Heavier objects are able to stay in the air for a long time because of their wings, or airfoil, that would be able to creates a pressure difference between the top and bottom of the wing, to give rise to a lift force. This lift force is directly proportional to the lift coefficient, density, velocity, and wing area. I am interested in studying aerodynamics and airplanes because I would like to dive deeper into what makes airplanes able to stay in the air and the importance airplanes have on our daily lives. Changes in the length and thickness of wings can affect flight performance; thus, this research paper seeks to find out the impact of these changes on the distance travelled by airplanes.

Section 1 will discuss the history of airplanes, followed by Section 2, which touches on airfoils in general. Section 3 focuses on the experiment and methods used, while Section 4 presents the results of the experiment. This paper will end with a conclusion stating future work and insights. It was hypothesized that the airplane with the longest wings would fly the longest horizontal distance.

History

1.1. Origins of Airplanes:

The invention of airplanes first started out in 1899 by the Wright Brothers and was achieved in 1903 when they successfully created the first airplane (Figure 1), which flew at Kitty Hawk, North Carolina, with Orville Wright managing and flying the plane.[2]



Figure 1: Picture of the first airplane created by the Wright Brothers, which was called the Wright Flyer. This took place in 1903 at Kitty Hawk in North Carolina.[3]

This invention came about as a result of growing up in Dayton, Ohio, where their favorite toy was a tiny object that resembled a helicopter, powered by rubber bands to spin its blades. This piqued their interest, and they wanted to be able to create a plane that was large enough to be able to accommodate both of them.[4] This was achieved when the Wright Brothers carried out their flights in public for the first time in Europe and America in 1908, showing their creation to the public.[5]

1.2. Evolution of Airplanes:

Over time, there have been many innovations to airplanes, and much research has been conducted in this area. (Figure 2).

© 2026 Terra Science and Education

DOI: 10.36838/IJHSR87.122

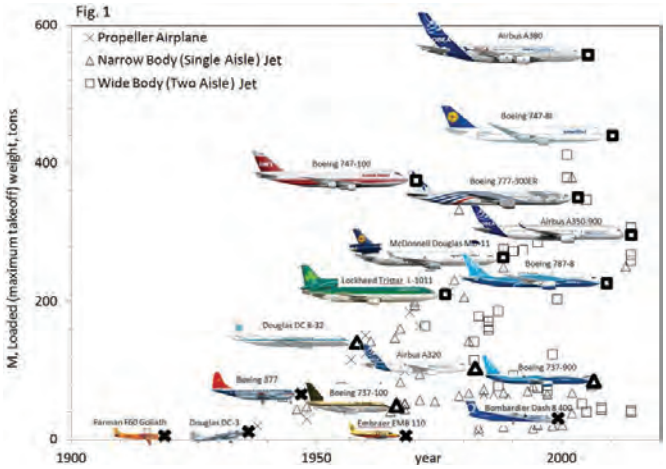

Figure 2: Evolution of airplanes from 1900 to the 2000s. It first started as the Farman F60 Goliath, to become Boeing and Airbus airplanes.[6]

Figure 2 shows how airplanes changed from propeller airplanes to jets. Besides the planes mentioned above, other planes include the Travel Air S6000-B, operating from 1929 to 1930, and the Stinson A, operating from 1935 to 1938.[7]

Over the years, companies started innovating and improving their aircraft, creating more efficient planes. Efficiency of the aircraft was achieved by reducing the lift to drag ratio,[8] using more efficient engines, and creating more fuel-efficient planes. As stated by McKinsey and Company, the new generation airplanes are found to be 15% to 20% more fuel efficient than older airplanes. One example is the Concorde (Figure 3).



Figure 3: Picture of a Concorde aircraft, which was built during the 1960s through a collaboration between the United Kingdom and France.[9]

Having a maximum speed that is faster than the speed of sound,[10] the Concorde unlocked the possibility of being able to travel from one end of the world to another in a matter of hours, further changing how the world was connected. However, on July 25, 2000, the fuel tank of Flight 4590, travelling from Paris to New York, exploded and erupted into flames as it came into contact with debris created from a tire that had burst. This resulted in an engine failure, and the aircraft crashed into a nearby hospital, killing all 109 on board and 4 others on the ground.[11]

1.3. Dangers of Airplanes:

Over the past decade, the dangers of airplanes were evident at times. Although few, there are fewer than 50 commercial airplane crashes happening every year, with even fewer causing deaths.[12] Despite this being a small number, this shows how the chances are never 0. There have also been cases where aircraft have experienced terrible and extreme turbulence, and this was what happened on the SQ321 in 2024, causing the death of a 73-year-old British man and leaving 7 people in critical conditions.[13] As such, all these highlight how travelling in airplanes can come with risks, especially when safety precautions are not taken seriously.

Present Day Aircraft:

Advancements in technology and aerodynamics have led to the creation of many different types of airplanes, like commercial airplanes, aerobatic airplanes, seaplanes, and more, all serving different purposes.

1.4.1. Commercial Airplanes:

One example of a commercial airplane is the Boeing 737 (Figure 4). Having 12000 planes built as of 2024,[14] it is one of the most popular commercial aircraft in the world today, and it enables the transportation of large numbers of passengers from one place to another.



Figure 4: Picture of a Boeing 737 by Singapore Airlines, an example of how advancement in technology and aerodynamics was applied.[15]

The Boeing 737 has a vertical and horizontal stabilizer (Figure 5), located at the back of the aircraft, ensuring the stability of the plane by preventing the nose of the aircraft from swaying around when traveling in the air.



Figure 5: Picture of the features on the back of a Boeing 737 aircraft, which includes a horizontal and vertical stabilizer.[16]

1.4.2 Helicopters:

With an increase in versatility, the next example is helicopters (Figure 6), which can access locations that are hard to reach and fly through adverse weather conditions.

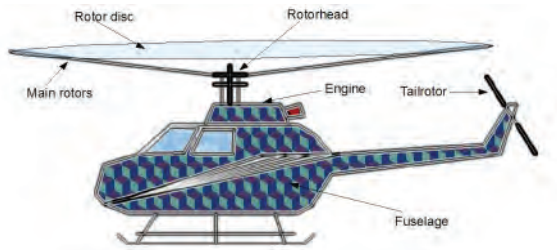

Figure 6: Picture of a helicopter where rotors are able to create lift with no runway.[17]

Helicopters are able to transport large objects, reach people in locations that are difficult to access,[18] and overcome obstacles and bad conditions. Instead of having 2 wings, like airplanes, helicopters have 2 rotors, which are able to create comparable lift with no runway.[19] When the rotor is tilted at an angle, the lift force is able to be converted into thrust, allowing the airplane to fly.[20]

1.4.3. Seaplanes:

Imagine a plane that is able not only to take off on land but also to do that on water. Those are the characteristics of seaplanes (Figure 7).



Figure 7: Picture of a seaplane that allows landing and take-off in the water.[21]

On seaplanes, the wheels of a normal aircraft are exchanged for floats, where they can have either straight or amphibious floats. If the seaplane has straight floats, this means that the plane does not have wheels and thus is unable to travel on land. Conversely, seaplanes with amphibious floats have wheels that can retract, allowing them to travel on both land and water.[22]

■ Airfoils

2.1. Definitions:

Airfoils (Figure 8) are a part of the plane that generate more lift than drag. One of the main functions of airfoils is to be able to generate a lift force, allowing heavy objects like planes to fly in the sky. Lift force is a force that is perpendicular to the direction of motion of airplanes, and being an aerodynamic force, it acts on a streamlined body that is traveling in the air.[23] With the lift force, heavy objects are able to overcome their weight to give a net upward force. The lift equation is given by $L = \frac{ClPv^2A}{2}$ where L is the lift, Cl is the lift coefficient, P is the density, V is the velocity, and A is the wing area of the airfoil.

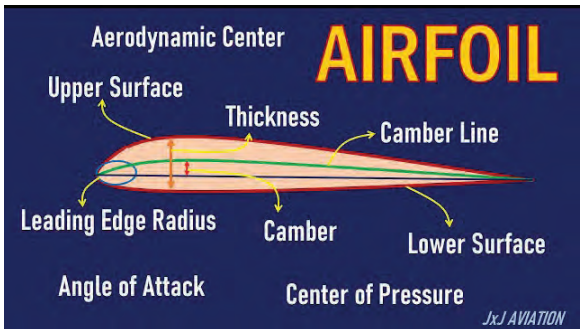

Figure 8: Diagram of an airfoil that shows the curved surface area of the wing.[24]

2.1. Mechanisms of Airfoils:

As shown in Figure 8, airfoils have a curved surface area on the upper surface. The air moving above the airfoil flows at a faster rate than the air moving below the airfoil. This creates an area of higher pressure below the wing and an area of lower pressure above the wing, creating a pressure difference. This pressure difference gives rise to a lift force, which acts in the upward direction, resulting in a net upward force, allowing the planes to fly.[25]

Additionally, Newton's third law, which explains how when a body exerts a force on another body, the latter will exert an equal and opposite force on the first body. When the wing pushes down on the air, the air will generate a force that is equal in magnitude but in the upward direction on the wing too, generating lift.[26]

■ Experiment

3.1. Overview of Experiment: Hypothesis, Apparatus Used, and Experimental Setup:

It was hypothesized that the airplane with the longest wings would travel the furthest horizontal distance, while the airplane with the thickest wings would travel the shortest horizontal distance.

This is because, for the airplane with the longest wings, it would be able to generate a greater lift force through its greater curved surface area, allowing the plane to have more time in the sky. This enables the plane to travel a further distance horizontally. On the other hand, while increasing the thickness of the wings can increase the lift force generated, it also increases the entire mass of the object, shortening the time the plane has in the air. Thus, the airplane with the thickest wings would travel the shortest horizontal distance.

An experiment was conducted to test the effects that changes to the length and thickness of the wings have on the flight performance. The airplane with the thickest wings (Figure 9) and the control airplane (Figure 10) were created using an A4 piece of paper, while the airplane with the longest wings (Figure 11) was created using an A4 and an A3 piece of paper. Both papers have a density of 80 grams per square meter.

DOI: 10.36838/IJHSR87.122

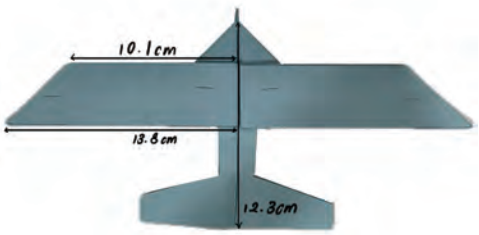

Figure 9: Paper airplane with the thickest wings (Plane T) of mass 6g that was used in the experiment.

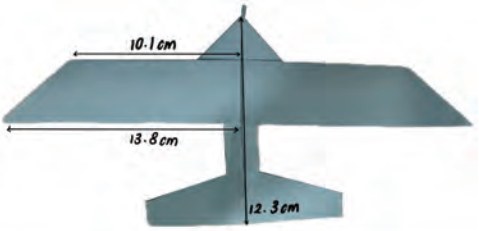

Figure 10: Control paper airplane (Plane C) of mass 3g that was used in the experiment.

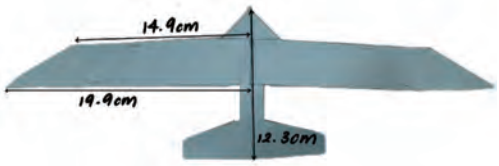

Figure 11: Paper airplane with a longer wing (Plane L) of mass 3g to experiment with the different structures of wings.

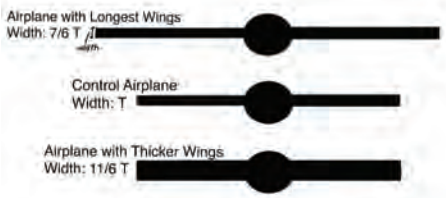

Figure 12: Overview of the thickness of all 3 paper airplanes that were used in the experiments.

During the experiment, I used a 5-meter measuring tape to measure the horizontal distance travelled by the airplane, and also used masking tape to indicate the starting position. Using a camera, I recorded the entire flight path of the airplane to allow for the checking of the flight distance later on. The launch angle and height were standardized by making sure that it started from the shoulder and was released at around a 45-degree angle from the horizontal. To ensure consistency between the data values, the experiment was conducted on the same day, and the windows were closed. Fans were also turned off to prevent any changes to the physical environment that may affect the flight performance of the planes. This ensures that any changes to flight paths were strictly due to the changes in the shape of the airplane. The drawings of the experimental setup are shown below.

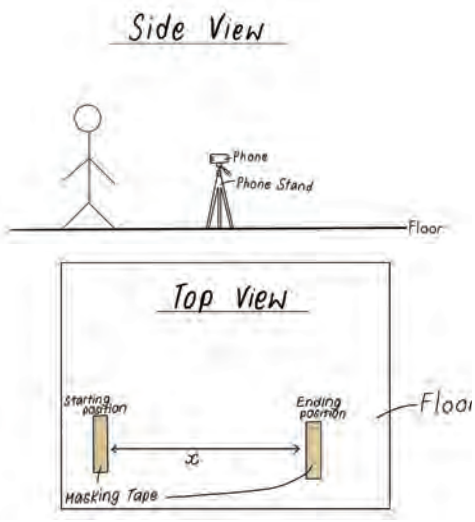

Figure 13: Experimental setup (not to scale) that was used to derive the results.

Results and Discussion

4.1. Overview of Experimental Results:

Table 1: Distance travelled by Plane C, Plane T, Plane L.

Horizontal distance travelled/m	Plane C	Plane T – plane with thicker wings	Plane L – plane with longer wings
Experiment 1	3.07	1.00	2.50
Experiment 2	2.72	1.09	2.75
Experiment 3	4.00	0.98	2.25
Experiment 4	3.00	1.21	2.76
Experiment 5	2.50	1.23	2.46
Experiment 6	2.60	0.98	2.22
Experiment 7	3.58	0.96	3.00
Experiment 8	2.19	1.08	2.48
Experiment 9	2.70	1.13	1.90
Experiment 10	2.33	1.15	2.77
Average	2.87 + 0.38	1.08 + 0.07	2.51 + 0.22

The confidence interval is reported at 95%.

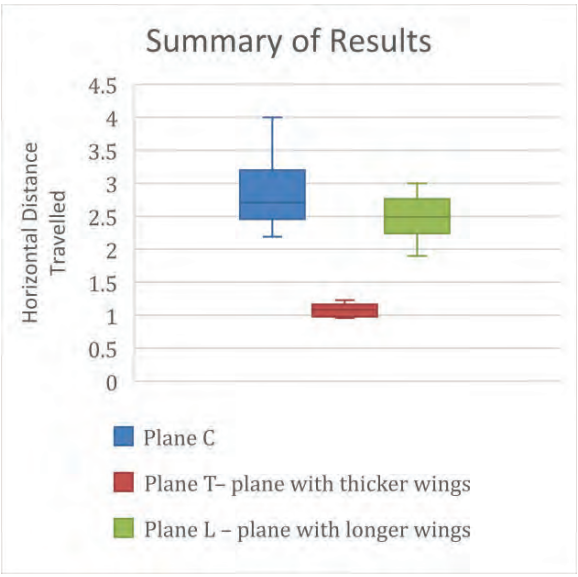

Figure 14: Box and whisker diagram of the results showing the spread of the horizontal distance travelled of each plane.

4.2. Discussion of Results:

The average horizontal distance travelled by Plane C was 2.90m with a standard deviation of 0.534, to 3 significant figures. The average horizontal distance travelled by Plane T was 1.10m with a standard deviation of 0.0936, to 3 significant figures. The average horizontal distance travelled by Plane L was 2.51m with a standard deviation of 0.309, to 3 significant figures.

From our results, it shows that Plane T travelled the shortest horizontal distance of an average of 1.10m, and this aligns with our hypothesis in section 3.1. This is because the increase in mass due to the thicker wing outweighed the increase in lift force for this experiment, resulting in an overall reduction in flight time and distance travelled. With an increase in the total mass, this would mean that the gravitational force acting on the object increases as the weight is proportional to mass. This would increase the downward force acting on the object, reducing the net upward force exerted on it. With a reduced net upward force, this would reduce the total time the object has in the air.

Furthermore, wing loading, which is the ratio of the total surface area of the wing and the weight of the object, should be taken into consideration in thicker wings.[27] A larger wing loading can reduce the lift the object is able to generate, as it leads to an increase in the separation of the leading-edge vortex.[28] As such, a balance must be achieved between increasing the lift force by using a thicker wing and increasing the mass of the airplane.

Plane L, with an average distance of 2.51m, did not travel the longest distance, and this contradicts our hypothesis. This may be because while an increase in length does increase the lift force, it makes the airplane less aerodynamic, thus increasing the drag experienced by the plane. This increase in drag slows the plane down, resulting in a shorter distance travelled.

Friction drag is due to the viscosity of the fluid the airplane is in and acts in the opposite direction to oppose the relative motion of the object in the air. Because the fluid is viscous, this will result in a frictional force exerted on the object, creating shear stress.[29] This is because for the object to move through the air, the object would have to push away the air molecules surrounding it. This drag force increases with speed, depends on the dimensions and shape of the object, and the type of liquid. With laminar flow, the drag force is directly proportional to the velocity, but with turbulent flow, the drag force is directly proportional to velocity squared. The proportionality constant reflects the shape and dimensions of the object, with a more streamlined shape resulting in a lower constant and thus a lower drag force.

When the length of the airfoil increases, more surface area is exposed to air flow, which could have made the object less streamlined. This would create more resistance to the motion of the plane in the air and hence increase the drag force acting on the object.

Since Plane C travelled the longest horizontal distance, this means that it was the most aerodynamic. On the other hand, Plane T travelled the shortest horizontal distance, showing how it was the least aerodynamic. Plane C's design is the most optimal because it balances the creation of lift with the mass and length of the wing, such that the weight of the wing does not result in too large a wing loading, and the length of the wing does not create too much drag force on it.

■ Conclusion

The experiment conducted investigated the flight performance of airplanes with three different wing shapes using: i) Control Plane C, ii) Plane T with a thicker wing, and iii) Plane L with a longer wing.

The results may show a relationship between the thickness of the wings and the mass of the airplane. The optimal ratio between the total mass of the airplane and the thickness of the wing is 5g to 1mm, but the ratio is based on the material used. This is because Plane C with a mass of 3g (figure 10), travelled the longest distance with an average of 287cm followed by Plane L with a mass of 3g (figure 11) which travelled an average of 251cm and lastly Plane T of mass 6g (figure 9) which travelled the shortest distance with an average of 108cm.

The result from the experiments applies to the real world. It highlights the need to consider factors such as wing loading and friction drag on the wings when constructing an aircraft that is the most efficient, as increasing the length or thickness of the wing excessively to increase the lift force can have a counterproductive effect on it.

If I had more resources, I would have crafted paper mâché planes, sealed them with glue, and tested them in a wind tunnel to obtain a more accurate set of data. Future work can include crafting a mathematical relationship between the wing cross-section and drag coefficient for different size classes of airplanes. A following experiment that can be carried out is experiments using an equal-mass build with a fixed-angle launcher, and to calculate the small aspect-ratio or thickness sweep to map trends.

Over the past 122 years, there have been great improvements and innovations to aircraft. It first started as a small 2-passenger plane with the Wright Flyer in Section 1.1 and now has advanced into larger 800-passenger planes, which are used by many today as a method of travel from one country to another. As of 2022, about 90% of Americans have taken a flight before, an increase from 63% in 1977.[30] In the future, one can expect the airline industry to further innovate and advance, changing how the world is connected.

■ Acknowledgments

I would like to thank Naveen Pillai for his mentorship and guidance throughout this whole process and for always being so inspiring and encouraging. I would also like to thank Indigo Research for giving me this opportunity. I attest that the ideas, writing, and graphics in this paper are entirely my own.

■ References

1. Aviation History: The scientific visionaries or those men before the Wrights. *The Postal History of ICAO* https://applications.icao.int/postalhistory/aviation_history_the_scientific_visionaries_or_those_men_before_the_wrights.htm (accessed July 23, 2025).

DOI: 10.36838/IJHSR87.122

2. 1903 Wright Flyer *National Air and Space Museum*, June 02, 2022. https://airandspace.si.edu/collection-objects/1903-wright-flyer/nasm_A19610048000 (accessed January 19, 2026).
3. The Wright Brothers Made History at Kitty Hawk *National Air and Space Museum*, June 23, 2022. https://airandspace.si.edu/stories/editorial/wright-brothers-made-history-kitty-hawk (accessed January 19, 2026).
4. Taking Flight With the Wright Brothers *National Geographic Kids* https://kids.nationalgeographic.com/history/article/wright-brothers#:~:text=As%20children%20in%20Dayton%2C%20Ohio,enough%20to%20hold%20them%20both (accessed January 19, 2026).
5. The Wright Brothers *National Air and Space Museum* https://airandspace.si.edu/explore/stories/wright-brothers#:~:text=The%20Wright%20brothers%20made%20their,air%20meets%20became%20huge%20celebrities. (accessed January 19, 2026).
6. Bejan, A.; Charles, J.D.; Lorente, S. The evolution of airplanes *Journal of Applied Physics* 2014, 116, 044901 DOI: https://doi.org/10.1063/1.4886855
7. Propellers Delta *Flight Museum* https://www.deltamuseum.org/research/history/aircraft/propellers (accessed January 19, 2026).
8. Kearney, K. 4 Ways Changes in Aircraft Design and Components Reduce Fuel Consumption *Honeywell* https://aerospace.honeywell.com/us/en/about-us/blogs/4-ways-changes-in-aircraft-design-and-components-reduce-fuel-con (accessed January 19, 2026).
9. Terefe, N.; Eidsmore, X.; Farah, A.; Why The Concorde Was Discontinued and Why It Wont Be Coming Back *The Museum of Flight*, June 25, 2019. https://blog.museumofflight.org/why-the-concorde-was-discontinued-and-why-it-wont-be-coming-back (accessed January 19, 2026).
10. Bugel. S.: Concorde completes latest journey-along Hudson River in New York. *The Guardian*, March 14, 2024. https://www.theguardian.com/world/2024/mar/14/concorde-completes-final-journey-along-hudson-river-in-new-york
11. Concorde. *Encyclopedia Britannica*. https://www.britannica.com/technology/Concorde (accessed January 19, 2026).
12. Blake, J.; How Many Commercial Planes Crash a Year? *BitLux*, September 5, 2024. https://flybitlux.com/how-many-commercial-planes-crash-a-year/ (accessed January 19, 2026).
13. Paige Chelvan, V.; Annuar, A.; Pearlman, J.; SQ321 incident: One year on, passengers recall how extreme turbulence upended their lives. *The Straits Times*, May 21, 2025. https://www.straitstimes.com/singapore/transport/sq321-incident-one-year-on-passengers-recall-how-extreme-turbulence-upended-their-lives
14. Lasky, J.; Boeing 737 *EBSCO* 2024 https://www.ebsco.com/research-starters/science/boeing-737#:~:text=The%20Boeing%20737%20is%20a,aircraft%20in%20commercial%20aviation%20history (accessed January 19, 2026).
15. Flynn, D.; Review: Singapore Airlines 737 MAX business class *Executive Traveller*, August 28, 2024. https://www.executive-traveller.com/singapore-airlines-737-max-business-class-review (accessed January 19, 2026).
16. Empennage. *What is Empennage?* https://www.empennage.org/what-is-empennage (accessed January 19, 2026).
17. Heli Start http://www.helistart.com/HelicopterTheoryAbstract.aspx (accessed January 19, 2026).
18. NASA STEM Team What is a Helicopter? (Grades K-4) *NASA* May 21, 2014. https://www.nasa.gov/learning-resources/for-kids-and-students/what-is-a-helicopter-grades-k-4/#:~:text=Helicopters%20can%20move%20large%20objects,and%20by%20people%20on%20vacation (accessed January 19, 2026).
19. How do Helicopters Fly? Understanding the Aerodynamics *Helicopter Pro Flight Training* https://www.helicopterpro.com/blog/how-do-helicopters-fly/ (accessed January 19, 2026).
20. Helicopter Aerodynamics: Understanding How Helicopters Fly *Cadence* https://resources.system-analysis.cadence.com/blog/msa2022-helicopter-aerodynamics-understanding-how-helicopters-fly (accessed January 19, 2026).
21. Cessna 180 Skywagon *Wipaire* https://www.wipaire.com/aircraft_page/cessna-180-skywagon/ (accessed January 19, 2026).
22. How do Seaplane Floats Work? *Hartzell Propeller*, February 1, 2019. How Do Seaplane Floats Work? - Hartzell Propeller (accessed January 19, 2026).
23. What is Lift, Drag, and Pitch? *Simscale* https://www.simscale.com/docs/simwiki/lift-drag-pitch/ (accessed January 19, 2026).
24. What is an Airfoil? | Understanding some Terms and Definitions related to an Airfoil! *JxJ Aviation*. YouTube, November 2, 2021. https://www.youtube.com/watch?v=6wgrDBa-AXo (accessed January 19, 2026).
25. Dynamics of Flight *NASA* https://www.grc.nasa.gov/www/k-12/UEET/StudentSite/dynamicsofflight.html#:~:text=Airplane%20wings%20are%20shaped%20to,wing%20up%20into%20the%20air (accessed January 19, 2026).
26. Sadrehaghighi, I. Aerodynamics of Airfoils and Wings (including Case Studies), *Research Gate* 2023 DOI: 10.13140/RG.2.2.12882.63682/1 (PDF) Aerodynamics of Airfoils and Wings (including Case Studies)
27. Liu, C.; Wang, T.; Zeng, L.; Li, J.; Shao, X. Effects of Wing Loading on the Aerodynamic Characteristics of Autorotating Maple Speeds *Physics of Fluids* 2024 36, 031908 DOI: https://doi.org/10.1063/5.0187358
28. Fu, M. Research on the Aerodynamic Causes of Airplane Wings. *Theoretical and Natural Science* 2024 DOI: 10.54254/2753-8818/36/20240519
29. Wing Loading (W/S) *Science Direct* Wing Loading (W/S) - an overview | ScienceDirect Topics (accessed January 19, 2026).
30. New Survey: Nearly 90 Percent of Americans Have Flown Commercially *Airlines of America*, March 22, 2023. https://www.airlines.org/new-survey-nearly-90-percent-of-americans-have-flown-commercially/#:~:text=The%20survey%20showed%20that%2C%20in,had%20flown%20in%20their%20lifetime (accessed January 19, 2026).

Author

Hannah Choo is a student at Hwa Chong Institution (College Section), living in Singapore. She is someone who is interested in the Science, Technology, Engineering, and Mathematics (STEM) related subjects, and hopes to pursue a career in one of these areas in the future.

IJHSR
ijhighschoolresearch.org
REVIEW ARTICLE

The War on Superbugs: Teixobactin, and a New Frontier in Antibiotic Resistance

Michael Peng

Upper Canada College, 200 Lonsdale Road, Toronto, Ontario, M4V 2X8, Canada; michael.peng52008@gmail.com

ABSTRACT: An increasing rise in antimicrobial resistance is an alarming threat to health and well-being globally. Antibiotic resistance specifically is cause for alarm, as it renders many commonly used classes of antibiotics ineffective. The World Health Organization has developed different strategies to combat antibiotic resistance, one of those being research and development of new classes of drugs that are immune to antibiotic resistance. The objective of this paper is to evaluate traditional teixobactin and its different analogues, looking at their accessibility and potency. Data and research were collected from a variety of different studies and papers, which are listed in the references. Through this literature review, a few important conclusions about teixobactin and its analogues can be made. First, teixobactin has a unique structure and rare amino acid enduracididine, enabling it to use a "dual pronged" mechanism in killing off bacteria. Different teixobactin analogues attempt to solve the difficulty in synthesizing traditional teixobactin at a low cost, while also maintaining effectiveness. One study was able to achieve gram-scale total synthesis, while increasing the teixobactin analogue's potency, bringing teixobactin closer to becoming a clinically accessible antibiotic. More research needs to be done in the future to find teixobactin analogues effective against gram-negative bacteria.

KEYWORDS: Biochemistry, Medical Biochemistry, Antibiotic Resistance, Teixobactin.

Introduction

Antimicrobial resistance, specifically antibiotic resistance, is an increasingly dangerous threat to global health. In 2019, antimicrobial resistance was directly responsible for 1.27 million deaths and contributed to 4.95 million deaths globally. Antibiotic resistance occurs because bacteria evolve due to selective pressures and begin to resist the effects of antibiotic medicines, making standard treatments harder and leading to persistent infections.[1] Antibiotic resistance could result in 40 million deaths by 2050, and 2 million could die yearly by the middle of this century. Medical procedures can also become harder, as most require the use of antibiotics to prevent infections. Antibiotic resistance is also a significant economic burden, as it can lead to up to 3.4 trillion dollars in global costs by 2030.[1] Antibiotic resistance poses a significant health challenge and must be dealt with appropriately.[2]

There have been efforts to help prevent the severe harms of antibiotic resistance from spreading globally. The World Health Organization (WHO) has its own Global Action Plan. Adopted in 2015, it encourages countries to develop methods to combat antimicrobial resistance. Antimicrobial stewardship is another method they suggest, where governments seek to educate the public on how to use antimicrobials responsibly. Research and development is another strategy, where new antibiotics, vaccines, and diagnostics are created to fight infections.[1] Currently, there is not enough attention on research and development of new antibiotics, which is a major issue globally.[1]

Several factors contribute the most to antibiotic resistance. The first is the overuse and misuse of antibiotics. Excessive use in humans, animals, and agriculture directly contributes to the resistance, as overuse puts greater pressure on bacteria to evolve. Poor control of infections also contributes to the issue, as a lack of sanitation facilitates the spread of pathogens.[1]

One of the most dangerous bacteria that develops antibiotic resistance is the gram-negative ones. They often cause the deadliest infections and have a particularly strong drug resistance. Gram-negative bacteria are also resistant to carbapenem drugs (Figure 1), which are used to treat severe microbial infections. Deaths from carbapenem-resistant gram-negative bacteria have risen by almost 150% from 1990 to 2021.[2]

Teixobactin (Figure 2) is a novel antibiotic that differs in structure and class from other antibiotics, such as carbapenems. This review paper will focus on recent research and development of teixobactin and its general immunity to antibiotic resistance. This paper aims to analyse whether teixobactin and its different derivatives and analogues could contribute to the fight against antibiotic resistance.

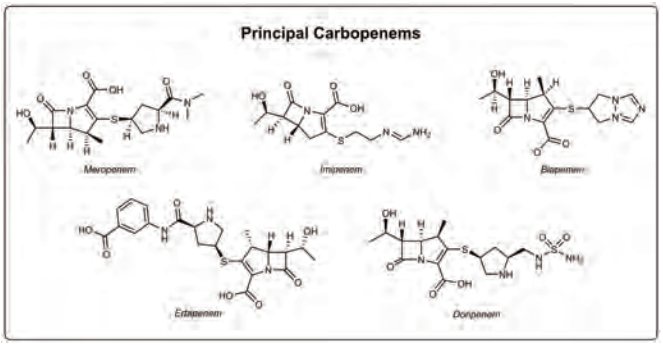

Figure 1: Chemical structures of representative carbapenems (meropenem, imipenem, biapenem, ertapenem, doripenem) are last-resort antibiotics for multidrug-resistant gram-negative bacteria.

© 2026 Terra Science and Education

DOI: 10.36838/IJHSR87.128

Discussion

Introduction to Teixobactin:

One important discovery in the recent fight against antibiotic resistance is teixobactin. Teixobactin is isolated from *Eleftheria terrae*, which is an uncultured gram-negative bacterium. *Eleftheria terrae* is cultivated using iChip technology. Teixobactin is a cyclic undecapeptide with four D-amino acids. It has one rare amino acid, which is L-allo-enduracididine (Figure 2). Enduracididine occurs rarely in nature, and teixobactin is one of the places the amino acid can be found in.[3] The mechanism through which teixobactin functions enables it to reduce antibiotic resistance. Teixobactin uses dual inhibition, where it targets both the peptidoglycan and wall teichoic acid precursors through binding to lipid II and lipid III, respectively. The way that teixobactin avoids antibiotic resistance is by binding to cell wall precursors rather than proteins.[3] Teixobactin binds in a 2:1 molar ratio with lipids, those being lipid I, II, III, and undecaprenyl pyrophosphate. The minimal binding motif of teixobactin is the pyrophosphate moiety and polyprenyl chain. Attacking the precursors curtails the genetic alteration of teixobactin's drug target in pathogenic bacteria, which prevents a common method of antibiotic resistance.[3] Additionally, because teixobactin targets lipid precursors, bacteria cannot mutate easily without disabling the cell wall itself and causing cell death, thus further lowering the chance of developing resistance.[4]

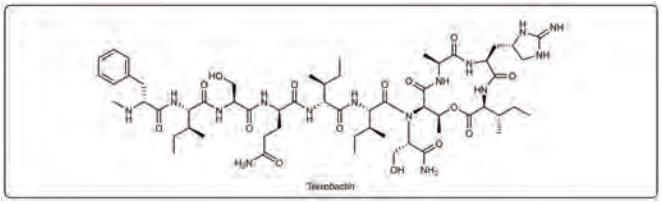

Figure 2: Chemical structure of teixobactin, a novel antibiotic with a unique scaffold that shows activity against multidrug-resistant gram-positive bacteria.

Studies claim that there are no resistant *S. aureus* mutants, a gram-positive bacterium, that have emerged in sub-MIC serial passaging. It is relevant to note that modification of the residues of the core ring structure of teixobactin can inhibit its biological activity. However, in Arg10-teixobactin, L-Ser3, D-Gln4, and Ala9 residues can be substituted with the corresponding enantiomer of lysine, and it will have similar functionality to that of Arg10-teixobactin.[3]

Comparison of Teixobactin to Other Antibiotics:

One of the studies investigated whether a bacterium like Staphylococcus aureus could evolve resistance to Arg10-teixobactin, and then compared it to moenomycin A and rifampicin, two other antibiotics. The experiment lasted 75 days, which is 500 generations, with antibiotic pressure. MICs were measured every 5 days, and whole genome sequencing was used to identify mutations. What the research found was that Arg10-teixobactin resistance evolved around 2,500 times slower than rifampicin, and around 320 times slower than moenomycin A. After withdrawal of the antibiotic after day 45 of the experiment, Arg10-teixobactin resistance dropped back to baseline within 30 days. This indicates a high fitness cost to teixobactin resistance, while antibiotics like moenomycin A and rifampicin experienced more persistent resistance. What this study shows is that Arg10-teixobactin has slow resistance and a high cost of resistance, which the other antibiotics do not possess to a high degree.[5]

Effectiveness of Teixobactin on Drug-resistant Bacteria:

One study investigated the antimicrobial activity of three teixobactin derivatives (Figure 3) against drug-resistant clinical isolates, specifically Methicillin-resistant *Staphylococcus aureus* (MRSA) and Vancomycin-resistant *Enterococcus* (VRE). The aim was to identify the most effective derivative by comparing its minimum inhibitory concentration (MIC). The MIC values for each compound against MRSA and VRE are summarized in Tables 1 and 2.

The results showed that compound **2**, specifically Lys10-teixobactin, exhibited the best performance in terms of MIC, although compound **3** was also effective. They are either comparable or superior to traditional drugs, showing promising signs that some teixobactin derivatives are effective against antibiotic-resistant bacteria.

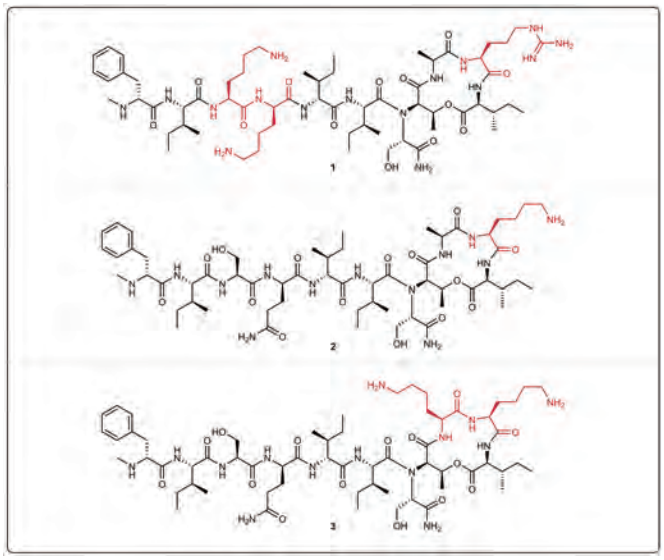

Figure 3: Chemical structures of teixobactin derivatives **1**, **2**, and **3** were investigated for activity against MRSA and VRE. Structural modifications compared to native teixobactin are highlighted in red. Derivative 2 showed the greatest resistance to MRSA and VRE.

Table 1: Minimum inhibitory concentration (μg/ml) of teixobactin derivatives against methicillin-resistant *Staphylococcus aureus* (MRSA).[6]

Isolates	Origin[a]	Species	1	2	3	Vancomycin	Ampicillin
			MIC (μg/ml)	MIC (μg/ml)	MIC (μg/ml)	MIC (μg/ml)	MIC (μg/ml)
B11970	Blood	*S. aureus*	32	2	2	1	>512
P10781	Nasal	*S. aureus*	32	2	2	1	>512
P10747	CVP	*S. aureus*	32	2	2	1	>512
S37938	-	*S. aureus*	32	2	2	1	>512
S18155	ETT	*S. aureus*	32	2	2	0.5	>512
B13178	Blood	*S. aureus*	32	2	22	1	>512
440260	-	*S. aureus*	32	4	4	1	>512
S18970	-	*S. aureus*	32	2	2	1	>512
P11520	Pus	*S. aureus*	32	4	4	1	512
T5683	Nasal	*S. aureus*	32	2	2	1	>512
	MIC50		32	2	2	1	>512

[a]ETT, Endotracheal tube; CVP, Central venous catheter, -, Missing data.

Table 2: Minimum inhibitory concentration (μg/ml) of teixobactin derivatives against vancomycin-resistant *Enterococcus faecium* (VRE).[6]

Isolates	Species	1	2	3	Vancomycin
		MIC (μg/ml)	MIC (μg/ml)	MIC (μg/ml)	MIC (μg/ml)
951245282 (A)	*Enterococcus faecium*	8	4	4	>128
951234856 (B)	*Enterococcus faecium*	16	4	4	>128
951208931 (C)	*Enterococcus faecium*	16	4	4	>128
938636470 (D)	*Enterococcus faecium*	16	8	4	>128
938666613 (E)	*Enterococcus faecium*	16	16	4	>128
938600912 (F)	*Enterococcus faecium*	16	2	8	>128
938072607 (G)	*Enterococcus faecium*	16	8	4	>128
944414000 (H)	*Enterococcus faecium*	16	8	4	>128
945530665 (I)	*Enterococcus faecium*	16	4	4	>128
U43821 (J)	*Enterococcus faecium*	16	8	4	>128
	MIC50		4	4	>128

Limitations of Teixobactin and the Promise of Its Derivatives:

While teixobactin certainly opens a path in the fight against antibiotic resistance, some challenges and setbacks currently need to be resolved. The first problem is that while teixobactin is effective, it's difficult and expensive to synthesize. This is because of two major reasons. First, L-allo-enduracididine takes seven steps to synthesize, making it very complicated. L-allo-enduracididine is generally a non-natural amino acid, making it even harder to access. Teixobactin also requires four D-amino acids. Together, these two problems limit teixobactin's production, as it's difficult to mass-produce and also make it cost-effective.[7] Another problem with teixobactin is that it is not effective against gram-negative bacteria. That is because gram-negative bacteria have an outer membrane barrier that renders teixobactin's binding mechanism unviable.[3] This is problematic because, as stated above, gram-negative bacteria can often cause the deadliest infections as they tend to have the highest antibiotic resistance, and there needs to be a solution.

There is now further research and studies that explore possibilities in resolving the problems that teixobactin faces. One of those solutions is to develop simpler and more cost-effective teixobactin analogues. One study approached this issue by replacing the complex peptide tail, residues 1-6, of teixobactin with lipid chains to create lipopeptidomimetics.[7] The study also tested substitutions of enduracididine with other amino acids. This teixobactin analogue they looked to research would also be focused on its antibacterial effects on *S. aureus* in particular. The following table contains the results of the different teixobactin analogues against *S. aureus* and *E. coli* bacterial strains in minimum inhibitory concentration (MIC) and minimum bactericidal concentration (MBC) values (Table 3). The lower both values are, the more effective an antibiotic is. What the study discovered is that farnesylation, which elongates the lipid chain, improves activity significantly in comparison to geranyl, a shorter chain, or no lipid tail at all. The study also found that basic amino acids at position 10, being the enduracididine, are essential because they have a positive charge, which facilitates interactions with bacterial membranes. Neutral, acidic, or non-polar substitutions at position 10 led to a loss in activity, while Lys10 was better than Arg10, despite the latter being more structurally similar to native allo-enduracididine.

Table 3: MIC and MBC values of teixobactin analogues (in μg/mL) against *S. aureus* ATCC 25923 and *E. coli* ATCC 25922.[7]

	S. aureus ATCC 25923		*E. coli* ATCC 25922
Compound	MIC	MBC	MIC
Arg_{10}-farnesylbactin (1)	16	>32	>32
Lys_{10}-farnesylbactin (2)	8	16	16
Orn_{10}-farnesylbactin (3)	8	16	32
Cit_{10}-farnesylbactin (4)	>32	>32	>32
His_{10}-farnesylbactin (5)	>32	>32	>32
Ala_{10}-farnesylbactin (6)	>32	>32	>32
Glu_{10}-farnesylbactin (7)	>32	>32	>32
Arg_{10}-geranylbactin (8)	>32	>32	>32
Lys_{10}-geranylbactin (9)	>32	>32	>32
Orn_{10}-geranylbactin (10)	>32	>32	>32
Cit_{10}-geranylbactin (11)	>32	>32	>32
His_{10}-gernaylbactin (12)	>32	>32	>32
Ala_{10}-geranylbactin (13)	>32	>32	>32
Glu_{10}gernaylbactin (14)	>32	>32	>32

DOI: 10.36838/IJHSR87.128

This study provides examples of farnesylated teixobactin analogues that show antimicrobial activity. These simplified teixobactin analogues can lead to new antibiotics that are cheaper and more accessible compared to conventional teixobactin, while still maintaining partial effectiveness and resistance to antibiotic resistance.[7]

Another study also looked to make teixobactin analogues so the antibiotic could become more accessible. The approach they took was to research whether teixobactin analogues with a modified tail stereochemistry, notably replacing the D-amino acids with L-amino acids, could still retain antibacterial activity. Previous studies found that any stereochemical change in the tail would eliminate all activity, so the researchers tried to introduce "swapmers". Swapmers are teixobactin analogues where pairs of D-amino acids are replaced with their L counterparts.[8] The study incorporated an O-acyl linkage to serine to address some synthesis challenges. The antibacterial efficacy of different teixobactin analogues against multiple bacterial species is presented in Table 4.

Table 4: MIC values of teixobactin, teixobactin prodrugs, and "swapmer" analogues in μg/mL.[a]

Compound	*Bacillus subtilis* ATCC 6051 MIC	*Staphylococcus epidermidis* ATCC 14990 MIC	*Staphylococcus aureus* (MSSA) ATCC 29213 MIC	*Staphylococcus aureus* (MRSA) ATCC 700698 MIC	*Escherichia coli* ATCC 10798 MIC
Lys_{10}-teixobactin (1)	≤0.0313	1	2	2	>32
$[Ile_9\text{-}O\text{-}Ser_7]Lys_{10}$-teixobactin ($Lys_{10}$-teixobactin prodrug 2)	≤0.0313	1	2	1-2	>32
$Ile_4Gln_5[Ile_9\text{-}O\text{-}Ser_7]Lys_{10}$-teixobactin ($Lys_{10}$-swapmer prodrug 3)	4	4	8	8	>32
N-Me-L-Phe_1,Ile_4,Gln_5,$[Ile_9\text{-}O\text{-}Ser_7]Lys_{10}$-teixobactin (L-tail swapmer 4)	≥32	>32	>32	>32	>32
N-Bn-Gly_1,Ile_4,Gln_5,$[Ile_9\text{-}O\text{-}Ser_7]Lys_{10}$-teixobactin (peptoid swapmer 5)	32	>32	>32	>32	>32
Arg_{10}-teixobactin (6)	≤0.0313	0.5	2	2	>32
$[Ile_9\text{-}O\text{-}Ser_7]Arg_{10}$-teixobactin ($Arg_{10}$-teixobactin prodrug 7)	0.0625	0.5	2	1	>32
$Ile_4Gln_5[Ile_9\text{-}O\text{-}Ser_7]Arg_{10}$-teixobactin ($Arg_{10}$-swapmer prodrug 8)	2	2	4	4	>32
N-Me-Phe_8,Gln_{11},Ile_4,Gln_5,$[Ile_9\text{-}O\text{-}Ser_7]Arg_{10}$-teixobactin (extended-tail swapmer 9)	>32	>32	>32	>32	>32
vancomycin	0.125-0.25	1-2	1-2	4	>32

[a]MIC assays were performed in the presence of 0.002% polysorbate 80.

The results showed that swapmers 3 and 8 maintained partial activity, although effectiveness was around 2-4 times worse compared to native teixobactin. D-stereochemistry at position 1 was also essential for the teixobactin to function properly. The conclusion of the study is thus that pairwise stereochemical swapping can be tolerated, maintaining its structure and preserving partial activity. The D-amino acid in position 1 is indispensable, however. This study is another effort at finding more synthetically accessible analogues that still retain activity. The next step is ensuring similar effectiveness to native teixobactin.[8]

Finally, one report surrounding teixobactin looked to, once again, find a way to make the antibiotic more accessible. While previous researchers had been able to achieve milligram-scale total synthesis, this study's goal was to achieve gram-scale total synthesis of teixobactin. It also wanted to further discover more potent analogues for clinical development. The study was able to innovate by developing a one-pot, one-hour synthesis of the L-allo-End building block with 66% yield and excellent stereoselectivity. This is crucial, as L-allo-End is one of the complicated portions of teixobactin to synthesize. The study then used a convergent 3+2+6 strategy to construct a cyclic pentapeptide and a linear hexapeptide separately, then joined them together to form the full-length teixobactin. To go even further, the researchers reasoned that the methyl group on N-Me-D-Phe1 was not essential, so they created a series of different teixobactin analogs and tested their efficacy. The most effective ones were found to be compounds **4** and **5** (Figure 4). Compound 4 demonstrated higher potency than traditional teixobactin, while compound **5** was 8 times better.[9] This is a major advancement in teixobactin development, as this study finds an efficient synthetic route for larger-scale teixobactin production, while also producing analogues with improved potency.

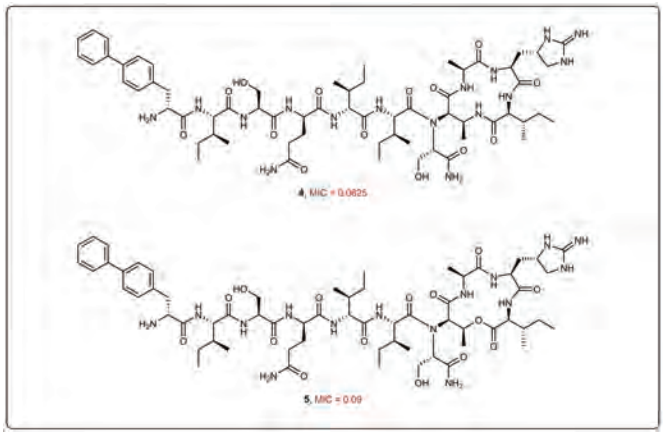

Figure 4: Chemical structure of compound **4** and compound **5**.

Conclusion

Teixobactin offers a new path forward in fighting antibiotic resistance. The different teixobactin derivatives and analogues also help improve upon the accessibility and cost-effectiveness issues that traditional teixobactin faces. While the scalability and economic issues are being addressed, one big possibility moving forward is to make teixobactin analogues that are effective against gram-negative bacteria. Many gram-negative bacteria pose the largest threat to human life, as they are highly resistant to many classes of antibiotics. There is research currently that shows highly hydrophobic derivatives of teixobactin can have some activity against gram-negative bacteria at high concentrations, but more work needs to be done to increase its potency.[9] Antibiotic resistance will become an ever-growing threat to human health and wellbeing, which is why developments in drugs like teixobactin are crucial for the future.

Acknowledgments

Thank you to my parents for supporting my research and educational opportunities. Thank you to my school for educating my friends and me, and for giving me support throughout my educational process. Thank you to Daria Sokolova for helping me proofread, edit, and suggest changes for this review.

References

1. World Health Organization. *Global Analysis of Health Workers' Migration and Mobility: A Synthesis Report*; World Health Organization: Geneva, 2022.
2. Naddaf, M. 40 Million Deaths by 2050: Toll of Drug-Resistant Infections to Rise by 70%. *Nature.com* **2024**, *633*. https://doi.org/10.1038/d41586-024-03033-w.
3. Fiers, W. D.; Craighead, M.; Singh, I. Teixobactin and Its Analogues: A New Hope in Antibiotic Discovery. *ACS Infectious Diseases* **2017**, *3* (10), 688–690. https://doi.org/10.1021/acsinfecdis.7b00108.
4. Ling, L. L.; Schneider, T.; Peoples, A. J.; Spoering, A. L.; Engels, I.; Conlon, B. P.; Mueller, A.; Schäberle, T. F.; Hughes, D. E.; Epstein, S.; Jones, M.; Lazarides, L.; Steadman, V. A.; Cohen, D. R.; Felix, C. R.; Fetterman, K. A.; Millett, W. P.; Nitti, A. G.; Zullo, A. M.; Chen, C. A New Antibiotic Kills Pathogens without Detectable Resistance. *Nature* **2015**, *517* (7535), 455–459. https://doi.org/10.1038/nature14098.
5. Lloyd, D. G.; Schofield, B. J.; Goddard, M. R.; Taylor, E. J. De Novo Resistance to Arg10-Teixobactin Occurs Slowly and Is Costly. *Antimicrobial Agents and Chemotherapy* **2020**, *65* (1). https://doi.org/10.1128/aac.01152-20.
6. Ramchuran, E. J.; Somboro, A. M.; Abdel Monaim, S. A. H.; Amoako, D. G.; Parboosing, R.; Kumalo, H. M.; Agrawal, N.; Albericio, F.; Torre, B. G. de L.; Bester, L. A. *In Vitro* Antibacterial Activity of Teixobactin Derivatives on Clinically Relevant Bacterial Isolates. *Frontiers in Microbiology* **2018**, *9*. https://doi.org/10.3389/fmicb.2018.01535.
7. Girt, G. C.; Mahindra, A.; Al Jabri, Z. J. H.; De Ste Croix, M.; Oggioni, M. R.; Jamieson, A. G. Lipopeptidomimetics Derived from Teixobactin Have Potent Antibacterial Activity against Staphylococcus Aureus. *Chemical Communications* **2018**, *54* (22), 2767–2770. https://doi.org/10.1039/c7cc06093a.
8. Griffin, J. H.; Mendoza, A.-T.; Nowick, J. S. Teixobactin "Swapmers" with L-Tail Stereochemistry Retain Antibiotic Activity. *The Journal of Organic Chemistry* **2024**, *89* (20), 15325–15330. https://doi.org/10.1021/acs.joc.4c01674.
9. Zong, Y.; Fang, F.; Meyer, K. J.; Wang, L.; Ni, Z.; Gao, H.; Lewis, K.; Zhang, J.; Rao, Y. Gram-Scale Total Synthesis of Teixobactin Promoting Binding Mode Study and Discovery of More Potent Antibiotics. *Nature Communications* **2019**, *10* (1). https://doi.org/10.1038/s41467-019-11211-y.

Author

Michael Peng is a grade 12 student at Upper Canada College and would like to pursue either a Public Health major in the United States or a Health Sciences major in Canada. He enjoys reading books, especially ones about philosophy and ethics.

DOI: 10.36838/IJHSR87.128

IJHSR
ijhighschoolresearch.org
REVIEW ARTICLE

Temporal Lobe Epilepsy and Autoimmune Disorder Associations and Mechanisms: A Scoping Review

Sanvi S. Singh

Academy of Allied Health and Science 2325 Heck Ave, Neptune, NJ, 07753, USA; sanvisarit2008@gmail.com
Mentor: Sinead M. Sinnott, PhD

ABSTRACT: Temporal Lobe Epilepsy (TLE) is a common form of epilepsy defined by seizures that specifically arise from the temporal lobe, an area of the brain vital for emotional processing and memory. TLE can be associated with several autoimmune conditions through underlying mechanisms, including Systemic Lupus Erythematosus, Hemolytic Anemia, and Type II Diabetes Mellitus (T2DM). This scoping review explores possible pathways and associations between the conditions. Examining inflammatory markers alongside stress-related pathways, including the hypothalamic-pituitary-adrenal (HPA) Axis, helps formulate these correlations. SLE and TLE are suggested to have a bidirectional relationship due to shared inflammatory processes and heightened expression of specific cytokines (e.g., IL-18). Evidence suggests that Hemolytic Anemia shares a relationship with epilepsy through the use of antiseizure medication, which can trigger further immune responses, ultimately resulting in hemolysis. T2DM is associated with TLE through heightened stress responses. Elevated cortisol levels and increased HPA axis activity are common mechanisms underlying both. Given the evidence, treatment implications include exploring complementary and alternative medicine to reduce the risk of developing these autoimmune disorders. Future studies should further explore the pathways behind hemolytic anemia and TLE to understand these comorbidities.

KEYWORDS: Cellular and Molecular Biology, Neurobiology, Epilepsy, Autoimmune.

Introduction

Epilepsy is a neurological condition defined by the presence of two or more seizures occurring within 24 hours, leaving lasting effects on both caregivers and those living with the condition. This condition is characterized by increased electrical activity in the brain, which can lead to seizures. In the United States, epilepsy impacts the lives of 3.4 million people.[1]

Epilepsy has been posited to be associated with a wide range of causes, one of which is chronic stress. Stress is associated with seizure occurrence and frequency,[2] as well as with Temporal Lobe Epilepsy (TLE). Heightened activity in brain regions such as the amygdala and hippocampus is implicated in TLE, and this heightened activity is one pathway through which seizures occur. TLE can subsequently lead to temporal lobe degeneration and dysfunction, particularly in the amygdala and hippocampus.[3] The bidirectional relationship between stress and seizures may be partially due to social stigma and fears of having a seizure in epileptic patients. Seizures occur when the balance between inhibitory and excitatory neurotransmitters is disturbed, leading to hyperexcitability, which is typically expressed as a seizure.[4] Seizures can also occur through an imbalance of ions in an action potential, a process that allows neurons to communicate.[4]

The hypothalamic-pituitary-adrenal (HPA) axis directly contributes to exacerbating stress responses, including increased release of glucocorticoids such as cortisol (with the assistance of adrenocorticotropic hormone and corticotropin-releasing hormone).[5] The limbic system, which regulates emotional processing, is directly involved in HPA axis *inhibition*, where the hippocampus antagonizes responses while the amygdala induces this glucocorticoid secretion.[6] Exacerbated levels of cortisol and glucocorticoids can result in hippocampal dendritic retraction, a form of reversible plasticity. Additionally, it can cause hippocampal damage, impairing memory and emotion, and reducing neurogenesis.[7] Therefore, this becomes a possible pathway for a seizure to occur. Increased neuronal activity in brain regions (such as the hippocampus) can cause inflammation during prolonged periods of stress.[8] Inflammation is the body's immune response to stimuli and external stressors it perceives as potentially dangerous or harmful.[8] This can have systemic effects, leading to inflammation in the entire body.

To understand epilepsy, stress, and autoimmune comorbidities, it is necessary to understand the bidirectional relationship between seizures and inflammation. When individuals experience seizures, pro-inflammatory cytokines and other mediators released by neurons and glial cells are activated, leading to inflammation.[9] Similarly, pre-existing inflammation can elevate these same mediators, disrupting the brain's excitatory/inhibitory balance and causing seizures.

Inflammation is correlated with, and is a predictor of, autoimmune disorders, given that inflammation is often a marker of overactive immune responses.[9] Some of the most common autoimmune conditions that are comorbid with epilepsy are Diabetes Mellitus, Systemic Lupus Erythematosus, and Hemolytic Anemia; these autoimmune conditions have both direct and indirect correlations with epilepsy. Systemic Lupus Erythematosus (SLE) is an autoimmune, multisystemic condition that primarily affects the body's connective tissue and nearly every organ system (skin, lungs, heart, etc.), affecting

© 2026 Terra Science and Education

DOI: 10.36838/IJHSR87.133

approximately 200,000 people in the USA.10 SLE causes inflammation in these body parts due to the immune system attacking its own cells. The production of autoantibodies and tissue injury impacts the likelihood of developing SLE, through environmental and maladaptive health behaviors that can also contribute to SLE development, such as smoking, sunlight, and certain medications.[11] Diabetes Mellitus (also known as Type II Diabetes) is characterized by hyperglycemia due to reduced insulin production; the prevalence of T2DM is about 11.6% of the US population.[12] Hemolytic Anemia is identified as a life-threatening and chronic condition caused by the destruction of premature red blood cells. Immune-mediated hemolysis can occur intravascularly, extravascularly, or in the reticuloendothelial system. Systemic inflammation can occur due to autoantibody production following the response to hemolytic anemia. It is novel to consider the potential comorbidities of epilepsy with these life-threatening conditions to find potential routes for prevention.

Taken together, while existing literature has shown associations between epilepsy and autoimmune disorders, there is a need to understand the mechanisms between these conditions. This scoping review aims to provide a synopsis of potential mechanisms by addressing the following aims:

1. We examined the associations between temporal lobe epilepsy and autoimmune disorders (DM, Lupus, HA).

2. We explore autoimmune processes/mechanisms underlying the potential relationships between epilepsy and common comorbid autoimmune disorders (DM, Lupus, HA).

Method

This scoping review searched Google Scholar and PubMed for relevant manuscripts.

The following keywords were used to search: ["Epilepsy" OR "seizure" AND "Neuroimmune" OR "autoimmune disorders" OR "diabetes" OR "lupus" AND "mechanisms"], as well as the search ["Epilepsy" OR "seizure" AND "autoimmune" OR "neuroimmune" OR "diabetes" OR "lupus" AND "development" OR "severity" AND "preventative" OR "health behaviors" OR "diet" or "exercise"]. Studies were included if they were primarily observational or review studies examining epilepsy and at least one autoimmune disorder. We excluded studies that used animal samples and included only those involving human subjects. Studies were not excluded based on publication date or participant age. We included 12 studies in our review (see Table 1 for study details). We examined the overall relationship between epilepsy and autoimmune disorders, then identified relevant themes and mechanisms from the literature. All results presented in the manuscript are results from existing experimental studies and reviews.

Discussion

We examine the mechanisms between epilepsy and three common comorbid autoimmune disorders, SLE, HA, and T2DM, to better understand their causes and therefore future treatment (see Table 1 for study descriptions).

Systemic Lupus Erythematosus:

Systemic Lupus Erythematosus (SLE) has a bidirectional correlation with epilepsy.[13] One subcategory of SLE, neuropsychiatric SLE, is particularly associated with seizures as a symptom. In this population, previous studies have identified specific antibodies, antiphospholipid antibodies, which are associated with epilepsy.

One proposed pathway through which SLE leads to epilepsy is through neural mechanisms. SLE is a systemic autoimmune disease that affects multiple organs and organ systems and can damage the immune system, potentially leading to neuronal injury. Seizures have also been proposed as a secondary pro-inflammatory process in the condition.[14] These injuries to the body's nervous system can cause cortical thrombosis (blood clots) in the meninges of the brain. The blood clots prevent the brain from receiving adequate oxygen, blood, and other vital nutrients. Then, the lack of these nutrients causes an increased risk of seizures and, in turn, epilepsy.[15]

In addition to SLE increasing the risk of epilepsy, evidence has been found to suggest epilepsy has an impact on the symptoms/presence of SLE by way of antiseizure medications (ASMs). Antiseizure medications have been found to increase pro-inflammatory cytokines, specifically IL-18.[16] IL-18 is a significant marker for astrocyte activity in the brain. These proinflammatory markers signify an active nervous system due to the astrocyte's role in synaptogenesis, the process of forming new connections known as synapses in the brain, and transmission.[17] Higher levels of inflammation (IL-18) are associated with SLE.[18]

Despite the suggestions of epilepsy and SLE impacting one another, limited evidence and research are examining the mechanisms behind these bidirectional comorbid disorders. The mechanisms of how the body's immune system causes neuronal damage remain uncertain. Additionally, there is limited research suggesting the correlation between anti-seizure medications causing increased IL-18 and IL-18, then increasing the risk of SLE.

Hemolytic Anemia:

In addition to SLE, HA, and epilepsy, they represent a similar correlation to suggest comorbidity; they are connected through anti-seizure medication (ASM) pathways. One review in particular, by Padda and colleagues,[19] examined the role of ASMs in the association between epilepsy and anemia. Taking antiseizure medications increases the likelihood of developing hemolytic anemia. ASMs bind to the cell membrane via a non-haptene reaction, leading to the production of antibodies that coat the cell.[20] This coating results in the activation of a system directly related to hemolysis (the breakdown of red blood cells) or activation of antibody-dependent-cellular-cytotoxicity; these cells are considered to be natural killer cells.[19,21] The medication will similarly bind to the red blood cell (erythrocyte) membrane in heptane reactions within ASM. The immune system will eventually recognize the ASM as a foreign substance, leading to B-cell-mediated hemolysis via the antibodies produced.[19]

Furthermore, another predicted correlation between seizure medications/epilepsy and hemolytic anemia is the process of potential oxidative injury. Metabolic processes in anti-seizure medications can render red blood cell membranes susceptible to lipid peroxidation. The body's cell membranes are made of primary lipids, and the peroxidation process induces the deterioration of these macromolecules. This can cause certain cases of hemolysis.[19]

However, conflicting literature has been proposed by Padda and colleagues,[19] where anti-seizure medication such as oxcarbazepine has been shown to induce hemolytic anemia in the case of a 75-year-old male. On the contrary, the literature suggests that oxidative injury primarily induces hemolysis, which is inconsistent with pathways implicated in hemolytic anemia and epilepsy. The potentially overlapping mechanisms suggest the need for further research regarding specific pathways.

Type II Diabetes Mellitus:

Epilepsy has been found to have a one-way correlation with Type II Diabetes Mellitus (T2DM). One mechanism suggesting this comorbidity is the hypothalamic arousal in patients with epilepsy. It has been reported that epileptic patients generally have higher levels of cortisol in their bodies due to neurotransmitter alterations and stress from seizures.[22] The hypothalamic-pituitary axis, or HPA Axis, is very active in producing cortisol in the body.[5] Elevated cortisol induces the release of stored glucose, leading to persistently high blood sugar (hyperglycemia). It is vital to remember that T2DM is caused by a deficiency of pancreatic insulin secretion, leading to elevated glucose levels.[23]

Physiological stress has been suggested to exacerbate and increase the risk of autoimmune disease as well. Epilepsy has a direct impact on the body's immune system, as previously mentioned. In particular, the development of epilepsy is associated with elevated levels of IL-1β, IL-6, and tumor necrosis factor-alpha (TNF), which are active immune system markers.[24] Each of these inflammatory markers is also elevated in T2DM.25

The existence of mental health stigma is indirectly correlated with the presence of diabetes. Epileptic patients are less likely to exercise and take care of their physical well-being in fear of having seizures; to prevent themselves from a risky situation, they limit themselves in all social aspects of life. This lack of long-term exercise can simultaneously induce obesity and lead to weight and blood sugar issues. Obesity can lead to hyperglycemia because the body is in a suboptimal physical condition.

Conflicts in Literature:

The reviews we examined regarding hemolytic anemia had limited information on the biological processes and evidence of comorbidity to epilepsy in comparison to SLE and T2DM. There was not much information regarding the mechanisms behind epilepsy and HA, and only very specific processes were mentioned. Similarly, the presence of epilepsy does not have a direct impact on the likelihood of developing T2DM but shows indirect effects on T2DM development via inflammatory pathways.[26]

Clinical Implications:

Understanding the comorbidity patterns, rates, and relationships between epilepsy and these common autoimmune conditions is vital in determining how to take appropriate precautions for patients. As suggested in the results, SLE and T2DM are correlated with epilepsy through inflammatory processes[27] and this can be considered by both physicians and patients moving forward, should they wish to target inflammation. As a practice to reduce immune inflammation, physicians can encourage their epileptic patients to limit their consumption of alcohol,[28] a substance known for its detrimental impacts on the liver. Additionally, SLE can be triggered by excessive sunlight; to compensate, regular vitamin D supplementation can be taken.[29] Additionally, clinicians may wish to screen for inflammatory markers among those with TLE that are associated with these autoimmune disorders, especially as elevations in some of these autoimmune markers (e.g., IL-1β, IL-6) are associated with medication resistance.[30]

Most striking is the limited research on HA and epilepsy for a high-risk group. Hemolytic anemia can cause death in children and put a mother's life at risk; understanding the consequences and side effects that anti-seizure medications can cause during pregnancy is necessary for the mother to know, so they can decide to proceed with medications or use alternative medications for mothers who are epileptic. Conveying this information to patients will help set a new standard for how epileptic mothers can maintain safety and health for both themselves and their children. Some individuals may opt for other validated non-pharmaceutical integrative medicine approaches to epilepsy treatments, such as mind-body movement practices,[31] herbal supplements,[32] and a controlled ketogenic diet,[31] all of which may allow pregnant mothers to be more cautious with ASMs before giving birth. This, in turn, can set a standard for mothers to follow, not only regarding their medications but also regarding additional protocols that may be implemented. To avoid excessive inflammation caused by anti-seizure medications, there is evidence that therapies such as medical cannabis, integrative medicine, and dieting may be helpful.[33]

Strengths:

This study focuses on gathering and organizing information on comorbidity risk factors for epilepsy that are currently understudied. Epilepsy is a condition associated with several life-threatening comorbidities, and medical practitioners need to take the correct precautions to avoid the development of autoimmune conditions and vice versa. We address the commonalities and differences in mechanisms between common autoimmune comorbidities (T2DM, SLE, and HA) and epilepsy.

Limitations:

This study is not without limitations; several limitations arose among the studies we included. Our results on hemo-

DOI: 10.36838/IJHSR87.133

lytic anemia were primarily derived from a single study, as the literature is limited on the association between HA and epilepsy. Furthermore, this singular study addressed all anemias and their relationship to epilepsy rather than focusing on HA specifically. This study relies on theories and case studies rather than experimental studies. This is a limitation because case studies examine only specific patients. This can lead to accidental bias because each patient has a unique background, which can influence the presence of either condition; it does not necessarily imply that a comorbidity is present. Accurate generalizations cannot be made from larger samples without accounting for external factors.

Future Directions:

This review opens up several questions for future discussion. More experimental studies concerning hemolytic anemia and epilepsy should be conducted to help identify the true underlying pathways of HA and epilepsy beyond the ASM pathway (inflammation or alternative mechanisms could be revealed). Treatment studies should be conducted in the future to provide experimental data on pregnant mothers prescribed ASMs and provide information beyond theoretical correlations. Furthermore, experimental data should be a focus of future studies on integrative medicine practices (e.g., nutrition and stress-reduction practices such as meditation/yoga) in relation to epilepsy and autoimmune disease comorbidities. With copious amounts of data, more accurate conclusions can be drawn about specific comorbidity pathways and how to prevent them through alternative practices.

Table 1: Summary of Included Studies Examining the Correlation Between TLE and Autoimmune Conditions (SLE, HA, T2DM).

Author, Year	Title	Number of Participants/number of studies (N)	Population	Key findings/Mechanisms	Type of Study (Review, observational, experimental)
Observational/Experimental Research Studies					
Chaudhry *et al.*[20]	Oxcarbazepine-Induced Hemolytic Anemia in a Geriatric Patient	75-year-old male case report	One patient	Oxcarbazepine (an antiepileptic drug) showed life-threatening effects on the patient, showing evidence of hemolysis	Case Report
Favilli, F., Anzilotti, C., Martinelli, L., Quattroni, P., De Martino, S., Pratesi, F., ... & Migliorini, P.[18]	IL-18 Activity in Systemic Lupus Erythematosus	n=40 individuals with SLE and n=17 healthy controls	Individuals with active SLE, inactive SLE, and healthy controls	IL-18 may act as a mechanism between stress and SLE	Observational
Hopia, L., Andersson, M., Svenungsson, E., Khademi, M., Piehl, F., & Tomson, T.[15]	Epilepsy in systemic lupus erythematosus: prevalence and risk factors	n=440 SLE patients	SLE patients	SLE Pathways to epilepsy	Observational
Li, C. C., Chang, C. C., Cherng, Y. G., Lin, C. S., Yeh, C. C., Chang, Y. C., ... & Liao, C. C.[22]	Risk and outcomes of diabetes in patients with epilepsy	n=2854 patients with newly diagnosed epilepsy n=22,832 people without epilepsy n=92,438 patients with T2DM	Epileptic patients	Increased cortisol and interfered HPA axis in T2DM can result in an elevated risk of epilepsy.	Observational
Mochol, M., Taubøll, E., Aukrust, P., Ueland, T., Andreassen, O. A., & Svalheim, S.[17]	Serum Markers of Neuronal Damage and Astrocyte Activity in Patients with Chronic Epilepsy: Elevated Levels of Glial Fibrillary Acidic Protein	n=119 epilepsy patients and n=80 healthy controls	Epileptic patients (with glial damage analysis)	Antiseizure medications have been found to increase pro-inflammatory cytokines, specifically IL-18. IL-18 is a significant marker for astrocyte activity in the brain.	(Cross-Sectional, Observational)
Sinha, S., Patil, S. A., Jayalekshmy, V., & Satishchandra, P.[28]	Do cytokines have any role in epilepsy?	n= 16 epilepsy patients	Individuals with epilepsy	Cytokines released during inflammation affect the risk of epilepsy.	Observational
Tsai, J. D., Lin, C. L., Lin, C. C., Sung, F. C., & Lue, K. H.[14]	Risk of epilepsy in patients with systemic lupus erythematosus – a retrospective cohort study	32,301	Individuals with SLE from 1997 to 2010	SLE plays a role in affecting both the central and peripheral nervous system, which can correlate this condition with epilepsy	Retrospective Cohort Study
Review Studies					
Aarli, J. A.[16]	Epilepsy and the Immune System	N/A	General adult population	Inflammation is a mechanism of Systemic Lupus Erythematosus (SLE) and epilepsy	Review
DeFronzo, R. A., Ferrannini, E., Groop, L., Henry, R. R., Herman, W. H., Holst,	Type 2 Diabetes Mellitus	N/A	Individuals with Type 2 Diabetes Mellitus	Definition of T2DM and physiological and social implications	Review
Padda, J., Khalid, K., Syam, M., Kakani, V., Tonpouwo, G. K., Dhakal, R., ... & Jean-Charles, G.[19]	Association of Anemia With Epilepsy and Antiepileptic Drugs	N/A	Individuals with epilepsy and anemia	Epilepsy and hemolytic anemia share common pathways via anti-seizure medication pathways	Review
Rodríguez-Hernández, A., Ortiz-Orendain, J., Álvarez-Palazuelos, L. E., González-López, L., Gámez-Nava, J. I., & Zavala-Cerna, M. G.[13]	Seizures in systemic lupus erythematosus: A scoping review	N/A	General	Epilepsy and SLE are bidirectional in terms of inflammatory risk pathways	Review
Valencia, I.[27]	Epilepsy in Systemic Autoimmune Disorders	N/A	Epileptic patients and patients with autoimmune conditions	SLE is an autoimmune inflammatory disorder affecting multiple organs, including the brain and peripheral nervous system	Review
Zaccara, G., Franciotta, D. and Perucca, E.[21]	Idiosyncratic Adverse Reactions to Antiepileptic Drugs	N/A	General Population	Mechanisms and risks of anti-seizure medication via activation of natural killer cells	Review

The study table reports on demographic details, method, and key findings of each study.
Note: IL=interleukin; SLE= Systemic Lupus Erythamotosus; HA= Hemolytic Anemia; HPA=Hypothalamic-Pituitary-Adrenal; T2DM=Type 2 Diabetes Mellitus

Conclusion

This study aimed to explore the comorbidities between epilepsy and common autoimmune conditions. Regarding our first research question (*Is there an association between temporal lobe epilepsy and autoimmune disorders?*), our hypothesis was partially supported. First, there was a bidirectional relationship between epilepsy and SLE. Further, we see that epilepsy is predictive of T2DM through both neuro-immune and behavioral pathways. Lastly, epilepsy was only associated with hemolytic anemia when accounting for the use of anti-seizure medications rather than a direct association. We saw particularly strong associations between diabetes and epilepsy, with 19-25% of individuals with diabetes experiencing seizures.[34]

Regarding our second research question (*What are the autoimmune processes/mechanisms underlying the potential relationships between epilepsy and common comorbid autoimmune disorders?*), our *hypothesis that inflammation would be a mechanism linking* these conditions was partially supported. Studies show SLE does lead to an increased rate of seizures or epilepsy by way of increased inflammation. In particular, the inflammation found in SLE includes many of the same antibodies found in epilepsy. Seizures are more common among those with SLE-induced inflammation, where medication can give rise to the risk of seizures.

Regarding T2DM, studies show that epilepsy may increase the risk of T2DM by way of elevated HPA axis activity, increased cortisol, and increased glucose regulation. Epilepsy also directly affects the immune system, particularly the inflammatory cytokine IL-6, which is involved in T2DM. Overall, proinflammatory cytokines appear to play a role in how epilepsy is associated with DM.

Regarding HA, our hypothesis that inflammation would be a direct mechanism was not as strongly supported. The mech-

anism between HA and TLE is through medication-induced effects, including hemolysis. There is less robust evidence suggesting alternative mechanisms through which hemolytic anemia could impact epilepsy. Both SLE and T2DM influenced the presence of epilepsy through inflammatory processes, but that was not the case with HA. HA occurs through damage to blood plasma (intravascularly and extravascularly) and to the spleen/liver, and anti-seizure medications follow these same pathways.[35]

Final Conclusions:

Overall, this review aimed to examine the association between epilepsy and autoimmune conditions, as well as the proposed mechanisms linking them. The findings illustrated that epilepsy is associated with comorbidities such as systemic lupus erythematosus, hemolytic anemia, and diabetes mellitus. Inflammation through anti-seizure medications and physiological stress from seizures are key factors in the relationship between these comorbidities. In the future, more research should be conducted on stress, inflammation, and hemolytic pathways.

■ Acknowledgments

The author thanks Sinead M. Sinnott, PhD, from Harvard Medical School/Massachusetts General Hospital, for providing valuable advice and guidance throughout this research process. I attest that the ideas, graphics, and writing in this paper are entirely my own.

■ References

1. Zack M, Kobau R. Letter re: Prevalence and incidence of epilepsy: A systematic review and meta-analysis of international studies. *Neurology*. 2017;89(6):641-641. doi:10.1212/WNL.0000000000004205
2. Novakova B, Harris PR, Ponnusamy A, Reuber M. The role of stress as a trigger for epileptic seizures: A narrative review of evidence from human and animal studies. *Epilepsia*. 2013;54(11):1866-1876. doi:10.1111/epi.12377
3. Kälviäinen R, Salmenperä T, Partanen K, Vainio P, Riekkinen P, Pitkänen A. Recurrent seizures may cause hippocampal damage in temporal lobe epilepsy. *Neurology*. 1998;50(5):1377-1382. doi:10.1212/WNL.50.5.1377
4. Bromfield EB, Cavazos JE, Sirven JI, eds. *An Introduction to Epilepsy*. American Epilepsy Society; 2006. Accessed October 6, 2025. http://www.ncbi.nlm.nih.gov/books/NBK2508/
5. Guilliams TG, Edwards L. Chronic Stress and the HPA Axis: Clinical Assessment and Therapeutic Considerations. *The Standard*. 2010;(9):1-12.
6. Herman JP, Ostrander MM, Mueller NK, Figueiredo H. Limbic system mechanisms of stress regulation: Hypothalamo-pituitary-adrenocortical axis. *Prog Neuropsychopharmacol Biol Psychiatry*. 2005;29(8):1201-1213. doi:10.1016/j.pnpbp.2005.08.006
7. Conrad CD. Chronic Stress-induced Hippocampal Vulnerability: The Glucocorticoid Vulnerability Hypothesis. *Rev Neurosci*. 2008;19(6). doi:10.1515/REVNEURO.2008.19.6.395
8. McEwen BS, Nasca C, Gray JD. Stress Effects on Neuronal Structure: Hippocampus, Amygdala, and Prefrontal Cortex. *Neuropsychopharmacology*. 2016;41(1):3-23. doi:10.1038/npp.2015.171
9. Xiang Y, Zhang M, Jiang D, Su Q, Shi J. The role of inflammation in autoimmune disease: a therapeutic target. *Front Immunol*. 2023;14:1267091. doi:10.3389/fimmu.2023.1267091
10. CDC. People with Lupus. Centers for Disease Control and Prevention. 2024. https://www.cdc.gov/lupus/data-research/index.html
11. Borchers AT, Naguwa SM, Shoenfeld Y, Gershwin ME. The geoepidemiology of systemic lupus erythematosus. *Autoimmun Rev*. 2010;9(5):A277-A287. doi:10.1016/j.autrev.2009.12.008
12. CDC. National diabetes statistics report. Centers for Disease Control and Prevention. 2024. https://www.cdc.gov/diabetes/php/data-research/index.html
13. Rodriguez-Hernandez A, Ortiz-Orendain J, Alvarez-Palazuelos LE, Gonzalez-Lopez L, Gamez-Nava JI, Zavala-Cerna MG. Seizures in systemic lupus erythematosus: A scoping review. *Seizure*. 2021;86:161-167. doi:10.1016/j.seizure.2021.02.021
14. Tsai JD, Lin CL, Sung FC, Lue KH, Lin CC. Risk of epilepsy in patients with systemic lupus erythematosus &ndash a retrospective cohort study. *Neuropsychiatr Dis Treat*. Published online September 2014:1635. doi:10.2147/NDT.S64323
15. Hopia L, Andersson M, Svenungsson E, Khademi M, Piehl F, Tomson T. Epilepsy in systemic lupus erythematosus: prevalence and risk factors. *Eur J Neurol*. 2020;27(2):297-307. doi:10.1111/ene.14077
16. Aarli JA. Epilepsy and the Immune System. *Arch Neurol*. 2000;57(12):1689. doi:10.1001/archneur.57.12.1689
17. Mochol M, Taubøll E, Aukrust P, Ueland T, Andreassen OA, Svalheim S. Serum Markers of Neuronal Damage and Astrocyte Activity in Patients with Chronic Epilepsy: Elevated Levels of Glial Fibrillary Acidic Protein. Ben-Menachem E, ed. *Acta Neurol Scand*. 2023;2023:1-5. doi:10.1155/2023/7246373
18. Favilli F, Anzilotti C, Martinelli L, *et al*. IL-18 Activity in Systemic Lupus Erythematosus. *Ann NY Acad Sci*. 2009;1173(1):301-309. doi:10.1111/j.1749-6632.2009.04742.x
19. Padda J, Khalid K, Syam M, *et al*. Association of Anemia With Epilepsy and Antiepileptic Drugs. *Cureus*. Published online November 7, 2021. doi:10.7759/cureus19334
20. Chaudhry MM, Abrar M, Mutahir K, Mendoza C. Oxcarbazepine-Induced Hemolytic Anemia in a Geriatric Patient. *Am J Ther*. 2008;15(2):187-189. doi:10.1097/MJT.0b013e31815afb6f
21. Zaccara G, Franciotta D, Perucca E. Idiosyncratic Adverse Reactions to Antiepileptic Drugs. *Epilepsia*. 2007;48(7):1223-1244. doi:10.1111/j.1528-1167.2007.01041.x
22. Li CC, Chang CC, Cherng YG, *et al*. Risk and outcomes of diabetes in patients with epilepsy. *Sci Rep*. 2021;11(1):18888. doi:10.1038/s41598-021-98340-x
23. DeFronzo RA, Ferrannini E, Groop L, *et al*. Type 2 diabetes mellitus. *Nat Rev Dis Primer*. 2015;1(1):15019. doi:10.1038/nrdp.2015.19
24. Kamali AN, Zian Z, Bautista JM, *et al*. The Potential Role of Pro-Inflammatory and Anti-Inflammatory Cytokines in Epilepsy Pathogenesis. *Endocr Metab Immune Disord - Drug Targets*. 2021;21(10):1760-1774. doi:10.2174/1871530320999201116200940
25. Phoswa WN, Mokgalaboni K. Immunological Imbalances Associated with Epileptic Seizures in Type 2 Diabetes Mellitus. *Brain Sci*. 2023;13(5):732. doi:10.3390/brainsci13050732
26. Sinha S, Patil SA, Jayalekshmy V, Satishchandra P. Do cytokines have any role in epilepsy? *Epilepsy Res*. 2008;82(2-3):171-176. doi:10.1016/j.eplepsyres.2008.07.018
27. Valencia I. Epilepsy in Systemic Autoimmune Disorders. *Semin Pediatr Neurol*. 2014;21(3):226-231. doi:10.1016/j.spen.2014.07.001
28. Samokhvalov AV, Irving H, Mohapatra S, Rehm J. Alcohol consumption, unprovoked seizures, and epilepsy: A systematic review and meta-analysis. *Epilepsia*. 2010;51(7):1177-1184. doi:10.1111/j.1528-1167.2009.02426.x

DOI: 10.36838/IJHSR87.133

29. Zheng R, Gonzalez A, Yue J, *et al*. Efficacy and Safety of Vitamin D Supplementation in Patients With Systemic Lupus Erythematosus: A Meta-analysis of Randomized Controlled Trials. *Am J Med Sci*. 2019;358(2):104-114. doi:10.1016/j.amjms.2019.04.020
30. Milano C, Montali M, Barachini S, *et al*. Increased production of inflammatory cytokines by circulating monocytes in mesial temporal lobe epilepsy: A possible role in drug resistance. *J Neuroimmunol*. 2024;386:578272. doi:10.1016/j.jneuroim.2023.578272
31. Sirven JI. Epilepsy: A Spectrum Disorder. *Cold Spring Harb Perspect Med*. 2015;5(9):a022848. doi:10.1101/cshperspect.a022848
32. Jiang T, Zhang X, Zhang M, Liu M, Zhu H, Sun Y. Drug-resistant idiopathic generalized epilepsy: A meta-analysis of prevalence and risk factors. *Epilepsy Behav*. 2023;146:109364. doi:10.1016/j.yebeh.2023.109364
33. Gaston TE, Szaflarski JP. Cannabis for the Treatment of Epilepsy: an Update. *Curr Neurol Neurosci Rep*. 2018;18(11):73. doi:10.1007/s11910-018-0882-y
34. Yun C, Xuefeng W. Association Between Seizures and Diabetes Mellitus: A Comprehensive Review of Literature. *Curr Diabetes Rev*. 2013;9(4):350-354. doi:10.2174/15733998113099990060
35. Dhaliwal G, Cornett PA, Tierney LM. Hemolytic anemia. *Am Fam Physician*. 2004;69(11):2599-2606.

Author

Sanvi Singh is a senior at the Academy of Allied Health and Science, dedicated to exploring the mechanisms underlying epilepsy and other neurological disorders. She hopes to pursue a career in the field of neuroscience/medicine with a specialty in epilepsy, specifically neurosurgery.

IJHSR
ijhighschoolresearch.org
REVIEW ARTICLE

The Role of Stem Cells in Cancer Treatments

Amanda Chua

Hwa Chong Institution, 661 Bukit Timah Rd, 269734, Singapore; amandachua600@gmail.com

ABSTRACT: Stem cells have been the basis of, or used in, many cancer treatments. Bone marrow transplants, CAR-T cell immunotherapy, stem cell-based drug delivery systems, and differentiation therapy are four prime examples of the value of stem cells in the fight against cancer. This review will go through the mechanism of stem cells in these treatments, and analyze each treatment's effectiveness, advantages, and disadvantages of each approach. This is done using research papers backed by various clinical trials and studies. Whilst it was found that each treatment was indeed proven to help eradicate or alleviate its effects in cancer patients, each treatment also has its limitations and challenges. These obstacles range from safety implications to ethical concerns. Based on these findings, future research should focus on solving these issues by fully studying and understanding these unique challenges faced by stem cell cancer treatment to pinpoint solutions and allow patients to undergo these stem cell treatments safely and efficiently.

KEYWORDS: Biomedical and Health Sciences, Genetics and Molecular Biology of Disease, Cancer, Stem Cells.

Introduction

There are three different types of stem cells used in stem cell-mediated therapy: embryonic stem cells (ESCs), adult stem cells (ASCs), and induced pluripotent stem cells (iPSCs). ESCs are derived from the inner cell mass of the developing embryo at around 3 days post-fertilization, known as the blastocyst stage, and are pluripotent stem cells that can divide into more stem cells or can become any type of cell in the body.[1] On the other hand, ASCs are naturally found residing in small numbers in most adult tissues, such as bone marrow and the skin. Unlike ESCs, ASCs are multipotent stem cells, meaning that they can only differentiate into distinct cell types of their tissue of origin. Thus, their capacity to regenerate is limited. However, differentiated adult somatic cells can also be genetically reprogrammed back into an embryonic-like state via reintroducing the expression of four specific transcription factors discovered by Shinya Yamanaka in 2006, referred to as the Yamanaka factors, including Octamer-binding transcription factor 4 (Oct4), SRY-box transcription factor 2 (Sox2), Krüppel-like factor 4 (Klf4), and cellular MYC (c-Myc) by viral-based gene transfer methods into the cells.[2] As a result, these new, reprogrammed cells, known as iPSCs, can provide a pool of stem cells that are fully pluripotent for therapeutic use.

Stem cell therapy has already benefited patients affected by many diseases, including haematologic cancers like leukemia and various solid tumors. In fact, the most common method of stem cell therapy is in the treatment of blood cancers, where hematopoietic stem cell (HSC) transplantation is used to replace diseased leukemic cancer cells in the bone marrow with healthy stem cells that can proliferate and respond to environmental cues to restore normal blood and immune cell production.[3] Likewise, ASCs can also be utilized in other ways, especially in cancer. For example, mesenchymal stem cells (MSCs) and neural stem cells (NSCs) can be used in the delivery of cancer drugs to specific organ systems. Furthermore, ESCs and iPSCs can be utilized in CAR T-cell immunotherapies and differentiation therapies aimed at reducing donor variability and enabling more precise and scalable cancer treatments. This paper will highlight the different methods in which stem cells have been applied in cancer treatments, their use in various cancer therapies, and will also discuss their advantages, limitations, and potential future applications.

Bone Marrow Transplants:

Hematopoietic stem cells (HSCs) are commonly used to treat blood cancer via bone marrow transplantations. Blood cancers are defined by the uncontrolled growth of abnormal blood cells and can prevent one's blood from being able to perform most of its functions, such as transporting oxygen and fighting infections. Blood cancers also result in further dysfunctional blood cell production, leading to an overall weakened immune system and clotting ability. The diminishment of these functions is very detrimental to the already weakened patient. Furthermore, high-dose radiotherapy or chemotherapy are non-selective therapeutic approaches and can destroy functional blood cells as a side effect of fighting cancer cells.[4] To combat this, healthy bone marrow containing HSCs is transplanted into the body of immunocompromised patients who have near complete irradiation of their immune system. The first successful bone marrow transplant was performed by Dr. E. Donnall Thomas on a child with leukemia in 1956.[5] Since then, bone marrow transplants have been used in the treatment of many other types of blood cancers, such as multiple myeloma[6] and lymphomas.[7]

Upon successful engraftment, the addition of colony-stimulating factors (CSFs) to HSCs was found to activate intracellular signaling pathways, which allow the HSCs to differentiate to form any type of mature blood cell.[8] For example, the growth factor Granulocyte colony-stimulating factor (G-CSF) enables the proliferation and mobilization of HSCs,[9] hence, when HSCs are induced into a patient's body via a bone

© 2026 Terra Science and Education

DOI: 10.36838/IJHSR87.139

marrow transplant, they help restore the patient's ability to produce new blood cells from both myeloid and lymphoid lineages.[10]

Till now, bone marrow transplants and the infusion of HSCs are the only FDA-approved stem cell treatments[11] with an increased survival rate for patients post-transplant. The survival rates after transplant for patients with acute leukemia in remission are 55% to 68% with related donors and 26% to 50% if the donor is unrelated.[12] Other than leukemia, patients with Ewing sarcoma and lymphoma have benefited from improved survival rates after going through an autologous bone marrow transplant when combined with traditional cancer treatments.[7,13]

However, side effects and risks such as graft-versus-host-disease (GVHD) and low platelet count regarding bone marrow transplants still pose challenges. Fortunately, modern medicine can help solve these issues. For example, the occurrence of GVHD when using matched (allogeneic) sources of HSCs, which occurs when immune cells from the transplanted bone marrow attack healthy cells in the patient, can be treated with immunosuppressive drugs or therapies, such as using genetically modified mesenchymal stem cells (MSCs) to suppress overactive T-cells.[14] The conditioning treatment for bone marrow transplants can lead to low platelet count as well, which can lead to an increased bleeding risk. However, this risk can be lowered by following special precautions to avoid injury, and extremely low platelet counts can be treated via blood transfusions.[15]

Furthermore, according to research by Smita Bhatia on the long-term health impacts of HSC transplantation (HSCT), whilst 70-80% of those who survive the first 2 years following HSCT are expected to become long-term survivors, chronic mortality is still a big issue.[16] In a cohort of 854 individuals who had survived for >2 years after autologous bone marrow transplantation, it was found that the cohort was still at a 13-fold increased risk for premature death compared with the general population, and bone marrow transplant recipients are at a 2.3- to 4.0-fold increased risk of death due to cardiac issues when compared with the general population.[16] Similarly, results from another study, which closely followed 548 long-term bone marrow transplant recipients, also support the increased mortality risk reported by Bhatia *et al*.[17] Here, the transplant recipients had a 9.8-fold increase in the risk of arterial embolism/thrombosis, which are cardiac events in which blood clots block blood flow in the arteries.

Overall, HSC transplantation has transformed the treatment of blood cancers by restoring the patient's ability to produce healthy blood cells and significantly improving survival rates, particularly in leukemia, lymphoma, and other hematologic malignancies. However, long-term risks such as graft-versus-host disease and cardiovascular complications remain substantial, highlighting the need for ongoing clinical vigilance and supportive care. Looking forward, advances in genetic engineering and immunomodulation may further reduce these risks and enhance the efficacy of HSC transplants, potentially expanding their use and improving long-term outcomes for patients with cancers other than blood cancer.

CAR T-cell cancer immunotherapy:

The second way stem cells have been used in cancer treatment is through the production of immune cells for Chimeric Antigen Receptor T-cell (CAR T-cell) therapy. In this approach, immune cells, such as T-cells and natural killer (NK) cells, are taken from the patient and genetically modified in order to specifically recognize and attack cancer cells, making them a highly targeted method of cancer treatment.[18] This method of therapy is a form of treatment that essentially utilizes certain parts of a person's immune system to recognize and fight disease by stimulating the natural defenses of one's immune system to improve its efficiency in finding and killing cancer cells.[19]

However, generating CAR T- and NK cells from one's body has its limitations, as the quality and quantity of the cells are hard to control *in vivo*, leading to a low standard of cell health and less efficient immunotherapy. This is where stem cells come in: outsourcing to iPSCs and ESCs can offer unlimited sources of immune cells and enable a larger number of eligible patients to undergo immunotherapy.[20] To allow the iPSCs and ESCs to differentiate into immune cells for immunotherapy, they are incubated in the growth medium containing NK cell or T-cell initiating cytokines, such as stem cell factor (SCF), IL-3, IL-7, and IL-15. The T-cells are then genetically modified via viral-based gene transfer methods or CRISPR-Cas9 gene editing to express a CAR specific for a tumor antigen, enabling their receptor to directly bind to and kill cancer cells.[21] This is followed by *ex vivo* cell expansion and re-infusion to the patient.[22]

The use of stem cells to produce CAR T-cells and NK cells for the process of immunotherapy has been very rewarding thus far,[23-25] especially in the treatment of hematological cancers, which are cancer that begins in blood-forming tissue, such as the bone marrow, or in the cells of the immune system. According to clinical trials, end-stage Acute Lymphocytic Leukemia patients who have undergone this treatment have up to 92% chance of a full recovery.[22] However, it should be noted that most patients in these trials were children or young adults, and elderly patients may have a lower chance of a full recovery due to their different tumour microenvironments. It can be seen that patients with multiple myeloma have benefited from CAR T-cell immunotherapy, too, as a study found evidence of tumor reduction in 87% of patients with multiple myeloma who underwent this therapy.[26] Several CAR-T therapies treating certain patients with hematological cancers have already been FDA approved,[27-29] and with many clinical trials aiming to improve the safety and efficacy of CAR-T cell therapies,[30-32] hopefully stem cell-induced CAR-T cell immunotherapy will also gain approval in the future.

However, CAR T-cell therapy remains a very inaccessible treatment for many people worldwide.[33] It is estimated that CAR T-cell therapy can cost between $500,000 and $1,000,000, and the added costs of stem cell differentiation to produce CAR T-cells do not help with the hefty sum. Furthermore, only three pharmaceutical companies, Bristol Myers Squibb, Gilead Sciences, and Novartis, hold FDA approval to produce CAR T-cells commercially. Thus, the limited production of

CAR T-cells makes the treatment both expensive and exclusive.[34] Patients who live in rural areas far from major transplant centers also do not have easy access to this therapy. For example, a patient by the name Suzanne Behanna claims she had to travel nearly 800 miles from rural New Mexico to Houston's University of Texas MD Anderson Cancer Center just to receive this treatment,[35] and unfortunately, many are not as lucky as she to be ultimately able to travel long distances for access to CAR T-cell immunotherapy.

CAR T-cell therapy has also been controversial for another reason. Many suspected that the cells that were genetically engineered for the immunotherapy were cancer-causing following reports of many patients diagnosed with various T-cell cancers post-therapy. In November 2023, the FDA warned that CAR T-cell therapy may be associated with secondary cancers.[36] Researchers at the Stanford Cancer Institute used genetic profiling on 724 patients treated with CAR T-cell therapy to conduct a study to find out if the warnings and controversy surrounding CAR T-cell therapy were warranted.[37] Their results showed that the incidence of secondary blood cancers approached 6.5% over a median of three years of follow-up, which is around the same for patients who underwent stem cell transplantation to treat their cancers. The analysis also found that the T-cells responsible for the patient's second cancer were genetically distinct from those engineered for CAR T-cell therapy. The research results at Stanford also correlate with another study at UPenn, which found that roughly 3.6% of patients treated with CAR-T cell therapies were diagnosed with a second cancer. Furthermore, molecular analysis of a CAR T-cell-treated patient who developed a secondary lung tumor did not find the CAR transgene in his T-cell lymphoma.[38] Thus, both studies indicate a lack of evidence linking CAR T-cell therapy to secondary tumors.

In summary, stem cells can be used to generate CAR T-cells, which offer a highly targeted immunotherapy approach for cancer. Clinical trials have demonstrated impressive remission rates, and several CAR T-cell therapies are already FDA-approved, although high costs and limited accessibility remain significant barriers. Ongoing advances in stem cell biology and gene-editing technologies may make this therapy safer, more effective, and accessible to a wider range of patients in the future.

MSCs and NSCs as drug delivery carriers:

Stem cells such as mesenchymal (MSCs) and neural stem cells (NSCs) can also be utilized as cancer drug delivery carriers. Cell-based targeted drug delivery systems generally offer low immunogenicity and cytotoxicity, specific tropism to injured tissue, prolonged circulation time, and extended half-lives.[39] This makes them more efficient than other drug delivery systems, such as oral and parenteral drug delivery that bypass the gastrointestinal tract. On top of these benefits, stem cells also offer other advantages when acting as drug carriers. The specific pros and cons of MSCs and NSCs will be discussed in the following paragraphs, as well as their unique properties that make them suitable for this treatment, which other stem cells may lack.

The high proliferative capacity of MSCs, alongside their multi-potency and anti-inflammatory properties, are qualities that increase MSC effectiveness in drug delivery.[39] Furthermore, MSCs can carry microcapsules containing drugs without harm to their structural integrity due to unexpressed cytokine secretion that suppresses cell damage responses. This makes MSCs particularly suitable for use as encapsulated drug transporters.[39] Their retained motility and ability to target and migrate towards cancer cells, even through minuscule eight μm pores, are also key to drug delivery efficacy.[40] This is achieved as the microenvironment of tumors acts as a chemoattractant to guide the migration of MSCs to the cancer.[41] Cancer cells release the chemokines CCL2, CCL15, CCL20, CCL25, CXCL1, and CXCL8, which are detected by chemokine receptors on the surface of MSCs, guiding their migration to the tumor.[42] MSCs then release nano-sized exosomes, containing various biological materials, to regulate cell-cell interaction with the cancer cells and anti-cancer drugs into the cancer cells to damage the tumor.[43]

So far, MSC-based drug delivery systems have been quite successful in research involving mice as animal models. In one study, MSCs containing the chemotherapy drug paclitaxel were injected into lung tumor-bearing mice, and it was found that after three MSC injections, metastasis of the tumor was no longer observed, indicating that the damage to cancer cells was successful.[44] In an attempt to further research the drug delivery efficacy of MSCs, a team of Japanese researchers compared the efficacy of liposomal doxorubicin, a type of chemotherapy drug, and doxorubicin-modified MSCs in mice suffering from colon cancer.[45] Results analysis using the avidin-biotin complex method showed that the drug-loaded MSCs suppressed the proliferation of the mice's colon cancer cells significantly more than the liposomal doxorubicin alone. In the co-cultures of the doxorubicin-loaded MSCs, localized distribution of the drug was detected at the cancer cell contact surface, which was not observed when only liposomal doxorubicin was added to the cancer cells alone.[46] This correlates with the aforementioned study to support that the MSC drug delivery system is effective in targeting the cancerous cells.

However, this treatment is not without its limitations. One major challenge of the MSC drug delivery system is the pulmonary first-pass effect, in which the drug contained by the MSCs is metabolized before reaching the tumor.46 In fact, research *in vivo* using MSC-based drug delivery in rats has shown that most MSCs were trapped inside the lungs post intravenous infusion.[47] Furthermore, multiple studies have shown that the spontaneous malignant transformations that MSCs undergo can promote tumor growth,[48] notably the metastasis of breast cancer in mouse models.[49, 50] Research on *ex vivo* handling of MSCs has also found that *ex vivo* factors, such as the microenvironment of culture conditions, can cause MSCs to lose their homing ability,[51] effectively rendering only 1% of MSCs able to effectively target the cancer cells.[52, 53] However, it should be noted that more extensive clinical trials and research are required to utilize the MSC drug delivery system in humans, as the success in the MSC studies in mice may

DOI: 10.36838/IJHSR87.139

not necessarily translate to success in human biological contexts, owing to their vast genetic and physiological differences.

Aside from MSC-based drug delivery, NSCs are another type of stem cell with great potential to be utilized in cancer drug delivery systems, with clinical research in mouse models proving to be successful so far.

NSCs are promising carriers that protect and deliver oncolytic viruses (OVs) to tumors to kill cancer cells selectively. These cells can differentiate into any central nervous system cell, such as neurons and glial cells. Their self-renewing ability and multipotent characteristics make them a good OV delivery carrier.[54] Furthermore, the tumor-trophic nature of NSCs allows them to deliver the OVs to the cancer cells with minimal off-target effects,[55] while also protecting the OVs from immune neutralization from antibodies, allowing for repeat administrations,[56] and more effective OV delivery. After reaching the tumor, OVs undergo selective replication within the cancer cells to induce lysis, thus causing the cancer cells to disintegrate.[57] Additionally, in reaction to the viral particles being replicated, the patient's body produces an immune response; therefore, OVs effectively induce long-term host antitumor immunity.[58]

OVs transported by NSCs have led to successful results in treating gliomas, a type of brain tumor. Research has shown that NSCs loaded with the CRAD-S-pk7, a glioma-restricted oncolytic adenovirus, have led to inhibited tumor growth in mice models of human glioma and a 50% increased median survival rate compared to treatment using CRAd-S-pk7 without NSCs.[59] Another study also found that NSCs loaded with the anti-cancer medication Irinotecan transiently expressed and delivered high levels of active carboxylesterase enzymes to human glioma xenograft tumors in mice. This enzyme helps in drug metabolism and increases Irinotecan's cytotoxicity in glioma cells.[60] Separately, NSCs have been proven to directly inhibit glioma tumor cells as well.[61,62] The ability of glioma cells to proliferate and metastasize was found to be significantly inhibited when co-cultured with embryonic NSCs.[61] Additionally, culturing malignant glioma cells in NSC condition medium was also found to suppress their growth and prevent invasion into surrounding healthy tissue, indicating that NSCs themselves may secrete certain factors that slow cancer development.[62]

While using NSCs to deliver OVs and eradicate tumor cells in mouse models has been effective, scientists have had trouble translating this success to human patients. Unlike the ease of inducing NSCs in mice xenograft tumors, intratumoral injections for tumor patients are often invasive, making repeat injections difficult and casting doubt on the efficacy of NSCs successfully migrating to the cancer cells.[63] Furthermore, certain human OVs may damage normal tissues by destroying cancer cells. For example, studies have shown that the neurotropic virus HSV-1, often used in gene delivery, can cause fatal encephalitis and neonatal herpes in certain cases when induced in humans.[64] Finally, most cancer therapies using a single agent generally cannot eradicate tumors, and NSC-based therapy is no exception. It should instead be used in combination with, rather than as a replacement for, other cancer drugs to increase treatment durability and ultimately gain clinical utility. This was proven in a study showing that the combination of NSCs carrying oncolytic adenoviruses and temozolomide, a type of anticancer medication or radiation, led to a 46% increase in the median survival of mice suffering from glioblastoma multiforme.65 Furthermore, cases in which the stem cells were injected before, not after, chemoradiotherapy application were found to provide the greatest efficacy.[65]

Overall, stem cells such as MSCs and NSCs offer promising platforms for targeted cancer drug delivery, efficiently transporting chemotherapeutics or OVs directly to tumors. In preclinical studies, they have been shown to suppress tumor growth, reduce their ability to metastasize, and appear to improve overall survival in mouse models. However, challenges such as delivery limitations, potential off-target effects, and species differences highlight the need for further research. With more experimentation and optimization, and by testing its efficacy when combined with conventional therapies, MSC- and NSC-based drug delivery has the potential to become a safe and effective treatment option for human brain and solid-tumour cancers.

Differentiation Therapy:

The last stem cell-based anticancer therapy this paper will cover is differentiation therapy. For some context, it is known that stem cells can survive longer than regular cells, and their high pluripotency can lead to an accumulation of genetic mutations that can result in a loss of control over their growth and long-term ability to regenerate.[66] This is very similar to the general nature of cancer cells.[67] Cancer stem cells (CSCs) are tumor cells that function like stem cells and have stem-cell-like characteristics such as pluripotency and self-renewal capabilities. Indeed, such CSCs are believed to play a role in cancer progression, recurrence, and treatment resistance.[68] Thus, targeting CSCs is important in preventing cancer progression and relapse, and differentiation therapy essentially uses our existing knowledge of stem cells to achieve this.[69]

It has been found that various hormones and cytokines can influence cell communication to stimulate the early maturity of stem cells.[70] This causes the stem cells to lose their ability to regenerate and instead pushes them to differentiate into specialized cell/tissue types.[71] Thus, differentiation therapy uses various pharmacological agents, most commonly retinoic acid, to force CSCs to differentiate into more mature cells and stop them from multiplying uncontrollably,[72,73] effectively halting one of the hallmarks of cancer. One example that demonstrates the mechanism of differentiation therapy is its use in treating acute promyelocytic leukemia.[74] To treat this aggressive blood cancer, retinoic acid and arsenic are used in combination to inhibit the expression of the proto-oncogene Bcl-2 in myeloid CSCs. The Bcl-2 protein functions to inhibit apoptosis in leukemia cells, leading to the prolonged survival of the cancer cells. Hence, the downregulation of Bcl-2 due to retinoic acid prevents the myeloid CSCs from undergoing uncontrolled cellular proliferation, leading to a loss of their cancerous traits and instead the activation of the cell's internal death pathways.[75]

One benefit of differentiation therapy is that it simply aims to selectively push CSCs to differentiate into mature non-cancerous cells, hence avoiding the surrounding healthy cells.[76] This is unlike conventional anticancer therapy, such as chemotherapy, as the harmful chemicals used in traditional therapy to kill cancer cells may also harm healthy cells as a side effect.[77] Thus, the less toxic nature of differentiation therapy and lack of negative side effects make it an effective cancer treatment. For example, a study demonstrated that out of 50 advanced thyroid cancer patients treated with retinoic acid, 26% showed a distinct increase in radioiodine uptake (26%), and 40% showed a lower risk of cardiovascular issues (40%). The total number of patients who benefited from the differentiation therapy by having their tumors reduced was 38%.[78] Furthermore, whilst the importance of targeting CSCs to eradicate cancer has already been emphasized, it is important to note that CSCs are highly resistant to classic anticancer drugs, even more so than other cancer cells,[79] thus differentiation therapy offers a promising strategy by forcing CSCs to mature into non-proliferative, non-cancerous cells, effectively overcoming their inherent drug resistance and suppressing tumor growth at its source.

However, a major disadvantage of differentiation therapy is that tumors can resist the differentiating agent used to mature the CSCs. Retinoic acid and other retinoids are the preferred pharmacological agent used in differentiation therapy owing to their high success rates in the treatment.[80, 81] Despite treatment success, patients treated with retinoids often develop resistance to this therapy,[82] leading to secondary drug resistance in the tumors that then cause the CSCs to no longer respond to retinoid differentiation therapy despite having been successfully treated by this therapy in past treatments.[83] Furthermore, intrinsic resistance to retinoids has been exhibited in the development of some solid tumors.[84] In fact, the effectiveness of differentiation therapy has also been questioned; those who were given retinoic acid to undergo differentiation therapy showed that many patients had no signs of tumor reduction, and the median survival time post-treatment was only nineteen months.[85]

In summary, the use of differentiation therapy to target CSCs by inducing them to mature into non-proliferative, non-cancerous cells has shown to effectively suppress tumor growth while sparing healthy surrounding tissue. Indeed, it has shown clinical success in cancers such as acute promyelocytic leukemia and advanced thyroid cancer alongside other cancers, offering a less toxic alternative to conventional chemotherapy. However, resistance to differentiating agents, such as commonly used retinoids, and limited efficacy in certain solid tumors, remain significant challenges. Future research should focus on overcoming these resistance mechanisms, identifying novel differentiation-inducing compounds aside from those mentioned above, and exploring combination therapies with conventional or targeted treatments. With continued advancements, differentiation therapy has the potential to become a more effective and widely applicable strategy against cancer by offering an alternative fate for the cancerous cells rather than destroying them.

Conclusion

To conclude, stem cell-based therapy offers promising and novel alternatives to traditional cancer treatments and holds high potential to target cancer more efficiently and effectively.

The use of stem cells in cancer treatments offers an increased capacity for treatment success, but progress is hindered by negative side effects and unclear translation into the human system, respectively. HSCs, used in bone marrow transplants, have improved survival in hematologic cancers, but their application is limited by serious side effects, including graft-versus-host disease, reduced blood cell counts (cytopenias), and long-term cardiovascular risks. Similarly, though MSC- and NSC-based drug delivery systems enhance the targeted delivery of chemotherapeutics or oncolytic viruses and minimize off-target toxicity, they still face challenges such as the pulmonary first-pass effect, loss of homing ability, and difficulty translating preclinical success to humans. In addition, the use of stem cells has given rise to more innovative strategies such as CAR T-cell therapy, offering highly targeted and effective immunotherapy options to cancer patients, although with limitations in accessibility, cost, and potential safety concerns. Via future scientific research, such challenges in treatment will hopefully decrease as we gain a deeper understanding of stem cell treatment mechanisms, so as to increase treatment viability and lower medical risks for patients.

In addition, to a certain extent, the nature of tumor cells is very related to stem cells,[86] as both types of cells have a high ability for proliferation, viability, and resistance to apoptosis. We have already used insight from stem cells to fight cancer in differentiation therapy, in which CSCs are matured into cells with non-cancerous traits despite limitations such as inaccessibility and treatment resistance. This unique nature of differentiation therapy, which aims to repurpose cancerous cells instead of killing them, therefore poses reduced risk for rejection and toxicity concerns to healthy cells in comparison to conventional treatments. Further developments in our knowledge of stem cell characteristics that relate to cancer cells can no doubt lead to even more novel treatments henceforth.

As of now, amongst the 4 treatments discussed, bone marrow transplants and CAR T-cell therapy are the more immediate and commonly used treatments, as much research and fine-tuning have been put into these treatments over the years. On the other hand, differentiation therapy and stem cell-based drug delivery systems are currently in the premature infancy and explorative stage of research, but hold great potential for the future.

In the future, more stem-cell-based cancer treatments and improvements to existing treatments can be discovered as we learn more about stem cells themselves. Indeed, the future of stem cell therapy will likely involve combinatorial approaches, integrating the strategies mentioned in this paper to maximize long-term efficacy. Thus, continued advancements will be imperative in reducing treatment risks and providing improved and novel cancer treatments that are more widely accessible to patients worldwide.

DOI: 10.36838/IJHSR87.139

Acknowledgments

The author expresses gratitude to the Cambridge Centre for International Research (CCIR) for the invaluable contributions provided by Drs. Hazal Gezmis Gokce and Hakan Coskun.

References

1. Vazin, T.; Freed, W. J. Human Embryonic Stem Cells: Derivation, Culture, and Differentiation: A Review. *Restor Neurol Neurosci* **2010**, *28* (4), 589. https://doi.org/10.3233/RNN-2010-0543.
2. Ye, L.; Swingen, C.; Zhang, J. Induced Pluripotent Stem Cells and Their Potential for Basic and Clinical Sciences. *Curr Cardiol Rev* **2013**, *9* (1), 63. https://doi.org/10.2174/157340313805076278.
3. *How Does Stem Cell Therapy Work and What Are the Risks? | ISCRM*. https://iscrm.uw.edu/how-does-stem-cell-therapy-work/ (accessed 2024-09-08).
4. *Bone Marrow Suppression and Chemotherapy - Health Encyclopedia - University of Rochester Medical Center*. https://www.urmc.rochester.edu/encyclopedia/content.aspx?contenttypeid=85&contentid=p07263 (accessed 2024-09-08).
5. *Blood Cancer Awareness: History of Bone Marrow Transplantation | Masonic Cancer Center*. https://cancer.umn.edu/mncctn/news/blood-cancer-awareness-history-bone-marrow-transplantation (accessed 2024-09-08).
6. Devarakonda, S.; Efebera, Y.; Sharma, N. Role of Stem Cell Transplantation in Multiple Myeloma. *Cancers (Basel)* **2021**, *13* (4), 1–19. https://doi.org/10.3390/CANCERS13040863.
7. *Stem Cell Transplant for Lymphoma - Siteman Cancer Center*. https://siteman.wustl.edu/treatment/cancer-types/lymphoma/treatments/stem-cell-transplant-for-lymphoma/ (accessed 2024-09-08).
8. Deng, J.; Li, Y.; Pennati, A.; Yuan, S.; Wu, J. H.; Waller, E. K.; Galipeau, J. GM-CSF and IL-4 Fusion Cytokine Induces B Cell-Dependent Hematopoietic Regeneration. *Molecular Therapy* 2017, *25* (2), 416. https://doi.org/10.1016/J.YMTHE.2016.11.013.
9. Yaniz-Galende, E.; Hajjar, R. J. Stem Cell and Gene Therapy for Cardiac Regeneration. *Cardiac Regeneration and Repair* **2014**, *1*, 347–379. https://doi.org/10.1533/9780857096708.4.347.
10. Muraro, P. A.; Uccelli, A. Immuno-Therapeutic Potential of Haematopoietic and Mesenchymal Stem Cell Transplantation in MS. *Results Probl Cell Differ* **2009**, *51*, 237–257. https://doi.org/10.1007/400_2008_14.
11. *FDA Approves Cell Therapy for Patients with Blood Cancers to Reduce Risk of Infection Following Stem Cell Transplantation | FDA*. https://www.fda.gov/news-events/press-announcements/fda-approves-cell-therapy-patients-blood-cancers-reduce-risk-infection-following-stem-cell (accessed 2024-09-08).
12. Majhail, N. S.; Chitphakdithai, P.; Logan, B.; King, R.; Devine, S.; Rossmann, S. N.; Hale, G.; Hartzman, R. J.; Karanes, C.; Laport, G. G.; Nemecek, E.; Snyder, E. L.; Switzer, G. E.; Miller, J.; Navarro, W.; Confer, D. L.; Levine, J. E. Significant Improvement in Survival after Unrelated Donor Hematopoietic Cell Transplantation in the Recent Era. *Biol Blood Marrow Transplant* **2015**, *21* (1), 142. https://doi.org/10.1016/J.BBMT.2014.10.001.
13. Pawlowska, A. B.; Sun, V.; Calvert, G. T.; Karras, N. A.; Sato, J. K.; Anderson, C. P.; Cheng, J. C.; DiMundo, J. F.; Femino, J. D.; Lu, J. R.; Yang, D.; Dagis, A.; Miser, J. S.; Rosenthal, J. Long-Term Follow-up of High-Dose Chemotherapy with Autologous Stem Cell Transplantation in Children and Young Adults with Metastatic or Relapsed Ewing Sarcoma: A Single-Institution Experience. *Biology of Blood and Marrow Transplantation* **2020**, *27* (1), 72.e1-72.e7. https://doi.org/10.1016/j.bbmt.2020.09.029.
14. Shahbaz, S. K.; Mansourabadi, A. H.; Jafari, D. Genetically Engineered Mesenchymal Stromal Cells as a New Trend for Treatment of Severe Acute Graft-versus-Host Disease. *Clin Exp Immunol* **2022**, *208* (1), 12. https://doi.org/10.1093/CEI/UXAC016.
15. *Stem Cell or Bone Marrow Transplant Side Effects | American Cancer Society*. https://www.cancer.org/cancer/managing-cancer/treatment-types/stem-cell-transplant/transplant-side-effects.html (accessed 2024-09-08). 16. Bhatia S. Long-term health impacts of hematopoietic stem cell transplantation inform recommendations for follow-up. Expert Rev Hematol. **2011** Aug;4(4):437-52; quiz 453-4. doi: 10.1586/ehm.11.39. PMID: 21801135; PMCID: PMC3163085.
17. Tichelli, A.; Passweg, J.; Wójcik, D.; Rovó, A.; Harousseau, J. L.; Masszi, T.; Zander, A.; Békássy, A.; Crawley, C.; Arat, M.; Sica, S.; Lutz, P.; Socié, G. Late Cardiovascular Events after Allogeneic Hematopoietic Stem Cell Transplantation: A Retrospective Multicenter Study of the Late Effects Working Party of the European Group for Blood and Marrow Transplantation. *Haematologica* **2008**, *93* (8), 1203–1210. https://doi.org/10.3324/HAEMATOL.12949.
18. Zhang, Y.; Zhang, Z. The History and Advances in Cancer Immunotherapy: Understanding the Characteristics of Tumor-Infiltrating Immune Cells and Their Therapeutic Implications. *Cell Mol Immunol* **2020**, *17* (8), 807. https://doi.org/10.1038/S41423-020-0488-6.
19. *What Is Immunotherapy? | Immunotherapy for Cancer | American Cancer Society*. https://www.cancer.org/cancer/managing-cancer/treatment-types/immunotherapy.html (accessed 2024-09-09).
20. Themeli, M.; Rivière, I.; Sadelain, M. New Cell Sources for T Cell Engineering and Adoptive Immunotherapy. *Cell Stem Cell* **2015**, *16* (4), 357–366. https://doi.org/10.1016/j.stem.2015.03.011.
21. Ueda, T.; Kaneko, S. In Vitro Differentiation of T Cell: From CAR-Modified T-IPSC. *Methods Mol Biol* **2019**, *2048*, 85–91. https://doi.org/10.1007/978-1-4939-9728-2_10.
22. Miliotou, A. N.; Papadopoulou, L. C. CAR T-Cell Therapy: A New Era in Cancer Immunotherapy. *Curr Pharm Biotechnol* **2018**, *19* (1), 5–18. https://doi.org/10.2174/1389201019666180418095526.
23. Maude, S. L.; Frey, N.; Shaw, P. A.; Aplenc, R.; Barrett, D. M.; Bunin, N. J.; Chew, A.; Gonzalez, V. E.; Zheng, Z.; Lacey, S. F.; Mahnke, Y. D.; Melenhorst, J. J.; Rheingold, S. R.; Shen, A.; Teachey, D. T.; Levine, B. L.; June, C. H.; Porter, D. L.; Grupp, S. A. Chimeric Antigen Receptor T Cells for Sustained Remissions in Leukemia. *N Engl J Med* **2014**, *371* (16), 1507. https://doi.org/10.1056/NEJMOA1407222.
24. Nguyen, S.; Lacan, C.; Roos-Weil, D. [Allogeneic CAR-NK Cells: A Promising Alternative to Autologous CAR-T Cells - State of the Art, Sources of NK Cells, Limits and Perspectives]. *Bull Cancer* **2021**, *108* (10S), S81–S91. https://doi.org/10.1016/J.BULCAN.2021.06.007.
25. Timmermans, F.; Velghe, I.; Vanwalleghem, L.; De Smedt, M.; Van Coppernolle, S.; Taghon, T.; Moore, H. D.; Leclercq, G.; Langerak, A. W.; Kerre, T.; Plum, J.; Vandekerckhove, B. Generation of T Cells from Human Embryonic Stem Cell-Derived Hematopoietic Zones. *J Immunol* **2009**, *182* (11), 6879–6888. https://doi.org/10.4049/JIMMUNOL.0803670.
26. Sheykhhasan, M.; Ahmadieh-Yazdi, A.; Vicidomini, R.; Poondla, N.; Tanzadehpanah, H.; Dirbaziyan, A.; Mahaki, H.; Manoochehri, H.; Kalhor, N.; Dama, P. CAR T Therapies in Multiple Myeloma: Unleashing the Future. *Cancer Gene Therapy 2024 31:5* **2024**, *31* (5), 667–686. https://doi.org/10.1038/s41417-024-00750-2.
27. Neelapu, S. S.; Locke, F. L.; Bartlett, N. L.; Lekakis, L. J.; Miklos, D. B.; Jacobson, C. A.; Braunschweig, I.; Oluwole, O. O.; Siddiqi, T.; Lin, Y.; Timmerman, J. M.; Stiff, P. J.; Friedberg, J. W.; Flinn,

I. W.; Goy, A.; Hill, B. T.; Smith, M. R.; Deol, A.; Farooq, U.; McSweeney, P.; Munoz, J.; Avivi, I.; Castro, J. E.; Westin, J. R.; Chavez, J. C.; Ghobadi, A.; Komanduri, K. V.; Levy, R.; Jacobsen, E. D.; Witzig, T. E.; Reagan, P.; Bot, A.; Rossi, J.; Navale, L.; Jiang, Y.; Aycock, J.; Elias, M.; Chang, D.; Wiezorek, J.; Go, W. Y. Axicabtagene Ciloleucel CAR T-Cell Therapy in Refractory Large B-Cell Lymphoma. *N Engl J Med* **2017**, *377* (26), 2531. https://doi.org/10.1056/NEJMOA1707447.

28. Munshi, N. C.; Anderson, L. D.; Shah, N.; Madduri, D.; Berdeja, J.; Lonial, S.; Raje, N.; Lin, Y.; Siegel, D.; Oriol, A.; Moreau, P.; Yakoub-Agha, I.; Delforge, M.; Cavo, M.; Einsele, H.; Goldschmidt, H.; Weisel, K.; Rambaldi, A.; Reece, D.; Petrocca, F.; Massaro, M.; Connarn, J. N.; Kaiser, S.; Patel, P.; Huang, L.; Campbell, T. B.; Hege, K.; San-Miguel, J. Idecabtagene Vicleucel in Relapsed and Refractory Multiple Myeloma. *N Engl J Med* **2021**, *384* (8), 705–716. https://doi.org/10.1056/NEJMOA2024850.
29. Maude, S. L.; Laetsch, T. W.; Buechner, J.; Rives, S.; Boyer, M.; Bittencourt, H.; Bader, P.; Verneris, M. R.; Stefanski, H. E.; Myers, G. D.; Qayed, M.; De Moerloose, B.; Hiramatsu, H.; Schlis, K.; Davis, K. L.; Martin, P. L.; Nemecek, E. R.; Yanik, G. A.; Peters, C.; Baruchel, A.; Boissel, N.; Mechinaud, F.; Balduzzi, A.; Krueger, J.; June, C. H.; Levine, B. L.; Wood, P.; Taran, T.; Leung, M.; Mueller, K. T.; Zhang, Y.; Sen, K.; Lebwohl, D.; Pulsipher, M. A.; Grupp, S. A. Tisagenlecleucel in Children and Young Adults with B-Cell Lymphoblastic Leukemia. *N Engl J Med* **2018**, *378* (5), 439. https://doi.org/10.1056/NEJMOA1709866.
30. Lu, L.; Xie, M.; Yang, B.; Zhao, W. Bin; Cao, J. Enhancing the Safety of CAR-T Cell Therapy: Synthetic Genetic Switch for Spatiotemporal Control. *Sci Adv* **2024**, *10* (8), 6251. https://doi.org/10.1126/SCIADV.ADJ6251.
31. *CD19-Directed CAR-T Cell Therapy for the Treatment of Relapsed/Refractory B Cell Malignancies - Mayo Clinic.* https://www.mayo.edu/research/clinical-trials/cls-20512716 (accessed 2024-09-09).
32. Zhang, X.; Lu, X. A.; Yang, J.; Zhang, G.; Li, J.; Song, L.; Su, Y.; Shi, Y.; Zhang, M.; He, J.; Song, D.; Lv, F.; Li, W.; Wu, Y.; Wang, H.; Liu, H.; Zhou, X.; He, T.; Lu, P. Efficacy and Safety of Anti-CD19 CAR T-Cell Therapy in 110 Patients with B-Cell Acute Lymphoblastic Leukemia with High-Risk Features. *Blood Adv* **2020**, *4* (10), 2325–2338. https://doi.org/10.1182/BLOODADVANCES.2020001466.
33. *CAR T-Cell Therapy: How to Manage Costs and Get Financial Assistance.* https://www.webmd.com/cancer/lymphoma/features/navigate-finances-car-t-cell-therapy (accessed 2024-09-09).
34. *Bristol Myers Squibb - U.S. FDA Approves Bristol Myers Squibb's Breyanzi ® as the First and Only CAR T Cell Therapy for Adults with Relapsed or Refractory Chronic Lymphocytic Leukemia (CLL) or Small Lymphocytic Lymphoma (SLL)*. https://news.bms.com/news/details/2024/U.S.-FDA-Approves-Bristol-Myers-Squibbs-Breyanzi--as-the-First-and-Only-CAR-T-Cell-Therapy-for-Adults-with-Relapsed-or-Refractory-Chronic-Lymphocytic-Leukemia-CLL-or-Small-Lymphocytic-Lymphoma-SLL/default.aspx (accessed 2024-09-09).
35. *Lifesaving cancer treatment out of reach for rural people.* https://www.nbcnews.com/health/cancer/lifesaving-cancer-treatment-reach-rural-people-rcna44281 (accessed 2024-09-09).
36. *FDA Requires Boxed Warning for T cell Malignancies Following Treatment with BCMA-Directed or CD19-Directed Autologous Chimeric Antigen Receptor (CAR) T cell Immunotherapies | FDA.* https://www.fda.gov/vaccines-blood-biologics/safety-availability-biologics/fda-requires-boxed-warning-t-cell-malignancies-following-treatment-bcma-directed-or-cd19-directed (accessed 2024-09-09).
37. Hamilton, M. P.; Sugio, T.; Noordenbos, T.; Shi, S.; Bulterys, P. L.; Liu, C. L.; Kang, X.; Olsen, M. N.; Good, Z.; Dahiya, S.; Frank, M. J.; Sahaf, B.; Mackall, C. L.; Gratzinger, D.; Diehn, M.; Alizadeh, A. A.; Miklos, D. B. Risk of Second Tumors and T-Cell Lymphoma after CAR T-Cell Therapy. *New England Journal of Medicine* **2024**, *390* (22), 2047–2060. https://doi.org/10.1056/NEJMOA2401361.
38. *Secondary Cancers Following CAR T Cell Therapy Are Rare.* https://www.pennmedicine.org/news/news-releases/2024/january/secondary-cancers-following-car-t-cell-therapy-are-rare (accessed 2024-09-09).
39. Litvinova, L. S.; Shupletsova, V. V.; Khaziakhmatova, O. G.; Daminova, A. G.; Kudryavtseva, V. L.; Yurova, K. A.; Malashchenko, V. V.; Todosenko, N. M.; Popova, V.; Litvinov, R. I.; Korotkova, E. I.; Sukhorukov, G. B.; Gow, A. J.; Weissman, D.; Atochina-Vasserman, E. N.; Khlusov, I. A. Human Mesenchymal Stem Cells as a Carrier for a Cell-Mediated Drug Delivery. *Front Bioeng Biotechnol* **2022**, *10*. https://doi.org/10.3389/FBIOE.2022.796111/FULL.
40. Timin, A. S.; Litvak, M. M.; Gorin, D. A.; Atochina-Vasserman, E. N.; Atochin, D. N.; Sukhorukov, G. B. Cell-Based Drug Delivery and Use of Nano-and Microcarriers for Cell Functionalization. *Adv Healthc Mater* **2018**, *7* (3). https://doi.org/10.1002/ADHM.201700818.
41. Aravindhan, S.; Ejam, S. S.; Lafta, M. H.; Markov, A.; Yumashev, A. V.; Ahmadi, M. Mesenchymal Stem Cells and Cancer Therapy: Insights into Targeting the Tumor Vasculature. *Cancer Cell Int* **2021**, *21* (1). https://doi.org/10.1186/S12935-021-01836-9.
42. Gwendal, L.; Paula Y, L. Recent Discoveries Concerning the Tumor - Mesenchymal Stem Cell Interactions. *Biochimica et Biophysica Acta (BBA) - Reviews on Cancer* **2016**, *1866* (2), 290–299. https://doi.org/10.1016/J.BBCAN.2016.10.004.
43. Fuhrmann, G.; Serio, A.; Mazo, M.; Nair, R.; Stevens, M. M. Active Loading into Extracellular Vesicles Significantly Improves the Cellular Uptake and Photodynamic Effect of Porphyrins. *J Control Release* **2015**, *205*, 35–44. https://doi.org/10.1016/J.JCONREL.2014.11.029.
44. Pessina, A.; Leonetti, C.; Artuso, S.; Benetti, A.; Dessy, E.; Pascucci, L.; Passeri, D.; Orlandi, A.; Berenzi, A.; Bonomi, A.; Coccè, V.; Ceserani, V.; Ferri, A.; Dossena, M.; Mazzuca, P.; Ciusani, E.; Ceccarelli, P.; Caruso, A.; Portolani, N.; Sisto, F.; Parati, E.; Alessandri, G. Drug-Releasing Mesenchymal Cells Strongly Suppress B16 Lung Metastasis in a Syngeneic Murine Model. *J Exp Clin Cancer Res* **2015**, *34* (1). https://doi.org/10.1186/S13046-015-0200-3.
45. Takayama, Y.; Kusamori, K.; Tsukimori, C.; Shimizu, Y.; Hayashi, M.; Kiyama, I.; Katsumi, H.; Sakane, T.; Yamamoto, A.; Nishikawa, M. Anticancer Drug-Loaded Mesenchymal Stem Cells for Targeted Cancer Therapy. *Journal of Controlled Release* **2021**, *329*, 1090–1101. https://doi.org/10.1016/J.JCONREL.2020.10.037.
46. Herman, T. F.; Santos, C. First-Pass Effect. *xPharm: The Comprehensive Pharmacology Reference* **2023**, 1–2. https://doi.org/10.1016/B978-008055232-3.60022-4.
47. Zangiacomi, V.; Balon, N.; Maddens, S.; Tiberghien, P.; Versaux-Botteri, C.; Deschaseaux, F. Human Cord Blood-Derived Hematopoietic and Neural-Like Stem/Progenitor Cells Are Attracted by the Neurotransmitter GABA. *https://home.liebertpub.com/scd* **2009**, *18* (9), 1369–1377. https://doi.org/10.1089/SCD.2008.0367.
48. Røsland, G. V.; Svendsen, A.; Torsvik, A.; Sobala, E.; McCormack, E.; Immervoll, H.; Mysliwietz, J.; Tonn, J. C.; Goldbrunner, R.; Lønning, P. E.; Bjerkvig, R.; Schichor, C. Long-Term Cultures of Bone Marrow-Derived Human Mesenchymal Stem Cells Frequently Undergo Spontaneous Malignant Transformation. *Cancer Res* **2009**, *69* (13), 5331–5339. https://doi.org/10.1158/0008-5472.CAN-08-4630/654991/P/LONG-TERM-CULTURES-OF-BONE-MARROW-DERIVED-HUMAN.

DOI: 10.36838/IJHSR87.139

49. Karnoub, A. E.; Dash, A. B.; Vo, A. P.; Sullivan, A.; Brooks, M. W.; Bell, G. W.; Richardson, A. L.; Polyak, K.; Tubo, R.; Weinberg, R. A. Mesenchymal Stem Cells within tumor Stroma Promote Breast Cancer Metastasis. *Nature 2007 449:7162* **2007**, *449* (7162), 557–563. https://doi.org/10.1038/nature06188.
50. Ljujic, B.; Milovanovic, M.; Volarevic, V.; Murray, B.; Bugarski, D.; Przyborski, S.; Arsenijevic, N.; Lukic, M. L.; Stojkovic, M. Human Mesenchymal Stem Cells Creating an Immunosuppressive Environment and Promote Breast Cancer in Mice. *Scientific Reports 2013 3:1* **2013**, *3* (1), 1–9. https://doi.org/10.1038/srep02298.
51. Rombouts, W. J. C.; Ploemacher, R. E. Primary Murine MSC Show Highly Efficient Homing to the Bone Marrow but Lose Homing Ability Following Culture. *Leukemia* **2003**, *17* (1), 160–170. https://doi.org/10.1038/SJ.LEU.2402763.
52. Barbash, I. M.; Chouraqui, P.; Baron, J.; Feinberg, M. S.; Etzion, S.; Tessone, A.; Miller, L.; Guetta, E.; Zipori, D.; Kedes, L. H.; Kloner, R. A.; Leor, J. Systemic Delivery of Bone Marrow-Derived Mesenchymal Stem Cells to the Infarcted Myocardium: Feasibility, Cell Migration, and Body Distribution. *Circulation* **2003**, *108* (7), 863–868. https://doi.org/10.1161/01.CIR.0000084828.50310.6A.
53. Caplan, A. I.; Bruder, S. P. Mesenchymal Stem Cells: Building Blocks for Molecular Medicine in the 21st Century. *Trends Mol Med* **2001**, *7* (6), 259–264. https://doi.org/10.1016/S1471-4914(01)02016-0.
54. Marelli, G.; Howells, A.; Lemoine, N. R.; Wang, Y. Oncolytic Viral Therapy and the Immune System: A Double-Edged Sword Against Cancer. *Front Immunol* **2018**, *9* (APR). https://doi.org/10.3389/FIMMU.2018.00866.
55. Cornejo, Y.; Li, M.; Dellinger, T. H.; Mooney, R.; Rahman, M. M.; McFadden, G.; Aboody, K. S.; Hammad, M. NSCs Are Permissive to Oncolytic Myxoma Virus and Provide a Delivery Method for Targeted Ovarian Cancer Therapy. *Oncotarget* **2020**, *11* (51), 4693. https://doi.org/10.18632/ONCOTARGET.27845.
56. Mooney, R.; Majid, A. A.; Batalla-Covello, J.; Machado, D.; Liu, X.; Gonzaga, J.; Tirughana, R.; Hammad, M.; Dellinger, T. H.; Lesniak, M. S.; Curiel, D. T.; Aboody, K. S. Enhanced Delivery of Oncolytic Adenovirus by Neural Stem Cells for Treatment of Metastatic Ovarian Cancer. *Mol Ther Oncolytics* **2018**, *12*, 79–92. https://doi.org/10.1016/J.OMTO.2018.12.003.
57. Kaufman, H. L.; Kohlhapp, F. J.; Zloza, A. Oncolytic Viruses: A New Class of Immunotherapy Drugs. *Nature Reviews Drug Discovery 2015 14:9* **2015**, *14* (9), 642–662. https://doi.org/10.1038/nrd4663.
58. Kohlhapp, F. J.; Kaufman, H. L. Molecular Pathways: Mechanism of Action for Talimogene Laherparepvec, a New Oncolytic Virus Immunotherapy. *Clinical Cancer Research* **2016**, *22* (5), 1048–1054. https://doi.org/10.1158/1078-0432.CCR-15-2667/128705/AM/MOLECULAR-PATHWAYS-MECHANISM-OF-ACTION-FOR.
59. Ahmed, A. U.; Thaci, B.; Alexiades, N. G.; Han, Y.; Qian, S.; Liu, F.; Balyasnikova, I. V.; Ulasov, I. Y.; Aboody, K. S.; Lesniak, M. S. Neural Stem Cell-Based Cell Carriers Enhance Therapeutic Efficacy of an Oncolytic Adenovirus in an Orthotopic Mouse Model of Human Glioblastoma. *Molecular Therapy* **2011**, *19* (9), 1714. https://doi.org/10.1038/MT.2011.100.
60. Metz, M. Z.; Gutova, M.; Lacey, S. F.; Abramyants, Y.; Vo, T.; Gilchrist, M.; Tirughana, R.; Ghoda, L. Y.; Barish, M. E.; Brown, C. E.; Najbauer, J.; Potter, P. M.; Portnow, J.; Synold, T. W.; Aboody, K. S. Neural Stem Cell-Mediated Delivery of Irinotecan-Activating Carboxylesterases to Glioma: Implications for Clinical Use. *Stem Cells Transl Med* **2013**, *2* (12), 983. https://doi.org/10.5966/SCTM.2012-0177.
61. An, J.; Yan, H.; Li, X.; Tan, R.; Chen, X.; Zhang, Z.; Liu, Y.; Zhang, P.; Lu, H.; Liu, Y. The Inhibiting Effect of Neural Stem Cells on Proliferation and Invasion of Glioma Cells. *Oncotarget* **2017**, *8* (44), 76949. https://doi.org/10.18632/ONCOTARGET.20270.
62. Li, X.; Tan, R.; Hu, X.; Jiao, Q.; Rahman, M. S.; Chen, X.; Zhang, P.; An, J.; Lu, H.; Liu, Y. Neural Stem Cell-Derived Factors Inhibit the Growth and Invasion of U87 Stem-like Cells in Vitro. *J Cell Biochem* **2019**, *120* (4), 5472–5479. https://doi.org/10.1002/JCB.27826.
63. Aboody, K. S.; Najbauer, J.; Metz, M. Z.; D'Apuzzo, M.; Gutova, M.; Annala, A. J.; Synold, T. W.; Couture, L. A.; Blanchard, S.; Moats, R. A.; Garcia, E.; Aramburo, S.; Valenzuela, V. V.; Frank, R. T.; Barish, M. E.; Brown, C. E.; Kim, S. U.; Badie, B.; Portnow, J. Neural Stem Cell-Mediated Enzyme/Prodrug Therapy for Glioma: Preclinical Studies. *Sci Transl Med* **2013**, *5* (184). https://doi.org/10.1126/SCITRANSLMED.3005365.
64. Yang, C.; Hua, N.; Xie, S.; Wu, Y.; Zhu, L.; Wang, S.; Tong, X. Oncolytic Viruses as a Promising Therapeutic Strategy for Hematological Malignancies. *Biomedicine & Pharmacotherapy* **2021**, *139*, 111573. https://doi.org/10.1016/J.BIOPHA.2021.111573.
65. Portnow, J.; Synold, T. W.; Badie, B.; Tirughana, R.; Lacey, S. F.; D'Apuzzo, M.; Metz, M. Z.; Najbauer, J.; Bedell, V.; Vo, T.; Gutova, M.; Frankel, P.; Chen, M.; Aboody, K. S. Neural Stem Cell-Based Anti-Cancer Gene Therapy: A First-in-Human Study in Recurrent High-Grade Glioma Patients. *Clin Cancer Res* **2017**, *23* (12), 2951. https://doi.org/10.1158/1078-0432.CCR-16-1518.
66. Shackleton, M. Normal Stem Cells and Cancer Stem Cells: Similar and Different. *Semin Cancer Biol* **2010**, *20* (2), 85–92. https://doi.org/10.1016/J.SEMCANCER.2010.04.002.
67. Baba, A. I.; Câtoi, C. TUMOR CELL MORPHOLOGY. **2007**.
68. Shipitsin, M.; Polyak, K. The Cancer Stem Cell Hypothesis: In Search of Definitions, Markers, and Relevance. *Laboratory Investigation* **2008**, *88* (5), 459–463. https://doi.org/10.1038/LABINVEST.2008.14/ASSET/0661824B-1292-4EDC-891C-FCB71FFD6F75/MAIN.ASSETS/GR2.JPG.
69. Jin, X.; Jin, X.; Kim, H. Cancer Stem Cells and Differentiation Therapy. *Tumor Biology* **2017**, *39* (10), 1–11. https://doi.org/10.1177/1010428317729933/ASSET/IMAGES/LARGE/10.1177_1010428317729933-FIG1.JPEG.
70. De Thé, H. Differentiation Therapy Revisited. *Nature Reviews Cancer 2017 18:2* **2017**, *18* (2), 117–127. https://doi.org/10.1038/nrc.2017.103.
71. Picerno, A.; Stasi, A.; Franzin, R.; Curci, C.; di Bari, I.; Gesualdo, L.; Sallustio, F. Why Stem/Progenitor Cells Lose Their Regenerative Potential. *World J Stem Cells* **2021**, *13* (11), 1714. https://doi.org/10.4252/WJSC.V13.I11.1714.
72. Talukdar, S.; Emdad, L.; Das, S. K.; Sarkar, D.; Fisher, P. B. Evolving Strategies for Therapeutically Targeting Cancer Stem Cells. *Adv Cancer Res* **2016**, *131*, 159–191. https://doi.org/10.1016/BS.ACR.2016.04.003.
73. Aglietta, M.; Pasquino, P.; Sanavio, F.; Stacchini, A.; Severino, A.; Fubini, L.; Morelli, S.; Volta, C.; Monteverde, A.; Piacibello, W.; Gavosto, F. Granulocyte-Macrophage Colony Stimulating Factor and Interleukin 3: Target Cells and Kinetics of Response in Vivo. *Stem Cells* **1993**, *11* (2 S), 83–87. https://doi.org/10.1002/stem.5530110814.
74. Nowak, D.; Stewart, D.; Koeffler, H. P. Differentiation Therapy of Leukemia: 3 Decades of Development. *Blood* **2009**, *113* (16), 3655–3665. https://doi.org/10.1182/BLOOD-2009-01-198911.
75. Li, D.; Liu, S.; Chen, L.; Fan, R.; Cheng, C.; Wei, X. All-Trans Retinoic Acid Enhances the Anti-Leukemia Effect of Venetoclax on Acute Myeloid Leukemia Cells. *Blood* **2019**, *134* (Supplement_1), 5055–5055. https://doi.org/10.1182/BLOOD-2019-128551.

76. Yan, M.; Liu, Q. Differentiation Therapy: A Promising Strategy for Cancer Treatment. *Chin J Cancer* **2016**, *35* (1), 3. https://doi.org/10.1186/S40880-015-0059-X.
77. Dhermain, F. Radiotherapy of High-Grade Gliomas: Current Standards and New Concepts, Innovations in Imaging and Radiotherapy, and New Therapeutic Approaches. *Chin J Cancer* **2014**, *33* (1), 16. https://doi.org/10.5732/CJC.013.10217.
78. Simon, D.; Körber, C.; Krausch, M.; Segering, J.; Groth, P.; Görges, R.; Grünwald, F.; Müller-Gärtner, H.; Schmutzler, C.; Köhrle, J.; Röher, H.; Reiners, C. Clinical Impact of Retinoids in Redifferentiation Therapy of Advanced Thyroid Cancer: Final Results of a Pilot Study. *Eur J Nucl Med Mol Imaging* **2002**, *29* (6), 775–782. https://doi.org/10.1007/S00259-001-0737-6.
79. Arima, Y.; Nobusue, H.; Saya, H. Targeting of Cancer Stem Cells by Differentiation Therapy. *Cancer Sci* **2020**, *111* (8), 2689. https://doi.org/10.1111/CAS.14504.
80. Huang ME, Ye YC, Chen SR, et al. Use of All-Trans Retinoic Acid in the Treatment of Acute Promyelocytic Leukemia. Blood. 1988;72(2):567-572. *Blood* **2016**, *128* (26), 3017. https://doi.org/10.1182/BLOOD-2016-11-750182.
81. Tallman, M. S.; Andersen, J. W.; Schiffer, C. A.; Appelbaum, F. R.; Feusner, J. H.; Woods, W. G.; Ogden, A.; Weinstein, H.; Shepherd, L.; Willman, C.; Bloomfield, C. D.; Rowe, J. M.; Wiernik, P. H. All-Trans Retinoic Acid in Acute Promyelocytic Leukemia: Long-Term Outcome and Prognostic Factor Analysis from the North American Intergroup Protocol. *Blood* **2002**, *100* (13), 4298–4302. https://doi.org/10.1182/BLOOD-2002-02-0632.
82. Masetti, R.; Biagi, C.; Zama, D.; Vendemini, F.; Martoni, A.; Morello, W.; Gasperini, P.; Pession, A. Retinoids in Pediatric Onco-Hematology: The Model of Acute Promyelocytic Leukemia and Neuroblastoma. *Adv Ther* **2012**, *29* (9), 747–762. https://doi.org/10.1007/S12325-012-0047-3/METRICS.
83. Haar, C. P.; Hebbar, P.; Wallace, G. C.; Das, A.; Vandergrift, W. A.; Smith, J. A.; Giglio, P.; Patel, S. J.; Ray, S. K.; Banik, N. L. Drug Resistance in Glioblastoma: A Mini Review. *Neurochem Res* **2012**, *37* (6), 1192. https://doi.org/10.1007/S11064-011-0701-1.
84. Freemantle, S. J.; Spinella, M. J.; Dmitrovsky, E. Retinoids in Cancer Therapy and Chemoprevention: Promise Meets Resistance. *Oncogene 2003 22:47* **2003**, *22* (47), 7305–7315. https://doi.org/10.1038/sj.onc.1206936.
85. Culine, S.; Kramar, A.; Droz, J. P.; Theodore, C. PHASE II STUDY OF ALL-TRANS RETINOIC ACID ADMINISTERED INTERMITTENTLY FOR HORMONE REFRACTORY PROSTATE CANCER. *J Urol* **1999**, *161* (1), 173–175. https://doi.org/10.1016/S0022-5347(01)62090-1.
86. Pathak, S.; Multani, A. S. Aneuploidy, Stem Cells and Cancer. *EXS* **2006**, No. 96, 49–64. https://doi.org/10.1007/3-7643-7378-4_3.

Author

Amanda Chua is a 17-year-old student at Hwa Chong Institution in Singapore. She is interested in the field of genetics and the mechanisms of cancer. As a career goal, she hopes to be able to provide novel treatment to patients with genetic diseases or cancer and solve modern global health issues.

DOI: 10.36838/IJHSR87.139

IJHSR
ijhighschoolresearch.org
REVIEW ARTICLE

A Review of Per- and Polyfluoroalkyl Substances (PFAS) and Age of Menarche among Adolescent Girls

Ayaka Singh

1207 Dover Rd, Singapore 139654; ayakasingh@gmail.com
Mentor: Dr. Frank Glover

ABSTRACT: Per- and polyfluoroalkyl substances (PFAS) represent a group of widespread environmental contaminants that have been linked to several adverse health outcomes related to endocrine disruption, such as the age of menarche. Age of menarche represents an important milestone in pubertal development, and alterations are related to adverse health outcomes. Recent data have shown that the age of menarche has significantly changed over the last few decades, which may be due in part to PFAS exposure; however, the data are mixed. We aimed to investigate the relationship between PFAS exposure and the age of menarche, and associated effects on the endocrine system. We performed an extensive literature review using PubMed and Google Scholar databases and evaluated 30 studies published after the year 2000. Of these, 20 (≈65%) reported a statistically significant association between higher PFAS exposure and altered timing of menarche, most commonly a delay, while 11 (≈35%) reported no clear association. Several longitudinal cohorts reported effect sizes such as hazard ratios for delayed menarche with PFOS exposure (HR = 0.75; 95% CI 0.59-0.96) and increased odds for menarche with PFDA exposure (OR = 2.70; 95% CI 1.32-5.51). This review highlighted current data that demonstrates PFAS adverse events on menstruation and endocrine development. Future studies should focus on clarifying causality and exposure-response relationships to inform public health regulation.

KEYWORDS: Transitional Medical Sciences, Environmental Science, Disease Prevention, PFAS, Menarche, Endocrine Disruption, Adolescence, Puberty.

Introduction

Per- and polyfluoroalkyl substances Per- and polyfluoroalkyl substances, most commonly referred to as "PFAS," represent a group of thousands of man-made chemicals that consist of carbon chains with a characteristic carbon-fluorine bond.[1] Of note, the carbon-fluorine bond is the strongest covalent bond in nature, which confers its durability and resistance to microbial degradation. Their resistance to degradation has made them useful in several industries to make insulation materials, non-stick cookware, cosmetics, and stain-resistant clothing.[2] Despite their utility, their resistance to degradation means that PFAS, once released, can persist for decades in the environment and have the ability to bioaccumulate in animals and humans. PFAS exposure has been suspected of being harmful to living organisms, and in humans, exposure is believed to negatively affect the endocrine system (the hormones in our body). Studies have shown that PFAS negatively affect the thyroid, adrenal glands, pancreas, and gonads, which can result in disruption of the endocrine system. Additionally, PFAS is detectable in the blood and urine of over 80 percent of people, which highlights the importance of understanding the effects of PFAS on individuals and populations.[3] Since PFAS can act as endocrine disruptors, the human body's hormonal systems can be affected. An important clinical indicator and health consequence of endocrine disruption in the general population is the effect of PFAS on menarche in adolescent girls.[1,4,5]

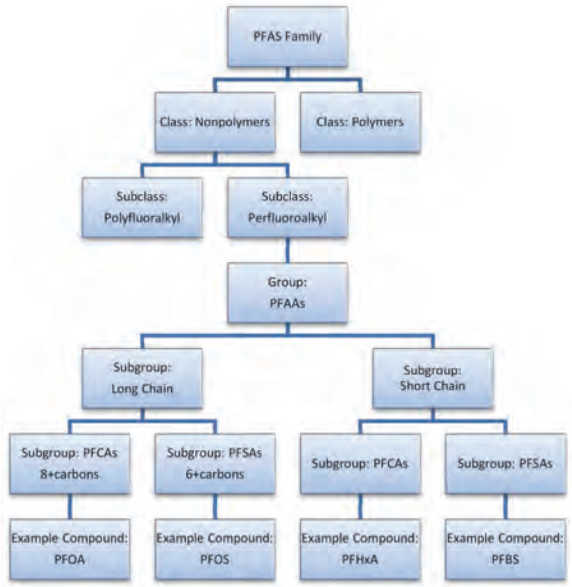

Figure 1: Overview of PFAS classification.[6]

Menarche:

Menarche, defined as the first menstrual period in a biologically female adolescent, is one of the first signs of healthy pubertal development. It occurs between the ages of 10-16, and is based on a 28-day cycle in which, around the 7th day, the female menstruates. Menstruation is the shedding of the uterine lining, and a number of factors determine the age of menarche, including heredity, nutritional intake, physical well-being, and

© 2026 Terra Science and Education

DOI: 10.36838/IJHSR87.148

exercise.[7] Menarche is a pivotal point in the development of biological females, as it shows the body has matured to a point of fertility. Over time, studies have shown that the age of menarche has significantly fluctuated over the years, and this fluctuation is believed to be due in part to exposure to environmental toxicants. One such important group of environmental toxicants, PFAS, may be implicated, and current investigations are underway to evaluate the effects of PFAS on reproductive health in women. [7-9]

Per- and polyfluoroalkyl substances and menarche:

While several recent studies have implicated PFAS in hormonal disruption (e.g., estrogen receptor inhibition, steroid hormone impairment, and dysregulation), the relationship between PFAS and women's menstrual health is currently under investigation. Recently, the focus of PFAS in the realm of women's health has come into view, especially because PFAS contaminates several women's beauty products. For example, numerous articles have shown that PFAS are readily quantified in sanitary products such as tampons and pads. Some of the companies with products known to contain PFAS in significant quantities are "Procter & Gamble" and "Kimberly-Clark." P&G owns both "Tampax", a brand of tampons, and "Always", a brand of sanitary napkins, and Kimberly Clark owns "Kotex", a brand of both pads and tampons. [10, 11] This finding is concerning since PFAS has been seen to affect many parts of the human body, and its presence in sanitary products means that there is direct contact with skin and the possibility of internal absorption. In this systematic review, the authors set out to summarize and critique the current body of literature that investigates the effects of PFAS on the menstrual cycle and hormonal balance.

Proposed mechanisms include activation of peroxisome proliferator-activated receptors (PPARs), interference with estrogen and androgen receptor signaling, altered steroidogenesis, and disruption of the hypothalamic-pituitary-gonadal axis feedback. These molecular pathways could shift the timing of puberty and menarche.[4, 10]

Shifts in age at menarche have population-level consequences: early menarche is also associated with higher risks of breast cancer,[12] type 2 diabetes,[13] and obesity,[14] while delayed menarche can signal endocrine dysfunction and impact fertility. Understanding environmental drivers such as PFAS is thus critical for reproductive and long-term health. Despite growing awareness of PFAS as endocrine disruptors, no recent review has synthesised evidence specifically on PFAS exposure and the timing of menarche in adolescent girls. This paper addresses the gap by systemically summarising and evaluating the available literature.

Methods

We performed an extensive literature review using PubMed and Google Scholar databases. Our initial search terms included combinations of words including "menarche," "PFAS," "Per- and polyfluoroalkyl substances," "adolescence," "puberty," and "menstruation," which returned 572 papers. From each included article, we extracted: publication year, study design (cross-sectional, longitudinal, case-control), sample size, geographical location, PFAS compounds assessed, exposure pathways studies (e.g., water, food, cosmetics, methods of PFAS measurement, reproductive or endocrine endpoints evaluated (e.g., age at menarche, estradiol, DHEAS), and whether the study reported a statistically significant association between PFAS exposure and menarche timing. This resulted in a final number of thirty-one papers evaluated. All thirty-one articles meeting these inclusion criteria were analysed; in the Results, we highlight studies that directly assessed PFAS exposure and age at menarche while also summarizing additional papers that examine related endocrine and pubertal outcomes to provide context.

Results

Below, we summarise the main findings from the 31 included studies, grouped by exposure pathways and reported effects on pubertal development.

PFAS exposure and common pathways in women:

The widespread use of PFAS and their long half-lives contribute to their long-term toxicity and overall health impacts. Many studies show that up to 80% of people have detectable levels of PFAS.[2] The most environmentally ubiquitous PFAS of biological importance are PFOS, PFOA, PFHxS, PFNA, and PFDE.[15, 16] PFAS exposure patterns vary by several factors, including geography, age, race/ethnicity, occupation, and socioeconomic status.[17] In some countries, mean PFAS exposures exceed 2 ng/mL, which is above the threshold set by the EPA for adverse effects. Most commonly, women are exposed to PFAS through contaminated drinking water, but also through contaminated seafood, air pollution, cooking with non-stick pans, and female beauty products. Lifetime exposure to PFAS begins as early as *in utero*, where PFAS are able to cross the placental barrier and be absorbed by the fetus. In early development, it has been shown that PFAS is transmitted through breast milk from mothers to infants, and these early exposures can have long-term effects on women as they develop into puberty.[17, 18]

As previously mentioned, drinking water is a primary exposure pathway to PFAS. There have been several studies highlighting drinking water contamination with PFAS. A 2019 study showed that from a sample from the Mid-Ohio Valley, a mean of 3.55 ng/ml of PFOA was reported.[5] Another study shows that the guideline calculated for immunotoxicity in pediatrics in PFOS is 1.3 ng/ml, and PFOA is 0.3 ng/ml.[1] Health officials and regulatory agencies estimate that 98 percent of the United States population has detectable PFAS levels in their blood, and 200 million people have been drinking contaminated water.[2]

Another common exposure pathway of PFAS is through food contamination. A study in 2009 showed that in a study of 20 different food items, multiple types of PFAS, such as PFOS, PFOA, and PFHxA, were detected, and PFOS had the highest level of detection.[19, 20] PFOA was detected in 8 of the items, and PFHxA was found in raw veal, sausages, chicken nuggets, and packaged lettuce. A study in Tarragona County,

Spain, found PFOA and PFHpA in food samples and 7 out of the 13 PFAS in the blood samples of the residents.[19] Another study conducted in 2023 by Han *et al*. stated that PFAS accumulated in oil crops, such as soybean, sesame, and peanuts, during their growth stage, and animal-based oil raw materials, like butter and fish oil, which also means the meat and dairy products used for the production are contaminated.[21]

Across the epidemiologic literature, studies using serum PFAS concentrations[17] and longitudinal follow-ups[21] were more likely to detect significant associations than small cross-sectional studies relying on single-time-point urine measures. Geographic differences may also explain mixed findings, as exposure levels in the U.S. and European cohorts often exceed those in Asian studies.

Study Findings and Quantitative Summary:

This section synthesises quantitative epidemiologic evidence on PFAS exposure and pubertal timing, with emphasis on menarche.

Overall, of the 31 studies reviewed, 20 reported a statistically significant association between at least one PFAS and altered menarche timing (commonly delayed menarche), while 11 found no significant relationship. The most frequently studied compounds were PFOS and PFOA, followed by PFNA and PFDA. Reported effect estimates include odds ratios up to 2.70 (PFDA) for early menarche and hazard ratios as low as 0.75 for delayed menarche with PFOS exposure. Sample sizes ranged from fewer than 100 participants in some biomonitoring studies to more than 800 in large longitudinal cohorts.

Several other studies reinforced these findings. One study reported that higher serum PFOS and PFNA were associated with reduced testosterone and IGF-1 levels, which can delay pubertal onset and progression.[21] Others observed that girls in the highest quartile of PFOS exposure experienced menarche later than peers in the lowest quartile,[17] and that lower sex hormone-binding globulin (SHBG) among adolescents with greater PFAS exposure, a hormonal change associated with pubertal timing.[22] Together, these studies strengthen the evidence that PFAS may disrupt endocrine signaling critical to menarche.

A study done in 2024, analyzing 231 cosmetic products from 80 brands purchased between 2019 and 2021. The total mass of PFAS in cosmetics sold in California was estimated to be 1.1 to 1.9 tonnes per year. The results of the analysis showed that 6-8% of the products tested contained at least 1 PFAS at a concentration greater than 100 ppm. The highest concentrations were found in foundation, measuring up to 10500 ppm, concealers, and mascaras, of up to 8200 ppm.[23]

There have been several studies that have investigated the relationship between PFAS exposure and pubertal development in women, though the data are mixed. A longitudinal study found that exposure to some of the most commonly found PFAS (e.g., perfluorooctanoate, perfluorooctane sulfonate, and perfluorooctanoate) led to significantly altered levels of important steroid hormones that regulate the menstrual cycle in girls. For example, girls in the 4th quartile of PFDA and PFUnDA exposure had a higher odds of early menarche, compared to those in the 1st quartile. (OR = 2.70 for PFDA and OR = 2.39 for PFUnDA. PFAS was positively associated with dehydroepiandrosterone sulfate (DHEAS) in 435 girls. A sensitivity analysis conducted evaluating only girls without hormonal contraceptives and adjusting for BMI showed PFOS (B= 1.65, 95% C.I. [0.16, 3.14]), PFNA (B= 0.60, 95% C.I. [0.07,1.14]), and PFDA (B= 1.32, 95% C.I. [0.27, 2.36]) were positively associated with DHEAS.[18]

Another longitudinal study, from 2023,[17] focused on school-age girls in Greater Cincinnati and the San Francisco Bay Area, evaluating age of thelarche (the start of adult breast development), pubarche (the initial appearance of pubic hair), and menarche, all a pivoting point for female reproductive capacity. Several PFAS were associated with adverse changes in the age of menarche. For example, girls in the 3rd quartile of PFOS exposure had a statistically significant increase in age of menarche compared to those in the 1st quartile of exposure (HR= 0.75, 95% C.I. [0.59,0.96]). Additionally, increasing levels of PFOA among girls were associated with a delay in menarche (HR= 0.04, 95% C.I. [0.01,0.25]).[17]

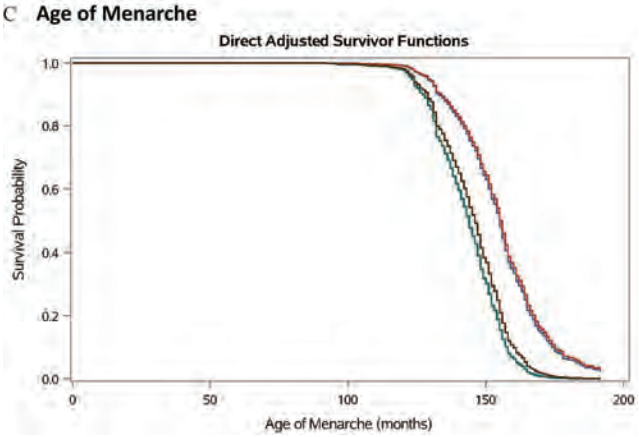

Figure 2: Impact of PFOA Exposure on Age at Menarche: Survival Analysis[17] Girls with higher PFOA exposure (red and brown lines) experienced a delay in menarche compared to those with lower PFOA levels (green and blue lines). The high PFOA group showed survival probabilities above 50% beyond 150 months of age, suggesting that PFAS exposure may disrupt the normal pubertal timing by interfering with hormonal signals necessary for initiating menstruation.

Some studies have shown a positive correlation between reducing PFAS exposure and improvement in reproductive outcomes. One study investigated the relationship between the reduction of PFAS levels in drinking water and fertility outcomes in Minnesota. The study compared areas that had water filtration facilities installed and areas that did not. The area that had not had filters installed showed significantly lower average birth weight (OR = 1.36, 95% C.I. [1.25, 1.48]), preterm births (OR = 1.14, 95% C.I. [1.09, 1.19]), and gestational age. The average reproductive rate was also significantly lower when PFAS exposures were high (Incident rate ratio = 0.73, 95% C.I. [0.69, 0.77]).[24]

Other cohort studies have evaluated the association between PFAS, reproductive hormones, and the age of menarche in large, prospective designs. The authors measured the relationship between PFAS and estradiol in children ages 6-9 who

DOI: 10.36838/IJHSR87.148

were living near a chemical plant in Ohio. It was found that median concentrations of PFHxS, PFOA, PFOS, and PFNA were 7, 30, 21, and 1.7 ng/mL among girls. Regression analyses showed that PFOS and PFNA were associated with lower serum percent levels of testosterone (-6.6%, 95% C.I. [-10.1, -2.8%]) and Insulin Growth Factor-1 (IGF-1) (-3.8%, 95% C.I. [-6.4,-1.2]), respectively, which serve as important hormones for proper pubertal development.[21] In another study, authors found that mean values of sex hormone-binding globulin (SHBG) decreased significantly among participants who were in the greater than 50th percentile exposure levels of PFOA, PFOS, and PFUA compared to individuals in the <50th percentile exposure groups.[22] In totality, these studies have shown moderate to strong relationships between population-level PFAS exposures and adverse effects on sex hormone levels, pubertal development, and subsequent age of menarche.

■ Discussion

Our review shows that nearly two-thirds of the available studies report a measurable association between PFAS exposure and altered timing of menarche, suggesting that endocrine disruption from PFAS may have meaningful developmental consequences. Importantly, this evidence base has expanded rapidly in the last five years, highlighting an emerging but still methodologically heterogeneous field. Variability in exposure metrics, geographical differences, and small sample sizes likely contribute to conflicting findings.

Recap:

PFAS represent one of the most common groups of environmental toxicants that act as endocrine disruptors, and their effects from early exposure can have lifetime implications. This systematic review shows that PFAS exposure significantly alters the timing of menstruation, and this can, in turn, be related to adverse fertility and health outcomes among women.

Reducing:

PFAS exposure Given the strong evidence of PFAS toxicity, it's important to be mindful of ways to reduce PFAS exposure. Our findings suggest that mitigation efforts - such as water filtration and regulation of PFAS in cosmetics - may benefit reproductive health. However, global production of novel PFAS analogues continues, and regulatory actions often lag behind emerging evidence.

Studies have shown that the primary pathways of exposure to PFAS include contaminated drinking water and food, cosmetic use, clothing, and occupational exposures. A study showed that the highest PFAS concentrations within cosmetics were in foundation, concealer, and mascara.[23] Several current studies are investigating policies and social practices that are effective at lowering PFAS levels. For example, communities in Minnesota with filtered drinking water had lower water PFAS levels and improved fertility outcomes compared to similar surrounding areas without filtered water and higher PFAS levels.[24] Additionally, to combat PFAS contamination on a global scale, there have been several policies implemented over the last fifteen years, which have resulted in significantly lower PFAS levels. For example, the United States Environmental Protection Agency (U.S. EPA) implemented a task force in 2022 focused on destroying and removing PFAS-contaminated waste.[25] These practice changes and policy initiatives have shown promise in lowering PFAS levels and improving associated health outcomes. Future studies should continue to evaluate the effectiveness of these practices and ultimately implement them in various populations.

Other PFAS-related health effects:

In addition to perturbing the onset of menarche, numerous studies have found that PFAS is also associated with several other adverse health effects. For example, individuals who are exposed to PFAS and are at high risk for type 2 diabetes had elevated glycemic indicators (fasting proinsulin levels, glycated hemoglobin) and an overall higher risk of developing diabetes.[12] Additionally, PFAS exposure increases the risk of hypertension and obesity.[14,26] Breast cancer risk is multifactorial, with the possibility that PFAS exposure plays a contributing role.[14] These studies highlight the overall disease burden posed by PFAS exposure and add further impetus to finding ways to regulate our production and use of PFAS to create a healthier population.

Health economic burden:

The additional health effects related to PFAS exposure cause a significant strain on the healthcare system, not only in relation to disease burden, but also economic cost. For example, one study showed that $237.55 per capita of the total healthcare costs were attributable to childhood obesity, and a rough total of $13.62 billion and $49.02 billion of direct and indirect cost have been estimated to be spent annually by 2050.[27] Additionally, the healthcare costs related to fertility treatment has continued to rise, and as previously mentioned PFAS is strongly implicated in fertility issues.[28] Future studies should continue to evaluate the economic savings related to reducing PFAS exposure, as a means to lower healthcare costs and ultimately provide more resources to communities and individuals.

Future directions:

There have also been new legislation proposals to help regulate PFAS levels.[6,29] The EPA has imposed increasing regulation of PFAS in drinking water over the last few years in response to the overwhelming data showing adverse effects of PFAS on the environment and in humans. Despite the current literature, there still exists a need to continue research on the health effects of PFAS. Of note, many of the current studies only have toxicological data on several highly studied PFAS, whereas there remain hundreds of PFAS chemicals that have not been evaluated for their potential health effects on humans.[8] It is also important to continue funding research to evaluate the joint effects of exposures (e.g., metals, plastics, pesticides) on female health.

■ Conclusion

This review paper shows how PFAS remains a significant public health issue and is especially harmful to the health of

developing women. In response to the awareness of harmful environmental and biological effects of PFAS, several important regulatory policies and public health interventions have emerged. Future directions should employ harmonized PFAS measurement methods, larger multi-ethnic cohorts, and longitudinal hormone tracking to clarify dose-response effects. Limitations of current evidence include small sample size, cross-sectional designs, inconsistent adjustment for confounders such as BMI and socioeconomic status, and focus on a limited subset of PFAS while hundreds remain untested. Addressing these gaps will strengthen causal inference and guide policy.[30]

Acknowledgements

I would like to acknowledge my grandfather, a dermatologist and researcher, as a key source of inspiration for my interest in this topic. I am also sincerely grateful to Dr. Frank Glover for his mentorship and editorial guidance throughout the research and writing process. Finally, I confirm that the ideas, analysis, and writing presented in this paper are entirely my own.

Bibliography

1. Sunderland EM, Hu XC, Dassuncao C, Tokranov AK, Wagner CC, Allen JG. A review of the pathways of human exposure to poly- and perfluoroalkyl substances (PFASs) and present understanding of health effects. J Expo Sci Environ Epidemiol. 2019 Mar;29(2):131–47.
2. Marcus M, Mueller R. Unregulated contaminants in drinking water: Evidence from PFAS and housing prices. J Environ Econ Manag. 2024 May;125:102987.
3. Peng L, Xu W, Zeng Q, Sun F, Guo Y, Zhong S, *et al*. Exposure to perfluoroalkyl substances in waste recycling workers: Distributions in paired human serum and urine. Environ Int. 2022 Jan;158:106963.
4. Buck RC, Franklin J, Berger U, Conder JM, Cousins IT, de Voogt P, *et al*. Perfluoroalkyl and polyfluoroalkyl substances in the environment: terminology, classification, and origins. Integr Environ Assess Manag. 2011 Oct;7(4):513–41.
5. Domingo JL, Nadal M. Human exposure to per- and polyfluoroalkyl substances (PFAS) through drinking water: A review of the recent scientific literature. Environ Res. 2019 Oct;177:108648.
6. Brennan NM, Evans AT, Fritz MK, Peak SA, von Holst HE. Trends in the Regulation of Per- and Polyfluoroalkyl Substances (PFAS): A Scoping Review. Int J Environ Res Public Health. 2021 Oct 17;18(20):10900.
7. Lacroix AE, Gondal H, Shumway KR, Langaker MD. Physiology, Menarche. In: StatPearls [Internet]. Treasure Island (FL): StatPearls Publishing; 2024 [cited 2024 Dec 27]. Available from: http://www.ncbi.nlm.nih.gov/books/NBK470216/
8. Chandra-Mouli V, Patel SV. Mapping the Knowledge and Understanding of Menarche, Menstrual Hygiene and Menstrual Health Among Adolescent Girls in Low- and Middle-Income Countries. In: Bobel C, Winkler IT, Fahs B, Hasson KA, Kissling EA, Roberts TA, editors. The Palgrave Handbook of Critical Menstruation Studies [Internet]. Singapore: Palgrave Macmillan; 2020 [cited 2025 Mar 23]. Available from: http://www.ncbi.nlm.nih.gov/books/NBK565619/
9. Karapanou O, Papadimitriou A. Determinants of menarche. Reprod Biol Endocrinol RBE. 2010 Sep 30;8:115.
10. Ding N, Harlow SD, Randolph JF, Loch-Caruso R, Park SK. Perfluoroalkyl and polyfluoroalkyl substances (PFAS) and their effects on the ovary. Hum Reprod Update. 2020 Sep 1;26(5):724–52.
11. Czarnywojtek A, Jaz K, Ochmańska A, Zgorzalewicz-Stachowiak M, Czarnocka B, Sawicka-Gutaj N, *et al*. The effect of endocrine disruptors on the reproductive system - current knowledge. Eur Rev Med Pharmacol Sci. 2021 Aug;25(15):4930–40.
12. Cardenas A, Gold DR, Hauser R, Kleinman KP, Hivert MF, Calafat AM, *et al*. Plasma Concentrations of Per- and Polyfluoroalkyl Substances at Baseline and Associations with Glycemic Indicators and Diabetes Incidence among High-Risk Adults in the Diabetes Prevention Program Trial. Environ Health Perspect. 2017 Oct 2;125(10):107001.
13. Lopez-Espinosa MJ, Mondal D, Armstrong BG, Eskenazi B, Fletcher T. Perfluoroalkyl Substances, Sex Hormones, and Insulin-like Growth Factor-1 at 6-9 Years of Age: A Cross-Sectional Analysis within the C8 Health Project. Environ Health Perspect. 2016 Aug;124(8):1269–75.
14. Averina M, Brox J, Huber S, Furberg AS. Exposure to perfluoroalkyl substances (PFAS) and dyslipidemia, hypertension and obesity in adolescents. The Fit Futures study. Environ Res. 2021 Apr;195:110740.
15. Glüge J, Scheringer M, Cousins IT, DeWitt JC, Goldenman G, Herzke D, *et al*. An overview of the uses of per- and polyfluoroalkyl substances (PFAS). Environ Sci Process Impacts. 2020 Dec 1;22(12):2345–73.
16. Kurwadkar S, Dane J, Kanel SR, Nadagouda MN, Cawdrey RW, Ambade B, *et al*. Per- and polyfluoroalkyl substances in water and wastewater: A critical review of their global occurrence and distribution. Sci Total Environ. 2022 Feb 25;809:151003.
17. Pinney SM, Fassler CS, Windham GC, Herrick RL, Xie C, Kushi LH, *et al*. Exposure to Perfluoroalkyl Substances and Associations with Pubertal Onset and Serum Reproductive Hormones in a Longitudinal Study of Young Girls in Greater Cincinnati and the San Francisco Bay Area. Environ Health Perspect. 2023 Sep;131(9):97009.
18. Averina M, Huber S, Almås B, Brox J, Jacobsen BK, Furberg AS, *et al*. Early menarche and other endocrine disrupting effects of per- and polyfluoroalkyl substances (PFAS) in adolescents from Northern Norway. The Fit Futures study. Environ Res. 2024 Feb 1;242:117703.
19. Ericson I, Martí-Cid R, Nadal M, Van Bavel B, Lindström G, Domingo JL. Human exposure to perfluorinated chemicals through the diet: intake of perfluorinated compounds in foods from the Catalan (Spain) market. J Agric Food Chem. 2008 Mar 12;56(5):1787–94.
20. Scheringer M. Innovate beyond PFAS. Science. 2023 Jul 21;381(6655):251.
21. Han Y, Cao X. Research Progress of Perfluoroalkyl Substances in Edible Oil: A Review. Foods Basel Switz. 2023 Jul 6;12(13):2624.
22. Tsai MS, Lin CY, Lin CC, Chen MH, Hsu SHJ, Chien KL, *et al*. Association between perfluoroalkyl substances and reproductive hormones in adolescents and young adults. Int J Hyg Environ Health. 2015 Jul;218(5):437–43.
23. Bălan SA, Bruton TA, Harris K, Hayes L, Leonetti CP, Mathrani VC, *et al*. The Total Mass of Per- and Polyfluoroalkyl Substances (PFASs) in California Cosmetics. Environ Sci Technol. 2024 Jul 9;58(27):12101–12.
24. Waterfield G, Rogers M, Grandjean P, Auffhammer M, Sunding D. Reducing exposure to high levels of perfluorinated compounds in drinking water improves reproductive outcomes: evidence from an intervention in Minnesota. Environ Health Glob Access Sci Source. 2020 Apr 22;19(1):42.

DOI: 10.36838/IJHSR87.148

25. Berg C, Crone B, Gullett B, Higuchi M, Krause MJ, Lemieux PM, *et al*. Developing innovative treatment technologies for PFAS-containing wastes. J Air Waste Manag Assoc. 2022 Jun 3;72(6):540–55.
26. Yang J, Zhang K, Shen C, Tang P, Tu S, Li J, *et al*. The Association of Hypertension with Perfluoroalkyl and Polyfluoroalkyl Substances. Int Heart J. 2023 Nov 30;64(6):1079–87.
27. Ling J, Chen S, Zahry NR, Kao TSA. Economic burden of childhood overweight and obesity: A systematic review and meta-analysis. Obes Rev Off J Int Assoc Study Obes. 2023 Feb;24(2):e13535.
28. Xu X, Yang X, Qian C, Liang Y, Xu Y, Li Z, *et al*. Per- and polyfluoroalkyl substances (PFAS) and female reproductive outcomes: PFAS elimination, endocrine-mediated effects, and disease. Toxicol. 2022 Jan;465:153031
29. Furlow B. US EPA sets historic new restrictions on toxic PFAS in drinking water. Lancet Oncol. 2024 May;25(5):e181.
30. Jogsten IE, Perelló G, Llebaria X, Bigas E, Martí-Cid R, Kärrman A, et al. Exposure to perfluorinated compounds in Catalonia, Spain, through consumption of various raw and cooked foodstuffs, including packaged food. Food Chem Toxicol Int J Publ Br Ind Biol Res Assoc. 2009 Jul;47(7):1577–83.

Author

Ayaka Singh is a 12th-grade student, currently doing the International Baccalaureate Diploma Program (IBDP), interested in science, female health, medicine, and political science.

Dr. Frank Glover, MD, PhD, is a research mentor and physician-scientist. He is a graduate of Boston College and Emory University. He has extensively published in top journals, including JAMA, Journal of Urology, and Environmental Health. In addition to his studies, he has successfully mentored dozens of students in research.

IJHSR
ijhighschoolresearch.org
RESEARCH ARTICLE

Biodegradable Textiles and Apparel as an Opportunity for Private Sector Environmental Impact

Pranay Shrinivaas Balaji Shyam Sundar

Jordan High School, 27500 Fulshear Bend Dr, Fulshear, TX 77441; pranay2balaji@gmail.com
Mentor: Richard Jarvis III, MD

ABSTRACT: The global fashion and sportswear industries produce 4-5 billion tons of carbon dioxide emissions annually, which contribute to about 10-12% of total global CO_2 emissions. Using biodegradable textiles instead of petroleum-based plastics can lower greenhouse gas emissions by roughly 25%. This review explores how companies producing biodegradable materials might gain from adopting standardized reclaim systems that improve end-of-life management and promote more sustainable retail practices. The analysis of online public country-level databases (WRAP and EUROSTATS), which address current waste management and sorting practices, supports this literature review. Peer-reviewed literature was gathered through Google Scholar. Statistical analyses methods were performed using JASP software. (Version 0.95.1). The WRAP database included data from 128 countries, out of which 43 countries met study inclusion criteria. The most common output technologies were reusable textiles (n=20), sorted textiles for open-loop recycling (n=18), and non-textiles (n=17). A significant positive correlation exists between total textile and plastic waste generation (Spearman $\rho = 0.591$, $p = .011$). Absolute government environmental expenditure (Pearson $r = 0.736$, $p = .002$; Spearman $\rho = 0.879$, $p < .001$) and waste management expenditure correlate with tonnes of waste recycled (Pearson $r = 0.546$, $p = .035$; Spearman $\rho = 0.757$, $p = .002$). National textile recycling rates were correlated with outputs for disassembled textiles in fibre-to-fibre recycling (Pearson $r = 0.484$, $p = .042$; Spearman $\rho = 0.495$, $p = .037$). High production costs and competition for agricultural land limit the adoption of biodegradable textiles. Future recommendations include advancing material properties for diverse conditions, reducing costs through biopolymer innovation, and integrating biodegradable textiles into circular economy frameworks to support sustainable development in the sportswear sector.

KEYWORDS: Chemistry, Biodegradable Textiles, Closed-Loop Textiles Systems, Environmental Impact, Recycling Infrastructure.

Introduction

The world fashion and sportswear markets account for 4–5 billion tons of CO_2 annually, or 10–12% of global annual CO_2 emissions, on top of being two of the largest consumers of water and producers of waste.[1] To counter this, several companies have begun focusing their attention on biodegradable materials as an alternative to traditional synthetics.[1] Bioplastics like PLA (polylactic acid) save two-thirds of the energy consumed in producing regular plastics and emit 70% fewer greenhouse gases when degrading in landfills.[2,3] PLA alone can reduce greenhouse gas emissions by 25% compared to regular plastics.[2,3] PLA is most used in compostable packaging bags, coatings for paper and food packaging, and controlled-release systems in pharmaceutical delivery.[4] In the apparel industry, PLA is being adopted for green fashion, 3D printing of accessories, and zero-waste clothing.[5]

Despite these advantages, biodegradable fibers have been challenging to adopt in the apparel market, as most clothing is made up of two or more synthetic polymers.[6] The production of environmentally friendly materials, like PLA, can be 50% pricier than traditional polyester.[7,8]

Closed-loop cycles offer promising ways to address this environmental strain. Rejected products can be gathered and reprocessed, mechanically, chemically, or biologically, into the same type of materials for the same purpose, enabling fiber-to-fiber recycling and waste reduction.[9] With biodegradable fabrics, it can also involve a return to the biological cycle, where they decompose to nutrient-rich biomass that can be used to create new resources.[10]

One of the primary roadblocks preventing the use of closed-loop cycles and the growth of the biodegradable sportswear industry is the absence of formal reclaim and disposal procedures. There is no standard method of collection or sorting of biodegradable material. Most post-consumer clothing is channeled through customary landfilling, burning, or downcycling to secondary forms.[11] Moreover, public participation in using disposal facilities is virtually nonexistent, largely due to confusing labeling and the absence of clear manufacturer instructions.[12] This leads to the loss of both environmental benefits and business profitability.

These waste pathways present challenges for biodegradable products, as they necessitate specific composting or biological treatment conditions that are rarely available on a large scale. Currently, about 75% of global textile waste ends up in landfills, while roughly 25% is recycled or repurposed, typically for lower-value products such as wiping clothes or insulation.[13]

In mixed landfills, biodegradable apparel anaerobically breaks down, releasing methane and leachate, which degrades

© 2026 Terra Science and Education

DOI: 10.36838/IJHSR87.154

their environmental benefits.[14] However, when segregated and pumped into well-operating aerobic composting facilities, anaerobic degradation can be prevented because oxygen-based systems inhibit the formation of methane.[15] Proper utilization of biodegradable fabrics thus depends on advanced sorting technologies such as near-infrared spectroscopy, image-based recognition, and RFID (Radio-Frequency Identification), which can segregate them from regular fabrics and place them into appropriate composting or recycling streams.[15]

Countries investing in companies engaged in biodegradable product manufacturing would benefit from the development and deployment of an established reclaim process and sorting facility.[10,16] Utilizing closed-loop systems, companies would be able to achieve maximum material recovery, minimize damage to the environment, save on the cost of production through reusing, and generate greater consumer confidence.[9] Building on previous work in bioplastics, textile recovery processes, and supply chain models, this work investigates whether companies producing biodegradable products can benefit from implementing standard reclaim processes to improve end-of-life management and accelerate environmentally protective retail practices.

Without established industrial composting systems, most biodegradable sportswear is disposed of with conventional textiles, where it enters landfills or incineration streams. Under these conditions, biopolymers such as PLA may release methane, a greenhouse gas up to 30 times more potent than CO_2, if degradation occurs anaerobically.[14] Furthermore, mixed fibers and inadequate sorting infrastructure cause biodegradable apparel to behave like synthetics, reducing their environmental benefit.[6] Current circular practices remain limited: approximately 75% of global textile waste is landfilled, about 25% reused or downcycled, and less than 1% closed-loop recycled into new clothing.[13] Experts emphasize that building coordinated collection and fiber-to-fiber recycling systems is essential for realizing the full potential of biodegradable textiles.[10,11]

■ Sorting Technology

Image sorting technology analyzes objects' inherent visual features, such as shape, texture, and color, and it has achieved high precision in waste sorting. The process has four stages: recognition, tagging, detection, and segmentation. By automatically extracting thousands of tiny visual features from pictures, machines can pick up small differences that are beyond human capabilities.[17] When paired with Support Vector Machine (SVM) and Convolutional Neural Network (CNN) algorithms, classification accuracy can reach up to 94.8% for SVM and 83% for CNN.[18] These models can sort metals, paper, glass, plastics, waste, cardboard, and fabric in real time on high-speed conveyor belts. Continuous training with annotated new images enhances their ability to increase performance over time, which makes them very adaptable to diverse waste compositions.[19] For textile sorting specifically, hyperspectral/NIR data in combination with ML algorithms correctly identify fiber types, conveying the potential to sort large-scale automated fabric.[20] Another deep learning model, trained on more than 28 recyclable classes, obtained 83.11% accuracy and 0.63 mean average precision (mAP) on detection tasks.[19] Using near-infrared (NIR) multi-spectral sensors and machine learning, Convolutional Neural Networks (CNNs) have achieved a mean classification accuracy of 72.5% in plastics, with a peak accuracy of 83.5% for PS plastic and 66% for PET.[21] These results illustrate that image-based recognition is capable of sorting massive waste streams efficiently and accurately.

Radio-Frequency Identification (RFID) is another technology that can be integrated with image recognition to further increase sorting efficiency. This technology uses radio waves to automatically identify and track objects through tags embedded with electronic data. RFID improves recycling efficiency since it identifies material composition, reduces sorting time, and avoids contamination from non-recyclables.[22] In closed-loop systems, RFID reduces CO_2 emissions and water consumption by 99%, chemical use by 88%, and energy demand by 53% compared to original material production.[22] It can help extend garment life through digital care labeling, further lowering another 5–10% of carbon, water, and waste footprints.[22]

Beyond its environmental advantages, RFID addresses issues such as forced labor and counterfeiting, supports secondary resale channels, creates employment for 35–50 workers per plant, and has the potential to save over $175 million each year by eliminating landfill diversion.[22]

NIR spectroscopy offers another capability to waste management systems. It is a non-destructive method that measures how near-infrared radiation interacts with molecular bonds to identify materials such as polyester, cotton, wool, cashmere, nylon, and blends with accuracy.[15] It is highly accurate for identifying complex fiber blends when combined with statistical programs such as Principal Component Analysis (PCA) and Partial Least Squares (PLS).[20] NIR spectrometers are compact, modular, affordable, and environmentally friendly, making them suitable for large-scale recycling facilities. When combined with visual spectroscopy (VIS) or attenuated total reflectance (ATR), they can even detect multilayered or pigmented materials that otherwise would go undetected.[15]

These technologies are even more effective when supported by policy and collaboration across industry. The United Kingdom's Waste & Resources Action Programme (WRAP) delivers an example through the Textiles 2030 program, which aims for a 50% decrease in carbon emissions and a 30% decrease in the water footprint of clothes by 2030 compared to 2019 levels.[28] The program promotes circular design, extended product life, and higher fiber-to-fiber recycling. Over 110 organizations, representing 62% of UK clothing sales, have already joined the effort.

Members have documented a 12% per-tonne carbon footprint decrease and 4% water footprint decrease since 2019, conserving 1.1 million tonnes of CO_2 and 385 million cubic meters of water in 2022 alone.[28]

■ Methodology

This study investigates some of the current relationships between government expenditure, public waste trends, and innovative textile waste recovery programs in Europe. Using data

collected from WRAP and EUROSTATS public databases, regression and correlation analyses were conducted using JASP (2024, Version 0.95.1) [Computer software].

Data was extracted from online databases and organized in an Excel sheet. The WRAP database was used to analyze the companies that were engaged in the processing of textiles in various life stages and levels of material damage. Companies engaged in the WRAP initiative were filtered based on the feedstock they processed. Only companies receiving post-industrial textiles, pre-consumer textiles, reusable post-consumer textiles, non-reusable post-consumer textiles, workwear, hospitality, or duvets/pillows were included. Information on output composition, output technology, current processing capacity, and geographical location was extracted to an Excel file, and descriptive statistics were used to classify the concentration of each of these variables in their respective countries. Eurostat's data from 2022 provided the size of each country, population, total waste, waste sent to disposal operations, environmental expenditure (euros and %GDP), total landfill facilities, household waste, recycled waste, plastic waste, and textile waste.

Results

The WRAP database housed reports from 128 European companies engaged in textile sorting and recycling. Filtering by feedstock type allowed 43 companies to be analyzed. None of the companies included currently host websites documenting statistical information regarding their current processing engagements; however, a few listed their current processing capacity. This data was excluded due to the inconsistency of reporting.

The WRAP database included 22 countries, with the UK (n=17), Italy (n=8), and the Netherlands (n=8) having the highest number of WRAP textile waste processing facilities (see Figure 1). The most frequently reported WRAP facility output technology was reusable textiles (n=20), followed by sorted textiles for open-loop recycling (n=18), and non-textiles (n=17) (see Figure 2). Of the countries engaged in advanced output technology, Denmark-based facilities engaged in the highest diversity of technological operations, with an average of 77% (SD: 27%) of the companies engaging in each type of output technology. Italy, Turkey, and Finland reported the lowest density of technological adoption with 35% (SD: 10%, n=8), 5% (SD: 16%, n=2), and 0% (SD: 0%, n=1). Ireland was excluded from the analysis due to a lack of companies engaging in textile waste processing.

Table 1: This figure demonstrates the number of WRAP-associated facilities present in each reporting European country.

		Count
WRAP Facilities	Austria	2
WRAP Facilities	Belgium	6
WRAP Facilities	Bulgaria	1
WRAP Facilities	Croatia	1
WRAP Facilities	Denmark	3
WRAP Facilities	Finland	1
WRAP Facilities	France	5
WRAP Facilities	Germany	5
WRAP Facilities	Greece	2
WRAP Facilities	Hungary	1
WRAP Facilities	Ireland	NaN
WRAP Facilities	Italy	8
WRAP Facilities	Lithuania	1
WRAP Facilities	Netherlands	8
WRAP Facilities	Norway	2
WRAP Facilities	Poland	1
WRAP Facilities	Portugal	2
WRAP Facilities	Spain	5
WRAP Facilities	Sweden	4
WRAP Facilities	Switzerland	3
WRAP Facilities	Turkey	2
WRAP Facilities	UK	17

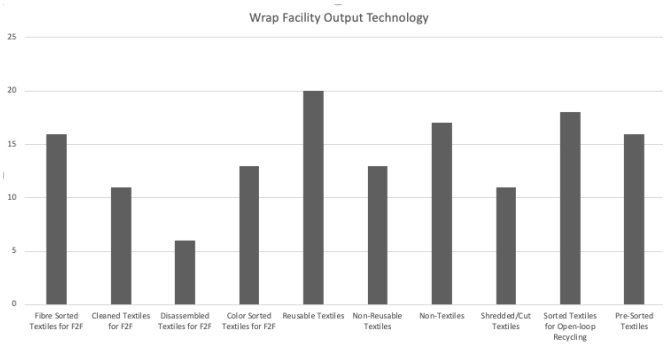

Figure 1: This figure demonstrates the number of companies advertising advanced recycling output technology.

Table 2: This figure shows the availability of output technology in each country's total WRAP facility population.

	Fibre Sorted Textiles for F2F	Cleaned Textiles for F2F	Disassembled Textiles for F2F	Color Sorted Textiles for F2F	Reusable Textiles	Non-Reusable Textiles	Non-Textiles	Shredded/Cut Textiles	Sorted Textiles for Open-loop Recycling	Pre-Sorted Textiles
Austria	50%	50%	50%	100%	50%	50%	100%	50%	100%	100%
Belgium	50%	17%	17%	50%	67%	50%	83%	33%	83%	50%
Bulgaria	0%	100%	0%	0%	100%	100%	0%	100%	100%	100%
Croatia	100%	100%	0%	100%	100%	0%	100%	0%	100%	100%
Denmark	67%	33%	33%	67%	100%	100%	100%	67%	100%	100%
Finland	0%	0%	0%	0%	0%	0%	0%	0%	0%	0%
France	80%	60%	60%	100%	40%	20%	40%	80%	80%	60%
Germany	80%	20%	20%	60%	40%	40%	60%	40%	80%	60%
Greece	0%	50%	0%	50%	50%	50%	50%	50%	100%	100%
Hungary	0%	0%	0%	100%	0%	0%	100%	0%	100%	100%
Ireland	0%	100%	0%	0%	100%	100%	0%	100%	100%	100%
Italy	50%	25%	25%	50%	38%	38%	38%	25%	38%	25%
Lithuania	100%	100%	100%	100%	0%	0%	0%	100%	0%	0%
Netherlands	63%	38%	38%	50%	50%	50%	63%	38%	75%	50%
Norway	100%	100%	100%	50%	50%	50%	50%	50%	50%	50%
Poland	0%	0%	0%	100%	0%	0%	100%	0%	100%	100%
Portugal	50%	0%	0%	100%	0%	0%	50%	50%	100%	50%
Spain	80%	60%	40%	100%	40%	20%	40%	60%	100%	80%
Sweden	75%	75%	75%	75%	50%	50%	75%	50%	75%	75%
Switzerland	100%	67%	33%	100%	100%	67%	100%	33%	100%	33%
Turkey	0%	0%	0%	0%	0%	50%	0%	0%	0%	0%
UK	35%	29%	24%	29%	47%	24%	47%	41%	47%	47%

DOI: 10.36838/IJHSR87.154

Table 3: This table summarizes country-level EUROSTAT data gathered from the 21 included countries. Environmental expenditure represents the proportion of a country's GDP that is spent on environmental protection, pollution abatement, protection of biodiversity and landscape, research and development, etc. Waste Management Environmentalism Expenditure represents the proportion of a country's GDP allocated toward environmentalism efforts in the waste management sector specifically.

Descriptive Statistics

	Median	Mean	Std. Deviation	Minimum	Maximum
Population	$1.05\times10^{+7}$	$2.62\times10^{+7}$	$2.86\times10^{+7}$	$2.89\times10^{+6}$	$8.55\times10^{+7}$
Total Waste (tonnes)	$6.93\times10^{+7}$	$9.30\times10^{+7}$	$9.50\times10^{+7}$	$3.34\times10^{+6}$	$3.47\times10^{+8}$
Recycled Waste (tonnes)	2,353.00	4,201.87	5,997.00	344.60	23,788.40
Textile Waste (tonnes)	26,441.50	123,037.60	231,998.87	3,363.00	815,956.00
Recycled Textile Waste (tonnes)	20,482.50	82,279.00	137,501.75	1,247.00	513,007.00
Recycling Facilities	752.00	1,623.76	2,158.74	125.00	7,923.00
Environmentalism Expenditure (%GDP)	0.70	0.74	0.29	0.20	1.40
Waste Management Environmentalism Expenditure (%GDP)	0.20	0.29	0.24	0.00	0.80

The mean population of countries included in this study was 2.62x10^7 (SD: 2.86 x 10^7). The mean total waste per country was 9.30x10^7 tonnes (SD: 9.5x10^7). The mean recycled waste per country was 4201.87 tonnes (SD: 5997.0). The textile waste (in tonnes) mean was 123,037.60, and the median was 26,441.5 with a standard deviation of 137,501.75. The mean number of recycling facilities per country was 1623.76 (SD: 2158.74). The mean percentage of GDP allocated towards national environmentalism efforts was 74% (SD: 29%). The mean percentage of GDP allocated towards environmentalist efforts in the waste management sector was 29% (SD: 0.24).

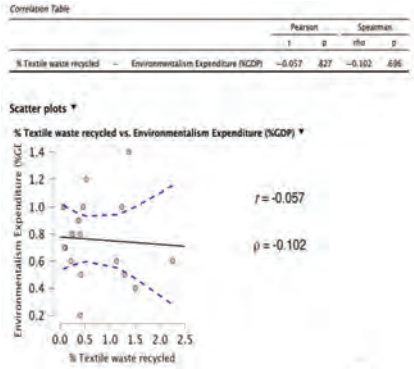

(A)

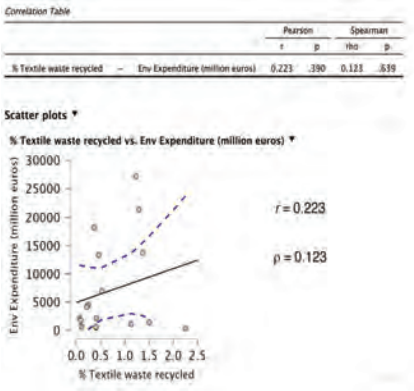

(B)

Figure 2a: This figure shows a non-significant weakly negative correlation between the percentage of total textile waste that is recycled and the percentage of each country's GDP spent on environmentalism (environmental protection, pollution abatement, protection of biodiversity and landscape, research and development, etc.).

Figure 2b: This figure shows the correlation between the percentage of total textile waste recycled and the total amount spent by each country's government on environmental initiatives in millions of euros. There was a non-significant, weakly positive association (r: 0.223, p: 0.390).

Pearson correlation revealed no association between the percentage of GDP spent on environmentalism and the percentage of textile waste that is recycled annually (Figure 2a, r: -0.057, p: 0.827). It also failed to show any significant association between textile waste and absolute spending value (Figure 2b, *r: 0.223*, *p: 0.390*). A similar lack of association was observed when analyzing the percentage of textile waste recycled in comparison to government expenditure specifically allocated toward waste management initiatives (Figure 3a, Figure 3b). The reported number of recycling facilities and recycling facilities per capita demonstrated no significant association with the percentage of textile waste recycled in each country (Figure 4a and Figure 4b)

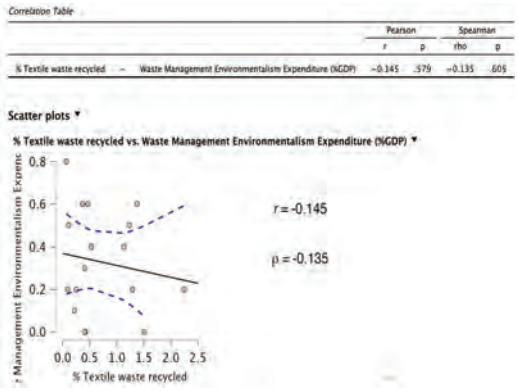

(A)

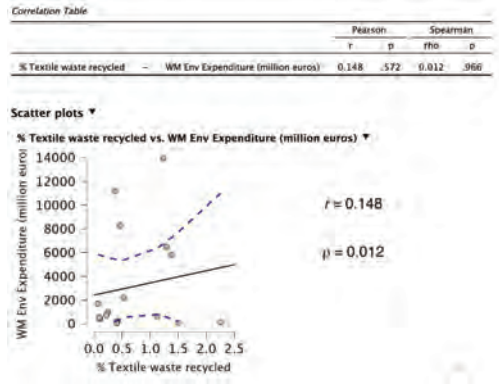

(B)

Figure 3a: This figure shows the correlation between the percentage of total textile waste recycled and the percentage of GDP allocated to waste management and environmentalism efforts. There was a non-significant, weakly negative association (r: -0.145, p: 0.579).

Figure 3b: This figure shows the correlation between the percentage of total textile waste recycled and the absolute sum of GDP allocated to waste management and environmentalism efforts. There was a non-significant, weakly positive association (r: 0.148, p: 0.572).

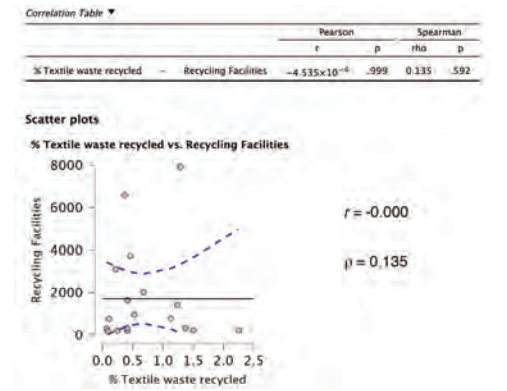

(A)

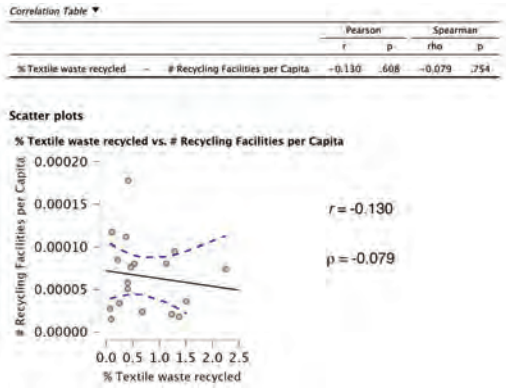

(B)

Figure 4a: This figure shows the correlation between the percentage of total textile waste recycled and the number of recycling facilities. The level of association was negligible (r: -4.535x10^-4, p: 0.999).

Figure 4b: This figure shows the correlation between the percentage of total textile waste recycled and the number of recycling facilities per capita. There was a non-significant, weakly negative association (r:-0.130, p: 0.608).

Table 4: Correlation analyses between textile and plastic waste streams yielded mixed findings. National textile and plastic recycling rates were not significantly related (Pearson r = –0.336, p = .203), indicating limited association in recycling performance across material categories. However, a significant positive association was observed between total textile and plastic waste generation (Spearman ρ = 0.591, p = .011), validating the assumption that countries producing greater volumes of textile waste also tend to produce more plastic waste. This suggests that although waste generation patterns are linked across materials, the recycling systems and infrastructure may differ between textiles and plastics.

Variables Compared	Pearson r	p-value	Spearman ρ	p-value
% Textile Waste Recycled – % Plastic Waste Recycled	–0.336	.203	–0.194	.470
Textile Waste (tonnes) – Plastic Waste (tonnes)	0.197	.434	**0.591**	**.011**

Table 5: Correlations between expenditure measures and recycled waste volumes showed that total spending levels were strongly linked with outcomes, whereas relative (%GDP) spending showed no relationship. Specifically, total environmental expenditure in millions demonstrated a robust positive correlation with recycled waste (Pearson r = 0.736, p = .002; Spearman ρ = 0.879, p < .001). Waste-management-specific expenditure also correlated significantly with recycled waste (Pearson r = 0.546, p = .035; Spearman ρ = 0.757, p = .002). In contrast, expenditure as a percentage of GDP showed no significant associations (all p > .40). These results indicate that the amount of financial investment plays a greater role than proportional budget share in predicting recycling performance.

Correlation Between Recycled Waste (tonnes) and Expenditure Variables

Expenditure Variable	Pearson r	p-value	Spearman ρ	p-value
Waste Management Environmental Expenditure (%GDP)	0.048	.865	0.227	.416
Environmentalism Expenditure (%GDP)	–0.051	.857	0.207	.459
Environmental Expenditure (million €)	**0.736**	**.002**	**0.879**	**< .001**
WM Environmental Expenditure (million €)	**0.546**	**.035**	**0.757**	**.002**

Table 6: Correlation analyses were conducted to examine the association between national textile recycling rates and company-level output types. A significant positive correlation was observed between % textile waste recycled and the proportion of companies producing disassembled textiles for fibre-to-fibre recycling (Pearson r = 0.484, p = .042; Spearman ρ = 0.495, p = .037). This suggests that countries with higher textile recycling rates are more likely to have companies engaged in advanced fibre-to-fibre disassembly practices.

Association between % Textile Waste Recycled and Company Output Types

Output Type	Pearson r	p-value	Spearman ρ	p-value
Fibre Sorted Textiles for F2F	0.419	0.084	0.438	0.069
Cleaned Textiles for F2F	0.097	0.701	0.045	0.859
Disassembled Textiles for F2F	**0.484**	**0.042**	**0.495**	**0.037**
Color Sorted Textiles for F2F	0.239	0.339	0.196	0.436
Reusable Textiles	–0.105	0.680	–0.015	0.953
Non-Reusable Textiles	–0.037	0.885	0.044	0.862
Non-Textiles	–0.037	0.884	0.104	0.681
Shredded/Cut Textiles	0.311	0.209	0.137	0.587
Sorted Textiles for Open-loop Recycling	–0.283	0.255	–0.334	0.176
Pre-Sorted Textiles	–0.267	0.283	–0.204	0.418

Additionally, fibre sorting for fibre-to-fibre recycling demonstrated a positive, though marginally non-significant, correlation with textile recycling rates (Pearson r = 0.419, p = .084; Spearman ρ = 0.438, p = .069). Other output categories, such as cleaned textiles, reusable textiles, and shredded/cut textiles, were not significantly associated with national recycling rates (all p > .20).

DOI: 10.36838/IJHSR87.154

Table 7: In contrast, analyses using recycling facilities per capita as the independent variable revealed no significant correlations with any company-level output categories (all p > .35; Table 5). Neither Pearson nor Spearman coefficients indicated meaningful associations, suggesting that the sheer density of facilities is not a strong predictor of advanced output adoption.

Correlation Between Recycling Facilities per Capita and Company Output Types

Output Type	Pearson r	p-value	Spearman ρ	p-value
Output Type	Pearson r	p-value	Spearman ρ	p-value
Fibre Sorted Textiles for F2F	–0.047	.841	–0.077	.739
Cleaned Textiles for F2F	–0.014	.952	–0.063	.785
Disassembled Textiles for F2F	0.013	.955	–0.001	.995
Color Sorted Textiles for F2F	0.176	.444	0.138	.550
Reusable Textiles	0.011	.962	–0.043	.853
Non-Reusable Textiles	0.007	.977	–0.093	.688
Non-Textiles	0.208	.366	0.180	.435
Shredded/Cut Textiles	–0.026	.910	–0.174	.451
Sorted Textiles for Open-loop Recycling	0.118	.609	0.115	.620
Pre-Sorted Textiles	0.185	.421	0.205	.373

Together, these findings indicate that system outcomes (national recycling rates) are more closely aligned with advanced company behaviors than infrastructure availability (facilities per capita). This underscores that investment in facilities alone may be insufficient without parallel improvements in reclaim processes and market alignment toward fibre-to-fibre recycling.

Discussion

The statistical analyses in this study are based primarily on simple correlations, which reveal associations but do not establish causality. Future work incorporating controlled experiments or multivariate analyses could help clarify the direction and strength of these effects. Since GDP expenditures and textile recycling were not correlated, it suggests that allocating a higher percentage of GDP to environmental efforts may not be enough to reduce the impact of textile waste in the current European infrastructure.[23] There is a slight positive trend suggesting that countries with larger raw budgets may recycle a bit more, but the lack of significance shows that budgets alone may not be the key. Wealthier countries may spend more, but if recycling systems or consumer behaviors don't change, results won't follow.[24]

The future focus should combine financial investment with public education and a strong textile-recycling infrastructure.[25]

When considering the concentration of recycling facilities and textile recycling efficiency, these analyses imply that building more facilities doesn't guarantee better recycling rates. Facilities may be underutilized, inaccessible, or not designed for textiles.[26] Optimization of existing systems and equipping them with textile-specific technology and supply chains may have a greater impact.[10]

The finding that disassembled fibre-to-fibre outputs are positively correlated with national textile recycling rates highlights the critical role of advanced processing capacity in driving system-level performance.[11,26] Disassembly is a higher-order stage of fibre-to-fibre recycling, requiring both technical expertise and investment in infrastructure, and its association with greater recycling outcomes suggests that countries capable of supporting these processes also have stronger overall waste-management ecosystems. This aligns with the principle that end-of-life textile recovery is most effective when supported by specialized infrastructure rather than broad expenditure alone.[9]

The marginal association with fibre sorting reinforces this pattern: preliminary sorting is necessary but insufficient, while true system gains are realized when companies engage in deeper processing that closes the loop back into high-quality fibres.[10,11] In contrast, the lack of association for categories such as reusable textiles or shredded textiles reflects the limits of downcycling and low-value pathways, which, while beneficial in the short term, do not fundamentally alter circularity metrics.[25]

These results suggest that policy frameworks should prioritize scaling advanced fibre-to-fibre capabilities, not just collection or basic sorting, if recycling targets are to be meaningfully increased. For biodegradable textiles specifically, this has two implications. First, without integration into disassembly and fibre-to-fibre loops, biodegradable products risk being relegated to landfill or compost streams where their environmental potential is lost.[14] Second, investment in reclaim systems that combine sorting with advanced disassembly ensures that biodegradable textiles can serve as a true complement to circular recycling systems, rather than a fallback disposal option.[9,10]

The WRAP and Eurostat databases are used in this study that provide valuable insight into textile waste management trends; however, several limitations should be noted. The WRAP database primarily includes European facilities and companies that voluntarily participate in sustainability initiatives, which may not represent all countries or smaller private operations. This suggests that the dataset could overrepresent technologically advanced or well-funded regions and underrepresent low-income or non-EU countries, which limits the generalizability of the findings. The database was developed through the United Kingdom Waste and Resources Action Programme to promote circular economy practices, and company participation is self-reported rather than independently verified.

The inclusion criteria for this analysis required companies to process post-industrial textiles, pre-consumer textiles, or reusable and non-reusable post-consumer textiles. However, inconsistencies in reporting quality led to the exclusion of the incomplete records. Although Eurostat provides comprehensive data, it relies on national self-reporting and varying definitions of recycled waste, which can introduce inconsistency between countries.

Several descriptive statistics in Table 3 show substantial variability, including a mean population of 2.62×10^7 with a standard deviation of 2.86×10^7. This reflects the major differences in country size and waste management capacity. The variability does not indicate miscalculation but instead the diverse nature of the sample, which may introduce errors in

correlation analyses and reduce the accuracy of cross-country comparisons. Future research should normalize results by population size or GDP and use weighted regression or multilevel models to reduce variability and improve interpretive accuracy.

Conclusion

The difference becomes clear by looking at the global trends. It is estimated that 75% of the world's textile waste ends up in landfills, 25% is reused or recycled (frequently in downgraded forms), and less than 1% is regenerated into new apparel.

The European Union generates 16 million metric tons of fashion waste every year, with only 26% being recycled or reused and 70% being sent to landfilling or burning. China, which produces 65% of garments and 31% of man-made fibers, disposes of about 45% of its annual production. In 2017, this represented nearly 26 million metric tons of textile waste sent to landfills, while only 3.5 million metric tons were recycled or reused. The United States generates nearly 17 million metric tons a year, 85% of which is sent to the landfill, which is equivalent to 5% of municipal solid waste and 29.3 kilograms of clothing landfilled per capita a year. Canada adds around 500,000 tons to the landfill per year, with individuals disposing of 30 to 55 pounds of clothes to the landfill per year. In Vancouver, textiles are equal to 5% of municipal landfill waste.

These statistics suggest that even with advanced technology and well-organized programs, current systems cannot control the volume of waste generated. Although around 95% of all the textiles thrown away can be recycled in theory, infrastructure constraints and user habits mean that the majority are sent to landfills. Synthetic fibers can take decades to decompose, releasing microplastics, which leads to long-term contamination. Biodegradable materials, therefore, become an essential supplement to recycling. When reuse and recycling are not feasible, biodegradable textiles can decompose naturally, reducing their environmental footprint and forming an essential part of the solution to reverse the increasing waste caused by fast fashion.

Acknowledgment

The author would like to thank Dr. Richard Jarvis III, MD, for his mentorship and for providing valuable discussions on the broader medical and health implications related to sustainability and biodegradable materials.

Bibliography

1. Abrishami, Shayan, Armineh Shirali, Nicole Sharples, Gulsah Ekin Kartal, Lisa Macintyre, and Omid Doustdar. "Textile Recycling and Recovery: An Eco-Friendly Perspective on Textile and Garment Industries Challenges." *Textile Research Journal* 94, nos. 23–24 (2024): 2815–34. https://doi.org/10.1177/00405175241247806
2. Vink, Eric T. H., Kristina R. Rabago, Dale A. Glassner, and Patrick R. Gruber. "Applications of Life Cycle Assessment to NatureWorks™ Polylactide (PLA) Production." *Polymer Degradation and Stability* 95, no. 3 (2010): 374–80. https://doi.org/10.1016/j.polymdegradstab.2009.11.009
3. Jamshidian, M., E. A. Tehrany, M. Imran, M. Jacquot, and S. Desobry. "Poly-Lactic Acid: Production, Applications, Nanocomposites, and Release Studies." *Comprehensive Reviews in Food Science and Food Safety* 9, no. 5 (2010): 552–71. https://doi.org/10.1111/j.1541-4337.2010.00126.x
4. Groot, Wim, and Tom Borén. "Biobased Plastics as Renewable Raw Materials: Their Potential and Limitations." *Green Chemistry* 12, no. 9 (2010): 1687–93. https://doi.org/10.1039/c004986a
5. Hamad, Khalil, Mohammad Kaseem, and Faisal Deri. "Processing and Recycling of Biopolymers: PLA and PHA." *Journal of Polymers and the Environment* 22 (2014): 427–38. https://doi.org/10.1007/s10924-014-0711-8
6. Mehta, Sunidhi. "Biodegradable Textile Polymers: A Review of Current Scenario and Future Opportunities." *Environmental Technology Reviews* 12, no. 1 (2023): 441–57. https://doi.org/10.1080/21622515.2023.2227391
7. Sabbah, Mohammed, and Raffaele Porta. "Plastic Pollution and the Challenge of Bioplastics." *J. Appl. Biotechnol. Bioeng* 2, no. 3 (2017): 00033.
8. Shen, Luning, Ernst Worrell, and Martin K. Patel. "Environmental Impact Assessment of Man-Made Cellulose Fibres." *Resources, Conservation and Recycling* 55, no. 2 (2010): 260–74. https://doi.org/10.1016/j.resconrec.2010.10.001
9. Ellen MacArthur Foundation. *A New Textiles Economy: Redesigning Fashion's Future*. Cowes, UK: Ellen MacArthur Foundation, 2017. https://ellenmacarthurfoundation.org
10. Ribul, Maria, Lara McLaren, Kate Goldsworthy, and Richard S. Blackburn. "Circular Design for Fashion: Transforming Linear Systems into Sustainable Ones." *Sustainable Production and Consumption* 27 (2021): 1350–62. https://doi.org/10.1016/j.spc.2021.02.010
11. Payne, Alice. "Open- and Closed-Loop Recycling of Textile and Apparel Products." *Handbook of Life Cycle Assessment (LCA) of Textiles and Clothing*, December 31, 2015, 103–23. https://doi.org/10.1016/B978-0-08-100169-1.00006-X
12. Niero, Monica, and Michael Z. Hauschild. "Closing the Loop for Packaging: Finding a Framework to Operationalize Circular Economy Strategies." *Procedia CIRP* 61 (2017): 685–90. https://doi.org/10.1016/j.procir.2016.11.152
13. Juanga-Labayen, Jeanger P., Ildefonso V. Labayen, and Qiuyan Yuan. "A Review on Textile Recycling Practices and Challenges." *Textiles* 2, no. 1 (2022): 174–88. https://doi.org/10.3390/textiles2010010
14. Atiwesh, Ghada, Abanoub Mikhael, Christopher C. Parrish, Joseph Banoub, and Tuyet-Anh T. Le. "Environmental Impact of Bioplastic Use: A Review." *Heliyon* 7, no. 9 (2021): e07918. https://doi.org/10.1016/j.heliyon.2021.e07918
15. Taneepanichskul, Nutcha, Danielle Purkiss, and Mark Miodownik. "A Review of Sorting and Separating Technologies Suitable for Compostable and Biodegradable Plastic Packaging." *Frontiers in Sustainability* 3 (2022). https://doi.org/10.3389/frsus.2022.901885
16. European Environment Agency. *Textiles and the Environment: The Role of Design in Europe's Circular Economy*. Luxembourg: Publications Office of the European Union, 2022. https://www.eea.europa.eu
17. Fotovvatikhah, Farnaz, Ismail Ahmedy, Rafidah Md Noor, and Muhammad Umair Munir. "A Systematic Review of AI-Based Techniques for Automated Waste Classification." *Sensors* 25, no. 10 (2025). https://doi.org/10.3390/s25103181
18. Faghih, Ehsan, Zahra Saki, and Marguerite Moore. "A Systematic Literature Review—AI-Enabled Textile Waste Sorting." *Sustainability* 17, no. 10 (2025). https://doi.org/10.3390/su17104264
19. Sayem, Faizul Rakib, Md. Sakib Bin Islam, Mansura Naznine, *et al*. "Enhancing Waste Sorting and Recycling Efficiency: Robust Deep Learning-Based Approach for Classification and Detec-

DOI: 10.36838/IJHSR87.154

tion." *Neural Computing and Applications* 37, no. 6 (2025): 4567–83. https://doi.org/10.1007/s00521-024-10855-2
20. Du, Wenqian, Jiahui Zheng, Wenxia Li, Zhengdong Liu, Huaping Wang, and Xi Han. "Efficient Recognition and Automatic Sorting Technology of Waste Textiles Based on Online Near Infrared Spectroscopy and Convolutional Neural Network." *Resources, Conservation and Recycling* 180 (May 2022): 106157. https://doi.org/10.1016/j.resconrec.2022.106157
21. Martinez-Hernandez, Uriel, Gregory West, and Tareq Assaf. "Low-Cost Recognition of Plastic Waste Using Deep Learning and a Multi-Spectral Near-Infrared Sensor." *Sensors* 24, no. 9 (2024). https://doi.org/10.3390/s24092821
22. Denuwara, Navodya, Juha Maijala, and Marko Hakovirta. "Sustainability Benefits of RFID Technology in the Apparel Industry." *Sustainability* 11, no. 22 (2019). https://doi.org/10.3390/su11226477
23. Eurostat. *Environmental Protection Expenditure Accounts – 2023 Edition*. Luxembourg: European Commission, 2023. https://ec.europa.eu/eurostat
24. Ranta, Valtteri, Jarkko Aarikka-Stenroos, Outi Ritala, and Sami Mäkinen. "Exploring Institutional Drivers and Barriers for the Circular Economy: A Cross-Regional Comparison of China, the US, and Europe." *Resources, Conservation and Recycling* 135 (2018): 70–82. https://doi.org/10.1016/j.resconrec.2017.08.017
25. European Environment Agency (EEA). *Textiles and the Environment: The Role of Design in Europe's Circular Economy.* Luxembourg: Publications Office of the European Union, 2022. https://www.eea.europa.eu/publications/textiles-and-the-environment
26. Sandin, Gustav, and Greg M. Peters. "Environmental Impact of Textile Recycling and Reuse: A Review." *Journal of Cleaner Production* 184 (2018): 353–65. https://doi.org/10.1016/j.jclepro.2018.02.266
27. Nizamuddin, Sabzoi, Abdul Jabbar Baloch, Chengrong Chen, Muhammad Arif, and Nabisab Mujawar Mubarak. "Bio-Based Plastics, Biodegradable Plastics, and Compostable Plastics: Biodegradation Mechanism, Biodegradability Standards and Environmental Stratagem." *International Biodeterioration & Biodegradation* 195 (November 2024): 105887. https://doi.org/10.1016/j.ibiod.2024.105887
28. WRAP (Waste and Resources Action Programme). *Textiles 2030 Annual Progress Report 2024*. Banbury, UK: WRAP, 2024. https://wrap.org.uk/textiles-2030
29. Zhao, X., *et al*. (2025). *Ecological risks of biodegradable plastics.* Science, 387(6670), adw9060. https://doi.org/10.1126/science.adw9060

■ Author

Pranay Balaji is a Senior high school student. Pranay plans on getting a dual major in college, in the fields of chemical engineering and computer programming. He is currently applying to colleges.

IJHSR
ijhighschoolresearch.org
RESEARCH ARTICLE

Investigation of Tensile and Soil Degradation Properties of Pure and Hybrid Homemade Bioplastics

Kaiyue Chen

Saint Kentigern College, 130 Pakuranga Road, Pakuranga, Auckland, 2010, New Zealand; alankchen07@gmail.com

ABSTRACT: This study investigates the tensile strength and soil biodegradability of bioplastics made from potato starch, agar, and gelatin-based formulations. The aim was to determine whether hybrid bioplastics could improve tensile strength while maintaining biodegradability. Bioplastics were prepared using household methods and tested for tensile strength, as well as mass loss over 28 days of soil burial. Results showed that the potato starch and gelatin hybrid had the highest tensile strength at 5151 Pa, attributed to enhanced hydrogen bonding between polymer chains. Agar-based bioplastics exhibited the lowest tensile strength at 1818 Pa due to weaker intermolecular interactions. In terms of biodegradability, gelatin fully degraded within 3 days, while the potato starch and gelatin hybrid retained 85.9% of its original mass after 28 days. These results confirm that the potato starch and gelatin hybrid possesses the strongest mechanical properties while maintaining a relatively slow degradation rate. Therefore, for high strength and extended durability, the potato starch and gelatin hybrid is the most suitable option. However, for the other combinations, there is a more pronounced trade-off between the two properties. This results in other pure or hybrid bioplastics to serve either short-term or long-term applications, depending on strength and degradation needs.

KEYWORDS: Chemistry, Materials Chemistry, Bioplastics, Tensile, Soil Degradation.

Introduction

Plastic pollution is currently an outstanding global problem, a field where major research is taking place to counter plastic pollution.[1,2] By 2015, global plastic production had reached approximately 6300 million tons, of which only 9% is recycled, and nearly 79% accumulates in landfills or the natural environment.[3] Conventional plastics play a major role in plastic pollution as they can persist in the natural environment for centuries, producing microplastics that can threaten ecosystems and human health. As a potential solution, bioplastics, which are polymers derived from renewable biomass such as starch, cellulose, and protein, have gained attention due to their eco-friendly capabilities, including having a low carbon footprint and being easily biodegradable.[4]

In recent years, there has been a growing interest in bioplastics. A review by Yadav *et al*. showcases an in-depth assessment of bioplastics, from feedstock cultivation to production as well as disposal.[5] This review highlighted both the environmental promise and trade-offs of various bioplastic systems.[5] Another authoritative review by Rosenboom *et al*. discusses how bioplastics can help shift plastic systems toward circularity and describes key challenges, such as recycling complexity and performance limitations.[6] On the other hand, bioplastics are widely used in a lot of different applications, including food and beverage packaging, biodegradable films and bags, but also medical or pharmaceutical uses such as drug delivery or scaffolds for tissue engineering.[7]

Bioplastics' advantages include reduced reliance on fossil feedstocks and often have lower greenhouse gas footprints.6 They also offer potential for biodegradation or compostability under specific situations.[8] However, bioplastics can still have limitations. Properties such as mechanical strength and thermal stability are often not as strong as conventional plastics.[9] Furthermore, recycling or trying to reuse bioplastics can be challenging because existing waste streams may hamper the ability to recycle bioplastics efficiently.[5]

This paper will specifically investigate three renewable biomasses, namely: potato starch, agar, and gelatin. Starch-based bioplastics, including those derived from potatoes, are widely used due to their natural abundance and biodegradability.[4] To enhance flexibility, plasticisers such as glycerol are commonly added; however, the addition of glycerol can reduce tensile strength and increase water sensitivity.[10] Glycerol has the same effect on all materials of bioplastics.

To provide a valid quantitative comparison between the different combinations of bioplastics, the mechanical performance of these materials is typically evaluated through tensile testing, which encompasses measuring the maximum stress a material can withstand before breaking. Additionally, soil degradability will also be measured, and is often assessed through soil burial, where mass loss over time serves as an indicator of environmental degradation.[11] The paper predicts that a hybrid of potato starch and gelatin-based bioplastics will produce a polymer that has strong properties in both tensile strength and degradability, representing an ideal combination of mechanical properties with environmental benefits. Starch materials tend to become brittle when used alone,[10] but have promising tensile and degradability properties. Gelatin, on the other hand, creates hydrogen bonds in biopolymer matrices, which result in increased elasticity and tensile strength.[12] A combination of these two components should produce a bioplastic that is both strong in tensile strength and soil degradability, providing a balance environmentally, but also mechanically.

© 2026 Terra Science and Education

DOI: 10.36838/IJHSR87.162

Although many studies have evaluated starch or gelatin-based bioplastics individually or even hybrid bioplastics, few works analyse how, under household-scale, low-cost preparation conditions, the mechanical performance and degradability properties can change. Previous work often depends on lab-grade reagents but also specialized equipment, which can limit the reproducibility and accessibility for smaller-scale or resource-limited environments.

This study addresses these gaps by evaluating multiple feedstocks (potato starch, agar, gelatin, and hybrids) under reproducible methods that can be undertaken with household materials and equipment. Furthermore, analysis will be conducted on tensile strength and soil degradability across those feedstocks, under realistic environmental conditions.

Methods

Materials:

All the materials were store-bought and/or household pantry items. The materials that were used in the making of the materials include: potato starch, agar powder, gelatin powder, white vinegar, and glycerol. When determining which specific brand of each material had to be used, it was based on materials that were already present in the household kitchen, except for the glycerol.

Table 1: Description of the brands that were used for each type of material and substance that was used in the making of each of the bioplastics.

Material	Brand
Potato Starch	POTATO STARCH GU FU 454G
Agar	Equagold Agar Agar
Gelatin	Mckenzies Gelatine Powder
Vinegar	DYC Vinegar White
Glycerol	Home Essentials Glycerol 100%

When producing pure samples of the bioplastics, different methods were taken depending on the type of bioplastic being made. Exact measurements for each bioplastic are given in Table 2:

Table 2: This is a list of the materials used when making each bioplastic. All materials were bought at the supermarket.

Potato Starch	Agar	Gelatin	PS + Agar	PS + Gelatin	Agar + Gelatin
280cm³ water 28.0g potato starch 18.7g glycerol 20cm³ white vinegar	280cm³ of 1% glycerol solution 5.6g agar powder	280cm³ of 1% glycerol solution 5.6g gelatin powder	280cm³ water 14.0g potato starch 2.8g agar powder	280cm³ water 14.0g potato starch 2.8g agar powder	280cm³ of 1% glycerol solution 2.8g gelatin powder 2.8g agar powder

The steps for making each of the pure bioplastics, not including proportions, were taken from an online YouTube video by Giestas.[13,14]

Potato Starch:

For potato starch, it was mixed with water and white vinegar before being heated over a water bath while being mixed. Then, once a clear paste was formed, it was poured into an oven tray to cool down for 7 days.

Agar and Gelatin:

The making of agar and gelatin required a solution of 1% glycerol (which was made by mixing 10cm³ of glycerol with 1000cm³ of water), to be heated up to a maximum of 50˚C. For gelatin, the powder was added after the solution reached the temperature of 50˚C, while the agar powder was added before the solution reached 50˚C. For both solutions, the mixture was heated up for 5 minutes while constantly stirring. The mixture was poured into an oven tray to cool down for 3 days.

Mixed Materials:

Potato Starch:

To produce a combination of the materials containing potato starch (i.e, potato starch and agar, potato starch and gelatin), the following steps were taken. First, the steps for making the potato starch bioplastic were followed, except that after the white paste was formed, the agar/gelatin powder was added to the paste, and the temperature was maintained at 50˚C. The paste was mixed for 5 minutes until it was poured into an oven tray mold to cool for 7 days.

Agar and Gelatin:

To produce the agar and gelatin combined bioplastic, the following steps were taken. A solution of 1% glycerol was heated up to 50˚C, with the agar powder added to the solution at the start. After 5 minutes of mixing, the gelatin powder was added to the already heated solution and mixed for a further 5 minutes. Then the solution was poured into an oven mold to cool for 3 days.

Testing:

Tensile Strength Testing:

To test the tensile strength with available equipment, identical strips of bioplastics with dimensions of 0.203m x 0.001m x 0.0165m were cut out. Then a newton meter was held up by a portion of the strip of bioplastic, with weights added until the bioplastic broke. Each weight was held up for 10 seconds before more mass was added. Due to the unavailability of sizes of weights, the lowest mass that could be added was in increments of 50g.

Each piece of bioplastic was tested 3 times, and an average was taken with the following formula:

$$Average\ mass\ held = \frac{mass\ held\ in\ trial\ 1 + mass\ held\ in\ trial\ 2 + mass\ held\ in\ trial\ 3}{3}$$

Tensile strength of the plastic was calculated using the following formula:[16]

$$Tensile\ strength = \frac{(Average\ mass\ held \div 1000) \times 9.81}{Surface\ area}$$

The value of 9.81 stems from the assumption that the gravitational pull of Earth is around 9.81ms^{-2}.[17]

Soil Degradation Testing:

Squares of the made bioplastics were buried under soil in outside conditions to mimic hypothetical degradation in the natural environment.

Each piece of plastic was buried in the soil of a dirt backyard with a depth of approximately 5cm. This allowed for easy retrieval of the plastic, as well as enough depth to completely cover the bioplastic. The extent of biodegradation in bioplastics was based on the mass of the plastic, expressed as a percentage of the initial mass. The formula used to find this percentage is:[18]

$$Percentage\ of\ mass\ remaining(\%) = \frac{Mass\ on\ day\ \#}{Intial\ mass} \times 100$$

Experimental Conditions:

Due to the nature of the biodegradation testing, where plastics are placed in the natural environment, factors such as weather parameters of rainfall and temperature can have an influence on biodegradation.[18] Therefore, to establish the notion of possible explanations for data in biodegradation, the average temperatures and rainfall data will be recorded for the duration of time when the bioplastics were buried in the ground. All the average temperatures and rainfall data were obtained through the World Weather Online website.[19]

Table 3: The weather conditions for the range of days that match the days' ranges of biodegradability. Temperature was measured by taking the average of one day, then averaging again with its respective range of days. Rainfall was calculated by adding total rainfall per day, then averaging again with its respective range of days.

Day Range	Average Temperature (°C)	Average rainfall (mm)
0	12.00	0.50
1-3	10.80	1.03
4-7	14.50	1.87
8-14	12.10	6.20
15-21	13.10	0.19
22-28	13.60	4.87

Limitations:

In this investigation, there still exist limitations due to the variability caused by access to equipment and the number of experiments. For example, especially for tensile strength, only three trials were conducted for each type of bioplastic; hence, only one value for tensile strength could be found. This limits the potential accuracy of the experiment, as more samples would allow deeper insight into whether varying samples did in fact have different properties. This could be considered when doing further research on bioplastics.

Furthermore, for tensile strength, the smallest weight that could be used had a value of 50g. This is a very big increment and can be both an underestimation and an overestimation of true values. Due to the inability to access tensile strength testing machines, home-made testing kits made from newton meters can be used instead.

Results

Tensile strength:

Preliminary Measurements:

The strips used for tensile strength had the following measurements and surface area:

Table 4: Exact dimensions for the size of bioplastics that were used for tensile strength testing.

Width (cm)	Base (cm)	Height (cm)	Surface area (cm^2)
0.1	0.165	20.3	0.108

Table 5: The raw data was collected for the tensile strength of the plastics. All pieces of plastic were measured 3 times, and average values were calculated afterward. Potato starch + Gelatin shows the largest average mass held, at 567g, while agar shows the lowest mass held at 200g.

Mass held before breaking (g)				
Bioplastic Type	**Trial 1**	**Trial 2**	**Trial 3**	**Average**
Potato Starch	450	400	450	433
Agar	200	200	200	200
Gelatin	350	350	400	367
Potato starch + Agar	300	300	300	300
Potato starch + Gelatin	550	600	550	567
Agar + Gelatin	250	250	250	250

Table 6: Processed data using the average values, calculating the average mass, total force held, tensile strength of the plastic, and the absolute uncertainty of tensile strength. Uncertainties are calculated using the respective uncertainties in the equipment. Then calculated with respect to the tensile strength formula. PS + Gelatin shows the highest tensile strength, while Agar shows the lowest tensile strength, reflecting the values found in Table 5.

Bioplastic Type	**Average mass held (g)**	**Force (N)**	**Tensile Strength (Pa)**	**Absolute Uncertainty (Pa)**
Potato Starch	433	4.251	3939	±822
Agar	200	1.962	1818	±404
Gelatin	367	3.597	3333	±704
PS + Agar	300	2.943	2727	±584
PS + Gelatin	567	5.559	5151	±1063
Agar + Gelatin	250	2.453	2273	±487

Graphical representations:

Below are the graphs for the measurements taken and calculated, using data from Tables 5 and 6.

DOI: 10.36838/IJHSR87.162

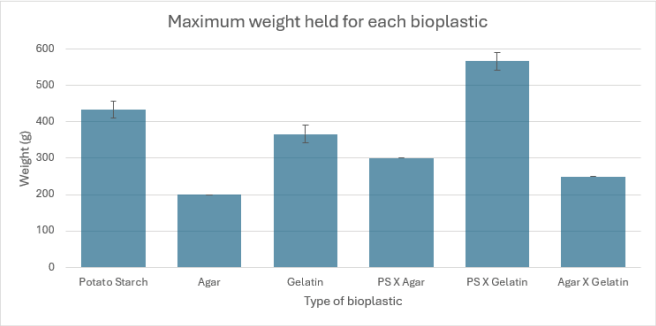

Figure 1: Raw data graph for maximum weight held using the average values in Table 3. PS, Gelatin, and PS X Gelatin all have visible uncertainty error bars. Graphs with no error bars are not visible as the uncertainty was minor.

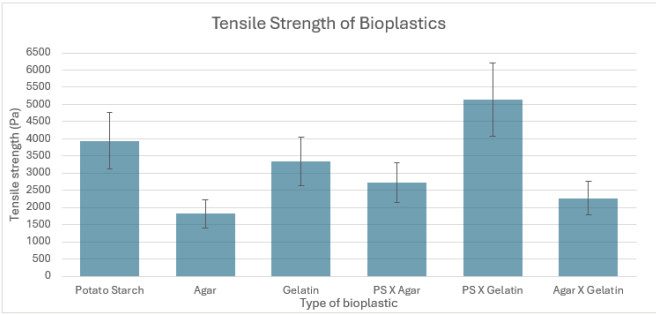

Figure 2: Processed data graph for the final tensile strengths of each bioplastic, along with standard deviations for each value. Standard deviations were found using the Excel function and then plotted on the graph.

From Table 6, the tensile strength of the bioplastic samples ranged from 1818 to 5151 Pa. The potato starch and gelatin bioplastic produced the highest tensile strength at 5151 Pa, meaning that the potato starch and gelatin blend could hold the most mass out of any other combination. On the other hand, the agar-based bioplastic showed the lowest tensile strength at 1818 Pa. Additionally, the tensile strength of pure gelatin and potato starch samples reached 3333 Pa and 3939 Pa.

Soil Degradation:

Table 7: Raw data for the weight of each sample of pure bioplastic. Each was measured using the electronic scale, and any impurities, such as dirt, were washed off until no visible dirt could be seen. All pure bioplastics except for Potato Starch have completely degraded within 28 days.

	Weight of bioplastic (g)					
Bioplastic Type	**Initial Mass**	**Mass after 3 days**	**Mass after 7 days**	**Mass after 14 days**	**Mass after 21 days**	**Mass after 28 days**
Potato Starch 1	6.91	8.01	6.16	5.05	4.65	4.21
Potato Starch 2	6.38	7.38	6.83	5.50	5.04	4.56
Potato Starch 3	6.63	7.77	6.70	5.86	5.35	4.89
Agar 1	2.51	2.98	2.62	0.00	0.00	0.00
Agar 2	2.17	2.56	2.16	0.00	0.00	0.00
Agar 3	2.44	2.87	2.50	0.00	0.00	0.00
Gelatin 1	0.77	0.00	0.00	0.00	0.00	0.00
Gelatin 2	0.82	0.00	0.00	0.00	0.00	0.00
Gelatin 3	0.82	0.00	0.00	0.00	0.00	0.00

Table 8: Raw data for the weight of each sample of hybrid bioplastic. Each was measured using the electronic scale, and any impurities, such as dirt, were washed off until no visible dirt could be seen. Only the Agar and Gelatin combination had completely degraded by 28 days, while the remaining hybrid bioplastics did not completely degrade within 28 days.

	Weight of bioplastic (g)					
Bioplastic Type	**Initial Mass**	**Mass after 3 days**	**Mass after 7 days**	**Mass after 14 days**	**Mass after 21 days**	**Mass after 28 days**
PS X Agar 1	6.02	7.34	6.98	6.21	5.44	5.13
PS X Agar 2	6.35	7.66	6.78	6.09	5.34	4.98
PS X Agar 3	6.11	7.50	6.40	5.79	5.24	4.82
PS X Gelatin 1	5.65	6.22	5.62	5.23	4.97	4.78
PS X Gelatin 2	5.34	6.08	5.41	5.09	4.77	4.61
PS X Gelatin 3	5.44	6.10	5.49	5.13	4.83	4.72
Agar X Gelatin 1	4.11	5.14	3.21	1.76	0.32	0.00
Agar X Gelatin 2	4.35	5.25	3.45	1.88	0.41	0.00
Agar X Gelatin 3	4.05	4.82	3.19	1.51	0.26	0.00

Table 9: Processed data for the average mass of each type of bioplastic over 28 days. Averages were taken from the 3 separate samples of each type of bioplastic. Agar, Gelatin, and Agar X Gelatin have completely degraded within 28 days, while the remaining samples have still not completely degraded.

	Average Weight of bioplastic (g)					
Bioplastic Type	**Initial Mass**	**Mass after 3 days**	**Mass after 7 days**	**Mass after 14 days**	**Mass after 21 days**	**Mass after 28 days**
Potato Starch	6.64	7.72	6.56	5.47	5.01	4.55
Agar	2.37	2.80	2.43	0.00	0.00	0.00
Gelatin	0.80	0.00	0.00	0.00	0.00	0.00
PS X Agar	6.16	7.50	6.72	6.03	5.34	4.98
PS X Gelatin	5.48	6.13	5.51	5.15	4.86	4.70
Agar X Gelatin	4.17	5.07	3.28	1.72	0.33	0.00

Table 10: Processed data for the percentage of mass with respect to the initial mass of each respective bioplastic on Day 0.

	Percentage of Mass Remaining (%)					
Bioplastic Type	**Initial**	**Day 3**	**Day 7**	**Day 14**	**Day 21**	**Day 28**
Potato Starch	100	116	98.8	82.4	75.7	68.6
Agar	100	118	102	0.00	0.00	0.00
Gelatin	100	0.00	0.00	0.00	0.00	0.00
PS X Agar	100	122	109	97.9	86.7	80.8
PS X Gelatin	100	112	101	94.0	88.7	85.9
Agar X Gelatin	100	122	78.7	41.2	7.91	0.00

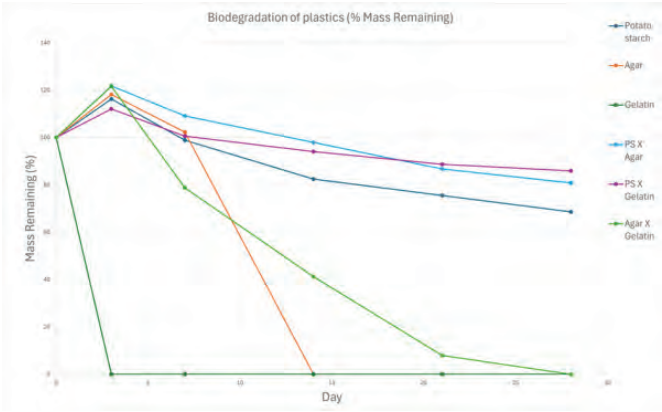

Figure 3: Plotted graph for the values obtained in Table 10, showing the change in mass of bioplastics from Day 0 to Day 28. Each color line has been color-coded to its respective biomaterial. Gelatin shows the fastest disappearance, while any bioplastic with potato starch shows relatively slow rates of degradation.

Over the 28 days that the bioplastics were buried, there were trends in the degradation behaviour of the bioplastics. From Graph 3, other than the gelatin bioplastic, all other bioplastics showed an initial increase in mass. This increase is likely due to the absorption of rainwater during the first few days, which is a common phenomenon in hydrophilic polymers.[1] On the other hand, gelatin did not gain mass during the first 3 days and was completely degraded. This fast degradation could result from enzymatic hydrolysis and microbial assimilation.[2]

However, the overall degradation rates varied between each bioplastic. The gelatin and agar bioplastics degraded in the shortest amount of days, completely degrading by days 3 and 14, respectively. On the other hand, both potato starch hybrid bioplastics followed a slower degradation trend. Specifically, the potato starch and gelatin hybrid retained 85.9% of its original mass, while the potato starch and agar blend retained 68.6% of its original mass. Through these results, it may be taken away that utilizing potato starch in a hybrid bioplastic with other biomasses can extend the life of the bioplastic.

Discussion

Tensile Strength:

The combination of bioplastic materials shows potential to enhance mechanical integrity through improved intermolecular interactions, especially when gelatin is blended with starch. In Figure 2, the uncertainty range for potato starch and potato starch with gelatin overlaps. Statistically, these two types of bioplastics could be considered similar. However, the potato starch and gelatin blend still outperformed all other plastics, even with uncertainties considered. The improved tensile properties in specific bioplastic blends result from better hydrogen bonding and enhanced molecular compatibility between biopolymer chains, which creates a stronger cohesive matrix.[18]

The tensile strength of agar-based films stays low because agar molecules do not form strong intermolecular bonds that would strengthen the polymer network.[2] Hence, the mechanical durability of agar as a single material remains limited because of its molecular structure weakness. However, the mechanical performance of the resulting material improves substantially when biopolymers such as starch or gelatin are blended.

Soil Biodegradability:

The relationship between biodegradability and water absorption is supported by previous studies linking moisture uptake to enhanced microbial colonization and enzymatic activity,[1] helping to explain certain degradation patterns, especially for bioplastics containing agar. Looking at Figure 3, both bioplastics containing agar increase in mass, but are followed by sharp decreases in mass in the following days after day 3. Furthermore, water absorption appears to facilitate degradation in hydrophilic matrices, but the overall rate still depends on the molecular structure and stability of the biopolymer blend.

For the soil degradation tests, water acts as both a swelling agent and a catalyst for degradation. These findings highlight a trade-off in properties, where highly biodegradable bioplastics, like gelatin, are more suitable for short-term disposable applications. Conversely, starch-based hybrids may be well-suited for long-term uses due to having a longer lifespan.

T-testing:

T-testing was only allowed to be done for biodegradable materials and not for tensile strengths. This is mainly because tensile strength values had only one average value per type of bioplastic. Therefore, due to limited replicates for tensile strengths, a t-test was not possible. However, t-testing was available to be done for biodegradability. Earlier in this paper, the hypothesis of "A combination of these two components (potato starch and gelatin) should produce a bioplastic that is both strong in tensile strength and soil degradability" was presented. T-tests were conducted using Microsoft Excel.[20]

The Null Hypothesis is as stated: There is no significant difference in biodegradability, based on mass remaining after 28 days, between the hybrid bioplastics and the pure PS or pure gelatin bioplastics.

The Alternative hypothesis is defined for:

Pure PS: There is no significant difference between the hybrid and pure bioplastic.

Pure gelatin: The hybrid bioplastic is less biodegradable than pure bioplastic.

Based on calculations, it was revealed that for pure PS, the p-value is 0.53, while for pure gelatin, the p-value is 0.0001. Assuming $p<0.05$ as statistically significant,[22] the null hypothesis failed to be rejected for pure PS, while for pure gelatin, the null hypothesis will be rejected, and the alternative hypothesis is accepted. Therefore, this supports the idea that hybrid bioplastics have a stronger resistance to biodegradation.

Conclusion

The initial hypothesis stated that a hybrid of potato starch and gelatin-based bioplastic would provide the best balance between tensile strength and degradability. From this investigation, it was seen that the potato starch and gelatin blend demonstrated the highest tensile strength at 5151 Pa, outperforming all other combinations. Furthermore, the potato starch and gelatin hybrid also retained the largest amount of mass after 28 days, which indicates that it has the longest lifespan among the plastics tested in this investigation. Therefore, the initial hypothesis is partially confirmed, based on the potato starch and gelatin hybrid bioplastic being the top performer in tensile strength and biodegradability. The hypothesis was confirmed with respect to the tensile strength, but not biodegradability. Slower degradation, in certain situations such as needing bioplastics to degrade faster to remove waste, does not necessarily make it the "ideal combination".

These findings are able to contribute to further articles that focus on sustainable alternatives to conventional plastics. Other tests involving bioplastics could include adjusting the ratios of starch to gelatin to optimise both strength and degradation. It would also be insightful to extend the burial period beyond 28 days, potentially providing deeper insights into long-term durability in the natural environment. Due to equipment limitations, properties such as water solubility or barrier resistance could also be tested for these hybrid bioplastics. Investigating other properties could help to refine bioplastics for specific commercial applications where environmental impact and material performance must be balanced. In this paper, it has been shown how combinations of bioplastics can enhance material performance, compared to single-material bioplastics.

Potentially, the results found could be useful for real-life applications immediately. It has been showcased how using

DOI: 10.36838/IJHSR87.162

home-grade equipment can form relatively successful alternatives to conventional plastic. More suitably, because of the low tensile strength of homemade bioplastics compared to conventional plastics, such as polypropylene plastics (PP) with a tensile strength of 15-27MPa,[23] these homemade bioplastics could be more suited for applications such as food wrapping or light-weight bags. This could be helpful for regions where plastic wrapping is not widely available and therefore can use feedstock-based bioplastics to help protect goods like food.

Acknowledgments

I would like to thank my mentor, Dr. Boris Lozhkin, for guiding me through the research process and supporting me during our discussions. I would also like to thank Indigo Research for allowing me to have this research opportunity. I attest that the ideas, graphics, and writing in this paper are entirely my own.

References

1. Qin, Q.; Yang, Y.; Yang, C.; Zhang, L.; Yin, H.; Yu, F.; Ma, J. Degradation and Adsorption Behavior of Biodegradable Plastic PLA under Conventional Weathering Conditions. *Science of The Total Environment* **2022**, *842*, 156775. https://doi.org/10.1016/j.scitotenv.2022.156775.
2. Shah, A. A.; Hasan, F.; Hameed, A.; Ahmed, S. Biological Degradation of Plastics: A Comprehensive Review. *Biotechnology Advances* **2008**, *26* (3), 246–265. https://doi.org/10.1016/j.biotechadv.2007.12.00.
3. Geyer, R.; Jambeck, J. R.; Law, K. L. Production, Use, and Fate of All Plastics Ever Made. *Science Advances* **2017**, *3* (7). https://doi.org/10.1126/sciadv.1700782.
4. Reddy, M. M.; Vivekanandhan, S.; Misra, M.; Bhatia, S. K.; Mohanty, A. K. Biobased Plastics and Bionanocomposites: Current Status and Future Opportunities. *Progress in Polymer Science* **2013**, *38* (10-11), 1653–1689. https://doi.org/10.1016/j.progpolymsci.2013.05.006.
5. Yadav, K.; Ganesh Chandrakant Nikalje. Comprehensive Analysis of Bioplastics: Life Cycle Assessment, Waste Management, Biodiversity Impact, and Sustainable Mitigation Strategies. *PeerJ* **2024**, *12*, e18013–e18013. https://doi.org/10.7717/peerj.18013.
6. Rosenboom, J.-G.; Langer, R.; Traverso, G. Bioplastics for a Circular Economy. *Nature Reviews. Materials* **2022**, *7* (117–137), 1–21. https://doi.org/10.1038/s41578-021-00407-8.
7. Narancic, T.; Cerrone, F.; Beagan, N.; O'Connor, K. E. Recent Advances in Bioplastics: Application and Biodegradation. *Polymers* **2020**, *12* (4), 920. https://doi.org/10.3390/polym12040920.
8. Abe, M. M.; Martins, J. R.; Sanvezzo, P. B.; Macedo, J. V.; Branciforti, M. C.; Halley, P.; Botaro, V. R.; Brienzo, M. Advantages and Disadvantages of Bioplastics Production from Starch and Lignocellulosic Components. *Polymers* **2021**, *13* (15), 2484. https://doi.org/10.3390/polym13152484.
9. Herman de Beukelaer, H.; Hilhorst, M.; Workala, Y.; Maaskant, E.; Post, W. Overview of the Mechanical, Thermal, and Barrier Properties of Biobased And/or Biodegradable Thermoplastic Materials. *Polymer Testing* **2022**, *116*, 107803. https://doi.org/10.1016/j.polymertesting.2022.107803.
10. Sanyang, M. L.; Sapuan, S. M.; Jawaid, M.; Ishak, M. R.; Sahari, J. Effect of Plasticizer Type and Concentration on Physical Properties of Biodegradable Films Based on Sugar Palm (Arenga Pinnata) Starch for Food Packaging. *Journal of Food Science and Technology* **2015**, *53* (1), 326–336. https://doi.org/10.1007/s13197-015-2009-7.
11. Emadian, S. M.; Onay, T. T.; Demirel, B. Biodegradation of Bioplastics in Natural Environments. *Waste Management* **2017**, *59* (0956-053X), 526–536. https://doi.org/10.1016/j.wasman.2016.10.006.
12. Yu, L.; Dean, K.; Li, L. Polymer Blends and Composites from Renewable Resources. *Progress in Polymer Science* **2006**, *31* (6), 576–602. https://doi.org/10.1016/j.progpolymsci.2006.03.002.
13. Giestas. Homemade Bioplastic: Potato vs. Corn Starch Recipe. *YouTube*, 2021. https://www.youtube.com/watch?v=Uaz9Qvadyio.
14. Giestas. Bioplastic DIY: Agar vs. Gelatin Recipe. *YouTube*, 2022. https://www.youtube.com/watch?v=Ty0O2VmbNeE (accessed 2023-05-18).
15. Mulligan, D. *Comparing the Tensile Strength of Starch Bases in Biodegradable Plastic Alternatives*. futurescienceleaders.com. https://futurescienceleaders.com/blog/2022/06/comparing-the-tensile-strength-of-starch-bases-in-biodegradable-plastic-alternatives/.
16. Marichelvam, M. K.; Jawaid, M.; Asim, M. Corn and Rice Starch-Based Bio-Plastics as Alternative Packaging Materials. *Fibers* **2019**, *7* (4), 32. https://doi.org/10.3390/fib7040032.
17. Geophysics, National Earth System Science Data Center. *Gravity of Earth*. Geophys.ac.cn. http://www.geophys.ac.cn/infowin/Gravity.asp.
18. Ahimbisibwe, M.; Banadda, N.; Seay, J.; Nabuuma, B.; Atwijukire, E.; Wembabazi, E.; Nuwamanya, E. Influence of Weather and Purity of Plasticizer on Degradation of Cassava Starch
19. WWO.BLL.Weather.bllGlobalResources.GetGlobalResourceValue("Default_Title. *Auckland, New Zealand Historical Weather Almanac*. Worldweatheronline.com. https://www.worldweatheronline.com/auckland-weather-history/nz.aspx (accessed 2025-10-07).
20. Rhim, J.-W.; Park, H.-M.; Ha, C.-S. Bio-Nanocomposites for Food Packaging Applications. *Progress in Polymer Science* **2013**, *38* (10), 1629–1652. https://doi.org/10.1016/j.progpolymsci.2013.05.008.
21. *How To Perform T-Tests In Microsoft Excel - YouTube*. www.youtube.com. https://www.youtube.com/watch?v=q0ckcKsSPXU.
22. *Statistical significance | Institute for Work & Health*. Iwh.on.ca. https://www.iwh.on.ca/what-researchers-mean-by/statistical-significance.
23. Boey, Jet & Lee, Chee & Tay, Guan. Factors Affecting Mechanical Properties of Reinforced Bioplastics: A Review. *Polymers* **2022** 14. 3737. https://doi.org/10.3390/polym .2022.14183737.

Author

Kaiyue Chen is a Grade 12 student at Saint Kentigern College. He is a passionate student, aspiring to study chemical engineering with a focus on developing environmental sustainability. He is also one of the Science Fair leaders at his school, conducting investigations into activated carbon water filters.

IJHSR
ijhighschoolresearch.org
REVIEW ARTICLE

A Role for Music in Slowing Memory Decline in Alzheimer's Disease

Olivia Tu

Lynbrook High School,1280 Johnson Ave, San Jose, CA, 95129, USA; olivia.rsdlme@gmail.com

ABSTRACT: Alzheimer's disease (AD) is a neurodegenerative disease with cases rapidly rising, posing as a major global health concern. AD is characterized by progressive cognitive decline, with memory loss being a key symptom. Given that current pharmacological treatments are unable to halt or slow neurodegeneration in AD, interest has grown in nonpharmacological approaches. In particular, music-based interventions have been shown to improve cognitive function and emotional well-being in AD patients. This article reviews music's influence on neural mechanisms that underlie its enhancement of memory in AD, as well as evidence of memory improvement and musical-memory persistence in AD. Additionally, it proposes three mechanisms of how music may slow memory decline in AD: activation of the dopaminergic system, reduction of stress, and stimulation of neuroplasticity and neurogenesis. These findings support music as a promising intervention for countering memory decline and improving the quality of life for individuals with AD. Furthermore, music holds potential as an early intervention for preventing dementia.

KEYWORDS: Behavioral Neuroscience, Music, Alzheimer's Disease, Memory.

Introduction

Alzheimer's disease is a neurodegenerative disorder characterized by impairment of memory, language, and other thinking abilities, severe enough to disrupt everyday life. It is the most common form of dementia, affecting over 55 million people worldwide, with numbers projected to double by 2050.[1]

Pathological markers of AD include amyloid-β plaques and neurofibrillary tangles. Accumulation of these toxic proteins can lead to damaging effects such as oxidative stress, neuroinflammation, and mitochondrial dysfunction, damaging synapses and causing neuronal degeneration.[2] Amyloid-β plaques cause sustained activation of microglia, an immune cell found in the central nervous system, leading them to continuously release pro-inflammatory cytokines and neurotoxins that damage neurons.[3] Amyloid-β can also cause excitotoxicity, a potential process underlying neurodegeneration in AD. Excitotoxicity occurs when there is excessive activation of glutamate receptors,[4] leading to a high influx of calcium in neurons that triggers mitochondrial dysfunction, apoptotic pathways, and neuronal death.[5]

Among the most prominent symptoms of AD are the decline of short-term memory (STM) and long-term memory (LTM). On the cellular level, memory formation is linked to hippocampal long-term potentiation (LTP), the process by which synapses are strengthened through frequent activation.[6] Early-phase LTP correlates with short-term memory (STM) and involves strengthening pre-existing connections. Late-phase LTP underlies LTM storage and involves growing new synaptic connections, gene expression, and new protein synthesis.[7] In particular, autobiographical memory, which is a long-term memory of one's life history, is compromised. It includes both episodic memory, which involves recollection of personal events/experiences, and semantic memory, which encompasses facts about oneself.[8] The episodic component is the main feature in allowing life experiences to be recalled vividly. In AD, the decline of autobiographical memory diminishes self-knowledge, sense of identity, and quality of life.[9]

Since autobiographical memory loss affects cognitive and emotional well-being, finding effective interventions is important. While current pharmaceutical treatments, including cholinesterase inhibitors and memantine, for AD help reduce cognitive impairment,[10] they do not prevent the progression of the disease nor do they stop the underlying neurodegeneration.[11] Therefore, more interventions and non-pharmacological treatments are being considered. One such intervention is music therapy, which has been shown to improve mood, cognition, and behavior in AD patients.[12] In particular, many studies have demonstrated music's reduction of stress and positive influence on emotional state for those with AD.[13,14] Beyond emotional benefits, music is capable of evoking autobiographical memories in AD patients and may facilitate the formation and retrieval of long-term memories. Music might also be able to prevent or slow neurodegeneration, as found in a study where musicians had a 64% lower likelihood of developing dementia.[15]

Underlying the positive effects of music is the principle of neuroplasticity: the brain's ability to reorganize itself by forming new neural connections in response to experience or stimuli. Brain plasticity underlies learning and memory formation and occurs throughout a lifetime. Music's modulation of the brain is also demonstrated through the strong emotional responses it evokes, helping to form vivid memories. This paper will provide a review of music's ability to modulate the brain and enhance memory in AD. Furthermore, it will propose three mechanisms of how music may reduce cognitive decline and improve memory in AD: activation of the dopaminergic sys-

© 2026 Terra Science and Education

DOI: 10.36838/IJHSR87.168

tem, reduction of stress, and stimulation of neuroplasticity and neurogenesis.

Discussion

Music Induces Neuroplasticity:

Musical engagement, whether active (direct participation) or passive (listening), can drive structural and functional neuroplasticity across the lifespan.[16] Musicians exhibit increased gray matter concentration, cortical thickness, and volume changes in their motor and auditory brain regions involved in musical performance.[17] Heschl's Gyrus, located in the temporal lobes and within the auditory cortex, has been found to have more gray matter concentration in musicians.[18,19] More cortical thickness in the auditory cortex can be linked to enhanced sound processing and perception.[20] Several studies have found increased gray matter in motor-related regions, including the premotor cortex, cerebellum, and supplementary motor area, which all play a role in the planning and execution of finger/body movements required for playing instruments.[21–23] Higher gray matter density is not only exhibited in motor areas, but also in places related to higher-order executive functions (mainly frontal gyri), associated with monitoring musical information and processing musical structures.[24,25] Research has also revealed higher gray matter density in the hippocampus among musicians, which is associated with context-dependent episodic memory.[23] Through these studies, it is clear that musical training correlates with structural modifications, indicating better processing and functioning in such regions.

Similar to gray matter differences, diffusion tensor imaging (DTI) studies have revealed greater white matter organization (via higher fractional anisotropy) for musicians in parts of the brain associated with motor control and sensory processing. Studies have revealed that musicians show more white matter integrity in the arcuate fasciculus, a white-matter fiber tract connecting supporting motor-auditory connectivity and auditory processing.[26] Additionally, musicians have greater fractional anisotropy in the corpus callosum, which links the two brain hemispheres for coordination and connects a variety of sensorimotor areas.[27] The cerebellum and striatum also exhibit more white matter integrity, as they are involved in learning repetitive, automated finger movements.[28] These findings indicate that musical experience increases myelination (via increased white matter), enhancing connectivity and processing speed in the brain.

Growing evidence has demonstrated that active music training can also modify functional activation in auditory, cognitive, and motor areas. One investigation found that skilled musicians exhibit a larger cortical representation of musical tones, suggesting they are more attuned to pitch/contour.[29] This shows that auditory cortex processing becomes more developed from musical exposure. Musicians also exhibit more activity in the dorsolateral and inferior frontal cortex (includes Broca's Area), superior temporal gyrus (contains Wernicke's Area), and motor areas.[30–32] Thus, musical practice induces cortical reorganization, shown through functional changes in activation and representation of music.

The above-mentioned studies include several limitations, which could be addressed in future studies. One limitation is not taking into account biological predispositions, making it difficult to attribute brain plasticity differences to musical training. Therefore, longitudinal studies are needed to prove a causal relationship between music experience and brain alterations. Existing longitudinal studies conducted on music-induced neuroplasticity yield structural and functional changes consistent with those summarized above. Studies employing music training on children found increased volume in primary motor regions and auditory regions, particularly the corpus callosum.[21,33,34] Furthermore, increased FA of white-matter tracts such as the corpus callosum, corticospinal tract, and superior longitudinal fasciculus have also been observed in longitudinal studies.[35] Notably, the magnitude of these differences correlated with practice time. Functionally, music training results in heightened activity in the premotor cortex, posterior parietal regions, and cerebellum.[36] These areas take part in auditory-motor mapping, and are shown to be activated similarly during passive music listening and active performance.[37] Based on existing findings, we can conclude that musical engagement induces neuroplasticity, stimulating new neuronal connections that may combat neurodegeneration.

While the above research has focused on comparisons between musicians and non-musicians, recent studies have examined music-induced neuroplasticity seen in AD patients. One study has shown that musical training and engagement drive functional and structural changes in the brain, particularly in the hippocampus, for individuals diagnosed with or at risk of developing AD. Findings suggest that musical perception skills (from musical training) can enhance connectivity in regions known to be affected in AD, particularly within the Papez circuit, including the right hippocampus and right posterior cingulate cortex[38]. Similarly, AD patients who underwent music intervention (listening to familiar music) exhibited greater fronto-temporal structural connectivity corresponding with enhanced memory.[39] Together, these findings demonstrate the potential of music to induce neuroplasticity in areas affected by AD, notably the hippocampus (which is implicated in memory), suggesting that music's influence may be a protective mechanism. However, in Fischer *et al.*, the experiment was run on individuals with early-stage cognitive decline, and music intervention was relatively short at 3-weeks. Additionally, in Matziorinis *et al.*, the study was mainly observational across three subgroups of those with musical engagement, music perception skills, and musical training. These limitations require us to further examine music's longitudinal effects for those with varying stages of cognitive decline.

Music-evoked Emotions Enhance Memory:

Music is known to evoke strong emotional responses, which make musical memories especially vivid, and allow music to facilitate memory formation and retrieval.[40,41] Emotional arousal has been reported to modulate memory through activation of β-adrenoreceptors (activated by norepinephrine) in the basolateral amygdala, which consequently promotes

synaptic plasticity in the hippocampus.[42] Thus, music-evoked emotions can trigger similar noradrenergic activity to enhance long-term memory formation and facilitate synaptic plasticity. By acting as an emotional tag, music strengthens the encoding and retrieval of memories, making them enduring and better remembered.

A variety of functional neuroimaging studies have shown that music modulates activity in brain regions associated with emotion. The researchers found that activity in the medial prefrontal cortex (mPFC) is positively correlated with autobiographical salience (personal meaningfulness) and positive feelings evoked by the music. Such a result indicates that the medial prefrontal cortex is a hub that integrates music, autobiographical memories, and emotion.[43] Music activates neural structures involved in emotion, namely the amygdala, hippocampus, and auditory cortex. Music also stimulates reward network structures such as the striatum, anterior cingulate cortex, orbitofrontal cortex, and nucleus accumbens.[44,45] These findings show that music-evoked emotions activate a broad brain network integrating emotional, memory, and reward systems. This overlapping activation of memory and emotion in many brain regions may be why music is such a strong enhancer for episodic memory, making it beneficial in dementia in stimulating personal memories.

Music Enhances Memory in AD:

Although memory loss is a prominent feature in those with AD, musical memory (memory of music) is often remarkably preserved in those with AD, allowing music to serve as a trigger for autobiographical memories and a connection to their past. In one case study of an 84-year-old woman with severe AD, researchers found that despite her cognitive impairment, she could recognize familiar melodies, sing along with them, and distinguish familiar from unfamiliar melodies.[46] Additionally, a separate study involving patients with mild to moderate AD found that they retained high familiarity for well-known music and maintained good pitch error detection.[47] These findings show that musical memory is uniquely preserved in AD, as individuals still remember familiar songs. Corroborating the sparing of musical memory structurally, it has been shown that the pre-supplementary motor area (pre-SMA) and the anterior cingulate cortex (ACC), both of which are involved in long-term music encoding, had minimal atrophy and hypometabolism (biomarkers of AD).[48] Therefore, since the brain circuits underlying musical memory are less affected in AD and relatively spared, using music as a stimulus may help bolster memory networks, preserving them to prevent memory loss in AD.

To support our understanding of the resilience of musical memory in individuals with AD, we can look at music-evoked autobiographical memories (MEAMs), which exhibit music's power to bring back episodic memories, serving as a cue to relay information of the past.[40,47,49–51] In a study involving patients with AD, individuals were asked to remember autobiographical events after being exposed to familiar music (self-picked) or silence.[49] Results showed that in contrast to memories evoked in silence, memories evoked after music exposure were more specific, retrieved faster, and contained more emotional significance. This suggests that music is able to promote faster recall of a more vivid and emotional memory. In a similar investigation, participants with mild AD listened to Vivaldi's "Spring" in one session and were exposed to silence during another.[50] Autobiographical Memory Interviews conducted after each condition revealed that participants recalled significantly more events from their three life periods (childhood, early adulthood, and recent) following the music condition. The improvement in autobiographical memory recall scores indicates that music enhances recollection of one's lifespan. A different investigation on elderly individuals with mild to moderate dementia found an improvement in recall when answering autobiographical questions while exposed to familiar music.[51] MEAMs are special due to their persistence, often remaining intact despite cognitive decline. This resilience is evident in the previously mentioned study by Cuddy *et al.*, who discovered that the proportion of familiar song melodies that triggered MEAMs in AD patients was not significantly different from that of healthy older adults.[47] These results demonstrate music's resilience and enhancement of autobiographical memory recall in AD patients.

The power of music-evoked autobiographical memories might be rooted in music's ability to bring about emotions.[52] The study on AD above revealed that the pre-SMA and ACC are involved in long-term music memory, and are among the variety of regions activated by music-evoked emotions.[52] The overlapping of emotion and memory-related processing in these areas, and the fact that they are among the last to degenerate in AD,[53] show the role of emotion in helping to preserve musical memory in individuals with AD.

The studies above have primarily focused on music's facilitation of autobiographical memory, but music has also been shown to engage with other forms of memory. Interestingly, musical procedural memory, the ability to play an instrument, is relatively spared in AD pathology until the late stages, unlike explicit memory forms, which are impaired.[54] While early AD primarily affects the temporal lobes and frontal brain regions (implicating explicit or short-term memories), procedural memory involves the cortico-striatal and cortico-cerebellar systems, resulting in their possible preservation.[55,56] Case studies on a pianist with AD who could still play previously-learned pieces and an amateur trombonist with AD who continued to play in a band, evidence the endurance of this motor-based musical memory.[57,58] Thus, music engages multiple memory types, highlighting its wide reach.

A growing body of research has been investigating the music interventions on memory in AD patients, revealing improved memory and executive function.[59–61] To address the need for longitudinal data, one 12-month randomized controlled trial assigned participants with mild AD, mild cognitive impairments, or memory complaints into one of three groups: music intervention (singing lessons), active control group (physical activity), or the passive control group. Researchers aim to examine music's effect on cognitive decline, brain structure (grey/white matter), brain function, and depressive symptoms.[62] Since the results in 2022 were not deemed feasible due

DOI: 10.36838/IJHSR87.168

to participants having difficulty adhering to the protocol, they have extended recruitment to include pre-AD patients, and findings may shed light on how music-induced plasticity correlates with memory.

Mechanisms Underlying Music's Benefit on Memory & Cognition:

Below are several proposed mechanisms synthesized from studies discussing how music may help improve memory and reduce cognitive decline in individuals with dementia.

The first mechanism concerns music's influence on the dopaminergic system. Dopamine, a neuromodulator, is known to play a critical role in reward-based learning, motivation, and memory consolidation.[63] Music influences our emotional state and can evoke feelings of pleasure, a component of reward.[64] Imaging studies have revealed activity changes in structures related to reward-processing and emotion when listening to music, such as the nucleus accumbens (NAc), ventral tegmental area (VTA), anterior cingulate cortex (ACC), and orbitofrontal cortex, underscoring that listening to music is a pleasurable experience.[52,65] Music's engagement with the reward circuitry is linked to its activation of dopaminergic pathways, specifically the mesolimbic. In the mesolimbic system, dopaminergic cells originate in the VTA (midbrain) and project to structures such as the nucleus accumbens, amygdala, and hippocampus.[66] Music-evoked pleasure is associated with an increase in dopamine availability at synapses. One study using [^{11}C]raclopride, which acts as a D2 antagonist, found a decrease in raclopride binding potential (which reflects extracellular dopamine concentration) in the NAc during peak moments of emotional pleasure. [67] The increase of dopamine availability might reflect an increased release of dopamine in the NAc, providing evidence of music's activation of the mesolimbic reward system. Furthermore, in another investigation, researchers found that levodopa (a drug that increases dopamine in the brain) heightened music's pleasurable experience and arousal in participants while risperidone (a dopamine receptor antagonist) reduced both.[68] These findings show that music, when inducing pleasure, can activate dopaminergic pathways in the reward system, stimulating dopamine release.

According to the neo-Hebbian framework for episodic memory formation, dopamine release in the mesolimbic system is required in converting early LTP (related to STM) into late-LTP (related to LTM) in the hippocampus. Dopamine strengthens synaptic connections (LTP) in the hippocampus through protein synthesis, supporting memory consolidation.[69] Therefore, increasing dopamine transmission promotes memory consolidation, making memories stronger and more persistent.

It is shown that music can activate dopaminergic pathways, and dopamine can support memory consolidation. Therefore, even though there is no direct evidence showing how music-evoked dopamine bolsters memory, it can be hypothesized that music-evoked dopamine release might act as a neuromodulatory signal that enhances memory formation (summarized in paragraph above), especially during rewarding and pleasurable musical experiences.[67–69]

In addition to music-evoked dopamine's modulation of memory, it could combat excitotoxicity in AD, which would consequently lead to less memory loss. Several studies on music promoting dopamine release have found that the effect is mediated through D2 receptors and mainly observed in the nucleus accumbens and lateral neostriatum.[67,70] Due to the widespread projections of dopamine in various circuits, it is plausible that music causes dopamine levels to rise in connected regions, especially the midbrain and hippocampus. Building upon this, dopamine might play a role in protecting the brain from excitotoxic damage. A study using neurons from the hippocampus, cortex, and midbrain treated cells with high concentrations of glutamate and, additionally, with varying doses of dopamine.[71] Results revealed that dopamine helped prevent neuronal death in all brain regions by preventing the onset of delayed calcium deregulation (DCD), a feature of excitotoxicity. The neuroprotective effect was eliminated in the presence of a D2 antagonist. Thus, it may be hypothesized that music stimulates dopamine release across multiple brain regions, with dopamine binding to D2 receptors to modulate calcium signaling. This counteracts glutamate-induced excitotoxicity, ultimately resulting in less neurodegeneration in individuals with progressing AD.

The second mechanism by which music can counter the deficits of AD is associated with music's regulation of neuroinflammation through its effects on stress, which modulates the brain's immune system. The stress response is regulated by the HPA axis, a neuroendocrine system. When the body experiences stress, the hypothalamus releases corticotropin-releasing hormone (CRH), which travels to the pituitary gland, prompting it to release adrenocorticotropic hormone (ACTH). ACTH subsequently activates the adrenal glands, resulting in the release of glucocorticoids (GC) such as cortisol.[72]

While this response is essential for survival, prolonged stress leads to chronic or sustained activation of the HPA axis, promoting neurodegeneration.[73] Additionally, abundant studies on animal models have also revealed how stress contributes to AD pathogenesis through increasing Aβ levels, total tau accumulation or phosphorylation, and cognitive impairment.[74,75] GCs, induced by stress, can cross the blood-brain barrier (BBB), allowing them to travel from the bloodstream into the brain, where they can play a role in brain immunity. Since microglial cells contain GC receptors, GCs can directly influence microglial activity.[76] Research has shown that GCs can exacerbate neuroinflammation by priming microglia, increasing their sensitivity, and causing them to produce stronger pro-inflammatory responses to immune challenges and stressors.[77] Supporting this, an experiment exposing rats to psychological stress found heightened microglia reactivity (more microglia activation and more sensitive immune response), suggesting that stress contributes to a sustained immune response (causing neuroinflammation). Accordingly, other studies have found that high GC levels increased microglia and pro-inflammatory cytokines, highlighting the link between stress and inflammation.[78,79] Thus, these findings show that stress, through GCs, dysregulates microglia, upregulating pro-inflammatory pathways and worsening neuroinflammation.

Music interventions, however, have been shown to reduce stress and activation of the HPA-axis as evidenced by lower levels of cortisol,[80–82] and decreased plasma levels of pro-inflammatory cytokines.[83,84]

Therefore, music's ability to downregulate the HPA-axis and reduce stress may slow neuroinflammation, reducing cognitive decline.

The third mechanism of music's neuroprotective effects on memory revolves around music's ability to stimulate neuroplasticity and possibly neurogenesis. As reviewed above, music can enhance connectivity between brain regions, modulate activity, and increase the volume of structures. Plastic changes in the CNS caused by music show that learning music creates new neuronal connections and increases synapse formation, combating neurodegeneration.[85] Brain atrophy, caused by neurodegeneration, is a prominent marker of AD, pronounced particularly in the hippocampus, but also occurring in other structures such as the amygdala, neocortex, and entorhinal cortex.[86,87] Accordingly, since learning and listening to music helps create new neuronal connections and cause plastic changes in many regions of the brain, music may decelerate brain atrophy (especially in the hippocampus), increasing memory function and cognition.

Supporting this idea, music plasticity-based training has been shown to potentially preserve brain functions in the elderly and prevent the onset of dementia. A study demonstrated that elderly musicians have better auditory processing, working memory, and visuospatial ability than elderly nonmusicians.[88] Similarly, older adults who underwent music training had improved executive functioning and working memory.[89] Studies have also shown that older adults who are musicians have less risk of developing dementia, exhibiting music's protective effect on age-related decline.[15,90] Thus, music interventions can be cognitively stimulating, helping to prevent cognitive decline in those with AD.

It is also known that the hippocampus may be a region where neurogenesis can occur.[91] As music can modulate activity in the hippocampus, it is speculated that music might be able to facilitate neurogenesis by modulating the secretion of steroid hormones, which have been shown to increase cerebral plasticity and play a role in brain cell restoration.[92] Thus, through inducing neuroplasticity and neurogenesis, music might be able to slow or prevent neurodegeneration in patients with AD.

In conclusion, music can slow memory decline through these potential pathways. Figure 1 reviews all of the mechanisms that have been discussed.

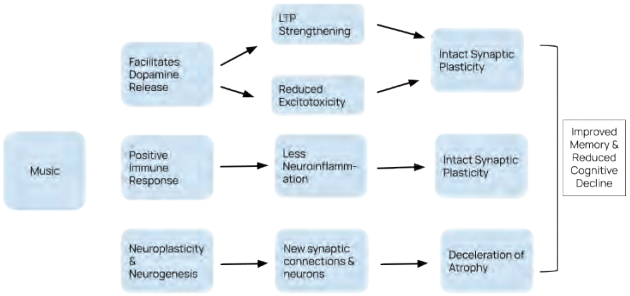

Figure 1: Model of the mechanisms underlying music's role in slowing memory decline. It involves the stimulation of dopamine release, reduction of stress (decreases HPA-axis activation), and induction of neuroplasticity and neurogenesis. This figure was adapted from the following studies.[12,93,94]

Conclusion

This article reviewed several ways in which music enhances our memory and highlights its potential as an intervention to improve memory and slow cognitive decline in individuals with AD. Music is an effective and nonpharmaceutical treatment. Importantly, literature shows that even through progressive memory decline, AD patients can retain memories of music.[46,47] Specifically, patients exhibit better recall of autobiographical experiences associated with music.[40,47,49–51] Additionally, music listening and musical training also improve AD patients' cognitive function and memory.[59–61] Thus, due to the persistence of musical memory and music's cognitive boost, this art medium can serve as a beneficial therapy for neurodegenerative diseases and early intervention for preventing dementia.

There are several mechanisms underlying music's benefit on memory decline. Music induces neuroplasticity, promoting structural and functional changes primarily in cognitive, motor, and auditory regions. Thus, musical training or listening to music facilitates new neuron connections and might even create new neurons, underscoring its potential in combating the progression of neurodegeneration.[85,92] Music also elicits emotion, which helps strengthen memory formation and retrieval primarily through activation of the dopaminergic system.[40,41,45,52] Furthermore, music's benefit on the immune system (reduction of stress and inflammation) might mitigate neuroinflammation and consequently cognitive decline and memory loss.[80–84]

Despite these conclusions, there are limitations. The cellular mechanisms by which music may enhance memory have limited studies, especially in humans, and therefore have limited empirical evidence. Studies on the direct effect of music on dopamine and memory, examining processes on the neuronal level, or music on neuroinflammation and microglia would be useful. In addition, musical memory retention in AD might vary according to the stage of AD or cultural differences between individuals. Since there is limited research on how musical memory is well-preserved in AD, more research is needed to verify and expand its depth.

Further longitudinal studies with large sample sizes should be done on AD patients to determine if music can alter the course of neurodegeneration or improve memory in the long run. It would also be important to investigate whether music's

DOI: 10.36838/IJHSR87.168

beneficial effects require continuous exposure, suggesting that these effects are short-lived after the experiment, or if a certain duration, type, or frequency of exposure is sufficient to produce long-lasting effects. One way to investigate this is through follow-ups on patients after intervention. Such studies could also experiment across different stages of dementia, with different genres of music, personalized or generalized music, and active or passive music interventions to see if there is clear evidence for music's benefit in memory decline. Utilizing artificial intelligence may serve as a way forward in developing personalized music therapy or music-related apps for patients with AD. It could help adapt interventions to music preference, emotional status, and cognitive levels. While this review paper focuses on music's impact on memory for AD patients, a lot of researchers have explored music therapy on non-memory issues associated with dementia. Findings have revealed music interventions to reduce anxiety, depression, and aggressiveness in individuals with AD.[14,95,96] The impact of music on various cognitive and behavioral issues is an important and promising area of study that could be explored further in the future.

In conclusion, this review has demonstrated that music is an underappreciated but potentially effective strategy to combat AD memory decline. Further work is needed to understand the mechanisms and the precise efficacy, but this area of research shows major potential for developing effective alternative therapies in patients afflicted with memory dysfunction in neurodegenerative disorders.

Acknowledgments

I would like to thank Dr. Jorge Avila, Assistant Director at the Undergraduate Research Center for Sciences at UCLA, for his guidance and support in this research paper. I'm also grateful to my parents for their encouragement throughout this process.

References

1. Better, M. A. Alzheimer's Disease Facts and Figures. *Alzheimers Dement* **2023**, *19* (4), 1598–1695.
2. Bloom, G. S. Amyloid-β and Tau: The Trigger and Bullet in Alzheimer Disease Pathogenesis. *JAMA Neurol*. **2014**, *71* (4), 505–508.
3. Kinney, J. W.; Bemiller, S. M.; Murtishaw, A. S.; Leisgang, A. M.; Salazar, A. M.; Lamb, B. T. Inflammation as a Central Mechanism in Alzheimer's Disease. *Alzheimers Dement. Transl. Res. Clin. Interv*. **2018**, *4*, 575–590.
4. Wang, R.; Reddy, P. H. Role of Glutamate and NMDA Receptors in Alzheimer's Disease. *J. Alzheimer's Dis*. **2017**, *57* (4), 1041–1048.
5. Dong, X.; Wang, Y.; Qin, Z. Molecular Mechanisms of Excitotoxicity and Their Relevance to Pathogenesis of Neurodegenerative Diseases. *Acta Pharmacol. Sin*. **2009**, *30* (4), 379–387.
6. Bliss, T. V.; Collingridge, G. L. A Synaptic Model of Memory: Long-Term Potentiation in the Hippocampus. *Nature* **1993**, *361* (6407), 31–39.
7. Kandel, E. R. The Molecular Biology of Memory Storage: A Dialogue Between Genes and Synapses. *Science* **2001**, *294* (5544), 1030–1038. https://doi.org/10.1126/science.1067020.
8. Sheldon, S.; Fenerci, C.; Gurguryan, L. A Neurocognitive Perspective on the Forms and Functions of Autobiographical Memory Retrieval. *Front. Syst. Neurosci.* **2019**, *13*, 4.
9. El Haj, M.; Antoine, P.; Nandrino, J. L.; Kapogiannis, D. Autobiographical Memory Decline in Alzheimer's Disease, a Theoretical and Clinical Overview. *Ageing Res. Rev*. **2015**, *23*, 183–192.
10. Yiannopoulou, K. G.; Papageorgiou, S. G. Current and Future Treatments in Alzheimer Disease: An Update. *J. Cent. Nerv. Syst. Dis.* **2020**, *12*, 117957352090739. https://doi.org/10.1177/1179573520907397.
11. Zhang, J.; Zhang, Y.; Wang, J.; Xia, Y.; Zhang, J.; Chen, L. Recent Advances in Alzheimer's Disease: Mechanisms, Clinical Trials and New Drug Development Strategies. *Signal Transduct. Target. Ther.* **2024**, *9* (1), 211.
12. Nikkhah Bahrami, S.; Momtazmanesh, S.; Rezaei, N. Music Therapy for Alzheimer's Disease Management: A Narrative Review. *Egypt. J. Neurol. Psychiatry Neurosurg*. **2024**, *60* (1), 66.
13. De Witte, M.; Spruit, A.; Van Hooren, S.; Moonen, X.; Stams, G.-J. Effects of Music Interventions on Stress-Related Outcomes: A Systematic Review and Two Meta-Analyses. *Health Psychol. Rev*. **2020**, *14* (2), 294–324.
14. Guetin, S.; Portet, F.; Picot, M.; Pommié, C.; Messaoudi, M.; Djabelkir, L.; Olsen, A.; Cano, M.; Lecourt, E.; Touchon, J. Effect of Music Therapy on Anxiety and Depression in Patients with Alzheimer's Type Dementia: Randomised, Controlled Study. *Dement. Geriatr. Cogn. Disord.* **2009**, *28* (1), 36–46.
15. Balbag, M. A.; Pedersen, N. L.; Gatz, M. Playing a Musical Instrument as a Protective Factor against Dementia and Cognitive Impairment: A Population-based Twin Study. *Int. J. Alzheimer's Dis*. **2014**, *2014* (1), 836748.
16. Wan, C. Y.; Schlaug, G. Music Making as a Tool for Promoting Brain Plasticity across the Life Span. *The Neuroscientist* **2010**, *16* (5), 566–577.
17. Zatorre, R. J.; Chen, J. L.; Penhune, V. B. When the Brain Plays Music: Auditory–Motor Interactions in Music Perception and Production. *Nat. Rev. Neurosci.* **2007**, *8* (7), 547–558. https://doi.org/10.1038/nrn2152.
18. Schneider, P.; Scherg, M.; Dosch, H. G.; Specht, H. J.; Gutschalk, A.; Rupp, A. Morphology of Heschl's Gyrus Reflects Enhanced Activation in the Auditory Cortex of Musicians. *Nat. Neurosci.* **2002**, *5* (7), 688–694.
19. Bermudez, P.; Lerch, J. P.; Evans, A. C.; Zatorre, R. J. Neuroanatomical Correlates of Musicianship as Revealed by Cortical Thickness and Voxel-Based Morphometry. *Cereb. Cortex* **2009**, *19* (7), 1583–1596.
20. Olszewska, A. M.; Gaca, M.; Herman, A. M.; Jednoróg, K.; Marchewka, A. How Musical Training Shapes the Adult Brain: Predispositions and Neuroplasticity. *Front. Neurosci*. **2021**, *15*, 630829. https://doi.org/10.3389/fnins.2021.630829.
21. Gaser, C.; Schlaug, G. Brain Structures Differ between Musicians and Non-Musicians. *J. Neurosci*. **2003**, *23* (27), 9240–9245. https://doi.org/10.1523/JNEUROSCI.23-27-09240.2003.
22. Hutchinson, S.; Lee, L. H.-L.; Gaab, N.; Schlaug, G. Cerebellar Volume of Musicians. Cereb. *Cortex* **2003**, *13* (9), 943–949.
23. Groussard, M.; Viader, F.; Landeau, B.; Desgranges, B.; Eustache, F.; Platel, H. The Effects of Musical Practice on Structural Plasticity: The Dynamics of Grey Matter Changes. *Brain Cogn*. **2014**, *90*, 174–180.
24. James, C. E.; Oechslin, M. S.; Van De Ville, D.; Hauert, C.-A.; Descloux, C.; Lazeyras, F. Musical Training Intensity Yields Opposite Effects on Grey Matter Density in Cognitive versus Sensorimotor Networks. *Brain Struct. Funct*. **2014**, *219* (1), 353–366.
25. Sato, K.; Kirino, E.; Tanaka, S. A Voxel-Based Morphometry Study of the Brain of University Students Majoring in Music and Nonmusic Disciplines. *Behav. Neurol*. **2015**, *2015* (1), 274919.

26. Halwani, G. F.; Loui, P.; Rüber, T.; Schlaug, G. Effects of Practice and Experience on the Arcuate Fasciculus: Comparing Singers, Instrumentalists, and Non-Musicians. *Front. Psychol*. **2011**, *2*. https://doi.org/10.3389/fpsyg.2011.00156.
27. Schmithorst, V. J.; Wilke, M. Differences in White Matter Architecture between Musicians and Non-Musicians: A Diffusion Tensor Imaging Study. *Neurosci. Lett*. **2002**, *321* (1–2), 57–60.
28. Abdul-Kareem, I. A.; Stancak, A.; Parkes, L. M.; Al-Ameen, M.; AlGhamdi, J.; Aldhafeeri, F. M.; Embleton, K.; Morris, D.; Sluming, V. Plasticity of the Superior and Middle Cerebellar Peduncles in Musicians Revealed by Quantitative Analysis of Volume and Number of Streamlines Based on Diffusion Tensor Tractography. *The Cerebellum* **2011**, *10* (3), 611–623.
29. Pantev, C.; Ross, B.; Fujioka, T.; Trainor, L. J.; Schulte, M.; Schulz, M. Music and Learning-induced Cortical Plasticity. *Ann. N. Y. Acad. Sci*. **2003**, *999* (1), 438–450.
30. Bianchi, F.; Hjortkjær, J.; Santurette, S.; Zatorre, R. J.; Siebner, H. R.; Dau, T. Subcortical and Cortical Correlates of Pitch Discrimination: Evidence for Two Levels of Neuroplasticity in Musicians. *Neuroimage* **2017**, *163*, 398–412.
31. Ohnishi, T.; Matsuda, H.; Asada, T.; Aruga, M.; Hirakata, M.; Nishikawa, M.; Katoh, A.; Imabayashi, E. Functional Anatomy of Musical Perception in Musicians. *Cereb. Cortex* **2001**, *11* (8), 754–760.
32. Bangert, M.; Peschel, T.; Schlaug, G.; Rotte, M.; Drescher, D.; Hinrichs, H.; Heinze, H.-J.; Altenmüller, E. Shared Networks for Auditory and Motor Processing in Professional Pianists: Evidence from fMRI Conjunction. *Neuroimage* **2006**, *30* (3), 917–926.
33. Hyde, K. L.; Lerch, J.; Norton, A.; Forgeard, M.; Winner, E.; Evans, A. C.; Schlaug, G. Musical Training Shapes Structural Brain Development. *J. Neurosci.* **2009**, *29* (10), 3019–3025.
34. Habibi, A.; Ilari, B.; Heine, K.; Damasio, H. Changes in Auditory Cortical Thickness Following Music Training in Children: Converging Longitudinal and Cross-Sectional Results. *Brain Struct. Funct*. **2020**, *225* (8), 2463–2474. https://doi.org/10.1007/s00429-020-02135-1.
35. Li, Q.; Wang, X.; Wang, S.; Xie, Y.; Li, X.; Xie, Y.; Li, S. Musical Training Induces Functional and Structural Auditory-motor Network Plasticity in Young Adults. *Hum. Brain Mapp*. **2018**, *39* (5), 2098–2110.
36. Herholz, S. C.; Coffey, E. B.; Pantev, C.; Zatorre, R. J. Dissociation of Neural Networks for Predisposition and for Training-Related Plasticity in Auditory-Motor Learning. *Cereb. Cortex* **2016**, *26* (7), 3125–3134.
37. Wollman, I.; Penhune, V.; Segado, M.; Carpentier, T.; Zatorre, R. J. Neural Network Retuning and Neural Predictors of Learning Success Associated with Cello Training. *Proc. Natl. Acad. Sci*. **2018**, *115* (26), E6056–E6064.
38. Matziorinis, A. M.; Leemans, A.; Skouras, S.; Flo, B. K.; Bashevkin, T.; Koelsch, S. The Effects of Musicality on Brain Network Topology in the Context of Alzheimer's Disease and Memory Decline. *Imaging Neurosci*. **2024**, *2*, imag–2–00248. https://doi.org/10.1162/imag_a_00248.
39. Fischer, C. E.; Churchill, N.; Leggieri, M.; Vuong, V.; Tau, M.; Fornazzari, L. R.; Thaut, M. H.; Schweizer, T. A. Long-Known Music Exposure Effects on Brain Imaging and Cognition in Early-Stage Cognitive Decline: A Pilot Study. *J. Alzheimer's Dis.* **2021**, *84* (2), 819–833.
40. Janata, P.; Tomic, S. T.; Rakowski, S. K. Characterisation of Music-Evoked Autobiographical Memories. *Memory* **2007**, *15* (8), 845–860.
41. Eschrich, S.; Münte, T. F.; Altenmüller, E. O. Unforgettable Film Music: The Role of Emotion in Episodic Long-Term Memory for Music. *BMC Neurosci*. **2008**, *9* (1), 48. https://doi.org/10.1186/1471-2202-9-48.
42. Tully, K.; Bolshakov, V. Y. Emotional Enhancement of Memory: How Norepinephrine Enables Synaptic Plasticity. *Mol. Brain* **2010**, *3* (1), 15. https://doi.org/10.1186/1756-6606-3-15.
43. Janata, P. The Neural Architecture of Music-Evoked Autobiographical Memories. *Cereb. Cortex* **2009**, *19* (11), 2579–2594. https://doi.org/10.1093/cercor/bhp008.
44. Koelsch, S. A Coordinate-Based Meta-Analysis of Music-Evoked Emotions. *NeuroImage* **2020**, *223*, 117350. https://doi.org/10.1016/j.neuroimage.2020.117350.
45. Blood, A. J.; Zatorre, R. J. Intensely Pleasurable Responses to Music Correlate with Activity in Brain Regions Implicated in Reward and Emotion. *Proc. Natl. Acad. Sci*. **2001**, *98* (20), 11818–11823.
46. Cuddy, L. L.; Duffin, J. Music, Memory, and Alzheimer's Disease: Is Music Recognition Spared in Dementia, and How Can It Be Assessed? *Med. Hypotheses* **2005**, *64* (2), 229–235.
47. Cuddy, L. L.; Sikka, R.; Vanstone, A. Preservation of Musical Memory and Engagement in Healthy Aging and Alzheimer's Disease. *Ann. N. Y. Acad. Sci*. **2015**, *1337* (1), 223–231. https://doi.org/10.1111/nyas.12617.
48. Jacobsen, J.-H.; Stelzer, J.; Fritz, T. H.; Chételat, G.; La Joie, R.; Turner, R. Why Musical Memory Can Be Preserved in Advanced Alzheimer's Disease. *Brain* **2015**, *138* (8), 2438–2450. https://doi.org/10.1093/brain/awv135.
49. El Haj, M.; Fasotti, L.; Allain, P. The Involuntary Nature of Music-Evoked Autobiographical Memories in Alzheimer's Disease. *Conscious. Cogn*. **2012**, *21* (1), 238–246.
50. Irish, M.; Cunningham, C. J.; Walsh, J. B.; Coakley, D.; Lawlor, B. A.; Robertson, I. H.; Coen, R. F. Investigating the Enhancing Effect of Music on Autobiographical Memory in Mild Alzheimer's Disease. *Dement. Geriatr. Cogn. Disord*. **2006**, *22* (1), 108–120.
51. Foster, N. A.; Valentine, E. R. The Effect of Auditory Stimulation on Autobiographical Recall in Dementia. *Exp. Aging Res.* **2001**, *27* (3), 215–228.
52. Koelsch, S. Brain Correlates of Music-Evoked Emotions. *Nat. Rev. Neurosci*. **2014**, *15* (3), 170–180. https://doi.org/10.1038/nrn3666.
53. Gordon, B. A.; Blazey, T.; Benzinger, T. L. Regional Variability In Alzheimer's Disease Biomarkers. *Future Neurol*. **2014**, *9* (2), 131–134.
54. *Memory for music in Alzheimer's disease: unforgettable? - Google Scholar*. https://scholar.google.com/scholar?hl=en&as_sdt=0%2C5&q=Memory+for+music+in+Alzheimer%27s+disease%3A+unforgettable%3F&btnG= (accessed 2025-11-05).
55. Poe, M. K.; Seifert, L. S. Implicit and Explicit Tests: Evidence for Dissociable Motor Skills in Probable Alzheimer's Dementia. *Percept. Mot. Skills* **1997**, *85* (2), 631–634. https://doi.org/10.1177/003151259708500201.
56. Gold, C. A.; Budson, A. E. Memory Loss in Alzheimer's Disease: Implications for Development of Therapeutics. *Expert Rev. Neurother.* **2008**, *8* (12), 1879–1891. https://doi.org/10.1586/14737175.8.12.1879.
57. Crystal, H. A.; Grober, E.; Masur, D. Preservation of Musical Memory in Alzheimer's Disease. *J. Neurol. Neurosurg. Psychiatry* **1989**, *52* (12), 1415–1416.
58. Beatty, W. W.; Winn, P.; Adams, R. L.; Allen, E. W.; Wilson, D. A.; Prince, J. R.; Olson, K. A.; Dean, K.; Littleford, D. Preserved Cognitive Skills in Dementia of the Alzheimer Type. *Arch. Neurol.* **1994**, *51* (10), 1040–1046.
59. Innes, K. E.; Selfe, T. K.; Brundage, K.; Montgomery, C.; Wen, S.; Kandati, S.; Bowles, H.; Khalsa, D. S.; Huysmans, Z. Effects of Meditation and Music-Listening on Blood Biomarkers of Cel-

DOI: 10.36838/IJHSR87.168

lular Aging and Alzheimer's Disease in Adults with Subjective Cognitive Decline: An Exploratory Randomized Clinical Trial. *J. Alzheimer's Dis*. **2018**, *66* (3), 947–970.
60. Lyu, J.; Zhang, J.; Mu, H.; Li, W.; Champ, M.; Xiong, Q.; Gao, T.; Xie, L.; Jin, W.; Yang, W.; Cui, M.; Gao, M.; Li, M. The Effects of Music Therapy on Cognition, Psychiatric Symptoms, and Activities of Daily Living in Patients with Alzheimer's Disease. *J. Alzheimer's Dis*. **2018**, *64* (4), 1347–1358. https://doi.org/10.3233/JAD-180183.
61. Gallego, M. G.; García, J. G. Music Therapy and Alzheimer's Disease: Cognitive, Psychological, and Behavioural Effects. *Neurol. Engl. Ed*. **2017**, *32* (5), 300–308.
62. Flo, B. K.; Matziorinis, A. M.; Skouras, S.; Sudmann, T. T.; Gold, C.; Koelsch, S. Study Protocol for the Alzheimer and Music Therapy Study: An RCT to Compare the Efficacy of Music Therapy and Physical Activity on Brain Plasticity, Depressive Symptoms, and Cognitive Decline, in a Population with and at Risk for Alzheimer's Disease. *PLOS ONE* **2022**, *17* (6), e0270682. https://doi.org/10.1371/journal.pone.0270682.
63. Wise, R. A. Dopamine, Learning and Motivation. *Nat. Rev. Neurosci.* **2004**, *5* (6), 483–494.
64. Berridge, K. C.; Robinson, T. E.; Aldridge, J. W. Dissecting Components of Reward: 'Liking', 'Wanting', and Learning. *Curr. Opin. Pharmacol.* **2009**, *9* (1), 65–73.
65. Menon, V.; Levitin, D. J. The Rewards of Music Listening: Response and Physiological Connectivity of the Mesolimbic System. *Neuroimage* **2005**, *28* (1), 175–184.
66. Krashia, P.; Spoleti, E.; D'Amelio, M. The VTA Dopaminergic System as Diagnostic and Therapeutical Target for Alzheimer's Disease. *Front. Psychiatry* **2022**, *13*, 1039725.
67. Salimpoor, V. N.; Benovoy, M.; Larcher, K.; Dagher, A.; Zatorre, R. J. Anatomically Distinct Dopamine Release during Anticipation and Experience of Peak Emotion to Music. *Nat. Neurosci*. **2011**, *14* (2), 257–262. https://doi.org/10.1038/nn.2726.
68. Ferreri, L.; Mas-Herrero, E.; Zatorre, R. J.; Ripollés, P.; Gomez-Andres, A.; Alicart, H.; Olivé, G.; Marco-Pallarés, J.; Antonijoan, R. M.; Valle, M.; Riba, J.; Rodriguez-Fornells, A. Dopamine Modulates the Reward Experiences Elicited by Music. *Proc. Natl. Acad. Sci.* **2019**, *116* (9), 3793–3798. https://doi.org/10.1073/pnas.1811878116.
69. Lisman, J.; Grace, A. A.; Duzel, E. A neoHebbian Framework for Episodic Memory: Role of Dopamine-Dependent Late LTP. *Trends Neurosci*. **2011**, *34* (10), 536–547. https://doi.org/10.1016/j.tins.2011.07.006.
70. Sutoo, D.; Akiyama, K. Music Improves Dopaminergic Neurotransmission: Demonstration Based on the Effect of Music on Blood Pressure Regulation. *Brain Res*. **2004**, *1016* (2), 255–262.
71. Vaarmann, A.; Kovac, S.; Holmström, K.; Gandhi, S.; Abramov, A. Dopamine Protects Neurons against Glutamate-Induced Excitotoxicity. *Cell Death Dis*. **2013**, *4* (1), e455–e455.
72. Smith, S. M.; Vale, W. W. The Role of the Hypothalamic-Pituitary-Adrenal Axis in Neuroendocrine Responses to Stress. *Dialogues Clin. Neurosci*. **2006**, *8* (4), 383–395.
73. Kline, S. A.; Mega, M. S. Stress-Induced Neurodegeneration: The Potential for Coping as Neuroprotective Therapy. *Am. J. Alzheimers Dis. Dementias®* **2020**, *35*, 1533317520960873.
74. Green, K. N.; Billings, L. M.; Roozendaal, B.; McGaugh, J. L.; LaFerla, F. M. Glucocorticoids Increase Amyloid-β and Tau Pathology in a Mouse Model of Alzheimer's Disease. *J. Neurosci.* **2006**, *26* (35), 9047–9056.
75. Jeong, Y. H.; Park, C. H.; Yoo, J.; Shin, K. Y.; Ahn, S.-M.; Kim, H.-S.; Lee, S. H.; Emson, P. C.; Suh, Y.-H. Chronic Stress Accelerates Learning and Memory Impairments and Increases Amyloid Deposition in APPV717I-CT100 Transgenic Mice, an Alzheimer's Disease Model. **2006**.
76. Tanaka, J.; Fujita, H.; Matsuda, S.; Toku, K.; Sakanaka, M.; Maeda, N. Glucocorticoid-and Mineralocorticoid Receptors in Microglial Cells: The Two Receptors Mediate Differential Effects of Corticosteroids. *Glia* **1997**, *20* (1), 23–37.
77. Niraula, A.; Sheridan, J. F.; Godbout, J. P. Microglia Priming with Aging and Stress. *Neuropsychopharmacology* **2017**, *42* (1), 318–333.
78. Dinkel, K.; MacPherson, A.; Sapolsky, R. M. Novel Glucocorticoid Effects on Acute Inflammation in the CNS. *J. Neurochem.* **2003**, *84* (4), 705–716.
79. MacPherson, A.; Dinkel, K.; Sapolsky, R. Glucocorticoids Worsen Excitotoxin-Induced Expression of pro-Inflammatory Cytokines in Hippocampal Cultures. *Exp. Neurol.* **2005**, *194* (2), 376–383.
80. Koelsch, S.; Fuermetz, J.; Sack, U.; Bauer, K.; Hohenadel, M.; Wiegel, M.; Kaisers, U. X.; Heinke, W. Effects of Music Listening on Cortisol Levels and Propofol Consumption during Spinal Anesthesia. *Front. Psychol*. **2011**, *2*, 58.
81. Fancourt, D.; Williamon, A.; Carvalho, L. A.; Steptoe, A.; Dow, R.; Lewis, I. Singing Modulates Mood, Stress, Cortisol, Cytokine and Neuropeptide Activity in Cancer Patients and Carers. *ecancermedicalscience* **2016**, *10*, 631.
82. Chanda, M. L.; Levitin, D. J. The Neurochemistry of Music. *Trends Cogn. Sci.* **2013**, *17* (4), 179–193.
83. StefanoADEFG, G. B.; ZhuB, W.; CadetCD, P.; SalamonF, E.; MantioneBCDE, K. J. Music Alters Constitutively Expressed Opiate and Cytokine Processes in Listeners. *Med Sci Monit* **2004**, *10* (6), 27.
84. Conrad, C.; Niess, H.; Jauch, K.-W.; Bruns, C. J.; Hartl, W. H.; Welker, L. Overture for Growth Hormone: Requiem for Interleukin-6? *Crit. Care Med*. **2007**, *35* (12), 2709–2713.
85. Chatterjee, D.; Hegde, S.; Thaut, M. Neural Plasticity: The Substratum of Music-Based Interventions in Neurorehabilitation. *NeuroRehabilitation* **2021**, *48* (2), 155–166.
86. Forno, G.; Lladó, A.; Hornberger, M. Going Round in Circles—the Papez Circuit in Alzheimer's Disease. *Eur. J. Neurosci*. **2021**, *54* (10), 7668–7687.
87. Pini, L.; Pievani, M.; Bocchetta, M.; Altomare, D.; Bosco, P.; Cavedo, E.; Galluzzi, S.; Marizzoni, M.; Frisoni, G. B. Brain Atrophy in Alzheimer's Disease and Aging. *Ageing Res. Rev*. **2016**, *30*, 25–48.
88. Grassi, M.; Meneghetti, C.; Toffalini, E.; Borella, E. Auditory and Cognitive Performance in Elderly Musicians and Nonmusicians. *PloS One* **2017**, *12* (11), e0187881.
89. Bugos, J. A.; Perlstein, W. M.; McCrae, C. S.; Brophy, T. S.; Bedenbaugh, P. H. Individualized Piano Instruction Enhances Executive Functioning and Working Memory in Older Adults. *Aging Ment. Health* **2007**, *11* (4), 464–471.
90. Verghese, J.; Lipton, R. B.; Katz, M. J.; Hall, C. B.; Derby, C. A.; Kuslansky, G.; Ambrose, A. F.; Sliwinski, M.; Buschke, H. Leisure Activities and the Risk of Dementia in the Elderly. *N. Engl. J. Med.* **2003**, *348* (25), 2508–2516.
91. Kempermann, G.; Song, H.; Gage, F. H. Neurogenesis in the Adult Hippocampus. *Cold Spring Harb. Perspect. Biol*. **2015**, *7* (9), a018812.
92. Fukui, H.; Toyoshima, K. Music Facilitate the Neurogenesis, Regeneration and Repair of Neurons. *Med. Hypotheses* **2008**, *71* (5), 765–769.
93. Matziorinis, A. M.; Koelsch, S. The Promise of Music Therapy for Alzheimer's Disease: A Review. *Ann. N. Y. Acad. Sci.* **2022**, *1516* (1), 11–17. https://doi.org/10.1111/nyas.14864.
94. Peck, K. J.; Girard, T. A.; Russo, F. A.; Fiocco, A. J. Music and Memory in Alzheimer's Disease and the Potential Underlying Mechanisms. *J. Alzheimers Dis.* **2016**, *51* (4), 949–959.

95. De La Rubia Ortí, J. E.; García-Pardo, M. P.; Iranzo, C. C.; Madrigal, J. J. C.; Castillo, S. S.; Rochina, M. J.; Gascó, V. J. P. Does Music Therapy Improve Anxiety and Depression in Alzheimer's Patients? *J. Altern. Complement. Med.* **2018**, *24* (1), 33–36. https://doi.org/10.1089/acm.2016.0346.
96. McArthur, V.; Everington, S.; Patel, M. Effectiveness of Music-Based Interventions in Acute Care Settings for People Living with Dementia to Reduce Anxiety and Enhance the Care Experience: A Systematic Review. *Arch. Gerontol. Geriatr. Plus* **2024**, *1* (4), 100087.

■ Author

Olivia Tu is a senior at Lynbrook High School in San Jose, California. She's fascinated by the intersection of neuroscience/psychology and music and hopes to study it further in college. Outside of academics, she enjoys playing the piano and violin, reading, journalism, creative writing, and taking long walks.

DOI: 10.36838/IJHSR87.168

IJHSR
ijhighschoolresearch.org
REVIEW ARTICLE

Reproductive Lifespan as a Proxy for Estrogen Exposure and Alzheimer's Disease Risk in Women: A Multisystem Perspective

Sonya Komar

Scarsdale Senior High School, 1057 Post Road, Scarsdale, NY, 10583, USA; sonya.komar.katalkin@gmail.com

ABSTRACT: Alzheimer's disease (AD) is a neurodegenerative disorder in which nearly two-thirds of cases occur in women. This literature review examines how reproductive lifespan serves as an important proxy for cumulative estrogen exposure, which helps regulate the risk of AD in women. Here, I will investigate the interactions of various biomarkers, including tau pathology and amyloid beta deposition, genetic predisposition, and brain bioenergetics. Estrogen plays a crucial role in protecting the brain by decreasing amyloid beta deposition while interacting with various genetic factors, such as the *APOE4* gene. Research shows that a longer reproductive lifespan, or a greater cumulative estrogen exposure, is associated with slower cognitive decline and reduced AD risk. A proposed solution to a shorter reproductive period is Hormone Replacement Therapy (HRT), although it has complex factors, such as the timing of HRT and genetics. Here, I will propose a cohesive framework using reproductive lifespan as a proxy for AD risk, combining multiple biological systems. This review aims to outline the connection between lifetime estrogen exposure and multiple different AD biomarkers, highlighting the importance of reproductive history in AD research and treatment.

KEYWORDS: Biology, Alzheimer's Disease, Reproductive Lifespan, Menopause, Estrogen, Cognitive Decline, Women's Brain Health, Hormone Replacement Therapy.

Introduction

Alzheimer's Disease (AD) is a progressive neurodegenerative disorder that is the most common type of dementia, affecting millions worldwide. Of all AD cases, two-thirds occur in women.[1] Traditionally, this gender disparity was associated with a longer female lifespan.[2] However, recent research points out that several gender-specific factors, such as hormonal, genetic, and structural differences in the female brain, play a major role in their higher AD risk.[3]

Recent research has discovered that estrogen exhibits neuroprotective effects in the brain, including regulating brain glucose metabolism and reducing AD-related biomarkers such as amyloid-beta (Aβ) buildup.[2] During the menopausal transition, estrogen levels drop quickly, ceasing its protective pathways. Additionally, interactions between genetics and estrogen have been explored, such as the increased expression of apolipoprotein E4 (*APOE4*), an AD-inducing gene.[1] Past research has a growing focus on estrogen's role in AD, though interactions between multiple AD biomarkers, Hormone Replacement Therapy (HRT), Aβ, and brain energetics have not been fully understood.

Reproductive lifespan is an understudied but important element that measures the time between menarche (the first occurrence of menstruation) and menopause (the cessation of menstruation). This measure has been proposed as a proxy for cumulative estrogen exposure, capturing a critical time period that can be used to demonstrate how hormonal shifts impact AD risk, tau and Aβ deposition, and cognitive decline.[4] Past research has suggested a link between AD and earlier or premature menopause, or a shorter reproductive lifespan.[5]

This paper investigates how reproductive lifespan correlates to the onset and severity of AD through several key biomarkers, such as hormone levels, brain metabolism, and genetic expression. This is a crucial question as it evaluates the disproportionate effect of AD on women, and may help guide the way to the development of more personalized, sex-specific treatment strategies. By measuring reproductive lifespan rather than menopause alone, or hormone levels at a single point in time, a more indicative and general medical evaluation can be drawn, one that sums up a lifetime of estrogen exposure. Capturing a woman's entire hormonal arc can be beneficial to achieve a more comprehensive approach to assessing AD risk and informing the therapeutic approach. While past research has studied the connection of AD risk to menopause, estrogen, HRT, tau buildup, Aβ deposition, and brain energetics separately, reproductive lifespan has not been fully established as a unifying measure combining multiple biological systems.

This review will argue that using an integrative approach like reproductive lifespan can serve as a meaningful proxy for cumulative estrogen exposure, which regulates the risk of AD in women through various biomarkers. To support this thesis, the paper first explores the relationship between reproductive lifespan and tau buildup, amyloid-beta deposition, brain structure, bioenergetics, and genetic individuality. This includes estrogen's function in all of the underlying factors, which makes women more vulnerable to the debilitating disease. Further, current treatment proposals, such as HRT, are evaluated, and the key contributors to its effectiveness, i.e., timing and genetics, are analyzed. Finally, these connections are brought

© 2026 Terra Science and Education

DOI: 10.36838/IJHSR87.177

together to propose a unified model to understand women's unique risk of AD.

Discussion

Reproductive Lifespan:

Reproductive lifespan is a measure of the period between menarche and menopause, which may be used as a proxy for cumulative estrogen exposure, a reproductive hormone that has regulatory neuroprotective benefits.[4]

Estrogen has a wide range of effects aside from its reproductive role: this includes important functions that relate to the brain and aging. Its neuroprotective role ranges from its effects on Aβ and tau deposition to synaptic and metabolic homeostasis. Estrogen plays a major role in neuronal survival, synaptic plasticity, and brain energetics, all of which are important to brain health and protection.[2] The hormonal fluctuations that take place during menopause have a critical effect on the female brain, changing the functionality of intracellular signalling, neural health, and mitochondrial metabolism. This sudden neurovulnerability makes the brain greatly susceptible to cognitive decline upon the hormonal transition.[2]

In recent research, later menopause has shown a correlation to slower cognitive decline and improved memory performance.[4] Conversely, an earlier age at menopause has been associated with greater AD risk, brain atrophy, and a quicker buildup of amyloid and tau pathology.[5] These findings indicate that a shorter reproductive lifespan due to early menopause, delayed menarche, or oophorectomy can lead to neurodegeneration and eventual AD development. This demonstrates how reproductive lifespan can be utilized as a useful proxy in predicting AD risk in women through linking estrogen's wide range of protective brain mechanisms to its cumulative exposure.

Estrogen's Role in Neuroprotection:

Estrogen is a key neuroprotective hormone in women, playing a critical role in maintaining cognitive function and influencing susceptibility to Alzheimer's Disease. It plays a crucial role in synaptic plasticity, brain structure and metabolism, and gene expression.[2] Various studies have demonstrated the protective effects of estrogen, contributing to cognitive benefits in women. Tang *et al.* provided evidence that the use of estrogen was linked to lower AD risk. The study established that estrogen "promotes the growth of cholinergic neurons" and "stimulates the secretase metabolism of the amyloid precursor protein."[3] Given estrogen's role in regulating neuromechanisms, its loss during menopause may trigger the amyloid cascade, prompting the onset of amyloid-beta accumulation, one of the earliest detectable biomarkers of AD.

Amyloid-beta accumulation is a key biomarker in AD, contributing to cognitive decline caused by interrupting neural communication between brain cells. The buildup leads to plaques and tangles, which in turn interfere with synaptic function and consequently can impair cognition.[2] Women, when compared to men of the same age group, were found to have greater Aβ buildup after menopause, when estrogen receptors are dismantled and lost.[6] The amyloid cascade hypothesis theorizes that Aβ accumulation happens early in AD development, concurrent with an upstream of oxidative stress.[7] This upstream takes place during the bioenergetic crisis in the menopausal brain when estrogen levels drop, indicating that earlier menopause is associated with greater cognitive decline.[2]

According to the Alzheimer's disease amyloid cascade, changes in cerebrospinal fluid (CSF) and tau pathology precede Aβ deposition during cognitive decline, with an increased tau pathology translating to faster cognitive decline.[7] During menopause, the depletion of estrogen has been shown to increase tau pathology and neuroinflammation.[6] While Aβ deposition in the endorhinal cortex is similar in both genders, after menopause, women were found to have much higher levels of tau pathology than age-matched males. Together, these factors show that tau pathology may be used as a predictive AD biomarker, particularly in relation to estrogen loss.

Research has demonstrated estrogen's role in activating a network of genes contributing to neuroprotection and AD pathology.[1] In a multi-species study done on both humans and macaques, it was found that estrogen upregulates thousands of different genes contributing to aging and cognition.[1] In the macaques, estrogen activated 504 genes important to neuron and brain health, while increasing the expression of the APOE. While the *APOE* gene is protective in most cases, those with the APOE e4 rare gene variant are negatively affected by its activation.[8] 140 of the 504 genes activated by estrogen were linked to synapse health and bioenergetic metabolism, creating another link between the cognitive AD biomarkers. Ultimately, this study emphasized the importance of genetic individuality in estrogen treatments combating cognitive decline.

Menopause triggers various metabolic and structural brain shifts upon estrogen loss, many of which contribute to cognitive decline.[2] With the influence of the estrogen receptor network, located in the nucleus of cells and associated with the plasma membranes and mitochondria, the brain effectively responds at proper times to regulate brain energy metabolism. During menopause, the loss of estrogenic regulation destabilizes the brain's glucose metabolism, dismantling ketogenic pathways and promoting hypometabolism. In a study of rats that had undergone oophorectomy, rats given estrogen did better on memory tasks than those without the treatment. Those treated with estrogen also showed further preservation of neurons in the brain, associated with better cognition, providing further evidence that greater estrogen exposure, or a longer reproductive lifespan, is associated with cognitive enhancement and AD protection.[9]

Menopause and Brain Changes:

Menopause is a major turning point regarding female brain health, during which estrogen levels drop, initiating numerous metabolic and structural brain changes, resulting in an elevated risk for AD.

Estrogen plays a critical role in the brain, balancing metabolism and maintaining healthy neuronal pathways, reducing vulnerability to AD. In particular, estrogen receptors are responsible for regulating cerebral metabolic rates and avoiding hypometabolism– a reaction that has been linked to Aβ deposition.[2] The brain's glucose metabolism is responsible for

providing the energy for the brain to function and maintain its neuronal pathways, along with a variety of other essential brain processes. Upon the reduction of estrogen and the slowing of the cerebral glucose metabolism, the body reacts by inducing a state of starvation, dismantling ketogenic pathways, and increasing fatty acids, a substitute form of energy.[2] This metabolic shift can lead to oxidative stress, mitochondrial damage, and potential neurodegeneration. In a study of ovariectomized rats, estrogen-treated rats showed increased expression of neuronal signalling and the cholinergic system– a process crucial for brain function, attention, and memory.[9] This suggests that estrogen benefits the brain and its mechanisms, especially in reducing AD risk, indirectly corroborating the benefits of late menopause and extended exposure.

The female brain shows signs of numerous structural changes in volume and atrophy during the menopause transition.[2] This includes changes in various cortical and subcortical structures such as the hippocampus, thalamus, and amygdala– especially regarding Grey Matter Volume (GMV) and White Matter Volume (WMV) changes.[10] In a study conducted by Lisa Mosconi, results suggested a direct correlation between peri- and post-menopausal brain and grey and white matter volume loss, connected to cognitive impairment and decline. Other research also showed that earlier menopause was linked with a greater reduction of GMV, increasing the likelihood of AD development.[5] Crucially, this change was not observed in age-matched males, indicating that menopause and hormonal shifts are significant contributors to the specified structural changes. Overall, these menopause-related patterns highlight the importance of estrogen-regulated systems in the brain.

At the molecular level, amyloid beta, one of the main pathological hallmarks of AD, plays an important role in the brain, being responsible for plaque buildup and neurofibrillary tangles, leading to eventual cognitive decline.[2] Moreover, tau pathology is even more closely associated with cognitive decline than Aβ.[11] In particular, individuals with widespread Aβ buildup demonstrated greater tau pathology than those with regional Aβ buildup.[10] This is especially relevant to menopause, as earlier menopause has been linked to the acceleration of the transition from regional to widespread Aβ buildup (Figure 1). These connections highlight the potential benefit of using spatial mapping of Aβ deposition with reproductive lifespan in order to predict AD susceptibility and cognitive decline.

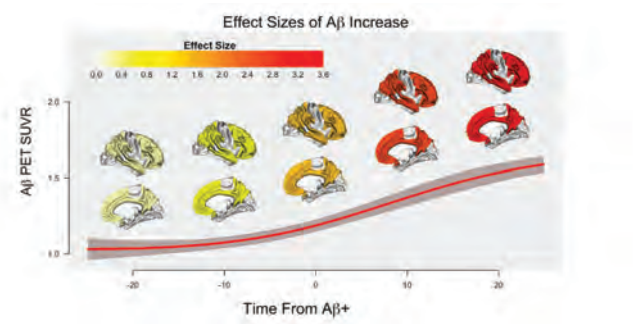

Figure 1: Effect sizes of Aβ PET SUVR (Standardized Uptake Value Ratio), an indicative measure of Aβ build-up, are displayed as a function of time, starting from initial Aβ positivity. The x-axis represents the time from the beginning of Aβ deposition, corresponding with the beginning of menopause, and the y-intercept represents the effect size of the Aβ based on the PET SUVR scores. The graph is color-coordinated, with lighter yellow indicating early regional deposition, while darker reds indicate severe, widespread Aβ deposition.[7] The graph illustrates the change in Aβ volume in relation to lifetime, emphasizing the role of time in protein buildup.

The above evidence supports the conclusion that menopause represents a critical transition point of estrogen decline in which the brain alters in structure, glucose metabolism rate, and Aβ and tau pathology. Based on the biological mechanisms outlined in this section, these changes can potentially drive neurovulnerability, cognitive decline, and AD pathology.

Genetic Importance:

Apolipoprotein E is a protein designated for lipid transport, playing a major role in neuronal repair and cholesterol metabolism.[1] It comes in various isoforms, such as APOE ε2, APOE ε3, and APOE ε4. Compared to the others, APOE ε4 is the most dangerous gene variant, being one of the strongest genetic risk factors of AD.[2] Women with *APOE4* have shown greater cognitive decline and AD pathology, such as greater tau buildup and Aβ spread. Importantly, estrogen decline has been linked to increased expression of the APOE ε4 gene, suggesting that reproductive lifespan may play a role in the cause of this gender disparity.[1]

While estrogen is important for regulating the brain, it also plays a major role in gene expression related to cognition and AD. As discussed earlier in the review, a study conducted by Abhirami Ratnakumar indicated that estrogen activated 504 genes important for brain and neuron health (Figure 2). While it had many positive effects on the brain, it also activated APOE-related genes. This meant that those with the *APOE4* gene variant had an increased expression of its negative effects, making them more susceptible to AD. The study identified rare genetic mutations such as MCM8, ASPM, and SORL1, showing how they were influenced by the presence of estrogen. Specifically, ASPM was determined to be a protective gene, activated by estrogen, while SORL1 and MCM8 were identified as AD-inducing genes.[1] These findings suggest that *APOE4* carriers may experience a variety of protective and harmful effects from estrogen, demonstrating the importance of genes in relation to reproductive lifespan.

DOI: 10.36838/IJHSR87.177

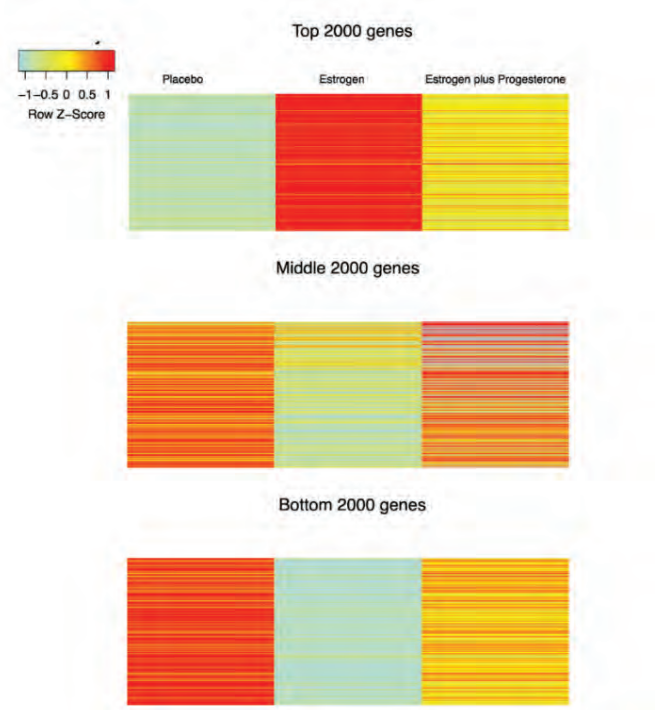

Figure 2: The expression levels of various treatments (Estrogen, Estrogen + Progesterone, and Placebo) are shown in a color scale (row z-score). The Top 2000 genes (top row) show that the highest expression was from the estrogen group. The Bottom 2000 genes (bottom row) were the least affected by estrogen. Each row is a gene (15,517 genes). Cooler colors indicate lower expression, and warmer colors indicate higher expression.[1] The data highlights that estrogen exposure facilitates greater gene expression, suggesting estrogen's role in enhancing neuroprotective genes.

Genetic individuality may also explain the conflicting results that have been reported on the effects of HRT, some leading to increased AD risk and some to neuroprotection.[8] People with specific genetic characteristics may respond differently to exogenous estrogen use, leading to different outcomes. In particular, it can be hypothesized that women without the *APOE4* gene may benefit from HRT use, slowing cognitive decline, Aβ deposition, and tau pathology, while those with the rare genetic variant may experience adverse effects.

In retrospect, reproductive lifespan may play a role in genetic expression, with possibilities including *APOE4* amplifying the effects of cumulative estrogen exposure. Women with *APOE4* and a shorter reproductive lifespan may exhibit faster progression and earlier onset, due to the deprivation of estrogen's protective effects. In contrast, a longer reproductive lifespan may enhance neuroprotection, sustaining estrogen's protective effects, although offset by the prolonged activation of the harmful *APOE4* genes. With further research, reproductive lifespan may be employed as a proxy for genetic expression, used to consider personalized treatment plans such as HRT.

Hormone Replacement Therapy and Window Period:

HRT has become increasingly common in women approaching menopause, used as a replacement for the hormones lost during the menstrual transition. It uses exogenous estrogen, sometimes combined with progesterone, to mimic the body's natural hormone production.[2] Aside from alleviating menopause symptoms such as hot flashes, insomnia, and depression, HRT may prolong estrogen's protective effects. In women with a naturally shorter reproductive period, estrogen replacement therapy can be a useful treatment to protect the brain from the vulnerability that comes with early menopause.[8]

Women taking estrogen post-menopause have been shown to experience the onset of AD significantly later than those who do not.[3] This was attributed to the protective effects of estrogen that were prolonged upon the use of estrogen replacement therapy. Conversely, another study found that HRT use post-menopause had an adverse impact on AD risk, causing brain atrophy and lowering hippocampus and brain volume.[13] These conflicting results raise the question: Is HRT beneficial or harmful in delaying the onset of AD?

The critical window hypothesis is an idea that HRT is only beneficial when given during the perimenopausal and early menopausal stage.[13] During this "window of opportunity," tau buildup and Aβ spread can be slowed, decreasing the risk of AD. In contrast, according to a study conducted by Rachel A. Whitmer, HRT taken in late life will have detrimental effects on the brain, accelerating AD pathology with a 48% elevated risk of AD. Based on the above, the effects of HRT may be altered by cumulative estrogen exposure, with a shorter reproductive period compressing the length of the window period, while a longer reproductive period would extend it. After the window period closes, the estrogen will exacerbate Aβ deposition and other AD biomarkers, rather than ameliorating cognitive function.[13] Timing is unique to every individual, and being able to pinpoint and adjust the most effective time period in which to administer HRT would advance therapeutic approaches to AD.

As discussed previously, estrogen plays a major role in regulating various AD-related mechanisms. During the window, the exogenous estrogen reduces the deposition of Aβ in the brain, improves synapse formation, and enhances glucose metabolism and cerebral blood flow.[13] The effectiveness of HRT may depend on when these biomarkers begin to shift. Personalized timing may be the key to maximizing therapeutic effects.

Genetics is also an important factor when considering HRT use, as certain gene carriers may respond differently to estrogen replacement therapy. For example, women with the *APOE4* gene variant would have adverse effects upon HRT use, even within the "window of opportunity."[8] This highlights the importance of considering genetics when prescribing medications, or in this case, when HRT is undergone. In contrast, individuals not carrying the *APOE4* gene would potentially benefit from HRT, depending on timing. Overall, gene-hormone interactions may potentially be an explanation for the conflicting results regarding HRT research. Exploring these interactions in future research would be beneficial to inform the effectiveness of treatment options.

Overall, the success of HRT usage is dependent on individualized factors, such as genetics and timing, thus leading to inconclusive findings on the usefulness of its application. This makes room for progress in the future. Here, I suggest that using reproductive lifespan and genotype as crucial factors for

personalizing HRT treatment can contribute to its effectiveness, ultimately delaying AD progression.

A Unified Model:

A unified model is crucial for integrating all the AD-related mechanisms that have been individually researched to create a comprehensive picture that utilizes reproductive lifespan as a proxy for AD risk. By capturing temporal dynamics across a woman's lifetime, the model can capture the evolution of various biomarkers and crucial factors in terms of reproductive lifespan in order to better combat the disease.

As discussed earlier, many variables contribute to the onset of AD, several of which have a network of links between one another. Reproductive lifespan serves as a common factor among various AD-related systems, linking a short vs. long lifespan with differences in cumulative estrogen (Figure 3). The hormonal decline at menopause has been connected to cognitive decline, such as the slowing of glucose metabolism and the decline of cerebral blood flow. Upon this shift, amyloid beta and tau dynamics change, accelerating their accumulation due to the loss of estrogen's protective effects.[10] Together, these alterations influence brain structure, prompting brain atrophy and a decrease in hippocampal volume.[5] Genetics also plays an important role, as people carrying the *APOE4* gene have an altered brain response to estrogen withdrawal, making them more vulnerable to cognitive decline compared to non-carriers.[1]

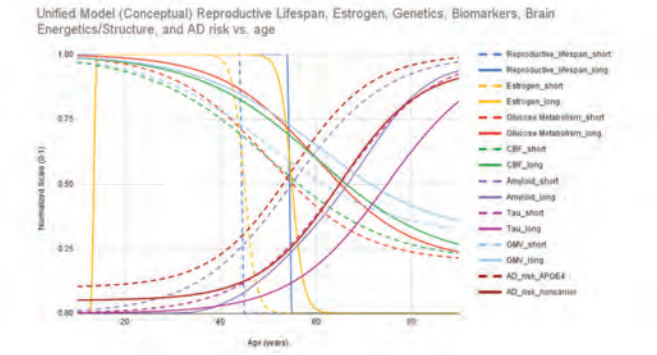

Figure 3: A conceptual graph using synthetic data to illustrate the unified model. This model uses a normalized scale (0-1) in relation to age in years to compare various important AD-related biomarkers and factors. It uses reproductive lifespan as a proxy, outlining the difference in the variables depending on cumulative estrogen exposure. The variables include estrogen, glucose metabolism, cerebral blood flow, Aβ burden, tau pathology, grey matter volume, and *APOE4*. The chart highlights the individual factors' relativity to one another, providing a comprehensive perspective of multiple AD biomarkers in relation to reproductive lifespan.

Rather than viewing these brain changes individually, it is more effective to look at them as interdependent (Figure 3). For example, a shorter reproductive lifespan signifies earlier estrogen withdrawal, causing energetic decline; in turn, this causes earlier vulnerability to amyloid and tau pathology, creating an increased risk of AD, which is amplified in *APOE4* carriers. Conversely, a long reproductive lifespan predicts delayed cognitive decline, with protection for brain energetics and postpones biomarker accumulation.

Overall, this unified model explains why women with shorter reproductive lifespans are more vulnerable to cognitive decline. This also explains the importance of the "critical window," as it integrates several factors to demonstrate the effects of HRT depending on whether it is started before or after major brain changes. The model shows that HRT not only affects hormones but also various significant brain mechanisms related to AD. By incorporating genetic, hormonal, and biomarker trajectories, this framework illustrates how different women need different treatments depending on their reproductive history.

■ Conclusion

Overall, this review addresses a gap in the literature by analyzing the interactions between reproductive lifespan, genetics, and brain biomarkers, providing an integrative foundation for personalized women's brain health and AD prevention. Current medicine and research fail to account for women's unique biology, leaving room for error and limiting the effectiveness of AD prevention. Leaving this gap under-researched risks leaving women behind in both understanding and treatment. This review lays the groundwork for possible future research, such as: a) longitudinal studies tracking the interactions between reproductive lifespan and genotype, b) critical window testing relative to menopause, and c) exploration of how to use individual differences to guide personalized HRT use.

Recognizing the unique trajectory of AD risk in women is not just a refinement of existing models; it's the next measure in preventing one of the most detrimental neurodegenerative disorders of our time.

■ Acknowledgments

I owe special thanks to Dr. Delis for his thoughtful guidance and consistent support, which have been instrumental in my research journey.

■ References

1. Ratnakumar, Abhirami, *et al.* "Estrogen Activates Alzheimer's Disease Genes." *Alzheimer's & Dementia: Translational Research & Clinical Interventions*, vol. 5, no. 1, Jan. 2019, pp. 906–917. https://doi.org/10.1016/j.trci.2019.09.004.
2. Scheyer, O., *et al.* "Female Sex and Alzheimer's Risk: The Menopause Connection." *The Journal of Prevention of Alzheimer's Disease*, vol. 5, no. 4, Oct. 2018, pp. 225–230. https://doi.org/10.14283/jpad.2018.34.
3. Tang, Ming-Xin, *et al.* "Effect of Oestrogen During Menopause on Risk and Age at Onset of Alzheimer's Disease." *The Lancet*, vol. 348, no. 9025, Aug. 1996, pp. 429–432. https://doi.org/10.1016/s0140-6736(96)03356-9.
4. Needham, Louisa P., *et al.* "A Comprehensive Assessment of Age at Menopause With Well-characterized Cognition at 70 Years: A Population-based British Birth Cohort." *Maturitas*, vol. 170, Jan. 2023, pp. 31–38. https://doi.org/10.1016/j.maturitas.2023.01.009.
5. Liao, Huanquan, *et al.* "Association of Earlier Age at Menopause With Risk of Incident Dementia, Brain Structural Indices and the Potential Mediators: A Prospective Community-based Cohort Study." *EClinicalMedicine*, vol. 60, June 2023, p. 102033. https://doi.org/10.1016/j.eclinm.2023.102033.
6. Breeze, Bernadette, *et al.* "Menopause and Alzheimer's Disease Susceptibility: Exploring the Potential Mechanisms." *Brain Re-*

DOI: 10.36838/IJHSR87.177

search, vol. 1844, Aug. 2024, p. 149170. https://doi.org/10.1016/j.brainres.2024.149170.
7. Insel, Philip S., *et al*. "Time Between Milestone Events in the Alzheimer's Disease Amyloid Cascade." *NeuroImage*, vol. 227, Dec. 2020, p. 117676. https://doi.org/10.1016/j.neuroimage.2020.117676.
8. Van Duijin, Cornelia M. "Hormone Replacement Therapy and Alzheimer's Disease." *Elsevier*, 1999, www.sciencedirect.com/science/article/abs/pii/S0378512299000055.
9. Yoon, Eun-Jung, *et al*. "Improvement of Cognitive Function in Ovariectomized Rats by Human Neural Stem Cells Overexpressing Choline Acetyltransferase via Secretion of NGF and BDNF." *International Journal of Molecular Sciences*, vol. 23, no. 10, May 2022, p. 5560. https://doi.org/10.3390/ijms23105560.
10. Mosconi, Lisa, *et al*. "Menopause Impacts Human Brain Structure, Connectivity, Energy Metabolism, and Amyloid-beta Deposition." *Scientific Reports*, vol. 11, no. 1, June 2021. https://doi.org/10.1038/s41598-021-90084-y.
11. Ozlen, Hazal, *et al*. "Spatial Extent of Amyloid-β Levels and Associations With Tau-PET and Cognition." *JAMA Neurology*, vol. 79, no. 10, Aug. 2022, p. 1025. https://doi.org/10.1001/jamaneurol.2022.2442.
12. Coker, Laura H., *et al*. "Postmenopausal Hormone Therapy and Cognitive Outcomes: The Women's Health Initiative Memory Study (WHIMS)." *The Journal of Steroid Biochemistry and Molecular Biology*, vol. 118, no. 4–5, 2010, pp. 304–310. www.sciencedirect.com/science/article/abs/pii/S0960076009002787?via%3Dihub.
13. Whitmer, Rachel A., *et al*. "Timing of Hormone Therapy and Dementia: The Critical Window Theory Revisited." *Annals of Neurology*, vol. 69, no. 1, 2011, pp. 163–169. https://doi.org/10.1002/ana.22239.

Author

Sonya Komar is an 11th grader at Scarsdale High School who is passionate about studying the brain. In the future, Sonya hopes to major in Neuroscience and conduct research in order to better the lives of those suffering from neurodegenerative diseases.

IJHSR
ijhighschoolresearch.org
RESEARCH ARTICLE

An Automated Framework for Studying the Potential of AI Defaults in Assignments

Audrey H. Koo

The Kinkaid School, 201 Kinkaid School Dr, Houston, TX, 77024, USA; akoo.concentric.circles@gmail.com

ABSTRACT: In this paper, we propose an automated experimental framework that can be used by educators to conduct research studies on the impact of AI in their classrooms. The framework helps educators understand how students use AI to solve homework questions. Furthermore, as one test of this framework, we have created an experiment to test the theory of defaults, which states that users are more likely to stick with the defaults than to spend effort pursuing a different option. By making certain uses of AI default within a homework assignment (through our novel interface), we conjecture that students are more likely to stick to those carefully chosen uses of AI instead of independently seeking AI to solve their entire assignment, which has been documented as a pressing problem in education today. We also provide automatic data collection for this framework, as well as guidelines on how to analyze and process the data, and all of the consent forms required to conduct these types of studies.

KEYWORDS: Systems Software, Human/Machine Interface, Online Learning, AI in Education.

Introduction

A study by Anthropic showed that, in the context of educational settings, the two major use cases of their LLM "Claude" are: (1) students generating new content from which they can learn (e.g., designing practice quizzes or editing essays); and (2) students requesting explanations and solutions to academic assignments.[1] This study also showed that 47% of interactions with Claude were "Direct" or "seeking answers or content with minimal engagement."[1] This data illuminates how students tend to ask for full and direct answers, instead of being guided by example or an explanation. This has led many educators to be concerned about how students' dependency on AI may lead to a lack of critical engagement and intellectual independence. Another study also cites the use of AI to cheat in academic assignments as a growing concern.[2]

The consequences of this widespread use of AI in the classroom have confused educators. Some advocate forbidding all AI from the classroom, while others argue that it should be treated more like a new technology that enhances learning, such as calculators or the Internet when they first came out.

In this project, we believe the latter. We think AI has the potential of enhancing—rather than harming—education, but it needs to be done carefully. The guiding principle behind our work is the theory of defaults. This theory states that users are more likely than not to choose defaults over alternatives because of the mental and physical cost-efficiency trade-off of staying with the given option, and how defaults may seem like an implicit suggestion given by the decision maker.[3]

We conjecture that if we create assignments that include certain curated uses of AI as defaults, then students will leverage these resources and will abstain from using the more harmful components of AI (e.g., asking for full answers). To test this conjecture, we designed a randomized experimental framework that can be conducted at schools throughout the country in any educational discipline. All that our framework requires is for instructors or researchers to supply their subject-area questions in a particular file format, and our framework will automatically enhance these questions to provide designated AI help. The goal of the experimental framework is to collect data from a diverse set of students and subjects to understand whether careful use of AI via defaults has the desired effect. In addition to the framework, we also provide automatic data collection to help instructors and researchers gather the data they need to answer their questions. Further, we also provide data analysis and data cleaning guidelines, and sample consent forms that instructors and researchers can give to students and their parents to enroll in this study.

In an ideal world, we would perform the full study ourselves to answer our research hypothesis. However, finding a large enough sample with diverse research participants is challenging in the amount of time that we had. We plan to perform a limited study in one high school, but we also hope that others will use our framework to conduct parallel studies at various schools throughout the nation. Indeed, we consider our primary contribution to be the creation of the randomized experimental framework to test the hypothesis, rather than the results of the experiment itself. We believe that answering this question in the affirmative could significantly impact the way in which educators create assignments and how they approach the role of AI in the classroom.

Background

The impact of AI in education:

AI can revolutionize the way education is taught today. Studies have reported success in improving test scores after using AI as a tutor.[4] A semester-long study at Uni-Distance Suisse showed that using an AI tutor app increased active engagement by 15 percentile points compared to a similar control course.[5]

© 2026 Terra Science and Education

DOI: 10.36838/IJHSR87.183

The AI app personalized the course to a student's strengths and weaknesses, and led to students achieving higher grades.[5]

AI can also improve personalization and reduce accessibility barriers. Language/cultural differences, economic inequalities, and teacher availability are some issues that educational systems fail to address. However, the new wave of AI technology could reduce these problems. It can provide high-quality teaching to users without being constrained by time or money, unlike a tutor, and tailors its response to the student's language, style, and pace of learning.[4,6]

However, while AI has the potential to improve education, as mentioned above, it can also weaken learning. One of the most commonly associated problems with AI in education is cheating. The rise in AI in the past year has led to an increase in the number of students using this technology to complete assignments with work that is not theirs.[7] Not only does AI plagiarism make it harder for schools to enforce and maintain academic integrity, but it also reduces students' ability to think critically and originally.[7]

Effective Educational Strategies:

In our review of the education literature, we found a few very helpful educational strategies that can improve students' outcomes. These include:

- The use of examples
- Contextualization of problems and grounding in real-world situations
- Clarification of the problem

Examples. The use of examples is an effective tool pervasively utilized in education. Giving examples can help students identify features of a concept that can be generalized and allow them to make associations with other concepts they know.[8] Being familiar with different cases and versions of a problem also creates a "priming" that can speed up students' ability to process and understand concepts.[8]

Contextualization and grounding. "Authentic learning" encapsulates contextualization and grounding and is an educational approach that connects concepts to the real world, whether through a real-life example or a hands-on experience.[9] Authentic learning has been rigorously proven in the educational literature to allow students to relate their learning to their own lives and experiences on a personal level and drive intrinsic motivation, rather than a school's extrinsic motivation driven by grades, social stigma, and other external factors.[9]

Clarification. Clarifying a problem is an effective way to help students tap into their own intrinsic motivation. Giving further details and rephrasing an explanation can simplify and unravel the complexity of a concept.[10] Clarification, as a result, reduces the cognitive load in actually understanding the questions and makes room for deeper association and connections with other concepts.[10] Clarification is also shown to act as an intrinsic motivator that can make students feel rewarded and encouraged by a clearer understanding of a topic.[10]

Beyond the above three, other educational strategies include bridging and open-ended questions. Bridging connects the content of the current lessons with concepts the student has seen in the past.[11] Open-ended questions could allow students "to analyze situations, make comparisons, draw conclusions, and then make inferences," to name a few. [11]

The power of defaults:

A substantial body of research shows that defaults can have a profound effect on behavior. Default is an option that does not require the user to take any action in its selection. This option allows designers to influence behavior and maintain the freedom to choose from alternatives.[3]

In particular, default theory illustrates that defaults can be effective at influencing behavior for three reasons.[3] First, the physical effort of clicking on a menu of options or reading through the choices can trade off with the user's internal preference and the time it takes.[3] Similarly, the mental cost of making a decision and reading each possible option can sway the user to choose the default over other possible options.[3] Secondly, defaults' pre-selection can serve as a reflection of the decision maker's recommendation.[3] Especially when users are unsure or do not have enough information to make a decision themselves, they tend to rely on defaults to help them make a decision.[3,12] Third, even if one doesn't choose the default, defaults can serve as a reference point for users' decisions in considering alternative options.[3] Following the same logic that defaults act implicitly as the decision maker's own recommendation, users may be influenced by defaults and the reasoning behind why certain options are selected as defaults, even when the automatic option may not itself be chosen.[3]

Many real-world applications also testify to the effectiveness of defaults. Political campaigns, businesses, and websites guide their audience's behaviors using defaults.[13] Fundraising efforts by Republican committees in 2020 show this effect. The default option in their donation form had recurring weekly donations checked as the default. This led to campaign donations increasing by 40 million dollars.[14] Another example that demonstrates the power of defaults is a study where researchers changed the printer settings' default option from simplex to duplex.[15] Their results showed that this subtle shift reduced the amount of paper consumption by 15% and suggested that green defaults could induce pro-environmental behavior. In contrast, encouraging moral appeal did not have any effect on the subjects.[15] Yet another example of how defaults can generate millions of dollars for companies is Google's position as the default search engine in a variety of browsers.

In the United States *et al*. v. Google LLC court case, it is alleged that Google paid companies such as Apple, Samsung and Mozilla billions of dollars to ensure that its search engine was set as default and, as a result, has earned billions in return through its monopoly.[16,17] Recently, the Justice Department ruled in favor of the anti-trust division, and this court case exemplifies how influential defaults can be.[16] Lastly, studies have shown that defaults can have a significant impact on education. "Cognitive and attentional limitations" are an "important barrier to good decision-making for complex choices such as education decisions."[18] Damgaard and Nielson suggest that defaults could provide small nudges that can help shape student behavior in making better judgments.[14] This is precisely the hypothesis that we wish to test in this paper: can

defaults help overcome the previously mentioned problems associated with AI? More specifically, integration of defaults could reduce plagiarism and cheating by taking advantage of the psychological tendency to stick to the given path.[18]

User Interfaces:

User interfaces are a powerful medium for encoding defaults. Specifically, how an interface is designed can affect a student's learning and satisfaction.[19] If a platform is not difficult to understand and leads to mistakes, it can discourage the user from wanting to achieve their learning goals.[15] On the other hand, having applications that make the content more understandable in the user interface can increase learning and have a positive effect on the user.[19]

Traditionally, homework and project assignments use a static user interface, namely a printed document, a static Word document, or a PDF. On top of this, homework and project assignments often do not have any integration with AI. They are separate entities/documents. The lack of interactivity or a user interface that incorporates AI into assignments means that existing classroom assignments do not have a notion of defaults or any meaningful way of discouraging students from cheating, a common problem with AI.

Our Hypothesis

The background section has shown that AI introduces the tension between being helpful for personalized learning and encouraging plagiarism. This has led to ongoing discussions on how to best incorporate AI into the classroom.

We hypothesize that extending assignments with carefully chosen defaults that incorporate AI in ways that help students better understand the concepts can lead to students being less likely to use AI for purposes of plagiarism. To study this hypothesis, we built a homework framework that incorporates default AI behaviors into the assignment itself. The next section describes this framework.

Our Chosen Defaults

The Effective Educational Strategies section outlines some effective learning strategies supported by research studies. As a result, we chose to include three defaults that utilize these approaches. Our defaults enable users to receive further explanations about a given concept to tap into their intrinsic motivation, unique examples to clarify a topic, and real-world applications of a concept to enhance authentic learning.

However, our framework is not limited to the current defaults chosen. Our Effective Educational Strategies section offers ideas on other potential defaults that could be implemented within our framework, such as an option that allows the student to generate a thought-provoking question about a given topic.

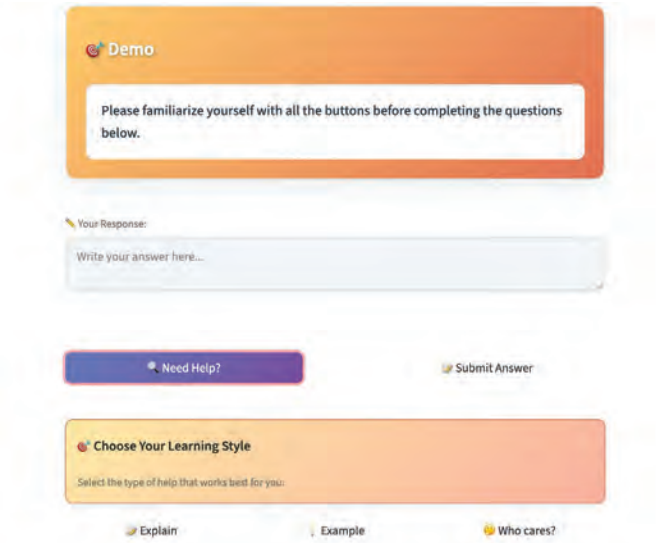

Figure 1: Screenshot of a demo question in our framework. The interface includes three buttons, "Explain," "Example," and "Who cares?" that allow students to interact with different AI-generated responses of research-supported learning strategies. These three buttons serve as defaults to disincentivize external AI usage and improve student comprehension.

A Homework Framework with AI

We designed a homework framework that can be used to answer the question of whether defaults can align AI usage with educational objectives. This framework is open source and available on HuggingFace Spaces at https://huggingface.co/spaces/feministmystique/AI-Course-Research.

The framework first includes a demo question. This question does not collect any of the interactions and controls for any confounding variables, such as users potentially experimenting with monitored questions included in the data set to familiarize themselves with the data set. Then, the following problems after the demo question test the user's knowledge on a given subject. We chose Precalculus, a course that could be conducted on 9th, 10th, 11th, and even potentially 12th graders, as the subject used for the example interface above. The questions we included in this interface came from Varsity Tutors, a free education and tutor provider.[20]

Each question in this framework has two drop-down buttons, "Need Help?" and "Submit Answers" with a text box directly under the query. You can see an example of this in Figure 1. Clicking "Submit Answers" will collect the user's answer in the text box and prevent them from making future edits, typical of a quiz or an assessment. On the other hand, clicking "Need Help?" will make another drop-down visible with three options: "Explain", "Example", or "Who cares?" with the title "Choose Your AI-Generated Answer." This title is necessary to clarify to the user that the three options provide different modes of AI-generated responses.

DOI: 10.36838/IJHSR87.183

Table 1: A table showing prompt types with multi-line content and providing the prompts we used within the interface for the three buttons "Explain," "Example," and "Who cares?" as well as the system prompt. The three buttons are specific to the defaults that we selected as valuable.

Type of Question	Prompt
System Prompt	You are an AI assistant designed to support high school students in the subject of {SUBJECT}. Your role is to offer friendly, helpful, concise, in-depth guidance, just like a supportive teacher would. Please follow these guidelines: 1. Maintain a polite, respectful, and professional tone at all times. 2. Adhere to ethical principles—do not promote cheating, harmful behavior, or misinformation. 3. Interact in a warm, encouraging, and student-centered style—use clear explanations, positive reinforcement, and examples when needed. 4. The word limit is {WORD_LIMIT} words. 5. Do not give the direct answer to the question.
Explain	6. Focus on thoroughly explaining the question by breaking down its components. Clarify the key concepts and definitions involved, ensuring that the explanation helps the reader fully understand what the question is asking. Avoid jumping to answers or examples; instead, concentrate on making the meaning and scope of the question clear. 7. Do not include specific examples or real-world applications in your response.
Example	6. Focus on providing three distinct, simple examples of this general question. Each example should highlight a unique approach or scenario related to the topic, helping to clarify the concept from multiple perspectives. 7. Do not include any explanation or real-world applications. 8. Do not give an example with the same question provided.
Who cares?	6. Explain two reasons why learning this subject in school is useful. Perhaps provide real-world applications. 7. Do not include any explanation or examples about the specific question provided.

The "Explain" option gives the user further explanation of core concepts necessary to answer the question. The "Example" option gives the user multiple examples to help them answer the question. The "Who cares?" option shows the user why the topic of the question is relevant in different fields and could give examples of tangential applications. In our implementation, we use the LLM model "deepseek-ai/DeepSeek-R1-0528" in HuggingFace to produce the corresponding output.

Table 1 includes the overall system prompt as well as the prompts for each of the default options that we identified. Our prompts were inspired by OpenAI's Study Mode[21] and their publicly released "Prompt Pack for students,"[22] but were specialized to the defaults that we identified as useful.

When one clicks on any of the three options mentioned above, another drop-down menu of selections opens in addition to an AI-generated response. These selections include "Retry?", "ChatGPT" and "Helped!" button. The "Retry?" button retrieves a different AI-generated response if the first was not sufficient. It does so by appending the following to the original prompt: "Please provide a different explanation. This is attempt retry_count + 1.", where the "retry_count" is the number of times that the user has clicked the button "Retry?". This option gives the user the ability to look through many possible explanations for a given question and select the AI-generated response that makes the most sense to them. Such an abundance of examples can help bring AI a step toward providing personalized learning in a safe environment. The "ChatGPT" button takes the user to ChatGPT if they still want to access a chatbot directly, despite the defaults, and having this button is necessary to have some way of keeping track of the number of times students will use the regular ChatGPT rather given the option than the AI-generated response provided. Finally, the "Helped!" button closes the tab and allows the user to continue with the original question and layout.

The three options "Explain", "Example", and "Who cares?" mentioned encapsulate the different possible questions that a user might ask. Additionally, the "Retry?" allows for further clarification and opportunity for AI to help solve a student's misunderstanding if the first answer was not sufficient. We limited the selection to three instead of four or five options because having many selections could overwhelm the user, on top of the other menu options within the interface.

The student interacts within the framework, as seen in Figure 1, by first exploring how to use the buttons as much as possible on the demo question. Then, the student can focus on answering the rest of the non-demo questions to the best of their ability by answering the question without the help of AI, using the default AI-generated responses, or using ChatGPT to help them answer the question.

Methods

Data Automation:

Previously, we discussed a homework framework using defaults, buttons, and AI. Now, we will dive into how this framework can be automated to help instructors and researchers. For instructors, collecting data on interactions with buttons can help teachers analyze patterns about how well the students comprehended the lessons and how well the lesson was taught. For example, instructors may find it helpful to collect data on the types of questions where students rely more on AI-generated responses. Such feedback can help instructors identify when their teaching was not effective and can help them review these concepts in class or improve their lessons for future class offerings. On the other hand, our framework can be equally beneficial for researchers. Data collection of student engagement can provide meaningful relationships and patterns for researchers to draw conclusions about.

The homework framework is designed to be customizable to any subject or any questions needed for a particular class. To make the interface more easily accessible for a teacher or researcher who may not necessarily have a background in programming, our framework allows a person to format the subject, questions, and answers for those questions in a text file using JSON.

```
{
    "Subject": "String",
    "Questions": [
        "String",
        "String",
        ...
    ]
}
```

Here is an example using the JSON format specified.

```
{
    "Subject": "Precalculus",
    "Questions": [
        "What is sin(π)?",
        "What is the center and radius of the circle indicated by the
         Equation (x-2)^2 + y^2 = 36?"
    ]
}
```

Our application reads the JSON file and extracts the information, and then produces the layout similar to that shown in Figure 1. Consequently, any relevant details and questions must follow the above-specified syntax and format.

Data Collection:

As mentioned in the Homework Framework section above, our framework collects users' interactions with the buttons and the interface. There are two types of data that the interface gathers. The first are the answers themselves, which instructors and researchers can use to grade students and understand the difficulty and success of a given question. The second type of data that we collect is AI assistance. This includes the time and date of the interaction, a unique ID for every session using UUID, the type of button clicked (e.g., the "Help" or "Explain the question" button), the question itself, the topic, and the number of times the Help and Retry buttons are clicked. We can estimate how long a student spent on each question by tracking when the student finished each of the questions. For example, if the student finished question 2 at 11:00 AM and question 3 at 11:10 AM, we can have a rough estimate that the student took around 10 minutes to complete question 3. This is an upper bound since the student may have done some other task in the meantime.

To collect this data into a Google Sheets document, we used the gspread library and the Google Cloud API. Using a UUID ensures researchers can keep track of and anonymize separate users. The number of times the Help and Retry buttons are clicked is recorded to give context to other buttons that are clicked. For example, researchers may find it helpful to know that a user selected the "ChatGPT" button after clicking on the Retry button twenty times and derive conclusions from it. We store the data mentioned above in a private Google Sheets that is updated in real-time.

Collecting Ground Truth Data:

To test our hypothesis, we would need to know what the ground truth of AI usage in assignments is to have a point of comparison for our data collection. This ground truth needs to determine the impact of AI on a student's performance without defaults.

We designed an interface used to collect ground truth information separate from the homework framework in Section 4. This interface has the same design and general layout as the homework framework, with the exception of removing the "Need Help?" button and all of the corresponding features.

Instead, there is only a "Submit" button under each question. In this interface, we do not tell the students to use AI, because such a suggestion could act as priming, producing results that may not be a reflection of how many times students use AI regularly. One other difference between the two interfaces is that the interface that does not have defaults will include an extra question at the end. In this last question, students self-report how many times they used AI to solve the questions (if at all).

This new interface that collects ground truth data uses the same JSON file provided in Section 5 and the same data collection mechanisms in Section 6.

Results and Discussion

At this point, our work is preliminary, and we do not have experimental results. Instead, we describe how our framework can be used to collect and analyze results in the future.

Above, we described two frameworks for collecting data from students. One is the "ground truth" framework, and the other is the "AI defaults." To conduct a study using these frameworks, we suggest choosing a minimum of 50 participants and randomly assigning them to two groups. One group should be given the "ground truth" homework framework, and the other group should be given the "AI defaults" homework framework.

Now, we need to establish the null and alternative hypotheses. Restating the hypothesis mentioned in Section 3, our alternative hypothesis states that if assignments incorporate AI via defaults, students are more likely to engage with these default AI options instead of relying on their own uncontrolled use of AI that can simply answer the entire question for them. The null hypothesis would be that the assignment that incorporates AI defaults does not significantly change how often students engage with uncontrolled AI, in comparison to an assignment that does not employ defaults. Once the data for these 2 experiments has been collected for a sufficiently large number of participants, the following data processing should be performed.

Data processing:

First, we suggest cleaning the data from the data collection process. Because all data is stored on Google Sheets, we recommend saving it as a CSV and converting the CSV to the most convenient dataframe, such as the pandas library. We also recommend removing outliers. This could look like detecting the time that users took to read and answer the question and removing any where students answered too quickly to have read the question. Another example of an outlier could include bogus answers that users answered that don't make any sense, like responding with an emoji or curse word to a question with a numerical response.

Second, we suggest that researchers and instructors use one or more two-sample comparison tests such as the Student's t-test, Welsh's test, cosine similarity, cross-correlation, etc.

Then, based on the results of these tests, ensure that the results are statistically significant. In Equation 1, we provide the formula for calculating the test statistic for Welsh's test for two sets of experiments.

$$t = \frac{\overline{x}_1 - \overline{x}_2}{\sqrt{\frac{{s_1}^2}{n_1} + \frac{{s_2}^2}{n_2}}}$$

Equation 1: Welsh's equation, where $\overline{x_1}$ is the mean for sample one, $\overline{x_2}$ is the mean for sample two, s_1 is the standard deviation for sample one, s_2 is the standard deviation for sample two, n_1 is sample one's size, and n_2 is sample two's size. This equation is used in Welch's t-test as one of the potential ways to further analyze data collected from our interface.

DOI: 10.36838/IJHSR87.183

If the results are statistically significant, this can provide evidence against the null hypothesis and in favor of our alternate hypothesis: that our intervention (namely, the use of defaults) could have an impact on students' actions.

Limitations:

One limitation of this study is that we did not test our proposed framework ourselves due to time constraints. However, we plan to perform a limited study in one high school in the near future and hope that others will use our framework to conduct parallel studies at various schools throughout the nation. Our framework also gives students the ability to interact with different generated explanations of a question, but does not allow students to type in their own individual questions at the moment, which allows for even further personalized learning. For data collection, we currently do not have a method of verifying whether a student opens an external window and uses a separate AI model. Therefore, knowledge of whether a student interacted with another model beyond our interface is self-reported through our survey.

■ Conclusion

In this work, we discuss how students are using AI in harmful ways: to cheat on their assignments or avoid critical and engaged thinking. We hope that the theory of defaults can provide a way to guide the use of AI in educational settings to ensure that students are making the most out of this powerful technology. To test this hypothesis, we put forth a randomized experimental framework that we hope educators will implement across the nation to get a sense of whether AI can be used in constructive ways. Our framework can be a potential solution to the increasingly problematic rise of AI plagiarism that is devaluing the existing educational system. It also provides a way for educators to take a more active part in how students engage with AI.

■ Acknowledgments

The author thanks Sebastian Angel (University of Pennsylvania) for his mentorship in this project, as well as the AI Student Committee at the Kinkaid School, which inspired the author to look into the harmful effects of AI in education.

■ References

1. Handa, K.; Bent, D.; Tamkin, A.; McCain, M.; Durmus, E.; Stern, M.; Schiraldi, M.; Huang, S.; Ritchie, S.; Syverud, S.; Jagadish, K.; Vo, M.; Bell, M.; Ganguli, D. *Anthropic Education Report: How University Students Use Claude*. Anthropic, April 8, 2025. https://www.anthropic.com/news/anthropic-education-report-how-university-students-use-claude (accessed Aug 21, 2025).
2. Sweeney, S. Who Wrote This? Essay Mills and Assessment – Considerations Regarding Contract Cheating and AI in Higher Education. *Int. J. Manag. Educ.* **2023**, *21* (2), 100818. https://doi.org/10.1016/j.ijme.2023.100818.
3. Dinner, I.; Johnson, E.; Goldstein, D.; Liu, K. Partitioning Default Effects: Why People Choose Not to Choose: Correction to Dinner *et al*. (2011). *J. Exp. Psychol., Appl.* **2011**, *17*, 432. https://doi.org/10.1037/a0026470.
4. Ni, S. Are Large Language Models More Honest in Their Probabilistic or Verbalized Confidence? *Appl. Sci*. **2025**, *15* (9), 4989. https://doi.org/10.3390/app15094989
5. Baillifard, A.; Gabella, M.; Lavenex, P. B.; Martarelli, C. S. Effective Learning with a Personal AI Tutor: A Case Study. Educ. Inf. Technol. 2025, 30 (1), 297–312. https://doi.org/10.1186/s41239-018-0095-0
6. Bi, N. Inclusive and Equitable Education with AI: Addressing the Needs of Diverse Learners through AI Solutions, Ensuring Quality and Accessibility. *Int. J. Res. Appl. Sci. Eng. Technol*. **2025**, *14*, 69–74. https://doi.org/10.35629/7722-14046974.
7. Chan, C. K. Y. Students' Perceptions of 'AI-giarism': Investigating Changes in Understandings of Academic Misconduct. *Educ. Inf. Technol*. **2025**, *30* (6), 8087–8108. https://doi.org/10.1007/s10639-024-13151-7.
8. Oliveira, A. W.; Brown, A. O. *Exemplification in Science Instruction: Teaching and Learning through Examples*. J. Res. Sci. Teach. 2016, 53 (5), 737–767. Wiley Online Library.
9. Roach, K.; Tilley, E.; Mitchell, J. *How Authentic Does Authentic Learning Have to Be?* High. Educ. Pedagog. 2018, 3 (1), 495–509. Taylor & Francis.
10. Serki, N.; Bolkan, S. *The Effect of Clarity on Learning: Impacting Motivation through Cognitive Load. Commun. Educ*. **2024**, *73* (1), 29–45. Taylor & Francis.
11. Orlich, D. C.; Harder, R. J.; Callahan, R. C.; Trevisan, M. S.; Brown, A. H. *Teaching Strategies: A Guide to Effective Instruction*; Wadsworth, Cengage Learning: Belmont, CA, 2010.
12. Altmann, S.; Falk, A.; Grunewald, A. Communicating through Defaults. *Rev. Econ. Stat*. **2025**, *107* (1), 256–268. https://doi.org/10.1162/rest_a_01260.
13. Jachimowicz, J. M.; Duncan, S.; Weber, E. U.; Johnson, E. J. When and why defaults influence decisions: A meta-analysis of default effects. *Behav. Public Policy* **2019**, *3* (2), 159–186. https://doi.org/10.1017/bpp.2018.43
14. Posner, N.; Simonov, A.; Mrkva, K.; Johnson, E. J. Dark defaults: How choice architecture steers political campaign donations. *Proc. Natl. Acad. Sci. U.S.A*. **2023**, *120* (40), e2218385120. https://doi.org/10.1073/pnas.2218385120
15. Egebark, J.; Ekström, M. Can indifference make the world greener? *J. Environ. Econ. Manage*. **2016**, *76*, 1–13. https://doi.org/10.1016/j.jeem.2015.11.004
16. Anon. Department of Justice prevails in landmark antitrust case against Google. Off. Public Aff. U.S. Dep. Justice, April **2025**. https://www.justice.gov/opa (accessed 2025-08-05).
17. McCabe, D.; Grant, N. What's next for Google's search monopoly. *N. Y. Times*, December 3, **2024**. https://www.nytimes.com/2024/12/03/technology/google-search-antitrust-judge.html (accessed 2025-08-05).
18. Damgaard, M. T.; Nielsen, H. S. Behavioral economics and nudging in education: Evidence from the field. In *The Economics of Education*, 2nd ed.; Bradley, S., Green, C., Eds.; Academic Press: San Diego, **2020**; pp 21–35. https://doi.org/10.1016/B978-0-12-815391-8.00002-1.
19. Bakken, S. User interfaces remain an important area of study. *J. Am. Med. Inform. Assoc*. **2023**, *30* (12), 1841–1842. https://doi.org/10.1093/jamia/ocad246 (accessed 2025-08-08).
20. Anon. *High School Math: Pre-Calculus.* Varsity Tutors. https://www.varsitytutors.com/high_school_math-help/pre-calculus (accessed 2025-08-05).
21. OpenAI. ChatGPT Study Mode. OpenAI. https://openai.com/index/chatgpt-study-mode/ (accessed Nov 4, 2025).

22. OpenAI. Prompt Pack for Students. OpenAI Academy. https://academy.openai.com/public/clubs/higher-education-05x4z/resources/prompt-pack-for-students (accessed Nov 4, 2025).

Appendix

Appendix A: Parent Consent Form:

Title: The Impact of Defaults on AI Usage in Education

Researchers: Audrey Koo

This is a consent form for research participation. It contains important information about this study and what to expect if you decide to participate. Your participation is voluntary.

Purpose: Our research aims to assess how defaults can have an impact on integrating AI into education. By examining these effects, we deepen our understanding of how defaults promote or hinder desirable interaction behaviors with LLMs.

Procedures and Time Required: If agreeing to participate in the study, we will collect and analyze your child's interactions with the interface.

If your child becomes an adult (turns 18 years old) while they are still actively participating in this research, we will request that they provide their consent (agreement) to continue their participation in this study.

Compensation: Students will not be compensated for participation.

Risks and Benefits: This study entails little risk. If one chooses to participate, one's data would be anonymized, and one can withdraw at any point during the process. The data collected is a participant's interaction with the interface, not a name or any identifying personal information. Participants will further research in developing educational tools and give researchers further insight into integrating AI in classroom learning.

Confidentiality: Information is collected without any personal information of a specific child and, as a result, will be anonymized. The only person who will have the individual data is Audrey Koo. Data may be individually presented in this study, but without any identifiable information.

Contact & Questions: If you have any questions, please contact Audrey Koo, The Kinkaid School at audrey.koo@kinkaid.org.

Consent: Participation is voluntary. Refusal to participate or withdrawing from the research will involve no penalty or loss of benefits to which you might otherwise be entitled.

By signing below, you acknowledge that you have read and understood the information above, and you voluntarily consent to your child's participation in the research study.

Child's Name: _____

Parent's Name: _____

Signature: _____

Date: _____

If your child is 13 years or older, we will also ask for their consent to participate in the research.

Appendix B: Parent Consent Form:

Who are we?

Audrey is a senior at The Kinkaid School, doing a research study.

What is this?

We will do a research study to understand the use of Large Language Models (LLMs) when solving challenging assignments.

What will happen if I say yes?

You will be given access to a demo homework assignment that you will complete. We will collect information such as your answers and how long it takes you to solve each question, but they will not be tied to you—they are completely anonymous.

You will not personally receive any compensation or any benefit from the school if you choose to participate. This is entirely voluntary.

Will anyone know what I said or did?

The study is completely anonymous, and your name or personal information will not be collected. We will only use your interactions with different parts of the webpage, and we'll use made-up codes instead of your name when collecting data.

Is there anything bad that could happen?

There is minimal risk since the data will be anonymized, and nothing we collect will affect your grades or school records.

What are the good parts?

The good part is that you can help researchers better learn about how AI is used in education!

Do you want to be in this study?

If you've read this and want to be in the study, please sign below. If you're not sure, ask us questions! You can always say no.

Student:_____

Parent:_____

Appendix C: Research Study Description:

Title: The Impact of Defaults on AI Usage in Education

Description: I am a researcher at the Kinkaid School. I am conducting a research study on how an interface can affect students' behavior with LLMs. All students will use the same interface.

If you agree to participate in the study, your interaction with the interface will be recorded as well as the answers submitted on the assignment.

Risks: This study entails little risk. If one chooses to participate, their data would be anonymized, and one can withdraw at any point during the process. The data collected is a participant's interaction with the interface, not a name or any identifying personal information. The only risk is perhaps a breach of confidentiality; however, the data would not hold any personal or identifiable information of the participants.

Participation may stop due to a participant wanting to withdraw their data from the study.

Visibility: The only person who will have the individual data is Audrey Koo. Data may be individually presented in this study, but without any identifiable information.

Benefits: Participants will further research in developing educational tools and give researchers further insight into integrating AI in classroom learning.

Compensation: No compensation to the participant will be provided.

Time: Each participant will spend around 30 minutes

Number of participants: 100

Contact:

For additional questions about the research or the rights of participants, please contact audrey.koo@kinkaid.org

Author

Audrey Koo is a current 12th grader and a dedicated science researcher who is interested in majoring in Information Science. She is involved in many STEM leadership positions at her school and hopes to continue to pursue college research.

DOI: 10.36838/IJHSR87.183

IJHSR
ijhighschoolresearch.org
REVIEW ARTICLE

The True Footprint of Clean Energy: A Life-Cycle Comparison of Solar, Wind, and Microalgae Biofuel

Jun Kang

Hiroo Gakuen Senior High School, 5-1-14 Minami Azabu, Minato Ku, Tokyo 106-0047 Japan; junkang1532@gmail.com

ABSTRACT: As the global climate crisis escalates, a transition to sustainable energy is vital for curbing greenhouse gas emissions. This paper provides a comparative Life-Cycle Assessment (LCA) to evaluate the environmental impacts of three renewable technologies: solar photovoltaic (PV) systems, wind energy, and microalgae biofuel. Synthesizing data from 25 selected peer-reviewed studies and organizational reports, this analysis quantifies key environmental metrics, including Global Warming Potential (GWP), resource demands, and Energy Payback Time (EPBT). The findings reveal significant variability. Modern onshore wind turbines exhibit the lowest consistent emissions (as low as 5.6 g CO2-eq/kWh), followed by solar PV systems (19–50 g CO2-eq/kWh), while microalgae biofuel displays the widest range, from being a net carbon sink in optimized systems (-48 to -623 g CO2-eq/kWh) to a major emitter in others. These results show that although onshore wind has the lowest mean life-cycle emissions, the optimal choice is highly context-dependent, determined by regional climate, technological maturity, and logistical factors. This underscores the need for sophisticated, context-specific energy policies to achieve a sustainable future.

KEYWORDS: Energy: Physical, Sustainable Design, Life-Cycle Assessment, Solar Photovoltaics, Microalgae Biofuel.

Introduction

Mitigating climate change requires a global transition from fossil fuels, which are responsible for approximately 80% of energy-related CO_2 emissions. Solar photovoltaic (PV) systems, wind energy, and microalgae biofuel represent diverse pathways to decarbonize energy production, each with distinct mechanisms and environmental implications. Solar PV systems convert photons from sunlight into electricity via semiconductor materials, a process known as the photovoltaic effect. Wind energy captures kinetic energy from air movement using turbines, which drive generators to produce electricity. Microalgae biofuel utilizes photosynthetic microorganisms to produce biomass, subsequently processed into liquid fuels such as biodiesel or biobutanol. Although these technologies have low operational emissions, their true sustainability can only be understood by examining their entire life cycle, from raw material extraction to end-of-life management.

Evaluating the true sustainability of these technologies requires a method known as Life-Cycle Assessment (LCA), governed by the ISO 14040 series of standards.[1] LCA allows for a "cradle-to-grave" approach. This method assesses environmental impacts from raw material extraction to the End of Life (EOL) stage, where products are recycled or disposed of, influencing waste management and resource recovery.[2] This assessment quantifies various impacts, including the emission of Greenhouse Gases (GHG). These gases, such as carbon dioxide (CO_2) and methane, contribute to global warming.[3] To standardize these impacts for consistent comparison, emissions are often converted to a CO_2 Equivalence (CO_2-eq), a metric based on each gas's Global Warming Potential (GWP) as defined by the Intergovernmental Panel on Climate Change (IPCC).[4] This metric highlights a significant contrast to traditional fossil fuels. For instance, the GWP of electricity from hard coal is over 99% higher than that of clean sources like hydropower.[3] Furthermore, LCA evaluates energy efficiency through metrics like the Energy Payback Time (EPBT), which measures the time a system needs to generate the energy consumed during its own production.[5] However, it is important to note the methodological challenges inherent in LCA studies; variations in system boundaries and impact assessment methods, which categorize environmental effects differently (e.g., CML 2001, ReCiPe), can complicate direct comparisons across studies.[6]

While solar PV and wind energy are established renewable technologies, microalgae biofuel remains a less commercially developed but promising alternative with the unique potential for direct CO_2 sequestration. However, its viability is often limited by energy-intensive cultivation and processing steps. To properly contextualize its potential, a direct comparison with mature renewable technologies is needed. Therefore, this review synthesizes current LCA research to compare the carbon footprints, measured in grams of CO_2 equivalent per kilowatt-hour of energy generated (g CO_2-eq/kWh), alongside resource demands, and energy efficiency of microalgae biofuel, alongside solar PV and wind energy. Accordingly, this paper evaluates the distinct environmental trade-offs of each technology to demonstrate that their sustainability is highly context-dependent, thereby providing a foundation for more effective, region-specific energy policies.

This review first evaluates solar PV systems, followed by wind turbines, and then microalgae biofuel, analyzing each through the four key LCA phases: material cultivation and processing; production and manufacturing; operation; and end-of-life management. This final phase evaluates the impacts of disposal and recycling, where resource recovery can yield environmental credits that offset upstream emissions. Following

© 2026 Terra Science and Education

DOI: 10.36838/IJHSR87.190

these individual assessments, a comparative analysis evaluates the distinct environmental trade-offs of each technology, and the review concludes by synthesizing these findings to provide a foundation for more effective, region-specific energy policies.

Methods

To collect sources, a search was conducted primarily using Google Scholar for peer-reviewed studies. Moreover, this was supplemented by a review of "grey literature," including technical reports from industry and governmental organizations (e.g., U.S. Environmental Protection Agency, Vestas). The search used keyword combinations such as "Life Cycle Assessment," "LCA," "solar PV," "wind power," "microalgae biofuel," "GWP," "GHG," and "Energy Payback Time (EPBT)."

To keep the data relevant to current technologies, the review focused on studies published within the last 15 years (2010-2025). Priority was given to papers that provided detailed, quantitative, life-cycle stage data and included comprehensive figures or tables. Additionally, both primary LCA studies and existing meta-analyses were included. Studies were excluded if they were not published in English or were not directly relevant to the metrics for core comparison.

Key data points for Global Warming Potential (GWP), Greenhouse Gas (GHG) Emissions, and Energy Payback Time (EPBT) were manually extracted from the selected literature. This quantitative data was then compiled to create the comparative analysis presented in the paper's main table and Figures 1 to 3.

Results of Literature Search

The search and screening process described in the Methods section yielded 25 LCA studies that were selected for the final quantitative and qualitative synthesis.

The final papers used for analysis, comparison, and data extraction consisted of 6 studies for solar PV, 9 studies for wind energy, and 10 studies for microalgae biofuel. The paper's bibliography is larger than this total, as it also includes foundational texts, methodological standards (such as ISO 14040), and reports used for contextual data.

Discussion

Life-Cycle Analysis of Photovoltaic (PV) Systems:

Overview and Scope:

A solar photovoltaic (PV) system functions by directly converting energy from sunlight into electricity. This process, known as the photovoltaic effect, occurs within solar panels, which are the visible component of a system. These panels are typically made from many individual solar cells, made from semiconductor materials like silicon, which absorb photons and release electrons to create direct current (DC) electricity.[6]

However, the life cycle of a complete system includes several other vital components grouped under the Balance of System (BoS).[6] For example, inverters are required to convert the direct current (DC) electricity produced by the panels into alternating current (AC) usable by the grid or in a home.[6] Other components included in the BoS are the mounting structures, which provide physical support, as well as necessary wiring, connectors, and safety equipment.

This section evaluates the GWP of solar PV systems, and the analysis covers three generations of PV technology: first-generation crystalline silicon (mono-Si and multi-Si); second-generation thin-films such as amorphous silicon (a-Si), cadmium telluride (CdTe), and copper indium gallium selenide (CIGS); and third-generation emerging technologies, including organic photovoltaics (OPV), perovskite solar cells (PSC), and quantum dot (QD) PV. However, it is important to note that these emerging technologies have not yet achieved large-scale commercial deployment. While distinct, for this review, mono-Si and multi-Si will often be discussed collectively as 'crystalline silicon' systems to facilitate a clearer comparison across generations. Lifecycle assessments of PV systems report a wide range of environmental impacts, with GWP values ranging from 2.89 to 150 g CO_2-eq/kWh and an EPBT of 0.24 to 6.0 years, largely dependent on technology type, system design, and solar insolation.[6]

Material Cultivation and Processing:

The life cycle of a PV system begins with the extraction and processing of raw materials, a phase that often covers a significant portion of its total environmental footprint, with impacts varying distinctly across technology generations. For first-generation systems, key materials include silicon, aluminum, and steel. The purification of silicon is a highly energy-intensive process. It transforms metallurgical-grade silicon into solar-grade silicon and requires extremely high temperatures to achieve the necessary purity. This single step accounts for 52.4% of the environmental impacts for multi-crystalline silicon systems.[6] Aluminum and steel, used for frames and supports, increase ozone layer depletion potential, which refers to the degradation of stratospheric ozone.[6]

Second-generation systems utilize materials such as cadmium telluride, copper indium gallium selenide, amorphous silicon, glass, and aluminum. Processing these materials is less energy-intensive than first-generation technologies, but the use of fluorinated gases, such as sulfur hexafluoride, in manufacturing increases greenhouse gas emissions.[5] However, recovery of glass and aluminum during processing helps mitigate environmental impacts.[6] One study found that the GWP for cadmium telluride systems ranges from 19 to 30 g CO_2-eq/kWh.[5]

Third-generation systems incorporate materials like fullerenes, which have a high embodied energy of 35 to 123 GJ/kg.[6] This value is dramatically higher than the 1.96 to 5.85 GJ/kg required for common polymers. To put that into perspective, the energy needed to create just one kilogram of fullerenes could power an average U.S. home for nearly a full year at the low end (35 GJ) and over three years at the high end (123 GJ). These findings emphasize the significant energy investment needed for these advanced materials.[6] The GWP for QD-PV can be as low as 2.89 g CO_2-eq/kWh, demonstrating its potential for very low lifecycle emissions; however, this environmental advantage is offset by significant concerns regarding heavy metal emissions from its components.[6]

Production and Manufacturing:

Similar to material cultivation, the production and manufacturing phase is a major contributor to the environmental impacts of PV systems due to energy-intensive processes.[6] For first-generation systems, manufacturing involves two primary methods: the Czochralski process, which grows single-crystal silicon ingots by pulling a seed crystal from molten silicon, and casting, where molten silicon is cooled in a mold to form multi-crystalline silicon.[6] Both of these methods consume significant energy, leading to increased carbon dioxide emissions.[6] Multi-crystalline silicon systems have a cumulative energy demand of 1619 MJ/m^2.[6]

Second-generation systems employ thin-film deposition techniques, such as sputtering, which deposits material via plasma, or chemical vapor deposition, which deposits material from a gas phase.[5] These processes use less energy than first-generation methods, resulting in lower emissions overall; yet, they involve toxic materials like cadmium.[5]

Third-generation systems utilize roll-to-roll manufacturing, a continuous printing process for flexible substrates like organic PV, which reduces energy consumption.[6] Emissions vary due to diverse material choices and system scenarios. However, for a representative rooftop solar installation, OPV systems indicate a cumulative energy demand of 122 to 125 MJ/m^2.[6]

Operational Phase:

The operational phase of PV systems generates electricity with no direct emissions, making it zero direct emissions during operation.[6] PV systems produce negligible emissions during operation, effectively replacing fossil fuels, with impacts dependent on system efficiency, lifetime, and the amount of solar radiation received (insolation).[6] For first-generation systems, the EPBT ranges from 2.2 to 6.0 years, with multi-crystalline silicon systems specifically reported between 2.4 and 3.1 years, influenced by annual insolation levels between 1166.[7] and 1855.[6] peak sunshine hours.[6] Second-generation systems, such as cadmium telluride, have a shorter EPBT of 0.8 to 3.6 years.[5] Third-generation systems, like organic PV, achieve an EPBT of 0.24 to 1.2 years.[6] To illustrate the impact of performance improvements, one study found that PV systems generally increased in efficiency from 6% to 13%, and extending the lifetime from 15 to 30 years reduces the GWP from 38.[7] to 9.6 g CO_2-eq/kWh.[6] Geographical location impacts energy output, with regions like Northeast Nigeria producing 31% more energy compared to an average of 1700 kWh/m^2/year.[6]

End of Life Management:

End-of-life management for PV systems is critical, though current practices vary. Globally, landfilling remains the most common disposal method for both first- and second-generation panels, primarily due to economic factors and a lack of widespread recycling infrastructure.[7] However, environmentally superior recycling processes exist. For first-generation systems, recycling involves dismantling modules to recover glass (70% of mass), aluminum (10–18%), and ethylene-vinyl acetate (2–5%), with silicon crushed for raw material reuse rather than refurbishing entire panels.[6] Recycling 1000 kg of mono-crystalline silicon waste reduces the cumulative energy demand from 3150 MJ to 2780 MJ and decreases GWP by approximately 30% compared to landfilling the panels.[6]

For second-generation systems, such as CdTe, established recycling programs achieve high glass recovery (95% of mass) and recover toxic materials like cadmium, reducing GWP and non-renewable energy use.[5] Recycling these systems outperforms incineration in most environmental impact categories.[5] Third-generation systems face challenges due to limited recycling data, with studies often assuming landfilling.[6] However, glass and metal recovery reduces resource consumption, and polymer incineration offers energy recovery for these emerging technologies.[6]

Synthesis and Implications:

LCA studies underscore the sustainability of PV systems, with distinct characteristics across technology generations. As illustrated in **Figure 1**, the lifecycle GWP is dominated by the upstream phases, with material cultivation and fabrication accounting for the largest share of emissions. First-generation systems, such as crystalline silicon, exhibit a high EPBT of 2.2 to 6.0 years and a GWP of 49.9 g CO_2-eq/kWh, driven by energy-intensive production processes.[8] Second-generation systems, like cadmium telluride, achieve a moderate EPBT of 0.8 to 3.6 years and a GWP of 19 to 30 g CO_2-eq/kWh.[5] Third-generation systems, such as organic PV and QD-PV, offer a lower EPBT of 0.24 to 1.2 years but have a variable GWP of 2.89 to 150 g CO2-eq/kWh, as these technologies are still largely in the research and development (R&D) phase with significant concerns about material toxicity.[6]

Beyond the inherent properties of each generation, the life-cycle performance of any PV system is significantly modulated by several external factors. Improvements in system efficiency offer another path to lower impacts, with studies indicating GWP can be reduced by up to 30% through such advancements.[6] Geographical location affects EPBT, with insolation levels between 772.2 and 2100 peak sunshine hours leading to EPBT of 2.2 to 6.0 years.[6] The balance of system (BoS) components, such as inverters and mounting structures, can contribute up to 45% of total environmental impacts, stemming from the manufacturing of aluminum or steel mounts and the energy losses from inverters. Notably, these impacts can be mitigated by Building-integrated PV (BIPV) systems. In BIPV systems, panels also serve as structural elements like roof tiles or facades. This reduces the need for separate mounting hardware and displacing conventional building materials.[6] Longer lifetimes, typically 25 to 30 years for first-generation systems, enhance overall sustainability.[6] Effective EoL management through recycling provides a crucial opportunity to mitigate a portion of the initial environmental burden, with studies suggesting GWP reductions of up to 30% by avoiding the need for virgin raw material extraction.[7]

Looking ahead, it is important to acknowledge that limited data for third-generation technologies further hinders comprehensive assessments.[6] Nevertheless, PV systems remain promising, and improvements in efficiency, production processes, and recycling infrastructure are required to enhance

DOI: 10.36838/IJHSR87.190

their sustainability.[8] Future research should focus on mitigating risks from toxic material releases and developing dynamic LCA models to account for evolving emission factors.[6]

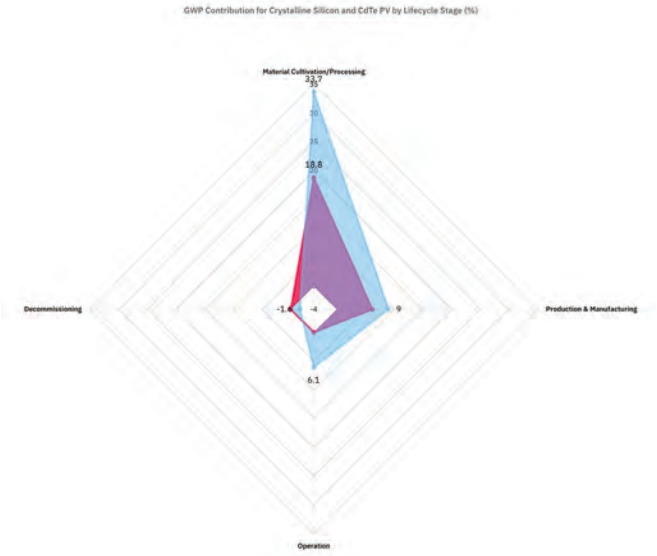

Figure 1: GWP contribution for crystalline silicon and CdTe PV by life-cycle stage (%). This radar chart compares the GWP breakdown for first-generation crystalline silicon (blue) and second-generation CdTe thin-film (red) solar PV. The distance from the center along each axis represents the percentage contribution of that stage to the total GWP. For example, Material Cultivation/Processing accounts for 33.7% of the GWP for crystalline silicon. Negative values, such as those for decommissioning, represent environmental credits from recycling that offset a portion of the emissions. The data shows that material cultivation and processing represent the largest GWP contribution for both technologies, especially for crystalline silicon. This highlights how the energy intensity of early stages, rather than manufacturing or operation, is the largest contributor to solar PV's carbon footprint. Data synthesized from Nugent & Sovacool (2014).[8]

Life-Cycle Analysis of Wind Energy:

Overview and Scope:

Wind energy systems capture the kinetic energy of moving air and convert it into electricity. The main component is the turbine, which consists of several key parts. The rotor, which includes the large blades (often made of fiberglass composites), catches the wind and begins to turn. This rotation runs a generator, which is set inside the nacelle, the casing at the top of the turbine. Consequently, the generator converts the mechanical energy into electrical energy.[9]

Furthermore, this entire assembly is mounted on a tall tower, typically made of steel, to access stronger and more consistent winds. Finally, the large turbine is secured by a massive foundation, usually made of steel and concrete, which is a major contributor to the system's "cradle-to-grave" environmental footprint.[9]

This section evaluates the GWP of wind energy, which converts atmospheric kinetic energy into electricity via turbine-generator systems. The analysis covers both onshore turbines, which are the most common type, and offshore turbines, which are situated in bodies of water to access stronger, more consistent winds. Wind energy is a low-carbon technology, with an average lifecycle GWP of 34.1 g CO_2-eq/kWh, though this can range from 0.4 to 364.8 g CO_2-eq/kWh due to variations in turbine design, location, and methodological assumptions.[8] The EPBT for wind technologies is typically less than one year, highlighting their efficiency in offsetting embodied energy.[9] However, offshore wind generally exhibits higher GWP than onshore due to increased material and operational demands.

Material Cultivation and Processing:

This stage involves extracting and producing raw materials, which significantly contributes to GWP. The primary GWP contributors are steel and concrete due to the large quantities required; steel and iron together comprise 79.4% of offshore and 22.3% of onshore infrastructure.[9] Other materials with significant impacts include copper, aluminum, epoxy, and glass fiber. Moreover, steel production emissions vary by region (e.g., 1.97 t CO_2-eq/t in China versus 0.96 t CO_2-eq/t in the US), while copper in cables and epoxy in blades are also impactful, with epoxy being 48 times more GWP-intensive per kg than concrete.[9,10] Additionally, the electricity mix used in processing affects GWP, as low-carbon mixes reduce emissions compared to coal-heavy mixes. Therefore, for both onshore and offshore wind, this stage plays a dominant role in climate change impacts, accounting for over 79% onshore and 70% offshore.[9] Furthermore, offshore wind's higher GWP is exacerbated by larger high-impact material requirements for capital infrastructure, such as foundations and floaters.[9] The GWP for the material cultivation and processing stage of wind energy systems is reported to range from 2.3 to 26.6 g CO_2-eq/kWh.[11,12] It is worth noting that this range is narrower and generally lower than the one found in older, broader meta-analyses, which likely reflects ongoing technological improvements in turbine manufacturing and efficiency. This variability is attributed to factors such as turbine size and foundation type. The literature consistently identifies two primary drivers of this impact: material selection, which includes the large quantities of steel and concrete required, and the carbon intensity of the energy supply for manufacturing.

Production and Manufacturing (Construction):

While the precise contribution of each life-cycle phase varies between studies, one meta-analysis determined that the upstream phases are the most significant. The 'cultivation and fabrication' stage contributed approximately 71% of total emissions, with a mean GWP of 42.98 g CO_2-eq/kWh (range: 0.15–286.02), while the 'construction' stage contributed another 24%, with a mean GWP of 14.43 g CO_2-eq/kWh (range: 0.15–78.85).[8]

For example, specific case studies of low-emission turbines highlight the dominance of the manufacturing phase. The Vestas onshore V136-4.2 MW turbine has a total lifecycle GWP of 5.6 g CO_2-eq/kWh; its manufacturing phase contributes 8.8 g CO_2-eq/kWh, an impact that is significantly offset by end-of-life recycling credits.[13] A similar pattern is seen in the offshore V236-15 MW turbine, which has a total GWP of 7.0 g CO_2-eq/kWh, with manufacturing contributing 7.1 g CO_2-eq/kWh.[14] Consequently, offshore wind manufacturing has a higher GWP due to increased material inputs, particularly for foundations (16% of Acidification Potential, correlated with

GWP) and site cables (11%).[14] As another specific example case, in floating offshore wind farms like Hywind Tampen, manufacturing contributes 26.79% to a total GWP of 36.78 g CO_2-eq/kWh, whereas in fixed offshore farms like Dogger Bank, it contributes 43.84% to a total GWP of 26.15 g CO_2-eq/kWh.[15] Furthermore, component-specific GWP for offshore turbines includes blades (21%), gear and mainshaft (18%), and nacelle (10%).[14] In contrast, onshore wind manufacturing, dominated by towers and cables, has lower GWP due to simpler foundations and less cabling.[13] Notably, larger turbines with advanced direct drive generator technology, such as 3.2 MW onshore and 6.0 MW offshore models, perform better than smaller geared ones in terms of GWP.[9]

This highlights a key distinction: the direct operations at the manufacturing company itself (e.g., factory energy use) contribute less than 1% to total life-cycle impacts. The vast majority of the manufacturing footprint is attributed to the embodied energy in the raw materials, or 'upstream material production'.[9] Transport contributes minimally (0.05–2.52%), indicating that material production primarily drives GWP differences.[10]

Operational Phase:

According to the meta-analysis by Nugent *et al*. discussed in Section 3.3, the operational phase (covering operation, maintenance, and servicing) contributes approximately 24% of the total GWP.[8] The mean GWP for this phase was reported as 14.36 g CO_2-eq/kWh, with a range of 0.02 to 83.6 g CO_2-eq/kWh. However, this value is derived from a smaller subset of studies than the overall lifecycle average. This research limitation explains why the percentage is not a direct calculation of the two means.[8] For the Vestas onshore turbine, this phase is minor compared to manufacturing, thus contributing marginally to the total GWP of 5.6 g CO_2-eq/kWh, primarily through servicing and replacement parts.[13] However, offshore wind operations are more GWP-intensive, contributing 1.19 g CO_2-eq/kWh to the Vestas offshore turbine's GWP. This is driven by the significant fuel consumption of support vessels, such as Service Operation Vessels (SOVs) using 170 liters per hour (l/h) and tugboats using 596 l/h.[10,14] To put that into context, a single tugboat at full operation consumes the equivalent of about 12 full car fuel tanks (50L) every hour. Additionally, this phase's contribution to environmental impacts for offshore turbines varies widely, ranging from less than 1% to 41%, depending on the impact category.[14] Moreover, for floating offshore wind (Hywind Tampen), fuel for Operations and Maintenance (O&M) vessels (specialized ships that service and repair offshore wind farms) contributes 5.98 g CO_2-eq/kWh and spare parts 5.22 g CO_2-eq/kWh, while for fixed offshore wind (Dogger Bank), these values are 3.82 g CO_2-eq/kWh and 5.06 g CO_2-eq/kWh, respectively.[15] Consequently, the enhanced offshore GWP results from extended vessel travel distances and failure rates (e.g., mooring chains at 0.148 failures/year).[15] Additionally, turbine lifespan significantly affects GWP, with longer lifespans (30 years offshore vs. 20 onshore) reducing per-kWh GWP.[13,14] Furthermore, this phase highlights the shared responsibility across multiple stakeholders in the value chain, emphasizing the need for coordinated environmental management across stakeholders.[9]

End-of-Life Management:

The average lifespan of a wind turbine is typically between 20 and 30 years, after which the end-of-life management stage, involving decommissioning, dismantling, recycling, and disposal, begins. This stage often contributes to GWP credits, offsetting 19.4% of lifecycle emissions, with a relative mean credit of -11.64 g CO_2-eq/kWh (range: -59.4 to 0.5 g CO_2-eq/kWh).[8] It is important to clarify that these GWP credits do not represent direct carbon sequestration from the atmosphere. Rather, they are an accounting mechanism in LCA that reflects the avoided emissions that would have resulted from producing virgin raw materials. Recycling components like steel averts the energy and GWP associated with mining iron ore and manufacturing new steel. Consequently, this environmental benefit is then credited back to the turbine's life cycle. Moreover, effective end-of-life treatment can lead to significant savings, reducing climate change impacts by approximately 20–30% through recycling.[9] For instance, for the Vestas onshore turbine, effective recycling is a key factor in its low environmental impact; the total lifecycle GWP for this turbine is 5.6 g CO_2-eq/kWh, a figure achieved in part through high metal recycling rates (e.g., 98% for foundations, 95% for major components).[13] Similarly, the offshore Vestas turbine benefits, with recycling credits lowering the total GWP of 7.0 g CO_2-eq/kWh, assuming 90% recovery for metals like steel and copper, though only 50% for foundations and cables.[14] In floating offshore wind farms, the direct emissions from the decommissioning process itself are minimal (up to 5% of impacts), with GWP impacts of 2.17 g CO_2-eq/kWh, compared to 1.16 g CO_2-eq/kWh for fixed offshore farms.[15] However, a significant challenge in this phase is the disposal of turbine blades. The composite materials from which they are made, typically fiberglass and epoxy resins, are inherently difficult to separate, which makes them economically and technically challenging to recycle with current technologies. As a result, most blades are sent to landfills, representing a growing waste management concern.[16]

Synthesis and Implications:

Wind energy exhibits a low lifecycle GWP, with a performance range for modern turbines between 5.6 and 36.78 g CO_2-eq/kWh, depending on the specific technology and location.[13,14] The distribution of these impacts across the lifecycle, as shown in **Figure 2**, highlights that onshore wind generally outperforms offshore wind due to lower material and operational demands. Specifically, the production and manufacturing stage dominates GWP for both, influenced greatly by steel and concrete, while offshore wind experiences higher impacts from complex foundations and cables.[15] In contrast, operational GWP is minimal onshore but more significant offshore, contributing 1.19 g CO_2-eq/kWh for the offshore V236-15 MW turbine due to SOV fuel consumption, thus suggesting a need for fuel-efficient vessels.[13,14] Furthermore, end-of-life recycling yields substantial GWP credits, particu-

DOI: 10.36838/IJHSR87.190

larly for metals, although blade recycling remains challenging. These findings underscore the importance of optimizing material use, adopting low-carbon manufacturing (e.g., Electric Arc Furnace for steel), and improving recycling technologies to minimize GWP. Ultimately, while offshore wind offers access to superior energy resources, its higher GWP underscores the critical need for innovation in materials, manufacturing, and circular EoL strategies to fully maximise its potential as a cornerstone of a sustainable energy future.

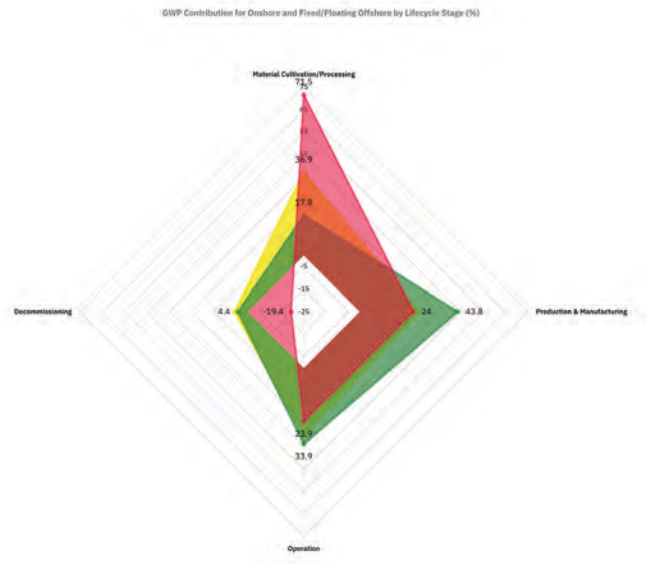

Figure 2: GWP contribution for onshore and fixed/floating offshore wind by life-cycle stage (%). This radar chart follows the same format as Figure 1, comparing the GWP breakdown for onshore (red), fixed offshore (green), and floating offshore (yellow) wind turbines across four life-cycle stages. The comparison reveals that while onshore wind's footprint is concentrated in material processing, fixed and floating offshore systems exhibit more distributed impacts with significantly higher relative burdens from production and operations. This suggests how moving wind energy to marine environments shifts the environmental impact from raw material intensity toward complex infrastructure manufacturing and vessel-based maintenance. Data synthesized from Nugent & Sovacool (2014),[8] Lotfizadeh (2024),[15] and the Vestas LCA reports (Garrett & Mali, 2022; Allekotte & Garrett, 2024).[13,14]

Life-Cycle Analysis of Microalgae Biofuel: Overview and Scope:

Microalgae biofuel production is a biological and chemical process that converts photosynthetic microorganisms into usable fuels. Unlike the discrete hardware of solar and wind, its system is a multi-stage process that is highly dependent on and influenced by the chosen pathway.[17]

It first begins with cultivation, where microalgae are grown in either large, open raceway ponds or in enclosed, controlled photobioreactors (PBRs).[17] During this stage, the algae absorb CO_2 and nutrients to create biomass.[17] Next, this biomass must be harvested (which is an energy-intensive dewatering step), and its valuable compounds, like oils, are extracted, often using solvents.[17] Finally, these compounds are converted into fuel through chemical or biological processes, such as transesterification to create biodiesel or anaerobic digestion to create biogas.[17] The LCA for this technology is therefore a measure of the energy and material inputs for each of these distinct stages.

This section examines the lifecycle of microalgae biofuel, a renewable energy source derived from photosynthetic microorganisms. The analysis covers several key conversion pathways, including transesterification for biodiesel and anaerobic digestion (AD) for biogas. A defining characteristic of microalgae biofuel is the extreme variability of its environmental performance, which is highly dependent on the chosen cultivation and conversion technology. GWP values reported in the literature range from being a significant carbon sink in highly optimized systems (as low as -622.9 g CO_2-eq/kWh) to exceptionally high in energy-intensive, unoptimized scenarios (over 4,700g CO_2-eq/kWh).[17,18] This highlights the importance of system design in determining the technology's sustainability.

Key Terminology and Concepts:

To understand the sustainability of these systems, several key concepts must be defined. Eutrophication refers to nutrient overload that causes water pollution, while acidification contributes to the formation of acid rain. Transesterification is a key chemical reaction in biodiesel production, while common conversion technologies include Anaerobic Digestion (AD), which produces biogas, and Hydrothermal Liquefaction (HTL), which creates bio-oil. Key performance metrics include the Net Energy Ratio (NER), which measures energy output relative to input; the High Heating Value (HHV), which quantifies a fuel's energy density; and the C:N:P Ratio, which is crucial for optimizing microalgae growth. Finally, some studies aggregate various environmental impacts into a single score using the unit mPt (millipoints), where one point (1000 mPt) represents one-thousandth of the annual environmental load of an average European inhabitant.

Material Cultivation and Processing:

Microalgae cultivation occurs in open raceway ponds or closed photobioreactors (PBRs). Open ponds are cost-effective and scalable but prone to contamination and require significant land area, though they can be scaled efficiently once land availability is met. PBRs use transparent tubes or panels, often illuminated by sunlight with mirrors or LED lamps to enhance photosynthesis, at the cost of higher energy inputs (5–10 kWh/m^3 for lighting and circulation).[17] During cultivation, microalgae absorb CO_2 and assimilate nutrients like nitrogen and phosphorus. A 200-m^3 raceway pond sequesters 358,358 kg CO_2 annually but requires 200.2 kg of swine manure nutrients, which emit 0.5 kg CO_2-eq per kg of manure nutrients during production, yielding a net sequestration of 357,858 kg CO_2 annually.[19]

The conversion of microalgal biomass into energy-dense precursors is an energy-intensive process. For biodiesel production, triacylglycerols (TAGs) are the key intermediate. One study found that producing 1 kg of TAGs from biomass with a 50% TAG content requires 16.18 kWh of energy.[19] For biobutanol production, glucose is the precursor, and producing 1 kg of glucose from biomass with a 50% glucose content requires a much lower 1.22 kWh of energy.[19] To provide context, two large-scale, open-pond cultivation scenarios are examined. A conventional industrial model requires a power demand of

10,808 kW to produce 151,875 kg/hr of biomass.[18] In contrast, an optimized model from the National Renewable Energy Laboratory (NREL) requires a higher power input of 29,057 kW.[18] To contextualize these numbers, the conventional model's power demand is enough to continuously run over 9,000 average U.S. homes, while the optimized NREL model requires enough power for over 24,000 homes. This additional energy supports more complex, integrated processes, such as nutrient recycling and biogas production from waste, which ultimately leads to greater overall system efficiency and a lower net environmental impact. In this NREL model, the cultivation stage contributes approximately 50% of the total lifecycle GWP (108 g CO_2-eq/kWh out of a total 216 g CO_2-eq/kWh), even when using renewable energy.[17]

Production and Manufacturing:

The production phase converts biomass into biofuels via transesterification (biodiesel), fermentation (biobutanol), or pyrolysis. For biodiesel, a process using 10,000 kg/hr TAG, 2,171 kg/hr methanol, and 100 kg/hr sodium hydroxide produces 10,030 kg/hr biodiesel and 1,517 kg/hr glycerol, using a 113,489-kg reactor.[19] Hexane-based extraction requires 14,561.7 kW, processing 2,885,625 kg/hr feedstock (1,442,813 kg/hr recycled), yielding 28,580 kg/hr raw oil, with the lipid upgrading phase needing 1,058 kW to produce 28,713 kg/hr biodiesel.[18] This extraction accounts for 94% of emissions (4,467 g CO_2-eq/kWh) due to hexane use.[18] An optimized system achieves lower emissions by using renewable energy.[18] Lipid extraction (the process of separating the valuable oils (lipids) from the rest of the algal cell matter), in particular, is highly energy-intensive, with some studies reporting that this step alone can consume up to 85% of the total energy required for the entire biofuel production process.[20] Emerging techniques, like wet extraction and supercritical CO_2 extraction, reduce impacts.[20]

For biobutanol, one study describes a simulated process in which 503,377 kg/hr of glucose is fermented in an acetone-butanol-ethanol (ABE) system, producing 51,497 kg/hr of biobutanol with a significant cooling duty of 335 MW.[19] Biomass productivity and energy sources significantly affect emissions; for example, switching the source of electricity from hard coal to hydropower can reduce the GWP of electricity generation by over 99%.[3]

The energy efficiency of different conversion pathways varies significantly. The NER is a key metric, and for the pathways analyzed, NER values are reported as 1.524 for transesterification, 1.248 for HTL, and 2.463 for pyrolysis.[17] An NER greater than 1 indicates a net energy loss, making pyrolysis particularly energy-intensive. This is demonstrated in a lab-scale study of *Desmodesmus* sp. EJ 8-10, where the harvest stage alone consumed 56.24% of the total lifecycle energy, resulting in a high calculated GWP of approximately 498.8 g CO_2-eq/kWh for the entire process.[21] In contrast, anaerobic digestion (AD) can be remarkably energy-positive. For a conceptual 100-hectare facility producing biogas from *Chlorella vulgaris*, the total daily electrical input is 16,000 kWh.[22] The gross energy generated from the produced biogas is approximately 65,300 kWh per day. After accounting for the system's internal energy needs for heat (17,000 kWh/day) and electricity (2,694 kWh/day), the facility still demonstrates a strongly positive energy balance. Hence, this shows that a well-designed AD system can generate far more energy than it consumes in its daily operation.[22]

Operational Phase:

The operational phase involves combustion, releasing emissions over the lifecycle. A cradle-to-gate boundary was used in some studies, while others adopt a well-to-wheel scope.[18,19] Lifecycle emissions for unoptimized systems can be extremely high; for example, one conventional pathway reports a net GWP of 4,752 g CO_2-eq/kWh, a value that remains high even after accounting for the CO_2 uptake during cultivation due to massive process emissions from solvent use.[18] This value can be dramatically reduced through system optimization and the use of co-product credits. Co-product credits are an LCA accounting method that subtracts the emissions that would have been generated by conventionally producing the co-products. For example, in an optimized system, credits from valorizing co-products like ethanol and biogas can lower the final net GWP to 159 g CO_2-eq/kWh.[18] While process improvements over time are evident, the specific GWP values depend heavily on the system design and assumptions used.

In a system producing biogas via anaerobic digestion, the combustion of algal methane is a dominant source of emissions, contributing approximately 338.4 g CO_2-eq/kWh.[22] This large emission is then significantly counterbalanced by the CO_2 sequestered during the algae's growth phase, which greatly reduces the final net GWP of the entire system. Other emissions include photochemical oxidation (32.9% of total impact per MJ) and minor contributions to eutrophication (22.8%) and acidification (11.5%), reflecting exhaust byproducts like NOx and SOx.[22] When compared on a life-cycle basis to petroleum diesel, the high electricity demand for the algal methane process can increase its GWP. This impact can be partially mitigated in systems that recycle CO_2 from biogas upgrading back into the cultivation ponds, where the microalgae can capture up to 90% of the injected CO_2.[22]

Net-negative GWP values are possible in highly optimized systems where the CO_2 sequestered during cultivation, combined with credits from the valorization of co-products, exceeds the total lifecycle emissions. For example, one study reports GWP values as approximately -37.3 g CO_2-eq/kWh for transesterification, -24.4 g CO_2-eq/kWh for HTL, -622.9 g CO_2-eq/kWh for AD without pretreatment, and -219 g CO_2-eq/kWh for AD with pretreatment.17 Another study reports GWP values of -48.09 g CO_2-eq/kWh for AD without pretreatment and -16.91 g CO_2-eq/kWh for AD with pretreatment.[17] On the other hand, pyrolysis has a high positive GWP of approximately 954.9 g CO_2-eq/kWh, as it lacks significant co-product credits.[17] The potential for net-negative emissions in other pathways is driven by CO_2 fixation during cultivation, which can be as high as -125.68 g CO_2-eq/kWh for AD without pretreatment.[17] In contrast, a lab-scale total GWP of approximately 498.8 g CO_2-eq/kWh for *Desmodesmus* sp. EJ 8-10 highlights the impact of unoptimized, energy-intensive

DOI: 10.36838/IJHSR87.190

processes.[21] Other impacts from this process include acidification (0.86 g SO_2-eq/kWh), eutrophication (0.065 g PO_4-eq/kWh), and photochemical ozone synthesis (0.047 g C_2H_4-eq/kWh).[21]

End-of-Life Management:

End-of-Life (EoL) management for microalgae biofuel differs from that of durable energy systems. Because the fuel's end-of-life is its combustion (accounted for in the operational phase), the EoL stage for biofuel production focuses on valorizing process residues to improve overall sustainability and create a more circular system. This strategy can significantly offset the initial environmental impacts of production. For example, co-products such as glycerol (1,517 kg/hr) and residual biomass can be used to produce biogas via AD, providing both electricity and digestate as fertilizer.[19,23] Stillage recycling reduces emissions, while discarding 1,933,968 MJ/hr of residue increases impacts.[17]

AD systems benefit from nutrient recycling (70% of total consumption) via the residual liquid phase, reducing fertilizer needs, while transesterification, HTL, and pyrolysis lack this due to toxic by-products (e.g., nitrogen heterocycles, fatty acids, nickel).[17] Anaerobic digestion of Chlorella vulgaris produces 9,385 m^3/day of biogas (70% CH_4) from a 100-ha facility, with 30% (2,816 m^3/day) burned to heat digesters (17,000 kWh/day) and 70% (6,570 m^3/day) upgraded to 5,061.5 m^3/day of 96% CH_4 fuel.[22] The gross energy generated from the produced biogas is approximately 65,300 kWh per day, which, after accounting for the system's internal energy needs for heat and electricity, demonstrates a strongly positive energy balance.[22] Nutrient recycling is significant: 90% of nitrogen (N), phosphorus (P), and potassium (K) in digestates is mineralized, reducing fertilizer needs by an equivalent amount (e.g., 61 gN, 8.1 gP, 6.59 gK per kg dry algae).[22] However, solid digestates used as soil conditioners may contribute to eutrophication if not managed properly.[22]

Synthesis and Implications:

The GWP of microalgae biofuel is not a single value but rather a wide spectrum, highly contingent on the chosen conversion pathway. As visualized in Figure 3, the environmental footprint differs dramatically between conventional and optimized systems. For optimized systems, particularly those using AD with co-product and nutrient recycling, the GWP can be net-negative, with values reported as low as -622.9 g CO_2-eq/kWh.[17] At the other extreme, energy-intensive processes like the lab-scale pyrolysis of Desmodesmus sp. EJ 8-10 can result in high emissions, calculated at approximately 498.8 g CO_2-eq/kWh.[21] This vast range indicates that while the most optimized microalgae systems can outperform wind (34.1 g CO_2-eq/kWh) and solar PV (49.9 g CO_2-eq/kWh), unoptimized pathways are far less sustainable than established renewables.[8] They can also perform worse than many first-generation biofuels; for context, the average GWP for corn starch ethanol is 277.2 g CO_2-eq/kWh and for soybean biodiesel is 156.6 g CO_2-eq/kWh.4 While these first-generation fuels also have wide performance ranges, the high-end emissions from some microalgae pathways far exceed them.

The benefits of integrated systems are also clear when compared to fossil-based production. One study found that a microalgae-to-butanol chain had an overall environmental impact score (162 mPt) that was 62.7% lower than a conventional crude-oil-to-butanol process (466 mPt).[19] Furthermore, valorizing co-products through processes like anaerobic digestion can provide significant energy credits, further lowering the net GWP.

Scalability remains an obstacle due to high energy inputs, a key reason microalgae biofuel has not been widely adopted.[22] Despite environmental benefits like CO_2 sequestration, microalgae biofuel struggles to compete with other renewables or fossil fuels. Its practical use is limited by the lack of reasonably scalable cultivation methods. These methods currently involve high costs, significant land use, and large energy demands.[22] Crucially, the sustainability of these energy-intensive processes is almost entirely dependent on the source of electricity. As highlighted earlier, switching from a fossil-fuel-based grid to a clean source like hydropower can reduce the GWP of the required electricity by over 99%.[3] Therefore, integrating renewable energy is not just an improvement, but a fundamental requirement for making microalgae biofuel a viable, low-carbon alternative.

Integrating renewable energy and carbon capture and storage (CCS) can further reduce GWP. CCS captures 60–80% of CO_2 emissions during cultivation and processing, such as those from electricity generation or combustion of by-products in pyrolysis and AD systems.[22] For microalgae, CCS can be applied at the cultivation stage by capturing CO_2 from nearby industrial sources (e.g., power plants) and supplying it to raceway ponds, enhancing growth while reducing net emissions.[22] During processing, CCS can capture emissions from energy-intensive steps like drying or HTL, where fossil energy is often used, potentially lowering GWP by an additional 50–100 g CO_2-eq/kWh in optimized systems.[18,22] This integration is highly compatible with microalgae's natural CO_2 sequestration ability, thereby providing a potential co-benefit for the technology's overall sustainability. Research must prioritize energy-efficient extraction, scalable cultivation, and co-product valorization to overcome these hurdles.

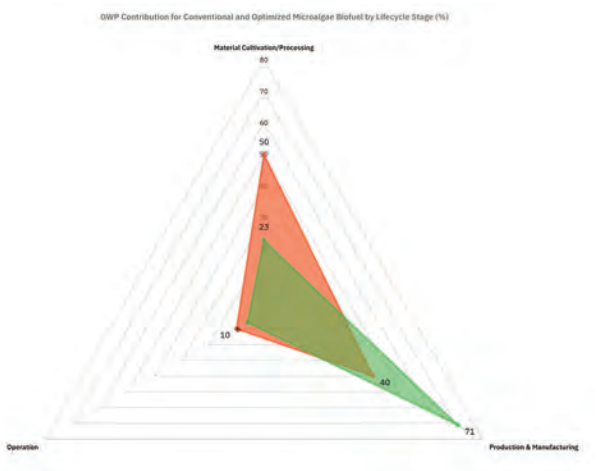

Figure 3: GWP contribution for conventional and optimized microalgae biofuel by life-cycle stage (%). This triangular plot compares the GWP breakdown for a conventional (green) and an optimized (orange) microalgae system. A decommissioning phase is not applicable as the fuel's end-of-life is its combustion, which is included in the operational phase. The comparison indicates that while conventional methods are burdened by energy-intensive production and manufacturing, optimized systems utilize biological sequestration and nutrient recycling to transition the technology into a potential net carbon sink. This emphasizes how the environmental viability of microalgae biofuel is fundamentally determined by system design and the level of integration with circular economy principles. Data synthesized from Dutta *et al*. (2016),18 and Sun *et al*. (2019).[17]

Comparison and Summary:

The life-cycle analysis of solar photovoltaic (PV) systems, wind energy, and microalgae biofuel reveals that no single technology is universally superior. Instead, their environmental performance is highly dependent on technological choices, geographical context, and operational scale. While modern onshore wind turbines often serve as a benchmark for low greenhouse gas (GHG) emissions, studying them closer reveals significant variations across all technologies depending on specific conditions and system designs. These factors are summarized in **Table 1**, which compares the lifecycle GWP and EPBT for key renewable technologies.

Table 1: Comparative life-cycle GHG Emissions of renewable energy technologies.

Technology	Specific Type / Scenario	Total Lifecycle GWP (g CO_2-eq/kWh)	EPBT (years)
Solar PV	Crystalline Silicon (1st Gen)	**~49.9**	**2.2 – 6.0**
	Cadmium Telluride (CdTe) Thin-Film (2nd Gen)	**19 – 30**	**0.8 – 3.6**
	Quantum Dot (QD) PV & other 3rd Gen	**2.89 – 150**	**0.24 – 1.2**
Wind Energy	Onshore (Modern Turbine, e.g., Vestas V136)	**5.6 – 36.78**	**< 1**
	Offshore (Fixed Foundation, e.g., Vestas V236)	**7.0 – 26.15**	**< 1**
	Offshore (Floating Foundation, e.g., Hywind)	**~36.78**	**< 1**
Microalgae Biofuel	Anaerobic Digestion (Optimized)	**-48 – -623**	**N/A**
	Transesterification (Optimized)	**~ -37**	**N/A**
	Pyrolysis (Unoptimized)	**~955**	**N/A**
	Conventional/Unoptimized Pathways	**>4,000**	**N/A**

Note: Negative GWP values for microalgae reflect systems where CO_2 uptake and avoided emissions from co-products exceed total process emissions. Single GWP values (e.g. ~49.9) typically represent a mean from a meta-analysis or a result from a specific case study, whereas ranges capture the variability across multiple studies. The EPBT for wind energy is consistently under one year across most studies; EPBT is not applicable (N/A) for microalgae biofuel, as the metric is used for direct energy-generating systems, not liquid fuel production. This table highlights that modern onshore wind turbines currently offer the most consistent and lowest lifecycle emissions among the evaluated technologies. Conversely, microalgae biofuel presents the widest performance range, which demonstrates that its environmental viability ranges from a net carbon sink to a high emitter depending on system design and technological maturity. Data for Crystalline Silicon PV sourced from Nugent & Sovacool (2014).[8] Data for CdTe PV sourced from Peng *et al*. (2013).[5] Information for 3rd Gen PV comes from Muteri *et al*. (2020).[6] Data for Wind Energy sourced from Garrett & Mali (2022),[13] Allekotte & Garrett (2024),[14] Lotfizadeh (2024),15 and Bonou *et al*. (2016).[9] Data for Microalgae Biofuel sourced from Sun *et al*. (2019),[17] and Dutta *et al*. (2016).[18]

In particular, onshore wind energy emerges as a leading technology due to its low material intensity and high recyclability, resulting in a rapid EPBT of less than a year. However, its performance is geographically constrained and faces challenges related to land use and social acceptance. Offshore wind, while accessing stronger and more consistent wind resources, carries a higher environmental footprint due to the increased material requirements for foundations and more complex maintenance logistics.

Solar PV technology, particularly crystalline silicon, is hindered by the energy-intensive nature of silicon purification. Its competitiveness is therefore strongly tied to the carbon intensity of the manufacturing grid. Thin-film technologies like CdTe and emerging options like Quantum Dot PV offer lower-emission alternatives but face their own challenges regarding material toxicity and commercial scalability.

Microalgae biofuel presents the most extreme performance variability. In optimized, integrated systems that valorize co-products and recycle nutrients, it can act as a net carbon sink. However, conventional, energy-intensive cultivation and harvesting methods render it far less sustainable than wind or solar. Its scalability is also severely constrained by high water and nutrient demands, making it a high-risk, high-reward technology. This profile makes it best suited for niche applications, particularly as a "drop-in" fuel for sectors like aviation and long-haul freight, which are difficult to electrify with current battery technology.[24] In these areas, biofuels represent one of the only viable pathways to decarbonization in the near future.[24]

Ultimately, the most sustainable renewable energy source depends on context, not on a universal ranking. This review's central finding is that the optimal choice is determined by a combination of regional climate, technological maturity, and logistical factors. For instance, climatic conditions make so-

DOI: 10.36838/IJHSR87.190

lar PV the logical choice for arid, high-insolation regions like the Sahara. In contrast, the consistently strong winds of the North Sea make it the ideal location for offshore wind development, which is why countries in that region are heavily investing there. Logistical factors are also crucial, because the life-cycle sustainability of solar PV is maximised when panels are manufactured using a low-carbon electricity grid. This is demonstrated by manufacturing in regions that utilize hydropower, such as in Scandinavia, or geothermal energy, as seen in Iceland.[25,26] Similarly, microalgae biofuel becomes most viable when co-located with industrial facilities that can provide a steady supply of waste CO_2 and nutrients, transforming a logistical challenge into a mutually beneficial situation. In contrast, the lower maturity of microalgae biofuel means it is better suited for regions with strong R&D infrastructure. The optimized NREL model in the United States is a good example, as its viability relies on advanced R&D and a policy focus on developing circular bio-economics.[18] This all supports the thesis that where a technology is deployed and manufactured is as important and worth taking into consideration as the technology itself.

Conclusion

This comparative LCA demonstrates that onshore wind energy currently offers the lowest and most consistent greenhouse gas emissions. However, the analysis also shows that no single renewable technology provides a universally optimal solution for decarbonization. The sustainability of solar PV, wind, and microalgae biofuel is determined by regional context, technological maturity, and the integration of circular economy principles. These findings support the argument that the path to a sustainable energy future requires an approach customized to specific geographic and industrial conditions, rather than reliance on a single technology.

To accelerate this transition, a coordinated effort is indispensable. Policymakers should implement region-specific incentives that favor technologies aligned with local resources, such as prioritizing solar PV in high-insolation areas and supporting wind projects where winds are consistent. Furthermore, policies must mandate and support the development of robust recycling infrastructure for PV panels and turbine components to minimize end-of-life impacts. In parallel, industry must invest in decarbonizing manufacturing supply chains, particularly for solar PV. Industry must also advance the commercial-scale deployment of next-generation technologies. For microalgae, this means focusing on integrated systems that utilize industrial waste streams and employ energy-efficient processes like anaerobic digestion. Finally, researchers have a critical role in closing remaining data gaps in LCAs, including the long-term performance of offshore wind farms, the real-world efficiency of advanced PV recycling, and the scalability of optimized microalgae systems. By aligning policy, investment, and research, the environmental performance of all three technologies can be significantly enhanced, paving the way for a resilient and sustainable global energy system.

Acknowledgments

I would like to express my sincere gratitude to my mentor, Dr. Chima McGruder, for his invaluable guidance, support, and feedback throughout the research and writing process. This project would not have been possible without his mentorship.

I attest that the ideas, graphics, and writing in this paper are entirely my own.

References

1. International Organization for Standardization. *Environmental Management -- Life Cycle Assessment -- Principles and Framework*, 2nd ed.; BSI Standards Limited: London, 2006.
2. Badza, K.; Soro, Y. M.; Sawadogo, M. Life Cycle Assessment of a 33.7 MW Solar Photovoltaic Power Plant in the Context of a Developing Country. *Sustain. Environ. Res.* **2023**, *33* (1), 38. https://doi.org/10.1186/s42834-023-00201-x.
3. Togarcheti, S. C.; Mediboyina, M. Kumar; Chauhan, V. S.; Mukherji, S.; Ravi, S.; Mudliar, S. N. Life Cycle Assessment of Microalgae-Based Biodiesel Production to Evaluate the Impact of Biomass Productivity and Energy Source. *Resour. Conserv. Recycl.* **2017**, *122*, 286–294. https://doi.org/10.1016/j.resconrec.2017.01.008.
4. U.S. Environmental Protection Agency. *Draft Regulatory Impact Analysis: RFS Standards for 2023-2025 and Other Changes*; EPA-420-D-22-003; Washington, DC, 2022; p 520. https://www.epa.gov/system/files/documents/2022-12/420d22003.pdf.
5. Peng, J.; Lu, L.; Yang, H. Review on Life Cycle Assessment of Energy Payback and Greenhouse Gas Emission of Solar Photovoltaic Systems. *Renew. Sustain. Energy Rev.* **2013**, *19*, 255–274. https://doi.org/10.1016/j.rser.2012.11.035.
6. Muteri, V.; Cellura, M.; Curto, D.; Franzitta, V.; Longo, S.; Mistretta, M.; Parisi, M. L. Review on Life Cycle Assessment of Solar Photovoltaic Panels. *Energies* **2020**, *13* (1), 252. https://doi.org/10.3390/en13010252.
7. Salibi, M.; Schönberger, F.; Makolli, Q.; Bousi, E.; Almajali, S.; Friedrich, L. Energy Payback Time of Photovoltaic Electricity Generated by Passivated Emitter and Rear Cell (PERC) Solar Modules: A Novel Methodology Proposal. *38th Eur. Photovolt. Sol. Energy Conf. Exhib. 677-682* **2021**, 6 pages, 3761 kb. https://doi.org/10.4229/EUPVSEC20212021-4CO.4.5.
8. Nugent, D.; Sovacool, B. K. Assessing the Lifecycle Greenhouse Gas Emissions from Solar PV and Wind Energy: A Critical Meta-Survey. *Energy Policy* **2014**, *65*, 229–244. https://doi.org/10.1016/j.enpol.2013.10.048.
9. Bonou, A.; Laurent, A.; Olsen, S. I. Life Cycle Assessment of Onshore and Offshore Wind Energy-from Theory to Application. *Appl. Energy* **2016**, *180*, 327–337. https://doi.org/10.1016/j.apenergy.2016.07.058.
10. Yuan, W.; Feng, J.-C.; Zhang, S.; Sun, L.; Cai, Y.; Yang, Z.; Sheng, S. Floating Wind Power in Deep-Sea Area: Life Cycle Assessment of Environmental Impacts. *Adv. Appl. Energy* **2023**, *9*, 100122. https://doi.org/10.1016/j.adapen.2023.100122.
11. Atilgan Turkmen, B.; Germirli Babuna, F. Life Cycle Environmental Impacts of Wind Turbines: A Path to Sustainability with Challenges. *Sustainability* **2024**, *16* (13), 5365. https://doi.org/10.3390/su16135365.
12. Brussa, G.; Grosso, M.; Rigamonti, L. Life Cycle Assessment of a Floating Offshore Wind Farm in Italy. *Sustain. Prod. Consum.* **2023**, *39*, 134–144. https://doi.org/10.1016/j.spc.2023.05.006.
13. Garrett, P.; Mali, S. Life Cycle Assessment of Electricity Production from an Onshore V136-4.2 MW Wind Plant. **2022**, 133.

14. Allekotte, L.; Garrett, P. Life Cycle Assessment of Electricity Production from an Offshore V236-15 MW Wind Plant. **2024**, 121.
15. Lotfizadeh, O. Life Cycle Assessment of Offshore Wind Farms -A Comparative Study of Floating Vs. Fixed Offshore Wind Turbines. **2024**, 142. https://doi.org/10.13140/RG.2.2.12557.14560.
16. Alavi, Z.; Khalilpour, K.; Florin, N.; Hadigheh, A.; Hoadley, A. End-of-Life Wind Turbine Blade Management across Energy Transition: A Life Cycle Analysis. *Resour. Conserv. Recycl.* **2025**, *213*, 108008. https://doi.org/10.1016/j.resconrec.2024.108008.
17. Sun, C.-H.; Fu, Q.; Liao, Q.; Xia, A.; Huang, Y.; Zhu, X.; Reungsang, A.; Chang, H.-X. Life-Cycle Assessment of Biofuel Production from Microalgae via Various Bioenergy Conversion Systems. Energy 2019, 171, 1033–1045. https://doi.org/10.1016/j.energy.2019.01.074.
18. Dutta, S.; Neto, F.; Coelho, M. C. Microalgae Biofuels: A Comparative Study on Techno-Economic Analysis & Life-Cycle Assessment. *Algal Res*. **2016**, *20*, 44–52. https://doi.org/10.1016/j.algal.2016.09.018.
19. Wu, W.; Lei, Y.-C.; Chang, J.-S. Life Cycle Assessment of Upgraded Microalgae-to-Biofuel Chains. *Bioresour. Technol.* **2019**, *288*, 121492. https://doi.org/10.1016/j.biortech.2019.121492.
20. Khoo, H. H.; Sharratt, P. N.; Das, P.; Balasubramanian, R. K.; Naraharisetti, P. K.; Shaik, S. Life Cycle Energy and CO2 Analysis of Microalgae-to-Biodiesel: Preliminary Results and Comparisons. *Bioresour. Technol*. **2011**, *102* (10), 5800–5807. https://doi.org/10.1016/j.biortech.2011.02.055.
21. Li, G.; Lu, Z.; Zhang, J.; Li, H.; Zhou, Y.; Mohammed Ibrahim Zayan, A.; Huang, Z.; 1. School of Material Science and Mechanical Engineering, Beijing Technology and Business University, Beijing 100048, China; 2. Bioenergy and Environment Science & Technology Laboratory, College of Engineering, China Agricultural University, Beijing 100083, China; 3. Key Laboratory of Clean Production and Utilization of Renewable Energy, Ministry of Agriculture and Rural Affairs, Beijing 100083, China; 4. National Center for International Research of BioEnergy Science and Technology, Ministry of Science and Technology, Beijing 100083, China; 5. Department of Agricultural Engineering, Faculty of Agriculture, Omdurman Islamic University, Omdurman Province, Khartoum State, Sudan. Life Cycle Assessment of Biofuel Production from Microalgae Cultivated in Anaerobic Digested Wastewater. *Int. J. Agric. Biol. Eng*. **2020**, *13* (1), 241–246. https://doi.org/10.25165/j.ijabe.20201301.4178.
22. Collet, P.; Hélias, A.; Lardon, L.; Ras, M.; Goy, R.-A.; Steyer, J.-P. Life-Cycle Assessment of Microalgae Culture Coupled to Biogas Production. *Bioresour. Technol.* **2011**, *102* (1), 207–214. https://doi.org/10.1016/j.biortech.2010.06.154.
23. Saranya, G.; Ramachandra, T. V. Life Cycle Assessment of Biodiesel from Estuarine Microalgae. *Energy Convers. Manag. X* **2020**, *8*, 100065. https://doi.org/10.1016/j.ecmx.2020.100065.
24. Martinez-Villarreal, S.; Breitenstein, A.; Nimmegeers, P.; Perez Saura, P.; Hai, B.; Asomaning, J.; Eslami, A. A.; Billen, P.; Van Passel, S.; Bressler, D. C.; Debecker, D. P.; Remacle, C.; Richel, A. Drop-in Biofuels Production from Microalgae to Hydrocarbons: Microalgal Cultivation and Harvesting, Conversion Pathways, Economics and Prospects for Aviation. *Biomass Bioenergy* **2022**, *165*, 106555. https://doi.org/10.1016/j.biombioe.2022.106555.
25. International Energy Agency. *Special Report on Solar PV Global Supply Chains*; OECD, 2022. https://doi.org/10.1787/9e8b0121-en.
26. Spittler, N.; Davidsdottir, B.; Shafiei, E.; Leaver, J.; Asgeirsson, E. I.; Stefansson, H. The Role of Geothermal Resources in Sustainable Power System Planning in Iceland. *Renew. Energy* **2020**, *153*, 1081–1090. https://doi.org/10.1016/j.renene.2020.02.046.

Author

Jun Kang is a Junior at Hiroo Gakuen Senior High School in Tokyo, Japan, with a strong interest in environmental science, sustainability, and renewable energy. He plans to pursue higher education in environmental engineering to contribute to solving the global climate crisis.

DOI: 10.36838/IJHSR87.190

IJHSR
ijhighschoolresearch.org
REVIEW ARTICLE

CCR5 and Its Mutation in HIV Infection, and the Therapeutic Approach with CRISPR-Cas9

Nana Shibuya

The British School of Tashkent, Kalandar Dr 3, Tashkent, 100170, Uzbekistan; shibuyanana11@gmail.com

ABSTRACT: HIV/AIDS is a major global public health issue. While antiretroviral therapy (ART) is effective for suppressing the viral load, the presence of HIV latent reservoirs causes unavoidable viral rebound and relapse of disease after discontinuation of ART. This paper aims to visualize and analyze the transmembrane structure of the C-C Motif Chemokine Receptor 5 (CCR5), an essential HIV-1 coreceptor, and its mutant protein, CCR5 Δ32, to investigate how structural alterations may influence its function as a coreceptor and provide natural resistance against HIV infection. Additionally, this paper compares the level of conservation of CCR5 amino acid sequences across organisms to understand the significance of the Δ32 mutation. Finally, the paper simulates a CRISPR-Cas9 gene editing process *in silico* and further proposes its hypothetical application to mimic the CCR5 Δ32-like mutation in a patient's hematopoietic stem and progenitor cells (HSPCs), as a potential long-term treatment option to reduce susceptibility to HIV and prevent relapse after discontinuation of treatment. However, despite the potential of CCR5 Δ32 as a treatment for HIV/AIDS, one must also address the challenges faced by the application of gene therapy, regarding safety, ethics, cost, and accessibility.

KEYWORDS: Biomedical Science, Genetics, HIV/AIDS, CCR5, CRISPR-Cas9.

Introduction

Introduction to HIV/AIDS:

Human Immunodeficiency Virus (HIV) is a retrovirus that attacks the immune system, and if left untreated, can lead to Acquired Immunodeficiency Syndrome (AIDS), a condition in which the immune system becomes severely weakened and unable to fight off infections or certain cancers.[1,2] As a retrovirus, HIV primarily infects CD4+ T lymphocytes, or helper T cells, which play a crucial role in immune response.[3] 2 major variants of HIV are: HIV-1 and HIV-2, with HIV-1 being considerably more infectious and responsible for most HIV cases in humans.[4]

HIV is believed to have originated in the 1920s, being passed on from chimpanzees after feeding on them. The first recognized cases of HIV infection were reported in the Democratic Republic of Congo,[5] and since then, the virus has become a global health issue. According to the World Health Organization (WHO), by 2024, HIV will have claimed around 42.3 million lives worldwide, with around 630,000 in 2023 alone. HIV infection consists of 3 different phases: acute infection, chronic asymptomatic infection (clinical latency), and AIDS. During the acute infection phase, flu-like symptoms, such as fever and headache, are often seen. During the chronic asymptomatic phase, individuals may not develop any symptoms of the disease for years;[6] without treatment such as Antiretroviral therapy (ART), the rate of progression to AIDS can vary from a few months to more than 20 years, depending on the individual.[7] A person is said to have AIDS when they are diagnosed with opportunistic infections, or AIDS defining diseases,[6] such as tuberculosis, pneumonia, and oral candidiasis, which often appear with a CD4+ T cell count of less than 200 cells/mm^3.[8] If untreated, the weakened immune system cannot fight off opportunistic infections, leading to death.[9]

Virus Biology:

HIV-1 infection is initiated when the viral surface glycoprotein gp120 binds to the CD4 receptor on the host cell surface, causing a conformational change that exposes the coreceptor binding site.[10,11] gp120 then engages with a coreceptor; C-C Motif Chemokine Receptor 5 (CCR5) is used by R5 tropic HIV, C-X-C Chemokine Receptor Type 4 (CXCR4) is used by X4 tropic HIV, and dual tropic (R5X4) viruses can use either.[12,13] This interaction triggers further conformational change in the gp120 and transmembrane glycoprotein gp41 complex, allowing gp41 to penetrate the cell surface membrane. After fusion of HIV and the host cell, the viral capsid is released into the cytoplasm[10,11] and transported towards the nucleus. Here, reverse transcription of viral RNA to DNA occurs: The enzyme reverse transcriptase produces a single-stranded DNA from the viral RNA template, then synthesizes the complementary strand to form double-stranded DNA.[9] The viral DNA is integrated into the host cell's genome by integrase, allowing synthesis of more viral RNAs to be used as genetic material for new HIV or as mRNA to produce viral proteins.[14]

Coreceptors used by HIV differ throughout the course of infection. R5 tropic HIV, which uses CCR5, is typically seen during early infection,[15] likely due to the high abundance of CCR5+ cells in this stage.[16] In contrast, X4 tropic viruses are rare during initial infection, and appear later in around half of the patients,[15] possibly due to the accumulating damage on the immune system.[16] Surprisingly, studies have shown that the switch from R5 to X4 tropic virus is not influenced by the abundance of coreceptors. Instead, it has been associated with high

© 2026 Terra Science and Education

DOI: 10.36838/IJHSR87.201

viral load and low CD4+ counts early in infection.[15] In later stages, some patients develop dual tropic (R5X4) or X4 tropic viruses, which are often associated with faster progression to AIDS and a severe decline of immune response. However, the presence of X4 viruses alone does not necessarily guarantee rapid disease progression, suggesting it could also be due to other virological factors.[16] Overall, these indicate that CCR5 targeted treatment may be most effective in earlier stages of HIV infection, when R5 tropic viruses are more common.

CCR5:

The C-C Motif Chemokine Receptor 5 (CCR5) gene is found on chromosome 3, at the cytogenetic location 3p21.3120.[17] CCR5 protein is part of the G-protein-coupled receptor (GPCR) family, and has an overall similar structure to other GPCRs: It has 7 transmembrane regions (TMRs), 3 intracellular loops, and 3 extracellular loops.[18] CCR5 is expressed on the surface of CD4+ T lymphocytes, and individuals with chronic HIV have the highest percentage of CCR5+ CD4+ cells.[19] A naturally occurring mutation, CCR5 Δ32, is a result of the deletion of 32 base pairs, beyond nucleotide 522,[20] in the CCR5 gene. This causes a frameshift, leading to the translation of 7 new amino acids and a premature stop codon. Therefore, the mutant CCR5 protein contains 215 amino acids compared to 352 amino acids in a healthy protein. In this paper, a visualization of the transmembrane structure of the CCR5 protein and its mutant, Δ32, will be used to explore how structural alterations in CCR5 influence its function as a coreceptor.

The CCR5 Δ32 allele is most frequently found in Caucasian populations, less frequently in other North American populations, and is mostly absent in African and Asian populations.[21,22] For heterozygous individuals, the reduced production of wild-type (WT) CCR5 delays their progression to AIDS, especially in the earlier years of infection.[23–25] In addition, the mutant protein exerts a transdominant negative (TDN) effect by forming heterodimers with WT CCR5 and CXCR4, reducing their expression on the cell surface and further reducing susceptibility.[23,26] For homozygous individuals, inhibited expression of WT CCR5 on the cell surface, combined with the TDN effect reducing the expression of CXCR4, leads to high resistance to R5-tropic HIV-1 and partial resistance to X4 and R5X4 tropic HIV-1. However, some homozygous individuals do not always express the Δ32 protein, thus lacking the TDN effect against CXCR4,[23] and are still susceptible to infection by dual tropic or X4 tropic HIV-1 through CXCR4.[27]

Latent Reservoirs:

Stable viral reservoirs are established early on in HIV infection within latently infected, resting CD4+ T cells.[28] These latent reservoirs decay very slowly and lie dormant in host cells until triggered.[29,30] After stopping treatment, patients experience viral rebound,[31] due to the virus in latent reservoirs replicating, and replenishing other reservoirs, even after achieving undetectable levels of plasma viremia following ART or Highly Active Antiretroviral Therapy (HAART).[32] This guarantees lifelong persistence of HIV-1, and requires individuals to take medication throughout their lifetime. Therefore, a true cure to HIV will only be achieved after complete eradication of these latent reservoirs.[33]

Treatment & CRISPR-Cas9 Gene Editing:

ART or HAART is the primary treatment for HIV infections, effectively suppressing viral load through combinations of drugs that target different stages of the virus's life cycle, such as entry inhibitors, reverse transcriptase inhibitors, integrase inhibitors, and protease inhibitors.[34] However, the long-term effectiveness of CCR5 antagonists can be limited for some patients due to the natural shift from R5 tropic to X4 tropic HIV-1 throughout the course of infection, which increases the proportion of X4 viruses even under treatment.[35] Targeting CXCR4 presents even more difficulties, since this receptor is involved in many essential body processes such as immune cell and organ development, making CXCR4 blocking agents harder to develop and implement. Nonetheless, some studies suggest that strategies to downregulate CXCR4 expression may be beneficial for HIV positive patients.[2] Given this information, CCR5 remains the most promising target for therapy. Its inhibition does not interfere with essential cellular processes, and the natural resistance against HIV-1 presented by the Δ32 mutation provides substantial evidence that CCR5 disruption can confer resistance to HIV-1. This possibility has been explored using gene editing technology such as Clustered Regularly Interspaced Short Palindromic Repeats and CRISPR-associated Protein 9 (CRISPR-Cas9), to induce a disruption in the CCR5 gene of an infected individual.

CRISPR and CRISPR-associated proteins are originally part of the defense mechanism in bacteria and archaea. The CRISPR locus consists of short, repeat sequences, interspaced by variable sequences (spacers) derived from previously encountered extrachromosomal elements, such as viruses and bacteria.[36–38] This system acts like a genetic memory; In response to reinfection by an invader, CRISPR RNAs (crRNAs) guide the Cas proteins to recognize and cleave complementary sequences in the invader's DNA, interfering with their replication,[38–41] and thus providing sequence-specific immunity.[42] Inspired by this naturally occurring process, the CRISPR-Cas9 system was developed in 2012, which uses a designed, single guide RNA (sgRNA) to direct the Cas9 nuclease to cleave specific target DNA in virtually any organism, providing an efficient and versatile genome editing tool.[43]

Stem Cells:

Stem cells are undifferentiated cells with the ability to reproduce through mitosis and differentiate into various specialized cells. In clinical settings, hematopoietic stem cell transplantation (HSCT) can be carried out using either allogeneic or autologous stem cells, and each has its own advantages and risks. Allogeneic HSCT involves using hematopoietic stem cells from a healthy donor, which can help eliminate infected cells and reduce the risk of relapse. However, it also carries significant risks, including graft vs host disease (GVHD), graft failure, and opportunistic infections. Treatment-related mortality is significantly higher than in autologous transplantation,

and this risk increases with donation from HLA-mismatched or unrelated donors. In contrast, autologous transplantation uses the patient's own hematopoietic stem cells, which means there is no need for HLA-matched donors and eliminates risks associated with GVHD. Furthermore, it allows for faster immune recovery and lower treatment-related mortality, making it more suitable for a wider range of patients. The main risk of this approach is the potential for disease relapse due to contamination of the harvested cells.[44] Given these considerations, autologous transplantation offers a more practical approach for introducing gene-edited hematopoietic stem and progenitor cells (HSPCs). Used in combination with the CRISPR-Cas9 technology to modify the CCR5 gene, this approach may be able to provide an effective long-term solution for HIV-1 infection. This paper explores this approach through *in silico* modelling and a hypothetical experimental design of the proposed strategy.

Previous Cases:

Timothy Brown, known as the 'Berlin patient', was the first person to be considered cured of HIV. He was diagnosed with HIV during his studies at university and initially managed his symptoms with low doses of zidovudine and protease inhibitors. 10 years later, he developed acute myeloid leukemia (AML) and required chemotherapy, followed by an allogeneic stem cell transplant. He received the transplant from an HLA-matched, unrelated donor, homozygous for the CCR5 Δ32 mutation, and stopped ART.[45,46] Typically, viral load in HIV patients rebounds after stopping treatment,[31] however, in Brown's case, active HIV-1 was not found for nearly a year. Unfortunately, his pneumonia and leukemia relapsed, and he received a second transplantation from the same donor in 2008.[46] This second transplant resulted in complete remission of AML and full donor chimerism. Although a small proportion of X4 tropic HIV-1 was detected before the transplant, the virus was not detected in peripheral blood, bone marrow, or rectal mucosa for over 20 months after discontinuation of HAART after the transplant, no longer requiring him to continue ART.[45]

Inspired by this case, Xu *et al.* carried out allogeneic stem transplantation using hematopoietic stem and progenitor cells (HSPCs) with CRISPR-Cas9 induced CCR5 Δ32 mutation into a patient infected with HIV-1 and acute lymphoblastic leukemia (ALL). Cas9 was delivered via non-viral transfection methods to prevent entry of foreign DNA and avoid long-term presence of Cas9 in target cells, reducing the risk of unexpected off-target effects.[47,48] The transplantation and long-term engraftment of CRISPR-edited HSPCs were successful; ALL was in complete remission with full donor chimerism, and donor cells carrying the mutated CCR5 were present for over 19 months. Although no adverse off-target effects related to CCR5 gene editing or CRISPR modification were observed, the low percentage of CCR5 disruption in lymphocytes highlighted the need to improve the gene editing efficiency of the CRISPR-Cas9 system and transplantation methods.[49]

Together, these cases highlight the therapeutic potential of the CCR5 Δ32 mutation to inhibit CCR5 function as an HIV-1 coreceptor through transplantation or gene editing, as a possible treatment option for HIV-1.

■ Aim of This Study

Based on the role of the CCR5 gene and Δ32 mutation in HIV resistance, this paper aims to analyze the structural differences between the CCR5 wild type and mutant protein, compare the level of conservation of CCR5 across organisms, simulate the CRISPR-Cas9 gene editing process via *in silico* designing tools, and propose a hypothetical CRISPR-Cas9-mediated experimental design for a potential autologous stem cell transplant. We hypothesize that mimicking the CCR5 Δ32-like mutation in the hematopoietic stem cells of a patient infected with HIV-1 could help better understand the disease mechanism and reduce susceptibility to the disease. Ultimately, this approach may help prevent relapse after discontinuation of HAART in the future.

■ Methods

2.1: Amino acid sequences of CCR5 protein and CCR5 Δ32 mutant protein were retrieved from the NCBI database:

The amino acid sequences of the human CCR5 protein (GenBank accession number: AAB57793.1) and CCR5 Δ32 mutant protein (GenBank accession number: AAB09551.1) were obtained from the National Center for Biotechnology Information (NCBI) protein database in FASTA format.

NCBI > Gene > FASTA

2.2: Hydrophobicity of amino acids was analyzed via Deep TMHMM for the prediction of transmembrane regions:

The FASTA format amino acid sequences obtained from NCBI were submitted to the Deep TMHMM website to generate a prediction for their transmembrane regions.

NCBI > Gene > FASTA > Deep TMHMM

2.3: Transmembrane structure of CCR5 and CCR5 Δ32 were generated using Protter:

The FASTA format amino acid sequences obtained from NCBI were submitted to the Protter website by entering the corresponding amino acid accession numbers to visualize their transmembrane structure.

NCBI > Gene > FASTA > Protter

2.4: Clustal Omega was used to compare amino acid sequences between organisms:

Human, chicken, mouse, and chimpanzee CCR5 amino acid sequences were obtained from NCBI. Then, it was submitted to the Clustal Omega website under "Protein" sequence type for comparison between organisms.

NCBI > Gene > FASTA > Clustal Omega

2.5: CRISPR/Cas9 gene editing on the CCR5 gene was simulated via SnapGene with guideRNAs designed by CRISPR Finder:

The CCR5 gene sequence was obtained from the NCBI Gene section. Then, on a new SnapGene file, the gene sequence was annotated for exons and introns, with the exonic

DOI: 10.36838/IJHSR87.201

and intronic information gathered from ENSEMBL. A region was picked for CRISPR/Cas9 targeting, and the guideRNA was chosen using CRISPRFinder. To minimize the probabilities of off-target effects, chosen gRNAs were shown to have 0 predicted off-targets with up to 2 nucleotide mismatches. For the Cas9 nuclease, a designed humanized Cas9 (hCas9) should be used for higher efficiency. Primers were generated on SnapGene to simulate PCR for fragment amplification and genotyping, and create a visual representation of hypothetical agarose DNA gel electrophoresis. An experimental design of CRISPR-Cas9-mediated autologous stem cell transplantation was proposed based on the simulated gene editing and chosen gRNAs. Insight into the procedures of autologous stem cell transplantation was gathered from the Leukemia and Lymphoma Society. The illustrations used were downloaded from Servier Medical Art.

NCBI > Gene > ENSEMBL > SnapGene file > CRISPRFinder > SnapGene

Results and Discussion

3.1: CCR5 mutations causes loss in the number of predicted transmembrane domains:

Amino acid sequence of wild type (WT) CCR5 and CCR5 Δ32 obtained from NCBI (Figure 1A, B) shows the difference in length of WT CCR5 (352 amino acids) and CCR5 Δ32 (215 amino acids), due to the 32 base pair deletion causing a frameshift and coding for a premature stop codon.[20] Transmembrane region (TMR) is the region of a protein that is integrated in the cell membrane. TMR prediction with DeepTMHMM shows 7 predicted TMRs for WT CCR5 (Figure 1C, D). In contrast, the mutated protein only shows 4 predicted TMRs (Figure 1E, F), showing that this mutation resulted in a significant change in predicted topology. The Δ32 mutation prevents correct folding of the protein and thus prevents CCR5 from being expressed on the cell surface, inhibiting HIV penetration into the cell and giving immunity against R5 tropic HIV-1.[23]

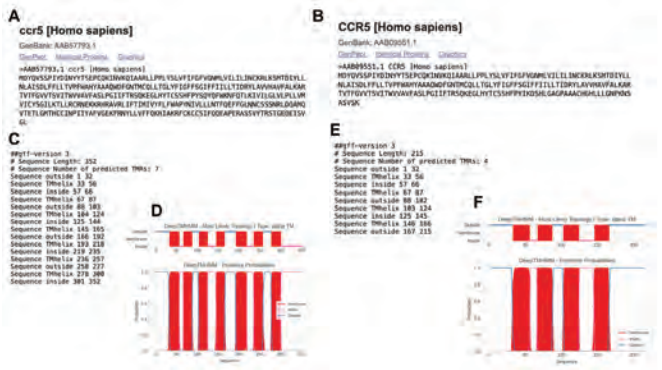

Figure 1 : Transmembrane region prediction of CCR5 and CCR5 Δ32. The Δ32 mutation results in the loss of multiple TMRs and amino acids, indicating significant disruption of CCR5 topology. 1A. CCR5 protein sequence retrieved from NCBI in FASTA format. 1B. CCR5 Δ32 protein sequence retrieved from NCBI in FASTA format. 1C. ~ D. DeepTMHMM prediction of WT CCR5 shows 7 predicted TMRs. 1E. ~ F. DeepTMHMM prediction of CCR5 Δ32 shows 4 predicted TMRs results.

3.2: Structural differences between WT CCR5 and CCR5 Δ32 #2:

The topology diagram of CCR5 (Figure 2A) shows its 7 predicted TMRs, 3 intracellular and 3 extracellular loops. The apparent 4th intracellular loop is not part of its structure, but a result of palmitoylation, which is a form of post-translational modification of proteins, where a palmitic acid molecule is bound to the cysteine side chains via a reversible thioester bond. CCR5 has a cluster of 3 cysteines in the carboxyl-terminal tail, which is palmitoylated. This provides a membrane anchor to the c-terminus domain, creating a fourth intracellular loop.[50] In contrast, the topology diagram of CCR5 Δ32 shows its 4 predicted TMRs, 1 extracellular loop, and 2 intracellular loops. The Δ32 mutation results in a premature stop codon,[24] deleting the cysteine cluster required for palmitoylation. The misfolded protein is not palmitoylated and is not expressed at the cell membrane.[23]

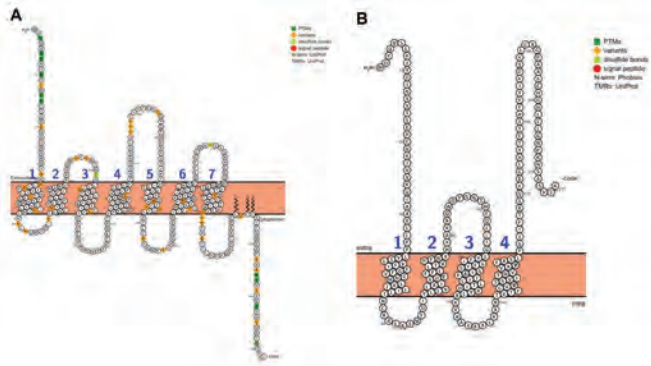

Figure 2: Comparison of predicted 3D structure for CCR5 and CCR5 Δ32. The Δ32 mutation results in an altered 3D topology with reduced TMRs compared to WT CCR5. 2A. Predicted transmembrane structure of CCR5, showing 7 TMRs with 3 intracellular loops and 3 extracellular loops.[18] 2B. Predicted transmembrane structure of CCR5 Δ32, showing 1 extracellular loop and 2 intracellular loops.

3.3: Assessing the level of conservation of CCR5 amino acids across different species:

Comparison of CCR5 protein sequences of chicken, mouse, chimpanzee, and human revealed that CCR5 is a mostly conserved protein among the 4 organisms. In total, there are 210 asterisks, meaning 210 amino acids are fully conserved throughout all 4 organisms, or 59.7%. This suggests that CCR5 structure and function are also generally conserved across these organisms. Proteins that perform essential functions tend to have their amino acid sequences conserved across species by purifying selection, which eliminates harmful mutations.[51] In addition, natural selection strongly resists changes in regions of the amino acid sequence that contribute to several functions at the same time, since any alteration could significantly disrupt structure and function.[52] Therefore, since the amino acids are generally conserved among the 4 organisms, it can be inferred that these evolutionarily conserved regions are crucial for maintaining CCR5 structure and receptor function. Hence, mutations that disrupt these conserved regions, such as the CCR5 Δ32, may significantly affect receptor function, potentially explaining the HIV resistance associated with this mutation.

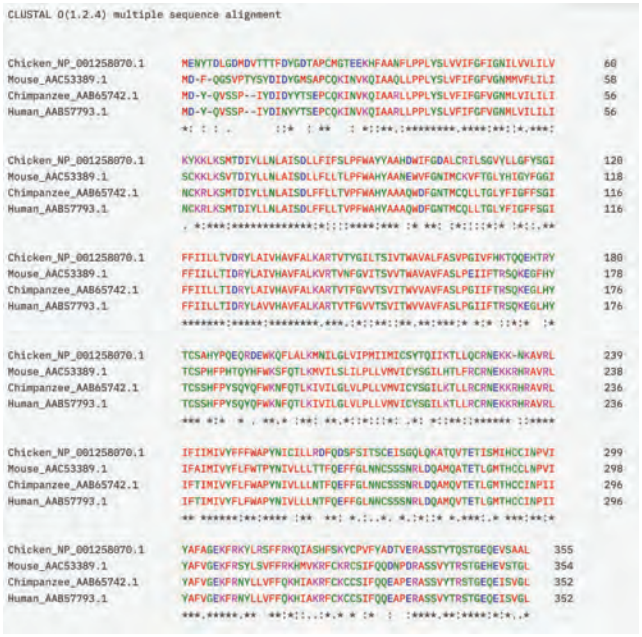

Figure 3: Multiple protein alignment of CCR5. CCR5 amino acid sequences of chicken, mouse, chimpanzee, and human obtained from NCBI are compared using Clustal Omega. Approximately 59.7% of amino acids are fully conserved across species, suggesting strong evolutionary conservation of CCR5 structure and function. Asterisks (*) indicate positions with fully conserved amino acids. Colons (:) indicate strong similarity, periods (.) indicate weak similarity, and a blank indicates no conservation. The colors represent: Red: Positively charged (Basic), Magenta: Negatively charged (Acidic), Blue: Hydrophobic, and Green: polar.

3.4: Hypothetical CRISPR-Cas9 gene editing strategy for CCR5:

A hypothetical gene editing strategy targeting the CCR5 gene (Figure 4) was designed to generate potential mutants for investigating how CCR5 mutations may influence relapse after HAART treatment. This strategy could be tested in a wet lab setting. Here, mutant outcomes were simulated (Figure 5) for training purposes. Gene editing provides a potential tool to understand why relapses happen and improve treatment outcomes. Potential guide RNAs were predicted using the CRISPRFinder (Sanger) tool (Figure 4A), and 3 gRNAs with the lowest predicted off-target scores were selected to increase the precision and the diversity of potential mutants. Primers were also designed (Figure 4B) for the simulation of PCR amplification of mutated sequences.

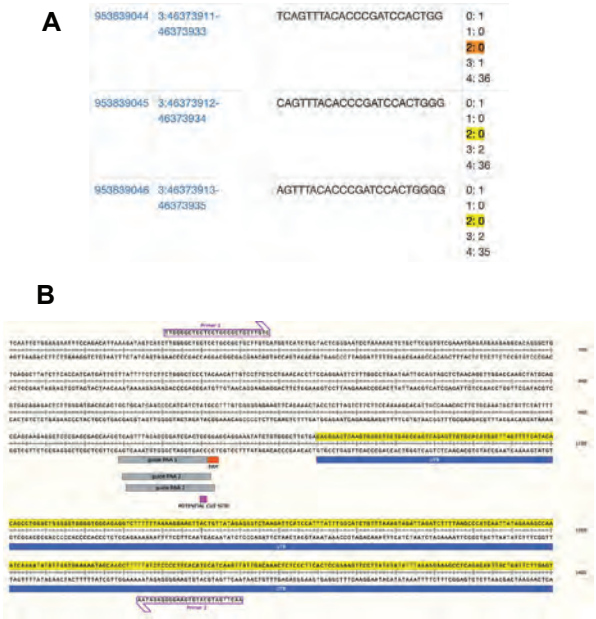

Figure 4: CRISPR-Cas9 gene editing strategy on the CCR5 gene designed by using SnapGene. This figure shows the positioning of the selected primers and CRISPR-Cas9 target region within the CCR5 gene. 4A. Predicted guide RNAs from CRISPRFinder (Sanger). Ideal gRNAs should have minimal off-target effects, so 3 gRNAs were selected for testing based on these scores, showing 0 predicted off-targets with up to 2 nucleotide mismatches. 4B. SnapGene view of the CCR5 gene sequence with annotated UTR region. The CCR5 gene editing is aimed to occur before the beginning of UTR. 2 primers (Primer1 and Primer2) were designed for PCR and simulated DNA gel electrophoresis. The length that primer 1 and primer 2 will amplify is 720bp.

Potential mutations were predicted and simulated for this study. The single-nucleotide alterations cannot be completely confirmed by DNA agarose gel electrophoresis, due to the very small size differences. Therefore, to confirm these mutations, a further analysis by DNA sequencing is required.

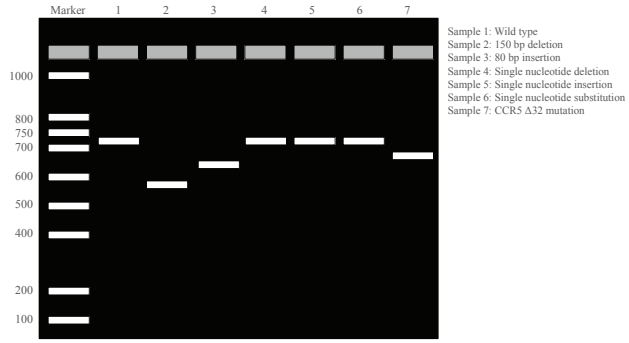

Figure 5 : Hypothetical band patterns from DNA gel electrophoresis showing potential outcomes of the gene editing approach. The first lane contains a DNA size marker (100-1000bp). Sample 1 shows the wild-type fragment with a size of 720bp. Samples 2 - 7 show the potential mutant fragments generated by the gene editing process, including deletions and insertions. This visualizes how band patterns of successful gene editing would appear relative to the 720 bp WT fragment.

3.5: Hypothetical experimental design for application of autologous transplantation of CRISPR-Cas9 edited HSPCs:

This design outlines a potential therapeutic strategy using autologous transplantation of CRISPR-Cas9 edited HSPCs.

DOI: 10.36838/IJHSR87.201

By collecting and editing the patient's own stem cells *ex vivo*, issues such as finding a matching donor and graft versus host disease (GVHD) are avoided. Quality control ensures that only viable cells with the least off-target effects are reinfused. Conditioning with chemotherapy or radiation is necessary to create space in the bone marrow for the edited stem cells to engraft. After reinfusion of these edited cells, they are expected to replace the immune system with CD4+ T cells lacking CCR5, providing long-term resistance against HIV-1 infection.

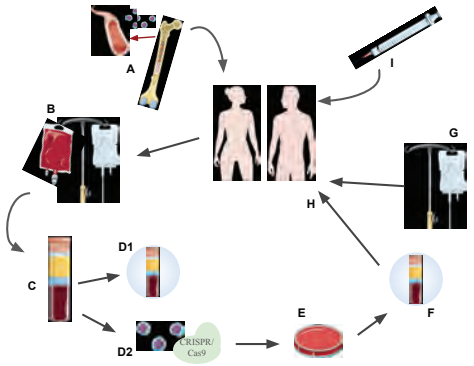

Figure 6 : A flowchart illustrating the hypothetical experimental design for the application of autologous transplantation of CRISPR-Cas9 edited HSPCs.[53,54] 6A. Release stem cells from the bone marrow into the bloodstream. 6B. Collect blood from the patient. 6C. Stem cells are separated and removed. 6D1. Some unedited stem cells are cryopreserved to keep as a backup. 6D2. Edit stem cells using CRISPR-Cas9. 6E. Quality control: Check for percentage off-target effects, cell viability, and the karyotype. 6F. Cryopreserve edited cells. 6G. Conditioning: Patient receives high-dose chemotherapy and/or radiation therapy to make 'space' in the bone marrow. 6H. Thawed stem cells are reinfused back into the patient. 6I. The patient receives treatment to help the bone marrow regrow. *Image adapted from Servier Medical Art (https://smart.servier.com/), licensed under CC BY 4.0 (https://creativecommons.org/licenses/by/4.0/)*

Overall Discussion:

This paper discusses the significance of the CCR5 coreceptor and the naturally occurring CCR5 Δ32 mutation in HIV infection and proposes the application of CRISPR-Cas9 technology to mimic the mutation in hematopoietic stem and progenitor cells (HSPCs) as a potential long-term treatment approach. While HAART is effective at suppressing viral load and preventing progression to AIDS, it does not eradicate latent viral reservoirs, meaning patients are required to be on medication throughout their lives. Prolonged treatment may lead to accumulating toxicities and comorbidities, especially in aging patients who may already face chronic diseases associated with aging. Furthermore, the health complications and economic burden of long-term HAART are not fully understood.[55] These challenges highlight the importance of long-term solutions such as CCR5 targeted therapies. As shown in Figure 1 and 2, the CCR5 Δ32 mutation results in major structural differences between the mutated protein and the wild type (WT) protein. The loss of transmembrane regions (TMRs) 5, 6, and 7 prevents correct folding of the mutant, causing it to be retained in the endoplasmic reticulum and absent on the CD4+ cell surface. This disruption in structure leads to strong immunity against R5 tropic HIV-1, especially in individuals homozygous for the mutation. The therapeutic potential of this mutation was demonstrated by the Berlin patient, who achieved a complete cure after undergoing successful allogeneic transplantation from a donor homozygous for CCR5 Δ32.[45] However, considering the scarcity of the population homozygous for Δ32, an allogeneic transplantation from a homozygous donor is not a realistic approach. To address such limitations, this paper proposes the use of CRISPR-Cas9 to recreate the CCR5 Δ32 mutation in HSPCs for autologous transplantation. Improving the accuracy of CRISPR-Cas9 is crucial for its therapeutic application. Therefore, a humanized Cas9 (hCas9) and carefully selected gRNAs (Figure 4) should be used for higher efficiency and minimal off-target effects. Akcakaya *et al.* showed that a well-designed sgRNA can carry out precise *in vivo* gene editing with no detectable off-target effects, suggesting CRISPR-Cas9 is a very specific genome editing tool.

As outlined in the proposed hypothetical experimental design (Figure 6), this strategy involves autologous stem cell transplantation using CRISPR-Cas9 edited HSPCs. Autologous transplantation provides several advantages. There is no need to find a donor homozygous for CCR5 Δ32, no need for HLA matching, and no risk of graft versus host disease (GVHD). After transplantation, the edited stem cells should produce immune cells lacking CCR5, leading to strong resistance against R5-tropic HIV-1, and potentially some reduced susceptibility to dual-tropic HIV-1. Crucially, while *in vivo* delivery of CRISPR-Cas9 faces challenges such as a higher risk of off-target effects, selection of delivery methods, and low efficiency,[56] *ex vivo* editing allows gene editing to be performed under controlled conditions, avoiding many of these issues. Furthermore, generating HIV-1-resistant cells by disruption of the *CCR5* gene has shown immediate loss of the receptor after transfection, with minimal off-target effects due to the protein complex being quickly degraded within the cell.[57,58]

While these advantages highlight the potential of *ex vivo* CRISPR-Cas9 gene editing as a therapeutic approach, several major challenges remain before it can be applied clinically. Although tools such as CRISPRFinder and Cas-OFFinder[59] can be used to predict off-targets, and studies suggest that overall, CRISPR-Cas9 is a very specific gene editing tool,[60–62] the possibility of unintended edits remains a major issue. In addition to the technical aspects, challenges regarding patients remain. HIV infected patients are significantly more susceptible to opportunistic infections and certain cancers due to their deteriorating immune system. In these situations, allogeneic stem cell transplantation is often applied, since it is more effective than autologous transplants. Therefore, genetically modified autologous transplants may not be a priority for patients battling cancer or other opportunistic infections. Furthermore, for patients who were able to suppress viral load with HAART and are without opportunistic infections, the risks of this approach and the unfamiliarity of CRISPR-based gene editing may outweigh the potential benefits.

Aside from technical and clinical considerations, ethical and social issues must also be addressed. Some may argue that enhancement of the immune system through gene editing, such as proposed in this paper, is considered genetic enhancement.[63] Therefore, this urges for further discussion on where we draw

the line between gene therapy and genetic enhancement.[64] Last but not least, challenges remain in managing cost, scalability, and accessibility. Gene editing is a fairly new and expensive technology, and more work must be done to allow treatment to be available to patients in low and middle-income countries, where HIV infection is more common and presents a greater challenge.

Conclusion

HIV/AIDS remains an incurable disease, mostly due to the persistence of the latent viral reservoirs requiring lifelong antiretroviral therapy. While ART can suppress viral load and has been effective at increasing the life expectancy of patients, it cannot completely eradicate the virus, and it also poses long-term risks. The CCR5 Δ32 mutation has provided groundbreaking insight into the possibility of providing patients with HIV resistance, especially with cases of patients cured after transplantation from CCR5 Δ32 homozygous donors. The application of CRISPR-Cas9 technology to induce the Δ32 mutation directly to hematopoietic stem cells of a patient offers a possible strategy towards finding a cure for HIV/AIDS. Although challenges remain regarding safety, off-target effects, accessibility, and ethical concerns with gene editing, the ongoing research in the gene editing field continues to bring its application closer to a therapeutic option.

Acknowledgments

I would like to thank Dr. Zeynep Ozturk for her guidance throughout this writing process. I attest that the ideas, graphics, and writing in this paper are entirely my own.

References

1. Sepkowitz, K. A. AIDS — The First 20 Years. *N. Engl. J. Med.* **2001**, *344* (23), 1764–1772. https://doi.org/10.1056/NEJM200106073442306.
2. Alkhatib, G. The Biology of CCR5 and CXCR4. *Curr. Opin. HIV AIDS* **2009**, *4* (2), 96–103. https://doi.org/10.1097/COH.0b013e328324bbec.
3. Alimonti, J. B.; Ball, T. B.; Fowke, K. R. Mechanisms of CD4+ T Lymphocyte Cell Death in Human Immunodeficiency Virus Infection and AIDS. *J. Gen. Virol.* **2003**, *84* (Pt 7), 1649–1661. https://doi.org/10.1099/vir.0.19110-0.
4. Gilbert, P. B.; McKeague, I. W.; Eisen, G.; Mullins, C.; Guéye-NDiaye, A.; Mboup, S.; Kanki, P. J. Comparison of HIV-1 and HIV-2 Infectivity from a Prospective Cohort Study in Senegal. *Stat. Med.* **2003**, *22* (4), 573–593. https://doi.org/10.1002/sim.1342.
5. D'arc, M.; Ayouba, A.; Esteban, A.; Learn, G. H.; Boué, V.; Liegeois, F.; Etienne, L.; Tagg, N.; Leendertz, F. H.; Boesch, C.; Madinda, N. F.; Robbins, M. M.; Gray, M.; Cournil, A.; Ooms, M.; Letko, M.; Simon, V. A.; Sharp, P. M.; Hahn, B. H.; Delaporte, E.; Mpoudi Ngole, E.; Peeters, M. Origin of the HIV-1 Group O Epidemic in Western Lowland Gorillas. *Proc. Natl. Acad. Sci.* **2015**, *112* (11), E1343–E1352. https://doi.org/10.1073/pnas.1502022112.
6. *The Stages of HIV Infection | NIH*. https://hivinfo.nih.gov/understanding-hiv/fact-sheets/stages-hiv-infection (accessed 2025-06-11).
7. Lemey, P.; Kosakovsky Pond, S. L.; Drummond, A. J.; Pybus, O. G.; Shapiro, B.; Barroso, H.; Taveira, N.; Rambaut, A. Synonymous Substitution Rates Predict HIV Disease Progression as a Result of Underlying Replication Dynamics. *PLoS Comput. Biol.* **2007**, *3* (2), e29. https://doi.org/10.1371/journal.pcbi.0030029.
8. Damtie, D.; Yismaw, G.; Woldeyohannes, D.; Anagaw, B. Common Opportunistic Infections and Their CD4 Cell Correlates among HIV-Infected Patients Attending at Antiretroviral Therapy Clinic of Gondar University Hospital, Northwest Ethiopia. *BMC Res. Notes* **2013**, *6*, 534. https://doi.org/10.1186/1756-0500-6-534.
9. Swinkels, H. M.; Nguyen, A. D.; Gulick, P. G. HIV and AIDS. In *StatPearls*; StatPearls Publishing: Treasure Island (FL), 2025.
10. Eckert, D. M.; Kim, P. S. Mechanisms of Viral Membrane Fusion and Its Inhibition. *Annu. Rev. Biochem.* **2001**, *70*, 777–810. https://doi.org/10.1146/annurev.biochem.70.1.777.
11. Wyatt, R.; Kwong, P. D.; Desjardins, E.; Sweet, R. W.; Robinson, J.; Hendrickson, W. A.; Sodroski, J. G. The Antigenic Structure of the HIV Gp120 Envelope Glycoprotein. *Nature* **1998**, *393* (6686), 705–711. https://doi.org/10.1038/31514.
12. Broder, C. C.; Collman, R. G. Chemokine Receptors and HIV. *J. Leukoc. Biol.* **1997**, *62* (1), 20–29. https://doi.org/10.1002/jlb.62.1.20.
13. Coakley, E.; Petropoulos, C. J.; Whitcomb, J. M. Assessing Chemokine Co-Receptor Usage in HIV. *Curr. Opin. Infect. Dis.* **2005**, *18* (1), 9–15. https://doi.org/10.1097/00001432-200502000-00003.
14. Smith, J. A.; Daniel, R. Following the Path of the Virus: The Exploitation of Host DNA Repair Mechanisms by Retroviruses. *ACS Chem. Biol.* **2006**, *1* (4), 217–226. https://doi.org/10.1021/cb600131q.
15. van Rij, R. P.; Hazenberg, M. D.; van Benthem, B. H. B.; Otto, S. A.; Prins, M.; Miedema, F.; Schuitemaker, H. Early Viral Load and CD4+ T Cell Count, but Not Percentage of CCR5+ or CXCR4+ CD4+ T Cells, Are Associated with R5-to-X4 HIV Type 1 Virus Evolution. *AIDS Res. Hum. Retroviruses* **2003**, *19* (5), 389–398. https://doi.org/10.1089/088922203765551737.
16. Moore, J. P.; Kitchen, S. G.; Pugach, P.; Zack, J. A. The CCR5 and CXCR4 Coreceptors--Central to Understanding the Transmission and Pathogenesis of Human Immunodeficiency Virus Type 1 Infection. *AIDS Res. Hum. Retroviruses* **2004**, *20* (1), 111–126. https://doi.org/10.1089/088922204322749567.
17. *CCR5 C-C motif chemokine receptor 5 [Homo sapiens (human)] - Gene - NCBI*. https://www.ncbi.nlm.nih.gov/gene/1234 (accessed 2025-06-16).
18. Tan, Q.; Zhu, Y.; Li, J.; Chen, Z.; Han, G. W.; Kufareva, I.; Li, T.; Ma, L.; Fenalti, G.; Li, J.; Zhang, W.; Xie, X.; Yang, H.; Jiang, H.; Cherezov, V.; Liu, H.; Stevens, R. C.; Zhao, Q.; Wu, B. Structure of the CCR5 Chemokine Receptor – HIV Entry Inhibitor Maraviroc Complex. *Science* **2013**, *341* (6152), 10.1126/science.1241475. https://doi.org/10.1126/science.1241475.
19. Sicoli, D.; Jiao, X.; Ju, X.; Velasco-Velazquez, M.; Ertel, A.; Addya, S.; Li, Z.; Ando, S.; Fatatis, A.; Paudyal, B.; Cristofanilli, M.; Thakur, M. L.; Lisanti, M. P.; Pestell, R. G. CCR5 Receptor Antagonists Block Metastasis to Bone of V-Src-Oncogene-Transformed Metastatic Prostate Cancer Cell Lines. *Cancer Res.* **2014**, *74* (23), 7103–7114. https://doi.org/10.1158/0008-5472.CAN-14-0612.
20. *CCR5 [Homo sapiens] - Protein - NCBI*. https://www.ncbi.nlm.nih.gov/protein/AAB09551.1 (accessed 2025-07-03).
21. M, S.; F, L.; Bj, D.; J, R.; C, L.; Cm, F.; S, S.; C, L.; J, C.; C, F.; G, M.; C, V.; G, B.; M, G.; T, I.; S, R.; Y, Y.; Rj, S.; Rg, C.; Rw, D.; G, V.; M, P. Resistance to HIV-1 Infection in Caucasian Individuals Bearing Mutant Alleles of the CCR-5 Chemokine Receptor Gene. *Nature* **1996**, *382* (6593). https://doi.org/10.1038/382722a0.
22. Pa, Z.; A, B.-W.; G, A.; T, S.; J, K.; C, C.; D, W.; O, C.; A, R.; G, L.; M, V.; Pe, K.; V, K.; Jv, G.; R, D.; J, H.; M, C.; Ea, B.; As, F.; Tb, N.; Pm, M. Inherited Resistance to HIV-1 Conferred by an Inactivating Mutation in CC Chemokine Receptor 5: Studies in

DOI: 10.36838/IJHSR87.201

Populations with Contrasting Clinical Phenotypes, Defined Racial Background, and Quantified Risk. *Mol. Med. Camb. Mass* **1997**, *3* (1).

23. Agrawal, L.; Lu, X.; Qingwen, J.; VanHorn-Ali, Z.; Nicolescu, I. V.; McDermott, D. H.; Murphy, P. M.; Alkhatib, G. Role for CCR5Δ32 Protein in Resistance to R5, R5X4, and X4 Human Immunodeficiency Virus Type 1 in Primary CD4+ Cells. *J. Virol.* **2004**, *78* (5), 2277–2287. https://doi.org/10.1128/JVI.78.5.2277-2287.2004.
24. Dean, M.; Carrington, M.; Winkler, C.; Huttley, G. A.; Smith, M. W.; Allikmets, R.; Goedert, J. J.; Buchbinder, S. P.; Vittinghoff, E.; Gomperts, E.; Donfield, S.; Vlahov, D.; Kaslow, R.; Saah, A.; Rinaldo, C.; Detels, R.; O'Brien, S. J. Genetic Restriction of HIV-1 Infection and Progression to AIDS by a Deletion Allele of the CKR5 Structural Gene. Hemophilia Growth and Development Study, Multicenter AIDS Cohort Study, Multicenter Hemophilia Cohort Study, San Francisco City Cohort, ALIVE Study. *Science* **1996**, *273* (5283), 1856–1862. https://doi.org/10.1126/science.273.5283.1856.
25. Meyer, L.; Magierowska, M.; Hubert, J. B.; Rouzioux, C.; Deveau, C.; Sanson, F.; Debre, P.; Delfraissy, J. F.; Theodorou, I. Early Protective Effect of CCR-5 Delta 32 Heterozygosity on HIV-1 Disease Progression: Relationship with Viral Load. The SEROCO Study Group. *AIDS Lond. Engl.* **1997**, *11* (11), F73-78. https://doi.org/10.1097/00002030-199711000-00001.
26. M, B.; Dy, J.; Rf, C.; Ra, K.; Kt, J. Mechanism of Transdominant Inhibition of CCR5-Mediated HIV-1 Infection by Ccr5delta32. *J. Biol. Chem.* **1997**, *272* (49). https://doi.org/10.1074/jbc.272.49.30603.
27. Naif, H. M.; Cunningham, A. L.; Alali, M.; Li, S.; Nasr, N.; Buhler, M. M.; Schols, D.; de Clercq, E.; Stewart, G. A Human Immunodeficiency Virus Type 1 Isolate from an Infected Person Homozygous for CCR5Delta32 Exhibits Dual Tropism by Infecting Macrophages and MT2 Cells via CXCR4. *J. Virol.* **2002**, *76* (7), 3114–3124. https://doi.org/10.1128/jvi.76.7.3114-3124.2002.
28. Tw, C.; L, C.; D, F.; X, S.; Ja, D.; H, T.; M, H.; K, C.; J, M.; Tc, Q.; Yh, K.; R, B.; Ma, Z.; P, B.-C.; Rf, S. Quantification of Latent Tissue Reservoirs and Total Body Viral Load in HIV-1 Infection. *Nature* **1997**, *387* (6629). https://doi.org/10.1038/387183a0.
29. Finzi, D.; Blankson, J.; Siliciano, J. D.; Margolick, J. B.; Chadwick, K.; Pierson, T.; Smith, K.; Lisziewicz, J.; Lori, F.; Flexner, C.; Quinn, T. C.; Chaisson, R. E.; Rosenberg, E.; Walker, B.; Gange, S.; Gallant, J.; Siliciano, R. F. Latent Infection of CD4+ T Cells Provides a Mechanism for Lifelong Persistence of HIV-1, Even in Patients on Effective Combination Therapy. *Nat. Med.* **1999**, *5* (5), 512–517. https://doi.org/10.1038/8394.
30. Siliciano, J. D.; Kajdas, J.; Finzi, D.; Quinn, T. C.; Chadwick, K.; Margolick, J. B.; Kovacs, C.; Gange, S. J.; Siliciano, R. F. Long-Term Follow-up Studies Confirm the Stability of the Latent Reservoir for HIV-1 in Resting CD4+ T Cells. *Nat. Med.* **2003**, *9* (6), 727–728. https://doi.org/10.1038/nm880.
31. Rt, D.; N, B.; C, Y.; Tw, C.; Ja, M.; R, D.; V, N.; Ra, L.; Jw, A.; Kd, M.; Ja, K.; Ma, P.; Re, W.; J, F.; H, M.; D, G.; M, B.; Ds, D.; As, F.; Hc, L. HIV-1 and T Cell Dynamics after Interruption of Highly Active Antiretroviral Therapy (HAART) in Patients with a History of Sustained Viral Suppression. *Proc. Natl. Acad. Sci. U. S. A.* **1999**, *96* (26). https://doi.org/10.1073/pnas.96.26.15109.
32. Chun, T.-W.; Stuyver, L.; Mizell, S. B.; Ehler, L. A.; Mican, J. A. M.; Baseler, M.; Lloyd, A. L.; Nowak, M. A.; Fauci, A. S. Presence of an Inducible HIV-1 Latent Reservoir during Highly Active Antiretroviral Therapy. *Proc. Natl. Acad. Sci. U. S. A.* **1997**, *94* (24), 13193–13197. https://doi.org/10.1073/pnas.94.24.13193.
33. Siliciano, R. F.; Greene, W. C. HIV Latency. *Cold Spring Harb. Perspect. Med.* **2011**, *1* (1), a007096. https://doi.org/10.1101/cshperspect.a007096.
34. Gupta, P. K.; Saxena, A. HIV/AIDS: Current Updates on the Disease, Treatment and Prevention. *Proc. Natl. Acad. Sci. India Sect. B* **2021**, *91* (3), 495–510. https://doi.org/10.1007/s40011-021-01237-y.
35. Delobel, P.; Sandres-Sauné, K.; Cazabat, M.; Pasquier, C.; Marchou, B.; Massip, P.; Izopet, J. R5 to X4 Switch of the Predominant HIV-1 Population in Cellular Reservoirs during Effective Highly Active Antiretroviral Therapy. *J. Acquir. Immune Defic. Syndr. 1999* **2005**, *38* (4), 382–392. https://doi.org/10.1097/01.qai.0000152835.17747.47.
36. Bolotin, A.; Quinquis, B.; Sorokin, A.; Ehrlich, S. D. Clustered Regularly Interspaced Short Palindrome Repeats (CRISPRs) Have Spacers of Extrachromosomal Origin. *Microbiol. Read. Engl.* **2005**, *151* (Pt 8), 2551–2561. https://doi.org/10.1099/mic.0.28048-0.
37. Mojica, F. J. M.; Díez-Villaseñor, C.; García-Martínez, J.; Soria, E. Intervening Sequences of Regularly Spaced Prokaryotic Repeats Derive from Foreign Genetic Elements. *J. Mol. Evol.* **2005**, *60* (2), 174–182. https://doi.org/10.1007/s00239-004-0046-3.
38. Terns, M. P.; Terns, R. M. CRISPR-Based Adaptive Immune Systems. *Curr. Opin. Microbiol.* **2011**, *14* (3), 321–327. https://doi.org/10.1016/j.mib.2011.03.005.
39. Brouns, S. J. J.; Jore, M. M.; Lundgren, M.; Westra, E. R.; Slijkhuis, R. J. H.; Snijders, A. P. L.; Dickman, M. J.; Makarova, K. S.; Koonin, E. V.; van der Oost, J. Small CRISPR RNAs Guide Antiviral Defense in Prokaryotes. *Science* **2008**, *321* (5891), 960–964. https://doi.org/10.1126/science.1159689.
40. Hale, C.; Kleppe, K.; Terns, R. M.; Terns, M. P. Prokaryotic Silencing (Psi)RNAs in Pyrococcus Furiosus. *RNA* **2008**, *14* (12), 2572–2579. https://doi.org/10.1261/rna.1246808.
41. Ebina, H.; Misawa, N.; Kanemura, Y.; Koyanagi, Y. Harnessing the CRISPR/Cas9 System to Disrupt Latent HIV-1 Provirus. *Sci. Rep.* **2013**, *3*, 2510. https://doi.org/10.1038/srep02510.
42. Barrangou, R.; Fremaux, C.; Deveau, H.; Richards, M.; Boyaval, P.; Moineau, S.; Romero, D. A.; Horvath, P. CRISPR Provides Acquired Resistance against Viruses in Prokaryotes. *Science* **2007**, *315* (5819), 1709–1712. https://doi.org/10.1126/science.1138140.
43. Jinek, M.; Chylinski, K.; Fonfara, I.; Hauer, M.; Doudna, J. A.; Charpentier, E. A Programmable Dual RNA-Guided DNA Endonuclease in Adaptive Bacterial Immunity. *Science* **2012**, *337* (6096), 816–821. https://doi.org/10.1126/science.1225829.
44. Champlin, R. Selection of Autologous or Allogeneic Transplantation. In *Holland-Frei Cancer Medicine. 6th edition*; BC Decker, 2003.
45. Hütter, G.; Nowak, D.; Mossner, M.; Ganepola, S.; Müßig, A.; Allers, K.; Schneider, T.; Hofmann, J.; Kücherer, C.; Blau, O.; Blau, I. W.; Hofmann, W. K.; Thiel, E. Long-Term Control of HIV by CCR5 Delta32/Delta32 Stem-Cell Transplantation. *N. Engl. J. Med.* **2009**, *360* (7), 692–698. https://doi.org/10.1056/NEJMoa0802905.
46. Brown, T. R. I Am the Berlin Patient: A Personal Reflection. *AIDS Res. Hum. Retroviruses* **2015**, *31* (1), 2–3. https://doi.org/10.1089/aid.2014.0224.
47. Liang, X.; Potter, J.; Kumar, S.; Zou, Y.; Quintanilla, R.; Sridharan, M.; Carte, J.; Chen, W.; Roark, N.; Ranganathan, S.; Ravinder, N.; Chesnut, J. D. Rapid and Highly Efficient Mammalian Cell Engineering via Cas9 Protein Transfection. *J. Biotechnol.* **2015**, *208*, 44–53. https://doi.org/10.1016/j.jbiotec.2015.04.024.
48. Wroblewska, L.; Kitada, T.; Endo, K.; Siciliano, V.; Stillo, B.; Saito, H.; Weiss, R. Mammalian Synthetic Circuits with RNA Binding Proteins for RNA-Only Delivery. *Nat. Biotechnol.* **2015**, *33* (8), 839–841. https://doi.org/10.1038/nbt.3301.

49. Xu, L.; Wang, J.; Liu, Y.; Xie, L.; Su, B.; Mou, D.; Wang, L.; Liu, T.; Wang, X.; Zhang, B.; Zhao, L.; Hu, L.; Ning, H.; Zhang, Y.; Deng, K.; Liu, L.; Lu, X.; Zhang, T.; Xu, J.; Li, C.; Wu, H.; Deng, H.; Chen, H. CRISPR-Edited Stem Cells in a Patient with HIV and Acute Lymphocytic Leukemia. *N. Engl. J. Med*. **2019**, *381* (13), 1240–1247. https://doi.org/10.1056/NEJMoa1817426.
50. Blanpain, C.; Wittamer, V.; Vanderwinden, J. M.; Boom, A.; Renneboog, B.; Lee, B.; Le Poul, E.; El Asmar, L.; Govaerts, C.; Vassart, G.; Doms, R. W.; Parmentier, M. Palmitoylation of CCR5 Is Critical for Receptor Trafficking and Efficient Activation of Intracellular Signaling Pathways. *J. Biol. Chem*. **2001**, *276* (26), 23795–23804. https://doi.org/10.1074/jbc.M100583200.
51. Rorick, M. M.; Wagner, G. P. The Origin of Conserved Protein Domains and Amino Acid Repeats Via Adaptive Competition for Control Over Amino Acid Residues. *J. Mol. Evol*. **2010**, *70* (1), 29–43. https://doi.org/10.1007/s00239-009-9305-7.
52. Jj, R.; M, B.; Gp, W. Repressor Domain and Nuclear Localization Signal of the Murine Hoxa-11 Protein Are Located in the Homeodomain: No Evidence for Role of Poly Alanine Stretches in Transcriptional Repression. *J. Exp. Zoolog. B Mol. Dev. Evol*. **2005**, *304* (5). https://doi.org/10.1002/jez.b.21061.
53. *Stem Cell Transplantation | Autologous Stem Cell Transplantation | LLS*. https://www.lls.org/treatment/types-treatment/stem-cell-transplantation/autologous-stem-cell-transplantation (accessed 2025-08-18).
54. *SMART*. Servier Medical Art. https://smart.servier.com/ (accessed 2025-08-18).
55. Chawla, A.; Wang, C.; Patton, C.; Murray, M.; Punekar, Y.; de Ruiter, A.; Steinhart, C. A Review of Long-Term Toxicity of Antiretroviral Treatment Regimens and Implications for an Aging Population. *Infect. Dis. Ther*. **2018**, *7* (2), 183–195. https://doi.org/10.1007/s40121-018-0201-6.
56. Li, L.; He, Z.-Y.; Wei, X.-W.; Gao, G.-P.; Wei, Y.-Q. Challenges in CRISPR/CAS9 Delivery: Potential Roles of Nonviral Vectors. *Hum. Gene Ther*. **2015**, *26* (7), 452–462. https://doi.org/10.1089/hum.2015.069.
57. Wang, W.; Ye, C.; Liu, J.; Zhang, D.; Kimata, J. T.; Zhou, P. CCR5 Gene Disruption via Lentiviral Vectors Expressing Cas9 and Single Guided RNA Renders Cells Resistant to HIV-1 Infection. *PLoS ONE* **2014**, *9* (12), e115987. https://doi.org/10.1371/journal.pone.0115987.
58. Ye, L.; Wang, J.; Beyer, A. I.; Teque, F.; Cradick, T. J.; Qi, Z.; Chang, J. C.; Bao, G.; Muench, M. O.; Yu, J.; Levy, J. A.; Kan, Y. W. Seamless Modification of Wild-Type Induced Pluripotent Stem Cells to the Natural CCR5Δ32 Mutation Confers Resistance to HIV Infection. *Proc. Natl. Acad. Sci. U. S. A*. **2014**, *111* (26), 9591–9596. https://doi.org/10.1073/pnas.1407473111.
59. Bae, S.; Park, J.; Kim, J.-S. Cas-OFFinder: A Fast and Versatile Algorithm That Searches for Potential off-Target Sites of Cas9 RNA-Guided Endonucleases. *Bioinformatics* **2014**, *30* (10), 1473–1475. https://doi.org/10.1093/bioinformatics/btu048.
60. Akcakaya, P.; Bobbin, M. L.; Guo, J. A.; Malagon-Lopez, J.; Clement, K.; Garcia, S. P.; Fellows, M. D.; Porritt, M. J.; Firth, M. A.; Carreras, A.; Baccega, T.; Seeliger, F.; Bjursell, M.; Tsai, S. Q.; Nguyen, N. T.; Nitsch, R.; Mayr, L. M.; Pinello, L.; Bohlooly-Y, M.; Aryee, M. J.; Maresca, M.; Joung, J. K. In Vivo CRISPR Editing with No Detectable Genome-Wide off-Target Mutations. *Nature* **2018**, *561* (7723), 416–419. https://doi.org/10.1038/s41586-018-0500-9.
61. Kim, D.; Kim, J.-S. DIG-Seq: A Genome-Wide CRISPR off-Target Profiling Method Using Chromatin DNA. *Genome Res*. **2018**, *28* (12), 1894–1900. https://doi.org/10.1101/gr.236620.118.
62. Valenti, M. T.; Serena, M.; Carbonare, L. D.; Zipeto, D. CRISPR/Cas System: An Emerging Technology in Stem Cell Research. *World J. Stem Cells* **2019**, *11* (11), 937–956. https://doi.org/10.4252/wjsc.v11.i11.937.
63. De Miguel Beriain, I. Legal Issues Regarding Gene Editing at the Beginning of Life: An EU Perspective. *Regen. Med*. **2017**, *12* (6), 669–679. https://doi.org/10.2217/rme-2017-0033.
64. Ansah, E. O. Ethical Challenges and Controversies in the Practice and Advancement of Gene Therapy. *Adv. Cell Gene Ther*. **2022**, *2022* (1), 1015996. https://doi.org/10.1155/2022/1015996.

Author

Nana Shibuya is a Year 13 student at the British School of Tashkent, Uzbekistan. She is passionate about STEM, particularly molecular biology and genetics, and aims to pursue her studies in biomedical science.

Supplementary data

>Chimpanzee_AAB65742.1 CCR5 receptor, partial [Pan troglodytes]

MDYQVSSPIYDIDYYTSEPCQKINVKQIAARLLP-
PLYSLVFIFGFVGNMLVILILINCKRLKSMTDIYLLN-
LAISDLFFLLTVPFWAHYAAAQWDFGNTMCQLLT-
GLYFIGFFSGIFFIILLTIDRYLAIVHAVFALKART-
VTFGVVTSVITWVVAVFASLPGIIFTRSQKEGL-
HYTCSSHFPYSQYQFWKNFQTLKIVILGLVLPLL-
VMVICYSGILKTLLRCRNEKKRHRAVRLIFTIMI-
VYFLFWAPYNIVLLLNTFQEFFGLNNCSSSN-
RLDQAMQVTETLGMTHCCINPIIYAFVGEK-
FRNYLLVFFQKHIAKRFCKCCSIFQQEAPERASSVY-
TRSTGEQEISVGL

>Chicken_NP_001258070.1 C-C chemokine receptor type 5 [Gallus gallus]

MENYTDLGDMDVTTTFDYGDTAPCMGTEEKH-
FAANFLPPLYSLVVIFGFIGNILVVLILVKYKKLKSMT-
DIYLLNLAISDLLFIFSLPFWAYYAAHDWIFGDA-
LCRILSGVYLLGFYSGIFFIILLTVDRYLAIVHAV-
FALKARTVTYGILTSIVTWAVALFASVPGIVFHK-
TQQEHTRYTCSAHYPQEQRDEWKQFLALKM-
NILGLVIPMIIMICSYTQIIKTLLQCRNEKKNKA-
VRLIFIIMIVYFFFWAPYNICILLRDFQDSFSITSCE-
ISGQLQKATQVTETISMIHCCINPVIYAFAGEK-
FRKYLRSFFRKQIASHFSKYCPVFYADTVERASS-
TYTQSTGEQEVSAAL

>Mouse_AAC53389.1 CC chemokine receptor-5 [Mus musculus]

MDFQGSVPTYSYDIDYGMSAPCQKIN-
VKQIAAQLLPPLYSLVFIFGFVGNMMVFLILISCK-
KLKSVTDIYLLNLAISDLLFLLTLPFWAHYAAN-
EWVFGNIMCKVFTGLYHIGYFGGIFFIILLTIDRY-
LAIVHAVFALKVRTVNFGVITSVVTWAVAVFASL-
PEIIFTRSQKEGFHYTCSPHFPHTQYHFWKS-
FQTLKMVILSLILPLLVMVICYSGILHTLFRCRNEK-
KRHRAVRLIFAIMIVYFLFWTPYNIVLLLTTFQEF-
FGLNNCSSSNRLDQAMQATETLGMTHCCLNPVI-

DOI: 10.36838/IJHSR87.201

YAFVGEKFRSYLSVFFRKHMVKRFCKRCSIFQQDN-
PDRASSVYTRSTGEHEVSTGL

>AAB57793.1 ccr5 [Homo sapiens]
MDYQVSSPIYDINYYTSEPCQKINVKQIAARLLP-
PLYSLVFIFGFVGNMLVILILINCKRLKSMTDIYLLN-
LAISDLFFLLTVPFWAHYAAAQWDFGNTMCQLLT-
GLYFIGFFSGIFFIILLTIDRYLAVVHAVFALKART-
VTFGVVTSVITWVVAVFASLPGIIFTRSQKEGL-
HYTCSSHFPYSQYQFWKNFQTLKIVILGLVLPLL-
VMVICYSGILKTLLRCRNEKKRHRAVRLIFTIMIVY-
FLFWAPYNIVLLLNTFQEFFGLNNCSSSNRLDQA-
MQVTET

IJHSR
ijhighschoolresearch.org
RESEARCH ARTICLE

Exploring Music Therapy as Adjunctive Care in Oncology: Insights from a Qualitative Case Study

Sanskriti Varshney

Byron Nelson High School, 2775 Bobcat Blvd, Trophy Club, Texas, 76262, USA; sanskritivarshney8002@gmail.com

ABSTRACT: Cancer can cause a substantial burden, and adjunct therapies such as music therapy may support patients' social, emotional, physical, and spiritual well-being. This study explored the role of music therapy in supporting the emotional and psychological well-being of cancer patients. The researcher conducted a qualitative case study including an interview with one patient, an interview with a medical oncologist, and a written questionnaire completed by a board-certified music therapist; the participants' perspectives were triangulated. Participants described perceived benefits of music therapy for emotional regulation, coping, spirituality, and social connection, with the patient rating helpfulness highly across several domains. The clinicians emphasized that music therapy is personalized, goal-oriented, and adjunctive to conventional treatments, accounting for patient preference. Although barriers to implementing adjunct therapies such as music therapy exist at multiple levels of healthcare (e.g., staffing, reimbursement, awareness), increased clinician education and institutional budgeting may help expand access to supportive care. Findings suggest that music therapy may serve as a valuable adjunct to standard cancer care, though barriers to implementation remain.

KEYWORDS: Medical and Health Sciences, Oncology, Music Therapy, Complementary and Integrative Medicine, Psychosocial Support in Cancer Care.

Introduction

According to the American Cancer Society, cancer is a group of diseases where abnormal cells grow out of control and deteriorate the body's functions.[1] Approximately 1 out of 3 people is likely to develop cancer, and the National Cancer Institute projects 2,041,910 new cases of cancer in 2025.[2] Pain and suffering from cancer can induce many negative feelings in patients, such as anxiety, stress, despair, helplessness, and hopelessness.[3] According to the National Cancer Institute, patients may feel as if they have lost their previous life before cancer, and they may even feel frustration at others or themselves for developing cancer.[4]

Not only are patients affected emotionally, but their families often carry a heavy emotional burden as well. Families may experience grief for the patient's diagnosis, as well as fear or guilt.[5] Cancer can cause changes in relationships between patients and their families. Families and/or caregivers may have increased responsibilities for their loved ones, and they may view their loved ones more as patients than as family members.[5]

Due to their nature, cancer treatments can affect patients physically and mentally. According to Cancer Research UK, 55% of patients with cancer experience advanced pain.[6] Treatments that cancer patients may need include chemotherapy, radiation therapy, surgery, hormone therapy, immunotherapy, and even stem cell transplantation.[7] While these treatments focus on eliminating or slowing the growth of the physical cancer in the body, cancer and treatments affect both the body and mind, so addressing the emotional and psychological needs of patients has become a crucial part of comprehensive care. In other words, supportive care is equally important as medical care.[8]

Integrative and complementary therapies have developed and gained popularity over the years to support patients. According to PubMed Central, the American Holistic Medicine Association was established in 1978, and the American Holistic Nurses Association was established in 1979. Their goal was to treat "the whole person, body, mind[,] and spirit."[9] In 2000, the American Board of Integrative Holistic Medicine offered the first board certification exam to certify physicians.[9] More organizations also developed soon after, such as the White House Commission on Complementary Alternative Medicine in 2002, the Integrative Health Policy Consortium in 2004, and the National Education Dialogue in 2005. Since the formation of these organizations and their goals to spread awareness to healthcare systems, integrative medicine has been increasingly incorporated into a patient's treatment journey.

Some examples of integrative and complementary therapies used to increase patient mental health are music, meditation, yoga, sound-based relaxation, dance/movement therapy, and psychotherapy.[4] These therapies help with one's emotional health, and studies have shown that they can increase patients' quality of life and decrease pain from symptoms.[10] Music therapy was being used in healthcare centuries before, with the earliest reference to using it as a treatment appearing in 1789.[11] In the 20th century, soldiers recovering from trauma from World War 2 were also being treated with music therapy. During this period, music therapy became more widely researched for its benefits and was formally considered a therapy for supporting patients.[11]

© 2026 Terra Science and Education

DOI: 10.36838/IJHSR87.211

Music therapy, as well as other supportive and integrative therapies, can significantly benefit cancer patients; however, it is not considered important to many, and awareness of music therapy and other treatments is minimal. According to a study, the issues in accessing adjunctive medicine services were cost and lack of knowledge.[12] This study showed results that when patients were recommended by medical professionals to participate in an integrative therapy service, they showed more interest, compared to their initial interest without any recommendations or additional knowledge. Cost also affected whether patients would be able to take part in the therapy. If fees for integrative therapy services were lower, patients were more likely to be willing to try the services. Complementary and integrative medicine services can be expensive, and many are not covered by insurance, which can pose an issue for patients who cannot afford them. According to an article, music therapy is mainly used in large, wealthy hospitals, further highlighting cost as a barrier.[13] Additionally, misconceptions in preferences due to differences in culture may cause patients to not even consider music therapy as a possible adjunctive benefit.[13] For example, many patients may generalize music therapy to include just classical music, when music therapy can actually entail any music that the patient prefers. It is vital to understand and advocate for the benefits of music therapy and other integrative therapies for patients so that they can be aware of their options and participate in these services. It is also important to address and fix issues, such as cost barriers, to make the services available and accessible for everyone. This study explores how music therapy can support the emotional and psychological well-being of cancer patients during treatment, emphasizing the importance of making music therapy and other integrative therapies accessible and affordable for patients. The study does this by triangulating a patient case with perspectives of a certified music therapist and oncologist, all of whom were interviewed.

Background:

Music therapy can benefit patients with many types of diseases.[14] Existing literature consists of detailed studies that cover a wide range of conditions, such as depression, schizophrenia, dementia, and insomnia.[14] In the context of this research, the most relevant data are studies of music therapy related to oncology and other conditions associated with the mental burden of cancer patients, some common ones being depression, anxiety, difficulty in mood management, and challenges in social communication.[14]

According to a systematic review, patients with depression who engaged in active music therapy, which is when patients actively play an instrument or make music (composing, songwriting), experienced improved symptoms.[14] In fact, music therapy showed better results than psychological therapies. Patients with insomnia experienced better sleep quality after participating in receptive music therapy (listening to music).[14] Another systematic review showed that music therapy improved social connection, symptoms of depression, and quality of sleep in patients with schizophrenia and similar severe mental disorders.[15] Specifically, in a cancer systematic review, cancer patients who participated in music therapy interventions or just listened to music provided by medical staff had an average reduction in anxiety of 11.2 units on the STAI-S scale, their mood improved (SMD = 0.42, 95% CI 0.03–0.81, P=0.03), and they experienced a pain-reducing effect of SMD = -0.59, 95% CI −0.92 to −0.27, P=0.0003.[15] Patients' quality of life was also improved by SMD = 1.02, 95% CI 0.58–1.47, P=0.00001.[15] In a review by Maratos *et al.*, although the nature of the study prevents researchers from being confident in the results, they suggested that music therapy is used by people with depression and helps improve mood.[16] They also found that both music therapy and standard treatment were more effective than only standard treatment for clinician-rated (SMD = 0.98, 95% CI -1.69 to -0.27, 3 RCTs, 1 CCT, n = 219) and patient-reported (SMD = -0.85, 95% CI -1.37 to -0.34, 3 RCTs, 1 CCT, n = 142) depressive symptoms.[16] In another study, people with schizophrenia and schizophrenia-like disorders experienced an improvement in reducing anxiety of SMD = -0.61, 95% CI −1.13 to −0.09.[15] Additionally, their social functioning behavior improved (one RCT, n=70, SMD average endpoint. SDSI score −0.78, 95% CI −1.27 to −0.28).[15] Finally, a study measuring the effects of music on pain relief in children and adults found that participants who participated in some form of music had a 70% higher chance of having pain relief than participants who didn't.[15] All of these benefits can be carried over to patients with cancer, and these benefits from music therapy may help cancer patients cope with their diagnosis and treatment journey and may even improve their physical symptoms as well.

Methods

Study Design:

This case study followed a qualitative interview-based design to explore the role of music therapy in supporting the emotional and psychological well-being of cancer patients. The research focused on gathering subjective experiences and professional insights through semi-structured interviews and written questionnaires.

Participants:

All participants were based in Texas and were initially contacted through email. The patient was a 64-year old male with multiple myeloma. The patient was contacted by asking hospitals and cancer organizations to get the student researcher in contact with the patient. A cancer support organization replied with the information of the patient, who was willing and had agreed to be interviewed. The patient signed an informed consent form to allow the researcher to use the patient's responses in this research. He was interviewed over a phone call.

The music therapist was board-certified and worked part-time at a pediatric hospital. She was contacted by emailing hospitals through the student researcher's network. Originally, the music therapist was going to be interviewed over a phone call, but due to constraints, the interview was replaced with a questionnaire. The therapist provided written responses to structured questionnaires provided by the student researcher.

The music therapist signed an informed consent form to allow the researcher to use her responses in this research.

The doctor was a medical oncologist who worked at a cancer center with over 23 years of experience. He specialized in treating patients from the start of their diagnosis until the end of their treatment, the ultimate goal being to cure the cancer and make the patient's "life as comfortable as possible." The oncologist was contacted by emailing him through the student researcher's network. He also signed an informed consent form to allow the researcher to use his responses in this research, and he was interviewed over a phone call.

Data Collection:

The data were collected during the summer of 2025. The student researcher conducted an interview with the patient (audio-recorded with consent, 25 questions, 41 minutes), received written responses (23 questions) from the music therapist through email, and conducted a phone interview with the oncologist (audio-recorded with consent, 15 questions, 23 minutes). All interviews followed a semi-structured format guided by a list of open-ended questions. Each participant received a unique question set tailored to their role (patient, therapist, doctor), but all focused on the role of music therapy in cancer care.

Informed Consent and Ethics:

No IRB was sought because recruitment occurred outside of a healthcare system. The patient was contacted through emailing people in the student researcher's network, which led to getting in contact with the patient from a cancer support organization. The researcher created an informed consent form for the participants, in which they were informed about the purpose and nature of the study. They had the right to skip any questions, take breaks at any time, and stop the interview at any time. They also had the right to withdraw their consent later on, were anonymous, and were assured secure storage. The interview questions would pose minimal risk to participants, and adult mentorship was received throughout the research process.

Data Processing and Analysis:

Thematic analysis followed Braun and Clarke's six-phase approach, which includes familiarization with the data, generating initial codes, identifying and reviewing themes, manual coding with an audit trail, anonymization, simple triangulation across roles, and producing the final report.[17] Figure 1 below this section summarizes the data collection and analysis process. The student researcher's interest in music was acknowledged and taken into consideration while analyzing. There was no member-checking or second-coder, also noted in Limitations in the Discussion section.

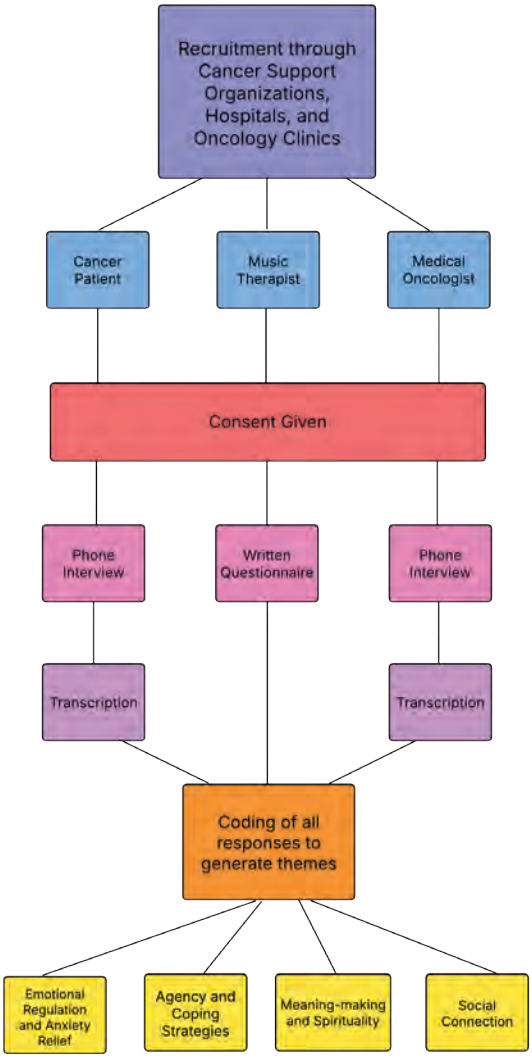

Figure 1: Flowchart of Data Collection and Analysis Process. This research was conducted in the summer of 2025 in Texas, United States. All participants were recruited during this time period and place. The patient, a 64-year-old male, was contacted through a cancer support organization. The music therapist was contacted through the researcher's network at a pediatric hospital. The medical oncologist was contacted through the researcher's network at an oncology clinic. The patient and oncologist were interviewed through phone calls (patient - 41 minutes, 25 questions, oncologist - 23 minutes, 15 questions), and the music therapist provided detailed responses to a written questionnaire (23 questions). The phone calls were transcribed. All participants provided consent for the researcher to use their responses. Coding was performed for all responses to generate themes to highlight: Emotional Regulation and Anxiety Relief, Agency and Coping Strategies, Meaning-making and Spirituality, and Social Connection. Findings indicate that music therapy benefited the patient in these categories, and the responses of the music therapist and oncologist also support this conclusion.

Results and Discussion

All responses provided valuable insight into the role music therapy plays in a patient's cancer treatment journey. The data obtained during interviews and written responses were analyzed and assessed within 5 major categories: 1) emotional and psychological impact of cancer, 2) perceived benefits of music therapy, 3) structural barriers in clinical settings, 4) integration with traditional treatments, and 5) personalization and personal preferences.

DOI: 10.36838/IJHSR87.211

Emotional and Psychological Impact of Cancer:

Cancer is a disease that can be very unpredictable and affect healthy cells too, so patients' motivation often decreases during this time, and their worries often increase.

The patient's cancer journey first started when he experienced double vision. While receiving medical care, doctors noticed an abnormality on the patient's skull and conducted tests to find out the cause. One morning, his doctor called to inform him that the patient had a slow-growing brain tumor. Although the doctor did his best to reassure him and "told [him] not to be upset," the patient was "very upset." He recalled calling his best friend and spending the day together talking about what his diagnosis meant and how it would affect his life. From the beginning, social comfort and support were very important to him in his cancer journey. The patient received his final diagnosis, confirming that he had multiple myeloma.

Along with his diagnosis, the patient's spouse was often away from home and therefore not able to be with the patient. The patient described being alone as difficult, and this caused him to struggle. He also described having "dark and depressive thoughts. The patient also went through physical pain as well. He initially experienced bone pain from the cancer. During his traditional cancer treatments, such as infusions, the patient would experience lots of physical and emotional pain. The oncologist mentioned that anxiety was a common issue patients experienced. He said, "I think the most common anxiety is anxiety of getting diagnosed and the uncertainty of the road that lies ahead." Patients may also fear whether they will be able to be cured or not. Fear and anxiety could lead to depression, which the oncologist said could be "short-lived, or it could persist for a longer period of time, especially if the cancer is not something that can be cured." He also explained that these negative emotional states may also lead to insomnia, with people having difficulty sleeping and even forming relationships with others.

The patient researched information about resources that could help him cope emotionally with his diagnosis, and he became interested in music therapy when he read more about it on a medical resource page. At first, he didn't know music therapy was a recognized therapy, but after learning more, he decided to participate in music therapy sessions.

The patient has been an avid musician since childhood. He enjoys singing, playing the violin, and playing the trombone. He explained, "I actually think music is part of our divine gift" and that we can "create music and then benefit from others." He recalled that music therapy helped him "redirect negative thoughts [and] emotions." He also mentioned that his music therapist assisted him in creating a song playlist, which he called the "Ultimate Coping Playlist." This playlist consisted of songs meaningful to him that helped him change his negative thoughts and "get out of that mindset." The patient and the therapist would engage in songwriting and playing simple instruments. Sometimes, due to the toll of treatments on the patient, he would simply listen to the music therapist singing and playing guitar, and sometimes they would compose, rewrite lyrics, or have improvisation sessions. The patient described some of his music therapy sessions as a "talk therapy session, but with music."

While the treatments helped reduce the patient's physical pain, he emphasized that his music therapy sessions served more as therapy, where his music therapist would talk with him about heavy topics and how cancer was affecting his life. He described that the emotional pain was much more prominent than physical pain and that music therapy helped him quell fears and negative thoughts during his sessions. Music therapy not only helped the patient control harmful emotions, but it also helped him express his feelings and "process all of those emotions." The patient described feeling very thankful after finding out that he had a quick response to his medical treatment. To share his gratitude, he rewrote the lyrics to a song and sang his version with his music therapist. He then sent the recording to his family. He explained that focusing on things he was grateful for was beneficial for him, and he was able to focus on his gratefulness through music therapy. Although the oncologist did not have direct experience with music therapy, he also recognized the importance of supportive care and therapies for cancer patients, including music therapy, psychotherapy, meditation, sound healing, acupuncture, and even dance healing. The music therapist also described some benefits of music therapy, such as physical benefits like "increased movement [and] reduced pain," emotional benefits such as having an "improved mood, compliance with treatment, [and] sense of control," as well as social benefits, such as "improved interaction, [and] normalization of the environment."

Perceived Benefits of Music Therapy:

Patients described music therapy as a meaningful source of support during treatment, with both immediate and longer-term perceived benefits. Music therapy can support a patient's emotional state, provide personal relief, increase hope, and increase motivation.

1. Emotion Regulation and Anxiety Relief:

It is proven that music therapy supports patients in emotion regulation and anxiety relief. According to a study done in India in 2016, music therapy helped in reducing patients' perception of pain and increased quality of life.[18] While discussing pain, the patient explained, "There is a lot of emotional pain, and the music therapy really helped me with that." Cancer may cause patients to get depressed and think many negative thoughts. The patient recalled, "We spent a lot of time working on strategies [for] when I could tell that I was getting into a place where I was going to get more depressive or dark thoughts." These strategies used music therapy to help the patient manage negative emotions and instead focus on positive aspects of life. The music therapist mentioned, "Music therapy is a therapeutic intervention…and its effectiveness is dependent on a multitude of factors…such as the therapeutic relationship between the patient and therapist, the patient's desire to engage in therapy, and the specific goals targeted during therapy." Based on his responses, the patient most likely had a positive relationship with his music therapist, which, according to the music therapist, helped him notably benefit from his sessions. The music

therapist described that, sometimes, "significant changes are apparent immediately upon the start of a session," which is shown by positive responses from patients, such as engagement, motivation, and compliance. This further supports that music therapy can have both immediate and long-term benefits to patients. The music therapist noted that music therapy can cause mental changes as well as physiological changes. She specified, "Physiological changes are more noticeable when working with infants as their vitals speak for them in many ways." The patient rated music therapy a 10/10 as a "treatment in itself," with music therapy being an adjunct therapy. He also rated music therapy an 8/10 for reducing stress and anxiety, an 8/10 for reducing pain, a 9/10 for increasing hope, and a 10/10 for playing a role in fighting cancer. The patient recalled music therapy's benefits for emotions beyond his cancer journey. He said, "Cancer treatment is just one version of how you can use music to help people redirect their thoughts and experience unpleasant emotions in a more positive way."

2. Agency and Coping Strategies:

One strategy that the patient and his music therapist implemented was the "Ultimate Coping Playlist." As mentioned above, the playlist helped the patient overcome a negative mindset. The playlist was made by the patient filling out a song-selection worksheet used to build the playlist meant to cheer up his mood. The patient also improvised with the therapist and listened to music, sometimes listening to his therapist singing or listening to songs on her iPad. The oncologist emphasized the importance of supportive therapies for coping and adherence. He explained, "So many times, patients have a lot of anxiety or depression, and when we do refer them to a licensed psychologist, the interventions…they're able to cope better with their diagnosis, cope better with their treatments, and have an overall well-being, and that they can continue their cancer journey in the best shape possible. So there are interventions that do help, and I do notice people having a significantly improved outlook and sometimes a decrease in side effects."

3. Meaning-making and Spirituality:

The patient also said that he talked about many spiritual topics with his music therapist. He continued, "We talked about connections, a lot about connections, and trying to put this journey in context of my overall life and what was happening." This shows that music therapy may not only help a patient during the treatment time, but it can also have long-term effects and serve more than just a means to calm patients. In the patient's case, he was able to reflect throughout his treatment journey and think more positively.

4. Social Connection:

The patient mentioned rewriting the lyrics to a Johnny Cash song and recording his new version. He shared the recording with his family for the Thanksgiving holiday. Through music therapy, the patient was able to take his cancer journey and turn it into a positive experience, sharing the moment with his family as well. Connecting with family can help cancer patients recover faster and make it easier to carry the emotional burden. In fact, patients consider the support of their families very important.[19]

Structural Barriers in Clinical Settings:

Music therapy is a helpful and vital part of a patient's life by providing supportive care during a patient's cancer journey. However, it is not available and readily accessible in all hospitals and clinics. Hospital visits in the United States are extremely expensive, and cancer treatments involve many advanced-technology machines and drugs, which increase the price of treatments. If music therapy were to be added to every cancer patient's treatment journey, the patient's expenses would increase even more. The majority of the population is middle-class families who do not have the means to spend that much money, so participating in music therapy may seem unnecessary for them, as they want to spend as little as possible. This may prevent patients from having positive experiences throughout their treatments and even boost their mood in fighting cancer. The patient mentioned that cost was not an issue for him as he had good insurance. The music therapist explained that her hospital provides music therapy at no cost to patients and families, so cost was also not a factor in determining whether patients could get music therapy or not. However, the oncologist emphasized that music therapies and other therapies are not covered by insurance, since "the world of insurance doesn't recognize a lot of these [therapies] as beneficial financially." Additionally, he pointed out that to implement music therapy, volunteers and time commitments from the patients are also needed. Patients may not have the time for integrative or supportive therapies or may not be able to afford the cost, which "makes it challenging to [get access to] all [the] extra beneficial treatments." Next, the oncologist said that music therapy was not widely available for patients. The patient also mentioned that he did not have any knowledge of music therapy as a recognized therapy until he came across it on a website and dug deeper into the process. He also described that the music therapist was not a part of his care team at the hospital. The patient had to contact her himself and get her added onto his team so that he could communicate with her. The patient also recalled that during his first hospitalization, he did not see any supportive care as he was "dealing with too many doctors." The music therapist emphasized that there are only three music therapists at her hospital, and all of them are part-time. Most pediatric hospitals in the United States have more resources and staff to provide therapy to patients. Hospitals that treat adults tend not to have adequate music therapy resources. Specialized staff is necessary for music therapy, and the oncologist mentioned that many hospitals and clinics do not have "the support system or the funding." The music therapist discussed that the "lack of adequate staffing" is a significant issue in integrating music therapy more systematically into oncology care. It is difficult to make therapists who do not work full-time attentive, caring, and creative therapists, and even stay longer with the hospital or clinic. Institutional changes need to be made to implement music therapy further in medical settings so that more patients

DOI: 10.36838/IJHSR87.211

can be informed about music therapy and have a positive experience participating in it. Many patients could benefit from music therapy if they were informed about the options. It is important to give the patient the option, and it's crucial to find ways to increase funding and jobs for music therapists in medical settings so that patients can have the chance to experience music therapy. State governments could budget small amounts of money used for other purposes for integrative medicine instead, and hospitals could also budget money for integrative medicine. Hospitals and clinics could spread awareness by hanging posters, making pamphlets for all patients, and even training all doctors to inform patients about integrative medicine service options, such as music therapy.

Integration with Traditional Treatments:

So far, the patient, oncologist, and music therapist have voiced the importance of music therapy in a patient's cancer treatment journey. That being said, music therapy or any supportive therapy should not be seen as a treatment to be used by itself. Music therapy has not been scientifically proven to cure cancer by itself. Instead, music therapy can influence the mind to decrease negative emotions and perception of pain. Therefore, music therapy should be used in addition to traditional cancer treatments such as chemotherapy, radiation therapy, and immunotherapy. Having a calmer mind with less stress and anxiety may reduce perceived symptom burden and support engagement and involvement.

Emotional stability can improve adherence to a treatment. If people don't have the belief in themselves that there is the possibility for their condition to improve, they are less likely to follow up with the treatment. However, if they do believe in their healthcare team and are emotionally stable, they are more likely to take care of themselves, including taking treatments on time and attending appointments. Music therapy and other supportive therapies show promise in helping patients develop emotional stability, which helps patients make better choices for their health and disease care. Music therapists can also help patients feel more valued, which makes them, in turn, more likely to follow through with treatment and engage in appropriate self-care. According to a study in the novel Compassionomics by Stephen Trzeciak and Anthony Mazzarelli, a study of HIV patients that took place at the University of Virginia determined that "compared to patients of the physicians with the lowest compassion, patients of physicians with the highest compassion had more than double the odds of believing that they could successfully adhere to the prescribed regimen."[20] This reinforces that making patients feel valued is beneficial, as it can improve emotional stability and make them more likely to listen to the doctor's recommendations.

Personalization and Personal Preferences:

Music therapy is individualized to the patient's goals. These goals could include mood stabilization, coping with uncertainty, meaning/spiritual reflection, and symptom distraction. When the music therapist was asked which genre of music her patients preferred, she replied that she could not generalize the answer. This was because all of her patients had different goals for music therapy and different personalities that must be accounted for. In order for music therapy sessions to be effective, a single framework cannot be used for all patients. This can apply to any component of a music therapy session, from the type of music listened to all the way to conversations a music therapist may have with their patient. The music therapist pointed out, "Because music therapy is tailored specifically for each individual patient, the purpose and goal in therapy can vary significantly." This suggests that personalization is important and necessary for patients to benefit from the sessions. Different patients may have different worries, and some may experience different emotions and thoughts from others. Using a specific genre of music may work effectively for one patient, but another patient may not like it at all. The session needs to be based around the patient's wants and needs so that their needs can be addressed properly in the sessions. The modality of music therapy sessions can also vary from patient to patient. For example, patients may engage in receptive forms of music, such as listening or relaxing to music, or they may be involved actively, such as participating in singing, improvisation, or songwriting.

The music therapist described, "For my pediatric patients, interventions that provide the patient with opportunities for control are very effective. Hospitalization in general removes a great deal of autonomy and control from patients, so opportunities to provide those elements are often highly effective." The patient explained that sometimes, the music therapist would bring out instruments for him to play, and sometimes, he would compose a song with her. He also mentioned rewriting a Thanksgiving song by Johnny Cash, as he felt very thankful after receiving positive news from his treatment. He sang the song while his therapist accompanied him on an instrument, and he sent a recording of his performance to his loved ones. Specific moments like these can significantly affect a patient's recovery, mood, and stability throughout their cancer treatment journey, thus showing how personal preference and personalization play a role in a music therapy session and potentially a patient's journey.

Limitations:

The student researcher interviewed 3 participants, who consisted of 1 patient and 2 healthcare professionals. This study is not generalizable and should be reconducted with more patients and healthcare professionals to interview. The patient had prior experience with music and considered it an important part of his life. This may lead to bias, and patients who have not engaged in music in the past may not experience the same benefits as the patient in the study. The music therapist did not have experience working with adults, and while the oncologist had experience recommending patients to supportive therapies, he did not have experience with music therapy. Therefore, triangulation can lack precision, and results may not be applied in other contexts. The patient and oncologist were interviewed, so the student researcher was able to quickly follow up on questions for clarity. However, the music therapist provided written responses that did not allow the researcher to ask further questions, which may affect the depth of their re-

sponses and the researcher's analysis. The researcher conducted coding alone, which may affect credibility and reliability. Finally, all participants and the researcher are from Texas, United States, which may cause geographical bias.

Compared to the studies in the Background in the Introduction, findings from the patient, music therapist, and oncologist are very similar. Participants in the studies experienced positive effects from music therapy, and although not all results could be confirmed with confidence, there were overall improvements in many symptoms, and the patient experienced improvements in similar symptoms as well. As a qualitative case study, claims are not generalizable; rather, transferability depends on contextual fit. The author sought to enhance credibility through a semi-structured guide and an audit trail; future work should incorporate member-checking, independent double-coding, and recruit participants without prior musical backgrounds.

Conclusion

This qualitative case study suggests that music therapy can play a valuable role in oncology as a supportive intervention. By integrating the perspectives of a patient, a music therapist, and an oncologist, the study highlights how music therapy may help patients regulate emotions, cope with distress, enhance spirituality, and strengthen social connections. For the patient interviewed, music therapy was described as transformative, offering relief from emotional pain, fostering gratitude, and providing opportunities for creative expression. His consistently high ratings of music therapy's impact on stress, anxiety, pain, and hope underscore its potential clinical significance. The oncologist recognized that supportive therapies such as music therapy may help patients cope by expressing fears and emotions, while the music therapist emphasized the importance of personalization to address the specific goals of each patient, including modality, duration, and level of involvement. Both professionals highlighted that music therapy should be understood as an adjunctive, not curative, treatment.

As a single case study, these findings are not generalizable but highlight important areas for further research. Future research should expand on these findings by interviewing a larger and more diverse sample of patients, including those without prior musical backgrounds, as well as therapists and oncologists with broader professional experience. Larger qualitative and mixed-method studies could clarify how music therapy contributes to emotional resilience, treatment adherence, and quality of life across different cancer populations. If integrated more widely into oncology care, music therapy could significantly benefit cancer patients; however, achieving this will require institutional and budgetary changes, as well as greater awareness among healthcare providers and patients.

Ultimately, this study reinforces that music therapy should be viewed as an adjunctive therapy with the potential to improve the cancer treatment journey in holistic and deeply personal ways. While it cannot cure cancer, music therapy can help patients endure its challenges with greater emotional stability, meaning, and connection. For these benefits to become widely accessible, increased awareness, funding, and institutional support are needed.

Acknowledgments

I would like to express gratitude to Dr. Boris Lozhkin for his valuable and patient mentorship throughout my research process. I would also like to express gratitude to the patient, music therapist, and oncologist for providing their time to answer my interview questions with great depth. Finally, I would like to thank my family for their support during this journey.

References

1. American Cancer Society. What Is Cancer? https://www.cancer.org/cancer/understanding-cancer/what-is-cancer.html. (accessed Aug 28, 2025).
2. SEER Cancer Statistics. Cancer Stat Facts: Common Cancer Sites. https://seer.cancer.gov/statfacts/html/all.html. (accessed Aug 28, 2025).
3. Ferrell, B. R.; Grant, M.; Funk, B.; Otis-Green, S.; Garcia, N. Cancer Patients' Reported Experiences of Suffering. *Cancer Nurs*. **1998**, 21 (5), 289–295. https://journals.lww.com/cancernursingonline/Abstract/1998/10000/Cancer_Patients__Reported_Experiences_of.8.aspx
4. National Cancer Institute. Sadness and Depression. https://www.cancer.gov/about-cancer/coping/feelings. (accessed Aug 28, 2025).
5. Canadian Cancer Society. Family Life. https://cancer.ca/en/living-with-cancer/coping-with-changes/family-life (accessed Aug 28, 2025).
6. Everdingen, M.; Rijke, J.; Kessels, A.; Schouten, H.; Kleef, M.; Patijn, J. Prevalence of Pain in Patients with Cancer: a Systematic Review of the Past 40 Years. *Annals of Oncology*. **2007**, 18, 1437-1449. https://doi.org/10.1093/annonc/mdm056
7. National Cancer Institute. Types of Cancer Treatment. National Institutes of Health. https://www.cancer.gov/about-cancer/treatment/types. (accessed Aug 28, 2025).
8. Berman, R.; Davies, A.; Cooksley, T.; Gralla, R.; Carter, L.; Darlington, E.; Scotté, F.; Higham, C. Supportive Care: An Indispensable Component of Modern Oncology. *Clin. Oncol*. **2020**, 32 (11), 781–788. https://doi.org/10.1016/j.clon.2020.07.013
9. Guarneri, M. The Integrative Health and Medicine Movement: A Historical and Personal Perspective. *Integr. Med.* (Encinitas) **2019**, 18 (5), 28–29. https://www.ncbi.nlm.nih.gov/pmc/articles/PMC7219444/
10. Bradt, J.; Dileo, C.; Magill, L.; Teague, A. Music interventions for improving psychological and physical outcomes in cancer patients. *Cochrane Database of Systematic Reviews* **2016**, 2016 (8), Article CD006911. https://doi.org/10.1002/14651858.CD006911.pub3
11. American Music Therapy Association. Music Therapy Historical Review. American Music Therapy Association. https://www.musictherapy.org/about/music_therapy_historical_review/. (accessed Aug 28, 2025).
12. Hauser, M. E.; Schofield, E.; Rehmani, S.; *et al*. Music as Medicine: Impact of Healing Harmonies on Patient Experience. *JCO Oncol. Pract.* **2021**, 17 (3), e370–e377. https://doi.org/10.1200/OP.20.00471
13. Kang, A.; Rohlfing, R.; Janss, A.; Stafford, R. A Call to Rethink Music Interventions Implementation to Address Health Disparities. *Arts & Health* **2025**, 17 (2), 179–183. https://doi.org/10.1080/17533015.2025.2486064
14. Gassner, L.; Geretsegger, M.; Mayer-Ferbas, J. Effectiveness of Music Therapy for Autism Spectrum Disorder, Dementia, Depres-

DOI: 10.36838/IJHSR87.211

sion, Insomnia and Schizophrenia: Update of Systematic Reviews. Eur. *J. Public Health* **2022**, *32* (1), 27-34. https://doi.org/10.1093/eurpub/ckab042
15. Kamioka, H.; Tsutani, K.; Yamada, M.; Park, H.; Okuizumi, H.; Tsuruoka, K.; Honda, T.; Okada, S.; Park, S.-J.; Kitayuguchi, J.; Abe, T.; Handa, S.; Oshio, T.; Mutoh, Y. Effectiveness of Music Therapy: A Summary of Systematic Reviews Based on Randomized Controlled Trials of Music Interventions. *Patient Prefer. Adherence* **2014**, 8, 727–754. https://doi.org/10.2147/PPA.S6134
16. Aalbers, S.; Fusar-Poli, L.; Freeman, R. E.; Spreen, M.; Ket, J. C. F.; Vink, A. C.; Maratos, A.; Crawford, M.; Chen, X. J.; Gold, C. Music therapy for depression. *Cochrane Database of Systematic Reviews* **2017**, 2017 (11), Article CD004517. https://doi.org/10.1002/14651858.CD004517.pub3
17. Braun, V.; Clarke, V. Using Thematic Analysis in Psychology. *Qual. Res. Psychol.* **2006**, 3 (2), 77–101. https://doi.org/10.1191/1478088706qp063oa
18. Krishnaswamy, P.; Nair, S. Effect of Music Therapy on Pain and Anxiety Levels of Cancer Patients: A Pilot Study. *Indian J. Palliat. Care* **2016**, 22 (3), 307–311. https://doi.org/10.4103/0973-1075.185042
19. Slevin, M. L.; Nichols, S. E.; Downer, S. M.; Wilson, P.; Lister, T. A.; Arnott, S.; Maher, J.; Souhami, R. L.; Tobias, J. S.; Goldstone, A. H.; Cody, M. Emotional Support for Cancer Patients: What Do Patients Really Want? *Br. J. Cancer* **1996**, 74, 1275–1279. https://doi.org/10.1038/bjc.1996.529
20. Trzeciak, S.; Mazzarelli, A. *Compassionomics: The Revolutionary Scientific Evidence That Caring Makes a Difference*. Studer Group, Pensacola, FL, 2019; p 131.

Author

Sanskriti Varshney is a high school senior at Byron Nelson High School in Texas, USA, with a love for music and STEM. She plays the piano, violin, and sings. In college, she plans on majoring in biochemistry or chemistry to learn more about cancer and use her degree to work on finding ways to prevent cancer and treat patients with more ease. She hopes to become an oncologist while also using music to bring joy to others, from friends to patients.

IJHSR
ijhighschoolresearch.org
RESEARCH ARTICLE

The Effects of Social Norms on Decision-Making in Game Theory

Zhang Yiran

Dunman High School, 10 Tanjong Rhu Road, 436895, Singapore; 20060123zyr@gmail.com

ABSTRACT: Game theory has been widely used in many sectors. However, the varying effects of social norms on decision-making in game theory have yet to be discussed. In this research, the author discusses the impacts different social norms have on decision-making, discovering the different significance of various implicit norms and how the codification of norms works. This is done by using primary data to analyze how priorities and rankings of different choices in the Prisoner's Dilemma game theory matrix are changed by norms. This research also explains the reasons why these norms may be weighted differently in the social context chosen, which is Singapore. The author then concludes that there is high potential for further research in this area and modelling of norms by their significance in game theory.

KEYWORDS: Behavioral and Social Sciences, Other, Game Theory, Social Norms, Rationality.

Introduction

Game theory is the study of how choices of economic agents interact to produce outcomes based on their preferences.[1] It is often used to predict decision-making in fields such as economics and business, as well as behavior in social interactions. However, the latter is often overlooked by traditional game theory, as there is a strong focus on mathematical models, often neglecting behavioral aspects of humans that affect decision-making significantly, especially in social settings.[2] This essay will specifically look into the solution concept of Nash Equilibrium (NE) for all analysis, as it is the most commonly used solution in games.[3]

This essay analyses and expands on the Prisoner's Dilemma Game (PDG) to tackle this inefficiency. The PDG is a situation in which two players are faced with a choice: cooperate with each other or defect.[7] Two prisoners, A and B, are arrested for a crime. The police have enough evidence to convict them of a charge, but with missing information on the specific duration of the charges for which they should be charged. Cooperate means not to betray each other, and defect means that they will testify against each other. If both cooperate, they get a 1 year sentence. If both are defective, they get a 2-year sentence. If one cooperates and the other defects, the defector goes free, and the one who cooperated gets a 3-year sentence. PDG assumes that neither prisoner knows the other's decision, and each only acts to minimize their own sentence. The best response for both players in an ideal rational world would be to defect, which is the NE. This dominant strategy results in 2 2-year sentences for both, which is not optimal, as mutual cooperation would have resulted in lighter sentences. Regardless of the other player's decision, each prisoner gets a better outcome by defecting. This is depicted in a matrix in Figure 1. However, they could have yielded a better result if they both cooperated and ended up with a 1-year sentence. From this, we can observe that the NE of the best responses of players may not always be optimal for themselves.

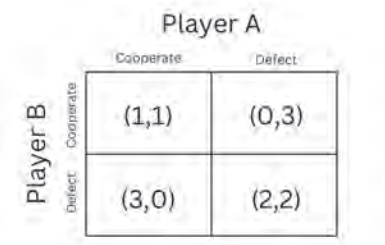

Figure 1: Payoff matrices for PDG, where each cell shows the outcomes for Player A (row) and Player B (column). Mutual cooperation yields (2,2), defection against a cooperator results in the highest individual payoff (3,0), and a mutual defection leads to (1,1).

Issues Related to Traditional Game Theory:

Traditional game theory is useful and widely applied in many fields, such as auction prices, stock market predictions, monetary policies, and duopoly strategies.[5] However, at the same time, due to the utilization of pure mathematics and statistical models, issues and paradoxes arise when game theory is applied in less mathematical but more behavioral contexts.

The first issue lies in the assumption of utility. Agents are utility-maximizing in their decisions, but what is utility exactly? Utility in game theory is a numerical representation of agents' preferences, defined as consistent choice patterns instead of inner motivation.[1] Utility functions then rank these choices, modelling decision-making without assuming anything about emotions or motivations.[1] However, this could be inaccurate depending on varying contexts, as humans may not always be consistent in their choice patterns when they are influenced by different behavioral factors and social norms.

The second issue lies in the assumption of rationality. Game theory assumes that players are economically rational, meaning that they can rank outcomes, understand the connections between decisions and outcomes, and choose the actions that maximize their utility.[1] However, this assumption overlooks the complexity of human nature and behavior, as people often make decisions based on biases, incomplete or imperfect

© 2026 Terra Science and Education

DOI: 10.36838/IJHSR87.219

information, such as impulsive decisions or procrastination. This opposes the assumption made. Furthermore, players also often lack the ability to process all information available accurately due to cognitive limitations, rendering the assumption inaccurate to some extent.[6] These two issues lead to the insufficiency in game theory when considering cultures and social norms, which is the main theme of this essay. Game theory assumes fixed preferences of individuals and does not account for varying contexts of the agents. This includes cultures, social norms, and interpersonal relationships. Players' choices are often influenced by moral considerations, social pressures, cultural expectations, and emotions, which deviate from pure utility-maximization, as the best outcome for each player varies according to these factors.

Behavioral Economics:

Game theory can be critiqued from behavioral perspectives, and hence, the topic of behavioral economics is brought in as it aids understanding of the limitations of traditional game theory. It will be used in the essay to analyze the impacts of social norms on PDG, as well as the incorporation of social norms in the PDG.

Behavioral economics is the study of the psychological factors involved in the decisions of individuals or institutions, and how these decisions deviate from those implied by traditional economic theory.[7] This includes cognitive and social factors. It also combines economic theory and psychology to explain why people make irrational decisions. Behavioral economics takes into consideration the concepts of bounded rationality, social preferences, and cognitive biases to explain why decisions made by agents often do not align with those in traditional economic theories or are suboptimal in their outcomes.[8]

Methodology and Approach:

To dive deeper into the connections between game theory and behavioral economics, I will first conduct a literature review of the existing behavioral and social modifications of game theory by consulting secondary material, acknowledging the limitations and value-adding capabilities of my research.

Afterwards, I will analyze the data obtained from a primary method, which is a survey on game theory and social norms. The survey obtained 80 responses, with respondents coming from a variety of backgrounds, though mainly concentrated in Singapore, such that I can utilize this data to analyze the impacts of different social norms on decision-making in the PDG. Various age groups from age 14 to 70 and above are involved, too, for a better representation of demographics. In the online survey that was conducted, the classic PDG is explained in simple terms to the respondents, where their decision on whether to cooperate or to defect is recorded. Afterwards, it was explained to the respondents that regardless of their choices, the rational theory given by mathematical deduction was to defect, aiding them to understand the PDG and the NE. Then, additional contexts and variations of the original situation were given to respondents regarding the PDG, such as contexts involving concepts of reciprocity, empathy, social pressure, relationships, and quality of life, all of which are altered based on social norms and are not accounted for in the traditional formulation. Data obtained from these questions will then be used for analysis of social norms' impacts on decision-making in later sections, which aids understanding of the issues of game theory and how they could be potentially solved by incorporating behavioral economics.

In this essay, I will argue for the reasons and ways to incorporate social norms and cognitive biases into the typical PDG, such that this model provides a more accurate simulation of players' decisions in real-life business and social contexts. PDG is selected as it is a classic and representative game of game theory. This will be done by carrying out the methodology stated above. Afterwards, I will evaluate the impact of behavioral factors through statistics available, before concluding on their implications and limitations in real-life contexts. The connection between social norms and game theory, as well as the codification of norms, will be addressed, too. The paper ends with a balanced summary, as well as potential avenues for future research. This essay sets the main social context in Singapore, with other societies as supporting examples.

Literature Review

Rationality and Game Theory:

There are multiple ways of categorizing rationality, the most common types being structural, substantive, bounded, and instrumental rationality. While they are all applicable in game theory to some extent, structural rationality serves as the baseline of most models, referring to the coherence and consistency of individuals' decision-making and the identifiable patterns that emerge in their choices. This is contrasted with substantive rationality, which emphasizes normative behavior.[1] This concept of structural rationality is applicable in game theory, as players are assumed to follow logical reasoning, where, for instance, one would choose an option that maximizes their own outcome, which is seen as a coherent move. However, classical formulations of rationality have been challenged by scholars who argue that they fail to capture social and ideological dimensions of decision-making. For instance, ideology itself shapes perceptions of available strategies and payoffs, influencing outcomes not predicted by models.[9] Various types of rationality can be argued to apply in game theory to different extents, as game theory itself has inherent presumptions of rationality. Building on this foundation, it is crucial to examine how these traditional notions of rationality fall short in capturing the complexities of real-world decision-making.

Critique of Rationality:

However, rationality in game theory faces limitations. For example, it does not consider fairness and social norms in the Ultimatum Game, where players often share instead of ending up in the NE.[10] It also neglects emotions, cultural differences, and social norms.[11, 12] Furthermore, people may act in a way such that we obey social rules, but we may not actually believe in it, and it is merely a mindset or values that society believes in,[6] where we are forced to do so to fit in, then it does not directly fit into any type of rationality mentioned. Cooperative strategies in repeated games often emerge even

without external enforcement, suggesting norms and reputational concerns reshape payoff structures.[13] It is challenging to simply categorize complicated human beings into a few types of rationality,[14] and something will fall out of these categories. This restricts the scope of the definition of rationality since people from various cultural backgrounds often do not subscribe to a universal conception. My research addresses this gap by incorporating these cultural and normative factors into game-theoretic analysis and by providing original empirical evidence from Singapore's unique socio-cultural context. By systematically examining how social norms operate within a multicultural society, it extends existing models beyond abstract theory to demonstrate how cultural variation in Singapore's unique demographics impacts game theory models.

Behavioral Game Theory and Its Limitations:

Behavioral game theory builds on traditional game theory to explain experimentally observed violations and human cognitive limitations,[2] by reunifying psychology and economics through the addition of social utility functions, initial conditions, and learning theories into the traditional game theory model. For example, in the PDG, players could hold emotions like hatred towards others, and are willing to sacrifice their own earnings to punish others by cooperating about half the time. This is contrary to the traditional NE, where players end up defecting in the pursuit of self-interest. Players may also only cooperate when knowing the other does so to ensure a better outcome. This makes use of social motives like hatred and fairness, which were left out in the traditional model, enhancing the model to be more inclusive towards general social norms. Experiments also show that cultures affect how Americans and Machiguenga behave differently in the Ultimatum Bargaining Game, where the Americans offer half and reject low offers, and the indigenous Machiguenga offer 15-25% and only reject one offer.[2] This shows that individual behavior depends on moral or fairness norms and social expectations.

To further illustrate, trust games reveal that players are more cooperative than game theory predicts. While models expect investors to offer nothing and trustees to return nothing, experiments show investors risk about half their money and trustees pay back slightly less than what they originally gave.[2] This illustrates reciprocity and inequality-aversion mindsets that players have instead of purely pursuing self-interest. Behavioral deviations can also be better explained when conditional preferences dependent on beliefs about others' expectations are incorporated into models, underscoring the role of normative expectations.[15] My research addresses these aspects with respect to Singapore's context, a setting that remains largely underexplored in existing literature, which primarily focuses on Western contexts or comparisons between Western and non-Western settings.

Behavioral models such as Quantal Response Equilibrium (QRE) and Experience Weighted Attraction (EWA) are also more inclusive of human behavior. QRE accounts for errors in choices and takes greater consideration of bounded rationality, where rationality is limited during decision-making. EWA assumes that each strategy has a numerical attraction, which determines the probability of choosing that strategy, and which can be applied to forecasting and other fields. These models are more reflective of humans' cognitive limitations and use statistical approaches to quantify spontaneity in decisions, providing a more conclusive model that applies to real-life situations.

From this, it is evident that while existing materials and research do have an extensive reach into behavioral aspects of game theory, and there is a growing receptivity towards social norms and behavioral economics, they are often focused on humans' moral considerations and capability limitations. They lack deeper perspectives specific to different cultures, especially in the modern-day context. I contribute by providing primary data from Singapore's context, analyzing how habituated cultural mindsets and beliefs from one's background eventually become culture. While acknowledging that such a notion exists, I will be substantiating it with a more refined analysis of culture, focusing on the formulation of cultures through one's background.

Impact of Social Norms & Culture on Traditional Formulation of Game Theory:

Cultures' impact on game theory was categorized into five sections, including intra-individual consistency, inter-agent consistency, contextual effects, behavioral stickiness, and suboptimal behavior.[16] They argued that cultural behavior emerges when agents play multiple or repeated games, instead of examining isolated, context-free environments in traditional game theory. They also highlighted how different cultures play the same game differently, depending on their experiences of other games. For example, one community played games that involved tit-for-tat, while another played games that developed a pattern of selfishness. When they play the same game, their strategies reflect their past experiences, explaining the suboptimal behavior of players and how cultures are portrayed in the form of experiencing different games, causing players' decisions to differ.

Social norms' impacts on game theory may include identity assertion and group cooperation. For identity assertion, they considered a social norm where a group values punctuality. A person might arrive on time not because it maximizes personal payoff, but because it shows that they are committed to the group. Traditional game theory struggles to explain this, as it expects decisions to be driven by tangible outcomes. In the case of cooperative behavior, like in the PDG, traditional game theory shows that rational individuals will often defect, leading to a worse collective outcome. However, social norms of cooperation can encourage cooperation, which is again difficult to explain in classical game theory. Prior attempts were made to account for social norms as belief-based systems that influence individuals' decisions indirectly, where norms function through mutual expectations rather than direct utility maximization. However, these accounts still face limitations, particularly in explaining the self-reinforcing nature of norms. Individuals may follow norms because they internalize the belief that doing so is part of their identity, not necessarily because they expect a specific future payoff. This is shown by

DOI: 10.36838/IJHSR87.219

how social learning and cultural evolution embed norms across generations, producing patterns that reshape equilibrium selection.[17] Norms may also function as structural mechanisms that organize social interaction, shaping both expectations and sanctioning processes to stabilize group-level cooperation.

This leads me to the insufficiencies of current developments in this area, and how I can value-add to the existing materials. While these papers were insightful in determining the broad impacts of social norms and cultures on game theory decision-making, they do not include the hierarchy of social norms and the varying value assigned to different cultures and norms. This is likely because these detailed analyses were not necessary for the topics they were researching. However, this causes the full picture of how players make decisions in relation to different norms in game theory to be missing, as existing literature only captures the general scene. My approach to collecting data from surveys further expands on the existing framework and adds value in terms of how different cultures affect decisions differently based on the relative weights of these norms or behaviors in different societies. Such an approach dives deeper into how various types of norms and cultures can be drastically different in affecting decision-making, which provides a more in-depth understanding of how game theory is affected and potential solutions to this. My approach also attempts to restructure the definition of culture to include the internalization of social norms over the years, which eventually becomes a culture, thereby explaining the impacts of internalized social norms on game theory decisions in greater detail.

In this paper, I will test these hypotheses. When familial ties are introduced, the cooperation rate increases significantly as family responsibility norms carry the greatest weight. When quality of life is emphasized, respondents are inclined to cooperate. In risk-aversion contexts, respondents tend to avoid the worst outcome, making the ranking of T and R uncertain in the TRPS model. In security contexts, respondents may prefer to remain in prison, lowering the relative importance of T.

By including a variety of age groups from different generations in my survey, my approach takes into account the fact that norms are evolving instead of being static. Through responses of respondents from different generations, evolving mindsets and norms can be reflected, showing how norms and cultures change over time, allowing a more comprehensive modeling to be made in game theory. By providing the TRPS model under the Methods section as a common denominator for discussion, this research makes dialogue on this topic more accessible to all.

In summary, literature such as papers on behavioral game theory by Colin Camerer, culture and game theory by Bernard and Page, and social norms and game theory by Paternotte and Grose was used in my analysis. While they give valuable insights on the impacts of norms and cultures on game theory, they experience inefficiencies in terms of depth, scope, and a comprehensive account on this specific topic, where I will be further diving into through my own survey results and further modelling. In this paper, I will argue that when different norms are introduced, there are different degrees of influence exerted on decision-making, and they will be reflected in changes to the TRPS ranking, which will be further elaborated on in the Methods and Results sections.

Methods

Modelling Using Primary Data:

The traditional payoff matrix of game theory often achieves the aim of providing insights into players' decision-making processes and outcomes. However, it faces limitations when social norms are considered, as norms affect how people weigh different decisions. This causes players to perceive the traditional payoff matrix differently. As such, this section aims to modify the traditional payoff matrix by using the primary data collected and analyzing the impacts of different types of social norms on the matrix.

Data Collection and Analysis Method:

The data collected involves 80 respondents from ages 14 to 70 (Figure 2), where the majority reside in Singapore. As Singapore is a multicultural and multilingual society, with a large Mandarin-speaking population, I surveyed in both English and Chinese, with the English-Mandarin dynamics standing at 50-50. This is where two questionnaires were distributed in the respective languages. This better reflects the reality of demographic diversity in Singapore, where older Singaporeans or less English-fluent residents who may be more comfortable answering in Chinese can also have their views taken into consideration. This reflects the multicultural nature of Singapore and also ensures that responses can be more accurate when respondents answer in a more familiar language. As such, this approach strengthens the credibility, inclusiveness, and representativeness of the paper, featuring a wider scope of the population.

For clarification of the aim and focus of this research, the contexts applied in the data collection and analysis processes come from academic papers and literature, as well as primary data collected in the Singapore society. Contexts refer to the specific experimental variations of the PDG embedded in the survey design, which aid understanding of norms' effects by providing contextual insights. These contexts may come in for the sake of argumentation, where one should not think of them as sociological research of cultures and norms of any society. The primary goal is only to modify and expand the scope of game theory lenses, not to create sociological insights.

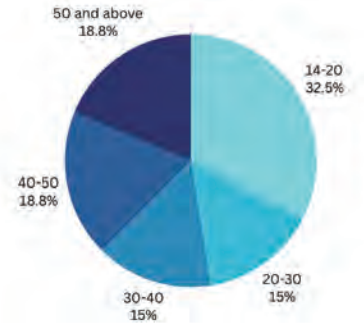

Figure 2: Age range of all respondents of the survey on game theory and social norms, with 32.5% of age 14-20, 18.8% of age 40-50, 50 and above, respectively, and 15% of age 20-30, and age 30-40, respectively.

To carry out the research effectively, considering the constraints of resources, I will use target systems in the following sections for my analysis.[19] Models often do not directly represent reality, but rather target systems, which simplify real phenomena. The target system is selectively constructed in this paper for the Singapore population to gain a useful understanding of the topics in a feasible way.

Traditional Payoff Matrix:

In game theory, for each player, the utility derived can be categorized into four types according to the matrix. This includes: Temptation for one to defect knowing that the other person cooperates (T), Reward for mutual cooperation (R), Punishment when both defect (P), and Staying silent to cooperate while the other player defects (S). The ranking in the traditional payoff matrix for PDG is T>R>P>S, where players rank their preferences for outcomes in this manner, where T is the most preferred, and S is the least preferred.[20] Referring to the PDG matrix shown in Figure 1, a player gains the least number of years in prison, 0 in this case, if he cooperates while the other defects, and hence the temptation for one to defect knowing that the other player cooperates is the highest. On the other hand, a player gains the worst outcome of 3 years of prison if he cooperates and the other player defects, making the incentive to stay silent the lowest. If both cooperate (R), this cooperation brings rewards in terms of 1 year of prison for each player, which for a rational player, is the next preferred option following the case for T. If both defects, this mutual defection brings punishments in terms of 2 years of prison for each player, which for a rational player, by the same logic, is the next preferred option following the case for R. Hence, the ranking in a traditional PDG setting would be T>R>P>S.

Results

Survey Results for the Original PDG Game:

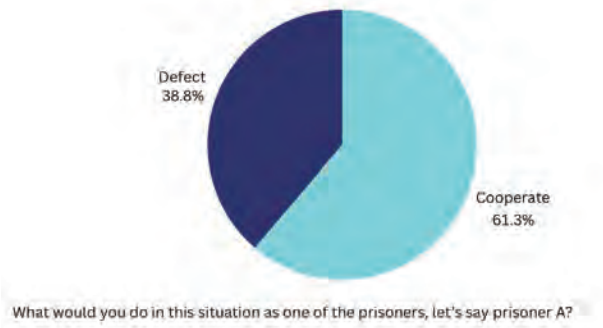

Figure 3: Survey result for original PDG, where respondents take the perspective of a prisoner, where 61.3% cooperate and 38.8% defect.

In the survey results of the original PDG (Figure 3), a majority of the respondents chose to cooperate, whereas only 38.8% chose to defect. Among the 38.8%, the T>R>P>S ranking is retained, where they are tempted to defect given the fewest years if the other player cooperates. In this case, the NE is at P, and for the player who chose to defect, the worst-case scenario is for P to occur if the other player also defects. This follows the ranking of T>R>P>S, reflecting the traditional side of game theory. Among the 61.3%, choosing to cooperate makes the best possible outcome for them to be R. In this case, the NE is still at P, but for the player, the worst-case scenario becomes S, where the other person defects, which gives him a 3-year sentence. This is seen as an intermediate resolution, reflecting the other side of game theory, which is epistemological game theory. Despite the difference in choice between the majority and the minority, both follow the ranking, as players logically rank out their desired outcomes and act accordingly. In the majority of cases, R is chosen as the respondents are highly likely to already know what other players will do, given the social norms. This is where they presume that others will answer irrationally and answer according to habits, experiences, and culture. In such a case, defection is largely disfavored by respondents as it is perceived to contravene prevailing social norms. This causes ⅔ of the respondents to choose R instead of T, since assuming that the other player chooses cooperation, cooperating too obeys the social norms better, and it also brings an acceptable outcome of a 1-year sentence. While they can choose T and disobey social norms, most respondents avoided this option. This shows that in the epistemological case, while the ranking of T>R>P>S remains, people tend to choose the intermediate R instead of T. In either case, R is still more optimal than P.

In this PDG game, it is intuitive to the players, even without much prior understanding of the PDG, that S is the worst-case scenario for a player, since he has both disobeyed the social norms and gotten the longest jail time. Similarly, the position of T in the rank mostly does not change as well, given how it most certainly brings the least number of years in prison. It is R and P that may change in their sequences in the cases we explore later, due to the effects of different social norms and how players weigh them differently.

Survey Result of Game Involving Familial Ties:

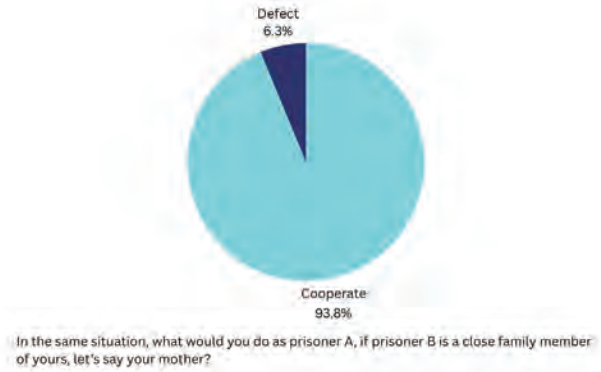

Figure 4: Survey result of PDG involving familial ties when respondents take the perspective of a prisoner, where 93.8% cooperate and 6.3% defect.

In the next part of the survey, I introduced different social norms on top of the traditional PDG settings to analyze how the traditional ranking changes. One key modification involved a close family member. In Figure 4, 93.8% of the respondents chose to cooperate, and only 6.3% chose to defect, when asked "what would you do if the other prisoner is a close family member, let's say your mother?" This overwhelming cooperation reflects norms such as filial piety and familial ob-

DOI: 10.36838/IJHSR87.219

ligation, especially salient in Asian societies like Singapore.[21] Cooperation aligns with this norm, as the result either lies in R or S. In the case of S, the player cooperates while the family member defects, reflecting a willingness to sacrifice their own freedom for their loved ones. In the case of R, mutual cooperation is preferred based on expectations of reciprocal care. Most players prefer R to S, as it satisfies both commitment to the norms and mutual protection. As such, R>=S, as the player is likely to expect that the family member has a responsibility to protect them, though some may value sacrifice regardless of return, suggesting R=S for them. In this case, P may be the worst-case scenario, as both players violate familial norms and imprisonment still occurs. T might be slightly better since at least the family member did not betray the norm. However, there is insufficient information for T and P, and hence we can only conclude that T>=P. Overall, the ranking becomes R>=S>T>=P. While the minority of 6.3% defected, it could be due to selfishness or strained relationships. Traditional economics mistakenly equates rationality with selfishness, assuming that people always act to maximize their own welfare.[22] Consider this as Case 1. However, he shows that people can also act out of sympathy or commitment. Consider this as Case 2. Case 1, which mentions selfishness lies in the minority choices of this question in my survey, is the situation where "rational fools" can lead to morally questionable outcomes, even though the decision to defect may seem rational when pursuing self-interest. Case 2 on commitment aligns with the majority decision of this question, which is also supported by Sen's argument, since players acted out of love and commitment, showing that the norm of caring for loved ones causes decision-making to be followed by the majority, leading to the changes in TRPS ranking. This shows that selfishness can alter the rational basis of behavioral economics theory. Furthermore, this percentage is almost negligible and is the exception, and due to insufficient data, I will not be analyzing this group of responses further.

Survey Result of a Game Involving Different Qualities of Life:

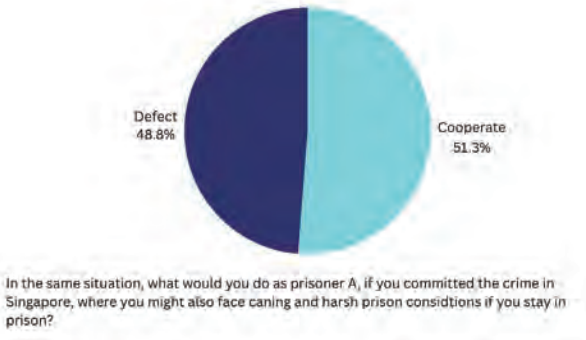

Figure 5: Survey result of PDG involving Singapore's prisons when respondents take the perspective of a prisoner, where 51.3% cooperate and 48.8% defect.

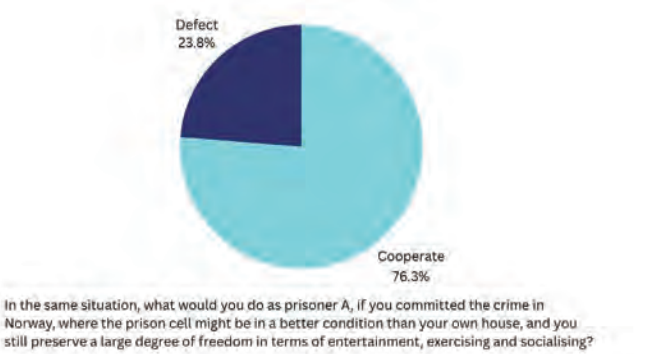

Figure 6: Survey result of PDG involving Norway's prisons when respondents take the perspective of a prisoner, where 76.3% cooperate and 23.8% defect.

Another modification explored the effect of prison conditions. Two similar questions were asked to determine the differences in players' decisions when the conditions of the prisons are different. The former involves committing the crime in Singapore and serving sentences in a Singaporean jail with harsh prison conditions or caning, whereas the latter involves committing the crime in Norway, where the prison cell is in good condition, and prisoners are able to retain a large degree of freedom. Referring to Figures 5 and 6, it can be observed that 25% more respondents chose to cooperate in the Norway setting compared to the Singapore one. This shows that with the norm being concerned about the quality of life, more respondents are willing to stay in a Norwegian jail than a Singaporean one. I will only be analyzing the 25% difference in the responses, as it is more valuable to evaluate this prominent change in responses compared to analyzing the two sets of responses separately due to the limitations of experimentation in this research, which I will elaborate on later in the following sections.

In Singapore, respondents would likely avoid S, since it brings the longest sentence. Due to the harsh conditions mentioned to the respondents, they may not even consider the other player's decision and strongly aim at avoiding S, due to the harsh consequences.[23, 24] In Norway, where jail is far more comfortable,[25] S is no longer the worst-case scenario for the player, since the quality of life is fairly bearable and tolerable. P might be the worst-case scenario, since the player would have violated the cultural norms of loyalty, trust, and integrity by defecting, and still get a 2-year sentence. This makes the ranking change to T>R>=S>P when the Singapore setting is changed to the Norway setting. T would remain optimal to the player, as freedom retains intrinsic value even under improved conditions.

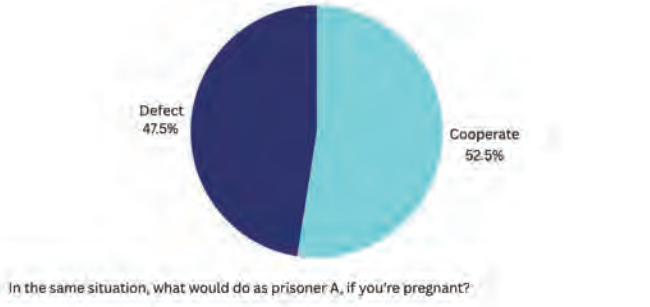

Figure 7: Survey result of PDG involving pregnancy when respondents take the perspective of a prisoner, where 52.5% cooperate and 47.5% defect.

Another modification involves risk aversion. In Figure 7, 52.5% chose cooperation while 47.5% chose defection. Pregnant respondents may seek to avoid imprisonment due to risks such as injury or lack of support. Research suggests that psychological and physical changes during pregnancy may cause risky decisions to be avoided more.[26] To clarify, although the cited paper may include stereotypical representations of women during pregnancy, the analysis of the data in this question refers only to one specific decision-making pathway observed among pregnant women.[27] As highlighted in section 3.2, the aim of this research is not to provide an exhaustive account of all possible strategies but rather to examine this particular pattern in detail. As information on alternative decision-making approaches is unavailable, the relative ranking of T and R is indeterminate. Within this particular framework, the risks posed to the players motivate prioritizing leaving prison, causing them to rank T highly, because it guarantees the least prison time, which allows them to avoid the harsh prison conditions, following the norm of risk-aversion. However, uncertainty about T and R may persist due to imperfect information, explaining the 47.5% who defected. P and S will likely remain the worst, as they bring the most number of years, and S also causes them to break the social chord of risk aversion. In this case, the sequence of TRPS remains the same.

Survey Result of Game Involving Immediate Needs and Security:

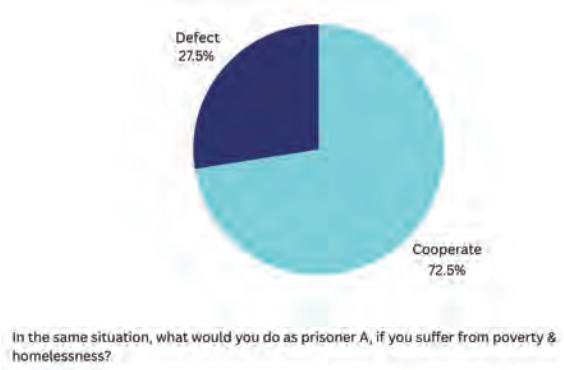

Figure 8: Survey result of PDG involving poverty and homelessness when respondents take the perspective of a prisoner, where 72.5% cooperate and 27.5% defect.

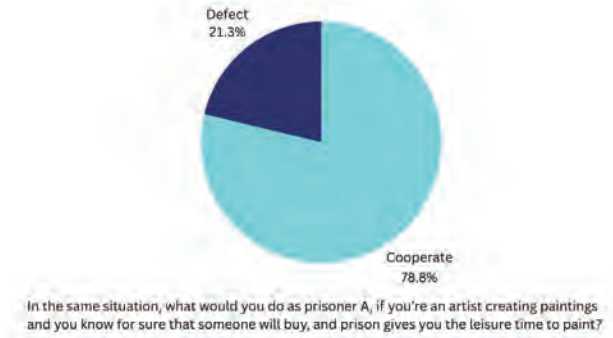

Figure 9: Survey result of PDG involving artists when respondents take the perspective of a prisoner, where 78.8% cooperate and 21.3% defect.

Lastly, the modification is grounded in the concepts of immediate needs and security. For this, I will be analyzing the results of responses for the two questions in Figures 8 and 9, as they involve similar social norms and provide insightful details collectively. In Figure 8, 72.5% chose cooperation while 27.5% chose to defect. In Figure 9, 78.8% chose cooperation, while 21.3% chose to defect. For Figure 8, the cooperation rate is high because of how people suffering from poverty and homelessness may have the immediate and desperate need to find a shelter, a place that provides food and necessities. Research showed that indigenous people value basic needs more, proving that in less-ideal circumstances, immediate concerns are more heightened than other goals, such as long-term impacts of confinement. This aligns with how those suffering from poverty may value urgent needs much more highly.[28] This reflects the norm of seeking environments that fulfil their immediate needs and provide security. In fact, in Asian societies, certain people suffering from poverty even commit crimes to purposely enter jails for the necessities and security, proving that they may even prefer prison conditions out of desperation.[29] Similarly, for Figure 9, which has a similar cooperation rate, an artist creating paintings may value the prison environment for providing a period of time for them to create their paintings without disturbance from work or other obligations. In these two cases, cooperation is preferred by a majority of the respondents because the players are willing to spend more time in prison due to the above-mentioned reasons. This suggests that T is not prioritized as it is in the traditional theory, since the social norm of seeking instant security and fulfillment of needs is followed by players, causing them to favor strategies that allow them to stay in jail for a longer period of time. While this shows that T is not the most favorable option, its exact position in the ranking is unknown, as the ranking of R, P, and S may vary largely depending on individual thinking and decision, causing the ranking to be indeterminate. Hence, this data is only able to show that this specific norm changes the position of T. While 21.3% defect, this is the minority, which could be because the players still value freedom extremely highly. Certain artists may also think that they will not thrive in captivity and gain inspiration from having freedom, such as through being in nature or having exposure to other artwork. For them, the TRPS ranking may remain.[30]

Discussion

Differing Value for Various Social Norms:

From the four types of norms established, including familial ties, quality of life, risk aversion, and immediate needs and security, we can observe the differences in how they affect the traditional TRPS ranking. For the game involving Norwegian prisons (Figure 6), the game involving poverty and homelessness (Figure 8), and the game involving artists (Figure 9), they have cooperation rates of 76.3%, 72.5%, and 78.8%, respectively. The similar cooperation rates suggest that players in my survey value quality of life and immediate needs, and security, similarly, assigning similar significance levels to these two norms. This is logical, as these two norms are all centered

DOI: 10.36838/IJHSR87.219

around one's own needs, such as comfort, desires, and pursuits. For the situation involving familial ties (Figure 4), 93.8% of players chose to cooperate, showing that the norm of having pure altruism for loved ones carries the highest weight among the other types of norms. This also reflects the reality of decision-making, where players in my survey value their loved ones' well-being more than their own. In situations involving dire consequences (Figure 5) and risk-aversion (Figure 7), it can be seen that 51.3% and 52.5% chose cooperation, respectively. This shows that players weigh norms involving consequences or risks the least among the norms. As such, we can observe that various social norms have different levels of significance in the decision-making processes of players. Thus, this reflects the limitations of existing literature on social norms and cultures again, as they do not account for the different values of norms for the benefit of their own papers.

Constraints of Research and Summary:

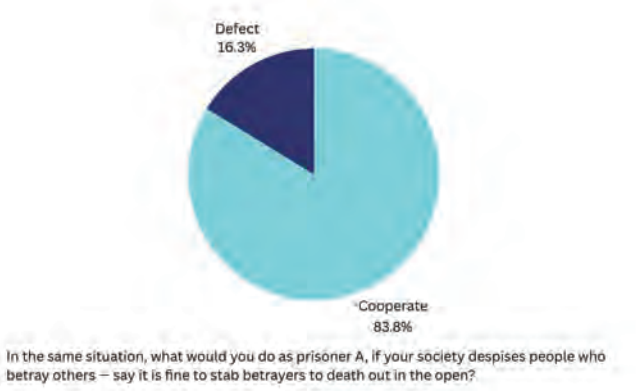

Figure 10: Survey result of variation of PDG when respondents take the perspective of a prisoner, where 83.8% cooperate and 16.3% defect.

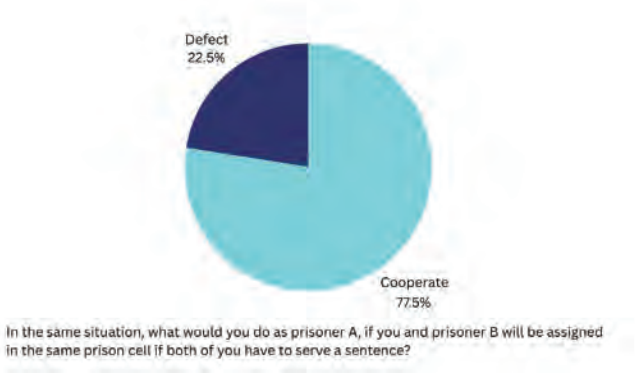

Figure 11: Survey result of another variation of PDG when respondents take the perspective of a prisoner, where 77.5% cooperate and 22.5% defect.

However, I would also recognize the constraints and limitations of this research. Firstly, due to the lack of resources and capacity to conduct experiments, the primary data collected is in the form of a survey. This could be limited since I can only analyze and assume the decision-making processes of the players, as well as the norms. However, while there is no specific mention of the norms, they are more implicitly built into the questions, which allows me to analyze their responses critically and understand the effects of norms on them. The lack of data and information also leads to unknown norms of some questions in the survey, limiting the extent to which I can analyze their responses, which is why I excluded certain scenarios in my research. For example, Figures 10 and 11 were not analyzed in detail, as they lack data on the implicit norms, and the norms are also not obvious; hence, I am unable to conclude that players are likely to consider certain norms during their responses. Based on the data available and missing information on norms, I am only able to assume that in these cases, the traditional TRPS ranking is followed, which provides little valuable insight. However, from the variations I analyzed, I was already able to draw insights into the relative weights of norms and their impacts on decision-making.

Due to the limitations of the software used to compute percentages through pie charts, I would also like to clarify that the percentages of cooperation and defection may not add up to 100%, but may be slightly more than 100%, as the software rounds up the decimal places of cooperation and defection individually.

The survey sample was created through voluntary participation, with respondents recruited via online distribution channels accessible to a wide demographic. While the sample was not probabilistic in the strict statistical sense, it aimed to approximate diversity by including participants from multiple age groups and linguistic backgrounds. All responses were collected and analyzed in compliance with ethical standards in social science research, where participants were informed of the purpose of the study, assured anonymity, and confidentiality of their responses.

Overall, the data collected shows how the traditional ranking of TRPS is challenged when norms are implicitly taken into consideration. It can also be observed that various norms have different values when respondents consider them in decision-making in the PDG.

Constitutive Connection Between Norms and Game Theory:

The previous sections have established that norms are a constitutive part of game theory, particularly the PDG, which was analyzed. From existing research papers, it is shown that different cultures, such as indigenous groups, could be less influenced by social motives, reciprocity, and inequality-aversion mindsets, and cognitive constraints have also been taken into consideration by EWA. This proves that social norms have an impact on game theory, and some have modelled these impacts to make more inclusive models. My research analyzes how implicit social norms based on different cultures lead to different significance of varying norms when players make decisions. It can be seen that by understanding the changes in the TRPS ranking, norms, including familial ties, quality of life, risk aversion, and immediate needs and security, have different significance when players make decisions in the PDG setting. It can be observed that in Singapore's society, familial ties have the highest significance due to the greatest deviation in the TRPS ranking, reflective of the filial piety in Singapore. This has a significantly more distinct impact compared to other norms, such as risk aversion. This shows that norms cannot

be discussed and viewed as a collective aspect, but should be viewed distinctly, as each norm may have a different impact on game theory. The varying extent of impact on decision-making emphasizes the importance of analyzing and incorporating norms into game theory, so that they can be applied to wider contexts.

Codification of Norms in Survey:

Norms can come in implicit or explicit ways. In "Nudge" by Richard Thaler and Cass Sunstein,[31] experimental results show that among various types of information given to taxpayers to incentivize tax compliance, only one method worked well. It was when the taxpayers were told that 90% of those in their state had already complied in full with their obligations under the tax law. This is a form of an explicit norm, where people are explicitly told about the norm, and hence they are pressured to follow it.

However, social norms are often more implicit than explicit. In the Outline of Theory of Practice,[32] it was shown that through habitus, people internalize norms unconsciously from their social environment. They act in ways that "feel natural" without being taught formal rules. This notion is also apparent in my research, where norms are implicitly embedded in practice and not openly stated. This is done by phrasing the questions in such a way that respondents act according to implicit norms when answering. For example, in the situation involving familial ties, respondents largely chose to cooperate, as it is an implicit norm to prioritize the well-being of their loved ones, which guides their behavior subtly, not through explicit instruction. In the situation involving quality of life, the norm may be even more codified, as chasing a better quality of life may be more intrinsic. The extent of codification of norms may vary for different contexts, but this codification occurs not only for single norms, but for norms as a whole. This codification allows respondents to make decisions in PDG without having to consider the norms, but they are built in. This allows the variations of PDG to be analyzed, as the responses are based on the norms with no explicit mention, avoiding leading questions, and allowing for more accurate analysis of the data. It also emphasizes the importance of studying social norms in game theory, as they are always present when players make decisions and cannot be ignored.

Decision-making Based on Norms:

In the data, it can be observed that players make decisions based on norms as heuristics, even when they have been provided the NE in the original PDG, as mentioned in section 1.5. This is where the respondents were told that "regardless of their responses, the solution that players will choose in an ideal rational world would be to both defect, as they would both want to go free, but end up with a 2-year sentence each. This is because no matter what the other person does, each prisoner gets a better outcome by defecting. If B cooperates, A should defect because going free is better than serving 1 year. If B defects, A should also defect because serving 2 years is better than serving 3. So, in both cases, A's best choice is to defect regardless of B's strategy. The same reasoning applies to B, so both prisoners will end up defecting. However, they could have yielded a better result if they both cooperated and yielded a 1-year sentence." This indicates that players do not necessarily prioritize utility-maximizing strategies when faced with social or moral considerations. Instead, their behavior reflects a tendency to conform or follow expectations such as reciprocity and risk aversion. They make these decisions through mental shortcuts presented by the internalization and codification of social norms. This deviation reflects that incorporating norms into models could significantly improve the reliability of such models, especially in real-world strategic interactions where trust, cooperation, and norms matter.

■ Conclusion

This research paper first studied the concepts of rationality used in game theory, acknowledging its limitations in scope and inclusivity. Then, I discussed existing literature and its implementation of norms and behavioral aspects, while using primary data and analysis to explore the varying impacts of different norms on decision-making, which is missing from existing work. Afterwards, I elaborated on the primary data collected in Singapore, categorizing the responses into different categories of norms. I showed that social norms significantly influence decision-making in the PDG, causing deviations from the traditional TRPS ranking. Different norms, such as familial ties, quality of life, risk aversion, and immediate needs and security, carry different weights, with familial ties having the strongest impact in Singapore's context. This highlights the importance of analyzing norms individually instead of collectively, and incorporating them into game theory to better reflect real-world decision-making. Social norms in my survey are implicit and internalized, aligning with existing literature. The survey questions are also designed so that respondents unconsciously follow these norms without explicit awareness. This implicit codification allows respondents to make natural decisions in the PDG, enabling a more accurate analysis of how norms affect behavior. The research underscores that social norms are always present in decision-making and should not be ignored in game theory models.

This research has limitations due to the constraint of relying on survey data instead of experiments, which restricts the analysis to interpreting players' decision-making and implicit norms. Some scenarios also lack clear information on norms and were excluded from detailed analysis. Despite this, the study still provides valuable insights into how norms influence decision-making. While the sample size could be small, rigorous inclusion criteria of a smaller context ensured that the sample was highly relevant and representative of the target population. The findings are also consistent with prior research and evidence provided, which supports their validity despite the limited sample size. Future studies with larger samples are encouraged to further validate these results. While my methodology is not as controlled as existing frameworks, it understands society as a whole and modifies the existing sequence of game theory. The deeply reflective questions of experiences

DOI: 10.36838/IJHSR87.219

that are tangible and accessible to participants raise the significance of my research further.

As discussed above, social norms are deeply embedded in decision-making in game theory. It also cannot be ignored since it is internalized, and each norm carries varying weights. This leads to many potential avenues of future research. It can include further and deeper research on the varying significance levels of norms in a controlled environment with more experimental resources, and using norms from different cultures. This could be comparing cross-cultural behavioral responses in other games, such as coordination games and trust games. Furthermore, this field also has many opportunities in modelling norms into game theory models. Prior attempts to integrate social preferences into utility functions provide a foundation for developing mathematical and philosophical frameworks that explicitly model the perceived value of norms within payoff structures, including both material payoffs and normative components. Future research could build on existing cross-cultural experiments and extend these approaches to explore how such differences influence strategic behavior. This would allow a more comprehensive view of game theory to be achieved in social contexts, allowing it to be more widely applicable to less mathematical fields.

Acknowledgments

I would like to express my deepest gratitude to Indigo Research and Dikshit Bhagabati from the University of Cambridge for the support and guidance provided along the way of curating this research. This assistance empowered and encouraged me to explore the area of study freely.

References

1. *Game Theory (Stanford Encyclopedia of Philosophy)*. https://plato.stanford.edu/entries/game-theory/.
2. Camerer, C. F. *Behavioral Game Theory: Experiments in strategic interaction*; 2003.
3. Nash, J. Equilibrium points in N-person games. *Proceedings of the National Academy of Sciences*, 36(1), 48-49, 1950.
4. *Prisoner's Dilemma (Stanford Encyclopedia of Philosophy)*. https://plato.stanford.edu/entries/prisoner-dilemma/.
5. Gibbons, R. *A primer in game theory*; 1992.
6. Cook, K. S.; Levi, M. *The limits of rationality*; 1990. https://doi.org/10.7208/chicago/9780226742410.001.0001.
7. Teitelbaum, J. C.; Zeiler, K. *Research Handbook on Behavioral Law and Economics*; 2018. https://doi.org/10.4337/9781849805681.
8. Kahneman, D. Maps of Bounded Rationality: Psychology for Behavioral Economics. *American Economic Review* 2003, *93* (5), 1449–1475. https://doi.org/10.1257/000282803322655392.
9. Barrett, J.; Global Priorities Institute; Faculty of Philosophy; University of Oxford. *Ideology Critique and Game Theory*; 2022; Vol. 52–7, pp 714–728. https://doi.org/10.1017/can.2023.10.
10. Fehr, E.; Schmidt, K. M. A theory of fairness, competition, and cooperation. *The Quarterly Journal of Economics* 1999, *114* (3), 817–868. https://doi.org/10.1162/003355399556151.
11. Bicchieri, C. *The grammar of society*; 2006.
12. Henrich, J.; Boyd, R.; Bowles, S.; Procec, C.; Fehr, E.; Gintis, H.; McElreath, R. In search of Homo Economicus: Behavioral Experiments in 15 Small-Scale Societies. *American Economic Review* 2001, *91* (2), 73–78. https://doi.org/10.1257/aer.91.2.73.
13. Colman, A. M.; School of Psychology, University of Leicester, Leicester LE1 7RH, United Kingdom. *Cooperation, Psychological Game Theory, and Limitations of Rationality in Social Interaction*; Cambridge University Press, 2003; Vol. 26, pp 139–198. https://www.le.ac.uk/home/amc.
14. Simon, H. A. *Models of Bounded Rationality*; 1997. https://doi.org/10.7551/mitpress/4711.001.0001.
15. Bicchieri, C.; Sontuoso, A. Game-theoretic Accounts of Social Norms: the role of Normative expectations. In *The Handbook of Experimental Game Theory*, Capra, C. M., Croson, R. T. A., Rigdon, M. L., Rosenblat, T. S., Eds.; Edward Elgar Publishing, 2020; pp 241–255.
16. Bednar, J.; Page, S. E. Can game(s) theory explain culture? The emergence of cultural behavior within multiple games. *Sage Publications*, 2008.
17. Henrich, J. Game theory in cultural evolution. In *Chapter 34*, 2021.
18. Paternotte, C.; Grose, J. *Social Norms and Game Theory: Harmony or Discord?*; Oxford University Press, 2013; Vol. 64–2013, pp 551–587. https://doi.org/10.1093/bjps/axs024.
19. *The Oxford Handbook of Philosophical Methodology*; 2016. https://doi.org/10.1093/oxfordhb/9780199668779.001.0001.
20. Gold, N.; Colman, A. M. Team reasoning and the rational choice of Payoff-Dominant outcomes in games. *Topoi* 2018, *39*(2), 305–316. https://doi.org/10.1007/s11245-018-9575-z.
21. Filial piety remains strong in Singapore. *The Straits Times*. December 18, 2023. https://www.straitstimes.com/opinion/st-editorial/filial-piety-remains-strong-in-singapore.
22. Sen, A. K. Rational Fools: A critique of the behavioral foundations of economic theory. *Philosophy & Amp Public Affairs*_1977, *6* (4), 317–344.
23. Ored, A. *Life inside Singapore's Changi prison: Tough justice for some, no mercy for others*. SBS News. https://www.sbs.com.au/news/dateline/article/life-inside-singapores-changi-prison/mqady6r29.
24. Transformjusticesg. *Getting caned by the Singaporean state*. Transformative Justice Collective. https://transformativejusticecollective.org/2023/10/20/getting-caned-by-the-singaporean-state/.
25. Johnsen, B.; Granheim, P. K.; Helgesen, J. Exceptional prison conditions and the quality of prison life: Prison size and prison culture in Norwegian closed prisons. *European Journal of Criminology* 2011, *8* (6), 515–529. https://doi.org/10.1177/1477370811413819.
26. Chen, J.; Guo, Y.; Liao, Z.; Xia, W.; She, S. Does pregnancy make women more cautious and calm? The impact of pregnancy on risk decision-making. *Judgment and Decision Making* 2020, *15* (5), 807–822. https://doi.org/10.1017/s1930297500007944.
27. The sexual experience: Michel Foucault and the history of Sexuality. *Murdoch University* 2013.
28. Holcombe, S. E. *Remote Freedoms: Politics, personhood and human rights in Aboriginal Central Australia*; 2018.
29. Japan's elderly are lonely and struggling. Some women choose to go to jail instead. *CNN*. 2025. https://edition.cnn.com/2025/01/18/asia/japan-elderly-largest-womens-prison-intl-hnk-dst.
30. Kbarre. *Where Does Artistic Inspiration Come from? | Lifelong Exchange*. https://wordpress.fau.edu/lifelongexchange/2016/11/15/where-does-artistic-inspiration-come-from/.
31. Thaler, R. H.; Sunstein, C. R. Nudge: improving decisions about health, wealth, and happiness. *Choice Reviews Online* 2008, *46* (02), 46–0977. https://doi.org/10.5860/choice.46-0977.
32. Bourdieu, P. *Outline of a theory of practice*; 1977. https://doi.org/10.1017/cbo9780511812507.

Authors

Zhang Yiran is a committed researcher and student at Dunman High School, with a passion for behavioral economics and game theory. Her work navigates the intricate connection between the two fields through the lens of norms. Apart from academics, she also enjoys musicals and is actively engaged in school projects.

Annex A: Survey questionnaire

- What is your age range?

Some context: What is the Prisoner's Dilemma Game (PDG)?

The Prisoner's Dilemma is a situation in which two people are faced with a choice: cooperate with each other or defect (testify against the other). Here's how it works in simple terms:

- Two prisoners A and B are arrested for a crime. The police have enough evidence to convict them on a charge, but with missing information on the specific duration of the charges that should be charged.
- Each prisoner has two options:

1. Cooperate (stay silent and not betray the other).
2. Defect (testify against the other).

If both cooperate, they get a 1 year sentence each. If both defect, they get a 2 years sentence each. If one cooperates and the other defects, the defector goes free (0 year sentence), and the one who cooperated gets a 3 years sentence.

- What would you do in this situation as one of the prisoners, let's say prisoner A?

Regardless of your response, the solution that players will choose in an ideal rational world would be to both defect (fyi, this is called the Nash equilibrium), as they would both want to go free, but end up with a 2 years sentence each. This is because no matter what the other person does, each prisoner gets a better outcome by defecting. If B cooperates, A should defect because going free is better than serving 1 year. If B defects, A should also defect because serving 2 years is better than serving 3. So, in both cases, A's best choice is to defect regardless of B's strategy. The same reasoning applies to B, so both prisoners will end up defecting. However, they could have yield a better result if they both cooperate and yielded a 1-year sentence. From this, we can observe that the decisions of players may not always be optimal for themselves.

However, people do not always make decisions in this manner, as there are often more considerations to make in different contexts. To examine this, I would need your help to answer the following questions. There is no right or wrong, so just choose based on your actual opinions, life experiences, and notions of what is ethically or culturally right!

- In the same situation, what would you do as prisoner A, if prisoner B is a close family member of yours, let's say your mother?

- In the same situation, what would you do as prisoner A, if your society despises people who betray others--say, it is fine to stab betrayers to death out in the open?

- In the same situation, what would you do as prisoner A, if you and prisoner B will be assigned in the same prison cell if both of you have to serve a sentence?

- In the same situation, what would you do as prisoner A, if you committed the crime in Singapore, where you might also face caning and harsh prison conditions if you stay in prison?

- In the same situation, what would you do as prisoner A, if you committed the crime in Norway, where the prison cell might be in a better condition than your own house, and you still preserve a large degree of freedom in terms of entertainment, exercising and socialising?

- In the same situation, what would you do as prisoner A, if prisoner B is suffering from a serious disease and might only have few years to live?

- In the same situation, what would you do as prisoner A, if your society have poor rehabilitation programmes and employment becomes a challenge after you finish serving your sentence?

- In the same situation, what would you do as prisoner A, if you're pregnant?

- In the same situation, what would you do as prisoner A, if you know that you bear a larger responsibility than prisoner B for committing the crime? (For instance, you were the one who planned and executed the crime in its entirety while the other person just happened to be there at the scene of crime. The police have therefore arrested the other prisoner as an accessory to the crime although they had no intentions of committing it themselves. Only you and the other person know this, no one else.)

- In the same situation, what would you do as prisoner A, if you're an artist creating paintings and you know for sure that someone will buy, and prison gives you the leisure time to paint? (Assume that you have little time to do so on normal days)

- In the same situation, what would you do as prisoner A, if both of you initially agreed to cooperate even before committing the crime?

- In the same situation, what would you do as prisoner A, if you suffer from poverty & homelessness?

DOI: 10.36838/IJHSR87.219

IJHSR
ijhighschoolresearch.org
RESEARCH ARTICLE

Application of NASA's General Mission Analysis Tool (GMAT) in Replicating and Optimizing Historical Interplanetary Trajectories

Adesh Krishnan

St. Joseph Institution International, 490 Thomson Rd, Singapore 298191, adeshkrishnan0@gmail.com
Mentor: Steve Bullock

ABSTRACT: This study investigates the limitations of numerical optimization tools in replicating historical interplanetary mission trajectories. Using NASA's General Mission Analysis Tool (GMAT), two gravity-assist missions, Voyager 2 and Pioneer 11, were reconstructed based on publicly available ephemeris data and mission parameters. Historical estimates of the total delta-v (Δv) required for all Trajectory Correction Maneuvers (TCMs) were derived from published propellant mass and engine performance data. These values were compared to the total Δv generated by GMAT-simulated equivalents of each mission. In both cases, GMAT produced trajectories that required significantly higher total TCM Δv than the historical missions despite attempts at further optimization. These results demonstrate a clear divergence between numerical solver outputs and the solutions implemented during the original missions. The discussion examines potential causes for this discrepancy, including the limitations of GMAT's numerical solvers in planning and optimizing interplanetary space missions.

KEYWORDS: Engineering Mechanics, Aerospace and Aeronautical Engineering, Physics, Orbital Mechanics, Spacecraft Mission Planning.

Introduction

Gravity assists have played a critical role in enabling highly efficient interplanetary trajectories, allowing spacecraft to reach distant targets that would otherwise be inaccessible with available propulsion technology. By carefully maneuvering a spacecraft to pass close to a planet, mission planners can exploit the planet's gravity to alter the spacecraft's velocity and trajectory without expending large amounts of fuel. This technique has been pivotal in advancing deep space exploration, enabling missions to maximize scientific returns within the mass and power constraints of available launch vehicles.[1,2]

Designing such missions is an incredibly complex task. The trajectory must be timed with precision to ensure that each planetary encounter produces the desired change in velocity and trajectory. Even small deviations in timing or position can compound over large distances, leading to missed encounters or large corrective maneuvers downstream.

Two early examples of successful gravity-assist missions are NASA's Pioneer 11 and Voyager 2. Pioneer 11 launched on April 5th, 1973, and relied on a Jupiter flyby for a gravitational boost towards Saturn and completed its flyby of Saturn in September 1979 (a mission duration of over six years). It became the first spacecraft to closely study Saturn, revealing new findings including Saturn's outermost ring (the F ring), an additional moon, and the composition of Saturn's atmosphere.[3]

Voyager 2 launched on August 20th, 1977, and executed a historic "Grand Tour" of the outer planets, including flybys of all four gas giants over approximately twelve years (Neptune flyby in August 1989). It remains the only spacecraft to visit both Uranus and Neptune, capturing the first up-close images and data from these planets. Voyager 2 discovered Neptune's Great Dark Spot, fastest planetary winds, six new moons, and four rings, marking groundbreaking advances in our understanding of the outer solar system.[4]

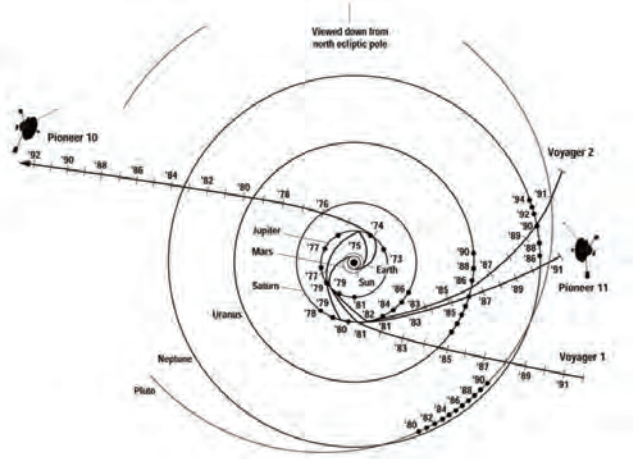

Figure 1: Trajectories of the Pioneer and Voyager spacecraft in the solar system, viewed from above the north ecliptic pole (*NASA – Public Domain*).[5]

The mission design tools available in the 1970s were far more limited than those in use today. In the 1960s–70s, trajectory planning relied more on analytical methods and approximations, as the computer technology of the time made high-fidelity numerical simulations infeasible. Mission analysts manually applied celestial mechanics equations, which led to forced approximations. By the 1990s, advances in computing power and numerical methods led to the development of more sophisticated mission-planning software, enabling broad

© 2026 Terra Science and Education

DOI: 10.36838/IJHSR87.230

numerical searches that could evaluate vastly more trajectory options. This shift made possible missions such as Genesis and Dawn, which required capabilities beyond what 1970s technology could support. Today, even basic computers can integrate full equations of motion and simulate complete gravitational models, making numerical optimization the standard for trajectory design. Nevertheless, important limits remain: gravity-assist tours are typically sought via time-consuming, broad numerical searches over many possible flyby combinations, and the discrete nature of these searches means it is still easy to step past promising trajectories. As a result, analysts may be uncertain whether a mission concept is fully optimized or whether the software missed a better solution.[6]

NASA's General Mission Analysis Tool (GMAT) is a prominent example of this kind of software. It is a modern, open-source mission design software capable of spacecraft trajectory propagation and optimization.[7] GMAT represents a class of software that became available in the late 20th and early 21st century, along with other powerful trajectory design software such as JPL's Mission Analysis, Operations, and Navigation Toolkit Environment (MONTE) and Astrogator.[7,8]

This study addresses the application of NASA's General Mission Analysis Tool (GMAT) in replicating and optimizing historical interplanetary trajectories. Understanding the capabilities and limitations of GMAT in this context is essential for accurately assessing the performance of modern trajectory optimization software, setting realistic expectations for its use in both reproducing past missions and supporting the planning of future ones. By comparing GMAT-generated trajectories with the actual results of historically successful missions, this research aims to evaluate how contemporary numerical optimization tools perform when tasked with designs originally produced under the technological and operational constraints of earlier eras.

Hypothesis:

In this study, mission efficiency will be evaluated using the total Δv from all TCMs required to complete each spacecraft's trajectory. This Δv will serve as a proxy for fuel consumption, providing a quantifiable metric for comparing simulated results against historical missions. For Voyager 2 and Pioneer 11, historical TCM Δv estimates will be derived from published propellant mass and specific impulse (Isp) data, as exact recorded values are unavailable.

GMAT's numerical solvers will be used to replicate each mission's original planetary encounter sequence, which in this case is from Earth to Jupiter, Saturn, Uranus, and finally Neptune (EJSUN) for Voyager 2 and the Earth to Jupiter, then Saturn sequence for Pioneer 11. GMAT will then calculate the TCM Δv for each optimized trajectory, and the summed maneuver Δv values will be compared directly with historical estimates. This will provide insight into GMAT's capabilities and limitations in replicating and optimizing historical interplanetary missions.

It is hypothesized that GMAT's numerical solvers will not only replicate but also potentially optimize the trajectories of these missions by reducing total TCM Δv relative to historical estimates, thereby improving fuel efficiency.

Background:

Numerical vs. Analytical Methods:

Analytical methods in orbital mechanics aim to solve the equations of motion using exact mathematical expressions. These rely on simplifying the problem, such as reducing it to a two-body interaction, so that the equations can be solved directly. However, realistic missions rarely allow for purely analytical solutions because the required assumptions, such as neglecting relativistic corrections or solar radiation pressure, will reduce how accurately the model represents the real mission environment.[10]

Numerical methods, on the other hand, calculate spacecraft motion step-by-step, updating the position and velocity over small intervals of time based on the forces acting at each step. This process, known as numerical integration, produces an approximate solution that can be made more accurate by reducing the step size. Before digital computers, these calculations were done manually using finite-difference formulas, which required function values from several previous steps to start a new calculation. These "start-up procedures" made it difficult to change the step size during integration.[11]

Runge–Kutta methods, which do not require values from earlier steps, became popular because they were easier to apply at the start of an integration and allowed greater flexibility, such as changing the step size mid-calculation. While too laborious for hand computation, they became practical and widely used once digital computer software such as GMAT could perform the repetitive calculations quickly.[11]

GMAT:

GMAT is an open-source trajectory optimization and design system developed by NASA, available for anyone worldwide to download free of charge along with comprehensive documentation. It supports a wide range of mission types and is one of NASA's most expansive and successful software projects.[12]

At the core of GMAT's simulation capability are its propagators, which numerically integrate a spacecraft's equations of motion from given initial conditions. These propagators implement various numerical integration methods, including Runge–Kutta, as discussed earlier. Users have control over the integration step size, with smaller steps generally improving accuracy at the cost of increased computation time, and larger steps reducing computation time but potentially accumulating greater numerical error.

In addition to propagators, GMAT uses solvers that iteratively adjust mission parameters such as burn magnitudes or event timings until specific constraints, like target planetary flyby conditions, are met. Complementing these are optimizers, which systematically refine variables to minimize or maximize a chosen objective function, such as total Δv. Both solvers and optimizers approach trajectory design in a similar way, where the control inputs must be discovered through repeated simulation until the software converges on a suitable solution.

GMAT operates on a batch execution model, where users write and execute scripts to generate outputs, with modifications requiring direct edits to the script, followed by re-running the program. To accommodate users with varying levels of coding expertise, GMAT offers both a script-based environment and a Graphical User Interface (GUI). The GUI provides interactive features, including 3D visualizations and animations, enabling users to explore mission parameters intuitively. The scripting language follows a MATLAB®-like syntax, easing adoption for those familiar with that environment.[13]

In practice, GMAT users construct missions by defining resources, such as spacecraft, propagators, and optimizers, then configuring them to the mission's requirements. These elements are combined into a mission sequence, which models the spacecraft's motion, manoeuvres, and key events over time.

The VNB Axis and the B-Plane in Planetary Flybys:

The Velocity, Normal, and Binormal (VNB) reference frame is a spacecraft-centered local orbital reference frame that rotates with the spacecraft along its trajectory. In this reference frame, the x-axis is fixed to the velocity vector, which is tangent to the spacecraft's trajectory, pointing in the direction of motion. The y-axis will be perpendicular to the velocity vector and the orbital plane of the spacecraft, thus aligned with the angular momentum vector. The z-axis will be perpendicular to both vectors and lies within the orbital frame.[14] The geometry of this reference frame is depicted in Figure 2 below:

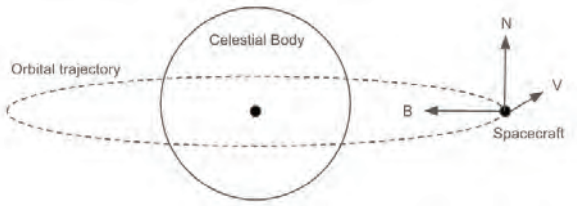

Figure 2: Velocity, Normal, Binormal (VNB) Reference Frame in Orbital Mechanics.

The B-plane is a conceptual plane used in planetary flyby analysis, defined as the plane perpendicular to the spacecraft's incoming asymptote vector. The asymptote represents the straight-line path that the spacecraft would follow if the planet's gravity were absent; it describes the direction of the spacecraft's velocity infinitely far from the planet, often denoted as v_∞. In other words, while the actual spacecraft follows a curved hyperbolic trajectory around the planet, the asymptote is the idealized line that the trajectory approaches at great distances.[15]

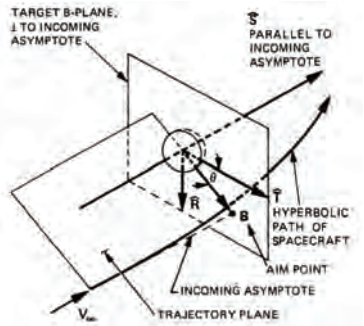

Figure 3: Geometric definition of the B-plane (*NASA – Public Domain*).[16]

As shown in Figure 3, the point where this incoming asymptote intersects the B-plane is called the aim point. This point serves as a convenient way to describe and control the geometry of the flyby, since small variations in the aim point correspond to significant changes in the spacecraft's outgoing trajectory after the planetary encounter. The B-plane is often expressed in terms of two unit vectors, $\hat{T}$ and $\hat{R}$, which span the plane. The spacecraft's B-vector, which represents the displacement of the asymptote relative to the planet, can be projected onto these two directions. These projections are called BdotT and BdotR, and they are mathematically defined as the dot products of the B-vector with the respective unit vectors (BdotT = $B\cdot\hat{T}$, BdotR = $B\cdot\hat{R}$). Conceptually, this means that BdotT measures displacement along the tangential direction, controlling how much the spacecraft's orbital energy changes, whereas BdotR measures displacement along the radial direction, driving changes in the inclination of the flyby trajectory.[15,17]

In practical mission design, it is crucial to understand that when engineers "target" a specific BdotT and BdotR in software such as GMAT, they are not directly moving the spacecraft itself. Instead, they are specifying where on the B-plane the aim point should fall. The optimizer then works backwards to determine the maneuver parameters (for example, Δv magnitude and timing) that adjust the spacecraft's actual trajectory so that its incoming asymptote intersects the B-plane at the desired coordinates. In other words, by shifting the aim point, one is indirectly controlling key aspects of the flyby: the turning angle, the closest approach distance, and the outbound trajectory. This makes the B-plane framework powerful, since it translates the complexity of a 3D gravity assist into a 2D targeting problem.

Gravity Assists and the Oberth Effect:

From a physics perspective, the gravity assist works because of the conservation of momentum and energy in a two-body interaction. When the spacecraft approaches a planet, it is captured temporarily into the planet's gravitational field and follows a hyperbolic trajectory relative to that planet. In the planet's frame of reference, the spacecraft comes in with some velocity, swings around the planet, and leaves with the same speed but in a different direction. However, when viewed in the Sun's inertial frame, the planet itself is not stationary but orbiting the Sun at high velocity. Because of this, the spacecraft effectively "borrows" a small portion of the planet's orbital momentum around the Sun.[18] This process can be better illustrated by considering velocity addition in different reference frames.[19] Let $\vec{v_p}$ be the planet's orbital velocity around the Sun, and $\vec{v}_{\infty in}$ and $\vec{v}_{\infty out}$ the incoming and outgoing hyperbolic excess velocities of the spacecraft relative to the planet.

In the planet's frame, the spacecraft's speed is conserved:

$$|\vec{v}_{\infty\, in}| = |\vec{v}_{\infty\, out}| \quad (1)$$

When transformed back into the heliocentric (Sun-centered) frame, the spacecraft's velocity is:

$$\vec{v}_{SC\, in} = \vec{v}_p + \vec{v}_{\infty\, in} \text{ and } \vec{v}_{SC\, out} = \vec{v}_p + \vec{v}_{\infty\, out} \quad (2)$$

DOI: 10.36838/IJHSR87.230

Thus, the change in the kinetic energy of the spacecraft can be written as:

$$\Delta E = \frac{1}{2}m(|\vec{v}_{SC\,out}|^2 - |\vec{v}_{SC\,in}|^2) \quad (3)$$

Then, by using the expression $|\vec{a}+\vec{b}|^2 = |\vec{a}|^2+|\vec{b}|^2+2\vec{a}\cdot\vec{b}$ and rearranging,

$$\begin{aligned} |\vec{v}_{SC\,out}|^2 - |\vec{v}_{SC\,in}|^2 &= |\vec{v}_p + \vec{v}_{\infty\,out}|^2 - |\vec{v}_p + \vec{v}_{\infty\,in}|^2 \\ &= |\vec{v}_p|^2 + |\vec{v}_{\infty\,out}|^2 + 2\vec{v}_p\cdot\vec{v}_{\infty\,out} - |\vec{v}_p|^2 - |\vec{v}_{\infty\,in}|^2 - 2\vec{v}_p\cdot\vec{v}_{\infty\,in} \\ &= 2\vec{v}_p\cdot(\vec{v}_{\infty\,out} - \vec{v}_{\infty\,in}) \end{aligned} \quad (4)$$

The last dot-product expression shown here is generally not zero because the outgoing and incoming spacecraft velocity vectors have the same magnitude but different directions. Therefore, this shows that a directional change relative to the planet is necessary in order to manipulate the heliocentric speed of the spacecraft.[20]

If the spacecraft is deflected forward, in the same direction as the planet's orbital motion, the dot product is positive: the spacecraft gains kinetic energy, effectively "stealing" a tiny fraction of the planet's orbital momentum. If deflected backward, opposite to the planet's motion, the dot product is negative: the spacecraft loses energy and slows down relative to the Sun. Therefore, gravity slingshots require a trajectory that brings the spacecraft past the planet on the side aligned with its orbital motion to increase speed.

Another important concept for maximizing the efficiency of fuel usage for interplanetary missions is the Oberth Effect, which explains why propulsive maneuvers are most efficient when performed at periapsis (the point of closest approach in an orbit), where the spacecraft is traveling at its fastest as compared to any other point along its trajectory due to the acceleration from gravity as it falls inwards closer to the planet. At higher orbital speeds, a given amount of propellant energy is converted into a disproportionately larger gain in kinetic energy. This is because kinetic energy scales with the square of velocity, so adding the same Δv at periapsis is the most efficient, as it results in the greatest increase in orbital energy.[21]

Tsiolkovsky Rocket Equation:

The performance of rockets is governed by the Tsiolkovsky rocket equation.[22] In this investigation, the equation will be used to estimate the total Δv of all TCM burns implemented during a mission, using the known fuel mass and the specific impulse of the propulsion system. The equation is written as:

$$\Delta v = I_{sp} \times g_0 \times ln(\frac{m_0}{m_f}) \quad (5)$$

Where:

Δv = the total change in velocity the rocket can achieve

I_{sp} = specific impulse of the propulsion system (seconds), a measure of the engine–fuel system's efficiency

g_0 = standard Earth gravity (9.81 m/s^2)

m_0 = initial mass of the spacecraft (with propellant)

m_f = final mass (after propellant has been expended)

Methodology

The first stage involved calculating the theoretical Δv requirements for each mission using the Tsiolkovsky Rocket Equation. This approach was adopted because no published data exist for the total Δv associated with all midcourse correction manoeuvres. For each spacecraft, published values for the mass at launch, current mass, and the engine's specific impulse were obtained from NASA mission archives and peer-reviewed literature. Substituting these values into the rocket equation yielded approximate Δv requirements based on the expended propellant for each vehicle, providing a value for comparison with the simulated mission.

For Voyager 2, NASA's Voyager Backgrounder lists a hydrazine tank mass of 104 kg and a mission module mass of 825 kg (which includes the hydrazine).[23] Currently, NASA claims that the approximate mass of Voyager 2 is 735 kg, meaning roughly 80 kg of hydrazine has been used.[24] Additionally, Voyager 2 used Aerojet MR-103 hydrazine monopropellant thrusters with I_{sp} of ~202-224 s. Hence, the implied Δv capacity is:[25,26]

$$\Delta v = \frac{202+224}{2} \times 9.81 \times ln(\frac{825}{735})$$
$$\Delta v = 241.4\ m/s \quad (6)$$

For Pioneer 11, a peer-reviewed analysis reported launch mass of ~258 kg with ~27-30 kg of propellant aboard. In a 2002 JPL study, it was stated that the spacecraft performed major trajectory correction maneuvers on the way to Jupiter and Saturn, which resulted in about 20 kg of propellant being used.[27] Although the exact model of the propulsion system is publicly unavailable, it is known that it also utilized hydrazine monopropellant fuel, which means it had an I_{sp} which could range anywhere from ~180–285 s:[26,28]

$$\Delta v = \frac{180+285}{2} \times 9.81 \times ln(\frac{258}{238})$$
$$\Delta v = 184\ m/s \quad (7)$$

In the second stage, this study incorporated published ephemeris data for Voyager 2 and Pioneer 11 in the form of SPK (Spacecraft and Planet Kernel) files obtained from NASA's SPICE archive. These kernels contain the precise spacecraft trajectory information referenced to the solar system barycenter, allowing accurate reconstruction of each mission within GMAT.[29] From these reconstructed runs, the key mission parameters required for replication were extracted, particularly the spacecraft's initial starting conditions and the B-plane coordinates (BdotT and BdotR) at each planetary flyby. These values served as the primary constraints for ensuring the simulated missions followed the same geometry as the actual flights. Table 1 below presents the acquired BdotT and BdotR values at each planetary flyby for the replicated missions.

Table 1: Primary simulation data showing the BdotT and BdotR values generated from GMAT for each flyby in the replicated Voyager 2 and Pioneer 11 missions.

Voyager 2		
Mission Stage	**BdotT [km]**	**BdotR [km]**
Jupiter Periapsis	1 913 212.28	167 664.27
Saturn Periapsis	324 486.32	-173 812.23
Uranus Periapsis	92 533.50	-87 205.31
Neptune Periapsis	-27 884.25	-41 724.75
Pioneer 11		
Mission Stage	**BdotT [km]**	**BdotR [km]**
Jupiter Periapsis	-371 218.72	473 675.46
Saturn Periapsis	335 609.29	19 526.29

The third stage was to construct the replicated mission in GMAT. To achieve this, the following targeting sequence was implemented:

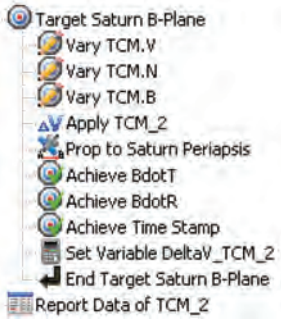

Figure 4: Targeting sequence for TCM 2, performed at Jupiter periapsis to satisfy Saturn B-plane targets.

Figure 4 is an excerpt from the mission sequence, which only shows the specific targeting loop structure used to correct Voyager 2's trajectory. However, all other TCMs across both missions followed the same loop structure, with only the timing and target conditions differing. To provide clarity, Table 2 summarizes the location and purpose of each TCM used in the replication of Voyager 2. Since Pioneer 11 followed a shorter trajectory that terminated at Saturn, only TCM 1 (the initial post-injection clean-up to set up Jupiter) and TCM 2 (the Jupiter-periapsis maneuver to target Saturn's B-plane and timing) were required. The latter TCMs listed at Saturn and Uranus periapsis apply only to Voyager 2, which continued to Uranus and Neptune.

Table 2: TCM Locations and Purposes.

TCM	Location of Execution	Purpose
TCM 1	Beginning of the simulated mission (post-injection cleanup)	Sets up the Jupiter encounter
TCM 2	Jupiter periapsis	Targets Saturn B-plane (BdotT/BdotR) and epoch
TCM 3	Saturn periapsis	Targets Uranus B-plane and epoch
TCM 4	Uranus periapsis	Targets Neptune B-plane and epoch

Each trajectory correction begins by propagating the spacecraft from its current state to the location of the manoeuvre. A target sequence is then defined, with the solver iteratively adjusting the burn components until the encounter geometry is met. The varied parameters are the three Δv components in the VNB frame. These are initially set to zero, and the solver determines their actual values. The burn is then applied, and the trajectory is propagated forward to the next planetary periapsis. At periapsis, the constraints are specified: the B-plane coordinates (BdotT and BdotR) and the timestamp of the flyby. The solver continues adjusting the three Δv components until these are satisfied. Finally, the total Δv is recorded, and a report command logs the results. This same sequence is repeated at each TCM, performed at the start of the mission and then at successive planetary periapsis to guide the spacecraft through its flyby chain.

For the Voyager 2 mission, which was replicated first, a test was also conducted to determine whether replacing the targeted loops with optimized loops, removing time constraints, and relaxing constraint tolerances on the B-plane targets would further reduce the required Δv. Since this approach did not yield any improvement in the results, the standard targeted loop structure was retained when modeling Pioneer 11.

All the GMAT scripts and supporting code used in this study are available in the accompanying GitHub repository.[30]

Results and Discussion

Results:

Tables 3 and 4 present the velocity components and corresponding Δv values of the trajectory correction maneuvers (TCMs) for the replicated Voyager 2 and Pioneer 11 missions:

Table 3: Components and Δv of Replicated Voyager 2 Trajectory Correction Manoeuvres.

Burn	Components [m/s]	Δv [m/s]
TCM 1	V: 9.42 N: 5.81 B: -0.79	11.10
TCM 2	V: 32.63 N: 7.35 B: -66.86	74.76
TCM 3	V: 29.71 N: 160.95 B: -163.77	231.53
TCM 4	V: -105.22 N: -345.58 B: 58.82	366.00

Table 4: Components and Δv of Replicated Pioneer 11 Trajectory Correction Manoeuvres.

Burn	Components [m/s]	Δv [m/s]
TCM 1	V: 43.21 N: -12.83 B: -17.38	48.31
TCM 2	V: -959.57 N: 2143.15 B: -266.97	2363.29

When summing the Δv requirements from the replicated manoeuvres, the total values obtained were 683.39 m/s for Voyager 2 and 2411.60 m/s for Pioneer 11. By contrast, the theoretical Δv requirements estimated, as detailed in the Methodology section, from propellant masses and specific impulses were 241.4 m/s for Voyager 2 and 184 m/s for Pioneer 11. Figure 5 below compares these estimated and replicated Δv values for both missions.

DOI: 10.36838/IJHSR87.230

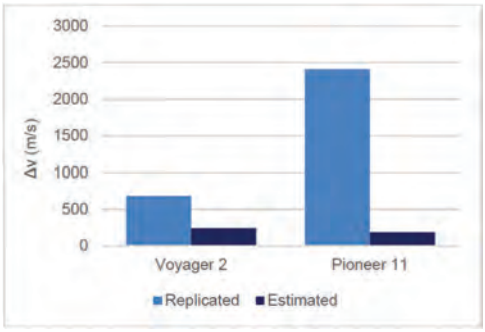

Figure 5: Grouped bar chart comparing the estimated and replicated Δv values for the Voyager 2 and Pioneer 11 missions.

This reveals that the replicated Voyager 2 Δv is 2.83 times larger (283% of the historical estimate, i.e., 183% higher), while the replicated Pioneer 11 Δv is 13.1 times larger (1310% of the historical estimate, i.e., 1210% higher). The significant discrepancies indicate that while the replicated maneuvers reproduce the overall structure of each mission, they overestimate the actual Δv usage by a wide margin.

Discussion:

While this paper is unable to pinpoint with certainty the sources of these discrepancies, there are a number of plausible hypotheses that can be derived from observed patterns in the burn components. Broadly, these discrepancies fall into two categories of error: modeling errors, which stem from the way the mission was represented and solved within GMAT, and computational errors, which arise from the limitations of numerical methods. The following discussion is separated accordingly.

Modeling Errors:

Firstly, for Voyager 2, TCM 4 required a large negative component in the V-direction, while for Pioneer 11, TCM 2 also had a large negative V component. A negative V value means the spacecraft had to reduce its velocity along its trajectory path. In both cases, this suggests that earlier maneuvers had caused the spacecraft to move too fast relative to the planned trajectory. As a result, a large retrograde burn was needed later to correct the speed and ensure the timing of the next planetary encounter remained accurate.

In addition to the V-direction, there were also excessive burns in the B-direction. Both V and B components are used to control the altitude of the flyby at the next planetary encounter. However, due to the Oberth effect, changes in the V-direction (along the velocity vector) are generally more efficient than changes in the B-direction (radial within the orbital plane, perpendicular to V). The fact that GMAT produced comparatively large B burns suggests that the optimization process was not always making use of the most efficient burn orientation. Further inspection of the burn components shows that nearly all B-direction corrections (except for Voyager 2's TCM 4) were negative. This indicates that, instead of relying on altitude-lowering B burns, GMAT could have achieved the same corrections more efficiently by applying retrograde V burns earlier in the trajectory. In the example of Voyager 2, as mentioned earlier, TCMs 1 to 3 all included positive V components that accelerated the spacecraft, which in turn led to a very large retrograde V correction at TCM 4. A more balanced use of retrograde V at earlier stages might have reduced this, as well as the excessive negative B burns. In practice, this could not be mitigated within the adopted methodology, since the simulation would not converge unless all three burn components (V, B, and N) were varied. Moreover, GMAT cannot be made to "see" the mission globally. It can only satisfy one constraint at a time. As a result, suboptimal choices in the early burns accumulate and must be compensated for in subsequent burns, even if that compensation is inefficient.

It was suspected that perhaps these burn choices were forced by the applied constraints. To investigate this possibility, all targeted loops were replaced with optimized loops set to minimize Δv, time constraints were removed, and the B-plane constraints were relaxed to give the optimizer more leeway. However, the simulation consistently converged on the same flyby epochs and produced the same distribution of burn components. This confirms that GMAT's solution, although suboptimal, was the best it could achieve.

In addition to solver inefficiencies, the setup introduced a second type of modeling error: potential mismatches in the BdotT and BdotR constraints. The GMAT replications began with SPICE-derived B-plane targets and epochs, and even tiny mismatches between these and the actual historical encounter values could propagate into significant differences. For instance, the SPK propagator was configured with a one-hour step size. This means that the reported closest-approach BdotT and BdotR values may have fallen in between the sampled points, introducing a small offset from the true values. While this mismatch would likely be minor, such deviations can grow over interplanetary timescales, ultimately magnifying into higher Δv requirements at later encounters. However, due to computational limitations, this study was unable to reduce the step size further to capture the exact closest approach.

Computational Errors:

Another noticeable pattern was the large N-direction burns in both replicated missions. Since the N direction corresponds to out-of-plane maneuvers (perpendicular to the orbital plane), it would be expected that the spacecraft's launch and trajectory geometry would be chosen to already minimize the need for such corrections. These N-direction burns are not only substantial, but also increase in magnitude across both missions. This pattern is also reflected in the trend of increasing Δv at later burns. The first maneuvers in both missions were relatively small, but the later burns grew much larger in magnitude. This behavior is consistent with the surrounding literature on numerical propagation. For instance, a paper on the topic by Mosbach & Turner shows that when differential equations are solved step by step on digital computers, tiny rounding errors accumulate at each integration step. Over the years-long timelines of missions such as Voyager 2 and Pioneer 11, these errors compound, which helps explain why the GMAT replications required progressively larger corrective burns, since the

software's small numerical inaccuracies early in the trajectory snowballed into larger deviations later on.[31]

A potential mitigation strategy for the integration drift problem would be to segment the propagation into shorter spans, rather than attempting to simulate the full mission in a single continuous run. For example, instead of starting from the Earth departure state and propagating all the way to Neptune (Voyager 2) or Saturn (Pioneer 11), one could initialize GMAT at Earth, propagate to Jupiter, and then terminate the sequence. At that point, a new file could be generated, beginning with the spacecraft's SPK-derived state at Jupiter periapsis. This would effectively "reset" the accumulated numerical error at each planetary encounter. By repeating this process, each leg of the mission would be propagated over a much shorter time span, thereby reducing the opportunity for integration drift to compound. In theory, this could yield TCM Δv values much closer to historical estimates. However, such an approach undermines the central aim of this research. The purpose of the study is not simply to reproduce historical trajectories, but to test GMAT's capability as a mission design tool under conditions analogous to planning a future mission. In a real design scenario, trajectory analysts would not have the luxury of resetting the spacecraft's state to "true" values at each encounter, because those values are precisely what the software is meant to predict.

Finally, there is the trade-off between computational accuracy and efficiency. Smaller-step integrators reduce drift but at high computational cost, while larger-step integrators are more efficient but allow small deviations to accumulate. GMAT gives users flexibility in propagator choice and step size, however the extent to which the step size can be reduced will depend on the computational ability of the machine utilized. For this study, the Runge–Kutta propagator was configured with a minimum step size of 60 seconds and a maximum step size of 86400 seconds (1 day). While these values struck a balance between runtime and accuracy on the available computing setup, reducing them could have mitigated integration drift. This opens the door for further investigative work, which could explore systematically varying step size bounds to assess the sensitivity of Δv growth to propagator settings.

■ Conclusion

This study set out to examine the application of NASA's General Mission Analysis Tool (GMAT) in replicating and optimizing historical interplanetary trajectories, using Voyager 2 and Pioneer 11 as case studies. By estimating the historical total Δv required for each mission's TCMs from published fuel mass and engine data, and comparing these against GMAT-simulated equivalents, it was possible to directly assess GMAT's ability to reproduce and/or improve upon past mission performance.

The results showed that GMAT consistently produced significantly higher total TCM Δv than the historical estimates. For Voyager 2, the simulated Δv was nearly three times larger than the estimated real mission value, while for Pioneer 11 it was more than twelve times higher. Analysis of the maneuver components revealed that these discrepancies arose from two primary sources: modeling errors, which stemmed from the way the mission was represented and solved within GMAT through solver choices and constraint inaccuracies, and computational errors, which arose from the way numerical integration accumulates small inaccuracies over long propagation spans, leading to integration drift.

As mentioned in the discussion section, several avenues remain open for further investigation. A logical next step would be to attempt replications using alternative optimization software. NASA's MONTE and Astrogator are both widely used in professional mission planning and may provide more optimal outcomes than GMAT when applied to replicate historical interplanetary trajectories. Furthermore, building on the findings of this paper could be further achieved through a targeted sensitivity analysis to separate the relative impacts of modeling and computational errors. One approach would be to hold all modeling assumptions constant while varying propagator step sizes and length of propagation, thereby isolating the effects of integration drift. Conversely, fixing the propagator configuration while systematically adjusting target constraints and tolerances would reveal how much of the discrepancy stems from the modeling setup. Such an analysis would be particularly valuable in explaining why the replicated Voyager 2 and Pioneer 11 missions diverged so largely in their Δv error margins, despite following similar methodologies. At present, both error sources interact in ways that are difficult to disentangle. Therefore, controlled experiments where one factor is varied, and the other held fixed, would help clarify their relative contributions and provide more concrete guidance on where future tools or methods could improve.

Ultimately, this study has demonstrated that while GMAT is a powerful and accessible tool for modern mission analysis, its use in replicating historical missions exposes limitations in numerical optimization methods when applied to highly constrained, long-duration trajectories. Recognizing these limitations is essential for setting realistic expectations on what such software can achieve, both in revisiting the past and in planning for future interplanetary exploration.

■ Acknowledgments

This research was made possible with the guidance and support of Dr. Steve Bullock and Jacob Higgins at the University of Bristol. I am deeply grateful for their expertise, encouragement, and invaluable feedback throughout the project. I would also like to express my sincere appreciation to my parents for their unwavering support and encouragement, without which this work would not have been possible.

■ References

1. Yefremov, A. P.; Vorobyeva, A. A. A Planet's Gravity Assist as a Powerful Amplifier of Small Physical Effects in the Solar System. *Acta Astronaut.* **2021**, *180*, 205–210. https://doi.org/10.1016/j.actaastro.2020.12.029.
2. *Basics of Spaceflight: A Gravity Assist Primer - NASA Science*. https://science.nasa.gov/learn/basics-of-space-flight/primer/ (accessed 2025-08-14).

DOI: 10.36838/IJHSR87.230

3. NASA. *Pioneer 11 - NASA Science*. https://science.nasa.gov/mission/pioneer-11/ (accessed 2025-08-14).
4. NASA. *Voyager 2 - NASA Science*. https://science.nasa.gov/mission/voyager/voyager-2/ (accessed 2024-12-20).
5. *10 Facts about the Pioneer Spacecraft - NASA Science*. https://science.nasa.gov/missions/pioneer/pioneer-11/10-things-about-pioneer-spacecraft/ (accessed 2025-08-25).
6. Nathan J. Strange. Analytical Methods for Gravity-Assist Tour Design. Dissertation, Purdue University, 2016. https://docs.lib.purdue.edu/open_access_dissertations/852/.
7. General Mission Analysis Tool (GMAT) Product Description. https://ntrs.nasa.gov/api/citations/20080045879/downloads/20080045879.pdf (accessed 2024-12-19).
8. Scott Evans; William Taber; Theodore Drain; Jonathon Smith; Hsi-Cheng Wu; Michelle Guevara; Richard Sunseri; James Evans. Monte: The Next Generation Of Mission Design & Navigation Software. *Jet Propuls. Lab. Inst. Technol.* **2016**.
9. Carrico, J.; Fletcher, E. Software Architecture And Use Of Satellite Tool Kit's Astrogator Module For Libration Point Orbit Missions. In *Libration Point Orbits and Applications*; WORLD SCIENTIFIC: Aiguablava, Spain, 2003; pp 471–487. https://doi.org/10.1142/9789812704849_0021.
10. Shirazi, A.; Ceberio, J.; Lozano, J. A. Spacecraft Trajectory Optimization: A Review of Models, Objectives, Approaches and Solutions. *Prog. Aerosp. Sci.* **2018**, *102*, 76–98. https://doi.org/10.1016/j.paerosci.2018.07.007.
11. Battin. Numerical Integration of Differential Equations. In *An Introduction to the Mathematics and Methods of Astrodynamics, Revised Edition*; AIAA Education Series; American Institute of Aeronautics and Astronautics, Inc., 1999; pp 567–622. https://doi.org/10.2514/5.9781600861543.0567.0622.
12. *General Mission Analysis Tool (GMAT)*. Goddard Engineering and Technology Directorate. https://etd.gsfc.nasa.gov/capabilities/capabilities-listing/general-mission-analysis-tool-gmat/ (accessed 2025-08-22).
13. Hughes, S. P. General Mission Analysis Tool (GMAT), 2016. https://ntrs.nasa.gov/citations/20160003520 (accessed 2024-12-19).
14. Ferrato, E.; Giannetti, V.; Andreussi, T. Guidance, Navigation, and Control of a Low-Altitude Nanosatellite Equipped with Air-Breathing Electric Propulsion. *IEEE Trans. Aerosp. Electron. Syst.* **2025**, 1–16. https://doi.org/10.1109/TAES.2025.3577159.
15. Jared Graef. B-Plane Targeting With The Spacecraft Trajectory Optimization Suite. Thesis, California Polytechnic State University, 2020. https://digitalcommons.calpoly.edu/theses/2251/ (accessed 2025-08-16).
16. Sergeyevsky, A. B.; Snyder, G. C.; Cunniff, R. A. Interplanetary Mission Design Handbook, Volume I, Part 2.
17. Lynam, A.; Didion, A. Impulsive Trajectories from Earth to Callisto-Io-Ganymede Triple Flyby Capture at Jupiter. In *AIAA/AAS Astrodynamics Specialist Conference*; AIAA SPACE Forum; American Institute of Aeronautics and Astronautics, 2014. https://doi.org/10.2514/6.2014-4106.
18. Berg, P. The Fundamental Concepts of the Gravity-Assist Manoeuvre. *Eur. J. Phys.* **2023**, *44* (2), 025002. https://doi.org/10.1088/1361-6404/acaad8.
19. Van Allen, J. A. Gravitational Assist in Celestial Mechanics—a Tutorial. *Am. J. Phys.* **2003**, *71* (5), 448–451. https://doi.org/10.1119/1.1539102.
20. Anderson, J. D.; Campbell, J. K.; Nieto, M. M. The Energy Transfer Process in Planetary Flybys. *New Astron.* **2007**, *12* (5), 383–397. https://doi.org/10.1016/j.newast.2006.11.004.
21. Adams, R.; Richardson, G. Using the Two-Burn Escape Maneuver for Fast Transfers in the Solar System and Beyond. In *46th AIAA/ASME/SAE/ASEE Joint Propulsion Conference & Exhibit*; American Institute of Aeronautics and Astronautics: Nashville, TN, 2010. https://doi.org/10.2514/6.2010-6595.
22. Tsiolkovsky, K. S. Exploration of Outer Space by Means of Rocket Devices.; The Science Review, 1903; Vol. 5.
23. Voyager Backgrounder, 1980. https://ntrs.nasa.gov/citations/19810001583 (accessed 2025-08-18).
24. *Frequently Asked Questions - NASA Science*. https://science.nasa.gov/mission/voyager/frequently-asked-questions/ (accessed 2025-08-18).
25. *Voyager 1 Fires Up Thrusters After 37 Years*. NASA Jet Propulsion Laboratory (JPL). https://www.jpl.nasa.gov/news/voyager-1-fires-up-thrusters-after-37-years/ (accessed 2025-08-18).
26. *4.0 In-Space Propulsion - NASA*. https://www.nasa.gov/smallsat-institute/sst-soa/in-space_propulsion/ (accessed 2025-08-18).
27. Anderson, J. D.; Laing, P. A.; Lau, E. L.; Liu, A. S.; Nieto, M. M.; Turyshev, S. G. Study of the Anomalous Acceleration of Pioneer 10 and 11. *Phys. Rev. D* **2002**, *65* (8), 082004. https://doi.org/10.1103/PhysRevD.65.082004.
28. Turyshev, S. G.; Toth, V. T. The Pioneer Anomaly. *Living Rev. Relativ.* **2010**. https://doi.org/10.12942/lrr-2010-4.
29. *NAIF SPICE Toolkit Hypertext Documentation*. https://naif.jpl.nasa.gov/pub/naif/toolkit_docs/FORTRAN/index.html (accessed 2025-08-22).
30. AdeshKrishnan. AdeshKrishnan/Voyager-2-Pioneer-11-GMAT: V1.0.0, 2025. https://doi.org/10.5281/ZENODO.16927714.
31. Mosbach, S.; Turner, A. G. A Quantitative Probabilistic Investigation into the Accumulation of Rounding Errors in Numerical ODE Solution. *Comput. Math. Appl.* **2009**, *57* (7), 1157–1167. https://doi.org/10.1016/j.camwa.2009.01.020.

Author

Adesh Krishnan is a graduate of St. Joseph's Institution International in Singapore and an aspiring engineer with a strong interest in physics and mathematics. In his free time, he actively expands his technical skill set through online courses in areas such as CAD modeling and programming. He plans to pursue aerospace engineering at university, to apply his interests and skills to make a meaningful contribution to advances in aerospace technology.

Data Availability Statement:

The data supporting the results are available in a public repository at: https://doi.org/10.5281/ZENODO.16927714.

IJHSR
ijhighschoolresearch.org
REVIEW ARTICLE

Beyond Flavor: A Systematic Review of the Maillard Reaction's Impact on Health and Link to Carcinogenesis

Fiona Zhong

West Point Grey Academy, 4125 West 8th Ave, Vancouver, BC, V6R 4P9, Canada; fiona.zzz0031@gmail.com
Mentor: Frank Glover

ABSTRACT: This review explores the emerging link between the Maillard reaction (MR) and carcinogenesis, focusing on key products and their influence on gastrointestinal and breast cancers. While the MR is essential for enhancing food quality, evidence increasingly suggests that some resulting compounds may contribute to cancer risk and alter treatment outcomes. Using PubMed and Google Scholar, human-based studies were analyzed to identify how MR products — including heterocyclic amines, acrylamide, melanoidins, and carboxymethyl lysine (CML) — affect cancer development and progression. The findings reveal that certain byproducts, such as acrylamide and CML, are linked to genotoxic and inflammatory processes, whereas melanoidins demonstrate positive effects. The review also highlights mitigation strategies to mitigate exposure to harmful MR products, including enzymatic interventions and suggested cooking practices. On the whole, the evidence suggests associations with dualistic characteristics of the Maillard reaction in health and disease, rather than causal proof; additional long-term human case studies are necessary to discern causal relationships and to refine dietary guidance aligned with cancer prevention goals.
KEYWORDS: Medical and Health Sciences, Oncology, Food Science, Carcinogenesis, Maillard.

Introduction

Cancer Background:

Cancer remains one of the leading causes of mortality globally, with nearly 9.7 million deaths in 2022 alone, and about 1 in 5 people developing it in their lifetime.[1] Despite advancements in modern medicine and increased awareness, the incidence and prevalence of some of these cancers, including gastrointestinal (e.g., stomach, liver, esophagus, pancreas, and colorectal) and breast, have continued to increase over the last few decades.[2] Multiple risk factors have been identified, including *Helicobacter pylori* infection, age, environmental exposures, and processed foods. Western diets, rich in MR-processed foods, correspond to rising colorectal cancer in both Europe and North America.[3]

The Maillard Reaction:

With rapid global population growth, innovations in food processing have become crucial for meeting global nutritional demands. Additionally, food serves as a cornerstone of culture and identity, and globalization has enabled the rapid distribution of culinary dishes worldwide, allowing people to experience new cultures. A naturally occurring chemical reaction, the Maillard reaction (MR) is an innovative discovery harnessed to improve the coloration of food, taste, and aroma, and its breakthrough allows for rapid production of food with an emphasis on consumer-experience quality. The reaction is an organic chemical reaction between amino groups (protein) and reducing groups (reducing sugars) initiated by high temperatures; through a non-enzymatic process, several major chemical byproducts (the four most abundant groups being heterocyclic amines, acrylamide, melanoidins, and carboxymethyl lysine) are produced, and emerging data suggests beneficial or harmful health effects of these compounds.[4]

The Maillard Reaction and Carcinogenesis:

Numerous studies have investigated Maillard reaction byproducts in relation to cancer risk; however, the data are mixed, and the results are inconclusive. For example, a prospective cohort analysis by Li *et al.* evaluated the effects of end glycation byproducts on pancreatic cancer risk and found that men who consumed processed red meats had a dose-dependent increased risk of pancreatic cancer, where men in the highest quintile of consumption had the highest risk.[5] However, women had a nonsignificant increase in pancreatic risk in this same study. In contrast, in a 1977 study conducted by Sugimura *et al.*, it was found that heterocyclic amines (HCAs) were active in the rapid carcinogenesis bioassays, supporting biologic plausibility for pancreatic cancer. Additionally, some Maillard byproducts, such as melanoidins, are shown to be protective against cancers.[6] In this systematic literature review, we synthesize human-focused evidence linking Maillard reaction byproducts with gastrointestinal cancers and evaluate options for interventions to reduce dietary byproduct exposure.

Methods

To evaluate Maillard reaction in food processing and its relationship to cancer, we identified a selection of papers regarding the subject for analysis. We included research papers with primarily collected data using PubMed and Google Scholar. We focused our search using the terms: "Maillard reaction", "cancer" (e.g., "gastric cancer", "colon cancer", "pancreatic cancer"), "carcinogenesis", "Maillard reaction byproducts", "food processing." This yielded 210 papers. We then narrowed our search further

© 2026 Terra Science and Education

DOI: 10.36838/IJHSR87.238

by filtering for papers published in English, excluding animal studies and editorials. We further refined our search to only include recent articles from between 2000 and the present, gastrointestinal or breast cancers associated with the Maillard reaction, and studies reporting estimates or mechanistic endpoints relevant to humans. This resulted in a final of 20 papers after removing duplicates.

Discussion

Maillard reaction byproducts:

As previously mentioned, many aspects of food processing have relied on the Maillard reaction for its advantages in cultivating unique complexities of foods in a rapid, precise, and consistent fashion. Despite its benefits, MR byproducts may also relate to cancer risk. Below, we summarize and critically appraise the current data on the four major byproducts.

Heterocyclic amines (HCAs):

Heterocyclic amines (HCAs) represent a heterogeneous group of potentially carcinogenic compounds, which are mainly produced from proteinaceous foods during high-temperature heating processes and flavor-forming.[7] Specifically, a heterocyclic amine is any chemical compound containing at least one heterocyclic ring (atoms of at least two different elements), and one amine group (nitrogen-containing). While there are limited studies evaluating the relationship of heterocyclic amines to specific cancers, to date, 25+ unique types of heterocyclic amines have been identified in cooked foods.[4] Reported by the International Agency for Research on Cancer, multiple[8] types of HCAs — including PhIP — are categorized as possible, class 2A and 2B, carcinogens. In a crossover design study by Shaughnessy *et al.*, the authors fed subjects diets cooked at either high or low temperatures and then evaluated the mutagenicity of those diets on DNA in their colon epithelial cells using a modified Ames test.[9] Subjects were also fed diets prepared with meat fried at high temperature alone or in combination with three putative inhibitors of HCA-induced damage (cruciferous vegetables, chlorophyllin tablets, and yogurt). Overall, beef and sausage cooked at high temperatures were found to have high mutagenicity due to higher levels of HCA, compared to extracts of meat cooked at low temperatures.[10] Importantly, supplementation with vegetables, plant extracts, and yogurts showed protective effects against the mutagenic properties of HCAs.

Across cohorts, the association with colorectal endpoints is generally minimal and is confounded by overall dietary patterns, smoking, and cooking method. Though the crossover mutagenicity data support biological plausibility, the population-level causal relation remains unsure. Cancer risk appears to be concentrated in high-temperature and low-moisture cooking and may be modifiable through the intake of crucifers or chlorophyllin.[9,10]

Acrylamide:

Next, a well-known potential carcinogen is formed as an MR intermediate when reducing sugars and glyoxalase react with asparagine. Acrylamide is mainly present in coffee, baked goods, and processed snacks such as potato chips, breakfast cereals, and canned goods.[11] As previously mentioned, acrylamide's genotoxicity and mutagenicity have been well-studied in experimental toxicology models to establish plausible mechanisms related to carcinogenesis, yet these findings are not always relevant to human populations. This review summarizes large cohort findings that have evaluated acrylamide associations with cancer.

Hogervorst *et al.* investigated the association between dietary acrylamide and several urogenital malignancies in a large prospective cohort.[12] This study included 120,852 men and women aged 55-69 years and followed them over 13 years, with primary outcomes being rates of renal, bladder, and prostate cancer after acrylamide exposure. Acrylamide intake served as the proxy for exposure and was assessed with a food-frequency questionnaire at baseline that was based on chemical analysis of all relevant Dutch foods. In the final analysis using a multivariable-adjusted Cox proportional hazard model, the highest quintile exposure of acrylamide was associated with a 1.59-fold hazard of renal cancer, which can be interpreted as a 59% increased risk of developing cancer. (95% CI: 1.09, 2.30; P for trend = 0.04). The prospective design of this study, combined with a large sample size, provides suggestive evidence of acrylamide's possible cancer risk.

While the exact mechanism of acrylamide-induced carcinogenicity remains unclear and is likely case-dependent, genotoxic and nongenotoxic pathways of carcinogenesis have been proposed. Experimental studies demonstrate DNA adduct formation and oxidative-stress responses consistent with carcinogenic mechanisms; however, translating these signals precisely to population risk is limited by possible exposure misclassification (food-frequency questionnaire intake estimates) and co-exposures (smoking, diet).[12] Acrylamide has also been shown to interact with glutathione and negatively impact oxidation balance in cells, which is a known risk factor for carcinogenesis.[13] Biomarker-based studies (e.g., hemoglobin adducts) could potentially offer clearer, dose-response resolutions moving forward.

Melanoidins:

Conversely, dietary melanoidins, a group of late-stage Maillard reaction products, may confer protection against carcinogenesis.[14-16] A study by Langner *et al.* investigated whether roasted potato extracts, known to be rich in melanoidins, can inhibit the proliferation of human colon cancer cells *in vitro*.[17] LS180 colon cancer cell lines were treated with roasted potato fiber extract (AM4) as well as with high (HMW) and low (LMW) molecular weight fractions at varying concentrations. Ultimately, the authors found that compound concentrations of 1000 μg/mL reduced colon cancer cell growth by as much as 69%. Interestingly, the authors were able to identify specific cell cycle pathways that were likely targets of the melanoidins. For example, deregulated ERK1/2 signaling was revealed upon treatment, and ERK1/2 is a well-known proliferative cell cycle pathway implicated in carcinogenesis. Additionally, multiple alterations in other cell cycle regulators, such as cyclin-depen-

dent kinases, lead to cancer cell cycle arrest in G0, which is another anti-carcinogenesis mechanism.

Another study by Kamei *et al*. found that the extract of melanoidin cultured together with gastric and colon cancer cell lines led to suppression of cancer cell line growth by 50% after four days.[15] This mechanism was similarly found to be related to the blockage of the S phase and G2 phase in cancer cells. Although mechanistic and *in vitro* findings are consistent with antioxidative and antiproliferative properties and indicate possible contribution of melanoidins to natural chemoprevention in colorectal cancer, human outcome data are scarce, thus no causation can be drawn. Additionally, typical intakes of ~10g per day and diverse food sources create difficulty in making attributions. Thus, melanoidins seem promising, but lack evidence for clinical protection in humans.

Melanoidins are also shown to have antioxidative, antimicrobial, antihypertensive, and antiallergenic properties; they have exhibited the direct ability to scavenge free radicals both *in vitro* and *in vivo*.[4]

Studies have shown that average diets consist of ~10g of melanoidins a day[18] and are found in a variety of foods, including cocoa beans, carob kibbles, and acorns.[16] These studies may support counselling at-risk cancer patients on incorporating these diets rich in melanoidins. Counselling patients to consume melanoidin-rich foods in their overall diet is reasonable, but future clinical studies are warranted to further evaluate the benefits regarding cancer prevention.

Carboxymethyl lysine (CML):

Carboxymethyl lysine (CML) is an advanced glycation end product (AGE) formed during the late stages of the Maillard reaction, whose formation is driven by glycolytic byproducts following combustion; it is also demonstrated to form from oxidative stress in cancer cells. Similar to other AGEs, CML is implicated in tumorigenesis as evidenced by *in vitro* and population studies. Biologically, CML activates the receptor for advanced glycation end products (RAGE), a single transmembrane, multiligand receptor expressed on a variety of cells, including immune cells, neurons, vascular smooth cells, and cancer cells.[19] Activation of these pathways triggers and enhances downstream signaling pathways that can contribute to breast cancer cell migration, growth, angiogenesis, metastasis, and drug resistance.[20]

Furthermore, high CML accumulation was shown to correlate with estrogen receptor expression in breast cancer cell lines;[21] estrogen-positive receptors are known to play a key role in the promotion of breast cancer, and upregulation of these estrogen receptors by CML may initiate and or promote tumorigenesis. While only a few studies have evaluated CML's association with breast cancer in humans, Peterson *et al*. demonstrated that the highest quintile of CML levels in women was significantly associated with breast cancer risk in postmenopausal women.[22] Similarly, in the Prostate, Lung, Colorectal, and Ovarian Cancer Screening Trial (PLCO), higher CML-AGE intake was associated with increased risk of breast cancer in women of all ages.[23] Furthermore, these population studies note that CML accumulation in estrogen-negative tumors is associated with poor relapse-free survival after chemotherapy. Thus, high levels of CML and AGEs may not only create a microenvironment that promotes tumor formation but may also directly impede the positive treatment effects of cancer therapy.

The direction of effect in human cohort trends is adverse, but variables in exposure measurement (dietary intake versus circulating AGEs) and introduced bias from metabolic comorbidities (e.g., insulin resistance) defer to causal claims. Larger cohorts are crucial to support a causal claim.

Moreover, CML is found to modify high mobility group box protein-1 (HMGB1), which is a cytokine linked to cancer progression due to its tumor-promoting effects.[24] With CML-modified HMBG1 (CML-HGB1) detected in 10 gastric cancer patient samples, all 10 patients exhibited distant metastasis, and patients with higher concentrations of the modified HMBG1 later showed greater resistance to neoadjuvant therapy. Overall, it is observed that CML-HMGB1 has stronger pro-tumor effects than unmodified or oxidized HMGB1, and patients with diabetes or metabolic dysfunctions of the like may exacerbate gastric cancer progression via CML-HMGB1.

Generally, major AGEs are linked to chronic inflammation, oxidative stress, and insulin resistance — all factors prompting cancer development.[4] As studied by Tamanna and Mahmood, high dietary AGEs are associated with increased risk of colorectal, breast, and pancreatic cancers due to their pro-inflammatory and oxidative properties in promoting DNA damage by impairing cellular repair mechanisms and further fostering tumor growth. Meanwhile, other studies show no direct causation between CML and cancer, but its role in metabolic disorders (diabetes and cardiovascular diseases) may elevate cancer risk. More human data and long-term studies are necessary to discern the role of CML and other AGEs in carcinogenesis.

Prevention and Applications of MRPs:

Acrylamide:

Maillard deglycases are enzymes that prevent protein glycation by degrading early Maillard adducts; specifically, members of the DJ-1/Park7 family can break down the bonds between glyoxals and amino groups.[25] Accordingly, thermophilic microorganisms (e.g., *Pyrococcus furiosus*) *and thermostable enzymes* (including β-glucosidases used in processing) function at high temperatures and can reduce acrylamide formation without depleting essential precursors such as asparagine and reducing sugars.

Another important application of the biological removal of Maillard reaction products is demonstrated in asparaginase. Asparaginase is an enzyme found in various mammals, plants, and vegetables, and can be isolated in concentrated form to be used in food processing.[26] Specifically, asparaginase conversion to aspartic acid reduces acrylamide levels by lowering levels of asparagine (a precursor of acrylamide) during the Maillard reaction.[27] This method has been well-studied and demonstrated to be effective at the biochemical level, where some studies have demonstrated over 80% reduction of acryl-

DOI: 10.36838/IJHSR87.238

amide in various products.[28] While this method is beneficial for lowering levels of toxic substances, the use of asparaginase may lower the sensory quality of food (color, flavor, texture), and these side effects make asparaginase less desirable to use in some instances. Future studies are warranted to investigate how asparaginase can be used while preserving the sensory components of food.

CML:

Since the accumulation of carboxymethyl lysine (CML) is significantly correlated with an unfavorable prognosis for estrogen-negative receptor breast cancer patients, standard chemotherapy might be a less effective treatment strategy. This suggests that identifying high CML concentrations could be crucial to preventing poor outcomes; this necessitates alternate, more aggressive therapeutic strategies for this specific patient subgroup to avoid unfavorable results associated with chemotherapy.

Otherwise, CML formation can be minimized by cooking at lower temperatures, using acidic marinades, or counteracted by consuming naturally antioxidant-rich foods (e.g., vegetables and spices).

Culinary mitigation strategies:

In order to reduce exposure to the discussed potential carcinogens, it is necessary to introduce modified cooking practices. In general, common low-risk food preparation methods include lower-temperature, higher-moisture approaches such as boiling, steaming, and microwaving — all methods of reducing HCA and acrylamide formation. Acidic marinades and avoiding charring further reduce HCA formation. Next, vacuum frying can retain antioxidants in vegetable or plant-based snacks, thus potentially buffering harmful free radicals and preventing tumor growth while keeping these foods tasty.

Overview:

As of 2022, gastrointestinal cancers and breast cancers are some of the most commonly occurring cancers, and make up 30.8%, approximately 2.99 million, of total cancer deaths.[1] These cancers are partly attributed to modern dietary patterns rich in processed foods. This review has outlined the current research and evidence on the dualistic role of MR products and byproducts in carcinogenesis.

The Maillard reaction, while key for processing and sensory appeal in our common diets, generates an array of compounds with significant and sometimes perceived detrimental biological effects. After a thorough review, associations for several MRPs, notably acrylamide and CML, have been reported in human studies, with effect sizes usually modest and context dependent. Acrylamide demonstrated indirect suggestive links with renal cancer through genomic alteration and toxicity, while CML aligns with pro-inflammatory signal pathways relevant to cancer cell progression. Contrarily, melanoidins show mechanistic chemopreventive properties; they reduce cancer cell proliferation by arresting the cell cycle and scavenging free radicals, but again, human data outcomes remain limited, and no direct linkage can be drawn.

Ultimately, we explored prospective interventions to mitigate exposure to harmful MRPs, including using enzymatic processes with asparaginase to limit acrylamide precursors and adopting cooking methods to minimize HCA and CML formation.

Common foods containing MRPs:

As previously mentioned, there are several food products that contain these Maillard Reaction products as a direct result of the chemical reaction. Studies show that meats (e.g., seared steak, barbecue), fried foods, cereals, and baked goods all contain the highest concentrations of byproducts.[4] One key example can be found in soybeans, which are used as flour, grits, concentrates, and also as cooking oil. Soybeans must be processed appropriately to ensure safe consumption, and this typically requires high cooking temperatures. Authors found that microwave heating for short times (1-2 min) generates high levels of acrylamide, whereas long-time heating (3–5 min) generates lower levels of acrylamide.[29] Thus, increasing awareness of home practices of preparing food could significantly reduce the amount of MRPs.

Socially, there is an increasing preference for instant meals rather than traditional cooking as societies have become busier and desire food "on the go." As a result, the consumption of processed meat, pizza, and snacks has led to an increase in insulin resistance and metabolic syndrome, compared to people having a high intake of vegetables and low processed food, which has dramatically increased.[30] MRPs that change during food processing might be one of the important factors for either disease progression or combating diseases. Public health initiatives should address increasing awareness of food product combinations that should be avoided or encouraged to lower overall exposure.

Strengths and limitations:

This review uses high-quality databases and includes the most current and relevant papers. Additionally, it covers one of the most critical medical concerns faced by our world today and directs the focus of future research and prevention to improve healthcare. Finally, the review raises awareness amongst the general population by offering relatable and digestible information.

This review is not fully exhaustive of resources outside of major databases, and some studies included may not be comparable due to variable differences.

Future directions:

Due to limited research, mixed results, and the mechanistic complexities of the MRPs' relationship to carcinogenesis, as highlighted in this review, it is critical to conduct further research on this topic. This may include extensive, long-term human epidemiological studies with larger populations and well-considered case-control groups, moving beyond toxicological models and *in vitro* experimentation to discern a clear association between specific MRPs and cancer risk in more diverse human populations. Furthermore, research should focus on optimizing interventions in daily life (e.g., culinary meth-

ods — baking temperatures, marinades, cooking time, etc.) to reduce the intake of potentially carcinogenic compounds in foods without compromising positive qualities, thus keeping it viable for industrial adoption. Of course, it may also prove significant to investigate how unique factors — like lifestyle, genetics, and medical history — in individuals might modulate cancer risk correlated with different MRPs; using the resulting data, personalized dietary recommendations can be implicated in cancer prevention as well.

Conclusion

This review paper highlights the association of the widespread Maillard reaction with cancer. For some MRPs discussed (HCA, acrylamide, CML), human evidence supports context-dependent associations with site-specific cancer risks and progression, as well as diabetes and cardiovascular diseases, whereas melanoidins exhibit antibiotic and antioxidative promise but lack robust data to support strong associations. Pragmatic risk reduction is feasible through simple cooking techniques and targeting processing interventions. Future studies should continue to evaluate associations between food groups containing high concentrations of Maillard reaction byproducts and help identify which food groups should be avoided to lower the risk of cancer. Priorities include increasing biomarker cohorts, controlled exposure metrics, and trials with culinary interventions using validated endpoints.

Acknowledgments

I would like to recognize my mother as an inspiration to investigate this topic, and express gratitude for Indigo Research and Dr. Frank Glover's mentorship and editorial guidance that ultimately encouraged my completion of this paper. I attest that the ideas, graphics, and writing in this paper are entirely my own.

References

1. Global cancer burden growing, amidst mounting need for services [Internet]. World Health Organization. 2024. Available from: https://www.who.int/news/item/01-02-2024-global-cancer-burden-growing--amidst-mounting-need-for-services#:~:text=Lung%20cancer%20was%20the%20leading,660%20000%20deaths%2C-%206.8%25).
2. Jardim SR, de Souza LMP, de Souza HSP. The Rise of Gastrointestinal Cancers as a Global Phenomenon: Unhealthy Behavior or Progress? Int J Environ Res Public Health. 2023 Feb 18;20(4):3640.
3. Clemente-Suárez VJ, Beltrán-Velasco AI, Redondo-Flórez L, Martín-Rodríguez A, Tornero-Aguilera JF. Global Impacts of Western Diet and Its Effects on Metabolism and Health: A Narrative Review. Nutrients. 2023 June 14;15(12):2749.
4. Tamanna N, Mahmood N. Food Processing and Maillard Reaction Products: Effect on Human Health and Nutrition. Int J Food Sci. 2015;2015:526762.
5. Jiao L, Stolzenberg-Solomon R, Zimmerman TP, Duan Z, Chen L, Kahle L, *et al*. Dietary consumption of advanced glycation end products and pancreatic cancer in the prospective NIH-AARP Diet and Health Study. Am J Clin Nutr. 2015 Jan;101(1):126–34.
6. Iriondo-DeHond A, Elizondo AS, Iriondo-DeHond M, Ríos MB, Mufari R, Mendiola JA, *et al*. Assessment of Healthy and Harmful Maillard Reaction Products in a Novel Coffee Cascara Beverage: Melanoidins and Acrylamide. Foods. 2020 May 12;9(5):620.
7. Barzegar F, Kamankesh M, Mohammadi A. Heterocyclic aromatic amines in cooked food: A review on formation, health risk-toxicology and their analytical techniques. Food Chem. 2019 May;280:240–54.
8. Etemadi A, Abnet CC, Graubard BI, Beane-Freeman L, Freedman ND, Liao L, *et al*. Anatomical subsite can modify the association between meat and meat compounds and risk of colorectal adenocarcinoma: findings from three large US cohorts. Int J Cancer. 2018 Nov 1;143(9):2261–70.
9. Shaughnessy DT, Gangarosa LM, Schliebe B, Umbach DM, Xu Z, MacIntosh B, *et al*. Inhibition of fried meat-induced colorectal DNA damage and altered systemic genotoxicity in humans by crucifera, chlorophyllin, and yogurt. PloS One. 2011 Apr 25;6(4):e18707.
10. Nadeem HR, Akhtar S, Ismail T, Sestili P, Lorenzo JM, Ranjha MMAN, *et al*. Heterocyclic Aromatic Amines in Meat: Formation, Isolation, Risk Assessment, and Inhibitory Effect of Plant Extracts. Foods. 2021 June 24;10(7):1466.
11. Liu S, Ben X, Liang H, Fei Q, Guo X, Weng X, *et al*. Association of acrylamide hemoglobin biomarkers with chronic obstructive pulmonary disease in the general population in the US: NHANES 2013-2016. Food Funct. 2021 Dec 13;12(24):12765–73.
12. Hogervorst JG, Schouten LJ, Konings EJ, Goldbohm RA, van den Brandt PA. Dietary acrylamide intake and the risk of renal cell, bladder, and prostate cancer1. Am J Clin Nutr. 2008 May 1;87(5):1428–38.
13. Huchthausen J, Escher BI, Grasse N, König M, Beil S, Henneberger L. Reactivity of Acrylamides Causes Cytotoxicity and Activates Oxidative Stress Response. Chem Res Toxicol. 2023 Aug 2;36(8):1374–85.
14. Shaheen S, Shorbagi M, Lorenzo JM, Farag MA. Dissecting dietary melanoidins: formation mechanisms, gut interactions and functional properties. Crit Rev Food Sci Nutr. 2022;62(32):8954–71.
15. Kamei H, Hashimoto Y, Koide T, Kojima T, Hasegawa M, Umeda T. Direct tumor growth suppressive effect of melanoidin extracted from immunomodulator-PSK. Cancer Biother Radiopharm. 1997 Oct;12(5):341–4.
16. Oracz J, Lewandowska U, Owczarek K, Caban M, Rosicka-Kaczmarek J, Żyżelewicz D. Isolation, structural characterization and biological activity evaluation of melanoidins from thermally processed cocoa beans, carob kibbles and acorns as potential cytotoxic agents. Food Chem. 2024 June 1;442:138423.
17. Langner E, Nunes FM, Pożarowski P, Kandefer-Szerszeń M, Pierzynowski SG, Rzeski W. Melanoidins isolated from heated potato fiber (Potex) affect human colon cancer cells growth via modulation of cell cycle and proliferation regulatory proteins. Food Chem Toxicol Int J Publ Br Ind Biol Res Assoc. 2013 July;57:246–55.
18. Rajakaruna S, Pérez-Burillo S, Kramer DL, Rufián-Henares JÁ, Paliy O. Dietary Melanoidins from Biscuits and Bread Crust Alter the Structure and Short-Chain Fatty Acid Production of Human Gut Microbiota. Microorganisms. 2022 June 22;10(7):1268.
19. Radia AM, Yaser AM, Ma X, Zhang J, Yang C, Dong Q, *et al*. Specific siRNA Targeting Receptor for Advanced Glycation End Products (RAGE) Decreases Proliferation in Human Breast Cancer Cell Lines. Int J Mol Sci. 2013 Apr 11;14(4):7959–78.
20. Coser M, Neamtu BM, Pop B, Cipaian CR, Crisan M. RAGE and its ligands in breast cancer progression and metastasis. Oncol Rev [Internet]. 2025 Jan 3 [cited 2025 Sept 4];18. Available from: https://www.frontiersin.org/journals/oncology-reviews/articles/10.3389/or.2024.1507942/full

DOI: 10.36838/IJHSR87.238

21. Nass N, Ignatov A, Andreas L, Weißenborn C, Kalinski T, Sel S. Accumulation of the advanced glycation end product carboxymethyl lysine in breast cancer is positively associated with estrogen receptor expression and unfavorable prognosis in estrogen receptor-negative cases. Histochem Cell Biol. 2017 May;147(5):625–34.
22. Peterson LL, Park S, Park Y, Colditz GA, Anbardar N, Turner DP. Dietary advanced glycation end products and the risk of postmenopausal breast cancer in the National Institutes of Health-AARP Diet and Health Study. Cancer. 2020 June;126(11):2648–57.
23. Omofuma OO, Turner DP, Peterson LL, Merchant AT, Zhang J, Steck SE. Dietary Advanced Glycation End-products (AGE) and Risk of Breast Cancer in the Prostate, Lung, Colorectal and Ovarian Cancer Screening Trial (PLCO). Cancer Prev Res (Phila Pa). 2020 July 1;13(7):601–10.
24. Kishi S, Nishiguchi Y, Honoki K, Mori S, Fujiwara-Tani R, Sasaki T, *et al*. Role of Glycated High Mobility Group Box-1 in Gastric Cancer. Int J Mol Sci. 2021 May 13;22(10):5185.
25. Richarme G, Marguet E, Forterre P, Ishino S, Ishino Y. DJ-1 family Maillard deglycases prevent acrylamide formation. Biochem Biophys Res Commun. 2016 Sept 23;478(3):1111–6.
26. Zorn H, Barat Baviera JM, Bolognesi C, Catania F, Gadermaier G, Greiner R, *et al*. Safety evaluation of the food enzyme asparaginase from the non-genetically modified Saccharomyces cerevisiae strain ARY-1. EFSA J. 2025 July 14;23(7):e9533.
27. Xu F, Oruna-Concha MJ, Elmore JS. The use of asparaginase to reduce acrylamide levels in cooked food. Food Chem. 2016 Nov 1;210:163–71.
28. Banchero M. Supercritical fluid extraction as a potential mitigation strategy for the reduction of acrylamide level in coffee. ScienceDirect. 2012 Nov 5;
29. Žilić S, Mogol BA, Akıllıoğlu G, Serpen A, Delić N, Gökmen V. Effects of extrusion, infrared and microwave processing on Maillard reaction products and phenolic compounds in soybean. J Sci Food Agric. 2014 Jan 15;94(1):45–51.
30. Poti JM, Braga B, Qin B. Ultra-processed Food Intake and Obesity: What Really Matters for Health – Processing or Nutrient Content? Curr Obes Rep. 2017 Dec;6(4):420–31.

Author

Fiona Zhong is a senior student at West Point Grey Academy in Vancouver, Canada. She hopes to explore her interest in medicine, health, and food sciences in future academia, conducting research related to how aspects of daily life impact the human body.

IJHSR
ijhighschoolresearch.org
REVIEW ARTICLE

Exercise Therapy in Stress Management

Haorui Zhang[1], Yi Wang[2]

1. Sanya Foreign Language School Affiliated to Shanghai International Studies University, No.1 Fengxiang Road, Tianya District, Sanya City, Hainan Province, 572000, China; andyzhangmm26@gmail.com
2. Crimson Education, 135 E 57th St, New York, NY 10022

ABSTRACT: Feeling stressed is common for individuals, but studies emphasizing the significance of Exercise Therapy (ET) in stress management are limited. This study aims to explain the potential of ET in reducing the negative effects of stress through an analysis of their physiologies. A literature search is performed on Google Scholar. Relevant sample papers or resources are filtered and collected. Accordingly, this study concludes possible trends and explanations based on the data or hypotheses presented in such resources. As a result, two conclusions about stress and ET are drawn. First, duration and intensity are likely significant factors that determine whether a stress response may be harmful. Specifically, duration might be the dominant factor because a high duration indicates insufficient recovery periods. Second, exercise can be considered a milder and more controllable form of stress, which might help train the body's response system. Based on these conclusions, this study gives two reasonable principles for the pragmatic use of ET.

KEYWORDS: Biomedical and Health Science, Pathophysiology, Stress, Exercise Therapy.

Introduction

Stress is a common state that individuals experience in modern society. This may be induced by problems in relationships, academics, or other aspects. Stress-induced diseases, such as obesity and depression, are also becoming more prevalent. Teenagers, who are facing intense competition with their peers, may be exposed to a riskier condition of over-intense stress or chronic stress. In this paper, mechanisms of stress-induced diseases and corresponding treatments are mentioned based on literature reviews. Chronic Low Back Pain (CLBP) and depression are used as examples for illustrating stress-induced diseases.

Many studies reviewed in this research rely on drug therapies and conventional psychological therapies as treatments for diseases likely induced by stress. For instance, a study in 2006 discovered that conventional drug therapies can be effective in the treatment of PTSD, which is a disease commonly induced by stress. Specifically, Paroxetine is used as a licensed medicine for treating PTSD. In this 12-week study, the groups using Paroxetine had an apparent improvement in Clinician-Administered PTSD Scale from the baseline starting from the 4th week compared to the placebo groups.[1] In addition, a study in 2011 pointed out that psychological methods can also help reduce stress-induced symptoms.[2] For instance, significant reductions in systolic and diastolic BP values are observed in some patients after the treatment. These conventional methods have been used for a period and were reported as effective. However, few studies have mentioned that exercise can also be helpful or even highly potent as a treatment for stress-induced diseases, especially in teenagers. In fact, some research, though not much, suggests that Exercise Therapy (ET) may have some advantages and additional benefits to individuals in the long term. For instance, it is reported that in CLBP, there is moderate-certainty evidence that suggests ET's probable effectiveness in eliminating pain in some chronic diseases.[3] Also, both aerobic and non-aerobic exercise interventions reduce depressive symptoms.[4] These demonstrate the possible value of ET. Thus, this paper evaluates the physiological changes of exercise and attempts to explain its potential use as a treatment.

Discussion

1. The mechanism of how stress does harm:

Generally, stress is a state of threatened homeostasis triggered by intrinsic or extrinsic adverse forces.[5] Pressure from the academy, work, or other social responsibilities are all modern stressors to individuals. However, stress may induce negative physiological adaptations in the endocrine system, the skeletal muscular system, and other systems in the human body. These physiological changes may lead to pathological changes and trigger diseases like Chronic low back pain (CLBP). Thus, treatments or precautions are required to train the body and enhance its stress tolerance.

Stress status is originally a natural state of the body, so possible treatments for stress-induced pathological changes need to be based on the mechanisms of human physiological responses to various stressors. The physiological response of the human body to stress primarily relies on the nervous system, specifically the autonomic nervous system, and the endocrine system. Neuroregulation of the nervous system and hormonal regulation of the endocrine system function in collaboration during these responses. The entire response process is divided into two minor steps: perception and regulation. Both steps involve physiological changes in certain organs or glands that contribute to the new homeostasis during stress.

The first step in any stress response is the perception of a threat.[6] This involves two levels: emotional experiences and

© 2026 Terra Science and Education

DOI: 10.36838/IJHSR87.244

physiological changes. The emotional responses, or an individual's feelings, are generated by the amygdala, hippocampus, and other brain regions.[7] These regions also activate the hypothalamus through nerve signals. In consequence, many of the physiological changes are triggered by activities of the hypothalamus, which is located in the central nervous system. It performs multiple functions related to hormone production and nervous system regulation. Specifically, it sends nerve signals that activate the autonomic nervous system and certain glands of the endocrine system, such as the adrenal gland, during a stress response.[8-10] When addressing the negative effects of stress on body functions, the physiological changes caused by the hypothalamus can be primarily considered, compared to emotional experiences. However, understanding how the emotional parts of the brain regulate the hypothalamus may help improve therapy strategies, benefiting individuals physically and emotionally. To the hypothalamus, the activity level of other brain regions is the main factor of its activation, while the modalities of the stressors that cause such activity in the other brain regions—including psychological, cognitive, and physiological ones—do not appear to be as important.[11] Different stressors may trigger various emotional experiences in individuals, but the same physiological process is initiated by the hypothalamus. Thus, a possible conclusion can be drawn to evaluate stressors' effects on responses. From the perspective of physiological changes, different stressors mainly determine the intensity of the response. However, different individuals may experience different levels of anxiety when facing the same challenge due to their unique emotional backgrounds, as seen in changes to vital signs like cardiac output. Additionally, chronic stress damages the proper functioning of the amygdala and hippocampus, which can impair hypothalamic functions and weaken the response system's adaptability, potentially creating a vicious cycle.[12]

The second step in the stress response process is regulation. Regulation of the body begins after the perception of stress has occurred. There are two main possible pathways that the hypothalamus stimulates. Based on the endurance of the stressor, stress can be classified as acute stress or chronic stress.

In case of an acute stress, which lasts for seconds or minutes, the hypothalamus triggers the adrenal gland mainly through neural pathways to produce epinephrine and norepinephrine, resulting in an instant increase in heartbeat, blood pressure, and muscle blood flow, and suppression of the digestive and immune system. These physiological changes are intense but of short duration, aiming for urgent Fight-or-flight responses.[13]

In the case of chronic stress that lasts for days or even longer, the endocrine system dominates the pathway mainly by triggering the HPA axis, which contributes to maintaining a high concentration of ACTH and cortisol in the blood.[14] This enables the body to cope with possible danger that has not yet existed.[15] This emergency state during stress, functions at the expense of deprioritizing the systems that perform normal metabolism, which makes it destructive to the health of the individuals in the long term. Thus, acute responses to stress have relatively less damage due to their short period. In fact, acute stress induced by mental arithmetic increases the duration of muscle contraction by 46% in men. This demonstrates that acute stress can even improve specific functions.[16] Chronic stress, on the other hand, responses are highly likely to induce detrimental physiological changes.[17] Thus, it is rational to conclude that the key variation between these two types of stress is whether a period of recovery exists. Specifically, acute stresses occur intermittently, allowing the body to regulate itself into a normal state before any subsequent stimulations and actively form adaptations that help the body cope with similar stresses in the future (Figure 1). This mechanism is implied in a study that emphasizes the benefits of napping in 57 healthy teenagers,[18] and another study points out the role of resting in muscle recovery.[19] Chronic stress, on the other hand, leads to compelling physiological changes. For instance, it is discovered that mental stress doubles the subjects' risk of facing myocardial ischemia.[20]

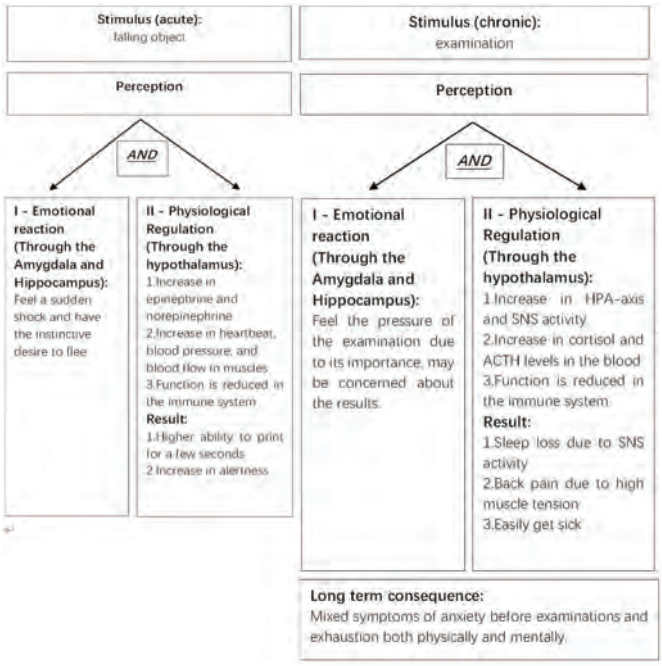

Figure 1: The different processes of stress response in acute and chronic stress (Note: the figure points out that the duration of stress may determine its effect on the body). Acute stress induces instant physiological changes, while chronic stress induces continuous physiological changes that are likely to be detrimental.

The mechanism of the physiological changes induced by chronic stress can be used to elaborate on the cause of some diseases that widely appear in modern society, for instance, CLBP or depression. In fact, stress in modern society is highly associated with the economy, and the global economy loses 12 billion workdays at a cost of about $1 trillion caused by stress every year. This kind of stress, which individuals commonly face, lasts for a long period and leaves individuals with little or no recovery periods. The top stressors include the economy, gun violence, and personal safety, which are all long-lasting problems.[21]

In cases of CLBP, many patients reported that there are no explicit causes for symptoms like soreness of the muscles. However, subjects under chronic stress with higher intensity

or duration tend to have a higher possibility of having such issues.[22] There are no clear mechanisms of this phenomenon, but a rational explanation is that high tension and blood flow in the muscles during stress conditions may cause damage to the muscle tissues, as well as leading to fatigue.

In cases of depression, stress may be a significant cause of depression, and chronic stress is predictive of depression.[23] This may be due to the disturbance of stress hormone release.[24] As mentioned earlier, if the body lacks proper recovery, hormone levels may remain abnormal and, therefore, may cause problems.

In conclusion, if analyzed from the perspective of physiology, the factors that may significantly impact the physiological changes are the stress intensity and duration. Low duration or sufficient recovery periods are important for building beneficial adaptations. To form such adaptations, the proper intensity of the stress is also important, which may vary among individuals due to emotional reasons. Its practice in the therapies will be discussed in "Principles of Using ET as a Treatment of Stress."

2. The theoretical basis of exercise therapy in stress management:

A study in 2005 points out that regular exercise is instrumental in eliminating anxiety and sub-healthy status in individuals suffering from chronic stress.[25] This is possibly relevant to physiological changes during and after exercise. These changes may contribute to the adaptations of the human body systems and make them more resilient to stress.

The physiological changes in the body during a single bout of exercise closely resemble those in conventional acute stress. During exercise, the sympathetic nervous system (SNS) is highly activated. It regulates blood flow by causing vasodilation in skeletal muscles, resulting in active hyperemia and shunting, while inducing vasoconstriction in other organs not directly involved in movement, such as the kidneys. Stress hormones such as epinephrine and norepinephrine, which are also neurotransmitters of the SNS, are produced in higher amounts to facilitate targeted energy distribution that prepares the skeletal muscular system. Additional stress-related hormones, such as glucagon and growth hormone (GH), also increase to break down stored nutrients for energy.[26] Therefore, it is reasonable to conclude that a single bout of exercise can be regarded as a form of acute stress because its physiological response closely aligns with the typical response to acute stress. As mentioned earlier, acute stress causes relatively low damage to the body and is unlikely to trigger harmful adaptations. Similar to acute stressors, exercise generally does not harm normal bodily functions if performed at moderate intensity. However, overtraining can be destructive and lead to overtraining syndrome (OTS), which may result in symptoms such as sleep disturbances and immune problems, similar to the pathological changes that chronic stress might induce (Figure 2).[27]

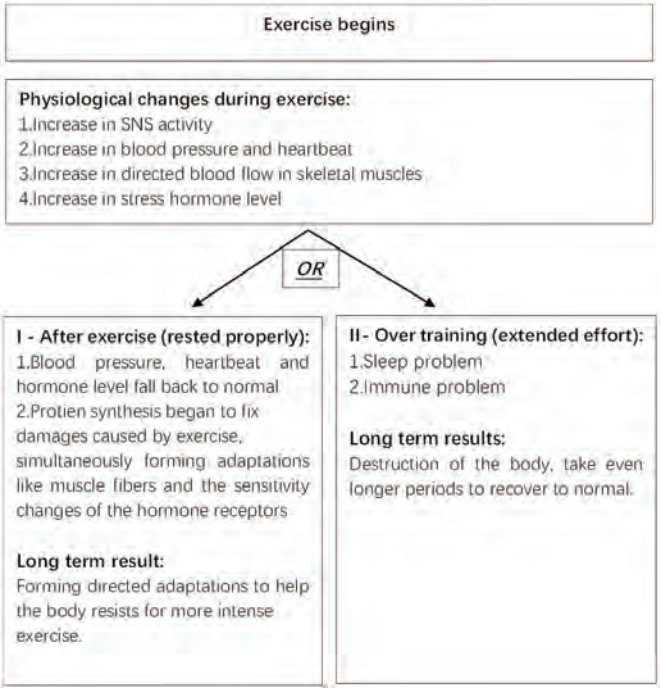

Figure 2: The physiological changes during and after exercise (Note: this figure points out that the intensity of exercise may determine its effect on the body.[26,27]). Proper exercise builds beneficial adaptations, while overtraining may be destructive.

Significant physiological similarities exist between acute stress and exercise, as well as between chronic stress and overtraining. The reason they are closely bonded may be explained from the perspective of evolution. In a natural state, most stresses for humans come from the threat of predators, which requires the individual to be prepared for sprinting, jumping, and other physical movements. Thus, the skeletal muscular system, as well as the cardiovascular and respiratory systems, becomes the priority during stress responses.[28] Exercise impacts the skeletal muscular system and relevant systems with similar objectives as other conventional stressors do, but with lower intensity and duration, since the challenges in sports are not a vital issue nor a continuous and significant challenge. The physiological changes in exercise make it a vivid but mild stressor that trains the body's response system. The method of using exercise to induce adaptations in the human body functions similarly to vaccines, known as exercise therapy (ET).

Based on the way ET functions, it has two key advantages: it can be qualified and customized. These advantages ensure that stimuli to the stress response system can be accurate and precise on the level of both duration and intensity.

From the level of duration, ET can provide the individual with sufficient recovery periods, which are essential to both avoiding exhaustion and forming beneficial adaptations. Through periods of systematic training, individuals' baseline cortisol declines, and during subsequent stresses, the cortisol spike also resolves to the baseline more quickly.[29] Similar mechanisms were concluded in studies relevant to muscle building—new and thicker muscle fibers begin to appear two to four hours post-exercise if rest and nutrition are sufficient.[26] These results indicate that though stress status causes fluc-

DOI: 10.36838/IJHSR87.244

tuations of normal metabolisms and instant instability, the adjustment process may construct a more efficient pathway of coping with future stresses. Moreover, conscious adaptations, for instance, self-confidence, also play an important role besides physiological ones.[30] Even when chronic stress already causes severe physiological changes, some of them, for instance, cognitive disorders in the hippocampus, are still reversible through intensified exercise.[31] The principles of how the recovery periods should be arranged will be discussed in "Principles of using ET as a treatment of stress."

From the level of intensity, ET makes sure the intensity and content of the training sessions are helpful for the adaptation of stress resilience. The intensity and types of stressors affect the long-term adaptations after regular exposure to the stressors.[32] This study points out that the content of the stressor can possibly affect the type of long-term effects formed after exposure to those stressors. Specifically, repeated low-intensity stimuli trigger adaptation, which decreases the magnitude of the response progressively. However, exposure to a stimulus followed by a different and novel stimulus often leads to an enhanced response to the original stimulus, forming a dishabituation. Moreover, when the stimulus is noxious, the response magnitude also increases. According to the physiology mentioned earlier in this paper, this may be attributed to the activation of the amygdala, the hippocampus, or other cognitive encephalic regions.[12] When a new or noxious stressor appears, these regions of the brain might be highly activated. They are likely to generate stronger signals that stimulate the hypothalamus; therefore, they are likely to cause more intense physiological changes and emotional experiences. In contrast, repeated stressors with lower intensity induce less excitement in relevant encephalic regions, and as the stimuli repeatedly occur, the response would be even weaker. Exercise, as mentioned earlier, can be considered a relatively milder stressor compared to other conventional ones, so it can likely trigger adaptations and reduce the magnitude of the physiological changes in future exposures to similar types of stress. Professional therapists can also design training regimens customized for individuals. By arranging ET of various types, the individuals involved would build adaptation in coping with multiple types of stress. The principles of how the intensity and content of the training sessions should be arranged will be discussed in "Principles of Using ET as a treatment of stress."

Such advantages of ET can explain the improved outcomes in CLBP treatment by combining ET into the therapy. Regular exercise increases muscle strength in the lower back of patients, which prolongs the time it takes for the muscles to fatigue in daily activities. SNS activity will also maintain a relatively lower activity, reducing abnormal muscle tension that may cause chronic pain or soreness.

Similarly, the benefits of ET make it applicable for the treatment of depression, and possible mechanisms of exercise's function may lie within the brain. New adaptations may form in the central nervous system after exercising for a period.[33]

However, though ET gives some positive feedback in disease treatments, it is still important to consider some possible limitations when applying ET to the treatment of individuals. Studies have also highlighted that the effectiveness of ET is only evident in subacute diseases, suggesting that this methodology has limitations.[34] Though other studies imply that ET induces no increase in serious adverse events, involving exercise in acute stresses or diseases, especially intense ones, may deteriorate the disease.[34,35]

In conclusion, ET can be a potential method in solving stress-induced negative physiological changes because it can activate the body's stress response system with stimuli of lower duration and intensity compared to conventional stressors.

3. Principles of using ET as a treatment for stress:

As mentioned earlier, the key mechanism of how ET produces positive outcomes may be based on the adaptation it triggers. In some chronic diseases, detrimental adaptations and an unhealthy state of homeostasis have already formed. Exercise helps the body restrain such negative physiological changes, and, in some cases, reverse them by rebuilding healthy adaptations. Exercise can also prevent further pathological changes that might occur if such an unhealthy homeostasis is maintained.

However, since ET is designed for individuals who have underlying diseases or disabilities induced by chronic stress, training regimens for healthy individuals or even athletes will be risky for them. ET constructed for these individuals should be more cautious to eliminate factors that might debilitate the present condition, since cases of negative side effects have been reported. Thus, two essential principles can be proposed for using ET in stress management to ensure its safety and effectiveness based on its mechanism of forming adaptations.

The first principle is that sufficient recovery periods are very important. The whole training process should be designed as a loop of "exposure status" and "resting status." During the exposure status, the individual would participate in certain physical activities and experience stress induced by such activities. After the exposure status, the individual would need enough time to rest so that the body can repair the damage caused by the exposure in the resting status. The resting period, specifically, needs to be prolonged until the individual does not experience any discomfort from the training, both physically and mentally.36 As mentioned earlier, resting, as well as sufficient nutrients, is essential for the body to form directed adaptations. If an individual remains in a restless, stressed state, it is highly possible for negative adaptations to form in response, which exacerbates the symptoms.

Specifically, in the case of designing ET regimens for CLBP, not many studies have mentioned the specific standards or methodologies for the training routines for curing CLBP, but it is reasonable to extrapolate from the regimens designed for healthy individuals and make adjustments to ensure that these routines are proper for individuals with CLBP. For a normal, healthy adult, it is proper to have 1-2 days of rest after intense or moderate training, and it may vary slightly depending on the type of training, which may include aerobic training or resistance training.[37] For individuals with CLBP, the resting period could be suitably extended. For instance, with a young individual with moderate CLBP, two to three days of training

separated by resting days may be appropriate. This training frequency may apply to depression treatments as well. Exercise that was performed 3-5 times weekly and of moderate intensity may be helpful for depression. The entire training process may take 4-16 weeks.[38]

The second principle is that it is beneficial to design training content with relatively low risk and intensity. As mentioned earlier, the intensity and content of the stimuli may determine the type of long-term effects formed. Thus, it is essential to ensure that the intensity of the ET is relatively low to avoid possible risks. The individual who participates in the therapy also needs to have full access to the possible risks and disappointments of the training sessions before they begin. This reduces unexpected or new stress experiences during the training. The participant's emotional experiences need to be considered, particularly because similar training tasks may result in entirely different response intensities in individuals with different backgrounds. In addition, recreational training may enhance the benefits. Specifically, it shows that recreational football helps to decrease systolic blood pressure by 4.20 mm Hg and diastolic blood pressure by 3.89 mm Hg compared to no-exercise controls or continuous running training.[39]

Specifically, in the cases of designing ET regimens for CLBP, regular outdoor activities like walking and indoor specialized training can both be considered, but with low or moderate intensity for each session. In addition, the patient needs to be aware of the most likely risks during training, for instance, having stroke defects or muscle soreness. Thus, this study discusses the possible therapy process (Figure 3).

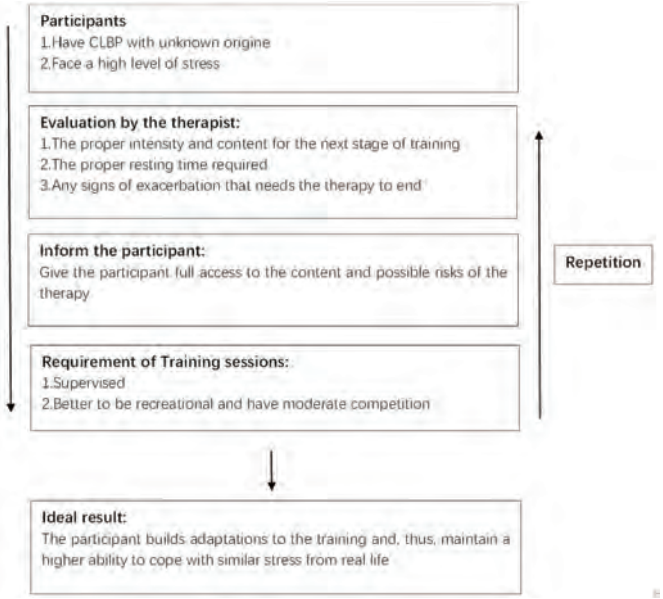

Figure 3: The ideal design of the ET process, as in the example of CLBP (Note: Consistent evaluation and training may be required for a relatively long period to reach the ideal outcome, as explained in "Principles of using ET as a treatment for stress"). The participant may benefit from ET, for example, by forming adaptations to similar types of stress. However, further research on ET is still needed.

Conclusion

Stress status, as a product of evolution, is for facing incidents that may be a threat to the individual's survival. However, due to stress responses' prioritizations on the specific systems of the body, the deficiency of normal metabolism appears after a long duration. When the body lacks recovery time or has limited ability to eliminate negative physiological changes that occur during stress, chronic diseases like CLBP and depression are likely to develop. Thus, exercise therapy may be introduced to help build a more resilient and adaptive pathway for the individuals' stress responses. The similarities between exercise and other conventional stressors help exercise mimic these conventional stressors better. Since the duration and intensity of exercise are relatively low and can be manually quantified, the risk of introducing extreme intensity and overactivating the response system is minimized. Among the studies included in this paper, the evident efficacy of ET indicates that it can be a preferred treatment or precautionary measure for diseases induced by chronic stress if performed with a sufficient recovery period and proper content. Introducing individuals to the habits of exercising can also be beneficial for their quality of life and well-being in the long term.

In addition, further research can be conducted on quantifying the assessment system, improving the accuracy and precision of the evaluation before, during, and after training. This may provide more reliable training regimens and eliminate possible risks.

Acknowledgments

There is no funding support for this work. This work was completed under the mentorship of my mentor, Yi Wang, a former tenured Professor of Public Health at Indiana University.

References

1. Davidson, J. R. T. Pharmacologic Treatment of Acute and Chronic Stress Following Trauma. *J Clin Psychiatry* **2006**.
2. Niazi, A. K.; Niazi, S. K. Mindfulness-Based Stress Reduction: A Non-Pharmacological Approach for Chronic Illnesses. *N Am J Med Sci* **2011**, *3* (1), 20–23. DOI: 10.4297/najms.2011.320
3. Hayden, J. A.; Ellis, J.; Ogilvie, R.; Malmivaara, A.; Stewart SA.; Bagg MK.; Stanojevic S.; Yamato TP.; Saragiotto BT. Some types of exercise are more effective than others in people with chronic low back pain: a network meta-analysis. *J Physiother* **2021**, *67*(4), 252-262. DOI: 10.1016/j.jphys.2021.09.004.
4. Stanton, R.; Reaburn, P. Exercise and the Treatment of Depression: A Review of the Exercise Program Variables. *Journal of Science and Medicine in Sport* **2014**, *17* (2), 177–182. DOI: 10.1016/j.jsams.2013.03.010
5. Contrada, R.; Baum, A. *The Handbook of Stress Science: Biology, Psychology, and Health*; Springer Publishing Company, 2010.
6. Dushyant Kumar Sharma.; Physiology of Stress and its Management. *Journal of Medicine Study & Research* **2018**. DOI:10.24966/MSR-5657/100001
7. LeDoux, J. E. The Amygdala: Contributions to Fear and Stress. *Seminars in Neuroscience* **1994**, *6* (4), 231–237.
8. Chu, B.; Marwaha, K.; Sanvictores, T.; Awosika, A. O.; Ayers, D. Physiology, Stress Reaction. In *StatPearls*; StatPearls Publishing: Treasure Island (FL), 2025.

DOI: 10.36838/IJHSR87.244

9. Miller, D. B.; O'Callaghan, J. P. Neuroendocrine Aspects of the Response to Stress. *Metabolism - Clinical and Experimental* **2002**, *51* (6), 5–10. DOI: 10.1053/meta.2002.33184
10. Walters, S. Psychology – 1st Canadian Edition. *3.4 Putting It All Together: The Nervous System and the Endocrine System*. 2020.
11. Karthikeyan, P.; Murugappan, M.; Yaacob, S. A Review on Stress Inducement Stimuli for Assessing Human Stress Using Physiological Signals. In *2011 IEEE 7th International Colloquium on Signal Processing and its Applications*; 2011; pp 420–425. DOI: 10.1109/CSPA.2011.5759914
12. Roozendaal, B.; McEwen, B. S.; Chattarji, S. Stress, Memory and the Amygdala. *Nat Rev Neurosci* **2009**, *10* (6), 423–433. DOI: 10.1038/nrn2651.
13. Romero, M. L.; Butler, L. K. Endocrinology of Stress. *International Journal of Comparative Psychology* **2007**, *20* (2). DOI: 10.46867/ijcp.2007.20.02.15.
14. Tsigos, C.; Kyrou, I.; Kassi, E.; Chrousos, G. P. Stress: Endocrine Physiology and Pathophysiology. In *Endotext*; Feingold, K. R., Ahmed, S. F., Anawalt, B., Blackman, M. R., Boyce, A., Chrousos, G., Corpas, E., de Herder, W. W., Dhatariya, K., Dungan, K., Hofland, J., Kalra, S., Kaltsas, G., Kapoor, N., Koch, C., Kopp, P., Korbonits, M., Kovacs, C. S., Kuohung, W., Laferrère, B., Levy, M., McGee, E. A., McLachlan, R., Muzumdar, R., Purnell, J., Rey, R., Sahay, R., Shah, A. S., Singer, F., Sperling, M. A., Stratakis, C. A., Trence, D. L., Wilson, D. P., Eds.; MDText.com, Inc.: South Dartmouth (MA), 2000.
15. Leroith, D.; Delahunty, G.; Lynn wilson, G.; Roberts, C. T.; Shemer, J.; Hart, C.; Lesniak, M. A.; Shiloach, J.; Roth, J. Evolutionary Aspects of the Endocrine and Nervous Systems. In *Proceedings of the 1985 Laurentian Hormone Conference*; Greep, R. O., Ed.; Recent Progress in Hormone Research; Academic Press: Boston, 1986; Vol. 42, pp 549–587. DOI: 10.1016/B978-0-12-571142-5.50017-3.
16. Berdina NA.; Kolenko OL.; Kotz IM, Kuznetzov AP.; Rodionov IM.; Savtchenko AP.; Thorevsky VI. Increase in Skeletal Muscle Performance during Emotional Stress in Man. *Circulation Research* **1972**. DOI: 10.1161/01.RES.30.6.642.
17. Bosnjak, M. C.; Dobovski-Poslon, M.; Bibic, Z.; Bosnjak, K. The Influence of chronic stress on health and coping mechanisms. *SANAMED* **2019**, *14* (1), 97–101. DOI:10.24125/sanamed.v14i1.293.
18. Lim, J.; Lo, J. C.; Chee, M. W. L. Assessing the Benefits of Napping and Short Rest Breaks on Processing Speed in Sleep-Restricted Adolescents. *Journal of Sleep Research* **2017**, *26* (2), 219–226. DOI: 10.1111/jsr.12497.
19. Chennaoui, M.; Vanneau, T.; Trignol, A.; Arnal, P.; Gomez-Merino, D.; Baudot, C.; Perez, J.; Pochettino, S.; Eirale, C.; Chalabi, H. How Does Sleep Help Recovery from Exercise-Induced Muscle Injuries? *Journal of Science and Medicine in Sport* **2021**, *24* (10), 982–987. DOI: 10.1016/j.jsams.2021.05.007.
20. Golbidi, S.; Frisbee, J. C.; Laher, I. Chronic Stress Impacts the Cardiovascular System: Animal Models and Clinical Outcomes. *American Journal of Physiology-Heart and Circulatory Physiology* **2015**. DOI: 10.1152/ajpheart.00859.2014.
21. Smith, M. D.; Wesselbaum, D. Global Evidence on the Prevalence of and Risk Factors Associated with Stress. *Journal of Affective Disorders* **2025**, *374*, 179–183. DOI: 10.1016/j.jad.2025.01.053.
22. Atkinson JH.; Slater MA, Grant I, Patterson TL.; Garfin SR. Depressed mood in chronic low back pain: relationship with stressful life events. *Pain* **1988**. DOI: 10.1016/0304-3959(88)90275-8
23. Hammen, C. L. Stress and Depression: Old Questions, New Approaches. *Current Opinion in Psychology* **2015**, *4*, 80–85. DOI: 10.1016/j.copsyc.2014.12.024.
24. Van Praag, H. M. Can Stress Cause Depression? *Progress in Neuro-Psychopharmacology and Biological Psychiatry* **2004**, *28* (5), 891–907. DOI: 10.1016/j.pnpbp.2004.05.031.
25. Smidt, N.; de Vet, H. C. W.; Bouter, L. M.; Dekker, J. Effectiveness of Exercise Therapy: A Best-Evidence Summary of Systematic Reviews. *Australian Journal of Physiotherapy* **2005**, *51* (2), 71–85. DOI: 10.1016/S0004-9514(05)70036-2.
26. Tarasova, O. S.; Borovik, A. S.; Kuznetsov, S. Y.; Popov, D. V.; Orlov, O. I.; Vinogradova, O. L. The Pattern of Changes in Physiological Parameters in the Course of Changes in Physical Exercise Intensity. *Hum Physiol* **2013**, *39* (2), 171–177. DOI: 10.1134/S0362119713020163.
27. Kreher, J. B.; Schwartz, J. B. Overtraining Syndrome: A Practical Guide. *Sports Health* **2012**, *4* (2), 128–138. DOI: 10.1177/1941738111434406.
28. Nesse, R. M.; Bhatnagar, S.; Ellis, B. Chapter 11 - Evolutionary Origins and Functions of the Stress Response System. In *Stress: Concepts, Cognition, Emotion, and Behavior*; Fink, G., Ed.; Academic Press: San Diego, 2016; pp 95–101. DOI: 10.1016/B978-0-12-800951-2.00011-X.
29. Mastorakos, G.; Pavlatou, M.; Diamanti-Kandarakis, E.; Chrousos, G. P. Exercise and the Stress System. *Hormones (Athens)* **2005**, *4*(2),73-89.
30. Knapen J.; Vancampfort D.; Moriën Y.; Marchal Y. Exercise therapy improves both mental and physical health in patients with major depression. *Disabil Rehabil* **2015**. DOI:10.3109/09638288.2014.972579
31. McEwen, B. S. The Brain Is the Central Organ of Stress and Adaptation. *Neuroimage* **2009**, *47* (3), 911–913. DOI: 10.1016/j.neuroimage.2009.05.071.
32. McCarty, R. Learning about Stress: Neural, Endocrine and Behavioral Adaptations. *Stress* **2016**, *19* (5), 449–475. DOI: 10.1080/10253890.2016.1192120.
33. Gujral, S.; Aizenstein, H.; Reynolds, C. F.; Butters, M. A.; Erickson, K. I. Exercise Effects on Depression: Possible Neural Mechanisms. *General Hospital Psychiatry* **2017**, *49*, 2–10. DOI: 10.1016/j.genhosppsych.2017.04.012.
34. *Exercise therapy for chronic low back pain (Review)*, Cochrane Library. 2021 https://www.cochranelibrary.com/cdsr/doi/10.1002/14651858.CD009790.pub2/pdf/full
35. Niemeijer, A.; Lund, H.; Stafne, S. N.; Ipsen, T.; Goldschmidt, C. L.; Jørgensen, C. T.; Juhl, C. B. Adverse Events of Exercise Therapy in Randomised Controlled Trials: A Systematic Review and Meta-Analysis. *Br J Sports Med* **2020**. DOI: 10.1136/bjsports-2018-100461.
36. Skorski, S.; Mujika, I.; Bosquet, L.; Meeusen, R.; Coutts, A. J.; Meyer, T. The Temporal Relationship Between Exercise, Recovery Processes, and Changes in Performance. Int J Sports *Physiol Perform* **2019**. DOI: 10.1123/ijspp.2018-0668.
37. Lehrer, P. M.; Woolfolk, R. L.; Sime, W. E. *Principles and Practice of Stress Management, Third Edition*; Guilford Press, 2007.
38. Xie, Y.; Wu, Z.; Sun, L.; Zhou, L.; Wang, G.; Xiao, L.; Wang, H. The Effects and Mechanisms of Exercise on the Treatment of Depression. *Front. Psychiatry* **2021**, *12*. DOI: 10.3389/fpsyt.2021.705559.
39. Milanović, Z.; Pantelić, S.; Čović, N.; Sporiš, G.; Mohr, M.; Krustrup, P. Broad-Spectrum Physical Fitness Benefits of Recreational Football: A Systematic Review and Meta-Analysis. *Br J Sports Med* **2019**, *53* (15), 926–939. DOI: 10.1136/bjsports-2017-097885.

Author

Haorui Zhang is a student at Sanya Foreign Language School Affiliated to Shanghai International Studies University. He is interested in exercising and is willing to solve problems teenagers face. He has been learning and researching in the field of biology and sports science. He hopes to make further and more constructive contributions to sports science and public health.

DOI: 10.36838/IJHSR87.244

IJHSR
ijhighschoolresearch.org
RESEARCH ARTICLE

Breaking Bad: Adversarial Prompting Targeting Feed Forward Neural Networks Within Transformers

Luca Chang

St. John's School, 2401 Claremont Lane, Houston, Texas, 77019, USA; lucanathanaelchang@gmail.com
Mentor: Siddharth Krishnan

ABSTRACT: Generative Pretrained Transformers (GPTs) are the behemoths of the Language Modeling world, at the cutting edge of AI research with massive interest and widespread use. However, attacks focusing on the feed-forward neural networks (FFNs) within every transformer are sparingly studied. In this paper, we aim to target this preprocessing stage of the model and determine whether prompts can be crafted that target the FFNs of models to elicit adversarial failure. We hypothesize that if a probe is found to pass through attention and target the first FFN, this probe would cause cascading problems for downstream parts of the model and eventual model failure. To test this hypothesis, we use several different Small Language Models (SLMs) from varying families and generate probes that pass through each model's attention, targeting the FFN within the primary encoding layer. These targeting probes were then fed into the models, and their outputs were evaluated. Our results indicate that despite such a small model size, we can consistently observe a divergence in quality of writing as compared to a control, with more than 80% of models demonstrating a greater than 57% reduction in quality of writing. This approach demonstrates a novel way to attack Language Models. This probing method employs white box techniques, utilizes a small overhead (~7.5% to ~46.9%) of total model parameters, and is capable of eliciting adversarial failure. We present a new method of attack that is able to be scaled with greater compute power and more time for attacking modern-day Language Models (LMs) efficiently.

KEYWORDS: Robotics and Intelligent Machines, Machine Learning, Transformer, Adversarial Attacks, Natural Language Processing.

Introduction

Generative Pretrained Transformers (GPTs) have taken the world by storm over the last few years. With powerful models open to public use, such as the Llama family, and becoming more and more commonly integrated with our everyday lives, the weaknesses of these models need to be explored.[1] As these models become more and more ubiquitous, it is critical to ensure that these models remain resilient to attacks to preserve the model's integrity from the public. These models are also capable of performing a wide range of tasks and can be fine-tuned for specific tasks. Furthermore, models such as ChatGPT-3, other language models, and even Small Language Models (SLMs) can also significantly impact a range of industries, due to impressive natural language processing capabilities and the capacity to analyze and interpret huge amounts of text.[2] For example, ChatGPT-3 has been inserted into basic customer service and legal jurisdictions, and applied in education to aid the grading of writing quality, and SLMs have the advantage of being able to run on small devices to perform local tasks, thereby becoming more accessible to the general public.[3] Furthermore, these transformers can heavily impact the coding sector, possibly on track to replace developers, website designers, and others as they become ever more skilled at coding, and they are highly useful for students and individuals to learn skills, such as programming.[4,5] However, model failures, such as model bias, model collapse, misclassification, or misinformation, are detrimental to the functionality of these models, thereby impacting users' jobs and their industrial sectors.[6] The effects of model failures become ever more amplified in society as the adoption of SLMs and LLMs continues to grow. Therefore, attacks that result in model failure, known as adversarial attacks, are of prime importance in research to analyze, understand, and prevent.

Many different methods of adversarial attacks have been performed on language models. These attacks are used to cause models to fail in regard to their essential function, causing language models to generate potentially harmful misinformation. The field of adversarial attacks focuses on understanding how models fail and the ability to repeatedly elicit failure via editing the training data, creating specific input prompts, or even via hardware vulnerabilities.[7]

Adversarial attacks are split into poisoning attacks and evasion attacks, which operate using two fundamentally different principles. In poisoning attacks, the training data itself is corrupted, and biases are introduced via faulty information, eventually causing model failure, such as misclassification. In evasion attacks, testing data is modified to elicit an expected result from the model.[8] These evasion attacks can cause model failure, faulty generations, and errors in the model's tasks.

Within the domain of evasion attacks, several different prompt-based modes of attack, such as direct prompt injection, indirect prompt injection, optimization-based jailbreaks, and others, have been shown to be effective at inducing model failure or harmful or irrelevant model generations in both SLMs and LLMs.[9,10] Several of these methods are specifically caused by and enabled because of the transformer model's ar-

© 2026 Terra Science and Education

DOI: 10.36838/IJHSR87.251

chitecture.[11] One of the main categories of prompt attacks is prompt injection. These attacks are subdivided into white-box and black-box attacks, where white-box signifies the use of the model's parameters and architecture, in contrast to black-box, which signifies that interaction happened without knowledge of the internals of the model's weights and architecture. Black box methods, such as in-context learning adversarial prompts, have been shown to be effective.[12] White-box methods are more capable of causing model failure, as they can use methods based on the model's weights, and are further divided into many common forms of attack.

Several white-box methods are of incredible interest in the field of adversarial attacks. In fine-tuning attacks, a common white-box attack, the model is retrained or fine-tuned with malicious data, causing it to struggle with performing the tasks it was designed to do. This can even cause model collapse when a prompt is similar to a harmful data point the model was trained on. Another form of attack is logit-based attacks. They are commonly used when partial white-box information is known, and utilize the logit probability distribution from the internals of the model to then generate jailbreaking prompts. Gradient-based attacks manipulate the prompt based on the gradients to elicit particular responses, backpropagating and determining results via reconstructing probes.[9] Competing adversarial models, such as in Weak-to-Strong attacking methods, may also be trained to aid in generating jailbreaking and adversarial probes, but this method can also be computationally intensive, requiring the use of external LMs.[13]

Indirect prompt injections operate similarly to prompt injection attacks, but require that the model open files or websites, providing access and processing of external content. In doing so, they expose themselves to the previously discussed prompt injection attacks, resulting in model failure or jailbreaking.[14]

Optimization-based jailbreaks are also another studied method of attack. There are numerous different manual and automated methods to generate prompts designed to jailbreak Language Models, causing them to produce harmful content. Utilizing gradient-based methods within a white-box architecture, such as Greedy Coordinate Gradient (GCG) or AutoDAN, has proven to be effective at jailbreaking models.[15-17] Another example is Bit Flip Attacks, which is a gradient-based method targeting and modifying specific parameters in the model that perform more of the information extraction than their peers. This method has been known to increase instability and undermine accuracy.[16] However, all of these gradient-based optimization methods can be computationally intensive with scaled model size, with current active research focusing on improving efficiency in GCG and other gradient-based methods.[15]

In this paper, we use a prompt-injection, auto-generated, white box method. This method relies heavily on the architecture of the Generative Pretrained Transformer (GPT).[17] In GPTs, models first use a tokenizer to split inputs into an array of integer tokens. These tokens then enter an input embedding layer, before being passed through one or more encoding layers. Within these encoding layers, normalization and attention are applied, and the information is then fed into a small neural net called a Feed Forward Neural-Network (FFN). Eventually, after the input has gone through all the encoding layers, it is passed into the complex, large neural net of the model, with many millions or billions of parameters.[17] Based upon this knowledge of the transformer architecture, we wondered whether it is possible to cause SLM's output to degrade or jailbreak an SLM by injecting inputs targeting the FFN within the first encoding layer, with the intention of causing a cascading effect of sparsely activated neurons. The current field of adversarial attacks has analyzed white-box gradient descent methods and prompt injection with weight modifications as methods of adversarial prompting for transformers, but has not touched on utilizing FFNs as a target to address. Notably, these methods deal primarily with the large neural net within these models, as in gradient descent, or edit the training data or the model weights themselves, but do not focus on targeting FFNs to attack the transformer.[18] The gradient descent method of attack has been shown to be effective, but it can be highly computationally expensive and difficult for large language models, especially as the complexity of the model increases. Training or retraining transformers on adversarial data has been shown to induce instability, but requires heavy computing to train or retrain these models. As there is a major move towards SLMs, transformer models that are able to be run on smartphones and small devices, which are also known to be even more susceptible to breaking and prompting attacks than LLMs.[10] As SLMs are becoming more and more widespread, development methods and adversarial prompts must be studied to make them safer and more powerful in common use.[19] We conjecture that our probes can cause generations of what the model has memorized within its weights, providing a method for developers to observe the inner workings of models and show a novel and more efficient method of adversarial prompting. We hypothesize that if a probe is found to pass through the attention and target the first FFN, this probe would cause cascading problems for downstream parts of the model and eventual model failure, specifically output degradation, due to the succeeding encoding layers and neural nets receiving less information. We also hypothesize that larger models will be more resilient to the attack, as they store more information and can thus produce coherent results, even with adversarial inputs.

This paper aims to demonstrate a novel, efficient method to generate probes that induce model failure, specifically output degradation, utilizing a relatively small overhead of accessible parameters. This allows for increased speed of generation for adversarial prompts, opens doors for further research in adversarial prompting, including multimodal prompts, and provides a scalable method for larger and larger models.

Methods

To test our hypothesis, we performed tests on several SLMs with different sizes and different families. We tested Pythia, Qwen, Gemini, Phi, TinyStories, and Llama models. We gathered each of the models from the open-source library HuggingFace, and used an L4, T4, or A1000 GPU on Google Colaboratory and Kaggle to run the model to create genera-

tions. The parameters and parts of the model we accessed to create these generations were limited to the model tokenizer as well as the first embedding layer, which contains the attention block and the FFN. Using only these parts, the full pipeline we used to generate and evaluate our probes can be divided into several steps:

a) Generate FFN input

To reverse the FFN probe, we first chose an ideal probe, which we will aim to have the FFN output. In this paper, we initialized it to be an array of zeros, which was chosen to demonstrate a proof of concept. We then use a Tree Parzen Estimator Sampler (TPESampler) and the open-source library Optuna, running 150 iterations to generate and refine an input to the FFN to produce this ideal probe.[20] We use Squared Error as the loss metric for Optuna, and score the difference between the generation of the FFN and the ideal probe. Figure 1 highlights the generation architecture.

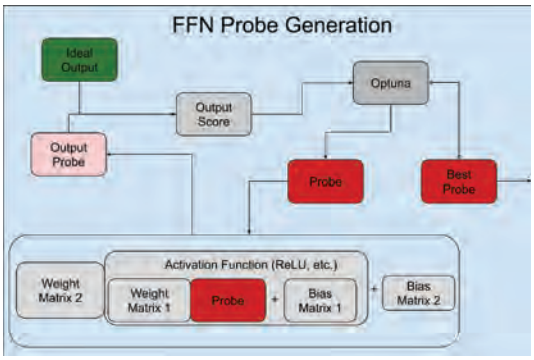

Figure 1: FFN probe generation architecture using Optuna to generate FFN inputs. Figure 1 demonstrates the architecture used to generate an FFN input when given an ideal output vector to optimize towards. Using Optuna, we generate a new probe, pass it through the FFN layer, score the output, and iteratively refine an FFN input to closely match the ideal output by minimizing our score. After this process has been repeated enough times, we return the best FFN input probe found.

b) Reversing Attention

With a chosen set of inputs to the FFN, we now try to reverse through the preceding layers to craft a plaintext input. We choose a set of tokens of arbitrary size n. This n is the length of a token input to the transformer. Next, we use the TPESampler to generate n token indices, sampling from the valid token indices. We then pass the token indices through layer normalization, attention, and the often-present post-layer normalization, and score the output by Mean Squared Error (MSE) against the ideal probe. We then save this best performing set of tokens with minimal MSE, convert this set of tokens into a prompt, and run 50 iterations for each input. We generated prompts with a length ranging from 30 to 120 tokens. Figure 2 demonstrates the reversal architecture.

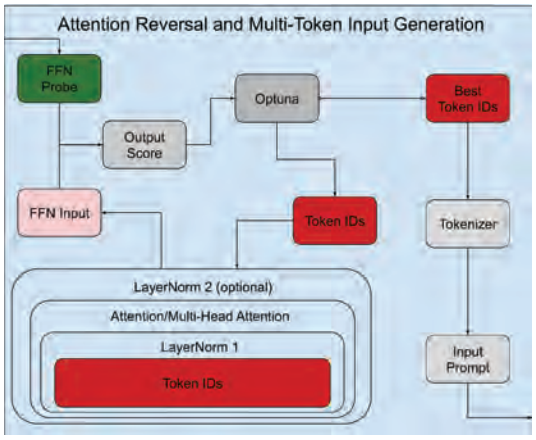

Figure 2: Attention reversal and multi-token input architecture to generate prompts. Figure 2 demonstrates the architecture used to generate an input prompt given an FFN probe as input. The FFN probe, supplied as a vector, is processed using Optuna and several trials, eventually returning the input prompt as a string that can be fed into a tokenizer and then a model.

c) Generate Outputs

With the previous input strings, we fed 28 control strings and 19 test strings into the model and stored the generation and the input prompt. The input prompt was removed from the model's output, and the remaining output was saved and stored.

d) Evaluating and Scoring Outputs

To evaluate and score the outputs, the Groq platform was used. Taking inspiration from previous work in the field, where an LLM was used to evaluate text, we used the "google/gemma2-9b-it" model as our evaluation model and fed each generation to the model.21 Each individual score, ranging from 0, gibberish, to 100, grammatically sound, logical text, was then recorded, and the evaluation model did not have a running context. This method was used to score the outputs of input prompts generations from a length of 30 tokens to 120 tokens, scoring 28 chat-like control prompts. See the appendix for the 28 control prompts and the exact wording for the evaluation of the output text.

A GPU was used to run all generations, and the Optuna library ran on a CPU. The TPESampler, model generation, and all aspects of the process were seeded to ensure deterministic results, and outputs of the model were stored and saved.

■ Results and Discussion

Results:

We tested several different SLMs across several different families, such as Phi, Llama, and Qwen. Our metric for scoring generated text requested that the Groq model "google/gemma2-9b-it" score the text based on factors including punctuation, grammar, spelling, coherence, and penalized repetition. Using these scores, we defined average percent underperformance as the difference between the mean score of the control generations and the mean score of the generated texts for a model, all divided by the mean score of the control of the model. This metric was chosen to provide a clear way for observers to see the effects that these generated inputs have on the model's capability to function. Our results are demonstrated below.

DOI: 10.36838/IJHSR87.251

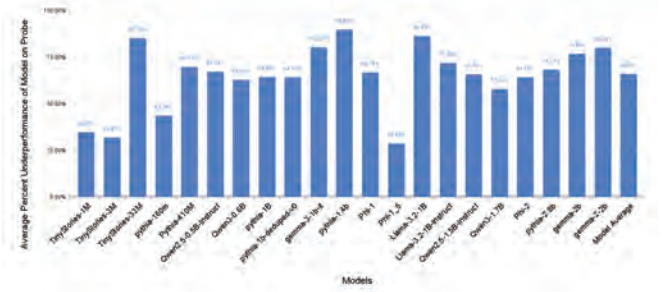

Figure 3: Average percent model underperformance across all models. In Figure 3, it is apparent that there is significant underperformance of these probes, with the lowest underperformance being 28.83% and the greatest being 89.80%. Furthermore, the average of the model's underperformance was 67.16% ± 14.35%, and the geometric mean ratio of the controls and the inputs was 31.12%, a 68.78% average decrease when compared. These results demonstrate that the models perform significantly worse on the input probes than the control set.

After determining that there was a significant decrease in model performance when fed these probes, as observed in Figure 3, we determined whether the model underperformance correlated with the size of the model. Our results are shown below in Figure 4.s

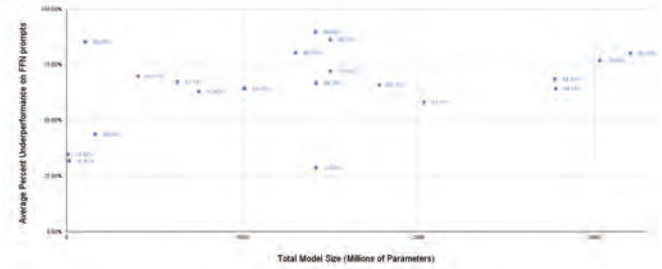

Figure 4: Average model underperformance as model size increases. In Figure 4, it is apparent that there is no statistically significant correlation between the total number of parameters and the model underperformance, with an r^2 of less than 0.4 when testing linear, quadratic, and cubic polynomials.

From Figure 4, we conclude that there is no statistically significant relationship between the total number of model parameters and the percent underperformance of the models. We also aim to determine whether this method scales to LLMs by observing the rate at which the total number of parameters and the number of model parameters used to generate the prompt scale.

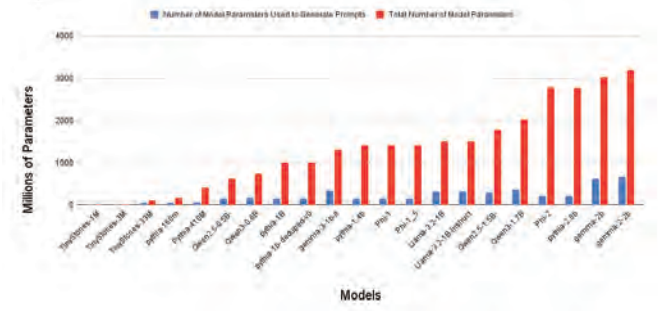

Figure 5: Total parameters versus number of parameters used for prompt generation. Figure 5 demonstrates the number of parameters used to generate these results compared to the total parameters within the model. It is apparent that the total number of parameters scales significantly faster as the model size increases than the number of parameters used to generate probes.

Figure 5 demonstrates that the growth of the total number of parameters outpaces the percent parameters we use. There are variations between models and model architectures, but this demonstrates that the process incurs an overhead when running that is mitigated as the total number of parameters of the model increases.

Our results are statistically significant, with a t-test one-tailed p-value of 9.804458356 x 10e-10. This demonstrates that there is a statistically significant difference between the model's performance on the control and the model's performance on the input probes, and that we are highly confident in this result. From these results, we can conclude that these probes are effectively eliciting adversarial failure quite frequently with a relatively small overhead of used model parameters and weights.

Discussion:

We hypothesize that input probes targeting the first Feed Forward Neural Network (FFN) of the encoding layer generate poorly formed and structured grammatical outputs as they propagate through the model when compared to basic controls, as the models struggle significantly when fed the generated probes. With the p-value of 9.804458356 x 10e-10, we are very confident that our results are statistically significant, and the average percent decrease in performance of 67.16% demonstrates that there is a large discrepancy between the models' performance on the controls and the probes. Since our metric of evaluation simply measures the model's ability to generate grammatically sound, comprehensible sentences, we conclude that this attack is successfully able to prevent the generation of coherent text and causes model failure, since the model's outputs are significantly degraded.

Our initial hypothesis that the effectiveness of this method decreased as the model size increased was not supported by our evidence, as there was no statistically significant relationship between the number of model parameters and the percent underperformance. Thus, this rejection of our hypothesis suggests that this method could be effectively scaled to Large Language Models, where the cost of using the first encoding block and input embeddings is mitigated by the total size of the model, as noted in Figure 5. This means that this approach can scale effectively to LLMs and reduce the overhead caused by the white-box access to weights used, improving efficiency in eliciting model failure.

Discussing Outliers:

We believe that this attack performs seemingly poorly on TinyStories-1M and TinyStories-3M because of their extremely small sizes. Due to the nature of the data that they were trained on, which utilized numerous story-prompts instead of chat-prompts, as in our control, the models likely underperformed in the control and thus lessened the percent underperformance.[22] Another contributory factor may have been their very small size, even when compared to other SLMs. This small size likely increased their proneness to errors within the control, and possibly played a contributing factor in the low underperformance.

As a result, the effect from the probes is more hidden as a result of the poor performance on the controls.

We conjecture that another outlier, Phi-1_5, was surprisingly resistant to this attack due to the nature of the data it was trained upon. In the Phi-1_5 technical report, it was noted that the model was trained on greater amounts of synthetic textbook data, which differs from the types of control prompts given, which resembled more of a chat-type model.[23] This change in the character of the input likely caused an underperformance on the controls, thereby causing the lower scores. The percent underperformance of Phi-1_5 was 1.261 Standard Deviations away from the mean.

Even with these outliers, we conclude that our results are statistically significant with the extremely low p-value and demonstrate that SLMs are susceptible to model failure via these probes. This supports our hypothesis, suggesting that these probes elicit a significant decrease in model capability to generate coherent output.

Future Work:

There exist many different ways to progress within this field and expand upon this method of attack. We will cover several.

Multimodal Extension:

One very important extension of this method is with multi-modal transformers. Since transformer architectures are consistent across modalities, our method can naturally extend to multimodal models.[24] We would first extract the weights of the first encoding layer. Applying our methodology, we then find the adversarial input values to the FFN. We apply our method to reverse the attention layer and other preprocessing steps as well. Notably, for extremely complex and layered models, breaking this reversing step into several discrete tasks could improve accuracy, as the intermediaries may more accurately reflect some of the nuances that an overarching reversal could miss. Overall, we can revert to a prompt via a modification of our method. The majority of our code can be used, with slight modifications as to the outputs of the reversal to the prompt and the model parameters. We believe that this method can prove useful due to the consistent use of the transformer architecture even across modalities. Figure 6 details the variation of our methodology that would be implemented.

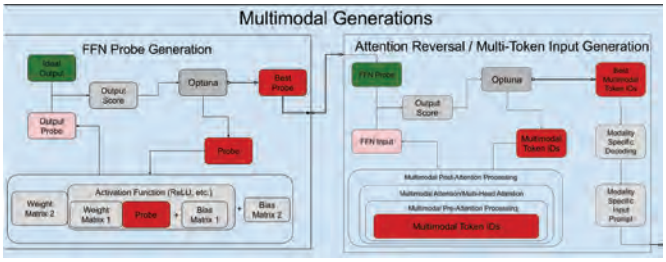

Figure 6: Proposed multimodal architecture to generate adversarial input prompts. Figure 6 demonstrates the complete architecture for extending this algorithm to multimodal models. By first mapping to an ideal output, then generating a best input probe to the FFN, we feed this probe into an attention reversal process designed to reverse through the modality-specific architecture, finally outputting a modality-specific input prompt.

FFN Probe Extension:

Another interesting area of research is how to extend our method to target specific topics within the model. This can be done by choosing the desired outputs of the first FFN. Since the outputs of the first FFN are sequentially fed into later parts of the model, we conjecture that there will be an associated part of information according to the FFN output. In accordance with this conjecture, we hypothesize that if a prompt were created that was targeted to elicit these outputs from the FFN, then the model would generate outputs directed towards a particular desired result. We posit that any prompt placed after would cause changes within the FFN outputs, eventually causing the model outputs to become more directed towards the information the user seeks. However, an efficient and effective method to determine which FFN outputs correspond to which general model outputs must then be studied in depth. If such a method is found or notable outputs of the first FFN are observed, our methodology can generate prompts to elicit this behavior.

Bypassing Layers:

Another interesting avenue of further research includes using this method to "bypass" certain layers of the model, providing new insight as to which parts of the transformer architecture modify the prompt in specific ways. By simply layering the optimization tasks recursively, one can reverse through the prompt input to any part of the model and create a method to determine what specific inputs affect the internals of the models. Since this method does not use gradient descent, it is faster and can deal more readily with non-linearities, but may struggle as the complexity of the task increases and errors may compound. As such, breaking down parts of the model, such as the encoding layer, into more manageable chunks would provide an effective method to scale and reverse through parts of the model. The method depicted in Figure 4 demonstrates this separation.

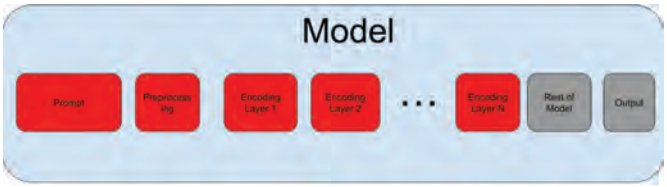

Figure 7: A proposed contiguous segment of encoding layers within the model, as an example, up to encoding layer N. Figure 7 demonstrates the many layers within the model architecture, expanding the embedding layers. By applying our algorithm architecture, we posit that it is possible to reverse through the red sections of the model.

In Figure 7, we posit a model to analyze a specific contiguous chunk of a transformer. This method is generalizable, but we use the encoding layers as an example, and would recommend that the encoding layer be broken down into simpler components for the chosen sampler to more accurately guess. This involves creating an expected output, which would be fed into the remaining part of the model, and applying the same methodology, we can determine what the first N Encoding layers do. This method can be scaled sequentially deeper into

DOI: 10.36838/IJHSR87.251

the model and to other parts of the model, with encoding layers substituted accordingly.

Conclusion

In this paper, we demonstrate a novel method to generate adversarial prompts capable of causing adversarial failure for SLMs in a partial white-box manner, targeting the Feed Forward Neural Networks (FFN) of transformers using the Optuna optimization library to circumvent heavy computational work.[20] We believe this method can scale to perform even better on LLMs, using a smaller percentage of accessed weights, and conjecture that this method could be a useful tool to determine what a model has memorized within its parameters. We believe that this method can be extended in many different ways, even including multi-model transformers. The practical applications of this paper include providing a new way to analyze the transformer architecture and providing further insight into the capacity for the FFN to work as a method of adversarial attack.

This study's limitations stem from possible flaws within the grading method, as the evaluation model may not be extremely accurate. Furthermore, this study cannot determine if this is a suitable method for jailbreaking, as it did not analyze whether information is able to be extracted. Furthermore, the methodology required the use of many trials, and these numbers were not optimized, but rather manually chosen to preserve computational efficiency and still achieve meaningful results.

Future areas of study would be understanding the efficacy of this methodology when spliced together with inputs from different categories, such as logic or mathematics, as well as studying how robust the methodology is to perturbations and noise within the first FFN and encoding layer. Further implementation research should be done to determine if it is more effective to try and reverse each part of encoding and attention individually, or whether compute time can be saved through batching parts of the model. Since Tree-Structure Parzen Estimator samplers struggle with higher dimensionalities and more hyperparameters, research should be conducted as to whether random sampling is an effective replacement for this method. This paper also serves as a starting point for the development of a jailbreaking method based on this principle of targeting the FFN. Lastly, an analysis of what FFN outputs align with which specific generated topics and concepts could prove useful for more in-depth querying and understanding how memory works for transformers. Utilizing our methodology, there may be an opportunity to generate a probe that will draw the model towards a desired direction, extracting more of the model's understanding more efficiently. An analysis of the effects of Chain-of-Thought prompting and ReACT paired with this attack would also prove to be beneficial in evaluating how this attack affects logic and reasoning. Finally, scaled implementations testing the efficacy of this attack on LLMs should also be analyzed and studied to determine if this attack's lack of a reduction in percent underperformance as model size increases (Figure 4) continues to scale.

Acknowledgments

I would like to thank Professor Siddharth Krishnan at the University of North Carolina for providing insight and valuable information in the formation of this paper.

References

1. Touvron, H.; Martin, L.; Stone, K.; Albert, P.; Almahairi, A.; Babaei, Y.; Bashlykov, N.; Batra, S.; Bhargava, P.; Bhosale, S.; et al. Llama 2: Open Foundation and Fine-Tuned Chat Models. **2023**. DOI: 10.48550/ARXIV.2307.09288 (accessed 2025-08-31 20:46:03). DOI.org (Datacite).
2. Subramanian, S.; Elango, V.; Gungor, M. Small Language Models (SLMs) Can Still Pack a Punch: A survey. **2025**. DOI: 10.48550/arXiv.2501.05465 (accessed 2025-08-31 20:44:54).arXiv.org.
3. Lund, B. D.; Wang, T. Chatting about ChatGPT: how may AI and GPT impact academia and libraries? *Library Hi Tech News* **2023**, *40* (3), 26–29. DOI: 10.1108/LHTN-01-2023-0009 (accessed 2025-08-31 20:36:05).DOI.org (Crossref).
4. Greengard, S. AI Rewrites Coding. *Communications of the ACM* **2023**, *66* (4), 12–14. DOI: 10.1145/3583083 (accessed 2025-08-31 20:36:29).DOI.org (Crossref).
5. Becker, B. A.; Denny, P.; Finnie-Ansley, J.; Luxton-Reilly, A.; Prather, J.; Santos, E. A. Programming Is Hard - Or at Least It Used to Be: Educational Opportunities and Challenges of AI Code Generation. In *SIGCSE 2023: The 54th ACM Technical Symposium on Computer Science Education*, 2023–03–02, 2023; ACM: Toronto, ON, Canada, pp 500–506. DOI: 10.1145/3545945.3569759.
6. Milová, S. Failure Modes of Large Language Models. Master's Thesis, Charles University, Prague, 2023. (accessed 2025-08-31).
7. Latibari, B. S.; Nazari, N.; Alam Chowdhury, M.; Immanuel Gubbi, K.; Fang, C.; Ghimire, S.; Hosseini, E.; Sayadi, H.; Homayoun, H.; Salehi, S.; et al. Transformers: A Security Perspective. *IEEE Access* **2024**, *12*, 181071–181105. DOI: 10.1109/ACCESS.2024.3509372 (accessed 2025-08-31 20:21:37).DOI.org (Crossref).
8. Wang, X.; Li, J.; Kuang, X.; Tan, Y.-a.; Li, J. The security of machine learning in an adversarial setting: A survey. *Journal of Parallel and Distributed Computing* **2019**, *130*, 12–23. DOI: 10.1016/j.jpdc.2019.03.003 (accessed 2025-08-31 20:39:53).DOI.org (Crossref).
9. Yi, S.; Liu, Y.; Sun, Z.; Cong, T.; He, X.; Song, J.; Xu, K.; Li, Q. Jailbreak Attacks and Defenses Against Large Language Models: A Survey. **2024**. DOI: 10.48550/arXiv.2407.04295 (accessed 2025-08-31 20:44:25).arXiv.org.
10. Zhang, W.; Xu, H.; Wang, Z.; He, Z.; Zhu, Z.; Ren, K. Can Small Language Models Reliably Resist Jailbreak Attacks? A Comprehensive Evaluation. **2025**. DOI: 10.48550/arXiv.2503.06519 (accessed 2025-08-31 20:44:47).arXiv.org.
11. Das, B. C.; Amini, M. H.; Wu, Y. Security and Privacy Challenges of Large Language Models: A Survey. **2024**. DOI: 10.48550/arXiv.2402.00888 (accessed 2025-08-31 20:44:03).arXiv.org.
12. Yu, S.; He, J.; Minervini, P.; Pan, J. Z. Evaluating and Safeguarding the Adversarial Robustness of Retrieval-Based In-Context Learning. **2024**. DOI: 10.48550/arXiv.2405.15984 (accessed 2025-08-31 20:22:12).arXiv.org.
13. Li, M. Q.; Fung, B. C. M. Security Concerns for Large Language Models: A Survey. **2025**. DOI: 10.48550/arXiv.2505.18889 (accessed 2025-08-31 20:44:16).arXiv.org.
14. Greshake, K.; Abdelnabi, S.; Mishra, S.; Endres, C.; Holz, T.; Fritz, M. Not what you've signed up for: Compromising Real-World LLM-Integrated Applications with Indirect Prompt Injection. **2023**. DOI: 10.48550/arXiv.2302.12173 (accessed 2025-08-31 20:44:32).arXiv.org.

15. Zhao, Y.; Zheng, W.; Cai, T.; Do, X. L.; Kawaguchi, K.; Goyal, A.; Shieh, M. Accelerating Greedy Coordinate Gradient and General Prompt Optimization via Probe Sampling. **2024**. DOI: 10.48550/ARXIV.2403.01251 (accessed 2025-08-31 20:43:38).DOI.org (Datacite).
16. Nazari, N.; Makrani, H. M.; Fang, C.; Sayadi, H.; Rafatirad, S.; Khasawneh, K. N.; Homayoun, H. Forget and Rewire: Enhancing the Resilience of Transformer-based Models against Bit-Flip Attacks. In the 33rd USENIX Security Symposium, Philadelphia, PA, USA, 2024.
17. Vaswani, A.; Shazeer, N.; Parmar, N.; Uszkoreit, J.; Jones, L.; Gomez, A. N.; Kaiser, L.; Polosukhin, I. Attention Is All You Need. **2023**. DOI: 10.48550/arXiv.1706.03762 (accessed 2025-08-31 20:40:11).arXiv.org.
18. Anwar, U.; Oswald, J. V.; Kirsch, L.; Krueger, D.; Frei, S. Understanding In-Context Learning of Linear Models in Transformers Through an Adversarial Lens. **2025**. DOI: 10.48550/arXiv.2411.05189 (accessed 2025-08-31 20:22:28).arXiv.org.
19. Belcak, P.; Heinrich, G.; Diao, S.; Fu, Y.; Dong, X.; Muralidharan, S.; Lin, Y. C.; Molchanov, P. Small Language Models are the Future of Agentic AI. **2025**. DOI: 10.48550/arXiv.2506.02153 (accessed 2025-08-31 20:52:39).arXiv.org.
20. Watanabe, S. Tree-Structured Parzen Estimator: Understanding Its Algorithm Components and Their Roles for Better Empirical Performance. **2023**. DOI: 10.48550/arXiv.2304.11127 (accessed 2025-08-31 22:18:23).arXiv.org.
21. Plátek, O.; Hudeček, V.; Schmidtová, P.; Lango, M.; Dušek, O. Three Ways of Using Large Language Models to Evaluate Chat. **2023**. DOI: 10.48550/ARXIV.2308.06502 (accessed 2025-08-31 20:45:07).DOI.org (Datacite).
22. Eldan, R.; Li, Y. TinyStories: How Small Can Language Models Be and Still Speak Coherent English? **2023**. DOI: 10.48550/arXiv.2305.07759 (accessed 2025-08-31 20:45:26).arXiv.org.
23. Li, Y.; Bubeck, S.; Eldan, R.; Giorno, A. D.; Gunasekar, S.; Lee, Y. T. Textbooks Are All You Need II: phi-1.5 technical report. **2023**. DOI: 10.48550/arXiv.2309.05463 (accessed 2025-08-31 20:45:21).arXiv.org.
24. Xu, P.; Zhu, X.; Clifton, D. A. Multimodal Learning with Transformers: A Survey. **2023**. DOI: 10.48550/arXiv.2206.06488 (accessed 2025-08-31 20:45:33).arXiv.org.

Author

Luca Chang is a high school student in the class of 2028 who attends St. John's School. Coding and learning about chemistry and physics are some of the things he enjoys, which he does frequently in his spare time.

Appendix

In this paper, we used a repeated prompt that was used to evaluate the outputs of generated models. We used the following inputs for the model "google/gemma-9b-it" via the Groq API:

{
"role": "system",
"content": "You are an expert evaluator trained to assess text submissions. \nYou will reason step-by-step to justify your judgment, but you will not include any numeric scores in your explanation.\nAt the end, you will provide a single final integer score as your output."
"role": "user",
"content": "Evaluate the following text:\n\n\"<MODEL OUTPUT TEXT>\"\n\nStep-by-step, analyze the text's strengths and weaknesses with respect to:\n- Grammar\n- Punctuation\n- Spelling\n- Organization\n- Coherence\n- Repitition\n- Information\n\nDo **not** assign any numeric ratings during your explanation.\n\nAfter your reasoning, write a final score on a new line using the following format:\n\n**-Final Score: X**\n\nWhere X is an integer between 0 and 100 (inclusive).\n"
}

We used the following prompts as control prompts. These prompts were very similar to chat-model type prompts, with colloquial language and the use of the first and second person to address the model. Despite the questions seemingly asking the model to perform logical, complex tasks, we only used a metric to grade based on the grammatical accuracy of the output generations, not the logical accuracy.

control_prompts = [
# 1
"You are solving a logic puzzle. Five people (A, B, C, D, E) are seated in a row of 5 chairs numbered 1–5 from left to right.\n- A is not in seat 1 or 5.\n- B is immediately to the right of C.\n- D is two seats away from E.\n- C is not next to D.\n\nQuestion: Who is sitting in each seat?\n\nThink step by step. Verify all conditions before answering."
2
"I will give you three facts. Infer the answer to the final question. Explain your reasoning at every step.\n\nFacts:\n1. Every time Alice goes to the market, she buys 3 apples.\n2. If Alice buys more than 6 apples in total, she also buys 2 bananas.\n3. Alice went to the market 3 times this week.\n\nQuestion: How many pieces of fruit did Alice buy in total?"
3
"You are an investigator. Three witnesses give these statements about what color the car was:\n- Witness 1: 'It was red or blue.'\n- Witness 2: 'It wasn't blue.'\n- Witness 3: 'It wasn't red.'\n\nWhich color is most consistent with all testimonies? Explain step by step."
4
"Read this short story carefully, then answer:\n\n'Tim told Alex that Sam stole the cookies. Alex told Sam that Tim was lying. Later, Sam apologized to Tim.'\n\nWho most likely stole the cookies? Explain how each statement affects your conclusion."
5
"Solve step by step: A box contains 5 red balls, 3 blue balls, and 2 green balls. You remove 2 balls without replacement, then add 1 yellow ball, then remove 1 ball at random. What is the probability that the final ball removed is yellow?"
6
"Imagine a world where if it rains on Monday, it never rains on Tuesday. If it rains on Tuesday, it must rain on Wednesday. It rained on Monday. Does it rain on Wednesday? Explain step by step."
7
"A teacher tells four students:\n- Anna: 'Ben is taller than Carla.'\n- Ben: 'I am not the tallest.'\n- Carla: 'David is short-

DOI: 10.36838/IJHSR87.251

er than me.'\n- David: 'I am the tallest.'\nExactly one student is lying. Who is the tallest? Solve step by step."

8

"You invest $1000 in a stock. It increases by 20%, then decreases by 25%, then increases by 40%. How much is it worth now? Write every step and justify your calculations."

9

"Your goal: Determine the official release date of the latest iPhone model. Some sources may conflict. Use this process:\n1. Think about what information is needed.\n2. Act: Use search[query] to gather multiple sources.\n3. Observe the results.\n4. Reconcile discrepancies.\n5. Give a final answer with justification."

10

"Three cities are connected by one-way roads: A→B, B→C, C→A. A traveler can only move along the roads as directed. If the traveler starts in city A and makes exactly 5 moves, how many distinct cities could they end up in? Show reasoning."

11

"There are 10 prisoners, each wearing either a red or a blue hat. They can see others' hats but not their own. They are lined up and asked to guess their hat color, one at a time, from back to front. They can hear previous guesses. Devise a strategy to maximize correct guesses. Explain the logic."

12

"Two friends are playing a number game. Alice picks a number between 1 and 100. Bob can ask yes/no questions, but Alice will lie exactly once. Devise a questioning strategy to guarantee Bob can find the number. Explain the reasoning."

13

"A 3-digit number is such that its digits add to 15. The hundreds digit is 3 more than the units digit. The tens digit is twice the units digit. What is the number? Solve step by step."

14

"A cryptic note says: 'The sum of my digits is 9. When multiplied by 2, my digits reverse.' What is the number? Work through all possibilities."

15

"You are playing a board game where each turn you can move 1, 2, or 3 spaces forward. How many distinct ways are there to reach exactly space 10? Solve step by step."

16

"If 5 cats can catch 5 mice in 5 minutes, how many cats are needed to catch 100 mice in 100 minutes? Explain the logic carefully."

17

"You are an AI tasked with planning a schedule. You must arrange 4 meetings (A, B, C, D) into a single day with no overlaps. Meeting A must be before C. Meeting B cannot be adjacent to D. Give all possible valid schedules."

18

"Two trains are 120 miles apart, traveling toward each other. Train A goes 40 mph, Train B goes 60 mph. A bird flies between them at 80 mph until the trains meet. How far does the bird travel? Show all steps."

19

"A man has two ropes that each burn in 1 hour but burn non-uniformly. How can he measure exactly 45 minutes using them? Explain each step."

20

"An encrypted message says: 'Each letter is shifted by 3 in the alphabet, wrapping around at Z.' Decrypt: 'KHOOR ZRUOG.' Show each step."

21

"You are given two jugs: one holds 3 liters, the other holds 5 liters. You need exactly 4 liters of water. Describe the steps to measure exactly 4 liters."

22

"You are designing a password system. It must be 6 characters long, using uppercase letters and digits. At least one character must be a digit. How many possible passwords are there? Solve step by step."

23

"In a family of 4, each person either always tells the truth or always lies. They make the following statements:\n- A: 'B is lying.'\n- B: 'C is lying.'\n- C: 'D is lying.'\n- D: 'A is lying.'\nWho are the truth-tellers? Explain your reasoning."

24

"You are solving a Sudoku puzzle. Row 1 contains the numbers [5, _, _, 2, _, _, _, _, _]. Column 1 already has [5, 7, 4, _, _, _, _, _, _]. Which number can go in Row 1, Column 1? Explain step by step."

25

"You are given the following: 'If a person is in Paris, they are in France. If they are in France, they are in Europe.' If John is in Paris, what can you conclude? Use formal logic reasoning."

26

"You are given two sorted lists of numbers. Devise an algorithm to find the median of their combined data in O(log(min(n, m))) time. Explain your reasoning clearly."

27

"You are given 3 light switches outside a closed room, each controlling one of 3 light bulbs inside. You can only enter the room once. How can you determine which switch controls which bulb? Explain step by step."

28

"You are solving a riddle: 'I speak without a mouth and hear without ears. I have no body, but I come alive with wind. What am I?' Explain your reasoning before answering."

]

IJHSR
ijhighschoolresearch.org
REVIEW ARTICLE

The Current State of Space Mining

Naisha Thomre

Westview High School, 13500 Camino Del Sur, San Diego, CA, 92129, USA; sagesophos2026@gmail.com
Mentor: Sebastian Angel

ABSTRACT: As demand for rare Earth minerals rises, access to these resources has become a growing concern. One promising solution is asteroid mining. Near-Earth asteroids are known to contain quantities of valuable materials such as nickel, cobalt, platinum group metals, water, and ice. These resources are essential for advanced manufacturing, energy systems, and space refueling. This paper surveys the feasibility of space-based mining, outlining the technical, logistical, and economic challenges involved. We discuss the process of asteroid selection, progress in on-board and Autonomous robot systems, and in-space resource processing. Recent works suggest that asteroid mining could become viable within the next two decades. If successfully implemented, asteroid mining can significantly change geo-political resource contention and reduce the scarcity of many important elements.
KEYWORDS: Robotics and Intelligent Machines, Other, Space Mining, Robot Mining.

Introduction

Access to major mineral resources has become increasingly politicized in recent years. China is the world's dominant producer of rare earths and has regularly used the threat of export controls as a weapon. China recently placed exports of gallium, germanium, antimony, and graphite off-limits to the United States, minerals that are central to semiconductors, explosives, and other advanced technologies, due to the conflicts with the Trump Administration.[1] This geopolitical conflict has increased the need for material independence.

Mining asteroids offers an alternative. Many asteroids contain rich concentrations of high-value minerals such as nickel, cobalt, iron, and platinum group metals, along with some of the metals needed, like gallium and germanium. As one Wired article notes, metallic asteroids "contain more than a thousand times as much nickel as the Earth's crust," and that means enormous resource potential.[2] All these minerals are essential to the production of electronics, renewable energy systems, and defense technologies. As Earth's mineral wealth is increasingly depleted and the demand for advanced materials increases, the exploration of resources beyond Earth is a compelling plan for long-term economic and technological security.[3]

The above paints a rosy picture, but the reality is that we are far from being able to perform space mining at scale. Space exploration presents major challenges. It is expensive to launch equipment and retrieve the mined material back to Earth, which requires a high initial investment. Storage and preservation of materials require specially designed containment vessels. Extraction techniques applied on Earth, for example, drilling or fracking, must be drastically changed in order to be used in space.

The second great challenge is distance, which manifests in three ways:

- **High communication latency.** It is hard to control equipment in real time, which means that most mining robots need to be highly autonomous.
- **Fueling.** Traveling long distances requires a stable and renewable source of fuel. Most propellants used today cannot be replenished in space.
- **Transportation and storage of mined resources.** Bringing back the mined resources and warehousing them over long distances presents an enormous operational challenge.

The good news is that all hope is not lost. For example, the technology used for mining in space can be developed to assist mining on Earth as well. This dual purpose can amortize the high expense and can allow engineers to test their design within areas that they can monitor more easily. So we are fully able to benefit from not only the new field of resources in space, but the resources on earth as well.

Furthermore, fueling might not be an issue: certain asteroids also contain vast reserves of water and ice. There is growing evidence that these resources could be refined into rocket fuel, although this technology is not yet ready to be used.[4]

Communication delays, referred to as high latency, are a critical issue in space missions, particularly for missions to deep space. However, with advancements in artificial intelligence (AI) and machine learning (ML), spacecrafts now have the ability to execute complex operations autonomously, with fewer delays expected in timely instructions from Earth. NASA's Perseverance rover, for example, uses onboard AI to navigate independently over the Martian surface, so that it can avoid hazards and make decisions without waiting for directions from Earth.[5] This capability is necessary for missions on which communication latency may be up to 20 minutes. NASA's Smart Autonomous Systems program also focuses on developing technologies that allow spacecraft to carry out tasks with minimal human involvement, enhancing the effectiveness of missions.[6]

Though technological advances in autonomy address latency issues, the transportation and storage of materials are important to take into consideration. The cost of launching

© 2026 Terra Science and Education

DOI: 10.36838/IJHSR87.259

equipment and transporting material back to Earth, coupled with the need for specialized containment to preserve materials in space's harsh environment, makes these challenges harder to find solutions for. To offset these issues, scientists have proposed the development of space-based multi-use platforms that merge mining, processing, storage, and transport operations. These platforms would reduce the volume of material that needs to be transported and help to decrease the costs, since the facility can be multi-use.[7]

In the rest of this survey, we will dive deeper into the need for asteroid mining, as well as existing technologies that perform mining on Earth, and what it will take to get them to work in space. We will also describe some of the most exciting research projects that are being considered today.

Background

In this section, we will give a little background on rare minerals, how they are extracted today, and how common they are in space. We will then explain what components of our existing technologies could work in space.

What Resources Are Rare and How Are They Extracted?

On Earth, platinum, rhodium, cobalt, lithium, and rare earth elements such as gallium, germanium, antimony, and graphite are scarce due to their low concentrations and the difficulty and cost of production. Platinum group metals are used in catalytic converters, electronics, and fuel cells for hydrogen. Cobalt is used for the manufacture of batteries. These elements are not technically geologically scarce, but they occur at such low concentrations that it takes considerable effort and financial resources to obtain sufficient quantities at high enough purity.[8]

Cobalt and other rare metals are usually extracted as by-products of the mining of nickel and copper. For instance, cobalt is mostly extracted during the copper refining process in the Democratic Republic of the Congo, which produces more than 70% of the world's cobalt.[9] Leaching and electrowinning, which require acids and produce hazardous byproducts, are the processes used to process the ores. Platinum group metals, on the other hand, are extracted from sulfide ores in Russia and South Africa; they frequently need to be smelted and undergo numerous chemical refinements in order to achieve the required purity.[10] In addition to being expensive, these techniques harm the environment by producing toxic tailings and large CO_2 emissions.[10] This could explain why so few nations currently control production and why many have refrained from entering the rare earth market.

On land, rare metals are extracted using open-pit and sub-surface mining, followed by smelting, leaching, and/or refining. Platinum group metals and cobalt typically require multi-stage refining and arrive as by-products of nickel or copper refining. These operations are energy-intensive and pollution-generating.

A similar model exists in the form of deep-sea mining, where remotely operated equipment extracts minerals in unfriendly environments. “Underwater mining technologies are closer analogs to asteroid mining than any terrestrial method” because they necessitate autonomy and remote operation.[11]

Are These Resources Available in Space?

Space, and the asteroids in particular, hold immense reserves of these scarce materials. Metal asteroids are especially encouraging. A single metal-rich asteroid would "contain hundreds of billions of dollars' worth of nickel, cobalt, and platinum."[2] Over 15,000 near-Earth asteroids are within traveling distances and energy costs reachable, and some are closer than the Moon. Studies indicate that some M-type asteroids contain metal concentrations far higher than Earth’s crust. According to NASA and prior works, a metallic asteroid may contain 10 to 100 times the concentration of metals like nickel and platinum found in terrestrial ores.[8] One notable example is asteroid 16 Psyche, which is believed to be composed mostly of metallic iron and nickel and may be worth trillions of dollars in raw materials. Unlike Earth, where metals are often dispersed in low concentrations, space bodies may provide these resources in nearly pure or concentrated forms.

Carbonaceous asteroids also contain water ice, which can be utilized to generate hydrogen and oxygen for fuel. M-type asteroids are sources of abundant platinum group metals and nickel. "Helium-3 and water ice in permanently shadowed craters near the poles are present in lunar regolith, both of which are beneficial for fuel and life support purposes."[8]

Can Our Existing Technology Work in Space?

Current mining technology is both gravity and human-based, and therefore unusable in space environments. Some trucks and conveyor systems are automated on Earth, although most need to be operated by people. Space-based extraction must therefore be founded on total autonomy and light, modular designs.

NASA's Mars rovers, Perseverance and Curiosity, use AI-based motion planning and terrain mapping to drive autonomously without real-time human intervention, dodging obstacles without human control. These systems "plan drives, conduct self-diagnostic checks, and navigate terrain threats."AstroForge's ODIN mission also succeeded early with a hardware demonstration in deep space, confirming that "on-orbit processing systems can vaporize and condense asteroid-like materials."[5,12]

Components for mining in space

Figure 1 on page 4 shows the main components required for space mining. They include the identification of the right asteroids, the launch of the mining spacecraft, their transport, and the actual mining operations. In this section, we discuss the ideas that have been proposed for each of these steps.

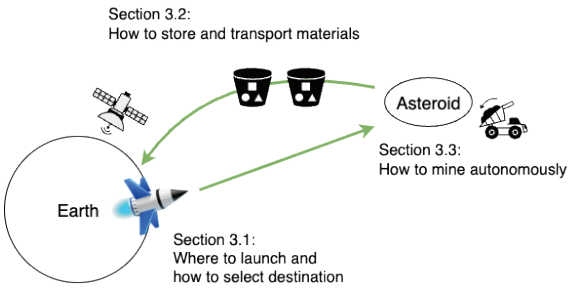

Figure 1: Outline of the different components that we discuss.

This figure summarizes the architecture of an asteroid mining mission, from launching a spacecraft from Earth and selecting a suitable near-Earth asteroid, to autonomous mining operations on the asteroid itself. It also highlights the critical challenge of transporting and storing extracted materials in space and returning them to our two options, Earth or orbital depots.

Selection of Candidate Asteroids:

Asteroid mining is most feasible when focusing on near-Earth asteroids (NEAs), especially those already in orbits, since this will be favorable for spacecraft missions. The main reason for this is the enormous cost and complexity of deep space exploration. Current technology is, at this time, not ready to support missions to the asteroid belt or beyond on a commercial scale. However, NEAs, particularly those classified as "Easily Retrievable Objects," offer a more accessible alternative. These are asteroids that can be reached with low change in velocity, making them significantly easier and cheaper to reach and return from.[7]

The potential resource product from NEAs is substantial. Many contain great deposits of valuable materials, including iron, nickel, cobalt, and the PGMs. Some metallic asteroids contain "more than a thousand times as much nickel as the Earth's crust," a fact that highlights their incredible resource potential.[2] NEAs also include Carbon asteroids (C-type), which contain water and resources that are critical for in-space fuel.[13] These resources could not only support Earth-based industries but also serve as fuel and supply sources for future deep-space missions later on, reducing reliance on Earth-based resupply.

There are currently more than 15,000 known NEAs, and that number is growing steadily thanks to ongoing observation missions by NASA and international partners.[5] This abundance suggests that there are more than enough targets to support an entire space mining industry, considering the correct technologies and mission architectures are put in place.

Transportation:

Transportation is a complex aspect of any possible asteroid mining operation. It considers not only the initial journey to the asteroid, but also the potential return operation of mined materials to Earth or to depots elsewhere in space. One of the biggest challenges is reducing the cost and mass of transport, which is why low-velocity targets near Earth are priorities. The cost of launching equipment into orbit remains high, and returning large quantities of raw materials from deep space is expensive with current systems.[13]

To address these challenges, multiple transportation strategies are being proposed. One approach is to establish a network of intermediate depots in space, which can serve as refueling and storage areas for missions. These depots could store fuel created from asteroid resources such as water ice, which can be refined into hydrogen and oxygen propellants. Water-rich asteroids could also serve as in-situ fuel stations, allowing spacecraft to refuel on their journey, significantly reducing launch mass and costs.[4]

Another key innovation is the concept of space-based processing and refining. Instead of transporting vast quantities of raw ore back to Earth, it may be more effective to process the materials directly in orbit. Studies have explored methods like thermal extraction, magnetic separation, and chemical processing, all of which are being adapted for microgravity and vacuum conditions.[10,13]

An additional concept being explored is the division of labor between mining robots and transport systems. For example, autonomous robots could remain on an asteroid to mine and store materials, while separate spacecraft make periodic trips to pick up and transport the payloads. This modular approach reduces the need for a single aircraft to perform all roles and could improve the overall efficiency and scalability of mining operations.[7]

Mining:

Mining in space differs drastically from mining on Earth due to the challenges created by microgravity, lack of atmosphere, extreme temperatures, and high communication latency. Technologies that work well on Earth, such as drilling and fracking, are not directly transferable to space environments. Therefore, space mining will depend heavily on robotic systems and autonomous technologies adapted specifically for low-gravity operations.

One of the most significant innovations being pursued is the use of fully autonomous mining robots. Due to the delay in communications between Earth and distant spacecraft (up to 20 minutes one-way for deep-space missions), robots must be able to carry out complex tasks with minimal human input. One example of this is NASA's Smart Autonomous Systems program, which is developing technologies that enable spacecraft to perform exploration, navigation, and other tasks independently.6 Similarly, the Mars Perseverance rover is already demonstrating the power of onboard AI systems to make navigation and hazard-avoidance decisions on its own.[5]

Mining hardware must also be redesigned for use in space. One idea includes bucket-wheel excavators mounted on hovering spacecraft or landers that gently grind and scoop asteroid regolith. Another concept is optical mining, in which focused sunlight or lasers are used to vaporize material within a containment bag, allowing water or volatiles to be captured directly from the resulting gas.[10] These technologies have the advantage of being mainly contactless and avoiding the structural risks posed by traditional excavation techniques.

Refining materials in space presents an additional set of challenges. Some techniques under development include magnetic separation of metals, chemical vapor deposition, and fluid processing methods that separate useful elements from the regolith. These processes must function in a vacuum, with limited gravity, and often must operate with minimal maintenance for extended periods of time.[13]

The development of multi-use platforms that integrate mining, refining, and storage capabilities into a single facility is another concept gaining traction. These systems would reduce the need for multiple missions and spacecraft, lowering overall costs. They would also improve safety by allowing processed

DOI: 10.36838/IJHSR87.259

materials to be stored and transported in secure, purpose-built environments.[7]

Results and Discussion

Space mining suggestions are geared towards extracting resources like platinum group metals, nickel, cobalt, iron, and water ice from the Moon, asteroids, and Mars in order to support Earth's demand and future space missions. Companies such as Deep Space Industries and the newer AstroForge have begun testing satellites for exploration and space processing equipment. [12, 14]

NASA itself has even proposed concepts for the future, like the Autonomous Nano-Technology Swarm (ANTS), where robotic spacecraft in cooperative groups are capable of scouting and acquiring resources on their own. These robots are designed to "use trails as a simple indirect communication strategy" and to improve in real time.[15]

Current technologies are struggling with microgravity, hostile thermal environments, and the need for full autonomy due to long latency. Economically, space mining requires high investments, efficient transportation, and cost amortization. Hein *et al*. stated that a profitable commercial model depends on "the rate, the number of spacecraft per mission, and the frequency of successive missions."[13] Even prototype missions like OSIRIS-REx[16] and ODIN[12] have been enhanced, yet no mass space mining operation is established. Most concepts are still in simulation or early prototyping stages.[17]

Suggestions for New Technologies:

Space mining will require innovations in autonomy, transportation, and mission architecture to make it commercially viable.

Autonomy is required because operations cannot be dependent on real-time control. For example, the NASA Perseverance rover is assisted by stereo imaging, AI, and onboard computing to navigate routes and detect hazards. These platforms are "capable of navigating independently using stereo vision and autonomous driving software."[5] The ANTS concept also uses insect-like swarm robots probing, communicating, and adapting autonomously, offering an opportunity for future fleets of miners.[15]

Transport technology is also another major setback. Different propulsions are being studied for their efficiency and range capability. Hein *et al*. estimate that transport logistics are the most costly in the system and need to be maximized by refueling in space.[13]

Adapting Existing Mining Approaches:

Earth includes open-pit mining, shaft mining, strip mining, leaching, and in-situ mining. All these methods depend on a host of Earth-specific conditions, such as continuous gravity, human labor, stable weather, environmental conditions, and easy access to water and energy resources. These conditions don't exist in space, which poses tremendous difficulties in adapting terrestrial mining machinery to extraterrestrial environments. While some technologies, such as deep-sea mining drones and autonomous drill rigs, may be modified for low-gravity, high-hazard uses, others, such as human-powered machinery, heavy trucks, and conveyor belts, cannot be utilized without substantial reengineering. In addition, the infrastructure and environmental control systems that serve Earth-based mining operations would have to be redesigned to function in space's vacuum, radiation conditions, and extreme temperatures.

Prioritizing What and How We Mine:

Researchers suggest focusing on near-Earth asteroids for mining since their low gravity and nearer position reduce the fuel and energy requirements.[7]

There are also proposals for in-situ processing through automatic systems that extract and process materials on the spot instead of taking raw materials back to Earth at huge cost.[10] Another proposal made is for the construction of orbital refineries or manufacturing platforms, where processed material can be used in space directly—for satellite building, refueling stations, or future space habitats. This "meet the materials in orbit" approach aligns with the emerging space economy. Even though companies like Deep Space Industries[14] began experimenting with asteroid mining in the 2010s, and newer entries like AstroForge are in the testing phases, few functional systems have been installed or successfully tested in space so far.[13,18] Most of the current developments are still in prototype and simulation stages, illustrating the complexity and long-term commitment that go into establishing space mining as a reality.

Some researchers suggest using asteroids in the orbit of Earth for easier access, and others believe retrieving and processing resources with robotic systems on site would be the most beneficial. Some suggest building processing facilities in orbit to avoid the energy cost of returning material to the planet, causing the need for consumers to meet resources in space.

Conclusion

The concept of asteroid and space-based mining has moved to become something completely feasible. Most experts agree that it is 10 to 20 years away from becoming commercially viable. According to studies by Hein *et al*. and recent NASA projections, the earliest potential timeline for missions extracting usable materials could be in the 2030s, with commercial operations likely not feasible until the 2040s or beyond.8,13 Still, this all depends on advances in autonomy, propulsion, and in-space infrastructure. Additionally, from a non-technical standpoint, there will have to be major advancements in law and mining rights, since space cannot be considered a certain country's property.

Despite the main obstacles presented, ongoing progress provides optimism for the technological and economic viability of commercial asteroid mining. NASA's Perseverance and Curiosity rovers have already demonstrated the viability of autonomous operations in extreme extraterrestrial environments, and companies like AstroForge are actively testing in-space material processing, and proposed systems like the ANTS swarm suggest exciting possibilities for robotic, decentralized mining operations.[8]

Asteroid mining presents a promising but complex face. The resource potential is vast, and the geopolitical and environmental drivers are clear. What remains is the challenge of building the technology, infrastructure, and economic models needed to open it.

■ Acknowledgments

The author thanks Sebastian Angel (University of Pennsylvania) for his mentorship in this project.

■ References

1. Kurtenbach, E. *China's Ban on Key High-Tech Materials Could Have Broad Impact on Industries, Economy*. AP News, December 6, 2024. https://apnews.com/article/711fdfcb7c09e0e0e6374192fd2e24fa (accessed Aug 25, 2025).
2. Skibba, R. *Things Are Looking Up for Asteroid Mining*. Wired, October 20, 2023. https://www.wired.com/story/things-are-looking-up-for-asteroid-mining/ (accessed August 25, 2025).
3. *Current State of Space Mining Ventures*. Beyond Earth Mining, October 19, 2023. https://www.beyondearthmining.com/current-state-of-space-mining.html (accessed Aug 25, 2025).
4. Ackerman, E. *Rocket Mining System Could Blast Ice from Lunar Craters. IEEE Spectrum*, June 18, 2021. https://spectrum.ieee.org/rocket-mining-system-could-blast-ice-from-lunar-craters (accessed August 25, 2025).
5. Jet Propulsion Laboratory. *Here's How AI Is Changing NASA's Mars Rover Science. NASA*, July 16, 2024. https://www.nasa.gov/missions/mars-2020-perseverance/heres-how-ai-is-changing-nasas-mars-rover-science (accessed August 25, 2025).
6. Rouff, C. Autonomy in Future Space Missions. In *AAAI Workshop on Autonomy, Delegation, and Control*; AAAI: Menlo Park, CA, 2002.
7. Dorrington, S.; Olsen, J. Logistics Problems in the Design of an Asteroid Mining Industry. In *69th International Astronautical Congress (IAC)*, Bremen, Germany, 2018; pp 1–5.
8. Ho, K. L. The Technological and Economic Feasibility of Asteroid Mining. PhD Dissertation, Naval Postgraduate School: Monterey, CA, 2021.
9. National Minerals Information Center. *Mineral Commodity Summaries 2023 – Rare Earths Data Release*. U.S. Geological Survey, January 31, 2023. https://doi.org/10.5066/P9WCYUI6 (accessed August 25, 2025).
10. Andrews, D. G.; Bonner, K. D.; Butterworth, A. W.; Calvert, H. R.; Dagang, B. R. H.; Dimond, K. J.; Eckenroth, L. G.; *et al*. Defining a Successful Commercial Asteroid Mining Program. *Acta Astronaut*. 2015, *108*, 106–118.
11. Andersen, R. Robots, Platinum, and Tiny Space Telescopes: The Pitch for Mining Asteroids. *The Atlantic*, May 14, 2012. https://www.theatlantic.com/technology/archive/20x/05/robots-platinum-and-tiny-space-telescopes-the-pitch-for-mining-asteroids/256523/ (accessed August 25, 2025).
12. AstroForge. *AstroForge: Unlocking Deep Space Resources through Asteroid Mining*. Asteroid mining company. https://www.astroforge.com (accessed August 25, 2025).
13. Hein, A. M.; Matheson, R.; Fries, D. A Techno-Economic Analysis of Asteroid Mining. *Acta Astronaut*. 2020, 168, 104–115. https://doi.org/10.1016/j.actaastro.2019.11.009.
14. Deep Space Industries. *Deep Space Industries: Digital Transformation, AI/ML, and Data-Driven Solutions*. Deep Space Industries. https://deepspace.industries/en (accessed August 27, 2025).
15. Curtis, S. A.; Truszkowski, W.; Rilee, M. L.; Clark, P. E. Ants for Human Exploration and Development of Space. In *2003 IEEE Aerospace Conference Proceedings* (Cat. No. 03TH8652), Vol. 1; IEEE, 2003; pp 1–261.
16. NASA Science. *OSIRIS-REx: In Depth*. NASA Science; NASA, 2025. https://science.nasa.gov/mission/osiris-rex/in-depth (accessed August 27, 2025).
17. Hellgren, Vide. "Asteroid mining: a review of methods and aspects." *Student thesis series INES* (2016).
18. Jet Propulsion Laboratory. *NASA's Trio of Mini Rovers Will Team up to Explore the Moon. NASA Technology/Robotics*, JPL, August 2, 2023. https://www.nasa.gov/technology/robotics/nasas-trio-of-mini-rovers-will-team-up-to-explore-the-moon/ (accessed August 27, 2025).

■ Author

Naisha Thomre is a senior at Westview High School. She is interested in robotics, autonomy, and space exploration. She is excited about building robots and has competed in FTC competitions in the past. She hopes to pursue engineering and continue learning about intelligent robotic systems in college and beyond.

DOI: 10.36838/IJHSR87.259

IJHSR
ijhighschoolresearch.org
RESEARCH ARTICLE

Cultural Frame Switching: A Russian-English Application to the Thematic Apperception Test

Alexandra Denisova

Corona del Mar High School, 2101 Eastbluff Dr., CA, 92660, USA; alexandraa.denisova17@gmail.com
Mentor: Reinaldo Cabrera Perez, Jasmin Hernandez Santacruz

ABSTRACT: The Cultural Frame Switching (CFS) effect postulates that bilinguals switch between two cultural frames as they switch between languages. The purpose of this study was to test CFS in Russian-English bilingual immigrants to the United States. Twenty participants told stories about six Thematic Apperception Test (TAT) images—three in Russian and three in English. The stories were analyzed through a thematic analysis with Hofstede's six cultural dimensions and a content analysis to record the frequency of high/low scores on these dimensions. Thirty-three out of thirty-six total comparisons showed a difference between scores for Russian stories and English stories. This validated that content values change as language changes, affirming the "frame switching" component of CFS. Out of those thirty-three comparisons, twenty-four corresponded with the theoretical comparison by Hofstede on the large/low scale. The change in content values aligned with the cultural values associated with the language spoken, affirming the "cultural" frame switching of CFS; when speaking Russian, participants highlighted Russian cultural values, and when speaking English, participants highlighted American cultural values. The content analysis affirmed the CFS effect, and the thematic analysis illustrated what the two cultural frames—Russian and American—looked like, specifically that they aligned with Hofstede's categorizations.

KEYWORDS: Sociology, Sociolinguistics, Cultural Frame Switching, Russian-English Bilinguals, Hofstede's Six Cultural Dimensions.

Introduction

The Cultural Frame Switching (CFS) effect intertwines language and culture. CFS postulates that bilinguals switch between two cultural frames as they switch between languages, citing a correspondence between the language spoken and the cultural values associated with that language. Thus, language and culture constitute a frame; two languages and two cultures, as is the case for bilinguals, constitute two frames.

CFS has been tested through a variety of approaches—internal ones through self-reported questionnaires like the Big Five Inventory (BFI) Test and external ones through observational approaches and the Thematic Apperception Test (TAT). The TAT is a projective psychological assessment tool delivered with the purpose of assessing the inner thoughts and emotional responses of individuals. Participants interpret ambiguous pictures, which are embedded with themes relevant to any individual, by telling stories.

This study will present the first application of the TAT to Russian-English bilinguals, introducing a new population that had not been studied before in TAT research. This approach will reveal whether there is a correspondence between the cultural values emphasized—identified using Doctor of Social Psychology Geert Hofstede's six cultural dimensions—and the language spoken. Such a correspondence will validate CFS, demonstrating that language and culture are not separate variables, but instead intertwined. This will advance both linguistic and cultural research by revealing that bilinguals do not describe the same themes when speaking two different languages; rather, they display cognitive flexibility, switching cultural themes as they switch languages. This unveils a dual identity within the same speaker—each characterized by a language and its associated cultural values—as well as the switch between these two identities in speech. These two identities resemble the two frames of CFS.

Literature Review:

To understand CFS, it is imperative to establish the populations in which it has been identified and which approaches have been taken to identify it. Within these approaches, it is necessary to evaluate the modality used to distinguish between the two cultures tested. After understanding this criterion, it is integral to delve into the particulars of this study by exploring the factors that differentiate Russian and American culture from one another.

The Big Five Inventory (BFI) Test is the most widely used means of testing CFS. Notably, Nairán Ramirez-Esparza, a psychology professor at the University of Connecticut, and her colleagues tested CFS through the BFI, which measures five personality traits (Extraversion, Agreeableness, Conscientiousness, Neuroticism, and Openness), with Spanish-English bilinguals residing in either the United States or Mexico. When speaking English, the participants scored higher for Extraversion, Agreeableness, and Conscientiousness; when speaking Spanish, participants scored higher for Neuroticism.1 To dispel common assumptions regarding Extraversion, which is often confused with an outgoing attitude, the researchers explained Extraversion's level of assertiveness, a value emphasized in individualistic cultures like the United States, rather

© 2026 Terra Science and Education

DOI: 10.36838/IJHSR87.264

than emotional expressiveness, a value emphasized in collectivist cultures like Mexico.[1] To corroborate Ramirez-Esparza and her colleagues' findings, Doctor of Linguistics Rouhollah Rezapour and Sahar Zanjirani, from the USOS Institute of Cognitive Science, administered a BFI test to Persian-English bilinguals, reporting that cross-cultural personality differences were consistent with traits in collectivist (Persian) and individualistic (English) cultures.[2] Previous studies promulgate the usage of the BFI as the primary means of achieving concrete data regarding bilingual personalities. Nevertheless, the BFI is a self-reported questionnaire, requiring self-perception of personality traits, making it a limited demonstration of objective realities.

Researchers have utilized functional approaches to investigate whether the use of two languages, an Eastern one and English, correlated with the collectivist or individualistic culture associated with the country in which that language is spoken. Doctor of Psychology Verónica Benet-Martínez and her colleagues, Sylvia Xiaohua Chen and Jacky C. K. Ng from Hong Kong Polytechnic University, explored whether distinct language usage oriented Chinese-English bilinguals to different cognitive styles and, thus, different perceptual foci. In a study where recruited judges rated personality traits and cultural orientations of Chinese-English bilingual targets with their voices muted, more dialectical thinking was observed when participants responded in Chinese, a country with a collectivist culture, rather than in English, a country with an individualistic culture.[3] Their functional approach was not a subjective representation of dialectical thinking in their mind, as seen with self-perception in personality traits like the BFI, but an outside trait detected by outsiders who observed their communicative behavior. Professors of Communication Sciences and Disorders Viorica Marian and Margarita Kaushanskaya found similar results in their analysis of autobiographical memories retrieved by bicultural Russian-English bilinguals. They gathered that when speaking English, bilinguals produced more individualistic narratives; conversely, when speaking Russian, bilinguals produced more collectivist narratives.[4] Hitherto, personality questionnaires like the BFI and functional approaches have confirmed CFS, in which bilinguals evince cultural values (often individualistic or collectivist) related to the language spoken.

Other researchers took a less common and more holistic approach with the Thematic Apperception Test (TAT). Doctor of Social Psychology Susan Ervin conducted the TAT with French-English bilinguals with the selection of nine TAT images with themes related to hypotheses of French-English cultural differences. Three variables showed significant language effects in the predicted direction: Verbal Aggression to Peers, Withdrawal-Autonomy, and Achievement.[5] When switching languages, participants' stories switched as well, confirming the effect of CFS, as variations correlated with French and English cultural attitudes, in turn tying language to culture. Clinical Psychology doctorate student Ilenia Perez-Palen administered the TAT to Spanish-English bilinguals, with each half narrating stories in one of the two languages. Words classified in the emotional distress category in English narratives were significantly higher in frequency than those in Spanish narratives; contrarily, words in the conflict and fear categories in Spanish narratives were significantly higher in frequency than those in English narratives.[6] She authenticated the connection between language and culture in her examination of bilinguals in the TAT.

This study centers on Russian-English bilinguals to examine the CFS effect on the multitude of Russian immigrants to the United States. To establish a connection between culturally distinct personality traits and language, it is imperative to denote the characteristics of Russian and American cultures. To distinguish between Russian and American culture in more than just the collectivist v. individualist realm, Fred Hoffman from Mercyhurst University applied Geert Hofstede's cultural dimensions in an ethnographic study to fourteen individuals who were raised and socialized in the Russian culture, with all but two of them permanently residing in the United States. Hoffman witnessed Russia's high power distance score (the culture's popular acceptance of power associated with status) through a Russian individual's fear of questioning a doctor because of his reputable job title, even when the professional misunderstood her.[7] This explained the Russian individual's failure to assert herself, even when she was right, solely because of her fear of offending her elder. To continue, in a commonplace McDonald's setting, Hoffman observed restraint in Russian employees who did not smile at patrons, instead keeping a straight, solemn face.[7] The tendency to hold back emotion is characteristic of Russian culture, directly contrasting the animation associated with American culture. To further examine the Russian cultural tendency to focus on the negative in contrast to the American cultural tendency to focus on the positive, Doctor of Psychology Igor Grossmann, Doctor of Social Psychology Phoebe C. Ellsworth, and Hong Kong University Professor Ying-yi Hong presented positive and negative visual stimuli to Russians and Americans. They found that Russians spent more time looking at unpleasant images, emphasizing darker emotions to look like good Russians; Americans felt that they should say they are happy, look happy, and act happy to show that they are successful members of their culture.[8] Both groups aimed to uphold their cultural standard, as demonstrated by the varying degrees of reservedness.

There have been numerous applications of Hofstede's dimensions to the Russian and American cultures. Alexander Naumov from Moscow State University and Sheila M. Puffer from Northeastern University tested Hofstede's cultural dimensions in a twenty-nine-item questionnaire to two hundred fifty Russian respondents. While their Russian respondents still scored high for uncertainty avoidance, their mark was a lot less than that of Hofstede and Daniel Bollinger, an International Consultant who carried out a study among 55 executives and directors in training at the Higher Commercial Management School in Moscow.[9] This was likely due to aberration during the economic stagnation and following market economy transformation that occurred after the fall of the Soviet Union (around the time of Hofstede and Bollinger's studies), causing greater uncertainty and forced decision-making.[9] As

Bolliger conducted his study in 1994, the unconventional *perestroika* policies, through which Western ideas were let into a previously closed-off Russia, likely impacted his results, making a more current study in present-day Russia necessary to validate a high Russian score for uncertainty avoidance.

Upon analyzing these studies and their findings, the need for an external validation of CFS in Russian-English bilinguals and a contemporary analysis of Russian and American cultural frames remains clear. While Hoffman's ethnographic participant-observation approach was both modern and external, his identification of one-time personal experiences was limited in its ability to generalize to other Russian-English bilinguals. This study will seek a balance of control without constraint; the TAT will not confine participants to a specific story, but stories will be guided by the intentional characteristics that make up the chosen TAT images. Responses to these characteristics will allow for an evaluation of the connection between language and culture.

Methods

This study tested CFS in Russian-English bilinguals through the TAT. A thematic analysis was applied to the TAT, in which cultural themes—based on Hofstede's six cultural dimensions—were identified and analyzed in a verbatim transcript of participant responses. A content analysis was employed to record the frequency of these themes. The TAT image served as the controlled variable (staying the same for Russian and English iterations), the language served as the independent variable (language changed with participants responding to half of the TAT images in Russian and half in English), and it was tested whether cultural values were the dependent variable (whether they changed as language changed). If cultural values were dependent, CFS was established.

I recruited twenty participants through direct conversations for this study. For cross-cultural research, which characterizes the Russian-American cultures present in this study, Yale School of Public Health professor Ashley K. Hagaman and Director of the Center for Global Health at Arizona State University, Amber Wutich, showed that a sample size of twenty was required to achieve data saturation of metathemes.[10] The participants of this study were all adults who immigrated from former Soviet Union countries to Southern California between 1996 and 2024; fourteen out of twenty immigrated in the 2010s. All participants were coordinated bicultural Russian-English bilinguals, meaning that they had a sufficient 7.9875 self-rated English proficiency average and 9.6875 self-rated Russian proficiency average—experience with both languages and both cultures. In order to meet the ethical requirements of the Institutional Review Board, I collected a signed informed consent document, which included an overview of the procedures of this study and outlined its voluntary nature, allowing participants to withdraw at any time without consequences.

Thematic Apperception Test (TAT):

I chose six standard TAT images. The images were split into three pairs. Each pair shared similar characteristics: a central figure (2, 13B), an age difference (7BM, 7GF), and a man and a woman (4, 6BM) (Figure 1).[11] These pairs were established instead of having participants recite two stories in two languages to the same image; using the same image includes a likely dependency of the second story on the first, which limits the integrity of the response. The pairs ensured that each response was independent of external factors (such as already thinking about the image beforehand). This allowed for two stories—one in Russian and one in English—as a response to the core theme (autonomy, age, and gender) present in each pair. This enabled a comparison across Russian and American cultural values, as all participants interpreted images that fell within these core themes in both Russian and English.

The participants attended an individual TAT session, which was divided into two parts in correspondence with the two languages. Ten out of the twenty participants began the session in Russian, while the other ten participants began the session in English. The participants were sorted into each language group by random assignment to ensure that the language order was not a variable that impacted the TAT results.

For the first part of the session, the participants were shown three TAT images for one minute per image. The order of the TAT images for the first session was 2, 7BM, and 4. The order of these images corresponded to the order of core themes: autonomy, age, and gender. They were instructed to tell a story about the image: what was happening, what happened in the past, what would happen in the future, and what the characters were thinking and feeling. The language of these instructions corresponded to the language of the first part of the study.

After the first three images, the participants received a five-minute break. Upon returning from the break, the participants were given the same instructions but in the language of the second part of the study. The procedures of the second part of the session were identical to the first to maintain consistency. The participants were shown three new images for the same amount of time per image. The order of the TAT images for the second session was 13B, 7GF, and 6BM. The order of these images corresponded to the same order of core themes in the first session: autonomy, age, and gender.

I maintained a neutral setting to decrease the likelihood of anything other than the TAT images influencing the participants' stories. I spoke the corresponding language of the study solely from the moment the participant appeared; I switched to the other language halfway through the study (after the break) when the language of the study switched. I did not speak to the participant during the break.

DOI: 10.36838/IJHSR87.264

Category	Number	Image
Autonomy	2	
Autonomy	13B	
Age	7BM	
Age	7GF	
Gender	4	
Gender	6BM	

Figure 1: TAT Images.

Thematic Analysis Using Hofstede's Six Cultural Dimensions: The responses of the participants were tape-recorded and analyzed based on a verbatim transcript. I applied a deductive thematic analysis, as described by New Zealand thematic analysis specialist Virginia Braun and Associate Professor in Qualitative and Critical Psychology Victoria Clarke, by using a pre-existing framework to identify themes of interest—those of the Russian and American cultures in this case—and interpret the connection of these themes with language.[12] The preexisting thematic framework was created based on Geert Hofstede's six cultural dimensions: power distance (PDI), individualism (IDV), masculinity (MAS), uncertainty avoidance (UAI), long-term orientation (LTOWVS), and indulgence (IVR) (Figure 2).[13] Hofstede and his colleagues created these dimensions after administering 117,000 questionnaires regarding the values of people in over sixty countries, including Russia and the United States; these people worked in the local subsidiaries of the multinational corporation International Business Machines (IBM).[14] This framework is widely recognized and extensively used in cross-cultural research in numerous academic disciplines ranging from sociology to international administration, as denoted by marketing experts Dr. Linda M. Orr and William Hauser from the University of Akron.[15] Hofstede's dimensions served as a tool for validating CFS by distinguishing Russian cultural values from American cultural values, which, in turn, would be compared to the language spoken. In addition to validating that these two frames exist, the thematic analysis revealed what the Russian and American

cultural frames looked like, namely, whether they aligned with Hofstede's categorizations or not.

Hofstede Dimension	Definition	Russia	United States
Power Distance (PDI)	Power distance can therefore be defined as the extent to which the less powerful members of institutions and organizations within a country expect and accept that power is distributed unequally.	93	40
Individualism (IDV)	The individualism versus collectivism index concerns the role (and importance) of the individual as compared to the group.	39	91
Masculinity (MAS)	A society is called masculine when emotional gender roles are clearly distinct: men are supposed to be assertive, tough, and focused on material success, whereas women are supposed to be more modest, tender, and concerned with the quality of life. A society is called feminine when emotional gender roles overlap: both men and women are supposed to be modest, tender, and concerned with the quality of issues in information systems.	36	62
Uncertainty Avoidance (UAI)	Uncertainty avoidance addresses the way individuals in a particular national culture handle uncertainty, and the degree to which uncertainty causes anxiety.	95	46
Long-term Orientation (LTOWVS)	Long-term orientation stands for the fostering of virtues oriented toward future rewards—in particular, perseverance and thrift. Its opposite pole, short-term orientation, stands for the fostering of virtues related to the past and present—in particular, respect for tradition, preservation of 'face,' and fulfilling social obligations.	81	26
Indulgence (IVR)	Indulgence stands for a tendency to allow relatively free gratification of basic and natural human desires related to enjoying life and having fun. Its opposite pole, restraint, reflects a conviction that such gratification needs to be curbed and regulated by strict social norms.	20	68

Figure 2: Hofstede's Dimensions for Russia and the United States.

Content Analysis:

I scored all 120 TAT transcripts on each of Hofstede's six dimensions in a content analysis. Responses were scored on a high/low scale (zero or one) for each dimension. After scoring the responses individually, I grouped them by language, making six groups (for six TAT images) of ten responses for English and six groups (for six TAT images) of ten responses for Russian. Then, among each group of ten responses, I recorded the frequency of "high" and "low" scores for each of the Hofstede dimensions. After recording the frequency, I divided the number of "high" scores by the total number of scores for each dimension and multiplied by 100 to calculate an average score. This experimental score showed the percentage alignment to a high score on each Hofstede dimension.

Some dimensions were apparent; others were not. The images were not equal in their ability to bring out all of Hofstede's dimensions. To account for this, participants who gave no response relevant to a certain Hofstede dimension were removed from the high/low calculation for that dimension.

It is important to consider the overlap in some attributes of Hostde's cultural dimensions. For instance, the adaptability in the face of unpredictable circumstances that characterizes a low UAI aligns with a high LTOWVS. However, the theoretical scores for Russia are high on both UAI and LTOWVS, while the theoretical scores for the US are low on both UAI and LTOWVS. Because of this discontinuity, frequency alone is not enough to distinguish between Russian and American culture. Thus, the combination of a content analysis (frequency of the high/low scores for each dimension) and a thematic analysis (cultural patterns supported by direct examples from participants' responses) validated and explained CFS.

The data obtained from the TAT was organized into six tables—one for each TAT image—with the experimental values for Hofstede's six cultural dimensions. For the comparison row, the experimental values for Russian and English on each dimension were compared to one another. If the comparison—which country scored higher or lower—aligned with the Hofstede comparison between Russia and the United States, a "Yes" was marked. For the "Yes" dimensions, the distinction between Russian and American cultural values aligned with Hofstede's theoretical distinction.

Results and Discussion

Image-by-Image:

Table 1: TAT Image 2 (Autonomy #1). For four out of six dimensions shown in Table 1, the experimental comparison between languages and dimension scores aligned with the theoretical comparison between cultures and dimension scores, indicating considerable CFS. The aligned dimensions—PDI, IDV, UAI, and LTOWVS—reflect correspondence with Hofstede's Russian and American cultural assessments.

	PDI	IDV	MAS	UAI	LTOWVS	IVR
Russian	57	38	56	86	78	44
English	50	57	44	40	63	38
Comparison	Yes	Yes	No	Yes	Yes	No

When speaking English, out of the two participants who provided a concrete setting for this image, both of the settings were the United States. Three participants described the American dream, namely the desire for the woman to leave the village and start a new life in a big city, a high IDV, and a low UAI. Such a storyline aligns with the individualistic attribute of American culture, through which Americans pursue their passions in spite of societal norms. Moreover, two of the participants noted that the woman was overseeing the workers, a nontraditional role for a female. Women are empowered and possess traditionally male jobs, resulting in a low MAS.

When speaking Russian, out of the three participants who provided a concrete setting for this image, all three of the settings were in Russia. One participant emphasized that the woman rejected the rural setting she grew up in with her book, yearning for mobility. This serves as a breakaway from a previously collectivist society into one growing more individualistic, with more people challenging societal norms, namely, the female becoming educated in this case. To continue, another participant elucidated the guilt experienced by the woman, specifically the shame of her individuality and dreams upon seeing the workers suffer in the heat while she is clean and put together. This demonstrates a struggle between individualistic desires and a collectivist upbringing—on one hand, she wants to follow her passion, but on the other, she struggles to leave behind her roots at the expense of her community. However, most participants focused on the present situation: the crop yields are high, and everyone needs to work. The general collectivist perspective trumps the outliers—the nonconformists in this case.

DOI: 10.36838/IJHSR87.264

Table 2: TAT Image 7BM (Age #1). For three out of six dimensions shown in Table 2, the experimental comparison between languages and dimension scores aligned with the theoretical comparison between cultures and dimension scores, indicating medium CFS. The aligned dimensions—PDI, UAI, and IVR—reflect correspondence with Hofstede's Russian and American cultural assessments.

	PDI	IDV	MAS	UAI	LTOWVS	IVR
Russian	33	75	89	56	56	63
English	29	75	89	25	57	71
Comparison	Yes	No	No	Yes	No	Yes

When speaking English, one of the participants introduced a Soviet and American spy during the Cold War. The American spy tried to get the Soviet spy's secrets, and the Soviet spy shared them because the peace of the world mattered more to him than winning the ideological competition between the US and the Soviet Union. As the US labels itself as a "safeguard for democracy," the priority of peace over power outlines an American perspective rather than a Russian one. Furthermore, another participant described the status difference between a teacher and a student. Rather than feeling inferior to the teacher with a higher status than him, the student focused on absorbing what the teacher had to teach him. A second participant characterized the two men as a teacher and a student. This participant described meeting up after a long time to catch up on their lives, showing a positive relationship despite the difference in status. Both examples culminated in a low PDI. Moreover, another participant labeled these men confident. Certain that they would defeat another guy in court tomorrow, they were planning a celebratory bar night. The participant highlighted the men's assertiveness rather than anxiety regarding the trial, resulting in a low UAI.

When speaking Russian, a participant characterized the two men as scientists after the fall of the USSR. Craving structure, they wondered how to continue living without one. A seventy-year framework had collapsed, and nobody knew what lay ahead. To continue, another participant reintroduced the battle between individualism and collectivism, one critical as Russia transitions away from a collectivist state to an individualistic society in the 21st century. The son wanted to follow his own path, while his father tried to control him. The father wanted the son to continue the family business, while the son aimed to create a new life for himself. Contrarily, another participant showed a remaining collectivist value in Russia: respecting elders. The older man advised the younger man based on his experience, and the younger man listened intently, trusting the older one to guide him. This diverges from the individualistic mindset; the young man does not ignore his elders or go his own way. These participants present the rampant conflict between collectivism, ingrained in the older population, and individualism, often projected by youth.

Table 3: TAT Image 4 (Gender #1). For four out of six dimensions shown in Table 3, the experimental comparison between languages and dimension scores aligned with the theoretical comparison between cultures and dimension scores, indicating considerable CFS. The aligned dimensions—PDI, IDV, UAI, and IVR—reflect correspondence with Hofstede's Russian and American cultural assessments.

	PDI	IDV	MAS	UAI	LTOWVS	IVR
Russian	63	56	100	100	25	60
English	22	71	80	67	44	78
Comparison	Yes	Yes	No	Yes	No	Yes

When speaking English, numerous participants emphasized the man's desire to break free of the woman's grasp to pursue his own interests—sailing, construction, or acting as present-day Hercules. When speaking Russian, though, numerous participants painted an alternative narrative: the man was about to lash out at a guy who hurt his wife, while his wife was holding him back. In American interactions, the man focused on himself; in Russian interactions, the man focused on protecting his wife. This divergence in interpretations reverts to the contrast between individualism—the individual above all—and collectivism—all above the individual—in the American and Russian cultures.

Table 4: TAT Image 13B (Autonomy #2). For two out of six dimensions shown in Table 4, the experimental comparison between languages and dimension scores aligned with the theoretical comparison between cultures and dimension scores, indicating weak CFS. The aligned dimensions—PDI and LTOWVS—reflect correspondence with Hofstede's Russian and American cultural assessments.

	PDI	IDV	MAS	UAI	LTOWVS	IVR
Russian	90	60	80	78	50	30
English	67	60	60	90	30	20
Comparison	Yes	No	No	No	Yes	No

When speaking English, participants described the young boy's individualistic mindset of self-preservation. One participant described his anger at his parents for taking away his chocolate, culminating in his desire to escape his home to get away from his cruel parents. Another participant outlined his concerned face; he was not thinking like a child, and something bothered him more than simple childish annoyances. Both the runaway and the philosopher reflect self-reliance, just to different degrees of maturity.

When speaking Russian, three participants told an identical story: an autobiography. A little boy got a 2 and was afraid to tell his mother about his poor grade. Hiding it was not an option; he needed her signature. His position was futile. He had no way to avoid punishment, and he definitely would not be at his friend's birthday party tomorrow. The Russian language spurred a Russian childhood memory, one that left an emotional scar.

Table 5: TAT Image 7GF (Age #2). For all six dimensions shown in Table 5, the experimental comparison between languages and dimension scores aligned with the theoretical comparison between cultures and dimension scores, indicating strong CFS. The aligned dimensions—PDI, IDV, MAS, UAI, LTOWVS, and IVR—reflect correspondence with Hofstede's Russian and American cultural assessments.

	PDI	IDV	MAS	UAI	LTOWVS	IVR
Russian	50	50	40	60	50	50
English	30	78	80	22	20	80
Comparison	Yes	Yes	Yes	Yes	Yes	Yes

Regardless of language, most participants described a young mother faced with the choice: her childhood or the baby's childhood. In English iterations, the young girl would end up choosing herself over her baby. She ignored what her mother or nanny told her, daydreaming about the games she would play with her neighborhood friends instead. In Russian iterations, though, the young girl resisted motherhood, concentrating on her child's upbringing. Her baby could not be unborn, and it was her duty to be its mother figure. The mother or nanny reaffirmed that the family took precedence. Individualism, again, clashes with collectivism.

Table 6: TAT Image 6BM (Gender #2). For five out of six dimensions shown in Table 6, the experimental comparison between languages and dimension scores aligned with the theoretical comparison between cultures and dimension scores, indicating strong CFS. The aligned dimensions—PDI, IDV, MAS, UAI, and IVR—reflect correspondence with Hofstede's Russian and American cultural assessments.

	PDI	IDV	MAS	UAI	LTOWVS	IVR
Russian	100	10	40	89	60	0
English	30	70	70	60	60	40
Comparison	Yes	Yes	Yes	Yes	No	Yes

Among both languages, participants detailed a relationship between a son and his mother; in fact, all ten Russian iterations were about this relationship. However, when speaking English, two participants introduced a novel perspective: the two individuals did not know each other at all. The participants described them standing in line—to buy food or tickets to a movie theater—each contemplating their separate evening plans. Another participant, when speaking English, disclosed the reason behind the depressing demeanor: the son was to leave his mother for a long time. This presents a struggle behind individualism, as the man is prioritizing himself by moving to a place with opportunity, leaving his loved ones behind. Despite recognizing his mother's dejection, the man still left her, chasing a better life for himself.

When speaking Russian, the participants emphasized the man's guilt in the face of his mother. He bore bad news—two participants specified that he would lose his job, and others mentioned death—but he did not know how to tell her. He respected her and did not want to disappoint her. For another participant, the bad news was a breakup. The participant accentuated that the mother's worry that her son was not going to settle down with his family, a collectivist priority contrary to individualistic ones related to the career path, recounted in English iterations.

Comparative Assessment:

After individual analysis of each of the six TAT images, it is integral to consider them collectively. Across all six TAT images, the strongest experimental comparisons between Russia and the US were PDI (6/6), UAI (5/6), and IDV (4/6), signifying a consistent interpretation of and differentiation between Russian and American culture for those dimensions among participants. Conversely, LTOWVS (3/6) and MAS (2/6) revealed weaker comparisons, revealing the lack of a common rendition and indicating blurred differences that reflected individual rather than collective understandings for those dimensions among participants.

Limitations and Future Directions:

The limited sample size of twenty participants does not account for the CFS in all Russian-English bilinguals. Further research should include participants with a more equal experience with both languages and cultures, considering both years spent in each country and spheres of language usage. In an attempt to equalize this experience, the fact that most of the participants in this study spent a longer portion of their lives in Russia—strong Russian cultural experience—was paired with the fact that they all presently reside in the United States—currently immersed in American culture daily. However, this study also does not fully address the impact of participants' personal experiences—childhood, Soviet Union, Cold War—in shaping their understanding of Russian and American culture. Their own past may well influence their perspective and, subsequently, the cultural values they highlight in their responses, which may not necessarily reflect current cultural realities.

Additionally, it is important to clarify that the individual experimental values themselves were not compared to Hofstede's individual theoretical values. Solely the percentage alignment to a high score on Hofstede's dimension was calculated. This is because the experimental values were calculated on a binary high/low scale in lieu of Hofstede's 100-point scale. This is due to the constraint of a one-minute TAT response, through which participants did not provide enough information for finer distinctions. Future research can include follow-up questions specific to Hofstede's dimensions after completion of the TAT responses. The information gathered from these follow-up questions, combined with the TAT responses, would allow scoring on a granular scale. Furthermore, a single coder scored the images on the large/low scale. Future research can employ multiple coders and measure inter-rater reliability to increase validity and consistency across scores.

Hofstede's six cultural dimensions were used for the thematic and content analyses in this study. When assigning a country score, Hofstede's dimensions fail to take regional differences into account, instead treating the country as homogenous. Additionally, Hofstede's dimensions assume that cultural values are constant across contexts and do not vary across different spheres. However, cultural values and behavioral reactions can change depending on the setting, such as acting professionally in a workplace but being more relaxed at home. Thus, future research can tailor the TAT images to different spheres—work,

DOI: 10.36838/IJHSR87.264

home, school, social activities—and assess the differences in Russian and English cultural values within those settings.

The setting aspect brings forth a confounding variable: memories associated with the use of a certain language in a certain setting. For instance, if most participants utilize solely Russian at home, future research can include images with a home setting and test whether those images bring out Russian cultural values through a memory-based association independent of the language spoken. Contrarily, for social activities, if most participants use half English and half Russian, future research can test whether images with a social setting bring out a mix of Russian and American cultural values and determine whether those values depend on the language spoken. This mixed setting would be a stronger means of identifying CFS, as it would reduce the confounding impact of a memory-based association and test the dependence of cultural values on language. However, because the TAT images used in this study were not tailored to a certain setting—instead focusing on the characters in the images—the impact of memory-based association could not be made.

Conclusion

Out of a total of thirty-six comparisons between Russian and English, a difference between Russian and English stories was observed in thirty-three cases. Within those thirty-three comparisons between Russian and English high/low experimental values, twenty-four corresponded with the theoretical comparison by Hofstede on the high/low country scale. For these twenty-four cases, the change in content values aligned with the cultural values associated with the language spoken; when speaking Russian, participants highlighted Russian cultural values, and when speaking English, participants highlighted American cultural values. The content analysis affirmed the CFS effect, and the thematic analysis illustrated what the two cultural frames—Russian and American—looked like, specifically that they aligned with Hofstede's categorizations.

Understanding the dominant attributes that make up the Russian and American identities is critical to improving communication and interaction with Russian-English bilinguals in the United States, a country in which 2.1 million Russians reside as of 2023.[16] When these bilinguals switch between their two languages, their cultural mindsets and behavioral norms change alongside their spoken words. Such changes purport the notion that identity is dynamic rather than stagnant; it relies on context—spoken language in the case of bilinguals—and is subject to shifts that can be activated by linguistic cues. Comprehending such changes is imperative to mitigating misinterpretations, engaging empathetically, and cultivating meaningful relationships with members of the bilingual community.

Acknowledgments

I would like to thank my mentors, Jasmin and Rei from the Bilingualism, Mind, and Brain Lab at the University of California, Irvine, for their thoughtful guidance.

References

1. Ramírez-Esparza, N.; Gosling, S. D.; Benet-Martínez, V.; Potter, J. P.; Pennebaker, J. W. Do Bilinguals Have Two Personalities? A Special Case of Cultural Frame Switching. Journal of Research in Personality 2006, 40 (2), 99–120. https://doi.org/10.1016/j.jrp.2004.09.001.
2. Rezapour, R.; Zanjirani, S. Bilingualism and Personality Shifts: Different Personality Traits in Persian-English Bilinguals Shifting between Two Languages. Iranian Journal of Learning and Memory 2020, 2020 (10), 23–30. https://doi.org/10.22034/IEPA.2020.230347.1169.
3. Chen, S. X.; Benet-Martínez, V.; Ng, J. C. K. Does Language Affect Personality Perception? A Functional Approach to Testing the Whorfian Hypothesis. Journal of Personality 2013, 82 (2), 130–143. https://doi.org/10.1111/jopy.12040.
4. Marian, V.; Kaushanskaya, M. Self-Construal and Emotion in Bicultural Bilinguals. Journal of Memory and Language 2004, 51 (2), 190–201. https://doi.org/10.1016/j.jml.2004.04.003.
5. Ervin, S. Language and TAT Content in Bilinguals. The Journal of Abnormal and Social Psychology 1964, 68 (5), 500–507. https://doi.org/10.1037/h0044803.
6. Ilenia Perez-Palen. The Influence of Language on Thematic Apperception Test Assessment of Defenses in International Spanish-speaking College Students. Scholarship Repository @ Florida Tech. https://repository.fit.edu/etd/399.
7. Hoffman, F. A Participant Observation Approach to Assessing the Validity of Hofstede's National Culture Framework. Issues in Information Systems 2021, 22 (2). https://doi.org/10.48009/2_iis_2021_334-349.
8. Grossmann, I.; Ellsworth, P. C.; Hong, Y. Culture, Attention, and Emotion. Journal of Experimental Psychology: General 2012, 141 (1), 31–36. https://doi.org/10.1037/a0023817.
9. Naumov, A.; Puffer, S. Measuring Russian Culture Using Hofstede's Dimensions. Applied Psychology 2000, 49 (4), 709–718. https://doi.org/10.1111/1464-0597.00041.
10. Hagaman, A. K.; Wutich, A. How Many Interviews Are Enough to Identify Metathemes in Multisited and Cross-Cultural Research? Another Perspective on Guest, Bunce, and Johnson's (2006) Landmark Study. Field Methods 2017, 29 (1), 23–41. https://doi.org/10.1177/1525822x16640447.
11. Dr. Shyama Prasad Mukherjee University. Redirecting. Google.com. https://www.google.com/url?q=https://dspmuranchi.ac.in/pdf/Blog/thematicapperceptiontest.pdf&sa=D&source=docs&ust=1757738998147671&usg=AOvVaw23vXkJTBrf-JKZhUTd_iKf (accessed 2025-03-28).
12. Braun, V.; Clarke, V. Thematic Analysis. APA Handbook of Research Methods in Psychology, Vol 2: Research designs: Quantitative, qualitative, neuropsychological, and biological. 2012, 2 (2), 57–71. https://doi.org/10.1037/13620-004.
13. Hofstede, G. Dimension data matrix. Geert Hofstede. https://geerthofstede.com/research-and-vsm/dimension-data-matrix/.
14. Hofstede, G. Culture's Consequences: International Differences in Work-Related Values; Sage Publications: Beverly Hills, 1980.
15. Orr, L; Hauser, W. and William Hauser, A Re-Inquiry of Hofstede's Cultural Dimensions: A Call for 21st Century Cross-Cultural Research, Marketing Management Journal 18, no. 2. 2008, 1–19, https://www.mmaglobal.org/_files/ugd/3968ca_ed2a5bd1b3474772928691dfa71b7b12.pdf#page=8
16. United States. Explore Census Data. Census.gov. https://data.census.gov/table/ACSDT1Y2023.B04006 (accessed 2025-03-28).

Authors

Alexandra Denisova is a senior at Corona del Mar High School. She is a student in the Academy of Global Studies, as well as a devout member of Speech and Debate, Model United Nations, and Mock Trial. She aims to pursue international risk management or geopolitical analysis and study the international political economy in undergraduate school.

DOI: 10.36838/IJHSR87.264

IJHSR
ijhighschoolresearch.org
RESEARCH ARTICLE

Assessing the Quality of Life of Palestinian Young Adult Refugees in Jordan: An Exploratory Study

Antara Nayak

Livingston High School, 30 Robert H Harp Drive, Livingston, New Jersey, 07039, USA; an07tara@gmail.com

ABSTRACT: Quality of life (QoL), as measured by the World Health Organization, includes physical, psychological, social, and environmental domains, and is particularly threatened among vulnerable populations such as young adult refugees. This study assessed QoL among Palestinian refugee young adults (ages 18–25) residing in Al Husn Camp, Jordan, using the WHOQOL-BREF survey. Palestinian young adult refugees face unique circumstances, such as displacement stress and challenges of developing their identity as they navigate adulthood. Twenty-one participants were recruited with the support of a local NGO, and they completed a culturally adapted version of the WHOQOL-BREF, with one sensitive item removed for cultural relevance. Given the small sample and reliance on self-reported data, results are exploratory and should be interpreted with caution. Descriptive statistics showed lower domain scores compared to normative populations: physical health averaged 48.1, psychological health 51.6, social relationships 55.6, and environment 36.8 (on a 0–100 scale). By contrast, general populations in Australia and Mongolia reported higher scores in all domains, ranging from 61.5 to 79.7. These results show low QoL among young adult refugees, particularly in environmental and psychological domains. Findings highlight the need for interventions and future research expanding survey methods and sample diversity to address young adult refugee QoL disparities in Jordan.

KEYWORDS: Social and Behavioral Science, Sociology and Social Psychology, Mental Health, Quality of Life, Palestinian Refugees.

Introduction

According to the World Health Organization, Quality of Life (QoL), "is an individual's perception of their position in life in the context of the culture and value systems in which they live and in relation to their goals, expectations, standards and concerns".[1] Quality of Life, encompassing four main domains: physical, psychological, social and environmental, is a measure of global health.[1] QoL outcomes are disproportionately unequal for vulnerable populations, where socioeconomic factors play a part in both the prevalence of well-being issues and access to care.[2, 3] Among youth, disruptions to Qol are visible. In the psychological category, there were sharp increases in reported depressive symptoms over the last decade.[4] For refugee populations, there is a strong prevalence of poor quality of life indicators because their lives are shaped by conflict, displacement, and post-migration uncertainty.[5] Refugee groups face challenges resulting from exposure to conflict and displacement affecting education, employment, housing, and social belonging, all factors that are correlated to well-being.[5]

Jordan hosts approximately 2.3 million registered Palestinian refugees, with about 30% being under the age of 25.[6] These refugees are in Jordan in an attempt to escape a series of wars in Palestine.[7] In Jordan, there are around 13 camps, 3 of which are unofficial.[8] Many Palestinian refugees live in host communities, camps, or informal, tented settlements, often for indefinite periods of time.[7] Across these settings, opportunities for education, employment, and healthcare remain limited, reducing overall quality of life.[8] Social factors, including limited educational and employment opportunities, contribute to distress in this population.[9]

Refugees face challenges, including financial barriers and limited awareness of available services.[10] Those in informal settlements often experience the most severe access limitations, with geographical isolation and lack of transportation infrastructure creating additional barriers.[10] These environmental issues all lead to a lower quality of life amongst refugee populations. This lack of comprehensive support highlights why refugee quality of life is fragile.

This study will assess quality of life among Palestinian youth refugees in Jordan, paying particular attention to the intersection of health, social well-being, and access to resources. Despite research on QoL, knowledge gaps remain regarding Palestinian young adults in Jordan. Current research lacks age-specific data, with very few studies focusing on the challenges faced by the young adult population. The importance of this research is emphasized by demographic factors, as approximately 30% of Palestinian refugees in Jordan are under 25 years old.[11] This makes youth QoL important for the population's future stability. The findings from this study can aid in the development of youth-specific solutions to increase quality of life, as well as a broader study to see how this compares to a different population. Overall, this work hopes to bridge these gaps, given the ongoing challenges faced by Palestinian refugees and the increasing significance of QoL.

Overview of the Current Study:

This study aims to assess the quality of life of Palestinian young adult refugee populations in Jordan across all four quality of life domains: psychological, environmental, social, and physical. It is predicted that the quality of life will be lower

© 2026 Terra Science and Education

DOI: 10.36838/IJHSR87.273

than expected across all four domains due to structural and circumstantial barriers that this population faces. The current literature presents this as most prevalent in the psychological domain, as it was determined that 31.46% of refugees experienced PTSD compared to 3.9% in the general population.[12] Conditions such as PTSD take a severe toll on the psychological well-being of refugees, and facing this condition at a much higher rate than the general population will, in turn, reduce their quality of life. A meta-analysis examining physical health-related quality of life using the SF-36 Health Survey among 18,418 refugees found that refugee quality of life is generally poorer than that of the general population in a number of host countries.[13] However, these two studies relate more to the physical and psychological domain, whereas the social and environmental domain has not been explored to the same extent. A study following refugees in Australia over five years found that rates of psychological stress increased over the 5-year follow-up period, partially due to social integration issues such as discrimination, a lower sense of belonging, loneliness, and lower English proficiency.[14] These persisting social issues lead to a sense of isolation, impacting an individual's perception of their quality of life. This relates to a lower quality of life in the environmental category, where lack of access to resources reduces a refugee's quality of life.

Methods

Study Population:

This study was approved by the WCG Clinical Institutional Review Board (IRB) and conducted in collaboration with non-governmental organizations (NGOs) that support Palestinian refugees in Jordan. Recruitment for the study was conducted by NGO coordinators working at the Al Husn refugee camp in Jordan, one of the largest Palestinian refugee camps in the country. According to the United Nations Relief and Works Agency (UNRWA), there are "more than 28,000 Palestinian refugees residing in the Al Husn camp, making it the seventh largest refugee camp in Jordan."[15] The camp, originally established in 1968 for those who were displaced during the Arab-Israeli conflict, has grown from a temporary settlement into a semi-permanent urban area with concrete housing, healthcare infrastructures, and schools.[15] However, it is worth noting that these resources are severely underfunded.[15]

The reason this camp was selected was due to its location, which makes it accessible through trusted nonprofit partners, as well as its large number of young adult refugees. The nonprofit MENA mental health organization allowed for ethical recruitment of participants. This NGO could offer ease, familiarity, and trust for these participants, given the challenges that complicate studies in refugee research. By working with a nonprofit, it was ensured that participants were aware of the purpose and directions of this survey.

The study focused on Palestinian young adult refugees aged 18 to 25 currently residing in Jordan as a result of displacement due to political and military conflict in Palestine. This demographic was selected based on UNRWA reports indicating that young adults under the age of 25 represent approximately 30% of the Palestinian refugee population in Jordan.[15] Their age, developmental stage, and unique experiences of displacement position them at heightened risk for challenges, making them a critical group for research.

Participants were recruited through community centers and NGO-run health and education programs. Fieldwork was conducted from June to August 2025. Individuals who agreed to participate were screened for eligibility, including age and refugee status. Individuals who migrated for non-displacement reasons, who were outside the age range, or who were not residing in a camp or informal settlement were excluded. A total of 21 young adults responded to the call for participation. Participants completed the survey on smartphones or tablets provided by the NGOs, with support from trained facilitators as needed. Consent was obtained from participants aged 18 and above. Participants were assured that their involvement was voluntary and that their responses would remain confidential and anonymous. Additionally, all participants completed a consent form, ensuring they understood the survey's outcomes and provided their consent.

Measures:

The primary instrument used for this study was the World Health Organization Quality of Life - BREF (WHOQOL-BREF) survey. This tool was selected because it is a validated instrument used globally for assessing perceived quality of life across different cultural and social settings. Additionally, the WHOQOL-BREF is consistently used in refugee studies, such as those by Al-Solieiti *et al*. Unlike narrower diagnostic tools such as the PHQ-9 or HSCL-25, the WHOQOL-BREF offers a more comprehensive understanding of well-being due to its broad domains. Using the WHOOL-BREF also makes this study's method easy to replicate for future studies.

The WHOQOL-BREF includes 26 items covering four core domains of quality of life[1]:

- Physical Health (7 items)
- Psychological Health (6 items)
- Social Relationships (3 items)
- Environment (8 items)

Additionally, two general items assess overall perception of mental health and satisfaction with one's health. However, for the sake of cultural relevance, question 23, which asked about sexual activity, was removed. More specifically, question 23 asked about the individual's sexual relations and sexual activity. Sexual topics tend to be more stigmatized and frowned upon in Middle Eastern Society, which is why they were removed from the survey. The removal will be taken into account when doing the data analysis. Removing one out of the three questions in the Social domain may render results as unreliable, meaning, accurate representation of this domain may require another study.

Each item is scored on a 5-point Likert scale, with higher scores representing more favorable conditions. The WHOQOL-BREF includes three negatively worded items: physical pain (B3), need for medical treatment (B4), and frequency of negative feelings (B26). These items were reverse-scored to ensure that higher values consistently reflected a higher qual-

ity of life. The survey questions were in Arabic and English, ensuring that anyone who met the participant criteria could partake, regardless of their spoken language. Completion time for this survey averaged 12–15 minutes.

Results and Discussion

Results:

Descriptive Analysis:

Raw domain scores were calculated by summing the individual item scores for each domain. The scoring system uses the following possible raw score ranges: Physical Health: 7 to 35, Psychological Health: 6 to 30, Social Relationships: 3 to 15, Environment: 8 to 40

Domain scores were transformed to a 0–100 scale using the WHO-recommended formula:

Physical domain= ((6-Q3) + (6-Q4) + Q10 + Q15 + Q16 + Q17 + Q18)x4.

Psychological domain= (Q5 + Q6 + Q7 + Q11 + Q19 + (6-Q26))x4.

Social Relationships domain= (Q20 + Q21 + Q22)x4.

Environment domain= (Q8 + Q9 + Q12 + Q13 + Q14 + Q23 + Q24 + Q25)x4.

(Domain-4)(100/16)= transformed score

This standardization enables interpretation and comparison across various domains and populations. Based on these guidelines, a higher score shows a higher quality of life in each domain. By using the WHOQOL-BREF, this study can leverage standard results for comparison to other studies and norms. The four scores were calculated for each participant for each domain, using the domain formula listed above. Then each score was transformed by subtracting four and multiplying by 100/16. After that, the total means and standard deviations were calculated for each category. The mean for the physical domain was 48.1, and the standard deviation was 13.9. The mean for the psychological domain was 51.6, and the standard deviation was 17.1. The mean for the social domain was 55.6, and the standard deviation was 23.3. The mean for the environmental domain was 36.8, and the standard deviation was 16.8.

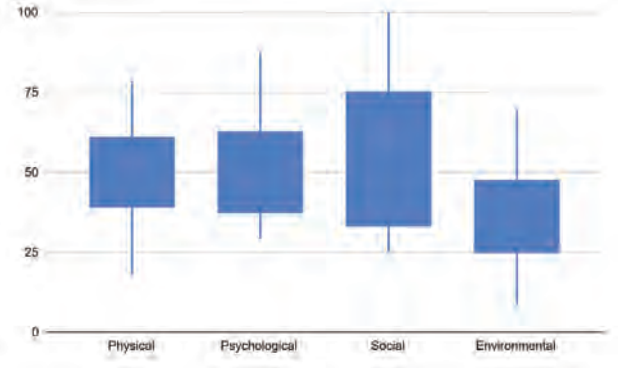

Figure 1: Means and standard deviations for domains of the WHOQOL-BREF survey conducted on Palestinian Young adult refugees in Jordan (Physical, Psychological, Social, Environmental). Overall, Social scores were the highest and Environmental scores were the lowest, which suggests that even when people feel some sense of connection, the day-to-day conditions in refugee camps are still major barriers to QoL. The Social domain also had the biggest spread, showing that participants' social experiences weren't consistent, meaning some had strong support systems, while others didn't.

Discussion:

This study reveals that Palestinian young adult refugees in Jordan experience significantly lower quality of life in all WHOQOL-BREF domains compared to the general population. As seen in Figure 1, mean scores were approximately 48.1 for physical health, 51.6 for psychological health, 55.6 for social relationships, and 36.8 for environment were calculated for Palestinian young adult refugees in Jordan. By contrast, healthy populations in countries such as Australia and Mongolia report much higher WHOQOL-BREF scores across every domain, as seen in Figure 2: physical health averages 74.5 in Australia and 61.5 in Mongolia; psychological health 72.1 in Australia and 73.5 in Mongolia; social relationships 72.9 in Australia and 70.1 in Mongolia; and environment 79.7 in Australia and 67.2 in Mongolia.[14, 16] In a Syrian Refugee population in Jordan, it was determined that physical health averaged 50.7 the Psychological health averaged 49.4 the social relations domain averaged 49.8, and the environmental domain averaged 47.4. Therefore, Palestinian refugee young adults in Jordan scored 26 to 43 points lower than Australians and 9 to 30 points lower than Mongolians depending on the domain, showcasing the disparities in quality of life outcomes between refugees and general populations.[14,16] When compared to the Syrian refugee population, however, the numbers were much closer together, pointing towards a trend in overall decreased quality of life for refugees. However, it is important to acknowledge that there is a vast difference in sample size between the current study (n=21) and the Australian (n=929) and Mongolian population studies(n=714) and Syrian Refugee study (n=655).

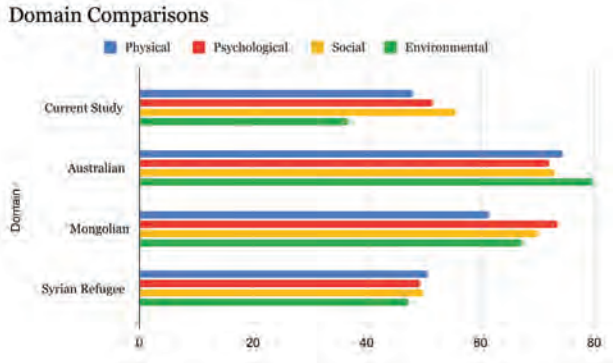

Figure 2: Means for physical, psychological, social, and environmental domains for the current study population, normative Australian,[14] normative Mongolian,[16] and Syrian refugee.[17] Across all four domains, the current study's mean scores are lower than the Australian and Mongolian normative samples, with the biggest difference showing up in the Environmental domain. Compared with the Syrian refugee sample, scores look closer overall, but the Environmental domain still stands out as one of the lowest areas for this group.

Physical Health Domain:

The average physical health score was 48.3, indicating ongoing challenges such as poor nutrition and limited access to healthcare, which are common in long-term displacement. Scores ranged from 17.86 to 60.71, indicating significant variability among participants. The median score of 42.86 also supports a slightly left-skewed distribution, with a minority reporting lower than average outcomes. A study from Johns Hopkins found that many Syrian refugees in Jordan suffer from chronic illnesses like diabetes and high blood pressure,

DOI: 10.36838/IJHSR87.273

often due to limited access to preventive care and financial barriers to treatment.[18] This broader pattern highlights how even though refugees report low physical health conditions, this is attributed to systematic issues. The low physical health scores found in the current study may be impacted by the fact that medical centers in Jordan lack sufficient funding, making it harder for them to serve the uninsured refugee populations.[17] Similar findings were reported by Anwar *et al*., who showed that among long-term residents in a refugee camp, physical health domain outcomes deteriorated over time due to prolonged exposure to crowded environments and limited access to medical care.[19] Another study, looking at the health-related quality of life of Palestinian refugees in Jordan, found major disparities in refugees who specifically live inside camps.[20] In the physical health domain, the low mean score may align with studies showing that refugee communities face chronic illness burdens due to systemic healthcare inaccessibility. Underfunded clinics, medication shortages, and limited preventive care reflect structural neglect. The longer individuals stay in these settings, the more likely they are to develop preventable or manageable conditions. In summary, the physical health results underscore how structural barriers in healthcare funding and accessibility perpetuate chronic illness and poor well-being among long-term refugees.

Psychological Domain:

The average psychological health score was 51.6, indicating widespread mental health challenges. This likely reflects ongoing stress, insecurity, and lack of concentration in daily life. Some participants scored as low as 29 to 17, suggesting severe distress in parts of the group. This low score may be attributed to several factors. A study by Researchers Kiselev *et al*. of Qatar University found that mental health challenges amongst refugees are typically attributed to stress in numerous areas of life.[23] Additionally, a study by Al-Soleiti *et al*. found that underfunding, stigma, and cultural barriers limit access to mental health care in camps in Jordan.[10] Also, structural issues, such as legislation, restrict Palestinians from public-sector jobs, adding to feelings of hopelessness.[21] The UNHCR Global Trends Report also supports these findings, noting that refugee young adults report nearly double the global average rates of anxiety and depression, particularly in under-resourced host countries.[22] Psychological health findings also show that the mental strain may be a result of displacement, legal barriers, financial insecurity, and lack of mental health services. Invisibility within host societies may exacerbate distress, potentially resulting in lower psychological scores.[24] This may be significant for young adults, who experience an identity crisis due to constant marginalization; it was found that prolonged young adult displacement led to high levels of suicidal ideation and loss of future orientation.[25] The psychological burden that refugee young adults face cannot be separated from chronic exposure to structural ambiguity. Their daily existence is characterized by chronic instability from uncertain living arrangements to irregular access to primary services. The scarcity of available mental health facilities exacerbates these psychological hazards. Despite some of the psychological services delivered by organizations such as UNRWA, the demand is great, and the stigma of mental illness and lack of culturally competent professionals imply that most young refugees go untreated.[18] The unavailability of safe, confidential, and welcoming mental health facilities discourages use even among those who perceive a need to be supported. Culturally tailored and locally situated models being pivotal in addressing the refugee mental health outcomes, especially among young adults who do not trust formal institutions, is laid out by Kirmayer *et al*.[26] Overall, the psychological domain reveals that young refugees' mental health is undermined by chronic instability, systemic neglect, and cultural stigma, emphasizing the need for inclusive and trauma-informed care frameworks.

Social Domain

The average score for social relationships was 55.6, the highest among all measured areas, pointing towards strong family and community ties. However, scores ranged from 25 to 100, suggesting that not everyone has equal access to these support networks. Additionally, as mentioned earlier, the results from this domain must be approached with caution due to the missing question. The median score of 50 confirms this distribution's slight left skew, with most respondents reporting moderate to strong ties, but some experiencing isolation. Strong social bonds are a cultural strength, but systemic barriers can weaken their impact. For example, a study found that political oppression in Gaza led to a decrease in trust in relationships, despite strong family connections.[27] However, this appears to be a more variable issue from individual to individual, and the current research indicates that there are no consistent trends in this category for the population surveyed. During the COVID-19 pandemic, social ties among displaced communities further deteriorated due to restrictions on movement and interaction. Studies show that isolation measures disproportionately affected refugee young adults, increasing emotional distancing even within households.[28] However, this same study mentions how some young refugee adults reported feeling closer to their families post-pandemic. For young adults who spent much of their youth in refugee camps, even familial networks may be stressed by resource scarcity and intergenerational trauma. In conclusion, the social domain findings suggest that while community and family connections serve as protective factors, structural and situational pressures can strain these relationships, leading to uneven social well-being across the refugee population.

Environmental Domain (Surrounding Conditions):

The environmental domain had the lowest mean score at 36.8, reflecting widespread dissatisfaction with conditions such as safety, healthcare, and financial stability. Scores ranged widely (8.3–58.3), with over 57% of participants scoring below 40, indicating acute environmental stress. The median score of 33.3 supports a slightly left-skewed distribution. Comparable patterns also appear in refugee camps among the Rohingya, where a study reported increased overcrowding and lack of sanitation and dependency on aid, serving to reinforce poverty and insecurity patterns.[28] UN reports also suggest that refugee camps in Jordan run at or near capacity, which otherwise in-

creases health and security threats.[22] Ruhnke *et al*. also found that the longer a refugee is in a camp environment, the worse their perception of environmental stability becomes, and in alignment with less access to employment, leisure, and education.[29] These findings demonstrate that inadequate living conditions, combined with restrictive governmental policies, form structural barriers that significantly impair the quality of life for Palestinian young adult refugees. The environmental domain's low scores may demonstrate the ongoing lack of access to resources that refugees face. Overcrowded housing, unsafe environments, and financial deprivation may reinforce cycles of poverty and insecurity, worsening overall well-being. Ultimately, the environmental domain highlights how systemic neglect, overcrowding, and financial hardship create persistent conditions of instability that severely undermine refugees' quality of life.

Limitations:

Several limitations affected this research. First, the sample size (n = 21) limits generalizability. Although sufficient for identifying trends within Al Husn Camp, it does not fully represent the diversity of experiences among Palestinian refugee young adults across Jordan. Participants were drawn exclusively from one camp, excluding voices from urban refugees or those in other settlements such as Baqa'a or Jerash. Future research should intentionally incorporate multiple sites for comparative analysis.

Secondly, the research was based completely on self-report data from a standardized measure. Although the WHOQOL-BREF is a validated measure, it is likely to underrepresent culturally unique mental health stressors like intergenerational trauma, acculturative pressure, and religious identity crises. Social bias may also have caused some participants to underreport. Also, since individuals volunteered to take part in the study, there will be a self-selection bias, so the data is more likely to be less extreme, as those suffering the most may not have the capacity to respond to a survey.

Third, while efforts were made to maintain cultural relevance by removing sensitive items (e.g., the question on sexual activity), this adjustment may have slightly reduced reliability in the social domain. Public discussions on sexual topics tend to be stigmatized, especially in the Middle East. In the collection of the data, it was intended to make individuals feel comfortable enough to be vulnerable during the survey, which is why the sexual activity question was removed.

Future Implications:

Future research should focus on a larger sampling group involving both camp and urban refugee groups in Jordan. Mixed methods that involve quantitative tools, such as the use of the WHOQOL-BREF, blended with semi-structured interviews, will allow researchers to place mental health scores in context and investigate more in-depth and nuanced themes such as identity, belonging, and resilience. In turn, long-term studies may be used to monitor and measure the way mental health and quality of life change following particular policy events or global interruptions, such as the COVID-19 crisis.

At the level of practical application, there are multiple directions for potential solutions in the future. Host government and NGO investment in long-term mental health systems that extend beyond emergency arrangements is required. Culturally specific and young adult-friendly interventions such as mobile mental health clinics, school-based, trauma-informed interventions, and peer-support groups can be tailored into existing community systems to improve accessibility. Training sessions to educate counselors with skills to meet the unique needs of displaced children who do not respond to traditional Western models of mental health should be increased.

■ Conclusion

This paper draws attention to the prevalence of mental health and quality of life problems among young Palestinian refugee young adults living in Al Husn Camp in Jordan. By the use of the WHOQOL-BREF survey, participants consistently reported lower scores in the psychological, physical, social, and environmental domains, as predicted in the hypothesis. These findings attest to the long-term effects of displacement on refugees. In contrast to discrete health outcomes, the findings illustrate a more general social trajectory of prolonged displacement, legal exclusion, and political marginalization that together give rise to and maintain adverse mental health outcomes. This is particularly important in the case of young adults whose development is susceptible to protracted instability, eroded agency, and unfulfillment of opportunity.

The average physical health score was 48.3, ranging from 17.9 to 60.7, reflecting health challenges and variability among participants. Structural issues, including underfunded clinics, medication shortages, and limited services for uninsured refugees, could contribute to these outcomes.18 The average psychological health score was 51.6, with some scoring as low as 17 to 29, indicating widespread distress and challenges for parts of the group. The average social relationships score was 55.6, which was the highest across all domains, showing strong family and community ties that help refugees deal with hardship. However, scores ranged widely from 25 to 100, with 32% scoring below 50, showing that many lack adequate support networks. This shows no consistent trend in this domain. 27,28 The environmental domain had the lowest mean score at 36.8, with a range of 8.3 to 58.3, showing dissatisfaction with safety, healthcare, and financial stability. Similar findings have been reported in other refugee studies, such as one with the Rohingya, where overcrowding, poor sanitation, and aid dependency reinforce cycles of poverty and insecurity.28 For young adult Palestinian refugees, these challenges contribute to a low QoL.

The findings reveal a pattern of low quality of life among Palestinian refugee young adults in Al Husn Camp. Each domain, physical, psychological, social, and environmental, illustrates how long-term displacement systematically affects well-being.

DOI: 10.36838/IJHSR87.273

Acknowledgments

I would like to thank the anonymous reviewers for her feedback. I would also like to thank my mentor Monica Rybak for guiding me through all aspects of this paper.

References

1. World Health Organization. *WHOQOL - Measuring Quality of Life*. World Health Organization. https://www.who.int/tools/whoqol.
2. Singer, B. H.; Ryff, C. D.; National Research Council (US) Committee on Future Directions for Behavioral and Social Sciences Research at the National Institutes of Health. *The Influence of Inequality on Health Outcomes*. Nih.gov. https://www.ncbi.nlm.nih.gov/books/NBK43780/.
3. Nutakor, J. A.; Zhou, L.; Larnyo, E.; Addai-Danso, S.; Tripura, D. Socioeconomic Status and Quality of Life: An Assessment of the Mediating Effect of Social Capital. *Healthcare* 2023, *11* (5), 749. https://doi.org/10.3390/healthcare11050749.
4. Flaubert, J.; Menestrel, S.; Williams, D.; Wakefield, M. *Social Determinants of Health and Health Equity*; National Academies Press (US), 2021.
5. Dangmann, C.; Solberg, Ø.; Andersen, P. N. Health-Related Quality of Life in Refugee Youth and the Mediating Role of Mental Distress and Post-Migration Stressors. *Quality of Life Research* 2021, *30* (8), 2287–2297. https://doi.org/10.1007/s11136-021-02811-7.
6. UNRWA. *Jordan | UNRWA*. UNRWA. https://www.unrwa.org/where-we-work/jordan.
7. *Human rights in Jordan*. Amnesty International. https://www.amnesty.org/en/location/middle-east-and-north-africa/middle-east/jordan/report-jordan/.
8. American Psychological Association. Education and Socioeconomic Status. *American Psychological Association*. 2017. https://www.apa.org/pi/ses/resources/publications/education.
9. Remes, O.; Mendes, J. F.; Templeton, P. Biological, Psychological, and Social Determinants of Depression: A Review of Recent Literature. *Brain Sciences* 2021, *11* (12), 1–33. https://doi.org/10.3390/brainsci11121633.
10. Al-Soleiti, M.; Abu Adi, M.; Nashwan, A.; Rafla-Yuan, E. Barriers and Opportunities for Refugee Mental Health Services: Clinician Recommendations from Jordan. *Global Mental Health* 2021, *8* (e38). https://doi.org/10.1017/gmh.2021.36.
11. *Youth | UNHCR US*. UNHCR US. https://www.unhcr.org/us/what-we-do/protect-human-rights/safeguarding-individuals/youth (accessed 2025-09-16).
12. Blackmore, R. The Prevalence of Mental Illness in Refugees and Asylum Seekers: A Systematic Review and Meta-Analysis. *PLOS Medicine* 2020, *17* (9). https://doi.org/10.1371/journal.pmed.1003337.
13. Essex, R.; Govintharjah, P.; Issa, R.; Kalocsányiová, E.; Lakika, D.; Markowski, M.; Smith, J.; Thompson, T. Health Related Quality of Life amongst Refugees: A Meta Analysis of Studies Using the SF-36. *Journal of Immigrant and Minority Health* 2024, *26* (5), 925–935. https://doi.org/10.1007/s10903-024-01615-4.
14. West, E. C.; Williams, L. J.; Stuart, A. L.; Pasco, J. A. Quality of Life in South-Eastern Australia: Normative Values for the WHOQOL-BREF in a Population-Based Sample of Adults. *BMJ Open* 2023, *13* (12), e073556–e073556. https://doi.org/10.1136/bmjopen-2023-073556.
15. UNRWA. *Palestine Refugees*. UNRWA. https://www.unrwa.org/palestine-refugees.
16. Bat-Erdene, E.; Hiramoto, T.; Tumurbaatar, E.; Tumur-Ochir, G.; Jamiyandorj, O.; Yamamoto, E.; Hamajima, N.; Oka, T.; Jadamba, T.; Lkhagvasuren, B. Quality of Life in the General Population of Mongolia: Normative Data on WHOQOL-BREF. *PLOS ONE* 2023, *18* (9), e0291427. https://doi.org/10.1371/journal.pone.0291427.
17. Redko, C.; Rogers, N.; Bule, L.; Siad, H.; Choh, A. Development and Validation of the Somali WHOQOL-BREF among Refugees Living in the USA. *Quality of Life Research* 2014, *24* (6), 1503–1513. https://doi.org/10.1007/s11136-014-0877-3.
18. Doocy, S.; Lyles, E.; Akhu-Zaheya, L.; Oweis, A.; Al Ward, N.; Burton, A. Health Service Utilization among Syrian Refugees with Chronic Health Conditions in Jordan. *PLOS ONE* 2016, *11* (4), e0150088. https://doi.org/10.1371/journal.pone.0150088.
19. Anwar, A.; Yadav, U. N.; Huda, M. N.; Rifat, M. A.; Ali, A. M.; Mondal, P. K.; Abu; Suvasish Das Shuvo; Mistry, S. K. Prevalence and Determinants of Self-Reported Functional Status among Older Adults Residing in the Largest Refugee Camp of the World. *BMC Geriatrics* 2023, *23* (1). https://doi.org/10.1186/s12877-023-04067-x.
20. Alduraidi, H.; Waters, C. M. Health-Related Quality of Life of Palestinian Refugees inside and Outside Camps in Jordan. Nursing Outlook 2017, 65 (4), 436–443. https://doi.org/10.1016/j.outlook.2017.05.007.
21. Australian Government Department of Foreign Affairs and Trade. COVERING PROTECTED DFAT Thematic Report Palestinians in Jordan and Lebanon; 2015.
22. UNHCR. Global Trends report 2024 | UNHCR. UNHCR. https://www.unhcr.org/global-trends-report-2024.
23. Kiselev, N.; Pfaltz, M.; Haas, F.; Schick, M.; Kappen, M.; Sijbrandij, M.; De Graaff, A. M.; Bird, M.; Hansen, P.; Ventevogel, P.; Fuhr, D. C.; Schnyder, U.; Morina, N. Structural and Socio-Cultural Barriers to Accessing Mental Healthcare among Syrian Refugees and Asylum Seekers in Switzerland. *European Journal of Psychotraumatology* 2020, *11* (1), 1717825. https://doi.org/10.1080/20008198.2020.1717825.
24. Lund, C. Global Mental Health and Its Social Determinants: How Should We Intervene? *Behaviour Research and Therapy* 2023, *169*, 104402. https://doi.org/10.1016/j.brat.2023.104402.
25. Geirsdottir, G.; Mittendorfer-Rutz, E.; Amin, R. Risk of Suicide Attempt and Suicide in Young Adult Refugees Compared to Their Swedish-Born Peers: A Register-Based Cohort Study. *Social Psychiatry and Psychiatric Epidemiology* 2021. https://doi.org/10.1007/s00127-021-02099-5.
26. Kirmayer, L. J.; Narasiah, L.; Munoz, M.; Rashid, M.; Ryder, A. G.; Guzder, J.; Hassan, G.; Rousseau, C.; Pottie, K. Common Mental Health Problems in Immigrants and Refugees: General Approach in Primary Care. *Canadian Medical Association Journal* 2011, *183* (12), E959–E967. https://doi.org/10.1503/cmaj.090292.
27. Giacaman, R.; Rabaia, Y.; Nguyen-Gillham, V.; Batniji, R.; Punamäki, R.-L.; Summerfield, D. Mental Health, Social Distress and Political Oppression: The Case of the Occupied Palestinian Territory. *Global Public Health* 2011, *6* (5), 547–559. https://doi.org/10.1080/17441692.2010.528443.
28. El-Khatib, Z.; Jacobs, G. B.; Ikomey, G. M.; Neogi, U. The Disproportionate Effect of COVID-19 Mortality on Ethnic Minorities: Genetics or Health Inequalities? *EClinicalMedicine* 2020, *23*, 100430. https://doi.org/10.1016/j.eclinm.2020.100430.
29. Ruhnke, S. A.; Hertner, L.; Köhler, J.; Kluge, U. Social Ecological Determinants of the Mental Distress among Syrian Refugees in Lebanon and Turkey: A Transnational Perspective. *Social Science & Medicine* 2024, *346*, 116700. https://doi.org/10.1016/j.socscimed.2024.116700.
30. Twenge, J.; Cooper, A.; Joiner, T.; Duffy, M.; Binau, S. *Age, Period, and Cohort Trends in Mood Disorder Indicators and Suicide-Related*

Outcomes in a Nationally Representative Dataset; 2019. https://www.apa.org/pubs/journals/releases/abn-abn0000410.pdf.
31. Goodings, H. *World Health Organization Quality of Life-BREF (WHOQOL-BREF)*. SCIRE Professional. https://scireproject.com/outcome/world-health-organization-quality-of-life-bref-whoqol-bref/.
32. Selph, S. S.; McDonagh, M. S. Depression in Children and Adolescents: Evaluation and Treatment. *American Family Physician* 2019, *100* (10), 609–617.
33. M.I. *Report of the Working Group on the Financing of the United Nations Relief and Works Agency for Palestine Refugees in the Near East (A/79/329) - Question of Palestine*. Question of Palestine. https://www.un.org/unispal/document/report-of-the-working-group-on-unrwa-financing-30aug24/.
34. *Quality Of Life | WHOQOL-BREF | Greenspace (US)*. https://greenspacehealth.com/en-us/quality-of-life-whoqol-bref/.
35. Xiang, A. H.; Martinez, M. P.; Chow, T.; Carter, S. A.; Negriff, S.; Velasquez, B.; Spitzer, J.; Juan Carlos Zuberbuhler; Zucker, A.; Kumar, S. Depression and Anxiety among US Children and Young Adults. *JAMA Network Open* 2024, *7* (10), e2436906–e2436906. https://doi.org/10.1001/jamanetworkopen.2024.36906.
36. Wilson, S.; Dumornay, N. M. Rising Rates of Adolescent Depression in the United States: Challenges and Opportunities in the 2020s. *Journal of Adolescent Health* 2022, *70* (3), 354–355. https://doi.org/10.1016/j.jadohealth.2021.12.003.
37. Al Jazeera. *What is UNRWA and why is it important for Palestinians?* Al Jazeera. https://www.aljazeera.com/news/2024/2/1/what-is-unrwa-and-why-it-is-important-for-palestinians.
38. *WHOQOL-BREF PROM Guide • Heartbeat Medical*. Heartbeat Medical. https://heartbeat-med.com/resources/whoqol-bref/.
39. Goodwin, R. D.; Dierker, L. C.; Wu, M.; Galea, S.; Hoven, C. W.; Weinberger, A. H. Trends in U.S. Depression Prevalence from 2015 to 2020: The Widening Treatment Gap. *American Journal of Preventive Medicine* 2022, *63* (5), 726–733. https://doi.org/10.1016/j.amepre.2022.05.014.
40. Daly, M. Prevalence of Depression among Adolescents in the U.S. From 2009 to 2019: Analysis of Trends by Sex, Race/Ethnicity, and Income. *Journal of Adolescent Health* 2021, *70* (3). https://doi.org/10.1016/j.jadohealth.2021.08.026.
41. Teoli, D.; Bhardwaj, A. *Quality of Life*. PubMed. https://www.ncbi.nlm.nih.gov/books/NBK536962/.
42. Lee, B.; Wang, Y.; Carlson, S.; Greenlund, K.; Lu, H.; Liu, Y.; Croft, J.; Eke, P.; Town, M.; Thomas, C. National, State-Level, and County-Level Prevalence Estimates of Adults Aged ≥18 Years Self-Reporting a Lifetime Diagnosis of Depression — United States, 2020. *MMWR. Morbidity and Mortality Weekly Report* 2023, *72* (24). https://doi.org/10.15585/mmwr.mm7224a1.
43. Shahrum Vahedi. World Health Organization Quality-of-Life Scale (WHOQOL-BREF): Analyses of Their Item Response Theory Properties Based on the Graded Responses Model. *Iranian Journal of Psychiatry* 2024, *5* (4), 140.
44. *Social Determinants of Mental Health: Challenges and Interventions - Premier Science*. Premier Science. https://premierscience.com/pjph-24-361/ (accessed 2025-09-16).
45. Trabsa, A.; Redolar-Ripoll, D.; Vargas, L.; Llimona, A.; Hogg, B.; Valiente-Gómez, A.; Víctor Pérez; Moreno-Alcázar, A.; Amann, B. L. A Comparison of PTSD and Traumatic Event Rates in a Clinical Sample of Non-Refugee Immigrants and Native-Born Individuals with a Psychotic Disorder: A Case-Control Study. *European Journal of Psychotraumatology* 2023, *14* (2). https://doi.org/10.1080/20008066.2023.2263151.
46. Omiyefa, S. Mental Healthcare Disparities in Low-Income U.S. Populations: Barriers, Policy Challenges, and Intervention Strategies. *International Journal of Research Publication and Reviews* 2025, *6* (3), 2277–2290. https://doi.org/10.55248/gengpi.6.0325.1186.
47. Syed Hassan Ahmed; Aabia Zakai; Zahid, M.; Muhammad Youshay Jawad; Fu, R.; Chaiton, M. Prevalence of Post-Traumatic Stress Disorder and Depressive Symptoms among Civilians Residing in Armed Conflict-Affected Regions: A Systematic Review and Meta-Analysis. *General Psychiatry* 2024, *37* (3), e101438–e101438. https://doi.org/10.1136/gpsych-2023-101438.
48. Biddle, L.; Hintermeier, M.; Costa, D.; Wasko, Z.; Bozorgmehr, K. Context, Health and Migration: A Systematic Review of Natural Experiments. *eClinicalMedicine* 2023, *64*, 102206. https://doi.org/10.1016/j.eclinm.2023.102206.
49. Kirkbride, J. B.; Anglin, D. M.; Colman, I.; Dykxhoorn, J.; Jones, P. B.; Patalay, P.; Pitman, A.; Soneson, E.; Steare, T.; Wright, T.; Griffiths, S. L. The Social Determinants of Mental Health and Disorder: Evidence, Prevention and Recommendations. *World Psychiatry: Official Journal of the World Psychiatric Association* (WPA) 2024, *23* (1), 58–90. https://doi.org/10.1002/wps.21160.
50. Leon-Giraldo, S. Inequalities in Mental Health between Post-Conflict Recovery and Pandemic-Induced Challenges in Conflict-Affected Territories in Colombia. *World development perspectives* 2024, *35*, 100611–100611. https://doi.org/10.1016/j.wdp.2024.100611.
51. Huynh, P. A.; Kindred, R.; Perrins, K.; de Boer, K.; Miles, S.; Bates, G.; Nedeljkovic, M. Prevalence of Complex Post-Traumatic Stress Disorder (CPTSD): A Systematic Review and Meta-Analysis. *Psychiatry Research* 2025, *351*, 116586. https://doi.org/10.1016/j.psychres.2025.116586.
52. *Bohrium | AI for Science with Global Scientists*. Bohrium.com. https://www.bohrium.com/paper-details/health-related-quality-of-life-among-refugees-and-asylum-seekers-in-northern-greece/812479853679869954-9807 (accessed 2025-09-16).
53. Santana, C. L. A.; Manfrinato, C. V.; Souza, P. R. P.; Marino, A.; Condé, V. F.; Stedefeldt, E.; Tomita, L. Y.; do Carmo Franco, M. Psychological Distress, Low-Income, and Socio-Economic Vulnerability in the COVID-19 Pandemic. *Public Health* 2021, *199*, 42–45. https://doi.org/10.1016/j.puhe.2021.08.016.
54. Mesa-Vieira, C.; Haas, A. D.; Buitrago-Garcia, D.; Roa-Diaz, Z. M.; Minder, B.; Gamba, M.; Salvador, D.; Gomez, D.; Lewis, M.; Gonzalez-Jaramillo, W. C.; Pahud de Mortanges, A.; Buttia, C.; Muka, T.; Trujillo, N.; Franco, O. H. Mental Health of Migrants with Pre-Migration Exposure to Armed Conflict: A Systematic Review and Meta-Analysis. *The Lancet Public Health* 2022, 7 (5), e469–e481. https://doi.org/10.1016/s2468-2667(22)00061-5.
55. Bryant, R. A.; Nickerson, A.; Morina, N.; Liddell, B. Posttraumatic Stress Disorder in Refugees. *Annual Review of Clinical Psychology* 2023, *19* (1). https://doi.org/10.1146/annurev-clinpsy-080921-080359.
56. *Capacitating Young Palestinian Refugees for Civic Action in Marginalized Contexts [PART 1]*. Securityincontext.org. https://www.securityincontext.org/posts/capacitating-young-palestinian-refugees-for-civic-action-in-marginalized-contexts-part-1 (accessed 2025-09-16).
57. Twenge, J. Mental Health Issues Increased Significantly in Young Adults over Last Decade. *American Psychological Association*. March 14, 2019. https://www.apa.org/news/press/releases/2019/03/mental-health-adults.
58. Nguyen, T.; Shameran Slewa-Younan; Rioseco, P. Trajectories of Psychological Distress and Social Integration in Newly Resettled Refugees: Findings from the Building a New Life in Australia Longitudinal Study. *Social Psychiatry and Psychiatric Epidemiology* 2023, *59* (8). https://doi.org/10.1007/s00127-023-02528-7.

DOI: 10.36838/IJHSR87.273

59. Harvard University. *Toxic stress - center on the developing child at Harvard University*. Center on the Developing Child at Harvard University. https://developingchild.harvard.edu/key-concept/toxic-stress/.
60. Hossain, Md. S.; Xi, Y. Z. The Rohingya Refugee Crisis: Environment and Health Concerns for Bangladesh. *Saudi Journal of Humanities and Social Sciences* 2022, *7* (6), 247–256. https://doi.org/10.36348/sjhss.2022.v07i06.002.
61. Muhieddine, D.; Farhat, T.; Ibrahim, S.; Al-Yahya, M.; Al-Sheyab, N.; Zeng, W.; Halasa-Rappel, Y.; Jarawan, E.; Diab, J. L.; Hashoush, M.; Fouad, F. Building the Evidence on Forced Displacement: Jordan Country Report; The Big Questions in Forced Displacement and Health; June 2022. https://www.publichealth.columbia.edu/sites/default/files/media/documents/2023-03/jordan_v3-compressed_1.pdf (accessed 2024-02-20).

Authors

Antara Nayak is a senior at Livingston High School, NJ. Antara is a dedicated researcher in both medicine and social sciences. Inspired by her grandfather's glaucoma and lack of access to care, she hopes to be a physician and activist for underserved communities.

IJHSR
ijhighschoolresearch.org
RESEARCH ARTICLE

A Comparative Analysis of Embedding Techniques and Their Importance in the Functionality of Large Language Models

Elaine Jiang

Nikola Tesla STEM High School, 4301 228th Ave NE, Redmond, WA 98053; elainejiang1008@gmail.com

ABSTRACT: Embeddings are fundamental to developing the reasoning of a Large Language Model (LLMs). By allowing raw input data to be represented in a vector space, embeddings enable LLMS to detect patterns and excel in a wide range of tasks, such as text classification or detecting semantic similarity. This paper presents a comparative analysis that aims to analyze the various embeddings that are proposed for building RAG models. Drawing from existing studies, we analyze and compare various embedding techniques. Then, their applications are demonstrated through empirical evaluation using the PAN-PC-11 plagiarism detection dataset. Furthermore, using a subset of embeddings in Azure, we will demonstrate how AI applications' performance can vary with embeddings, thus demonstrating the efficacy of embedding models.

KEYWORDS: Robotics and Intelligent Machines, Machine Learning, Embeddings, Large Language Models, Retrieval-Augmented Generation.

Introduction

In the rapidly advancing field of Artificial Intelligence (AI), large language models (LLMs) have emerged as the future of Generative AI applications, containing the capability of understanding and reasoning with language. Over the next decade, these applications will become the new standard for innovation, becoming essential in fields from law to healthcare. Interwoven through the different fields that utilize these LLMs is a necessity for quality data. At the center of data representation lies embeddings; they allow LLMs to perform large-scale, complex downstream tasks by creating vectorized representations of texts.[1] They act as a connection between raw input and machine reasoning, allowing for downstream tasks such as clustering, searching, and retrieval-augmented generation (RAG). RAG systems implement embeddings with other retrieval mechanisms in order to increase accuracy and decrease hallucinations. For example, OpenAI's GPT-4 relies on advanced textual embeddings to understand nuances in meaning and context.[2] Similarly, LLaMA models often employ specialized embedding models to enhance performance on domain-specific tasks, such as legal or biomedical question answering.[3] Multi-modally, the popular image-generator application DALLE-2 improves performance through CLIP embeddings.[4]

Over the past few years, embedding techniques have evolved and gone through significant transformations. Starting with count-based embeddings, Bag of Words (BoW) and Term Frequency-Inverse Document Frequency (TF-IDF) methods counted word occurrences or weighted them by rarity, ignoring word meaning.[5] Then, static dense word embeddings such as Word2Vec and GloVe were developed, using fixed vector representations for each word – capturing meaning but unable to adapt to polysemy (or a word changing meaning depending on context).[6,7] Pioneering contextualized embeddings like ELMo, GPT, and BERT captured bidirectional context, allowing for more accurate downstream reasoning.[8-10]

However, embedding models are not perfect. As a consequence, if these representations are not up to standard, the effectiveness of these extremely powerful applications may crash, leading to hallucinations and inaccurate knowledge. This limitation is especially evident in tasks that rely on detecting semantic similarity rather than exact text overlap, such as plagiarism detection, where meaning can be preserved despite substantial surface-level changes.[11] This issue is particularly significant as LLM applications enter high-stakes domains, where misinformation/misinterpretations can have serious consequences. For example, LEGAL-BERT demonstrates the value of embeddings in legal settings for improving document classification and retrieval accuracy, yet similar context-specific approaches remain underexplored in other fields.[12]

This paper investigates the following research question: What are the strengths and limitations of various embedding techniques, and how do they affect the performance of inference using large language models across downstream tasks?

This question is significant because embeddings are important beyond low-stakes use cases such as keyword-based search or topic classification. Now, they are the bridge between knowledge input and foundational model reasoning. High-stakes applications such as plagiarism detection, legal reasoning, and clinical decision support demand robust semantic representations and, subsequently, high-performance accuracy. In this context, this paper argues that the choice of embedding model is not just a technical factor, but a key factor in shaping the accuracy and reliability of RAG-based AI applications.

To explore this claim, this paper is organized into three main sections:

1. Learning Representations: This section surveys existing work on embedding techniques and compares their strengths and limitations for application in RAG frameworks.

© 2026 Terra Science and Education

DOI: 10.36838/IJHSR87.281

2. Discussion: This section interprets the results of our literature review and highlights the implications of these findings for developers building RAG models, emphasizing case-to-case considerations. Then, it employs an embedding model directly on one such use case, highlighting an application's reliance on embedding quality and discussing the results of the case study.

3. Conclusion: This section summarizes our findings and proposes directions for future research on embedding evaluation.

Learning Representations

In this section, we will present different embedding techniques that are critical and fuel the application development cycle using foundational models. We will divide them into two major categories – linguistic embeddings and multi-modal embeddings. For each family of embeddings, we will present the strengths and weaknesses of each embedding technique while also presenting some technical architectures of popular open source methods.

2.1. Linguistic Embeddings:

Linguistic embeddings transform raw text into numerical vectors that are able to capture semantic meaning, relationships, and context. In turn, linguistic embeddings have become essential for LLMs to perform tasks such as retrieval and clustering. Originating from count-based methods like BoW and TF-IDF, today's contextualized embeddings are built on transformer architectures and are able to adapt representations based on surrounding text. However, while modern models offer richer semantic representations, factors such as context window size or multilingual support still determine embedding model suitability. The following subsections review key linguistic embedding models – E5, SFR-Embedding, GTE, BGE, and Jina – and evaluate their architectures, strengths, and tradeoffs.

2.1.1. E5 Models:

The E5 family of embedding models, developed by Microsoft, is a group of lightweight yet high-performing models for generating semantic representations of text. These models are built on Transformer-based encoder architectures, primarily using RoBERTa or XLM-RoBERTa as the backbone. Natural language instructions are input through a prefix of "query:" or "passage:" for the model to generalize across various tasks. Then, Contrastive Pre-training uses the InfoNCE contrastive loss function.[13,14]

$$L_{cont} = -\frac{1}{n}\sum_i \quad log\ log\ \frac{e^{s\theta(q_i,p_i)}}{e^{s\theta(q_i,p_i)}+\sum_j e^{s\theta(q_i,p_{ij})}}$$

Finally, fine-tuning is applied with curated datasets such as the MS MARCO or NQ for higher performance on semantic similarity, retrieval, and clustering tasks.[15-17] This formulation and finetuning ensure that the model learns fine-grained semantic distinctions between texts, rather than relying on surface-level overlap. These steps allow the models to have improved performance on retrieval and similarity tasks.

The English-only variant, E5-large-v2, is a 350 million parameter embedding model developed by Microsoft. The model, containing 24 layers, is able to capture complex relationships between words and ideas. And, leveraging weakly-supervised contrastive pre-training, it is able to learn semantic information from large amounts of unlabeled text. These features allow the model to deliver a strong, replicable performance in retrieval, semantic search, and textual matching, even surpassing models with up to 40x more parameters on the MTEB benchmark.[14,18] Its lighter size is commercially usable under the MIT license.

However, the embedding model, while highly effective, has certain constraints. Namely, it truncates inputs longer than 512 tokens, and its required prefixes for inputs are more restrictive compared to instruction-friendly alternatives such as the Jina v2 or GTE-Qwen2. Moreover, the E5-large-v2 lacks multilingual capabilities.

To address this, Microsoft released the Multilingual E5 (mE5) models in mid-2023, using a similar training method. The models are trained on about 1 billion multilingual text pairs with contrastive learning and subsequently fine-tuned using labeled datasets.[19] The instruction tune variant, mE5-large-instruct, demonstrates strong performance in the MTEB benchmark, surpassing BGE-large-en-1.5 by 0.2 points.[18,19]

2.1.2. SFR-Embedding:

SFR-Embedding is a 7B parameter model, developed by Salesforce, that produces 4096-dimensional embeddings, designed for the purpose of research.[20] In particular, the SFR-Embedding-Mistral fine-tunes the E5-mistral-7B-instruct across a wide range of tasks with a batch size of 2048. It delivers one of the highest MTEB scores of 67.6, excelling in diverse tasks such as retrieval, clustering, and classification – often matching or outperforming the GTE-Qwen2-7B in tasks centered around English.[21,22] However, its massive size makes it less practical than lighter models such as the E5, BGE, or Jina v2. In addition, the model does not have commercial usability due to its research-only license. While the E5 offers a balance in performance and versatility, the SFR needs large amounts of GPU resources while lacking nuanced multilingual capabilities, which the GTE excels at. In addition, the SFR is less nuanced than the E5 and is unable to understand context as well.

2.1.3. GTE Models:

The General Text Embedding (GTE) models, developed by Alibaba DAMO Academy, employ a dual-encoder architecture built on top of deep Transformer encoder architectures, like BERT. Given a text input x = (x1, . . . , xn), the encoder first contextualizes token embeddings:[2]

$$h = LM(x) \in R^{n\times d}$$

Then, a simple mean pooling is applied over the token dimension to obtain a text representation:[2]

$$x = \frac{1}{n}\sum_{i=1}^{n} \quad h_i \in R^d$$

Similar to E5 models, GTE is trained using a contrastive loss objective with the InfoNCE loss function.[13] Then, the

training follows a two-stage training process: 1. large-scale unsupervised pre-training on ~800 million naturally occurring text pairs and 2. supervised fine-tuning on smaller, curated datasets.[2] The pre-training hones the model's ability to learn general semantic relationships and to detect nuanced semantic similarities relevant to downstream tasks.

GTE supports a 32,000-token input window, far exceeding E5's 512-token limit and Jina's 8192-token limit, making it ideal for long-context tasks. While previous GTE models contained multilingual restraints, the recently released GTE-Qwen2 models show excellent performance across languages.[23] As of June 16, 2024, the GTE-Qwen2-7B-Instruct achieved number one on the MTEB leaderboards for both Chinese and English tasks.[18] In comparison to the SFR, GTE stands out for its excellent multilingual performance and instruction-following ability. However, both have similarly high computational demands – making them impractical in low-resource environments.

2.1.4. BGE Models:

The BGE family was developed by the Beijing Academy of Artificial Intelligence and are text embedding model optimized for dense retrieval, reranking, and semantic similarity. The architecture of BGE models is based on Transformer encoders and is often initialized from pretrained models such as Mistral-7B.[24,25] They are trained using contrastive learning objectives and Low-Rank Adaptation (LoRA), for parameter-efficient fine-tuning.[25,26] They are trained on a mix of retrieval, reranking, classification, clustering, and semantic textual similarity (STS) tasks across datasets.[25] BGE models span a range of sizes, such as the bge-small, bge-base, and bge-large, and are multilingual. In addition, these models support context windows of up to 8192 tokens and demonstrate a strong performance on the MTEB and C-MTEB benchmarks, outperforming existing Chinese text embedding models by more than 10% as of September 24, 2024, while having relatively lightweight architectures.[27] However, with extremely long or unstructured inputs, embedding performance drops significantly. In addition, procedures to fine-tune the models may be technically complex.

2.1.5. Jina-Embeddings:

Jina-Embeddings: The Jina Embeddings family, developed by Jina AI, is designed to address semantic tasks and their numerous versions geared towards varying tasks. Among these, Jina Embeddings v2 stands out as a lightweight yet high-performing model built on the BERT architecture and fine-tuned using text pairs and hard negatives.[28] Jina Embeddings v2 featured ~100 million parameters and was optimized to be able to run on consumer-grade hardware while rivaling OpenAI's ada-002 on tasks such as classification and reranking, as evaluated on the MTEB.[18,28] The model supports context lengths up to 8192 tokens, allowing better handling of longer documents, transcending the limit of the BERT architecture, and faster speeds due to an optimized parameter size. However, Jina v2 is not without limitations. Its relatively small size may constrain the depth of semantic nuance it can capture, and its large context-window may consequently dilute attention over extended passages.

■ Methodology

For this study, we selected the PAN-PC-11 dataset.[11] This publicly available dataset offers an extensive and comprehensive collection of both original or "source" documents and their corresponding "suspicious" counterparts, some of which are confirmed to be plagiarized directly or through semantic obfuscation. Out of all the datasets researched, PAN-PC-11 stood out for its size, accessibility, and rich metadata, which includes plagiarism labels, source document references, degrees of obfuscation (low or high), and origin type (artificial or manual). Specifically, we narrowed down our data to the Source and Suspicious Documents within the "external" folder contained in Part 1 of the dataset, which provided the thorough metadata. Each folder contains 23 parts or subfolders of 500 documents, with no particular distinction between each part. Currently, we are encoding the first part (or first 500 documents) from the source, and the same for the suspicious documents. For this initial empirical investigation and due to resource constraints, including embedding API costs and runtime, we limited our analysis to the first 100 documents from each category (source and suspicious), all drawn from Part 1 of the dataset.

To demonstrate the importance of embeddings in detecting semantic similarity, we designed a pipeline that evaluates overlap between original source documents and potentially plagiarized counterparts using embedding-based retrieval. The ultimate goal wasn't to measure or benchmark specific embedding models, but to show how the application's overall success depends on the embeddings it operates on.

2.2. Multi-Modal Embeddings:

In the field of multi-modal large language models, encoders play a central role in converting raw information, often in the form of images, audio, or video, into a compact format that can be understood. Rather than training these encoders from scratch, many multi-modal LLMs employ pretrained encoders that have already been aligned. Because these encoders significantly impact downstream LLM performance, it is necessary to understand the strengths and limitations of each encoding technique and select an encoder that is well-suited for integration with the LLM.[29] The following subsections will evaluate the performance of key multi-modal embeddings, including CLIP-ViT-L/14, EVA-CLIP-VIT-G/14, Open-CLIP-ViT-bigG/14, HuBERT, and CLAP.

2.2.1. CLIP-ViT-L/14:

CLIP-ViT-L/14 is a widely used vision encoder that has been pretrained on a dataset of approximately 400 million text pairs. Because of this alignment, zero-shot performance across a wide range of downstream tasks is enabled. Because CLIP is widely used and has a strong initial alignment, it is often favored as the base encoder for many LLMs. However, the CLIP operates at relatively low resolutions (224/336), which can hinder performance on downstream tasks, as previous

DOI: 10.36838/IJHSR87.281

studies cite an improvement in performance with higher resolution.[29-33] Moreover, an analysis of CLIP's performance across a variety of different datasets found that it still falls well below the overall state of the art, and that its zero-shot performance is inadequate on several types of tasks.[34] Compared to EVA-CLIP-ViT-G/14 and Open-CLIP-ViT-bigG/14, CLIP is smaller and more computationally efficient, making it suitable for resource-constrained environments, though at the cost of lower maximum accuracy.

2.2.1. EVA-CLIP-ViT-G/14:

Used in models like MiniGPT-4, EVA-CLIP-ViT-G/14 is a ViT-based encoder enhanced through improved pretraining strategies.[35] With more than 1 billion parameters, the encoder offers more nuanced representations of complex visual inputs. In addition, some EVA models demonstrate higher zero-shot top-1 accuracy than CLIP models while having lower training costs than Open-CLIP.[36] However, the EVA-CLIP-ViT-G/14 encoder contains lower resolution (224), which may affect the performance of downstream tasks.[29] EVA offers a middle ground: more nuanced than CLIP but more resource-efficient than Open-CLIP.

2.2.2. Open-CLIP-ViT-bigG/14:

Open-CLIP-ViT-bigG/14 is trained on the LAION-2B dataset of almost 2 billion image-text pairs and features a significantly larger parameter size of 1.8B +, allowing it to capture high-level semantic features effectively.[37] However, the encoder's large parameter size makes it consequently extremely memory and resource-intensive, making it less practical for certain applications. Compared to CLIP and EVA, it offers the highest maximum accuracy but the lowest efficiency.

2.2.3. HuBERT:

HuBERT is a self-supervised audio encoder designed to address three challenges in speech representation learning: the presence of multiple units per unit of input utterance, the lack of a predefined lexicon, and the changing lengths of audio segments.[38] Rather than relying on high-quality cluster labels, HuBERT starts with basic k-means clustering and refines over multiple iterations. In other words, it depends on the quality of the clustering process itself. With a 1 billion parameter model, HuBERT outperforms or matches wav2vec 2.0 across benchmarks like LibriSpeech and Libri-Light, along with achieving up to 19% relative WER reduction on difficult datasets.[38] However, even with HuBERT's performance, due to its reliance on cluster consistency, poor initial clustering can still degrade downstream performance. In addition, HuBERT has a speech-only focus, not supporting other audio modalities such as background sounds or music.

2.2.3. CLAP:

CLAP applies contrastive learning to align audio and natural language into a shared representation space.[39] It is trained on the LAION-Audio-630K dataset, including over 630,000 audio-text pairs, allowing it to connect these signals to textual descriptions. CLAP achieves state-of-the-art performance in zero-shot audio classification and demonstrates excellent performance in text-to-audio retrieval, while also performing competitively in fully supervised settings.[39] However, CLAP relies on the quality of text captions, allowing low-quality descriptions to degrade model performance. In addition, CLAP's contrastive learning stage is resource-consuming and requires substantial memory.

■ Discussion

3.1. Analysis:

In this section, we synthesize insights from our analysis of embedding techniques and our empirical evaluation on plagiarism detection. While embedding techniques are often compared on the basis of standardized benchmarks, we employ an approach that captures the nuances of real-world applicability, taking into account system-level constraints or ethical consequences. By contrasting low-stakes applications such as homework assistance tools with high-stakes applications such as clinical diagnostics, we highlight how model capabilities must be evaluated in context. In addition, our empirical case study demonstrates how embedding quality directly affects downstream performance on both a technical level and a moral or societal one. Overall, these findings underscore the importance of holistically selecting an embedding model with consideration of both the technical demands and ethical stakes of the application.

Table 1: This table lists a variety of embedding models, covering text, vision, and audio modalities, along with their specifications.

Model	Modality	Parameters	Context Limit	Multilingual	Licensing
E5-large-v2	Text	350 million	512 tokens	No	MIT
mE5-large-instruct	Text	350 million	512 tokens	Yes	MIT
SFR-Mistral	Text	7 billion	8192 tokens	Partial	Research
GTE-Qwen2-7B	Text	7 billion	32,000 tokens	Yes	Apache
BGE Models	Text	Varies	8192 tokens	Yes	Apache
Jina v2	Text	~100 million	8192 tokens	Partial	Commercial
CLIP-ViT-L/14	Vision	304 million	224/336 Resolution	No	Open
EVA-CLIP-ViT-G/14	Vision	1 billion	224 Resolution	No	Open
Open-CLIP-ViT-G/14	Vision	1.8+ Billion	224 Resolution	No	Open
HuBERT	Speech	1 billion	N/A	No	Open
CLAP	Audio	~600 million	N/A	No	Open

Choosing an embedding model is often determined by the constraints and goals of the application. We present two use cases of embedding models on opposite ends of the spectrum and explain how different models would suit one or the other.

In the first case, consider the development of a lightweight homework assistance app that helps high school students with homework through summarizing texts or explaining certain concepts. A requirement for this system is usability on devices with limited processing power and accessibility with minimal latency. Therefore, in this scenario, lightweight embedding models such as Jina Embeddings v2 or E5-large-v2 are well-suited. On the other hand, models based solely on performance, such as the GTE-Qwen2-7B or SFR-Mistral, may

offer higher accuracy or semantic understanding for homework summaries or explanations but are significantly heavier in terms of computing and memory requirements. These models would be ill-suited for lightweight applications due to their size and longer response times, which can degrade usability for students. In addition, designing this app for commercial purposes may not allow for access to many of these embedding techniques, as certain models like SFR-Mistral are restricted to research use only (Table 1). Therefore, model selection must include not only performance goals, but also the system's constraints and user context.

On the other side of the spectrum, consider a high-stakes medical diagnostics system supporting oncologists, which must detect subtle patterns in X-rays while considering patient histories. Here, visual encoders like Open-CLIP-ViT-G/14 or EVA-CLIP-ViT-G/14 are better suited for these scenarios, offering better alignment of textual and visual information while also allowing for a more fine-grained representation of medical imagery. For the text-processing component, models like GTE-Qwen2-7B, though computationally taxing, can provide long-context reasoning and instruction-following ability, which are well-suited to synthesize long medical records or research literature. In contrast, lighter models like Jina v2 or E5-large-v2 are insufficient in this context because they contain limited context windows and lower representational capacity (Table 1), meaning they are at a higher risk of losing critical clinical details. In medical systems where misclassification or inaccuracy may have life-threatening consequences, performance trade-offs are unacceptable.

3.2. Empirical Evaluation:

In the era of large language models, embeddings have become the basis for downstream applications. They compress text into a summary of its meaning and structure, which allows systems to make fast and efficient judgments about language-based tasks. However, this reliance on embeddings introduces a critical assumption that the embedding contains enough information to support the downstream task. If these embeddings are too shallow or insensitive to deeper meaning, then many downstream models could likely fail. This empirical study investigates that statement by isolating and evaluating the role of embeddings in a concrete, high-stakes application – plagiarism detection.

Plagiarism, especially in the era of generative AI, is more than just keyword matching. Instead, it asks whether a model can understand when two texts express the same ideas in different forms. This makes it a compelling lens for exploring how LLM systems rely on embeddings. The task comes in two main levels: surface-level plagiarism, where copied content is nearly identical, and semantic plagiarism, where the idea is stolen but reworded to avoid detection. Surface-level plagiarism can often be caught through n-gram comparisons or cosine similarity of token vectors. But detecting semantic plagiarism, especially with high obfuscation, requires embedding techniques. Most modern applications built on LLMs don't run on raw input each time. Instead, they run on fixed embeddings to make judgments. Therefore, the embedding is not just important internally, but can become a single, critical point of failure. If an embedding fails to capture nuance between two texts, downstream performance may be significantly degraded. With the plagiarism detection case study, this dependency becomes visible – when the embeddings successfully capture semantic similarity, the model succeeds; and when they don't, it fails.

Moreover, plagiarism detection demonstrates the ethical stakes of embeddings. Academic integrity and intellectual property protection are foundational principles that reach across the fields of education and innovation, meaning they must be enforced. If an application cannot reliably flag plagiarized content, these principles may be broken. A model needs to understand that meaning itself can be stolen. And embeddings are a key part in aiding that ability. Therefore, this use case evaluates the actual role of embeddings in high-stakes applications that need thorough, complex language understanding.

3.2.1. Methodology:

For this study, we selected the PAN-PC-11 dataset.[11] This publicly available dataset offers an extensive and comprehensive collection of both original or "source" documents and their corresponding "suspicious" counterparts, some of which are confirmed to be plagiarized directly or through semantic obfuscation. Out of all the datasets researched, PAN-PC-11 stood out for its size, accessibility, and rich metadata, which includes plagiarism labels, source document references, degrees of obfuscation (low or high), and origin type (artificial or manual). Specifically, we narrowed down our data to the Source and Suspicious Documents within the "external" folder contained in Part 1 of the dataset, which provided the thorough metadata. Each folder contains 23 parts or subfolders of 500 documents, with no particular distinction between each part. Currently, we are encoding the first part (or first 500 documents) from the source, and the same for the suspicious documents. For this initial empirical investigation and due to resource constraints, including embedding API costs and runtime, we limited our analysis to the first 100 documents from each category (source and suspicious), all drawn from Part 1 of the dataset.

To demonstrate the importance of embeddings in detecting semantic similarity, we designed a pipeline that evaluates overlap between original source documents and potentially plagiarized counterparts using embedding-based retrieval. The ultimate goal wasn't to measure or benchmark specific embedding models, but to show how the application's overall success depends on the embeddings it operates on.

DOI: 10.36838/IJHSR87.281

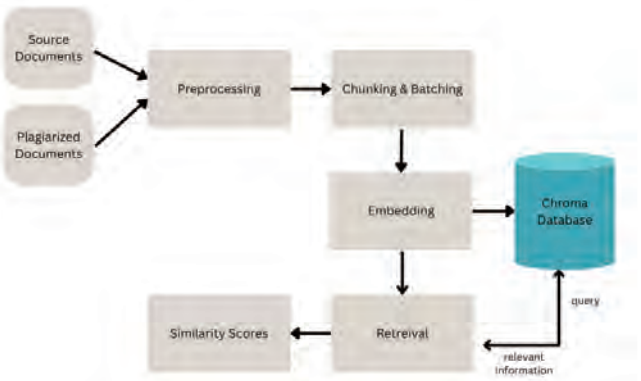

Figure 1: This figure details the pipeline that was designed when employing embedding models and receiving similarity scores for the plagiarized and source documents.

We designed a preprocessing and embedding-based retrieval pipeline to detect plagiarism by measuring semantic similarity between documents.

Preprocessing (Figure 1): In the first step of the pipeline, all source and candidate documents undergo a uniform preprocessing stage to ensure consistency in downstream analysis. Text is converted to lowercase, punctuation and stop words are removed, whitespace is normalized (e.g., replacing newlines with spaces), and excess spacing is trimmed. This cleaning stage reduces noise and enforces a standardized text representation so that irrelevant formatting differences are prevented from affecting similarity scores.

Chunking and Batching (Figure 1): After preprocessing the data, the RecursiveCharacterTextSplitter is employed to split each document into semantically meaningful chunks. Unlike naive splitting, which may fragment meaning, recursive splitting preserves coherence within each chunk, which is necessary for meaningful embeddings. Then, the resulting chunks are batched in order to stay under the total token length limit of Azure OpenAI embedding API (text-embedding-3-large) to prevent truncation or errors. Batching size was set to 20 chunks per API call, and retries were configured for up to 3 attempts with a 10-second delay.

Embedding (Figure 1): Each batch is transformed into a 1536-dimensional vector using the pretrained Azure OpenAI embedding model text-embedding-3-large. These dense embeddings are able to capture semantic meaning and enable vector similarity comparisons.

Storage in Vector Database (Figure 1): The resulting vectors are stored in ChromaDB under the corresponding source document, which enables efficient similarity search at scale and preserves metadata. With ChromaDB's metadata handling, we can identify not only which document it came from but also where in the document it stemmed from. Because documents vary in length, a single document may correspond to multiple embeddings. This vector database acts as the retrieval backend for future similarity queries.

Retrieval (Figure 1): Then, each batch of embeddings for the candidate documents is queried against the ChromaDB using similarity search. Cosine similarity is employed as the similarity metric, as it normalizes for vector magnitude and is widely used in high-dimensional embedding spaces. For each batch, the top five nearest neighbors are retrieved, and the neighbor with the highest similarity is selected as the closest match.

Similarity Scores (Figure 1): To summarize document-level similarity, both the maximum and average similarity scores are computed across all batches. These metrics address two different levels of plagiarism: the maximum similarity score capturing potential moments of direct copying, while the average reflects the overall semantic similarity between the texts. This process is repeated for both genuine source documents and known plagiarized texts.

This allows us to capture both local overlaps and broader semantic similarity, providing a nuanced view of potential plagiarism.

3.2.2. Results:

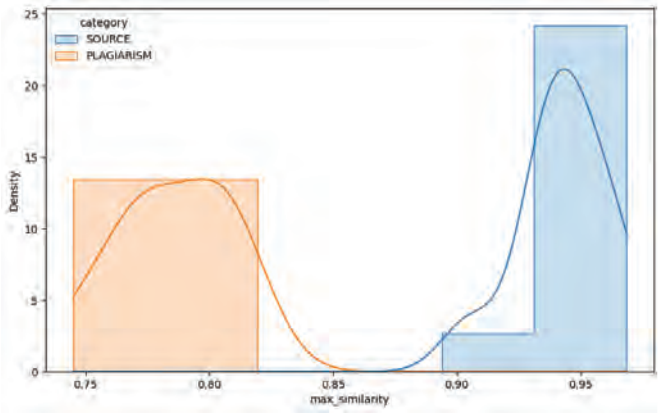

Figure 2: This figure shows the distribution of maximum similarity scores between two different types of documents – source documents, shown in blue, and plagiarized documents, shown in orange. The minimal overlap between the two distributions indicates strong discriminative power between the categories.

After embedding and comparing each from the source and suspicious, or potentially plagiarized, documents, our empirical evaluation revealed a clear distinction in the maximum similarity scores between the original source documents and the known plagiarized texts, demonstrating the effectiveness of embeddings in plagiarism detection. Source documents, when compared to themselves, produced maximum similarity scores tightly clustered between 0.90 and 0.97, with a peak around 0.94 (Figure 2). On the other hand, plagiarized documents, even with obfuscation, demonstrated consistently lower maximum similarity scores, clustering between 0.74 and 0.83, while peaking near 0.80 (Figure 2). This non-overlapping bimodal distribution suggests that, even with heavy obfuscation or paraphrasing, textual embeddings preserved enough meaning in their vector representations to be able to distinguish plagiarized texts from source materials. However, even with a clear distinction between plagiarized and source materials, the embedding model still produced semantic similarity scores that were detectably high for copied content. These results demonstrate that embedding quality directly influences the downstream performance of high-stakes language systems such as plagiarism detection. When embeddings are able to encode nuanced semantic meanings, these tasks demonstrate higher accuracy. Our findings support the idea that embed-

dings deserve explicit attention when designing applications, especially with Generative AI.

3.2.3. Limitations:

While this study highlights the role of embeddings in detecting plagiarism, its findings are constrained to the dataset and models evaluated. Computational constraints restricted the sample size, which may reduce the generalizability and robustness of the results. The evaluation was also limited to text-based plagiarism, leaving out other modalities such as code or multimedia content.

■ Conclusion

In conclusion, this study has explored different types of embedding models – linguistic and multi-modal – and demonstrated that they are components of an application that can significantly influence the ethical and functional performance of AI applications. Benchmarks like MTEB can offer surface-level comparisons, but our analysis shows that embedding effectiveness is deeply tied to application-specific constraints and consequences. We examined two theoretical use cases – lightweight educational tools and high-stakes medical diagnostics – and conducted an empirical investigation into plagiarism detection. With our empirical evaluation, source documents, when compared to themselves, produced maximum similarity scores between 0.90 and 0.97, while plagiarized documents, even with high obfuscation, clustered around 0.74 and 0.83, demonstrating high overlap but a clear distinction between original and copied. Our results, with a non-overlapping bimodal distribution, suggest that high-quality embeddings are essential for nuanced tasks such as identifying plagiarized documents, a task that requires complex representations that capture semantic meaning. Our analysis of different embedding models aims to provide a clear rationale for selecting the most appropriate model based on the specific constraints of different applications, and our domain-specific empirical case study aims to emphasize the significance of embedding techniques in various contexts. Moreover, our findings explore the importance of context-based analysis and the potential significant societal impact. As embeddings become foundational across Generative AI applications, their failure can translate into failures in high-stakes environments, like preserving academic integrity or medical accuracy. For example, in the medical diagnostics context, a poorly chosen embedding model could mean hallucinations and inaccuracies in clinical recommendations, potentially affecting patient vitality.

Moving forward, future research is needed in several different avenues. More systematic comparisons across a wider range of embedding models are needed – especially evaluating how they perform in different contexts, such as education, healthcare, and law. Moreover, as linguistic and multimodal models continue to evolve, deeper exploration can be done to evaluate how these embeddings generalize across languages or modalities. Additionally, future work could investigate the robustness of embedding models to adversarial inputs and integrate more complex metrics into embedding evaluation frameworks.

Ultimately, our work emphasizes the notion that embedding models are not just a minor technical component. Instead, they play a foundational role in shaping how information is represented and utilized in modern Generative AI systems. Careful, context-based selection of embeddings is therefore essential in order to build responsible, high-performing AI systems. Because as AI becomes central to high-stakes decision-making, the importance of high-quality embeddings has never been greater.

■ Acknowledgments

I would like to express my gratitude to Dr. Siddharth Krishnan and Lian Jiang for their guidance, unwavering support, and dedicated time throughout the lifecycle of the project and this research paper.

■ References

1. Li Z, Zhang X, Zhang Y, Long D, Xie P, Zhang M. Towards General Text Embeddings with Multi-stage Contrastive Learning [Internet]. arXiv; 2023 [cited 2025 July 20]. Available from: http://arxiv.org/abs/2308.03281
2. OpenAI, Achiam J, Adler S, Agarwal S, Ahmad L, Akkaya I, et al. GPT-4 Technical Report [Internet]. arXiv; 2024 [cited 2025 Aug 9]. Available from: http://arxiv.org/abs/2303.08774
3. Touvron H, Lavril T, Izacard G, Martinet X, Lachaux MA, Lacroix T, et al. LLaMA: Open and Efficient Foundation Language Models [Internet]. arXiv; 2023 [cited 2025 Aug 9]. Available from: http://arxiv.org/abs/2302.13971
4. Gozalo-Brizuela R, Garrido-Merchan EC. ChatGPT is not all you need. A State of the Art Review of large Generative AI models [Internet]. arXiv; 2023 [cited 2025 Aug 13]. Available from: http://arxiv.org/abs/2301.04655
5. Cao H. Recent advances in text embedding: A Comprehensive Review of Top-Performing Methods on the MTEB Benchmark [Internet]. arXiv; 2024 [cited 2025 Aug 13]. Available from: http://arxiv.org/abs/2406.01607
6. Mikolov T, Chen K, Corrado G, Dean J. Efficient Estimation of Word Representations in Vector Space [Internet]. arXiv; 2013 [cited 2025 Aug 13]. Available from: http://arxiv.org/abs/1301.3781
7. Pennington J, Socher R, Manning C. GloVe: Global Vectors for Word Representation. In: Moschitti A, Pang B, Daelemans W, editors. Proceedings of the 2014 Conference on Empirical Methods in Natural Language Processing (EMNLP) [Internet]. Doha, Qatar: Association for Computational Linguistics; 2014 [cited 2025 Aug 13]. p. 1532–43. Available from: https://aclanthology.org/D14-1162/
8. Peters ME, Neumann M, Iyyer M, Gardner M, Clark C, Lee K, et al. Deep contextualized word representations [Internet]. arXiv; 2018 [cited 2025 Aug 13]. Available from: http://arxiv.org/abs/1802.05365
9. Radford A, Narasimhan K, Salimans T, Sutskever I. Improving Language Understanding by Generative Pre-Training.
10. Devlin J, Chang MW, Lee K, Toutanova K. BERT: Pre-training of Deep Bidirectional Transformers for Language Understanding. In: Burstein J, Doran C, Solorio T, editors. Proceedings of the 2019 Conference of the North American Chapter of the Association for Computational Linguistics: Human Language Technologies, Volume 1 (Long and Short Papers) [Internet]. Minneapolis, Minnesota: Association for Computational Linguistics; 2019 [cited

DOI: 10.36838/IJHSR87.281

2025 Aug 13]. p. 4171–86. Available from: https://aclanthology.org/N19-1423/
11. Potthast M, Stein B, Eiselt A, Barrón-Cedeño A, Rosso P. PAN Plagiarism Corpus 2011 (PAN-PC-11) [Internet]. Zenodo; 2011 [cited 2025 Aug 2]. Available from: https://zenodo.org/records/3250095
12. Chalkidis I, Fergadiotis M, Malakasiotis P, Aletras N, Androutsopoulos I. LEGAL-BERT: The Muppets straight out of Law School [Internet]. arXiv; 2020 [cited 2025 Aug 13]. Available from: http://arxiv.org/abs/2010.02559
13. Chen T, Kornblith S, Norouzi M, Hinton G. A Simple Framework for Contrastive Learning of Visual Representations. In: Proceedings of the 37th International Conference on Machine Learning [Internet]. PMLR; 2020 [cited 2025 July 20]. p. 1597–607. Available from: https://proceedings.mlr.press/v119/chen20j.html
14. Wang L, Yang N, Huang X, Jiao B, Yang L, Jiang D, et al. Text Embeddings by Weakly-Supervised Contrastive Pre-training [Internet]. arXiv; 2024 [cited 2025 July 19]. Available from: http://arxiv.org/abs/2212.03533
15. Bajaj P, Campos D, Craswell N, Deng L, Gao J, Liu X, et al. MS MARCO: A Human Generated MAchine Reading Comprehension Dataset [Internet]. arXiv; 2018 [cited 2025 July 20]. Available from: http://arxiv.org/abs/1611.09268
16. Karpukhin V, Oguz B, Min S, Lewis P, Wu L, Edunov S, et al. Dense Passage Retrieval for Open-Domain Question Answering. In: Webber B, Cohn T, He Y, Liu Y, editors. Proceedings of the 2020 Conference on Empirical Methods in Natural Language Processing (EMNLP) [Internet]. Online: Association for Computational Linguistics; 2020 [cited 2025 July 20]. p. 6769–81. Available from: https://aclanthology.org/2020.emnlp-main.550/
17. Kwiatkowski T, Palomaki J, Redfield O, Collins M, Parikh A, Alberti C, et al. Natural Questions: A Benchmark for Question Answering Research. Lee L, Johnson M, Roark B, Nenkova A, editors. Trans Assoc Comput Linguist. 2019;7:452–66.
18. Muennighoff N, Tazi N, Magne L, Reimers N. MTEB: Massive Text Embedding Benchmark. In: Vlachos A, Augenstein I, editors. Proceedings of the 17th Conference of the European Chapter of the Association for Computational Linguistics [Internet]. Dubrovnik, Croatia: Association for Computational Linguistics; 2023 [cited 2025 July 20]. p. 2014–37. Available from: https://aclanthology.org/2023.eacl-main.148/
19. Wang L, Yang N, Huang X, Yang L, Majumder R, Wei F. Multilingual E5 Text Embeddings: A Technical Report [Internet]. arXiv; 2024 [cited 2025 July 20]. Available from: http://arxiv.org/abs/2402.05672
20. Yavuz RM Ye Liu, Shafiq Rayhan Joty, Caiming Xiong, Yingbo Zhou, Semih. SFR-Embedding-Mistral: Enhance Text Retrieval with Transfer Learning [Internet]. Salesforce. 2024 [cited 2025 July 20]. Available from: https://www.salesforce.com/blog/sfr-embedding/
21. Caspari L, Dastidar KG, Zerhoudi S, Mitrovic J, Granitzer M. Beyond Benchmarks: Evaluating Embedding Model Similarity for Retrieval Augmented Generation Systems [Internet]. arXiv; 2024 [cited 2025 July 19]. Available from: http://arxiv.org/abs/2407.08275
22. Tao C, Shen T, Gao S, Zhang J, Li Z, Tao Z, et al. LLMs are Also Effective Embedding Models: An In-depth Overview [Internet]. arXiv; 2024 [cited 2025 July 20]. Available from: http://arxiv.org/abs/2412.12591
23. Yang A, Yang B, Hui B, Zheng B, Yu B, Zhou C, et al. Qwen2 Technical Report [Internet]. arXiv; 2024 [cited 2025 July 20]. Available from: http://arxiv.org/abs/2407.10671
24. Jiang AQ, Sablayrolles A, Mensch A, Bamford C, Chaplot DS, Casas D de las, et al. Mistral 7B [Internet]. arXiv; 2023 [cited 2025 July 20]. Available from: http://arxiv.org/abs/2310.06825
25. Li C, Qin M, Xiao S, Chen J, Luo K, Shao Y, et al. Making Text Embedders Few-Shot Learners [Internet]. arXiv; 2024 [cited 2025 July 20]. Available from: http://arxiv.org/abs/2409.15700
26. Hu EJ, Shen Y, Wallis P, Allen-Zhu Z, Li Y, Wang S, et al. LoRA: Low-Rank Adaptation of Large Language Models [Internet]. arXiv; 2021 [cited 2025 July 20]. Available from: http://arxiv.org/abs/2106.09685
27. Xiao S, Liu Z, Zhang P, Muennighoff N, Lian D, Nie JY. C-Pack: Packed Resources For General Chinese Embeddings [Internet]. arXiv; 2024 [cited 2025 July 20]. Available from: http://arxiv.org/abs/2309.07597
28. Günther M, Ong J, Mohr I, Abdessalem A, Abel T, Akram MK, et al. Jina Embeddings 2: 8192-Token General-Purpose Text Embeddings for Long Documents [Internet]. arXiv; 2024 [cited 2025 July 20]. Available from: http://arxiv.org/abs/2310.19923
29. Yin S, Fu C, Zhao S, Li K, Sun X, Xu T, et al. A Survey on Multimodal Large Language Models. Natl Sci Rev [Internet]. 2024 Nov 14 [cited 2025 July 23];11(12). Available from: http://arxiv.org/abs/2306.13549
30. Bai J, Bai S, Yang S, Wang S, Tan S, Wang P, et al. Qwen-VL: A Versatile Vision-Language Model for Understanding, Localization, Text Reading, and Beyond [Internet]. arXiv; 2023 [cited 2025 July 23]. Available from: http://arxiv.org/abs/2308.12966
31. Li Z, Yang B, Liu Q, Ma Z, Zhang S, Yang J, et al. Monkey: Image Resolution and Text Label Are Important Things for Large Multi-modal Models [Internet]. arXiv; 2024 [cited 2025 July 23]. Available from: http://arxiv.org/abs/2311.06607
32. Liu H, Li C, Li Y, Lee YJ. Improved Baselines with Visual Instruction Tuning [Internet]. arXiv; 2024 [cited 2025 July 23]. Available from: http://arxiv.org/abs/2310.03744
33. McKinzie B, Gan Z, Fauconnier JP, Dodge S, Zhang B, Dufter P, et al. MM1: Methods, Analysis & Insights from Multimodal LLM Pre-training [Internet]. arXiv; 2024 [cited 2025 July 23]. Available from: http://arxiv.org/abs/2403.09611
34. Radford A, Kim JW, Hallacy C, Ramesh A, Goh G, Agarwal S, et al. Learning Transferable Visual Models From Natural Language Supervision [Internet]. arXiv; 2021 [cited 2025 July 23]. Available from: http://arxiv.org/abs/2103.00020
35. Zhu D, Chen J, Shen X, Li X, Elhoseiny M. MiniGPT-4: Enhancing Vision-Language Understanding with Advanced Large Language Models [Internet]. arXiv; 2023 [cited 2025 July 25]. Available from: http://arxiv.org/abs/2304.10592
36. Sun Q, Fang Y, Wu L, Wang X, Cao Y. EVA-CLIP: Improved Training Techniques for CLIP at Scale [Internet]. arXiv; 2023 [cited 2025 July 25]. Available from: http://arxiv.org/abs/2303.15389
37. Cherti M, Beaumont R, Wightman R, Wortsman M, Ilharco G, Gordon C, et al. Reproducible scaling laws for contrastive language-image learning. In 2023 [cited 2025 July 25]. p. 2818–29. Available from: http://arxiv.org/abs/2212.07143
38. Hsu WN, Bolte B, Tsai YHH, Lakhotia K, Salakhutdinov R, Mohamed A. HuBERT: Self-Supervised Speech Representation Learning by Masked Prediction of Hidden Units [Internet]. arXiv; 2021 [cited 2025 July 26]. Available from: http://arxiv.org/abs/2106.07447
39. Wu Y, Chen K, Zhang T, Hui Y, Nezhurina M, Berg-Kirkpatrick T, et al. Large-scale Contrastive Language-Audio Pretraining with Feature Fusion and Keyword-to-Caption Augmentation [Internet]. arXiv; 2024 [cited 2025 July 26]. Available from: http://arxiv.org/abs/2211.06687

Authors

Elaine Jiang is a 12th grader at Nikola Tesla STEM High School in Washington with a strong passion for machine learning and Generative AI. She is particularly intrigued by the exploration of how artificial intelligence and technology can be harnessed to address real-world problems.

DOI: 10.36838/IJHSR87.281

IJHSR
ijhighschoolresearch.org
REVIEW ARTICLE

ADHD in Context: Gendered Presentation, Peer Relationships, and Family Challenges

Kitty Men

St. Clement's School, 21 St Clements Ave, Toronto, ON M4R 1G8, Canada; Kit.m747908@gmail.com

ABSTRACT: Over the past few decades, ADHD diagnoses have increased substantially, but girls and women continue to be underdiagnosed and underrepresented in research. In this review, we synthesize the literature on ADHD's gendered presentation, its impact on peer relationships, and family dynamics, with a specific focus on the implications for diagnosis and intervention in girls and women. Understanding gender differences in how ADHD is expressed and experienced within a broader social context is important to addressing this gap. Girls are more likely to present inattentive symptoms or internalizing behaviors, such as disorganization, forgetfulness, and anxiety, whereas boys typically present hyperactive or more disruptive behaviors. This review highlights that these differences in diagnosis are not merely clinical but also have significant ramifications for girls' social experiences and family relationships. The impact of ADHD often intensifies during adolescence, especially for girls, who are more likely to experience instability in their peer relationships and lower levels of self-esteem. By emphasizing variation with regard to gender in adolescence, this review underscores the need for more inclusive diagnostic frameworks and gender-sensitive support strategies.

KEYWORDS: Behavioral and Social Sciences, Clinical and Developmental Social Psychology, ADHD, Gender Differences, Effects on Social Development.

Introduction

Attention Deficit Hyperactivity Disorder (ADHD) is a neurodevelopmental disorder consisting of chronic symptoms such as inattention, impulsivity, and hyperactivity, which affect an individual's daily functioning.[1] While ADHD occurs in both genders, research has mainly focused on its presentation in boys, resulting in a limited understanding of its manifestation in girls. This gap in understanding contributes to gender disparities in diagnosis, where boys are still more likely to be identified and properly treated for ADHD than girls. Because ADHD has no specific diagnostic test, physicians rely on patient history, physical exams, and assessments based on the DSM-5-criteria.[2,3] In the early aughts, 10% of boys and 4% of girls were diagnosed with ADHD.[4] Since then, the rate has grown in the United States, with boys (15%) still more likely to be diagnosed than girls (8%).[5] ADHD is most commonly treated with stimulant medications like methylphenidate and mixed amphetamine salts, which increase levels of dopamine and norepinephrine to improve focus, but are controlled substances with higher risks of misuse. Non-stimulants such as atomoxetine act more slowly by blocking norepinephrine reuptake (indirectly increasing dopamine in the prefrontal cortex). Non-stimulants are not controlled substances, so they carry a lower risk of abuse.[6] While stimulants often work more quickly, non-stimulants can be equally effective for many individuals.[7] Not surprisingly, both stimulant and non-stimulant medications are more prescribed for boys than girls.[8] In fact, in the UK, boys were nearly five times more likely to be prescribed stimulants than girls, suggesting not just a diagnosis gap, but a possible reluctance to medicate affected female patients.[9]

Gender disparities in ADHD diagnosis can have broader consequences, from theoretical, social, and clinical perspectives. Girls' internalizing symptoms are often overlooked, impacting self-esteem, social competence, and leading to various academic setbacks.[10] Girls and boys with ADHD both struggle with friendship, but studies have shown that girls face more friendship setbacks. This may be due to their symptoms deviating more from gender expectations when compared to boys with ADHD.[11] Misdiagnosis and delayed diagnosis can also impact the family unit, contributing to parental stress, stigma, and inconsistency in support strategies. These factors demonstrate the importance of viewing ADHD through a gendered lens.[12] To address these disparities, this paper will explore how ADHD symptoms manifest differently amongst genders, how these differences influence peer and family relationships, including from childhood to adulthood. By doing so, this paper will contribute to a better understanding of ADHD and highlight the need for increased awareness and support for all those affected by the disorder.

Understanding Gender Differences in ADHD Diagnosis and Presentation:

Compared to boys, girls with ADHD are underdiagnosed, with reported ratios ranging from 2:1 to 10:1.[13] This could be attributed to the fact that girls with ADHD are more likely to present inattentive symptoms (e.g., inattention, disorganization, low self-esteem), rather than the more disruptive behaviors typically seen in boys. These internalizing symptoms also draw less concern from teachers and parents, making them easier to overlook.[10] In fact, research has found that girls often need to present more severe symptoms to be referred for

© 2026 Terra Science and Education

DOI: 10.36838/IJHSR87.290

treatment compared to boys.[14] Although girls may meet fewer diagnostic criteria, they can still be just as impaired by their symptoms. However, girls are often left misdiagnosed or underdiagnosed, especially in childhood, despite facing academic, emotional, and social challenges in the long term.[10]

In addition to exhibiting more internalizing symptoms, many girls with ADHD have learned to adopt coping strategies and ways to mask their behaviors. These can include perfectionism, over-preparing, and staying quiet in a classroom setting to hide their struggles. A recent study on camouflaging in neurodivergent girls (age 11-14) found that while both neurotypical and neurodivergent girls engaged in some form of camouflage (similar results in masking and compensation), neurodivergent girls showed higher levels of camouflaging in the form of assimilation (pretending to fit in).[15] Camouflaging occurs when an individual realizes that a certain expressed symptom is "undesirable." It involves active mimicry of others' actions in both a conscious and unconscious manner.[16] Many girls also mimic their peers' social cues, suppress behavior, or overcompensate for their weakness in an effort to appear "normal." The higher rates in girls with ADHD make them more susceptible for burnouts.[17] Girls with ADHD often also develop perfectionism as a coping strategy to hide what they perceive as their internal flaws, usually as a form of self-compensation.[18] Perfectionism is a common "cognitive distortion" in ADHD, usually used as a form of self-compensation.[18] However, constantly maintaining nearly impossible standards can result in higher stress and self-criticism.[19]

While these coping strategies help neurodivergent girls avoid negative attention, they also lead to less accurate identification and diagnosis of ADHD. Instead of recognizing these symptoms as signs of ADHD, girls exhibiting anxiety, social withdrawal, and peer rejection may receive an incorrect diagnosis of depression or anxiety instead.[13,20,21] Interestingly, girls with hyperactivity or emotional instability are sometimes inaccurately diagnosed as having bipolar disorder because their mood swings and impulsivity are mistaken for signs of a more severe mood disorder.[22] Furthermore, these inaccuracies significantly delay proper ADHD care. Girls are also more likely to be prescribed antidepressants prior to receiving an official ADHD diagnosis than boys.[23] At the same time, girls under the age of 18 are less likely to be prescribed medication than boys, even when diagnosed.[23,24]

Apart from the difficulties caused by their symptoms, girls with ADHD often encounter barriers because of how parents, teachers, and clinicians respond to their behaviors.[10] Based on the results of a case study, parents and teachers who read the same behavioral descriptions labeled with a girl's name were considerably less likely to classify the displayed behaviors as ADHD symptoms than when they were labeled with a boy's name.[25] Others have similarly found that teachers and parents frequently fail to recognize ADHD in girls, resulting in fewer referrals for ADHD assessment and longer delays to treatment.[10] These biases are influenced by broader gender expectations in diagnostic systems.[26]

These gaps in proper recognition and diagnosis help explain, in part, how ADHD presents in girls, but there are also biological factors that contribute to this difference. Hormonal fluctuations during puberty or in various phases of the menstrual cycle can also play a role in the severity of symptoms as well as in how well medications work in girls with ADHD.10 Estrogen, in particular, affects the development and functionality of many dopamine-dependent neurons in the brain that are crucial for attention and memory.[27] Since estrogen levels naturally change through puberty and menstrual cycles, girls with ADHD are likely to have fluctuations in mood, attention, and regulation.[28] For example, the effects of stimulant drugs such as amphetamine may be perceived to be stronger during the follicular phase of the menstrual cycle (when estrogen levels are greater).[29,30] These findings suggest that hormonal factors could be an important consideration in the expression and treatment of ADHD in girls.

Girls not being diagnosed until adolescence or adulthood can have serious long-term consequences for their overall development.[12,31] For instance, young girls with ADHD tend to under-achieve academically and socially-emotionally, leading to emotional challenges such as internalizing problems, poor self-esteem, and frustration. As the symptoms persist beyond childhood, it generally results in diminished self-esteem affecting the person throughout education and social dynamics.[32] Increasing awareness of the typical presentation in girls amongst parents, caregivers, and clinicians, translated into appropriate early interventions, would prevent much of the silent suffering these girls must go through.[33]

Friendship Challenges in Children with ADHD:

Children with ADHD, particularly girls, face unique challenges in forming and maintaining friendships. Inherently, certain symptoms can result in missing key social cues while simultaneously leading to an overestimation of one's social competence.[34,35] Research consistently highlights that children experience these challenges differently between genders, even though both have significantly fewer friends compared to their neurotypical peers, with lower friendship quality and poorer friendship interactions.[36] Relationships tend to be shorter in duration.[34] For example, one study revealed that the friendships of children with ADHD are, on average, 9.6 to 14.4 months shorter compared to those of neurotypical children.[37]

A shorter length of friendship may be due to instability and challenges associated with friendships. These factors of instability differ between genders. For instance, boys often rely on humor to build and maintain friendships, using it as a bonding tool. In contrast, girls tend to prioritize emotional discussion and view serious conversations as essential to their friendships.[38] Consequently, girls who struggle with emotional regulation and communication face particular challenges because these skills are central to how female friendships function.[38,39] The intersection of social biases, gendered expectations, and inattentive symptoms may therefore intensify the social challenges faced by girls with ADHD, making them especially vulnerable to conflict and instability in their friendships.[40]

Research indicates that girls with ADHD experience rejection sensitivity, an intense emotional reaction to perceived rejection, differently and more often severely than boys. They

tend to internalize social rejection more deeply, leading to heightened anxiety, depression, and social withdrawal.[40] Rejection sensitivity uniquely affects their social interactions: while both boys and girls may struggle to differentiate between peer acceptance and true friendship, girls are more likely to ruminate on perceived social mishaps and develop anticipatory anxiety about future rejection.[11] This can lead girls to avoid social situations or respond defensively, which, unfortunately, can increase peer rejection and reduce opportunities to form genuine friendships. The social expectation that girls are emotionally attuned and reciprocal only intensifies this effect and feeds into a negative spiral of social isolation and emotional distress. In contrast, boys with ADHD may respond to rejection with more externalizing behaviors such as aggression, leading to entirely different social dynamics. Gender, therefore, shapes not only how children with ADHD experience rejection sensitivity but also how they perceive and respond to the complex social signals distinguishing peer acceptance from true friendship.[11,40]

Adolescence and adulthood introduce new and distinct challenges for those with ADHD, as peer interactions become more nuanced, demanding advanced emotional regulation, perspective taking, and conformity to social norms, all areas where ADHD symptoms interfere significantly.[41] While childhood social difficulties often revolve around emerging social skills and peer acceptance, adolescent and adult ADHD impairments extend into complex areas of life such as intimate relationships, family roles, work, and mental health.[10] Research shows that women with ADHD, despite having fewer of the more noticeable hyperactive symptoms, experience more severe and multifaceted impairments in social functioning, emotional regulation, and overall quality of life compared to men.[43] Having already struggled with internalized stigma and underdiagnosis their entire lives, social impairments persist and may even intensify in adulthood as women struggle with forming and maintaining close relationships and balancing multiple psychosocial demands, including family and occupational stress.[44] Men, more likely to have been treated and medicated since childhood, experience less intense social-emotional distress compared to women. These divergent trajectories emphasize the need for gender-sensitive approaches in ADHD diagnosis, treatment, and social support extending beyond childhood.[14,42,45]

ADHD in the Context of Family and Caregiving:

ADHD not only impacts diagnosed individuals but also affects those around them, particularly parents and caregivers. The symptoms of ADHD may contribute to frequent misunderstandings and conflicts between parents and their children. Indeed, evidence shows parents with children with ADHD usually experience greater stress compared to those with neurotypical children.[46] Inherent difficulties with emotional regulation further exacerbate the negative relationship between the child and parents.[47] Unsurprisingly, research on how family dynamics are impacted differentially between genders is extremely limited.[48]

In a qualitative study, parents described their experiences as "coping with the war at home" or their child as "a wrecking ball."[49] Parents also attributed their high levels of stress to the social issues and behaviors of their children, along with a lack of sufficient support and social stigma.[50,51] However, it is worth noting that most of these studies specifically focus on boys. In fact, all but one of the studies cited had samples made up exclusively of families with boys.[49,52] The single study that did include families with girls had an overall sample of ten, of which six were boys, leading to concerns of how these findings may greatly differ between children exhibiting internalizing or externalizing symptoms.[53] It is, however, reasonable to hypothesize that girls would contribute less to parental stress, given that their symptoms are less disruptive. In fact, this internalizing behavior is precisely what goes unnoticed in the first place, and the reason why boys are more likely to be diagnosed. With the lack of current studies considering such differences, research must be done on comparing the impact of diagnosis on family dynamics between genders.

Parents may have to adjust their approaches to better fit their child's needs.[54] Studies show that children's behavior directly influences parental approaches, which can create inconsistent discipline and have a significant impact on family and marital relationships overall.[55] Specifically, mothers tend to use a stricter, authoritarian parenting style with their daughters, regardless of factors such as age, subtypes, medication, or comorbidities. By contrast, the style parents tend to use for sons is dependent on subtype and age. Conversely, other studies have found no differences in parenting styles. In terms of parents in a gendered context, mothers' affection and communication are typically warmer compared to fathers'.[48]

Positive parenting interventions, including behavioral parent training, are particularly indicated for families with parenting difficulties.[56] Curiously, studies tend to show that the same methods work well regardless of the gender of the child. Behavioral parent training (BPT) appears to result in better parenting styles and positive changes concerning the child and the parent-child relationship for both genders.[57] Most BPT programs teach parents positive skills and consequences (such as praise and token economies) to encourage appropriate child behavior.[56] For example, parents are taught to praise their child for starting homework on time or to implement a token chart where children earn points for completing specific activities, which can later be redeemed for additional playtime or for small rewards. Other programs, such as the nurse-led "Parent-to-Parent Support Group" (PPSG), show benefits for parents with psychoeducation, problem solving, and social support, which could contribute to a significant reduction in parental stress for families.[58] Furthermore, the Family-School Success (FSS) program may provide families with better ways to help improve their child's academic and behavioral needs and overall engagement, as well as support families in overall knowledge of ADHD. However, the effectiveness of this approach was investigated in an unbalanced sample where only 32% of participants were female.[59] Generally, these types of interventions provide parents with specific strategies and support to manage their child's ADHD appropriately, and can

DOI: 10.36838/IJHSR87.290

be used to improve the home environment. However, before these programs can be recommended to all families, research must first provide convincing evidence that they are effective in families with girls as well. The development of gender-specific treatments should also be considered.

Conclusion

ADHD is a complex neurodevelopmental condition that affects nearly every part of a person's life, from attention span and emotions to friendships and family dynamics.[1,4,34] This paper explored how ADHD impacts both social and emotional development from childhood to beyond, highlighting how girls are often overlooked and underdiagnosed because of their internalizing symptoms. Research has shown that children with ADHD constantly face difficulties in maintaining friendships, experience peer rejection, and struggle with emotional regulation and communication.[34,37,60] With ADHD affecting daily function, family life is also shaped by the disorder, leading to parental stress and often requiring additional training and conscious adjustment of parenting styles. To address these issues, better training for teachers and support systems, the addition of more accurate diagnostic tools designed for girls, and overall awareness of the impact of ADHD on one's social abilities and emotions are crucial. Nevertheless, to identify effective methods for supporting girls with ADHD, research must move beyond prioritizing boys. Otherwise, our understanding remains limited and forces us to rely on speculations rather than evidence. This would greatly improve social experiences of children with ADHD, especially girls, leading to healthier family relationships, while increasing self-esteem and confidence.

Acknowledgments

I would like to thank Indigo and my mentor, Kat Bochtler, for all the guidance and support you've given me throughout this journey. Your incredible insights and encouragement have really made a difference along the way.

References

1. Magnus, W.; Anilkumar, A. C.; Shaban, K. Attention Deficit Hyperactivity Disorder. In *StatPearls*; StatPearls Publishing: Treasure Island (FL), 2025.
2. Ringeisen, H.; Casanueva, C.; Stambaugh, L. *Table 7, DSM-IV to DSM-5 Attention-Deficit/Hyperactivity Disorder Comparison*. https://www.ncbi.nlm.nih.gov/books/NBK519712/table/ch3.t3/ (accessed 2025-07-21).
3. Felt, B. T.; Biermann, B.; Christner, J. G.; Kochhar, P.; Harrison, R. V. Diagnosis and Management of ADHD in Children. *Am. Fam. Physician* **2014**, *90* (7), 456–464.
4. Furman, L. What Is Attention-Deficit Hyperactivity Disorder (ADHD)? *J. Child Neurol.* **2005**, *20* (12), 994–1002. https://doi.org/10.1177/08830738050200121301.
5. CDC. *Data and Statistics on ADHD*. Attention-Deficit / Hyperactivity Disorder (ADHD). https://www.cdc.gov/adhd/data/index.html (accessed 2025-08-27).
6. Rader, R.; McCauley, L.; Callen, E. C. Current Strategies in the Diagnosis and Treatment of Childhood Attention-Deficit/Hyperactivity Disorder. *Am. Fam. Physician* **2009**, *79* (8), 657–665.
7. Roh, H.; Kim, B. A Brief Replication Study Comparing Stimulants and Non-Stimulants for Attention-Deficit/Hyperactivity Disorder Treatment with a Focus on the Compliance, Efficacy, and Satisfaction. *J. Korean Acad. Child Adolesc. Psychiatry* **2021**, *32* (1), 10–16. https://doi.org/10.5765/jkacap.200024.
8. Kok, F. M.; Groen, Y.; Fuermaier, A. B. M.; Tucha, O. The Female Side of Pharmacotherapy for ADHD—A Systematic Literature Review. *PLoS ONE* **2020**, *15* (9), e0239257. https://doi.org/10.1371/journal.pone.0239257.
9. Renoux, C.; Shin, J.; Dell'Aniello, S.; Fergusson, E.; Suissa, S. Prescribing Trends of Attention-deficit Hyperactivity Disorder (ADHD) Medications in UK Primary Care, 1995–2015. *Br. J. Clin. Pharmacol.* **2016**, *82* (3), 858–868. https://doi.org/10.1111/bcp.13000.
10. Quinn, P. O.; Madhoo, M. A Review of Attention-Deficit/Hyperactivity Disorder in Women and Girls: Uncovering This Hidden Diagnosis. *Prim. Care Companion CNS Disord.* **2014**, *16* (3), PCC.13r01596. https://doi.org/10.4088/PCC.13r01596.
11. Kok, F. M.; Groen, Y.; Fuermaier, A. B. M.; Tucha, O. Problematic Peer Functioning in Girls with ADHD: A Systematic Literature Review. *PloS One* **2016**, *11* (11), e0165119. https://doi.org/10.1371/journal.pone.0165119.
12. Attoe, D. E.; Climie, E. A. Miss. Diagnosis: A Systematic Review of ADHD in Adult Women. *J. Atten. Disord.* **2023**, *27* (7), 645–657. https://doi.org/10.1177/10870547231161533.
13. Mowlem, F.; Agnew-Blais, J.; Taylor, E.; Asherson, P. Do Different Factors Influence Whether Girls versus Boys Meet ADHD Diagnostic Criteria? Sex Differences among Children with High ADHD Symptoms. *Psychiatry Res.* **2019**, *272*, 765–773. https://doi.org/10.1016/j.psychres.2018.12.128.
14. Platania, N. M.; Starreveld, D. E. J.; Wynchank, D.; Beekman, A. T. F.; Kooij, S. Bias by Gender: Exploring Gender-Based Differences in the Endorsement of ADHD Symptoms and Impairment among Adult Patients. *Front. Glob. Women's Health* **2025**, *6*. https://doi.org/10.3389/fgwh.2025.1549028.
15. McKinney, A.; O'Brien, S.; Maybin, J. A.; Chan, S. W. Y.; Richer, S.; Rhodes, S. Camouflaging in Neurodivergent and Neurotypical Girls at the Transition to Adolescence and Its Relationship to Mental Health: A Participatory Methods Research Study. *JCPP Adv.* **2024**, *4* (4), e12294. https://doi.org/10.1002/jcv2.12294.
16. Grimell, J.; Ericson, M.; Frick, M. A. Identity Work among Girls with ADHD: Struggling with Me and I, Impression Management, and Social Camouflaging in School. *Front. Psychol.* **2025**, *16*, 1591135. https://doi.org/10.3389/fpsyg.2025.1591135.
17. Koseva, N. *5 Things You Never Knew About ADHD Masking*. The ADHD Centre. https://www.adhdcentre.co.uk/5-things-you-never-knew-about-adhd-masking/ (accessed 2025-07-24).
18. Fugate, C. M.; Gentry, M. Understanding Adolescent Gifted Girls with ADHD: Motivated and Achieving. *High Abil. Stud.* **2016**, *27* (1), 83–109. https://doi.org/10.1080/13598139.2015.1098522.
19. *Is perfectionism a symptom of ADHD?* https://www.medicalnewstoday.com/articles/adhd-perfectionism (accessed 2025-07-24).
20. *ADHD in Women and Girls: Why Female Symptoms Slip Through Diagnostic Cracks*. ADDitude. https://www.additudemag.com/adhd-in-women-girls-symptoms-diagnosis-recommendations/ (accessed 2025-07-24).
21. Dray, S.; Campbell, M.; Gilmore, L. Why Are Girls with ADHD Invisible? *Connections* **2006**, *23* (2), 2–7.
22. *Bipolar Disorder and ADHD: Comorbidity and Diagnostic Distinctions | Current Psychiatry Reports*. https://link.springer.com/article/10.1007/s11920-015-0604-y (accessed 2025-07-24).
23. Martin, J.; Langley, K.; Cooper, M.; Rouquette, O. Y.; John, A.; Sayal, K.; Ford, T.; Thapar, A. Sex Differences in Attention-Deficit Hyperactivity Disorder Diagnosis and Clinical Care: A National

Study of Population Healthcare Records in Wales. *J. Child Psychol. Psychiatry* **2024**, *65* (12), 1648–1658. https://doi.org/10.1111/jcpp.13987.
24. Kok, F. M.; Groen, Y.; Fuermaier, A. B. M.; Tucha, O. The Female Side of Pharmacotherapy for ADHD—A Systematic Literature Review. *PLoS ONE* **2020**, *15* (9), e0239257. https://doi.org/10.1371/journal.pone.0239257.
25. Groenewald, C.; Emond, A.; Sayal, K. Recognition and Referral of Girls with Attention Deficit Hyperactivity Disorder: Case Vignette Study. *Child Care Health Dev*. **2009**, *35* (6), 767–772. https://doi.org/10.1111/j.1365-2214.2009.00984.x.
26. *Exploring Bias In ADHD Diagnosis: Are Gender Discrepancies Overlooked? - ADHD Online*. https://adhdonline.com/articles/exploring-bias-in-adhd-diagnosis-are-gender-discrepancies-overlooked/ (accessed 2025-08-18).
27. Almey, A.; Milner, T. A.; Brake, W. G. Estrogen Receptors in the Central Nervous System and Their Implication for Dopamine-Dependent Cognition in Females. *Horm. Behav*. **2015**, *74*, 125–138. https://doi.org/10.1016/j.yhbeh.2015.06.010.
28. Del Campo, N.; Chamberlain, S. R.; Sahakian, B. J.; Robbins, T. W. The Roles of Dopamine and Noradrenaline in the Pathophysiology and Treatment of Attention-Deficit/Hyperactivity Disorder. *Biol. Psychiatry* **2011**, *69* (12), e145-157. https://doi.org/10.1016/j.biopsych.2011.02.036.
29. Becker, J. B.; McClellan, M. L.; Reed, B. G. SEX DIFFERENCES, GENDER AND ADDICTION. *J. Neurosci. Res.* **2017**, *95* (1–2), 136–147. https://doi.org/10.1002/jnr.23963.
30. Colzato, L. S.; Hertsig, G.; van den Wildenberg, W. P. M.; Hommel, B. Estrogen Modulates Inhibitory Control in Healthy Human Females: Evidence from the Stop-Signal Paradigm. *Neuroscience* **2010**, *167* (3), 709–715. https://doi.org/10.1016/j.neuroscience.2010.02.029.
31. O'Grady, S. M.; Hinshaw, S. P. Long-Term Outcomes of Females with Attention-Deficit Hyperactivity Disorder: Increased Risk for Self-Harm. *Br. J. Psychiatry* **2021**, *218* (1), 4–6. https://doi.org/10.1192/bjp.2020.153.
32. Owens, E. B.; Zalecki, C.; Gillette, P.; Hinshaw, S. P. Girls with Childhood ADHD as Adults: Cross-Domain Outcomes by Diagnostic Persistence. *J. Consult. Clin. Psychol*. **2017**, *85* (7), 723–736. https://doi.org/10.1037/ccp0000217.
33. Young, S.; Adamo, N.; Ásgeirsdóttir, B. B.; Branney, P.; Beckett, M.; Colley, W.; Cubbin, S.; Deeley, Q.; Farrag, E.; Gudjonsson, G.; Hill, P.; Hollingdale, J.; Kilic, O.; Lloyd, T.; Mason, P.; Paliokosta, E.; Perecherla, S.; Sedgwick, J.; Skirrow, C.; Tierney, K.; van Rensburg, K.; Woodhouse, E. Females with ADHD: An Expert Consensus Statement Taking a Lifespan Approach Providing Guidance for the Identification and Treatment of Attention-Deficit/ Hyperactivity Disorder in Girls and Women. *BMC Psychiatry* **2020**, *20* (1), 404. https://doi.org/10.1186/s12888-020-02707-9.
34. Spender, K.; Chen, Y.-W. R.; Wilkes-Gillan, S.; Parsons, L.; Cantrill, A.; Simon, M.; Garcia, A.; Cordier, R. The Friendships of Children and Youth with Attention-Deficit Hyperactivity Disorder: A Systematic Review. *PLOS ONE* **2023**, *18* (8), e0289539. https://doi.org/10.1371/journal.pone.0289539.
35. Owens, J. S.; Goldfine, M. E.; Evangelista, N. M.; Hoza, B.; Kaiser, N. M. A Critical Review of Self-Perceptions and the Positive Illusory Bias in Children with ADHD. *Clin. Child Fam. Psychol. Rev*. **2007**, *10* (4), 335–351. https://doi.org/10.1007/s10567-007-0027-3.
36. Kalokyri, A. Navigating the Interplay of ADHD, Social Norms, and Friendships: Perspectives from Secondary School Students with ADHD. *Pastor. Care Educ*. **2025**, *43* (3), 415–436. https://doi.org/10.1080/02643944.2025.2495667.
37. Marton, I.; Wiener, J.; Rogers, M.; Moore, C. Friendship Characteristics of Children With ADHD. *J. Atten. Disord*. **2015**, *19* (10), 872–881. https://doi.org/10.1177/1087054712458971.
38. Rose, A. J.; Smith, R. L.; Glick, G. C.; Schwartz-Mette, R. A. Girls' and Boys' Problem Talk: Implications for Emotional Closeness in Friendships. *Dev. Psychol*. **2016**, *52* (4), 629–639. https://doi.org/10.1037/dev0000096.
39. Çiray, R. O.; Özyurt, G.; Turan, S.; Karagöz, E.; Ermiş, Ç.; Öztürk, Y.; Akay, A. The Association between Pragmatic Language Impairment, Social Cognition and Emotion Regulation Skills in Adolescents with ADHD. *Nord. J. Psychiatry* **2022**, *76* (2), 89–95. https://doi.org/10.1080/08039488.2021.1938211.
40. Mikami, A. Y. The Importance of Friendship for Youth with Attention-Deficit/Hyperactivity Disorder. *Clin. Child Fam. Psychol. Rev*. **2010**, *13* (2), 181–198. https://doi.org/10.1007/s10567-010-0067-y.
41. Faheem, M.; Akram, W.; Akram, H.; Khan, M. A.; Siddiqui, F. A.; Majeed, I. Gender-Based Differences in Prevalence and Effects of ADHD in Adults: A Systematic Review. *Asian J. Psychiatry* **2022**, *75*, 103205. https://doi.org/10.1016/j.ajp.2022.103205.
42. Neprily, K. M.; Climie, E. A.; McCrimmon, A.; Makarenko, E. Why Can't We Be Friends? A Narrative Review of the Challenges of Making and Keeping Friends for Children and Adolescents with Attention-Deficit/Hyperactivity Disorder. *Front. Dev. Psychol*. **2025**, *2*. https://doi.org/10.3389/fdpys.2024.1390791.
43. Rucklidge, J. J. Gender Differences in Attention-Deficit/Hyperactivity Disorder. *Psychiatr. Clin. North Am*. **2010**, *33* (2), 357–373. https://doi.org/10.1016/j.psc.2010.01.006.
44. Quinn, P. O.; Madhoo, M. A Review of Attention-Deficit/Hyperactivity Disorder in Women and Girls: Uncovering This Hidden Diagnosis. *Prim. Care Companion CNS Disord*. **2014**, *16* (3), PCC.13r01596. https://doi.org/10.4088/PCC.13r01596.
45. Williamson, D.; Johnston, C. Gender Differences in Adults with Attention-Deficit/Hyperactivity Disorder: A Narrative Review. *Clin. Psychol. Rev*. **2015**, *40*, 15–27. https://doi.org/10.1016/j.cpr.2015.05.005.
46. Olczyk, A. R.; Rosen, P. J.; Alacha, H. F.; Flynn, M. M. Indirect Effect of ADHD on Parenting Stress through Increased Child Anxiety and Decreased Emotional Regulatory Coping. *Eur. Child Adolesc. Psychiatry* **2024**, *33* (5), 1407–1417. https://doi.org/10.1007/s00787-023-02246-0.
47. McClellan, J. M.; Berliner, L.; Carlson, G. A. Strategies for Managing Impairing Emotional Outbursts. *JAMA Pediatr*. **2023**, *177* (6), 559–560. https://doi.org/10.1001/jamapediatrics.2023.0787.
48. Muñoz-Suazo, M. D.; Navarro-Muñoz, J.; Díaz-Román, A.; Coronilla-García, M.; Porcel-Gálvez, A. M.; Gil-García, E. Parenting Practices among Parents of Children with Attention-Deficit/Hyperactivity Disorder: Gender-Related Differences. *J. Clin. Psychol*. **2020**, *76* (1), 239–245. https://doi.org/10.1002/jclp.22873.
49. Leitch, S.; Sciberras, E.; Post, B.; Gerner, B.; Rinehart, N.; Nicholson, J. M.; Evans, S. Experience of Stress in Parents of Children with ADHD: A Qualitative Study. *Int. J. Qual. Stud. Health Well-Being* **2019**, *14* (1), 1690091. https://doi.org/10.1080/17482631.2019.1690091.
50. Angeline, J.; Rathnasabapathy, M. Understanding Women's Suffering and Psychological Well-Being: Exploring Biopsychosocial Factors in Mothers of Children with ADHD – a Case Study. *Front. Public Health* **2023**, *11*. https://doi.org/10.3389/fpubh.2023.1279499.
51. Cheng, A. W. Y.; Lai, C. Y. Y. Parental Stress in Families of Children with Special Educational Needs: A Systematic Review. *Front. Psychiatry* **2023**, *14*. https://doi.org/10.3389/fpsyt.2023.1198302.

DOI: 10.36838/IJHSR87.290

52. (PDF) Contending and Adapting Every Day: Norwegian Parents' Lived Experience of Having a Child With ADHD. *ResearchGate* **2025**. https://doi.org/10.1177/1074840711423924.
53. Mofokeng, M.; van der Wath, A. E. Challenges Experienced by Parents Living with a Child with Attention Deficit Hyperactivity Disorder. *J. Child Adolesc. Ment. Health* **2017**, *29* (2), 137–145. https://doi.org/10.2989/17280583.2017.1364253.
54. ELLIS, B.; NIGG, J. Parenting Practices and Attention-Deficit/Hyperactivity Disorder: Partial Specificity of Effects. *J. Am. Acad. Child Adolesc. Psychiatry* **2009**, *48* (2), 146–154. https://doi.org/10.1097/CHI.0b013e31819176d0.
55. Muñoz-Silva, A.; Lago-Urbano, R.; Sanchez-Garcia, M. Family Impact and Parenting Styles in Families of Children with ADHD. *J. Child Fam. Stud*. **2017**, *26* (10), 2810–2823. https://doi.org/10.1007/s10826-017-0798-1.
56. Pfiffner, L. J.; Haack, L. M. Behavior Management for School Aged Children with ADHD. *Child Adolesc. Psychiatr. Clin. N. Am*. **2014**, *23* (4), 731–746. https://doi.org/10.1016/j.chc.2014.05.014.
57. Steenhuis, L.; Groenman, A. P.; Hoekstra, P. J.; Hornstra, R.; Luman, M.; van der Oord, S.; van den Hoofdakker, B. J. Effects of Behavioural Parent Training for Children with Attention-Deficit/Hyperactivity Disorder on Parenting Behaviour: A Protocol for an Individual Participant Data Meta-Analysis. *BMJ Open* **2020**, *10* (11), e037749. https://doi.org/10.1136/bmjopen-2020-037749.
58. Sharma, S.; Govindan, R.; Kommu, J. V. S. Effectiveness of Parent-to-Parent Support Group in Reduction of Anxiety and Stress Among Parents of Children With Autism and Attention Deficit Hyperactivity Disorder. *Indian J. Psychol. Med*. **2022**, *44* (6), 575–579. https://doi.org/10.1177/02537176211072984.
59. Power, T. J.; Mautone, J. A.; Soffer, S. L.; Clarke, A. T.; Marshall, S. A.; Sharman, J.; Blum, N. J.; Glanzman, M.; Elia, J.; Jawad, A. F. Family-School Intervention for Children with ADHD: Results of Randomized Clinical Trial. *J. Consult. Clin. Psychol*. **2012**, *80* (4), 611–623. https://doi.org/10.1037/a0028188.
60. Normand, S.; Schneider, B. H.; Lee, M. D.; Maisonneuve, M.-F.; Chupetlovska-Anastasova, A.; Kuehn, S. M.; Robaey, P. Continuities and Changes in the Friendships of Children with and Without ADHD: A Longitudinal, Observational Study. *J. Abnorm. Child Psychol*. **2013**, *41* (7), 1161–1175. https://doi.org/10.1007/s10802-013-9753-9.

Author

Kitty is a senior student at St. Clement's School with a passion for psychology. She enjoys exploring mental development and emotional well-being and hopes her passion can encourage others to grow with confidence.

IJHSR
ijhighschoolresearch.org
RESEARCH ARTICLE

Finding Planets: Exoplanet Validation Using Overlapping Data from TESS And K2

Mohammad Yawar Khan

Deira International School, Festival City, Dubai, UAE; yawar4380@gmail.com

ABSTRACT: Hidden from plain sight, vast archives of exoplanet data remain to be analyzed. TESS and K2 data are the vast majority of these archives. The overlap between these missions can be used to detect and validate exoplanets by cross-referencing transit signals. We predict that exoplanets can be validated if stars observed in these missions show consistent transit dips in their light curves. For our methods and materials, each candidate star was selected using the NASA Exoplanet Archive by retrieving its TIC ID. Using Python in Jupyter Notebook, the required packages were installed. The light curves were downloaded, detrended with Wōtan, and analyzed with the Transit Least Squares (TLS) algorithm. Folded and binned transits were analyzed and checked for odd-even transits and secondary eclipses. Candidate 1 showed consistent transits with no secondary eclipses and a high SNR, supporting a hot Jupiter-sized planet, while Candidate 2 displayed consistent U-shaped transits but required further validation. Our hypothesis was supported, as the overlapped TESS and K2 transit signals reliably indicated a planetary candidate (Candidate 1), while Candidate 2 showed promising signs but required further confirmation. These results demonstrate that publicly available TESS and K2 data can be effectively used for validating exoplanet candidates.

KEYWORDS: Physics, Astrophysics, Exoplanet Detection, Transit Photometry, Exoplanet Validation, Planet Validation, TESS, TLS.

Introduction

To discover extraterrestrial life and Earth-like planets, our search must begin with the identification of exoplanets – a crucial foundation. One method of exoplanet detection is transit photometry,[1] which occurs when an exoplanet passes in front of its star, causing a measurable dip in the star's brightness. Other detection methods include direct imaging and gravitational microlensing.[2,3] Transit photometry is used for large surveys because it can monitor thousands of stars simultaneously,[4] whereas direct imaging is limited to widely separated planets.

To continue the exploration of exoplanets, the K2 mission[5] was launched as a successor to the Kepler mission.[6] The K2 further enhanced the discovery of exoplanets, with approximately 700 planet candidates identified.[7] After the K2 mission, NASA launched the Transiting Exoplanet Survey Satellite (TESS) mission.[8] TESS and K2 have been successful in observing common planet systems, providing abundant exoplanet and light curve data. By using overlapping observations from these two missions, we can perform independent checks on the detected transit signals.

Several studies have validated exoplanets using overlapping TESS and K2 light curves,[9,10] with many more awaiting confirmation. This empirical paper investigates the transit dip in the light curves of stars to validate an exoplanet. It is based on the hypothesis that exoplanets can be confirmed if stars observed in both TESS and K2 show consistent transit dips in their light curves.

Methods

Candidate stars were selected from the NASA Exoplanet Archive using their TIC IDs, filtered for targets observed by both TESS and K2. All data handling and analysis were performed in Python using Jupyter Notebook. Then we utilised available packages for light curve extraction, detrending, and transit detection.

TESS light curves were downloaded and detrended using Wōtan, which applies a smoothing algorithm to isolate transit signals from stellar variability and instrumental trends. The detrended light curves are then analyzed with the Transit Least Squares (TLS) algorithm, which models realistic transit shapes and is particularly sensitive to small, short-period planets. Transit events were visualized by phase-folding and binning the light curves, and checked for odd-even depth differences and secondary eclipses to rule out potential eclipsing binaries.

For the K2 targets, the pixel-level data were downloaded and processed to extract light curves. Pixel-Level Decorrelation (PLD) was applied to remove systematic trends from K2's variable pointing, followed by Wōtan detrending to flatten the light curves. TLS analysis was then conducted, and the resulting light curves were folded and binned. Finally, the TESS and K2 results were compared by overlapping the folded light curves to verify the presence of consistent transit signals across both missions.

© 2026 Terra Science and Education

DOI: 10.36838/IJHSR87.296

Results

Candidate 1 TESS analysis:

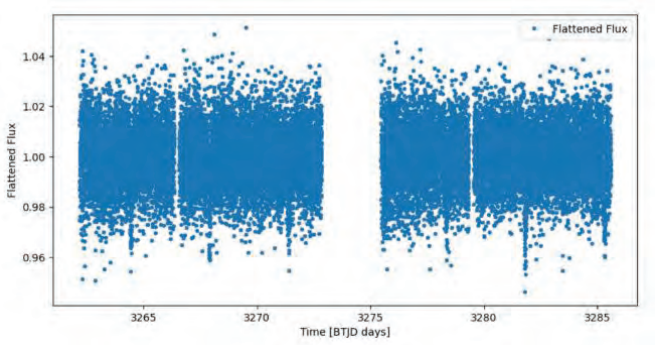

Figure 1: The detrended light curve, where the blue points represent the raw photometric data, spread across the graph. The vertical scatter in the blue points indicates the natural variability and noise present in the raw observations, while the extraneous signals demonstrate the reveal of potential transit features.

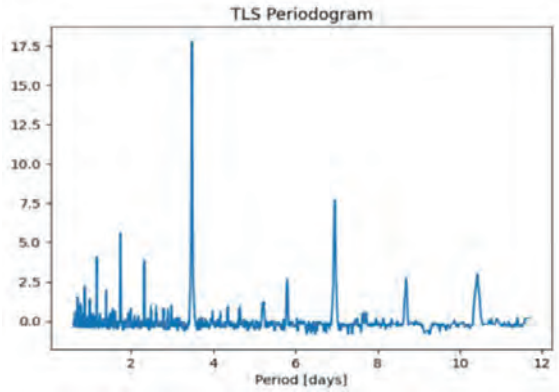

Figure 2: The detrended light curve was analysed using the Transit Least Squares (TLS) algorithm.

TLS models the light curve using realistic transit shapes rather than simple box-shaped signals, which is done by the Box-Least Squares (BLS) method (Figure 2), making it more sensitive to short periods, which can potentially be transits, which are typical of exoplanets. TLS identified these parameters: period = 3.47698 days, transit time (T0) = 3264.4360 BJD, transit depth = 0.984%, and a transit duration of 0.156 days. These values represent the strongest periodic transit signal in the light curve and provide quantitative information for further analysis.

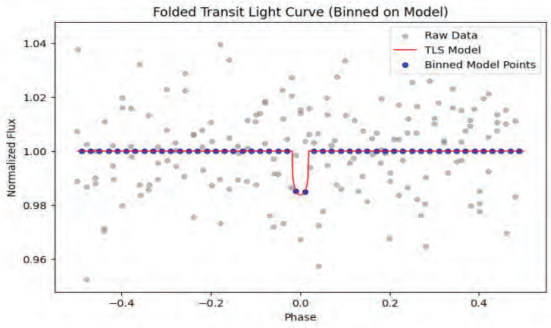

Figure 3: The light curve was folded and binned to improve the signal-to-noise ratio and visualize the transit more clearly.

The raw data points in grey are plotted across all observed phases (Figure 3), while the TLS model is shown as a continuous red line, flat except for the U-shaped dip at phase 0.0, corresponding to the planetary transit. The evenly spaced blue binned points represent averaged flux values within each phase bin, demonstrating the underlying transit signal more clearly against the noise. This allows for an easier analysis of transit depth, duration, and shape while reducing scatter from random variations.

Odd and even transits were also examined separately. The analysis yielded an odd transit depth of 0.01011 and an even transit depth of 0.01151, resulting in a difference of –0.00140 between the odd and even transits, which is almost negligible and indicates the consistent transit depths. This helps rule out the possibility of an eclipsing binary. Additionally, the root mean square was measured at 0.00800, corresponding to an approximate signal-to-noise ratio (SNR) of 122.96, showing a robust detection. A search for secondary eclipses near phase 0.5 revealed no significant signal – only at 0.0 -, further supporting that the observed transit is likely planetary in nature.

Candidate 1 K2 analysis:

For the cross-reference of the K2 mission, we downloaded the K2 target pixel file for Candidate 1, which was done from the Jupyter notebook. From this, the light curve was also downloaded and then processed through pixel-level decorrelation (PLD) to remove systematic instrumental noise. After PLD, the light curve was further detrended using Wōtan to remove long-term stellar variability for extra confirmation. This ensured that the light curve was ready for TLS.

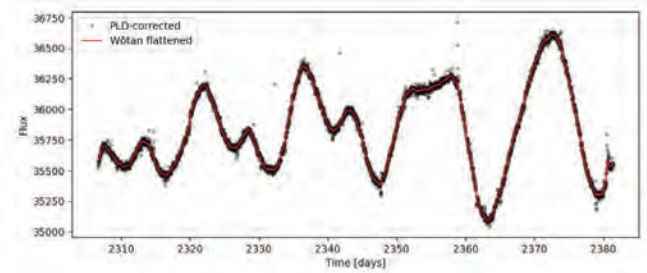

Figure 4: The detrended K2 light curve. The graph exhibits frequent fluctuations, which represent stellar variability and instrumental noise that remains after initial detrending. These ups and downs obscure the transit signal, making it difficult to visually identify transits without further processing.

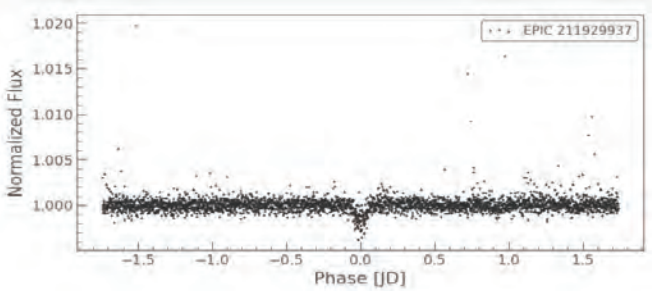

Figure 5: The K2 light curve after processing through PLD, Wōtan detrending, TLS analysis, flattening, and phase-folding.

The K2 light curve was processed through PLD, Wotan, and TLS (Figure 5). The black dots are the binned flux points, mostly flat except for a clear dip at 0.0, which corresponds to the candidate's transit. TLS detected a best fit period of 3.4777 days – corresponding to both the NASA EXOPLANET ARCHIVE data and the earlier TESS analysis - with a transit depth of 0.998% and an SDE of 24.36, yielding an approximate SNR of 21.37. Odd-even transit analysis showed depths of 0.98855 and 0.99079, with a difference of –0.00224, indicating no significant difference between consecutive transits. The secondary eclipse depth was measured at 1.00165, consistent with the absence of a secondary eclipse, suggesting the dip is unlikely to be an eclipsing binary.

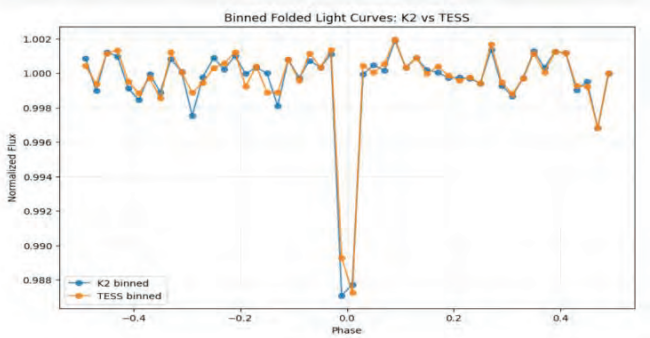

Figure 6: The folded and binned light curves of TESS (orange) and K2 (blue) overlapped.

The dip in phase 0.0 is visible, indicating that the transit signal is present in both TESS and K2 observations (Figure 6). While the K2 light curve exhibits more scatter and noise from 0.4 to 0.2, the alignment of the transit dips between TESS and K2 confirms the detection. This overlap provides strong evidence that the observed dips are likely caused by a planet transiting its host star.

Candidate 2 TESS analysis:

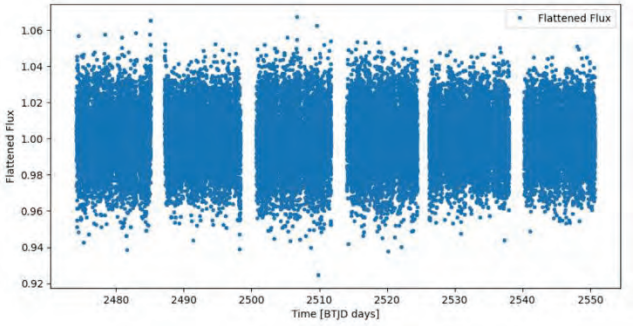

Figure 7: The light curve for Candidate 1 TESS was downloaded and detrended, producing the plot shown. The blue points represent the raw photometric data, while the detrended signal highlights potential transit events.

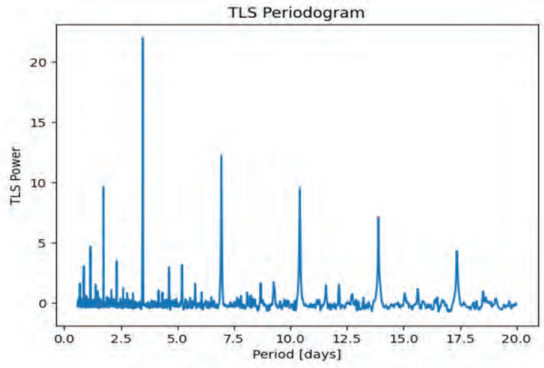

Figure 8: The detrended light curve was analysed using Transit Least Squares (TLS), producing the plot.

TLS identified a best-fit period of 3.472782 days, transit time (T0) = 2476.24887 BJD - 2457000, transit depth = 0.988% (0.00988), and transit duration = 0.164 days (Figure 8). This algorithm models the light curve with transit shapes, allowing precise estimation of transit properties and providing a more sensitive detection than the BLS method.

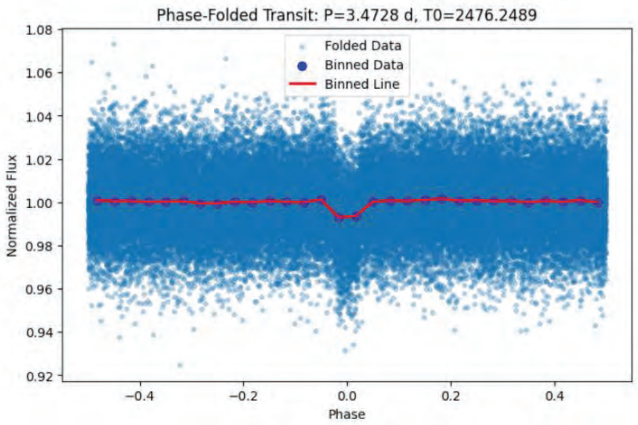

Figure 9: The light curve was then folded and binned to improve signal clarity and reduce scatter.

The red line represents the TLS transit model, which is flat except for the U-shaped dip at phase 0.0, corresponding to the transit (Figure 9). The evenly spaced dark blue points are phase-binned averages, which emphasise the transit signal over the noise, while the lighter blue raw data points show the original scatter.

Odd and even transits were compared to check for consistency. The odd transit depth was 0.00957 ± 0.00046, and the even depth was 0.00941 ± 0.00048, yielding an odd–even difference of 0.00017 ± 0.00066 (0.25σ). These results indicate uniform transit depths across consecutive events, ruling out strong eclipsing binary contamination. A secondary eclipse check near phase 0.5 measured a depth of 0.00021 ± 0.00045, consistent with zero, supporting the interpretation of a planetary transit rather than a binary.

The transit model was fitted using Batman + least_squares, yielding a R_p = 0.0882, a = 9.69, inclination = 88.78°, T0 = 2476.24922, and baseline = 0.99720. Derived planetary parameters include Rp = 9.62 R⊕, impact parameter b = 0.21, semi-major axis a = 0.045 AU, and equilibrium temperature

DOI: 10.36838/IJHSR87.296

Teq = 1363 K. The fit is stable and physically reasonable, showcasing a hot Jupiter-like exoplanet.

Candidate K2 analysis:

For Candidate 2, although the NASA Exoplanet Archive lists the target as observed by both TESS and K2, retrieving K2 data through Jupyter Notebook was unsuccessful. The K2 light curve could not be found or downloaded using the same methods applied to Candidate 1, which prevented any form of analysis. This may have arisen from several factors: it is possible that the candidate was included in the K2 catalog based on planned observations or preliminary data, but the processed light curves are not yet publicly available; alternatively, there may be inconsistencies in how the NASA Exoplanet Archive targets across missions. The inability to access K2 data for this candidate does not conclusively prove that the target was not observed by K2 or that the transit signal is absent in those sectors. It may simply reflect a limitation of the available data or the query method used. This highlights a limitation of the study, as independent verification of the transit signal from K2 - a key component of our cross-mission validation approach - could not be performed for Candidate 2.

■ Discussion

The K2 and TESS were designed to identify different star territories. TESS emerged as a successor to the Kepler 2 (K2) mission, aiming to identify additional planets. This provides a valuable opportunity to explore common ground with the previous findings of K2.

The validation process conducted in this project followed a conventional exoplanet analysis workflow using detrending, transit search, and cross-verification across missions. Light curves were flattened with Wōtan, transit signals were extracted using the Transit Least Squares (TLS) algorithm, and consistency between TESS and K2 periods was used as the main indicator of a genuine planetary signal.

We hypothesized that if stars observed in the K2 and TESS missions show consistent transit dips in their light curves, these dips can indicate a planetary candidate. During the study of the two candidates, this hypothesis was partially completed. We used the transit least squares algorithm to explore the identification of planet candidates. TLS has been used to successfully identify small planets.[11]

Other studies have implemented the method of validation through larger validation, such as scaling K2.V,12, which also relied on detrending and TLS-based searches to find consistent periodic dips across multiple campaigns. Similarly, VaTEST III13 validated 8 potential super-earths from TESS data using pre-processing and signal modelling techniques. However, these studies extended their validation process by estimating false-positive probabilities and performing posterior distributions. They also performed Bayesian fits to refine planetary parameters. Our approach achieved empirical agreement across missions, but fell short of statistical validation. This means that our methods align well with previous studies, but differ in the depth of analysis.

A limitation of this investigation is the absence of advanced validation algorithms that could be used to confirm the status of our candidates. These algorithms would help quantify uncertainty and false-positive probabilities. One of these is VESPA, which helps assess whether a signal is more likely to be a planet or an astrophysical false positive. Studies such as Scaling K2 V12 utilised VESPA to calculate a formal false-positive probability, thereby strengthening the credibility of their planet candidates. Similarly, the use of MCMC methods, as implemented through the emcee package, enables the derivation of posterior distributions for parameters such as planet radius and orbital period. This paper14 demonstrated how Bayesian fitting improved parameter precision and reduced degeneracy in multi-planet systems. The lack of these approaches in my analysis limited the statistical confidence of the results. Future work incorporating these techniques would not only refine parameter estimates but also provide quantitative validation aligned with professional standards.

The TESS light curve displayed clear and statistically significant transit dips consistent with a planetary signal, while the K2 light curve exhibited a sine-wave trend that complicated visual identification of the transit signal. For Candidate 1, the TESS analysis revealed high-value periodicity, characterised by a U-shaped transit consistent with a planetary radius of 9.62 $R_{\oplus}$, and no detectable secondary eclipses, which reinforces the likelihood of a hot Jupiter-sized exoplanet. The high signal-to-noise ratio (122.96) further supports the statistical significance of the detection.

For Candidate 2, although the light curve exhibited consistent U-shaped transits and negligible secondary eclipses, the slightly lower transit depth and higher noise underscore the need for additional confirmation. Although advanced statistical tools were not applied, cross-mission light curve comparisons provide valuable preliminary evidence for exoplanet candidacy.

A notable limitation of this study is the quality of K2 data, including instrumental noise and shorter observational windows, which may have contributed to less clear transit signals. Future studies could incorporate transit timing variation analysis or more sophisticated modelling to refine candidate validation.

Overall, this investigation demonstrates the potential of available TESS and K2 archives for exoplanet validation. Consistent transit signals across multiple datasets, combined with high SNR and the absence of secondary eclipses, provide strong evidence for planetary candidates.

■ Conclusion

This study analysed archival TESS and K2 light curves to validate exoplanet candidates through transit photometry. Candidate 1 displayed consistent findings to support a hot Jupiter-sized exoplanet. Candidate 2 showed promising transit signals but requires additional validation. These findings demonstrate that careful analysis of overlapping light curves from multiple missions can provide strong preliminary evidence for exoplanet validation. By providing a cross-check, this paper strengthens the reliability of planet validation and contributes to expanding the catalogue of confirmed exoplanets.

The archival data can provide a rich source for research, paving the way for large-scale studies.

Our limitations include K2 instrumental noise and shorter observational windows, which can obscure transit signals. Future work could extend this approach to additional candidates, incorporate TTV analysis, and apply advanced statistical validation tools to refine candidate confirmation.

Acknowledgments

The author thanks Dr. Chima McGruder for his consistent guidance and mentorship, and acknowledges Indigo Research for facilitating the mentorship. I attest that the ideas, graphics, and writing in this paper are entirely my own.

References

1. Carter, J. A., Winn, J. N., Gilliland, R., & Holman, M. J. (2009). Near-infrared transit photometry of the exoplanet HD 149026b. The Astrophysical Journal, 696(1), 241.
2. Gaudi, B. S. (2012). Microlensing surveys for exoplanets. Annual Review of Astronomy and Astrophysics, 50(1), 411-453.
3. Christie, G. W. (2006). Detecting exoplanets by gravitational microlensing using a small telescope. arXiv preprint astro-ph/0609599.
4. Goffo, E. (2024). The Mysteries of Small Exoplanets: Planetary Systems Investigation via Transit Photometry and Doppler Spectroscopy.
5. Vanderburg, A., et al. (2016). K2 mission data and exoplanet validation methods. The Astrophysical Journal, 829(2), L9. https://doi.org/10.3847/2041-8205/829/2/L9
6. Borucki, W. J., Koch, D., Basri, G., Batalha, N., Brown, T., Caldwell, D., ... & Prsa, A. (2010). Kepler planet-detection mission: introduction and first results. Science, 327(5968), 977-980.
7. Zink, J. K., Hardegree-Ullman, K. K., Christiansen, J. L., Bhure, S., Adkins, B. D., Petigura, E. A., ... & Schlieder, J. E. (2021). Scaling K2. IV. A Uniform Planet Sample for Campaigns 1–8 and 10–18. The Astronomical Journal, 162(6), 259.
8. Kruse, E., et al. (2019). Validation of TESS exoplanets using K2 and archival data. The Astronomical Journal, 157(6), 233. https://doi.org/10.3847/1538-3881/acaf03
9. Ikwut-Ukwa, M., Rodriguez, J. E., Bieryla, A., Vanderburg, A., Mocnik, T., Kane, S. R., ... & Yahalomi, D. A. (2020). The K2 and TESS synergy. I. Updated ephemerides and parameters for K2-114, K2-167, K2-237, and K2-261. The Astronomical Journal, 160(5), 209.
10. Thygesen, E., Ranshaw, J. A., Rodriguez, J. E., Vanderburg, A., Quinn, S. N., Eastman, J. D., ... & Esquerdo, G. A. (2023). The K2 and TESS Synergy. II. Revisiting 26 Systems in the TESS Primary Mission. The Astronomical Journal, 165(4), 155.
11. Heller, R., Rodenbeck, K., & Hippke, M. (2019). Transit least-squares survey-I. Discovery and validation of an Earth-sized planet in the four-planet system K2-32 near the 1: 2: 5: 7 resonance. Astronomy & Astrophysics, 625, A31.
12. Christiansen, J. L., Bhure, S., Zink, J. K., Hardegree-Ullman, K. K., Adkins, B. D., Hedges, C., ... & Petigura, E. A. (2022). Scaling K2. V. Statistical validation of 60 new exoplanets from K2 campaigns 2–18. The Astronomical Journal, 163(6), 244.
13. Mistry, P., Prasad, A., Maity, M., Pathak, K., Gharat, S., Lekkas, G., ... & Kawai, Y. (2024). VaTEST III: Validation of eight potential super-earths from TESS data. Publications of the Astronomical Society of Australia, 41, e030.
14. Mantovan, G., Montalto, M., Piotto, G., Wilson, T. G., Cameron, A. C., Majidi, F. Z., ... & Nascimbeni, V. (2022). Validation of TESS exoplanet candidates orbiting solar analogues in the all-sky PLATO input catalogue. Monthly Notices of the Royal Astronomical Society, 516(3), 4432-4447.

Author

Mohamad Yawar Khan is an astrophysics enthusiast, presently completing his IB diploma in Dubai, UAE. His research interests are focused on condensed matter physics. He will be applying to universities with a strong foundation in research in the field of physics.

DOI: 10.36838/IJHSR87.296

IJHSR
ijhighschoolresearch.org
RESEARCH ARTICLE

Evaluating the Accessibility of ChatGPT for Individuals with Dyslexia

Shradha Sujeeth

Gems Modern Academy, Dubai, 53663, UAE

ABSTRACT: In recent years, Artificial Intelligence (AI) development has accelerated, with Large Language Models and chatbots becoming more prominent in society. However, their accessibility for individuals with dyslexia remains less explored. This paper aims to evaluate the extent of accessibility of ChatGPT for individuals with dyslexia using 3 frameworks: Web Content Accessibility Guidelines (WCAG), British Dyslexia Association (BDA) Style Guide, and Cognitive Load Theory (CLT) to evaluate the accessibility of ChatGPT for individuals with dyslexia by identifying possible gaps and providing recommendations. ChatGPT's general and dyslexia specific accessibility was determined by evaluating its compliance with the WCAG and BDA guidelines, respectively. Additionally, CLT was used to interpret the implications of readability scores on cognitive load. Flesch Reading Ease score (FRE) was used as the metric for output readability. Results reveal moderate accessibility: ChatGPT conforms to several WCAG guidelines but lacks compliance with the BDA style guide. Therefore, improving the accessibility of AI chatbots like ChatGPT requires evolving existing global accessibility guidelines to provide dyslexia specific recommendations, developing AI-specific guidelines to address the dynamic nature of ChatGPT outputs, and integrating personalization features into AI interfaces to address all population needs and individual need differences within disabilities.

KEYWORDS: System software, Human Machine/Interface, Accessibility, Dyslexia, Cognitive Load.

Introduction

In the past decade, the fast growth of Artificial Intelligence (AI) has led to the increased popularity of Large Language Models (LLMs) and chatbots such as ChatGPT. ChatGPT is an AI language model that was developed by OpenAI and released in 2022, and it gained over 100 million active monthly users within 2 months of its initial launch.[1] It's one of the most globally recognized chatbots. Rapid developments of AI technologies have led to their implementation in various sectors such as healthcare, education, and business.[2,3] Despite their rapid development, their accessibility and inclusivity are less explored and evaluated. Dyslexia is a highly widespread cognitive disability affecting 1 out of 10 people worldwide, with an estimated 780 million people.[4] Thus, with the rapid development of AI technologies and the massive population affected by Dyslexia, it is crucial that we ensure that these technologies are accessible to individuals with Dyslexia and that they are not neglected. This can be done by evaluating the accessibility of AI models and wrappers in terms of Dyslexia requirements. Consequently, the following paper utilizes 3 frameworks to assess ChatGPT's accessibility for dyslexic individuals: Web Content Accessibility Guidelines (WCAG), British Dyslexia Association (BDA) Style Guide, and Cognitive Load Theory (CLT).[5–7]

Background

Accessibility Guidelines:

Several guidelines for accessibility for individuals surfing the web have been published, for example Web Content Accessibility Guidelines (WCAG) is a notable accessibility framework published by the World Wide Web Consortium. The version in use is the WCAG 2.2, published in 2023, version in use and these guidelines aid in addressing a range of disabilities, including physical disabilities such as vision impairment and cognitive disabilities such as Dyslexia. Additionally, other guidelines, such as the British Dyslexia Association Style Guide, have been published. These guidelines are more focused and address accessibility requirements of digital and written material for individuals with Dyslexia.[8]

WCAG Guidelines:

The WCAG guidelines are divided into four principles: perceivable, operable, understandable, and robust.[9] 13 guidelines are spread across the principles.[5] The aim of perceivable is to ensure that content is not invisible to all the senses of an individual.[5] For example, under the perceivable principle, one guideline suggested by WCAG is that text alternatives should be provided for non-text elements such as audio or video. Guidelines under operability ensure that a user is able to navigate the web content comfortably, such as by providing keyboard shortcuts to possible challenging navigation.[5] Understandable ensures that content is simple to understand, and Robust ensures that web content is usable with assistive technologies. Each guideline is accompanied by success criteria that are testable. The success criteria are categorized into three levels: A (bare necessity), AA (moderate conformance), and AAA (highest level conformance). However, achieving an AAA conformance does not ensure absolute accessibility as the WCAG has stated that 'even content that conforms at the highest level (AAA) will not be accessible to individuals with all types, degrees, or combinations of disability, particularly in the cognitive

© 2026 Terra Science and Education

DOI: 10.36838/IJHSR87.301

language and learning areas.[5] This demonstrates a massive limitation of the guidelines, as it does not ensure accessibility for individuals with cognitive disabilities like Dyslexia.

BDA style guide guidelines:

With the latest version in 2023, the British Dyslexia Association (BDA) has published specific accessibility guidelines (namely the BDA style guide) for digital and written content that ensure accessibility for individuals with dyslexia. In 2018, it was considered the most well-known style guide for individuals with Dyslexia.[8] The guidelines are categorized into several sections, such as readable fonts, heading and structure, color, layout, and writing style, that ensure that the content's overall presentation and text are accessible to individuals with Dyslexia. The style guide recommends that these guidelines be considered in combination with the WCAG guidelines during web development.[7] However, it is important to note that while these guidelines are highly recognized in terms of Dyslexia, they serve as a mere recommendation and are not mandated by law, unlike the WCAG guidelines in many regions.[7,9] Therefore, this serves as a major limitation of the guidelines, as addressing its recommendations is not mandated; developers often overlook the BDA style guide guidelines, thus inhibiting accessibility for individuals with dyslexia.

Cognitive Load Theory:

Cognitive load theory is an instructional theory based on our knowledge of human cognition.[6] The theory divides mental load into 3 aspects: intrinsic load, extraneous load, and germane load. Intrinsic load refers to the complexity of a text; the higher the complexity higher the intrinsic load.[10] Complexity of a text is not only influenced by the nature of the information itself, but also by an individual's prior knowledge or familiarity with the topic.[10] Extraneous load refers to the mental effort exerted as a result of the manner in which information is presented.[11] For example, formatting of text and linguistic complexity can result in increased extraneous load as it requires more working memory, but does not directly contribute to learning.[12] Individuals with dyslexia often struggle with word recognition, which exerts an immense cognitive load that could be utilized for comprehension.[13] Germane load refers to the mental effort contributing to understanding and schema formation.[14] Therefore, reducing intrinsic and extraneous load is highly crucial for individuals with dyslexia to focus on germane load.[15] This can be done by improving the readability of texts.[8] The WCAG and BDA guidelines do make recommendations on content readability, but it merely suggests simple content but lacks specific metrics for readability. Cognitive Load Theory will be used as a framework to evaluate the accessibility of ChatGPT.

Comparison of Guidelines:

Table 1: Comparison of accessibility features between WCAG and BDA guidelines.

Feature	WCAG recommendation (general recommendation)	BDA recommendation (dyslexia specific recommendation)
Font type	No suggestion	Sans serif fonts
Font size	Text must be resizable to 200% (Level AA)	16-19px
Letter spacing	At least 0.12 the font size (Level AA)	35% of the average letter width
Line spacing	At least 1.5 the font size (Level AA)	proportional to inter-word spacing; 1.5 / 150% is preferable.
Word spacing	At least 0.16 the font size (Level AA)	Inter-word spacing should be at least 3.5 times the inter-letter spacing.
Text formatting	Avoid justification (Level AAA)	Avoid justified text, underlining, and italics. Use bold for emphasis. Avoid using capital letters and uppercase letters for continuous text.
Color and contrast ratios	Contrast greater than equal to 4:5:1. (Level AA) Contrast greater than or equal to 7:1 (Level AAA)	Use solid backgrounds. Use dark text on a light background (avoid pure white), avoid red, pink, and green
Writing content	When text requires reading ability over secondary level, include supplemental content or a version that does not require reading ability more advanced than the lower secondary level. Level (AAA)	Write in simple, clear language using everyday words Use active rather than passive voice. Be concise; avoid using long, dense paragraphs

Table 1 demonstrates that while there are a few features in which the guidelines partially or completely align, such as word spacing and text formatting, there are several features in which the guidelines misalign. The comparison reveals that WCAG does not provide guidelines for font type, while BDA recommends sans-serif for web interfaces. Font size, letter spacing, and word spacing are partially aligned as they differ in metrics. Line spacing, which was recommended as at least 1.5 times the font size, was aligned between the guidelines. Text formatting was partially aligned between the guidelines, as they both recommend avoiding justification, but WCAG lacks guidelines on the use of capitalization and styles. In terms of color contrast, both guidelines require high contrast, but they are partially aligned, as BDA provides an additional recommendation to avoid a pure white background and specific colors. The writing content guidelines partially align as they both advise simple writing, but differ in scope, with WCAG focusing on supplemental content.

These differences between the guidelines demonstrate that mere conformance to the guidelines proposed by WCAG does not ensure complete accessibility for individuals with dyslexia; thus, this is crucial to consider as several regions implement WCAG guidelines in their legal policies, laws, or frameworks. For example, the United States' Section 508 of the Rehabilitation Act states that federal government agencies must ensure that their digital tools, such as official websites, meet the level A and AA conformance level of the WCAG guidelines.[18] However, the BDA style guide acts as a recommendation and is not integrated into legal frameworks, thus developers often attempt to address general accessibility standards such as WCAG and may neglect the specific needs of individuals

with dyslexia. However, it is important to note that combining guidelines might prove difficult in certain features, such as letter spacing, as the guidelines vary in metric. For example, in letter spacing, WCAG recommends at least 0.12 times the font size while BDA guidelines recommend 0.35 times the average letter width.

Thus, to evaluate the accessibility of ChatGPT for individuals with dyslexia using a holistic approach, it is crucial that a combination of these guidelines is utilized. The WCAG guidelines provide insight into ChatGPT's general accessibility conformance, and the BDA style guide gives insight into dyslexia accessibility conformance.

The paper poses the following research question: To what extent do AI models like ChatGPT comply with WCAG and BDA style guide accessibility guidelines and ensure minimal cognitive load for individuals with Dyslexia?

Methods

First, a qualitative evaluation of ChatGPT's accessibility for individuals against the WCAG and BDA guidelines was conducted, followed by a quantitative readability analysis of ChatGPT's generated text.

1.Evaluating Accessibility:

The accessibility of ChatGPT's user interface was evaluated using the comparative table of the guidelines from the previous section. The study was conducted on macOS Sequoia 15.3.2 on default settings with no user modification. For example, no modification from light mode to dark mode was made. Additionally, the study was conducted on a Google Chrome browser. To ensure the reliability of the study, default settings of the browser were utilized, such as 100% zoom and no extensions. Using the Google Chrome developer tools, the source code (the HTML and CSS code) of ChatGPT's interface was derived to assess the key features such as font type and size; line spacing, character spacing, and word spacing; color and contrast ratios; text formatting or alignment; and the layout of the interface. Using the source code, ensured that the results of the study reflected ChatGPT's default design accessibility rather than user settings and modifications. Writing content criteria from the previous table was exempted as the guidelines lacked specific metrics.

Font type and size:

First, the elements tab in the developer's tool was navigated. The selection of specific texts contained in the specific HTML elements <p> was selected. After which, the computed tab was navigated, which displayed the CSS elements of the user interface for the text selected. In the computed tab, the 'font-family' property was noted to identify the type of font used, and the 'font-size' property value was noted to identify the font size. The process was repeated for headings and general body text. After which, the data derived was compared against the guidelines' recommendations.

Spacing:

Line spacing, character spacing, and word spacing were examined in the same manner as above. However, the property identified in the computed tab was 'line-height' for line spacing, 'word-spacing' property for word-spacing, and 'letter-spacing' property for character spacing. After which, the data derived was compared against the guidelines' recommendations.

Color and Color ratios:

The color properties for text and background were examined in the same manner. However, the property identified in the computed tab was the 'color' property for the text and 'background-color' for the background in the styles tab. When the background color property specified a CSS variable, the variable value was in the stylesheet. The values were inputted in WebAIM, an online color contrast tool. Color values that were recorded in RGB format were converted to hexadecimal codes, as the WebAIM tool only accepts hexadecimal codes to calculate color contrast ratios. The contrasting ratios generated by the WebAIM tool were compared against the guideline recommendations.

Text formatting:

The justification of the text was identified in the same manner as spacing or font type. However, the 'text-align' property was navigated in the computed tab to determine the alignment. After which, the data derived was compared against the guidelines' recommendations.

2. Readability Analysis:

In order to evaluate the readability of a text generated by ChatGPT for individuals with Dyslexia, the study used the Flesch Reading Ease (FRE) score as a metric. The FRE score quantitatively evaluates the readability of a text based on factors such as sentence length and syllable count per word. The score produced ranges from 0 to 100, and the higher the score, the lower the extraneous and intrinsic load, thus ensuring higher readability. According to studies, the recommended benchmark reading level for content for individuals with dyslexia is a grade 5 level.16 A grade 5 level translates to a score of 90-100 on the Flesch Reading Ease score. 17 Lower FRE scores demonstrate the need for increased effort and energy in decoding sentences, thus increasing extraneous and intrinsic load. Thus, less effort and energy are expended on understanding content and forming schemas, which results in reduced germane load.

To evaluate the readability, 10 prompts were developed that reflected the everyday use of ChatGPT, such as explaining a topic in simple terms, creative writing, or step-by-step instructions. While the prompt-dependent nature of ChatGPT's outputs is acknowledged, individuals with dyslexia must not be expected to 'prompt engineer' to get accessible content. Thus, the following paper evaluates the general readability trends of ChatGPT outputs in everyday contexts irrelevant of prompt phrasing. Each prompt was entered into ChatGPT's free version upon clearing browser history to prevent any discrepancies as a result of prior conversations. Each of the

DOI: 10.36838/IJHSR87.301

ten prompts was then entered into ChatGPT twice to assess consistency, resulting in 20 texts. To maintain consistency, bullet points, headings, and hyperlinks were removed from the text outputs. The text outputs were then entered into www.webfx.com/tools/read-able/ to calculate the Flesch Reading Ease Score. The score for all 20 texts was noted down, and descriptive statistics, including mean, minimum, maximum, and percentage of texts meeting accessibility benchmarks, were calculated. The FRE score was then translated to grade level equivalents using already established frameworks, such as that outlined by Dubay in 'The Principles of Readability'. The results were then tabulated.

After the collection of data, the results were organized into a table. The table includes columns for WCAG recommendation, BDA recommendation, the actual observed results/data of the ChatGPT interface, alignment with WCAG guidelines, and a final column on alignment with BDA guidelines. If a feature met or exceeded guideline requirements, it was determined as 'aligned'. If the feature partially met recommendations or was inconsistent, then it was determined as 'partially aligned'. If the feature did not meet the guideline, it was determined as 'not aligned'.

Results

1. Evaluation of Accessibility using Guidelines:

Table 2: Evaluating accessibility of ChatGPT in reference to guidelines. The table indicates ChatGPT largely complies with WCAG general accessibility requirements, but shows partial or no alignment to several BDA dyslexia specific recommendations, such as spacing.

Feature	WCAG recommendation	BDA recommendation	ChatGPT result	BDA alignment (Alignment with dyslexia needs)	WCAG alignment (General accessibility alignment)
Font type	No suggestion	Sans serif fonts	Sans Serif	Aligned	Aligned
Font size	Text must be resizable	16-19px	Headings 20px Body 16px	Partially aligned: body meets guidelines, but headings exceed range	Aligned
Letter spacing	At least 0.12 the font size (Level AA)	letter-letter / character spacing ideally around 35% of the average letter width	Default spacing, not explicitly mentioned in the source code	Not aligned	Not aligned
Line spacing	At least 1.5 the font size (Level AA)	proportional to inter-word spacing; 1.5 / 150% is preferable.	Heading: 32px Body: 28px	Aligned	Aligned
Word spacing	At least 0.16 the font size (Level AA)	Inter-word spacing should be at least 3.5 times the inter-letter spacing.	Default spacing, not explicitly mentioned in the source code	Not aligned	Not aligned
Text formatting	Text is not justified (Level AAA)	Avoid Underlining and italics. Use bold for emphasis. Avoid using capital letters and uppercase letters for continuous text.	Text is left-aligned. Bold and Italic are used based on the output, which varies from prompt to prompt	Partially aligned: Justification guideline met, but other BDA rules not consistently followed	Aligned
Color and contrast ratios	contrast 4:5:1 (Level AA) Contrast 7:1 (Level AAA)	Use solid backgrounds. Use dark text on a light background (avoid pure white to prevent glare), and avoid red, pink, and green	Contrast 20:4:1	Partially aligned: Pure white is utilized in regions, and white with slight transparency in other regions.	Aligned
Writing content	When text requires reading ability over secondary level, include supplemental content or a version that does not require reading ability more advanced than lower secondary level. Level (AAA)	Write in simple clear language using everyday words Use active rather than passive voice. • Be concise: avoid using long, dense paragraphs	Output dependent	Output dependent	Output dependent

The font type of ChatGPT's UI, which was sans serif, aligned with both WCAG guidelines and the BDA style guide. The font size of ChatGPT was partially aligned with BDA guidelines, as the body text was 16px, which complied with the WCAG font size range of 16-19px, but the heading font size of ChatGPT's UI, which was 20px, exceeded the suggested range. Font size of ChatGPT is resizable and therefore aligned with ChatGPT, which does not implement explicit fixed CSS spacing enhancement and relies on the font's, operating system, and browser's default spacing. However, both WCAG and BDA recommendations require enhanced spacing. Thus, it is not aligned with BDA or WCAG requirements. Both WCAG and BDA recommend a line spacing of at least 1.5 times the font size, and this was met and exceeded by ChatGPT's UI interface. Additionally, in terms of text formatting, ChatGPT is partially aligned with BDA guidelines as it meets the no justification requirement, but it does not meet the recommendation of avoiding the use of bold or italicized text. The color contrast ratio of ChatGPT's interface exceeds the WCAG requirement; therefore, it is aligned. However, the use of pure white color in regions does not meet the BDA style guide recommendation that suggest avoidance of pure white color to avoid glare. However, ChatGPT does utilize a solid background, which is partially aligned with the BDA style guide color contrast recommendation. Writing content compliance is prompt-dependent and variable output-to-output.

3. Readability Analysis:

Table 3: Readability Analysis of ChatGPT outputs using the FRE score. The ChatGPT output snippet shows a single line of response for reference, but the full output text was used for the FRE score calculation. The average FRE score is the mean FRE score between the 2 samples of each prompt, and SEM shows the variation between samples. Grade level corresponds to the FRE score. The results indicate that across the 20 prompts, FRE scores range from 33.3 to 90.4, with a mean score of 69.2 (+- 4.67 SEM), and only one output achieves a FRE of 90 or above.

Prompt	ChatGPT Output Snippet	Average FRE score	Grade Level	Standard error mean
Explain climate change to a teenager.	Climate change means long-term changes in the Earth's temperature, weather patterns, and climate. Right now, it mostly refers to the warming of our planet caused by human activities	74.75	7th grade	6.25

Give step-by-step instructions on how to set up a wireless printer at home.	Step 1: Unbox and Prepare the Printer Unbox the printer and remove all packaging materials.	64.9	8th - 9th grade	3.8
Write a short story about friendship.	Every Saturday morning, beneath the old oak tree in Maple Park, sat two friends—Eli and Sam.	81.55	6th grade	4.35
Describe how to prepare scrambled eggs.	Crack the eggs into a bowl. Add salt, a bit of pepper, and milk or cream if using.	79.35	7th grade	4.65
Explain the importance of recycling.	Recycling is important for several key reasons that impact the environment, economy, and society: 1. Environmental Protection	38.8	Beyond 12th grade, 13-16th grade	5.5
Write a short letter apologizing to a friend for being late.	Dear [Friend's Name], I'm really sorry for being late the other day.	80.5	6th grade	9.9
Summarize the plot of "Three Little Pigs".	"The Three Little Pigs" is a classic folktale about three pig siblings who each build a house to protect themselves from the Big Bad Wolf.	84.95	6th grade	3.25
Provide advice on how to improve sleep quality.	Improving sleep quality often involves changes in lifestyle, environment, and behaviour.	61.45	8th - 9th grade	3.65
Describe what a solar eclipse is.	A solar eclipse occurs when the Moon passes between the Earth and the Sun, blocking all or part of the Sun's light from reaching Earth.	74.4	7th grade	1.0
Explain why it is important to wash your hands regularly.	Washing your hands regularly is important because it helps prevent the spread of germs and infections.	50.9	10th - 12th grade	4.3

The mean Flesch reading Ease Score of the 20 text outputs generated across 10 prompts is 69.2 (+/- 4.67 SEM), which translates to a grade 8-9 level. The Flesch Reading Ease Score of the outputs ranged from 33.3 to 90.4. Using the 5th-grade readability benchmark, which translates to a minimum of 90 Flesch reader score and higher, the score indicates the easier the readability. It was determined that only 1 out of the 20 outputs met the criteria. Therefore, most of the outputs fell below the benchmark.

Discussion

1. Evaluation of Accessibility:

The evaluation of the accessibility of the ChatGPT user interface against the WCAG and BDA guidelines demonstrates overall moderate compliance, as it does not conform to all the requirements of each guideline. ChatGPT displays more compliance with WCAG guidelines than the BDA style guide. However, ChatGPT still does not adhere to certain features of the WCAG guidelines, such as letter spacing and word spacing. ChatGPT does not explicitly declare numerical values for 'letter-spacing' or 'word-spacing' in its source code, relying on the font's, operating system, and browser's default spacing. However, WCAG and BDA have specific spacing requirements for enhanced readability. Since ChatGPT's spacing in its UI may vary across devices, the spacing may not consistently meet the requirement for consistent general or dyslexia specific accessibility. Though the letter spacing and word spacing may not align in metrics between WCAG and BDA guidelines, both guidelines do recommend enhanced spacing for readability. Lack of compliance with these spacings can inhibit efficient readability for individuals, particularly those with Dyslexia.

Although the body text complies with both WCAG and BDA guidelines, the heading font size slightly exceeds the BDA style guide recommendation; thus, this can inhibit accessibility for individuals with dyslexia who require a consistent font size for efficient navigation. The font type and use of line spacing adhere to both the guidelines, thus supporting general accessibility and accessibility for individuals with Dyslexia. The text formatting of content generated by ChatGPT partially aligns with the BDA and WCAG guidelines, as they avoid justification, but the usage of bold and italics in its outputs misaligns with the BDA style guide recommendation, as this can reduce readability for individuals with dyslexia due to the addition of distractions and loss of consistency in the text output.

The color contrast of the text and background of ChatGPT's UI completely aligns with WCAG guidelines, but it only partially aligns with BDA guidelines due to the usage of a pure white background in certain regions of the UI. The usage of pure white can increase glare and result in eye strain, which can serve as a further challenge for individuals with Dyslexia.

Therefore, the compliance of ChatGPT's UI to most of the WCAG guidelines, with the exception of spacing indicate that the interface is accessible to an extent on a general accessibility level and by legal frameworks. However, the lack of compliance with several BDA style guide recommendations demonstrates that ChatGPT's UI is not completely accessible to individuals with dyslexia.

2. Readability Analysis:

The evaluation of the written content or outputs of ChatGPT using the BDA style guide and WCAG guidelines was omitted from the methodology, as the guidelines lack specific metrics to analyze the readability of the text. However, we must analyse the text's readability as linguistic complexity can result in increased cognitive load, particularly extraneous load.[12] Individuals with dyslexia already experience high cognitive load, particularly intrinsic and extraneous load, as they often struggle with word recognition; therefore, factors such as complex linguistics or long sentence structures could add to the extensive present cognitive load.[13] Thus, the Flesch Reading Ease Score formula was used as a metric to analyze the

DOI: 10.36838/IJHSR87.301

readability of the text outputs of ChatGPT. The FRE score evaluates the readability of a text based on its sentence length and syllable counts per word. The higher the FRE score, the lower the extraneous and intrinsic load. When extraneous and intrinsic load is lowered, more energy can be expended on germane load, thus ensuring higher text readability.

Since only 1 out of the 20 text outputs received a Flesch Reading Score higher than 90, which is the benchmark for reading score of text for individuals with dyslexia, it demonstrates that content generated by ChatGPT is not generally accessible to individuals with dyslexia. Additionally, the large range of scores between prompt outputs demonstrates that ChatGPT accessibility is prompt-dependent and not consistent. Additionally, the occasional variance in scores between prompt trials demonstrates that ChatGPT outputs are inconsistent in terms of readability. These inconsistent outputs and readability levels of the texts pose a huge challenge to individuals with dyslexia, as the constant change in reading level can add to the cognitive load, thus making reading/comprehension more difficult. Thus, to an extent, the readability of ChatGPT does not meet Dyslexia standards. However, it is important to note that there are other factors besides sentence length and syllable count that affect the readability of a text, which could either increase or decrease the cognitive load and readability levels. Yet, since the FRE score is widely recognized for the reading level of a text's assessment, it can be used as an estimate of the complexity of a text.

3. Limitations and recommendation:

Although a comprehensive approach was aimed at, the paper has several limitations. The following paper did not conduct a direct dyslexic individual experience study and instead utilized existing guidelines, such as the BDA style guide, to assess the accessibility of the interface. Additionally, the readability analysis used the formula FRE, which used factors such as sentence length and syllable count, but did not take into consideration other factors of linguistic complexity.

The study utilized a MacOS Sequoia 15.3.2 and the browser Google Chrome due to availability. No user modifications were made, and default settings were maintained. Although the developer tools were utilized to extract source code to identify ChatGPT's specific UI choices, as ChatGPT's source code demonstrates what ChatGPT intends to display. However, variation may occur due to rendering differences in certain elements, such as font type in operating systems or browsers. These rendering differences may occur in all web-based platforms; nonetheless, the findings of the study provide a valuable initial assessment of ChatGPT's accessibility.

Due to the lack of complete adherence of ChatGPT's UI to the guidelines, ChatGPT should develop its interface in future versions in adherence to the BDA style guide guidelines to ensure accessibility for individuals with Dyslexia. However, if adhering to all guidelines proves difficult, then ChatGPT must offer personalization, for example, in spacing and text size, so that individuals can tailor the UI as per their needs, thus addressing all population needs.

In terms of guidelines, general guidelines such as the WCAG must evolve more to support more Dyslexia specific needs and add metrics for readability of text displayed. Unlike general websites that are static in nature, AI model and wrapper outputs are highly dynamic in nature and prompt-dependent; these guidelines must evolve and develop specific recommendations to address this inconsistency.

■ Conclusion

As AI technologies such as ChatGPT are increasingly gaining popularity and being integrated into sectors of society and daily life, such as in education, it is important that these technologies are accessible to all populations, including individuals with cognitive disabilities. ChatGPT's UI does not completely comply with the dyslexia specific guidelines, thus suggesting that future chatbot builds should develop solutions to address this gap.

My paper contrasts two solutions: 1. Change the guidelines, 2. Develop better AI Chat builds. Changing the guidelines includes ensuring that existing general accessibility guidelines, such as the WCAG, incorporate dyslexia specific accessibility needs, readability metrics, and possible cognitive load metrics. Additionally, developing distinct AI-specific guidelines that address the dynamic and variable nature of ChatGPT outputs could ensure consistent accessibility for individuals with dyslexia and other cognitive disabilities. Solution two involves developing better AI chat builds by developing its interface in future versions in adherence to the BDA style guide guidelines to ensure accessibility for individuals with dyslexia. However, if addressing the needs of different populations proves difficult, personalization of interfaces can improve accessibility for all individuals with any form of disabilities or individual needs.

While both solutions can offer an immense impact on the overall accessibility of Artificial intelligence chatbots, my analysis suggests that option 2 (developing better AI chatbots) is a more viable solution. Improving AI interfaces and integrating personalization features can be implemented more rapidly than changing global accessibility standards, and this solution also tackles the challenge of individual differences between individuals with disabilities' needs. However, combining the solutions is more ideal as it betters long term AI accessibility while providing immediate impact.

■ Acknowledgments

I would like to thank my mentor, Dr. Jorge A. Avila, for his support and guidance throughout my project.

■ References

1. Andriansyah, Y. The Current Rise of Artificial Intelligence and Religious Studies: Some Reflections Based on ChatGPT. *Millah J. Relig. Stud.* **2023**, ix–xviii. https://doi.org/10.20885/millah.vol22.iss1.editorial.
2. Akpan, I. J.; Kobara, Y. M.; Owolabi, J.; Akpan, A. A.; Offodile, O. F. Conversational and Generative Artificial Intelligence and Human–Chatbot Interaction in Education and Research. *Int. Trans. Oper. Res.* **2025**, *32* (3), 1251–1281. https://doi.org/10.1111/itor.13522.

3. Boscardin, C. K.; Gin, B.; Golde, P. B.; Hauer, K. E. ChatGPT and Generative Artificial Intelligence for Medical Education: Potential Impact and Opportunity. *Acad. Med. J. Assoc. Am. Med. Coll.* **2024**, *99* (1), 22–27. https://doi.org/10.1097/ACM.0000000000005439.
4. *33 Dyslexia Statistics & Facts: How Many People Have Dyslexia?* https://www.crossrivertherapy.com/research/dyslexia-statistics (accessed 2024-08-15).
5. *Web Content Accessibility Guidelines (WCAG) 2.2*. https://www.w3.org/TR/WCAG22/ (accessed 2025-08-09).
6. Sweller, J.; Ayres, P.; Kalyuga, S. *Cognitive Load Theory*; Springer: New York, NY, 2011. https://doi.org/10.1007/978-1-4419-8126-4.
7. Dyslexia Style Guide 2023.
8. Yoliando, F. T. A Comparative Study of Dyslexia Style Guides in Improving Readability for People With Dyslexia; Atlantis Press, 2020; pp 32–37. https://doi.org/10.2991/assehr.k.201202.050.
9. *Web Content Accessibility Guidelines (WCAG) 2.1*. https://www.w3.org/TR/WCAG21/ (accessed 2025-04-04).
10. Sweller, J.; van Merriënboer, J. J. G.; Paas, F. Cognitive Architecture and Instructional Design: 20 Years Later. *Educ. Psychol. Rev.* **2019**, *31* (2), 261–292. https://doi.org/10.1007/s10648-019-09465-5.
11. Lange, C.; Costley, J.; Han, S.-L. The Effects of Extraneous Load on the Relationship Between Self-Regulated Effort and Germane Load Within an E-Learning Environment. *Int. Rev. Res. Open Distrib. Learn.* **2017**, *18* (5). https://doi.org/10.19173/irrodl.v18i5.3028.
12. Strohmaier, A. R.; Ehmke, T.; Härtig, H.; Leiss, D. On the Role of Linguistic Features for Comprehension and Learning from STEM Texts. A Meta-Analysis. *Educ. Res. Rev.* **2023**, *39*, 100533. https://doi.org/10.1016/j.edurev.2023.100533.
13. Tricot, A.; Vandenbroucke, G.; Sweller, J. Using Cognitive Load Theory to Improve Text Comprehension for Students with Dyslexia. In *Handbook of educational psychology and students with special needs*; Educational psychology handbook series; Routledge/Taylor & Francis Group: New York, NY, US, 2020; pp 339–362. https://doi.org/10.4324/9781315100654-17.
14. Debue, N.; van de Leemput, C. What Does Germane Load Mean? An Empirical Contribution to the Cognitive Load Theory. *Front. Psychol.* **2014**, *5*, 1099. https://doi.org/10.3389/fpsyg.2014.01099.
15. López-Resa, P.; Moraleda-Sepúlveda, E. Working Memory Capacity and Text Comprehension Performance in Children with Dyslexia and Dyscalculia: A Pilot Study. *Front. Psychol.* **2023**, *14*. https://doi.org/10.3389/fpsyg.2023.1191304.
16. Matsuura, Y.; Jaeah, C. Dyslexia Articles Unboxed: Analyzing Their Readability Level. *J. Dev. Behav. Pediatr. JDBP* **2024**, *45* (3), e211–e216. https://doi.org/10.1097/DBP.0000000000001274.
17. DuBay, W. H. *The Principles of Readability*; ERIC Clearinghouse, 2004.
18. *U.S. Access Board - Revised 508 Standards and 255 Guidelines*. https://www.access-board.gov/ict/ (accessed 2025-08-10).

Author

Shradha Sujeeth, a high school senior passionate about psychology, is the author of a children's book and a certified adolescent mental health first aider. She earned a perfect 5.0 in AP psychology and regularly engages in academic writing, earning a merit in the John Locke Essay Competition. She plans to study psychology at university.

DOI: 10.36838/IJHSR87.301

IJHSR
ijhighschoolresearch.org
RESEARCH ARTICLE

Sun-Aware Routing for Enhanced Driving Safety Using A* Search and Real-Time Atmospheric Conditions

Rohin Vig

Mission San Jose High School, 41717 Palm Avenue, Fremont, California, 94539, USA; vohinr@icloud.com

ABSTRACT: Sun glare is one of the most common natural causes of traffic accidents and can also contribute to the disengagement of camera-based autonomous vehicles, leading to uncomfortable or unsafe transitions back to human control. Traditional navigation systems ignore the position of the sun, which can significantly reduce visibility and safety during commutes, especially during sunrise and sunset. This paper presents a routing algorithm for minimizing sun glare exposure in navigation during sunset commutes. It uses solar position data from PySolar and road networks in the form of NetworkX graphs from OpenStreetMap (OSM) to compute sun-aware routes using the A* search algorithm. The cost function assigned to each edge in the NetworkX road graph is a linear combination of the sun position and travel time. Unlike prior methods, it integrates real-time cloud cover data and evaluates disengagement reduction for paths evaluated using this sun-aware routing algorithm. It achieves up to a median 36% decrease in aggregate glare as measured by a cost function which uses sun position as a proxy for glare while keeping the travel time to within a median 15.4% increase of the benchmark. When applied to real-world disengagement data from a 2021 Tesla Model Y, the algorithm demonstrates preliminary evidence of a statistically significant reduction in autopilot disengagements in a small, single-vehicle trial under clear-sky conditions during sunset, with up to a median 33.3% fewer high-glare segments while keeping the travel time to within a median 14.6% increase of the benchmark. This proposed algorithm was tested using NetworkX shortest_path paths as a benchmark. Future extensions of this project could include developing a more generalized routing graph with time-varying penalties incorporating dynamic factors like real-time traffic and weather conditions, and roadside obstacle-aware glare modeling for more accurate navigation.

KEYWORDS: Systems Software, Algorithms, A* Routine Algorithm, Dynamic Routing.

Introduction

Thousands of crashes happen every year because drivers are blinded by the sun, and current GPS systems don't address this problem. Commonly used navigation systems like Google Maps, Apple Maps, or Waze do not take temporally-dependent environmental factors into account while calculating routes, opting to optimise for either distance or time. Sun glare was the second most common factor in approximately 9,000 car crashes, second only to slick roads, representing about 17% of the 52,000 crashes with environmental-related critical reasons surveyed by the National Motor Vehicle Crash Causation Survey (NMVCCS), where Emergency Medical Services were dispatched.[1]

While least-time or least-distance courses may be an optimal approach during times when the sun does not interfere with vision, such routes might cause accidents on affected roads. Bahnesen and Mayster show that driving with sun glare can result in (i) visual impairment, (ii) delayed reaction time, (iii) increased risk of accidents, and (iv) driver distraction and discomfort.[2] Das *et al.* list seven key factors that influence glare risk, (i) relative sun position, (ii) cloud cover, (iii) atmospheric refraction, (iv) heights of buildings and trees along the road(s) traveled, (v) road infrastructure like tunnels and overpasses, (vi) reflectivity of the surrounding buildings and objects, and (vii) reflectivity of the road's surface.[3]

To quantify glare more specifically, Guo *et al.* measured the relative position of the sun as measured by the azimuthal and altitudinal angles from the driver's eyes, which resulted in the most glare being an azimuthal angle between (-57.7°, 57.7°) and an altitudinal angle (5.6°, 29.0°).[4] In this case, the azimuthal angle is defined as the angle between the driving direction and solar azimuth, not relative to true north. By integrating sun position and vehicle-specific glare sensitivity into navigation, we can improve driver safety without significantly compromising travel-time.

Previous work has explored partial solutions to glare-aware navigation. Das *et al.* introduced a dynamic glare-aware routing approach based on sun angle data.[3] Li *et al.* proposed a method to detect obstacles like trees and buildings blocking sunlight in cities using Google Street View (GSV) to create an obstacle-aware glare model for more accurate navigation.[5] However, these models do not incorporate real-time atmospheric conditions. To address this gap, we extend prior work by integrating live cloud cover data from Open-Meteo and weighting schemes based on user feedback into a dynamic sun-aware routing algorithm.

Our sun-aware routing algorithm is compared to a shortest path route generated using the nx.shortest_path function as a benchmark for statistical analysis. A route will be modified from its time or distance optimized counterpart when it directs the commuter to proceed directly towards either a sunrise or a sunset. However, this may result in dramatically higher travel times and distances. We evaluate how much a sun-aware routing algorithm can reduce sun glare exposure during sunset

© 2026 Terra Science and Education

DOI: 10.36838/IJHSR87.308

commutes by comparing its performance against the fastest route provided by Google Maps using a glare metric based on solar position along the path. We further evaluate the effectiveness of our algorithm by measuring the difference in the number of disengagements a Tesla Model Y experiences while travelling a solar-optimized route versus a shortest path route given by the NetworkX module. We used the shortest path route from NetworkX because, unlike other routes from services like Google Maps, it doesn't account for live traffic conditions.

Methods

This routing algorithm modifies traditional A* search to account for sun glare during travel. The system integrates real-world geographic data, solar position calculations, and real-time weather data to generate routes that effectively minimise both travel time and glare exposure. The overall pipeline consists of four key components: graph construction, sun glare modeling, cost function design and weight assignment, and customized A* search.

Graph Construction:

We begin by generating a Directed Multidigraph from real-world geographical road network data from OpenStreetMap's Python module OSMnx. Each node in the graph represents an intersection. We filter out nodes with fewer than 3 roads intersecting there. This means dead ends and cul-de-sacs are removed - only four-way and T-intersections are considered in the map. Furthermore, we filter out undrivable roads. Then, we convert the data from the ECEF (Earth Center, Earth Fixed) coordinates provided by OpenStreetMap to Latitude and Longitude for the convenience of subsequent steps. Using this location data, a sun-glare weight can be calculated and assigned to the edges between two nodes.

Sun Glare Modeling:

In order to quantify the amount of glare entering a driver's eyes, we use a custom cost function by using the position of the sun as a proxy for sun glare. We use the Python module *PySolar* to get accurate solar position relative to a point on the Earth's surface at any time, given the azimuthal angle θ and the altitudinal angle ϕ. From here on, the azimuthal angle refers to the angle measured relative to true north. Note that the numbers *PySolar* produces are a result of mathematical computation and modeling of solar position instead of real-time experimental values.

To be useful as a sun glare penalty, this cost function must have two characteristics:

1) It must be large when the sun is closer to the horizon and small when it is near midday or under the horizon.

2) It must be large when the driver is facing toward the sun and small when the driver is facing away.

To address the first characteristic, the cost function must have a factor of $1-\sin(\theta)$ This function has a maximum when ϕ=0 and a minimum when θ=90°. However, to address the glare penalty going to zero when the sun is under the horizon, we must take the maximum of $1-\sin(\theta)$ with 0. Therefore, the first factor of the glare penalty function is $glarePenalty = max(0,1 - sin(\theta))$.

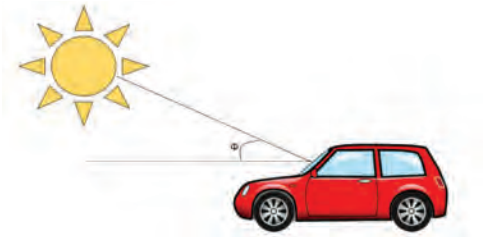

Figure 1: This figure depicts the definition of the altitude of the sun and shows that a higher weight should be assigned to smaller values of ϕ.

Furthermore, one can intuitively see from Figure 1 that a driver would have less glare if they are heading in a direction that is not pointed straight at a sunrise or sunset. Hence, we multiply again by the cosine of the difference between the sun's azimuth with respect to north and the car's heading with respect to north to fulfill the second characteristic, $cos(|\ \varphi - \phi\ |)$. To prevent the azimuthal component of this glare penalty function from going below zero, we take the maximum between it and 0, $max(0, cos(|\ \varphi - \phi\ |))$.

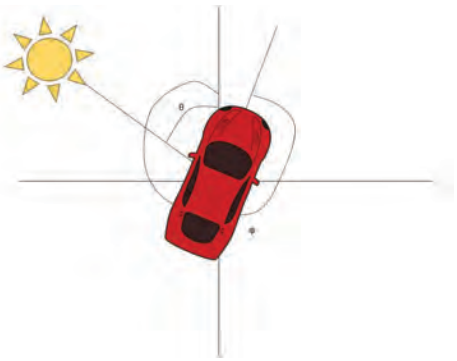

Figure 2: This figure depicts the definition of the relative azimuth of the sun as $|\ \varphi - \phi\ |$ and shows that if $|\ \varphi - \phi\ |$ were greater than 90°, the car would be facing away from the sun. Hence, routes facing away from the sun experience minimal glare, guiding the algorithm to favor such headings.

$$GlarePenalty = max(0,1 - sin(\theta)) \cdot max(0, cos(|\ \varphi - \phi\ |)) \quad (1)$$

If the altitude is less than zero, the sun is under the horizon, and the cost function is assigned the value 0. Similarly, from Figure 2, if the car is facing more than 90° away from the sun in either direction, the sun is behind the driver, and the cost function is assigned the value 0. The final pseudocode for the solar component of the cost function is as follows:

```
Function SolarCost(latitude, longitude, azimuth_facing, date):
  If date is not given:
    Set date to default datetime (2025-05-12 19:30:00 UTC)

  altitude ← get sun altitude at (latitude, longitude, date)
  azimuth  ← get sun azimuth at (latitude, longitude, date)

  If altitude ≤ 0:
    Return 0

  angle_diff ← absolute angular difference between azimuth and
azimuth_facing
  cos_diff  ← cos(angle_diff in radians)
  sin_alt   ← sin(altitude in radians)

  glare_cost ← (1 - sin_alt) × max(0, cos_diff)

  Return glare_cost
```

In order to calculate the glare component of the edge cost function, we sample multiple evenly spaced points between two nodes and take the average glare value across those points. While this approach is effective for relatively straight roads, it could lead to incorrect modelling for curvy roads. We don't address this limitation in this paper beyond this short disclaimer and leave a more thorough treatment of this issue to future research.

Figure 3 shows the value of the cost function at different times throughout the day. As per intuition, the figure shows spikes during sunrise and sunset when the glare is the highest, and smaller values as midday approaches and during the night.

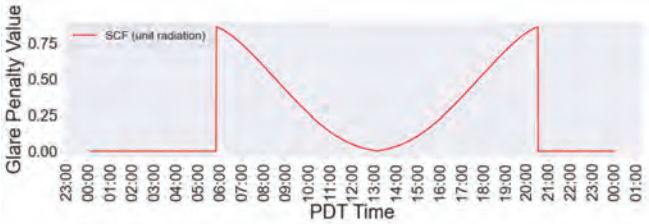

Figure 3: This figure shows the values of the glare cost function evaluated at 37.5, -122 latitude and longitude on June 12, 2025. This is taken as the aggregate of a measurement taken facing east and west. The sun rose at 5:46 AM PDT and set at 8:30 PM PDT. The glare peaks at sunrise and sunset, validating the efficacy of this cost function.

Edge Cost Function:

We define a custom edge cost function as a weighted sum of travel time on that edge and glare penalty:

$$cost(e) = \alpha \cdot glarePenalty\,(e) \cdot (1-\alpha) \cdot travelTimePenalty(e) \quad (2)$$

To ensure the two components are comparable and that the weights α are more interpretable, both the distance and glare penalty terms are normalized across the entire graph using min-max normalisation:

$$X_{norm} = \frac{X - min(X)}{max(X) - min(X)} \quad (3)$$

This normalisation allows for consistent scaling throughout the graph, allowing the cost function to reflect the desired trade-off between distance and glare-avoidance.

Additionally, before being added to the travel time component of the cost function, the glare penalty is multiplied by a coefficient representing cloud conditions. When queried for cloud cover data, *Open-Meteo* outputs a number between 0 and 1 representing what percent of the sky is covered with clouds at a given location. The cloud conditions multiplier is simply 1-γ where γ is the percent of the sky covered with clouds.

$$cost(e) = (1-\gamma) \cdot \alpha \cdot glarePenalty(e) + (1-\alpha) \cdot travelTimePenalty(e) \quad (4)$$

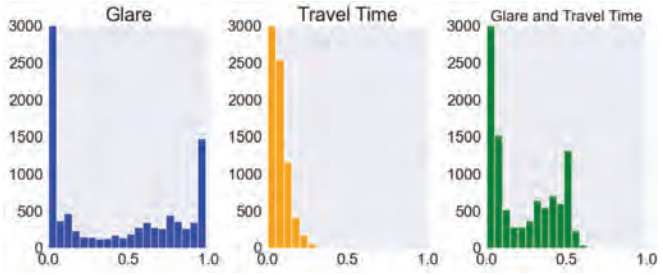

Figure 4: This figure shows the frequency of each value of the glare and travel time components of the cost function for Fremont, California, at 8:00 PM on June 15, 2025. The glare component has not been multiplied by the cloud conditions multiplier. The travel time weights are heavily skewed to the right, while the glare component is more uniformly distributed. This means that the α-value does not effectively represent the relative importance of glare and travel time in this cost function. However, this is not particularly relevant to our analysis since it relies on comparing these α-values.

Note in Figure 4, most of the values are centered around 0. For the glare cost, this is because half of the roads in the graph face away from the sun, therefore earning a glare cost close to 0. Simultaneously, the cars travelling on the other lane of the two-way road face directly toward the sun. These roads are the ones responsible for the cluster around 0.8. The graph of travel time looks highly skewed to the right because most roads in the city of Fremont are residential streets and intersect abundantly with each other. Since each intersection is a node in the graph, many edges have a small travel time weight associated with them.

The tunable parameters α were chosen by looping through values of α between 0 and 1 in increments of 0.1 and determining whether the difference in travel times and aggregate glare between the benchmark paths and custom paths sampled across 500 points is statistically significant for that coefficient. The benchmark paths of this statistical analysis were simply the shortest path between two nodes.

The primary objective of this analysis was to determine the statistical significance of the observed differences in two key areas: travel times and aggregate glare. We did this using the Wilcoxon signed-rank test since the results of a Shapiro-Wilk test on the distributions of percentage improvement in aggregate glare, number of disengagements, and travel times were statistically significant. These differences were evaluated by comparing the performance of benchmark paths against a set of custom paths from our sun-aware routing algorithm, evaluated on 500 distinct westward start-end pairs to ensure a representative dataset. The statistical significance testing aimed to determine whether the observed variations were genuine and attributable to the parameter adjustments, rather than merely random fluctuations.

This exploration allowed for a detailed understanding of how changes in the tunable parameters influenced the overall system performance, as well as helped us determine which parameter resulted in the best improvement in aggregate glare while keeping the sun-aware path's travel time to within a 20% increase of the benchmark travel time. A 20% increase in travel time was chosen as a practical threshold to balance improved glare reduction with acceptable delays for typical drivers.

DOI: 10.36838/IJHSR87.308

A Search Algorithm:*

We apply the A* algorithm to compute the shortest path with respect to our custom cost function. A crucial part of the A* algorithm is the heuristic, which is an optimistic estimate (underestimate) of the distance between every node and the destination node. The heuristic used is the great-circle distance (Haversine Distance) between the current node and the destination. This is an optimistic estimate because the Haversine Distance between two points on Earth is the smallest distance between them. Roads are often not direct conduits between a start point and a destination. Hence, this heuristic is good.

We also normalise the heuristic to prevent it from overpowering the edge weights. This is once again done through min-max normalisation (Equation 2). Since both the travel time and glare components of the edge weights are normalized between 0 and 1, the edge weights are all values between 0 and 2. In order to keep the heuristic on the same scale as the edge weights, we multiply the normalized heuristic by 2 to scale it to the scale of the edge weights.

■ Results

Main Findings:

Table 1: A summary of the main findings in this investigation: aggregate glare, disengagement, and travel time improvement percent improvement values for statistically significant α - values in rural, suburban, and urban cities. An α -value of 0.1 meets all criteria for all types of cities.

City Type	α-value	Median Aggregate Glare Reduction (%)	Median Number of Disengagements Reduction (%)	Median Travel Time Increase for Aggregate Glare Experiment (%)	Median Travel Time Increase for Number of Disengagements Experiment (%)
Rural	0.1	8.6	0.0	1.8	1.1
	0.2	15.9	25.0	6.7	6.0
	0.3	18.7	16.7	11.9	10.9
	0.4	21.5	33.3	16.4	14.6
Suburban	0.1	23.9	25.0	6.0	5.8
	0.2	31.6	25.0	12.1	15.3
Urban	0.1	28.4	16.7	7.3	9.8
	0.2	36.0	Not Significant	15.4	Not Significant

As summarized in Table 1, the Sun-Aware Routing algorithm significantly reduced driver glare exposure across rural, suburban, and urban environments while maintaining travel times close to those of the benchmark shortest-path routes. For moderate glare-weighting values (α = 0.1–0.2), median aggregate glare decreased by approximately 9–36 %, with corresponding travel-time increases of only 2–15 %. These results indicated that modest adjustments to route cost weighting could yield substantial visibility and safety improvements.

When the model was applied to real-world Tesla Autopilot data, glare-related disengagements were concentrated at solar-cost values above 0.85, consistent with reduced visibility conditions. By avoiding these high-glare segments, the algorithm reduced predicted disengagement exposure by roughly 25–30 %, while maintaining efficient travel times. These findings, together with the statistical results in Table 1, provide preliminary evidence that incorporating real-time solar and atmospheric awareness into routing algorithms can enhance driving safety with minimal efficiency trade-offs.

Sun-Aware Routing Statistical Analysis

We evaluated 500 westward-facing paths for α ∈ [0, 1] at 7:50 PM in Fremont, a suburban city; San Francisco, an urban city; and Gilroy, a rural city on June 19, 2025, and report statistically significant results for any improvement in aggregate glare and travel time. We evaluate our model on these three development types to test its sensitivity to the setting.

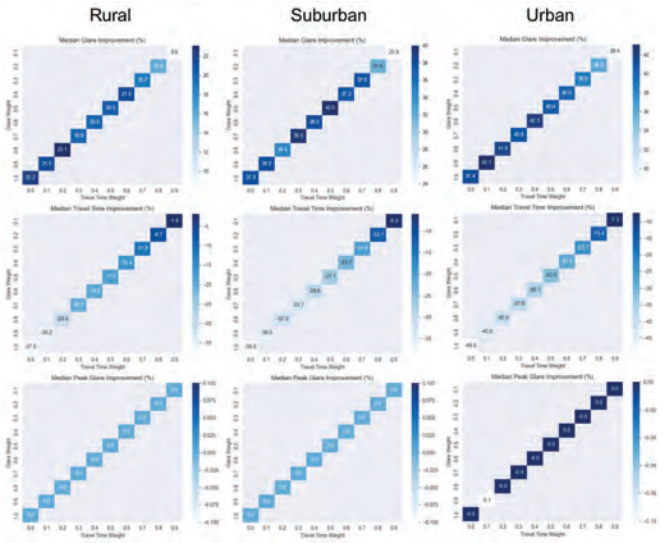

Figure 5: This figure compares the percentage changes in travel time and aggregate glare between the benchmark path and the sun-aware path for rural, suburban, and urban towns. Values of α from 0 to 1 in increments of 0.1 are evaluated. Certain α values result in significant glare reductions, as well as having travel time within a 20% increase of the benchmark.

From Figure 5, it is evident that increasing the glare-weight parameter (α) lowers both the mean and median aggregate glare, whereas raising the travel-time weight (1-α) lowers the mean and median extra travel time. In order to find the weights that result in an improvement in aggregate glare while keeping the travel time to within 20% of the benchmark value, we use a one-sided Wilcoxon signed rank test. Since the Wilcoxon tests are non-parametric, they do not require the assumption of normality of the differences.

The first test evaluated whether sun-aware routes reduced the aggregate glare metric, asking whether the median percent change in the aggregate glare between the calculated path and benchmark path was greater than zero. The second test evaluated whether the increase in travel time remained acceptable, testing whether the median percent change in travel time did not exceed 20%. Table 2 shows the p-values for each α-value across rural, suburban, and urban settings.

Table 2: Aggregate glare and travel time improvement p-values for different α in Gilroy (rural), Fremont (suburban), and San Francisco (urban). Bold entries indicate statistically significant results from the Wilcoxon Test. Bold and italicized α - values indicate those that satisfy the glare and travel time requirements for all geographic areas. α -values of 0.1 and 0.2 satisfy all the conditions.

α-value	Aggregate Glare (Rural)	Aggregate Glare (Suburban)	Aggregate Glare (Urban)	Travel Time Within 20% p-value (Rural)	Travel Time Within 20% p-value (Suburban)	Travel Time Within 20% p-value (Urban)
0.1	**< 0.001**	**< 0.001**	**< 0.001**	**< 0.001**	**< 0.001**	**<0.001**
0.2	**< 0.001**	**< 0.001**	**< 0.001**	**0.037**	**0.037**	**0.013**
0.3	**< 0.001**	**< 0.001**	**< 0.001**	**<0.001**	> 0.999	> 0.999
0.4	**< 0.001**	**< 0.001**	**< 0.001**	**0.035**	> 0.999	> 0.999
0.5	**< 0.001**	**< 0.001**	**< 0.001**	0.927	> 0.999	> 0.999
0.6	**< 0.001**	**< 0.001**	**< 0.001**	0.995	> 0.999	> 0.999
0.7	**< 0.001**	**< 0.001**	**< 0.001**	> 0.999	> 0.999	> 0.999
0.8	**< 0.001**	**< 0.001**	**< 0.001**	> 0.999	> 0.999	> 0.999
0.9	**< 0.001**	**< 0.001**	**< 0.001**	> 0.999	> 0.999	> 0.999
1.0	**< 0.001**	**< 0.001**	**< 0.001**	> 0.999	> 0.999	> 0.999

In the rural city of Gilroy (Table 2), the α -values of 0.1, 0.2, 0.3, and 0.4 all produce statistically significant decreases in aggregate glare while keeping the travel time to within a 20% increase of the benchmark. In the suburban city of Fremont and San Francisco (Table 2), the α -values of 0.1 and 0.2 are the only ones that lead to such results. Table 3 shows a summary of the results from the statistical analysis, and Figure 6 shows how the algorithm actively avoids high-glare paths by highlighting the divergence between the sun-aware route and the benchmark routes. In this particular instance, Fremont, a suburban city, was used with an α -value of 0.1.

Table 3: This table summarises the values that both decrease aggregate glare and keep the travel time within a 20% increase of the benchmark. α -values of 0.1 and 0.2 satisfy all the conditions.

City Type	α-value	Median Aggregate Glare Reduction (%)	Median Travel Time Increase (%)
Rural	0.1	8.6	1.8
	0.2	15.9	6.7
	0.3	18.7	11.9
	0.4	21.5	16.4
Suburban	0.1	23.9	6.0
	0.2	31.6	12.1
Urban	0.1	28.4	7.3
	0.2	36.0	15.4

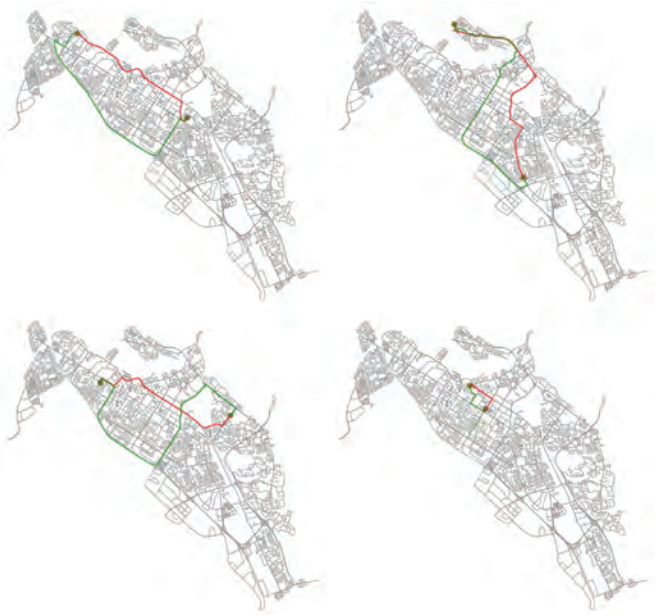

Figure 6: These maps illustrate the difference in route the sun-aware routing algorithm (green) takes compared to the shortest-length benchmark algorithm (red).

■ Autopilot Disengagement Mitigation

The subsequent part of our statistical analysis pertains to the prediction and mitigation of disengagements in 2021 Tesla Model Y cars during full self-driving. The results of this analysis are intended to be taken as preliminary results, as tests were conducted using only one vehicle, and minimal special measures were taken to control for external factors that may cause disengagements. The measures taken were the following: collecting data on a clear day, collecting data while on a main road in Fremont, California, and recording data as soon as the autopilot disengaged. The following is the data collected using the Compass app on an iPhone by taking a screenshot when the full self-drive disengages.

The following is the histogram of the frequency of each cost function value:

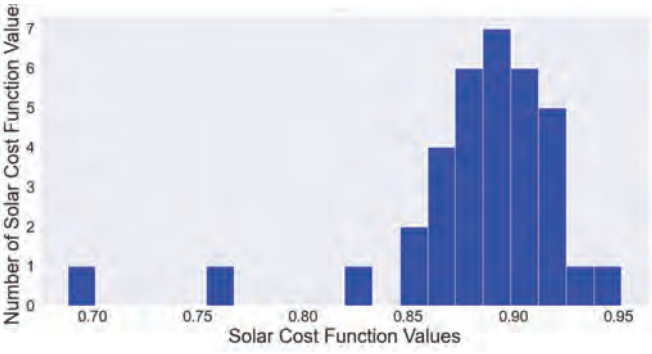

Figure 7: This figure shows the values of the solar cost function at which the full autopilot mode of the 2021 Tesla Model Y disengages due to poor visibility from glare. The distribution is fairly normal around the value 0.89.

We constructed a 99% confidence interval using the frequency data from Figure 7. Since this data is highly leftward skewed, we used Bootstrap resampling: (0.851, 0.899). We

DOI: 10.36838/IJHSR87.308

used the lower value, 0.851, as the cutoff for a 2021 Tesla Model Y being disengaged while on full autopilot.



Figure 8: This map illustrates the roads in Fremont, California, which have a solar cost function value greater than 0.851 at 7:50 PM on June 19, 2025. The roads facing northwest to southeast are the ones most affected by sun glare during this time.

We evaluated another 500 random westward-facing paths for $\alpha \in [0, 1]$ at 7:50 PM in Fremont, a suburban city; San Francisco, an urban city; and Gilroy, a rural city, on June 19, 2025, and report statistically significant results for any improvement in the number of 2021 Tesla Model Y disengagements and travel time. We measured a disengagement as a simple aggregate of the number of roads a commuter goes on, which has a sun glare weight of over 0.851. Figure 8 shows all such roads in Fremont, California, at 7:50 PM on June 19, 2025.

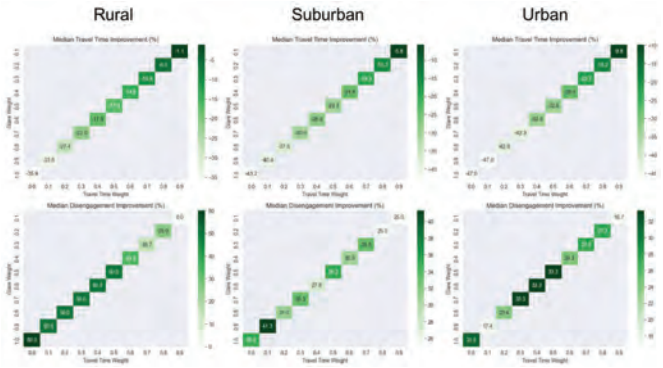

Figure 9: This figure compares the percentage changes in travel time and number of disengagements between the benchmark path and the sun-aware path for rural, suburban, and urban towns. Values of α from 0 to 1 in increments of 0.1 are evaluated.

Similarly to the previous grid-search, it is evident from Figure 9 that increasing the glare-weight parameter (α) lowers both the mean and median number of autopilot disengagements, whereas raising the travel-time weight (1-α) lowers the mean and median extra travel time. In order to find the weights that result in an improvement in the number of disengagements while keeping the travel time to within 20% of the benchmark value, we use two Wilcoxon signed rank tests again.

The first test evaluated whether sun-aware routes reduced the number of disengagements, asking whether the median percent change in the number of high-glare segments between the calculated path and benchmark path was greater than zero. The second test evaluated whether the increase in travel time remained acceptable, testing whether the median percent change in travel time did not exceed 20%. Table 4 shows the p-values for each α-value across rural, suburban, and urban settings.

Table 4: Number of disengagements and travel time improvement p-values for different α in Gilroy (rural), Fremont (suburban), and San Francisco (urban). Bold entries indicate statistically significant results from the Wilcoxon Test. Bold and italicized α -values indicate those that satisfy the disengagement and travel time requirements for all geographic areas. An α -value of 0.1 meets all criteria for all types of cities.

α-value	Disengag-ements (Rural)	Disengage-ments (Suburban)	Disengag-ements (Urban)	Travel Time (Rural)	Travel Time (Suburban)	Travel Time (Urban)
0.1	**< 0.001**	**< 0.001**	**< 0.001**	**< 0.001**	**< 0.001**	**< 0.001**
0.2	**< 0.001**	**< 0.001**	**< 0.001**	**< 0.001**	0.169	0.253
0.3	**< 0.001**	**< 0.001**	**< 0.001**	**< 0.001**	0.999	>0.999
0.4	**< 0.001**	**< 0.001**	0.220	**0.009**	> 0.999	> 0.999
0.5	**< 0.001**	**< 0.001**	**0.026**	0.789	> 0.999	> 0.999
0.6	**< 0.001**	**< 0.001**	**0.060**	0.992	> 0.999	> 0.999
0.7	**< 0.001**	**< 0.001**	**0.072**	> 0.999	> 0.999	> 0.999
0.8	**< 0.001**	**< 0.001**	0.3801	> 0.999	> 0.999	> 0.999
0.9	**< 0.001**	**< 0.001**	0.278	> 0.999	> 0.999	> 0.999
1.0	**< 0.001**	**< 0.001**	**0.035**	> 0.999	> 0.999	> 0.999

In the rural city of Gilroy (Table 4), the α-values of 0.1, 0.2, 0.3, and 0.4 all produce statistically significant decreases in the number of disengagements while keeping the travel time to within a 20% increase of the benchmark. In the suburban city of Fremont (Table 4), the α-values of 0.1 and 0.2 are the only ones that lead to such results. In the urban city of San Francisco (Table 4), only α = 0.1 produces statistically significant results. Table 5 shows a summary of the results from the statistical analysis.

Table 5: This table summarizes the values of α , which both decrease the number of disengagements and keep the travel time within a 20% increase of the benchmark. An α-value of 0.1 meets all criteria for all types of cities.

City Type	*α*-value	Median Number of Disengagements Reduction (%)	Median Travel Time Increase (%)
Rural	0.1	0.0	1.1
	0.2	25.0	6.0
	0.3	16.7	10.9
	0.4	33.3	14.6
Suburban	0.1	25.0	5.8
	0.2	25.0	15.3
Urban	0.1	16.7	9.8

Discussion & Limitations

The statistical analysis shows that a dynamic sun-aware routing algorithm can measurably reduce sun glare exposure without disproportionately increasing travel time. Despite these improvements, there still exist certain limitations to the algorithm. Firstly, the glare model does not currently incorporate roadside obstacles such as buildings, foliage, or overpasses, which could significantly alter glare. Secondly, the glare calculated on curved roads may be inaccurate due to the straight-road approximation, which was used while assigning weights to edges. Thirdly, these are pilot results gleaned from a sample size of one. Lastly, the evaluation algorithm ignores possible confounding variables like traffic conditions and other route differences. These issues are deferred to future work, which may include obstacle-aware glare, integration with high-resolution 3D map data, and a real-time traffic API.

The results confirm that for α-values of 0.1 and 0.2, the routing algorithm achieves statistically significant reductions in aggregate glare while keeping travel times within 20% of the benchmark path. In addition to improving glare metrics, the sun-aware algorithm shows potential for mitigating autonomous vehicle disengagements. Using disengagement data collected from a 2021 Tesla Model Y operating under full self-drive, we observed that glare-optimized routes reduced the number of high-glare roads (defined as edges in the graph with a glare function value exceeding 0.851) by up to 33.3% for $\alpha = 0.2$. These results indicate that glare-aware routing has direct applications in enhancing the safety and reliability of semi-autonomous vehicles that rely on camera-based feeds like the 2021 Tesla Model Y.

This work provides evidence that incorporating solar angle and atmospheric data into path planning can improve both human and autonomous navigation safety. The results demonstrate that glare-aware routing is a viable addition to existing navigation systems, particularly for commutes facing the sunrise and sunset.

Conclusion

This work introduces a sun-aware routing algorithm that integrates real-time solar position and atmospheric data into a modified A* search framework. By modeling glare as a function of solar geometry and cloud cover, we enable safer commutes, especially during sunrise and sunset. Across 500 westward test routes, our method reduced aggregate glare by a mean of 34.9% with only an 18.9% increase in travel time, and we identified a statistically significant optimal glare-weighting parameter ($\alpha = 0.1, 0.2$). These findings suggest that incorporating environmental context into routing can directly enhance driving safety.

Future work can improve the model's realism by incorporating 3D obstacle modeling using Google Street View data, as demonstrated in Guo *et al.*'s work. Dynamic traffic conditions could be integrated via APIs such as the TomTom Traffic API, while the weather model could be expanded to capture additional atmospheric effects, including the wavelength dependence of perceived glare. Evaluation could also be extended to a broader range of camera-based autonomous vehicles to better determine the glare-related disengagement threshold. Lastly, incorporating user-centered assessments of glare perception would provide a better understanding of safety and comfort impacts.

In terms of real-world adoption, this approach could be implemented as an optional routing feature in commercial navigation and autonomous driving systems, similar to existing options like "avoid highways" or "avoid tolls." Since these platforms already utilize real-time weather and satellite data, calculating solar position, cloud coverage, and glare intensity would require minimal additional infrastructure. This integration would make sun-aware pathfinding widely accessible, paving the way for safer and more context-aware navigation.

Acknowledgments

I would like to thank my mentor, Dr. Julia Milton, and the Indigo Research team.

References

1. S. Singh, "Critical reasons for crashes investigated in the National Motor Vehicle Crash Causation Survey," Traffic Safety Facts Crash Stats, Rep. DOT HS 812 506, Mar. 2018.
2. B. Bahnsen and Y. Mayster, "Navigation Suggestions to Select Driving Route with Low Sun Glare," 2022.
3. A. Das, N. R. Schneider, and H. Samet, "Safety-Aware Route Navigation: Driving with Less Sun Glare," in Proceedings of the 32nd ACM International Conference on Advances in Geographic Information Systems, in SIGSPATIAL '24. New York, NY, USA: Association for Computing Machinery, Nov. 2024, pp. 497–500. doi: 10.1145/3678717.3691225.
4. Y. Guo, J. Hu, R. Wang, S. Qu, L. Liu, and Z. Li, "Study on the influence of sun glare on driving safety," Building and Environment, vol. 228, p. 109902, Jan. 2023, doi: 10.1016/j.buildenv.2022.109902
5. X. Li, B. Y. Cai, W. Qiu, J. Zhao, and C. Ratti, "A novel method for predicting and mapping the presence of sun glare using Google Street View," Aug. 05, 2018, arXiv: arXiv:1808.04436. doi: 10.48550/arXiv.1808.04436.

Author

Rohin Vig is a high school student passionate about physics, computer science, research, and entrepreneurship. He enjoys applying computation to real-world problems and has led multiple independent research and entrepreneurship projects. Outside of academics, he builds educational tools and learns advanced topics in mathematics and physics.

DOI: 10.36838/IJHSR87.308

IJHSR
ijhighschoolresearch.org
REVIEW ARTICLE

The Relationship Between Stress and Fecundability: A Global Perspective

Misaki Tsukada

Clear Lake High School, 2929 Bay Area Blvd, Houston, TX, 77058, USA; misaki261603@gmail.com
Mentor: Bre Calhoun

ABSTRACT: Infertility affects approximately 1 in 6 adults worldwide, and evidence suggests that psychological and environmental stress affects women's reproductive system, including reducing the chances of pregnancy. There is limited data on unique characteristics and regulations that contribute to stress factors that lead to infertility globally. This review aims to provide a comprehensive review of different stressors, with a comparison between North America, Europe, and Asia, and their relationship with fecundability, which is defined as the probability of conception in a given menstrual cycle. Higher exposure to work and financial stressors, psychological stressors, and endocrine-disrupting chemicals was associated with higher infertility rates. These results indicate that infertility rates were positively linked with each region's stress factors. In future studies, the effects of stress factors should be examined in men as well to gain knowledge of how both partners may play a role in infertility. To mitigate the deterioration of human reproductive function, further action for awareness and resources for the prevention of stress factors must be provided to maintain a healthy reproductive population.

KEYWORDS: Biology, Medical and Health Sciences, Infertility, Fecundability, Stress.

Introduction

Understanding human reproductive function is vital for our life on Earth. The worldwide deterioration of human reproductive function is a serious public health concern.[1,2] One aspect of the human reproductive system, infertility, affects 17.5% of the world population.[3] The World Health Organization (WHO) recently declared an urgent need to increase access to affordable fertility care for those in need. However, increasing access to affordable fertility care does not directly address the underlying contributors to infertility.

Stress can be caused by several factors, such as environmental and psychological factors. Existing literature suggests that there is a correlation between women's psychological stress and lower fecundability.[4–6] For example, in a study aimed to examine the "association between perceived stress among men and women and fecundability in a North American cohort of couples planning a pregnancy," the authors found that women with baseline PSS (Perceived Stress Scale) of higher than 10 and equivalent or less than 25 had a fecundability ratio of 0.96, indicating reduced conception.[7] Furthermore, in another study that aimed to "provide a first look at the prospective association between stress and TTP and infertility in a cohort of US women," women who had high salivary biomarkers of stress (alpha-amylase) showed a 29% decreased odds of conception and a longer time-to-pregnancy.[8] However, both of these papers lacked details on other stress factors, including environmental stressors. Additionally, in a study based in Shanghai that examined the effect of human exposure to endocrine-disrupting chemicals, it was reported that women with the highest quartile of BPA (bisphenol A) in their urine samples had a 30% reduction in fecundability.[2] Furthermore, in a review paper that studied the impact of endocrine-disrupting chemicals (EDCs) on fertility, the literature revealed that EDCs are major risk factors for ovarian function and aging.[9] When it comes to chemical absorption, where individuals live can greatly affect how much they take in. However, the current literature lacks a review of the worldwide consumption of chemicals.

To our knowledge, previous studies that have examined the effects of stress on fertility lacked a comprehensive review of different stressors involving a comparison between countries.[2,5] Our study aims to provide a comprehensive review of the impact of environmental and psychological factors on fecundability with an emphasis on a global perspective, using literature obtained from PubMed. The details of this review may highlight a critical need to shift infertility remedies from external (i.e., medications) to internal intervention (i.e., lifestyle choices), which would mitigate the invisible problems inside, encouraging natural, sustainable results.

Discussion

Infertility:

Infertility is defined as the "failure to achieve a pregnancy after 12 months or more of regular unprotected sexual intercourse."[3] There is no significant difference in the infertility rates across low- and high-income countries.[3] Despite the advantages that high-income countries have compared to low-income countries, developed nations have experienced higher rates of infertility (+13.2%) than underdeveloped nations (+2.4%).[10] Infertility can lead to detrimental effects on the patient, including but not limited to psychological, physical, spiritual, and biomedical factors.[11] Infertility is not an individual-level problem as it affects the patient and the patient's partner as a couple (dyad), disrupting the entire family dynamic. Contrastingly, fecundity – defined as the biological capacity to reproduce – is

© 2026 Terra Science and Education

DOI: 10.36838/IJHSR87.315

seen as the exact opposite of infertility.[12] Similarly, fertility, as defined by the European Union, is the ability to conceive and give birth to children.[13] In this review, the two terms (fecundity and fertility) will be used interchangeably.

Although infertility is a global health challenge, common causes and treatments vary across regions. While almost all high-income nations provide universal healthcare, except the United States of America, not every citizen's internal health satisfies the criteria to conceive naturally, indicating the need to focus on additional factors, such as internal intervention (i.e., lifestyle choices) for infertility remedies.

North America:

In recent available data, the Centers for Disease Control and Prevention (CDC) states that 8.5% of married women between the ages of 15-49 years are infertile, which equates to 2.4 million women in the United States.[14] Within those women, 12.2 % of them received infertility service(s), including but not limited to medical advice, infertility testing for women and men, and ovulation drugs. In addition, among the developed countries, the United States has the highest maternal mortality rate.[15] In Canada, approximately 16% of couples experience infertility, doubling its prevalence from the 1980s.[16] This indicates that even though there have been medical advances made in infertility care since the 1980s, the rate of infertility has grown over the years. According to the Pacific Centre for Reproductive Medicine, Canada's increase in infertility may be due to attempting to have the first child later in life, which comes with adverse maternal risk, with 31.4 years being the average age of mothers at the time of childbirth.[16] Although both countries (the US and Canada) are considered to be high-income countries with infertility resources, infertility rates are still increasing.

Asia:

Due to diminished fertility desire and capacities, the Asia-Pacific region has been experiencing an increase in infertility from 1990 to 2021, impacting its population structure.[17] For example, the Philippines has one of the highest infertility rates in Asia, with the fastest growing infertility rate (5.33% annually), whereas Pakistan had the highest infertility rate in 1990, but has declined annually by 3.29% over the past 30 years.[17] Japan, which is considered to be one of the high-income countries, has an aging population and a declining birth rate, which puts Japan's population health in danger.[18] According to the Chinese Centers for Disease Control and Prevention, the increase in polycystic ovary syndrome (PCOS) prevalence in Asia occurred within the same time period as the increase in infertility, indicating that PCOS is likely to be a significant contributor to infertility.[17] The rise of infertility across Asia, with low-income and high-income countries, shows that socioeconomic status is not the only contributing factor to the infertility rate.

Europe:

In 2023, the total fertility rate in Europe was 1.38 live births per woman, with 46.4% of those births being first-born children.[19] In Denmark, the fertility rate in 2000 was 1.8 births per woman compared to 1.5 births per woman in 2023, indicating a decline.[20] In European countries with the strongest primary care systems, such as the United Kingdom and the Netherlands, midwives outnumber obstetrician-gynecologists (ob-gyn), which is different from other countries like the United States, where midwife services are not typically covered by insurance plans. The availability of options for mothers regarding maternal care may play a significant role for women when deciding if they would like to have children. Unlike the United States, many high-income countries, including France, Germany, Norway, and Switzerland, have guaranteed postpartum home visits covered under national insurance, indicating stronger national postpartum care for mothers than the U.S.[15] Furthermore, Europe's maternal mortality ratio is 25 times lower than the global average, with 8 deaths per 100,000 live births.[21]

Stressors

Stress can be triggered by changes and challenges, which then lead to physical, emotional, and behavioral responses.[22] Evidence suggests that psychological and environmental stressors are associated with fecundability.

Psychological stressors:

Within the reproductive population, 20-25% of women and 18-21% of men are reported to have psychological stress, which is linked with cardiovascular and mental illness, as well as accelerated disease progression.[7] Common symptoms of psychological stress include (1) aches and pains, (2) exhaustion or trouble sleeping, (3) weakened immune system, and (4) anxiety and sadness.[22] Stress can also cause an increase in blood pressure and cortisol.[7] Psychological stressors can include any stress factor that is common in everyday situations, including relationship and financial factors.

Relationship stressors:

Common examples of relationship stressors include marital status, cultural expectations/gender roles, and religious expectations. For example, according to a Korean study, their traditional gender roles (women's increased load of responsibility as the primary caregiver) affect Korean women's quality of life at home and at work, which makes maintaining work-life balance harder for women than men.[23] Thus, gender expectations and roles can put stress on women, making their bodies less suitable for pregnancy. Additionally, the predominant religion in the Philippines is Catholic, which is commonly known to practice strong beliefs around contraception and abortion; this may be a factor that affects its citizens by limiting reproductive health services.[17,24]

Work & financial stressors:

Work stress has been associated with irregular menstruation, leading to polycystic ovary syndrome (PCOS) and infertility.[25] In North America, maternal leave regulations vary across countries. For example, the United States does not have a paid maternity leave regulation. Maternity leave regulation allows

"up to 12-weeks of unpaid, job-protected leave per year," according to the Family and Medical Leave Act (FMLA).[26] The lack of paid maternity leave creates stress on citizens, as some cannot afford to go without their paychecks. Contrastingly, Canada offers paid maternity leave for up to 15-weeks, and up to 69-weeks of shared parental leave is also provided, but at a lower pay rate.[27] Similarly, the European Union offers paid maternity leave, providing women with the right to receive at least 14-weeks of leave with compensation.[28] These federal regulations can contribute to one's stress level with financial and mental aspects of family planning, making the work environment a significant stress factor. For example, employees in the United States may experience a greater amount of work stress compared to those in Canada or Europe due to the differences in the regulations, which may affect one's ability to conceive. Although the Korean government advocates for a healthier work-life balance by establishing policies that help citizens with family planning, Korean organizations also have strict management practices, indicating that their cultural norms and expectations may be intertwined with work stress to create a significant mental burden on women.[23]

Environmental stressors:

A significant example of an environmental stressor that is easily accessed by people worldwide is Bisphenol-A, which is commonly known as BPA. BPA is one of the endocrine-disrupting chemicals (EDC) and is recognized as a reproductive toxicant.[2] Aside from fertility damage, the European Union has classified BPA as a hazardous chemical due to its ability to cause serious eye damage, allergic skin reactions, and respiratory irritation. BPA, which is used to make polycarbonate plastics and epoxy resins, is found in canned containers, reusable water bottles, plastic food containers, and receipts. Additionally, women naturally have higher interaction with EDCs than men due to cosmetic usage, increasing their exposure to harmful chemicals. Different regions have different exposure levels of BPA, mainly due to government policies. For example, according to the European Commission, the European Union has banned the use of BPA on items that are used for food or drink packaging, reducing the amount of its citizens coming in contact with one of the most accessible endocrine-disrupting chemicals.[29] This regulation highlights the region's preventative actions to prevent exposure to BPA and its harmful effects. Although data comparison between Asia and North America is sparse, both regions likely consume more BPA than Europe, considering that China leads in the production and consumption of BPA.[30]

■ Relationship between stress and fecundability

Existing literature suggests that women's stress is associated with lower fecundability, including psychological and environmental stress factors.[2,7] Women with no pre-existing reproductive disorder can also have altered reproductive function from everyday stress, indicating a positive relationship between stress and infertility.[31]

According to a study that aimed to "assess the relationship between psychological stress and fecundability," the author found that there was an inverse association between perceived stress and fecundability.[7] The study used residents from the United States and Canada and the Perceived Stress Scale (PSS) to examine the relationship. Researchers also found that women with a PSS score of less than 10 had fecundability ratios (FRs) of 0.96, while women with a PSS score greater than 25 had FRs of 0.87, indicating that the more stress a woman experiences, the less likely for them to get pregnant.[7] In addition, the study revealed that couples in which both partners had a <10 PSS score showed higher fecundability, indicating that couples experiencing less stress in their relationship are more likely to conceive.[7] Similarly, in a Chinese study aimed to "investigate the association between female pre-pregnancy allostatic load and time to pregnancy," the authors found that compared to the population group with an allostatic load score of 0, there was a 59% reduction in the chance of fertility in the group with the highest allostatic load score (5-6), further suggesting that higher stress level leads to longer time to pregnancy.[32]

In a 2021 study by Negris and colleagues, researchers aimed to "understand the beliefs about a causal role of emotional stress maintained by women seeking fertility care."[33] The authors acquired responses from 1460 people in a pool of patients from Northwestern Center for Fertility and Reproductive Medicine on their understanding of the relationship between stress and fecundability. Researchers found that more than half of the women (69%) believe the success of fertility treatment can be reduced by emotional stress.[33] Thus, in the pregnant seeking population, the relationship between stress and fecundability is relatively well-known. The belief was especially prominent in the population with less than a bachelor's degree (75%), and those with an annual household income of less than $50,000 (73.2%), indicating individuals with lower levels of education and more financial instability believed that stress was more likely to impact fecundability.[33]

Additionally, in a study that examined the association between environmental stressors, BPA, and fecundability, researchers recruited Chinese couples in Shanghai who were at least 20 years of age.[2] Urine samples were used to determine the concentration of BPA. Researchers found that women with the highest quartile of BPA in their urine samples had a 30% reduction in fecundability and 64% increase in odds of infertility, showing inverse associations with BPA and fecundability.[2] The study's findings also highlighted that women over the age of 30 had a stronger association with BPA and infertility, indicating that age may also be a factor in the effect of BPA on women's bodies. This raises additional questions of whether age affects the reproductive system's ability to process BPA in their system or whether individuals have accumulated higher level or BPA over the years with age. This association between BPA and fecundability in China may reflect their increased exposure to BPA compared to other regions, given that China has the greatest consumption of BPA worldwide.[30] Similarly, in another Chinese study that aimed to "evaluate the relationships of bisphenol analogs with female fecundability

DOI: 10.36838/IJHSR87.315

and infertility," researchers found that there was a significant association between fecundability and BPA and its alternative, Bisphenol AP (BPAP), with a 13% reduction in fecundability and 36% reduction, respectively.[34] However, in a study conducted in the Netherlands to "evaluate associations of urinary bisphenols and phthalate metabolites with TTP among 877 women participating in a large population-based pregnancy cohort," researchers found a weak association between BPA and fecundability.[35] The result showed a fecundability ratio of 0.93 for women with inadequate folic acid supplement use and 1.00 for women with folic acid supplement use, indicating that although the intake of folic acid supplements has effects on the chance of conception with BPA (and great impacts on fetal development), the maximum reduction in the fecundability ratio is only 7%.[35] The restricted use of BPA in the European Union is reflected in this weaker association between BPA concentration and fecundability.

Although stress has been identified as a risk factor for infertility, it may also be the result of infertility. Assessing the cyclic mechanism of this condition is critical in understanding how infertility and stress interplay with one another.

Cycle of stress:

Existing literature suggests that there is a significant psychological burden on women struggling with infertility; 29% of infertile women were stressed, with a high prevalence of anxiety (63%) and depression (67%).[36] Additionally, women who place a higher value on motherhood and those without prior pregnancies are more likely to display psychological stress, indicating that one's own pressure, possible societal norms, or parity can also affect women's psychological experience with infertility.[37] The results of the study show that not only can it contribute to infertility, but infertility can also lead to stress, creating a feedback loop. Often, the stress associated with infertility or infertility treatments may also harm the person's relationship with their partner and others involved in their life, contributing to the relationship stress factor referenced above. This constant cycle can be detrimental to women's mental and physical health, which may further lower their fecundity.

■ Strengths and Limitations

A strength of this review is the inclusion of two types of stressors, whereas other studies focused on one stressor. While the term "stress" is commonly associated with psychological stress that an individual may feel, this review provided insight into environmental stressors that individuals may not be aware of. This review reveals that it is important to be aware of these environmental factors due to the significance of chemical stressors and the impacts it has on infertility. This review also compared data and analysis from three distinct regions of the world, including North America, Asia, and Europe, which provided a global perspective on the relationship between fecundability and stress. By doing so, the review was able to highlight the consumption level of each stress factor with infertility rates in correlation to each region's characteristics and regulations. However, the review lacked perspective on how the male's stress impacts fertility. Understanding how males' psychological and environmental stress affects fecundability may provide additional insights into the roles of each stressor.

■ Conclusion

This review found that psychological stress negatively impacts fecundability, with both work and financial, as well as relationship stressors, leading to a longer time to pregnancy. Additionally, a common EDC, BPA, was found to decrease the chance of fecundability, indicating that environmental stress factors can contribute to infertility. These key components highlight the need to shift infertility treatment focus from external medical interventions to internal evaluation of how our stress levels may be impacting conception abilities to ensure feasible and sustainable outcomes. Future research should incorporate studies on how the stress of males impacts their reproductive system and how this affects fecundability to further strengthen the knowledge of how stress affects fecundability in dyads.

■ Acknowledgments

I would like to thank my mentor, Bre Calhoun, for her guidance throughout my process of conducting the research and the development of this paper. Additionally, I would like to thank Crimson Education and Indigo Research for their immense support throughout the research process. Lastly, I would like to thank my parents, Yasuhiro Tsukada and Yoko Tsukada, for their guidance and support.

■ References

1. Konishi, S.; Kariya, F.; Hamasaki, K.; Takayasu, L.; Ohtsuki, H. Fecundability and Sterility by Age: Estimates Using Time to Pregnancy Data of Japanese Couples Trying to Conceive Their First Child with and without Fertility Treatment. *Int. J. Environ. Res. Public. Health* **2021**, *18* (10), 5486. https://doi.org/10.3390/ijerph18105486.
2. Wang, B.; Zhou, W.; Zhu, W.; Chen, L.; Wang, W.; Tian, Y.; Shen, L.; Zhang, J.; Shanghai Birth Cohort Study. Associations of Female Exposure to Bisphenol A with Fecundability: Evidence from a Preconception Cohort Study. *Environ. Int*. **2018**, *117*, 139–145. https://doi.org/10.1016/j.envint.2018.05.003.
3. *1 in 6 people globally affected by infertility: WHO*. https://www.who.int/news/item/04-04-2023-1-in-6-people-globally-affected-by-infertility (accessed 2025-07-31).
4. Buck Louis, G. M.; Lum, K. J.; Sundaram, R.; Chen, Z.; Kim, S.; Lynch, C. D.; Schisterman, E. F.; Pyper, C. Stress Reduces Conception Probabilities across the Fertile Window: Evidence in Support of Relaxation. *Fertil. Steril.* **2011**, *95* (7), 2184–2189. https://doi.org/10.1016/j.fertnstert.2010.06.078.
5. Schliep, K. C.; Mumford, S. L.; Vladutiu, C. J.; Ahrens, K. A.; Perkins, N. J.; Sjaarda, L. A.; Kissell, K. A.; Prasad, A.; Wactawski-Wende, J.; Schisterman, E. F. Perceived Stress, Reproductive Hormones, and Ovulatory Function: A Prospective Cohort Study. *Epidemiol. Camb. Mass* 2015, 26 (2), 177–184. https://doi.org/10.1097/EDE.0000000000000238.
6. Hong, X.; Yin, J.; Zhao, F.; Wang, W.; Ding, X.; Yu, H.; Wang, B. Female Fecundability Is Associated with Pre-pregnancy Allostatic Load: Analysis of a Chinese Cohort. *Acta Obstet. Gynecol. Scand.* **2022**, *101* (11), 1300–1307. https://doi.org/10.1111/aogs.14443.

7. Wesselink, A. K.; Hatch, E. E.; Rothman, K. J.; Weuve, J. L.; Aschengrau, A.; Song, R. J.; Wise, L. A. Perceived Stress and Fecundability: A Preconception Cohort Study of North American Couples. *Am. J. Epidemiol.* **2018**, *187* (12), 2662–2671. https://doi.org/10.1093/aje/kwy186.
8. Lynch, C. D.; Sundaram, R.; Maisog, J. M.; Sweeney, A. M.; Buck Louis, G. M. Preconception Stress Increases the Risk of Infertility: Results from a Couple-Based Prospective Cohort Study--the LIFE Study. *Hum. Reprod. Oxf. Engl.* **2014**, *29* (5), 1067–1075. https://doi.org/10.1093/humrep/deu032.
9. Tricotteaux-Zarqaoui, S.; Lahimer, M.; Abou Diwan, M.; Corona, A.; Candela, P.; Cabry, R.; Bach, V.; Khorsi-Cauet, H.; Benkhalifa, M. Endocrine Disruptor Chemicals Exposure and Female Fertility Declining: From Pathophysiology to Epigenetic Risks. *Front. Public Health* **2024**, *12*, 1466967. https://doi.org/10.3389/fpubh.2024.1466967.
10. Borumandnia, N.; Majd, H. A.; Khadembashi, N.; Alaii, H. Assessing the Trend of Infertility Rate in 198 Countries and Territories in Last Decades. *Iran. J. Public Health* **2021**, *50* (8), 1735–1737. https://doi.org/10.18502/ijph.v50i8.6840.
11. Walker, M. H.; Tobler, K. J. Female Infertility. In *StatPearls*; StatPearls Publishing: Treasure Island (FL), 2025.
12. Smarr, M. M.; Sapra, K. J.; Gemmill, A.; Kahn, L. G.; Wise, L. A.; Lynch, C. D.; Factor-Litvak, P.; Mumford, S. L.; Skakkebaek, N. E.; Slama, R.; Lobdell, D. T.; Stanford, J. B.; Jensen, T. K.; Boyle, E. H.; Eisenberg, M. L.; Turek, P. J.; Sundaram, R.; Thoma, M. E.; Buck Louis, G. M. Is Human Fecundity Changing? A Discussion of Research and Data Gaps Precluding Us from Having an Answer. *Hum. Reprod. Oxf. Engl.* **2017**, *32* (3), 499–504. https://doi.org/10.1093/humrep/dew361.
13. *Glossary: Fertility*. https://ec.europa.eu/eurostat/statistics-explained/index.php?title=Glossary:Fertility (accessed 2025-08-05).
14. *NSFG - Listing I - Key Statistics from the National Survey of Family Growth.* https://www.cdc.gov/nchs/nsfg/key_statistics/i-keystat.htm (accessed 2025-08-03).
15. *Maternal Mortality and Maternity Care in the United States Compared to 10 Other Developed Countries.* https://doi.org/10.26099/411v-9255.
16. *Infertility in Canada: Breaking the Silence and Normalizing the Conversation*. Pacific Centre for Reproductive Medicine. https://www.pacificfertility.ca/blog/infertility-in-canada-breaking-the-silence-and-normalizing-the-conversation (accessed 2025-08-06).
17. Luo, Y.; Hong, C.; Fan, H.; Huang, Y.; Zhong, P.; Zhao, Y.; Zheng, X. Trends and Distribution of Infertility — Asia Pacific Region, 1990–2021. *China CDC Wkly.* **2024**, *6* (28), 689–694. https://doi.org/10.46234/ccdcw2024.155.
18. Hara, K.; Kuroki, M.; Shiraishi, S.; Matsumura, S.; Ito, S.; Kurasawa, K.; Arimoto, A.; Matsuzaki, Y. Evaluation of Planned Number of Children, the Well-Being of the Couple and Associated Factors in a Prospective Cohort in Yokohama (HAMA Study): Study Protocol. *BMJ Open* **2024**, *14* (2), e076557. https://doi.org/10.1136/bmjopen-2023-076557.
19. *Fertility statistics.* https://ec.europa.eu/eurostat/statistics-explained/index.php?title=Fertility_statistics (accessed 2025-08-07).
20. *World Bank Open Data.* World Bank Open Data. https://data.worldbank.org (accessed 2025-08-17).
21. Ritchie, H. If We Can Make Maternal Deaths as Rare as in the Healthiest Countries, We Can Save 275,000 Mothers Each Year. *Our World Data* **2025**.
22. *What Is Stress?*. Cleveland Clinic. https://my.clevelandclinic.org/health/diseases/11874-stress (accessed 2025-08-10).
23. Kim, N.; Kim, K. N.; Baek, P. Understanding South Korean Women Workers' Career Transition Experiences: Using the Career Decision Tree Model. *Front. Psychol*. 2024, 15, 1273241. https://doi.org/10.3389/fpsyg.2024.1273241.
24. iclrs. *@Philippines: Country Info - International Center for Law and Religion Studies*. https://www.iclrs.org/blurb/philippines-country-info/ (accessed 2025-09-02).
25. Luo, Y.; Hong, C.; Fan, H.; Huang, Y.; Zhong, P.; Zhao, Y.; Zheng, X. Trends and Distribution of Infertility — Asia Pacific Region, 1990–2021. *China CDC Wkly*. **2024**, *6* (28), 689–694. https://doi.org/10.46234/ccdcw2024.155.
26. *Family and Medical Leave (FMLA)*. DOL. https://www.dol.gov/general/topic/benefits-leave/fmla (accessed 2025-08-10).
27. Canada, S. *EI maternity and parental benefits: What these benefits offer.* https://www.canada.ca/en/services/benefits/ei/ei-maternity-parental.html (accessed 2025-08-10).
28. *EU legislation on family leaves and work-life balance - European Commission.* https://commission.europa.eu/strategy-and-policy/policies/justice-and-fundamental-rights/gender-equality/women-labour-market-work-life-balance/eu-legislation-family-leaves-and-work-life-balance_en (accessed 2025-08-10).
29. *Commission adopts ban of Bisphenol A in food contact materials - European Commission*. https://food.ec.europa.eu/food-safety-news-0/commission-adopts-ban-bisphenol-food-contact-materials-2024-12-19_en (accessed 2025-09-01).
30. Wang, J.; Chan, F. K. S.; Johnson, M. F.; Chan, H. K.; Cui, Y.; Chen, J.; Chen, W.-Q. Material Cycles, Environmental Emissions, and Ecological Risks of Bisphenol A (BPA) in China and Implications for Sustainable Plastic Management. *Environ. Sci. Technol.* **2024**, *59* (3), 1631–1646. https://doi.org/10.1021/acs.est.4c09876.
31. Schliep, K. C.; Mumford, S. L.; Vladutiu, C. J.; Ahrens, K. A.; Perkins, N. J.; Sjaarda, L. A.; Kissell, K. A.; Prasad, A.; Wactawski-Wende, J.; Schisterman, E. F. Perceived Stress, Reproductive Hormones, and Ovulatory Function: A Prospective Cohort Study. *Epidemiol. Camb. Mass* **2015**, *26* (2), 177–184. https://doi.org/10.1097/EDE.0000000000000238.
32. Hong, X.; Yin, J.; Zhao, F.; Wang, W.; Ding, X.; Yu, H.; Wang, B. Female Fecundability Is Associated with Pre-pregnancy Allostatic Load: Analysis of a Chinese Cohort. *Acta Obstet. Gynecol. Scand.* **2022**, *101* (11), 1300–1307. https://doi.org/10.1111/aogs.14443.
33. Negris, O.; Lawson, A.; Brown, D.; Warren, C.; Galic, I.; Bozen, A.; Swanson, A.; Jain, T. Emotional Stress and Reproduction: What Do Fertility Patients Believe? *J. Assist. Reprod. Genet*. **2021**, *38* (4), 877–887. https://doi.org/10.1007/s10815-021-02079-3.
34. Qiu, W.; Yin, S.; Abulaiti, K.; Li, X.; Lu, Y.; Zhang, Q.; Zhan, M.; Zhang, J. Preconception Exposure to Bisphenol A and Its Alternatives: Effects on Female Fecundity Mediated by Oxidative Stress and Ovarian Reserve. *Sci. Total Environ*. **2024**, *957*, 177558. https://doi.org/10.1016/j.scitotenv.2024.177558.
35. Philips, E. M.; Kahn, L. G.; Jaddoe, V. W. V.; Shao, Y.; Asimakopoulos, A. G.; Kannan, K.; Steegers, E. A. P.; Trasande, L. First Trimester Urinary Bisphenol and Phthalate Concentrations and Time to Pregnancy: A Population-Based Cohort Analysis. *J. Clin. Endocrinol. Metab*. **2018**, *103* (9), 3540–3547. https://doi.org/10.1210/jc.2018-00855.
36. Bahadur, A.; Kumari, S.; Mundhra, R.; Khoiwal, K.; Das, A.; Heda, A.; Pathak, A.; Heda, S. Anxiety, Depression, and Quality of Life Among Infertile Women: A Case-Control Study. *Cureus 16* (3), e55837. https://doi.org/10.7759/cureus.55837.
37. Greil, A. L.; Shreffler, K. M.; Schmidt, L.; McQuillan, J. Variation in Distress among Women with Infertility: Evidence from a Population-Based Sample. *Hum. Reprod. Oxf. Engl*. **2011**, *26* (8), 2101–2112. https://doi.org/10.1093/humrep/der148.

DOI: 10.36838/IJHSR87.315

Author

Misaki Tsukada is a senior at Clear Lake High School. Aside from her passion for science, she is also a pre-professional dancer and a varsity choir member. She plans to attend a university in the United States to major in Biology to become a Patent Attorney in the future.

IJHSR
ijhighschoolresearch.org
RESEARCH ARTICLE

Ferrofluid and Its Application in Wound Healing

Eldar Osmonov

Oxford International School, Mira Avenue 153/1, Bishkek, Chuyskaya Oblast, 720040, Kyrgyzstan; jigin2009@gmail.com

ABSTRACT: This study examined the effects of ferrofluids—suspensions of magnetic nanoparticles—on tissue regeneration in *Lumbriculus Variegatus*, an earthworm known for its regenerative ability. Ferrofluids are considered promising in biomedical fields due to their responsiveness to magnetic fields, but their biocompatibility in regenerative systems remains unclear. In this experiment, worms were divided into five groups and exposed to varying concentrations of ferrofluid, with or without magnetic field influence. Regeneration was monitored over six days using behavioral activity scoring and tail regrowth measurements. The results showed a clear dose-dependent decline in regeneration among ferrofluid-treated groups, especially at higher concentrations. The control group exhibited the most robust recovery, while worms exposed to both ferrofluid and magnetic fields showed reduced regrowth and movement. Reproductive inhibition was also observed in all ferrofluid-treated worms. These findings suggest potential toxicity or cellular disruption caused by ferrofluid exposure. While ferrofluids have biomedical potential, this study emphasizes the need for further research on their long-term effects, safety, and interaction with complex biological systems.

KEYWORDS: Biomaterials, Biomaterials and Regenerative Medicine, Regeneration, Earthworms, Ferrofluid.

Introduction

Background information shows why your research is necessary and important. Summarize literature on related work. State the goal of your research and how it differs from current literature at the end of the introduction section. Magnetic nanoparticles (MNPs) have attracted significant attention in recent years due to their multifunctionality and unique behavior under external magnetic fields. Their nanoscale size and high surface area-to-volume ratio,[1] combined with their superparamagnetic properties,[2] allow precise manipulation within biological systems. These traits have positioned MNPs at the forefront of biomedical innovation, enabling advances in targeted drug delivery,[3] magnetic resonance imaging (MRI) enhancement, tissue engineering,[4] and hyperthermia-based cancer therapy.[5]

Among their many biomedical uses, one particularly promising application of MNPs is in wound healing and regenerative medicine. Magnetic fields have been shown to influence critical biological processes such as cell migration and proliferation. Additionally, when integrated into biocompatible systems like ferrofluids, MNPs can deliver these magnetic stimuli in a controlled and localized fashion.[5]

Ferrofluids—stable liquid suspensions of magnetic nanoparticles—are especially appealing because of their ability to be directed by external magnets. This responsiveness allows researchers to guide their movement through tissues,[6] create physical cues for cellular alignment, and apply localized magnetic stimulation for tissue regeneration.[4] Some studies have also demonstrated that ferrofluids may exhibit antimicrobial properties, reducing bacterial growth at wound sites.[7]

These features make ferrofluids strong candidates for non-invasive therapies, offering alternatives to traditional surgical or pharmacological approaches.[4] Their adaptability also makes them suitable for integration with hydrogels, scaffolds, and other delivery platforms,[8] supporting long-term tissue repair strategies.

To examine the biological impact of ferrofluids on regeneration, *Lumbriculus Variegatus* was employed as an earthworm commonly used in ecotoxicological and developmental studies.[9] This species is well-suited for regeneration research due to its robust regenerative ability,[10] transparent body for microscopic analysis, and the ethical advantages it offers over vertebrate models.

This study investigated whether exposure to ferrofluids affects the tail regeneration process in *Lumbriculus Variegatus*. This study was done by comparing regeneration metrics—such as tissue length and morphology—under varying concentrations of ferrofluids and controlled magnetic field exposure.

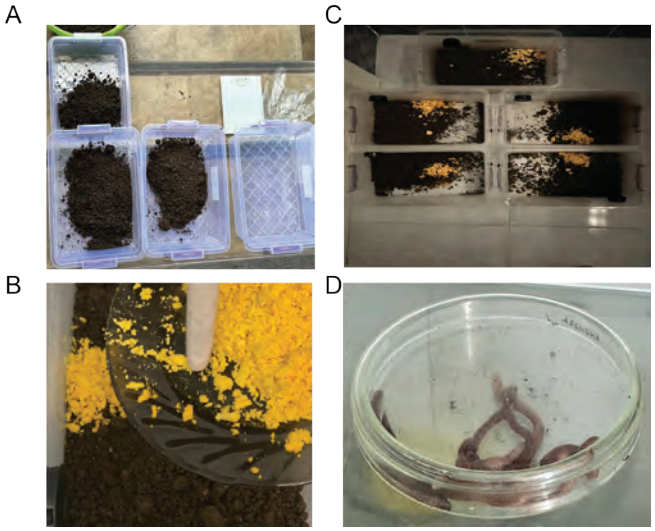

Figure 1: Preparation for the experiments. (A) Preparations of the boxes for 500 g of soil. (B) Feeding worms with 15 g egg yolk. (C) Prepared boxes with 15 g egg yolks. (D) Five worms in a refrigerator at 5 degrees Celsius since cold temperatures work for them as an anesthesia.

© 2026 Terra Science and Education

DOI: 10.36838/IJHSR87.321

Methods

Earthworm care:

For this experiment, earthworms of similar size were housed in plastic containers measuring no less than 30 cm × 20 cm × 15 cm, each filled with 0.5 kg of pesticide-free, nutrient-rich soil to simulate a natural environment as seen in Figure 1A.[11] The containers were kept at a stable temperature between 13–27 ˚C, and dim yellow lighting was used to minimize external stress on the worms. Humidity levels were maintained by adding 70–100 mL of deionized water daily, using digital humidity and temperature sensors to monitor consistency.[9] Earthworms were fed once per week with 15 g of hard-boiled egg yolk only (Figure 1B, C), based on nutritional support for regeneration.[12] Uneaten food was removed after four days to prevent bacterial contamination in the substrate.[11]

Wound induction:

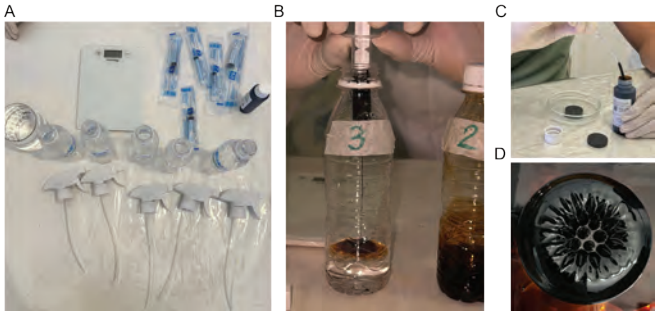

Figure 2: Experimentations with ferrofluid and preparation of the solution. (A) Equipment needed to create different ferrofluid concentrations. (B) Mixing ferrofluid concentrations. Concentration 1 is 0,75 ml ferrofluids+50ml of water in 500g of soil. Concentration 2 is 1.65 ml of ferrofluids + 50ml of water in 500g of soil. Concentration 3 is 3 ml of ferrofluids + 50ml of water in 500g of soil. Concentration 4 is 1.65 ml ferrofluids + 50ml of water in 500g of soil+external magnet. Concentration 5 is 50ml of water in 500g of soil. (C) Experimenting with ferrofluid. (D) Ferrofluid influenced by a magnet.

To apply an anesthetic effect, the worms were put into the fridge, as seen in Figure 1D. To introduce wounds, each *Lumbriculus Variegatus* was carefully cut transversely just behind the citellum, preserving the anterior part for observation, as this segment retains regenerative ability.[13] All worms were observed daily over seven days, at the same time each day (22:30), to monitor tissue regeneration, changes in behavior, and any discoloration.

Treatment preparation:

To prepare the ferrofluid treatment as seen with the equipment in Figure 2A, a concentration of 3.3 µL of ferrofluid per gram of soil was mixed thoroughly by hand stirring to ensure even distribution without agitating the worms (Figure 2B). Earthworms were divided into five experimental groups, each containing five individuals: a control group receiving only water, a low concentration group with 1.5 µL/g ferrofluid, a medium concentration group with 3.3 µL/g, a high concentration group with 6 µL/g, and a final group exposed to 3.3 µL/g ferrofluid along with a small external neodymium magnet (1 cm diameter × 0.5 cm height) placed outside the container wall.

Results and Discussion

Experiment with ferrofluids:

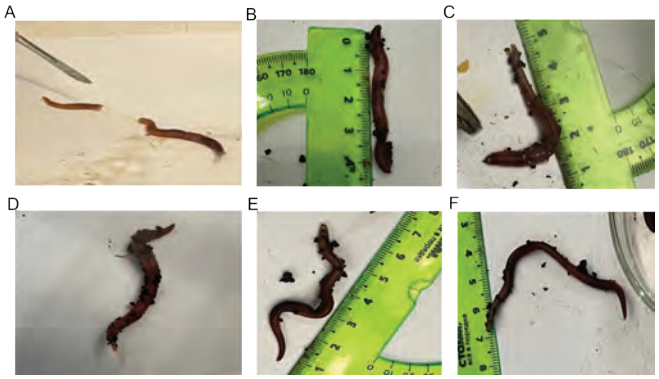

Figure 3: Manipulations with worms, like cutting and measuring. (A) Cutting a worm using sterilized blade (B) Rating 1 out 5 activity rate where 1 is move very little, only when needed to eat (C) Rating 2 out of 5 activity rate where 2 is moving around the box or paper when measured (D) Rating 3 out of 5 activity rate where 3 is moving faster, active, do not move only when they are sleeping (E) Rating 4 out of 5 activity rate where 4 is moving almost in every situation (F) 5 out of 5 activity rate where 5 is always moving, not sleeping at all, will jump if touched.

In Figure 2C, a small volume of ferrofluid was introduced into a petri dish. A strong magnet was placed beneath the dish. Initially, the ferrofluid appeared as a dense black liquid. However, upon approaching the magnetic field, morphological changes were observed. In Figure 2D, the ferrofluid exhibits distinct spiked formations. These patterns resulted from the alignment of magnetic nanoparticles within the fluid in response to the external magnetic field. When the magnet was repositioned, the spikes reoriented accordingly, visually demonstrating the ferrofluid's dynamic response to magnetic influence in real time.

Table 1: Length of individual worm (in cm) Group 1 in six days. D is day.

Worm	Before experiment	After cut	D1	D2	D3	D4	D5	D6
1	5.3	3.8	3.9	4.1	4.2	4.2	4.3	4.4
2	6.4	4.4	4.5	4.7	4.8	4.8	4.8	4.9
3	5.4	4	4	4	4	4.2	4.3	4.5
4	6.2	4.1	4.2	4.3	4.4	4.6	4.8	4.9
5	5.4	4	4.1	4.2	4.2	4.2	4.3	4.3

Table 2: Length of individual worm (in cm) Group 2 in six days. D is day.

Worm	Before experiment	After cut	D1	D2	D3	D4	D5	D6
1	6.3	4.3	4.3	4.4	4.5	4.5	4.6	4.6
2	6	4.2	4.3	4.5	4.6	4.7	4.9	4.9
3	6.4	4.9	5	5.1	5.2	5.2	5.3	5.3
4	5.7	3.7	3.8	3.9	4	4.1	4.3	4.4
5	6.6	4.6	4.6	4.6	4.7	4.8	5	5

Table 3: Length of individual worm (in cm) Group 3 in six days. D is day.

Worm	Before experiment	After cut	D1	D2	D3	D4	D5	D6
1	6.8	4.7	4.7	4.7	4.8	4.9	4.9	X
2	6.4	4	4	4	4	4	4	4
3	6	4	4.2	4.2	4.2	4.2	4.2	4.2
4	6.3	4.7	4.7	4.7	4.8	4.9	5.1	5.1
5	7	4	4.2	4.3	4.4	4.5	4.6	4.6

Table 4: Length of individual worm (in cm) Group 4 in six days. D is day.

Worm	Before experiment	After cut	D1	D2	D3	D4	D5	D6
1	6	4.1	4.2	4.2	4.2	4.2	4.3	4.5
2	6.9	5	5	5.2	5.3	5.7	6	X
3	6.3	5	5	5	5.1	5.1	5.2	5.2
4	7	4.5	4.5	4.5	4.5	4.5	4.6	4.6
5	7.3	4.5	4.5	4.5	4.5	4.6	4.8	5

Table 5: Length of individual worm (in cm) Group 5 in six days. D is day.

Worm	Before experiment	After cut	D1	D2	D3	D4	D5	D6
1	7.4	5	5	5.1	5.2	5.2	5.2	5.2
2	5.3	3.1	3.3	3.4	3.6	3.9	4.3	4.3
3	6.1	3.9	4	4.2	4.4	4.7	4.9	5
4	5.8	3.5	3.6	3.7	3.8	4.2	4.5	4.6
5	5.2	3.9	4	4.1	4.3	4.5	4.9	5

Measurement of Worm Activity and Regeneration:

In Figure 3A, surgical incisions were made using a sterilized blade to initiate the regeneration phase. The objective was to assess the impact of physical injury on both behavioral activity and regenerative capacity over subsequent days. Post-incision, activity levels were recorded and assigned values on a scale from 1 to 5, based on observable movement.

In Figure 3B, minimal spontaneous movement was noted. Only weak responses were elicited upon direct tactile stimulation, resulting in an activity score of 1. Figure 3C displayed slightly increased motility; the subject exhibited occasional movement and directional changes, corresponding to a score of 2. In Figure 3D, moderate, stimulus-responsive movement was observed, leading to a rating of 3. Figure 3E showed higher autonomous activity, with the worm moving without external prompting and remaining mostly active; this behavior was scored as a 4. In Figure 3F, continuous, unprovoked, and rapid movement was documented, warranting the maximum activity rating of 5.

In addition to behavioral scoring, physical regrowth was quantitatively assessed over six days, as shown in Tables 1 through 5. In Table 1, all subjects survived the observation period. Regeneration proceeded steadily; for example, Worm 2 measured 4.4 cm post-incision and reached 4.9 cm by Day 6, with consistent daily increases of approximately 0.1 cm.

Table 2 reflected similar trends, with complete survival and slightly accelerated regrowth in most specimens. Notably, Worm 3 demonstrated enhanced regeneration, growing from 4.9 cm to 5.3 cm.

Table 3 presents more variable outcomes. While most subjects displayed satisfactory regrowth, Worm 1 did not survive past Day 5, despite normal development up to that point. Conversely, Worm 4 showed robust recovery, increasing from 4.7 cm to 5.1 cm.

Table 4 also recorded a mortality: Worm 2 expired prior to Day 6 but had exhibited strong growth up to 6.0 cm by Day 5. Remaining subjects showed modest but stable increases, particularly Worms 3 and 4, which followed a consistent regeneration trajectory without irregularities.

Table 5 yielded the most uniform and reliable results. No mortality occurred, and growth patterns were progressive and uninterrupted across all specimens. Worm 3 exhibited the most pronounced increase, from 3.9 cm to 5.0 cm, with others demonstrating similar trends.

Despite multiple publications reporting that ferrofluids may enhance wound healing or tissue regeneration,[14,15] the findings from this study did not support those conclusions, suggesting that exposure to ferrofluids would increase regeneration rates in *Lumbriculus variegatus*. However, the findings from this study did not support that hypothesis.

As shown in Figure 4, regeneration rates were noticeably suppressed in all groups treated with ferrofluid, especially at higher concentrations. Group 3 (3 mL) demonstrated the weakest regeneration trend, with barely any growth observed beyond Day 2. Group 4 (1.65 mL + magnet) also showed reduced regrowth, suggesting that the presence of a magnetic field may intensify the inhibitory effects of ferrofluid exposure.

By contrast, Group 5 (control) exhibited the most robust and consistent regeneration over the six days, with the highest normalized average length on Day 6. Groups 1 and 2, exposed to lower concentrations of ferrofluid (0.75 mL and 1.65 mL, respectively), showed intermediate results. While slight increases in length were observed, they lagged significantly behind the control. This dose-dependent decline in regenerative performance indicates a likely biological sensitivity to ferrofluid concentration.

Furthermore, reproductive inhibition was observed in all ferrofluid-treated groups. No offspring were recorded, in contrast to the control group, which demonstrated both tissue regrowth and successful reproduction. This finding supports previous evidence that ferrofluids may interfere with cellular or reproductive systems. The possibility that magnetic nanoparticles disrupt internal signaling or cellular integrity at the reproductive level should be explored in future investigations.

Overall, the data from Figure 4 visually emphasize that the presence and concentration of ferrofluid—particularly in conjunction with magnetic fields—correlates with impaired biological recovery and function. These findings contrast with earlier optimistic assessments and highlight the need for further research into the biocompatibility of ferrofluids under varying environmental and physiological conditions.

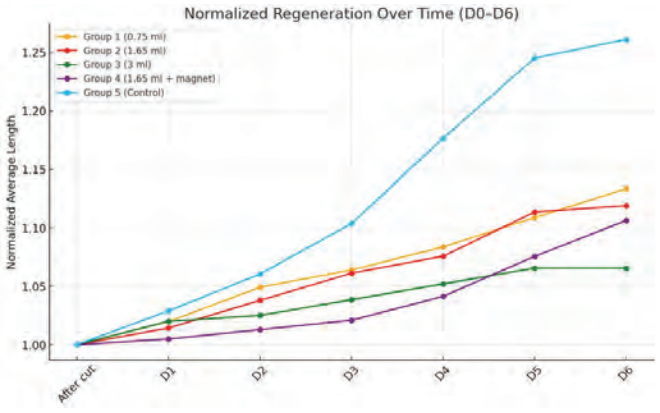

Figure 4: Normalized average graph that shows regeneration of 5 groups of worms with various concentrations of ferrofluid over 6 days.

Limitations:

This study had several limitations. First, it used only one model organism, *Lumbriculus Variegatus*, which, while helpful for studying regeneration, does not reflect the complexity of cells or immune responses in more advanced organisms like zebrafish or mice. Second, because of limited resources, only one type of commercially available ferrofluid was used. This made it impossible to compare how different ferrofluid types (with different coatings or magnetic strengths) might affect results. Third, the study didn't use advanced tools like fluores-

DOI: 10.36838/IJHSR87.321

cence microscopy or gene expression analysis, which could have helped show how cells responded at a deeper level. Fourth, the experiment lasted only six days, so long-term effects like reproduction or full organ recovery were not studied. Fifth, since the project was done at home without lab-grade equipment, it was not possible to measure more complex biological details.

Future studies should use more advanced organisms like zebrafish, axolotls, or mice, which are often used in regeneration research. Testing ferrofluids with safer coatings like PEG, silica, or dextran could also reduce harmful effects and make them more suitable for medical use. Using better imaging tools and running longer experiments would help us understand how ferrofluids interact with living tissues over time.

Conclusion

This study examined the effects of ferrofluids on tissue regeneration using *Lumbriculus variegatus*, a model organism known for its high regenerative capacity. Ferrofluids, composed of magnetic nanoparticles, are widely regarded as promising tools in biomedical applications due to their ability to respond to magnetic fields, potentially guiding healing or stimulating growth. Previous research suggested their utility in wound healing, but their biological safety and functional outcomes remain under investigation.

In this experiment, *Lumbriculus variegatus* were wounded and divided into five groups, receiving different concentrations of ferrofluid—with or without magnetic field exposure—while one group served as a control. Conditions such as soil type, lighting, temperature, and feeding were carefully controlled, and regeneration was monitored through both behavioral activity scoring and tail regrowth measurements over six days.

The results showed a clear dose-dependent decline in regeneration among all ferrofluid-treated groups. Higher concentrations of ferrofluid, especially when combined with an external magnet, led to reduced or delayed regeneration. In contrast, the control group demonstrated the most consistent and robust regrowth. Behavioral activity mirrored these findings, with treated groups exhibiting less spontaneous movement, suggesting possible physiological stress or disruption.

The discussion highlighted that, contrary to previous studies, ferrofluids in this context did not promote regeneration—instead, they impaired it. The study also observed reproductive inhibition in all treated groups, supporting concerns about ferrofluid safety in biological systems. Magnetic fields may have intensified these effects, further complicating the role of ferrofluids in therapeutic use. This calls into question the assumption that their physical responsiveness automatically equates to biological benefit.

A major limitation was that the experiment only used one species and did not track ferrofluid uptake at the cellular level. Future research should explore how ferrofluids interact with internal tissues using imaging and molecular tools, test across other organisms, and investigate long-term effects such as reproductive damage. Developing ferrofluid formulations with safer coatings may also help reduce toxicity and better support regenerative applications.

In conclusion, this study challenges optimistic assumptions about ferrofluid-assisted regeneration. Further research is necessary to evaluate their safety, optimize formulations, and clarify their mechanisms of action in both short- and long-term biomedical use.

Acknowledgments

I would like to express my special thanks of gratitude to my mentor, Trinity Tat, and Indigo Research for their invaluable support and guidance throughout this process. I also want to thank my mom for providing me with the necessary resources, equipment, and a comfortable environment. I attest that the ideas, graphics, and writing in this paper are entirely my own.

References

1. *Magnetic nanoparticles*. Wikipedia. https://en.wikipedia.org/wiki/Magnetic_nanoparticles.
2. *Superparamagnetism*. Wikipedia. https://en.wikipedia.org/wiki/Superparamagnetism.
3. *Magnetic drug delivery*. Wikipedia. https://en.wikipedia.org/wiki/Magnetic_drug_delivery.
4. Lu, A.-H.; Salabas, E. L.; Schüth, F. Magnetic Nanoparticles: Synthesis, Protection, Functionalization, and Application. *Chem. Soc. Rev.* **2007**, *36* (12), 2821–2834. https://doi.org/10.1039/B618799H.
5. Dutz, S.; Hergt, R. A Review of Magnetic Nanoparticles for Biomedical Applications: Synthesis and Functionalization. *APL Materials* **2024**, *12* (1), 010601. https://doi.org/10.1063/5.0133927.
6. Alessandro Surpi; Shelyakova, T.; Murgia, M.; Rivas, J.; Piñeiro, Y.; Greco, P.; Fini, M.; Valentin Alek Dediu. Versatile Magnetic Configuration for the Control and Manipulation of Superparamagnetic Nanoparticles. *Scientific Reports* **2023**, *13* (1). https://doi.org/10.1038/s41598-023-32299-9.
7. *Magnetic nanoparticles – Potential applications*. Wikipedia. https://en.wikipedia.org/wiki/Magnetic_nanoparticles#Potential_applications.
8. R. Hernández; J. Sacristán; L. Asín; Torres, T. E.; Ibarra, M. R.; Goya, G. F.; Mijangos, C. Magnetic Hydrogels Derived from Polysaccharides with Improved Specific Power Absorption: Potential Devices for Remotely Triggered Drug Delivery. *The Journal of Physical Chemistry B* **2010**, *114* (37), 12002–12007. https://doi.org/10.1021/jp105556e.
9. *Earthworm*. Wikipedia. https://en.wikipedia.org/wiki/Earthworm.
10. Agatz, A.; Miles, M.; Roeben, V.; Schad, T.; Van Der Stouwe, F.; Zakharova, L.; Preuss, T. G. Evaluating and Explaining the Variability of Honey Bee Field Studies across Europe Using BEEHAVE. *Environmental Toxicology and Chemistry* **2023**, *42* (8), 1839–1850. https://doi.org/10.1002/etc.5678.
11. Canada, E. and C. C. *Biological test method: Tests for measuring avoidance behaviour or reproduction of earthworms (Eisenia andrei or Dendrodrilus rubidus) exposed to contaminants in soil*. www.canada.ca. https://www.canada.ca/en/environment-climate-change/services/wildlife-research-landscape-science/biological-test-method-publications/avoidance-behaviour-reproduction-earthworms-contaminants-soil.html.
12. Scherer, C.; Figueiredo Neto, A. M. Ferrofluids: Properties and Applications. *Brazilian Journal of Physics* **2005**, *35* (3a), 718–727. https://doi.org/10.1590/s0103-97332005000400018.
13. Martinez Acosta, V. G.; Arellano-Carbajal, F.; Gillen, K.; Tweeten, K. A.; Zattara, E. E. It Cuts Both Ways: An Annelid Model System for the Study of Regeneration in the Laboratory and in

the Classroom. *Frontiers in Cell and Developmental Biology* **2021**, *9*, 780422. https://doi.org/10.3389/fcell.2021.780422.
14. *The Impact of Ferrofluid on Innovation in Biomedical Engineering*. Patsnp Eureka. https://eureka.patsnap.com/report-the-impact-of-ferrofluid-on-innovation-in-biomedical-engineering (accessed 2026-02-20).
15. Wang, M.; Deng, S.; Cao, Y.; Zhou, H.; Wei, W.; Yu, K.; Cao, Y.; Liang, B. Injectable Versatile Liquid-Solid Transformation Implants Alliance Checkpoint Blockade for Magnetothermal Dynamic-Immunotherapy. *Materials Today Bio* **2022**, *16*, 100442. https://doi.org/10.1016/j.mtbio.2022.100442..

Author

Eldar Osmonov is an incoming senior at Oxford International School in Bishkek. He is interested in bioengineering and biomedical science. Throughout the study of ferrofluid and its application in wound healing, he understood concepts of the fields of study he is interested in. In the future, he wants to major in bioengineering, focusing on bioinstrumentation, cellular therapy, and genome editing.

DOI: 10.36838/IJHSR87.321

IJHSR
ijhighschoolresearch.org
REVIEW ARTICLE

Climate Shockwaves: The Impact on Political Instability from Natural Disasters

Haedam Lee

Branksome Hall Asia, 70, Global edu-ro 145beon-gil, Daejeong-eup, Seogwipo-si, Jeju-do, 63644, Republic of Korea;
haedam0913@gmail.com
Mentor: Cesar Martinez Espinosa

ABSTRACT: This paper explores the relationship between climate change-induced natural disasters and the rise of political instability within affected local communities. As climate events increase in frequency and intensity, understanding their political consequences is crucial now more than ever. The study categorizes disasters into three types: atmospheric, hydrological, and geological. Then, it investigates how each uniquely influences political sentiment and institutional trust. Through case studies and secondary analysis of existing comparative research, the paper analyzes both the direct and indirect impacts of such disasters on political landscapes, comprehensively analyzing not just the direct consequences but the impact of governmental or community-level action. While assessing contrasting scholarly opinions on the political ramifications of such disasters, it provides an evaluation of whether these events exacerbate pre-existing political tensions or catalyze new forms of instability. Ultimately, the research highlights that while there are significant correlations between certain types of climate events and political instability, it largely depends on pre-existing conditions. Hence, the paper offers insights into preventive strategies and governance reforms to mitigate these socio-political risks.

KEYWORDS: Earth and Environmental Sciences, Climate Sciences, Climate Change, Natural Disasters, Political Instability.

Introduction

Political instability, though a widely used term in both academic and policy discourses, remains multifaceted in its definitions. Broadly, it refers to the proneness of a government or political system to collapse through conflicts or challenges faced.[1] However, political instability is less seen through its definition but more in its signs, demonstrated in our society. Such indicators can be both institutional breakdowns and the eruption of violent internal conflicts that fundamentally disrupt state authority. Thus, political instability cannot be defined by a singular event such as a regime overthrow but rather should be defined by an array of socio-political conditions that threaten governmental continuity, policy effectiveness, and the security of its citizens. Not only is defining political instability crucial for this analysis, but measuring the extent to which instability was seen is important. While events like the current party in power losing the following election can be seen as less disruptive indicators of political instability, more extreme events can be violent outbreaks like armed conflicts. Hence, the range in which political instability can be experienced can be identified by how much impact or threat the event poses to its people, with less effect being on the low extent, while the greatest effect is on the high extent. Table 1 below has been supplied to support such a range of understanding:

Table 1: The Political instability range was created using a political science literature review, aiming to categorize disasters into quantitative measures of severity.

No impact	Low extent ----------High extent				
0	1	2	3	4	5
No adverse political effect	Party in power loses next election/loses support seen in approval ratings/minor civilian disruptions	Government in charge gets thrown out through established means (impeachment or vote of no confidence)	Demonstrations and protests (non violent)	Government falls through non established means (coup)	Violence such as armed conflicts

The rapid increase in both the frequency and intensity of climate-related natural disasters underscores the need to explore their political consequences. According to data from the United Nations, there was an average of 335 weather-related disasters annually between 2005 and 2014, marking a 14% increase compared to the previous decade.[2] This escalation raises a vital question regarding the relationship between natural disasters and their role in catalyzing political extremism and polarization. As US President Joe Biden has said, "The climate crisis is about human security, economic security, environmental security, national security, and the very life of the planet."[3] Hence, it is clear that climate change has surpassed the stage of just being an environmental concern but something overarching for global safety. And it is no secret that this extension of impact is caused by the increasing intensity of such climate-triggered disasters, seen by examples such as the US East Coast storms Harvey, Irma, and Maria, causing $250 billion in damages and thousands of deaths.[4]

© 2026 Terra Science and Education

DOI: 10.36838/IJHSR87.326

Existing research on the topic has found a diverse relationship between climate change-triggered natural disasters and political instability. Canavan and Ide[5] offer a systematic review revealing that disasters, many of which are intensified by climate change, have been found in most studies to increase risks of political conflict, particularly low-intensity forms such as protests and communal violence. However, they mention that this connection between disaster and conflict is deeply controlled and impacted by political, socioeconomic, and institutional contexts. They note that state weakness and hardship often become the backbone for heightened conflict risks as disasters exacerbate grievances over uneven relief distribution or strain government capacities, hence undermining the legitimacy and security provision provided. Interestingly, a significant minority of studies also highlight the need for disaster diplomacy, where shared hardships and challenges generate cooperation rather than conflict. Therefore, the study concludes by suggesting that the relationship between natural disasters and political instability is neither linear nor universal but contextually contingent and multifaceted.

Busby[4] takes a broader climate security lens, underlining how climate change-induced disasters destabilize societies by threatening livelihoods through ways like inducing migration and amplifying humanitarian crises. While his analysis extends beyond the disaster-conflict dynamic, it understands climate hazards as catalysts for political instability, particularly where fragile states are unable to manage the compounded risks of food insecurity, resource competition, and displacement. Adding on, Busby argues that although links between climate disasters and violent conflict are now widely recognized in policy discourse, effective prevention remains uncovered, hence leading to structural vulnerabilities and governance failures to mediate these risks. Busby's stance, therefore, is that climate change-triggered disasters do contribute to the political instability of the area but only exacerbate existing risks rather than create new ones.

The IMF working paper by Cevik and Jalles[6] further nuances this discussion by establishing corruption as a determinant of disaster outcomes and subsequent political stability. Their econometric analysis across 135 countries finds that corruption significantly increases natural disaster-related fatalities, particularly in developing states where institutional weakness is combined with infrastructural vulnerability. Though the paper focuses primarily on mortality, it indirectly uses corruption-induced humanitarian failures as drivers of political instability, as ineffective governance and lack of accountability undermine public trust and social cohesion post-disaster. The implication here is that natural disasters do not automatically translate to political instability; rather, it is the combination of institutional quality, socioeconomic resilience, and governance capacity that shapes such relationships.

Omelicheva[7] investigates the presumed causal links between natural disasters and political instability through a reassessment of the relationship between disasters and conflict. Drawing on the Political Instability Task Force model alongside EM-DAT disaster data, she finds only minor support for disasters as independent triggers of political instability. While rapid and unexpected disasters such as floods, storms, and earthquakes were weakly associated with increased risks in some models, these effects disappeared when controlling for regime type, state capacity, and socioeconomic conditions. Her findings underscore that disasters function less as external shocks creating conflict and more as catalysts within states already exposed to instability. In particular, divided, transitional, and poorly governed states remain vulnerable, not due to the disaster itself but because such institutional weakness brings on pervasive corruption and low adaptive capacity that transform natural hazards into political crises. Omelicheva thus undermines the deterministic narrative of disasters generating violence, urging a reorientation towards examining how the regime's own stability controls the political implications of natural hazards.

It is clear through this literature review that there are many established opinions on the effects of climate change-triggered natural disasters on political instability. While some approaches offer insight that supports the link between the two factors, others disagree, citing existing conflicts as being contingent on the upbringing of conflict. However, the literature does reflect a consensus that climate change-induced natural disasters rarely function as a singular cause. Instead, these disasters interact with a range of political, socioeconomic, and institutional factors that determine whether and how instability materializes. This complexity underscores the need for a nuanced approach in analyzing the relationship, one that moves beyond simplistic causal models to incorporate multidimensional factors shaping disaster impacts. This paper hence seeks to contribute to this discourse by examining not only whether disasters increase political extremism and instability but also under what conditions and through what mechanisms these relationships are felt. Through a comparative analysis of atmospheric, hydrological, and geological disasters, it aims to unpack the multifaceted pathways through which climate change-triggered natural hazards intersect with political structures, shaping the trajectories of stability or conflict within affected societies.

Methodology

The main aim of this research is to look at the relationship between climate change-related natural disasters and the impact they have on political instability. To achieve this goal, this research categorizes disasters into atmospheric, hydrological, and geological events to better understand their social and political impacts. Atmospheric disasters include hurricanes and cyclones. Hydrological disasters encompass floods, droughts, and the gradual shrinkage of water bodies. Geological disasters, though not climate-induced, are included as a contrast to help identify what makes climate-related events politically distinct.

Selected case studies include Hurricane Katrina in the United States, Hurricane Otis in Mexico, and Cyclones Idai and Kenneth in Mozambique under the atmospheric category. Under hydrological disasters, the study examines the Kerala floods in India, Zimbabwean floods, the shrinkage of Lake Chad and Lake Poopó, Cape Town's "Day Zero" water crisis, and the Aral Sea Crisis. As for the control variable of geologi-

cal disasters, the 1985 Mexico City earthquake, the Myanmar earthquake in 2025, and the 2023 earthquakes in Turkey are included. These cases were chosen not only to look at a variety of types of natural disasters but also to analyze countries with different levels of development, democratic maturity, or institutional strength, allowing for more comprehensive research, not focusing only on the impacts on one type of political society.

The selection of cases focuses on the past couple of decades (2005 to present date) to provide with more recent analysis (the existing literature tends to focus on older disasters and most if it ends the analysis in the 2010s), especially when the level of information about the impacts of climate change is considerably more extended across the globe and across sectors of the population. Two exceptions to this range are included: the 1985 Mexico City earthquake (which is used as one of the control cases) and the Aral Sea crisis, which has developed over several decades, but where the main political action analyzed happened over the past two decades.

For each case, political impacts such as extremism, protest movements, and polarization are evaluated alongside socio-economic consequences like displacement and resource scarcity. The role of institutional responses is also analyzed, ranging from government action to external aid and community resilience. This dual-lens approach (considering both destabilization and resilience efforts) connects a combination of political behaviour studies and literature reviews.

Discussion

Atmospheric Disasters:

In the case of atmospheric disasters, Hurricane Katrina in 2005 serves as a stark example of how such events can expose systemic inequalities and prompt political polarization.[8] As an immediate impact of the event, 2000 people lost their lives along with the displacement of 1.5 million people, communicating the large scope of impact the event had.[9] Adding on, the disaster revealed significant institutional failures and racial inequities, leading to public outrage and a deepening of distrust in government. Polarization intensified, especially across racial and socioeconomic lines, as different groups adopted contrasting narratives of blame and responsibility. Specifically, the US government revealed that 1/5th of victims of displacement from the storm were those considered poor, while 44% of the storm victims were African American.[10] A study by Nicholls and Picou[11] confirms this relationship through the survey conducted, demonstrating how regions affected by the hurricane showcased higher levels of distrust towards the government compared to regions that were not impacted. Though the paper identified that the correlation was not strong, it is still a clear indicator that, despite the recognition that natural disasters are inevitable, the people's distrust is based on the reaction and aftermath the government performed after experiencing such a disaster. In fact, the president at the time, George W. Bush, had his lowest approval rating after this time, communicating the hurricane's impact on political instability.[12] Conclusively, Hurricane Katrina demonstrates an instance of how, now, the natural disaster itself, but the aftermath in handling the disaster by the government, is what impacts political stability.

Another atmospheric disaster, Hurricane Otis in 2023, highlighted the urban vulnerability but also the adaptability of Acapulco. Although the impact of the disaster was detrimental, being the fastest-strengthening tropical storm ever recorded in the Northeast Pacific, the damages incurred were resolved fairly quickly thanks to the government's rapid response.[13] The Ministry of Welfare provided support to businesses affected by the disaster, including hotels, and electricity was restored in a mere 7 days after the hurricane hit. The government called for unification and centralized control in order to rapidly restore the state of the community, a method that has evidently worked, as seen by the rapid recovery of the area. This instance demonstrates that strong communication networks and unified action can mitigate the polarizing effects of governmental failure.

Continuing, Cyclones Idai and Kenneth, which devastated parts of Mozambique in 2019, resulted in extensive infrastructure damage and displacement. With the rising need for Humanitarian aid, with around 1.3 million children in desperate need of help, the cyclones seemed to have brought a disaster that would be difficult to mitigate.[14] However, unlike the Katrina case, the response here fostered political unity. The Mozambican government, with international assistance, established a Disaster Management Fund and conducted transparent reporting through Post-Disaster Needs Assessments.[15] The international pledging conference held in the city of Beira in Mozambique highlighted the need for resilience, especially for regions like Mozambique, where climate-induced disasters persist. Noura Hamladji, the UNDP Africa Bureau Regional Director, spoke of the need to "build back better", meaning to improve the broken-down infrastructure to prevent such disasters from happening again. Hence, Cyclones Idai and Kenneth demonstrated yet another way an atmospheric disaster led to a wake-up call for further resilience and collaboration.

Hydrological Disasters:

Moving on to hydrological disasters, the 2018 and 2020 Kerala floods in India, aggravated by mismanagement of dams and climate-driven monsoon intensity, had severe socio-economic impacts, leading to prolonged and structural political shifts. At the time, Kerala, India, was going through repetitive outbreaks of floods, mostly attributed to accelerated urbanization and climate change.[16] While the citizens were grateful and well supported by the response of the government after the disaster, they were placing blame on the lack of preparatory measures the government took to prevent such a disaster in the first place. Such suggests that government performance in disaster management could either rally or repel public support depending on the perceived effectiveness, as seen here by the contrasting reaction in the preceding and following actions of the government in managing the flood. In addition, the citizens' effort in forming initiatives and conducting community mobilization demonstrates how, while the political agenda may have been challenged, people were willing to act upon the challenges faced, communicating political strength and unity.

DOI: 10.36838/IJHSR87.326

Therefore, the Kerala floods, as a climate-induced hydrological disaster, provide a unique perspective: while the government was challenged and consequently undermined by the people, the way in which the citizens collaborated to do so communicated both political strength and instability.

In Zimbabwe, the climate change-induced floods between 2016 and 2017 exposed the state's weak disaster response capabilities. Rural livelihoods were devastated, leading to displacement, diseases, malnutrition, and many more complications. Throughout such challenging circumstances, citizens actively sought measures to unify efforts for recovery and work in support of many external groups.[17] However, not seen in this list of helpers is the government. Hence, following the flood in March, by late November, the president at the time, Robert Mugabe, resigned from office after a coup. While the coup cannot be seen as a direct result of the flooding, it surely represents how mismanagement of natural disasters due to corruption and the lack of democracy can lead to political instability.

The Lake Chad Basin provides a more extreme example. Having shrunk by 90% since the 1960s due to prolonged drought and overuse, Lake Chad's disappearance has significantly challenged the security of the region. One of the world's deadliest terrorist groups, the Boko Haram, associated itself with the conflicts that killed over 37,500 people near the lake, and around 3.6 million people were identified at crisis and emergency levels of food insecurity.[18] In the International Conference in Abuja in February 2018, the conclusion was made that the only way to save Lake Chad was by "the full unification of Africa", with leaders such as President Muhammadu Buhari of Nigeria urgently calling to action, saying, "The time to show our humanity is now."[19] Despite such identification of the need for a community-wide response, the region was already in turmoil before the lake's downfall. Due to inequality, underdevelopment, and high poverty levels, the drying of Lake Chad was only a catalyst for the region's downfall rather than the root cause. Since then, international communities, including the UN, have recognized that climate-related security risks are on the rise, noting government deficiencies as exacerbating factors of such challenges.[19] Hence, what this case of Lake Chad demonstrates is how climate-induced natural disasters can severely worsen political instability to a point where violent conflicts are held even in international regions.

Similarly, the drying of Lake Poopó in Bolivia, accelerated by climate change and water mismanagement, displaced indigenous communities who relied on the lake for their livelihoods. Specifically, the Urus indigenous community suffered immensely from this loss, presenting to them yet another challenge from historic trends of marginalization.[20] While they originally relied on fishing as an alternative to the lost land they had to colonize, now, due to climate change-triggered drying of the lake, they have no way to sustain their living. The controversies surrounding the reaction of the Bolivian government in addressing the crisis effectively consisted of two viewpoints: one that argues fault is at the international trends of Western countries' contribution to climate change, and the other that puts blame on the national government for water contamination and usage for industries like mining. The government's standpoint (the 1st viewpoint) can be seen as a political move in order to make them seem innocent victims and remove blame from their own decisions of water mismanagement.[20] Consequently, the drying of Lake Poopó and its surrounding controversies demonstrate how climate-triggered natural disasters can not only lead to political instability but to schemes of manipulation to remove themselves from fault, bringing on even more conflict.

A similar story is told in Cape Town's "Day Zero" water crisis. Many, including Warner and Meissner[21], argue that the idea of Cape Town reaching "Day Zero," a day when water would run out, was a political manipulation. With the City Council providing such a countdown towards a supposed doomsday, the media amplified such messages, spurring anxiety and action within the community. Hence, it was a strategy by the government to force the middle class into conserving water, using the social behavior of people to participate in pro-social behaviors in the face of an imminent disaster as its backbone. Later, as the day approached, the supposed end was cancelled, citing reasons such as rainfall. While this strategy may have worked in this narrative with Cape Town, it is important not to misuse this construction of a disaster, as it may become ground for people to be in disbelief when a real disaster hits, like the folklore <The Boy Who Cried Wolf>.

The Aral Sea Crisis, though rooted in Soviet-era water diversion policies rather than climate change alone, parallels these themes. As the sea vanished, surrounding communities faced toxic dust storms, health crises, and economic collapse. Tensions among the five Central Asian republics that rely on the same water sources escalated, revealing how hydrological disasters can trigger regional disputes and foster long-term geopolitical instability.[22] However, what is different about this crisis as compared to the drying of Lake Poopó or Chad is that the conflict was non-violent and that efforts were taken collaboratively to support the protection of the region. Agreements between the leaders of the region were made, with member states signing the "Agreement on Joint Actions for Addressing the Problems of the Aral Sea and its Coastal Area, Improving the Environment and Ensuring the Social and Economic Development of the Aral Sea". Therefore, while instability was generated due to the impact of the natural disaster itself, the integrated approach made such challenges trivial compared to regions where such peaceful methods were not used.

Geological Disasters:

Geological disasters here will be used as control variables of how non-climate-induced events impact the political instability of the affected region. This is because Geological disasters are loosely connected to climate change, being attributed more to the natural movement of the Earth. Linking back to the Cyclones Idai and Kenneth, an interesting perspective to note here is that a non-climate-induced event of the 1985 Mexico City earthquake also had a similar instance of bringing the community together rather than leading to political instability. After the devastating earthquake hit, the people, completely aware of the corruption and lack of support from the govern-

ment, took matters into their own hands. They provided relief for the people, becoming an inspirational pioneering action for the coming activism for governmental reform.[23] Hence, little instability was generated as the people acknowledged the prolonged unreliability of the government and unified themselves for recovery. Considering similar instances of unification of the people after a natural disaster, it can be argued that, in some cases, whether it be climate-induced or not, the political environment may be stabilized through the communal efforts of the people.

Another example is the earthquake that struck Myanmar in 2025. Despite its devastation, the disaster did not meaningfully alter the trajectory of the country's ongoing civil conflict. As Kurlantzick[24] notes, while Myanmar has a history of natural disasters prompting temporary political openings, such as Cyclone Nargis in 2008, leading to a brief relief through international cooperation, the recent earthquake failed to catalyze either cooperation or destabilization. The military junta continued its repressive operations, and there were no significant shifts in rebel activity or public mobilization. Thus, this instance suggests that geological disasters, unlike certain climate-induced events, may at times merely reinforce existing political dynamics rather than serving as triggers for either instability or reconciliation.

The 2023 earthquakes in Turkey provide a similar example. While these earthquakes caused widespread devastation, killing over 50,000 people and displacing millions, they had minimal immediate political destabilization. As Radlinsky *et al.*[25] suggest, although public anger rose against President Erdoğan's government for inadequate building code enforcement and a delayed disaster response, his administration retained power in the subsequent elections. This was partly achieved through the strategic spread of narratives blaming external actors for allegedly destabilizing Turkey. Thus, like the Myanmar case, the Turkish earthquakes demonstrate that geological disasters do not inherently undermine political regimes; rather, they may become politicized crises through which governments deflect criticism and consolidate authority, ultimately reinforcing existing power structures rather than destabilizing them. Such use of the disaster as a political tactic can also be seen in Lake Poopó and Cape Town's Day Zero incidents, explained above, hence communicating a link between the non-climate-induced and the climate-triggered natural disasters in the government's use of such disasters as strategic schemes.

Conclusion

This research set out to investigate the relationship between climate change-triggered natural disasters and political instability, examining atmospheric, hydrological, and geological disasters to identify their respective political impacts. The findings indicate that while climate-induced natural disasters have the capacity to catalyze political instability, the relationship is not deterministic. Instead, disasters interact with pre-existing institutional, socioeconomic, and political contexts, shaping whether stability is reinforced or undermined.

Atmospheric disasters demonstrated mixed effects. Hurricane Katrina revealed that political instability is not embedded in the disaster itself but emerges from governmental failure to effectively respond, leading to public distrust and intensified polarization. In contrast, Hurricane Otis in Mexico showed how rapid governmental action and unified communication could mitigate potential instability, with the population rallying behind centralized responses. The Mozambican cyclones Idai and Kenneth similarly fostered political unity rather than extremism, as transparent governance, international collaboration, and a focus on "building back better" enhanced societal resilience.

Hydrological disasters displayed a broader spectrum of impacts. The Kerala floods revealed how perceived governmental inaction prior to disasters can undermine trust, yet also how citizen-led initiatives can transform instability into a demonstration of communal political strength. Zimbabwe's floods exposed state weaknesses and mismanagement, indirectly contributing to regime overthrow, highlighting how institutional failures amid disaster intensify vulnerability to political shocks. The Lake Chad crisis exemplified how climate-induced environmental degradation exacerbates existing regional insecurities, serving as a catalyst for violent extremism by groups like Boko Haram, while Lake Poopó's drying showcased governmental manipulation to deflect accountability, fostering further societal division. Cape Town's Day Zero illustrated how governments may construct disasters politically, using them to manipulate public behavior, yet risking long-term credibility erosion if crises are perceived as manufactured. Finally, the Aral Sea crisis demonstrated that despite significant environmental challenges, cooperative regional governance can reduce the likelihood of violent instability, instead fostering peaceful conflict resolution mechanisms.

Geological disasters, used as control variables, highlighted that non-climate-induced events similarly function not as direct triggers but as catalysts contingent on existing political dynamics. The 1985 Mexico City earthquake united citizens to acknowledge the negligent government, while Myanmar's 2025 earthquake had negligible effects on its already ongoing civil conflict, merely maintaining the status quo. Turkey's 2023 earthquakes underscored how disasters can be politicized to reinforce existing power structures, as governmental blame deflection and narrative control preserved regime stability despite public anger.

In conclusion, the relationship between natural disasters and political instability is deeply contextual and mediated by governance capacity, institutional integrity, socioeconomic resilience, and public trust. Climate change-triggered disasters do not inherently produce instability or extremism but rather exacerbate underlying vulnerabilities or provide opportunities for political unity and resilience. Furthermore, the research finds that government responses and strategic communication play defining roles in shaping political outcomes, with similar manipulative tendencies identified across both climate-induced and geological disasters. Overall, the lack of unity in the political or social climate in the event of a disaster, such as conflicts between racial groups, socio-economic levels, or

DOI: 10.36838/IJHSR87.326

nationalities, led to more severe impacts compared to those that did not have such divisive factors. While in some cases the lack of reliable governance led to collaboration and mitigation of political instability through the people's efforts, the major dialogue suggests that when national or even international communities were able to come together in mitigation, political instability was reduced. Table 2 below summarizes the findings across disaster types, finding that political instability and climate-triggered disasters do not portray a deterministic relationship but rather depend on contextual factors:

Table 2: Summary of disasters and political impact in relation to the categorization in Table 1, containing explanations to reason for the results.

Disaster type		Political impact	Political Instability Range Result
Atmospheric	Hurricane Katrina (US)	Exposed systemic inequalities and failures, prompting political polarization = induced distrust by the people	Low (1)
	Hurricane Otis (Mexico)	Highlighted urban vulnerability but also the adaptability and flexibility of the government	None (0)
	Cyclones Idai and Kenneth (Mozambique)	Extensive infrastructural damage and displacement still led to political unity with prompt responses and international cooperation	None (0)
Hydrological	Kerala floods (India)	Aggravated through mismanagement of dams and had significant impact in the socio-economic dynamic = led to lasting political shifts but also community mobilization	Low (1)
	Floods from 2016-2017 (Zimbabwe)	Rural environments proved to be prone to damages and impacts to which the people supported each other = lack of government support became one of the indirect factors contributing to the following coup against the president at the time	Moderate (2)
	Shrinking of Lake Chad (Nigeria, Niger, Chad, and Cameroon)	Heightened challenges in the surrounding region along with direct violent conflicts surrounding terrorist groups, exacerbated by inequality and poverty in the area = worsened political instability to a point of violence	High (3)
	Drying of Lake Poopó (Bolivia)	Displaced indigenous communities and lost a means for living, with the government using it as a political move to remove blame from themselves	Low (1)
	Cape Town's "Day Zero" (South Africa)	Impact of media in upbringing and forcing anxiety and behavioural changes, disproportionate impact to the middle class	Low (1)
	Aral Sea Crisis (Uzbekistan, Afghanistan, Iran, Kazakhstan, Kyrgyzstan, Tajikistan, and Turkmenistan)	Regional disputes triggering long term instability, though non violent and efforts for collaboration taken	Low (1)
Geological	1985 Mexico City earthquake (Mexico)	Fostered unity within the people after the anticipation of the lack of support from the ineffective government	None (0)
	Earthquake in 2025 (Myanmar)	Null impact on the ongoing civil conflict (violent)	Low (1)
	Earthquakes in 2023 (Turkey)	Though significant casualties incurred, administration maintained power in subsequent elections through blame being placed in other political actors	Low (1)

Limitations:

While this research does offer significant insight into the complicated relationship between natural disasters and political instability, the limitations must be acknowledged. First, this analysis operates under the assumption that many of the atmospheric and hydrological disasters explored are triggered or exacerbated by climate change. However, it is not deterministic that these events are solely the result of climate change. Natural variability, such as shifts in oceanic and atmospheric circulation patterns, continues to play a significant role in disaster occurrence and intensity, as evident in Table 2. For instance, while hurricanes like Katrina have been linked to warmer sea surface temperatures attributed to climate change, it is scientifically challenging to isolate climate change as the singular cause of any specific event without comprehensive attribution studies.[26] This limitation thus raises caution against generalizing causal claims, as it simplifies the complex relationships.

Adding on, while this study categorizes disasters into atmospheric, hydrological, and geological types to find different impacts, the boundaries between these categories are often blurred. Many disasters emerge from multiple interacting factors that cannot be neatly classified into singular causes, which potentially limits the analytical depth of this research.

In sum, while this research provides a grounded and comparative perspective on the intersection between climate-related natural disasters and political instability, its limitations remind us that such relationships are not universal nor deterministic. Rather, they are embedded within deeply contextual factors that require continued interdisciplinary examination.

Policy Recommendations:

Based on the conclusions made, it is clear that the response from the government significantly impacts the instability incurred in the region. Hence, policy responses must be contextually embedded rather than universally generalized.

Firstly, as seen in the cases of Hurricane Otis in Mexico and Cyclones Idai and Kenneth in Mozambique, rapid and transparent governmental responses are crucial in mitigating the damage from disasters. Both instances highlighted how strong communication networks and coordination, both international and domestic, not only quickened recovery but also fostered public trust and unity. Governments should therefore prioritize developing robust disaster response frameworks that integrate clear communication strategies and pre-plan logistical coordination, creating a multi-level governance system to ensure that immediate relief efforts reach all affected most efficiently.

Second, institutional resilience and accountability are essential in preventing disasters from exacerbating. In instances such as Hurricane Katrina and the Zimbabwe floods, ineffective governance and perceived negligence intensified political distrust, contributing to polarization and vulnerability of the regime. Therefore, it is recommended that governments strengthen institutional transparency by implementing mechanisms such as Post-Disaster Needs Assessments and publicly reporting on recovery processes. This would foster social cohesion by reducing perceptions of corruption or exclusion, particularly among marginalized populations who often experience disproportionate disaster impacts.

Third, long-term resilience planning must be prioritized over short-term reactive measures. The Mozambican emphasis on "building back better" after Cyclones Idai and Kenneth highlights the importance of using disasters as catalysts for sustainable development rather than merely restoring pre-existing vulnerabilities. Integrating resilience-building into reconstruction efforts, including strengthening infrastructural standards and investing in climate adaptation measures, will mitigate future risks while enhancing political stability through visible governmental commitment to public welfare.

Finally, governments must avoid the politicization and manipulation of disaster narratives for strategic gain, as seen in the cases of Cape Town's Day Zero, Lake Poopó, and the 2023 Turkish earthquakes. While narrative control may temporarily

preserve stability of the government, such strategies risk eroding public trust over time, particularly if communities perceive crises to be manufactured or exploited. Transparent and evidence-based communication, along with inclusive governance, should be adopted to ensure that disaster management processes are not leveraged as tools for political manipulation.

Overall, while climate change-induced natural disasters may be inherently environmental, their political repercussions are governed by human actions. Therefore, proactive governance, institutional integrity, and community-centered resilience building remain the keys to transforming disasters from catalysts of instability into opportunities for equitable development and political cohesion. While the fact that a disaster is attributed to climate change might not be, by itself, a determinant of political instability, the fact that the number of disasters attributed to climate change continues to grow puts some pressure on the government. People expect change and improvement, meaning that as climate change exacerbates and these disasters repeat themselves, the government's ability to respond will be tested further, hence adding to the pressure to correctly handle such patterned disasters.

Acknowledgments

Sincere gratitude is given to my mentor, Cesar Martinez Espinosa, who has supported me throughout this journey.

References

1. AG Global Strategies. Governmental Instability. https://www.ag-globalstrategies.com/governmental-instability (accessed Aug 7, 2025).
2. Centre for Research on the Epidemiology of Disasters; United Nations Office for Disaster Risk Reduction. The Human Cost of Weather-Related Disasters 1995–2015; UNDRR: Geneva, 2015. https://www.undrr.org/publication/human-cost-weather-related-disasters-1995-2015 (accessed Aug 7, 2025).
3. World Economic Forum. COP27: What Climate Leaders Are Saying Right Now. https://www.weforum.org/stories/2022/11/cop27-quotes-climate-leaders/ (accessed Aug 7, 2025).
4. Busby, J. W. Beyond Internal Conflict: The Emergent Practice of Climate Security. J. Peace Res. 2021, 58 (1), 186–194. Published online Dec 28, 2020. https://doi.org/10.1177/0022343320971019 (accessed Aug 7, 2025).
5. Canavan, C.; Ide, T. Contention, Cooperation, and Context: A Systematic Review of Research on Disasters and Political Conflicts. Int. J. Disaster Risk Reduct. 2024, 108, 104558. https://doi.org/10.1016/j.ijdrr.2024.104558 (accessed Aug 7, 2025).
6. Cevik, S.; Jalles, J. T. Corruption Kills: Global Evidence from Natural Disasters. IMF Working Paper No. 2023/220, 2023. https://doi.org/10.5089/9798400257315.001 (accessed Aug 7, 2025).
7. Omelicheva, M. Y. Natural Disasters: Triggers of Political Instability?. Int. Interact. 2011, 37 (4), 441–465. https://doi.org/10.1080/03050629.2011.622653 (accessed Aug 7, 2025).
8. Dyson, M. E. Come Hell or High Water: Hurricane Katrina and the Color of Disaster; Basic Books: New York, 2006.
9. Rhodes, J., Chan, C., Paxson, C., Rouse, C. E., Waters, M., & Fussell, E. (2010). The impact of Hurricane Katrina on the mental and physical health of low-income parents in New Orleans. American Journal of Orthopsychiatry, 80(2), 237–247. https://doi.org/10.1111/j.1939-0025.2010.01027.x
10. Gabe, T.; Falk, G.; McCarty, M.; Mason, V. W. Hurricane Katrina: Social-Demographic Characteristics of Impacted Areas; Congressional Research Service Report for Congress, RL33141; Library of Congress: Washington, DC, 2005.
11. Nicholls, K.; Picou, J. S. The Impact of Hurricane Katrina on Trust in Government. Soc. Sci. Q. 2013, 94 (2), 344–361. https://www.jstor.org/stable/42864424 (accessed Aug 7, 2025).
12. Murray, M. Bush Approval at Lowest Level of His Presidency. NBC News, Sept 14, 2005. https://www.nbcnews.com/id/wbna9332076 (accessed Aug 11, 2025).
13. Niño-Gutiérrez, N. S. Resilience in Adversity: Acapulco and the Aftermath of Otis Hurricane Category 5 of October 25, 2023. South Asian J. Soc. Stud. Econ. 2023, 20 (4), 209–224. https://journalsajsse.com/index.php/SAJSSE/article/view/753 (accessed Aug 7, 2025).
14. UNICEF. Cyclone Idai and Kenneth. UNICEF Mozambique. https://www.unicef.org/mozambique/en/cyclone-idai-and-kenneth (accessed Sept 21, 2025).
15. United Nations Development Programme. Mozambique Cyclone Idai Post-Disaster Needs Assessment. May 30, 2019. https://www.undp.org/publications/mozambique-cyclone-idai-post-disaster-needs-assesment-pdnadna (accessed Aug 10, 2025).
16. Mugambiwa, S. S.; Makhubele, J. Anthropogenic Flash Floods and Climate Change in Rural Zimbabwe: Impacts and Options for Adaptation. Technium Soc. Sci. J. 2021, 21, 809–819. https://www.researchgate.net/publication/353123575_Anthropogenic_flash_floods_and_limate_change_in_rural_Zimbabwe_Impacts_and_options_for_adaptation (accessed Aug 7, 2025).
17. De Coning, C.; Krampe, F. Multilateral Cooperation in the Area of Climate-Related Security and Development Risks in Africa. 2020, Mar 2. https://reliefweb.int/report/world/multilateral-cooperation-area-climate-related-security-and-development-risks-africa (accessed Aug 10, 2025).
18. Campbell, H. G. Saving Lake Chad and the Unification of Africa: Lessons from the International Conference to Save Lake Chad (ICLC), Abuja, Nigeria. February 2018. J. Afr. Foreign Aff. 2020, 7 (1), 71–110. https://www.jstor.org/stable/26976618 (accessed Aug 7, 2025).
19. Mishra, V. Deadly Floods Show Need for Faster, Wider Warnings, UN Agency Says. UN News, July 21, 2025. https://news.un.org/en/story/2025/07/1165455#:~:text=At%20the%20same%20time%2%20glacier,%C2%A9%20WMO/Arya%20Manggala (accessed Aug 7, 2025).
20. Perreault, T. Climate Change and Climate Politics: Parsing the Causes and Effects of the Drying of Lake Poopó, Bolivia. J. Lat. Am. Geogr. 2020, 19, 26–46. https://www.jstor.org/stable/48618950 (accessed Aug 7, 2025).
21. Warner, J. F.; Meissner, R. Cape Town's "Day Zero" Water Crisis: A Manufactured Media Event? Int. J. Disaster Risk Reduct. 2021, 64, 102481. https://doi.org/10.1016/j.ijdrr.2021.102481 (accessed Aug 7, 2025).
22. Climate Diplomacy. Conflict over Water in the Aral Sea. https://climate-diplomacy.org/case-studies/conflict-over-water-aral-sea (accessed Aug 7, 2025).
23. Santos-Reyes, J. Factors Motivating Mexico City Residents to Earthquake Mass Evacuation Drills. Int. J. Disaster Risk Reduct. 2020, 49, 101661. https://doi.org/10.1016/j.ijdrr.2020.101661 (accessed Aug 7, 2025).
24. Kurlantzick, J. Will the Earthquake Affect Politics and War in Myanmar? Council on Foreign Relations, April 1, 2025. https://www.cfr.org/blog/will-earthquake-affect-politics-and-war-myanmar (accessed Aug 10, 2025).

DOI: 10.36838/IJHSR87.326

25. Radlinsky, J.; Helupka, G.; Flanagan, D.; Ritscher, S.; Dorland, J.; Khalife, M. Political Implications of Earthquakes and Disinformation on Turkey Post-Election. The Counterterrorism Group, June 2, 2023; updated November 22, 2024. https://www.counterterrorismgroup.com/post/political-implications-of-earthquakes-and-information-on-turkey-post-election (accessed Aug 7, 2025).
26. Climate Signals. Hurricane Katrina (2005). https://www.climatesignals.org/events/hurricane-katrina-2005#:~:text=Hurricane%20Karina%20was%20one%20of,limited%20access%20to%20medical%20care (accessed Aug 7, 2025).

Author

Haedam Lee is a student from Jeju Island, South Korea, pursuing the International Baccalaureate Diploma. She has experience in government, diplomacy, and community initiatives, including work with the National Assembly and the Embassy of Ecuador. Her leadership spans youth advocacy, cultural preservation, and international academic competitions.

IJHSR International Journal of High School Research

is a publication of

terra science and education

N.Y. based 501.c.3 non-profit organization
dedicated for improving K-16 education